NASA TECHNICAL TRANSLATION NASA TT F-12,172

NASA TT F-12,172

HANDBOOK OF ELASTIC STABILITY
(REVISED AND SUPPLEMENTED)

Kuranishi Masatsugu
Naka Takao
Yoshiki Masao
Hayashi Shigeru
Sugano Makoto
Hirai Atsushi

Translation of "Cone Dansei Antei Yoran"
Corona Press, Tokyo, 1958, 686 pages

N69-34698
(ACCESSION NUMBER)
(PAGES)
(NASA CR OR TMX OR AD NUMBER)
(THRU)
1
(CODE)
32
(CATEGORY)
FACILITY FORM 602

AUG 1969
RECEIVED
NASA STI FACILITY
INPUT BRANCH

NATIONAL AERONAUTICS AND SPACE ADMINISTRATION
WASHINGTON, D.C. 20546 JULY 1969

PREFACE TO THE FIRST EDITION

In September 1947, the Column Research Council of Engineering Foundations of the United States sent a letter to Professor Kameyama Naoto of the First Engineering Department of Tokyo University. It read: "We would like to obtain cooperation in carrying out exhaustive research pertaining to the problems of elastic instability which possess extremely complex properties, and hope to produce indices suitable for design purposes. For this reason, in connection with these problems, we would very much like to receive reports published after 1942; i.e., in the period after the war began, reports on research that has been completed, but as yet unreported, and information concerning research being conducted at the present time." Specialists in our country had long been keenly aware that research on problems in elastic instability was extremely important, and for this reason they used this as an opportunity to propose to the Japan Science Research Council the establishment of a Column Research Special Committee. At the end of the same year this committee was organized.

This was a group consisting of 22 members from throughout the country. It was divided into five groups in promoting this research, namely the Investigation Liaison Section (survey of materials, collection and filing, English translation and printing, liaison), the First Sectional Research Committee (research on columns, dense columns, trusses, arches and frames as structural elements), the Second Sectional Research Committee (study of plates and reinforced plates as structural elements), the Third Sectional Research Committee (investigation of spheres and shells as structural elements), and the Fourth Sectional Research Committee (investigation of adjustable support columns for mine pillars). Meetings were held almost every month, and in addition to publishing research results, in accordance with the requests from the Column Research Council of The United States, 78 reports of averaging 400 pages each were translated into English and submitted to that council. Since that time, research liaison has developed between the Column Research Councils in both countries, and an exchange of reports has been continuing.

The above Column Research Special Committee, in performing its main function as an agency for the introduction of research on elastic stability theory in our country to foreign countries, decided to publish this handbook on elastic stability. The proposal of Professor Takefuji Yoshi of Tokyo University was the motification for the publication of this handbook. It began with the collection of materials on elastic stability which the late engineer Takahashi Shogen published as his graduation thesis from the Architectural Section of the Engineering Department of The Tokyo Imperial University in 1940. Unfortunately, Takahashi died only a few years after his graduation, and after that Sugano Makoto and Hisada Toshihiko continued on with his work. However, due to war damage part of the original manuscripts were burned, and scattered, and it was extremely difficult to bring them all together. The Committee recognized that this project would not only make it possible to gain a foothold in research on elastic stability theory, but also would be of great benefit directly to fields in applied engineering. For this reason, it was decided to take up this project,

to examine it through the committee members mentioned below, and to expand and complete the research and publish it. This is because such a book had not, up to the present time, then been published anywhere in the world.

General Theory	(Kuranishi Masatsugu)	Materials	(Naka Takao)
Frames [Rahmen]	(Sugano Makoto)	Arches	(Hirai Atsushi)
Plates	(Yoshiki Masao)	Shells	(Hayashi Shigeru)

In addition to respecting as much as possible the aim of Professor Takefuji's proposal to arrange the contents as loose-leaf materials, it was decided to add to each chapter a general discussion touching on the basic problems of elastic stability thus forming a guide to material, in order to adapt the handbook to conditions in our country, which at the time of this writing, was characterized by a general lack of literature pertaining to elastic stability. This book is thus completely different in aim from other books of this sort.

Owing to (1) the fervent cooperation of each member of the committee in planning the book and gathering the materials, (2) the supervision by Hayashi Shigeru over all matters pertaining to printing and publishing, (3) the fact that the extremely troublesome task of formulating requests to the Ministry of Education was accomplished rapidly, (4) to the fact that over a period of two years the Ministry provided financial support in publishing the results of our research and finally, owing to the sympathetic cooperation of Corona Publishers, this difficult project was completed in a relatively short period of time. In compiling and preparing the materials, much cooperation was received from the following persons, to whom we are very grateful: Akasaka Takashi, Kunio Takeshi, Hato Sukeyuki, Sumida Minoru, Takata Shuzo, Tamura Koichi, Nagai Tamotsu, Homma Yasuyuki, and Matsuoka Tsuyoshi.

Due to the nature of this book, it should be supplemented every year, and for this reason we would like to call the attention of the users to this fact and hope that it will be possible to revise the book further in the future. We in the committee sincerely hope to obtain the opinions of everyone in the field. Finally, we should like to point out that in the general discussions by each responsible member, the method of treating the problems and making explanations is not uniform. This is because in the compilation of this book, each part is considered as an original contribution from each committee member.

20 July 1951

Chairman of the Column Research Committee

Yuasa Kiichi

PREFACE TO SECOND REVISED AND ENLARGED EDITION

Already eight years have passed since the handbook on elastic stability was published by the Column Research Committee in October 1951. During this period, since the editorial policy with regard to this book was unprecedented in this field, the fact that it merited recognition and acclaim, both at home and abroad, was an honor to the members of the committee.

Later, the Column Research Special Committee that was established by the Japan Science Council was dissolved, but its research projects have been continued by the Column Research Committee. In vi[illegible] of the wishes expressed with regard to this book that have come from every a[illegible]a since the publication of the first edition, and the later developments in problems of elastic stability, it was decided among the authors of the first edition, to continue working on supplementing and revising the original. At first it was scheduled for one year after April 1957, but each author had his own functions and duties to perform, some traveled overseas on business during that interval, so that the edition was not ready until now.

In preparing this revised enlarged edition, the objective of the first edition revision was to collect as much data as possible that were published since the printing of the first edition, but due to such problems as the individual circumstances of each author described above, and difficulty with regard to the expansion and the contents of each section and problems in printing technology, it was impossible to completely coordinate the policy for expanding and collecting data with the data collection. Moreover, it was decided that in the expanded portions, each section would include its own text, data, and references. Consequently, an inconvenience arises in the sense that material on the same item may be scattered in two different places, but since this is primarily due to printing problems, the authors would appreciate the reader's understanding in this matter. However, it was decided to make indexing as convenient as possible, and the arrangement of the items follows the order in the first edition. Moreover, the positions of these items are indicated in the Table of Contents.

The major portions in which expansions were made, in addition to the literature on the subject, are as follows:

Section 2.

Chapter 3. Flexural Torsional Buckling

Materials:
- Constant Section Columns
- Eccentric Compression
- Lateral Buckling of Beam
- Flexural Torsional Buckling

Section 3.

3.1.11 Examples of Calculations Determining Buckling Load

Chapter 1.

Materials - Continuous materials

Rahmen (Rigid Frames)

Chapter 2.

Materials - Torsional Buckling of Langer Girders

Section 4.

Chapter 6. Sandwich Plates

Chapter 7. Plastic Buckling of Rectangular Plates

Materials: Isotropic Sandwich Plates

Sandwich plates with surface member isotropic, core member orthotropic.

Orthotropic Sandwich Plates

Corrugated

Materials: Bent Plates

Molding, Reinforced Plates

Cylinders

Elliptic cylinders

Spherical shells

Arc section cylinders

Shells with surface of hyperbolic paraboloid

Reinforcing curved plates

Reinforcing cylinders

Sandwich Circular Columns

7 December 1959

Chairman of the Column Research Committee Yoshiki Masao

SYMBOLS

A	Sectional area
a,b,	Side length of plate; 1/2 of main access of ellipse
a,b,c,	1/2 of main access of ellipsoid
B	$E \cdot I$ (flexural rigidity)
b,h	Width and height of rectangular section
C	Torsional rigidity
D	$\frac{Et^3}{12(1-\nu^2)}$ (flexural rigidity of plate)
d	Diameter (e.g. d_1 inner diameter, d_2 outside diameter)
E	Young's modulus
e	Eccentric distance
F	Force
f	Vibration number; allowable unit stress (e.g., f_c,f_k)
G	Modulus of rigidity
g	Gravity acceleration
H	Horizontal force (e.g., H_k buckling horizontal force)
I	Geometrical moment of inertia
I_p	Polar moment of inertia of area
i	Radius of gyration of area
J(); F()	Type 1, Type 2 Bessel functions
K	I/l = rigidity
k	Constant; rigidity ratio; subscript denoting buckling
L; U	External work; internal work
l	Length of member; span
l_k	Buckling length
M	Bending moment
M_x, M_y	Bending moment of plate
M_{xy}	Torsional moment of plate
m	Poisson's number; constant; mass
m, n	Half wave number
N_x, N_y	Axial force of plate
N_{xy}	Shearing force of plate
n	Constant
P	Concentrated force; concentrated load; axial force
P_k	Buckling load
P_e	Euler load of compression number
p; q	Normal; equally distributed load in direction of tangent
Q	Shearing force
R	Reaction; resultant (force)
r	radius (e.g., r_1 - inside radius; r_2 - outside radius)
S	Geometric moment of area
s	Length along axis of curve
T	Torsion moment
t	Thickness of member
u,v,w	Displacement in direction of x, y, z

V	Volume
v	Velocity
V; H	Vertical of reaction; horizontal component
W	Total load of member; concentrated load of beam
w	Deflection of plate
x,y,z	Coordinates
Z	Section modulus
α	Constant
β	Side length ratio (a/b) of plate; constant
γ	Shearing strain
δ	Deflection, displacement at specific point
ε	Normal strain
θ	Angle
λ	Slenderness ratio (l/i) (e.g., $\lambda_k = l_k/i$ = buckling slenderness ratio)
μ	Friction coefficient
ν	Poisson ratio; safety factor
ρ	Density; radius of curvature
σ	Normal stress; e.g., σ_k = normal strength of buckling compression)
σ_e	Euler stress of plate ($\pi^2 D/b^2 t$)
τ	Shear unit stress (e.g., τ_k = buckling shear unit stress)
ω	Angular velocity; $2_\pi f$; Buckling coefficient

TABLE OF CONTENTS

SECTION 1

		Page
Chapter 1.	General Remarks	
1.1.1.	Elastic Stability and Finite Deformation Theory	2
1.1.2.	Phenomena of Elastic Stability and Bodies Subject to It	3
Chapter 2.	Buckling	
1.2.1.	Buckling Deformation that can Occur in Bars, Plates and Shells	5
1.2.2.	Buckling Loads of Bars, Plates and Shells	8
1.2.3.	Deformation and Load After Buckling	18
1.2.4.	Buckling, Stability and Instability in Energy Theory	23
1.2.5.	The Case of Original Deflection	34
1.2.6.	Buckling Above the Proportional Limit	42
1.2.7.	Maximum Load After Buckling	46
1.2.8.	Buckling In Reinforced Members and Combined Members	49
1.2.9.	Buckling In Anisotropic Bars, Plates and Shells	52
1.2.10.	Buckling In Thick or Massive Bodies	53
1.2.11.	Natural Stress and Buckling	55
1.2.12.	Repeated Load and Buckling	56
1.2.13.	Dynamic Loads and Buckling	57
1.2.14.	Problems With Respect to Time, and Buckling	59
Chapter 3.	Elastic Stability Problems Other Than Buckling	
1.3.1.	Yield	60
1.3.2.	Jump Transition	61
1.3.3.	Vaulting Theory	62
1.3.4.	Combination Of Various Types of Problems in Elastic Stability	63
Chapter 4.	Determination By Calculation of Critical Buckling Values	
1.4.1.	Method Of Analysis	67
1.4.2.	Comparison Method	67
1.4.3.	Successive Approximations, Rayleigh's Equations	69
1.4.4.	Energy Methods, Ritz's Method, Ritz-Timoshenko Method	76
1.4.5.	Galerkin's Method	81
1.4.6.	Grammel's Method	82
1.4.7.	Temple, Weinstein and Trefftz-Newing Methods	86
1.4.8.	Method Using Integral Equations	88
1.4.9.	Finite Difference Method	89
1.4.10.	Perturbation Method	93
1.4.11.	The Method of Leased Squares	96
1.4.12.	Method of Series Expansion	97
1.4.13.	Lower Limit of Minimum Eigen Value of Compound System	98
1.4.14.	Method Using Approximation of Boundary Conditions	98
1.4.15.	Methods for Determining Buckling Loads in Frame Structures	99
1.4.16.	Determinations By Calculation of Buckling Strength	103

Page

Chapter 5. Experimental Determination of Buckling Load and Buckling Strength
1.5.1. Buckling Test Methods 107
1.5.2. Advice On Boundary Conditions 111
1.5.3. Relationship Between Deformation During Tests and Buckling Load 114
Chapter 6. Design and Strength as Related to Buckling and Other Factors
1.6.1. Strength Due to Buckling, Yielding, "Jump Transition" 118
1.6.2. Formulas for Buckling Strength, Safety Factors 119
1.6.3. Concerning Prevention of Buckling 122
1.6.4. Relationship Between Designs with Minimum Weight and Buckling 127
REFERENCES 129

SECTION 2
SOLID MEMBERS

Chapter 1. Compressive Members
2.1.1. Central Compressive Members Having Uniform Cross-Sections 133
2.1.2. Members of Non-Uniform Cross-Section 134
2.1.3. Non-Uniform Load 135
2.1.4. Buckling Unit Stress 137
2.1.5. Allowable Buckling Unit Stress of Centrally Compressed Members 145
2.1.6. Eccentrically Compressed Members 150
2.1.7. Ultimate Buckling Theory 155
2.1.8. Design Formulas Taking Load Eccentrically Into Consideration 158
Chapter 2. Lateral Buckling of Beams
2.2.1. Lateral Buckling of Tie Plates 162
2.2.2. Lateral Buckling of I-Beams 162
2.2.3. Design Formulas Taking Lateral Buckling Into Consideration... 165
Chapter 3. Buckling with Bending and Torsion
2.3.1. Shear Center 170
2.3.2. Buckling Coupled with Bending and Torsion 188
REFERENCES 307

SECTION 3
FRAMES AND ARCHES

Chapter 1. Frames (Continuous Members, Built-Up Members, Trusses Rigid Frames)
3.1.1. Historical Remarks 312
3.1.2. Methods of Stability Analysis 313
3.1.3. Classification of Frames 314
3.1.4. Hypotheses in Stability Analysis 316
3.1.5. Analysis Bases on the Deflection Angle Method 316
3.1.6. Solution by the Fixed Moment Method 319
3.1.7. Auxiliary Numerical Values 321
3.1.8. Abbreviated Method of Calculation for a Built-Up Compression Member 324

Page

3.1.9. Buckling Shear..... 327
3.1.10. Stiffening of Support Points..... 328
3.1.11. Examples of the Calculation of Buckling Load..... 329
REFERENCES..... 392
Chapter 2. Arch Bridges
3.2.1. Introductory Survey..... 396
3.2.2. Buckling of Solid Web Arches Due to Equally Distributed Loads. 398
3.2.3. Buckling of Solid Web Arch Due to Asymmetrically Distributed Load..... 405
REFERENCES..... 422

SECTION 4
PLATES

Chapter 1. History of Developments
Chapter 2. The Buckling of Flat Plates
4.2.1. Calculation of the Critical Buckling Point of Flat Plates..... 426
4.2.2. The Buckling of Rectangular Flat Plates..... 428
4.2.3. Buckling of Circular and Other Non-Rectangular Flat Plates.... 437
4.2.4. Orthotropic Plates..... 438
Chapter 3. Problems of Flat Plate After Buckling
4.3.1. Effective Width in the Case of a Compressive Load..... 441
4.3.2. Maximum Load of Rectangular Flat Plate Sustaining Compression and Other Matters..... 444
4.3.3. Tension Field Problems..... 446
Chapter 4. Reinforcing Plates
4.4.1. Buckling of Reinforcing Plates Sustaining Compression..... 449
4.4.2. Reinforcing Plates Sustaining Shearing Load and Bending Load.. 451
4.4.3. Maximum Load of Reinforcing Plates Undergoing Compression..... 451
Chapter 5. Flat Plate Structures
4.5.1. Buckling of Flat Plate Structures Under Compression..... 455
4.5.2. Considerations in Designing Flat Plate Structures..... 457
Chapter 6. Buckling of Sandwich Plates
Chapter 7. Plastic Buckling of Rectangular Plates
REFERENCES..... 575

SECTION 5
SHELLS

Chapter 1. Introduction
5.1.1. Shell Structures..... 587
5.1.2. Forms of Buckling that May Occur in Shells..... 587
Chapter 2. Buckling Theory of Shells
5.2.1. General Description of History [1-39]..... 591
5.2.2. Analytical Theory..... 594
Chapter 3. Buckling Phenomena and Buckling Load for Various Types of Shells..... 603
5.3.1. Buckling of Cylinders..... 603
5.3.2. Curved Plates..... 615
5.3.3. Buckling of Elliptical Cylinders..... 617
5.3.4. Buckling of Spherical Shells..... 617

Page

5.3.5. Elliptical Shells.... 621
5.3.6. Conical Shells..... 622
5.3.7. Reinforced Curved Plates..... 622
5.3.8. Buckling of Reinforced Cylinders..... 624
5.3.9. Reinforced Elliptical Cylinders..... 630
5.3.10 Corrugated Members..... 630
5.3.11. Torsion Yield Phenomena in Shells with Closed Cross-Sections.. 631
Chapter 4. Stress Conditions After The Buckling of Outer Plates in Reinforced Shells
5.4.1. Effective Width of Flat Outer Plates... 634
5.4.2. The Effective Width of Curved Plates..... 636
5.4.3. Analysis of Stress After The Buckling of the Outer Plates of Reinforced Shells Under the Bending Moment..... 640
5.4.4. Effects of Rivet Pitch on Compressive Strength of Reinforced Shells..... 641
5.4.5. Imperfect Tension Field in Curve Plate Section After Shear Buckling..... 643
Chapter 5. Breaking Strength of Reinforced Shells (With Particular Reference to Flexural Breaking Strength)..... 644
5.5.1. Effects of Outer Plates on Breaking Strength..... 644
5.5.2. On Boundary Conditions When Using Tests on Partial Structures In Lieu of Strength Tests on Complete Structures..... 646
5.5.3. Methods for Determining Breaking Moment..... 646
Chapter 6. Similarity Laws for Strength Tests Scale Models for Obtaining the Necessary Data For the Design of Tension Shell Structures..... 649

HANDBOOK OF ELASTIC STABILITY REVISED AND SUPPLEMENTED

ABSTRACT. An exhaustive mathematical treatment of the problem of elastic stability is presented. Direct and specific solutions are provided in formula and tabula form for each type of member (plate shell). Problems in the plaster area are discussed in considerable depth. General methods and numerical examples in the determination of the buckling load are also presented.

SECTION 1. GENERAL REMARKS

The purpose of this section is to outline the basic problems relating to /1* the theory on elastic stability. Since the direct and specific solutions for each type of member (plate, shell) and structure are given in detail in each section, here we shall not touch upon them. Instead, we have decided to discuss basic observations pertaining to problems of elastic stability, and to include as much as possible on the elements effecting stability problems and the practical aspects of the theory. Moreover, instead of dividing the discussion individually according to columns, plates and shells, we will refer to various problems while contrasting each of these. In this manner, this book is quite different in substance from previous works [1]-[10][1] although the title of the book is elastic stability, in actual practice, strength and change in rigidity based on elastic stability are important, so it would be inappropriate to consider stress only within the limits of elasticity. Instead, a discussion including the field of plasticity would be of even greater importance. Consequently we have decided to discuss problems in this area in considerable depth.

Moreover, since it is considered appropriate to discuss general method and theory for determining buckling load; i.e., numerical computation methods, within the general remarks, we have decided to introduce as many methods as possible, with regard to this point, and to use examples to make the explanation clearer.

---

[1]Figures in brackets refer to references at the end of the section. We have only cited the most representative works.

*Numbers in the margin indicate pagination in the foreign text.

CHAPTER 1

INTRODUCTION

1.1.1. Elastic Stability and Finite Deformation Theory

When a body undergoes elastic deformation by means of an external force, not only is the external force and the internal force caused by elasticity in a state of equilibrium, but normally this is a stable equilibrium. However, in a particular type of deformation, when this reaches a certain magnitude, or when the magnitudes of the external force corresponding to this becomes greater than the certain magnitude, the state of equilibrium no longer is stable and then either a separate type of deformation forms a stable equilibrium, or a rapid, great deformation takes place and damage to the body frequently occurs. Elastic stability theory deals with this type of problem.

The basic hypotheses that are normally used as a theory of elasticity determining elastic deformation and stress are (1) in the relationship between deformation or displacement and strain, the deformation is considered to be minute and linear, (2) The relationship between stress and strain is also considered to be linear, and (3) the equilibrium between the stresses themselves and with the external force may be established by the configuration and the state of the body prior to the deformation. The theory which is based on such basic hypotheses is called the theory of infinitesimal deformation. In this case, the deformations and stresses which are caused by the external force are all linear with respect to the external force (see Figure 1.1.1) form a stable equilibrium, and it is impossible to improve that with respect to the state of any external force, they are only in a single state of deformation. /2

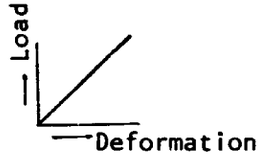

Figure 1.1.1

However, if considered carefully, since this theory corresponds to the case when the load is infinitesimal, and is regarded as indicating the direction in which a particular type of deformation will occur in the case when the condition changes from a state of a 0 load to one in which the beginning of the application of the load takes place, it can be said to be impractical. However, this theory is simple and its results, except in special cases,[1] are considerably close to actual deformation; i.e., they can be regarded in practice as a sufficient approximation so they are widely used in actual computations. Moreover, most of the theory of elasticity in ordinary elastic dynamics, material dynamics and structural dynamics belong to this theory of infinitesimal deformation.

In such a theory of infinitesimal deformation, since a stable state of equilibrium is constantly maintained, as described above, it cannot be used as a basic theory of elastic stability. It is thus necessary to consider the

[1]For example, the flexure of thin curved cylinders is a special case [67]. The general conditions responsible for this special case are still not clear.

case when none of the basic hypotheses will hold. We shall call such a theory a theory of finite deformation. According to it, as a result, the deformation which was caused by an external force is not necessarily always linear with respect to the external force, and it cannot be said that there is continuously a stable state of equilibrium. This also means that it is not true that a single state of deformation exists with respect to the state of a particular external force. Therefore, it is absolutely necessary to rely on this theory of finite deformation when considering elastic stability. Since the literature which discusses the finite deformation theory is extensive [11]--[16], we will not go into detail here.

1.1.2. Phenomena of Elastic Stability and Bodies Subject to It.

If finite deformation theory is followed, the following occurs, even considering simple cases. First of all, even when the deformation with respect to load increases monotonously, there are cases when the rate of increase in the load with respect to the deformations shown in Figures 1.1.2 and 1.1.3 rise gradually and cases when it decreases gradually. We shall collectively refer to these, which are shown in Figures 1.1.1 and 1.1.2 and 1.1.3, as the usual types, and will refer to them individually as the linear type, gradual load increase type, and gradual load decrease type respectively. However, since there are no cases in which an unstable equilibrium occurs with these types, they are not properly the subject of problems in elastic stability.

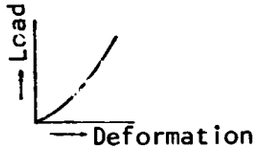

Figure 1.1.2

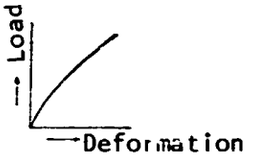

Figure 1.1.3

The cases which pose problems in elastic stability are those shown in Figures 1.1.4, 1.1.5 and 1.1.6, in which extremely large or extremely small load values are produced, and there occur points of deviation after which two states of equilibrium are present.

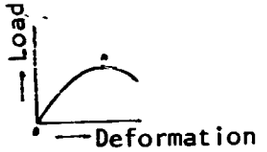

Figure 1.1.4

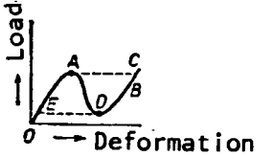

Figure 1.1.5

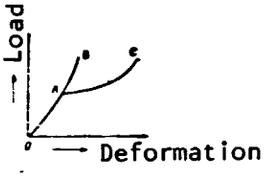

Figure 1.1.6

In cases such as those shown in Figure 1.1.4, in which when the maximum value is reached, the load can no longer be sustained, we shall call this "yield" and the maximum load in such a case will be called the "yield load."

There are also cases such as that in Figure 1.1.5, in which a maximum value (point A) and a minimum value (point D) are present. In such a case, /3

when the load is increased up to Point A, the deformation rapidly increases discontinuously and varies greatly up to Point B. Moreover, when a load is increased above this, it follows Line B-C and the deformation changes. When, conversely, the load is reduced from this state, it passes through Point B and reaches the Point D which is the minimum value. In this case, the deformation changes rapidly and moves to Point E. Then it follows Line E-O and returns to point O. We shall call this a "jump transition." Moreover, points A and D will be called respectively the Ascending and Descending jump transition loads.

In Figure 1.1.6, Point A is the separation point and after this two states of equilibrium along A-B and A-C are formed. Moreover, their states of deformation are different. Cases with such a point of separation will be called "buckling." Moreover, the load at this point of separation will be called the "buckling load." Normally the term "buckling" is used in a much wider sense, and includes cases in which a curve without a point of bifurcation is formed, which is close to the load-deformation curve with a bifurcation point and is due to load and other conditions. However, in the narrow sense, we shall adopt it as describing "pure" buckling. This buckling will form the central subject matter of the theory of elastic stability to be described below, and has been studied for the longest period of time and the most extensively. Moreover, only the simplest cases have been indicated above, and there are both instances in which the above cases are combined, and instances in which more complex cases may occur.

In discussing problems in elastic stability, it is by all means necessary to enter into the domain of finite deformation theory, but normally the phenomena that have been described above, appear in bodies such as slender bars, thin plates and shells, whose dimensions in the direction of more than one coordinate are extremely small in comparison with their dimensions in other directions. That is, the objects of investigation are bars, whose cross-section dimensions are much smaller than their dimensions lengthwise, plates whose thickness is much smaller than their length and width, and shells whose plate thickness is much smaller than their width, length and radius of curvature. In such cases, since there is a tendency for the displacement in the direction in which the dimensions are small to become great, it is easy for stability problems such as buckling to arise. Therefore in speaking of problems of elastic stability, these slender bars, thin plates and shells immediately become a problem. Consequently, it is easy to think that these alone are the subject matter of problems in elastic stability.

However, actually, such slender or thin bodies are not necessarily the only ones to be treated, and problems in elastic stability can arise even in thick or massive objects. For example, compression strength in lumber and Nakanishi Fujio's yield theory, etc. are clearly a type of stability problem, and one can consider that the mountain forming ability of the earth's crust, caveins in mine tunnels, etc., are related to stability problems. Elastic stability theory on such massive objects has not yet become the focus of attention, so except in special cases, there is no reason to discuss it here at any great length. Consequently, we shall discuss the above slender bars, thin plates, shells and combinations of these within the framework of the theory. Moreover, as related phenomena, we shall deal mainly with the above

buckling, yield, jump transition and items related to these.

CHAPTER 2

BUCKLING

1.2.1. Buckling Deformation that can Occur in Bars, Plates and Shells

Since buckling is the case in which a bifurcation point occurs, as described above, in the region immediately adjacent to this point, two states of /4
equilibrium are present. It is certain that one of the states of equilibrium is a form of deformation (that we shall call "direct form of deformation") which is present until the load is applied. The other state of equilibrium is a form of deformation (called "buckling form of deformation") which is different from the first and must be such that until it occurs, it is totally absent. Now we shall cite two or three examples of what can be considered as buckling deformation. Considering first an isotropic straight bar, we can consider the following table.

Table 1.2.1

Load Type	Straight Deformation	Buckling Deformation
1. Axial compression load	Straight Contraction	a. Bending b. Torsion
2. Bending load around one principal axis	Bending around principal axis	a. Bending around other principal axes b. Torsion
3. Torsion load	Torsion	a. Bending

The combination 1-a for this type of load and buckling deformation is called "column buckling." It has been treated the most extensively since the time of Euler [17] and is representative of buckling. When contrasting this with other types of buckling, we shall call it flexural buckling (Knickung). The combination 1-b was first published by H. Wagner [18] in 1928, and is a relatively recently developed theory. Consequently, even though it does actually occur quite considerably, it has not been the center of general interest. We shall call this torsional buckling (Verdrehung).

In the case of load type 2, if it is one which causes a bending moment, it can be either a couple load or a lateral load. However, it is impossible

for a and b in buckling deformation to occur independently. Buckling deformation appears as a combination 2-a-b. L. Prandtl [19] was the first to treat this and calls it lateral buckling (Kippung). Case 3-a was first discussed by Greenhill [20]. It appears in the case of a twisted slender wire.

In addition to the items indicated in this table, there are also cases of combinations of these loads, for example, one can conceive of 1-2 and 1-3 combinations. Moreover, it is also possible to have a pulling load in place of the compression load 1.

TABLE 1.2.2

Load Type	Straight Deformation	Type of Buckling Deformation
1. Axial compression load or uniform external pressure.	Contraction in which original form is generally maintained	a. bending (inside plane of gyration) b. bending (outside plane of gyration) c. torsion
2. Bending load inside plane of gyration	Bending in which original form is generally maintained	a. Bening toward outside plane of gyration b. Torsion
3. Uniform internal pressure inside plane of gyration or external pressure	Elongation or contraction in which original form is generally maintained	a. Inversion

Even in the case of a bar, different problems will arise with a bent bar. /5 For example, the cases indicated in Table 1.2.2 can be considered when the bar is circular, or part of it is.

In the combination 1-a in this table, the flexure (bending) occurs inside the plane of gyration, and is widely known as circular buckling [21]. We shall call this flexural buckling here. The combination 1-b-c- is considered to occur in the case of the toppling of an arch. Even in the case of 2, a and b occur in the form of toppling.

3-a was discussed by Biezeno [22]. It occurs in the form in which in the deformation of a circle, the inside and outside over the entire circumference are uniformly replaced by each other. He calls this Umstulpung (inversion).

In the case of a bent bar, it is possible for the load combination 1-2 to occur which causes toppling. Moreover, the helical spring, which is a type of bent bar, can, in its entirety, undergo the same type of buckling as a straight bar [23].

In addition to the simple cases listed above, there are also various combinations [112,113], but generally considerations of bars in the past have been confined to the range discussed above.

Structures in the form of continuous beams, trusses and rigid frames (Rahmen) are combinations of straight bars. Moreover, if we include bent bars, this would involve rigid frames which include the continuation of arches or arches themselves. These cases can also be considered as being the same forms of buckling deformation.

In the case of an isotropy in bars, since the relationship between the load type and the direct type of deformation is not as simple as it is above, different cases can arise. For example, a torsion load may occur due to tension, as in kinks in stranded wire, and as a result, it is possible for flexural buckling to occur.

The load in flat plates belongs to intra-plane load. This type changes from a type of deformation in which only deformation occurs inside the plane, to a type of deformation in which a deflection occurs in the direction towards the outside of the plane [24]. This is characteristic of plates, and while in addition buckling similar to that in bars may also occur, it is not intrinsic with plates, so we shall not consider it as buckling in plates. Compression load, shearing load and others can be considered as intra-plane loads of plates and since plates can have various configurations such as rectangular, circular, elliptical, with circular or elliptical holes; there are many problems related to these types.

Cases in which these plates have reinforcing members or structures in which flat plates are bonded together, pose problems and in this case while for the plate itself, only the deflection constitutes a form of buckling deformation, in reinforcing members or parts of flat plates, the type of buckling deformation occurring in bars may also appear. Since the latter can also occur in combination with the former, the problems that arise are considerably complex.

In the case of shells, there are those which are open and are viewed as curved plates, and those such as cylindrical shells, elliptical shells, conical shells and spherical shells which are partly or completely enclosed. Usually load states under which only stress resultants (Schnittkrafte) in shells may occur are considered as forms of direct deformation, and deformations such that a displacement of a direction perpendicular to the shell surface; i.e., deflection, is applied is considered as a form of buckling deformation [24].

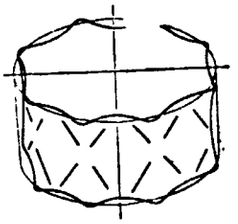

Figure 1.2.1

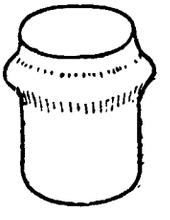

Figure 1.2.2

As in the case of flat plates, various problems arise depending on the configuration of the shell, the type of load, the presence or absence of a reinforcing member, an isotropy, etc., and the type of buckling load is that which accompanies deflection. However, on this basis it cannot be said that buckling deformation is limited to only one type. For example, when a cylinder sustains an axial compressive load, either of two types of deformation may occur, (1) when a diamond shaped surface such as that shown in Figure 1.2.1, or an axially symmetrical type of deformation in which the circumference is uniformly protruding or concave as shown in Figure 1.2.2. Consequently, it is necessary to consider carefully which type of buckling deformation may occur. Moreover, the form of buckling deformation characteristic in bars may also appear, but since it is not intrinsic to shells, it will not be considered here. Nevertheless, in the case of shells, it is necessary to consider carefully the fact that from this type of deformation, other types of deformation intrinsic to the shell itself may be induced. /6

1.2.2. Buckling Loads of Bars, Plates and Shells.

Since a buckling load is a load at a point of bifurcation, one should consider a possible new type of buckling deformation, and find a load due to which there is established an equilibrium which takes into account the infinitesimal deformation that occurs, when this new deformation is applied. In such a case, it is not possible to determine the relationship of the load to the deformation with respect to a large deformation which occurs after buckling but at least it is possible to determine the magnitude of the buckling load and the form of the deformation, as a type of buckling deformation.

Since in this case only an infinitesimal deformation is applied, it is impossible to employ without modification the relationships between displacement and strain, and strain and stress according to infinitesimal deformation theory, but the equation for the equilibrium of internal forces must be considered, not with respect to the original form of the body, but with respects to the deformed state. Nevertheless, this results in a linear differential equation for the deformation which is very convenient and relatively easy to solve.

The equation for equilibrium in the case when an infinitesimal displacement is applied as a form of buckling deformation is as follows. First, when a straight bar with a uniform section sustains a central compressive load P and a buckling load is generated, assuming the deflection to be v, since as shown in Figure 1.2.3, the lateral load has no effect except at the end of the bar, the following equation is obtained.

$$EI\frac{d^4v}{dx^4}+P\frac{d^2v}{dx^2}=0\ . \qquad (1.2.1)$$

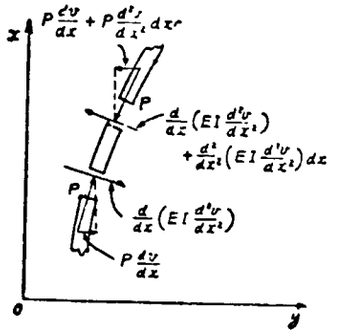

Figure 1.2 3

This case differs from ordinary infinitesimal deformation theory, in that the direction of the axial force and shear force, as shown in Figure 1.2.3, must be considered as the axial direction of the deformed bar, or a direction perpendicular to this.

As end conditions, if we appropriately combine

(1) Displacement 0 (v = 0), or

Lateral force $(EI\, d^3v/dx^3+P\, dv/dx=0)$ (A)

(2) Deflection 0 $(dv/dx=0)$, or

Bending moment 0 $(d^2v/dx^2=0)$

these may be given, at both ends as

(1) Rigid end $(v=0,\ dv/dx=0)$,

(2) Rotating end $(v=0,\ d^2v/dx^2=0)$, (B)

(3) Free end $(d^2v/dx^2=0,\ EI\, d^3v/dx^3+P\, dv/dx=0)$

In either case the end conditions are of the same order. Except when in the solution for the above differential equation which satisfies the end conditions, the identical with sign v=0, if P does not have a specific value (eigen value) a solution cannot be obtained. Moreover, this value of P is none other than the buckling load. Moreover, the solution v(x), the differential equation in this case (i.e., an eigen function) takes the shape of the initial deformation in this type of buckling deformation. In this case, an undetermined coefficient remains, but this does not mean that it is possible to employ a value of any size, it only means that the infinitesimal initial deformation is not quantitatively determined and can be understood only in terms of its configuration. /7

Below are several examples of the above.

When both ends are rotated

$$P=m^2\pi^2EI/L^2,\quad v=A\sin m\pi x/L,\quad m=1,\ 2,\ \cdots \tag{1.2.2}$$

When both ends are rigid

$$P=4m^2\pi^2EI/L^2,\quad v=A\,(1-\cos 2m\pi x/L),\quad m=1,\ 2,\ \cdots \tag{1.2.3}$$

$$P=4\times(2.048,\ \text{etc.}\times\pi^2EI/L^2,\quad v=A\,\{\sin(2\times 4.493\,x/L)+0.916\times 2\,x/L\},\ \text{etc.} \tag{1.2.4}$$

One end rigid, the other end rotating

$$P=2.048\pi^2EI/L^2, \text{ etc.} \quad v=A(\sin 4.493x/L+0.946x/L), \text{ etc.} \tag{1.2.5}$$

One end rigid, the other end free

$$P=(1/2+m)^2\pi^2EI/L^2, \quad v=A\left\{1-(-1)^m\sin\left(\frac{1}{2}+m\right)\pi x/L\right\}, \quad m=0,1,2,\cdots \tag{1.2.6}$$

What should be taken into particular account here is the fact that the equilibrium is considered in terms of finite deformation theory, which means that the free end does not involve a bending moment of 0 ($d^2v/dx^2 = 0$), a shear force of 0 ($d^3v/dx^3 = 0$). Actually in the above results, when the free end ($x = 0$), the bending moment is 0 ($d^2 v/dx^3 = 0$), but the shear force becomes EI $d^3v/dx^3 = (\pm)$ AEI $(1/2 + m)^3\pi^3/L^3$, which is not 0. That is, in the free end, the above lateral force should be 0. Moreover, considered in simple terms, if the shear force of 0 is considered as a condition for the free end, this would mean that the case is being treated in which the direction of the load varies with the deflection, as shown in Figure 1.2.5 as if the load operated in the direction of the deflected axis. Moreover, in the case of Figure 1.2.5, equilibrium is not considered in such a deformation so this type of buckling deformation is not established [10]. It is evidenced from this that what is meant by not employing the shear force is to employ the lateral force. Moreover, it is clear that it is necessary to consider carefully the fact that the magnitude of the load and the direction vary together with the buckling deformation.

Figure 1 2.4

Figure 1.2.5

As indicated by the above examples, numerous values obtained corresponding to the case when the buckling load is m = 1, 2, the actual buckling load that occurs should be a form of deformation with a stable equilibrium. From this point of view, the minimum value of m; i.e.,only the case of the minimum value for the buckling load represents the stable equilibrium for the type of buckling deformation. Consequently, only it can become the buckling load in the true sense. Moreover, since the section of a bar has two main axes, generally both of them must be considered together and when the end conditions are independent with respect to both main axes, it turns out that a buckling deformation occurs such that all the buckling loads for both main axes, the one with the low value obtains. The case in which the rotating end is around an axis in an arbitrary direction is solved as in example when the end conditions are related to both main axes [10]. /8

When the displacement is 0, and the lateral force is 0, the differential equation (1.2.1) above may be the following two-stage equation

$$EI\frac{d^2v}{dx^2}+Pv=0. \tag{1.2.7}$$

This equilibrium equation is found from the equilibrium of the moment due to the internal and external forces operating on the portion from the cross-section at point x of the bar to the end section. In this case, the moment which is Pv appears precisely because finite deformation is being considered. This means that in this case, the end conditions in both ends are

bending moment ($d^2v/dx^2 = 0$), or deflection 0 ($v = 0$), or
deflection angle ($dv/dx = 0$) (C)

and that only one of them can be used. Such a two-stage differential equation is easier to understand so this is the method that is normally used, in which the buckling load is determined by adding to this equation the added displacement at the ends, or the term based on the added lateral force. However, the method in (1.2.1) above is theoretically the correct one and since it is convenient when considering it in contrast with a flat plate, we have used it and noted it here.

The differential equation for equilibrium with respect to the torsional buckling due to the compressive load of a straight bar, is as follows [18].

$$EC_{bd}\frac{d^4\varphi}{dx^4}+\left(Pi_{sp}^2-GJ_T\right)\frac{d^2\varphi}{dx^2}=0. \tag{1.2.8}$$

It is possible to give the end conditions with respect to each end by the following combination:

(1) rotation 0 ($\phi = 0$,) or

rotation free around center of figure (D)

$$\left(EC_{bd}\,d^3\varphi/dx^3+\left(Pi_{sp}^2-GJ_T\right)d\varphi/dx-Pr_0^2\cdot 2\varphi/L=0\right)^{(3)(4)}$$

(2) end plain warp 0 $(d\varphi/dx=0)$

or end plain warp free $(d^2\varphi/dx^2=0)$

and the end conditions are determined by

(1) rigid end $(\varphi=0,\ d\varphi/dx=0)$

(2) spherical end $(d\varphi/dx=0,\quad EC_{bd}\,d^3\varphi/dx^3-Pr_0^2\cdot 2\varphi/L=0)$ (E)

(3) end where warp free $(\varphi=0,\ d^2\varphi/dx^2=0)$

In the case of problems arising when an axial load and a bending load are applied and a lateral buckling occurs, assuming that only I_y around the axis is very large, a simultaneous equation for v, ϕ is obtained [10] of the form

$$EI_z\frac{d^4v}{dx^4}+P\frac{d^2v}{dx^2}-\frac{d^2}{dx^2}(\varphi M)=0.$$

$$EC_{bs}\frac{d^4\varphi}{dx^4}+\left(Pi_{sp}^2-GJ_T\right)\frac{d^2\varphi}{dx^2}-M\frac{d^2v}{dx^2}=0. \qquad (1.2.9)$$ /9

The end conditions are a combination of (A)(D) above and this means that for both ends 4 conditions are applied due to (B)(E). That is, this is 6 for the displacement in the direction of the axes x, y, z at both ends (or external force) and rotation (or moment) but since the displacement in the direction of x, indirection of the z axis, and around axis y are not treated as problems here, we obtained the three end conditions; namely, the displacement in direction y (or lateral force) and the rotation around axis x, z (or bending or torsion moment). The terms $d\phi/dx$ (or $d^2\phi/dx^2$) indicating the relationship of the bending and torsion to this form the condition.

The case of a bent bar is essentially similar to that described above. Moreover, the case in which inversion buckling occurs is different from this. This is the main point in which curved bar and a straight bar are different, and in such a case, not only buckling but jump transition also occurs. (See Section 1.3.2).

When, in the case of a flat plate of uniform thickness, the load inside the plate is uniform, the equation for the equilibrium when an infinitesimal deflection w occurs, takes a shape similar to that of Equation (1.2.1), and assuming that $D = Et^3/12(1-\nu^2)$ when the compressive load is n_x, n_y, and the plane internal shear load is n_{xy}, we obtain

$$D\left(\frac{\partial^4w}{\partial x^4}+2\frac{\partial^4w}{\partial x^2\partial y^2}+\frac{\partial^4w}{\partial y^4}\right)+n_x\frac{\partial^2w}{\partial x^2}-2n_{xy}\frac{\partial^2w}{\partial x\partial y}+n_y\frac{\partial^2w}{\partial y^2}=0 . \qquad (1.2.10)$$

Assuming that this is a rectangle parallel to axes x and y, the end conditions with a periphery where x or y are constant are as follows, assuming t as the direction of the periphery and n as the normal

(1) deflection 0 (w = 0) or

lateral force 0 $\left(D\left\{\partial^3w/\partial n^3+(2-\nu)\partial^3w/\partial n\partial t^2\right\}+n_n\partial w/\partial n-n_{nt}\partial w/\partial t=0\right)$

(2) deflection 0 $(\partial w/\partial n=0)$ or (F)

bending moment 0 $(\partial^2w/\partial n^2+\nu\,\partial^2w/\partial t^2=0)$

and since the displacement in direction n,t or the stress resultant are taken into consideration from the beginning, the equation holds, so there is no problem. General considerations on this point are described later. Combining the above conditions, the end conditions become

(1) on rigid side $w=0,\ \partial w/\partial n=0,$

(2) rotating side $w=0,\ \partial^2 w/\partial n^2=0$

(3) on free side $\partial^2 w/\partial n^2+\nu\,\partial^2 w/\partial t^2=0,$ (G)

$$D\left\{\partial^2 w/\partial n^2+(2-\nu)\partial^2 w/\partial n.\,\partial t^2\right\}+n_n\partial w/\partial n-n_{nt}\partial w/\partial t=0.$$

In this case, for the lateral forces, in addition to the lateral shear stress resultants, the term is added which is based on the variations of the torsional moment as a corresponding shear stress resultant, and from the equilibrium in a finite deformation, the term based on the load is also added. The above equation (1.2.9) forms the equation for the condition in the case of a complex buckling deformation whereby the continuous terms from the difference between the centroid and the center of the shear is added [112,113].

Considering an example of the simplest case of buckling of a flat plate, where $n_x = n_{xy} = 0$, the four sides are x = 0, x = b, y = 0, y = L (assuming L > b) when the entire periphery is a rotating periphery, a solution for the above differential equation becomes /10

$$w=A\sin\pi x/b\sin m\pi y/L \qquad (m=1,2,\cdots) \tag{1.2.11}$$

the buckling load is

$$n_y=(mb/L+L/mb)^2\pi^2D/b^2. \tag{1.2.12}$$

In this case, the minimum value of m does not necessarily become the lowest value of n_y. Figure 1.2.6 indicates the case where m = 1, 2, ... with the term L/b (on the right side of the equation) as the abcissa. Consequently, m = 1 gives the lowest value of n_y when $L/b \leqq \sqrt{2}$, m = 2 gives the lowest value when $\sqrt{2} \leqq L/b = \sqrt{6}$ and generally, m = n gives the lowest value when $\sqrt{n(n-1)} \leqq L/b \leqq \sqrt{n(n+1)}$. Moreover, when m is large, the curve section where the lowest value is obtained becomes almost equal to 2π. Generally, it is possible to assume

(1.2.13)

$L/b<1$ when $n_y=(b/L+L/b)^2\pi^2D/b^2$

$L/b\geqq1$ when $n_y=4\pi^2D/b^2$

with L/b as the boundary giving the minimum value in the beginning. When the periphery conditions are different, the edge of the load as indicated in Figure 1.2.7 is the same as above. In this case the overall tendency is exactly the same as above, except that there is a difference in the value of L/b when it becomes an infinitesimally small value and in the infinitesimally small value. When the load edge becomes a rigid edge when L/b is small (L/b < 4), this is markedly greater than in the case when the load edge is a rotating edge, but when L/b becomes large, the influence of this load edge

becomes extremely small. In the same manner, when the load edge is a free edge, where L/b is small, the value is much smaller than the value when it is a rotating edge, but when L/b becomes large, it is considered that the influence where there is a load edge becomes small, but since this has not yet been computed, it is not indicated in the figure.

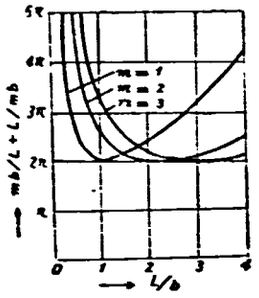

Figure 1.2.6

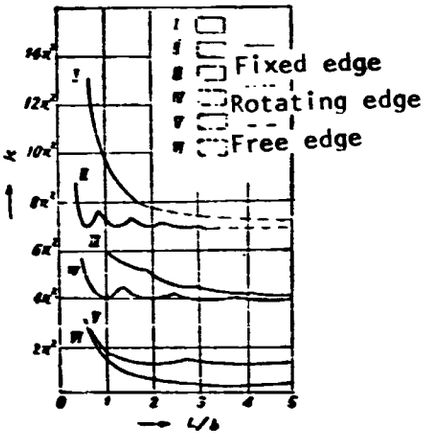

Figure 1.2.7

The case of a compressive load from four sides yields a result which is very similar. However, in the case of a shear load, it is difficult to obtain a solution algebraically for a rectangular plate, and only a case of an infinite zone can be obtained. But it is easy to imagine that it is similar in form.

In the case of a circular plate, since it is necessary to consider that the plane-internal stress resultants necessarily vary, the equilibrium differential equation with respect to deflection w in this case employs four coordinates, and assuming the tension to be positive with the regular n_n, n_θ [5], the equation becomes

$$D\left(\frac{\partial^2}{\partial r^2}+\frac{\partial}{r\partial r}+\frac{\partial^2}{r^2\partial\theta^2}\right)^2 w=\frac{\partial}{r\partial r}\left(rn_r\cdot\frac{\partial w}{\partial r}\right)+\frac{\partial}{r\partial r}\left(rn_{r\theta}\frac{\partial w}{r\partial\theta}\right) \qquad (1.2.14)$$

$$+\frac{\partial}{r\partial\theta}\left(n_{\theta r}\frac{\partial w}{\partial r}\right)+\frac{\partial}{r\partial\theta}\left(n_\theta\frac{\partial w}{r\partial\theta}\right)$$

and the periphery conditions on the side where r = constant are the same as in the case of a rectangular plate combining

(1) deflection 0 (w = 0) or /11

lateral force 0 $D\left\{\partial(\Delta w)/\partial r+(1-\nu)\partial(\partial^2 w/r\partial r\partial\theta-\partial w/r^2\partial\theta)/r\partial\theta\right\}$

$-n_r\partial w/\partial r-n_{r\theta}\partial w/r\partial\theta=0\Big)^*$ (H)

(2) deflection angle 0 $(\partial w/\partial r=0)$ or

bending moment $\left(\partial^2 w/\partial r^2+\nu\left\{\partial w/r\partial r+\partial^2 w/r^2\partial\theta^2\right\}=0\right)$

becoming

(1) at rigid side $w=0,\ \partial w/\partial r=0.$

(2) on rotating side $w=0,\ \partial^2 w/\partial r^2+\nu\left\{\partial w/r\partial r+\partial^2 w/r^2\partial\theta^2\right\}=0,$

(3) on free side $\partial^2 w/\partial r^2+\nu\left\{\partial w/r\partial r+\partial^2 w/r^2\partial\theta^2\right\}=0,$ (I)

$D\left\{\partial(\Delta w)/\partial r+(1-\nu)\partial(\partial^2 w/r\partial r\partial\theta-\partial w/r^2\partial\theta)/r\partial\theta\right\}$

$-n_r\partial w/\partial r-n_{r\theta}\partial w/r\partial\theta=0,$

This becomes more complicated in the case of shells. For example, three simultaneous differential equations are formed for u, v, and w, (3) from the equation of equilibrium for the internal cross-sectional forces in the case when a cylindrical shell sustains an axial compressive load, a bending load, a torsion load, and external pressure and the relationship between the displacement in directions x, y, z, u, v, w, and the sectional internal forces. Using the notation $N = Et/(1-\nu^2)$, $D = Et^3/12(1-\nu^2)$, $D/b^2N = k$,, $n_s/N = q_1$, $n_{x\phi}/N = q_2$, $pa/N = q_3$ with the differential ' $\alpha\partial/\partial x$, $\cdot\equiv\partial/\partial\phi$, we have

$$u''+\frac{1-\nu}{2}u\cdot\cdot+\frac{1+\nu}{2}u'\cdot+\nu w'+k\left(\frac{1-\nu}{2}u\cdot\cdot-w'''+\frac{1-\nu}{2}w'\cdot\right)+q_2u'\cdot+q_3(-u'\cdot+w')=0 \qquad (1.2.15)$$

$$\frac{1+\nu}{2}u'\cdot+v\cdot\cdot+\frac{1-\nu}{2}v''+w'+k\left(\frac{3}{2}(1-\nu)v''-\frac{3-\nu}{2}w'\cdot\right)-q_1v''+q_3(v'\cdot+w')=0$$

$$\nu u'+v\cdot+w+k\left(-\frac{1-\nu}{2}v'\cdot\cdot-u'''-\frac{2-\nu}{2}v''\cdot+w^{IV}+2w''\cdot\cdot+w\cdot\cdot\cdot\cdot+2w\cdot\cdot+w\right)+q_2w''+2q_2(v'-w'\cdot)+q_3(u'+w+w\cdot\cdot)=0$$

* $\Delta\equiv\partial^2/\partial r^2+\partial/r\partial r+\partial^2/r^2\partial\theta^2$

The terms underlined with a dotted line in the equation are those used by L. H. Donnell [26] for torsion load. Judgments by different authors on the importance of these terms in the equation differ, and there are differences which should be selected and which should be rejected. As contour conditions, there should be four each. For example, for x = a constant end plain, these conditions should be constructable by the combination /12

(1) displacement 0 in direction of diameter (w = 0), or

lateral force 0 $(Q_x+M_{x\varphi}/a-n_x w'/a-n_{x\varphi}\cdot w\cdot/a=0)$

(2) slope 0 (w′ = 0), in direction of generatrix or bending

moment (M_r = 0)

(3) Displacement 0 (u = 0), in direction of generatrix or (J)

axial force 0 $(n_x+n_{x\varphi}u\cdot/a=0)$

(4) Displacement 0 (v = 0), in direction of periphery or

lateral force inside plane 0 $(n_{x\varphi}-M_{x\varphi}/a+n_x v'/a=0)$

Normally even in the case of a fixed end, it is clear that w = 0, w′ = 0, or in a rotating end, w = 0, M_r = 0, but there are many cases in which the conditions (3) and (4) are not clearly given. For this reason, it is necessary to grasp clearly whether this is the actual thing, or the solution of the equation uses one of these. In a free end the condition

$$Q_x+M_{x\varphi}/a-n_x w'/a-n_{x\varphi}w\cdot/a=0,\quad M_x=0,\quad n_x+n_{x\varphi}u\cdot/a=0,\quad n_{x\varphi}-M_{x\varphi}/a+n_x v'/a=0$$

should hold. When this is not a cylinder, but a rectangular curved plate, (a cylinder cut along the generatrix), this forms a condition which is similar to the case of a flat plate on the lateral face.

Except in special cases, for example, L. H. Donnell's solution for torsional problems (it is very difficult to determine the eigen values and eigen functions from the above differential equations. In the case of a cylinder, assuming it to be extremely long, there are many cases in which a periodic solution in the lengthwise direction is satisfactory. In such a case, the end conditions do not pose a problem. However, even in such a periodic solution, since it is difficult to accurately express the form of buckling deformation, the solution should be found by satisfying it in a form which is mathematically easy to handle, namely u = A cos m ϕ cos λx/a. When the solution thus obtained is greater than a particular length, this results in being able to consider that the buckling load in the intrinsic buckling of the shell hardly changes at all. In cases shorter than this, the greater the shortness, the greater is the increase in the gradual buckling load (See Figure 1.2.8). [27]. In short cases, quantities such as rt/L^2 have a predominant influence. This tendency is exactly similar to the case of a rectangular flat plate, and is a characteristic of plates and shells as distinct from bars.

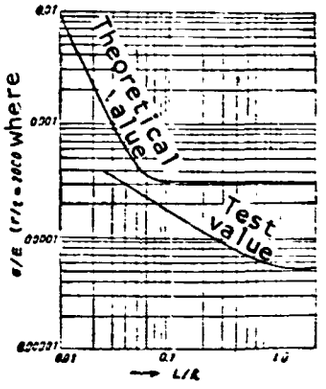

Figure 1.2.8

The results thus obtained should be considered as classic values. For example, in the case when a cylindrical shell is buckled by sustaining a compressive load, the buckling load has a value of about $\sigma_k a/Et = 0.6$, where σ_k is the compressive stress. However, in test results, the value is scattered between 0.1 and 0.4 and 0.2 can be considered as the average value. That is, it is about 1/3 of the classical theoretical value. The buckling load value for a shell thus is different from the case of a flat plate or a bar and there is a great difference between the classical theoretical value and the experimental value. This is also a characteristic peculiar to the buckling of shells.

Moreover, in cylindrical shells, in the case of an axially compressive load, considering even the intrinsic buckling of the shell itself, since, as stated above, there are two types of buckling deformation, it is necessary to determine which of these is manifested. Axially symmetrical deformation normally only occurs in a cylindrical shell which is relatively thick and has a high buckling compressive stress. In addition, when the cylindrical shell is long, the buckling should occur in the form characteristic of bars and actually appears in part of the results as a special case of the above solution. /13

What should be noted in particular for the case of shells, is that in the above methods, when determining the buckling load, the stresses prior to buckling are taken into account, but deformations and displacements prior to buckling are not considered. There are cases in which these cannot be overlooked in the case of shells. When this initial deformation is included in the equation, the deformation itself completely depends on finite deformation. In this event, this is a case with no point of bifurcation. The buckling of shells is thus not a simple matter, and since it is related to such things as jump transition, yield or vaulting, it is impossible to determine the buckling phenomenon adequately, only in terms of equilibrium in which the finite deformation is considered to be infinitesimal. Consequently, in such a case, it is necessary to deal with general finite deformation equations. Since this involves differential equations which are difficult to solve even when they are linear, and which become non-linear in this case, the method described above is impractical. For this reason, the energy method described below is used.

As described above, when restricting finite deformation to an infinitesimal value, in the methods of determining buckling load, the characteristic differences between rods and plates, and shells are characterized by the fact that when they are long, the buckling load decreases at an increasing rate in bars, but the buckling load in the case of the intrinsic buckling of plates and shells reaches a point where it no longer varies. The most characteristic fact concerning the difference between bars, plates and shells, is most clearly manifested in the case of the deformation occurring after buckling.

1.2.3. Deformation and Load After Buckling

Since we are dealing with deformations occurring after buckling, it is absolutely necessary to follow finite deformations. For this reason, since it is necessary to employ non-linear differential equations, this becomes extremely difficult, it is therefore necessary in very many cases to use a method of approximation, without following pure finite deformation theory and merely to determine the relationship between bowed and deformation up to a certain degree of deformation. When energy theory is utilized, this becomes relatively easy, and there are many cases in which such a treatment is used, but this point will be described later on.

Regarding deformation occurring after the buckling of a straight bar, following normal flexure theory (1.2.7) above, the bending moment is assumed to be proportional to the curvature, and if we decide to use the correct values from differential geometry for the curvature, we obtain the following equation. When one end is free and the other end is rigid, expressing the deflection at the free end as δ [4].

$$EI\frac{d^2v/dx^2}{\left\{1+(dv/dx)^2\right\}^{3/2}}+P(v-\delta)=0 \tag{1.2.16}$$

or using $dv/ds = \theta$ as a variable [1] and using length s along the bar axis in place of x, it is treated in the form

$$EI\frac{d^2\theta}{ds^2}+P\sin\theta=0 \tag{1.2.17}$$

and it is possible to determine the relationship between δ and P. The result has long been known under the name Elastica, the relationship between δ and P is shown in Figure 1.2.9, and naturally one proceeds from the bifurcation where there is a buckling load. The form of deformation is as shown in Figures 1.2.10 and 1.2.11. The a_1, a_2, and a_3 correspond to the curves m = 0 and b_1, b_2, b_3 correspond to m = 1. The curves m = 0, 1, 2, ... in Figure 1.2.9 are independent and not intersected. As described below, only m = 0 is the case of a stable equilibrium and m = 1, 2, ... is the case of unstable equilibrium. In the case where both ends are rotated, the deformation is as shown in Figures 1.2.12 and 1.2.13, deformations a_1, a_2, a_2 are stable, and the other b_1, b_2, b_3 are unstable. The relationship between load and deflection in the center is similar to that which is shown in Figure 1.2.9.

/14

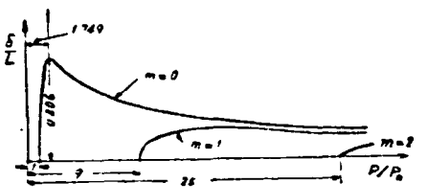

Figure 1.2.9.

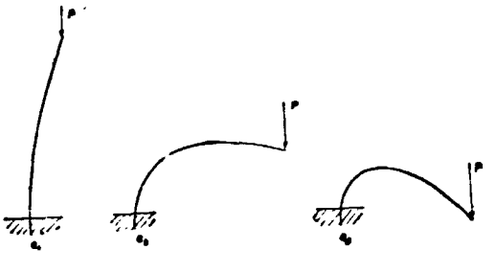

Figure 1.2.10.

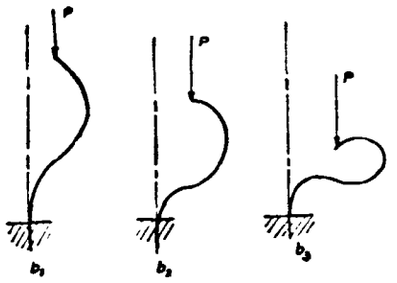

Figure 1.2.11.

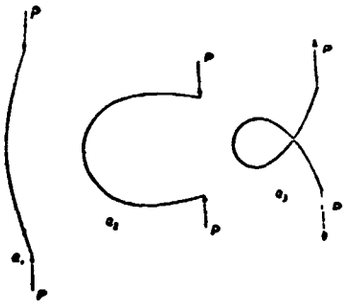

Figure 1.2.12.

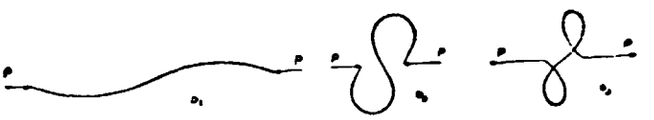

Figure 1.2.13.

Now the initial portion of the curve m = 0 in Figure 1.2.9 is almost a parabola, and the equation for the parabola is

$$P=P_k\left(1+\frac{1}{32}\cdot\frac{\pi^2\delta^2}{L^2}\right). \tag{1.2.18}$$

Consequently, when P increases 1% more than P_k, δ becomes 18% of column length L and the deformation increases markedly even in the case of a slight increase in load. Consequently, it can be considered that a very large deformation takes place with buckling load. And when this is an ordinary structural member, it cannot withstand such a deformation. Such a large deformation can be realized in the case of something like a human hair. Thus, as general theory, we can say that in flexural buckling due to the compressive load on a straight bar, in the case of buckling load, a large deformation occurs, even if the load is scarcely increased at all, and for this reason, rupture is caused. In other cases of buckling of a straight bar, it is considered that almost the same kind of tendencies appear, but apparently there are no clear cases of such tendencies. /15

In the case of a flat plate as described above, the case in which the deformation is so great, that the curvature must be expressed completely in terms

of finite deformation, is not treated here. We proceed from an equation constructed from the relationship of displacement and strain, assuming the deflection to be great. There are many cases in which during the process we either carry out an approximation or change over to the energy method [9]. In any case, in the event of a plate, it is extremely difficult to obtain substantial results. Only various types of results for the case in which some degree of approximation is allowable, have been published. The equilibrium equation for a flat plate end results obtained when it is assumed that within the displacement, only the deflection is assumed to be large, is as follows. F is Airy's stress function

$$\Delta\Delta F = E\left\{\left(\frac{\partial^2 w}{\partial x \partial y}\right)^2 - \frac{\partial^2 w}{\partial x^2}\frac{\partial^2 w}{\partial y^2}\right\} \tag{1.2.19}$$

$$D\Delta\Delta w = t\left\{\frac{\partial^2 F}{\partial y^2}\frac{\partial^2 w}{\partial x^2} + \frac{\partial^2 F}{\partial x^2}\frac{\partial^2 w}{\partial y^2} - 2\frac{\partial^2 F}{\partial x \partial y}\frac{\partial^2 w}{\partial x \partial y}\right\} \quad . \tag{1.2.20}$$

Using these equations, the results obtained which determine the relationship between the load and the deformation after buckling in a rectangular plate which sustains a compressive load in one direction, are shown in Figure 1.2.14. In many cases, instead of expressing it in this form, it is expressed as in Figures 1.2.15 and 1.2.16 in terms of the effective width (mittragende Breite) b_m. It is expressed by the following equations, in which it is made to agree approximately with the test results.

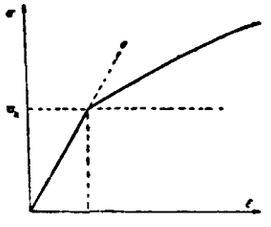

Figure 1.2.14

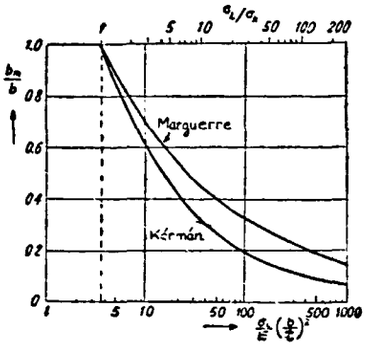

Figure 1.2.15

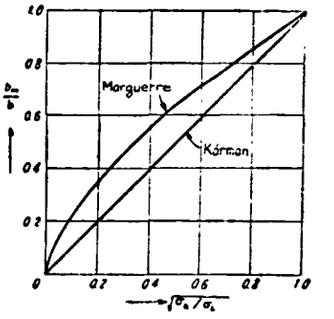

Figure 1.2.16

Karman's equation [29].

$$b_m/b = \sqrt{\sigma_k/\sigma_L} \tag{1.2.21}$$

Marguerre's equation [30].

$$b_m/b = \sqrt[3]{\sigma_k/\sigma_L} \tag{1.2.22}$$

where σ_L is the vertical compressive stress in the case of lateral force and σ_k is the buckling compressive stress.

In such a case, it is even more important to state in detail how the contour conditions are obtained, than in the case described above in the previous section. If not done, a great difference will appear in the results. Even in the case of the load side conditions [literal translation], it is possible to proceed in such a manner that in compression, the load on the compression side is uniformly distributed, or to have the load such that the displacement is uniform. Both of these have exactly the same meaning until buckling occurs, but the results are completely different after buckling occurs. The previous example is a case where displacement has a uniform distribution and since this is closest to cases which actually occur, normally this case is employed. If /16
we consider that the load has a uniform distribution, the increase in load after buckling, will be extremely slight and will be considered to yield a result which is close to that in the case of a bar.

In the results where with a side load, the displacement has a uniform distribution, the distribution of the external force on the load side becomes non-uniform after buckling occurs, and has the distribution shown in Figure 1.2.17. Immediately after buckling, this is almost a cosine curve and in the center is equivalent to the buckling stress, but after this, in the region of the contour, whereas the external forces increase gradually, conversely in the center section the external forces decrease. Since there is absolutely no deflection on the contour, the shrinkage is directly determined from the displacement, and the stress is determined. In the center portion, considering the effect of the deflection, it is necessary to perform the above calculations in order to determine the magnitude of the external force.

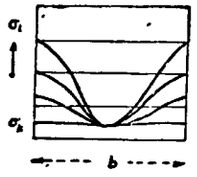

Figure 1.2.17

The relationship between deflection and load according to Kromm and Marguerre's calculations [31] is, assuming $w = f \sin \pi x/b \sin \pi y/\beta b$, $\sigma_p = P/tb$

$$\sigma_P/\sigma_k=(\beta^4+\beta^2+2)/4, \quad \text{or} \qquad (1.2.23)$$

$$\beta^2=(1+f^2\cdot\pi^2/4b^2\cdot E/\sigma_k)^{1/2}$$

Consequently, immediately after buckling, this forms a parabola

$$\frac{\sigma_F}{\sigma_i}=1+\frac{\pi^2}{8}\frac{E}{\sigma_k}\frac{f^2}{b^2} \qquad (1.2.24)$$

which is as shown in Figure 1.2.18. Let us compare this with the case of a bar. In a bar which sustains an axial compressive load, when both ends are rotating ends, $P/P_K = 1 + \pi^2/8\cdot\delta^2/L^2$. Here and in the above equation, if we compare the coefficients, δ/L^2 and f^2/b^2, the latter is E/σ_k times greater than the former. Since such a large contrast occurs, the increase in deflection with respect to the increase in load in the case of a plate, is not as marked as it is in the case of a bar.

Figure 1.2.18

In this manner, the relationship between deformation and load after buckling differs greatly in comparison with the case of a bar, and the load increases markedly after buckling can be said to be one of the major characteristics of the buckling of a flat plate.

Now let us consider as representative, the case in which a cylindrical shell sustains an axial compressive load, for the case of deformation after the buckling of a shell. In this case, in the buckling which causes axially symmetrical deformation, it is normal for the stress to be greater than a proportional limit, so this will be described below. First we shall discuss the case where a diamond-shaped deformation occurs.

We are considering deformation occurring after the buckling of a shell, but since as described above, there is already little certainty of a buckling load itself occurring, it would be strange indeed to continue the same policy as above in computing the deformation after buckling. The buckling values which have been computed in the past agree with the classical values, and according to Karman and Tsien [32] the deformation after buckling in the case of buckling due to the compressive load on a cylindrical shell produces a deflection which is in the form of a sine curve both laterally and longitudinally but when the deformation is great, it takes the diamond-shaped mentioned above. When we use $\varepsilon a/t$, in place of contraction ε in the overall direction of the axis, and $\sigma a/Et$ in place of the compressive strength σ, the relationship between the two of them is expressed as shown in Figure 1.2.19. Here, a is the diameter of the cylinder and t is the skin thickness. According to Karman, the /17
graph indicates that when increasing the load along OA in the graph, point A drops due to the imperfections in the test specimen, or on the other hand, energy is supplied due to vibration of the test apparatus, and from a point which does not reach buckling point A, the load suddenly jumps in the direction indicated by the dotted line and shifts to a point of low stability. In the case of a loading method, in which the load is varied in stages, the direction of this dotted line changes suddenly in the horizontal direction in the graph; it changes rapidly in a vertical direction when the displacement of the end is varied in stages, and changes suddenly in a slant direction in a case intermediate between these two (normally this belongs to the case when the elastic deformation, etc. of the test apparatus is taken into consideration). Karman maintains that the test results record the numerical value of point B which is the minimum value. This means that point B $\sigma a/Et = 0.194$ which agrees with the average value of the test result. The value for this point B is called by Karman the lower buckling value.

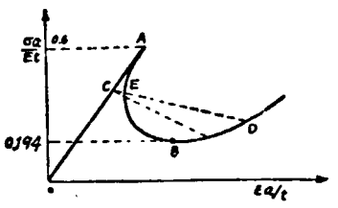

Figure 1.2.19

If conditions are as described above, for example since both points C and D are in a state of stable equilibrium, an unstable point of equilibrium, E should appear on line CD. In order to jump this unstable equilibrium point, considering that it becomes slightly lower due to the imperfection of the test piece, nevertheless we believe that a considerable

amount of energy must be supplied. Since we are considering a jump over this point, I have given it the name of "vaulting theory". A similar phenomenon occurs also in the buckling of other shells.

However, even considering the fact that there are reports [6] to the effect that the jumping phenomenon described in the Introduction clearly occurs in experiments in the case of a thin cylinder and a curved plate, we feel that it is groundless to view it as Karman does, as downward lower buckling value. It is believed that it is most valid to consider that the buckling load in a pure cylindrical shell is simultaneously the jump transition load described above. It is also surmised that its value is probably close to 1/2 the classical value. Moreover, due to the imperfection of the test specimens, the value can be considered to drop and for a dispersion to occur. However, a positive assertion cannot be made since an accurate solution has not yet been given. In any case, in the case of a shell, we believe that it is certain that the load for a state of equilibrium after buckling drops.

Summarizing the explanation given above for the loads of deformation after buckling, very marked characteristics are indicated, in which the buckling load in a bar is almost constant, the load increases in a flat plate, while in a shell, the result is that the load is reduced rapidly. This can be considered as the characteristic differences between bars, plates and shells. Of course, we are only talking here of representative cases, but when it comes to special configurations or complex conditions, these characteristics become blurred and nothing can be done about it. An example of this is the fact that a curved plate with a small curvature has characteristics similar to that of a flat plate.

1.2.4. Buckling, Stability and Instability in Energy Theory

Now let us consider the above buckling phenomena in terms of energy theory. A result of this is merely that we are viewing the same facts from a different point of view, but since judgments of stability and instability must be based on considerations of energy theory, the latter must be taken into account. First let us indicate the results of computations performed for the case when it is relatively easy to see what type of changes in overall energy occur in the case accompanying the buckling phenomenon. Considered generally in terms of energy, the case when the potential energy of the internal and external forces Π is an extreme value, is the state of equilibrium. /18

$$\delta \Pi = 0 \tag{1.2.25}$$

In infinitesimal deformation theory, in terms of the linear relationship between displacement, strain and stress, the maximum of the displacements for Π is of the second order and geometrically forms a quadratic parabola, so there is only a single extreme value. This constitutes the singularity of Kirchhoff's solution. When it comes to elastic stability theory which deals with finite deformation theory, the relationship between displacement and strain can no longer be considered as linear, and the strain energy; i.e., the potential energy becomes a high order parabola of the third order or above, and there are

two or more extreme value points. In the buckling problem, the case when two or more points of equilibrium are adjacent to each other corresponds to the point of bifurcation. In only determining the buckling load, the amount of the degree of displacement is still small even at the point of bifurcation, and, as has been explained already, a linear relationship can be used and the solution is relatively simple. However, since it is also relatively easy to determine the state at a point somewhat distant from the point of bifurcation, in terms of energy theory, we shall consider it on this point of view. Moreover, we shall proceed in our investigation assuming that $\delta\Pi = 0$ determines the point of equilibrium, and that there exists a stable equilibrium with Π = Min. i.e., $\delta^2\Pi > 0$.

First we shall consider as an example the case in which flexural buckling occurs due to an axial compressive load in a rod. When the rod deflection w is large in comparison with other displacements, the elongation ε_x of the center axis of the rod is

$$\varepsilon_x = \frac{\partial u}{\partial x} + \frac{1}{2}\left(\frac{\partial w}{\partial x}\right)^2 \tag{1.2.26}$$

and we consider a range of magnitudes of deformation such that the bending curvature κ_x is expressed by

$$\kappa_x = \partial^2 w / \partial x^2 \quad . \tag{1.2.27}$$

Next, assuming the displacement at one end to be 0, and the displacement at the other end to be only in the direction of the axis that is, eL, the average stress $\bar{\sigma}_x$ bar section is

$$\bar{\sigma}_x = E\varepsilon_x = E\left\{\frac{\partial u}{\partial x} + \frac{1}{2}\cdot\left(\frac{\partial w}{\partial x}\right)^2\right\} \quad . \tag{1.2.28}$$

and the strain energy A_i is as follows, with i as the two-dimensional diameter of the cross-section and F as the section area

$$A_i = \frac{EF}{2}\left[\int_0^L \left\{\frac{\partial u}{\partial x} + \frac{1}{2}\left(\frac{\partial w}{\partial x}\right)^2\right\}^2 dx + i^2\int_0^L \left(\frac{\partial^2 w}{\partial x^2}\right)^2 dx\right] \quad . \tag{1.2.29}$$

When the external force is a compressive force, $P = pF = -\bar{\sigma}_x F$, since the increase in the potential energy of the external force is -(pF)(eL), the overall increase in potential energy is

$$\Pi = \frac{EF}{2}\left[\int_0^L \left\{\frac{\partial u}{\partial x} + \frac{1}{2}\left(\frac{\partial w}{\partial x}\right)^2\right\}^2 dx + i^2\int_0^L \left(\frac{\partial^2 w}{\partial x^2}\right)^2 dx\right] - pFeL \quad . \tag{1.2.30}$$

Considering $\hat{\Pi}$ as the result of dividing this potential energy Π by EFL

$$\hat{\Pi} = \frac{\Pi}{EFL} = \frac{1}{2L}\int_0^L \left\{\frac{\partial u}{\partial x} + \frac{1}{2}\left(\frac{\partial w}{\partial x}\right)^2\right\}^2 dx + \frac{i^2}{2L}\int_0^L \left(\frac{\partial^2 w}{\partial x^2}\right)^2 dx - \frac{p}{E}e \quad . \tag{1.2.31}$$

Here we shall investigate the deformation of a bar where this is, from the condition Π = Min. in the vicinity of the buckling value or a value higher than this. /19

Assuming that one end of this rod (x = 0) has a displacement of 0 at the rotating end, the other end (x = L) is a rotating end, sustains the axial compressive load P and is assumed to be able to move only in the direction x. In such a case, the following two types can be considered as independent variables [33]. That is, we will take either the displacement of end (A) or the external force (B) as the independent variable.

Displacement where x = L, u(L) = -eL or [1] (1.2.32)

Compressive external force p = P/F

Since we are applying a hypothetical theory of displacement, we must follow the particulars that are involved. When employing variations of displacement, we are carrying out the variation in such a way that it is adapted to geometry, when, as in case number 1, the displacement of one end -eL is given, that point is not moved. However, in case 2, since an external force is applied to one end, displacement is possible and the work of the external force Pδu enters the calculations. Also, the fact that these are extremes of value must be established independently with respect to both u and w. Then, from the variations for u in equation (1.2.31) we have

$$\frac{\partial}{\partial x}\left\{\frac{\partial u}{\partial x}+\frac{1}{2}\left(\frac{\partial w}{\partial x}\right)^2\right\}=0. \tag{1.2.33}$$

The end condition is

$$u(0)=0,\ u(L)=eL \text{ or } \Big| \text{or } u(0)=0,\ \left[\partial u/\partial x+1/2\cdot(\partial w/\partial x)^2+p/E\right]_{x=L}=0\ . \tag{1.2.34}$$

Carrying out variation of the same equation for w, we have

$$-\frac{\partial w}{\partial x}\cdot\frac{\partial}{\partial x}\left\{\frac{\partial u}{\partial x}+\frac{1}{2}\left(\frac{\partial w}{\partial x}\right)^2\right\}-\left\{\frac{\partial u}{\partial x}+\frac{1}{2}\left(\frac{\partial w}{\partial x}\right)^2\right\}\frac{\partial^2 w}{\partial x^2}+i^2\frac{\partial^4 w}{\partial x^4}=0\ . \tag{1.2.35}$$

The end condition is

$$w(0)=w(L)=\left[\partial^2 w/\partial x^2\right]_{x=0}=\left[\partial^2 w/\partial x^2\right]_{x=L}=0\ . \tag{1.2.36}$$

These two simultaneous equations are not linear, but they are not difficult to solve, and from equation (1.2.33), we have

$$\left.\begin{aligned}\partial u/\partial x+1/2\cdot(\partial w/\partial x)^2&=\text{constant}\equiv -e_0\\ u&=u(0)-e_0x-\int_0^x\frac{1}{2}\cdot(\partial w/\partial x)^2dx\end{aligned}\right\}. \tag{1.2.37}$$

[1] The line was drawn between the two sides of this in order to contrast the two types.

Inserting this in equation (1.2.35) we obtain

$$\frac{\partial^4 w}{\partial x^4}+\frac{e_0}{i^2}\frac{\partial^2 w}{\partial x^2}=0 \quad . \tag{1.2.38}$$

The solution is, with $e_0/i^2 = \alpha^2$

$$w=f\sin\alpha x+g\cos\alpha x+f_1 x+g_1 \quad . \tag{1.2.39}$$

With respect to f, g, f_1, g , u(0), e_0, there are six end conditions

$$u(0)=0,\quad g+g_1=0,\quad g=0,\quad f\sin\alpha L+f_1 L=0,\quad f\alpha^2\sin\alpha L=0 \tag{1.2.40}$$

/20

$$-eL=u(0)-e_0 L-\int_0^L \frac{1}{2}\cdot(\partial w/\partial x)^2 dx \quad \text{or} \quad -e_0+p/E=0 \tag{1.2.41}$$

when $f_1 = g_1 = g = u(0) = 0$, one of the following two is obtained

(1) $f=0,\quad w=0$

$$e_0=e,\quad u=-ex \quad \text{or} \quad e_0=p/E,\quad u=-p/E\cdot x \tag{1.2.42}$$

(2) $f\neq 0,\quad w=f\sin\alpha x,\quad \alpha=\pi/L$

$$e_0=i^2\pi^2/L^2\equiv e^*,\quad u=-e^*x+\pi/8\cdot f^2/L\cdot\sin 2\pi x/L \quad . \tag{1.2.43}$$

There are two states of equilibrium, a straight state where f = 0 and a bent state where $f \neq 0$. In the straight state, this is determined by the p or e, but in the bent state, in the case of (A) where the end displacement is considered an independent variable, f is determined by e,

$$f^2/4L^2=e-e^* \quad . \tag{1.2.44}$$

In case (B) where the external force of the end is considered an independent variable, p itself is

$$p=Ee^*=p^* \tag{1.2.45}$$

a limit value is given, which is not exceeded. In this manner, we find from energy theory that there are two equilibriums, and two systems for determining them. Since there is a difference in the form of this, and that which is treated by ordinary energy methods, this point must be examined.

As stated initially Π is a minimum value; i.e., $\delta\Pi = 0$, $\delta^2\Pi > 0$, the condition for a stable equilibrium. Moreover, the conditions for determining accurately stability and instability from energy theory are as follows:

(1) The fact that the equilibrium is stable means that the potential energy in all adjacent states of deformation is greater than the value of the case of equilibrium.

(2) The fact that the equilibrium is unstable means that at least one minimum adjacent state of deformation is present, in which the potential energy is smaller.

(3) That there is an unstable equilibrium means that one minimum adjacent state of deformation is present, in which the potential energy is of the same magnitude, the potential energy is greater than the other adjacent states of deformation, and that there is absolutely no state present in which it is smaller. When this is the intermediate state of equilibrium in the change from equilibrium state (1) to state (2) it is called the limit of stability.

In order to determine the condition where $\hat{\Pi}$ described above is Min., u + δu, and w + δw is substituted for w and adjusting for the powers δu, δu [possibly a misprint], and excluding anything above the third order,

$$\Delta\hat{\Pi}=\hat{\Pi}(u+\delta u,\ w+\delta w)-\hat{\Pi}(u,w)=\delta\hat{\Pi}+\frac{1}{2}\delta^2\hat{\Pi}+\cdots \tag{1.2.46}$$

$$=-\frac{1}{L}\frac{p}{E}\delta u_{x=L}+\frac{1}{L}\int_0^L\left\{\frac{\partial u}{\partial x}+\frac{1}{2}\left(\frac{\partial w}{\partial x}\right)^2\right\}\delta\left(\frac{\partial u}{\partial x}\right)dx$$

$$+\frac{1}{L}\int_0^L\left[\left\{\frac{\partial u}{\partial x}+\frac{1}{2}\left(\frac{\partial w}{\partial x}\right)^2\right\}\frac{\partial w}{\partial x}\delta\left(\frac{\partial w}{\partial x}\right)+i^2\frac{\partial^2 w}{\partial x^2}\delta\left(\frac{\partial^2 w}{\partial x^2}\right)\right]dx$$

$$+\frac{1}{2L}\int_0^L\left[\delta\left(\frac{\partial u}{\partial x}\right)\right]^2dx$$

$$+\frac{1}{2L}\int_0^L\left[\left\{\frac{\partial u}{\partial x}+\frac{1}{2}\left(\frac{\partial w}{\partial x}\right)^2+\left(\frac{\partial w}{\partial x}\right)^2\right\}\left[\delta\left(\frac{\partial w}{\partial x}\right)\right]^2+i^2\left[\delta\left(\frac{\partial^2 w}{\partial x^2}\right)\right]^2\right]dx.$$

/21

The fact that the primary [1st order] term of 0 was already used in case of equilibrium. The stability condition is determined from the secondary [2nd order] terms. Using the results from δΠ = 0, in the case of a straight contraction, according to equation (1.2.42)

$$(\delta^2\hat{\Pi})_1=(\delta^2\hat{A}_i)_1=\frac{1}{L}\int_0^L\left\{-e\left[\delta\left(\frac{\partial w}{\partial x}\right)\right]^2+i^2\left[\delta\left(\frac{\partial^2 w}{\partial x^2}\right)\right]^2\right\}dx \tag{1.2.47}$$

$$+\frac{1}{L}\int_0^L\left[\delta\left(\frac{\partial u}{\partial x}\right)\right]^2dx.$$

Also, from the curved state, according to (1.2.43), we obtain

$$(\delta^2\hat{\Pi})_2=(\delta^2\hat{A}_i)_2=\frac{1}{L}\int_0^L\left\{\left(-e^*+\frac{\pi^2}{L^2}f^2\cos^2\frac{\pi x}{L}\right)\left[\delta\left(\frac{\partial w}{\partial x}\right)\right]^2+i^2\left[\delta\left(\frac{\partial^2 w}{\partial x^2}\right)\right]^2\right\}dx \tag{1.2.48}$$

$$+\frac{1}{L}\int_0^L\left[\delta\left(\frac{\partial u}{\partial x}\right)\right]^2dx.$$

When it comes to determining the limit of stability, the second variation is 0. However, since it does not become negative, the fact that $\delta^2\Pi = 0$ means that it is a minimum value. In such a special case, this is

$$\delta(\delta^2\hat{\Pi})=0. \tag{1.2.49}$$

This, in the present problem is

$$\partial^2(\delta u)/\partial x^2=0 \tag{1.2.50}$$

$$\partial^4(\delta w)/\partial x^4+e/i^2\cdot\partial^2(\delta w)/\partial x^2=0. \tag{1.2.51}$$

The end condition is

$$\left.\begin{aligned}&\delta w(0)=\delta w(L)=|\,\delta(\partial^2 w/\partial x^2)\,|_{x=0}=|\,\delta(\partial^2 w/\partial x^2)\,|_{x=L}=0,\quad \delta u(0)=0\\ &\delta u(L)=0 \quad \text{又}|\text{比} \quad |\,\delta(\partial u/\partial x)\,|_{x=L}=0\end{aligned}\right\} \tag{1.2.52}$$

so

$$\delta u=0,\qquad \delta w=\delta f\sin \pi x/L \tag{1.2.53}$$

satisfies the end condition. Consequently, when $\delta f \neq 0$, this is the case of an unstable equilibrium. Moreover, from equation (1.2.51), the limit value of e is

$$e_k=i^2\pi^2/L^2$$

meaning that $e_k = e^*$ and the bifurcation point of equilibrium matches with the limit of instability. /22

The results of determination of stability and instability are

(1) stable if the straight deformation from (1.2.47) is $e \leq e^*$.

(2) unstable if the straight deformation is $e > e^*$; i.e., if $\delta w = f \sin \pi x/L$ is included, $\delta^2\hat{\Pi} < 0$.

(3) as for the fact that the curved shape is stable where $e > e^*$, judging from equation (1.2.48), the portion

$$\frac{1}{L}\int_0^L\left[-e^*\left(\delta\frac{\partial w}{\partial x}\right)^2+i^2\left(\delta\frac{\partial^2 w}{\partial x^2}\right)^2\right]dx$$

is positive regardless of the shape assumed for δw. Moreover, since

$$\frac{\pi^2}{L^2}\int_0^L f^2\cos^2\frac{\pi x}{L}\left(\delta\frac{\partial w}{\partial x}\right)^2 dx$$

is also added. It is clear that $\delta^2\hat{\Pi} > 0$.

Here, using the method of determining the limit of stability mentioned above, we shall examine the relationship to the ordinary energy methods. In ordinary cases, this amounts to merely investigating properties at the stability limit; that is, in such a case, the transition from a direct form of deformation to a buckling form of deformation, is investigated. In such a case, this amounts to either investigating changes only in the internal energy where, as described above, the displacement of the end is fixed, or to consider the work of the external force, taking into account the displacement of the end. Deducting the total amount of work until the stability limit is reached, considering the energy newly applied at the stability limits as A_i and A_a for the internal and external forces, this is expressed at the stability limit by the following equation

$$A_i=0 \quad \text{or} \quad A_i-A_a=0 . \tag{1.2.54}$$

Writing the contraction at the stability limit $-\partial u/\partial x$ as e_0 and with the stress as p_0

$$A_i=\frac{EF}{2}\left[i^2\int_0^L\left(\frac{\partial^2 w}{\partial x^2}\right)^2 dx - e_0\int_0^L\left(\frac{\partial w}{\partial x}\right)^2 dx\right] \quad \text{or} \quad \begin{aligned} A_i&=\frac{EF}{2}i^2\int_0^L\left(\frac{\partial^2 w}{\partial x^2}\right)^2 dx, \\ A_a&=\frac{Fp_0}{2}\int_0^L\left(\frac{\partial w}{\partial x}\right)^2 dx . \end{aligned} \tag{1.2.55}$$

In this equation on the left, the term $(\partial w/\partial x)^4$ is not present, as in the case of equation (1.2.30). In the right equation, even though this is a curved state, it is assumed that strain energy due to elongation is not present (i.e., the total length does not change). However, for this reason, it is assumed that the end is displaced only

$$u_1=-\frac{1}{2}\cdot\int_0^L(\partial w/\partial x)^2 dx \cdot$$

The condition of a stability limit (1.2.54) is satisfied for a specific w(x), but in other forms of deformation

$$A_i>0 \quad \text{or} \quad A_i-A_a>0$$

Consequently, with this specific w(x), A_i or A_i - A_a becomes a minimum value. Therefore

$$\delta A_i=0 \quad \text{or} \quad \delta(A_i-A_a)=0. \tag{1.2.56}$$

That is, a double requirement for equation (1.2.54) and equation (1.2.56) exists. Written in the form of an equation

$$A_i=\frac{EF}{2}\left[i^2\int_0^L\left(\frac{\partial^2 w}{\partial x^2}\right)^2 dx - e_0\int_0^L\left(\frac{\partial w}{\partial x}\right)^2 dx\right]=\text{Min.}=0 \quad \text{or} \quad A_i-A_0=\frac{EFi^2}{2}\int_0^L\left(\frac{\partial^2 w}{\partial x^2}\right)^2 dx - \frac{Fp_0}{2}\int_0^L\left(\frac{\partial w}{\partial x}\right)^2 dx=\text{Min.}=0 \cdot \tag{1.2.57}$$ /23

This equation is a second order equation which is of the same order as w. Moreover, these equations agree with equation (1.2.47) above in which the condition is that $\delta^2\Pi$ is minimum. The only difference is that δw here is w. However, it is clear that the relationship to the second variation is clearer if the approach described above is taken into account. However, in the case of the present method, since it is expressed by the same equation, using the infinitesimal displacement at the stability limit, occasionally it is easy to commit an error. That is, the equation for the usual energy method does not employ the principle of a hypothetical displacement such as that described above, and is merely used for determining the stability limit.

The results described above become very easy to understand if, instead of using the variation method, the problem is to determine the normal minimum values, utilizing Ritz's [34] method. Ritz's equation, solving equations (1.2.33-36) is

$$w=f\sin\frac{\pi x}{L},\quad \frac{\partial u}{\partial x}+\frac{1}{2}\cdot\left(\frac{\partial w}{\partial x}\right)^2=e+\frac{\pi^2 f^2}{4L^2}.$$

The potential energy $\hat{\Pi}$ in this case is

$$\hat{\Pi}=\frac{1}{2L}\int_0^L\left\{\frac{\partial u}{\partial x}+\frac{1}{2}\left(\frac{\partial w}{\partial x}\right)^2\right\}^2dx+\frac{i^2}{2L}\int_0^L\left(\frac{\partial^2 w}{\partial x^2}\right)^2dx-\frac{p}{E}e \tag{1.2.58}$$

$$=\frac{1}{2}\left(e-\frac{\pi^2f^2}{4L^2}\right)^2+\frac{i^2\pi^4f^2}{4L^4}-\frac{p}{E}e=\frac{\pi^4f^4}{32L^4}-\frac{\pi^2f^2}{4L^2}(e-e^*)+\frac{e^2}{2}-\frac{p}{E}e=\text{Min.}$$

so, the equation for determining f and p in this state of equilibrium derives from the minimum condition for e, f.

$$\frac{\partial\hat{\Pi}}{\partial e}=e-\frac{\pi^2f^2}{4L^2}-\frac{p}{E}=0 \tag{1.2.59}$$

$$\frac{\partial\hat{\Pi}}{\partial f}=\frac{f\pi^2}{2L^2}\left(e^*-\left(e-\frac{\pi^2f^2}{4L^2}\right)\right)=0\ . \tag{1.2.60}$$

Then, for the state of equilibrium

(1) $$f=0.\quad p=Ee,\quad \text{or} \tag{1.2.61}$$

(2) $$f\neq0,\quad \frac{p}{E}=e-\frac{\pi^2f^2}{4L^2}=e^*=i^2\frac{\pi^2}{L^2}\ . \tag{1.2.62}$$

Stability is determined by the second variation, but here we shall do this by a second order differential. The value is

$$\frac{\partial^2\hat{\Pi}}{\partial e^2}=1,\quad \frac{\partial^2\hat{\Pi}}{\partial f^2}=\frac{\pi^2}{2L^2}\left(e^*-e+3\frac{\pi^2f^2}{4L^2}\right)\ . \tag{1.2.63}$$

Therefore, the state of equilibrium (1) is $\delta^2\hat{\Pi}>0$ where $e > e^*$ and is stable, but where $e < e^*$, it becomes $\delta^2\hat{\Pi}/\partial f^2 = \pi^2/2L^2$. $(e^* - e) < 0$, and is unstable. The state of equilibrium (2) exists where $e > e^*$ and since $\pi^2f^2/4L^2 = e - e^*$ $\partial^2\hat{\Pi}/\partial f^2 > 0$, it is stable. /24

In order to make the results of the above equation more easily understandable, we shall compute the strain energy $\hat{A}_i$ thus, with $\alpha = e/e^*$

$$\frac{\hat{A}_i}{e^{*2}} = \frac{1}{2}\xi^4 - \xi^2(\alpha - 1) + \frac{\alpha^2}{2}, \quad \text{where} \quad \xi = -\frac{f\pi}{2L\sqrt{e^*}}$$

so, with ξ on the x axis, α as a parameter, and $y = \hat{A}_i/e^{*2}$ on the y axis, we obtain Figure 1.2.20. The energy portion of the external force is not included in the $\hat{A}_i/e^{*2}$. This is done in order to make the graph more easily understandable. It can be easily seen from this graph, that where the transformation $f = 0$, with $\alpha = 1$ as limits, $\hat{A}_i$ varies from minimum to maximum value, while where $\alpha > 1$, the place where the minimum value appears in the portion where $f \neq 0$, is clearly seen.

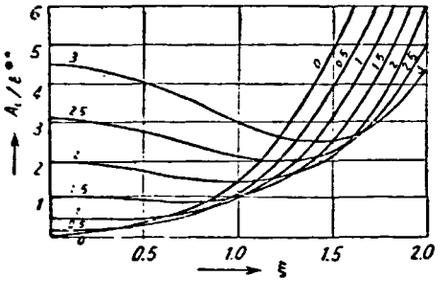

Figure 1.2.20.

This by itself is not very accurate, but it is proven by another method, that it agrees with the results described above, even if a large displacement is taken into account, or even if the correct variation treatment is used (4), that means that in the flexural buckling of a bar with both ends rotating or one end rigid and the other end free,

(1) deformation with uniform contraction and no deflection (i.e., direct form of deformation) is stable when there is less than a buckling load, but unstable when there is more than a buckling load.

(2) Within the range of a column length (excluding both ends), the form of deformation which causes a deflection with no inflection point is constantly stable as long as it is in a state of equilibrium (i.e., the form of buckling deformation with respect to the lowest buckling load).

(3) The type of deformation which causes an inflection point within the range of a column length is unstable, (i.e., the form of buckling deformation with respect to the second or greater buckling load above).

It is easy to misunderstand this problem of stability and instability since it is easy to think that given buckling, there is an immediate transition to an unstable state. If considered in terms of columns, there is the phenomenon according to which the buckling itself may shift to a stable equilibrium as described above, but in actual materials, and in the case of an eccentricity in the slenderness ratio, as described below, the yield phenomenon arises, and the buckling enters the instability region. Consequently, since cases of instability are observed immediately in the vicinity of buckling in experiments, it is reasonable that it is easy to have the misconception that buckling itself moves into an unstable state. However, the pure form of buckling is as described above, and it is certain that it moves to a state of equilibrium, and we wish to impress this on the reader's mind.

Apparently there are no results of careful investigation of stability and instability in the case of plates and shells. There are discussions of the case in which infinitesimal buckling deformation occurs in the vicinity of the point of bifurcation, but there are no discussions of stability in the very large buckling deformations in bars. However, it is easy to imagine that the conclusions would be the same as for the bars described above.

We shall describe concretely in detail the energy method as a numerical method of calculation of buckling load later on, and here we shall merely describe the fundamentals. First let us give a general consideration (3) to the general properties in the case of determining buckling load by the energy method in plates and shells. We assume that due to some external force system, the plate or shell undergoes plane-internal stress resultants n_{xI}, n_{yI}, n_{xyI}, and that the stress couples (Schnittmomente) M_{xI}, M_{yI}, M_{xyI} are all zero. In /25 order for such a state to obtain, it is necessary for an appropriate external force to be applied in the case of an appropriate contour condition. Otherwise, no buckling will occur such that a bifurcation point occurs. Assuming that the state sustaining n_{xI}, n_{yI} and n_{xyI} is the initial state, we shall attempt to determine the buckling load by investigating, in terms of energy, the case in which the state in which the displacements u, v, w are newly applied as a buckling deformation forms a stable equilibrium.

We assume that by virtue of the added displacements, u, v, w, the stress couples M_x, M_y, M_{xy}, M_{yx} and the lateral shearing force Q_x, Q_y are generated, and the plane internal stress resultants increase only by n_x, n_y, n_{xy}. However, we are considering only the range in which these values are markedly smaller in comparison with the original n_{xI}, n_{yI}, n_{xyI}. Moreover, since the contour conditions must be established for both the initial state and for the case in which an additional displacement is applied, with only the additional sectional internal forces, end conditions of the same order are satisfied. Although there is a constant solution for the case in which the additional displacement is zero overall, in the case of a special external force value, a finite solution is obtained, and this is a buckling load.

Expressing by ΔA_a the potential energy lost by the external forces due to u, v, w, we write this in the following manner

$$\Delta A_a = \Delta A_a^{(1)} + \Delta A_a^{(2)} + \Delta A_a^{(3)} + \cdots \tag{1.2.64}$$

Also, we will express the increase in strain energy ΔA_i as follows

$$\Delta A_i = \Delta A_i^{(1)} + \Delta A_i^{(2)} + \Delta A_i^{(3)} + \cdots \tag{1.2.65}$$

the indices (1), (2), and (3), indicate respectively the first, second and third order parts of u, v, and w. Then, judging from the above, since we assume that the initial state is a state of equlibrium,

$$\Delta A_i^{(1)} - \Delta A_a^{(1)} = 0 \tag{1.2.66}$$

Since $\Delta A_i^{(2)} - \Delta A_a^{(2)} > 0$, this is stable, and with respect to the stability limit

$$\Delta A_i^{(2)} - \Delta A_a^{(2)} = 0 \tag{1.2.67}$$

Moreover, in order to compute ΔA_i, we write the plane internal strain in the initial state as ε_{xI}, ε_{yI}, γ_{xyI}, the strain due to additional displacement as ε_x, ε_y, γ_{xy}, and the curvature in the center plane as κ_x, κ_y, κ_{xy}, and the plane element of center plane as dF

(1.2.68)

$$\Delta A_i = \int_F (n_{xI}\varepsilon_x + n_{yI}q_y + n_{xyI}\gamma_{xy})\,dF + \frac{1}{2}\int_F (n_x\varepsilon_x + n_y\varepsilon_y + n_{xy}\gamma_{xy})\,dF$$

$$+ \frac{1}{2}\int_F (M_x\kappa_x + M_y\kappa_y + 2M_{xy}\kappa_{xy})\,dF$$

Assuming that the relationships $n_x = N\varepsilon_x$, ..., $M_x = D\kappa_x$, obtained, and writing the relationship between strain component and displacement, using the indices (1), (2), ... with the same meaning as above, we obtain

$$\left.\begin{aligned} \varepsilon_x &= \varepsilon_x^{(1)} + \varepsilon_x^{(2)} + \cdots, \quad \cdots \\ \kappa_x &= \kappa_x^{(1)} + \kappa_x^{(2)} + \cdots, \quad \cdots \end{aligned}\right\} \tag{1.2.69}$$

$\Delta A_i^{(2)}$ is

$$\Delta A_i^{(2)} = \int_F (n_{xI}\varepsilon_x^{(2)} + n_{yI}\varepsilon_y^{(2)} + n_{xyI}\gamma_{xy}^{(2)})\,dF + \frac{1}{2}N\int_F (\varepsilon_x^{(1)2} + \varepsilon_y^{(1)2} + (1-\nu)\gamma_{xy}^{(1)2}/2)\,dF$$

$$+ \frac{1}{2}D\int_F (\kappa_x^{(1)2} + \kappa_y^{(1)2} + 2(1-\nu)\kappa_{xy}^{(1)2})\,dF \tag{1.2.70}$$

and since $N = Et/(1 - \nu^2)$, $D = Et^2/12\,(1 - \nu^2)$, we can write /26

$$\Delta A_i^{(2)} = J_1 + J_2 t + J_3 t^3 \tag{1.2.71}$$

J_1, J_2, and J_3 are values that are determined by the properties of the material, the size of the plate, and the form of buckling deformation, and J_2, J_3 always have a positive value. Inserting this into the equation for stability limit above,

$$-\Delta A_a^{(2)} + J_1 + J_2 t + J_3 t^3 = 0 \tag{1.2.72}$$

and $-\Delta A_a^{(2)}$, and J_1 are proportional to the load, consequently there are both cases in which this is positive or negative. When the load is small, the left side is always positive, and as the load is increased, cases arise in which this condition is satisfied. However, when the added displacement forms the plane internal strain, i.e., when $\varepsilon_x^{(1)} = \varepsilon_y^{(1)} = \gamma_{xy}^{(1)} = 0$, equation (1.2.72) becomes $\Delta A_a^{(2)} - J_1 = J_3 t^3$, and the buckling load is proportional to the third power of t. Moreover, the form of buckling deformation becomes irrelevant to the plate thickness. This is, in the case of the buckling of a flat plate,

the corrugated shape of the deformation is determined by the external configuration of the flat plate, and the fact that it is irrelevant to the plate thickness has already been noted above.

In the case of shells, it is difficult to have a general situation with no plane-internal strain, and the ratio between J_2 and J_3, due to the skin thickness of t comes to differ. That is, the corrugated shape of the deformation differs, and when t is small, this means that J_3 is large, i.e., a deformation is formed in which the number of corrugations is great. Moreover, the buckling load occasionally is proportional to the square of the skin thickness t (in the axial compressive load in a cylindrical shell), or proportional to 2.5 the power of t (the case of the torsional load in a cylindrical shell). Consequently, it is necessary to keep this in mind in determining the buckling load of a shell.

1.2.5. THE CASE OF ORIGINAL DEFLECTION

Above, we have described theoretically simple cases of buckling and for this reason, we have assumed even that the axially compressive load is a pure center load, that we had simple plane-internal stress resultants in plates and shells, and contrasted these with the cases in which no curvature variation (or negligible curvature variation) occurred. However, since it is an extremely difficult task to produce such a pure configuration, or to apply a load to the true center, it is necessary to consider that in actual cases, this "purity" is lost at least slightly. Consequently, it is absolutely necessary to take into consideration the influences due to the imperfections in the members and load eccentricity.

In order to express the imperfections in the members, we shall express this by the configuration of a physical body, and we will assume that the configuration from the beginning has, to a small degree, a buckling deformation component. For example, in making the contrast to the problem of flexural buckling due to axial compressive load in a straight bar, we assume that from the beginning, the straight bar is slightly bent. That is, the bar from the beginning has a configuration which should arise due to buckling. In such a case, in the relationship between the deformation of the body and the load, there is no case in which a bifurcation point arises due to buckling load, but since the form of buckling deformation gradually increases in size from the beginning, the curve with a cusp at the point of bifurcation will change into a smooth curve in the vicinity of it. In terms of equations, this is handled as follows:

We assume that there is a quantity, called here the original deflection, by which the initially present configuration deviates from a "pure" state, and that this quantity satisfies the contour conditions in the problem of buckling. This can be expressed by the sum obtained by multiplying an appropriate coefficient by the configuration of deformation (eigen function) corresponding to buckling loads, (eigen values) 1, 2, ... That is, expressing by w_0 the quanti-/27
ty by which the bar deviates from a pure condition, with c_1, c_2 as constants, this is expressed as follows:

$$w_0 = c_1 w_{01} + c_2 w_{02} + \cdots \tag{1.2.73}$$

w_{01}, w_{02} ... are the configurations of deformation (eigen functions) corresponding to the first, second ... buckling loads P_{k1}, P_{k2}, ... The fact that such an expansion is possible is proved mathematically, and when w_0 is given, c_1, c_2 are easily determined by the orthogonality between w_{01}, w_{02}, ...

Inserting this in the equilibrium equation, we obtain the following. Expressing the load as P,

$$H(w) + P\left\{G(w) + G(w_0)\right\} = 0 \tag{1.2.74}$$

H ( ), G ( ) are differential operators, and are the same as those which appear in buckling problems (see examples below). However, since w_{01}, w_{02}, are the eigen functions with respect to P_{k1}, P_{k2}, ... we obtain

$$H(w_{01}) + P_{k1} G(w_{01}) = 0, \qquad \text{etc.} \tag{1.2.75}$$

Assuming that the deflection in a bar whose initial deflection originally was c_1, w_{01}, is $w = k_1 c_1 w_{01}$ (where k_1, k_2 ... are constants)

$$k_1 c_1 H(w_{01}) + k_1 c_1 P G(w_{01}) + P c_1 G(w_{01}) = 0$$

or, since

$$-k_1 c_1 P_{k1} G(w_{01}) + k_1 c_1 P G(w_{01}) + P c_1 G(w_{01}) = 0$$

we obtain

$$k_1 = P/(P_{k1} - P) \tag{1.2.76}$$

Consequently similarly for initial $w_{01} = c_1 w_{01} + c_2 w_{02} + \ldots$, can be expressed as

$$w = \frac{P}{P_{k1} - P} c_1 w_{01} + \frac{P}{P_{k2} - P} c_2 w_{02} + \cdots \tag{1.2.77}$$

For example, in the case of a straight bar, in which both ends are rotating and sustained, an axially compressive load, $H(\ ) \equiv EI\partial^2/\partial x^2$, $G(\ ) = 1$

and since $P_{km} = m^2\pi^2 EI/L^2$, $w_{0m} = \sin m\pi x/L$

when the original deflection is

$$w_0 = c_1 \sin \pi x/L + c_2 \sin 2\pi x/L + \cdots$$

the deflection in the case of load P is

$$\frac{Pc_1}{\pi^2 EI/L^2-P}\sin\frac{\pi x}{L}+\frac{Pc_2}{4\pi^2 EI/L^2-P}\sin\frac{2\pi x}{L}+\cdots \tag{1.2.78}$$

Moreover, in the case of a flat plate, with a rotating circumference which sustains a compressive load in direction y, this is

$$H(\ )\equiv D\left(\frac{\partial^2}{\partial x^2}+\frac{\partial^2}{\partial y^2}\right)^2 \qquad G(\ )\equiv\frac{\partial^2}{\partial y^2}$$

Assuming that in direction x this is only a half-wave, using n_k in place of P_k

$$\left.\begin{aligned} n_{km}&=\frac{\pi^2 D}{b^2}\left(\frac{mb}{L}+\frac{L}{mb}\right)^2\\ w_{0m}&=\sin\frac{\pi x}{b}\sin\frac{m\pi y}{L}\end{aligned}\right\} \tag{1.2.79}$$

/28

therefore, assuming

$$w_0=\sin\frac{\pi x}{b}\left(c_1\sin\frac{\pi y}{L}+c_2\sin\frac{2\pi y}{L}+\cdots\right) \tag{1.2.80}$$

The deflection w in the case of load n_y is given by the following equation

$$\begin{aligned} w=\sin\frac{\pi x}{b}\Bigg(&\frac{n_y c_1}{\pi^2 D/b^2\cdot(b/L+L/b)^2-n_y}\sin\frac{\pi y}{L}\\ &+\frac{n_y c_1}{\pi^2 D/b^2\cdot(2b/L+L/2b)^2-n_y}\sin\frac{2\pi y}{L}+\cdots\Bigg)\end{aligned} \tag{1.2.81}$$

In the case of a rod, $P_{k1} < P_{k2} < \ldots$, so the term w_{0i} normally becomes markedly larger than the others, but in the case of a plate, the order of magnitude of n_{km} differs according to L/b and since the size comparison of these is not too great, various configurations develop due to the initial original deflection configuration. However, in any case, when the load approaches the lowest buckling load, the configuration of deformation corresponding to this becomes superior, and in the equation it approaches maximum.

Taking only the first term for the case of a bar, we obtain

$$w=Pc_1/(P_{k1}-P)\cdot\sin\pi x/L$$

Assuming a maximum value for w, i.e., assuming that the deflection in the center is w_1,

$$w_1=Pc_1/(P_{k1}-P) \tag{1.2.82}$$

or, since

$$w_0=w_1P_{k1}/P-w_1 \tag{1.2.83}$$

describing w_1 with respect to w_1/P, it forms a straight line, and it becomes possible to determine experimentally P_{k1} from the slope of that line (107). This method can also be expanded to the case of a flat plate, but since the several values for the buckling load such as those described above are close to each other, we cannot expect the formation of a perfect straight line. Moreover, as described below, there are problems in the case of a bar.

The above methods can also be applied approximately when the deformation increases relatively greatly. In such a case, assuming that the configuration of the buckling deformation hardly changes at all, the form of H ( ), G ( ) changes somewhat due to the increase in load and deformation, and as a result, in such a case, the value corresponding to the eigen value P_{km} is determined by the size of v_{om} or δ and is assumed to be P_{km}'. Then, it is considered that the relationship between w_{om} and P_{km}' in the case of a pure center load, is understood. However, in this case, since the rule of accumulation does not hold, it can only be applied to one type of configuration of superior deformation. For this, assuming the original deflection to be $c_1 w_{01}$, when the above $k_1 c_1$ is made δ, assuming that the eigen value becomes $P_{k1}'(\delta)$ since

$$\delta = k_1 c_1 = \frac{P c_1}{P_{k1}'(\delta) - P} \tag{1.2.84}$$

solving this for P, we have

/29

$$P = \frac{\delta}{\delta + c_1} P_{k1}'(\delta) \tag{1.2.85}$$

Therefore, when the relationship between δ, where $c_1 = 0$, and $P_{k1}'(\delta)$ is understood, the relationship between δ and P in the case of original deflection $c_1 w_{01}$ becomes $\delta/(\delta + c_1)$ times P_{k1}', so as shown in figure 1.2.21, it is easy to determine

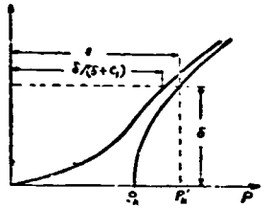

Figure 1.2.21

When the deformation progresses in this manner, even if original deflection c_1 is present, it approaches to the extent that it almost matches the curve $c_1 = 0$. This indicates that the same results will be obtained, even in the case of a rod, even if relatively precise calculations are performed using Equation (1.2.16). When considering the buckling load approximately as a problem, when there is no original deflection, when this is given in the form

$$P_{k1}' = P_{k1}(1 + a_1 \delta^2) \tag{1.2.86}$$

the relationship between P and δ given the original deflection $c_1 w_{01}$, is given by

$$P = P_{k1} \frac{\delta}{\delta + c_1}(1 + a_1 \delta^2) \tag{1.2.87}$$

when $c_1 \ll \delta$, it is possible to use the curve $c_1 = 0$. Using this fact, it is also possible to determine the values of P_{k1} from the relationship between P from the rest results and δ^2. This is Yoshiki Masao's δ^2 method (35) (see Section 1.5.3).

Now let us consider the influences in the case when the load is not in the pure center, but is applied eccentrically. We assume that the case of a straight bar sustaining an axially compressive load, with both ends rotating, and that a load is applied equally to both ends with an eccentricity e. In this case, since the lateral force within the body is still 0, it is possible to employ Equation (1.2.1). From this general solution, a solution should be derived which would satisfy the new contour conditions.

When a straight bar sustains an eccentric load, (x = 0) as the center of the rod, v is

$$v = e\left[\frac{\cos \alpha x}{\cos \alpha L/2} - 1\right], \qquad \text{where} \quad \alpha^2 = \frac{P}{EI} \tag{1.2.88}$$

The bending moment M is

$$M = P(v+e) = Pe\frac{\cos \alpha x}{\cos \alpha L/2} \tag{1.2.89}$$

The maximum deflection v_m, and the maximum bending moment M_m are respectively

$$v_m = e(\sec \alpha L/2 - 1)$$

$$M_m = Pe \sec \alpha L/2$$

Figure 1.2.22 indicates the relationship between this v_m and P.

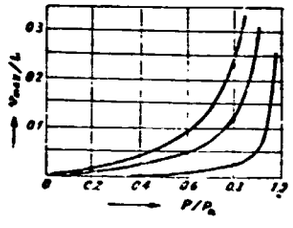

Figure 1.2.22

In such a case, it is possible to calculate algebraically as in the case of Figure 1.2.9 for large deformations after buckling. The results are as shown by Figure 1.2.23. Consequently, even in this case, as shown by Equation (1.2.87), the fact that the relationship between P and v_m can be expressed as a product of the two factors due to an increase in the eccentricity and deformation can be easily seen by comparing Figures 1.2.22 and 1.2.23. /30

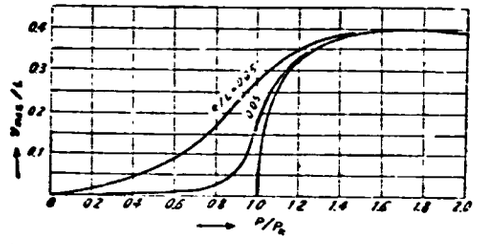

Figure 1.2.23

When the degree of eccentricity at both ends of the rod are different, assuming e $\pm$ d respectively as the degree of eccentricity

$$v=e\left\{\frac{\cos\alpha x}{\cos\alpha L/2}-1\right\}+d\left\{\frac{\sin\alpha x}{\sin\alpha L/2}-\frac{2x}{L}\right\}, \tag{1.2.90}$$

(1.2.91)

$$M=Pe\frac{\cos\alpha x}{\cos\alpha L/2}+Pd\frac{\sin\alpha x}{\sin\alpha L/2}, \qquad \text{where} \quad \alpha^2=\frac{P}{EI}$$

as can be seen from this equation, when e $\neq$ 0, from cos $\alpha L/2 = 0$, when $\alpha = \pi/L$ i.e., $P = \pi^2EI/L^2$, v, M become maximum and when e = o, from sin $\alpha L/2 = 0$, when $\alpha = 2\pi/L$, i.e., $P = 4\pi^2EI/L^2$, for the first time v, M become maximum. To consider that when the values of v, M become maximum, from the type of treatment given above, that this is a case of buckling load is satisfactory, since it matches the normal buckling load, but when e = 0, if the values do not become four times that of the normal ones, it would appear that bukling has not occurred. However, this is a mistake, and if the numerical equation is handled correctly, when $P = \pi^2EI/L^2$, buckling in the true sense of the word occurs, (9), (10). That is, even when e = 0, and $P = \pi^2EI/L^2$, A sin $\pi x/L$ [A is an unstable coefficient] is applied as a solution which satisfies the contour conditions, in addition to the solution for Equation (1.2.90). Therefore, the solution for v is

$$v=A\sin\frac{\pi x}{L}+d\left(\frac{\sin\pi x/L}{\sin\pi/2}-\frac{2x}{L}\right) \tag{1.2.92}$$

which means that the deflection of the form sin $\pi x/L$ can occur in any magnitude. This means none other than a true case of buckling. Zimmermann, in order to explain the same thing, proceeds from the statement to the effect that the values change rapidly when e $\rightarrow$ 0 and e = 0 is not a realization of a physical phenomenon (83). In any case, such a case is extremely easy to misunderstand and requires careful attention.

We assume that in the case of a rectangular plate, the four sides are rotating sides, and that the low eccentricity of the load end is of the form (e$\pm$d) sin $\pi x/b$ along the load edge. The reason such a distribution is employed is for solving the equations, but on the other hand, even assuming any eccentric distribution, if this is expanded to the series sin $m\pi x/b$, the term $m \geq 2$ does not become very important. A solution for deflection in such a case is

$$w=\frac{\sin\pi x/b}{\sqrt{1-4\pi^2D/b^2n_y}}\left\{e\left(\frac{\cos\alpha_1 y}{\cos\alpha_1 L/2}-\frac{\cos\alpha_2 y}{\cos\alpha_2 L/2}\right)+d\left(\frac{\sin\alpha_1 y}{\sin\alpha_1 L/2}-\frac{\sin\alpha_2 y}{\sin\alpha_2 L/2}\right)\right\} \tag{1.2.93}$$

where

$$\alpha_1,\alpha_2=-\frac{1}{2}\sqrt{\frac{n_x}{D}}\pm\sqrt{\frac{n_y}{4D}-\frac{\pi^2}{b^2}} \qquad \text{/31}$$

In such a case, where in $n_y < 4\pi^2 D/b^2$ since α_1, α_2 become complex numbers, it is necessary to perform the calculations using the appropriate treatment. Moreover, as in the case of a bar, if $e \neq 0$, when $n_{ym} = \pi^2 D/b^2 \cdot (L/b + b/L)^2$ from $\cos \alpha_1 L/2 = 0$, and when $d \neq 0$, when $n_{ym} = \pi^2 D/b^2 \cdot (L/2b + 2b/L)^2$ from $\sin \alpha_1 L/2 = 0$, w becomes infinitely large. However, in either case, true buckling occurs when $n_{yk} = \pi^2 D/b^2 \cdot (L/mb + mb/L)^2$ becomes a minimum value. Also, in this case, when $L/b > \sqrt{6}$, this true buckling constantly occurs earlier. Moreover, around $L/b > 3$, since the value of n_{ym} becomes large, the deflection due to eccentricity becomes relatively small, indicating that the influence of the end eccentricity is small. This means that these points indicate properties which are slightly different from the case of a bar. Next, what can be understood from equation (1.2.90) and (1.2.93) above, is that large e, d initially are superior deformations, but afterwards, from a certain point, a deformation becomes predominant which corresponds to a lower buckling load. Consequently, in a rod there are cases in which a deformation which initially is in the shape of an S, suddenly change into a bow-shaped deformation. In the case of a plate, there are cases in which the reverse situation obtains.

Now to explain the case in which there is simultaneously present, both original deflection and eccentricity, for the case of a rod. These two results can become overlapping when the deflection is small, so that the first term in Equation (1.2.77) and Equation (1.2.90) overlap with each other. In the case of an original deflection $c_1 \sin \pi x/L$, where there is an equal eccentricity e at both ends, if the maximum deflection v_m in the center is

$$v_m = \frac{Pc_1}{P_k - P} + e\left[\frac{1}{\cos\{\pi/2 \cdot \sqrt{P/P_k}\}} - 1\right], \quad \text{where } P_k = \frac{\pi^2 EI}{L^2} \tag{1.2.94}$$

The relationship between the deflection and the load, due to the size of c_1 and e, can be shown as in Figure 1.2.24. Of special note here is that the direction of deflection changes while it is in the process of reaching the buckling load. This has been observed from experiments, over a long period of time, but Zimmermann was the first to offer an explanation in terms of superimposition of the original deflection and eccentricity (83).

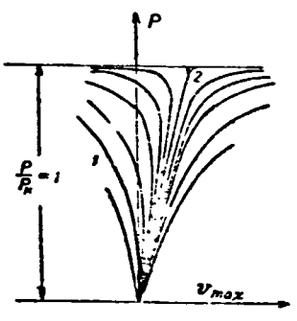

Figure 1.2.24

The fact that when $P \leq P_k$, $v_m = 0$ is responsible for this phenomenon, and assuming that in equation (1.2.94), $v_m = 0$, we obtain

$$\frac{e}{c_1} = -\frac{P}{P_k - P} \frac{\cos\{\pi/2 \cdot \sqrt{P/P_k}\}}{\cos\{\pi/2 \cdot \sqrt{P/P_k}\} - 1} \tag{1.2.95}$$

The case of curves 1 or 2 in Figure 1.2.24 form the limits for the value of e/c_1, and in the equation $v_m = 0$, but this is a case of $P = 0$ and $P = P_k$. Computing e/c_1 in such a case, when

$$-0.811 = -8/\pi^2 < e/c_1 < -\pi/4 = -0.785 \tag{1.2.96}$$

it can be seen that the deflection is reversed.

The same thing also occurs in the case of a flat plate. Moreover, in the /32
case of a flat plate, in addition to such a reversal, in the case of $\sqrt{2} < L/b < \sqrt{6}$, due to eccentricity, what was initially a curve-shaped deformation suddenly changes, and an S-shaped deformation predominates. Thereupon, in the vicinity of the center of the plate, what was initially deflected may return to 0. What should be noted in such cases, is, as can be seen from the above results, that the load when the direction of the deflection begins to change, is totally unrelated to the buckling load. Sometimes, reports are published which do not take cognizance of this relationship, so caution must be exercised.

The fact that deflection or waves occur early in tests on bars and plates can easily be explained by considering, as above, original deflection or load eccentricity. However, these do not have a direct relationship to buckling loads.

Even in cases where the load after pure buckling, as in plates, if consideration such as Equation (1.2.87) are taken into account, the relationship between load and deformation can be handled simultaneously, yielding a result which does not differ greatly from what has been described above. When the presence of original buckling is considered in such a manner, when a load edge is applied in a flat plate in such a manner that it is uniformly displaced, even under a buckling load, the effective width may become reduced. There are cases in which the effective width becomes less than the actual width even with respect to tensile load (36).

Since it is quite difficult to consider in general terms the case of deflection or eccentric loads in shells, we shall just offer two or three examples. Donnell (26) performs calculations considering original deflection in the case of the axial compression in a cylindrical shell. As will be described later, this was done in order to determine the buckling strength, but it did not adequately meet the objectives. In the case of axially symmetrical deformation in axial compression on a cylinder shell, due to lateral strain at the ends, where the cylinder radius should have increased, this is presented due to friction with the load plate, and Geckeler (37) calculates the fact that together with the load increase, large corrugations appear near the ends. This means that the deformation increases as shown in Figure 1.2.25 and when this results in a buckling load, it becomes infinitely large.

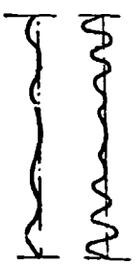

The term buckling is used to refer to all cases, not only of pure buckling such as that described in this section, but to those in which there is established a relationship between load and deformation, in which no bifurcation point occurs due to influences arising from imperfections of various types, but nevertheless undergoes a process very close to that of pure buckling. Consequently, when speaking in terms of buckling in this sense, even though the limits are not entirely clear, since in actual practice the concept is important, it is considered inappropriate to ignore buckling in this sense.

Figure

The problem of so-called buckling flexure (Knickbiegung) arises when from the beginning a certain original deflection or eccentricity is considerably large, or when not only axially compressive loads but bending loads are involved. The deflection is not proportional to the load, but becomes greater than proportional to it and in buckling loads, indicates a tendency to become maximum. Usually, when buckling flexure is in the process of occurring, a stress is formed which is greater than the proportional limit, the elasticity coefficient of the shell may change, or the shell may be destroyed owing to other types of buckling.

1.2.6. BUCKLING ABOVE THE PROPORTIONAL LIMIT

Now we consider a case in which the relationship between the stress and strain is no longer linear. This is important because in actual practice, there are many cases in which the stress has such values.

In this case, there is a difference in the elasticity coefficients in terms of the increase and decrease of stress as a property of the materials (correctly speaking, this cannot be said, but for convenience, we will assume this for the relationship between stress and strain). Usually in metal materials, in the case of tension or pure stress of compression, in the case of an increase in stress, the $d\sigma/d\varepsilon = E_c$ is smaller than Young's Modulus E, and its value changes according to the stress sigma. However, in the case of a decrease in stress, it is equal to Young's Modulus E, (Figure 1.2.26). Consequently, considering the case when the pure buckling occurs above the proportional limits, in the case of a slight bending, since on the inside of the bend the compressive strength increases, the elasticity coefficient in that portion is $d\sigma/d\varepsilon = E_c$, and on the outside of the bend, since the compressive strength decreases, the elasticity coefficient is equal to E. Considered in this manner and calculating according to normal bending theory, in the case of a rectangular cross-section (h x b) calling the position of the center axis h_1 from the inside edge of the bending, and h_2 from the outside edge

/33

$$h_1=\frac{\sqrt{E}\,h}{\sqrt{E}+\sqrt{E_c}}, \qquad h_2=\frac{\sqrt{E_c}\,h}{\sqrt{E}+\sqrt{E_c}} \tag{1.2.97}$$

expressing the flexural rigidity as $E_k I$ where $I = bh^3/12$), the values of E_k are given by the following equation (38)

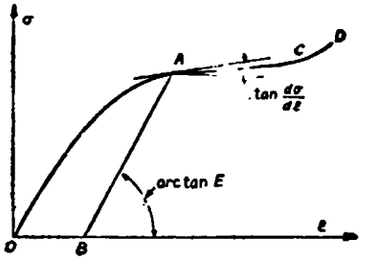

Figure 1.2.26

$$E_k=\frac{4EE_c}{(\sqrt{E}+\sqrt{E_c})^2} \tag{1.2.98}$$

Karman calls this E_k Knickmodul (we shall translate this here [in Japanese--translator's note] as "relative modulus of elasticity"). When the configuration of the cross-section is not a rectangle but another configuration, this relative modulus of elasticity changes slightly. In any case, the

equilibrium equation for buckling becomes

$$E_k I\frac{\partial^4 v}{\partial x^4}+P\frac{\partial^2 w}{dx^2}=0 \qquad (1.2.99)$$

and where this is E below the proportional limit, it merely changes to E_k. Therefore, when both ends are rotating ends, the buckling load P_k and the buckling stress σ_k are

$$P_k=\frac{\pi^2 E_k I}{L^2}, \quad \text{or} \quad \sigma_k=\frac{P_k}{F}=\frac{\pi^2 E}{\lambda^2}, \quad \text{where} \quad \lambda=\frac{L}{i} \qquad (1.2.100)$$

The results are as shown in Figure 1.2.27. The solid line indicates the results tested by Karman on a soft-steel column (38). Computed from the above equation, in the vicinity of the yield point, as shown by the dotted line in the graph, L/i should once become 0. However, the fact that, as shown in the graph, there is a smooth rise in the vicinity of the yield point, as Hartmann has pointed out, is due to the fact that the portion of the stress which rises immediately after bending begins in the vicinity of the yield point (CD in Figure 1.2.26) begins to have an effect, and the buckling strength increases. When such a short column sustains an eccentric load, assuming that the relationship between stress and strain in the case of an increase in compressive stress corresponding to the degree of deflection followed an actual curve, it is possible to compute the relationship between the average compressive stress σ_m and the deflection.

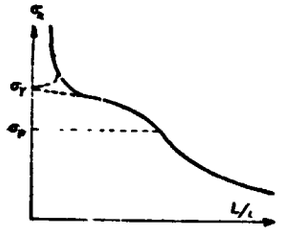

Figure 1.2.27

The results that Karmann obtained in calculating for various degrees of eccentricity in the case where σ_k = 31.35 kg/mm^2 are shown in Figure 1.2.28 (38). Although there is some problem in the hypothesis in the calculations (see Section 1.4.16) below), it is considered that there is not a very large error in the relationship between load and deflection. In particular, there is little error in the vicinity of infinitely large values of σ_m. As can be seen from the examples of computations, in the case of buckling greater than the proportional limit, when there is no eccentricity, the load decreases markedly when the buckling begins, and when there is eccentricity, the tendency is the same as this. However, it can be seen that the maximum values occur, and that the maximum values are reduced markedly owing to the amount of eccentricity. If this is compared with Figure 1.2.22 and 1.2.23 for the case below the proportional limits, there is a great difference and in this event, there were no cases in which the load decreased. However, even if σ_k is below the proportional limit, when the deflection increases, since a portion appears in which the compressive stress exceeds the proportional limit, it can be predicted that maximum values are present. Moreover, in that case, a configuration occurs such as shown in Figure 1.2.29 and even when there is a maximum value in the vicinity of this, there is a relatively slight variation, and there is no rapid change such as those shown in Figure 1.2.28.

/34

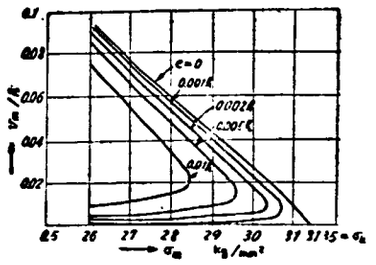

Figure 1.2.28

Consequently, in the case of the tests, when the buckling stress σ_k is above and below the proportional limits, the method of deflection differs greatly, being very rapid below the proportional limit and being relatively gentle and having a configuration close to that of a sine wave. while above the proportional limit it becomes bent into a shape such that it is rapidly "snapped" in the center.

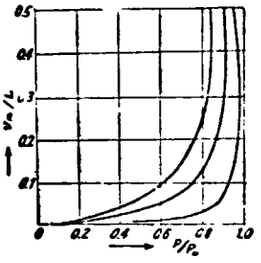

Figure 1.2.29

There are some people who believe that the load becomes a maximum value as above, when the maximum stress in the center section reaches the yield point, but as Hartmann has shown in actual calculations [8], this is not true.

Karmann determined, from the above calculations, the relationship between σ_k in the case where e = 0.005h, and λ = L/i, and indicated this in a graph such as that in Figure 1.2.30. The graph shows that the effect of eccentricity is very great when σ_k is between the proportional limit and the yield point. Moreover, the fact that almost all of the values from test results are performed with a center load are between e = 0.005h and e = 0, indicates that the above approach is quantitatively correct. Although calculations and tests have been carried out by this type of method for various sectional configurations and materials, this approach has always been shown to be correct.

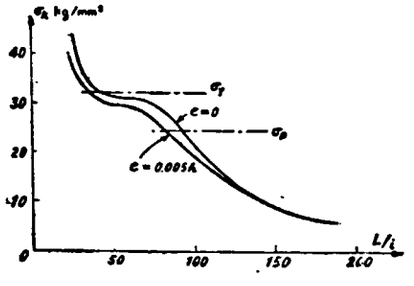

Figure 1.2.30

Instead of following Karman and using E_k as the relative modulus of elasticity, there are some who propose directly employing E_c. In test results, this is supported by the fact that the relative modulus of elasticity becomes smaller than E_k and is close to E_c (84). Also, when the curve for the buckling strength has been determined by tests, using Equation (1.2.100) in a converse manner, it is possible to determine the relative modulus of elasticity. Recently, it is claimed that E_c may be used as the relative modulus of elasticity in determining a load at the beginning of deflection (114).

In the case of plates, calculations have not been carried out for the case when the buckling load is greater than the proportional limit, such as in bars. However, when the stress in an orthogonal direction becomes small, it is possible to calculate this using Karman's relative modulus of elasticity mentioned above. Moreover, in the case of a plate, there are problems occurring after buckling, but when stresses greater than the proportional limit operate, it is anticipated that the drop in effective width will be very pronounced. In fact

/75

in Dickinson and Fischel's tests, (39) in a relatively thick plate where b/t = 49, in the case of a high buckling stress as shown by line A in Figure 1.2.31, the effective width is shown to drop much more rapidly than a normal curve (curve B in the figure).

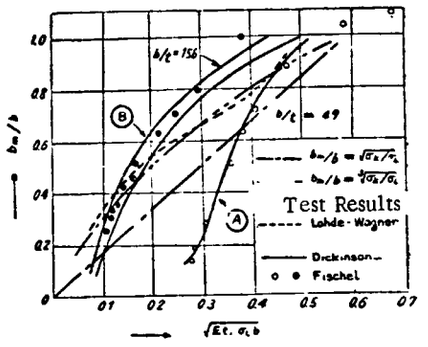

Figure 1.2.31

In the case of deformation after buckling, when cases arise in which the stress becomes greater than the proportional load inside the plate, corrugations remain due to buckling deformation, even after removing the load. We shall call this permanent buckling (40). This has become an object of research since when the degree of permanent buckling becomes greater than a certain limit, it is undesirable. (See Section 1.2.12 below.)

Since in shells, the stress varies i. two directions in the center plane, the relationship between stress and strain in the plastic region in such a case becomes necessary. However, it should not be as simple as in the case when the tension or compressive stress operate in only a single direction.

Geckeler uses the relative modulus of elasticity E_k determined by Karman for the case in which a cylindrical shell sustaining in axial compression undergoes axially symmetrical buckling deformation, carries out his computaticns considering that in the direction of the circumference, a modulus of elasticity E in which there is no change in Young's Modulus, obtains. Above the proportional limit, he shows that σ_k is proportional to the $\sqrt{E_k/E}$, the wave length decreases, being proportional to the $\sqrt[4]{E_k/E}$ (37). With respect to the same problem, Kuranishi Masatsugu (41) viewing the problem in terms of the additional stresses in the direction of the axis and the circumference, computed the buckling stress, allowing that it is due to $E_c = d\sigma/d\varepsilon$ in the sections which protrude outwards and that it follows Young's Modulus in the concave sections. By doing this, he felt that an optimum approximation would be obtained. As a result, in general, the buckling stresses were shown to be proportional to E_k/E, and to approximate the test values closer than Geckeler's results. Moreover, he was able to explain the fact that in this type of buckling deformation, usually only half a wave protrudes, and practically no concavity occurs. In addition, in the case of this type of buckling deformation, when there is a progression of one convex deformation, the load decreases. However, when, due to deformation, the cylinder wall becomes bent, and this bending "piles up", the loads again increase and become contiguous to each other, the second buckle appears, rising to almost the same load as in the beginning, and then the same thing is repeated.

Apparently not very many calculations have been carried out for the case in which when the stress in the case of other types of buckling deformations in cylindrical shells rises above the proportional limit, the buckling stress drops. Moreover, generally, when there are problems concerning above the proportional

limit when treating the results of buckling tests, these problems must not be overlooked. Otherwise, accurate results will not be obtained. For example, the author considers that Sechler (42), fails in his treatment of the results of flat plates, because he does not take this problem into consideration.

This buckling stress has been calculated (43) for the case in which the elasticity law is non-linear, such as in cast iron, as a problem similar to that which occurs above the proportional limit. This is important, depending on the type of material involved.

1.2.7. MAXIMUM LOAD AFTER BUCKLING

/36

After buckling has occurred, or in the case of eccentricity or initial deflection, the question as to the degree to which a load can be resisted after the deformation has progressed, is an extremely interesting question with regard to structural members. When a bar sustains axial compression, a load which is above the buckling load described above, cannot be expected in ordinary materials with practical dimensions. Moreover, the maximum load will drop somewhat due to eccentricity or original deflection, but it drops greatly above the proportional limit, and can be regarded as hardly dropping at all below the proportional limit. In cases which can be regarded as ordinary center load, results are obtained as indicated in Figure 1.2.30 in the previous section.

It is expected that this is the same in the case of other types of buckling in a bar, so generally the buckling load value itself is used as the maximum load after buckling in a bar (of course, the zone of plasticity is also taken into consideration). However, what must be carefully noted in this case, is that in the event of a thin section, a buckling appears which is not intrinsic to that of bars, but to that of plates or shells. In bars, this is normally called either local buckling or wall buckling, and care must be exercised in this matter since there are times when errors will occur due to its not having been taken into consideration. Moreover, it is possible for torsional buckling in additional to ordinary flexural buckling to occur in columns sustaining axial compression. When the torsional buckling occurs under a low load, since it becomes markedly smaller than what is normally considered to be buckling strength, it requires attention (44). Since this may occur only in open thin sections, it requires special attention in the case of such sections.

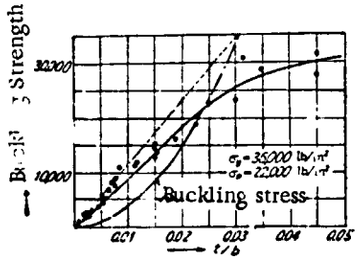

Figure 1.2.32

In the case of plates, computations for maximum load such as in bars, are not made. In the simplest case of rectangular plates sustaining a compressive load in one direction, judging from results of tests, what is indicated in Figure 1.2.32 occurs, this figure indicates the case of Duralumin (29) (45). When below the proportional limit, whereas the buckling stress is proportional to the square of t/b, the maximum average compressive strength, i.e., the buckling strength, is proportional to t/b. In other words, the maximum load is unrelated to b and results in being proportional

to t^2. This has been confirmed by experiments (85). Above the proportional limits, there is scarcely any difference between the buckling stress and the buckling strength, i.e., the maximum average compressive strength, and of course, is markedly lower than the buckling stress in the case when it is assumed that the elasticity modulus does not change (chain line in figure) (45).

In a rectangular plate sustaining a shear load, the ratio between the maximum load and the buckling load apparently is even higher than what is described above, but no clear results have been obtained in this regard. It has been investigated as the so-called theory of a semi-tensile field. In such a case of a plate, it becomes rather difficult to anticipate the maximum load with respect to various types of buckling.

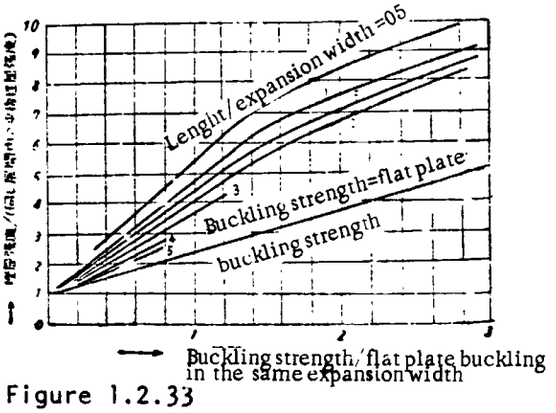

Figure 1.2.33

In the case of shell buckling, generally since this is treated as the theory of vaulting or jump transition, the buckling load should be regarded as the maximum load. Then, when a curved rectangular plate sustains a compressive load in the direction of the axis, due to bending in orthogonal directions, there are cases of increase and of decrease in load after buckling. Consequently, even if one attempts to adjust the test results, they appear as in Figure 1.2.33 (9). When b/r_0 is less than 0.1 ~ 0.2, the maximum load is larger than the buckling load, but when the curvature becomes greater than this, the buckling load and maximum load become almost equivalent, and appear to be as a load of the size of buckling load in a cylindrical shell. /37

There have been many attempts to calculate the maximum load for bars, plates and shells inclusively by following the hypothesis that in order to determine this maximum load, it should be treated as a load in which the maximum stress forms a load which is the yield point.

In the case of a bar, the maximum average compressive strength σ_m is determined by the following equation with the eccentricity e as in Southwell (46) or Smith's equation. Here, σ_y is the yield point stress, h_1 is the distance from the neutral axis to the most remote edge fiber.

$$\sigma_m=\sigma_y\Big/\left(1+\frac{eh_1}{i^2}\sec\left\{\sqrt{\frac{\sigma_y}{E}}\,\frac{L}{2i}\right\}\right) \qquad (1.2.101)$$

Moreover, assuming the so-called original deflection such as that in the equations of Perry or Robertson (46) as $c_1 \sin \pi x/L$, the fact that the maximum average compressive strength σ_m can be computed by the following equation shows that it belongs to this class.

$$\sigma_m=\frac{\sigma_y+(1+\eta)\sigma_x}{2}-\sqrt{\left\{\frac{\sigma_y+(1+\eta)\sigma_x}{2}\right\}^2-\sigma_y\sigma_x},\ \text{where}\ \eta=\frac{c_1 h_1}{b^2}. \tag{1.2.102}$$

In this manner, the values of e or c_1 are adjusted in order to agree with the test results. Moreover, the changes in modulus of elasticity are completely disregarded in this case even when above the proportional limit. Thereupon, it becomes possible to have a relatively good agreement with the test results. However, as explained above, this method is not theoretically correct.

The method which Karman attempted with respect to a rectangular plate with all sides rotating, sustaining a compressive load in one direction, is as follows. A plate width such that the compressive strength along the sides after buckling exactly becomes the buckling stress, is considered as the effective width (This is based on Karman's equation 1.2.21) given above for effective width. Of course, changes in the modulus of elasticity above the proportional limits are disregarded. When the stress along the sides becomes the yield point, the computations are carried out, assuming it to form the maximum load (29). Thereupon, we obtain

$$\sigma_m=\frac{\pi\sqrt{E\sigma_y}}{\sqrt{3(1-\nu^2)}}\frac{t}{b} \tag{1.2.103}$$

The results from this are indicated by the dotted line in Figure 1.2.32. They indicate a considerable difference from the solid line which is close to the test results. From the test results, as described above, in the case where $\sigma_m < \sigma P$, a form is obtained such that σp is used in place of σ_y in the above equation (45) and where $\sigma_m > \sigma_p$, there is a complete deviation from the straight line. Yamamoto Mineo and Kondo Kazuo have attempted to use the same approach of Karman's in order to determine the stress distribution (47). However, as can be seen by comparing with Figure 1.2.32, the results are the same as with Karman.

In any event, in both bars and shells, the changes in modulus of elasticity above the proportional limits are disregarded, and the assumption is made that when partial maximum stress becomes the yield point, this is the maximum load. /38
However, it is certain that such presuppositions are untrue, and can be allowed only in the event of results which are of good numerical approximation. Consequently, they should not be used in the case of a considerable numerical divergence. Attempts to make corrections for the fact that when the buckling stress has the conventional values, the latter are much higher than the test values, even in cylindrical shells sustaining a compressive load, following Donnell's computations in large deflection theory, are of the same nature (26). In this case, since not very satisfactory values are obtained in terms of results, it becomes necessary to eventually use an experimental equation.

1.2.8. BUCKLING IN REINFORCED MEMBERS AND COMBINED MEMBERS

The buckling load and buckling strength of bars, plates and shells, drops considerably when the length and breadth are large, so in order to prevent this, a reinforcing member (called a stiffener or anti-deflection member)is added, so that the member is divided into narrow sections and the buckling load is increased. Let us consider the effects of this.

In the case of bars, this means installing a supporting point between them, but when the rigidity of the support points is of a particular magnitude greater with respect to the deflection, the buckling load of the bar comes to have the same value as a bar in which the space between the support points is called the buckling length, i.e., the length between supporting points has a rotating end at both ends. (48). In this case, when the rigidity of the support points is smaller than this, the buckling length becomes greater than this, causing the buckling load to drop. Calculations have been made for such a case, in which the rotating rigidity of the support point is also taken into consideration. This is the same as the problems involved in combined members in which the bars between each span are connected by support points, and an elastic resistance is applied with respect to the deflection and rotation at the support point (S). For this reason, reinforced members in this sense can be handled as part of the problem involved with combined members.

When the number of support points is increased, a bar is obtained having elastic support of uniform distribution, then, when sustaining an axial compression, and a flexural buckling is generated, as in the case of deflection buckling of a flat plate, it turns out that the formation of several wave forms owing to the rigidity of the elastic support and the dimensions of the bar causes a minimum buckling load (49), (50). When there are many support points involved, this is frequently handled in terms of approximate values.

In the case of plates and shells, one can consider the installation of reinforced members, both longitudinally and laterally. For example, in the case of a rectangular flat plate with four rotating sides, with sustained compression in a longitudinal direction, it can be expected that it is more advantageous to install reinforced members longitudinally than laterally, considered in terms of the relationship between the aspect ratio (length and breadth ratio) and the buckling stress. In the case of a longitudinal reinforced member, it assumes part of the direct load, and is advantageous from this point of view. However, this in itself poses difficulties. When it comes to shells, the problems with such reinforcement are not simple and have not been treated in much detail. Problems of such reinforcement have been discussed only using approximation (51), or in the case of the closeness of reinforcing members in flat plates and shells, this is treated in terms of orthotropic plates and shells as described in the next section.

To the extent that in the above cases, the portions that are partitioned off by the reinforcing members are considered to be flat plates, when speaking about shells which have many reinforcing members, or plates themselves, even

after the buckling load, it is possible to increase the load as in the case of a flat plate. Ultimately, the effective width between the reinforcing member and the plate will become the same, forming a configuration which sustains an axial compressive load as a bar, and can be considered to resist until it is ruptured by the buckling.

When the attachment of the reinforcing member is a discontinuous coupling as in the case of rivets, the effect of the reinforcing member becomes small, and since there is no support between the rivets, the buckling load of the plate /39 decreases, and there are cases where buckling between rivets may occur. Moreover, depending upon the time, there are cases in which the effective width after buckling may rapidly decrease. Consequently, it is necessary to seriously reconsider what buckling will be crucial in this respect.

There are structures or members which can be considered as constructed from an assembly of simple bars, plates and shells, which are the basic members that we have been discussing up to the previous section. Structures having reinforcing members may be considered from this point of view, as combinations of plates or shells with bars. Constructions consisting of a combination of bars, include continuous beams, frame constructions and rigid joint constructions, etc. A combination of flat plates alone forms a structure such as Faltewerk (folded plate structure) or "plane wall".

These bar combinations can be classified as follows:

(1) Hinged frames. We assume that all joints are hinged. In such a case even when we consider that each member sustains only an axial force, and bending moment is not operating, when there is a load other than the deformation caused by the expansion of the member due to this axial force, it becomes possible for other types of buckling deformation to arise (4) (88). The simplest example of this is shown in Figure 1.2.34. At first, what had the shape indicated by the dotted lines, is transformed into the shape shown by the solid line, by buckling deformation. The conventional solution for buckling loads of such hinged frames, limits each member to being straight and to a pure central load, but, if, as a more practical approach to the problem, original deflection and eccentric loads are taken into consideration, this would mean that buckling would occur at a much lower load than the conventionally given buckling load, so caution must be exercised in such an approach.

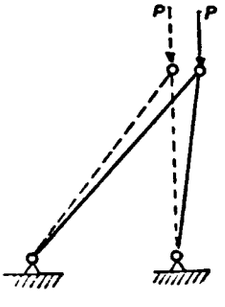

(2) Rigid joint frames. These are structures in which all joints are considered to be rigid. However, in this case, we can classify the problem into three types depending upon how we take into consideration the displacement of the joints and variation in member length.

(a) We assume that the joint is not displaced. Consequently, the length of the member, i.e., the distance between joints does not vary.

Figure 1.2.34

(b) Joint displacement is allowed, but variation in member length is disregarded.

(c) We take into consideration both the displacement of the joint and the variation in member length.

For example, when considering displacement in the direction of deflection of the support point in a continuous beam, normally we obtain (b). (See Figure 1.2.35). In addition, as a practical problem, the case shown in Figure 1.2.36 belongs to (b). However, considered in general, they all are examples of (c), but it is extremely rare when such a treatment is given, and conversely, in the overwhelming majority of cases, calculations for buckling loads of rigid joint frames are based on hypothesis (a) (86). However, as a result, since this is not always the safe thing to do, from a practical point of view, much more consideration must be given to the problem. For example, in the case of a construction such as that shown in Figure 1.2.37, the danger increases more. Ladder-type columns also belong under this classification so it is absolutely necessary to perform /40 calculations based on hypothesis (c).(4)(87). Even in other rigid joint structures, the influence of this load deformation is manifested (115).

Figure 1.2.35

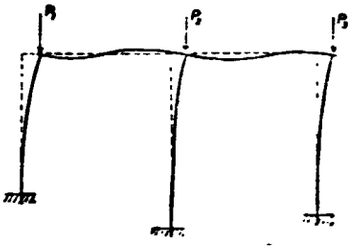

Figure 1.2.36

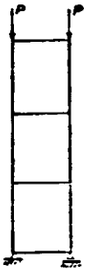

Figure 1.2.37

(3) Frames with elastic coupling. This is the case in which there is a plastic coupling, in which the coupling between the members at each joint is neither a hinge nor a rigid joint. A simple case of this is the case in which the variation in the angles of intersection between members is proportional to the moment transmitted (87). This can also be considered for the rotation and displacement of elastic support, of support points.

For the above cases, there is no particular problem with whether the structure itself is statically determinant or not. However, the methods of calculating statically indeterminant structures are all applied to the method for determining this buckling load. Moreover, in the case of the calculation of rigid joint structures, to determine a method for the treatment in the case when the stress becomes greater than the proportional limit, constitutes an important problem when determining actual strength through calculations, and for this reason two or three methods have been reported (89) (90) (See Section 1.4.15).

With regard to the case in which a folded plate structure made from a combination of flat plates sustains a compressive load in the direction of its folds, solutions have been made (45) for the case in which no consideration is

given to displacement of the corners constituting the folds, except for at their ends, assuming that the continuation in the lateral direction is similar to a rigid joint which transmits the moment without the angles of intersection changing. In those structures with appropriate dimensions, it is shown that even if they are open, their buckling load hardly drops at all, in comparison with a case of a closed cross-section configuration. It is quite difficult to perform calculations in the case of flat plates having reinforcing members, taking into account generally the displacements or the rotation of the corners. Moreover, when these coupling lines are rivets, buckling between rivets (116) corrugation buckling, etc. occur in addition to the influence from the rigidity.

The simplest and most widely-used combination of shells is the corrugated plate. The overall buckling in the corrugated plates has a property close to an orthotropic flat plate, however, one must pay heed to the fact that in the case where axial compression is sustained, the buckling becomes considerably smaller in comparison with [in proportion to] the buckling load of the number of closed cylinders. Considering this in terms of the curved plate of one part of a corrugated plate, since this takes the shape in which the conditions on the longitudinal side are such that the slope does not change, but the lateral force is 0, the buckling load drops. Such a fact must be taken into account carefully in the case of a structure consisting of the coupling together of curved plates. Below (Section 1.6.4), we shall discuss the specifics of such a case.

It should also be noted that buckling occurs due to internal pressure in items made from the coupling of two spherical sections (27) elliptical shells, and curved cylindrical tubes.

1.2.9. BUCKLING IN ANISOTROPIC BARS, PLATES AND SHELLS

There are cases in which the anisotropy of the material itself is treated, but actually, from a microscopic point of view, these are more frequently considered as homogeneously anisotropic. Lumber, plastics having fillers, reinforced concrete, steel cables, plates with reinforcing members, shells, and corrugated plates with a fine pitch pertain to these.

As for the property of anisotropy, there is not necessarily a match between the direction of the principle stresses and the direction of the principle strains. There are cases in which, since sheer strain, torsion, etc. occur due to compression and bending, buckling progresses, but no distinct point of bifurcation appears, i.e., as in the case of in original deflection. Moreover, adequate caution must be exercised since a rather unexpected type of buckling may occur causing flexural buckling due to the development of torsion due to tension. An example of the latter is kinks in electric wires and steel cables.

What is most often treated in the literature in the past concerning anisotropy is cases of longitudinal and lateral orthrotropy in plates and shells. In /41
such a case, if deflection buckling occurs due to compression or shear load, even if the longitudinal and lateral anisotropy are replaced, and even if there

is a difference in the corrugations that occur, they have the property that no differences in buckling load are caused, and for this reason show interesting results (91). When a shear load is applied to a rectangular flat plate, having diagonal anisotropy, two opposing directions can be conceived in the direction of the shear load, from the relationship with the strong direction in which there is anisotropy. By virtue of this there is a pronounced difference in the buckling load (9). However, it can be imagined from two or three tests that the maximum load does not differ very much due to this mutual opposition.

When a contour condition is given in an anisotropic body, attention is necessary, because depending on differences in contour conditions, e.g., (a) where the external force in the direction of the normal is 0 on the side of a rectangular flat plate sustaining compression in one direction and (b) where the displacement is 0, a considerable difference develops in the plane internal stresses, even before buckling occurs, and this will influence the buckling load.

1.2.10. BUCKLING IN THICK OR MASSIVE BODIES

What we have been treating up to now has been slender bars or thin plates or shells, or combinations of these, in which the dimensions in at least one direction are considerably smaller than the dimensions in the other directions. However, as we noted even in the Introduction, buckling does not occur only in such bodies, and there is the possibility of buckling occurring in semi-infinite bodies, infinite bodies with holes in them, massive bodies, thick bars, thick plates and shells.

Up to the present time, this type of buckling problem has scarcely been discussed. Here as an example of this, we shall consider in general buckling in the case of a flat plate sustaining a plane-internal load. Expressing the volume force as X_0, Y_0, and the stress within the body as σ_{xo}, σ_{yo}, τ_{xyo}, the following equilibrium equation is satisfied by infinitesimal deformation theory.

$$\partial\sigma_{xo}/\partial x+\partial\tau_{xyo}/\partial y+X_o=0 \qquad (1.2.104)$$

$$\partial\tau_{xyo}/\partial x+\partial\sigma_{yo}/\partial y+Y_o=0$$

We shall assume that the deformation which occurs in this case is infinitesimal and can be neglected. If we assume that it is possible for a new buckling displacement to occur, aside from this state of equilibrium, expressed by u_1, v_1, w_1, the buckling load is determined from the load in such an event, and buckling occurs. Assuming the stresses which are applied due to this additional displacement to be σ_{xI}, σ_{yI}, τ_{xyI}, if we determine the forces operating on the plane element dx dy in order to calculate the state of equilibrium, we obtain Figure 1.2.38. Assuming that X_0 and Y_0 are not related to the displacement, from the force in direction, x, y, z, the following equation is established, taking into consideration Equation (1.2.104), and ignoring the clearly infinitesimal quantity. Here Q_{xI}, Q_{yI} is the additional lateral shear force, and t is plate thickness.

$$\left.\begin{aligned}
&\frac{\partial}{\partial x}\left\{\sigma_{xI}+\tau_{xy0}\frac{\partial u_1}{\partial y}\right\}+\frac{\partial}{\partial y}\left\{\tau_{yxI}+\sigma_{y0}\frac{\partial u_1}{\partial y}\right\}=0\\
&\frac{\partial}{\partial x}\left\{\tau_{xyI}+\sigma_{x0}\frac{\partial v_1}{\partial x}\right\}+\frac{\partial}{\partial y}\left\{\sigma_{yI}+\tau_{yx0}\frac{\partial v_1}{\partial x}\right\}=0\\
&\frac{\partial}{\partial x}\left\{\sigma_{x0}t\frac{\partial w_1}{\partial x}+\tau_{xy0}\,t\,\frac{\partial w_1}{\partial y}+Q_{xI}\right\}+\frac{\partial}{\partial y}\left\{\tau_{yx0}t\frac{\partial w_1}{\partial x}+\sigma_{y0}t\frac{\partial w_1}{\partial y}+Q_{yI}\right\}=0
\end{aligned}\right\} \quad (1.2.105)$$

$$\left.\begin{aligned}
&\sigma_{xI}=\frac{E}{1-\nu^2}\left(\frac{\partial \xi_1}{\partial x}+\nu\frac{\partial \eta_1}{\partial x}\right), \qquad \sigma_{yI}=\frac{E}{1-\nu^2}\left(\frac{\partial \eta_1}{\partial y}+\nu\frac{\partial \xi_1}{\partial x}\right),\\
&\tau_{xyI}=\tau_{yxI}=\frac{E}{2(1+\nu)}\left(\frac{\partial \xi_1}{\partial y}+\frac{\partial \eta_1}{\partial x}\right)
\end{aligned}\right\} \quad (1.2.106)$$

/42

$$\xi_1=u_1-z\,\partial w_1/\partial x,, \qquad \eta_1=v_1-z\,\partial\, v_1/\partial y \quad (1.2.107)$$

$$Q_{xI}=\frac{\partial M_{xI}}{\partial x}+\frac{\partial M_{yxI}}{\partial y}, \qquad Q_{yI}=\frac{\partial M_{yI}}{\partial y}+\frac{\partial M_{xyI}}{\partial x} \quad (1.2.108)$$

Assuming

$$M_{xI}=\int_{-t/2}^{t/2}\sigma_{xI}z\,dz, \quad M_{yI}=\int_{-t/2}^{t/2}\sigma_{yI}z\,dz, \quad M_{xyI}=M_{yxI}=\int_{-t/2}^{t/2}\tau_{xyI}z\,dz \quad (1.2.109)$$

Equation (1.2.105) can be transformed as follows:

$$\left.\begin{aligned}
&\frac{E}{1-\nu^2}\left\{\frac{\partial^2 u_1}{\partial x^2}+\frac{1-\nu}{2}\frac{\partial^2 u_1}{\partial y^2}+\frac{1+\nu}{2}\frac{\partial^2 v_1}{\partial x\partial y}\right\}+\sigma_{y0}\frac{\partial^2 u_1}{\partial y^2}+\tau_{xy0}\frac{\partial^2 u_1}{\partial x\partial y}-Y_0\frac{\partial u_1}{\partial y}=0\\
&\frac{E}{1-\nu^2}\left\{\frac{\partial^2 v_1}{\partial y^2}+\frac{1-\nu}{2}\frac{\partial^2 v_1}{\partial x^2}+\frac{1+\nu}{2}\frac{\partial^2 u_1}{\partial x\partial y}\right\}+\sigma_{x0}\frac{\partial^2 v_1}{\partial x^2}+\tau_{yx0}\frac{\partial^2 v_1}{\partial x\partial y}-X_0\frac{\partial v_1}{\partial x}=0
\end{aligned}\right\} \quad (1.2.110)$$

$$\begin{aligned}
&-\frac{Et^2}{12(1-\nu^2)}\left\{\frac{\partial^4 w_1}{\partial x^4}+2\frac{\partial^4 w_1}{\partial x^2\partial y^2}+\frac{\partial^4 w_1}{\partial x^4}\right\}+\sigma_{x0}\frac{\partial^2 w_1}{\partial x^2}+2\tau_{xy0}\frac{\partial^2 w_1}{\partial y\partial x}\\
&\qquad+\sigma_{y0}\frac{\partial^2 w_1}{\partial y^2}-X_0\frac{\partial w_1}{\partial x}-Y_0\frac{\partial w_1}{\partial y}=0
\end{aligned} \quad (1.2.111)$$

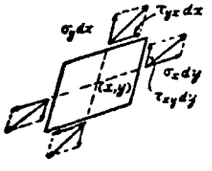

Figure 1.2.38

These equations are (1.2.110) for use of u_1, v_1 and (1.2.111) for w_1. For this reason, when the contour conditions are mutually irrelevant for u_1, v_1 and w_1, this solution can be obtained separately for u_1, v_1 and w_1. In this case, a solution of the form $w_1 = 0$, $u_1 \neq 0$, $v_1 \neq 0$, and $w_1 \neq 0$, $u_1 = 0$, $v_1 = 0$, is obtained. However, the case is also possible where $w_1 \neq 0$, $u_1 \neq 0$, $v_1 \neq 0$. That which considers only the section in equation (1.2.111) matches the normal equation for

the buckling of a flat plate. The problem here is a solution of the form $w_1 = 0$, $u_1 \neq 0$, $v_1 \neq 0$.

Since $E \gg \sigma_{xo}$, σ_{yo}, τ_{xyo}, the term with E in the above equation becomes large, but since in equation (1.2.111) the element Et^2/a^2 of the first term, with a as plate width is of the same size as $\sigma_{xo} \cdot \sigma_{yo}$, τ_{xyo}, it becomes very easy for this ordinary buckling problem to occur, meaning that wave-shaped irregularities are formed. However, in equation (1.2.110) since we consider that only the first term is much larger than the others, if the other terms are disregarded, buckling cannot occur. However, if that which is enclosed in parenthesis in the first term is very small, this becomes a quantity comparable with the third term. Such a case constitutes the present problem. Kappus merely touches on this problem in his paper (15).

We can consider as contour conditions $\sigma_I = 0$, $\tau_I = 0$ or $u_1 = 0$, $v_1 = 0$. Moreover, we wish to determine the eigen values of σ_{xo}, σ_{yo}, τ_{xyo} from the above equations. However, this is quite difficult from equations in such a form. However, this type of problem is considered necessary in actual practice, so a solution for it should be obtained. Moreover, the above form corresponds to plane stress, and a similar equation can be found for the state of plane strain. Hayashi Shigeru has indicated that it is possible to determine the buckling values in such cases as lumber, especially where the value of G is small, since even in the equation of the form of equation (1.2.110), the first term is of the same size as the other terms (52). /43

Moreover, there is considerable doubt as to whether in such problems, the initial deformation may be disregarded.

1 2.11. NATURAL STRESS AND BUCKLING

Occasionally, natural stresses (also called original stress, initial stress, thermal stress, etc.) are present within a body, which are not due to external forces, but are due to various factors, for example, to conditions at the time of forging, casting, or other processing, assembly or joining, due to shrinkage and swelling caused by heat and moisture, or due to partially undergoing plastic deformation.

In such a case, what is first considered is whether buckling arises in the body due to natural stress. For example, part of a cast object may be broken due to buckling. Moreover, there are cases in which a flat plate undergoes what is called "strain" meaning that from the beginning it has irregularities in it which cause buckling due to compressive stress, even if there is no bending moment present as an intrinsic natural stress. It is possible for a flat plate to undergo buckling in the case of even a slight rise in temperature, if it is rigid, so that the contour displacement is 0.

Next, the case can be considered in which differences in the buckling stresses arise due to the presence of natural stress. For example, when there exists a natural stress from compression from the beginning, this causes a decrease in the buckling stress. Even in the case of buckling between rivets,

it can be expected that this refers to the natural stress at the time of riveting. By conversely taking advantage of the influence of this natural stress, it is possible to increase the buckling load if first a natural tension stress is imparted. Hayashi Shigeru has calculated the tensioning applied to a saw used for lumber (53). In this, a natural tension stress is first imparted, in order to prevent buckling due to heat stress when sawing.

1.2.12. REPEATED LOAD AND BUCKLING

When a member has a very small degree of original deflection, or an eccentric load is operating on it, if it sustains a stress greater than the proportional limit locally, owing to a large degree of deformation, even if a buckling load is not attained, it is natural that the residual deflection which remains after the load has been removed to be greater than the original deflection. Consequently, when such a load is repeated many times, the original deflection, i.e., the residual deflection from the immediately preceding load gradually increases, and as a result, the maximum load which can be withstood gradually is reduced, rupture is caused, or local cracks develop, making the member unsuitable for use.

In the case of a bar, where there is little residual strain, the number of repetitions required for rupture to occur owing to the flexural buckling strength under a compressive load is quite large, and under the normally existing frequency of such repetition, it does not have to be taken into consideration. However, when the original deflection is rather large, or the load is high, the safe repetition frequency drops considerably so it is necessary to be treated as a problem.

In the case of a plate, the original deflection can be compared to the plate thickness, and since it is rather large, it is very easy for the above phenomena to occur. This is called permanent buckling and is generally treated as a problem in the case of a rectangular plate sustaining a compressive load in one direction (40). Moreover, this is undesirable in the outer plating of aircraft, so research on methods to prevent it is being conducted, and actually /44
is a problem which is considered very seriously. Figures 1.2.39 and 1.2.40 indicate the degree of magnitude of permanent buckling from examples of tests (40). Figure 1.2.39 shows the relationship between the edge member stress and the deflection (2 times the amplitude) with the maximum load edge member stress σ_a as a parameter in a case where the load has dropped after loading to a particular load (the value σ_a indicated in the figure for the edge member stress). Figure 1.2.40 indicates the result of expressing the relationship between the load (expressed by the maximum edge member stress σ_a) and the permanent buckling in the case where the value of the load when reading only the permanent buckling in such a case, is not only 0, but is measured using a load of a particular magnitude (σ_0) with σ_0 as a parameter. In this test, there is no repeated load, but judging from the increase in original deflection, when a load of greater than a particular degree has been applied, it can be predicted that the increase in deflection will become marked owing to repeated loads.

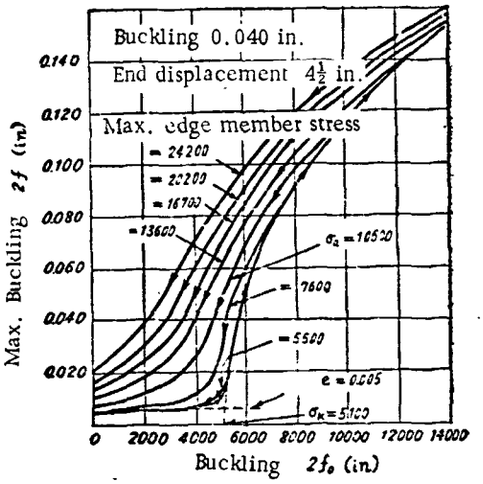

Figure 1.2.39

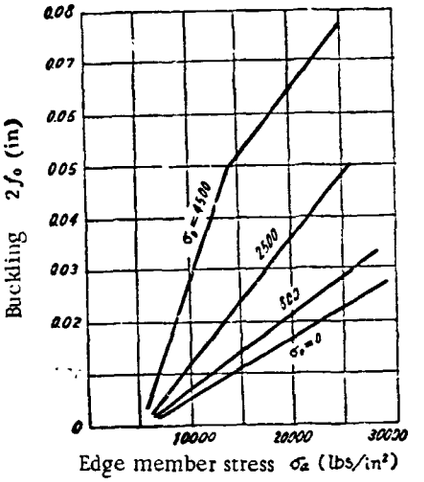

Figure 1.2.40

What must be noted in the case of an increase in the deflection of such a flat plate is, as shown by the examples in Figure 1.2.41, where the growing wave forms are a sine curve of close to 2 cycles, that the deformation C, which is a combination of the two sine waves, A, B, progresses, and consequently the large original deflection gradually increases at the end section.

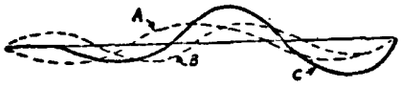

Figure 1.2.41

It was possible to ascertain from the above, that rupture is induced by repeating the load which accompanies buckling. As for rupture due to static load, it is possible to consider that whereas shear strength or separation strength constitute the limit with respect to tensile load, whereas buckling determines the strength with respect to compression load, and whereas, in the event of a repeated load, in tensile loads, etc., fatigue determines the strength, in compressive loads, buckling in the broad sense of the term becomes the standard for strength. Considered in this manner, rupture due to ordinary static loads is an extremely interesting problem.

1.2.13 DYNAMIC LOADS AND BUCKLING

Although it is certain that buckling phenomena also occur in the case of the application of a load dynamically, no success has yet been achieved in theoretically treating pure buckling. When a dynamic load is applied to a bar, /45 plate or shell, we proceed from an equation which assumes an original deflection of a constant degree. Expressing this original deflection by v_0, in the case of a bar, we proceed from

$$EI\frac{\partial^4 v}{\partial x^4}+P\frac{\partial^2 v}{\partial x^2}+\rho F\frac{\partial^2 v}{\partial t^2}+P\frac{\partial^2 v_0}{\partial x^2}=0 \tag{1.2.112}$$

This is also true for the case of a plate. Now, expanding the sum for the configuration (eigen function) of buckling deformation which satisfies profile conditions, where the original deflection v_0 is given. we obtain

$$v_0=c_1 v_{01}+c_2 v_{02}+\cdots \tag{1.2.113}$$

and we compute the deflection by P(t) for each term. Some people consider the case in which P is a constant value (54)(55), or handle this as a case in which $P = P_1 t$ or P is a triangle with respect to time, or varies according to a sine curve (56)(57)(58). Here the maximum value of v becomes the problem. When $P_0 < P_{k1}$, when a certain length of time is maintained, a value is reached which is equal to twice that of a static load. Vibration occurs when the load is removed, but this can also be calculated. When $P_0 > P_{k1}$, the deflection can increase to any degree along with time. Then, according to the loading rate, buckling deformation progresses corresponding to a high buckling load, which is not P_{k1} but above P_{k2}. With regard to this point, such deformation is rejected as unstable in the case of a static load, but in the case of a dynamic load, since it becomes the most marked phenomenon, depending upon conditions, it must be taken into consideration. In addition, an investigation has been carried out on the case where the load is eccentric (59). Moreover, research has been conducted on variations in the cycle of the lateral vibration of a bar, when it sustains a static axial load (60).

As for other types of problems, the case in which a particular mass collides with the end of a bar at the particular velocity has been treated. When the mass is extremely large, the end of the bar is displaced at a constant velocity. In such a case, according to experimental investigation (?17), it turns out that an axial force three times greater than the static buckling value occurs. When the slenderness ratio is small, and the region of plasticity is entered, since the plastic deformation is retarded due to the effect of the load velocity, it has been observed that the buckling load also increases. When the mass is finite, various cases arise depending upon the magnitude and velocity magnitude. This problem of collision is extremely difficult. Depending upon conditions, there are cases in which the colliding mass swings back several times (61). In the case of a bar moving and striking a firm wall, frequently a wave form remains due to plastic deformation (56).

Stability problems have also been dealt with, for the case in which a load is applied by vibration. That case in which consideration is given to variation in the vibration due to the axial load in the case of a vibrating bar has also been investigated. Even if, in this case, the load has a considerably higher value than the buckling load, if the time is short, this indicates that there is no great danger present (56). Moreover, when a static axial load is applied to a vibrating bar, the buckling load drops, owing to the vibration (62).

Aside from this, cases in which changes in the operating exte.nal forces occur accompanying displacement deformation may cause self-excited vibration, and for this reason are accompanied by unstable phenomena. For example, the collapse of the Takoma Bridge is an exemplification of this problem (63)(64).

1.2.14. PROBLEMS WITH RESPECT TO TIME, AND BUCKLING.

There are cases in which the deformation of materials changes depending upon time or their history. These include plastic deformation described in a previous section, changes in yield point due to load velocity, problems with creep, the Bauschinger effect and hysteresis. Moreover, the relationship of these to buckling has also been investigated to some extent. For example, it becomes possible to determine increase in buckling deformation due to creep, if we assume this to be a property of creep (65). /46

CHAPTER 3

ELASTIC STABILITY PROBLEMS OTHER THAN BUCKLING

As was mentioned in the introduction, it is possible for phenomena other than buckling to be involved in elastic stability problems. The most widely treated of these are "jump transition" and yield. In addition, there is Karman's jump transition theory which was introduced in order to explain the buckling of shells (32). We shall describe this briefly.

1.3.1. YIELD

This problem was first treated in Brazier's computations for the case in which a straight thin cylinder sustains a bending load (66). Generally, when something having the shape of a bent tube (part of a Torus) sustains bending, as Karman has shown in his investigation (67), from the time when the load is infinitesimally small, it is not possible to employ the infinitesimal deformation theory. Moreover, since this forms a flexural rigidity which is $(1 + 12\lambda^2)/(10 + 12\lambda^2)$ times that in the infinitesimal deformation theory (where $\lambda = Rt/a^2$, t is skin thickness, a is tube radius, R is bending radius), the smaller the bending radius R becomes, the greater is the reduction in the flexural rigidity. Beginning from Brazier's work on a straight tube, if we determine the relationship between the curvature 1/R in this case and the bending moment M, we obtain what is shown in Figure 1.3.1 in which there is one maximum value in the curve. The maximum bending moment, i.e., the yield bending moment M_k is calculated as follows:

$$M_k = \frac{2\sqrt{2}}{9} \frac{E\pi at^2}{\sqrt{1-\nu^2}} \tag{1.3.1}$$

The deformation of the cross-section of the tube in this case shows a deformation in the direction of the circumference in $v = 1/9 \cdot a \cos \theta$, and a displacement in the radius of $w = 2/9 \cdot a \sin 2\theta$, in the circular section a deformation is indicated in the form of a pseudo elipse in which the radius has increased and decreased only 2/9.

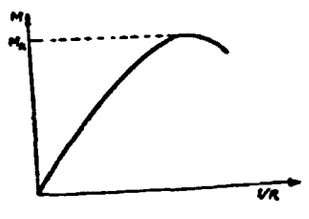

Figure 1.3.1

Heck (68) similarly computes the case of a bent tube with an elliptical cross-section. In this case, in the event of bending around the short axis, the radius of curvature of the wall is smaller than the neutral axis. At the most distant fiber, conversely there are cases in which a more dangerous section may occur on the inside wall surface than in the most remote fiber.

The calculations of Brazier and Heck above determine values for yield, but in each case, the results of tests, except in special cases, show that ordinary buckling, in which waves can occur on the wall surface, occurs prior to this yield load. That is, in tests, it does not go as far as this yield load. Since the buckling theoretical values according to classical theory are too high, the above yield load is lower than the buckling theory value and closer to the test values. However, I personally feel that it is necessary to consider that buckling actually does occur as a phenomenon. That is, if it is possible to correctly calculate the buckling load, it will be much lower than the yield load above. However, of course one should take into account the fact that the stress distribution inside the section varies somewhat from the influence of such as has been described above. /47

Even in square tubes and other thin sectioned objects, when a bending load is sustained, since the flexural rigidity decreases with an increase in the bending curvature, this phenomenon can be considered.

Ikeda Tsuyoshi has calculated and tested (69) the fact that even when a thin-skinned tube in the form of a square or equilateral triangle sustains torsion, this yield phenomenon also occurs.

Moreover, the maximum load in the case of flexural buckling due to the axial compressive load of a straight bar, described in the previous chapter, has a maximum value for the deflection load curve when the load is above the proportional limit, and even when it is below that limit. Since from that point there is no position of equilibrium, clearly this is a case of yield load. That is, the buckling strength of a column can be said to be the yield load.

1.3.2. JUMP TRANSITION

This occurs when, owing to progressive deformation, the equilibrium load becomes a maximum and a minimum, and when the load is variously changed, rapidly a great change in deformation occurs where this maximum or minimum value is present, and the state of equilibrium changes rapidly. We shall call the case of a maximum value the "ascending jump transition load" and the case of a minimum value, the "descending jump transition load". The problems occur only in a case of a rise or drop in the load, and in the case of a change in load, in the opposite direction, there is no problem.

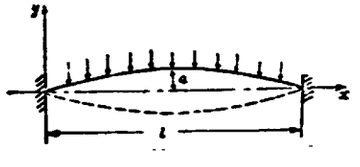

Figure 1.3.2

A famous example of this is shown in Figure 1.3.2, in which a girder with a small curvature sustains a lateral load of uniform distribution from its convex side (1). The relationship between the deflection in the center (a_1) and the load q is as shown in Figure 1.3.3. Using as an example the curve where m = 1/2 during ascension, the jump transition occurs from point A to B and then during descension, it occurs from point D to E. Moreover, as the form of the center line of the girder becomes $a_1/a \leq 0$, the convex curve occurs either above or below. Therefore, when

A→B, D→E, this relationship rapidly reverses.

$$u=\frac{5}{384}\frac{ql^4}{EI}\frac{1}{a},\qquad m=\frac{4I}{Fa^2} \tag{1.3.2}$$

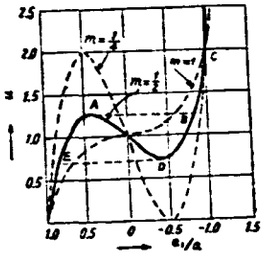

Figure 1.3.3.

Since the value of u in the case of an ascending or descending jump-transition load is

$$u=1\pm\sqrt{\frac{2}{27}\cdot\frac{(1-m)}{m^2}} \tag{1.3.3}$$

When m < 1/4, the descending jump-transition load is negative, and when the load drops, even if q = 0, the curve remains in the lower, convex form. Therefore, if q is not made less than 0, there is no jump to the upper convexity.

This type of jump phenomenon also occurs in other cases. For example, it is clearly observed when an external force is caused to operate uniformly on a circle inwards or upwards, (22) or when a circular plate or spherical shell with a uniform small curvature, sustains an external force. Also, when a cylindrical shell sustains an axial compressive load, and when diamond-shaped irregularities develop, the fact that this jump transition is considered to have occurred, is as explained above. /48

1.3.3. VAULTING THEORY

Karman advances to explain the fact that the test values for buckling due to axial compression in a cylindrical shell, or external pressure on a spherical shell, are much smaller than the theoretical values. The name "vaulting theory" is not Karman's term, but was invented by the present author for convenience. This refers to the fact that, for example, if we assume the relationship between the maximum concavity ε due to the external pressure p of a spherical shell, and the compressive stress σ due to external pressure, to be expressed as in Figure 1.3.4 (92). While A is the buckling load, before this value is reached, it passes from point C through B and then jumps to E, E_1 or E_2 When the load does not change, it changes horizontally, changes vertically when the contraction does not change, and changes diagonally in the case when there is a constant relationship between the load and contraction, and shifts in the direction of E, E_1, or E_2. When the magnitude Π of the overall potential energy in the case when the change follows this route CDE, is described with respect to contraction ε, we should obtain that which is shown in Figure 1.3.5. That is, at points C, E, there is a stable equilibrium whereas at point D, there is an unstable state of equilibrium.

In order to go beyond point D, a supply of energy from outside is necessary. It is assumed that this energy is supplied by vibration during the test. The difference in height between this C and D becomes somewhat smaller due to imperfection in the test sample, that is, the original deflection, eccentricity of

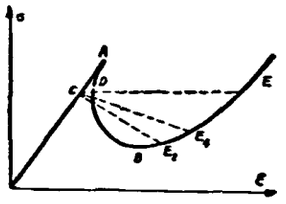

Figure 1.3.4

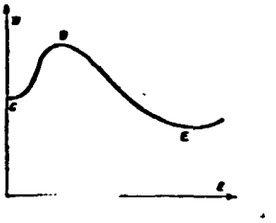

Figure 1.3.5

load, and non-homogeneity of the properties the material, and it is considered that it is easy for this vaulting to be caused. Consequently, one should consider that there is sufficient possibility for this phenomenon to take place.

Karman has given a rather reasonable explanation of vaulting itself, but what needs to be further discussed is what is the treatment occurring after this. He calls the load at the minimum point B in the curve in Figure 1.3.4, the lower buckling value and considers that this is the value that is recorded as the buckling load in the case of the tests. Moreover, this value agrees well with the test values in Karman's computation results. This was derived because occasionally the results agree, but is theoretically an unlogical approach. This point was already discussed at the end of Section 1.2.3 in detail. That is, this type of problem, if it were possible to perform correct calculations should be considered in such a form that there is an agreement between the buckling load and the ascending jump-transition load when there is a value which agrees with the test values. However, since vaulting theory itself can exist, we can say that in this regard, Karman's approach is interesting.

1.3.4. COMBINATION OF VARIOUS TYPES OF PROBLEMS IN ELASTIC STABILITY

It is not necessarily the case that the various types of problems in elastic stability that have been described above will occur singly, without relation to anything else. Sometimes two or more phenomena will occur simultaneously, or another phenomenon will become applied while one of these phenomena /49
is taking place, or there may be a transition to a new phenomenon.

For example, in such cases as when an elliptical tube sustains a bending load, deformation may increase due to the yield phenomenon, but before a maximum load is reached, buckling may occur, causing rupture. According to Heckt's computations (68) for such a case, the relationship between the second configuration and the limit of elastic stability is as shown in Figure 1.3.6. This figure notes the value of C with respect to the cross-section's eccentricity, $k^2 = (a^2 - b^2)/a^2$ where a, b are long and short radii

$$\sigma_k = C \cdot \frac{E}{1-\nu^2} \cdot \frac{1}{\rho}$$

writing the bending stress at the limit of stability as σ_k, (purely theoretical) and the radii of curvature of the long and short axes and of the cross-section ellipse as ρ_k, ρ_g, the indices g, k, indicate the values around the long and short axes. In this event, buckling may occur during the bending around the short axis, and the relationship between the deformation (bending curvature 1/R) and the load (bending moment M) is as shown in Figure 1.3.7. The yield load is point A, buckling occurs before it at point B, and the deformation proceeds following the curve BC.

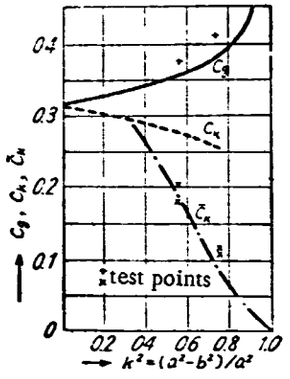

Figure 1.3.6

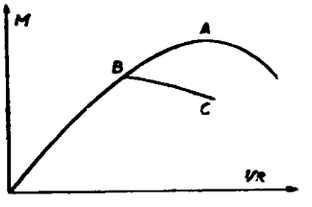

Figure 1.3.7

Cases have also been investigated in which, in the case of an elliptical tube sustaining axial compression, the buckling occurs first where the initial curvature is small. Then the load increases, and finally buckling occurs where the curvature is great (70).

In the case of Torus with a broad width, as shown in Figure 1.3.8, the relationship between the center load P in the outer direction and the deformation indicated by the rotation Ψ of the cross-section is calculated as shown in Figure 1.3.9 (22). At first, the shape is one in which the radius merely increases, but where at point A there is a load P_k, this is a buckling load which changes to a deformation with a rotation Ψ, and at the same time is a load causing jump transition to position B which is the position of reversal where $\Psi = 180°$. Moreover, when the load is caused to drop from this state, at first the radius merely contracts, but when rotation is begun at point C, at the same time, it jumps to point D. In this manner, the two points A, C are simultaneous, the buckling load and the jump-transition loads. Moreover, when the load in this case is slightly eccentric, it merely forms the jump-transition shown in Figure 1.3.10. If it becomes possible to correctly handle theoretically the buckling of a cylindrical shell sustaining an axial compression, it would probably also belong to this pattern. /50

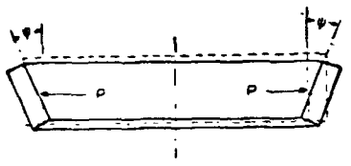

Figure 1.3.8

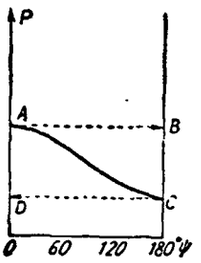

Figure 1.3.9

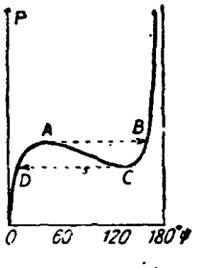

Figure 1.3.10

CHAPTER 4

DETERMINATION BY CALCULATION OF CRITICAL BUCKLING VALUES

Determination of buckling load, as already described in Section 1.2.2, is a problem of determining eigen values. In such a case, when this is a simple member, the eigen values are determined by a differential equation, or what is the same thing is determined by various other methods. In the case of a frame structure which is a combination of bars, the main problem is to find a solution of determinants of coefficients of a simultaneous equation of the same order from the beginning. In addition there are various other methods devised to do the same thing.

When it comes to problems after buckling, problems in yield, jump transition and vaulting, since there are many cases in which equations are used which are not linear, and which to some degree introduce finite deformation theory, it is difficult to describe their method of solution in general terms. Moreover, since there are various differences in the degree to which finite deformation theory is applied, depending upon the researcher and the object of investigation, we feel that it would be appropriate to touch on each of these individually, and for this reason will not deal with them at the moment. However, methods for calculating the buckling strength of a bar do have something in common with our presentation, so they are added at the end of this discussion.

The description of numerical computation methods for the eigen values in Sections 1.4.2 to 1.4.14 below is obtained primarily from the collection made by Collatz (71). In the methods for determining buckling loads in combined members consisting of bars, such as continuous columns, trusses and frames (Rahman's), we will only describe relatively new special methods.

Generally it first becomes possible to determine elastic stability and eigen values only after specifying the type of buckling deformation involved. Consequently, in the case when it is possible for an unspecified type of buckling deformation to be present at a low load, the results of initial calculations of it can have no meaning at all in actual practice. It is necessary to keep this point constantly in mind. For example, this would involve such things as the torsional buckling in the case of an axial compressive load on a bar.

The results presented below, up to Section 1.4.14 determine the buckling load in the case where it is below the proportional limits. That is, in the case of a bar, this merely amounts to calculating Euler's buckling load in a column. For sections where this is above the proportional limit, it is necessary either to use an elastic coefficient in place of E, or to make an approximation using an average value, taking this into consideration. Since this is quite difficult, it has not yet been adequately explained to this date.

1.4.1. METHOD OF ANALYSIS

This method involves finding a general solution which deals directly with the differential equations in Section 1.2.2, treats the eigen values as constants, and includes indeterminant coefficients. By including this in homogeneous end conditions, a primary homogeneous simultaneous equation is obtained for the indeterminant coefficients. As a condition for obtaining a solution where all of these indeterminant coefficients do not simultaneously become 0, we assume the coefficient determinant (S) to be 0. This is solved as an equation with eigen values treated as constants. The eigen values are determined, and then the eigen functions, i.e., the form of deformation, is determined from the solution of the differential equation (S) at that time. This method has been used for several different cases

1.4.2. COMPARISON METHOD /51

We shall consider a column as an example. When the cross-section of a column changes, the buckling load is necessarily larger than the buckling load of a column made with the weakest cross-section and should be smaller than the buckling load in a column constructed with the strongest cross-section. Moreover, when the compressive load differs due to the position of the cross-sections, the buckling load should be smaller than the value in the case when the compressive load is considered to be uniformly equal to its maximum value. Described in terms of an equation, this is as follows:

Differential equation for buckling of column. When

$$EI\frac{\partial^2 v}{\partial x^2}+Pv=0 \tag{1.4.1}$$

assuming P to be constant, the change in the axial force is assumed to be included in EI. Then, at all points x, when the relationship

$$EI_u \leqq EI \leqq EI_0 \tag{1.4.2}$$

obtains, and writing the eigen values from

$$EI_u\frac{\partial^2 v}{\partial x^2}+Pv=0, \qquad EI_0\frac{\partial^2 v}{\partial x^2}+Pv=0 \tag{1.4.3}$$

as P_{ku}, P_{ko}, respectively, when they have been determined, the eigen value P_k in equation (1.4.1) becomes

$$P_{ku} \leqq P_k \leqq P_{ko} \tag{1.4.4}$$

the method of comparison utilizes this. In particular, when using a constant value for EI_u, EI_0, since P_{ko}, P_{ku} are immediately understood, this is especially useful. Now let us consider this in slightly more general terms.

In the case of elastic stability, the following type of differential equation frequently appears:

$$\frac{d^2}{dx^2}\left(k_2(x)\frac{d^2y}{dx^2}\right)+\frac{d}{dx}\left(k_1(x)\frac{dy}{dx}\right)+k_0(x)y-\lambda p(x)y=0 \qquad (1.4.5)$$

Here $k_2(x)$, $k_1(x)$, $k_0(x)$, $p(x)$ are functions only of x, and are determined in accordance with the problems. The value of λ for obtaining a solution for y, where identically it is not 0, is the eigen value, and the solution for y in this case is an eigen function. In order of magnitude, we shall assign subscripts to λ, e.g., λ_1, λ_2..., and we shall write Equation (1.4.5) in more generalized form, as follows:

$$L[\varphi]+\lambda p\varphi=0 \qquad (1.4.6)$$

L[ ] indicates the differential operator. When what is compared with this is

$$L^*[\varphi]+\lambda p^*\varphi=0$$

We assume that the eigen value λ_n^* for this differential equation is understood. Then, for an arbitrary function ψ which satisfies the contour conditions, when

$$\int \varphi\, L^*[\varphi]dx \geq \int \varphi\, L[\varphi]dx \qquad (1.4.7)$$

$$\int p^*\varphi^2\,dx \leqq \int p\,\varphi^2\,dx \qquad (1.4.8)$$

obtain (these integrations indicate those carried out for the entire region of x. When not specifically mentioned below, the integration has this meaning), the eigen value λ_n in equation (1.4.6) forms the relationship /52

$$\lambda_n^* \geq \lambda_n \qquad (1.4.9)$$

As an example, we shall take the case of where we assume the contour condition to be the rotating end $f(0) = f(1) = f''(0) = f''(1) = 0$ with

$$[rf'']''+\lambda pf=0 \qquad (1.4.10)$$

corresponding to a non-uniform section and non-uniform compressive force.

Then, assuming the upper and lower limits of r and p to be r_0, r_u; p_0, p_u, i.e.,

$$0<r_u \leqq r \leqq r_0, \qquad 0<p_u \leqq p \leqq p_0$$

the differential equation that should be compared is that for a uniform cross-section and uniform compressive load.

$$[r_u f'']'' + \lambda p_0 f = 0, \qquad [r_0 f'']'' + \lambda p_u f = 0$$

and since it is understood that these eigen values are

$$\lambda_n^* = (n^4\pi^4/l^4)(r_u/p_0), \qquad \lambda_n^* = (n^4\pi^4/l^4)(r_0/p_u)$$

assuming $f_n^* = \sin n\pi x/1$ with

$$\frac{n^4\pi^4}{l^4}\frac{r_u}{p_0} \leqq \lambda_n \leqq \frac{n^4\pi^4}{l^4}\frac{r_0}{p_u}$$

the upper and lower limits of the nth eigen value λ_n corresponding to equation (1.4.10) is determined.

In the case of plates, in addition to this method, when an already known problem is attained by varying the domain, etc., it is possible to make a comparison by expanding this approach. Table 1.4.1 gives examples of this, and in the end of Section 1.4.4, an interesting application of the method is given.

1.4.3. SUCCESSIVE APPROXIMATIONS, RAYLEIGH'S EQUATIONS

This is the method for determining λ_1 in the case where, as a more generalized form of Equation (1.4.6) above, the differential operator M [ ] is introduced in place of p,

$$L[\varphi] + \lambda M[\varphi] = 0 \tag{1.4.11}$$

i.e., a method for determining the lowest eigen value. If special efforts are made, it is possible to find second order and higher eigen values. We shall begin by determining the lowest eigen values and eigen functions.

We shall begin from a completely arbitrarily selected function $F_0(x)$. That is, for F_0 only, it is not necessary to satisfy the boundary conditions. Then by solving an equation of the form

$$L[F_n] + M[F_{n-1}] = 0 \tag{1.4.12}$$

for the functions $f_1(x)$, $F_2(x)$,...$F_n(x)$, we continue with successively n = 1, 2.... In this case, it is necessary for F_1, F_2...F_n to satisfy the boundary conditions. then, assuming the nth approximate value of λ_1 to be $\Lambda_1^{(n)}$

$$\Lambda_1^{(n)} = \frac{\int F_n M[F_{n-1}]\,dx}{\int F_n M[F_n]\,dx} = \frac{-\int F_n L[F_n]\,dx}{\int F_n M[F_n]\,dx} \tag{1.4.13}$$ /53

Then it can be proved that すると $\Lambda_1^{(1)} \geq \Lambda_1^{(2)} \geq \cdots \geq \Lambda_1^{(n-1)} \geq \Lambda_1^{(n)} \geq \lambda_1$ In this manner, the upper limit of λ_1 is found and we proceed extracting λ_1. In this case

taking the point $x = x_m$ where F_n has a maximum value in place of the above integral, there are cases in which it is also possible to obtain a good approximation with

$$\lambda_1^{*(m)}=\left(\frac{M[F_{n-1}]}{M[F_n]}\right)_{x_m}=\left(\frac{-L[F_n]}{M[F_n]}\right)_{x_m} \tag{1.4.14}$$

Moreover, the F_n obtained in this manner is an approximation equation for the eigen function.

When in the form of Equation (1.4.6), M [F] = pF and when p is a continuous positive function, this becomes a problem. In this case, beginning from F0, we determine F_1, F_2, ... F_n from

$$L[F_n]+pF_{n-1}=0 \tag{1.4.15}$$

then, from

$$\mu_{2n}=\frac{\int pF_nF_{n-1}dx}{\int pF_n^2dx} \tag{1.4.16}$$

the approximation value of λ_1 is determined in the same way as in the case of Equation (1.4.13). Equation (1.4.16) is none other than that which is called normally Rayleigh's equation. However, in this case, it is calculated immediately from an arbitrary function, F_1 which satisfies the boundary condition and not as a successive approximation. That is, we shall write this as follows.

$$\mu_2=R(F_1)=\frac{-\int F_1L[F_1]dx}{\int pF_1^2dx}=\frac{\int pF_1F_0dx}{\int pF_1^2dx} \tag{1.4.17}$$

Moreover, in Equation (1.4.16) even numbered indices are used μ_2, ..., and those with odd numbered indices are assumed to be determined as follows.

$$\mu_1(F_1)=\frac{\int(L[F_1])^2/p\cdot dx}{-\int F_1L[F_1]dx}=\frac{\int pF_0^2dx}{\int pF_0F_1dx} \tag{1.4.18}$$

Whereupon we obtain $\mu_1\geq\mu_2\geq\mu_3\geq\cdots\geq\mu_{2n}\geq\lambda_1$

The upper limit of λ_1 can be understood from the above, but normally the following equation is used to determine its lower limits.

$$\lambda_1\geq\mu_{n+1}-\frac{\mu_n-\mu_{n+1}}{-1} \tag{1.4.19}$$

This l_2 is sufficient as a rough approximation to the lower limit of the secondary eigen value λ_2 but at least it should be $l_2 > \mu_{n+1}$. In order to obtain this rough approximation, l_2, it is convenient to use the results of the comparison methods in the previous section. For example, in the case of the problem $f'' + \lambda(1 + x) f = 0$, $f(0) = f(1) = 0$, since $1 \leq 1 + x \leq 2$, the eigen value in this problem should be between $f'' + \lambda f = 0$ and $f'' + 2\lambda f = 0$. Therefore this is $1/2\ n^2\pi^2 \leq \lambda_n \leq n^2\pi^2$. From these results, the rough approximations are as shown in the following table. /54

TABLE 1.4.1

Eigen value	Lower Limit	Upper Limit
λ_1	4.93 (−25 %)	9.87 (51 %)
λ_2	19.73 (−25 %)	39.48 (49 %)
λ_3	44.41 (−26 %)	88.83 (49 %)

The figures in parentheses in the table indicate the difference in percent from the true values. As can be seen by this, the approximation is too rough when attempting to determine approximate values by the comparison method, but the l_2 in the computations of Equation (1.4.20) above is satisfactory with such a value.

Now to give an example of the calculation of the approximate eigen values for this problem. First we introduce Rayleigh's equation. When we select for F_1 in Equation (1.4.17), the following form, the approximate values will be as shown in the right column and the percent of error is indicated in parentheses.

TABLE 1.4.2

F_1	R
$\sin \pi x$	$\frac{2}{3}\pi^2 = 6.5797$ (0.5 %)
$x - x^2$	$20/3 = 6.667$ (1.8 %)
$x - x^{0.8}$	6.617 (1.0 %)
$7x - 10x^2 + 3x^3$	6.5506 (0.03 %)

Now we shall try one step of a successive approximation. First, making $F_0 = 1$ randomly, since we obtain $F_1 = x(1 - x)(1 + x)/6$, from Equations (1.4.17), (1.4.18)

$$\mu_1 = \frac{3}{2} + \frac{17}{90} = \frac{135}{17} = 7.94 \quad (20\,\%)$$

$$\mu_2 = \frac{17}{90} + \frac{44}{1440} = \frac{272}{41} = 6.635 \quad (1.4\,\%)$$

From the above examples, when $l_2 = 19.73$ is used, the lower limit is determined and since

$$\lambda_1 \geq 6.635 - \frac{7.94 - 6.635}{19.73 + 6.635 - 1} = 5.975 \quad (-9\%)$$

we obtain $6.635 \geq \lambda_1 \geq 5.975$.

In order to obtain a slightly more satisfactory form, making $F_0 = x - x^2$ for F_0, since $F_1 = (7x - 10x^2 + 3x^3)/60$, since from Equations (1.4.17), (1.4.18) and (1.4.19) /55

$$\mu_1 = -\frac{1}{20} + \frac{4}{525} = \frac{105}{16} = 6.5625 \quad (0.2\%)$$

$$\mu_2 = \frac{4}{525} + \frac{3869}{3,326,400} = 6.55053 \quad (0.03\%)$$

$$6.55053 - \frac{6.5625 - 6.55053}{19.373 + 6.55053 - 1} = 6.5441 \quad (-0.06\%)$$

This becomes $6.5441 \leq \lambda_1 \leq 6.55053$, which is a sufficient value for engineering problems. When an accuracy better than this is desired F_2 should be determined proceeding from F_1.

It is not absolutely necessary to determine that F_1 is produced from $F_n - 1$ according to Equation (1.4.12) from the solution of a differential equation following normal methods, and sometimes it can be done by graphic solution, or by Mohr's method, or even Green's function or Cauchy's function, may be used.

Let us describe briefly how to determine Green's function G(x, s). We assume that the given differential equation is of the following shape

$$L[y] = p_0(x)\frac{d^n y}{dx^n} + p_1(x)\frac{d^{n-1}y}{dx^{n-1}} + \cdots + p_n(x)y = 0 \qquad (1.4.20)$$

As conditions on Green's function G(x,s)

(1) except when x = s,, L[G(x, s)] = 0

(2) where x = s, the differential coefficients for G(x, s) and up to the (n - 2) th order due to its x are finite and continuous.

(3) the differential coefficient for the (n - 1) order due to x is x = s, is discontinuous and where $x \to s$, it is

$$\left|\frac{d^{n-1}}{dx^{n-1}}G(x, s)\right|_{(x>s)} - \left|\frac{d^{n-1}}{dx^{n-1}}G(x, s)\right|_{(x<s)} \to \frac{1}{p_0(s)}$$

When the above G(x, s) is determined, the determination of F_n by Equation (1.4.2) becomes as follows, with x within the range of 0 and 1.

$$F_n(x)=\int_0^1 p(s)\cdot F_{n-1}(s)\cdot G(x,s)\,ds \tag{1.4.21}$$

When Green's function has been determined, when finding the lower limit of the first order eigen value, if we compute

$$\Gamma=\int_0^1\int_0^1 p(x)\cdot p(s)\cdot G^2(x,s)\,dx\,ds$$

since

$$\Gamma=\lambda_1^{-2}+\lambda_2^{-2}+\cdots>\lambda_1^{-2}+\lambda_2^{-2} \tag{1.4.22}$$

when we determine μ_{n+1} where $\mu_{n+1} > \lambda_1$

$$\Gamma>\mu_{n+1}^{-2}+\lambda_2^{-2} \tag{1.4.23}$$

Therefore, assuming /56

$$\frac{\lambda_2^2}{\mu_{n+1}^2}>\frac{1}{\mu_{n+1}^2\Gamma-1}\equiv J_n^2 \tag{1.4.24}$$

it is possible to calculate with

$$\mu_{n+1}-\lambda_1<\frac{\mu_n-\mu_{n+1}}{J_n-1} \tag{1.4.25}$$

For example, employing a beam supported at both ends as an example for determining G(x, s), EI d^4y/dx^4 = w(x), but considering only the left side, where $x < s - 1/2\varepsilon$, $x > s + 1/2\varepsilon$ since EI $d^4y/dx^4 = 0$, we allow respectively $y_1 = a_1 + b_1x + c_1x^2 + d_1x^3$, $y_2 = a_2 + b_2x + c_2x^2 + d_2x^3$ then, from condition (2) where $x = s$, $y_2 = y_1$, $dy_2/dx = dy_1/dx$, $d^2y_2/dx^2 = d^2y_1/dx^2$, in condition (3) EI d^3y_2/dx^3 = EI $d^3y_1/dx^3 + 1$, in addition as a terminal condition, introducing $y = 0$, $d^2y/dx^2 = 0$, where $x = 0$ and $x = 1$, the above constants, a_1, b_1, .. c_2, d_2 should be determined. Then, the deflection due to the distributed load which is w(x) and the concentrated load W(x) comes to be given by

$$y=\int_0^1 w(s)\cdot G(x,s)\,ds+W(s)\cdot G(x,s)$$

There are cases in which Cauchy's functions are more convenient than Green's functions. When Cauchy's function H(s, x) is used, the equation for determining F_n by successive approximation is

$$F_n(x)=\Phi(x)+\int_0^x H(s,x)\cdot p(s)\cdot F_{n-1}(s)\,ds \tag{1.4.26}$$

This $\Phi(x)$ is a general solution for L[y] = 0 and the constant was determined so that it met the terminal conditions.

Cauchy's function H(s, x) was determined by the following conditions with respect to Equation (1.4.20).

(1) L[H(s, x)] = 0

(2) where x = s, the differential coefficient for H(s, x) and up to the (n - 2) th order due to its x are 0.

(3) The differential coefficient $d^{n-1}H/dx^{n-1}$ of the (n - 1) order, due to x satisfies the following equation where x = s.

$$\frac{d^{n-1}H}{dx^{n-1}}=-\frac{1}{p_0(s)} \tag{1.4.27}$$

As an example, we linearly vary the flexural rigidity. Taking the case in which a uniformly distributed longitudinal load operates on a column with one end fixed and the other end free, we have the problem of determining the eigen value in

$$\frac{d}{dx}\left(x\frac{dv}{dx}\right)+\lambda xv=0$$

Therefore, $L[x] = xd^2v/dx^2 + dv/dx$, and the general solution is v = A log x + B. Therefore, both H(s, x) and $\Phi(x)$ are of this form. From condition (2), H(s, s) = 0, i.e., A log s + B = 0. From condition (3) where x = s, dH(s, x)/dx = -1/s, /57 therefore, A/s = -1/s, consequently A = -1, B = log s so H(s, x) = log s - log x, and ultimately the equation for the successive approximation in this case is

$$F_n(x)=A_n\log x+B_n+\int_0^x(\log s-\log x)\cdot s\cdot F_{n-1}(s)\,ds$$

As terminal conditions, where x = 1, v = 0, where x = 0, dv/dx = 0, and assuming $F_0(x) = 1$, $F_1(x)=A_1\log x+B_1+\int_0^x(\log s-\log x)\cdot s\cdot ds=A_1\log x+B_1-x^2/4$, , where x = 1, from $F_1(x) = 0$, $B_1 = 1/4$, where x = 0, $F_1'(x) = 0$ and $A_1/x - x/2 = 0$, $A_1 = 0$, consequently $F_1(x) = 1/4,(1 - x^2)$.

Similarly $F_2(x)=A_2\log x+B_2+\int_0^x\frac{1}{4}(\log s-\log x)\cdot s\cdot(1-s^2)ds=A_2\log x+B_2-x^2/16+x^4/64$, where x = 1, since $F_2(x) = 0$, $B_2 = 3/64$, where x = 0, since $F_2'(x) = 0$, since $A_2/x - x/8 + x^3/16 = 0$, $A_2 = 0$, consequently we obtain $F_2=3/64-x^2/16+x^4/16+x^4/64=(3-4x^2+x^4)/64$

Continuing this, we obtain

$$F_3=(19-27x^2+9x^4-x^6)/(4\cdot16\cdot36),\quad F_4=(211-304x^2+108x^4-16x^6+x^8)/(4\cdot16\cdot36\cdot64)$$

As an example of a graphic solution, the differential equation and the terminal conditions, are as follows.

$$EI\,d^2y/dx^2+\lambda py=0,\qquad x=0,\quad x=l\quad \text{で}\quad y=0$$

First, assuming $y = F_0$, we describe the curve pF_0/EI. The integration of this $F_1'' + F_0 \cdot p/EI = 0$, is carried out by graphic methods. This means to determine what is called in ordinary graphic dynamics as the bending moment when there is a distributed load F_0p/EI. We describe F_1p/EI from this F_1 integrated, and repeat the determination of F_2. Then, the following values are computed.

$$a_0=\int_0^l \frac{pF_0^2}{EI}dx,\qquad a_1=\int_0^l \frac{pF_0F_1}{EI}dx,\qquad a_2=\int_0^l \frac{pF_1^2}{EI}dx$$

The calculation of this integration may be carried out either graphically or by Simpson's method. We assume that the results are, for example

$$a_0=18.57\,l/EI_0,\quad a_1=1.615\,l^3/(EI_0)^2,\quad a_2=0.1407\,l^5/(EI_0)^3\ ,$$

Then

$$\mu_1=a_0/a_1=11.50\,EI_0/l^2,\quad \mu_2=a_1/a_2=11.48\,EI_0/l^2$$

Now with the rough lower limit of λ_2 as 1_2, computing from $EI_0y'' + \lambda y = 0$, assuming $1_2 = 4\pi^2EI_0/1^2$, since $\mu^2 - \lambda_1 \leq 0.01\ EI_0/1^2$, $11.47\ EI_0/1 \leq \lambda_1 \leq 11.48\ EI_0/1^2$, becomes the approximation solution.

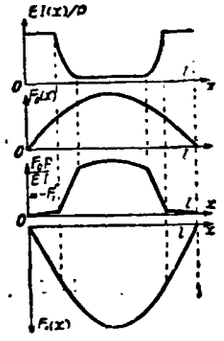

Figure 1.4.1

Next let us consider the determination of the second and third order eigen values. In this case, it is necessary to proceed from the case where the initially assumed function F_0 does not contain the constituents of first or other low order eigen functions from the beginning. For this reason, it is necessary to exclude the constituent first order eigen functions from the hypothesized F_0. For this reason if we assume that the first order normalized eigen function is ϕ_1, utilizing the orthogalness of the eigen function, it is necessary /58 to use as the function of the first approximation

$$F_0-\varphi_1(x)\int_0^l pF_0\cdot\varphi_1(x)\,dx \qquad (1.4.28)$$

since this is an approximation equation, this means that the first order eigen function component is not excluded, and each time that F_1, F_2 ... is determined, it is necessary to insure that by this procedure the first order eigen function component is excluded. Then, by means of this purification, in the approximation

equation the orthogalness with the first order eigen function is constantly guaranteed. By this method, if the eigen values are determined by the same method as the case of the first order eigen values described above, one approaches the true value (72).

1.4.4. ENERGY METHOD, RITZ'S METHOD, RITZ-TIMOSHENKO METHOD

It is considered that what is called the Ritz's method (34) was developed in the following manner. For example, under the boundary condition where there is a differential equation with the $L[\psi] + \lambda M[\psi] = 0$ of Equation (1.4.10). This forms Euler's equation for the problem of variation expressed by:

$$I(\varphi)=\int\left\{D[\varphi]+\lambda H[\varphi]\right\}dx=\text{Extreme value} \tag{1.4.29}$$

Assuming that F is the solution of (1.4.29), by the comparative function $\psi = f + \varepsilon\eta$ considering as far as the square of ε this becomes

$$\Delta I(\varphi)=I(f+\varepsilon\eta)-I(f)=\varepsilon\int\eta\left\{L[f]+\lambda M[f]\right\}dx+\underbrace{\text{boundary condition term}}+\varepsilon^2[\quad]+\cdots \tag{1.4.30}$$

This η should satisfy the boundary conditions which only assumes the "boundary condition" term to be 0. Then, when f is the solution of the differential equation, the ε terms become 0, and extreme values are obtained.

In the case of problems in elastic dynamics, the problem of extreme values in Equation (1.4.29) that coincides with the problem which is expressed by the theorem of hypothetical displacement indicating a minimum potential energy, or the theorem of a minimum strain work.

For example, when the original differential equation is the following self-following type equation which is the same as Equation (1.4.5),

$$L[f]+\lambda pf=(k_2f'')''+(k_1f')'-k_0f+\lambda pf=0 \tag{1.4.31}$$

The form of equation (1.4.28) becomes as follows

$$I(\varphi)=\int_{x_1}^{x}\left\{k_2(f'')^2+k_1(f')^2-(-k_0+\lambda p)f^2\right\}dx=\underbrace{\text{extreme value}}_{\text{extreme values}} \tag{1.4.32}$$

That which η should satisfy as a contour condition is

$$\left[k_2f''\eta'-(k_2f'')'\eta+k_1f'\eta\right]_{x_0}^{x_1}=0 \tag{.4.33}$$

Then, the comparison function $\phi = f + \varepsilon\eta$ satisfies only the same boundary conditions as ε. In Ritz's method, the comparison function ϕ is determined in such a manner that $I(\phi)$ approaches extreme values as much as possible, and normally the equation expressed below is used. /59

$$\varphi = \sum_{\nu=1}^{m} c_\nu \psi_\nu(x) \tag{1.4.34}$$

It is assumed that ψ_ν satisfies the following conditions:

(1) It satisfies the necessary conditions for η above.

(2) The integrals $\int D[\psi_\nu]dx$, $\int H[\psi_\nu]dx$ within the limits of possibility, can be differentiated. For example, if D is a first order differentiation, is continuous, and at least it can be spatially differentiated.

(3) They are mutually linearly dependent.

Now, considering $I\left[\sum_{\nu=1}^{m} c_\nu \psi_\nu\right]$ as functions of the variable c_ν, we determine the extreme values in this case. Consequently,

$$\partial I\left[\sum_{\nu=1}^{m} c_\nu \psi_\nu\right] \Big/ \partial c_\rho = 0, \quad (\rho = 1, 2, \cdots m) \tag{1.4.35}$$

In this case, since $I[\psi]$ is of the second order for ψ, Equation (1.4.35) becomes linear for c_ν and takes the form

$$\sum_{\nu=1}^{m} (a_{\rho\nu} - \Lambda b_{\rho\nu})\, c_\nu = 0, \quad (\rho = 1, 2, \cdots m) \tag{1.4.36}$$

Then, in order for all c_ν not to be 0, since the determinant must be 0,

$$\Delta_m(\Lambda) = \begin{vmatrix} a_{11} - \Lambda b_{11}, & a_{12} - \Lambda b_{12}, & \cdots, & a_{1m} - \Lambda b_{1m} \\ a_{21} - \Lambda b_{21}, & a_{22} - \Lambda b_{22}, & \cdots, & a_{2m} - \Lambda b_{2m} \\ & \cdots\cdots & & \\ & \cdots\cdots & & \\ a_{m1} - \Lambda b_{m1}, & a_{m2} - \Lambda b_{m2}, & \cdots, & a_{mm} - \Lambda b_{mm} \end{vmatrix} = 0 \tag{1.4.37}$$

and this is the case where $a_{\nu\rho} = a_{\rho\nu}$ and $b_{\nu\rho} = b_{\rho\nu}$. If this matrix equation is solved considering the equation for Λ, if its roots are arranged in order of magnitude, approximate values can be obtained for the eigen values where

$$L_1^{(m)} \leqq L_2^{(m)} \leqq L_3^{(m)} \leqq \cdots \leqq L_m^{(m)}$$

Then returning to Equation (1.4.36), the ratio between each of the c_ν corresponding to each eigen value is determined, and the approximate eigen functions are determined. We shall give an example of this for the latter part of section 1.4.6.

Determination of eigen values by the above equations (1.4.35) or (1.4.36) is called the energy method. Moreover, those methods which depend on the system expressed by Equations (1.4.44) and (1.4.45) described below are called the Ritz-Timoshenko Method and Timoshenko has used this method extensively in determining the buckling loads of bars and plates (1). By doing this he is simply determining values which are relatively close to a strict solution.

Now let us cite examples in the case of column problems using the Ritz-Timoshenko Method. We consider the case in which both the cross-section and the load vary. We assume that an external force at one end P is operating, /60
and that intermediately a force p which varies continuously is in operation. Then, the axial force S(x) in a cross-section x is

$$S(x)=P+\int_0^x p(x)dx=P+P_x, \qquad \int_0^l p(x)dx=P_0 \tag{1.4.38}$$

and it is possible to express $P = \nu P_0$. Considering a slightly bent condition deviating from a straight condition, the strain energy V is

$$V=\frac{1}{2}\int_0^l EI(x)\left(\frac{d^2v}{dx^2}\right)^2 dx \tag{1.4.39}$$

assuming that $1/\rho = d^2v/dx^2$. Loss in potential energy is caused due to the fact that the point of application of the external force drops. Assuming this to be T

$$T=\frac{1}{2}\int_0^l S(x)\left(\frac{dv}{dx}\right)^2 dx \tag{1.4.40}$$

Therefore, the overall potential energy Π is

$$\Pi=V-T=\int_0^l EI(x)\left(\frac{d^2v}{dx^2}\right)^2 dx-\int_0^l S(x)\left(\frac{dv}{dx}\right)^2 dx \tag{1.4.41}$$

However, this energy takes into account infinitesimal displacement from a state of straight contraction, so assuming that this is in a state of equilibrium, V - T = 0.

$$\int_0^l EI(x)\,(d^2v/dx^2)^2 dx-\int_0^l S(x)\,(dv/dx)^2 dx=0 \tag{1.4.42}$$

Introducing a correct value for this v, and determining the minimum value of P_0, the buckling load is determined. However, this v(x) is unknown. Assuming

$$v=c_1\varphi_1(x)+c_2\varphi_2(x)+\cdots \tag{1.4.43}$$

The $\psi(x)$ satisfy the terminal conditions for each, and approach the expected deformation. When they are mutually linear and independent, and are an infinite progression, they are determined in such a way that they converge. c_1, c_2 ... are unknown progressions, but we assume V - T = 0 and make our selection such that P_0 becomes minimum. Since v(x) is an approximate equation, actually V - T > 0 and an excessively large value is obtained for P_0.

$$V=V(c_1, c_2, \cdots), \quad T=P_0\cdot T'(c_1, c_2, \cdots)$$

The results of using the above function (1.4.43) are as follows, considering $S(x) = P_0 \cdot S(x)/P_0$.

$$P_0=V(c_1, c_2, \cdots)/T'(c_1, c_2, \cdots)$$

From this, by V - T = 0, when the minimum values are determined

$$\partial P_0/\partial c_\nu=0, \quad (\nu=1, 2, \cdots) \tag{1.4.44}$$

or,

$$\frac{\partial V}{\partial c_\nu}T'-\frac{\partial T'}{\partial c_\nu}V=0, \quad (\nu=1, 2, \cdots) \tag{1.4.45}$$

Consequently, n first order simultaneous equations of the same order are obtained with respect to end values of c. Then, assuming $c_\nu/c_1 = a_\nu$, (n - 1), first order simultaneous equations are obtained with respect to (n - 1) a_ν. This should be solved, a_ν determined and P_k calculated. /61

Below we give two examples of this method.

(1) In the case of a dead weight and terminal load with one end fixed and the other end free, using x = 0 as the fixed point, with the weight per unit length g, we obtain $S(x) = P + g(l - x)$. We assume the following shape for v

$$v=c(\cos\pi x/2l+a\cos 3\pi x/2l)$$

This does not satisfy the terminal conditions but since it differs only by a constant from that which satisfies these conditions, it is irrelevant in later calculations. Then, calculating V, T

$$V=c^2EI(1+81a^2)\pi^4/64l^3$$

Where, assuming $P/gl = \gamma$

$$P=\frac{\pi^2}{8}\frac{EI}{l^2}\frac{1+81a^2}{0.5+4.5a^2+(0.1487+0.6079a+2.1487a^2)/\gamma}$$

When solving for a, making this P minimum, $dP/da = 0$, $a^2 + (0.4019 + 1.4621\gamma)a - 0.01235 = 0$, therefore, assuming $g = 0$, $\gamma = \infty$, $a = 0$, and this agrees with Euler's equation. When $P = 0$, $\gamma = 0$, $a = 0.0287$, $(gl)_k = 7.84\ EI/l^2$ is obtained, which agrees with the known case. When $P = gl$, $\gamma = 1$, $a = 0.0066$, $P_k = (gl)_k = 1.90\ EI/l^2$.

(2) In the case of dead weight and terminal load, with both ends rotating, for one end assuming $x = 0$, $S(x)$ is the same as in the above example. We assume the following shape for V so that we satisfy $v = 0$, $v'' = 0$, when $x = 0$, $x = l$.

$$v=c(\sin\pi x/l+a\sin 2\pi x/l)$$

Computing from this, V, T

$$V=c^2EI(1+16a^2)\pi^4/4l^3$$

$$T=c^2P(1+4a^2)\pi^2/4l+c^2g(1+1.8012a+4a^2)\pi^2/8$$

Since $V = T$, with $P = \gamma \cdot gl$

$$P=\frac{\pi^2EI}{l^2}\frac{1+16a^2}{1+4a^2+(0.5+0.9006a+2a^2)/\gamma}$$

where $dP/da = 0$, $a^2 + (0.8327 + 1.6655\gamma)a - 0.0625 = 0$. When $g = 0$, when $\gamma = \infty$, and $a = 0$, this becomes Euler's equation. When $P = 0$, $\gamma = 0$, $a = 0.0093$, $(gl)_k = 1.88\ \pi^2EI/l^2 = 18.56\ EI/l^2$. When $P = gl$, $\gamma = 1$, $a = 0.02477$, and $P_k = 6.95\ EI/l^2$.

Moreover, when adopting this method, since there are cases when it is easy to determine the lower limit using the comparison method in Section 1.4.2, let us explain directly an example of this application.

We shall use an example in which a column of uniform cross-section with both ends rotating sustains a specific axial load. Assuming the form of the deformation to be $v = c(l^3x - 2lx^3 + x^4)$, /62

$$T=P/2\cdot\int_0^l(dv/dx)^2dx=Pc^2l^7\cdot 17/70,\quad V=EI/2\cdot\int_0^l(d^2v/dx^2)^2dx=EIc^2l^5\cdot 12/5.$$

Therefore, $P_k < 168/17\cdot EI/l^2 = 9.8823\ EI/l^2$. However, when there is a non-uniform cross-section from one side, since $EI(x)d^2v/dx^2 + Pv = 0$, if

$$I(x)\propto -v/d^2v/dx^2\propto l^2+lx-x^2$$

the above hypothesized deformation occurs. The rightmost maximum value in this case is $5l^2/4$ where $x = 1/2$. Therefore, assuming that this value is equivalent to I when it is uniform, since the column with the non-uniform cross-section, according to the above equation is a weaker one than this uniform column given

any cross-section, it has a smaller buckling value than the uniform column. Therefore, assuming

$$I(x)=4I_0(l^2+lx-x^2)/5l^2, \qquad v=c(l^3x-2lx^3+x^4)$$

Inserting this into the equilibrium differential equation

$$(48EI_0/5l^2-P)v=0, \qquad \text{Therefore} \quad P=\frac{48}{5}\cdot EI_0/l^2=9.6EI_0/l^2$$

Since this uniformly is necessarily smaller than anything with a cross-section I_0

$$9.6EI/l^2<P_L<9.8825EI/l^2$$

It is possible to determine the accuracy of this by comparing it wit. the strict solution. $\pi^2EI/l^2=9.8696EI/l^2$

1.4.5. GALERKIN'S METHOD

The starting point is the same as in the Ritz method, but the solution f rather than φ is expressed approximately as follows.

$$f(x)\approx\Psi(x)=\sum_{\nu=1}^{m}c_\nu\Psi_\nu(x) \tag{1.4.46}$$

The comparison function is selected from within the range expressed by Equation (1.4.46). Also, the function η is also determined from within this range. Next, an attempt is made to bring the right side of Equation (1.4.46) as close as possible to the solution f(x). That is, assuming $\varphi = f + \varepsilon\eta$, an attempt is made to have the first order term of ε 0. Then, Ψ_1, Ψ_2, ... Ψ_n are used alternately with η. Then, in place of Ritz's equation, it takes Galerkin's form (73).

$$\int\Psi_\rho\left\{L\left[\sum_{\nu=1}^{m}c_\nu\Psi_\nu\right]+\lambda M\left[\sum_{\nu=1}^{m}c_\nu\Psi_\nu\right]\right\}dx=0 \tag{1.4.47}$$

As for the term for the boundary conditions, now Ψ_ν must satisfy only the boundary conditions which are the same as f. That is, both

$$f=\sum_{\nu=1}^{m}c_\nu\Psi_\nu$$

must satisfy the boundary conditions. Otherwise, there will be an additional term in Equation (1.4.47). Consequently, the conditions which Ψ_ν must satisfy are as follows.

(1) All boundary conditions must be satisfied.

(2) Integration is possible only to the extent that $L(\Psi_\nu)$ and $M(\Psi_\nu)$ are formed. For example, when L [ ] is of the second order, it is necessary for

Ψ_ν to at least have a continuous first order and spatially continuous second order differential.

(3) They must be linearly independent.

When this is compared with Ritz's method, Equation (1.4.47) is more convenient practically than Equation (1.4.35) in the previous section. However, as for the conditions which are added to Ψ_ν, conditions (1) and (2) in this section are more important. In such a case, conditions (1), (2) in previous section are satisfactory, but given conditions (1),(2) in this section, they are unsatisfactory. For example, where $f'' + \lambda f = 0$, when $f(-1) = f(1) = 0$, assuming $\Psi_1 = 1 - |x|$, $\Psi_2 = (1 - |x|)x$, the conditions in the previous section are satisfied, but since the conditions in this section are not satisfied, Equation (1.4.47) cannot be used. If we make the following abbreviations, /63

$$a_{\rho\nu} = -\int \Psi_\rho L[\Psi_\nu]dx, \qquad b_{\rho\nu} = \int \Psi_\rho M[\Psi_\nu]dx \tag{1.4.48}$$

Galerkin's equation becomes as follows

$$\sum_{\nu=1}^{m} (a_{\rho\nu} - \lambda b_{\rho\nu}) c_\nu = 0, \qquad \rho = 1, 2, \cdots, m \tag{1.4.49}$$

From this, we write the root of λ in the equation in which the coefficient determinant of magnitude $L_1^{(m)}$, $L_2^{(m)}$, ..., $L_m^{(m)}$. Then, $L_1^{(1)}$ agrees with Rayleigh's values.

$$L_1^{(1)} = \frac{a_{11}}{b_{11}} = \frac{-\int \Psi_1 L[\Psi_1]dx}{\int \Psi_1 M[\Psi_1]dx} = R(\Psi) \tag{1.4.50}$$

1.4.6. GRAMMEL'S METHOD

The eigen value λ_1 in the successive approximation method in Section 1.4.3 has the following method, proceeding from Equations (1.4.17), (1.4.18) in that section.

$$\lambda_1 = \operatorname{Min} \mu_1(w) = \operatorname{Min} \frac{\int \frac{1}{p}\left(L[w]\right)^2 dx}{-\int w L[w]dx} \tag{1.4.51}$$

$$\lambda_1 = \operatorname{Min} \mu_2(w) = \operatorname{Min} \frac{-\int w L[w]dx}{\int p w^2 dx} \tag{1.4.52}$$

In this case, we employ Equation (1.4.52), and assuming that w has the form in the Equation (1.4.46), if we determine the conditions where for c_1, c_2, ... c_m,

we have a minimum value of $\mu_2(w)$, this forms Galerkin's method. In opposition tc this, employing Equation (1.4.51), assuming

$$w=\sum_{\nu=1}^{m} c_\nu \Psi_\nu(x) \tag{1.4.53}$$

We assume that Ψ_ν satisfies conditions (1), (2), (3) in Section 1.4.5 and for $c_1, c_2, \ldots c_m$, if we determine the condition where $\mu_1(w)$ is minimum, we obtain Grammel's equation, described in this section. Now, writing the denominators of Equation (1.4.51) as N, Z, if we minimize μ_1

$$\frac{\partial \mu_1(w)}{\partial c_\rho}=\frac{\partial \mu_1\left[\sum_{\nu=1}^{m} c_\nu \Psi_\nu\right]}{\partial c_\rho}=\frac{\partial (Z/N)}{\partial c_\rho}=\frac{\partial Z/\partial c_\rho-(Z/N)\cdot(\partial N/\partial c_\rho)}{N} \qquad \underline{/64}$$

$$=\frac{\partial Z/\partial c_\rho-\lambda\partial N/\partial c_\rho}{N}=0$$

Therefore

$$\frac{\partial}{\partial c_\rho}\int\left\{\frac{1}{p}\left(L\left[\sum_{\nu=1}^{m} c_\nu \Psi_\nu\right]\right)^2+\lambda\left(\sum_{\nu=1}^{m} c_\nu \Psi_\nu\right)\left(L\left[\sum_{\nu=1}^{m} c_\nu \Psi_\nu\right]\right)\right\}dx=0$$

$$\int\left[\frac{2}{p}L[\Psi_\rho]L\left(\sum_{\nu=1}^{m} c_\nu \Psi_\nu\right)+\lambda\left\{\Psi_\rho L\left[\sum_{\nu=1}^{m} c_\nu \Psi_\nu\right]+L[\Psi_\rho]\sum_{\nu=1}^{m} c_\nu \Psi_\nu\right\}\right]dx=0$$

Since the two terms inside the parentheses in the second term are equivalent

$$\int L[\Psi_\rho]\left\{\frac{1}{p}L\left[\sum_{\nu=1}^{m} c_\nu \Psi_\nu\right]+\lambda\sum_{\nu=1}^{m} c_\nu \Psi_\nu\right\}dx=0 \tag{1.4.54}$$

or

$$\sum_{\nu=1}^{m} c_\nu\int\frac{1}{p}L[\Psi_\rho]\left\{L[\Psi_\nu]+\lambda p\Psi_\nu\right\}dx=0, \tag{1.4.55}$$

$$\rho=1, 2, \cdots, m$$

This is similar to Galerkin's approach, but in place of Galerkin's Ψ_ρ it has a form in which $L(\Psi_\rho)/p$ is used.

Actually, the method used by Grammel to form an equation (93) begins from an appropriately selected function $\eta\nu(x)$ and from the relation

$$-L[\Psi_\nu]=p\eta_\nu \tag{1.4.56}$$

by integration, Ψ_ν should be determined. Moreover, when Green's function is understood, the calculation should proceed from

$$\Psi_\nu(x)=\int G(x,s)\cdot p(s)\cdot \eta_\nu(s)\,ds \tag{1.4.57}$$

Then, it is not necessary for η_ν to satisfy the boundary conditions. Then, Equation (1.4.55) becomes

$$\sum_{\nu=1}^{m} c_\nu \int p(x)\eta_\rho(x)\left\{\eta_\nu(x)-\lambda\int G(x,s)p(s)\eta_\nu(s)\,ds\right\}dx, \tag{1.4.58}$$

$$\rho=1, 2, \cdots, m$$

Taking only the first term of this, it becomes

$$\lambda=\frac{\int\frac{1}{p}\left(L[\Psi_1]\right)^2 dx}{-\int\Psi_1 L[\Psi_1]dx}=\mu_1(\Psi_1) \tag{1.4.59}$$

and agrees with the Equation (1.4.51) cited above. However, this Ψ_1 was computed from Equation (1.4.57).

Now we shall give examples for the three methods of Ritz, Galerkin, and Grammel discussed above. We shall employ the same problem as in the case of the successive approximation method. That is, the differential equation and contour conditions are /65

$$f''+\lambda(1+x)f=0, \quad f(0)=f(1)=0$$

In other words, this is the case of $L[\psi] = \psi''$, $p = (1 + x)$.

In Ritz-Galerkin's method

(a) $\Psi_1 = \sin i\pi x$, taking up to $i = 2$, $\Psi = c_1 \sin \pi x + c_2 \sin 2\pi x$, and from Equation (1.4.48), $\int \sin \pi x[\Psi''+\lambda(1+x)\Psi]dx=0$, $\int \sin 2\pi x[\Psi''+\lambda(1+x)\Psi]dx=0$. therefore

$$\left(\frac{\pi^2}{2}-\frac{3}{4}\lambda\right)c_1+\frac{8}{9\pi^2}c_2=0,$$

$$\frac{8}{9\pi^2}c_1+\left(2\pi^2-\frac{3}{8}\lambda\right)c_2=0$$

The roots of this determinant are $L_1=6.54846\,(0.001\,\%)$, $L_2=26.8316\,(1\,\%)$

(b) $\Psi = c_1(x - x^2) + c_2(x - x^3)$, the determinant is

$$0=\begin{vmatrix} -\frac{1}{3}+\frac{1}{20}\Lambda & -\frac{1}{2}+\frac{8}{105}\Lambda \\ -\frac{1}{2}+\frac{8}{105}\Lambda & -\frac{4}{5}+\frac{33}{280}\Lambda \end{vmatrix}$$

$$L_1=6.634\,(1.3\,\%), \qquad L_2=28.59\,(8\,\%)$$

Computing this by Grammel's method

(a) Using a rough equation, with $\eta_1 = 1$, $\eta_2 = x$, determining Ψ_ν from Equation (1.4.56), assuming that the contour conditions are satisfied, $\Psi_1 = (4x - 3x^2 - x^3)/6$, $\Psi_2 = (3x - 2x^3 - x^4)/12$ and computing from Equation (1.4.55), and making the substitution $\Lambda = 16\sigma$, the determinant is

$$0=\begin{vmatrix} \frac{3}{2}+\frac{34}{15}\sigma & \frac{5}{6}+\frac{37}{30}\sigma \\ \frac{5}{6}+\frac{37}{30}\sigma & \frac{7}{12}+\frac{99}{140}\sigma \end{vmatrix}$$

From this, finding the root of σ, and computing L_1, L_2

$$\Lambda_1=L_1^{(2)}=7.92\,(21\,\%), \qquad \Lambda_2=L_2^{(2)}=40.4$$

showing that the approximation is too unsatisfactory.

(b) Beginning from $\eta_1 = x - x^2$, $\eta_2 = x - x^3$, we obtain

$$\Psi_1=(7x-10x^2+3x^3)/60, \qquad \Psi_2=(10x-10x^3-5x^4+3x^5+2x^6)/60$$

making the substitution $\Lambda = 60\sigma$, and constructing a determinant

$$0=\begin{vmatrix} 42+384\sigma & 64+537\sigma \\ 64+537\sigma & 99+\frac{27720}{33}\sigma \end{vmatrix}$$

/66

From this root, if we compute $L_1^{(2)}$, $L_2^{(2)}$

$$\Lambda_1=L_1^{(2)}=6.5567\,(0.1\,\%), \qquad \Lambda_2=L_2^{(2)}=26.937\,(2\,\%)$$

(c) From $\eta_1 = \sin \pi x$, $\Psi_1'' = -p\eta_1$, assuming $\Psi_1(0) = \Psi_1(1) = 0$

$$\Psi_1=\left\{(1+x)\sin\pi x\right\}/\pi^2+2\,(\cos\pi x-1+2x)/\pi^3$$

From Equation (1.4.59)

$$L_1^{(3)}=3\pi^2/4\,(7/6+5/4\pi^2-16\pi^4)=6.555\,(0.1\,\%)$$

(d) From $\eta_1 = \sin \pi x$, $\eta_2 = \sin 2\pi x$

$$L_1^{(1)}=6.54840 \text{ (virtually no difference) } L_2^{(2)}=26.625 \text{ (1 \%)}$$

as can be understood from this, in Grammel's equation, the approximation is a step better than that of Ritz-Galerkin. This can be seen even if one considers the method of successive approximations. However, for this reason, considerable labor and calculations are required for such an improvement on the method of successive approximation.

1.4.7. TEMPLE, WEINSTEIN AND TREFFTZ-NEWING METHODS

(1) Temple's Method. This method satisfies the boundary conditions for w, in the case of the form of Equation (1.4.7), i.e., when $L[\psi] + \lambda p\psi = 0$, and selecting arbitrarily a function which nowhere throughout the range becomes 0, we utilize the fact that the upper and lower limits of the lowest eigen value are determined by

$$\left(\frac{-L[w]}{pw}\right)_{min} \leqq \lambda_1 \leqq \left(\frac{-L[w]}{pw}\right)_{max} \tag{1.4.60}$$

This has been proposed by many people, and Temple has generalized on it, (74). Consequently, when one proceeds by using $F_n(x)$ in the case of a successive approximation for w, it is possible to gradually restrict the interval between the upper and lower limits.

Kiesling (75) has proposed making an equation which includes a parameter k in the equation for w and utilizes for the lower limit a maximum due to the k in $[- L[w(k)]/pw(k)]_{min}$ and an min due to k in $[-L[w(k)]/pw(k)]_{max}$. However, it is necessary to restrict the region of k within the range which w satisfies the above conditions.

For example, where $EI\, d^2v/dx^2 + Pv = 0$, first we assume v_1, and when we proceed to determine by the method in Section 1.4.3, v_2 from $d^2v_2/dx_2 = -P/EI \cdot v_1$, the following relationship is established.

$$\left(\frac{v_n}{v_{n+1}}\right)_{min} < \frac{P_{k1}}{P} < \left(\frac{v_n}{v_{n+1}}\right)_{max} \tag{1.4.61}$$

Using $v_1 = 4\delta_1 x(1 - x)/l^2$ as an example, in the case of a uniform cross-section, we obtain

$$v_2=\frac{P\delta_1 lx}{3EI}\left(1-\frac{2x^2}{l^2}+\frac{x^3}{l^3}\right)=\frac{16\delta_2 x}{5l}\left(1-\frac{2x^2}{l^2}+\frac{x^3}{l^3}\right) \qquad v_3=\frac{16P\delta_2 l^2}{5EI}\left(\frac{x}{10l}-\frac{x^2}{6l^2}+\frac{x^5}{10l^5}-\frac{x^6}{30l^6}\right) \qquad \underline{/67}$$

Using v_1, v_1, since

$$\frac{v_1}{v_2}=\frac{12\,EI}{Pl^2}\,\frac{l^2x(l-x)}{x(l^2-2lx^2+x^2)}$$

Taking the maximum and minimum of this

$$\frac{9.6\,EI}{l^2}<P_1<\frac{12\,EI}{l^2} \qquad (1.4.62)$$

Moreover, taking v_2/v_3

$$\frac{v_2}{v_3}=\frac{10\,EI}{Pl^2}\,\frac{1-2x^2/l^2+x^3/l^3}{1-10x/6l+x^4/l^4-x^2/3l^2}$$

Using the maximum and minimum values of this,

$$\frac{9.63\,EI}{l^2}<P_1<\frac{10\,EI}{l^2}$$

The lower limits in this case can be determined by assuming the central deflection to be δ_1, δ_2, δ_3, ... in the case of v_1, v_2, v_3, ... and by assuming $v_1 = \delta_2$, $\delta_2 = \delta_3$.

The approximation in this method is not very good. According to Equations (1.4.17) and (1.4.18), with

$$\int_0^1 v_1^2\,dx=\delta_1^2\frac{32}{60},\qquad \int_0^1 v_1v_2\,dx=\delta_1^2\frac{4l^2}{3EI}\,\frac{17}{420},\qquad \int_0^1 v_2^2\,dx=\delta_1^2\frac{l^4}{9(EI)^2}\,\frac{93}{1890}$$

Therefore

$$\mu_1=\frac{EI}{l^2}9.88235,\qquad \mu_2=\frac{EI}{l^2}9.870768$$

Moreover, similarly to this case, when one calculates the lower limit from Equation (1.4.19), with l_2 = 39.2, this is 9.860708 EI/l^2.

As a result, even if only v_1, v_2 are used

$$9.86708\,EI/l^2<P_1<9.87097\,EI/l^2$$

Compared with the above equation (1.4.62), it can be said that the accuracy is completely incomparable.

(2) Weinstein's Method (76). When the problem is the same as in the previous section, in the form $L[\psi] + \lambda p\psi = 0$, selecting an arbitrary constant which will satisfy the boundary condition w, and calculating

$$R=-\frac{\int wL[w]dx}{\int pw^2dx},\quad \mu^2=\frac{\int\frac{1}{p}(L[w])^2dx}{\int pw^2dx} \tag{1.4.63}$$

It can be said that between $R-\sqrt{\mu^2-R^2}$ and $R+\sqrt{\mu^2-R^2}$, there is at least one eigen value λ (value closest to R). When it can be seen that R is closer to λ_1 than to λ_2, by other methods, it becomes possible to use $R-\sqrt{\mu^2-R^2}$ as the lower limit λ_1. However, this method fails if w is not close to an eigen function. However, it can be used even for a high order eigen value. /68

(3) Trefftz-Newing's Method for Determining Lower Limits (77). Similarly as above, we determine R, μ (where $\mu \geqq R \geqq \lambda_1$)

$$g=1-R/\mu \tag{1.4.64}$$

Moreover, we select rough approximations for the lower limits $l_1 = l_1^{(1)}$, l_2 with respect to λ_1, λ_2. Here it must be the case that $l_2 > R$. Then, by the following equation, it is possible to improve the lower limit by $l_1^{(1)}$, $l_1^{(2)}$ ..., $l_1^{(\nu)}$.

$$l_1^{(\nu+1)}=\mu-\mu\sqrt{\frac{l_2-l_1^{(\nu)}}{l_2-R}}\left\{g+2\sqrt{g}\sqrt{1-\sqrt{\frac{l_2-R}{l_2-l_1^{(\nu)}}}}\right\} \tag{1.4.65}$$

$$l_1^{(\nu)}\leqq\lambda_1\leqq R$$

Then (1.4.66)

is obtained.

1.4.8. METHOD USING INTEGRAL EQUATIONS

If one expresses the eigen value problem described above in terms of an integral equation, this becomes the problem of solving

$$\varphi(s)=\lambda\int K(s,t)\varphi(t)dt \tag{1.4.67}$$

This kernel K(s, t) can be written immediately if Green's function is known. For example, in the case of a simple problem, this becomes as follows

(1) When the differential equation is $f'' + \lambda pf = 0$ and the boundary conditions are $f(0) = f(a) = 0$

$$K(s,t)=\frac{t}{a}(a-s)\sqrt{p(s)p(t)}$$

(2) When the differential equation is $f''''+\lambda pf=0$ and the boundary conditions are $f(0)=f''(0)=f(a)=f''(a)=0$

$$K(s,t)=\frac{t(a-s)\{s(2a-s)-t^2\}}{6a}\sqrt{p(s)p(t)}$$

(3) When the differential equation is the same and the boundary conditions are

$$f(0)=f'(0)=f(a)=f'(a)=0$$

$$K(s,t)=\frac{t^2(a-s)^2(2st+at-3as)}{6a^3}\sqrt{p(s)p(t)}$$

(4) Similarly, when the boundary conditions are $f(0)=f'(0)=f''(a)=f'''(a)=0$

$$K(s,t)=\frac{t^2}{6}(3s-t)\sqrt{p(s)p(t)}$$

The above K(s, t) are with respect to $s \geq t$, and it is easy to determine that /69
which corresponds to $s \leq t$ from its symmetricity.

The above integral equations should be solved following this method. In order to convert to the integration to a sum by breaking up the entire region into parts, it is possible to use such accurate equations as the broken line equation, Simpson's equation and others. However, when using an accurate equation, one must not skip the point where the kernel is s = t. There are other methods of solution for the integral equations which can be used, and they are omitted here. Moreover, when the differential equation is of a complex form, or especially if it is a partial differential equation, the problem of determining Green's function itself is quite complicated.

1.4.9. FINITE DIFFERENCE METHOD

This method can be used for any linear differential equations, and is very effective in general application. In particular, in problems of plates, which involve eigen value problems and partial differential equations, even when difficulties are encountered using other methods, this method has the advantage that in some way it can be used to find an answer.

Dividing the region between x = a, x = b into n equal parts, we proceed from

$$h=(b-a)/n \tag{1.4.68}$$

and assume that the terminal conditions are given for x = a, x = b. We will write the eigen function values at

$$x_i=a+ih \quad (i=0, 1, 2, \cdots, n) \tag{1.4.69}$$

for each point of division as $f(x_i) = f_i$. Assuming that the given differential equation is

$$L[\varphi]+\lambda M[\varphi]=0 \tag{1.4.70}$$

If we compose a finite difference equation based on x_i, a primary simultaneous equation is established with respect to the unknown number F_i. For this reason, we replace the differentials by the finite difference table of the first approximation. That is

(1.4.71)

$$\left(\frac{dg}{dx}\right)_{x=x_i}=\frac{g(x_{i+1})-g(x_{i-1})}{2h}+\frac{1}{6}h^2m_3$$

$$\left(\frac{d^2g}{dx^2}\right)_{x=x_i}=\frac{g(x_{i+1})-2g(x_i)+g(x_{i-1})}{h^2}+\frac{1}{12}h^2m_4$$

$$\left[\frac{d}{dx}\left(p(x)\frac{dg}{dx}\right)\right]_{x=x_i}=\frac{p(x_{i+1/2})\{g(x_{i+1})-g(x_i)\}}{h^2}-\frac{p(x_{i-1/2})\{g(x_i)-g(x_{i-1})\}}{h^2}+h^2c$$

$$\left(\frac{d^3g}{dx^3}\right)_{x=x_i}=\frac{g(x_{i+2})-2g(x_{i+1})+2g(x_{i-1})-g(x_{i-2})}{2h^3}+\frac{17}{60}h^2m_5$$

$$\left(\frac{d^4g}{dx^4}\right)_{x=x_i}=\frac{g(x_{i+2})-4g(x_{i+1})+6g(x_i)-4g(x_{i-1})+g(x_{i-2})}{h^4}+\frac{17}{90}h^2m_6$$

$$\left[\frac{d^2}{dx^2}\left(p(x)\frac{d^2g}{dx^2}\right)\right]_{x=x_i}=\frac{1}{h^4}\Big[g(x_{i+2})p(x_{i+1})-2g(x_{i+1})\Big\{p(x_i)+p(x_{i+1})\Big\}$$
$$+g(x_i)\Big\{p(x_{i+1})+4p(x_i)+p(x_{i-1})\Big\}-2g(x_{i-1})\Big\{p(x_i)+p(x_{i-1})\Big\}$$
$$+g(x_{i-2})p(x_{i-1})\Big]+h^2c$$

In this case, m_0 indicates the upper limit of the entire region containing the points of division in the problem of the ρth order differential coefficient or $g(x)$. Moreover, c takes into account the effect due to p and its differential coefficient on the same thing. If one excludes the residual terms expressed by this mp or c, inserts them into a differential equation and writes $F_{(i)}$ in place of $g(x_i)$, and then for λ, writes Λ as the approximate value, the intended finite difference equation can be obtained. Then, it is possible to rewrite the boundary conditions as finite differences. For example, in place of $f'(b) = 0$, one writes $F_{n+1} - F_{n-1} = 0$. As a result, i will be outside of $i = 0$, $i = n$, but from the terminal conditions and the finite difference equation where $i = 0$ or $i = n$, by eliminating F_{-1} or F_{n+1}, it is possible to establish the $(n + 1)$ simultaneous equation for the unknown from F_0 to F_n. A multiple-ordered equation is obtained for Λ by means of the conditions for obtaining a solution in which everything from this F_0 to F_n is not 0, and with its determinant as 0. Arranging the solutions in order of magnitude, $\Lambda_1^{(n)}$, $\Lambda_2^{(n)}$, is obtained, and this $\Lambda_\rho^{(n)}$ is the approximate value of the ρth order eigen value. /70

There is also a method for adjusting Λ so that it satisfies the terminal conditions at one end, by successively calculating the equation, assuming that in this case the determinant is not 0, and that in addition to the terminal conditions at the other end, F_1 and other values are a constant such as 1.

In addition, two methods can be used to increase the approximation in this method by means of this finite difference equation.

(1) By making the mesh more finely differentiated.

(2) By using a high order approximation equation.

When the mesh is made more finely distributed, we assume that the relationship between n and $\Lambda_\rho^{(n)}$ becomes

$$\Lambda_\rho^{(n)} \approx \lambda_\rho - c/n^a \tag{1.4.72}$$

with c and a as constants, and when n is increased, it is possible to determine the value which is considered to be closest to λ_ρ.

However, generally when using this finite difference equation, caution must be exercised since, depending upon the type of problem, and the method for establishing the approximation equation, differences may arise, i.e., the approximation may approach the true value from above, or from below.

It is possible to give as an example the following, when employing a high order approximation equation.

$$\left(\frac{dg}{dx}\right)_{x=x_i} = \frac{-g(x_{i+2})+8g(x_{i+1})-8g(x_{i-1})+g(x_{i-2})}{12h} + \frac{h^4}{18}m_5$$

$$= \frac{1}{60h}\left\{g(x_{i+3})-9g(x_{i+2})+45g(x_{i+1})-45g(x_{i-1})+9g(x_{i-2})-g(x_{i-3})\right\} + \frac{47h^6}{2400}m_7$$

$$\left(\frac{d^2g}{dx^2}\right)_{x=x_i} = \frac{1}{12h^2}\left\{-g(x_{i+2})+16g(x_{i+1})-30g(x_i)+16g(x_{i-1})-g(x_{i-2})\right\} + \frac{h^4}{54}m_6$$

$$= \frac{1}{180h^2}\left\{2g(x_{i+3})-27g(x_{i+2})+270g(x_{i+1})-490g(x_i)+270g(x_{i-1})-27g(x_{i-2})+2g(x_{i-3})\right\}$$

$$+ \frac{47h^6}{8400}m_8$$

$$\left(\frac{d^3g}{dx^3}\right)_{x=x_i} = \frac{1}{8h^3}\left\{-g(x_{i+3})+8g(x_{i+2})-13g(x_{i+1})+13(x_{i-1})-8g(x_{i-2})+g(x_{i-3})\right\} + \frac{463h^4}{2520}m_7$$

$$\left(\frac{d^4g}{dx^4}\right)_{x=x_i} = \frac{1}{6h^4}\left\{-g(x_{i+3})+12g(x_{i+2})-39g(x_{i+1})+56g(x_i)-39g(x_{i-1})+12g(x_{i-2})-g(x_{i-3})\right\} \quad \underline{/71}$$

$$+ \frac{403h^4}{5040}m_8$$

As in the case of the first approximation, a simultaneous finite difference equation is obtained for F_i In this case, F_{-1}, F_{n+1} appear, but in order to be able to eliminate them as described above, the terminal portion cannot but be satisfied by the first approximation. This method is convenient, since the coefficients are correct without having to increase the degree of the algebraic equation for finding Λ, when raising the approximation by this method.

In the case of partial differential equations in plate problems, the grid points (x_i, y_k) are determined in the same manner as above, i.e.,

$$x=x_0+ih, \quad y=y_0+kl \quad (i,k=0, \pm 1, \pm 2, \cdots) \tag{1.4.74}$$

The points indicated by x_0, g_0) and length h, l can be freely selected, but in view of the boundary conditions, it is convenient to carry out the determination so that the approximation is satisfactory, and the boundary coincides as close as possible to the grid points mentioned above. As above, the approximation value of the eigen function f(x, y) at point (x_i, y_i) is F_{ik}. Then, in this case, when writing the finite difference table, the operation is simplified in the following "displacement operators" (Verschiebungsoperator) E_x, E_y are used. These operators were determined by

$$E_x g(x, y)=g(x+h, y), \quad E_x F_{i,k}=F_{i+1,k} \tag{1.4.75}$$

$$E_y g(x, y)=g(x, y+l), \quad E_y F_{i,k}=F_{i,k+1} \tag{1.4.76}$$

As a result, it is possible to calculate the operator formerly in the same way as an algebraic quantity; that is,

$$E_x^p g(x, y)=g(x+ph, y) \qquad E_y^{-p}(x, y)=g(x, y-pl) \qquad E_x^k E_y^m g(x, y)=g(x+kh, y+ml)$$

Then, for example, when writing $\partial^3 g/\partial x^2 \partial y$ indicating this except for the residual term, since

$$\left(\frac{\partial^2 g}{\partial x^2}\right)_{0,0} \approx \frac{1}{h^2}(y_{1,0}-2g_{0,0}+g_{-1,0})=\frac{1}{h^2}(E_x-2E_x^0+E_x^{-1})g_{0,0}$$

$$\left(\frac{\partial g}{\partial y}\right)_{0,0} \approx \frac{1}{2l}(g_{0,1}-g_{0,-1})=\frac{1}{2l}(E_y-E_y^{-1})\,g_{0,0}$$

It is possible to write

$$\left(\frac{\partial^3}{\partial x^2 \partial y} g\right)_{0,0} \approx \frac{1}{2h^2 l}(E_x-2E_x^0+E_x^{-1})\,(E_y-E_y^{-1})\,g_{0,0}$$

$$=\frac{1}{2h^2 l}(g_{1,1}-2g_{0,1}+g_{-1,1}+g_{1,-1}-2g_{0,-1}+g_{-1,-1})$$

Then, if we write the frequently occurring Δ, $\Delta\Delta$, we obtain the following, where h is assumed to be equal to 1.

$$\Delta g(x_0,y_0)=\frac{\partial^2 g(x_0,y_0)}{\partial x^2}+\frac{\partial^2 g(x_0,y_0)}{\partial y^2}=\frac{1}{h^2}(g_{1,0}+g_{0,1}+g_{-1,0}+g_{0,-1}-4y_{0,0})+\frac{1}{6}h^2m_4 \qquad /72$$

$$\Delta\Delta g(x_0,y_0)=\left(\frac{\partial^4}{\partial x^4}+2\frac{\partial^4}{\partial x^2\partial y^2}+\frac{\partial^4}{\partial y^4}\right)g(x_0,y_0)=\frac{1}{h^4}\{20g_{0,0}-8(g_{0,1}+g_{1,0}+g_{-1,0}+g_{0,-1})$$

$$+2(g_{1,1}+g_{1,-1}+g_{-1,1}+g_{-1,-1})+g_{0,2}+g_{2,0}+g_{-2,0}+g_{0,-2}\}+\text{const}\,h^2m_6$$

$$\Delta g(x_0,y_0)=\frac{1}{12h^2}\{-(g_{2,0}+g_{0,2}+g_{-2,0}+g_{0,-2})+16(g_{1,0}+g_{0,1}+g_{-1,0}+g_{0,-1})-60g_{0,0}\}+\frac{1}{27}h^4m_6$$

$$\Delta\Delta g(x_0,y_0)=\frac{1}{6h^4}\{-(g_{0,2}+g_{0,-2}+g_{2,0}+g_{-2,0})+14(g_{0,2}+g_{0,-2}+g_{2,0}+g_{-2,0})$$

$$-77(g_{0,1}+g_{0,-1}+g_{1,0}+g_{-1,0})+184g_{0,0}+20(g_{1,1}+g_{1,-1}+g_{-1,1}+g_{-1,-1})$$

$$-(g_{1,2}+g_{2,1}+g_{1,-2}+g_{2,-1}+g_{-1,2}+g_{-2,1}+g_{-1,-2}+g_{-2,-1})\}+\text{const}\,h^4m_8$$

The m_ρ in these equations indicates the upper limit of the maximum value of the ρth order partial differential coefficient at all grid points within this range. Also, in this case, only the required number of first order simultaneous equations occurs with respect to $F_{i,k}$. However, in the case of orders of approximations above the second order, if the boundary conditions are not satisfied by the first approximation, values of F for the grid points outside of the boundary will remain, causing the problem. Moreover, even in examples of numerical computation, it is of no interest to reduce the approximation for high order partial differential coefficients, so that they are lower than the low order ones. Conversely, the higher the order, the higher should be the approximation.

1.4.10. PERTURBATION METHOD

This method can be used when in solving $L^*[\varphi] + \lambda M^*[\varphi] = 0$, the correct solution is known for the case where there is only a slight difference in its coefficient. $L[\varphi] + \lambda K[\varphi] = 0$. In this case, it is necessary for the boundary conditions to be the same for both. The correct solution is known for

$$L^*[\varphi]+\lambda M^*[\varphi]=0 \qquad (1.4.80)$$

We write the eigen value as $\lambda_{n,o}$*, the eigen function as $f_{n,o}$.

In comparison with this, we assume that the original equation was written

$$L[\varphi]+\lambda M[\varphi]=L^*[\varphi]+\lambda M^*[\varphi]+N[\varphi]+\lambda K[\varphi]=0 \qquad (1.4.81)$$

* n,o is assumed to be single. When multiple, consult Courant-Hilbert (78).

Considering the parameter ε in writing,

$$L^*[\varphi]+\lambda M^*[\varphi]+\varepsilon N[\varphi]+\varepsilon\lambda K[\varphi]=0 \tag{1.4.82}$$

$\varepsilon = 0$ is Equation (1.4.80) where the correct solution is known. Where $\varepsilon = 1$, this becomes (1.4.81). Then, it is considered that the solution of Equation (1.4.81) is related to ε and it is assumed that it is possible for the eigen values and eigen functions to be expanded to the ascending powers of ε (general proof is difficult). i.e., /73

$$f_n=f_{n,0}+\varepsilon f_{n,1}+\varepsilon^2 f_{n,2}+\cdots, \qquad \lambda_n=\lambda_{n,0}+\varepsilon\lambda_{n,1}+\varepsilon^2\lambda_{n,2}+\cdots \tag{1.4.83}$$

We insert this in Equation (1.4.82). Then

$$\sum_{\nu=0}^{\infty}\varepsilon^\nu L^*[f_{n,\nu}]+\sum_{\nu=1}^{\infty}\varepsilon^\nu N[f_{n,\nu-1}]+\left(\sum_{\nu=0}^{\infty}\varepsilon^\nu\lambda_{n,\nu}\right)\left(\sum_{\nu=0}^{\infty}\varepsilon^\nu M^*[f_{n,\nu}]+\sum_{\nu=1}^{\infty}\varepsilon^\nu K[f_{n,\nu-1}]\right)=0$$

Correcting this, and arranging it for the ascending powers of ε, assuming each term to be 0,

From the coefficient ε^0

$$L^*[f_{n,0}]+\lambda_{n,0}M^*[f_{n,0}]=0 \tag{1.4.84}$$

From coefficient ε

$$L^*[f_{n,1}]+N[f_{n,0}]+\lambda_{n,0}(M^*[f_{n,1}]+K[f_{n,0}])+\lambda_{n,1}M^*[f_{n,0}]=0 \tag{1.4.85}$$

From coefficient ε^ν

$$L^*[f_{n,\nu}]+N[f_{n,\nu-1}]+\lambda_{n,\nu}M^*[f_{n,0}]+\sum_{p=1}^{\nu}\lambda_{n,\nu-p}(M^*[f_{n,p}]$$

$$+K[f_{n,p-1}])=0, \qquad (\nu=1, 2, \cdots,) \tag{1.4.86}$$

Since the initial equation (1.4.84) agrees with Equation (1.4.80), it is assumed that the following relationship is established for all functions g, h in which the properties of L* and M* satisfied the boundary conditions.

$$\int(gL^*[h]-hL^*[g])\,dx=0, \qquad \int(gM^*[h]-hM^*[g])\,dx=0, \tag{1.4.87}$$

Then, from Equation (1.4.85) (1.4.86), the unknown quantities $\lambda_{n,1}$, $f_{n,1}$, $\lambda_{n,2}$, $f_{n,2}$ ... are successively determined. That is, when equation (1.4.85) is multiplied by $f_{n,0}$ an integration is carried out for the entire range, employing Equation (1.4.87), since

$$\int f_{n,0}(L^*[f_{n,1}]+\lambda_{n,0}M^*[f_{n,1}])\,dx=\int f_{n,1}(L^*[f_{n,0}]+\lambda_{n,0}M^*[f_{n,0}])\,dx=0$$

The value of $\lambda_{n,1}$ is determined by the following equation

$$\lambda_{n,1}=-\frac{\int f_{n,0}(N[f_{n,0}]+\lambda_{n,0}K[f_{n,0}])\,dx}{\int f_{n,0}M^*[f_{n,0}]\,dx} \tag{1.4.88}$$

Similarly, $\lambda_{n,2}$ is as follows, when $\nu = 2$ in Equation (1.4.84) and it is multiplied by $f_{n,0}$ and integrated

$$\lambda_{n,2}=\frac{-\int f_{n,0}(N[f_{n,1}]+\lambda_{n,1}K[f_{n,0}]+\lambda_{n,1}M^*[f_{n,1}]+\lambda_{n,0}K[f_{n,1}])dx}{\int f_{n,0}M^*[f_{n,0}]\,dx} \tag{1.4.89}$$

Similarly, we can write $\lambda_{n,\nu}$ but usually there are many cases in which the equations as far as Equation (1.4.88) suffice. When it comes to Equation (1.4.89), it is necessary to know $f_{n,1}$. For this purpose it is necessary to solve for $f_{n,1}$ so that the boundary conditions aresatisfied, inserting the values of $\lambda_{n,1}$ in Equation (1.4.85). /74

As a special case, when K = 0, i.e., M* = M, and assuming simply p = p*, we assume that the solution is known for the following equation

$$L^*[\varphi]+\lambda p\varphi=0 \tag{1.4.90}$$

Then, we assume that

$$L[\varphi]+\lambda p\varphi=L^*[\varphi]+N[\varphi]+\lambda p\varphi=0$$

is used tc obtain the original solution

Then, Equations (1.4.88) and (1.4.89) become simple, as in the following equations.

$$\lambda_{n,1}=\frac{-\int f_{n,0}N[f_{n,1}]\,dx}{\int pf_{n,0}^2\,dx} \tag{1.4.91}$$

$$\lambda_{n,2}=\frac{-\int f_{n,0}(N[f_{n,1}]+\lambda_{n,1}pf_{n,1})\,dx}{\int pf_{n,0}^2\,dx} \tag{1.4.92}$$

In this case, it is possible to determine according to Courant-Hilbert (78) p 297, a solution which assumes that $f_{n,1}$ can be expanded by the eigen value function series, $f_{1,0}$, $f_{2,0}$...in Equation (1.4.90). That is, it corresponds to

Equation (1.4.85). When multiplying

$$L^*[f_{n,1}]+\lambda_{n,0}pf_{n,1}+(N[f_{n,0}]+\lambda_{n,1}pf_{n,0})=0 \tag{1.4.93}$$

by $f_{1,0}$ and integrating, and taking Equation (1.4.87) into consideration, also considering that $f_{1,0}$ is the solution of (1.4.90)

$$\int pf_{n,1}f_{i,0}dx=-\frac{\int f_{i,0}(N[f_{n,0}]+\lambda_{n,1}pf_{n,0})dx}{\lambda_{n,0}-\lambda_{i,0}} \tag{(}$$

Moreover, since the rule for expanding for $\sqrt{p}\,f_{i,0}/\sqrt{\int pf^2_{i,0}dx}$, where z $\sqrt{p}\,f_{n,1}$ is normalized is

$$\sqrt{p}\,f_{n,1}=\sum_i \frac{\sqrt{p}\,f_{i,0}}{\sqrt{\int pf_{i,0}^2dx}}\cdot\int\frac{\sqrt{p}\,f_{n,1}\sqrt{p}\,f_{i,0}dx}{\sqrt{\int pf_{i,0}^2dx}}$$

so it is found in

$$f_{n,1}=\sum_{\substack{i=1\\ i\neq n}}^{\infty}\frac{-\lambda_{n,1}\int pf_{n,0}f_{i,0}dx-\int f_{i,0}N[f_{n,0}]dx}{\lambda_{n,0}-\lambda_{i,0}}\cdot\frac{f_{i,0}}{\int pf_{i,0}^2dx} \tag{1.4.94}$$

By this it is possible to determine $f_{n,1}$ with the exception of $f_{n,0}$. Moreover, actually, since the term $f_{n,0}$ is not required, we can follow this procedure.

1.4.11. THE METHOD OF LEASED SQUARES

We assume that the eigen function f is an approximation equation of the following form

$$f(x)=\varphi(x, c_1, c_2, \cdots, c_n) \tag{1.4.95}$$

Moreover, we have satisfied the boundary conditions with x as a function. In order to determine c_1, ... and the approximate value of λ, i.e., Λ, we operate in such a way that the square of the error of the result of using ψ becomes a minimum. i.e., /75

$$I[\varphi]=\frac{\int(L[\varphi]+\Lambda M[\varphi])^2dx}{\int\varphi^2dx}=\text{Min.} \tag{1.4.96}$$

This denominator was added in order to normalize ψ, in order to agree with the common method of leased squares. Then, since the requirements of Equation

(1.4.96) become

$$\frac{\partial I}{\partial \Lambda}=0, \qquad \frac{\partial I}{\partial c_i}=0, \qquad (i=1, 2, \cdots, n) \tag{1.4.97}$$

by this, it is possible to determine Λ, c_1, c_2, ... c_n.

If ψ is a function w which already coincides well with the form of an eigen function, since $\partial I/\partial \Lambda = 0$, we obtain

$$\Lambda=\frac{-\int L[w]\cdot M[w]\,dx}{\int (M[w])^2\,dx} \tag{1.4.98}$$

when p = constant, this agrees with Rayleigh's equation, but when p is not a constant, it generally does not agree.

1.4.12. METHOD OF SERIES EXPANSION

When we assume that the eigen function can be expanded into a series, such as an exponential series or trigonometric series, it is possible to determine the eigen function as follows, i.e.

$$f(x)=\sum_{m=1}^{\infty} a_m \Psi_m(x) \tag{1.4.99}$$

We assume that this form $\Psi_m(x)$ already satisfies the boundary conditions. When this is inserted in $L[\psi] + \lambda M[\psi] = 0$, the results are expanded into a series as above.

$$L[\Psi_m]=\sum_{\nu=1} c_{m,\nu}\Psi_\nu, \qquad M[\Psi_m]=\sum_{\nu=1}^{\nu} d_{m,\nu}\Psi_\nu \tag{1.4.100}$$

Then, the differential equation becomes

$$\sum_{\nu=1}^{\nu}\Psi_\nu\left\{\sum_{m=1}^{\infty} a_m(c_{m,\nu}+\lambda d_{m,\nu})\right\}=0 \tag{1.4.101}$$

Now, considering the coefficient Ψ_ν should be 0, it is possible to form a first order linear equation for a_m. If we assume that the coefficient determinant is 0,

$$\Delta_n(\lambda)=\begin{vmatrix} c_{1,1}+\lambda d_{1,1}, & c_{1,2}+\lambda d_{1,2}, \cdots, & c_{1,n}+\lambda d_{1,n} \\ & \cdots\cdots & \\ c_{n,1}+\lambda d_{n,1}, & c_{n,2}+\lambda d_{n,2}, \cdots, & c_{n,n}+\lambda d_{n,n} \end{vmatrix}=0$$

An algebraic equation is obtained for λ . From this approximate values are obtained up to the initial n - order eigen value. (79) /76

Generally, it is not necessarily the case that this method will work smoothly. Good results are obtained when the method of selecting the series and for performing the equations is good. Pertaining to this type of method is that recently proposed by Takahashi (80).

1.4.13. LOWER LIMIT OF MINIMUM EIGEN VALUE OF COMPOUND SYSTEM.

We assume that when the differential equation is $L[\varphi] + \lambda p\nu\varphi = 0$, p is expressed as the sum of several functions. That is

$$p(x)=\sum_{\nu=1}^{n} p_\nu(x) \tag{1.4.103}$$

Moreover, we assume that we know the minimum eigen function $\lambda_1^{(\nu)}$ of $L[\psi] + \lambda p\varphi = 0$. Then, according to Dunkerley's equation, the lower limit of the minimum eigen value of $L[\varphi] + \lambda p\varphi = 0$ is determined by

$$\lambda_1 \geq 1/\left(\sum_{\nu=1}^{n} 1/\lambda_1^{(\nu)}\right) \tag{1.4.104}$$

When $L[\varphi]$ is the sum of many differential operators, $L_\rho[\varphi]$, and if we know the minimum eigenvalue $\lambda_1^{(\rho)}$, of $L[\varphi] + \lambda p\varphi = 0$, the lower limit of the minimum eigen value λ_1 of $L[\varphi] + \lambda p\varphi = 0$ is determined by

$$\lambda_1 \geq \sum_{\nu=1}^{n} \lambda_1^{(\nu)} \tag{1.4.105}$$

In buckling problems, this can be used when the external force system comes on, or the structure is a compound system.

1.4.14. METHOD USING APPROXIMATION OF BOUNDARY CONDITIONS

The methods described above were selected from those which satisfy as closely as possible the differential equations, from among those which satisfy the boundary conditions. There are also methods which satisfy the boundary conditions as closely as possible, by appropriately selecting such a function that would satisfy the differential equations. The following methods can be used as conditions for satisfying these boundary conditions as closely as possible. That is, the following methods are involved

(1) Point Selection Method

(2) Method of least squares. /77

(3) Series expansion method.

(1) In the point selection method, one merely satisfies the required conditions at several points on the boundary. One example of this is the attempt made by Sezawa in the case of a flat plate with a thick boundary (81), but the results were not a very good approximation.

(2) In the method of least squares, the determination is made on the basis of a condition according to which the sum (integration) of the square of the errors with respect to the boundary condition is minimized.

(3) In the series expansion method, the values of the combination of solutions of differential equation (s) on a boundary are, for example, expanded into a trigonometric series along the boundary, compared with the boundary conditions, and the values for each coefficient of that series are determined. A determinant is obtained for determining the eigen values from these equations. For example, that which Taylor uses to determine the buckling load on a rectangular plate with a fixed edge is an instance of this (82). Details are omitted on this from here since they are given on pages 452-455 of Kurinishi's book "Danseigiku" (Elasticity) (9).

1.4.15. METHODS FOR DETERMINING BUCKLING LOADS IN FRAME STRUCTURES

Various methods have been proposed for determining the buckling load in a structure consisting of a combination of bars by means of calculations. In this case, the method which can be used to calculate statically indeterminant stresses generally can be utilized in elastic stability problems. In the case of statically indeterminant stress, a general classification of methods can be made into those which utilized the stress of a member as an unknown quantity (statically indetermenant excessive quantity) and those which utilize deformation (displacement and rotation). Moreover, for each of them, in addition to the general method of composing a set of simultaneous first orders in equations for the unknown quantities and solving them, there are methods which proceed in stages, carry out sequential corrections, or utilize fixed points, or fixed values. Moreover, various specific methods have been devised for individual cases. Moreover, with regard to the structures themselves, there are both hinged joint frames and stiff joint frames. As has already been explained in Section 1.2.8, cases arise which depend on the ability of displacement of the joints, and the applicability of changes in member length.

In any case, following the general theory of buckling, given a particular load condition, in addition to the deformation that existed up until the time of that condition, we utilize the displacement and rotation of the joint as a new deformation with respect to the form of buckling deformation, and deter-

mine the state of equilibrium when this new deformation is applied, or taking into consideration the added internal forces (axial force, bending moment) we determine the conditions under which they develop in order for them to be in equilibrium with respect to the deformation, and formulate a homogeneous simultaneous equation. Then assuming its determinant to be 0, one may select the lowest values from its root as the buckling load.

In addition to this, there are several other methods which are essentially the same as the above. Kavanaugh's paper (86) is a collection of a relatively large number of these methods, together with a discussion of them. We will not attempt to present a general discussion of this problem here, but will instead describe relatively new special cases.

(1) Lundquist's Stiffness Method (89). Stiffness refers to the bending moment which must be applied to the end of a bar, in order to rotate one end, a of it only one radian in this case called absolute stiffness) or 1/4 radian (called relative stiffness), but here we shall call it "stiffness" without further qualification. There is a difference in its value, depending on the degree of restraint and axial load on the other end. We shall use S_{ab} to express the stiffness when the other end is thickened, S''_{ab} to express the stiffness when the other end is rotating, and S'_{ab} to express the general case, in which the other end is elastically restrained. Then S, S', S'' , result from multiplying the coefficients based on the axial load by EI/L. The ratio of the size of the bending moment occurring at one end b, due to the bending moment occurring at the other end a, to the first bending moment occurring at end a, we call the carryover factor. This will be denoted by c_{ab} when the other end /78 is a fixed end, by $C''_{ab}(=0)$, (when the other end is a rotating end) and by C'_{ab} in the case of general elastic restraint. This is also related to axial load, but the value of S, S'' , C, are already given in the form of a table (See Chapter 3.1).

Denoting by ik one of the members coming together at the joint i and by kh another one of the members coming together at joint k on the opposite side, the stiffness S'ik at end i of member ik can be expressed by the following equation

$$S'_{ik}=\frac{S_{ik}}{1-C_{ki}C_{ik}\sum_{h}S_{kh}/(S''_{ki}+\sum_{h}S'_{kh})} \qquad (1.4.106)$$

When this S'_{ik} is totalled for all of the members coming together at joint i, if $\sum_{k} S'_{ik}>0$ no buckling occurs. That is, ordinary deformation is stable. Then, $\sum_{k} S'_{ik} = 0$ is the limit of stability of this ordinary deformation. That is, the buckling load is determined from the condition

$$\sum_{k} S'_{ik}=0 \qquad (1.4.107)$$

In this case, since the influence of the other members starting from h in

in Equation (1.4.106) is calculated by an equation of the same form as Equation (1.4.106) and thus becomes involved, the influence of all members enters into Equation (1.4.107). Consequently, no matter which joint is selected as a joint, the same buckling load is involved. On this point, this is similar to the step method (Stufenverfahren) in the theory of static indeterminancy.

The above methods all involve the case in which there is no displacement of the joint. It is possible to expand this method to cover cases in which there is displacement of the joint, but one man, Lundquist, has determined that which is described above.

Moreover, the fact that Lundquist uses relative elasticity coefficient when discussing this method, and states that S, S', S'' , must be calculated, is of important significance. That is, the value of the parameter E which is which indicates the influence of the axial load, should be determined in accordance with the axial load P. The relative elasticity coefficient $\bar{E}$ proposed by Lundquist is calculated as follows.

$$\bar{E}=\frac{1}{\pi^2}\frac{P}{F}\left(\frac{L}{i\sqrt{c}}\right)^2 \tag{1.4.108}$$

Here $L/i\sqrt{c}$ is the effective slenderness ratio, i.e., the slenderness ratio obtained by dividing the buckling length $L\sqrt{c}$ by the sectional two-dimensional radius i. This value follows the Equation(s) for columns, and substitutes for that which is expressed as the function $P/F = \sigma k$. This method of indication is more practical than Karman's equation (1.4.52). Moreover, by employing $\bar{E}$ in this method, the buckling load of a frame becomes very close to the actual load. Otherwise, in the case of a single column, this would be the same thing as calculating only Euler's buckling load, and there would be the danger that it would be very remote from the actual buckling load.

(2) Lundquist's Series Method (89). This proceeds on the same basis as that which is described immediately above. A unit moment is applied to a joint b. In order to establish an equilibrium with this, a moment of -1 is distributed according to stiffness along the member which is connected to this joint. First, the end c of member bc converging at point b is fixed, then the restriction is removed, after which a bending moment is applied to the next member. /79
This procedure is the same as the Hardy Cross Method (44). Then the moment which returns to the original joint b is expressed as follows.

$$r=\sum_{c}\frac{C_{bc}S_{cd}C_{cb}S_{cb}}{(\sum_{d}S'_{cd}+S_{cb})(\sum_{c}S_{bc})} \tag{1.4.109}$$

$\sum_{c}$ indicates the sum for all members bc_1, bc_2, ... converging at point b,

$\sum_{d}$ indicates the sum of all c_i, d_1, c_id_2, ... for c_i. In order for ordinary deformation to be stable, it is necessary for a constant moment to operate on

each part. For this, it must be the case that $r < 1$. Consequently, $r = 1$ becomes the limit of stability. The S, S", C occurring in these calculations appear in the table. S' can be calculated from the equation (1.4.106). Also, in this case, it is easy to include $\bar{E}$ in the calculations.

(3) Hoff's Method (90). Hoff's Method is the same approach as the method based on the series used by Lundquist in the previous section, but it uses a different procedure, and there is some difference in the basis of explanation. By this method of Hoff's, using the load which is actually applied, and following the Hardy Cross Method (94), when one carries out the distribution of bending moments, the elimination of strain and brings about equilibrium, as a result, since the bending moments at each joint, in the case of elastic stability, converge to finite and unique values, the case when these moments no longer converge to finite values may be taken as the limits of stability.

One should notice that there are exceptional cases in which this convergence is only apparent. Even when this is unstable, there are cases in which the equilibrium is stable with respect to a particular series of changes, and forms a saddle point which is unstable with respect to other changes. In such a case, if one changes the order of elimination of restraints when using Cross's method, different values occur, so that this is immediately discernible, and actually it can be said that there are few cases in which such a situation would be encountered. However, since such a case is mathematically possible, it has been noted here.

Even with Hoff's method, it is easy to introduce the relative elasticity modulus $\bar{E}$ and perform calculations, and Hoff himself even gives examples of this.

(4) Hsu's Method (95). Hsu's approach is related to the methods described above. However, in this method, a particular member is selected, successive approximations are used to determine the overall stiffness from other members at joints at both ends of the selected member, and finally to determine the buckling load under the conditions of restraint of that member and to consider this as the limit of stability of the frame.

Assuming a member A, B that is to be investigated as a first approximation the other ends of the members connecting its ends AB, are fixed, and the overall stiffness from members other than AB, at A, B, is calculated. In this manner, it is possible to determine the degree of restraint at the end of each member.

As a second approximation, using the values determined by the first approximation for the overall stiffness of the other ends of the members connecting with the ends A, B of member AB, the overall stiffness from members other than AB at ends A, B is determined.

This procedure is repeated. It is a necessary condition of elastic stability that this should converge (however, it is not a sufficient condition). By doing this, when the total stiffness of the ends from the members is determined

as one finite value, the buckling load is determined for each member, as in a column having such elastic restraint. Then, if the buckling load is greater /80 than the actually applied load, one can judge that the frame is elastically stable.

1.4.16. DETERMINATIONS BY CALCULATION OF BUCKLING STRENGTH

This is generally carried out in the case of the flexural buckling of a column. There are very few cases in which it is used for other types of buckling. For this reason, we shall describe it only with respect to the flexural buckling of a column.

(1) Below Proportional Limit. In practice, the results of calculation of buckling load can be used witnout modification. Actually, when the deflection is increased, since a portion above the proportional limit will necessarily appear, the maximum values, i.e., the yield loads determined by applying the methods described below, is the buckling strength.

(2) The case in which the buckling strength is above the proportional limit, and there is a pure center load. In this case, that which is determined by Karman's theory described in Section 1.2.6 simultaneously becomes the maximum load. However, in the case of a column with a non-uniform cross-section, since this poses considerable difficulty, one cannot find many results of this being applied in such a case.

(3) The case in which buckling strength is above proportional limit, and there is original deflection and load eccentricity. In this case, considerable difficulties are encountered in attempting to perform calculations which will correspond faithfully to cases in which this actually occurs, so an appropriate simplification is made. The difficulty here lies in the fact that the stress-strain curves for a material have different paths in the case of a rise and a drop in stress. That which causes the drop in stress, extends gradually from the column center to the ends, and even in a single cross-section, it begins from the most remote tension fiber and gradually approaches the center. In addition, in any cross-section, the stress that is present when the drop in stress begins, is different at each point. Even if only one cross-section is considered, when the average compressive stress increases, the stress at each point should become as shown in Figure 1.4.1, in accordance with the distance from the neutral axis. The figure is an abbreviated diagram and OA_1B_1 indicates the distress-strain curve in the case when, as a material, there is an increase in stress. When the average compressive stress progresses from D_2 to D_3, O_2-O_2, O_3-O_3 correspond respectively to the neutral axes of bending, and the stress distribution in the cross-section should progress in the form $A_2C_2D_2B_2$ and $A_3C_3D_3B_3$. The range indicated by the h's in the diagram show the overall height of the cross-section. Then, the stress drops quickest in the most remote fiber, decreases along $A_1A_2A_3$, and since the drop in stress begins earlier, then this on the points on the inside, if we assume C_2, C_3 as the points where the drops in stress begin, they should appear on A_2C_2, and A_3C_3 respectively. In this way, it is possible to conceptualize the curves A_2, C_2, A_3C_3, but depending on the actual material, the cross-section configuration

and the degree of buckling deformation, when it comes to specifically calculating the value, this constitutes a very difficult task, and it is almost impossible to carry out. For this reason, simplification is required. It should be noted that those who have proposed simplifications in many cases have failed to present detailed explanations of their proposals.

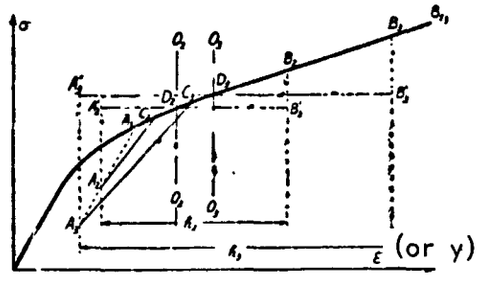

Figure 1.4.1

(4) Various proposals for simplification of stress-strain curves. /81

(a) Karman's Method (38). This is a simplification by Karman, which he carried out with respect to calculations of the relative modulus of elasticity of the proportional limit, for an eccentric column. Figure 1.4.2 corresponds to the illustration in Figure 1.4.1. That is, it is assumed that the tension side of bending causes a drop in the overall stress, and the stress which begins to cause a drop in stress is assumed to be equivalent to the average compressive stress. If this is compared with Figure 1.4.1, it can be seen that the differences constitute a considerable quantity. However, when the eccentric quantity is extremely small, it can be considered that the difference is not too great, and since Karman himself is performing calculations for such a case, in such an event, this can be considered as an appropriate simplification.

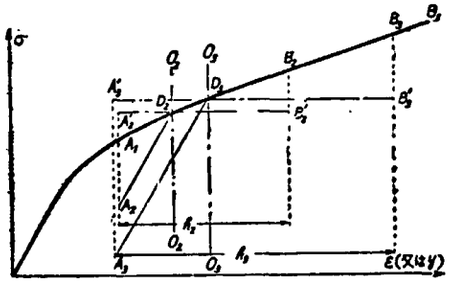

Figure 1.4.2

(b) Hoff's System (96). This system was developed in arranging the results of tests on the buckling load of rigid joint trusses that were carriedout jointly by two or three other persons together with Hoff. This method involves correctly estimating the stress which begins the drop in stress in the most remote fiber, determining the stress in the fiber as that which causes drop in stress from that point and on the bending tension side, assuming that there is linear variation from the neutral axis up to the stress in the most remote fiber. This means that, as shown in Figure 1.4.3, the distribution of the curve section expressed by the solid line $A_2D_2B_2$ $A_3D_3B_3$ is within this section. It can be seen from inspection and comparison with Figures 1.4.1, that the approximation in this system is quite satisfactory.

(c) System utilizing exactly the same curve in the case of a rise in stress with respect to the portion where there is a drop in stress. According to this method, when the eccentric throw is greater than the nuclear distance of the cross-section(s) since there are cases in which no drop in stress is actually present from the beginning, relatively correct results are obtained in cases when this is generally true. (Jesek calculated the case in which the eccentric throw by this method. (97).)

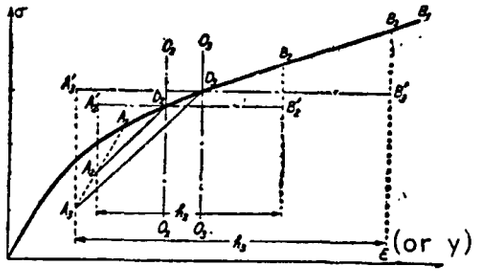

Figure 1.4.3

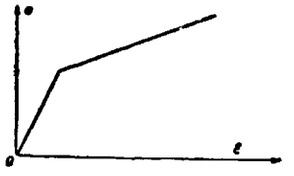

Figure 1.4.4

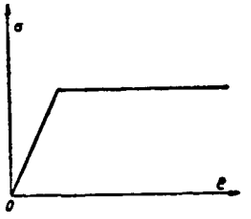

Figure 1.4.5

In addition to this system, there is an approach in which the stress-strain curve is also simplified.

(d) Ratzersdorfer's System. Ratzersdorfer, as shown in Figure 1.4.4, considers that the relationship between stress and strain forms a straight line with a different slope than Young's modulus even when above the proportional limit, or the yield point. He investigated the relationship between buckling stress, stress after buckling, and deformation, in such a case.

(e) System assuming perfect plasticity. This method, as shown in Figure 1.4.5, considers the case of perfect plasticity, which assumes that the stess is constant beyond the point of the proportional limit (also matches yield point). Jesek's calculations of buckling strength of a steel column, which were performed as part of a massive research effort, (97) were carried out on the basis of an investigation using this /82 method.

(5) Various Proposals for Simplification Relating to Changes in Direction of Column Length. It is extremely difficult to correctly estimate the stress-strain curve for each section of a column in the lengthwise direction and to introduce its values. For this reason, it is absolutely necessary to effect an appropriate simplification. Below we shall discuss 2 or 3 proposals.

(a) Karman's System. This is a procedure carried out by Karman in the same case as in the previous section (38). In this case, Karman has noticed that the center portion of the column is decisive for the strength of the column, and asserts that each portion of the column has a flexural rigidity which is calculated from the previous section (in the text) in accordance with the bending of each portion. This rigidity is determined by graphic solution.

(b) Roš-Brunner's Method (98). This procedure involves simplifying the determination of center curvature, given deflection of the column center line. The problem is solved if only the distribution of stress in the center section is accurately determined, and even if the deflection curve is eccentric, and can be maintained that a sine curve half wave is formed over the entire length of the column. In this case, Karman's method described above in (a) is used

for the [illegible]ibution of stress within the section.

([illegible]mann's System (9[illegible] This is a system which considers that the total length of a column is the length between the points in which, when there is no eccentricity, a column which is long by some length, reaches exactly the buckling load, forming a sine curve half wave and when there is eccentricity, the degree of deflection in the previous sine curve has a value exactly equal to the degree of eccentricity. In this manner, Hartmann assumes that one may treat only the distribution of stress in the center section, as mentioned previously in Section (b), and calculates the cases in which there are various degrees of eccentricity. In this case, the system outlined in (c) is used for the distribution of stress.

CHAPTER 5

EXPERIMENTAL DETERMINATION OF BUCKLING LOAD AND BUCKLING STRENGTH

There are cases when it is difficult to solve problems in elastic stability such as buckling only by calculation, and there are other cases in which calculation alone will not suffice. Moreover, there are also instances in which, in the case of actual structures, it is more reliable and more rapid to determine the properties of the structure through direct experimental research. For this reason, experimental research and investigation is being carried out for various cases.

In experimental research, even when systematically investigating a large number of topics, there are naturally limitations on extending the generality of the results outside of the range of the experiments, as long as the experiments are not accompanied by theoretical research. If errors are made in its application, and foolish errors may be made; moreover, even in the case of the tests themselves, there are cases in which it is difficult to formulate a correct judgment, owing to various imperfections occurring in carrying out the tests, and due to considerable differences and irregularities in the results obtained owing to the insolence of these irregularities. Consequently, to evaluate test results correctly, is a rather difficult problem. When it comes to experiments with actual structures, very frequently even more complications become involved, making judgments difficult. There are even cases when unrealistic tests may result due to the complexity of the test object itself or the test apparatus and frequently this results in conditions which were completely unexpected. It is necessary to pay adequate heed to these points.

1.5.1. BUCKLING TEST METHODS /83

In bars, columns, and shells, one carefully applies a load or an end displacement to combinations of these structures under their respective boundary conditions, and various specific methods have been adopted for investigating in detail the processes which take place up to their maximum loads.

The end conditions for flexural buckling due to compressive load on a bar, i.e., the end conditions for column tests usually involve rotating ends, but sometimes "flat seat" is used. The term "flat seat" involves finishing the end of a bar in the plane perpendicular to its axis, and applying a load to it by a load plate or a compression plate. Consequently, the end conditions are not very clear, but it is employed because the conditions are closer to that of a fixed end than a rotating end, and are simpler, or such a "flat seat" is used when the problem of buckling in a shell, or wall surface buckling is involved. The end condition coefficient is generally considered to be 2, whereas it is 4 for a fixed end. However, what is usually important in tests on columns is to have rotating ends, and to determine how to reduce eccentricity as a center load. Figures 1.5.1 through 1.5.3 (38)(100)(44) are examples of this.

The effects of such end conditions on the results are described later on.

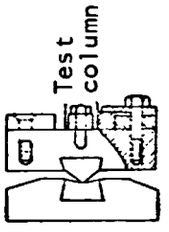

Figure 1.5.1

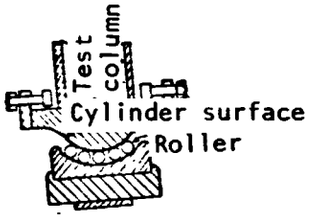

Figure 1.5.2

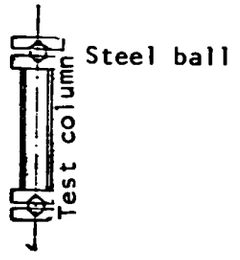

Figure 1.5.3

The method that is used to prove that the load is applied in the center without eccentricity involves measuring the deflection in the lateral direction, when a load to some degree has been applied, dropping the load when it is large, repeating the loading operation after controlling the position of the test object with respect to the load, and then, only after restricting the degree of deflection to within a certain limit, increasing the load up to the buckling load. In order to do this, normally a control apparatus is attached so that the end of the test piece can be displaced on the load plate. The devices on the sustaining faces of the test piece in the load plates shown in Figures 1.5.1 to 1.5.3 are for this purpose. However, there is considerable doubt whether such a method is appropriate for making corrections when there coexists both eccentricity and original deflection. This point will be discussed below in Section 1.5.3.

In this case, usually the column is placed upright and the testing apparatus is attached. Sometimes, it is attached horizontally to a horizontal test apparatus. However, in the case of the horizontal buckling in a beam, it is difficult to apply a load using a conventional materials tester. For this reason, frequently a special apparatus is produced and the load is applied directly using a load object.

For flat plates, the most usual case is that of the compressive load in one direction on a rectangular plate. In this case, difficulties arise in making the load edge strictly a rotating edge. For this reason, usually a "flat seat" is employed. It is considered that the effect of this is rather considerable when the aspect ratio [horizontal-vertical ratio] is below 2. Moreover, after buckling, the load is applied under conditions that the displacement is constant at the load end. This means that the load is applied by a load plate, such as that shown in the Figure 1.5.4 in Schumann-Back (85) tests. The condition that the load end displacement be constant is the boundary condition that is normally carried out both in theory and in testing plates and shells. Usually one desires to have, as a boundary condition for the side, a rotating edge condition.

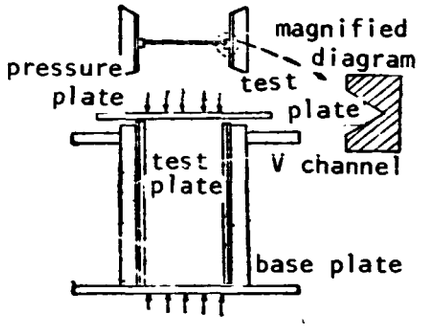

Figure 1.5.4

Schumann-Back normally employ a V channel, /84 as shown in Figure 1.5.4 in this method. There is also the method in which the end edge is cramped in a round rod. Or, as shown in Figure 1.5.5, the test is carried out with the test piece riveted to a reinforcing member. Neither case is perfect, and has its advantages and disadvantages. Consequently, since considerable differences arise in the test results, it is necessary to define clearly the test conditions and to utilize the results in this manner.

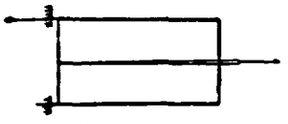

Figure 1.5.6

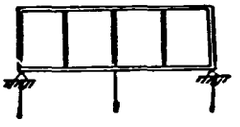

Figure 1.5.7

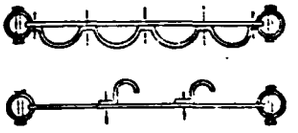

Figure 1.5.5

In the case of a shear load on a flat plate, usually the test object is riveted to edge members as shown in Figures 1.5.6 and 1.5.7 and normally the load is applied to the edge member. Consequently, the boundary conditions can be considered as intermediate between those of a rotating edge and those of a fixed edge.

The device developed by Marguerre (101), is considered to be relatively accurate as a method for applying a compressive or shear load to a flat plate. The apparatus is shown in Figure 1.5.8. According to this method, the plate is first fixed to a rail and the apparatus is designed so that the rail can be moved along the liner plate guide. Using the liner plates as a frame, it is possible to apply, either individually, or in combination, the compressive load and shear loads. He developed several kinds of test using this apparatus, in particular, he used it for tests on half tensile force fields.

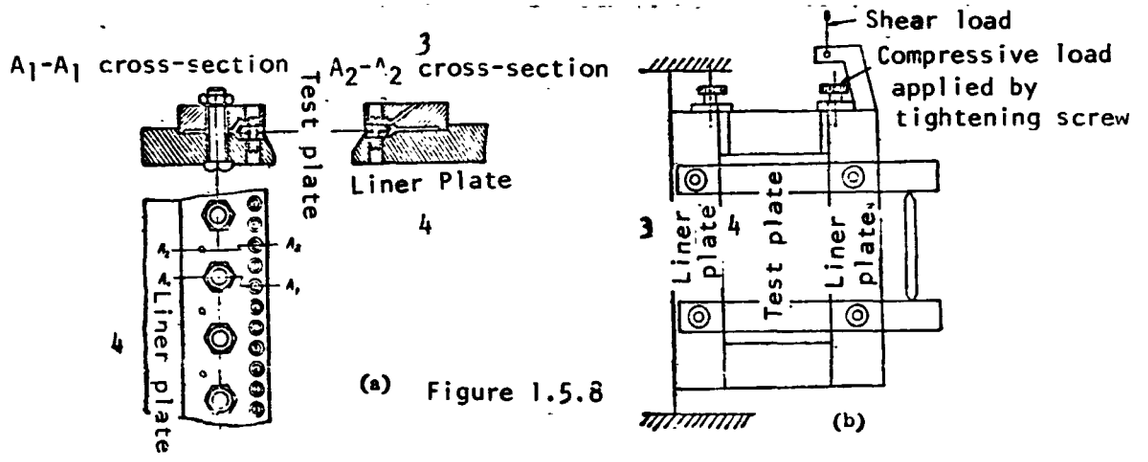

Figure 1.5.8

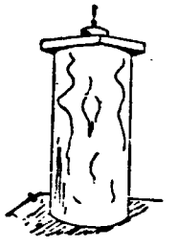

Figure 1.5.9

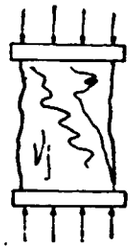

Figure 1.5.10

Normally in the case of shells, in compression tests on cylindrical shells, for the central axial load, a "flat seat" is used and the load is usually supplied /85 by a materials tester. That is, in most cases, an apparatus such as that shown in Figures 1.5.9 and 1.5.10 is employed. However, when the type of load differs, the procedure is not as simple as this, and special apparatus is required for each case.

If a cylindrical shell is considered in the manner of a beam, and a shear load and bending load are applied to the axis in a perpendicular manner, normally the load is supplied by an apparatus such as that shown in Figure 1.5.11. When applying a load that would twist the cylinder, usually it is riveted to a frame, and then placed on a torsion tester. A device that was designed in order to apply various types of loads to a cylindrical shell in any combination, is that shown in Figure 1.5.12, devised by Donnell for the National Advisory Committee for Aeronautics in the United States (102). By means of a crank which operates with 3° freedom, it is possible to apply 3 types of moment or a compressive load.

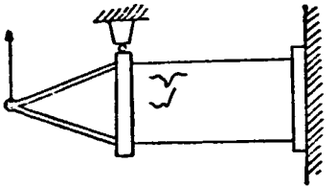

Figure 1.5.11

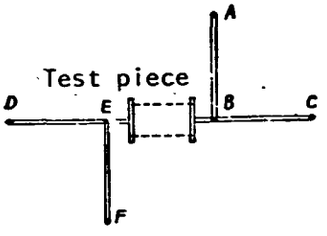

Figure 1.5.12

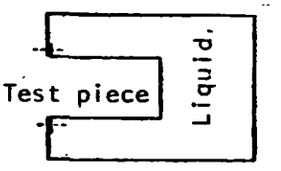

Figure 1.5.13

Tokugawa's method for applying external pressure to cylindrical shells is shown in Figure 1.5.13 (103). According to this method, the external pressure is applied by means of a liquid, and it is possible to observe the deformation of a test piece from inside.

In the case of a rectangular curved shell, when the curvature is small, the method can be used which is the same as that for flat plates, but the difficulties increase. A method was devised by Wenzek for this purpose (104). It involves using a test piece with cross-section configuration, consisting of 3 curved plates joined together by a longitudinal edge piece, as shown in Figure 1.5.14. Another approach is that of Ebner (105), in which the test piece is converted completely into a cylinder and the part between the reinforcing members is treated as a rectangular curved plate.

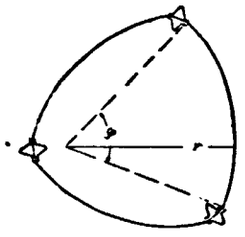

Figure 1.5.14

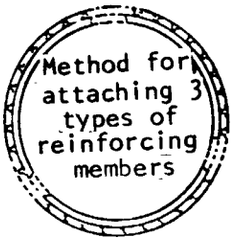

Figure 1.5.15

As far as the quantities that are determined in the tests are concerned, in the case of a bar, usually the maximum load is determined as the buckling load. When conducting detailed research, the relationship between the deflection and the load is determined before and after buckling. As described below, there is a method for determining buckling load from the relationship between the deflection under the buckling load and load, but it cannot be said that this method is necessarily reliable (See Section 1.5.3).

In the case of a plate, since the maximum load and the buckling load differ markedly, normally the deflection in the direction of the load is measured, and the point at which the apparent rigidity rapidly changes, is treated as the buckling load. Then, after the buckling load, the effective width is determined from the apparent rigidity, and finally the maximum load is determined. Moreover, the method proposed by Yoshiki Masao (35) described in Section 1.5.3 is employed to determine the buckling load, but when this is at the proportional limit or above, determinations of the buckling load cannot but be unreliable. In the case of shells, since jump transition and yield occur in addition to buckling, it is necessary to take this into consideration when conducting tests. In such cases, instead of gradually increasing the load, it is desirable to gradually change the displacements of the end plane. Then, if possible, it is desirable to follow the entire process in the case of the jump transition, (including portions under unstable equlibrium) but this is difficult both in experiments, and in practice. /86

Usually the maximum load, elasticity limit load, and deformations such as displacement and deflection are measured in the case of structures. Since in such a case, the number of places in which these must be measured increases, this is a cause for increase in difficulty. However, since it is important to determine what part is the basis for failure, it is necessary to measure in detail as much as possible, the deformation and the distribution of stresses. However, it is extremely difficult to determine the point of origin of this buckling, the time it took place, the place, and the relationship prior to and after buckling, and requires special knowledge and experience.

1.5.2. ADVICE ON BOUNDARY CONDITIONS

Making clear the boundary conditions on the test piece and the apparatus, when determining buckling load and other factors in the course of tests on test pieces, is important with regard to the utilization of the test results. However, from the standpoint of the tests, it is not only difficult to establish [illegible]nditions, but even to have a clear picture of what is involved. For [illegible]e must make efforts to ascertain as clearly as possible the

boundary conditions. It is important to investigate adequately the influences due to differences in boundary conditions.

(1) Load End Conditions. Load end conditions pose a special problem in the case of bars. Due to progress in test methods, it has become possible gradually to reduce the degree of eccentricity, and the relationship between the load and deflection of the bar now is approaching the ideal one. This is clear from the results shown in Figure 1.5.16. When this is below the proportional limit, since there is practically no influence with respect to the maximum load, there is little problem, but in the case of a buckling load above the proportional limit, since there is an influence, even on the maximum load, special care must be exercised. In order to reduce this eccentric throw [literally the degree of eccentricity], as described in the previous section, one should try to reduce as much as possible the deflection when the test load is applied. In the method for regulating the relative position of the load plate and test piece, if one does not reduce to a minimum the original deflection of the test piece, the effects described in Section 1.5.3 will occur, and the results may be confused. For this reason, a special caution is required.

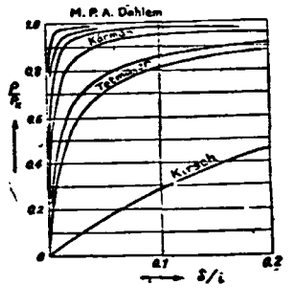

Figure 1.5.16

In the load terminal, there are practically no cases in which the end of the ordinary test piece will become the center of rotation of the rotating end. The space between the end of the test column and the center of rotation is the load plate, and since it is stiff, theoretically this means that one is conducting a test for the case in which a stiff section has become attached to the end of the column. For this reason, test results are obtained which differ from the buckling in the portion of the test column alone. It is necessary to correct this point. For this reason, as shown in Figure 1.5.17, a column of the same material as the test piece should be deflected along the curve running from point A' in the figure through point P, but in the case of load plate, the integral PA may be considered as a straight line in a direction tangential to P. Considering the length of $\overline{AA'}$ to be Δ, this is expressed by the equation, as Karman has calculated. /87

$$\Delta=\frac{\pi^2}{3}\left(\frac{\overline{AP}}{L}\right)^2 L \qquad (1.5.1)$$

In any case, the length of $\overline{AP}$ is somewhat smaller than L, so its influence is not very great.

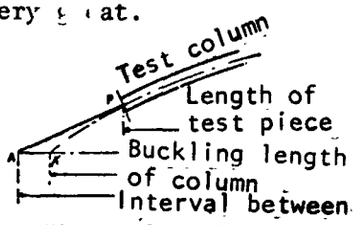

Figure 1.5.17

Next, what should be taken into consideration when utilizing a materials tester in order to apply a load, is that when it is constructed so that it is possible to control the horizontal movement of the load end, e.g., as in tension tests, or when it is constructed so that a particular point is used as the center and can

oscillate, changes in the buckling length of properties similar to those described above may also occur in parts of the test apparatus itself (106).

(2) Boundary Conditions on Load Edge. In buckling tests on flat plates and cylindrical shells, the conditions on the load edge involve the "flat seat" condition described in the previous section. Consequently, the end conditions are very unclear. Since it is impossible to regulate the degree of eccentricity, it is necessary from the very beginning to pay very close attention to the tooling of the end face, linearity, and angularity. If the linearity is not clearly defined, from the beginning, there is a loss in the uniform distribution of the load on the load edge, and when the angularity is poor, a similar adverse affect occurs with the eccentricity.

In the case of a rectangular plate, the effects due to differences in the condition oon the load edge, when the aspect ratio is below 2, but no consideration has been given to methods for correcting before this. When instead of a "flat seat" a profile is riveted along the load edge, if one does not be careful to make sure that symmetricity is maintained, it is possible for the load distribution to become uneven, or for the eccentricity to increase.

In the case of such closed section items as cylindrical shells, due to friction between the load plate and the test piece, displacement due to lateral strain (due to Poisson's ratio) becomes restricted, and from the very beginning, since this causes deflection deformation on the wall surface, it is necessary to be careful of changes in the buckling load due to this.

(3) Boundary Conditions on Ordinary Edge. Generally four quantities are involved in the boundary conditions for flat plates and shells. We shall assume that x, y are the plate surface, and z is a direction perpendicular to this. This condition involves regulation of the displacement, the axial force, or the shearing force, in the direction x, y, z and the regulation of the slope in the direction perpendicular tc the periphery, or of the bending moment around the periphery.

In the case of a rectangular flat plate, if we denote the edge by the direction y, the displacement in direction x is usually considered to be free. Sometimes, there are cases in which the displacement is considered to be 0. In order to clearly provide this, it is necessary to have a structure such as that shown in 1.5.8. Moreover, it is necessary to be careful that friction does not occur, so that displacement in the direction y may apply freely. Displacement in direction z, when regulated by a V channel, becomes as shown in Figure 1.5.18, and since this objective is not achievable, it is not any interest. Nevertheless, when employing the method of inserting the edge between the two cylinders as shown in Figure 1.5.19, the displacement is restricted, but the fact that the configuration shown id the figure is obtained due to the slope, means that there is no freedom, and since the bending moment is caused in such a case, the displacement approaches somewhat that of a fixed edge, rather than a condition of a rotating edge, and the buckling load rises. Moreover, for this reason, since friction is caused with respect to the displacement in the directions x, y, it is of no interest at this point. Actually, in the

case of a flat plate, the buckling load in Figures 1.5.18 and 1.5.19 show a difference of 1% to 2%, (85) (36).

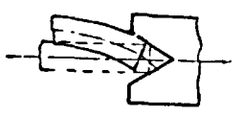

Figure 1.5.18

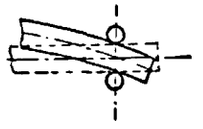

Figure 1.5.19

In the case of a shell, when using /88 the methods described in Figures 1.5.14 and 1.5.15, in the previous section as a test method for a curved rectangular plate, if one examines the test results, one sees that a considerable difference arises in the buckling load or in the change of the effective width after the buckling load.

1.5.3. RELATIONSHIP BETWEEN DEFORMATION DURING TESTS AND BUCKLING LOAD

As explained in Section 1.2.5, when there is original deflection in the test piece itself, or when there is an eccentric load, considerable deformation occurs even under buckling load. Literally, even with buckling load or less.

Consequently, in plates, rather pronounced wrinkles occur. However, this does not have any direct relationship to the buckling load. Nevertheless, it is possible to consider a method for determining the buckling load from the relationship between the way in which these wrinkles or deflections arise and progress; i.e., and load. However, considerable care is required for this purpose. We shall describe this below:

1. Karman's Method, Southwell's Method, Donnell's Method. Karman explains that when there is eccentricity, the relationship between the deflection, delta of a column and the load P can almost be considered that of a hyperbola, so, by means of the graph shown in Figure 1.5.20, it is possible to find the buckling load as one of it's asymptotes, (38). First, we take 3 points, A, B, C on the curve. Since it is considered that the direction of the asymptotes is vertical and horizontal, horizontal and vertical lines are drawn respectively from the 2 points, B, the point of intersection is determined; and when the 2 points, E, F are determined with ABF/ED, EBC/DF, this becomes one point on the asymptote. Consequently, the buckling load is determined from the horizontal line passing through F.

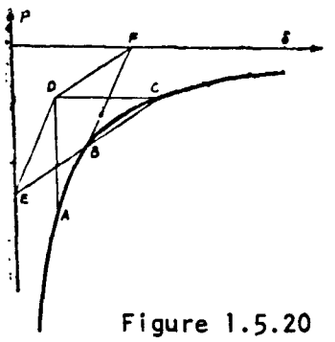

Figure 1.5.20

Southwell's approach concerns the case when a bar has original deflection and writing the original deflection as

$$c_1 \sin \pi x/L$$

the relationship between the center deflection δ and the load P, becomes

$$\delta = c_1 P/(P_k - P)$$

so, adjusting this, we can write

$$\delta=(\delta/P)P_k-c_1 \tag{1.5.2}$$

Consequently, since δ and δ/P have a linear relationship, when the test results are plotted as δ to δ/P as shown in Figure 1.5.21, it is possible to determine the buckling load from the slope (107).

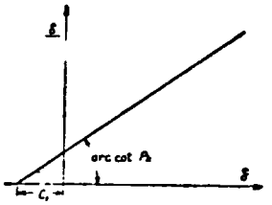

Figure 1.5.21

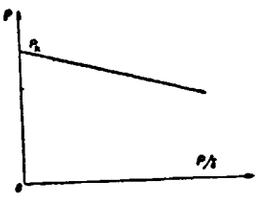

Figure 1.5.22

Donnell similarly transforms the equation for deflection and load in the case of original deflection, and obtains the following equation

$$P=P_k-c_1 P/\delta \tag{1.5.3}$$

Therefore, drawing the line P with respect to P/δ, from the value when $P/\delta = 0$, it is possible to determine the buckling load as $P = P_k$ (108).

In the case of plates, when there is original deflection, since the same equations hold, it is possible to use Southwell's and Donnell's methods. Moreover, Cox attempts to utilize the fact that the relationship between shrinkage and load with buckling load as boundary, becomes linear before and after it /89 respectively. (109).

In such cases, as Southwell has pointed out, it is necessary to bear in mind that the load or original deflection must be adequately large, it should be easy to measure the deflection with sufficient accuracy, and at the same time, the load should be below the proportional limit. Moreover, as described below, when both eccentricity and original deflection are present together, the basis for these methods becomes shaky. In the case of plates, since the difference between making determinations with a value of P_k and the buckling load of the next magnitude is small, even considering what was described in Section 1.2.5, it can be predicted that the determination of P_k will be difficult.

(2) Sezawa's Method. Sezawa, as a result of investigating the relationship between the axial compressive load of a column and the lateral vibration frequency, established that in the case of a buckling load P_k, the vibration number is 0, and then varies according to a linear relationship with the axial compressive load (60). For example, in the case of a column with both ends rotating, the relationship between the circular vibration P_m and the axial load

P is expressed by the following equation

$$p_{cr}^2=\frac{\pi^2}{\rho FL^2}\left(\frac{\pi^2 EI}{L^2}-P\right) \tag{1.5.4}$$

One example of test results for this is that shown in Figure 1.5.23 (the test results are on the dotted line).

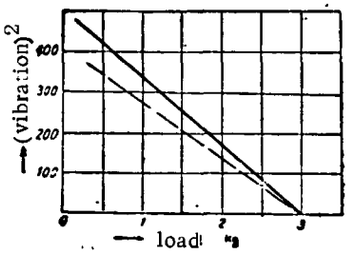

Figure 1.5.23

(3) δ^2 Method. This method was proposed by Yoshiki Masao (35). This method involves relationship between load and deformation after buckling in a flat plate. It is expressed by the following equation, as described in Section 1.2.5

$$P=P_k\left\{1+a\left(\frac{\delta}{b}\right)^2\right\} \tag{1.5.5}$$

Here, b is the plate width and a is a constant which depends upon the boundary condition, the aspect ratio of the plate, etc. For this reason, if one determines from tests the curve of the relationship between P and δ^2, one sees that P and δ^2 have a linear relationship where P is quite large, and when this is extended, so that the axis of P is crossed, this becomes equal to P_k.

In this case, when the stress is above the proportional limit, difficulties are experienced, and since when the aspect ratio is large, the difficulties described in the next section also become involved, some degree of caution is required in the utilization of this method.

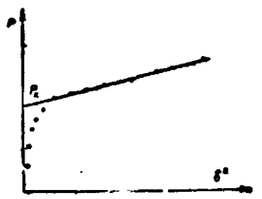

Figure 1.5.24

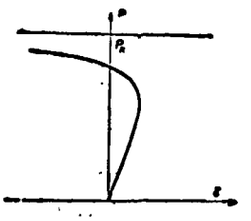

Figure 1.5.25

(4) Special Case of Change in Deflection when under Load. In the cases described above, either the degree of eccentricity is very small, even when the original deflection of the test piece is large, or the reverse is true, but as explained by figure 1.2.24, when the relationship between original deflection c_1 and eccentricity is expressed by the following equation for the case of a column, a reverse turn of the direction of deflection occurs, as shown by Figure 1.5.25.

$$-0.811<e/c_1<-0.785 \tag{1.5.6}$$

In such cases, methods such as those of Southwell are useless.

In addition, when the original deflection has the shape of an S, i.e., /90
when the shape of the deformation in the case of a second buckling load becomes included in large measure in the original deflection, the center axis, as shown in Figure 1.5.26 changes in the order 1, 2, 3, 4, 5, causing buckling. In such a case, good results cannot be obtained by the methods described above.

Figure 1.5.26

In the case of plates, in addition to the two cases mentioned above, the buckling deformation does not necessarily form a half wave length in the lengthwise direction, which is different from the case of bars. When a rectangular plate with four rotating sides sustains a compressive load in one direction, generally the plate becomes divided into shapes which are close to that of a square, and irregular wave forms are produced. Therefore, for example, in a rectangular plate with an aspect ratio close to 2, the deformation in the center longitudinal cross-section progresses, as shown by the Figures 1 2, 3, 4, in Figure 1.5.27. Due to this relationship, depending on the points measured, a reversal of deflection occurs.

Figure 1.5.27

The loads which cause a reversal of these deflections, do not have a direct relationship to the buckling load, as explained in detail in Section 1.2.5, so when conducting experiments, one must be careful not to select the initiation point of this reversal as buckling load, or to become confused by the effects of this reversal in the case when the δ^2 method is used.

As has been frequently mentioned, when the stress is above the proportional limit, since its influence involves factors in addition to those described above, caution must be exercised since it is very dangerous to utilize the method described in this section. In actual structures, there are many cases in which the stress goes above the proportional limit, so in structures with real dimensions, this point must be considered very carefully.

CHAPTER 6

DESIGN AND STRENGTH AS RELATED TO BUCKLING AND OTHER FACTORS

1.6.1. STRENGTH DUE TO BUCKLING, YIELDING, "JUMP TRANSITION"

The strength based on the buckling of the bar is the maximum load due to yielding, determined from the relationship between strength and stress, above the proportional limit of a material, as described in Section 1.2.7, i.e., it is the yield load. However, when the original deflection and load eccentricity are not very marked, this maximum load is almost equivalent to the buckling load. Of course, above the proportional limit, the buckling load takes into consideration changes in the elastic properties of the material. However, as explained in the previous chapter, it is quite difficult to determine this maximum load and above the buckling load in columns with a non-uniform cross-section, is quite complicated. In the buckling of bars, these properties have not been investigated concretely or in detail, except for the flexural buckling due to an axial compressive load, but it is not considered erroneous to believe that properties are shown which are exactly like those of the buckling of a column.

When a plate sustains a compressive load or a shearing load, and deflection buckling is caused, as described in Section 1.2.7, the maximum load, i.e., the strength becomes much larger than the buckling load. The conditions for determining this maximum load have not been studied concretely for such cases as bars. Usually one must rely on the results of experiments.

In the case of shells, since it is considered that it is most correct to maintain that the buckling load simultaneously is the ascending "jump transition" load, in this case, it may be considered to be the buckling load, i.e., the maximum load. Of course, in thin shells, when the stress is maintained /91
below the proportional limit, only the phenomenon of jump transition occurs unaccompanied by rupture phenomenon. For this reason, such properties are sometimes utilized.

In plates having reinforcing members, when the reinforcing members are weak, or they are very densely arranged, overall buckling occurs, and this approaches the properties of an orthotropic plate. In such a case, apparently the degree to which the maximum load is increased with respect to the buckling load is not very great, but the strength law is not very clear. When the reinforcing members are strong and not densely arranged, first the plate portion only buckles and it is considered that it withstands the load until the combination of the reduced effective width and the reinforcing members cause buckling as a column. This constitutes the strength of a plate having reinforcing members. This is the same both in the case when the plate sustains a compressive

load, and when it sustains a shearing load. However, cases of shearing load have not been concretely and clearly given.

The case of shells having reinforcing members has a relationship similar to this, and probably normally only the plate section buckles first. Problems most frequently arise in the case when the reduced effective width and the reinforcing members together cause bar-type buckling. Moreover, this is frequently handled as the case of an orthotropic shell. In any event, no one has succeeded in expressing strength by a simple equation.

In the case of structures consisting of a combination of plates and shells, since results which differ on various points with the basic cases described above occur, special care is required. In channel members which are viewed as a combination of plates, when the column buckling load with respect to the compressive load is markedly greater than the plate buckling load, the plate buckling load occurs first, but in this case, one cannot expect an increase above the buckling load having the properties of a plate (45).

The ascending jump transition load in the case when the yield load or deformation after jump transition is very great, and the stress is above the proportional limit, can be used as the maximum load or breaking load of the member or structure. Since the equations for this are explained in Chapter 2, they will not be repeated here.

Below, in this chapter, we shall examine problems relating to strength and design, primarily in terms of buckling.

1.6.2. FORMULAS FOR BUCKLING STRENGTH, SAFETY FACTORS

As has been described in the previous section, to determine theoretical formulas or equations for buckling strength, even if possible, is usually very difficult. For this reason, it is desirable to have them agree as closely as possible with the experiment results, and to express them as simply as possible. As a result, there is a large variety of design formulas for columns in which buckling is the central problem, and depending on the field of engineering involved, the preference for one type over the other differs. To cite several examples, we give below the simplest algebraic examples, with a and b as constants.

Tetmajer's Equation

$$\sigma_k = a - b(L/i) \tag{1.6.1}$$

DIN's Equation

$$\left.\begin{aligned} \sigma_k &= \sigma_y, && (L/i) < 60 \\ \sigma_k &= a - b(L/i), && 60 < (L/i) < 100 \\ \sigma_k &= \pi^2 E i^2 / L^2, && 100 < (L/i) \end{aligned}\right\} \tag{1.6.2}$$

Johnson's Equation

$$\sigma_k = \sigma_y - (\sigma_y^2/4\pi^2 E)(L/i)^2, \quad \sigma_k > \sigma > \sigma_y/2 \tag{1.6.3}$$

Rankine's Equation $$\sigma_k=\sigma_L/\{1+a(L/i)^2\} \tag{1.6.4}$$

More theoretical equations have the following form /92

Southwell's Equation $$\sigma_k=\sigma_y\Big/\left\{1+\frac{e\eta_1}{i^2}\sec\left(\sqrt{\frac{\sigma_k}{E}}\cdot\frac{L}{2i}\right)\right\} \tag{1.6.5}$$

Perry's Equation $$\sigma_k=\frac{\sigma_y+(1+\eta)\sigma_E}{2}-\sqrt{\left\{\frac{\sigma_y+(1+\eta)\sigma_E}{2}\right\}^2-\sigma_y\sigma_E}, \tag{1.6.6}$$

$$\sigma_E=\pi^2Ei^2/L^2, \qquad \eta=c_1\eta_1/i^2$$

Southwell, using a theoretical equation for the case of eccentricity e and Perry using equations for initial deflection $c_1 \sin \pi x/L$, established their formulas on the condition of the calculated maximum stress, with the extreme fiber from the neutral axis as η_1 is [illegible] to the yield point σ_y. Difficulties arise if E is used above the proportional limit, and the maximum load occurs in the case when it is equivalent to σ_y at the maximum stress, but if e, c_1 are appropriately selected, a practical formula is obtained (Refer to Section 1.2.7).

There are many cases in which this is handled by similar relationships depending upon whether the buckling is that of a bar, or other types, but it is not as convenient as the above.

In the case of flat plates, the maximum load becomes significantly greater than buckling load, but its limits can only be determined by experiment. However, the equation given by Kármán for the case when four edges are rotating, is

$$\sigma_{wk}=\pi\sqrt{E\sigma_y/3(1-\nu^2)}\cdot t/b \tag{1.6.7}$$

However, actually the σ_y in the equation should be made the proportional limit σ_p (See Figure 1.2.32). Moreover, when $\sigma_{wk} > \sigma_p$, this equation cannot be used at all. With regard to this section, equations for the case of columns have not been proposed (See Section 1.2.7), even in the case of other boundary conditions, only the same kind of equation can be used. In the case of shearing load, no appropriate equation has yet been formulated.

In shells, the buckling strength σ_{wk} is given by the following equation for the case of a cylindrical shell that generally is longer than a particular length with a radius a and a skin thickness t.

$$\sigma_{wk}=c\,E(t/a)^n \tag{1.6.8}$$

c, n are constants and n in the case of axial compression is n = 1, the torsional load with respect to the shearing stress is n = 1.35 - 1.5, in the case of external pressure, it is n = 2 with respect to a direct force in the direction of the circumference. Moreover, the values of c, according to experiment results, are respectively 0.3-0.2; 0.2-0.15; and 0.25. However, when the cylinder length is reduced, the influence of this is manifested (See Figure 1.2.8).

Generally, in the case of various types of buckling, when the load is a composite of two or more types of simple loads, we may express the buckling strength for each of these simple loads as σ_{k1}, σ_{k2}... and expressing the stress corresponding to the case when a maximum load is formed in the event that this compound load is sustained, as σ_1, σ_2,

$$\left(\frac{\sigma_1}{\sigma_{k1}}\right)^{n_1}+\left(\frac{\sigma_2}{\sigma_{k2}}\right)^{n_2}+\cdots=1 \tag{1.6.9}$$

is established, and is widely used. The n_1, n_2, ... are constants and frequently are equal to about 1 or 2.

The safety factor problem is important in design. This should be selected/93 by taking into consideration the rate of fluctuation of the original member with respect to its load resistance and the rate of fluctuation with respect to the value of the standard maximum of the load which is applied from outside. However, this has not been clearly measured, and frequently empirical values are used, as the result of which meaningless numbers are assigned to it. Moreover, as shown in the ω Method in formulas for columns, it is frequently the case that the allowable load is easily determined by means of a simple formula which includes the safety factor in experimental strength formulas. That is, the formula has the form

$$\sigma_{\text{allowable}} > P\,\omega/F \tag{1.6.10}$$

The design should be carried out in such a way that the value of ω is appropriately determined with respect to the slenderness ratio, and the computed value on the right side should be smaller than a specific allowable stress determined for the member. This equation can be further expanded, and in the case when the bending moment is simultaneously in effect, it is claimed that the following can be used, in which W is the section coefficient and the bending moment M does not take buckling bending into consideration.

$$\sigma_{\text{allowable}} < P\,\omega/F + M/W \tag{1.6.11}$$

This equation is widely used in architecture and civil engineering. However, apparently there are considerable arguments against it (4)(97).

Generally, it is very dangerous to employ the "safety factor" obtained by considering the stress value that is calculated with respect to the load is safe, since it is a certain percent with respect to the unique tensile strength

or the yield point of the material. Actually, one should consider that the maximum load is a certain percent with respect to the breaking load. This should be noted particularly in the case when buckling is also involved. Moreover, depending upon the standards, there are many cases in which, whereas it is natural to require that the rigidity of the member should be above a certain degree, there are standards which assume a load of a particular size, and state that the strength should be sufficient with respect to that load. In such case if one carries out a design which deviates from the customary dimensions, this is dangerous and requires caution.

Even though the concrete values for the safety factor itself are generally determined as indicated above, since there are differences depending upon the type of structure and the type of load, we shall not treat this here.

1.6.3. CONCERNING PREVENTION OF BUCKLING

Before each type of structure, or a part of them reaches a specific breaking load, or a predictable buckling load or buckling strength, it is desirable to reliably prevent the occurrence of other types of buckling or instability phenomena. Moreover, if this point is not clearly taken into account in design, an unpredicted instability will occur at a low load, and it is possible that unsuspected accidents such as breakage may occur, so this must be taken into careful consideration. From this point of view, we shall describe below several examples of the relationship between the rigidity of structural elements effecting buckling, and their dimensions.

(1) Rigidity of Intermediate Support Points on a Continuous Column. When a structure which is supported by having several support points at equidistant intervals on a single long bar sustains an axial compressive load, and buckling occurs, the maximum load when the distance between the support points is determined, is the buckling load, where the length between the support points is considered to be the buckling length. In order to have such a buckling load, it is necessary for there to be a rigidity of above a certain magnitude, so that the support points will not move laterally. When the rigidity is below this degree, the buckling load will decrease to a value lower than the above-mentioned maximum value. Denoting the spring coefficient indicating the rigidity at this support point as α, the overall length as 1, and the number of spans as m, the buckling load is $P_k = m^2\pi^2 EI/1^2$, and the value of α is necessary for this purpose, is given as /94

$$\alpha = mP/\beta l \qquad (1.6.12)$$

and the constant β with respect to the value of m has the numerical values indicated in the following table.

Table 1.5.1

m	2	3	4	5	6	7	9	11	∞
β	0.5	0.333	0.293	0.276	0.268	0.263	0.258	0.255	0.250

As frequently happens in such cases, the method which requires a load of P/100 as the strength of the part which constitutes the support point is open to debate.

(2) Prevention of Buckling in other Types of Columns. If one has knowledge concerning other types of buckling which should be prevented in such cases, it is possible to devise counter measures. It is sufficient to have knowledge concerning the presence of such buckling and the numerical values for the size of the load caused by it. In the other types of buckling which may occur in the case of the axial compressive load on a column are torsional buckling and wall surface buckling, so they will be described here.

(a) Prevention of Torsional Buckling. There are many cases in which torsional buckling occurs in open thin-walled sections, i.e., angle members and channel members (44). In order to prevent this buckling, the skin thickness should be made appropriately large (see next section), but in addition, the spaces between each open section are connected by cross pieces at appropriate intervals. Then, this forms a half-open sectional member, the torsional rigidity increases markedly, and it is possible to prevent torsional buckling.

(b) Prevention of Wall Surface Buckling. With regard to portions in which the wall surface is flat, one should make the buckling stress, considered as a flat plate, above the flexural buckling stress. For this purpose, as shown in Figure 1.6.1 for steel members, in section AB, considering that both edges are rotating edges,

$$b_1/t_1 < 35\{1+(L/i)/100\} \tag{1.6.13}$$

and in section AC, considering that one edge is free

$$b_2/t_2 < 14\{1+(L/i)/100\} \tag{1.6.14}$$

and ir EF, considering the rigidity of the support side to be small, this coefficient 14 should be 11. With regard to the curved section, as shown in Figure 1.6.2, compared with the buckling in the case of a cylindrical shell, one should have for section GH

$$r_3/t_3 < 25\{1+(L/i)/100\} \tag{1.6.15}$$

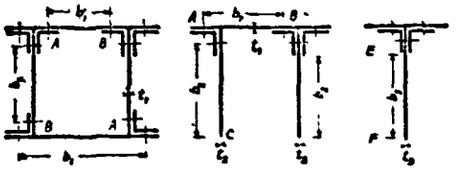

Figure 1.6.1

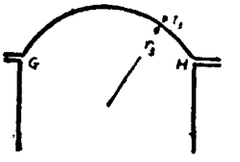

Figure 1.6.2

Moreover, in this case, it is important to have the conditions of support on the sides equal to that of a cylinder. In addition, for the buckling of walled surfaces in general, one should refer to methods for the prevention of buckling in plates and shells. Then, in order to maintain the boundary conditions, it is necessary to pay attention to the configuration on the end, and the method of coupling. Moreover, one should attempt to make it possible to skillfully employ reinforcing members. /95

(3) Arrangement and Rigidity of Flat Plate Reinforcing Members. When it is disadvantageous to have a broad flat plate width and only increase the skin thickness, reinforcing members are introduced in order to prevent a drop in the buckling load. Once the reinforcing members are added, it is desirable to increase the buckling load as far as the buckling stress of the flat plate, in which the integral between reinforcing members is considered as the width, and the edges are considered as rotating edges. This then is the maximum value in the case when, for the buckling load, the integral between the reinforcing members is made constant. The rigidity of the reinforcing members necessary for this purpose is as shown in Tables 1.5.2 to 1.5.4 in the case of a compressive load, and as in Figure 1.6.3, in the case of a shearing load. The measurement of this was carried out by Timoshenko (1) and are abbreviated values. Assuming $B = EI_r$, $D = Et^3/12\ (1 - \nu^2)$, $\beta = L/b$, $\delta = F/bt$ (plate width b, plate length L, cross-section area of reinforcing member F, geometrical moment of inertia I_r), the values of $\gamma = B/bD$ are given in the following tables.

Table 1.5.2

Case of 1 longitudinal reinforcing member (multiple 4)

β	δ=0.05	δ=0.10	δ=0.20
0.6	5	5	5
0.8	—	—	10
1.0	10	10	—
1.2	—	15	15
1.4	15	—	20
1.6	20	20	25
1.8	—	25	—
2.0	25	—	—

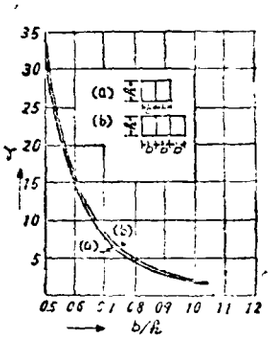

Figure 1.6.3

Table 1.5.3

Case of 2 longitudinal reinforcing members (multiple 9)

β	δ=0.05	δ=0.10
0.6	5	6.67
0.8	10	10

Table 1.5.4

Case of 1 lateral reinforcing member (multiple 1,)

$1,\left(\beta=1.41;\ (2/\beta+\beta/2)^2,(1/\beta+\beta)^2,\beta<1.41\right)$

β	0.5	0.60	0.70	0.80	0.90	1.0	1.2	1.41
γ	12.6	7.18	4.39	2.80	1.82	1.26	0.433	0

When longitudinal reinforcing members are thus included, the buckling axial force n_y becomes $m^2 4\pi^2 D/b^2$, and the buckling load increases in proportion to the square of the number of sections m. However, in lateral reinforcing members, this effect is very small, and when β = 0.5, while a reinforcing member with γ = 12.6 is added, the multiple is merely 2.96, and when β = 1.00, the multiple is 1.56. This means that the increase due to the reinforcing member /96 is slight. Therefore, it can be said that a lateral reinforcing member is an unsuitable method for directly preventing buckling of a flat plate. However, when the length of the longitudinal reinforcing member is increased, it becomes necessary to combine this with an appropriate lateral reinforcing member, and to measure the increase in buckling stress and buckling strength. Otherwise, very thick members will be required if only longitudinal reinforcing members are used.

In the case of shearing stress, as can be seen from Figure 1.6.3, using the width of one section for the b in $\gamma = B/bD$, is almost unrelated to the number of reinforcing members, and is determined by h/b (1).

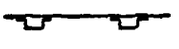

Figure 1.6.4

Figure 1.6.5

Moreover, when a reinforcing member is added, as shown in Figure 1.6.4, the width in terms of a flat plate becomes narrow, and since the torsional rigidity of the reinforcing member also increases, there is little worry about instability. In such objects as depicted in 1.6.5, since the rigidity of the reinforcing member itself with respect to torsion is small, caution must be exercised since it is easy for torsional buckling to occur.

In order to further increase the buckling load on a flat plate, it is possible to attach a corrugated plate, but in this case, as will be described in the next section, rather than employ the method of attachment shown in Figure 1.6.6,

it is more advantageous to employ the method shown in Figure 1.6.7 in which the buckling load due to compression for a corrugated plate is nigh.

Figure 1.6.6

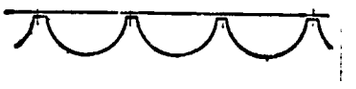

Figure 1.6.7

In order to prevent buckling of a part of a flat plate "escape holes" or "functional holes" with reinforcing edges are used. Or, instead of adding reinforcing members, channels are made with the plates themselves, or a protuberant section is prepared. There are still no results of experiments on this, but it is used in practice.

(4) Prevention of Buckling in Shells. As for the buckling of a shell, the buckling load in terms of a tube, is largest so for the cross-section configuration, one uses as much as possible, either a tube or a combination of part of a tube. In such cases, frequently it happens that the desired strength is not achieved. If caution is not exercised with respect to the boundary conditions, for example, in a corrugated plate as shown in Figure 1.6.8, which is viewed as a continuous connection of one part of a tube, owing to axial compressive load, the buckling stress for only the tube is unattainable This is because irregularities appear in the shape shown by the dotted line in the figure, and the boundary conditions on the edge have the form of an unvariable slope, and a free displacement, so that the buckling stress drops. For this reason, in such a case, as shown in Figure 1.6.9, in the connected parts of the curved surface shown by point A, it is necessary to find a way for the rigidity [stiffness] to appear in the configuration of the cross-section itself, such that the displacement is 0.

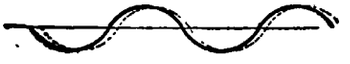

Figure 1.6.8

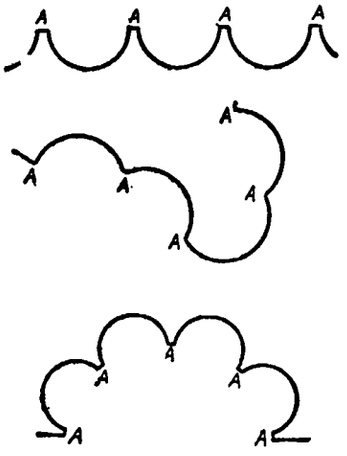

Figure 1.6.9

(5) Arrangement of Reinforcing Members of Shells. With regard to this case, there are no materials available such as those for a flat plate. Dschou's (51) results are quoted by Timoshenko (1) so one must refer to the latter's work. In addition to items with such a configuration, there are cases in which the problem of strength becomes important after the section of the plate has first buckled. Specific standards for such a case have not yet been clarified.

(6) Prevention of Buckling in Complex Structures. In the case of actual complex structures, the structural elements in which buckling should be prevented, and the types of buckling are numerous, and require extremely close attention. Especially when designing something which differs from conventional dimensions, this must be considered with great /97

care. As an example, we shall consider below the problem in which this must be considered for a plate girder.

In a plate girder, there is overall lateral buckling. Moreover, when accompanied by an axial load, flexural buckling and torsional buckling also pose problems. In any case, the girder is designed with overall buckling in mind, so it becomes necessary to prevent all other types of buckling. In this case, that which should be prevented can be described below for each section of the structure.

(a) In the edge members, it is necessary to take into consideration flexural buckling, torsional buckling, wall surface buckling, buckling between rivets, and in addition, loss in stiffness of connecting plates due to rivets.

(b) In the webs, one must take into consideration deflection buckling due to shearing load, deflection buckling due to bending load, buckling between rivets, and the influence of the reinforcing members used for this purpose. Moreover, depending upon the individual instance, deflection buckling in the parts connected with the reinforcing members also pose a problem.

(c) It is necessary to take into consideration the flexural buckling of the reinforcing member itself, when it is considered as a unit for inducing an external force onto the web, the torsional buckling, the wall surface buckling, and the buckling between rivets.

(d) It is necessary to take into consideration the flexural buckling, torsional buckling, wall surface buckling and buckling between rivets, in a reinforcing member which is considered as serving as a member for preventing deflection in the webs.

The explanations that have been given for these points should be considered as the standard.

1.6.5. RELATIONSHIP BETWEEN DESIGNS WITH MINIMUM WEIGHT AND BUCKLING.

Various conditions exist for having a minimum weight, but even given the same material with the same outer dimensions, it is possible to obtain a structure with minimum weight by selecting appropriately the form of the structure and regulating the dimensions and proportions.

Formerly, it was thought that a minimum dimension could be obtained by varying the sectional standard dimensions of a column or beam in the direction of the axis in such a way that the maximum stress was uniform. Even in pocketbooks this thought is expressed. However, in actuality, the dimensions and proportions within the cross-section itself are more important than this. The weight derived from the former method does not, in comparison with the case in which a uniform cross-section is used, drop by more than 1/2. However, when appropriate cross-section dimensions are used, it is easy to make this weight [drop] 1/100 in comparison with that which has a true cross-section. Consequently, this has a great advantage over the former method. As with regard to

the means of selecting these cross-section dimensions and proportions, the dimensions and proportions which should be selected come to be determined by the specific load (meaning such quantities as P/L^2, P/h^2, M/h^3, Q/h^2). And, moreover, the wall surface buckling strength becomes an important factor. Details on this can be found in the books (9)(10)(114) and the paper (111).

In terms of minimum weight, the limits on the prevention of buckling described in the previous section become an important element so it is necessary to adequately investigate these conditions. In any case, it is of the utmost importance to accurately understand what is meant by the true strength.

REFERENCES

1. Timoshenko, S., "Theory of Elastic Stability," 1936. /98
2. Timoshenko, S., "Stabilitatsprobleme der Elastizitat," in *Auerbach-Hort, Handbuch der phys. u. techn. Mechanik.* Bd. 4, 1 (1931), S. 81.
3. Flugge, W., "Statik und Dynamik der Schalen," 1934.
4. Ratzersdorfer, J., "Die Knickfestigkeit von Staben and Stabwerken," 1936.
5. Biezeno, C. B. and Grammel, R., "Technische Dynamik," 1940.
6. Mayer, R., "Die Knickfestigkeit," 1921.
7. Salmon, E. H. "Columns," 1921.
8. Hartmann, F., "Knickung, Kippung and Beulung," 1935.
9. Kuranishi, Masatsugu, "Danseigaku," (Elasticity), published by The Japan Mechanical Engineering Society (1948).
10. Kuranishi, Masatsugu, "Buckling Theory," unpublished.
11. Southwell, R. V., "Phil. Trans. A.," Vol. 213, p. 187.
12. Biezeno, C. B. and H. Hencky, "Proc. Acad. Sci. Amst.," Vol. 31 (1928), p. 569 and Vol. 32 (1929), p. 444.
13. Trefftz, E., "Proc. 3rd Intern. Congress for Appl. Mechn." Stockholm, Vo. Vol. 3 (1930), p. 44; and "Zeits, angew. Math. Mech." Bd. 13 (1933) S. 160.
14. Biot, M. A., "Proc. 5th Intern. Congress for Appl. Mech.," Cambridge, 1938.
15. Kappus, R., "Zeits. angew. Math. Mech.," Bd. 19 Nr. 5 u. 6, 1939.
16. Kotani Masao, "Dynamics of Continuous Bodies," *Iwanami Lectures, Mathematics.*
17. Euler, L., "Methodus in veniendi lineas curves maximi minimive propietate gaudentes Lausanne,", 1747.
18. Wagner, H., "Festschrift 25 Jahre Danzig T. H., 1928, S. 329.
19. Prandtl, L., "Kipperscheinungen, Nurnberg," 1899.
20. Greenhill, A. G., "Proc. Inst. Mech. Engrs.," London, 1883.
21. Levy, M., "Journ. math. pures et appl.," (Liouville,) 3 ser., tom. 10, 1884, p.5.
22. Grammel, R., "Zeits. angew. Math. Mech.," Bd. 3, 1923, S. 438; Bd. 7, 1927, S. 198.
23. Huribrink, E., "Zeits. V. D. I.," Bd. 54, 1910, S. 138.
24. Bryan, G. H. "Proc. London Math. Soc.," Vol. 22, 1891, p. 54.
25. Lorenz, R., "Zeits V. D. I.," Bd. 52, 1908, S. 1766.
26. Donnell, L. H., "Trans. Amer. Soc. Mech. Engrs.," Vol. 56, 1934, p. 795.
27. Karman, T. v. and Hsue-Shen Tsien, "Journ. of Aeron. Sci.," Vol. 7, 1940.
28. Karman, T. v., "Enzyklopadie der math," Wiss., Bd. 4, 4, 1919, S. 349.
29. Karman, T. v., E. E. Sechler and L. H. Donnell, "Trans. Amer. Soc. Mech. Engrs." Vol. 54, 1932, p. 53.
30. Marguerre, K., "Luftfahrforschung," Bd. 14, Nr. 3, S. 121; "Zeits angew. Math. Mech.," Bd. 16, 1936, S. 353.
31. A. Fromm and Marguerre, K., "Luftfahrforschung," Bd. 14, Nr. 12, S. 627.
32. Karman, T. v. and Hsue-Shen Tsien, "Journ. Aeron. Sci.," Vol. 8, 1941, p. 303.
33. Marguerre, K., "Zeits. angew. Math. Mech.," Bd. 18, Nr. 1, 1938, S. 57.
34. Ritz, W., "Crelle Journal," Vol. 135, 1909, p. 1.
35. Yoshiki Masao, "Journal of Applied Dynamics," Vol. 1, No. 6, 19.

36. Yamana, Masao; Matsuhira Sei, "Journal of the Japan Aeronautical Society," Vol. 5, No. 40, 1938; Shirato Minoru, Thesis, Tokyo University, Department of Aeronautics, 1939; Watanabe Shigehiro, "Journal of the Shipbuilding Society," No. 61, 1937.
37. Geckeler, J. W., "Zeits. angew. Math. Mech.," Bd. 8, 1928, S. 341.
38. Karman, T. v., "Forschungsarbeiten a. d. Ingw., Nr. 81, 1910. /99
39. Dickinson, H. B. and J. R. Fischel, "Journ. Aeron. Sci.," Vol. 6, p. 253.
40. Howlend, W. L. and P. E. Sandorff, "Journ. Aeron. Sci., Vol. 8, 7, 1941.
41. Kuranishi Masatsugu, "Applied Dynamics," Vol. 3, No. 18, 1945, p. 139.
42. Sechler, E. E. "Guggenheim Aeronautics Laboratory," C.I.T. Publ. No. 27.
43. Kakumae(?) Mutsuo, "A New Theory of Materials Dynamics," Industrial Graphics Publishers, 1941.
44. Kuranishi Masao, "Papers of the Japan Mechanical Engineering Society," Vol. 1, No. 5, 1935, p. 415.
45. Kuranishi Masao, "Journal of the Japan Aeronautical Society," Vol. 2, Nos. 3-5, 1935.
46. Pippard, A. J. S., "Aeroplane Structures," p. 213.
47. Yamamoto Mineo, Kondo Kazuo, "Reports of the Aeronautics Research Institute, No. 119.
48. Klemperer, W. B. and H. B. Gibbons, "Zeits. angew. Math. Mech.," Bd. 13, 1933, S. 251.
49. Zimmerman, H., "Die Knickfestigkeit eines Stabes mit elastischen Querstutzung," Berlin, 1906.
50. Chwalla, E., "Zeits. angew. Math. Mech.," Bd. 7, 1927, S. 276.
51. Dshou, D. D., "Luftfahrforschung," Bd. 11, 1935, S. 224.
52. Hayashi Shigeru, "On Compressive Instability Accompanying Slip Deformation" Published at a Meeting of the Society for Applied Dynamics.
53. Hayashi Shigeru, "Tensioning in a Circular Saw," *Applied Dynamics* Vol. 17, No. 8, 1948, p. 251.
54. Koning, C. and J. Taub, "Luftfahrforschung," Bd. 10, 1933, S. 55.
55. Taub, J., "Luftfahrforschung," Bd. 10, 1933, S. 65.
56. Kumai Toyoji, "Investigation of Excessive Vibration of a Column Due to Impact Load and of Impact Buckling Strength," Thesis, Osaka University, 1947.
57. Masada Senri, Paper read before the Japan Architectural Society, 1947; "High Speed Buckling of Columns," read before the Japan Applied Dynamics Society, 1948.
58. Suhara Jiro, read at the Kyushu University Engineering Department Conference on Stress Research.
59. Shibuya Takashi, Yamaguchi Kenji, "Journal of the Japan Aeronautical Society," Vol. 10, No. 98, 1943; Vol. 11, No. 115, 1944.
60. Sezawa Yoshio, "Papers of the Aeronautical Research Institute, No. 5, p. 39.
61. Imachi Isamu, "Applied Dynamics," Vol. 2, No. 8, p. 39.
62. Puwein, "Der Bauingenieur," Bd. 13, 1939.
63. Bleich, F., "Proc. Amer. Soc. Civil Engrs.," Vol. 74, No. 8, 1948-10).
64. Harai Atsushi, "On the Stability with Respect to Torsional Vibration of a Suspended Bridge," papers of the Japan Civil Engineering Society, 1949, March, p. 17.
65. Marin, J., "Journ. Appl. Phys.," Vol. 18, 1947-1, p. 103.
66. Brazier, L. G., "Aeron. Res. Comm. Rep. and Memo," No. 1081.

67. Karman, T. V., "Zeits, V. D. I.," Bd. 55, 1911, S. 1889.
68. Heck, O. S., "Luftfahrforschung," Bd. 14, 1987, S. 137.
69. Ikeda Tsuyoshi, "Journal of the Japan Aeronautical Society," Vol. 7, No. 61, May 1940, p. 426; Vol. 8, No. 79, Nov. 1941, p. 1183; Vol. 9, p. 84, April 1942, p. 455.
70. Shibuya Takashi, "Journal of the Japan Aeronautical Society," Vol. 7, No. 58, Feb. 1940, p. 97.
71. Collatz, L., "Zeits. angew. Math. Mech.," Bd. 19, Nr. 4, 1939, S. 224; Nr. 5, 1939, S. 297.
72. Mises, R. v. and H. Geiringer, "Zeits. angew. Math. Mech.," Bd. 9, 1929, S. 58.
73. Galerkin, B. G., "Wjestnik Ingenerow, Petrograd," Nr. 19, 1915.
74. Temple, J., "Proc. London Math. Soc., Ser. (2)," Vol. 29, 1929, p. 257.
75. Kiessling, F., "Zeits. angew. Math. Mech.," Bd. 10, 1930, S. 594.
76. Weinstein, D. H., "Proc. Nat. Acad. Sci.," Washington, Vol. 20, 1934, p. 529.
77. Newing, R. A., "Phil. Mag. (7)," Vol. 24, 1937, p. 114.
78. Courant, R. and Hiebert, D., "Methoden der math. Physik," Berlin, 1931.
79. Iguchi Roukozo, "Ing. Arch., Bd. 7, 1936, S. 207.
80. Takahashi Satoe, "Generalizations on Column Buckling Theory," Papers of The Japan Mechanical Engineering Society, Vol. 13, No. 45, 1947, p. 125.
81. Sezawa Yoshio, "Reports of the Aeronautical Research Institute," No. 69, April 1931.
82. Taylor, G. I., "Zeits. angew. Math. Mech.," Bd. 15, 1933, S. 147.
83. Zimmermann, H., "Lehre von Knicken auf neuer Grundlage," Berlin, 1930. /100
84. Shanley, F. R., "Journ. Aeron. Sci., Vol. 15, 1947.
85. Schuhmann, L. and G. Back, "Nat. Adv. Comm. Aeron. Techn. Rep. No. 356."
86. Kavanagh, T. C., "New York University, College of Engineering, Thesis, 1948.
87. Mises, R. v. and Ratzersdorfer, J., "Zeits. angew. Math. Mech.," Bd. 6, 1926, S. 181.
88. Mises, R. v. and Ratzersdorfer. J., "Zeits angew. Math. Mech.," Bd. 5, 1625, S. 218.
89. Lundquist, E. E., "Nat. Adv. Comm. Aeron. Techn. Note No. 617," 1937-10; ibid., No. 652, 1938-6; Ibid., No. 658, 1938-7.
90. Hoff, N. J., "Journ. Aeron. Sci.," Vol. 8, 1941, p. 115.
91. Seydel, E., "Ing. Arch," Bd. 4, 1933, S. 169.
92. Karman, T. v. and H. S. Tsien, "Journ Aeron. Sci., Vol. 7, 1939, p. 43.
93. Grammel, R., "Ing. Arch," Bd. 10, 1939, S. 35.
94. Cross, H., "Trans. Amer. Soc. Civil Engrs.," Vol. 96, 1932, p. 1.
95. Hsu, P. T., Cornell Univ. Exper. Sta. Bull. No. 36, 1947.
96. Hoff, N. J., B. A. Boley, S. V. Nards and S. Kaufman, "Amer. Soc. Civil Engrs." published 1948.
97. Ješek, K. "Die Festigkeit von Druckstaben aus Stahl," Wien, 1937.
98. Roš, M. and J. Brunner, "Proc. 2nd Intern. Congress f. Appl. Mech." Zurich, 1926, p. 368; Ibid., Berichte uber die 2. intern. Tagung f. Bruckenbau and Hochbau," Wien, 1929, S. 282.
99. Hartmann, F., "Zeits. osterr. Ing. u. Arch.-Verein," Bd. 85, 1933, S. 65.
100. Amer. Soc. Civil Engineers, "Special Committee Report," Trans. A.S.C.E., Vol. 89, 1926, p. 1485; Ibid., Vol. 95, 1931, p. 1152.

101. Marguerre, K., "Luftfahrforschung," Bd. 13, 7, S. 221.
102. Donnell, L. H., "Nat. Adv. Comm. Aeron. Techn. Rep. No. 479," 1933.
103. Tokugawa Takesade, "Papers of the Shipbuilding Society, No. 125 Suppl.," 1932, p. 151.
104. Wenzek, W. A., "Luftfahrforschung," Bd. 15, Nr. 7, 1938, S. 340.
105. Ebner, E., "Luftfahrforschung," Bd. 14, 1937, S. 93.
106. Hayashi Shigeru, "On the Effects of the Stiffness of Test Machines on Column Buckling," read at The Applied Dynamics Society.
107. Southwell, R. V., "Proc. Roy. Soc. London, Series A," Vol. 135, 1932.
108. Donnell, L. H., "S. Timoshenko 60th Anniv. Volume," 1938, p. 24.
109. Cox, H. L. and W. J. Glenshaw, "Inst. Engs. Shipb" Scotland, Vol. 81, 1937, p. 19.
110. DIN. E 4114, "Knick- und Bauvorschriften fur Stahlbau," 1. Entwurf, 1939.
111. Kuranishi Masatsugu, "Journal of the Shipbuilding Society," No. 56, 1935, p. 127.

SUPPLEMENTARY REFERENCES

112. Nylaneler, H., "Trans. of Roy. Inst. Tech., No. 28," Stockholm, 1949.
113. Kuranishi Masatsugu, "Reports of the Nihon University Engineering Institute, No. 1," 1952.
114. Shanley, F. R., "Weight-Strength Analysis of Airplane Structures," J. Wiley.
115. Kuranishi Masatsugu, "Proc. of 4th Jap. Nat. Congr. Appl. Mech.," p. 87-91 1954.
116. Kubo Tomai, "Research on Buckling of Riveted Plates," *Journal of the Japan Society for Applied Dynamics*, vol. 3, No. 19, 1950-10, pp. 157-167.
117. Dow and Hickman, "NACA T.N. No. 2139," Jan. 1950.

SECTION 2 /101

SOLID MEMBERS

CHAPTER 1

COMPRESSIVE MEMBERS

2.1.1. CENTRAL COMPRESSIVE MEMBERS HAVING U[illegible]FORM CROSS-SECTIONS

The limit value for the elastic buckling load of a member of uniform cross-section sustaining an axially compressive load, when neither end undergoes bending resistance

$$P_e=\frac{\pi^2 EI}{l^2}=\frac{\pi^2 B}{l^2} \qquad (2.1.1)$$

frequently becomes a standard. This is called Euler's buckling value for a member.*1 No great differences in practice are involved if the calculation is made that $\pi^2 = 9.87$. Even in cases where neither end resists horizontal forces, but do resist bending, the buckling value is P_e. Depending on changes in the conditions of support of the member, the buckling load for such cases can be determined if different numerical values are employed in place of π^2. That is, generally, it is possible to express the buckling load by

$$P_k=\frac{(m\pi)^2 EI}{l^2}=m^2 P_e \qquad (2.1.2)$$

The value of m is not necessarily an integer.

This comes to have the same state of deformation as the buckling wave form of an axially compressed member with both ends pinned, which has a member length of $l_k=l/m=\pi\sqrt{EI/P_k}$ when dealing with buckling deformation. Its buckling value is equal to Euler's buckling value. l_k is called the buckling length. It can be easily determined by observing the position of the inflection point arising in the bending of a member, with respect to simple member end conditions.

*1 Euler did not use the symbol EI but expressed this by Ekk and called it moment moment du ressort or moment de roideur. Van den Broek, "Limit Design," J. Wiley, 1948, p. 80.

TABLE 2.1.1*

State of support of member ends	Both ends pin-ended	Both ends fixed	One pin-ended end, other end fixed	One end free, other end fixed
Buckling deformation (member length l)	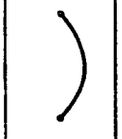	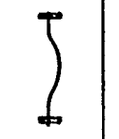	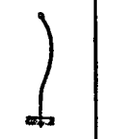	
Buckling length l_k	l	$0.5\,l$	$0.7\,l$	$2\,l$

As will be described later on, this is sufficient in the case of elastic buckling, but is not within non-elastic ranges. This operation at first sight seems to be meaningless, but since it can be related directly to Euler's load values, it is useful in clearly understanding buckling phenomenon and makes it easy to introduce the allowable values and safety factors necessary for actual design. Table 2.1.1 indicates simple cases of buckling length. Since the buckling length is determined for each buckling surface individually, the buckling lengths in direction x and direction y at right angles to it generally are not the same even within the same compressive member. /102

2.1.2. MEMBERS OF NON-UNIFORM CROSS-SECTION

There are cases in which, when the cross-section of a member is not constant, the buckling values are expressed in the form of Equation (2.1.2) and a buckling length $l_k = 1/m$ is used. The P_e in this case is the Euler buckling value for a member of equivalent cross-section which was arbitrarily selected and which has a member length 1. For the cross-section, either a maximum or minimum cross-section may be employed, or, on this basis, a hypothetical cross-section may be established. In the case of axial compression on a member with non-uniform cross section which is pin-ended on both ends, when the hypothetical cross-section is appropriately determined, it is possible to assume that the member length 1 is equivalent to l_k. In DIN Entwurf 2 E 4114 Section 8, an equation is given for calculating this using a constant geometrical moment of inertia such as

$$K = f(I_{min}/I_{max}) \cdot I_{max}$$

In the case of a I cross-section member of non-uniform depth with an extremely thin web. In Table 2.1.2, this function is expressed where $I_{min} \geq 0.04\ I_{max}$.

*This type of graphical representation is in J. W. Geckler's "Elastostatik, Handbuch der Physik IV, Springer, Berlin, (1928), S.283.

TABLE 2.1.2

Configuration of Member	$f(l_{min}/l_{max})$
	$0.34+0.66\sqrt{I_{min}/I_{max}}$
	$0.61+0.39\sqrt{I_{min}/I_{max}}$
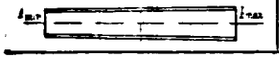	$0.20+0.80\sqrt{(I_{min}/I_{max})^{2}}$

2.1.3. NON-UNIFORM LOAD

It is difficult to express the buckling values in the case when the compressive force along the line of the axis varies. When the load varies at a constant degree over the entire length of the member axis, It is customary to employ as the buckling value, the value at the time of critical buckling at maximum load. When the variation is not constant, it is expressed by the stress of a suitable part. Even in such cases, there are times when a buckling length based on Equation (2.1.2), i.e., $l_k = 1/m$ is used. When the compressive force along an axis, where both ends are pin-ended, changes to a tensile force, for the value of l_k, an intermediate value is used, which is shorter than the total length l and longer than the length of the compressed part. When the end conditions of the member are complex, it is frequently difficult to determine the physical meaning of the buckling length. This is because it is difficult to express the phenomenon of buckling in its entirety in terms of buckling length, and as is clear from the definition, even though the magnitude of the load buckling value is immediately expressed from the buckling length, it is not necessarily the case that the buckling deformation will coincide with the deformation of a solid compressive member having a buckling length. Consequently, while it is possible to employ the buckling length in calculating the load or stress, when deformation is taken into account, the latter is not easily handled.

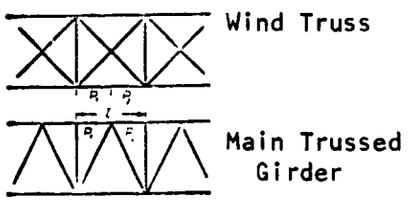

Figure 2.1.1

Figure 2.1.1 shows a member in which the joints cannot be freely moved to the sides. /103 In such a member, when the size of the compressive force on the left and right halves, considered from the center point, differs, if $P_1 > P_2$, it is possible to determine the buckling length by the following abbreviated formula with the load as P_1. This closely approximates the accurate value for buckling.

$$l_k = l(0.75+0.25\ P_2/P_1).$$

The above formula can also be used for tensile force, if the sign is made negative.

In a K truss column such as that shown in Figure 2.1.2, when the web member is made of solid angle steel, the buckling length, if $P_1 > P_2$ can be found from

$$l_k = l \cdot \left(0.84 + 0.16 \frac{P_2}{P_1}\right)$$

where the center load is P_1.

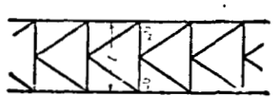

Figure 2.1.2

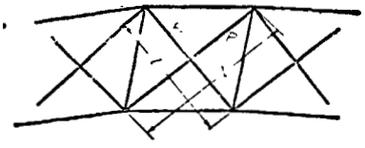

Figure 2.1.3.

If the members intersect, as shown in Figure 2.1.3, and one side is a compressive member (load P, member length l) and the other side is a tension member, (load P_1, member length l_t) if

$$\frac{P_t \cdot l}{P \cdot l_t} \geq 1$$

then one can use

$$l_k = 0.5\, l$$

In this case, there must be sufficient connection at the points of intersection, and it is necessary to employ rivets at least 1/3 of the rivets necessary for the connecting points of the compressive member. When

$$\frac{P_t \cdot l}{P \cdot l_t} < 1$$

one may use

$$l_k = l\sqrt{1 - 0.75 \frac{P_t \cdot l}{P \cdot l_t}}$$

In this case, it is necessary that at the points of intersection, the compressive members are adequately connected, and the geometrical moment of inertia is not weakened.

2.1.4. BUCKLING UNIT STRESS

In materials whose properties are characterized by the fact that the elasticity modulus and the Poisson ratio are related, and in which the proportional limit is present, the values of elastic buckling are calculated on the basis that in problems within that limit, these coefficients are assumed to take constant values irrespective of stress. The buckling unit stress which does not take into consideration the buckling values for the initial cross section of the member is called the average buckling unit stress.

$$\sigma_k = \frac{P_k}{A}. \tag{2.1.4}$$

In the case of a member with a constant cross section, σ_k is the unit stress wherein the part where P_k has a maximum value. In the case of a member with non-uniform cross-section, there are cases in which the size of σ_k changes in the direction of the member axis, and it becomes necessary to calculate σ_k in each cross-section, and to determine its maximum values. The necessity for determining the buckling unit stress is due to the fact that it contrasts directly with the properties of the material, e.g., the yield value, breaking value with respect to compression, etc. In materials such as carbon steel, in which yield phenomena clearly occur, it is frequently assumed that σ_k is not greater than its yield value. However, even in carbon steel, which has been strain-hardened, a distinct yield phenomenon is no longer observed, and in this case, with regard to σ_k, the stress for which the strain rapidly increases is made the limit. In Austenite steel, from the beginning of stress, there is no primary relationship between strain and stress. This is also true in concrete and lumber. There are methods which treat the modulus of that elasticity as a function of stress, in dealing with buckling problems in this kind of material. However, in ordinary calculations, the buckling load is calculated using constant coefficients.

In compressive members of soft steel used in structures, this can be /104
expressed as

$$\sigma_k = \frac{\pi^2 E}{\lambda^2} \tag{2.1.5}$$

within the proportional limit. The terms $\lambda = lk/i$ in the above equation are called the slenderness ratio. Equation (2.1.5) is sometimes called Euler's hyperbula, and is to be theoretically the maximum value of the compressive force of a slender member in which elastic buckling would occur. When the σ_k becomes greater than the proportional limit of the material, Equation (2.1.5) no longer expresses the actual resistance to compression of the member.

If the limits of resistance with respect to compression are expressed by the vague phenomena of large deformation, where $\lambda = 0$, the material should undergo large deformation at compression yield value $\sigma_{Y.P.}$, so a limit curve should be described with respect to compression between the proportional limit and $\sigma_{Y.P.}$ The shape of this limit curve is not based only on the properties of

the material, but is also related to the materials' configuration, and various curves have been cited from experiments. Various theories have been advanced by such people as Considére, Engesser, Jasinski, Kármán, Southwell, Chapmann to explain the experimental facts. Among them, the so-called Engesser-Kármán theory is the most popular at the present time. It is based on Considére's explanation. In the case of a steel column in a state of buckling and bending, with the part where the bending unit stress is 0 as the boundary, this is considered to be smaller than the modulus of elasticity E with respect to the bending compression unit stress (concave side of member) where the elasticity modulus E does not change with respect to the bending tensile unit stress (convex side of member). The reason for this is based on the results of single axis stress tests of soft steel, in which, when the stress exceeds the proportional limit, the proportional coefficients of stress and strain become smaller than the modulus of elasticity E below the proportional limit, with respect to increase in stress, whereas they become equal to E with respect to a decrease in stress.

According to this hypothesis, in place of the usual formula for buckling and bending,

$$E_r I \frac{d^2y}{dx^2} + Py = 0$$

is obtained. E_r is the coefficient which is inserted in place of E and is a function of the average unit stress of the member and the shape of the member. This becomes constant in a member of uniform sections, at any position in the direction of the member length. Within the elasticity range, if E_r is equal to E, it is possible to express all conditions by this formula. One may assume $E_r = E\zeta$, with $\zeta = 1$ within the elasticity range and $\zeta < 1$ in the non-elastic range. Using this form, Formula (2.1.5) becomes

$$\sigma_k = \frac{\pi^2 E \cdot}{\lambda^2} = \frac{\pi^2 E \zeta}{\lambda^2} \qquad (2.1.6)$$

ζ is related to the form of the cross-section, and there is less tendency for a decrease in where the cross-section is of compact form, than where it is of dispersed form. In Figure 2.1.4, changes in ζ above the limit of elasticity in section members and section members. This graph is of a test on soft steel St 37 with an elasticity limit of 2.05 t/cm^2. The compressive yield point of this material is 2.63 t/cm^2. However, the difference is not very great.

Bleich maintains that it is permissible to consider this to be constant in ordinary dimensions (1). If we assume that the slope of the curve of the compressive unit stress σ above the proportional limit and the strain ε to be /105

$$E_t = \frac{d\sigma}{d\varepsilon}$$

in a member with a rectangular cross-section, this is expressed as

$$E_r = 4EE_t/(\sqrt{E} + \sqrt{E_t})^2 \qquad (2.1.7)$$

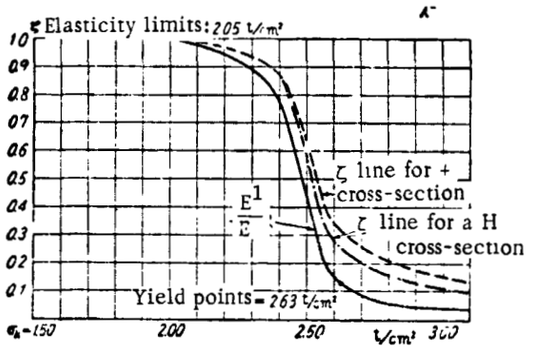

Figure 2.1.4.

and clearly values are obtained such that E E_r E_t. Such a E_r is called the reduced modulus or double modulus, and is useful in analyzing buckling tests above the proportional limits. However, in actual computations, often the tangent modulus E_i is used to determine the buckling unit stress. In such a case, this proves to be smaller than when E_r is used, and has the advantage of being a safer error, and making it possible to determine E_t by means of the load strain curve irrespective of the form of the member.

According to F. R. Shanley, in the initial period of buckling and bending,*1 deflection begins, due to the tangent modulus, and the load gradually increases. When the deflection increases, the tangent modulus soon reaches a constant value, and the load finally reaches a value which is given by the reduced modulus. It is not possible to determine the maximum load in the case when bending finally begins due to the central compressive load on an ideal column, using the tangent modulus. This is because up to this load, the column is perfectly straight, and the occurrence of bending is sudden. At this time, the sign of strain within the cross-section will not change. When the load becomes greater than the load indicated by the tangent modulus theory, bending immediately begins (2).

The experimental values come close to those which are usually given by the tangent modulus. This is considered to be due to various reasons. There are some cases in which the values from tests on columns having various member shapes, are processed and then used to calculate back to the values used for E_r or ζ in Equation (2.1.6). In such cases, the Tetmajer test and his linear equations are frequently referred to. This test covers soft steel members of section steel with various cross-sections and built-up steel with a compressive strength of 3.8 t/cm^2, and an elastic limit of 2.4 t/cm^2. The values obtained are

$$\lambda=10-105 \qquad \sigma_k=3.1-0.0114\lambda \quad \text{t/cm}^2$$

$$\lambda>105 \qquad \sigma_k=\frac{21.220}{\lambda^2} \quad \text{t/cm}^2$$

at $\lambda>105$, Euler's parabula is found, and the linear equation intercepts it rather than being tangent to it. Where λ is smaller, a method for processing

*1 F. R. Shanley's descriptions of this problem are carried in research literature published after item (2) in 1946. Column Paradox, Jour. Aero. Sciences, Vol. 13, No. 12 (1946-12), p. 678; Inelastic Column Theory, Jour. Aero. Sciences, Vol. 14, No. 5 (1947-5), pp. 261-267; Applied Column Theory, ASCE proc., scheduled for publication by (1949). Principles of Structural Design for Minimum Weight, Jour. Aero. Sciences (1949-3).

the test values by linear equation used by others besides Tetmajer. For example, T. H. Johnson maintains th.: the straight line is tangent to [literally "cuts"] Euler's parabula and at the curve with respect to a λ larger than this is effective (3). Generally, such a linear equation is of the type $\sigma_k = c_1 - c_2\lambda$. It is totally wrong to assign any sort of meaning to the constants c_1, c_2 in this equation. /106

The parabolic equation $\sigma_k = c_1 - c_2\lambda^2$ is also used in place of the linear equation. This is because, with the linear equation, it is difficult to obtain agreement with the elasticity limit, where $\lambda = 0$, at the yield point or the point of intersection with Euler's hyperbola, while if a parabula is used, the transition to Euler's hyperbola is achieved rather smoothly. The parabula for this equation was formulated early by J. B. Johnson, and in the case of carbon steel (0.10-0.15% C).

pin-ended at both ends $\sigma_k = 42{,}000 - 0.97\lambda^2$ lb/in²,

both ends flat $\sigma_k = 42{,}000 - 0.62\lambda^2$ lb/in².

One reason that the value of σ_k differs with respect to the same λ with different end conditions is that the l_k used for calculating λ is employed for the entire length of the member, irrespective of the end conditions. However, it is not this simple. The buckling length in the non-elastic range differs from the buckling length that is determined by theoretical calculations in the elastic range. Thus it is to be anticipated that the nature of the in the two above equations is rather complex. Figure 2.1.5 shows tests by Kármán comparing the buckling values of fixed and rotating ends. The abscissa uses l/i in place of while $m^2 = \sigma_k$ fixed end)/σ_k (rotating end) is expressed on the ordinate. When $l/i \leq 170$, since this ratio is for, this is equal to calculating the buckling length of a member with fixed ends, with $l_k = l/2$ and indicates Euler's elastic buckling value. However, where l/i 170, the buckling length of the fixed end members becomes $l_k = l/m$ and m becomes smaller than 2, especially when $l < 50$, this is $l_k = l$. That is, in the non-elastic range, the effect of the member end gradually becomes weaker with respect to the buckling length, and the fact that the coefficient (of) λ^2 in the two equations of J. B. Johnson given above is not to extreme, in spite of the difference in member end conditions, is due to the above reasons.

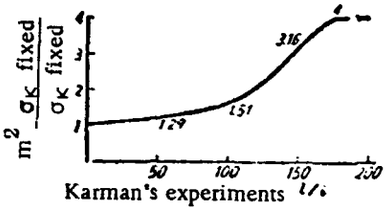

Karman's experiments

Christie's carbon steel (0.36% C) tests, Ostenfeld as

and the difference in the compressive strength expresses the fact that the smaller λ is, the greater is its effect. Nickel steel (<5% Ni) in comparison with carbon steel, resists a greater strength, the shorter the column. Schaller expresses this this by a linear f ula

The point of intersection of this formula with Euler's equation is = 86.

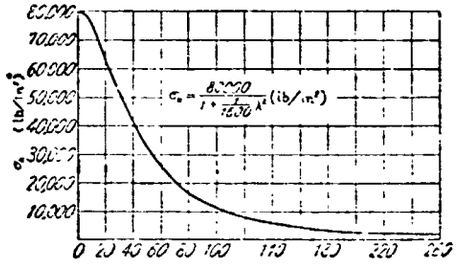

In the case of cast iron, when both ends are rounded, it is said that Rankine-Gordon's type of formula is suitable. This is shown in Figure 2.1.6.

$$\sigma_k = \frac{80{,}000}{1+\frac{\lambda^2}{1{,}600}} \quad \text{lb/in}^2.$$

Tetmajer has proposed linear equations for various members made of wood.

Figure 2.1.6.

$\lambda<100$ $\quad \sigma_k=0.293-0.00194\lambda$ t/cm², /107

$\lambda>100$ $\quad \sigma_k=987/\lambda^2$ 式中 $E=100$ t/cm².

Figure 2.1.7 indicates the relationship between the test values in this case and the above two formulas.

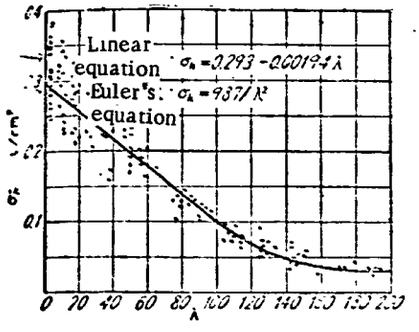

Figure 2.1.7.

The experimental grouping of the buckling unit stresses above, is divided into two regions: a short column range, and a long column range, or intwo three regions, including a range which is intermediate to these two. Usually the long column range is based on Euler's formula, while the other ranges are based on straight line formulas or parabolic formulas. In addition, methods for expressing the test values for the entire range by Rankine-Gordon's formula, and corrected eccentricity formulas have also been proposed. According to Ostenfeld's research, the straight line Euler's formula and parabolic Euler's formula agree well with the experiments, and are better than the corrected eccentricity formula, but he concludes that the Rankine-Gordon formula has a large average error (4). Roark makes a classification in two regions and states that the rupture value of a short column occurs when the unit bending edge stress due to direct pressure reaches a certain limit value. He explains that the limit value is the tensile yield point in structural steel, roughly the compression yield point in alloys, and at a point between the bending elasticity limit and the unit stress of rupture bending in lumber. He also states that there is a limit slenderness ratio which divides the short column and long column ranges (5).

In DIN Entwurf 2 E4114, with regard to soft steel (St 37) and low alloy structural steel (St 52), the buckling load in the case when an ideally central load is applied to an ideally linear member, and that member is ideally homogeneous, is called the ideal buckling load (ideale Knicklast) and the buckling load which deviates somewhat from this assumption is called the bearing load (Traglast, praktische Knicklast). If this is indicative of

Table 2.1.3

Circumference-length ratio λ	Ideal buckling stress σ_{kl}	Support stress σ_k	Circumference-length ratio λ	Ideal buckling stress σ_{kl}	Support stress σ_k
20	2,400	2,363	20	3,600	3,525
30	2,400	2,303	30	3,600	3,395
40	2,400	2,202	40	3,600	3,171
50	2,400	2,055	50	3,600	2,848
60	2,400	1,864	60	3,600	2,462
70	2,400	1,650	70	3,600	2,076
80	2,400	1,434	80	3,238	1,733
90	2,400	1,237	90	2,559	1,449
100	2,073	1,064	00	2,073	1,219
110	1,713	919	110	1,713	1,035
120	1,439	797	120	1,439	887
130	1,226	695	130	1,226	767
140	1,057	611	140	1,057	669
150	921	540	150	921	588
160	810	480	160	810	520
170	717	429	170	717	464
180	640	386	180	640	415
190	574	348	190	574	374
200	518	316	200	518	339
210	470	288	210	470	308
220	428	263	220	428	281
230	392	241	230	392	257
240	360	222	240	360	237
250	332	205	250	332	218

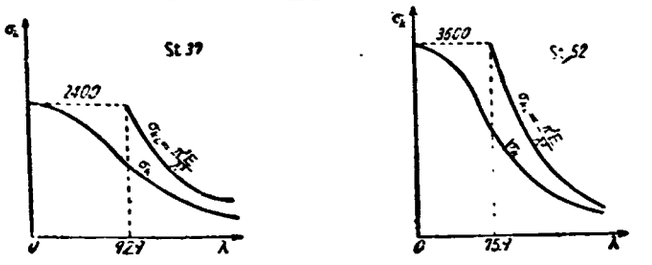

respect to λ, Table 2.1.3 is obtained. Below the strength characteristics of these types of steel are indicated.

E=2,100,000 kg/cm²,

G=810,000 kg/cm².

Yield point

St 37 σ_F=24–28 kg/mm²

St 52 (thickness less than 18mm) $\sigma_F \geq 36$ "

(>18–30 mm) $\sigma_F \geq 35$ "

(>30–50 mm) $\sigma_F \geq 34$ "

Tensile Strength

St 37	σ_B=37–45	kg/mm²
St 52 (thickness less than 18mm	σ_B=52–62	"
(>18–30 mm)	σ_B=52–64	"
(>30–50 mm)	σ_B=52–64	"

The standards for these constituents of these types of steel are given in Tables 2.1.4 and 2.1.5.

Number	Symbol	Refining method	Maximum quantity of components							
			Ladle analysis				Analysis of finished product			
			C	P	S	P+S	C	P	S	P+S
1	St 37.12	Thomas process	0.16	0.09	0.06	0.13	0.192	0.126	0.084	0.182
2		Siemens-Martin process	0.20	0.06	0.06	0.10	0.240	0.084	0.084	0.140

Component %	C	Si	Mn	Cu	S	P	S+P	Additive		
								Mn	Cr	Mo
St 52	≤0.20	≤0.50	≤1.2	≤0.55	≤0.06	≤0.06	≤0.10	0.30	0.40	0.20

In both types of steel, ST 37 and ST 52, there is no difference in the ideal buckling value within the range of Euler's hyperbola. This is because their E's are equal. Consequently, for long columns, there is not much benefit in using high yield point steel. However, in short columns, it is effective, and the DIN has a $\lambda < 92.9$ for this portion for ST 37, and a $\lambda < 75.9$ for ST 52, with constant values for the ideal buckling of minimum yield points of σ_F = 2,400 kg/cm² and σ_F = 3,600 kg/cm² respectively. Sometimes an approach is used where the short column area is considered as a horizontal line, and an immediate transition is made to an Euler hyperbola. This can be seen in Jezek's book (6). The bearing buckling value is lower than the ideal buckling /109 value. The [illegible: computation ?] of this value is based on Jezek's approach. Here, continually keeping the eccentricity of the load in mind, the edge unit stress of the cross-section due to buckling bending reaches the compressive yield point, and then is considered to extend over a certain range. Before explaining this approach in detail, let us show that it is possible to indicate approximately the bearing buckling value by Rankine-Gordon's formula.

For St 37

$$\sigma_k = \frac{2400}{1+1.4\left(\frac{\lambda}{100}\right)^2} \quad \text{kg/cm}^2, \tag{2.1.8}$$

For St 52

$$\sigma_k = \frac{3600}{1+2.2\left(\frac{\lambda}{100}\right)^2} \quad \text{kg/cm}^2. \tag{2.1.9}$$

where $\lambda = 0$, these formulas return to their respective yield points, and when λ is large, theysuccessively approximate Euler's curve. For example, the formula for St 37 has an error of about -6% for the bearing buckling value, where $\lambda = 100$ and +14% where $\lambda = 200$. In the St 52 formula, it is -8% where $\lambda = 100$, -8% where $\lambda = 200$, and +11% where $\lambda = 250$, but in both formulas, where $\lambda \to \infty$, $\sigma_k = 0$ is obtained, and this coincides with the bearing buckling value.

Considered from this point of view, Tetmajer's straight line allowable stress formulas which were defined in the regulations for the implementation of the laws for city architectural structures in our country for a long period of time are simple, and in this sense, should deserve review. I should like to add that in the present structural standards for architecture in our country (8) it is stated that as far as columns are concerned, long columns can be expressed by the Euler hyperbola, using the same procedure as the German standard which is older than that in DIN E 4114. As for short columns, it is possible to divide this into the method of expressing by straight line formula but the old German standard is based on the straight line formula and ours is based on the parabolic formula. These expressions are actually quite close to those obtained experimentally, but since in actual structures, various conditions differ from those in the laboratory, so that one can understand why the claim that it is more appropriate to determine the bearing load by keeping the eccentricity of load in mind, follows the lines laid down in DIN E 4114.

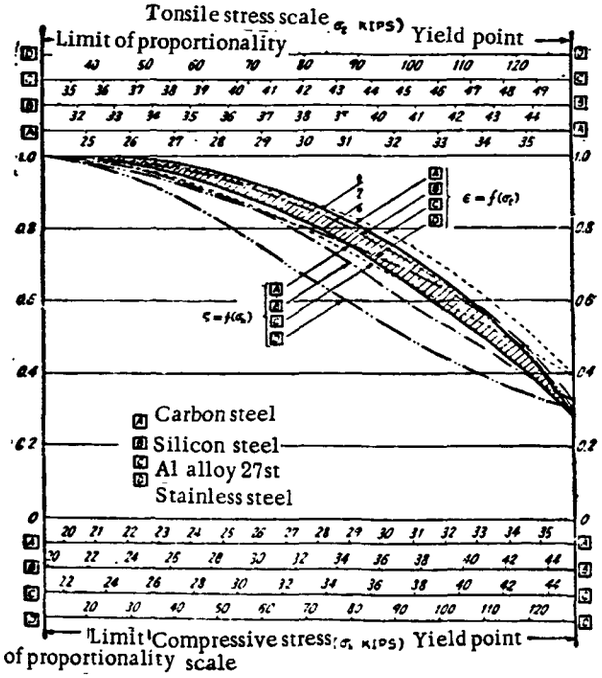

There is a very interesting section in Balog's criticism (10) of Moisseiff and Lienhard's paper (9), on the $\zeta = E_r/E$ in formula (2.1.6). E_i/E, E_c/E and E_t/E are all functions of the average unit stress σ within the plain of a number, but in steel and aluminum, E_c/E is greater than E_t/E and E_r/E is smaller than E_t/E. If we place the range of stress up to the yield point from the proportional load on the abscissa and graphically represent E_r/E and E_t/E a type of closed curve such as that shown in Figure 2.1.8 is described. In this case, since the range of stresses differs considerably in tension tests and compression tests, the device shown in the scale on the abscissa is used. The width between these closed curves, the higher the yield point and the wider the stress

/110

range, and if this is taken into consideration, it is possible to reduce it to a single functional relationship for various types of metal. When this relationship is determined for one type of metal, it is only necessary to conduct tension tests in order to determine E_r/E. Balog states that whereas determination of E_r/E by buckling tests is very inaccurate due to test errors, the E_t/E calculated in tension tests is accurate, and test is easy to conduct, and he recommends that ζ should be determined by this method. For example, using carbon steel as a standard, we shall indicate its closed curve by the hatched section in Figure 2.1.8. Expressing the yield point of this material as σ_{yc}, the range of stress of the proportional limits and the yield point as C_{yr}, the width of the closed curve at any point as η, the E_r/E belonging to other metals can be determined by first determining E_t/E experimentally by tension tests and then subtracting

$$\Psi = \frac{\sigma_{yr} X_{yr}}{\sigma_{yx} C_{yr}} \eta \qquad (2.1.10)$$

from this. Here σ_{yx} is the required tension yield point of the metal, X_{yr} is the range of stress between the proportional limit of the metal and the yield point. Assuming σ_{yc} = 36 kips/in^2, C_{yr} = 16.61 kips/in^2, where in silicone steel, σ_{yx} = 49 kips/in^2, X_{yr} = 25.12 kips/in^2, Ψ = 1.21η. In aluminum, σ_{yx} = 45 kips/in^2, X_{yr} = 24.07 kips/in^2 is obtained, so Ψ = 1.16η, and since in stainless steel σ_{yx} = 130 kips/in^2, X_{yr} = 120 kips/in^2, Ψ = 2.0η. These values match quite accurately the E_r/E obtained in tests.

2.1.5. ALLOWABLE BUCKLING UNIT STRESS OF CENTRALLY COMPRESSED MEMBERS

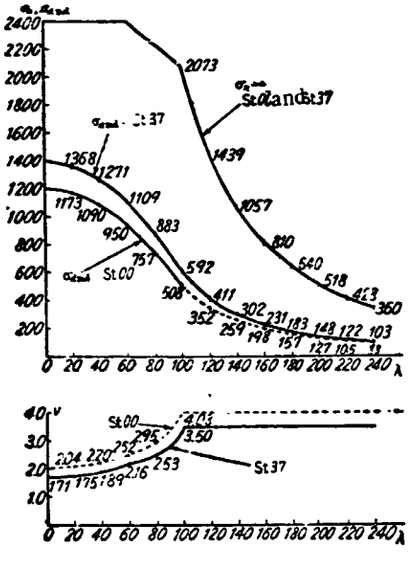

Figure 2.1.9

When the buckling bearing unit stress is divided by the safety factor, the allowable buckling unit stress is obtained. The formulas vary depending on the method of expressing the bearing unit stress. In the old German standards, the bearing stress is expressed by the Tetmajer-Euler formula. Within the range of the Euler curve, those for ST 37 and for St 52, with a safety factor of 3.5, maintain a constant value, and with respect to stresses above the proportional limit, the safety factor is gradually reduced from 3.5, and where λ = 0, i.e., the yield value of the material, it was 1.71 (11). In Figure 2.1.9, the safety factor ν is between λ = 0 and 100, and is shown to vary according to the two parabolic lines. In DIN Entwurf 2 E 4114, the bearing buckling value is determined, taking into consideration the eccentricity of the load, and with respect to this, the safety factor ν is 1.71 within the entire range of λ. Table 2.1.6

indicates the allowable buckling values obtained in this manner. In the old German standards, the long column range was in the form of an Euler's hyperbola, while in the short column range, it was a parabolic curve.

$$f_k = 1400 - 0.0808\lambda^2 \qquad 0 < \lambda < 100,$$

$$f_k = \frac{\pi^2 E}{\nu \cdot \lambda^2}, \qquad \nu = 3.5 \qquad \lambda > 100.$$

Table 2.1.6

Circumference-length ratio λ	St 37 Allowable stress (σ_{zul}=14,00)	Coefficient of buckling ratio ω	Circumference-length ratio λ	St 52 Allowable stress (σ_{zul}=21,00)	Coefficient of buckling ω
20	1,378	1,016	20	2,056	1,021
30	1,343	1,042	30	1,980	1,060
40	1,284	1,090	40	1,850	1,135
50	1,199	1,168	50	1,661	1,264
60	1,087	1,288	60	1,436	1,462
70	962	1,455	70	1,211	1,734
80	836	1,674	80	1,011	2,077
90	722	1,940	90	845	2,484
100	621	2,256	100	711	2,953
110	536	2,612	110	604	3,478
120	465	3,011	120	517	4,059
130	405	3,453	130	447	4,694
140	356	3,928	140	390	5,381
150	315	4,444	150	343	6,122
160	280	5,000	160	303	6,923
170	250	5,594	170	271	7,759
180	225	6,218	180	242	8,675
190	203	6,897	190	218	9,626
200	184	7,595	200	198	10,619
210	168	8,333	210	180	11,688
220	153	9,125	220	164	12,811
230	141	9,959	230	150	14,008
240	129	10,811	240	138	15,190
250	120	11,707	250	127	16,514

/111

The Japan architectural standards JES 3001 employs this form, and the allowable buckling values for a long load in structural steel is

$$\lambda \leqq 30 \qquad f_k = f_c,$$

$$30 < \lambda \leqq 100 \qquad f_k = f_c \left\{1 - 0.4\left(\frac{\lambda}{100}\right)^2\right\},$$

$$\lambda > 100 \qquad f_k = 0.6 f_c \Big/ \left(\frac{\lambda}{100}\right)^2.$$

The modulus of elasticity of steel is 2,100 t/cm^2.

The standards do not make clear how reinforced concrete structures should be treated, but in the case when the minimum diameter of a compressed member

of rectangular cross-section is less than 1/15 of the distance between the main support points, they stipulate that the inspection be made with respect to buckling.

In wooden structures, the short column range is expressed by a straight line formula. /112

$$\lambda \leqq 100 \qquad f_k = f_c(1-0.007\lambda),$$

$$\lambda > 100 \qquad f_k = 0.3 f_c \Big/ \left(\frac{\lambda}{100}\right)^2.$$

The differences in the type of material are simply included in the allowable compressive unit stress f_c, and the moduli of elasticity are defined as 70 for cryptomeria, 80 for cypress (henoki) and 90 t/cm^2 for pine.

When defining the allowable unit buckling stress as above, it is possible to calculate the buckling design by various methods. Expressing the load as P and the total cross-section area as A, we have the condition

$$\sigma = \frac{P}{A} < f_k$$

f_k has a value which differs according to the size of λ. The DIN uses a method according to which in performing calculations, instead of directly comparing σ with this f_k, it is compared with an allowable compressive unit stress f_c which has a constant value and is unrelated to λ. It uses

$$\omega = \frac{f_c}{f_k} > 1 \qquad (2.1.11)$$

Multiplying this by the compressive force P

$$\sigma_\omega = \frac{\omega P}{A} < f_c \qquad (2.1.12)$$

is used. This method is called -Verfahren, and is also used outside of Germany. Generally the method of increasing the load proportionally in this manner in performing calculations on structures, and contrasting it with a constant allowable unit stress, has several advantages. The fact that the safety factor in each part of the structure is maintained constant, taking the degree of influence of the load into consideration, is derived from the fact that it is possible to superimpose them linearly with respect to various load combinations. The allowable compressive unit stress for three types of steel is

for St 00 $f_c = 1.2$ t/cm^2,

for St 37 $f_c = 1.4$ t/cm^2,

for St 52 $f_c = 2.1$ t/cm^2.

Table 2.1.7

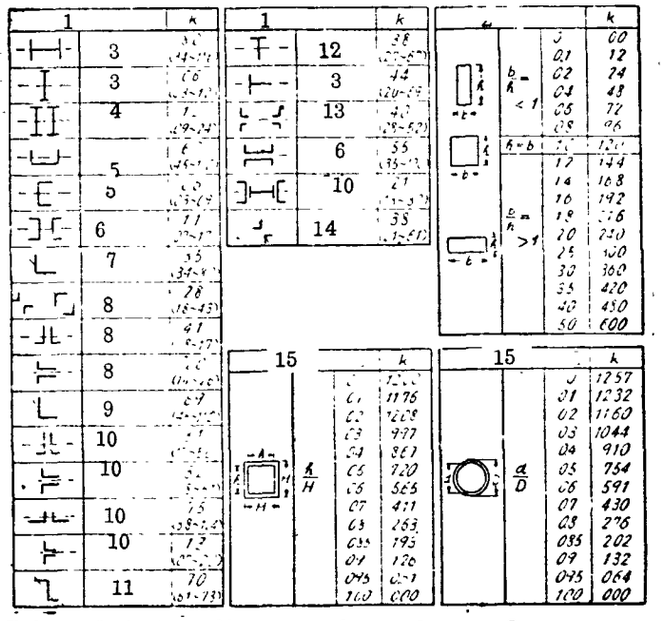

Key:
1. Cross-section configuration
2 Rectangular cross-section
3. I - beam
4. 2 I-beam
5. Channel
6. 2 - Channel
7. Equal sided angle
8. 2 - Equal sided angle
9. All equal sided angle
10. 2 - Unequal sided angle
11. Z shaped
12. T shaped
13. 4 - equal sided angle
14. 2-channel and I - beam box Nittestu catalogue
15. Hollow rectangular

Table 2.1.6 indicates the values of ω.

There is an abbreviated method (12) for determining the cross-section of a compressive member, using the configuration index k proposed by Gehler in his description in DIN Entwurf E 4114 (12). /113

$$k=\frac{A}{i^2}=\frac{I}{i^4}. \tag{2.1.13}$$

What is interesting here, is the fact that when the cross-section configuration is the same, the value of k is restored within a certain range for commercial lumber and combinations of it, so using its intermediate value, it is possible to determine the required cross-section area of the compressive member, or its geometrical moment of inertia. In Table 2.1.7, the average values of k and its range are quoted from volume II of the Textbook on Structures published by the Japan Architectural Society (13). Here, let us attempt an explanation following the method proposed by the Society. Assuming

$$\eta=\omega\left(\frac{\lambda}{100}\right)^2 \tag{2.1.14}$$

this is a quantity determined by ω and λ, but

$$\frac{\omega P}{A}\leq f_c \qquad\qquad \omega\leq\frac{Af_c}{P}=\frac{If_c}{i^2P}$$

Therefore

$$\eta\leq\frac{I\cdot f_c}{i^2\cdot P}\left(\frac{l_k/i}{100}\right)^2=k\left(\frac{l_k}{100}\right)^2\frac{f_c}{P} \tag{2.1.15}$$

Each item on the right side is determined ahead of time in designing, excluding k and the intermediate values of k are found from the table. Since ω and λ are numbers that are determined with respect to each other, if η is given, λ is also determined.

The following formula is used to determine the required cross section of a compressive member.

(2.1.16)

The accuracy of this abbreviated method depends on the value of k, but if the error is increased up to A_n, there is no effect. If carefully scrutinized, one can see that the actual required values are easily obtained.

Below is a comparison of various forms for the buckling allowable unit stress (lb./in.^{2})*1.

Table 2.1.8

	New York	Chicago	Philadelphia	Boston
Soft steel	$16{,}000-70\frac{l}{i}$	$16{,}000-70\frac{l}{i}$	$\frac{16{,}250}{1+\frac{l^2}{11000i^2}}$	$\frac{18{,}000}{1+\frac{l^2}{20{,}000i^2}}$
Cast iron	$9{,}000-40\frac{l}{i}$	$10{,}000-60\frac{l}{i}$	$\frac{11{,}160}{1+\frac{l^2}{400d^2}}$	$9{,}000-40\frac{l}{i}$

The forms for New York and Chicago are straight line formulas, whereas for Philadelphia and Boston are Rankine-Gordon formulas. However, in the California Administrative Code (14), the standards for the compressive members of structural steel are as follows. These standards define the calculation of stress by net cross-section.

When $1/i \leq 20$

rolled steel 20,000 lb./in.^{2}

cast steel 16,000 lb./in.^{2}

When $20 < 1/i \leq 120$ /114

$$f_k=17{,}000-0.485\frac{l^2}{i^2} \quad \text{lb/in}^2,$$

$$f_k=\frac{18{,}000}{1+\frac{l^2}{18000i^2}}\cdot\left(1.6-\frac{l}{200i}\right) \quad \text{lb/in}^2.$$

*1The forms given in the regulations for the implementation of the City Architectural laws published in our country are the same as for New York and Chicago indicated here.

This standard is expressed by a parabolic formula in the short column range, but in the long column range, it is expressed by a Rankine-Gordon deformation formula.*1 This improved formula was corrected so that [it] is 0 when 1/i = 320. The 1/i of main compression is restricted to below 180 and the secondary compressive member is also restricted to below 200.

Next, considering the buckling equation of a reinforced concrete column in terms of this standard,*2 when, for a minimum diameter d and column length l

$$l > 11d$$

the allowable buckling unit stress is determined by the following calculation.

$$f_k = f_c\left(1.33 - 0.03\frac{l}{d}\right).$$

Moreover, when the column undergoes a constant bending, it is restricted to

$$l < 24d$$

2.1.6. ECCENTRICALLY COMPRESSED MEMBERS

No member is completely homogeneous, and no member is completely devoid of flaws. There are no cases in which the compressive load of a column is not accompanied by some degree of eccentricity, and it is difficult to say that actually the line of the axis does not have an original bending. In a frame member (Rahmen), compressive stress and bending moments are both always involved. One may ask whether the equations and design formulas given for a centrally compressed member, such as those described up to this point, actually have any significance. Before touching on this question, let us first indicate the relationships between the eccentric compressive load and deflection that are given in various references. Figure 2.1.10 is given in R. V. Southwell's book (15). The ordinate expresses the terms that are proportional to the load, while the abscissa indicates the terms that are proportional to deflection. The uppermost curve is the relationship between deflection and load after the Euler load values in the case when the curvature of the deflection curve is accurately expressed for a centrally compressed load member, and this is frequently seen in other books. This curve is Euler's load value, and is tangent to the horizontal line when the deflection is 0. Moreover, the lowest curve is that which is obtained as a solution of the case when the curvature of the curve of deflection of an eccentrically compressed loaded member is determined by approximation, and a right angle hyperbola is described. When the load is 0, and there is deflection, this is due to original eccentricity. This curve /115 is also seen in many books. With the buckling load, the deflection becomes infinitely large, and long before it reaches the Euler load value, it is sur-

*1 This can be considered as a multiplication of the Rankine-Gordon formula and the Tetmajer formula.

*2 Standards 750, 755 in reference (14).

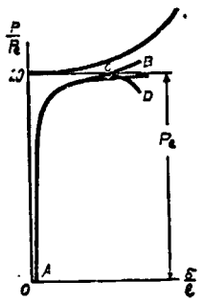

Figure 2.1.10

mised that the member will cut into the proportional limit or the yield point. Moreover, one feels a contradiction in using approximation equations for the curvature in considering these limits. Curve AB should correspond to this and a member with a small initial original curvature, undergoes an increase in load along the right angle hyperbola at the initial moment of deflection, but ultimately a curve is established which matches a curve determined by inaccurate equation of curvature.

Curve ACD further takes into account the stress as a property of the column material. We shall attempt to consider that the column is slender, the Euler limit values are low, and that the material does not undergo elasticity loss under direct compression. If the deflection increases, the bending P also increases and the point at which the bending edge unit stress ultimately reaches the elasticity limit is C. As long as the column is not extremely slender, point C is close to the Euler limit value. The resistance of the material will decrease prior to this, so that the curve from point C becomes distant from curve AB and moves downward. When curve ACD becomes horizontal, the stable equilibrium is lost. Viewed in this manner, the highest point of ACD is the rupture value, and this can be regarded as close to the Euler value. However, not only is it true that these two load values do not agree with each other, but only one of them can be expressed in elasticity theory, and the fact that they agree approximately also depends on the two conditions which arise in tests on a column which is loaded for a long period of time and accurately. The first of these conditions is that when the material no longer follows Hooke's law, the deflection has progressed considerably, and the second condition is that the considerable portion of the deflection of curve AB approaches the line expressing the Euler value.

In spite of this type of explanation of Southwell, numerical interpretations of ACB and ACD are not seen in his book, and the analytical properties of the curve itself are vague. In particular, ACB is a curve which should be expressed only by elasticity theory, but its inflection point appears as if it is at the point of bifurcation from the right angle hyperbola. Figure 2.1.11 is taken from the book by J. Ratzersdorfer (16). Where the eccentricity e/l is 0.01, and where it is 0.1, the curves have inflection points at Euler's load value. Such a graphic illustration is also found in K. Jezek's book, and in both cases, since there is no careful numerical treatment of them, they are both vague. In other words, these authors have focused on qualitative observations of these curves, and apparently do not consider them as important for buckling problems. On the other hand, this may be due to the fact that calculation of this curve involves troublesome and monotonous elliptical integration. A. Schleussner's book (17) is an important reference on this subject, and recently K. L. Ryder's paper and criticisms of it have appeared in "Transaction, A.S.C.E." (1948), pp. 40-78.

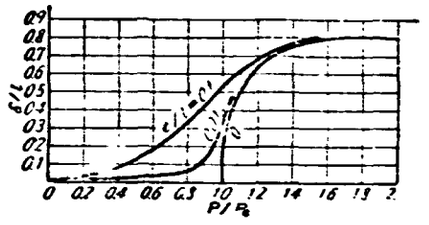

Figure 2.1.11

The deflection curve of a compressive member in which the load eccentricity and the member axis have initial curvature is expressed by using an approximation equation for curvature and expressing the extreme fiber stress of the convex and concave sides of the deflection by this (18)

$$\sigma=\sigma_a\left[1\pm\frac{c}{i^2}\left\{e_0\sec\frac{l}{2i}\sqrt{\frac{\sigma_a}{E}}+\frac{8Ee_1i^2}{l^2}\left(\sec\frac{l}{2i}\sqrt{\frac{\sigma_a}{E}}-1\right)\right\}\right].$$

In the equation, $\sigma_a = P/A$, c is the distance from the neutral axis of the section to the compressed extreme, e_0 is the eccentricity of the load and e_1 is assumed to form a parabula such that the initial curvature of the member axis is expressed by

$$y=e_1\left(1-\frac{4x^2}{l^2}\right)$$

/116

Here, assuming

$$\frac{e_0c}{i^2}=\frac{e_1c}{i^2}=0.03$$

and depicting the extreme fiber stress of the cross-section for the compressed side and the tension side, Figure 2.1.12 is obtained. In the case of a short column, it is easy for the extreme fiber stress on the convex and concave sides to reach the limit of elasticity such that this is expressed by the line 1/i = 30. In a column of intermediate length, only the concave side passes through the limit of elasticity, while the convex side finally reaches a maximum value under that condition. The resistance of the column at this time reaches its limit point before the convex side becomes a tensile stress. In the case of a long column, there is no case in which the extreme fiber stress passes through the limit of elasticity. The stress of the convex side sometimes becomes tension. The curve 1/i = 139 indicated by the dotted line is that obtained in Tetmajer's experiment (E. H. Salmon: Columns, p. 215.).

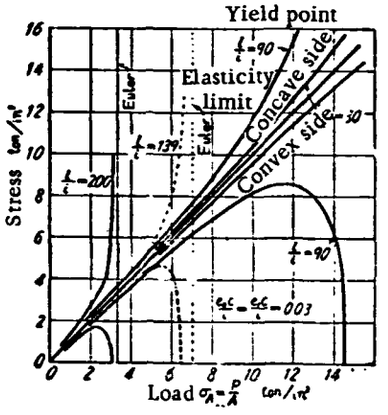

Figure 2.1.12

The maximum compressive extreme fiber stress in the case where the load eccentricity is e, the vertical stress is P, and the bending moment M = P·e. is operating, is expressed by the so-called Secant equation. S is the core distance.

$$\sigma=\frac{P}{A}\left(1+\frac{e}{s}\sec\frac{l}{2i}\sqrt{\frac{P}{AE}}\right). \qquad (2.1.17)$$

If in this equation we assume $\sigma_{Y.P.}$, and solve for P, the limit stress of a member with an eccentric load is determined (19).

Using ν as the safety factor, the allowable stress under such load conditions must be found from $P_f = P/\nu$. However, sometimes there are cases in which σ is restricted to a specific constant σ_{const} which is below $\sigma_{Y.P.}$, and by this means, P is determined.*2 In this case, a safety factor is not guaranteed such that $\nu = \sigma_{Y.P.}/\sigma_{const}$.

In a member with initial curvature, when the form of the axis is expressed by

$$y=a\sin\frac{\pi x}{l}$$

assuming load at both ends to be P

$$\sigma=\frac{P}{A}\left(1+\frac{a}{s}\cdot\frac{1}{1-\frac{P}{P}}\right).$$

In particular, if we assume that σ is equivalent to $\sigma_{Y.P.}$, it is possible to calculate the values of P. In this case, since $P_k = \pi^2 EI/1^2$, it is possible to determine the average compressive stress intensity $\sigma_a = P/A$ from <u>/117</u>

$$\sigma_{Y.P.}=\sigma_a\left(1+\frac{a}{s}\cdot\frac{1}{1-\frac{\sigma_a}{\pi^2 E}\frac{l^2}{i^2}}\right) \tag{2.1.18}$$

In the case of a [obliterated text: sine curve without initial curvature?] since the deflection which is applied by the load may be [obliterated text: determined by ?] the sine curve, assuming the added deflection at the center point of the column to be a_1, using Mohr's equation

$$\left(EI-\frac{Pl^2}{\pi^2}\right)a_1=\frac{Pl^2a}{\pi^2}. \tag{2.1.19}$$

The initial curvature at the column center point is $\pi^2 a/1$, and after deflection has occurred, since this becomes $\pi^2(a + a_1)/1^2$, if bending moment is also included in the change in curvature,

$$\frac{\pi^2(a+a_1)}{l^2}-\frac{\pi^2 a}{l^2}=\frac{M}{EI}=\frac{\sigma_m}{cE}.$$

The σ_m in the above equation is the extreme fiber stress which is based on the bending moment at position c from the neutral axis of the section. The actual extreme fiber stress becomes the sum of σ_m and the average stress intensity $\sigma_a = P/A$, $\sigma = \sigma_m + \sigma_a$, so

$$a_1=\left(\sigma-\frac{P}{A}\right)\frac{l^2}{\pi^2 cE}. \tag{2.1.20}$$

*1 According to the examples in footnotes on page 439 of R. V. Southwell, Theory of Elasticity, this method forms the basis for the design equations of the British Air Ministry.

From Equation (2.1.19) and Equation (2.1.20), if a_1 is eliminated, the following relationship is determined for the load P.

$$\left(EI-\frac{Pl^2}{\pi^2}\right)\left(\sigma-\frac{P}{A}\right)=Pac\,E.$$

solving this quadratic equation,

$$\sigma_a=\frac{1}{2}\left\{\left[\sigma+\sigma_e\left(1+\frac{a\cdot c}{i^2}\right)\right]\pm\sqrt{\left[\sigma+\sigma_e\left(1+\frac{a\cdot c}{i^2}\right)\right]^2-4\sigma\sigma_e}\right\} \tag{2.1.21}$$

In the above equation σ_e is Euler's buckling unit stress, i.e., P_e/A. If the extreme fiber stress σ is made to agree with a constant value, e.g., the limit of elasticity or the yield point $\sigma_{Y.P.}$, the average stress intensity σ_a is established. This formula is called the Wow formula and together with the Secant formula (16), it is frequently noted in reference works on buckling as a theoretical equation for determining the critical values of eccentric compressive load (20). Van den Broek skillfully utilized this formula to explain buckling of a straight member. If a = 0, the inside of the square root sign on the right side of the equation (2.1.21) becomes $[\sigma - \sigma_e]^2$ so if the sign in front of the square root sign is +, $a = \sigma_{Y.P.}$ Moreover, if - is used, $\sigma = \sigma_e$, i.e., it is possible to match this with Euler's buckling unit stress.

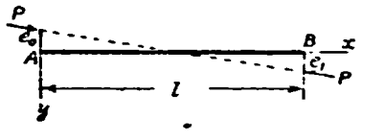

Figure 2.1.13

When the load curve intersects the material axis as shown in Figure 2.1.13, in a short column, the extreme fiber stress in the part where the bending moment of the member end is large, first reaches the yield point, and the resistance is determined by this. Assuming $e_0 > e_1$,

$$\frac{P}{A}=\frac{\sigma_{Y.P.}}{1+\frac{e_0}{s}}. \tag{2.1.22}$$ /118

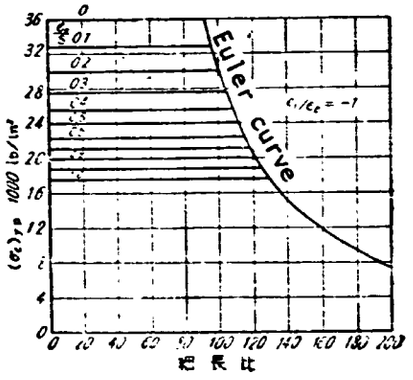

Figure 2.1.14

If the member length is large, the extreme fiber stress due to bending is

$$\sigma=\frac{P}{A}\left(1+\frac{e_0}{s}\,\frac{\sqrt{(e_1/e_0)^2-2(e_1/e_0)\cos\sqrt{P/EI}\cdot l+1}}{\sin\sqrt{P/EI}\cdot l}\right) \tag{2.1.23}$$

Assuming σ to be equal to $\sigma_{Y.P.}$, if e_1/e_0 and e_0/s are given, it is possible to determine P. When the load passes through the center of the member axis, $e_1/e_0 = -1$ and if the average compressive stress intensity P/A with regard to various e_0/s is expressed for the slenderness ratio l/i, Figure 2.1.14 is obtained. With

respect to the given e_0/s, in the short column region, P/A is constant, and is calculated from Equation (2.1.22). In the long column region, in this case, it agrees with Euler's hyperbola. When the absolute value of e_1/e_0, is smaller than 1, as the slenderness ratio from the portion expressed in Equation (2.1.22) increases, gradually this becomes expressed by the asymptotic curve which moves toward Euler's curve.

2.1.7 Ultimate Buckling Theory

Recently in general structural design, an ultimate strength is used as a basis, with respect to which the safety factor is established. This has come to be used in order to achieve the two objectives of reduction in weight and economy of materials. At the same time, it is used for planning the effective design of materials taking advantage of their special characteristics. With regard to buckling, this trend has been evidenced since before the establishment of DIN E 4114, and as a result, instead of determining the limit values by the conventional Euler's load and Tetmajer's straight line formula, and then determining the allowable stress intensity on the basis of this, it has become customary to use the support load as the basis. By means of this method, it has become possible to rationalize the safety factor.

In compressive members, for some reason or other, bending is always present. As for applicability to elasticity theory, it is systematic to consider the time at which, taking this quantity into consideration, the maximum extreme fiber stress reaches the yield point, to be the critical point of the member, and by this means, the critical load given by the Secant formula and the Wow formula is determined. However, according to experiments by many investigators of ultimate strength theory, even after the maximum extreme fiber stress, in the case of bending stress, reaches the yield point, it is known that an even greater load can be withstood. That is, the distribution of stress within the section reaches as far as the yield point inside, from the extreme fiber. The viewpoint of K. Jezek with regard to a steel column is similar to this, and Van den Broek has also developed a similar approach (21).

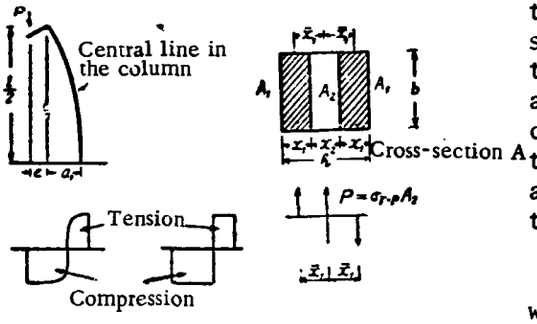

Figure 2.1.15

If we consider the case, such as that of soft steel, in which the stress strain curve is symmetric with respect to the compression side and the tension side, and the stress intensity, considering the column as having a rectangular cross-section, reaches the respective yield values, a stress distribution is obtained such as that shown in Figure 2.1.15.

From the equilibrium of stresses within the stresses

$$\sigma_{Y.P.}A_2 = P,$$

$$2\sigma_{Y.P.}A_1\tilde{x}_1 = P(e+a_1).$$

/119

If we assume that the added deflection a_1 is directly proportional to the square of the member length l

$$a_1 = kl^2.$$

using the symbols in the figure, and adjusting these equations

$$\frac{P}{A} = \frac{2\sigma_{r.p.}}{h}\left[\sqrt{\frac{h^2}{4} + (e+kl^2)^2} - (e+kl^2)\right]. \tag{2.1.24}$$

here the proportion coefficient is expressed by

$$k = \frac{\frac{h}{4}\left(\frac{A\sigma_{r.p.}}{P_1} - \frac{P_1}{A\sigma_{r.p.}}\right) - e}{l_1^2} \tag{2.1.25}$$

Here P_1 is the load value in the case of a member length of l_1 when in the above stress condition. In the above two equations, assuming in particular, e = 0, and eliminating k

$$\frac{P}{A} = 2\sigma_{r.p.}\left\{\sqrt{0.25 + \left[\frac{1}{4(l_1)^2}\left(\frac{A\sigma_{r.p.}}{P_1} - \frac{P_1}{A\sigma_{r.p.}}\right)\right]^2 l^4} - \frac{1}{4(l_1)^2}\left(\frac{A\sigma_{r.p.}}{P_1} - \frac{P_1}{A\sigma_{r.p.}}\right) l^2\right\}.$$

This equation covers the short column range. If we assume in the above equation that

$$\frac{P_1}{A} = \sigma_p \quad \cdots \quad \text{Proportional Limit}$$

the long column range is defined as that which is connected by this point.

$$\frac{P}{A} = 2\sigma_{r.p.}\left\{\sqrt{0.25 + \left[\frac{1}{4l_p^2}\left(\frac{\sigma_{r.p.}}{\sigma_p} - \frac{\sigma_p}{\sigma_{r.p.}}\right)\right]^2 l^4} - \frac{1}{4(l_p)^2}\left(\frac{\sigma_{r.p.}}{\sigma_p} - \frac{\sigma_p}{\sigma_{r.p.}}\right) l^2\right\}.$$

Moreover, if P_1 and l_1 are used as the values for the long column range, actually, since we can assume $P_1 = \pi^2 EI/l_1^2$

$$\frac{P}{A} = 2\sigma_{r.p.}\left[\sqrt{0.25 + \left(\frac{\sigma_{r.p.}^2 - \sigma_{1e}^2}{4\sigma_e \sigma_{r.p.}}\right)^2} - \frac{\sigma_{r.p.}^2 - \sigma_{1e}^2}{4\sigma_{r.p.}\sigma_e}\right]. \tag{2.1.26}$$

The σ_e and σ_{1e} in this equation are respectively the buckling values of Euler's theory for the member length l and l_1. When the member length becomes extremely long, Euler's value is expressed by the above equation, and when the member length is of an intermediate size, it expresses the stress conditions in the case of ductile equilibrium. Since P_1 and l_1 are of a magnitude selected in any long column range, if the point which agrees with Euler's equation is selected for the case when the member length is infinitely large ($l_1 \to \infty$), this becomes $\sigma_{1e} = 0$, so

$$\frac{P}{A}=\sigma_{Y.P}\left[\sqrt{1+\left(\frac{\sigma_{Y.P.}}{2\sigma_e}\right)^2}-\frac{\sigma_{Y.P.}}{2\sigma_e}\right]. \tag{2.1.27}$$

Equation (2.1.27) gives the critical buckling values in the case in which the sectional stress is in the yield state (tension and compression) due to buckling bending (Knickbiegung) and indicates a curve which is very similar to the support load in DIN E 4114. Figure 2.1.16 indicates tests on an aluminum Z section and calculation of this by equations (2.1.26), (2.1.27) and tangent modulus equations. /120

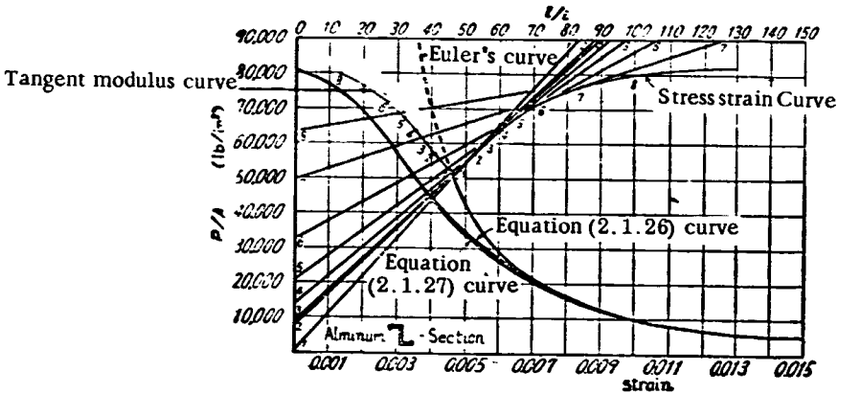

Figure 2.1.16

Assuming in Equation (2.1.25) that e = 0,

$$k=\frac{h(\sigma_{Y.P.}-\sigma_e^2/\sigma_{Y.P.})}{4\pi^2Ei^2}.$$

In Equation (2.1.27) in the case of an infinitely long column, since this matches Euler's curve, $\sigma_e = 0$ and

$$k=\frac{h\sigma_{Y.P.}}{4\pi^2Ei^2}$$

It is necessary to determine the appropriate values of k in such a way that the tangent modulus is exactly determined. As an example, in the case of a square cross-section member of aluminum alloy 24 ST where h = 5/8 in., $\sigma_{Y.P.}$ = 53,000 lb./in.^{2}, E = 10,640,000 lb/in^2

$$k = 0.00242$$

when e is present k is indicated by such a straight line formula as

$$k = 0.00242 + 0.0083e$$

When the column length increases the effect of e on the column resistance decreases, and becomes 0 in the case of infinite length.

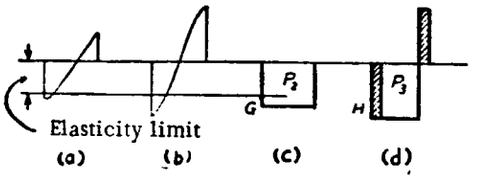

Figure 2.1.17

The distribution of sectional stress in an eccentrically compressed member is as shown in Figure 2.1.17. The ultimate resistance is expressed by (d). It changes to this state from states (a), (b). However, if this is a case of central compressive load, after reaching (c), it sud-- denly progresses to (d). The process from increase in load to decrease is gradual in the case of an eccentric load, and this tendency is greater, the greater the eccentricity. Equation (2.1.27) differs from the conventional Euler equation and is not affected by infinitesimal initial blending, load eccentricity, or other defects. The first two items on the top of Figure 2.1.18 represent a conventional explanation of bending stress, whereas the lower two graphically illustrate the case in which there coexists bending based on ultimate strength theory and bending and compression.*[1] /121

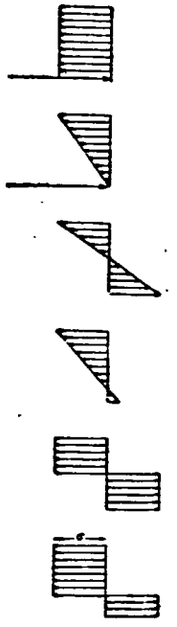

Figure 2.1.18

2.1.8. DESIGN FORMULAS TAKING LOAD ECCENTRICITY INTO CONSIDERATION

If the resistance of a member sustaining an eccentric compressive load is restrained to the case in which the extreme fiber stress reaches a specific value, e.g., the yield point, is elastic up to this point, and is determined as that for which Hooke's law holds the Secant formula is obtained.

$$\frac{P}{A}=\frac{\sigma}{1+\frac{ec}{i^2}\sec\frac{l}{2i}\sqrt{\frac{P}{AE}}}. \qquad (2.1.28)$$

*[1] Van den Broek notes the following:

Rankine's equation $P/A=\frac{\sigma}{1+\sigma l/ki}$.

Transformed Rankine's equation $P/A=\frac{\sigma}{1+\sigma/\sigma_k}$

The term l/i is not in the First Manual of Applied Mechanics published by Rankine in 1870 where it is 1/h, (Rankine died in 1872). h is called the minimum radius; moreover, in Miscellaneous Scientific Papers in Civil Engineering, 1/i is not seen. Limit Design, John Wiley and Sons, New York (1948), p. 110.

The method employed to determine the design load P, using $\sigma_{Y.P.}$ in place of in this formula and using νP in place of P, is the correct treatment of this formula, as Timoshenko has explained. However, it is necessary for the load eccentricity e to either be assumed, or determined by experiment. Nevertheless, the design load will not be immediately determined by solving these, since P is also included inside the denominator on the right side. It is convenient to prepare beforehand a numerical table for P/A for the case of when various eccentricities are present, in which case Equation (2.1.28) is used without modification. By using this, it is possible to immediately determine any safety factor ν when graphically displayed.

There are also many cases in which the Secant formula is used as a general buckling formula for compressive members. For example, Roark has provided the following formula for soft steel, structural silicone steel and structure nickel steel, as a standard for bridges.*1 For the allowable load P

$$\frac{\nu P}{A}=\frac{\sigma_{Y.P.}}{1+0.25\sec\left(\frac{\alpha l}{2i}\sqrt{\frac{\nu P}{EA}}\right)}.$$

in this formula, the characteristic feature is that the extent of eccentricity which can occur in a structure is expressed as a maximum of e/s = 0.25. The safety factor ν and the buckling length αl have different values depending on the conditions of connection of the member ends. $\sigma_{Y.P.}$ differs according to the material, being 32,000 in the case of carbon steel, 45,000 in structural silicone steel and 50,000 lb./in.^{2} in nickel steel. The magnitude of α is 0.75 in the case of a riveted end, and 0.875 in a pinned end. ν is as expressed in /122
Table 2.1.9 for section steel and built-up compression members.

TABLE 2.1.9

Material	Carbon steel		Structural silicon steel		Structural nickel steel	
Joint	Rivet end	Pin end	Rivet end	Pin end	Rivet end	Pin end
Risk factor	1.7	1.76	1.8	1.8	1.78	1.78
Limits of application l/i	>140		>130		>130	

In Germany, the ω method is used even in the case of eccentric loads. According to DIN Entwurf I E 4114 (1939-11-1), the bending unit stress and the compressive unit stress calculated by the ω method are added without modification.

$$\sigma_{bc}+\frac{\omega P}{A}\leqq f_c, \qquad (2.1.29)$$

$$\sigma_{bt}-\frac{P}{A}\leqq f_t. \qquad (2.1.30)$$

*1 J. Roark: Formulas for Stress and Strain (1938), p. 198.

σ_{bc} and σ_{bt} are respectively the compression and tensile unit stress due to bending. Formula (2.1.30) is necessary only when P is very small, or in the case of a ⅂ or ⊤ section member and is used in the case of

$$\sigma_{bt} > \sigma_{bc} + (\omega+1)\frac{P}{A} \tag{2.1.31}$$

in Equation (2.1.30)

$$\sigma_{bc} + \omega\frac{P}{A} = \frac{P}{A}\left(\frac{e}{s} + \omega\right) \leqq f_t \tag{2.1.32}$$

DIN Entwurf II E 4114 (1940-8-20) differs somewhat. The compressive and tensile unit extreme fiber stress based on the direct stress P and the bending moment M = P·e are calculated and it is ascertained whether this falls within the prescribed allowable values. In this calculation, it is not necessary to consider the deflection of the member. Next, buckling is analyzed, but when a precise calculation is not used, the following two formulas are employed.

When the member has a symmetrical cross-section or the section center of gravity is close to the tension extreme.

$$0.9\sigma_{bc} + \omega\frac{P}{A} \equiv \left(0.9\frac{e}{s_t} + \omega\right)\frac{P}{A} \leqq f_t. \tag{2.1.33}$$

when the center of gravity of the member cross-section is close to the compression extreme in addition to the above analysis

$$\frac{300+2\lambda}{1000}\cdot\sigma_{bt} + \omega\frac{P}{A} \equiv \left(\frac{300+2\lambda}{1000}\cdot\frac{e}{s_c} + \omega\right)\frac{P}{A} \leqq f_t. \tag{2.1.34}$$

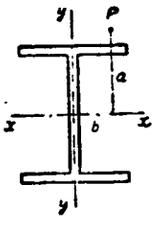

Figure 2.1.19

Figure 2.1.20

When the point of application of the load is on the principle axis, the following procedure is used. (Figure 2.1.20) When the distance between the point of application of force and axis xx is a, and the distance from axis yy is b, where

$$M_x = P\cdot a, \qquad M_y = P\cdot b$$

The analysis is carried out by inserting these values in Equations (2.1.33), (2.1.34). As in the Crane truss beam in Figure 2.1.20, in a member in which the compressed member sustains a compressive force P and a bending moment M_X and in which there is concern less buckling occur in the direction xx perpendicular to the stress plane, as long as

$$\sigma_{bc} \leqq \omega\frac{P}{A} \cdot$$

/123

it is possible to determine the dimensions approximately by Equation (2.1.33). In this case, for ω values are used with respect to the direction xx.

CHAPTER 2

LATERAL BUCKLING OF BEAMS

2.2.1. LATERAL BUCKLING OF TIE PLATES

In members which are employed primarily to resist bending stress, such as beams, the flexural stiffness B is increased much greater than the cross-section area. Naturally, the cross-section assumes a slender form. When this tendency is gradually strengthened, at a certain limit, the beam will suddenly collapse in a direction which is perpendicular to the bending stress plane. This is called lateral buckling. The higher the beam itself, the more slender it is, or the greater the span between the support point of the beams, the lower is the resistance value with respect to lateral buckling. This limit is usually expressed by the unit bending moment. In a rectangular cross-section beam sustaining pure bending, this is

$$M_k=\frac{\pi\sqrt{B_1C}}{l}$$

Here, B_1 is the flexural stiffness outside the plane of the plate, and C is the torsional stiffness. When the thickness of the plate is expressed as t_1, and the height is expressed by h, since

$$B_1=\frac{ht_1^3}{12}E, \qquad C=\frac{ht_1^3}{3}\left(1-0.630\frac{t_1}{h}\right)G$$

$$M_k=\frac{t_1^2}{lh}\sqrt{\left(1-0.630\frac{t_1}{h}\right)\frac{1}{2(1+\nu)}}\cdot\pi EZ.$$

Z is the section modulus, 1 is the span.

2.2.2. LATERAL BUCKLING OF I-BEAMS

This is expressed roughly by the same formula in the case of I steel beams. When section steel with both ends pure supports sustains pure bending, this is expressed by the following formula.

$$M_k=\frac{\pi\sqrt{B_1C}}{l}\sqrt{1+\pi^2\frac{a^2}{l^2}}=m\frac{\sqrt{B_1C}}{l}. \qquad (2.2.1)$$

Even if the support and load conditions change, if we express the maximum bending moment as M_k, it is possible to express it as shown in formula (2.2.1), where the value of M should be appropriately changed. Below, in Table 2.2.1 are several examples:

TABLE 2.2.1

The value of m

Condition of both ends		Simple support	Cantilever beam	Simple support	Simple support
Load condition		Simple Bending	Concentrated load on the free end	Concentrated load with center	Equally distributed load
$\frac{l^2}{a^2}=\frac{2C}{D}\frac{l^2}{h^2}$	0.1	21.4	44.3		
	0.4	15.9		21.6 $\frac{0.60}{1.70}$	17.9 $\frac{0.65}{1.53}$
	1.0	10.36	15.7		
	2.0	7.66	12.2		
	4.0	5.85	9.76	7.95 $\frac{0.63}{1.57}$	6.62 $\frac{0.69}{1.46}$
	6.0	5.11	8.69		
	8.0	4.70	8.03	6.40 $\frac{0.66}{1.50}$	5.34 $\frac{0.72}{1.40}$
	10	4.43	7.58		
	12	4.24	7.20		
	16	4.00	6.73	5.45 $\frac{0.71}{1.39}$	4.42 $\frac{0.76}{1.32}$
	20	3.83			
	24	3.73	5.87	5.21 $\frac{0.74}{1.82}$	4.22 $\frac{0.79}{1.29}$
	28	3.66			
	32	3.59		4.90 $\frac{0.76}{1.30}$	4.08 $\frac{0.80}{1.24}$
	36	3.55			
	40	3.51	5.64		
	48	3.46		4.[illegible] $\frac{}{1.25}$	3.94 $\frac{0.83}{1.20}$
	400	3.18		4.30 $\frac{0.92}{1.09}$	3.58 $\frac{0.94}{1.08}$
	∞	3.14			

(1),(2) The load is the value of m on the central axis. The upper and lower figures to the right in the same horizontal line in the table represent, respectively, the ratios of the load on the upper and lower flange to the load on the central axis

/124

B_1 is the flexural stiffness with respect to the outside of the principle of bending stress plain. Normally, in an I-section steel, this can be determined immediately from the catalog. In general it is equal to the sum of the bending stiffnesses inside the flange plane in two flanges.

$$B_1 \fallingdotseq \frac{b^2 t}{6} E. \qquad (2.2.2)$$

Here, the b is flange width, t is the average thickness of the flange

C is roughly

$$C = G\left(\frac{2}{3}bt^3+\frac{1}{3}ht_1^3\right). \qquad (2.2.3)$$

In this formula, h is the beam height, t_1 is web thickness. This was determined by considering an I section of steel as consisting of three plates. Since the I-section steel web and the flange fillets are thick, there are cases in which the value is made 25% greater than C above. E. Chwalla, on this basis, writes (95)

$$C=1.15G\left(\frac{2}{3}bt^3+\frac{1}{3}ht_1^3\right) \qquad /125$$

However, Timoshenko maintains (96) that even if these values differ considerably, their effects on the buckling stress is not very great. The A^2 in Formula (2.2.1) is the quantity which is directly proportional plane-internal stiffness of the flange and its torsional stiffness, and is

$$a^2=Dh^2/2C$$

Since D is the plane-internal flexural stiffness for 1 flange, normally there is no great difference in using 1/2 B_1. Consequently

$$\frac{l^2}{a^2}=\frac{16}{2(1+\nu)}\frac{t^2}{h^2}\frac{l^2}{b^2}.$$

In soft steel, since we can assume $\nu = 0.3$, it takes the following form

$$\frac{l^2}{a^2}=\frac{1}{0.16}\frac{t^2}{h^2}\frac{l^2}{b^2}.$$

If by this equation t/h is given, the size of l /a is determined by l /h .

In I steel, t/h is confined within a certain range. That is, in ordinary I steel, since t/h = 0.04,*1 we shall consider this case in particular. Assuming l/b = 30, $l^2/a^2 = 10$, and becomes m = 4.43 in Formula (2.2.1). According to Formula (2.2.2), $B_1 = Eb^3t/6$, and according to Formula (2.2.3), if $C = 2\,Gbt^3/3$

$$M_k=19300\frac{b^3t^2}{l}\ \text{kg-mm}.$$

Consequently, determining the extreme fiber stress as

$$Z=\frac{bt}{3h}(t^2+3h^2)$$

*1 In Japan Standard Regulations No. 26, G 15, I steel, this is t/h = 0.16 (I-75 x 75 x 8), 0.08 (I-100 x 75 x 8), 0.067 (I-150 x 75 x 9.5), 0.056 (I-180 x 100 x 10), 0.05 (I-200 x 100 x 10), 0.043 (I-300 x 150 x 13), 0.045 (I-400 x 150 x 18), 0.046 (I-500 x 190 x 23), 0.041 (I-600 x 190 x 25).

$$\sigma_k=\frac{M_k}{Z}=19300\cdot\frac{b}{l}\cdot\frac{3ht}{t^2+3h^2}=25.7 \text{ kg/mm}^2. \qquad /126$$

Since this value can be considered to be intermediate between the limit of elasticity and the yield point of the steel member, when the slenderness ratio $l/i = \sqrt{12}\, l/b$ with respect to the lateral buckling of the flange only, plane xz in Figure 2.2.1, is less than 100, i.e., if $l/b < 30$, it is considered to be within the range of plastic buckling.

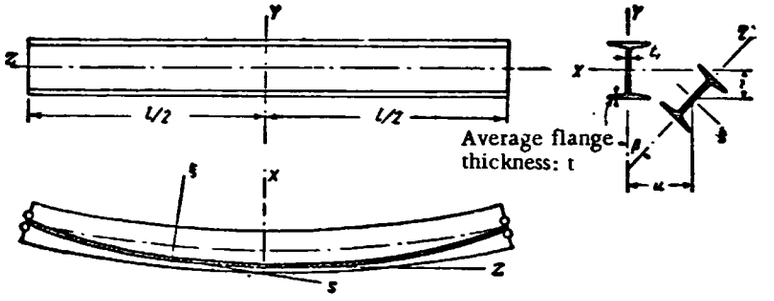

Figure 2.2.1

2.2.3. DESIGN FORMULAS TAKING LATERAL BUCKLING INTO CONSIDERATION

In the normal calculations of a beam, taking lateral buckling into account, and expressing by f the allowable compressive unit stress with respect to bending, it is necessary to perform the calculations in the form

$$M=\frac{f}{\kappa}\cdot Z$$

κ is the lateral buckling coefficient, and is greater than 1. Assuming B_1 and C to be constant

$$M : M_{30}=\frac{bm}{l} : \frac{bm_{30}}{l_{30}}.$$

Here, l_{30}, m_{30} and M_{30} are the values corresponding to formula (2.2.1) when l/b $l/b = 30$. Therefore,

$$M=\frac{30b}{l}\frac{m}{m_{30}}M_{30}.$$

Here if the values of m/m_{30} are accurately computed, we obtain the following as a rough approximation

$$(m/m_{30})=0.6+12\frac{b}{l}$$

Since this formula is within the safe range of error in design, the allowable bending moment may be expressed by

$$M=fZ\left(18\frac{b}{l}+360\frac{b^2}{l^2}\right)$$

It is possible to express the allowable lateral buckling bending unit stress f_k by

$$f_k=f\left(18\frac{b}{l}+360\frac{b^2}{l^2}\right).$$

κ Method. Assuming $f:f_k = \kappa$, in a beam sustaining elastic bending

$$\kappa=\frac{f}{f_k}=\frac{1}{18\frac{b}{l}+360\frac{b^2}{l^2}}>1.$$

Using this, as with the ω method in a centrally compressed member when
1/b > 30 $l/b>30$ のとき

$$\frac{\kappa M}{Z}<f$$

can be used.*1 This is called the κ method.

In a member sustaining bending and compression, there are cases when it is insufficient to only take into consideration bending due to eccentricity. In particular, in rigid frames (Rahmen) or statically indeterminant structures, a bending whose extent of the effect is equivalent to or greater than the axial compressive force, operates simultaneously, and in such cases, for approximate calculations, combined use of ω and κ methods is safest. /127

$$f>\omega\frac{P}{A}+\kappa\frac{M}{Z}.$$

The magnitude of κ is not, like ω, merely a variable of the slenderness ratio λ. That is, not only does κ differ according to 1/b but the load and support conditions also change. However, in many designs, when both ends are assumed to be a pure support, with pure bending, in most cases in practice, these calculations are on the safe side. In a pure cantilever in which tne load is applied to the upper edge, this value is insufficient.

A.I.S.C. Design Formula. According to the Specifications for Structural Steel of the American Institute of Steel Construction,*2

*1 This proposal was introduced by the author and by committee member Ishiguro Tokue for steel structural standards at a meeting of the Japan Architectural Society. In the instructions proposed, a method is described which expands on this. See publication of the Japan Architectural Society: Steel Structure Calculation Standards. (1950), pp. 94-99.

*2 A.I.S.C.: Specification for the Design, Fabrication and Erection of Structural Steel for Buildings (1949-6), chapter 3, article 15.

These formulas are as follows:

Edge tensile unit stress of rolled member, plate girder and built-up member ... 20,000 lb/in^2

Edge compressive unit stress of rolled member, plate girder and built-up member

$$\frac{lh}{bt} \leq 60 \quad \cdots \quad 20{,}000 \text{ lb/in}^2,$$

$$\frac{lh}{bt} > 600 \quad \cdots \quad \frac{12{,}000{,}000}{\frac{lh}{bt}} \text{ lb/in}^2.$$

According to this formula, e.g., if l/b = 30, this means that t/h = 0.05 becomes the limit. That is, when t/h is smaller than 0.05, assuming that elastic lateral buckling is caused, the allowable stress intensity is decreased in inverse proportion to lh/bt. This formula is immediately derived from Formula (2.2.1) by considering that the flange plate thickness is considerably smaller than the beam height.

2.2.4. DESIGN FORMULA TAKING INTO CONSIDERATION ONLY FLANGE BUCKLING

There is a simple formula which takes into consideration the flange buckling, plane xz in place of the overall lateral buckling of the beam. In most cases, this is the straight line formula.

$$\lambda = \sqrt{12}\,\frac{l}{b} \fallingdotseq 3.5\,\frac{l}{b}$$

In order to make this somewhat more theoretical, we shall employ the buckling length l_k taking into consideration the state of load distribution, without employing the total length of the flange for l. For example. When, a load of equal distribution is applied to a beam, since the distribution of the flange compressive force is parabolic,

$$l_k = 0.7\,l$$

is used. For example, for $\lambda < 100$,

$$\sigma_k = 48{,}000 - 210\,\lambda \quad \text{lb/in}^2 \qquad \text{/128}$$

Moreover, for $\lambda < 100$, Euler's formula is used. According to such a formula, in most cases the errors that are made are on the danger side. When h/b increases, the degree of danger increases markedly. However, as a general formula, since it is simple, there are many standards which use it.

Using the integral which is fixed with respect to the side displacement of a plate girder as the compressive force, we assume that

$$D=\frac{M}{I}S$$

operates. Here, S is the geometric moment of inertia with respect to the neutral axis of the flange section (includes flange plate, angle steel, part of web) M is the average value of the bending moment in the space in which it is necessary to take buckling into consideration. From this,

$$\frac{\omega_y D}{A} \leqq f.$$

ω_y is the coefficient ω determined by $\lambda_y = l_k/i_y$*1. That is, assuming the buckling unit stress with respect to λ_y to be f_k

$$\omega_y = f/f_k.$$

According to the American Railway Engineering Association

$$f=16{,}000-150\frac{l}{b} \quad \text{lb/in}^2$$

is used for the allowable unit stress.*2

In our Railroad Standards, the following*3 was used

Generally

$$f=1150-15\frac{l}{b} \quad \text{kg/cm}^2,$$

with beam connected to buckle plate

$$f=1150-10\frac{l}{b} \quad \text{kg/cm}^2.$$

Moreover, the tension side is taken as 1,200 kg/cm^2 irrespective of l/b with respect to the existing cross-section. Under existing railroad standards, a formula*4 is used which reduces this by the square of l/b.

---

*1 Stahlbau-Kalender, Ernst u. Sohn (1940), S. 191.

*2 Merriman, Wiggin: American Civil Engineers Handbook, 5th Edition (1945), p. 1185.

*3 Railroad and Bridge Design Specifications, Chapter 3, Article 11.

*4 Bridge Reference Charts, Kokuseido (1948), p. 80.

Generally,

$$f=1100-0.5\left(\frac{l}{b}\right)^2 \text{ kg/cm}^2.$$

When the beams are connected by buckle plates

$$f=1100-0.25\left(\frac{l}{b}\right)^2 \text{ kg/cm}^2. \qquad /129$$

In the California Administrative Code, it is as follows:

For rolled members, built-up members and beams,*1

$$\frac{l}{b}\leq 15 \quad \cdots f=20,000 \text{ lb/in}^2.$$

$$40>\frac{l}{b}>15 \quad \cdots f=\frac{22,500}{1+\frac{l^2}{1800\,b^2}} \text{ lb/in}^2.$$

2.2.5. LATERAL BUCKLING OF TIE SECTION HAVING ARC AXIS

If a pure bending moment is applied to both ends of a tie section having an arc axis with a radius r_0, the buckling bending (Knickbiegung) moment is

$$M_k=\frac{B_1+C}{2r_0}\pm\sqrt{\left(\frac{B_1-C}{2r_0}\right)^2+\frac{B_1C}{r_0^2}\frac{\pi^2}{\alpha^2}}. \qquad (2.2.4)$$

In the above equation, α is the angle at which both ends of the arc axis of the tie section is enclosed in the center. This equation corresponds to equation (2.2.1). That is, if $r_0 \to \infty$, $r_0\alpha = 1$, it agrees with equation (2.2.1).

That M_k has 2 values is determined by whether the direction in which the pure bending moment has effect causes the inside of the tie section to be the edge of compression or the outside to be the edge of compression. When the inside is the edge of compression, the lateral buckling resistance is great. When = , one root is 0. This expresses the fact that when bending occurs such that the outside is the edge of compression, rotation is caused on the diameter which connects the two ends.

*1 California Administrative Code, Title 21, Public Works, Article 804 (1948-9-1).

CHAPTER 3 (Supplement)

BUCKLING WITH BENDING AND TORSION

2.3.1. SHEAR CENTER

When a lateral load, which passes through the center of gravity of the cross-section of a member, is applied to that member, if the principal axes of the cross-section are biaxially symmetrical, or anti-symmetric lines, only deflection will occur, except when lateral buckling takes place. However, when only one of the principle axes of the cross-section is symmetrical, or no symmetrical line is formed, this is usually accompanied by torsion. This torsion is due to the shear force operating on the section, and the center of torsion forms the shear center. C. Bach discussed this a long time ago*1 If the lateral load passes through the shear center, torsion will not be caused. Consequently, the shear center can be defined as a point on a section, or a plane which is the same as that section, through which passes a shearing force such that the member does not undergo torsion. If this property is applied to a reciprocal theorem, it can be seen that the torsion around the shear center is pure torsion, and is not accompanied by deflection. The line which connects the shear centers of sections is called the shear center line. The shear center line of a straight beam is a single straight line. However, strictly speaking, since there are changes in the end conditions, support conditions, and in the distribution of load conditions and local shear forces, the shear center line of a straight beam should be considered slightly bent. This difference normally is very slight, so the shear center line is treated as a rotating center line.*2*3

---

*1 C. Bach: Versuche über die tätsächliche Widerstandsfähigkeit von Balken with ⊏-förmigen Querschnitten. Z. d. V.D.I. (1909), p. 1790.

*2 Timoshenko says that R. Maillart was the first to describe the concept of shear center and means of determining it. Timoshenko: History of Strength of Materials, (McCraw-Hill, 1953) p. 401.

*3 Here is a list of classical works on the subject:

R. Maillart: Schweiz, Bauztg., Vol. 77 (1921), p. 195; Vol. 79 (1922), p. 254.
C. Weber: Biegung u. Schub in geraden Balken, ZAMM, Vol. 4 (1924), p. 334.
A. Föppl and L. Föppl: Drang and Zwang, Vol. 2 (R. Oldenbourg, 1928), p. 121.
F. Bleich: Stahlhochbauten, Vol. 1. (J. Springer, Berlin, 1932), p. 79.
E. Trefftz: Über den Schubmittelpunkt in einem durch eine Einzellast gebogenen Balken. ZAMM, Vol. 15 (1935), p. 220.

The position of the shear center is constant with respect to the cross-section. It is necessary to know the state of flow of the shear force occurring on the section in order to determine its position. For this reason, according to bending theory, if the force equilibrium is determined, the conditions for the continuation of deformation and the [illegible word] are included, it is possible to obtain a solution which is close in terms of elastic dynamics. /131

In a beam sustaining bending, Jacob Bernoulli-Navier's plane-retention law is in effect. Denoting the principle axes of the section as x, y, arbitrary orthogonal axes passing through the center of gravity as X, Y, and the orthogonal angle between the X axis and the small x axis as θ, the stress σ_z in direction z of the member axis due to the bending moment M of the vector indicator, having a slope α with respect to the y axis, is expressed by the following equation. (Figure 2.3.1).

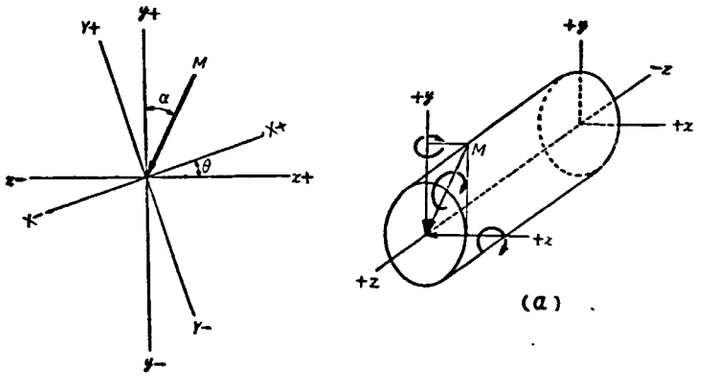

$$\sigma_z = \frac{M\sin\alpha \cdot y}{I_x} - \frac{M\cos\alpha \cdot x}{I_y}$$

$$= \frac{M(\sin\alpha \cdot y \cdot I_y - \cos\alpha \cdot x \cdot I_x)}{I_x I_y} \qquad (1)$$

Here I_X, I_Y are the geometrical moments of inertia with respect to the principal axis x, y. Since

$$X = x\cos\theta + y\sin\theta$$

$$Y = -x\sin\theta + y\cos\theta$$

By coordinate transformation,

$$I_X = \int_A Y^2 dA = \sin^2\theta \cdot I_y + \cos^2\theta \cdot I_x \qquad (2)$$

$$I_Y = \int_A X^2 dA = \cos^2\theta \cdot I_y + \sin^2\theta \cdot I_x \qquad (3)$$

$$I_{XY}=\int_{\Delta} XY dA=\sin\theta\cos\theta(I_x-I_y) \tag{4}$$

Therefore

$$2I_{XY}=\sin 2\theta\cdot(I_x-I_y) \tag{5}$$

$$I_X-I_Y=\cos 2\theta\cdot(I_x-I_y) \tag{6}$$

$$I_X+I_Y=I_x+I_y \tag{7}$$

Eliminating θ from (5) and (6), in substituting (7)

$$I_xI_y=I_XI_Y-I_{XY}^2 \tag{8}$$

Assuming that in equation (1) $\alpha + \theta = \pi/2$, $M \sin \alpha = M_X$

That is, this is the bending moment operating within plane Y_Z.

$$\sin\alpha=\sin\left(\frac{\pi}{2}-\theta\right)=\cos\theta,$$

$$\cos\alpha=\cos\left(\frac{\pi}{2}-\theta\right)=\sin\theta,$$

From (5) and (7),

$$I_x=\frac{I_X+I_Y}{2}+\frac{I_{XY}}{\sin 2\theta} \tag{9}$$

$$I_y=\frac{I_X+I_Y}{2}-\frac{I_{XY}}{\sin 2\theta} \tag{10}$$

From (5) and (6)

$$\frac{\cos 2\theta}{\sin 2\theta}=\frac{I_X-I_Y}{2I_{XY}} \tag{11}$$ /132

When these are inserted in equation (1), due to the bending moment around axis X,

$$\sigma_x=\frac{M_X(I_Y\cdot Y-X\cdot I_{XY})}{I_XI_Y-I_{XY}^2} \tag{12}$$

Similarly, assuming that $\alpha = -\theta$ in equation (1), with respect to the moment M_y around the axis Y,

(13)

$$\sigma_z=-\frac{M_Y(I_X\cdot X-Y\cdot I_{XY})}{I_XI_Y-I_{XY}^2}$$

If a division is made between the force $\sigma_{z(x)}$ in the direction of the axis due to the bending moment around the x axis, and the force $\sigma_{z(y)}$ in the direction of the axis due to the bending moment around the y axis, in equation (1)

$$\sigma_z=\sigma_{z(x)}+\sigma_{z(y)}=\frac{E\cdot y}{\rho_x}+\frac{E\cdot x}{\rho_y}$$

Assuming

$$\frac{1}{\rho_x}=\frac{d^2y}{dz^2},\quad \frac{1}{\rho_y}=\frac{d^2x}{dz^2}$$

(14)

$$\sigma_z=E\left(y\frac{d^2y}{dz^2}+x\frac{d^2x}{dz^2}\right)$$

Carrying out transformation of coordinates

(15)

$$\sigma_z=E\left(X\frac{d^2X}{dz^2}+Y\frac{d^2Y}{dz^2}\right)$$

If (12) and (15) have the same values, the curvature of the elastic lines of the member with respect to axis X and axis Y, due to M_X can be determined.

$$\frac{M_X\cdot I_Y}{I_XI_Y-I_{XY}^2}Y\quad\frac{M_X\cdot I_{XY}}{I_XI_Y-I_{XY}^2}X$$

$$=E\frac{d^2Y}{dz^2}Y+E\frac{d^2X}{dz^2}X$$

Assuming

$$\frac{d^2Y}{dz^2}=\frac{1}{\rho_X},\quad \frac{d^2X}{dz^2}=\frac{1}{\rho_Y}$$

On the basis of the assumption of plane support, these do not change depending on X, Y. Consequently

$$\frac{1}{\rho_X}=\frac{M_X\cdot I_Y}{E(I_XI_Y-I_{XY}^2)}\qquad(16)$$

$$\frac{1}{\rho_Y}=-\frac{M_X\cdot I_{XY}}{E(I_XI_Y-I_{XY}^2)}\qquad(17)$$

Here, the positive and negative signs for the curvatures, indicate whether the latter are concave or convex, where the elasticity lines are in the direction of the positive side of the coordinates. Similarly, if (13) and (15) are equivalent in value, the curvature of the elasticity lines of the mem-

ber with respect to axis X and axis Y due to M_Y is expressed as follows:

$$-\frac{M_Y \cdot I_X}{I_X I_Y - I_{XY}^2} X + \frac{M_Y \cdot I_{XY}}{I_X I_Y - I_{XY}^2} Y$$

$$= E\frac{d^2X}{dz^2} X + E\frac{d^2Y}{dz^2} Y$$

$$\frac{1}{\rho_X} = \frac{M_Y \cdot I_{XY}}{E(I_X I_Y - I_{XY}^2)} \tag{18}$$ /133

$$\frac{1}{\rho_Y} = -\frac{M_Y \cdot I_X}{E(I_X I_Y - I_{XY}^2)} \tag{19}$$

If it is assumed that in equation (1) $\sigma_Z = 0$, the straight line of the neutral axis can be determined.

$$y = \cot\alpha \cdot \frac{I_x}{I_y} \cdot x \tag{20}$$

The angle formed by the center axis and the bending moment M is a right angle when

$I_X/I_y = 1$, but is smaller than a right angle when

$I_X/I_y > 1$, and is larger than a right angle when

$I_X/I_y < 1$.

When the center axis is drawn onto the cross-section, the concept of positive or negative curvature becomes clear.

When a lateral load is applied to a member, not only bending stress, but shear stress also occurs. Its equilibrium, from elasticity theory is

$$\frac{\partial \sigma_z}{\partial z} + \frac{\partial \tau_{zx}}{\partial x} + \frac{\partial \tau_{zy}}{\partial y} = 0 \tag{21}$$

Therefore, assuming the derivatives of (1) to be

$$\frac{\partial \sigma_z}{\partial z} = \frac{dM_x}{dz}\frac{y}{I_x} + \frac{dM_y}{dz}\cdot\frac{x}{I_y}$$

$$\frac{dM_x}{dz} = Q_y, \quad \frac{dM_y}{dz} = Q_x$$

Where

$$\frac{\partial \tau_{zx}}{\partial x} + \frac{\partial \tau_{zy}}{\partial y} = -\left(\frac{Q_x}{I_y}\cdot x + \frac{Q_y}{I_x}\cdot y\right) \tag{22}$$

When there is no load in the direction of the X axis, $Q_X = 0$,

$$\frac{\partial \tau_{zx}}{\partial x}+\frac{\partial \tau_{zy}}{\partial y}=-\frac{Q_y}{I_x}y \tag{23}$$

Therefore, the equation for equilibrium with respect to portion A in Figure 2.3.2 is

$$\int_A \frac{\partial \tau_{zx}}{\partial x}dA+\int_A \frac{\partial \tau_{zy}}{\partial y}dA=-\frac{Q_y}{I_x}\int_y^{y_0} y dA$$

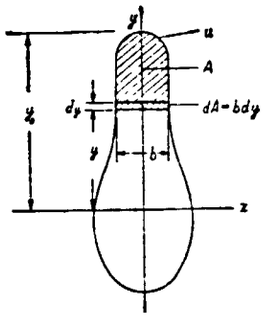

Figure 2.3.2

When Gauss's integration theorem is used for the right side of this equation, it is possible to convert the plane integral into a line integral.

$$\int_A \left(\frac{\partial \tau_{zx}}{\partial x}+\frac{\partial \tau_{zy}}{\partial y}\right)dA=\int_u \tau_u du \tag{24}$$

The right side is the integration along the other perimeter u of area A, and σ_u is the component of shear force at right angles to u. When no outer force is in effect around this, in sections other than that along b, $\tau_u = 0$, and assuming that τ_{zy} is the average value of τ_u in the section along the b, since the right side of (24) becomes $b\tau_{zy}$,

$$b\tau_{zy}=-\frac{Q_y}{I_x}\int_y^{y_0} y dA \qquad \text{/134}$$

In particular, assuming

$$S_x=\int_y^{y_0} y\, dA \tag{25}$$

$$\tau_{zy}=-\frac{Q_y S_x}{I_x b} \tag{26}$$

S_x is the primary moment of section A with respect to axis x. There is no part of (26) which differs from the normally employed equation for calculating shearing stress. What requires attention is the fact that τ_{zy} becomes the average value of τ_u within the range of b. If one considers that there is a change in the configuration of a cross-section, when a shearing force is sustained and also takes into account the flow of the shearing stress within the cross-section, and determines the shape of the function τ_u, including not only the equilibrium conditions, but the continuity and boundary conditions, the accurate value of τ_u can be determined. If one determines the accurate values of the shearing stress for a rectangular cross-section (Figure 2.3.3), the values shown in Table 1 are obtained.*1

*1 S. Timoshenko, J. N. Goodier: Theory of Elasticity, (McGraw-Hill, 1951), p. 326.

The shear stress is smaller in the center than in the surrounding parts. However, when s large, i.e., when the path of the shear flow is narrow, it can be se the difference between the center section and the surrounding sections is only a few percent. Consequently, in the case of a thin plate member, the magnitude of the shearing stress flowing along the center line of thickness is not greatly different from the average value, and may be considered as the principal shearing stress.

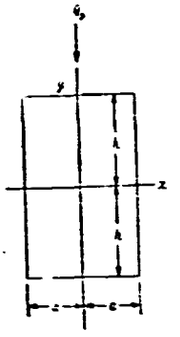

Table 1. Shearing Stress in Rectangular Cross-Section

Position	h/a	2	1	1/2	1/4
x = 0, y = 0	Adjusted value	0.983	0.940	0.856	0.805
x = a, y = 0	Adjusted value	1.033	1.126	1.396	1.988

Figure 2.3.3.

The numbers are the multipliers of the shearing stress 1.5 Q/A based on the equation (26), ν = 1/4.

Now we shall consider the principle shearing stress of thin sectioned steel such as that sh n Figure 2.3.4, having principle axis x, y. From this hypothesis, from the equilibrium of forces between du (a, b in Figure 2.3.1).

$$d(\tau t)dz+d\sigma_z(tdu)=0 \tag{27}$$

Therefore, when t is constant

$$\frac{d\tau}{du}=-\frac{d\sigma_z}{dz}=-\frac{Q_y}{I_x}y \tag{27a}$$

Here we assume $Q_x = 0$. If we integrate for area A having the diagonal shown in Figure 2.3.4

$$\tau t=-\frac{Q_y}{I_x}\int_A y\,dA$$
$$S_x=\int_A y\,dA \tag{28}$$

Where

$$\tau=-\frac{Q_y S_x}{I_x t} \qquad (29)$$ /135

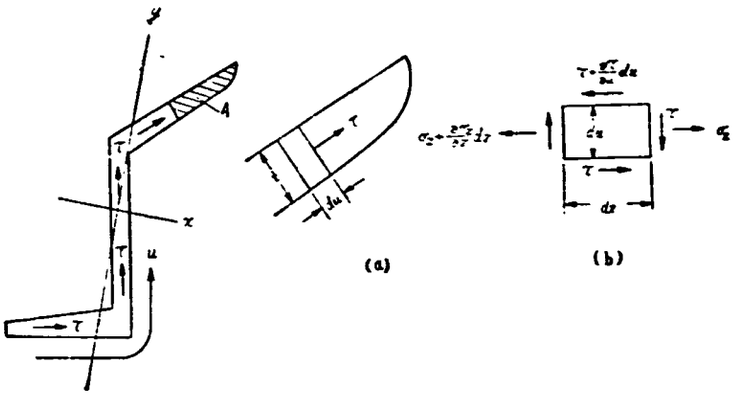

Figure 2.3.4

S_x is the geometric moment of inertia. Taking the integral in the direction of the center line. The size of τ is greater, the greater S_x and the smaller b. The starting point of the integration of S_x employs the size of the shearing stress, i.e., the point where S_x is already known.

$$S_x=S_0+S_{AB} \qquad (30)$$

Since normally in both end sections of an open cross-section, the shearing stress is 0, i.e., S = 0, this may be used as a starting point.

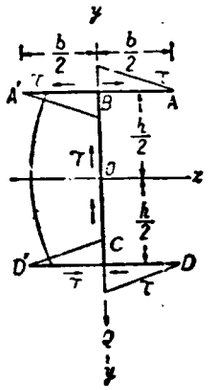

Figure 2.3.5

When the I cross-section (Figure 2.3.5) sustains a shearing stress Q_y passing through the center of gravity, in determining the primary moment with response to axis xx, it can be seen that the shearing stress in each of the four points, A, A', D, D' is 0. Consequently, assuming that for point A, u = 0, and determining the geometric moment of inertia for the integral AB

$$S_{AB}=\int_0^u yt\,du=\frac{h}{2}t\cdot u$$

Consequently for B

$$S_{(AB)B}=\frac{bh}{4}t$$

Similarly, from the integration of the interval A'B

$$S_{(A'B)B}=\frac{bh}{4}t$$

In integral BO

$$S_{B0}=2\cdot\frac{bh}{4}\cdot t+\int_{u=\frac{b}{2}}^{u=\frac{b}{2}+\frac{h}{2}-y}ytdu$$

$$=\frac{bht}{2}+\frac{t}{2}\left(\frac{h^2}{4}-y^2\right)$$

Consequently at point 0

$$S_{(B)0}=\frac{bht}{2}+\frac{th^2}{8} \qquad \underline{/136}$$

If the distribution of shearing stress is depicted using these, it becomes as shown in the figure. In the integral BC, the same results are obtained as with the conventional equations. Moreover, the shearing stress in the flange section parallel to axis xx is a straight line, the shearing stress in the web section perpendicular to the x axis is a parabola. The size of the shearing stress τ is determined from Equation (29). As can be seen from the direction of its flow, in flange AA', point B sustains tension and in flange DD', point C sustains compression.

From equation (27), since

$$\frac{d(\tau t)}{du}=-t\frac{d\sigma_z}{dz} \qquad (31)$$

If equation (12) is inserted into this and integrated, assuming

$$Q_Y = dM_X/dz$$

$$\tau t=-\frac{Q_Y}{I_xI_Y-I_{xY}^2}\left(I_Y\int_0^u Ytdu-I_{xY}\int_0^u Xtdu\right) \qquad (32)$$

Similarly, integrating, inserting (13), assuming $Q_X = dM_Y/dz$

$$\tau t=\frac{Q_X}{I_xI_Y-I_{xY}^2}\left(I_x\int_0^u Xtdu-I_{xY}\int_0^u Ytdu\right) \qquad (33)$$

Equation (32) is the general equation which expresses the shear flow of a thin skin open cross-section member corresponding to the shearing stress in direction Y, and equation (33) expresses this in correspondence with the shearing stress in direction X. It is possible to use these to determine the coordinates of the shear center. In this case, when the shearing stress passes through the shear center, the definition for the shear center is used, in which the cross-section does not undergo torsion. Shear force Q is divided into Q_X and Q_Y. The coordinate X of the shear stress is determined from the condition in which the sum of the moments formed by Q_Y and τt indicated in (32) is 0,

and the coordinate Y of the shear center is determined from the conditions in which the sum of the moments formed by Q_X and τ^t indicated in (33) is 0.

If the moment around the shear center is determined, the terms Q_X and Q_Y are not included. If the sum of the moments around the center of gravity is determined, the shear center is

$$X_0=\frac{1}{Q_Y}\int_u \tau t r du \tag{34}$$
$$=\frac{1}{I_X I_Y-I_{XY}^2}\left[-I_Y\int_u r du\int_0^u Y t du + I_{XY}\int_u r du\int_0^u X t du\right]$$

$$Y_0=\frac{1}{Q_X}\int_u \tau t r du \tag{35}$$
$$=\frac{1}{I_X I_Y-I_{XY}^2}\left[I_X\int_u r du\int_0^u X t du - I_{XY}\int_u r du\int_0^u Y t du\right]$$

The r in (34) and (35) expresses the length of the perpendicular line dropped from the center of gravity to the line tangent to the center line at point u on the center line of the cross-section, and the $\int_u$ indicates the inte- /137 gration along the total length of the center line.

When using the principal axis of the cross-section, since $I_{XY} = 0$,

$$x_0=-\frac{1}{I_x}\int_u r S_x du \tag{36}$$

$$y_0=\frac{1}{I_y}\int_u r S_y du \tag{37}$$

S_X and S_Y are the geometric moments of inertia around axis X and axis Y corresponding to the part u on the section.

As an example, we shall consider cold-shaped light channel steel, and will determine its shear center. (Figure 2.3.6). The plate thickness t is constant, and the roundness of the fillets is replaced by right angles. If we determine the center of gravity in order to draw the principle axis

$$C=\frac{b^2}{4(b+h)}$$

or

$$I_x=\frac{th^2}{12}(3b+h)$$

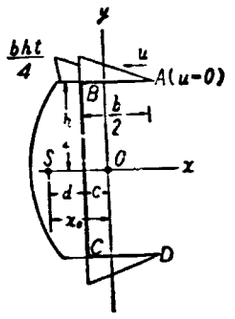

Figure 2.3.6

The magnitude of S_X is as follows, using examples of calculations of an I cross-section, with u = 0 for point A.

In integral AB $S_x=\frac{htu}{2}$, $r=\frac{h}{2}$

In integral BC $S_x=\frac{bht}{4}+\frac{t}{2}\left(\frac{h^2}{4}-y^2\right)$, $du=-dy$, $r=c$

In integral CD $S_x=\frac{bht}{4}-\frac{htx}{2}$, $du=dx$, $r=\frac{h}{2}$

Therefore,

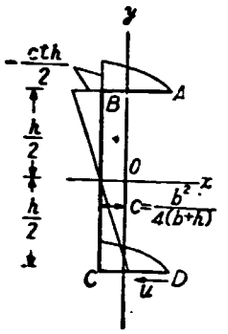

Figure 2.3.7

$$x_0=-\frac{1}{I_x}\int_u rS_x\,du$$

$$=-\frac{1}{I_x}\left[\int_0^{\frac{b}{2}}\frac{h}{2}\cdot\frac{ht}{2}\cdot u\,du+\int_{\frac{b}{2}}^{\frac{b}{2}+h}\left\{\frac{bht}{4}+\frac{t}{2}\left(\frac{h^2}{4}-y^2\right)\right\}c\cdot du\right.$$

$$\left.+\int_{u=\frac{b}{2}+h}^{u=\frac{b}{2}+h+\frac{b}{2}}\left(\frac{h}{2}\right)\left(\frac{bht}{2}-\frac{htx}{2}\right)dx\right]=-c-\frac{b^2h^2t}{16I_x}$$

Moreover, of course, $y_0 = 0$ and S_y becomes as shown by Figure 2.3.7. Therefore, in Figure 2.3.6

$$d=\frac{b^2h^2t}{16I_x}.$$

In cases in which it is easy to determine the principle axis in a thin-skinned open section member, the shear center is determined taking the principle axis as coordinate. The position of the shear center with respect to any coordinate axis is calculated by coordinate transformation. The following procedure is employed in order to determine the shear centers with respect to an arbitrary/138 coordinate axis, in the case of a member in which it is difficult to determine the principle axis. As an example, we shall perform calculations for that which is shown in Figure 2.3.8. We shall express the coordinates by the X axis and Y axis, and assume that the origin 0 later takes this as the center of gravity of this section. The coordinates of point B are expressed by m, n.

In Equations (34), (35), $\int_0^u Yt\,du$, $\int_0^u Xt\,du$

Begin integration with origin of u as first point A and point C, converge at point B, and calculations not carried out as far as point F, through point D.

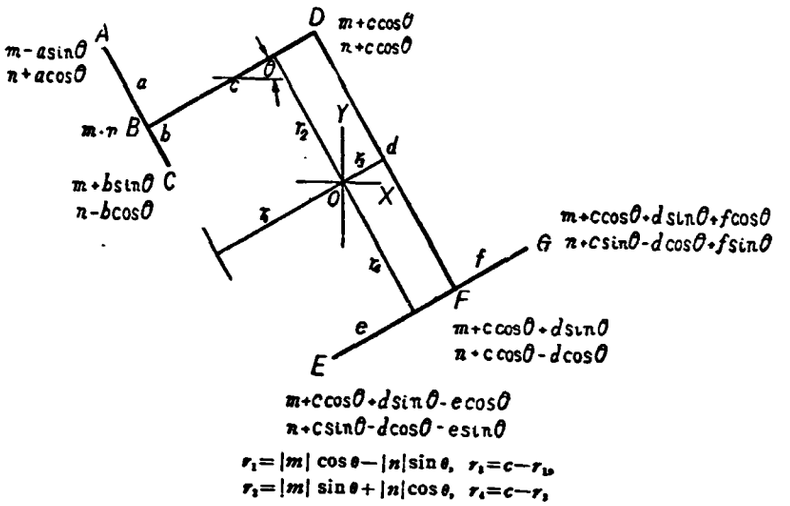

Figure 2.3.8

$$\int_{(AC)F} Yt\,du=(a+b+c+d)tn+\frac{t}{2}\cos\theta(a^2-b^2-d^2)$$

$$+\frac{ct}{2}\sin\theta\cdot(c+2d)=S_{(D)F}$$

Next, the integration is carried out with point E and point G as the origin of u, and for point F, respectively.

$$\int_{(E)F} Yt\,du=\frac{et}{2}(2n+2c\sin\theta-2d\cos\theta-e\sin\theta)=S_{(E)F}$$

$$\int_{(G)F} Yt\,du=\frac{ft}{2}(2n+2c\sin\theta-2d\cos\theta+f\sin\theta)=S_{(G)F}$$

From this, assuming $R_m=S_{(D)F}+S_{(E)F}+S_{(G)F}=0$

$$n=-[(a^2-b^2-d^2-2ed-2fd)\cos\theta+2(d+e+f)c\cdot\sin\theta \tag{38}$$
$$+c^2\sin\theta-e^2\sin\theta+f^2\sin\theta]/2l$$

Here l = a + b + c + d + e + f total length

$$\int_{(AC)F} Xt\,du=(a+b+c+d)tm-\frac{t}{2}\sin\theta(a^2-b^2-d^2)$$

$$+\frac{ct}{2}\cdot\cos\theta(c+2d)=S_{(D)F}$$

$$\int_{(E)F} Xt\,du=\frac{et}{2}(2m+2c\cos\theta+2d\sin\theta-e\cos\theta)=S_{(E)F} \qquad /139$$

$$\int_{(G)F} Xt\,du=\frac{ft}{2}(2m+2c\cos\theta+2d\sin\theta+f\cos\theta)=S_{(G)F}$$

Assuming $$R_m=S_{(D)F}+S_{(E)F}+S_{(G)F}=0$$

$$m=[(a^2-b^2-d^2-2ed-2fd)\sin\theta-2(d+e+f)c\cdot\cos\theta \qquad (39)$$
$$-c^2\cos\theta+e^2\cos\theta-f^2\cos\theta]/2l$$

m, n determine the coordinates of point B when point O is the center of gravity.

Next $$\int_a r\,du\int_0^u Yt\,du \quad \text{および} \quad \int_a r\,du\int_0^u Xt\,du$$

is calculated, but even in this case, the same path of integration is followed as before. Since here the integration from E and G has a direction which is the reverse of the path of integration from A, C, it is necessary to reverse the signs

$$R_X=\int_a r\,du\int_0^u Yt\,du \qquad (40)$$
$$=\left\{\frac{r_1t}{2}(a^2-b^2)-r_2t\left(a+b+\frac{c}{2}\right)c-r_3t\left(a+b+c+\frac{d}{2}\right)d+\frac{r_4t}{2}(e^2-f^2)\right\}n$$
$$+\frac{r_2t}{3}a^3\cos\theta+\frac{r_1t}{3}b^3\cos\theta-r_2tc\left\{\frac{1}{2}(a^2-b^2)\cos\theta+\frac{c^2}{6}\sin\theta\right\}$$
$$-r_3td\left\{\frac{1}{2}(a^2-b^2)\cos\theta+\frac{c^2}{2}\sin\theta+\frac{d}{2}\left(c\sin\theta-\frac{d}{3}\cos\theta\right)\right\}$$
$$+\frac{r_4t}{3}\left\{(e^2-f^2)(c\sin\theta-d\cos\theta)-\frac{2}{3}\sin\theta(e^3+f^3)\right\}$$

$$R_Y=\int_a r\,du\int_0^u Xt\,du \qquad (41)$$
$$=\left\{\frac{r_1t}{2}(a^2-b^2)\ -r_2t\left(a+b+\frac{c}{2}\right)c-r_3t\left(a+b+c+\frac{d}{2}\right)d+\frac{r_4t}{2}(e^2-f^2)\right\}m$$
$$\frac{t}{3}a^3\sin\theta-\frac{r_1t}{3}b^3\sin\theta-r_2tc\left\{-\frac{1}{2}(a^2-b^2)\sin\theta+\frac{c^2}{6}\cos\theta\right\}$$
$$-r_3td\left\{-\frac{1}{2}(a^2-b^2)\sin\theta+\frac{c^2}{2}\cos\theta+\frac{d}{2}\left(c\cos\theta+\frac{d}{3}\sin\theta\right)\right\}$$
$$+\frac{r_4t}{2}\left\{(e^2-f^2)(c\cos\theta+d\sin\theta)-\frac{2}{3}\cos\theta(e^3+f^3)\right\}$$

In the above equation

$$r_1=|m|\cos\theta-|n|\sin\theta \tag{42}$$

$$r_2=|m|\sin\theta+|n|\cos\theta \tag{43}$$

$$r_3=c-r_1. \tag{44}$$

$$r_4=d-r_2 \tag{45}$$

The shear center is expressed by the following equations, using the above /140

$$X_0=\frac{1}{I_xI_y-I_{xy}^2}\left[\ I_y\cdot R_x+I_{xy}\cdot R_y\right] \tag{46}$$

$$Y_0=\frac{1}{I_xI_y-I_{xy}^2}\left[I_x\cdot R_y-I_{xy}\cdot R_x\right] \tag{47}$$

Various open cross-sections are obtained from the sections in Figure 2.3.8.

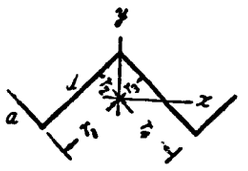

Figure 2.3.9

T shape $a=b,\quad b=e=f=0$

Corrugated shape $b=e=0,\quad a=f,\quad c=d$

Unequal sided angle shape $a=b=e=f=0,\quad c\neq d$

Equal sided angle shape $a=b=e=f=0,\quad c=d$

Lip angle shape $a=f=0,\quad b=e,\quad c=d$

Channel shape $a=b=f=0,\quad c=e$

Z shape $a=b=e=0,\quad c=f$

In the case of a corrugated member, assuming $l \fallingdotseq 2(a+d)$, $\theta = 45°$, the coordinates become the principle axis (Figure 2.3.9).

$$m=-[d^2\sin\theta+c(2d+c)\cos\theta]/2(c+d)$$

$$n=[d^2\cos\theta-c(2d+c)\sin\theta]/2(c+d)$$

$$R_x=\left\{-r_2t\cdot\frac{c^2}{2}-r_4t\left(c+\frac{d}{2}\right)d\right\}n$$

$$-r_2tc\cdot\frac{c^2}{6}\sin\theta-r_3td\left\{\frac{c^2}{2}\sin\theta+\frac{d}{2}\left(c\sin\theta-\frac{d}{3}\cos\theta\right)\right\}$$

$$R_y=\left\{-r_2t\cdot\frac{c^2}{2}-r_4t\left(c+\frac{d}{2}\right)d\right\}m$$

$$-r_2tc\cdot\frac{c^2}{6}\cos\theta-r_3td\left\{\frac{c^2}{2}\cos\theta+\frac{d}{2}\left(c\cos\theta+\frac{d}{3}\sin\theta\right)\right\}$$

In the case of an unequal sided angle member

$$m=-[d^2\sin\theta+c(2d+c)\cos\theta]/2(c+d)$$

$$n=[d^2\cos\theta-c(2d+c)\sin\theta]/2(c+d)$$

$$R_x=\left\{-r_1t\cdot\frac{c^2}{2}-r_3t\left(c+\frac{d}{2}\right)d\right\}n$$

$$-r_2tc\cdot\frac{c^2}{6}\sin\theta-r_3td\left\{\frac{c^2}{2}\sin\theta+\frac{d}{2}\left(c\sin\theta-\frac{d}{3}\cos\theta\right)\right\}$$

$$R_y=\left\{-r_1t\cdot\frac{c^2}{2}-r_3t\left(c+\frac{d}{2}\right)d\right\}m$$

$$-r_2tc\cdot\frac{c^2}{6}\cos\theta-r_3td\left\{\frac{c^2}{2}\cos\theta+\frac{d}{2}\left(c\cos\theta+\frac{d}{3}\sin\theta\right)\right\}$$

Assuming $\theta = 0$ (Figure 2.3.10)

$$m=-c(2d+c)/2(c+d)$$

$$n=d^2/2(c+d)$$

$$r_1=c(2d+c)/2(c+d)$$

$$r_2=d^2/2(c+d)$$

$$r_3=c-r_1=c^2/2(c+d)$$

/141

$$R_x=-\frac{1}{6}\frac{tc^2d^3}{c+d},\qquad R_y=\frac{1}{6}\frac{tc^3d^2}{c+d}$$

$$I_x=\frac{td^3}{12(c+d)^2}[4c^2+5cd+d^2]$$

$$I_y=\frac{tc^3}{12(c+d)^2}[4d^2+5cd+c^2]$$

$$I_{xy}=-\frac{c^2d^2t}{4(c+d)}$$

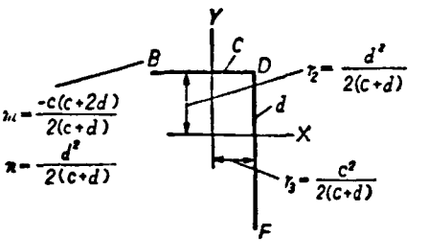

Figure 2.3.10

In the case of equal-sided angle members, in the above example, assuming $c \bar{\wedge} d \wedge h/2$, and $\theta = 45°$, (Figure 3.2.11), the coordinates become the principle axis and $X_0 = 0$, $Y_0 = h/4\sqrt{2}$. That is, the shear center becomes the point of intersection of the two sides.

When a lip HE is attached to the section in Figure 2.3.8, see Figure 2.3.12, assuming the geometric moment of area $\int Yt\,du$ or $\int Xt\,du$ is S_{HE}, the geometric moment of area of point E is $S_{(H)E}$. This is applied to S_{EF} according to Equation (30). S_{EF} has already been calculated.

$$S_{(H)xF}=S_{(H)x}+S_{xF}$$

The geometric moment of area at point F is

$$S_{(HE)F}=S_{(H)E}+S_{(E)F}$$

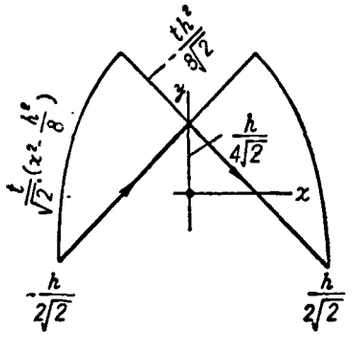

Figure 2.3.11

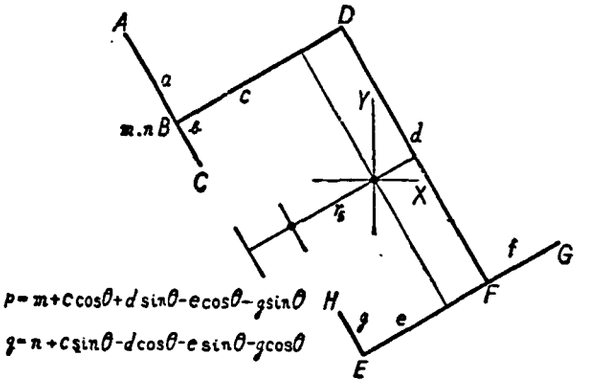

Figure 2.3.12

Consequently, owing to $$R_m=S_{(D)F}+S_{(HE)F}+S_{(G)F}=0$$

the position of the center of gravity, i.e., the magnitude of m, n is determined. Also

$$R_{HE}=\int_H^E rdu\cdot S_{HE}$$

$$R_{EF}=\int_E^F rdu\cdot S_{(H)EF}$$

$$=\int_E^F rdu(S_{(H)E}+S_{EF})$$

$$=\int_E^F rdu\cdot S_{(H)E}+\int_E^F rdu\cdot S_{EF}$$ /142

The second term on the right side has already been calculated. The first term becomes

$$\int_E^F rdu\,S_{(E)E}=S_{(H)E}\int_E^F rdu=S_{(H)E}r_4\int_E^F du$$

and is easy to find. In order to calculate the overall R, one should include the R_{HE} + R_{EF} determined here, in place of the R_{EF} used in the previous example.

In $$R_X=\int_u rdu\int_0^u Yt\,du$$

$$R_Y=\int_u rdu\int_0^u Xt\,du$$

following Timoshenko.[1]

---

[1]S. Timoshenko; Collected Papers (McGraw-Hill, 1953), p. 566.

Assuming

$$\int_0^u r\,du = w_u$$

$$R_Y = \int_u dw_u \int_0^u Xt\,du$$

$$= \left| w_u \int_0^u Xt\,du \right|_u - \int_u w_u Xt\,du$$

For the first term on the right side $\int_0^u Xt\,du$, since the coordinates pass through the center of gravity, we make the provision that it is 0 when u = 0 and when u is the ultimate end. Consequently

$$R_Y = -\int_u w_u Xt\,du$$

Similarly

$$R_X = -\int_u w_u Yt\,du$$

w_u is twice the area of the triangular zone connecting the center of gravity and the center line of the member cross-section. Such a quantity has force in section tdu at the point u and when we integrate for that which expresses the primary moment of this force over all of u, we obtain R. Wagner[1] in his first paper on the buckling accompanying torsion around a shear center introduces the quantity

$$w_u = \int_0^u r\,du$$

where he takes the center of r as the shear center. w_u expresses the degree of elongation w in the direction of the member axis with respect to the unit torsion angle per unit member length at position u of the member section sustaining torsion and w_n which has the same meaning with respect to the direction perpendicular to the center line of member thickness, i.e., with respect to the direction of thickness. In actual thin members, since w_n is quite smaller than w_u, it is possible to use w_u as w. Consequently, it can be seen that the w_u employed by Timoshenko has about the same substance as this. Denoting that which is taken around the shear center w_u as w_{su}, around the center of gravity as w_{0u}, the distance between the shear center and the center of gravity as s, and the solution formed by the tangent to the center line of the cross-section thickness with the straight line OS as β, we obtain

/143

$$w_{su} + w_{0u} = s \int_0^u \sin\beta t\,du = st_m p_u$$

Here, s the projection of the section thickness center line with respect to the line perpendicular to the straight line OS, and is the length corresponding to the range of integration Ou. t_m expresses the average thickness of the member thickness t in this integral. Consequently, the size of this has no relation to the locus of the center line.

[1] H. Wagner: Verdrehung und Knickung von offenen Profilen, Technische Hochschule Danzig 1904-1929, p. 329.

If the cross-section is not thin, the principle shear stress is not self-evident, so in order to determine τ_{xz}, τ_{yz}, it is necessary to follow a strict solution, and in this case, the Poisson ratio ν is related to the position of the shear center. Timoshenko's method of calculation for a semi-circle section member with a radius r (Figure 2.3.13) is as follows.[1]

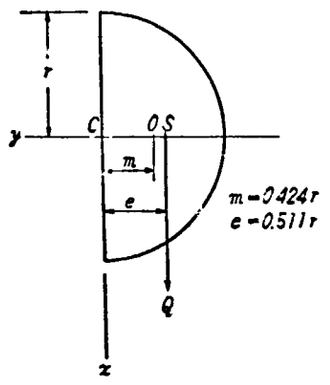

Figure 2.3.13

We place the origin of the coordinates at the center C of the circle. We denote the member length by 1. We assume that the shear stress operating on this section is equal to the shear stress

$$\tau_{zx}=\frac{(3+2\nu)P}{8(1+\nu)I}\left(r^2-x^2-\frac{1-2\nu}{3+2\nu}y^2\right)$$

$$\tau_{zy}=-\frac{(1+2\nu)Pxy}{4(1+\nu)I}$$

which occurs when a load P is operating in direction x on circular cection member with a center C. In the case of a semi-circle, we employ Q = P/2 in place of the P in the above equation. The moment due to this shearing stress with respect to the circle center C is

$$M_z=\int\int(\tau_{zx}y-\tau_{yz}x)dx\,dy$$

The position of load Q due to which point C does not rotate, is expressed by $2M_z/P$. Therefore, the center of gravity O of the semi-circle begins to rotate and its magnitude, ω_2, from the continuity condition

$$-G\frac{\partial}{\partial z}(2\omega_z)=\frac{\nu}{1+\nu}\frac{Py}{I}+C$$

is

$$\omega_z=\frac{\nu P(l-z)\cdot m}{EI}$$

Here, m is the distance of the center of gravity of the semi-circle,

$$m=0.424r$$ /144

In order to eliminate the rotation ω_z around the center of gravity, it is necessary to apply the torque in reverse. Moreover, in order to rotate a semi-circle cross-section member with a radius r, determined from Saint-Venant's calculations, by only a unit length θ, it is necessary to have a torsion moment.

$$M_t=0.296Gr^4\theta$$

Consequently, at position 1 - z, assuming

---

[1]S. Timoshenko, Theory of Elasticity (McGraw-Hill, 1951), p. 334.

$$\theta(l-z)=\omega_s$$

the size of the reverse torque M_t is understood. From this, the position at which load Q should be applied in order for the center of gravity O of the semi-circle not to twist, is

$$e=(M_s-M_t)\frac{2}{P}$$

This indicates the shear center S of a member with a semi-circle cross-section. If $\nu = 0.3$, $e = 0.511r$. This value agrees with the value calculated by A. G. Stevenson. E. Trefftz obtained a result where $e = 0.509r$. When only the condition of equilibrium of forces is taken into account, this is $e = 0.528r$. When a strict solution is used, the shear center must be called that point on a section, or on the same plane as the section, in which a lateral load operates so that the area around the center of gravity of the section of the members sustaining the lateral load that does not rotate. In any case this can be considered as a boundary condition.[1]

2.3.2. BUCKLING COUPLED WITH BENDING AND TORSION

Herbert Wagner first published on the torsional buckling around the shear center of an open section member in order to provide the foundations for design of this type of member, which is used in the structural members of metallic aircraft, as he states in the introduction to the Memorial Volume Commemorating the 25th Anniversary of the establishment of the Danzig Engineering College (1904-1924). Since the resistance to torsion of an open cross-section, where the member thickness is thin, is small, if it is used as a compression member, there are cases in which the member is twisted, buckles and collapses way below its Euler buckling value or yield point. Wagner's explanation states that the center of torsion matches the shear center, and according to later investigators[2] this is an extremely special case which should be treated as pure torsional b .ling. These investigators claim that generally the shear center and torsion center do not agree and that the bending and torsion are coupled. However, Wagner's conception is outstanding, and is of equally high value as Euler's observations on the buckling of columns, as expanded, the field of research on buckling, and has become the motivation for a wide variety of investigations. As a result, Euler's buckling, lateral buckling, and Wagner's buckling together form a single system. Each of them show a unique existence, and it has become clear that the general buckling of members is indicated by the combined values of the three.[3]

---

[1]W. R. Osgood: The center of shear again, JOURNAL OF APPLIED MECHANICS, Vol. 10 (1943), p. A-62.

[2]Robert Kappus: Drillknicken zentrisch gedruckter Stabe mit offenem Profil in elastischen Bereich, Luftfahrforschung, Bd. 14 (1937), p. 444.

[3]J. N. Goodier: Torsional and Flexural Buckling of Bars of Thin-Walled Open Section under Compressive and Bending Loads, Jr. Applied Mechanics, Vol. 9 (1942), P. A. 103.

We shall consider an open cross-section member such as that shown in Figure 2.3.14 following Wagner's initial paper. If a torsion feat is applied around the shear center line S, a shear flow indicated by the arrow in Figure 2.3.15 can be considered, for a member in which the length and center line of the thickness of the cross-section is expressed by z. The torsion angle between the two ends is denoted by ψ. Denoting by r the connecting line from the shear center to the point u on the section centerline, owing to the angle of rotation, ψ in both sections 1 and 3 of the member length z, the u points on the two sections will move with respect to each other by only rψ. Consequently, for the unit length, there is an angular displacement rψ/z. /145

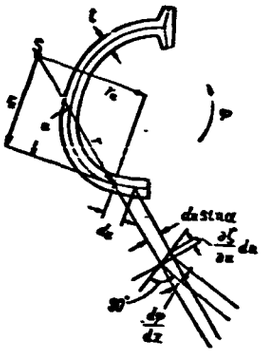

Figure 2.3.14

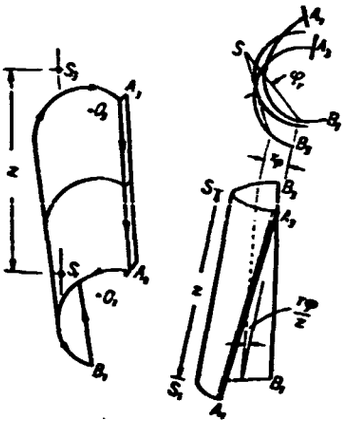

Figure 2.3.15

At points u, due to torsion, it can be seen that section 1 crosses with an angle rψ/z. In this case, the straight line uu is perpendicular to both end planes before and after the torsion. When ψ changes in the direction z, these are considered to have a torsion angle dψ with respect to each other considering the two sections in the space dz. (Figure 2.3.16) At first, when the member AB A_3B_3 is twisted, only dψ around the section center S, it becomes $A_1B_1A_3B_3$, and the uu_3 of the position r from the shear center becomes u_1u_3. $uu_1 = rd\psi$, uu_3, u_1u_3 are respectively right angles to the member section centerlines AB, A_1B_1. In order to determine the relative strain in the direction of the member axis before and after the torsion of the small strips with a length dz and a width du on the center line at point u, if these small strips are projected on the plane uu_3u_1, since the plane is perpendicular to r, and r has an intersection angle α AB and u, the graph shown in Figure 2.3.16 (a) is obtained. Since uu_1 is rdψ, angle uu_3u_1 becomes r dψ/dz, u_1u_1' has a slope r dψ/dz with respect to uu'. Consequently for the width $uu' = u_1u_1' = du \cdot \sin\alpha$, a difference in displacement of du sin α·r dψ/dz occurs. If r sin α = r_u, this difference becomes /146

$$du \sin\alpha \cdot r\frac{d\varphi}{dz} = \varphi' \cdot r_u \, du$$

If we denote by ζ the displacement of the section in the direction of the member axis, i.e., the degree of warp, with respect to the width du on the centerline,

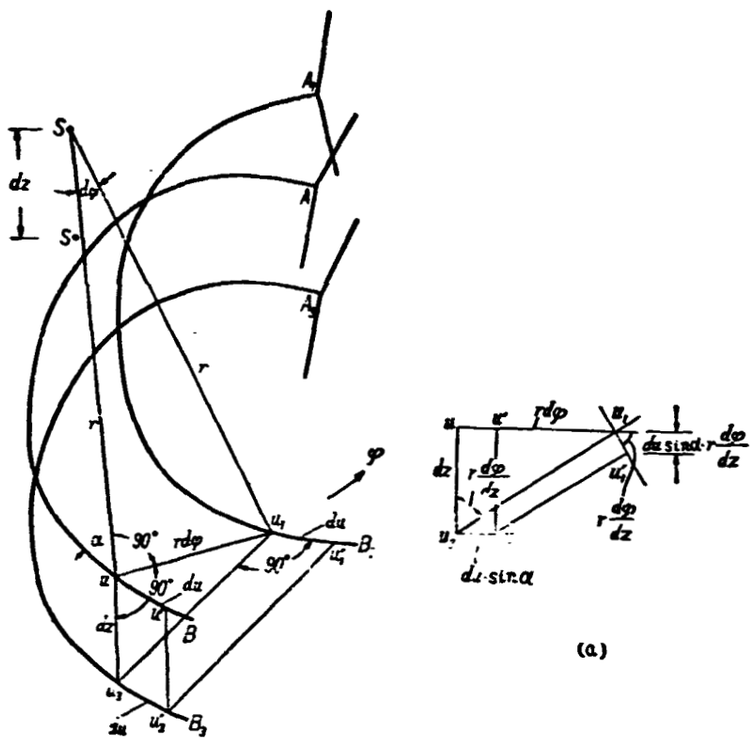

Figure 2.3.16

$$\frac{\partial \zeta}{\partial u} du = \varphi' \cdot r_n \, du$$

is established.

$$\frac{\partial \zeta}{\partial u} = r_n \cdot \varphi'$$

The displacement at an arbitrary point u on the centerline of thickness of the section is expressed by

$$\zeta_n = \varphi' \int r_n \, du$$

The origin of integration is determined later. Similarly, even in the direction of the normal to the section centerline, i.e., in the direction of thickness, there is displacement in the direction of the member axis, and writing $r_n = r \cos \alpha$

$$\frac{\partial \zeta}{\partial n} = r_n \cdot \varphi'$$

Therefore, the displacement of the points expressed by u, n on the member section is

$$\zeta=\zeta_u+\zeta_n=\varphi'\left(\int^u r_u\,du+\int_0^n r_n\,dn\right)\qquad=\varphi'(w_u+w_n)=\varphi'\cdot w \tag{1}$$

$$w_u=\int^u r_u\,du \tag{1a}$$

$$w_n=\int_0^n r_n\,du \tag{1b}$$

Here w is the degree of displacement of a section where $\psi' = 1$ in the direction of the member axis. Since r_n is constant in the direction of the normal to position u,

$$w_n=r_n\cdot n$$

The lower limit of integration in (1a) is assumed to be the position where the average of the displacements ζ_u in the direction of the member axis becomes 0. That is, the condition is

$$\int_A \zeta\,dA=0,\quad \text{よって}\quad \int_A w\,dA=0 \tag{1c}$$

moreover, since the average value of w_n is originally 0 /147

$$\int_A w_n\,dA=\int_u w_n t\cdot du=0 \tag{1d}$$

The $\int_A$ in the above equation indicates integration over the entire domain of the section while $\int_u$ integrates over the total length of the section thickness centerline.

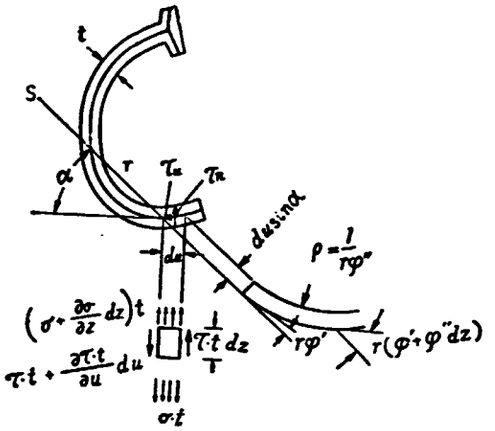

Figure 2.3.17

When ψ' is not constant, the short strip of width du sin α orthogonally projected on r of section du then has a curvature of

$$\rho=\frac{1}{r\varphi''}$$

(See Figure 2.3.17.) For this reason, elongation or contraction occurs in the direction of the member axis

$$de=r\varphi''\cdot du\sin\alpha$$

Denoting the stress in the direction of the member axis due to this as σ

$$\frac{\partial\sigma}{\partial u}=E\varphi''\cdot r_n$$

Therefore

$$\sigma = E\varphi'' \int^{u} r_u \, du$$

The change in σ in the direction n is

$$\frac{\partial \sigma}{\partial n} = E\varphi'' \cdot r_u$$

That is

$$\sigma = E\varphi'' \cdot r_u \cdot n$$

Therefore, adding these

$$\sigma = E\varphi'' \left(\int^{u} r_u \, du + r_u \cdot n \right) \tag{2}$$

Since there is no load in the direction of the axis

$$\int_A \sigma \cdot dA = 0 \tag{2a}$$

Comparing (2) with (1), (1a), we obtain

$$\sigma = E\varphi''(w_u + w_u) = E\varphi'' z \tag{2b}$$

Moreover, since the torsion has been applied around the shear center, from the definition of the shear center, σ does not form a bending moment.

Due to the presence of σ, resistance occurs with respect to torsion. Denoting the member length by l, the torsion moment around both ends by M, when the additional torsional moment $-dM_Z/dz = m$, from outside along the member axis is given, the strain energy of the member is

$$V = \frac{GJ_T}{2} \int_0^l \varphi'^2 \, dz + \frac{1}{2E} \int_0^l \int_A \sigma^2 \, dz \, dA \qquad \underline{/148}$$

The first term is based on Saint-Venant's torsional shear stress, and the second term is based on the direct stress described above. Moreover, when the point of position u on the section has a difference in the direction of z, shear stress also occurs, but the strain energy due to this is disregarded. From Equation (2b)

$$\frac{1}{2E} \int_0^l \int_A \sigma^2 \, dz \, dA = \frac{1}{2} E \int_A w^2 \, dA \int_0^l \varphi''^2 \, dz = \frac{1}{2} E C_{BT} \int_0^l \varphi''^2 \, dz \tag{3}$$

Here, we shall call this, following Wagner, Biegungs-verdrehungswiderstand (resistance to bending with torsion).[1]

---

[1] At first, Wagner used C_{bd} in place of C_{BT}, and claimed that this was in order to simplify expressing the integration. Moreover, later in the papers published jointly by Wagner and Pretschner at Lufo. (1934), C_{BT} and C_{bd} are mixed. As indicated below, different symbols are used by different authors. C* (Kappus), Γ (Goodier, Bleich), C_1 (Timoshenko), C_M (Kollbrunner, Meister).

(4)

$$C_{BT}=\int_A w^2 dA$$

In order to utilize the principle of hypothetical displacement, especially when both ends of the member are fixed, when the differential displacement $\delta\psi$ is given, according to the hypothesis,

Moreover since $z=0,\ z=l$ において $\delta\varphi=0,\ \delta\varphi'=0$

The following equation is established $\delta V=\delta T$

$$\frac{1}{2}GJ_T\int_0^l \delta(\varphi')^2 dz+\frac{1}{2}EC_{BT}\int_0^l \delta(\varphi''^2)dz$$

$$=\int_0^l m\,\delta\varphi\cdot dz$$

The end conditions of the member are included in order to calculate this. As a result,

$$\int_0^l(-GJ_T\varphi''+EC_{BT}\varphi''''-m)\delta\varphi\cdot dz=0$$

Since the above equation should hold with regard to any size $\delta\psi$,

$$EC_{BT}\cdot\varphi''''-GJ_T\cdot\varphi''\equiv m=-\frac{dM_z}{dz} \tag{5}$$

Integrated once, this becomes

$$-EC_{BT}\cdot\varphi'''+GJ_T\cdot\varphi'=M_z \tag{5a}$$

The derivation of this equation was carried out by Wagner, and is extremely elegant, but the differentiation calculations are troublesome. For this reason, we shall indicate below the method of the author which derives equation (5a) more easily.

We shall consider an overhanging beam (Figure 2.3.18) with a member length l[1]. We assume that a torsion moment M is applied to the front end, and an additional torsional $dM_z/dz\,dz$ in the middle, a torsion angle ϕ at the front end, and a torsion angle ψ at z. We shall take the section z from the tip, and calculate the work of the external forces in this section, and the strain energy due to the internal forces. The deformation in this case is assumed to be as /149

[1] We have taken as an example, the overhanging beam on page 174-180, of the article Verderhung und Knickung von offenen Profilen, Luftfahrforschung, Vol. XI (1934), published by H. Wagner and W. Pretschner which is frequently cited, as a thesis of Wagner's. The discussion below applies also to cases other than overhanging beams.

originally, and consider that the torsional moment (stress) and normal stress σ operating on the section at z to be the same as the external forces.

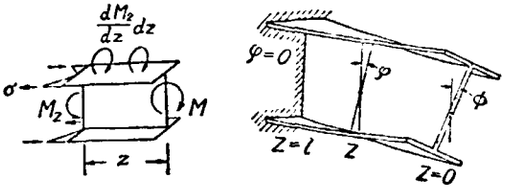

Figure 2.3.18

$$-\frac{1}{2}M\phi+\frac{1}{2}M_s\varphi-\frac{1}{2}\int_0^z\frac{dM_s}{dz}\cdot\varphi\,dz+\frac{1}{2}\int_A\sigma\cdot\zeta\,dA \qquad (6)$$
$$=\frac{EC_{BT}}{2}\int_0^z\left(\frac{d^2\varphi}{dz^2}\right)^2dz+\frac{GJ_T}{2}\int_0^z\left(\frac{d\varphi}{dz}\right)^2dz$$

The first term on the left side of the above equation is the work of the torsion moment of the free end, the second term is the work done by the stress torsion moment of the section [literally cut] end and the third term is the work done by the additional torsional moment. The fourth term is the work done by the normal stress based on the torsion working on the section [literally cut] plane and integration is carried out over the entire range of the section end plane.

If Equations (1) (2b), and (4) are used,

$$\int_A\sigma\cdot\zeta\cdot dA=\int_A E\varphi''w\cdot\varphi'\cdot w\,dA=EC_{BT}\cdot\varphi'\cdot\varphi'' \qquad (7)$$

Inserting (7) and differentiating equation (6) for z,

$$-\frac{1}{2}M_s\varphi'+\frac{EC_{BT}}{2}\varphi'\varphi'''+\frac{EC_{BT}}{2}\varphi''^2=-\frac{EC_{BT}}{2}\varphi''^2+\frac{GJ_T}{2}\varphi'^2$$

Leaving the term M_Z on the left side, transferring the other terms to the right side, and dividing by ψ', the same results are obtained as in Equation (5a).[1]

$$M_s=-EC_{BT}\varphi'''+GJ_T\varphi'$$

[1]Timoshenko first proposed this relation for the case of the lateral buckling of an I beam in 1905. Theory of Elastic Stability (McGraw-Hill, 1936), p. 257. Later, he expanded this method for the bending and torsion of thin-walled members of open cross-section. See Theory of Bending, Torsion and Buckling of Thin-Walled Members of Open Cross Section, Jr. Franklin Institute 239 (3,4,5), 201-219, 249-268, 343-361 (1945) and his Collected Papers (McGraw-Hill 1953), p. 576.

Also, differentiating this by z,

$$\frac{dM_u}{dz}=-EC_{BT}\varphi''''+GJ_T\varphi''$$

the equations for continuity of bending with torsion are determined if the torsion of a member occurring around the shear center, due to a load applied to the member is expressed by these equations, and if the relations expressing the bending of a member occurring on the principle axis is established and connected with these equations.

Generation of Shear Stress Based on Change in Normal Stress

When there is a change in the normal stress σ in direction z, a shear stress τ is generated together with this. We shall consider σ_u corresponding to the τ_u measured along the cross-section centerline, and τ_n corresponding to the σ_n measured at right angles to the cross-section centerline. From the equilibrium of the forces in the infinitesimal part with a width du, length dz, and thickness t

$$d(\tau_u\cdot t)=\frac{\partial\sigma_u}{\partial z}\cdot dA=E\varphi'''\cdot w_u\cdot dA \qquad \text{/150}$$

At position u

$$\tau_u\cdot t=E\varphi'''\int_0^u w_u\cdot t\,du \qquad (8)$$

the moment due to this shear stress is

$$M_u=\int_A \tau_u\cdot r_u\cdot dA=\int_u r_u\cdot du\cdot\tau_u t$$

$$=E\varphi'''\int_u r_u du\int_0^u w_u\cdot t\,du$$

Carrying out partial integration, using Equations (1) and (1a),

$$M_u=-E\varphi'''\int_A w_u^2\,dA=-E\varphi'''C_{BTu}$$

The shear stress based on the normal stress σ_n operates in direction n, and becomes a parabola.

Therefore $$M_n=-E\varphi'''\int w_n^2\,dA=-E\varphi'''C_{BTn}$$

$$M=M_u+M_n$$

and, assuming

$$C_{BT}=C_{BTu}+C_{BTn} \qquad (9)$$

This agrees with

$$C_{BT}=\int_A w^2\,dA$$

and

$$C_{BTu}=\int_A w_u^2\,dA \tag{10}$$

$$C_{BTn}=\int_A w_n^2\,dA \tag{11}$$

Moreover, the resultants of τ due to (8) are 0. They are essentially different from the τ indicated in Equations (32), (33) in the above section.

Calculation of C_{BT}

The following procedure is used in order to calculate C_{BT} by (9), (10), (11). According to (1a)

$$w_u=\int^u r_u\,du$$

but denoting the origin of this integration by u_0, the foot of the perpendicular to the member thickness centerline from the shear center, and denoting w_u at u_0 /151 by w_{u0} (Figure 2.3.19),

$$w_u=w_{u0}+\int_{u0}^{u} r_u\,du \tag{12}$$

Here w_{u0} is the value of w_u at points u_0 determined by the conditions of (1c). r_n is zero at this point. We assume that the case due to the path of integration in an upwards direction from u_0 as positive and that the case due to the path of integration in a direction downward from u_0 is negative. If we draw a line tangent to the centerline of the member thickness from the shear center S, and denote point of tangent by u_1, here, r_u is 0.

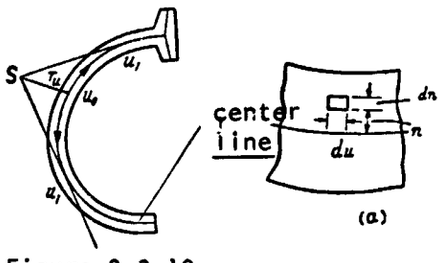

Figure 2.3.19

When within the range of integration, u passes over u_1, this is determined by the following equation (Figure 2.3.20)

$$w=w_0+\int_{u0}^{u1} r_u\,du-\int_{u1}^{u} r_u\,du \tag{13}$$

Moreover, when the u passes beyond the tangent point u_2

$$w=w_0+\int_{u_0}^{u_1} r_u\,du-\int_{u_1}^{u_2} r_u\,du+\int_{u_2}^{u} r_u\,du \tag{14}$$

We determine w below by the same method. When the configuration of the cross-section is determined by straight lines, (Figure 2.3.20 (a)), if u is on line Su_1, r_u is 0, and if line uu_1 is within the angle Su_1u_0, equation (12) is used, while if line uu_1 passes outside of angle Su_1u_0, equation (13) is used. The same is true below. Next, in order to calculate C_{BTn}, from equation (1b)

$$w_n=\int_{-\frac{n}{2}}^{\frac{n}{2}} r_n\,dn=r_n\cdot n$$

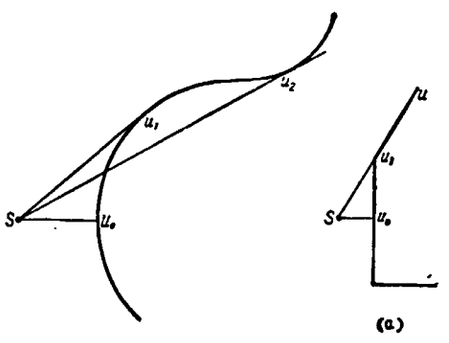

(a)

Figure 2.3.20

Inserting this in (11), (Figure 2.3.19 (a))

$$C_{Br_n}=\int_{\Delta} w_n^2\,dA=\int_u\int_{-\frac{t}{2}}^{\frac{t}{2}} w_n^2\,dn\cdot du$$

$$=\int_u\int_{-\frac{t}{2}}^{\frac{t}{2}} r_n^2\cdot n^2\,dn\cdot du=\frac{t^3}{12}\int_u r_n^2\,du$$

In a uniaxillary symmetrical cross-section member, there is a u_0 on the symmetric axis. Here, since the torsion extension of the cross-section is

$$w_{u_0}=0$$

Therefore, from (12)

$$w_u=\int_{u_0}^{u} r_u\,du$$

In the case of channel steel as in Figure 2.3.21, within the range u_0B, point B becomes the point of tangent, so

$$w_u-e\int_{u_0}^{u} du=ey$$

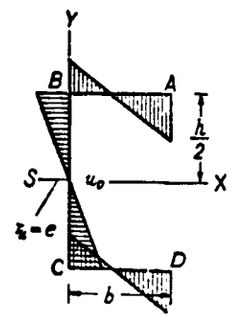

Figure 2.3.21

Therefore, at point B, this is eh/2. Moreover, /152 within the range BA

$$w_u=\frac{eh}{2}-\frac{h}{2}\int_e^x dx=\frac{eh}{2}-\frac{h}{2}(x-e)=eh-\frac{hx}{2}$$

At point A

$$w_u=\frac{h}{2}(e-b)$$

Within the range u_0C

$$w_u=-e\int_{u_0}^{u} du=e\int_0^y dy=ey$$

Therefore, at point C -eh/2

Since point C becomes the tangent point, within CD

$$w_u=\frac{hx}{2}-eh$$

At point D

$$w_u=\frac{h}{2}(b-e)$$

When $u \leqq u_1$, inserting equation (12) in (10)

$$C_{BT_u}=\int_u\left(w_0+\int_{u_0}^{u} r_u\,du\right)^2 t\,du \tag{15}$$

When $u < u \leqq u_2$, inse ting (13) in equation (10)

$$C_{BT_u}=C_{BT_{u_1}}+\int_u\left(w_0+\int_{u_0}^{u_1} r_u\,du-\int_{u_1}^{u} r_u\,du\right)^2 t\,du \tag{16}$$

Here

$$C_{BT_{u_1}}=\int_{u_0}^{u_1}\left(w_0+\int_{u_0}^{u} r_u\,du\right)^2 t\,du$$

When $u_2 < u \leqq u_3$, inserting (14) in equation (10)

$$C_{BT_u}=C_{BT_{u_2}}+\int_u\left(w_0+\int_{u_0}^{u_1} r_u\,du-\int_{u_1}^{u_2} r_u\,du+\int_{u_2}^{u} r_u\,du\right)^2 t\,du \tag{17}$$

Here

$$C_{BT_{u_2}}=C_{BT_{u_1}}+\int_{u_0}^{u_2}\left(w_0+\int_{u_0}^{u_1} r_u\,du-\int_{u_1}^{u} r_u\,du\right)^2 t\,du$$

Using these, the following procedure is obtained for determining C_{BTu} for the channel steel shown in Figure 2.3.21.

$$C_{BT_u}=\int_0^{\frac{h}{2}} e^2y^2t\,dy+\int_e^{e+b}\left(eh-\frac{hx}{2}\right)^2 t\,dx-\int_0^{-\frac{h}{2}} e^2y^2t\,dy$$

$$+\int_e^{e+b}\left(-eh+\frac{hx}{2}\right)^2 t\,dx$$

$$=\frac{th^2}{12}(e^2h+6be^2-6eb^2+2b^3)$$

Also, determining C_{BT_n} /153

$$C_{BT_n}=\int_u\frac{t^3}{12}r_u^2\,du=\frac{t^3}{12}\int_e^{e+b}x^2\,dx\times 2$$

$$+\frac{t^3}{12}\int_{-\frac{h}{2}}^{\frac{h}{2}} y^2\,dy=\frac{t^3b}{18}(3e^2+3eb+b^2)+\frac{t^3h^3}{144}$$

If we determine C_{BT} for I steel, Figure 2.3.22, we obtain the following

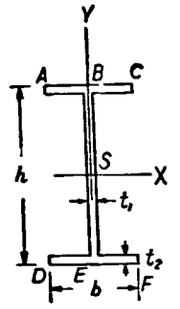

Figure 2.3.22

For EF, DE, AB, BC $\quad w_\omega = \frac{h}{2}x$

For AD

$$w_\omega = 0$$

$$C_{BT_\omega} = 4 \times \int_\omega \frac{h^2}{4} x^2 t_2 \, d\omega = \frac{b^3 t_2}{6}\left(\frac{h}{2}\right)^2 = I_y\left(\frac{h}{2}\right)^2$$

$$C_{BT_\omega} = \frac{1}{12}\left[t_2^3 \int_0^{\frac{b}{2}} x^2 dx\right] \times 4 + \frac{1}{12}\left[t_1^3 \int_0^{\frac{h}{2}} y^2 dy\right] \times 2$$

$$= \frac{t_2^3 b^3}{72} + \frac{t_1^3 h^3}{144}$$

Wagner's Buckling Values

When a compressive force is applied to solid angle steel as shown in Figure 2.3.23, it can be considered that deformations of type (a) or (b) occur. The reasons for this are (1) the possibility[1] of local buckling when two legs of angle steel are supported on three sides and a plate with one free side applies a compressive force to the two opposing symbol support sides, and (2) the possibility of buckling when, as a result of compression, torsion occurs around the shear center.

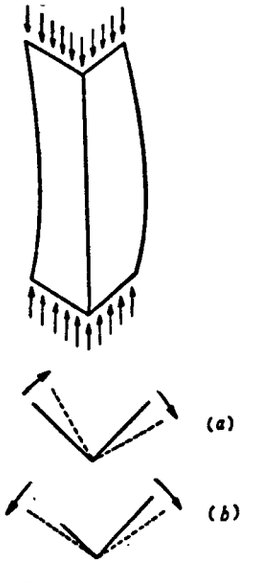

Figure 2.3.23

Case 2 does not differ in terms of deformation, from case 1, since it happens that in angle steel, the shear center is at the point of intersection of the two sides. If the energy required for the occurrence of (a), and for (b) is compared, since (b) requires only enough extra energy to change the configuration of the cross-section, usually, case (a) is treated as a problem in literature.

We shall consider the case in which a member sustaining a compressive force P undergoes torsion and then buckling. In this case, the torsion angle is infinitesimal and we assume that we can disregard the square of the term for it. If torsion occurs in a member, a normal stress σ and a shearing force τ accompanying it occur, but the resultant of σ in the direction of the member axis naturally is 0. Moreover, the effect of τ is to cause a pure torsion moment, and its magnitude, from (5a) is expressed by

[1]Timoshenko solved this problem for the first time in 1910. Theory of Elastic Stability (McGraw-Hill, 1936), p. 337.

$$M=-EC_{BT}\cdot\varphi'''+GJ_T\cdot\varphi'$$

Since the cross-section has an inclination $r\psi'$ at a postion r from the shear center, owing to twisting, a compressive force σ in the direction of the member axis produces a component at right angles to r where /154

$$\sigma \sin r\varphi' \fallingdotseq \sigma r\varphi'$$

Consequently, a torsion moment

$$M=\varphi' \int_A r^2\sigma A=\varphi'\cdot\sigma\cdot I_{SP}$$

occurs around the shear center. σ = P/A, $I_{SP} = \int_A r^2 dA$, I_{SP} are the extreme secondary moments around the shear center and assuming

$$i_{SP}^2=\frac{I_{SP}}{A} \tag{18}$$

and

$$M=\varphi'\cdot P\cdot i_{SP}^2 \tag{19}$$

When an elastic torsional resistance is present along the member, it is also necessary to add this. When a unit torsion angle is applied to a unit length, assuming that there is a torsion resistance β, β is considered as a type of spring constant. The torsion resistance moment per unit length due to this is $\beta\psi$, if this value is added to (5) and (19)

$$\varphi''''\cdot EC_{BT}+\varphi''(P\cdot i_{SP}^2-GJ_T)+\beta\cdot\varphi=0 \tag{20}$$

In the case of 2 ends with simple support, equation (20) is solved assuming the conditions

where $x=0,\ x=l, \qquad \varphi=0,\ \varphi''=0$

are satisfied. In this case, when $\beta = 0$, we assume $\psi = \psi_0 \sin \pi z/1$. γ_0 is the torsion angle in the center of the member. From this, assuming equation (20) to be an Eigen value of P, we obtain

$$P_w=\frac{1}{i_{SP}^2}\left(GJ_T+\frac{\pi^2}{l^2}EC_{BT}\right) \tag{21}$$

This is called Wagner's buckling value. When (18) is used

$$\sigma_w=\frac{1}{I_{SP}}\left(GJ_T+\frac{\pi^2}{l^2}EC_{BT}\right) \tag{22}$$

P_W, σ_W correspond respectively to Euler's buckling value (See article 2.1.1).

$$P_e=\frac{\pi^2EI}{l^2},\quad \sigma_e=\frac{\pi^2E}{\lambda^2}$$

When the spring constant β is present, with n an integer, the Eigen value becomes

$$P=\frac{1}{i_{SP}^2}\left(GJ_T+\frac{\pi^2\pi^2}{l^2}EC_{ST}+\frac{l^2}{\pi^2\pi^2}\cdot\beta\right) \tag{23}$$

Differentiating (23) for 1/n assuming 0, if we determine the member length l_1 giving a minimum value of P

$$l_1=\pi\sqrt{EC_{ST}/\beta} \tag{24}$$

If this value is inserted in (23), for $l > l_1$

$$P_{min}=\frac{1}{i_{SP}^2}(GJ_T+2\sqrt{EC_{ST}\beta}) \tag{25}$$

For $l \leq l_1$

$$P=\frac{1}{i_{SP}^2}\left(GJ_T+\frac{\pi^2}{l^2}EC_{ST}+\frac{l^2}{\pi^2}\beta\right) \tag{26}$$

/155

should be used. In Figure 2.3.24, $1/l_1$ is taken on the lateral axis, and P is taken on the longitudinal axis, and the buckling loads are indicated for various ends.

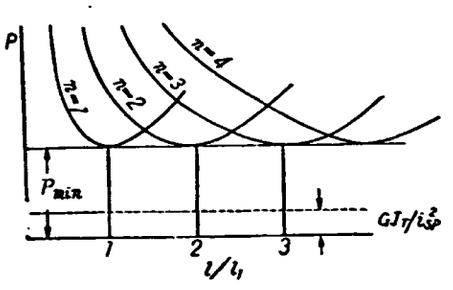

Figure 2.3.24

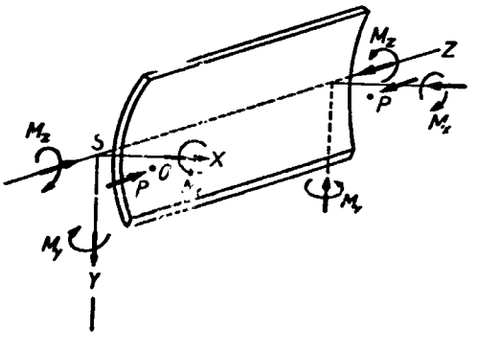

Figure 2.3.25

Compound Buckling from Central Compression, Simple Bending and Simple Torsion[1]

Let us consider the compounds bending and torsional buckling in the case when an axial force P acts on the center of gravity O in a thin-walled open section, such as that shown in Figure 2.3.25, a bending moment M_X, M_Y acts on the plane of the two principle axes and a torsion moment M_Z acts around the shear center axis.

We take the X, Y axes parallel to the principle axis, passing through the shear center S of the member before deformation. The Z is the shear center line. We assume that when the stresses acting on the cross-section are as shown in the figure, we are positive. That is, with regard to the planes of action of stress, viewing the end planes in the positive direction of the coordinates, we shall assume that for the normal stress P, this is positive when in the positive direction of the coordinates, and that for bending and torsional moments, combining the direction of rotation of the moments and the direction of rotation of the right twist and pointing a vector arrow in the direction of movement of the right twist, we assume that they are positive when the arrow is in the positive direction of the coordinates. In addition, we will aim the coordinates in terms of moments.

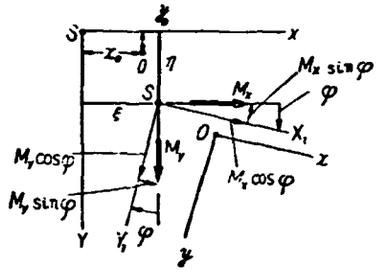

Figure 2.3.26

When the end planes of the member are viewed in the negative direction of the coordinates, the stresses which are in a direction opposite to that described above are positive. We express the principle axes of the cross-section as x, y, z; the geometrical moment of inertia around the x axis as I_x, the geometrical moment of inertia around the y axis as I_y. We denote by X_1, Y_1, Z_1 the coordinate axes related to the sheer center when X, Y, Z are fixed in space, and the cross-section moves together with the bending and torsional deformation of the member. We consider Z_1 and Z parallel. The turn angle ψ of X_1 with respect to X is positive in the case when it is in the direction of the positive range of Y, from the positive range of X, i.e., as shown in Figure 2.3.26. The value is extremely small, and it can be assumed that

$$\cos\varphi \fallingdotseq 1, \quad \sin\varphi \fallingdotseq \varphi$$

Since we are dealing with a thin-walled open section, we assume that the configuration does not change when the member is displaced. Expressing the movement of the shear center by ξ and η, the movement of the center of gravity O, with the coordinates of center of gravity x_0, y_0 /156

$$\xi + x_0\cos\varphi - y_0\sin\varphi - x_0 = \xi - y_0\varphi \tag{27}$$

[1]J. N. Goodier makes the same type explanation as this. Torsional and Flexural Buckling of Bars of Thin-Walled Open Section under Compressive and Bending Loads. Jr. Applied Mechanics, Vol. 9 (1942), p. A 103.

The author has attempted to construct a system where the direction of the external forces differs from that of Goodier.

$$\eta + x_0 \sin\varphi + y_0 \sin\varphi - y_0 = \eta + x_0\varphi \tag{28}$$

The movement of the center of gravity causes a bending moment due to the forces in the direction of the axes. That is, the bending moment that causes deflection in the plane XZ is

$$P(\eta + x_0\varphi) \tag{29}$$

The bending moment causing deflection in plane YZ is

$$P(\xi - y_0\varphi) \tag{30}$$

Since ψ is small, these are equal to the bending moment planes X_1Z_1, Y_1Z_1.

The bending moments M_X, M_Y and the torsion moment M_Z produce force components owing to displacement of the plane of action. As shown in Figure 2.3.26, M_X and M_Y are vector expressions and in the direction of X_1 there is $M_X \cos\psi$ and $M_Y \sin\psi$, while in the direction Y_1 there is $-M_X \sin\psi$ and $M_Y \cos\psi$. Moreover, as shown in Figure 2.3.27, due to M_Z this is $-M_z\frac{d\xi}{dz}$, in the direction of X_1 and $-M_z\frac{d\eta}{dz}$ in the direction of Y_1 but the former views the end plane XZ in the positive direction of Y so the sign is not changed, and becomes $-M_z\frac{d\xi}{dz}$ while the latter, since it views the end plane YZ in the negative direction of X, the sign is reversed, becoming $M_z\frac{d\eta}{dz}$. Therefore, the sum of the bending moments acting in X_1Z_1, bringing together the vectors in the direction of Y_1 is

$$-M_X \sin\varphi + M_Y \cos\varphi + M_z\frac{d\eta}{dz} = -M_X\varphi + M_Y + M_z\eta' \tag{31}$$

Similarly, the sum of the bending moments acting in plane Y_1Z_1, bringing together the vectors in X_1 is

$$M_X \cos\varphi + M_Y \sin\varphi - M_z\frac{d\xi}{dz} = M_X + M_Y\varphi - M_z\xi' \tag{32}$$

The equilibrium due to the bending moments is determined as follows, with ξ, η, and ψ as parameters.

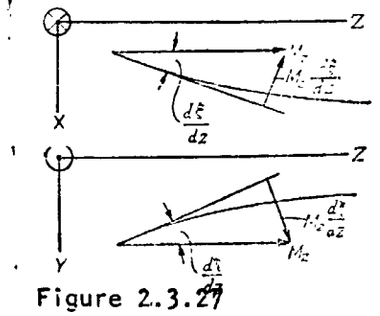

Figure 2.3.27

The equilibrium with respect to the bending moments acting in plane X_1Z_1 from (29) and (31) is

$$EI_y\xi'' + P(\xi - y_0\varphi) - M_X\varphi + M_Y + M_z\eta' = 0 \tag{33}$$

The equilibrium with respect to the bending moments acting in the plane Y_1Z_1, from (30) and (32) is

$$EI_z\eta''+P(\eta+x_0\varphi)-M_x-M_T\varphi-M_z\xi'=0 \tag{34}$$

The ξ'', η'' in (33) and (34) can be viewed as the curvature in the planes X_1Z_1, Y_1Z_1, since ψ is infinitesimally small.

Cover Page Title

We consider the following with regard to the torsion moment around these Z_1 axes. When the shear center moves only by ξ, η an arbitrary portion of an infinitesimally small area tdu on the section undergoes the following relative movement in comparison with before moving. Here, X_1Y_1 indicate the coordinates measured by the axes of the coordinates X_1Y_1 of the infinitesimally small area.

In direction X_1 /157

$$x_1-(x_1\cos\varphi+y_1\sin\varphi-\xi\cos\varphi-\eta\sin\varphi)=\xi-y_1\varphi \tag{35}$$

In direction Y_1

$$y_1-(-x_1\sin\varphi+y_1\cos\varphi+\xi\sin\varphi-\eta\cos\varphi)=\eta+x_1\varphi \tag{36}$$

Consequently, in plane X_1Z_1, the strip tdu has an inclination

$$\frac{d(\xi-y_1\varphi)}{dz}=\xi'-y_1\varphi'$$

and in plane Y_1Z_1, its inclination is (4")

$$\frac{d(\eta+x_1\varphi)}{dz}=\eta'+x_1\varphi'$$

Therefore, as shown in Figure 2.3.28, the normal stress σ acting on dA = tdu on the cross-section has the component

X_1 方向に分力 $-\sigma dA(\xi'-y_1\varphi')$ in the direction X_1 and a resultant

Y_1 方向に分力 $\sigma dA(\eta'+x_1\varphi')$ in the direction Y_1,

and this forms the torsion moment in the direction of the shear center.

That is, the torsion moment due to σdA is

$$dM=-[\sigma dA(\xi'-y_1\varphi')y_1-\sigma dA(\eta'+x_1\varphi')x_1]$$

Integrating this over the entire cross-section

$$M=-\int_A\{\sigma dA(\xi'-y_1\varphi')\cdot y_1-\sigma dA(\eta'+x_1\varphi')x_1\}$$

The σ in the above equation is the normal stress within the cross-section, and if the compressive stress is positive,

$$\sigma=\frac{P}{A}-\frac{M_T}{I_p}(x_1-x_0)+\frac{M_x}{I_e}(y_1-y_0) \tag{37}$$

Inserting this

$$M=-\left[\frac{P}{A}\int_{\Delta}\{(\xi'-y_1\varphi')y_1-(\eta'+x_1\varphi')x_1\}\,dA\right. \tag{38}$$

$$-\frac{M_Y}{I_y}\int_{\Delta}\{(\xi'-y_1\varphi')y_1-(\eta'+x_1\varphi')x_1\}(x_1-x_0)dA$$

$$\left.+\frac{M_X}{I_x}\int_{\Delta}\{(\xi'-y_1\varphi')y_1-(\eta'+x_1\varphi')x_1\}(y_1-y_0)dA\right]$$

In order to carry out the above calculations, we denote the coordinates related to the principal axis as x, y, and express the relationship with the coordinates X_1, Y_1 with respect to axes X_1, Y_1 by

$$x_1=x_0+x, \quad y_1=y_0+y$$

And, since[1]

$$\int_{\Delta}x_1\,dA=x_0A, \quad \int_{\Delta}y_1\,dA=y_0A, \quad \int_{\Delta}x_1^2\,dA=x_0^2A+I_y,$$

$$\int_{\Delta}y_1^2\,dA=y_0^2A+I_x, \quad \int_{\Delta}x_1y_1\,dA=x_0y_0A, \qquad \underline{/158}$$

$$\int_{\Delta}x_1^3\,dA=x_0^3A+3x_0I_y+H_y$$

$$\int_{\Delta}y_1^3\,dA=y_0^3A+3y_0I_x+H_x$$

$$\int_{\Delta}x_1^2y_1\,dA=x_0^2y_0A+y_0I_y+{}_xH_y$$

$$\int_{\Delta}y_1^2x_1\,dA=x_0y_0^2A+x_0I_x+{}_yH_x$$

$$H_y=\int_{\Delta}x^3\,dA, \quad H_x=\int_{\Delta}y^3\,dA, \quad {}_xH_y=\int_{\Delta}x^2y\,dA,$$

$${}_yH_x=\int_{\Delta}xy^2\,dA$$

Inserting this in (38), and adding M_Z, we obtain the following equation which expresses the total torsion moment.

$$-EC_{BT}\varphi''' + \left\{GJ_T - P\cdot i_{SP}^2 + M_Y\left(2x_0 + \frac{H_y + {}_yH_z}{I_y}\right) - M_X\left(2y_0 + \frac{H_x + {}_xH_y}{I_x}y\right)\right\}\varphi' + (Py_0 + M_X)\xi' - (Px_0 - M_T)\eta' = M_z \tag{39}$$

If we make the three equations (33), (34), and (39) simultaneous, the compound buckling values for bending and torsion with respect to a thin-walled open cross-section are determined.[1]

Flexure and Torsion of a Member with Lateral Load and Added Flexural Moment[2]

Given a member with a multi-lateral cross-section, made by welding together several thin plates, we denote its center of gravity by O (Figure 2.3.29). We denote by x and y the principal axes of the cross-section, and take z in the direction of the member axis. When a lateral load acts on this member, we assume that Navier's law is maintained, that the configuration of the cross-section is not deformed. Plate I which is at a distance R_1 from the center of gravity, taking as O_i the center of gravity due to the bending acting on that plate, rotates around the axes that are orthogonal to the plate. (Figure 2.3.29a). We denote by ε_i the elongation in direction Z in the center of gravity of the plate. Denoting by ζ_0, η_0, ψ the movement of the center of gravity O, the displacement of the center of gravity O_i of plate i is expressed by the distance $O_{i1}O_i' = s_i$ between the center of gravity O_{i1} after displacement and the projected point O_i' onto the plane of displacement of O_i. The curvature of plate

---

[1]The following relations are also obtained in the coefficients in the above cross-section.

$$I_{SP} = \int_A x_1^2\,dA + \int_A y_1^2\,dA = s^2A + I_x + I_y$$

I_{SP}, geometric moment of inertia around shear center.

S, distance between shear center and center of gravity.

$$\kappa_1 = H_y + {}_yH_z - x_0 I_{SP}$$
$$\kappa_2 = H_x + {}_xH_y - y_0 I_{SP}$$

κ_1, κ_2 are the section coefficients used by Goodier (Journal of Applied Mechanics, (1942), p. A106).

In a member with a cross-section in which the x axis is symmetrical,
$H_X = {}_xH_y = 0$
In a member with a cross-section in which the y axis is symmetrical,
$H_y = {}_yH_X = 0$
In a member with a cross-section in which both axes are symmetrical,
$H_X = H_y = {}_xH_y = {}_yH_X = 0$

[2]F. Bleich: Buckling Strength of Metal Structures (McGraw-Hill 1952), p. 107.

i becomes s_i''. From the continuity conditions of the plate,

$$\bar{\varepsilon}_{i-1}+a_{i-1}'s_{i-1}''=\bar{\varepsilon}_i-a_is_i'' \qquad (40)$$ /159

Denoting by ε the total average elongation of the plate and the total cross-section area by A

$$A\varepsilon=\sum_{i=1}^{n}Ai\,\bar{\varepsilon}_i$$

If we denote by

$$e_i=\bar{\varepsilon}_i-\varepsilon$$

the difference between the elongation in the center of gravity in each plate and the average elongation

From equation (40)

$$e_{i-1}+a_{i-1}'s_{i-1}''=e_i-a_is_i'' \qquad (41)$$

$$\sum_{i=1}^{n}A_ie_i=0 \qquad (42)$$

Since (41) and (42) are in equations related to ε_i, it is possible to solve this and to express this by the curvature s_i'' of each plate.

$$s_i=-\xi_0\sin\alpha_i+\eta_0\cos\alpha_i+\varphi r_i$$

$$s_i''=-\xi_0''\sin\alpha_i+\eta_0''\cos\alpha_i+\varphi''r_i$$

Assuming α_0 to be small and cos α_0 = 1 and sin α_0 =

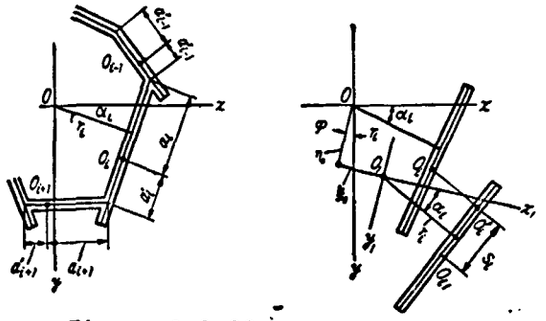

Figure 2.3.29

If this is used, the strain energy of the plate is

$$V_1=\sum_{i=1}^{n}\frac{1}{2}\int(EI_is_i''^2+EA_i\bar{\varepsilon}_i^2)dz \qquad (43)$$

$$=\frac{E}{2}\int\left[\sum_{i=1}^{n}(I_is_i''^2+A_i\varepsilon_i^2)+A\varepsilon^2\right]dz$$

$$=\frac{1}{2}\int(EI_y\xi_0''^2+EI_z\eta_0''^2+2ER_y\xi_0''\varphi''+2ER_z\eta_0''\varphi''$$

$$+ER_\omega\varphi''^2+EA\varepsilon^2)dz$$

If a strain energy

$$V_2=\frac{1}{2}GJ_T\varphi'^2dz$$

Due to the Saint-Venant's torsion moment is applied to this, this becomes the

total strain energy of the member. Moreover, the work of the load is expressed by

$$T=\int(\xi_0 q_x+\eta_0 q_y+\varphi m)dz$$

Q_X, q_Y and m are the lateral loads in directions x and y passing through the center of gravity, and the torsion moment. Consequently, the total potential energy in this member is

$$U=V_1+V_2-T \tag{44}$$

That the buckling condition formula is determined under the condition that the change in U due to the displacements $_0$, 0, , is minimum. Using the method of variation (44), the following four equations are obtained: /160

$$EI_y\xi_0''''+ER_y\varphi''''=q_x \tag{45}$$

$$EI_x\eta_0''''+ER_x\varphi'''=q_y \tag{46}$$

$$ER_y\xi_0''''+ER_x\eta_0''''+ER_\rho\varphi''''-GJ_T\varphi''=m \tag{47}$$

$$EA\varepsilon=0 \tag{48}$$

Here

$$q_x=-\frac{d^2M_y}{dz^2},\quad q_y=-\frac{d^2M_x}{dz^2},\quad m=-\frac{dM_z}{dz}$$

When a load in the direction of the axis does not act upon the member, (48) is constantly satisfied. In (45), (46), (47), writing

$$\xi_0=\xi-\frac{R_y}{I_y}\varphi \tag{49}$$

$$\eta_0=\eta-\frac{R_x}{I_x}\varphi \tag{50}$$

We obtained

$$EI_y\xi''''=q_x \tag{51}$$

$$EI_x\eta''''=q_y \tag{52}$$

$$E\left(R_\rho-\frac{R_y^2}{I_y}-\frac{R_x^2}{I_x}\right)\varphi''''-GJ_T\varphi'' \tag{53}$$
$$=m+y_0q_x-x_0q_y$$

$$R_\rho-\frac{R_y^2}{I_y}-\frac{R_x^2}{I_x}=C_{BT} \tag{54}$$

we obtain

$$-EC_{BT}\varphi''''+GJ_T\varphi''=-m-y_0q_x+x_0q_y \tag{55}$$

is of exactly the same form as (5a), so it can be seen that ξ, η are the degree of movement of the shear center, and the right side expresses the torsion moment around the shear center. As for the position of the shear center, writing $\xi_0 = 0$, $\eta_0 = 0$ in (49) and (50), the movement of the shear center when the center of gravity does not move is $\xi = R_y\psi/I_y$, $\eta = R_x\psi/I_x$, so the shear center is seen to be $x_s = R_x/I_x$, $y_s = R_y/I_y$.

Using the parameters , the strain energy becomes as follows

$$V=\frac{1}{2}\int_0^l (EI_y\xi''^2+EI_x\eta''^2+EC_{BT}\varphi''^2+GJ_T\varphi'^2+EA\xi'^2)dz \tag{56}$$

Denoting by T the work done by the load with respect to this, the total potential energy becomes

$$U = V - T$$

Member Sustaining Central Compressive Load

When a central compressive load P is sustained, with /161

$$\sigma=\frac{P}{A}$$

Then

$$T=\frac{1}{2}\int_0^l \left[P(\xi'^2+\eta'^2)+2Py_s\xi'\varphi'-2Px_s\eta'\varphi' +P\cdot i_{SP}^2\varphi'^2\right]dz \tag{57}$$

The x_s, y_s in the above equations are the coordinates of the shear center with respect to the principal axes. Therefore

$$U=\frac{1}{2}\int_0^l \left[EI_y\xi''^2+EI_x\eta''^2+EC_{BT}\varphi''^2+GJ_T\varphi'^2 -P(\xi'^2+\eta'^2)-2Py_s\xi'\varphi'+2Px_s\eta'\varphi'-P\cdot i_{SP}^2\varphi'^2\right]dz \tag{58}$$

If we carry out variations such that U is minimum for ξ, η, ψ

$$EI_y\xi''''+P\xi''+Py_s\varphi''=0 \tag{59}[1]$$

$$EI_x\eta''''+P\eta''-Px_s\varphi''=0 \tag{60}[2]$$

$$Py_s\xi''-Px_s\eta''+EC_{BT}\varphi''''+(Pi_{SP}^2-GJ_T)\varphi''=0 \tag{61}[3]$$

[1,2,3] Bleich maintains that these equations hold also within the non-elastic range and he uses E_t in place of E and G_t in place of G. (See Article 2.1.4.) Buckling Strength of Metal Structures, p.- 124.

The author devised a method which takes into consideration the non-elastic effect, based on the properties of the cross-section and published his findings in the collected papers of the 8th Joint Conference on Stress Dynamics (1958), p. 25.

(59), (60) and (61) correspond respecti· ly to (33), (34), and (39).

Compound Buckling Consisting of Central Compression, Simple Bending, Simple Torsion, Added Torsion, and Lateral Load.

If we differentiate (39), which twice differentiated (33) and (34) by z

$$EI_y\xi''''+P(\xi''-y_0\varphi'')-M_x\varphi''+M_z\eta''=0 \tag{62}$$

$$EI_z\eta''''+P(\eta''+x_0\varphi'')-M_T\varphi''-M_z\xi''=0 \tag{63}$$

$$-EC_{ST}\varphi''''+(GJ_T-P\cdot i_{SP}^2)\varphi''+(Py_0+M_x)\xi''-(P\cdot x_0-M_T)\eta''=0 \tag{64}$$

Comparing this with (59), (60), (61), if we insert the relations $x_0 = -x_S$, $y_0 = -y_S$,

$$EI_y\xi''''=-P(\xi''-y_0\varphi'')-M_x\varphi''+M_z\eta''+q_z \tag{65}$$

$$EI_z\eta''''=-P(\eta''+x_0\varphi'')+M_T\varphi''+M_z\xi''+q_y \tag{66}$$

$$-EC_{ST}\varphi''''+GJ_T\varphi''=P(i_{SP}^2\cdot\varphi''-y_0\xi''+x_0\eta'')-M_x\xi''+M_T\eta'' \tag{67}$$
$$+y_0q_z-x_0q_y-m$$

As can be seen from the right side of equation (67), the presence of a compressive force that acts to reduce the size of the torsion moment due to the distributive load. (65), (66), (67) are general equations.

In particular, assuming $P = M_Z = m = 0$, they express a lateral buckling equation. Moreover, assuming the loads other than M_X to be 0,

$$EI_y\xi''''=M_x\varphi'' \tag{68}$$

$$-EC_{ST}\varphi''''+GJ_T\varphi''=-M_x\xi'' \tag{69}$$

Differentiating (69) twice, /162

$$-EC_{ST}\varphi''''''+GJ_T\varphi''''=-M_x\xi''''=-\frac{M_x^2}{EI_y}\varphi'' \tag{69a}$$

Assuming a simple support at both ends of member length 1, writing

$$\varphi=C\cdot\sin\frac{\pi z}{l}$$

where z = 0, z = 1, = 0, so (69a) becomes

$$\frac{\pi^2}{l^2}\left(\frac{\pi^2}{l^2}EC_{BT}+GJ_T\right)=\frac{M_X^2}{EI_y} \tag{70}$$

Here

$$M_X=i_{SP}\sqrt{P_w P_{ex}} \tag{71}$$

$$P_w=\frac{1}{i_{SP}^2}\left(\frac{\pi^2}{l^2}EC_{BT}+GJ_T\right)$$

$$P_{ex}=\frac{\pi^2 EI_y}{l^2}$$

In an I beam, writing

$$C_{BT}=\frac{h^2 I_y}{4},\quad J_T=\frac{ht_1^3}{3}+\frac{2bt_2^3}{3},\quad B=EI_y,\quad D=\frac{B}{2},\quad C=GJ_T$$

Then

$$M_X=\frac{\pi}{l}\sqrt{BC}\sqrt{1+\frac{\pi^2 h^2}{l^2}\frac{D}{2C}}$$

This is exactly the same as Equation (2.2.1).

In a Member with a Cross-section with One Symmetrical Axis, one of the Principal Axes becomes a Symmetrical Axis

Denoting this by XX, the shear center and center of gravity are on this line. We draw an axis YY through the shear center.

From (33), (34), (39), we obtain the three equations respectively:

$$EI_y\xi''+P\xi=0 \tag{72}$$

$$EI_x\eta''+P(\eta+x_0\varphi)=0 \tag{73}$$

$$-EC_{BT}\varphi'''+(GJ_T-Pi_{SP}^2)\varphi'-Px_0\eta'=0 \tag{74}$$

From Equation (72) the Euler buckling load P_{eX} giving deflection in direction X is determined and from (73), (74), the flexural and torsional buckling values are obtained. In this deformation, there is a compounding only of the torsion and the movement in the direction of the Y axis. In the case where both ends have a simple support, according to the normal hypothesis, it is possible to write

$$\eta=C_2\sin\frac{n\pi z}{l},\qquad \varphi=C_3\sin\frac{n\pi z}{l}$$

At both ends, = = 0, '' = '' = 0. If this is inserted in (73),(74)

$$\left\{C_2\left(-\frac{\pi^2 EI_z}{l^2}+P\right)+C_3\cdot P\cdot x_0\right\}\sin\frac{\pi z}{l}=0 \qquad \text{/163}$$

$$\left[C_2 P\cdot x_0\frac{\pi}{l}+C_3\left\{-EC_{BT}\frac{\pi^3}{l^3}+(Pi_{SP}^2-GJ_T)\frac{\pi}{l}\right\}\right]\cos\frac{\pi z}{l}=0$$

In order for this to be simultaneous, in spite of C_2, C_3, its determinant must be 0.

$$\begin{vmatrix} -\frac{\pi^2 EI_z}{l^2}+P & P\cdot x_0 \\ P\cdot x_0 & -EC_{BT}\frac{\pi^2}{l^2}+P\cdot i_{SP}^2-GJ_T \end{vmatrix}=0$$

Solving this, for the compound buckling values

$$P=\frac{(P_w+P_{eT})\pm\sqrt{(P_w-P_{eT})^2+4\left(\frac{x_0}{i_{SP}}\right)^2 P_w P_{eT}}}{2\left\{1-\left(\frac{x_0}{i_{SP}}\right)^2\right\}} \qquad (75)$$

P_W is Wagner's buckling value, P_{eY} is Euler's buckling value with deflection in direction Y. Consequently, in a member with one axis symmetrical, there is no buckling value P_W.[1] P takes two values which are larger or smaller than either P_W or P_{eY}. In particular, when $x_0 = 0$, i.e., when the center of gravity agrees with the shear center, we obtain

(76)

$$P=\frac{(P_w+P_{eT})\pm(P_w-P_{eT})}{2}=P_w \text{ or } P_{eY}$$

In this case, the member has two axes symmetrical.

M. Kuranishi: Some Recent Investigation on the Elastic Stability of Bars, Report of the Research Institute of Technology, Nihon Univ. No. 1 (1952), p. 16. Okumura Toschie, Dissertation presented to Tokyo University: Stability of Members Sustaining Bending Moment and Axial Compressive Force. Publications of the Society for Civil Engineering, No. 33 (1956), p. 50.

Goodier indicates this point. Journal of Applied Mechanics (1942), p. A105.

Photographs 1(a) and 1(b) indicate buckling for the case in which a central compressive load is applied in an aluminum, lip-angle cross-section member.[1] /164 It can be seen that the crest lines are twisted in a straight manner.

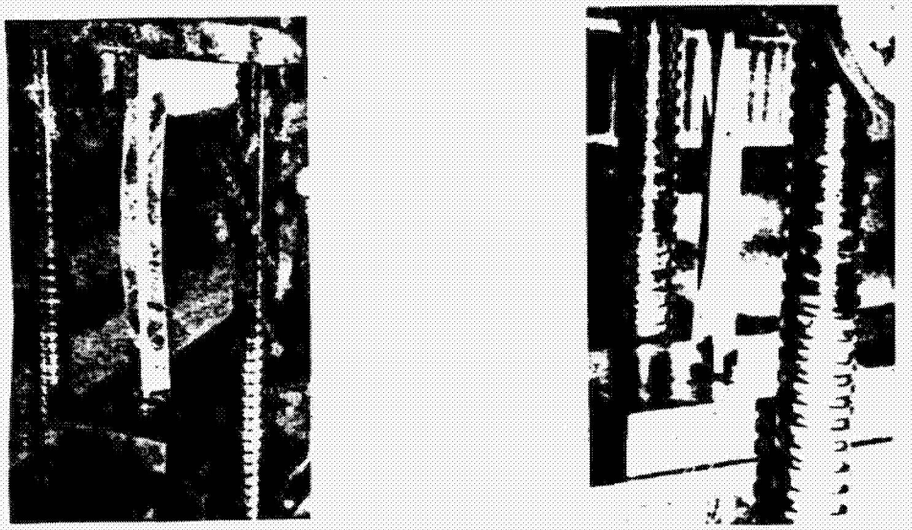

(a) (b)

Photograph 1

Case in which an eccentric compressive load is applied to a member having a cross-section with one symmetrical axis. Eccentricity in direction of axis XX (Figure 2.3.30).

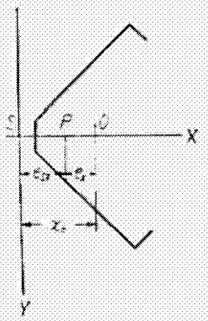

Figure 2.3.30

When a uniform eccentric compressive load is applied, assuming that in equations (33), (34) and (39) $x_0 = x_0$, $y_0 = 0$, $M_Y = P \cdot e_X$, $M_X = 0$, $e_{SX} = x_0 - e_X$, the following equations are obtained:

$$EI_y\xi'' + P\xi + P \cdot e_X = 0 \tag{77}$$

$$EI_x\eta'' + P\eta + P \cdot e_{SX} \cdot \varphi = 0 \tag{78}$$

$$-EC_{BT}\varphi''' + \left\{GJ_T - P \cdot i_{SP}^2 + P \cdot e_X\left(2x_0 + \frac{H_y + yH_z}{I_x}\right)\right\}\varphi' - P \cdot e_{SX} \cdot \eta' = 0 \tag{79}$$

[1]Experiment conducted by Kato Tsutomu under the author's guidance. Ph.D dissertation, Department of Physics, Tokyo University (1957).

Even in this case, equation (77) gives the buckling deformation in direction X, and the buckling value is

$$P_{eX}=\pi^2 EI_y/l^2$$

when the member has simple supports at both ends. (78) and (79) combine displacement in direction Y and twist.

$$P=\frac{(P_w+\alpha P_{eY})\mp\sqrt{(P_w-\alpha P_{eY})^2+4\left(\frac{e_{SX}}{i_{SP}}\right)^2 P_w P_{eY}}}{2\left\{\alpha-\left(\frac{e_{SX}}{i_{SP}}\right)^2\right\}} \tag{80}$$

Here

$$\alpha=1-\frac{e_X}{i_{SP}^2}\left(\frac{2x_0 I_y+H_y+{}_yH_z}{I_y}\right)$$

So, if in equation (80), $e_{SX}=0$,

$$P=\frac{P_w}{\alpha} \quad \text{または} \quad P_{eY}$$

is obtained

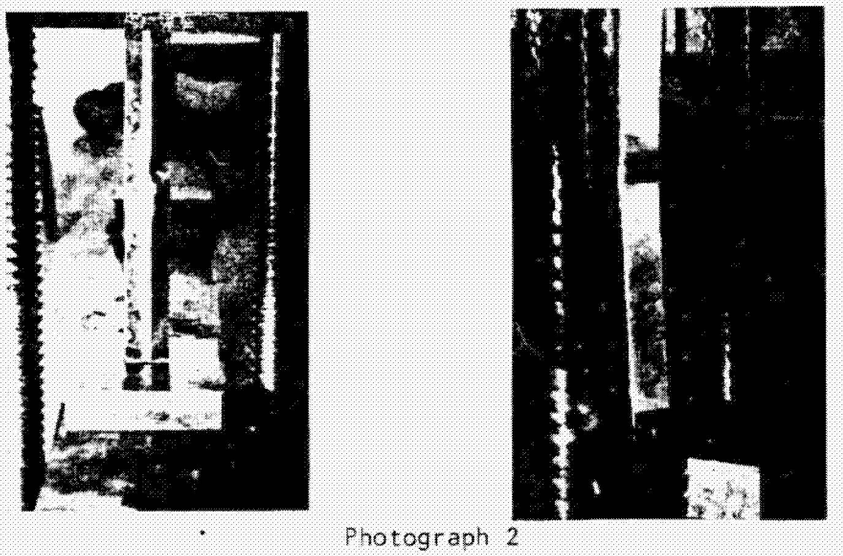

Photograph 2

That is, when an axial compressive force is applied to the shear center, any of the buckling values

$$P_{eX},\ P_{eY},\ P_w/\alpha$$

is obtained. When $\alpha = 1$, a buckling value P_W is obtained, but it is necessary for $e_X = 0$ or $x_0 = H_y = {}_yH_z = 0$ for this purpose. This condition indicates the /165 case of central compression of a bi-axially symmetrical open cross-section member.

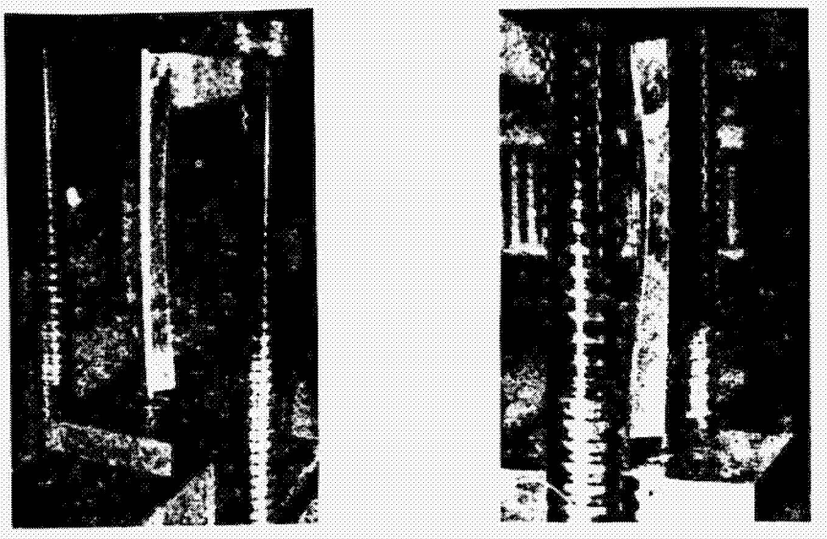

Photograph 3

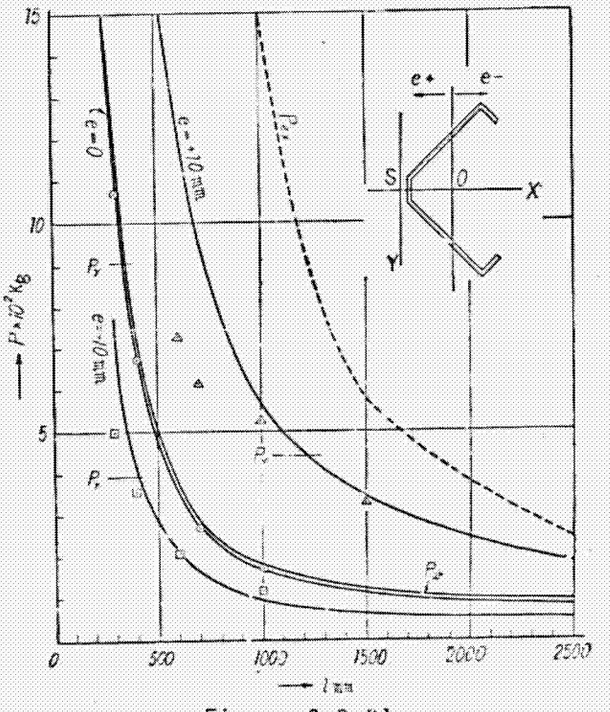

Figure 2.3.31

When the load point in Photograph 2 is between SO in Photograph 3, the load point is outside of the O in SO. Photograph 2 shows the reaching of the yield point with bending in direction of X, and the tendency for twisting cannot be seen. Photograph 3 shows bending and twisting in direction Y. Figure 2.3.31 /166

shows the results of tests on these members with simple support at both ends[1] Eccentricity in direction of YY axis (see Figure 2.3.32).

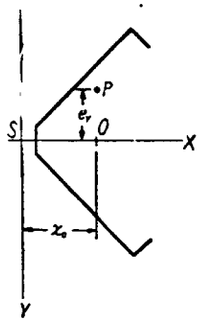

Figure 2.3.32

When a compressive load is applied in the direction of the axis YY from the center of gravity at a distance of e_Y, in equations (33), (34) and (39), we assume

$x_0=x_0$, $y_0=0$, $M_X=P\cdot e_Y$, $M_Y=0$

$$EI\xi''+P\xi-P\cdot e_Y\varphi=0 \tag{81}$$

$$EI\eta''+P(\eta+x_0\varphi)-P\cdot e_Y=0 \tag{82}$$

$$-EC_{BT}\varphi'''+(GJ_T-Pi_{SP}^2)\varphi'+P\cdot e_Y\xi'-P\cdot x_0\eta'=0 \tag{83}$$

In this case, when the three equations (81), (82), and (83) are linked, the buckling deformation involves bending in both directions X, Y and is accompanied by torsion. Further differentiating (82) by z, we eliminate the term $P\cdot e_Y$. In the case of a member with simple supports at both ends, assuming

$$\xi=C_1\sin\frac{\pi z}{l},\quad \eta=C_2\sin\frac{\pi z}{l},\quad \varphi=C_3\sin\frac{\pi z}{l}$$

so

$$(P-P_{eX})C_1-P\cdot e_Y C_3=0$$

$$(P-P_{eY})C_2+Px_0C_3=0$$

$$-P\cdot e_Y C_1+Px_0C_2+i_{SP}^2(P-P_w)C_3=0$$

In order for these to be made simultaneous despite the values of C_1, C_2, C_3,

$$\begin{vmatrix} P-P_{eX} & 0 & -P\cdot e_Y \\ 0 & P-P_{eY} & P\cdot x_0 \\ -P\cdot e_Y & P\cdot x_0 & i_{SP}^2(P-P_w) \end{vmatrix}=0$$

Solving this

$$\left(1-\frac{P_{eX}}{P}\right)\left(1-\frac{P_{eY}}{P}\right)\left(1-\frac{P_w}{P}\right)i_{SP}^2-\left(1-\frac{P_{eY}}{P}\right)e_Y^2-\left(1-\frac{P_{eX}}{P}\right)x_0^2=0 \tag{84}$$

If these three equations are solved for P, this will indicate the compound buckling value.

---

[1]See Kato Tsutomu's dissertation cited previously. Also Naka and Kato, Buckling of Solid Members (in Japanese). Tokyo University Press, 1959, p. 49.

The Case of Eccentricity (e_X, e_Y) on Both Axes (Figure 2.3.33).

In Equations (33), (34), and (39), if we assume

$$x_0=x_0,\ y_0=0,\ M_X=P\cdot e_Y,\ M_Y=P\cdot e_X$$

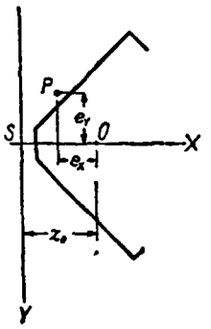

Figure 2.3.33

$$EI_y\xi''+P\xi-P\cdot e_Y\varphi+P\cdot e_X=0 \tag{85}$$

$$EI_x\eta''+P(\eta+x_0\varphi)-P\cdot e_Y-P\cdot e_X\varphi=0 \tag{86}$$

$$-EC_{ET}\varphi'''+\left\{GJ_T-P\cdot i_{SP}^2+P\cdot e_X\left(2x_0+\frac{H_y+yH_z}{I_y}\right)\right\}\varphi' \tag{87}$$
$$+(P\cdot y_0+P\cdot e_Y)\xi'-(P\cdot x_0-P\cdot e_X)\eta'=0$$

If we once differentiate (85) and (86) for z, the constant term Pe_X, $P\cdot e_Y$ are eliminated. That is /167

$$EI_y\xi'''+P\xi'-P\cdot e_Y\varphi'=0 \tag{88}$$

$$EI_x\eta'''+P(\eta'+x_0\varphi')-P\cdot e_X\varphi'=0 \tag{89}$$

Employing (87), (88) and (89) in the case where both ends have a simple support, if we insert

$$\xi=C_1\sin\frac{\pi z}{l},\quad \eta=C_2\sin\frac{\pi z}{l},\quad \varphi=C_3\sin\frac{\pi z}{l}$$

we obtain

$$(P-P_{eX})C_1+P\cdot e_Y\cdot C_3=0$$
$$(P-P_{eY})C_2-P(e_X-x_0)C_3=0$$
$$P\cdot e_Y\cdot C_1-P(e_X-x_0)C_2+i_{SP}^2\left\{P\left(1-\frac{e_X}{i_{SP}^2}\frac{H_y+yH_z}{I_y}\right)-P_w\right\}C_3=0$$

in order for these three equations to be simultaneous for any magnitude of C_1, C_2, C_3, the determinant becomes 0. From this

$$\begin{vmatrix} P-P_{eX} & 0 & P\cdot e_Y \\ 0 & P-P_{eY} & P(x_0-e_X) \\ P\cdot e_Y & P(x_0-e_X) & P\cdot i_{SP}^2\left\{\left(1-\frac{e_X}{i_{SP}^2}\frac{H_y+yH_z}{I_y}\right)-\frac{P_w}{P}\right\} \end{vmatrix}=0$$

Solving this

$$\left(1-\frac{P_{eX}}{P}\right)\left(1-\frac{P_{eY}}{P}\right)\left(\alpha-\frac{P_w}{P}\right)i_{SP}^2-\left(1-\frac{P_{eY}}{P}\right)e_Y^2-\left(1-\frac{Pe_X}{P}\right)(x_0-e_X)^2=0 \tag{90}$$

$$\alpha = 1 - \frac{e}{i_{SP}^2} \frac{H_y + {}_yH_x}{I_y}$$

If we assume $e_X = 0$ in equation (90), we obtain $\alpha = 1$, which agrees with (84).

Member with Two Symmetrical Axes Sustaining a Uniform Eccentric Compressive Force

In the case of a member with two axes that are symmetrical, $x_0 = y_0 = 0$, and $H_y = {}_yH_x = 0$. Therefore, since = 1, equation (90) becomes

$$\left(1 - \frac{P_{eX}}{P}\right)\left(1 - \frac{P_{eY}}{P}\right)\left(1 - \frac{P_w}{P}\right) i_{SP}^2 - \left(1 - \frac{P_{eY}}{P}\right) e_Y^2 - \left(1 - \frac{P_{eX}}{P}\right) e_X^2 = 0 \tag{91}$$

$$i_{SP}^2 = \frac{I_x + I_y}{A} = i_{max}^2 + i_{min}^2$$

Assuming $e_X = 0$ in this equation

$$1 - \frac{P_{eY}}{P} = 0 \tag{91a}$$

or

$$\left(1 - \frac{P_{eX}}{P}\right)\left(1 - \frac{P_w}{P}\right) i_{SP}^2 = e_Y^2 \tag{91b}$$

and from the top equation the buckling values of Pe_Y are obtained while from the lower equation, the compound buckling value including Pe_X, P_W is obtained. /168

The same argument has been given even where $e_Y = 0$, and if both e_X, e_Y are not 0, a compound flexural proportional buckling occurs in the directions of both X, Y. Kato has calculated carefully and graphically illustrated these buckling properties for the dimensions of commercial I steel.[1]

Eccentric Compressive Buckling of Sectional Steel

The case in which the eccentricities of compressive forces applied to both ends of a member are different is solved by maintaining that a central compressive load P (See Figure 2.3.34) and bending moments M_{X0}, M_{Xi} having a different magnitude simultaneously take effect. These bending moments are assumed to act on the inside of the web plane of I steel and a torsion moment M_Z is applied to both ends. Assuming

$$\frac{M_{xl}}{M_{x0}} = \beta$$

---

[1]Kato Tsutomu: Research on Steel Frame Constructions, Doctoral dissertation, Tokyo University Graduate School.

The support point reaction is

$$R=-(1-\beta)\frac{M_{X0}}{l}$$

The relation for deflection and torsion becomes as follows:

$$EI_y\xi''=-P\xi-M_{X0}\left\{1-(1-\beta)\frac{z}{l}\right\}\varphi \tag{92}$$

$$EI_x\eta''=-P\eta+M_{X0}\left\{1-(1-\beta)\frac{z}{l}\right\} \tag{93}$$

$$\begin{aligned}&-EC_{BT}\varphi'''+(GJ_T-P\cdot i_{SP}^2)\varphi'\\&=-M_z+M_{X0}\left\{1-(1-\beta)\frac{z}{l}\right\}\xi'-M_{X0}(1-\beta)\frac{\xi}{l}\end{aligned} \tag{94}$$

Equation (93) provides the unique solution P_{eY}. Consequently, the compound buckling is determined from the two equations (92) and (94).

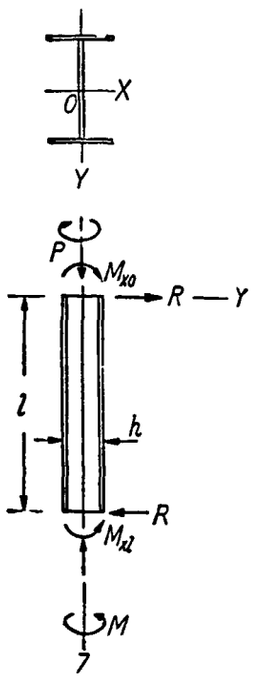

Figure 2.3.34

In the case where both ends have simple support, ξ, ψ are expressed by Fourier's series, and assuming[1]

$$\xi=l\sum_{n=1}^{\infty}\left(a_n\sin\frac{n\pi z}{l}\right) \tag{95}$$

$$\varphi=\frac{lM_{X0}}{GJ_T}\sum_{n=1}^{\infty}\left(b_n\sin\frac{n\pi z}{l}\right) \tag{96}$$

$$B=EI_y,\quad \alpha=\frac{R\cdot i_{SP}^2}{GJ_T},\quad \gamma=\frac{\pi^2}{l^2}\frac{EC_{BT}}{GJ_T}=\frac{\pi^2}{4}\frac{d^2}{l^2}\frac{B}{C},\quad C=GJ_T$$

Inserted in equation (94), the following equation is obtained.

$$-\frac{l^2\gamma}{\pi^2}\varphi'''+(1-\alpha)\varphi'=H\frac{M_{X0}}{C}-\frac{M_z}{C} \tag{97}$$ /169

In the above equation

$$H=(1-\beta)\sum\left(a_n\sin\frac{n\pi z}{l}\right)+\pi\left\{1-(1-\beta)\frac{z}{l}\right\}\sum_n\left(na_n\cos\frac{n\pi z}{l}\right) \tag{98}$$

---

[1] M. R. Horne: The Flexural-Torsional Buckling of Members of Symmetrical I-Section under Combined Thrust and Unequal Terminal Moments, The Quarterly Journal of Mechanics and Applied Mathematics, Vol. VII (1954), p. 410.

M_z is determined if Equation (97) is integrated from z = 0 to z = l.

$$M_s=\pi M_{x0}\sum_n(na_n\psi_n) \tag{99}$$

Here, when n is an odd number $\psi_n=\frac{4}{\pi^2}\frac{1-\beta}{n^2}$

where n is an even number $\psi_n=0$

Therefore, H is expressed by Fourier series

$$H=\sum_{m=1}^{\infty}\left[\sum_{n=1}^{\infty}a_n\{(1-\beta)\lambda_{nm}+n\pi\lambda'_{nm}\}\right]\cos\frac{m\pi z}{l}+\frac{M_s}{M_{x0}} \tag{100}$$

when n + m is odd $\lambda_{nm}=\frac{4}{\pi}\frac{n}{n^2-m^2}$

when n + m is even $\lambda_{nm}=0$

when n + m is odd $\lambda'_{nm}=\frac{4}{\pi^2}\frac{(1-\beta)(n^2+m^2)}{(n^2-m^2)^2}$

when n + m is even $n\neq m,\quad \lambda'_{nm}=0$

$$n=m,\quad \lambda'_{nm}=\frac{1+\beta}{2}$$

Inserting (96), (99), and (100) in equation (97), comparing the coefficient cos mπz/l

$$b_m=\frac{1}{\{(1-\alpha)+m^2\gamma\}}\left[\frac{8}{\pi^2}\frac{(1-\beta)}{m}\sum_n{}'\left\{\frac{n^3}{(n^2-m^2)^2}\right\}a_n+\frac{(1+\beta)}{2}a_m\right] \tag{101}$$

This connects the relations of the Fourier series a_n, b_m independently selective of (95), (96).

The Σ' in the equation indicates that summation should be carried out only when n + m is an odd number. Substituting (96) for the ψ in equation (92)

$$\xi''+\frac{\pi^2}{l^2}\frac{P}{P_{ex}}\xi=-\frac{\pi^2}{l}\left(\frac{M_{x0}}{M_s}\right)^2N \tag{102}$$

$$N=\left\{1-(1-\beta)\frac{z}{l}\right\}\sum_m\left(b_m\sin\frac{m\pi z}{l}\right) \tag{103}$$

$$M_s=-\frac{\pi}{l}\sqrt{BC},\qquad P_{ex}=\frac{\pi^2EI_y}{l^2}$$

Equation (103) is expressing N by Fourier series,

$$N=\sum_{n=1}^{\infty}\left[\sum_{m=1}^{\infty}b_m\mu_{nm}\right]\sin\frac{n\pi z}{l} \tag{104}$$ /170

Here

n + m odd number $\quad \mu_{nm}=\frac{8}{\pi^2}\frac{(1-\beta)nm}{(n^2-m^2)}$

n + m even number $\quad n\neq m,\quad \mu_{nm}=0$

$\quad n=m,\quad \mu_{nm}=\frac{1+\beta}{2}$

Here

$$\xi=l\left(\frac{M_{x0}}{M_{ex}}\right)^2\sum_{n=1}^{\infty}\left[a_n'\sin\frac{n\pi z}{l}\right] \tag{105}$$

If inserted in equation (102)

$$a_n'=\frac{1}{\left(n^2-\frac{P}{P_{ex}}\right)}\left\{\frac{8}{\pi^2}(1-\beta)n\sum_{m}'\left[\frac{m}{(n^2-m^2)^2}\right]b_m+\left(\frac{1+\beta}{2}\right)b_n\right\} \tag{106}$$

This equation again expresses the relationship of the Fourier series coefficients a_n, b_n. $\sum_{m}'$ means that adding summation should be carried out for m such that (n + m) becomes an odd number. If the a_n' here is used in place of the a_n, an even greater approximation is made to the deflection curve.

When the deflection curve is determined in this way, the buckling bending moment M_{X0} corresponding to the axial compressive force P is determined. The procedure follows the energy method.

The work due to compressive force P is, from (105)

$$T_P=\frac{P}{2}\int_0^l\left(\frac{d\xi}{dz}\right)^2dz=\frac{\pi^2}{4}\left(\frac{M_{x0}}{M_e}\right)^2Pl\sum_n\left[n^2a_n'^2\right] \tag{107}$$

Similarly, the work due to the bending moment M is

$$T_M=-\int_0^l M_{x0}\left\{1-(1-\beta)\frac{z}{l}\right\}\varphi\frac{d^2\xi}{dz^2}dz \tag{108}$$

$$=\frac{\pi^2}{2}\left(\frac{M_{x0}}{M_e}\right)^2P_{ex}l\sum_n\left[n^2a_n'^2\left(n^2-\frac{P}{P_{ex}}\right)\right]$$

With respect to this, the strain energy in the member is the bending strain energy

$$V_B=\frac{B}{2}\int_0^l\left(\frac{d^2\xi}{dz^2}\right)^2dz=\frac{\pi^2}{4}\left(\frac{M_{x0}}{M_e}\right)^2P_{ex}l\sum_n\left[n^2a_n'^2\right] \tag{109}$$

The strain energy of the normal stress of the flange due to torsion and extension is, from (96)

$$V_B' = \frac{Bh^2}{8}\int_0^l \varphi''^2 dz = \frac{\pi^2}{4}\left(\frac{M_{X0}}{M_e}\right)^2 \gamma P_{eX} l \sum_m [m^4 b_m^2] \tag{110}$$

The strain energy due to torsion is

$$V_T = \frac{C(1-\alpha)}{2}\int_0^l \varphi'^2 dz = \frac{\pi^2}{4}\left(\frac{M_{X0}}{M_e}\right)^2 (1-\alpha) P_{eX} l \sum_m [m^2 b_m^2] \tag{111}$$

$$T_P + T_M = V_B + V_B' + V_T \tag{112}$$

From this, the following relation between P and M_{X0} is determined /171

$$\left(\frac{M_{X0}}{M_e}\right)^2 \sum_n \left[\pi^2 a_n'^2 \left(\pi^2 - \frac{P}{P_{eX}}\right)\right] = \sum_m [\{(1-\alpha) + m^2\gamma\} m^2 b_m^2] \tag{113}$$

In order to determine a solution from the above equation, first P and β are determined, and then we hypothesize a Fourier series coefficient a_n for determining the form of the deflection curve. From this, b_m is calculated from (101). Table 2 gives the coefficients of a_n for calculating the numerical values within the large parentheses in equation (101). For example, when $\beta = 0$, assuming

From the table

are calculated.

Table 2. b_m in $\theta = \frac{lM_{X_3}}{C}\sum b_m \sin\frac{m\pi z}{l}$

	a_1	a_2	a_3	a_4	a_5	a_6
$b_1\{(1-\alpha)+\gamma\} = \sum(a_n \times$	.5000(1+β)	.7205(1−β)	0	.2306(1−β)	0	.1429(1−β)
$b_2\{(1-\alpha)+4\gamma\} = \sum(a_n \times$	.0450(1−β)	.5000(1+β)	.4377(1−β)	0	.1149(1−β)	0
$b_3\{(1-\alpha)+9\gamma\} = \sum(a_n \times$	0	.0865(1−β)	.5000(1+β)	.3529(1−β)	0	.0801(1−β)
$b_4\{(1-\alpha)+16\gamma\} = \sum(a_n \times$	.0009(1−β)	0	.1117(1−β)	.5000(1+β)	.3127(1−β)	0
$b_5\{(1-\alpha)+25\gamma\} = \sum(a_n \times$	0	.0029(1−β)	0	.1281(1−β)	.5000(1+β)	.2894(1−β)
$b_6\{(1-\alpha)+36\gamma\} = \sum(a_n \times$	.0001(1−β)	0	.0050(1−β)	0	.1396(1−β)	.5000(1+β)

Next, a_n' is determined by inserting these values in equation (106). Table 3 gives the coefficients of b_1, b_2, etc. in order to calculate the a_n' (n - P/P_{eX}); i.e., that which is contained within the large parentheses [trans. note: curly braces?] on the right side of equation (106). If b_m and a_n' are obtained, M_{X0} is determined by inserting them in equation (113). In order to get accurate values for these, one should follow the routine of taking the a_n' determined by (106), returning to (101) with this as a a_n and then calculating b_m.

Table 3. a_n' in $\xi=l\left(\frac{M_{x_0}}{M_{ex}}\right)^2\sum a_n'\sin\frac{n\pi z}{l}$

	b_1	b_2	b_3	b_4	b_5	b_6
$1-P/P_{ey}\}=\sum(b_m\times$	.5000(1+β)	.1801(1−β)	0	.0144(1−β)	0	.0040(1−β)
$1-P/P_{ex}\}=\sum(b_m\times$	.1801(1−β)	.5000(1+β)	.1945(1−β)	0	.0184(1−β)	0
$9-P/P_{ex}\}=\sum(b_m\times$	0	.1945(1−β)	.5000(1+β)	.1985(1−β)	0	.0200(1−β)
$16-P/P_{ex}\}=\sum(b_m\times$	.0144(1−β)	0	.1935(1−β)	.5000(1+β)	.2001(1−β)	0
$25-P/P_{ex}\}=\sum(b_m\times$	0	.0184(1−β)	0	.2001(1−β)	.5000(1+β)	.2010(1−β)
$36-P/P_{ex}\}=\sum(b_m\times$	.0040(1−β)	0	.0200(1−β)	0	.2010(1−β)	.5000(1+β)

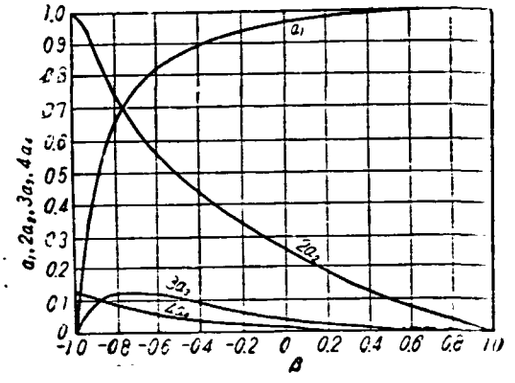

Figure 2.3.35

Figure 2.3.35 indicates the accurate values of a_1, $2a_1$, $3a_3$, $4a_4$, corresponding to the $\beta = M_X l/M_{XO}$ when $P = 0$, $\gamma = 0$. Since these are buckling deflection curves, the relative ratios for the coefficients a_n should be determined. Here, we assume

$$a_1^2+4a_2^2+9a_3^2+16a_4^2=1$$

When $P \neq 0$, a_1 is employed without modification, and if $(1 - P/P_{eX})$ is multiplied with the values of a_2, a_3, a_4, the approximate values of the relative ratio are determined. There is practically no effect of the degree of influence α of the torsional elongation or the bending torsion stiffness γ on the shape of the deflection curve. Consequently, Figure 2.3.35 can be used except in cases where $\beta = -1$. In table 1 and table 2, as one assumes that $\beta = -1$, and that the a_n for the even or odd number values for $n = 0$, the b_m for the odd number values or even number values of $m = 0$. Consequently, one mode has an odd number term a_n but the other mode has an even-numbered term; that is, when

/172

$$\gamma=0,\quad \frac{P}{P_{ex}}<0.77$$

The even-numbered term indicates the minimum buckling value, and when

$$\frac{P}{P_{ex}}>0.77$$

the odd-numbered term gives the minimum buckling value. When in the vicinity of $\beta = -1$, the convergence in calculation by the method of successive approximations, for the deflection curve is slow, but a buckling bending moment can be determined which is normally satisfactory.

When $\beta = 1$, the coefficients other than a_1 and b_1 become 0. Consequently, equations (113) becomes

$$\left(\frac{M_{x_0}}{M_e}\right)^2\frac{1}{\{(1-\alpha)+\gamma\}}+\frac{P}{P_{ex}}=1 \qquad (113a)$$

Since $M_{X0} = P \cdot e_Y$, equation (113a) is none other than (91b). Figure 2.3.36 depicts the relationship $(M_{X0}/M_e)^2/F$ for P/P_{eX} when in equation (113) we assume $\alpha = \gamma = 0$. It can be seen that this relationship is linear where $\beta = 1$, and that it is formed from two separate curves where $\beta = 1$.

Appended Table C_{BT}, JT

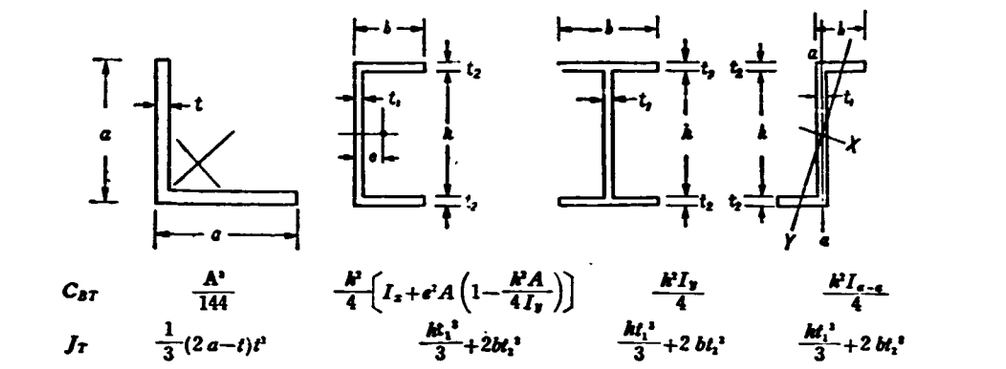

C_{BT}	$\frac{A^2}{144}$	$\frac{h^2}{4}\left[I_x+e^2A\left(1-\frac{h^2A}{4I_y}\right)\right]$	$\frac{h^2I_y}{4}$	$\frac{h^2I_{x-x}}{4}$
J_T	$\frac{1}{3}(2a-t)t^3$	$\frac{ht_1^3}{3}+2bt_2^3$	$\frac{ht_1^3}{3}+2bt_2^3$	$\frac{ht_1^3}{3}+2bt_2^3$

e . . . . distance from center of gravity

A . . . . cross-section area

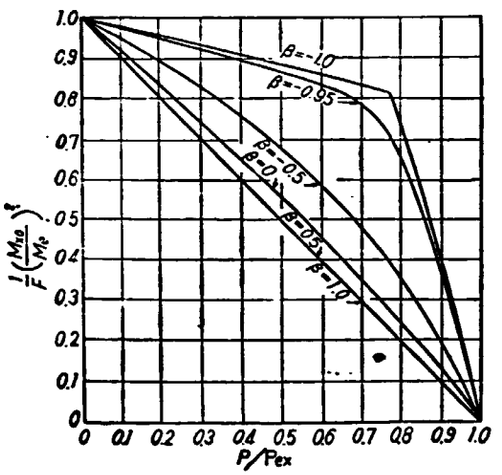

Figure 2.3.36

NUMBER	DIAGRAM & BOUNDARY CONDITIONS	FORMULA OR TABLE FOR RESULTS	REFERENCES, NOTES
1	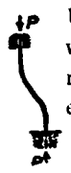 Upper end fixed with no lateral resistance, lower end fixed	$P_k=\frac{\pi^2 EI}{l^2}$	24 Based on Euler's solution. Center is point off in flexion.
2	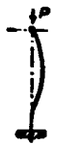 Upper end pin-ended, lower end fixed	$P_k=2.046\frac{\pi^2 EI}{l^2}$ More precisely, the coefficient is 2.04574	26
3	Spring constant c Upper end elastic support Lower end fixed	$P_k=\mu_0\frac{EI}{l^2}$ where μ_0 is first root of $\tan\mu=\mu\left(1-\frac{\mu}{c}\frac{EI}{l^2}\right)$	27
4	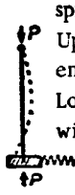 spring constant c Upper end rotating end Lower end fixed with elastic support	$P_k=\mu_0\frac{EI}{l_0}$ where μ_0 is first root of $\tan\mu\cdot\left(1+\frac{\mu}{c}\frac{EI}{l^2}\right)=\mu$	27
5	Column with upper end elastic support Coefficient of stiffness of upper end $c=\frac{H_0}{y_0}$, $c_1=\frac{M_0}{\theta_0}$ are the lateral H_0, M_0 resistance and resistance moments (i) $k_1=0$ Lateral resistance only (ii) $k=0$ Only bending resistance (iii) $k=\infty$ Deflection is 0 at upper end (iv) $k_1=\infty$ No inclincation at upper end	Buckling condition equation $\frac{k(m-\sin m)-m^3}{k(1-\cos m)}=\frac{m\sin m+k_1(1-\cos m)}{m\cos m+k_1\sin m}$ m is the figure below where $m^2\frac{EI}{l^2}=P_k$ $k=cl\Big/\frac{EI}{l^2}$, $k_1=\frac{c_1}{l^2}\Big/\frac{EI}{l^2}$ とする。 (i) $k=\frac{m^3}{m-\tan m}$ (a) (ii) $k_1=-\frac{m}{\tan m}$ (b) (iii) $k_1=\frac{m(\sin m-m\cos m)}{m\sin m+2\cos m-2}$ (c) (iv) $k=\frac{m^3\sin m}{m\sin m+2\cos m-2}$ (d) 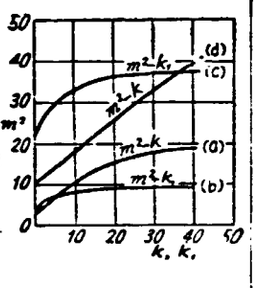	25

6

Column with both ends having elastic support

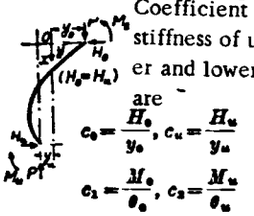

Coefficient of stiffness of upper and lower end are

$$c_0=\frac{H_0}{y_0},\ c_u=\frac{H_u}{y_u}$$

$$c_1=\frac{M_0}{\theta_0},\ c_2=\frac{M_u}{\theta_u}$$

H_0, H_u, M_0, M_u are the lateral resistance and resistance

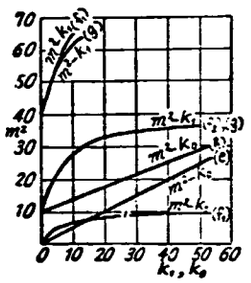

(i) $k_1=0$ Lateral resistance to both ends

(ii) $k_0=0$ Resistance moment on both ends

(iii) $k_0=\infty$ No deflecting at either end

(iv) $k_1=\infty$ Neither end declines

Buckling condition equation

$$\frac{m-\sin m+\frac{m^2(1+\alpha)}{k_0}}{1-\cos m+\frac{\beta m^2}{k_1}-\frac{\beta m^4(1+\alpha)}{k_1k_0}}$$

$$=\frac{\frac{m}{k_1}\sin m+1-\cos m}{\frac{m}{k_1}(\beta+\cos m)+\sin m}$$

where $m=\alpha l$

$$k_0=c_0l\Big/\frac{EI}{l^2},\quad k_1=\frac{c_1}{l}\Big/\frac{EI}{l^2},$$

$$\frac{c_0}{c_u}=\alpha,\quad \frac{c_1}{c_2}=\beta \quad \text{とする.}$$

where the stiffness at both ends is equivalent

$\alpha=\beta=1$

(e) $$\frac{m-\sin m+\frac{2m^2}{k_0}}{1-\cos m+\frac{m^2}{k_1}-\frac{2m^4}{k_1k_0}}$$

$$=\frac{\frac{m}{k_1}\sin m+1-\cos m}{\frac{m}{k_1}(1+\cos m)+\sin m}$$

(i) $\sin m=0$ deflection does not occur at either end

$m^2=\frac{1}{2}k_0$,

The resultants P_2H act on the line connecting both ends. Collapse (e)

(ii) $k_1=-\frac{m(\cos m\mp 1)}{\sin m}$ Complex sign negative (f_1), positive (f_2)

(iii) $(k_1)_1=2\left(\frac{m}{2}\right)^2\frac{\tan\frac{m}{2}}{\frac{m}{2}-\tan\frac{m}{2}}$ (g1)

$(k_1)_2=-2\frac{\frac{m}{2}}{\tan\frac{m}{2}}$ (g2)

(iv) $k_0=\frac{2m^2\sin m}{m\sin m-2(1-\cos m)}$ (h)

25

NUMBER	DIAGRAM & BOUNDARY CONDITIONS	FORMULA OR TABLE FOR RESULTS	REFERENCES, NOTES /175
7	Upper end free Lower end elastic, fixed.	$P_k=\mu_0\frac{EI}{l^2}$ where μ_0 $\mu\tan\mu=\frac{l}{\alpha EI}$ Here $\alpha=\frac{1}{k\cdot s}$ k: basic coefficient s: cross-section coefficient $k>0$ $P_k\fallingdotseq\frac{\pi^2EI}{(2l)^2\left(1+\frac{\alpha EI}{l^2}\right)^2}$	28 Same as in the case when link is increased only by $\Delta l=\alpha EI$
8	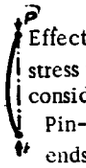 Effect of shearing stress taken into consideration. Pin-ended at both ends.	$P_k=\frac{P_e}{1+\frac{nP_e}{AG}}$ P_e: Euler load A: Cross-section area where n is constant based on shape of cross-section (i) rectangle $n=\frac{6}{5}$ (ii) circle $n=1.11$ (i) rectangle $n=\frac{\frac{6}{5}+\frac{3}{4}\nu}{1+\nu}$ $P_k=\frac{P_e}{1+\left(\frac{12}{5}+\frac{3\nu}{2}\right)\frac{\pi^2}{\lambda^2}}$ (Olsen) (iii) H cross-section ···H-··· 縦まわりの曲げ $P_k=\frac{P_e}{1+\left(\frac{12}{5}+\frac{3}{2}\nu\right)\frac{\pi^2}{\lambda^2}\frac{A}{A_f}}$ (Olsen) A_f: flange area	29 30 (i)(ii) Engesser (i)'(iii) Olsen
9	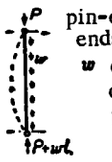 pin-ended at both ends w equally distributed load	$P_k+wl=\beta\frac{EI}{l^2}$ where $\beta=\frac{16.7}{1+1.36\gamma}+9.87$, $\gamma=\frac{P}{wl}$	31 Differential equation solved by series expansion
10	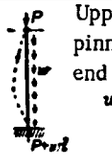 Upper end pinned, lower end fixed w is equally distributed load	$P_k+wl=\beta\frac{EI}{l^2}$ where $\beta=\frac{40.6}{1+2.6\gamma^{1.55}}+19.74$ $\gamma=\frac{P}{wl}$	31
11	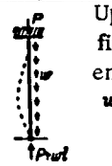 Upper end fixed, lower end pin-ended w is equally distributed load	$P_k+wl=\beta\frac{EI}{l^2}$ where $\beta=\frac{24.5}{1+1.68\gamma^{1.55}}+19.74$ $\gamma=\frac{P}{wl}$	31

NUMBER	DIAGRAM & BOUNDARY CONDITIONS	FORMULA OR TABLE FOR RESULTS	REFERENCES, /176 NOTES
12	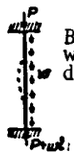 Both ends fixed. w is equally distributed load	$P_k+wl=\beta\frac{EI}{l^2}$ where $\beta=\frac{46.1}{1+2.4\tau}+39.48$ $\tau=\frac{P}{wl}$	31
13	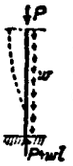 Upper end free, lower end fixed. w is equally distributed load	$P_k+wl=\beta\frac{EI}{l^2}$ where $\beta=\frac{5.38}{1+2.7\tau}+2.47$ when $\tau=\frac{P}{wl}$ $\tau=1$ $\beta=1.894$	31 32
14	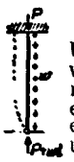 Upper end fixed with no lateral resistance, lower end pinned. w is equally distributed load.	$P_k+wl=\beta\frac{EI}{l^2}$ where $\beta=\frac{1}{1+1.43\tau}+2.47$ $\tau=\frac{P}{wl}$	31
15	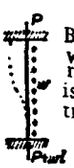 Both ends fixed with no lateral resistance, w is equally distributed load.	$P_k+wl=\beta\frac{EI}{l^2}$ where $\beta=\frac{9.06}{1+1.78\tau}+9.87$ $\tau=\frac{P}{wl}$	31
16	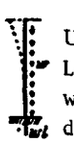 Upper end free. Lower end fixed. w is equally distributed load	$(wl)_k=7.85\frac{EI}{l^2}$	26
17	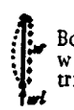 Both ends pinned. w is equally distributed load.	$(wl)_k=18.569\frac{EI}{l^2}$	26 Based on solution of idfferential equation. Solution obtained from general condition matrix.
18	Left end pinned. Right end fixed. w is equally distributed load	$(wl)_k=60.3\frac{EI}{l^2}$	31
19	Left end fixed. Right end pinned. w is equally distributed load	$(wl)_k=44.25\frac{EI}{l^2}$	31

NUMBER	DIAGRAM & BOUNDARY CONDITIONS	FORMULA OR TABLE FOR RESULTS	REFERENCES, NOTES /177
20	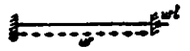 Both ends fixed. w is equally distributed load	$(wl)_k = 85.6\frac{EI}{l^2}$	31
21	Left end fixed. No lateral resistance. Right end fixed. w is equally distributed load.	$(wl)_k = 18.93\frac{EI}{l^2}$	31
22	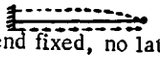 Left end fixed, no lateral resistance. Right end pinned. w is equally distributed load.	$(wl)_k = 3.47\frac{EI}{l^2}$	31
23	Compression load distribution Both ends pinned. Symmetrical distribution facing toward the center.	$\left(p_0\frac{l}{2}\right)_k = 31.5\frac{EI}{l^2}$	32
24	Compressive load distribution 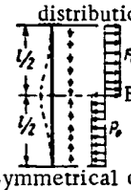 Both ends fixed. Symmetrical distribution facing center	$\left(p_0\frac{l}{2}\right)_k = 75.8\frac{EI}{l^2}$	32
25	Compressive load distribution Linear variation 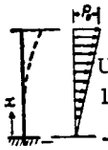 $p = p_0\frac{x}{l}$ Upper and free, lower end fixed.	$\left(p_0\frac{l}{2}\right)_k = 5.125\frac{EI}{l^2}$	32 Differential equation solved by series
26	Compressive load distribution $p = p_0\left(1-\frac{x}{l}\right)^n$ Upper end free. Lower end fixed.	$P_k = \alpha\frac{EI}{l^2}$ where P = total load $= \frac{p_0 l}{n+1}$ n: 0, 1, 2, 3 α: 7.837, 16.1, 27.3, 41.3	32 Solution of differential equation by Bessel function.

NUMBER	DIAGRAM & BOUNDARY CONDITIONS	FORMULA OR TABLE FOR RESULTS	REFERENCES, NOTES
27	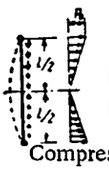 Pin-ended at both ends. Compressive load distribution	$\left(p_0\frac{l}{4}\right)_k=20.5\frac{EI}{l^3}$	32
28	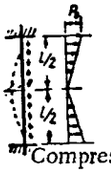 Both ends fixed. Compressive load distribution	$\left(p_0\frac{l}{4}\right)_k=54.0\frac{EI}{l^3}$	32
29	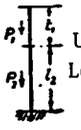 Upper end free. Lower end fixed.	Buckling condition equation $\tan l_2\sqrt{\frac{P_2}{EI}}\cdot\tan l_1\sqrt{\frac{P_1}{EI}}=\sqrt{\frac{P_2}{P_1}}$ Compressive force P_1 in integral l_1, compressive force P_2 in integral l_2.	33
30	Concentrated load at 2 points, lower end and center. 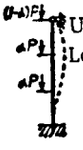 Upper end pinned. Lower end fixed.	(1) curve $y=c(2x^4-15ax^3+27a^2x^2)$ $P_k=\frac{EI}{(0.4285-0.1203\alpha)a^2}$ (2) curve $y=c(x^5-150x^3+72a^2x^3-108a^3x^2)$ $P_k=\frac{EI}{(0.4143-0.0573\alpha)a^2}$ $\alpha=0.5$ when (1) $P_k=2.714\frac{EI}{a^2}$ (2) $P_k=2.655\frac{EI}{a^2}$	34 Energy method
31	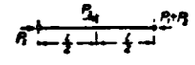 Pin-ended at both ends.	$(P_1+P_2)_k=\frac{4x^2}{l^2}EI$ x is lower table or lower formula $2\frac{\kappa x}{\tan\kappa x}+(1-\tau_1)\frac{x}{\tan x}=\frac{(1+\tau_1)^2}{3-\tau_1}$ where $\kappa=\sqrt{\frac{1-\tau_1}{2}}$ $\tau_1=\frac{\alpha-1}{\alpha+1}$	26

α	x
0	$\pi/2$
0.5	1.7185
1.0	1.8076
1.5	1.8670
2.0	1.9098
2.5	1.9415
3.0	1.9656
4.0	2.0010
9.0	2.0780
19.0	2.1180
∞	2.1602

$\alpha=P_2/P_1$

Approximate equation $\left(P_1+\frac{P_2}{2}\right)_k=\frac{\pi^2EI}{l^2}$ Error below 0.5%.

NUMBER	DIAGRAM & BOUNDARY CONDITIONS	FORMULA OR TABLE FOR RESULTS	REFERENCES, NOTES
32	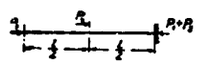 Left end free, right end fixed.	Buckling length l_k = 1 $\tau=\frac{1}{2-\sqrt{\beta}}$ where $\beta=P_2/(P_1+P_2)$ $(P_1+P_2)_k=\frac{4x^2}{l^2}EI$ $\alpha=P_2/P_1$ α: 0.0, 0.5, 1.0, 1.5, 2.0, 2.5, 3.0, 4.0, 9.0, 19.0, ∞ x: π/4, 0.9.98, 1.0618, 1.0903, 1.1475, 1.1934, 1.2307, 1.2871, 1.4196, 1.4934, 1.5708	26 /179
33	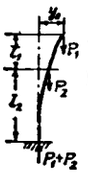 Upper end free. Lower end fixed.	Buckling conditions $\tan\alpha l_1 \tan\beta l_2=\frac{\beta}{\alpha}$ where $\alpha=\sqrt{\frac{P_1}{EI}}$, $\beta=\sqrt{\frac{P_1+P_2}{EI}}$	35
34	Pin-ended at both ends. 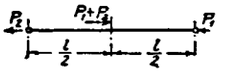 Tension Compression	Buckling length l_k = 1 P_2/P_1: 0, 0.2, 0.4, 0.6, 0.8, 1.0 τ: 0.729, 0.671, 0.616, 0.569, 0.527, 0.500 Approximation equation $\frac{P_1}{P_2}$ = 0.75 0.25 Positive: Compression on both sides. Negative: Tension on one side.	36
35	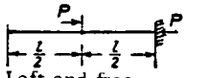 Left end free, Right end fixed.	$P_k=\frac{4\times(1.5708)^2}{l^2}EI$	36
36	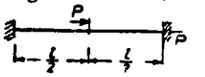 Both ends fixed.	$P_k=\frac{4\times(4.3128)^2}{l^2}EI$	36
37	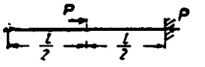 Left end free, Right end fixed.	$P_k=\frac{4\times(3.4401)^2}{l^2}EI$	36
38	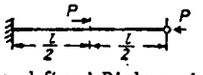 Left end fixed, Right end free.	$P_k=\frac{4\times(2.7779)^2}{l^2}EI$	36
39	General calculation of compression member.	(1) $\eta=k\left(\frac{l_k}{100}\right)^2\frac{f_c}{P}$ is computed where $k=\frac{A^2}{I}$ (2) The η corresponding to the ω from Tables, 44.1, 44.2 is determined. Slenderness ratio λ The required cross-section area A is determined from (3) A = P/f_c (4) This cross-section is analyzed byordinary methods	37

39

Table 44.1 TABLE OF STEEL STRUCTURE

λ		0	10	20	30	40	50	60	70	80	90
0	ω	1.00	1.00	1.00	1.04	1.07	1.11	1.17	1.24	1.34	1.48
	η	—	—	—	0.094	0.171	0.278	0.421	0.608	0.858	1.20
100	ω	1.67	2.02	2.40	2.82	3.27	3.75	4.27	4.82	5.40	6.02
	η	1.67	3.44	2.46	4.77	6.41	8.44	10.9	13.9	17.5	21.7
200	ω	6.67	7.35	8.07	8.82	9.60	10.42				
	η	26.7	32.4	39.1	46.7	55.3	65.1				

Table 44 2 TABLE OF WOODEN STRUCTURES

λ		0	10	20	30	40	50	60	70	80	90
0	ω	1.0	1.0	1.2	1.3	1.4	1.5	1.7	2.0	2.3	2.7
	η	—	—	0.048	0.117	0.224	0.375	0.612	0.980	1.47	2.11
100	ω	3..	4.0	4.8	5 6	6.5	7.5				
	η	3.30	4.84	6.91	9.46	12.7	16.9				

40

Round column which does not follow Hooke's law.

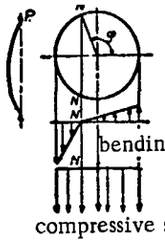

pin-ended at both ends

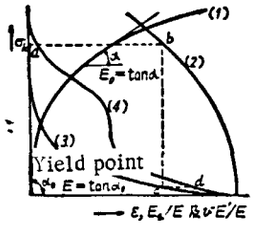

Reference Chart

(1) Compressive stress-strain curve determined. 38

(2) Determine the sloap E_0 = tan of the tangent drawn at the point on the curve (1) corresponding to the compressive

(3) Determine the $\sigma_c - E_0/E$ curve

(4) Draw the curve $E_0/E - \eta$ (Table 45.1).

(5) Draw the curve $E'/E - \varphi$ (Table 45.2).

The slenderness ratio λ_k causing buckling is

$$\lambda_k = \pi\sqrt{\frac{E'}{\sigma_k}}$$

Table 45.1 $\dfrac{E_0}{E} = 1 + \dfrac{\pi}{2}\dfrac{\cos\varphi}{\frac{1}{2}\sin^2\varphi - \frac{1}{2}\cos^2\varphi\left(\varphi - \frac{1}{2}\sin 2\varphi\right)}$

$\varphi°$	90	92	94	96	98	100	102	104	106
E_0/E	1.000	0.848	0.719	0.610	0.516	0.437	0.370	0.312	0.263
$\varphi°$	108	110	112	114	116	118	120	122	124
E_0/E	0.221	0.186	0.156	0.135	0.108	0.090	0.074	0.061	0.050
$\varphi°$	126	128	130	140	150	160	170	180	
E_0/E	0.041	0.033	0.026	0.008	0.002	0.0007	0.0001	0	

Table 45 2 $\dfrac{E'}{E} = 1 + 4\cos^2\varphi + \dfrac{4\cos\varphi}{\frac{1}{3}\sin^3\varphi - \frac{1}{2}\cos\varphi\left(\varphi - \frac{1}{2}\sin 2\varphi\right)} \times \left\{\frac{1}{8}\left(\varphi - \frac{1}{4}\sin 4\varphi\right) - \frac{2}{3}\cos\varphi\cdot\sin^3\varphi + \frac{1}{2}\cos^2\varphi\left(\varphi - \frac{1}{2}\sin 2\varphi\right)\right\}$

$\varphi°$	90	92	94	96	98	100	102	104	106
E_0'/E	1.000	0.920	0.844	0.772	0.705	0.641	0.590	0.542	0.503
$\varphi°$	108	110	112	114	116	118	120	122	124
E_0'/E	0.467	0.441	0.420	0.403	0.392	0.386	0.383	0.382	0.382
$\varphi°$	126	128	130	140	150	160	170	180	
E_0'/E	0.382	0 382	0.381	0.332	0.215	0.088	0.014	0	

NUMBER	DIAGRAM & BOUNDARY CONDITIONS	FORMULA OR TABLE FOR RESULTS	REFERENCES, NOTES
41	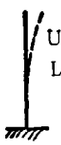 Upper end free. Lower end fixed.	$\sigma_k=\pi^2\frac{\alpha}{\lambda^2}$ α : Buckling coefficient Cast iron $\alpha=(1-\varepsilon)\frac{d\sigma_k}{d\varepsilon}$ (第46·1 図) ε is strain, Cox-Lang's stress strain $\varepsilon=\sigma/(a-b\sigma)$ Soft steel Elastic region $\alpha=(1-\varepsilon)E$ (Figure 46 2) One part yields, calculation by graphic equation 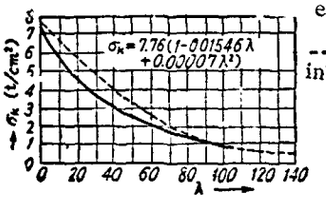 ---indicate that inTetmyer's equation $a=1380$, $b=190$ Figure 46.1 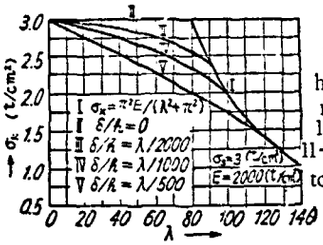 δ : maximum deflection h: minimum width of member cross-section l is Euler's value, $1-\sqrt{\frac{\sigma_k}{\sigma_E}}$ corresponding to the given deflections Figure 46.2	39
42	Reinforced Concrete Column, axial compression 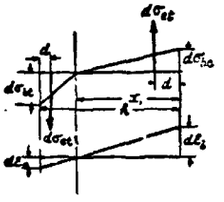 suffix b in concrete suffix e is reinforcing steel	(1) When the reinforcing steel is within the proportional limit, the buckling coefficient is $\alpha_k=4\left\{T_b x^3+E_b(1-x)^3\right\}$ $+6E_e p\left\{x^2+(1-x)^2-n\left(1-\frac{n}{2}\right)\right\}$ where $x=\frac{E_b p-E_e}{E_b-T_b}\left\{1-\sqrt{\frac{E_e p+T_b}{E_e p+E_b}}\right\}$, $n=\frac{2d}{h}$ E: Modulus of Elasticity, during reduction in force in concrete, in reinforcing steel, within proportional limit or during reduction in force, if a force is applied. T: Modulus of Elasticity, during application of force in concrete, above proprtional limits in reinforcing steel $p = A_e/bh$. A_e: Total cross-section area of reinforcing steel. $(1-x)^3\left\{+6p\left\{T_e x^2+E_e(1-x)^2\right\}\right.$ d: Reinforcing steel, skin thickness. (2) When the stress of the reinforcing steel exceeds the proportional limit.	41

NUMBER	DIAGRAM & BOUNDARY CONDITIONS	FORMULA OR TABLE FOR RESULTS	REFERENCES, NOTES
42	In this case, the figure to the right if obtained. Here, after the maximum stress in the concrete is reached, it is assumed that plastic deformation is applied until it is twice that value.	where $\alpha=\frac{1}{E_b-T_b}$ $\cdot\left\{m-\sqrt{m^2-(E_b-T_b)\left\{E_b+E_c p-(E_c-T_c)p\frac{n}{2}\right\}}\right\}$ $m=E_b+(T_c+E_c)\frac{p}{2}$ $\sigma_k=(1-p)\sigma_s+p\sigma_c \quad \frac{l}{i}=\pi\sqrt{\frac{\alpha_k}{\sigma_k}}$ 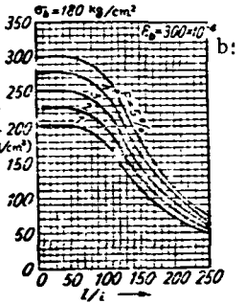 b: Maximum strain	
43	Generalized Column Boundary conditions are various.	$\sigma_k=c\pi^2 E\lambda^2$ Both ends fixed; Both ends pinned; One end fixed, other end free; One end fixed, other end free. c: 4; 1; 2; 1/4 Welded steel to tubular column $c=2$ Tension shell structure reinforcing member $c=1.7$	41
44	Short Column For the short column it is assumed (proportional limits) (buckling stress) (yield p int)	Test equation (1) $\sigma_k=\sigma_{kk}\left(\frac{l'i}{\pi\sqrt{E/\sigma_{kk}}}\right)^m$ l': buckling length k: Normally yield point, where wall surface buckling occurs, this is due the wall surface buckling strength. m: Constant where m = 1, line connected to Euler (sic) m = 2, Johnson's equation Test equation (2) $\sigma_k=\sigma_D(1-\alpha\lambda)$ σ_D, α constants soft steel $\sigma_D=31$ kg/mm² $\lambda<105$ $\alpha=0.00368$ hard steel $\sigma_D=33.5$ kg/mm² $\lambda<90$ $\alpha=0.00185$	41 from Tetmeyer
45	Round tube Wall surface buckling	$\sigma_k=\mu E\frac{t}{R}$ μ theroetically is =0.6, according to test values, = 0.3 as design safe = 0.18 is safe	41
45	Tubes, short columns	Duraluminum member $\sigma_k=3390-\frac{28.2}{\sqrt{c}}\frac{L}{i}$	41

NUMBER	DIAGRAM & BOUNDARY CONDITIONS	FORMULA OR TABLE FOR RESULTS	REFERENCES, NOTES
47	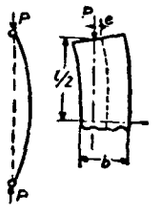 Pin-ended at both ends	$P_k=76\left(\frac{1}{2}-\frac{e}{b}\right)^2\frac{EI}{l^2}$ $\quad \frac{e}{b}=0\sim\frac{1}{2}$ $\frac{e}{b}\leqq\frac{1}{6}$ Correct solution when $l\sqrt{P_k/EI}/2$: 1.57 (e/b=0); 1.35 (1/24); 1.17 (2/24); 1.00 (3/24); 0.839 (4/24)	43 Solved by an eccentric compression member series based on material which cannot resist tensile force. Error within 3.5%.
48	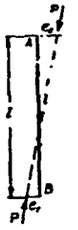 Pure support steel column	The average unit stress when s he maximum end fiber stress is equal to the yield point stress $\sigma_{Y.P.}$. is assumed to be $(\sigma_c)_{Y.P.}$ $(e_0 \geqq e_1)$ (i) In a short column, at member end A, a maximum bending moment is generated. $(\sigma_c)_{Y.P.}=\frac{\sigma_{Y.P.}}{1+\frac{e_0}{s}}$. (1) where s: radius of nucleus (ii) In a long column, in the intermediate cross-section, a maximum bending moment is generated. $(\sigma_c)_{Y.P.}=\frac{\sigma_{Y.P.}}{1+\frac{e_0}{s}\sqrt{\beta^2-2\beta\cos 2u+1}\cdot\operatorname{cosec}2u}$. (2) 但し $\beta=e_1/e_0$ $2u=\lambda\sqrt{\frac{(\sigma_c)_{Y.P.}}{E}}$. (iii) The critical value of conditions (i), (ii) is assumed to be (1) = (2). $\cos^{-1}\beta=\lambda\sqrt{\frac{(\sigma_c)_{Y.P.}}{E}}$. (3) $\beta=1.0\sim-1.0$ If we draw the curves, B they become as follows: where $E=30\cdot10^6$ lb/in², $\sigma_{Y.P.}=36{,}000$ lb/in²	42

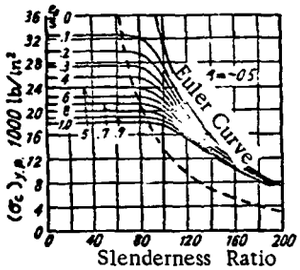

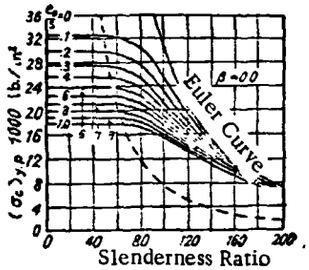

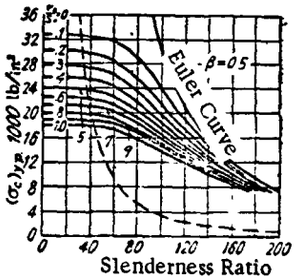

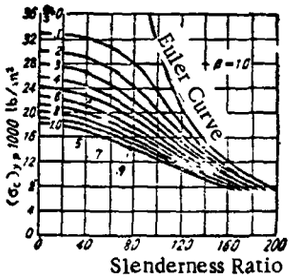

NUMBER	DIAGRAM & BOUNDARY CONDITIONS	FORMULA OR TABLE FOR RESULTS	REFERENCES, NOTES
48		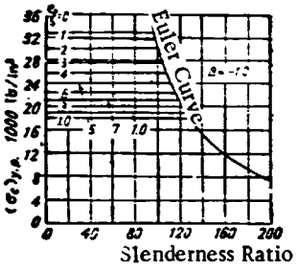 The broken lines indicate the condition (3).	
	Member where initial deflection 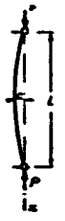 Simple support Steel column	$\sigma_{r.p.}=(\sigma_c)_{r.p.}\left[1+\frac{a}{s}\cdot\frac{1}{1-\frac{(\sigma_c)_{r.p.}}{\pi^2 E}\cdot\lambda^2}\right]$ (4) If the curves for $(\sigma_c)_{r.p.}-\lambda$ ⑦ are drawn 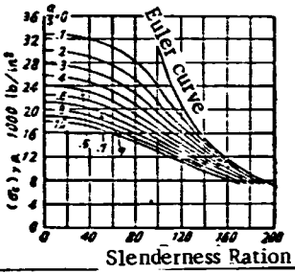	a considered infinitesimal
49	Long reinforced concrete column Simple support	$\frac{P_k}{P_c}=\alpha+(1-\alpha)\cos\frac{\pi}{290-3m}\lambda-\frac{b\lambda}{1+b\lambda}$ where $m=\frac{e}{k}$, P_c: Compressive breaking point, k: Radius of nucleus $\alpha=0.55+(0.048+0.0009\alpha)m$ $b=0.01\,m\{0.00032\sigma_B+0.01(5-p)\}$ σ_B: Concrete strength α: Reinforcement Ratio Applicable range: In short cross-section m ≦ 3, e ≦ 0 5h, ≦ λ 150	44 e is eccentricity h is cross-section
50	Long reinforcement concrete column. 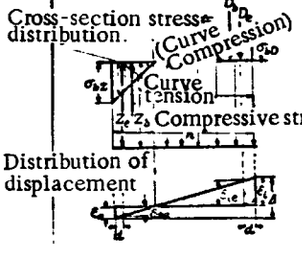	M_i is computed (related to elasticity range) $M_i=D_b S_1+D_e S_{e1}+Z_b S_2+Z_e S_{e2}$ We determine the maximum deflection and the eccentricity by graphic solution, where $M=M_1$ obtains. Where center deflection $\delta=\frac{l^2}{\pi^2}\frac{\Delta}{h}$ is assumed $M=P_k(\delta+e)$ If we determine the values with respect to e, given the following chart is obtained:	45 S_1, S_{e1}, S_2, S_{e2} are respectively the points of action and the distance from the neutral axis of the compenents D_b, D_e, Z_b, Ze.

NUMBER	DIAGRAM & BOUNDARY CONDITIONS	FORMULA OR TABLE FOR RESULTS	REFERENCES, NOTES
50	d is thickness of covering of reinforcement. The bending moment caused by stress: M_1 The bending moment caused by external force: M The downward stress expresses compression, upward stress expresses tension	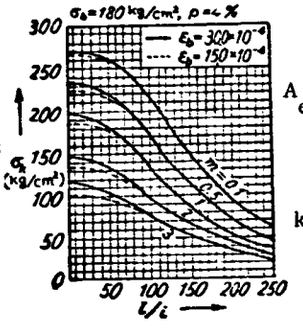 where $p=A_e/b\cdot h$. A_e = Total cross-section area of reinforcement $m=\frac{e}{k}$ k: Nucleus radius ε_b : Maximum strain of concrete	/185

COMBINED LOADS

番号	図及び境界条件	結果の式又は表	文献・備考
51	P column with both ends having elastic support, both ends pinned. The force of support is proportional to the displacement y. q = y.	$P_k=\frac{\pi^2 EI}{l^2}\left(m^2+\frac{\beta l^4}{m^2\pi EI}\right)$ m is the minimum integer which is larger that the values in the equation below, expressed as the number for the half-wave length of the buckled member. $\frac{1}{2}\left[\sqrt{1+\frac{4l^2}{\pi^2}\sqrt{\frac{\beta}{EI}}}-1\right]$	46
52	Member on elastic base. Both ends pinned. β : base coefficient $q=\beta y$	$P_k=\frac{\pi^2 EI}{l_k^2}$	47 Energy method, even when an independent elastic support is present, when there are more than three between the half-wave lengths, this equation

$\beta l^4/16EI$	0	1	3	5	10
l_k/l	1	0.927	0.819	0.741	0.615
$\beta l^4/16EI$	15	20	30	40	50
l_k/l	0.537	0.482	0.437	0.421	0.406
$\beta l^4/16EI$	75	100	200	300	500
l_k/l	0.376	0.351	0.286	0.263	0.235
$\beta l^4/16EI$	700	1000	1500	2000	3000
l_k/l	0.214	0.195	0.179	0.165	0.149
$\beta l^4/16EI$	4000	5000	8000	10,000	
l_k/l	0.140	0.132	0.117	0.110	

Number of half wave lengths in buckled form. $\frac{\beta l^4}{\pi^4 EI}=m^2(m+1)^2$

	$P_k=\pi^2\frac{EI}{l^2}n^2+\frac{\beta l^2}{\pi^2 n^2}$ $n=1,2,3\cdots$ $n=\frac{l}{\pi}\sqrt[4]{\frac{\beta}{EI}}$ An integer is taken from; The minimum value of P with respect to this n is taken to be P_k 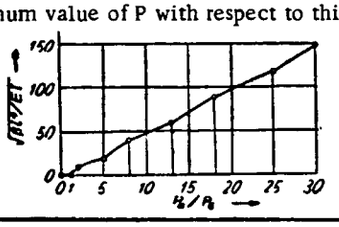	48

NUMBER	DIAGRAM & BOUNDARY CONDITIONS	FORMULA OR TABLE FOR RESULTS	REFERENCES, NOTES
53	Member on Elastic Base. 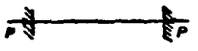 Both ends fixed. $q=\beta y$	Buckling condition equation $\frac{k_1}{k_2}=\frac{\tan k_2\frac{l}{2}}{\tan k_1\frac{l}{2}}$ 又は $=\frac{\tan k_1\frac{l}{2}}{\tan k_2\frac{l}{2}}$ ここに $k_1=\sqrt{\frac{P}{2EI}-\sqrt{\left(\frac{P}{2EI}\right)^2-\frac{\beta}{EI}}}$ $k_2=\sqrt{\frac{P}{2EI}+\sqrt{\left(\frac{P}{2EI}\right)^2-\frac{\beta}{EI}}}$ 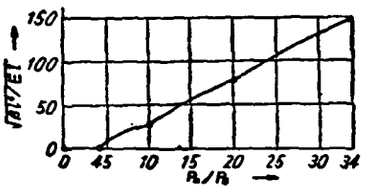 	48 Member width assumed to be b = 1.
54	Member on Elastic base. 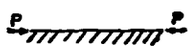 Both ends free. Base coefficient q = y.	Buckling equation $\left(\frac{P}{2EI}\right)^2>\frac{\beta}{EI}:\ \frac{\tan k_2\frac{l}{2}}{\tan k_1\frac{l}{2}}=\frac{k_2^2}{k_1^2}$ 又は $=\frac{k_1^2}{k_2^2}$ $k_1=\sqrt{\frac{P}{2EI}-\sqrt{\left(\frac{P}{2EI}\right)^2-\frac{\beta}{EI}}}$ $k_2=\sqrt{\frac{P}{2EI}+\sqrt{\left(\frac{P}{2EI}\right)^2-\frac{\beta}{EI}}}$ $\left(\frac{P}{2EI}\right)^2=\frac{\beta}{EI}:\ 3\sin kl\pm kl=0$ $\left(\frac{P}{2EI}\right)^2<\frac{\beta}{EI}:\ r\left(\sqrt{\frac{\beta}{EI}}-\frac{P}{EI}\right)\sinh\alpha l$ $\pm\alpha\left(\sqrt{\frac{\beta}{EI}}+\frac{P}{EI}\right)\sin\beta l=0$ $\alpha+ri=k_1 i,\quad -\alpha+ri=k_2 i.$ Generally, the minimum P_k is determined from the third equation. It becomes as shown in the chart below where (c) When is large, $P_k=\sqrt{\beta EI}$ 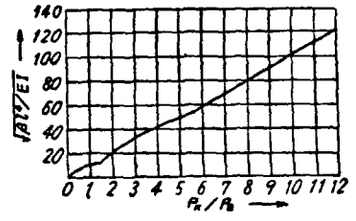 	49 Member width b = 1.

NUMBER	DIAGRAM & BOUNDARY CONDITIONS	FORMULA OR TABLE FOR RESULTS	REFERENCES, NOTES
55	Member sustaining elastic support from both sides 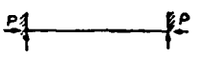 At both ends deflection = deflection angle = bending moment = 0	(1) Buckling shape $P_{1k}=4.796\{EA(EI)^{3/4}\beta^3\}^{2/3}$ (2) Buckling shape $P_{2k}=4.696\{EA(EI)^{3/2}\beta^3\}^{2/3}$ (3) Buckling shape $P_{3k}=\sqrt[4]{25.974\,E^2AI\beta^2}$ where in the case of (3) the boundary condition is only deflection= bneding moment = 0. = bending moment = 0.	50 Buckling of rails. Experimental values are used to determine the resistance force sustained by rails from a roadbed, and this is taken into consideration.
56	Member on elastic base. Both ends fixed, distributed load w	$\delta=l\sqrt[3]{\frac{w}{EI}}$, $\mu=\frac{wl}{P_k}$ $n=P_k/\sqrt[3]{w^2EI}$ Assuming μ: 0.1 | 0.2 | 0.4 | 0.6 | 1.0 | 1.2 | 1.36 δ: 1.589 | 2.012 | 2.567 | 2.975 | 3.463 | 3.967 | 4.354 n: 15.886 | 10.059 | 6.419 | 4.953 | 3.643 | 3.306 | 3.202	51 Buckling of rails. Denoting by l the buckling integral length P, w are determined and using n, l is determined Conversely, determining l, w, it is possible to determine the buckling load P corresponding to the integral length.
57	Infinitely long compressed member on elastic base. Base constant β; $q=\beta y$	Minimum buckling load is $P_k=2\sqrt{EI\cdot\beta}$ In this case, the buckling half-wave length is $L=\pi\sqrt[4]{\frac{E\cdot I}{\beta}}$	52
58	Member* partially sustaining elastic support 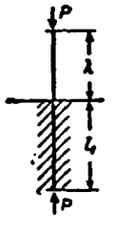 Base coefficient β $q=\beta y$ length of interval not sustaining elastic support	Buckling equations $\left(\frac{P}{2EI}\right)^2<\frac{\beta}{EI}$ のとき $a\tan al=\frac{2}{\alpha\tau}\frac{-(\alpha^2-3\alpha\tau^2)^2\sin^2\tau l_1+(3\alpha^2\tau-\tau^3)^2\sinh^2\alpha l_1}{-(\alpha^6-3\alpha\tau^2)\sin 2\tau l_1+(3\alpha^2\tau-\tau^3)\sinh 2\alpha l_1}$ where $\alpha=\sqrt{\sqrt{\frac{\beta}{4EI}}-\frac{P}{4EI}}$, $\tau=\sqrt{\sqrt{\frac{\beta}{4EI}}+\frac{P}{4EI}}$ $a^2=\frac{P}{EI}$ l_1 If l_1 is very large, $a\tan al=2\frac{\sqrt{\frac{\beta}{EI}}-a^2}{\sqrt{2\sqrt{\frac{\beta}{EI}}-a^2}}$ $\left(\frac{P}{2EI}\right)^2\geq\frac{\beta}{EI}$, This does not have a buckling value	53 Member length b = 1. *For example, a mast set in the ground.

/187

NUMBER	DIAGRAM & BOUNDARY CONDITIONS	FORMULA OR TABLE FOR RESULTS	REFERENCES, NOTES
59	A beam sustaining lateral load Q and axial compressive force P 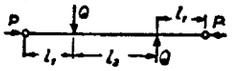 Pin-ended at both ends.	Solving the $\frac{d^2y}{dx^2}+\frac{P}{EI}y+\frac{M}{EI}=0$* and assuming the differential displacement to be $P_k=4\frac{\pi^2EI}{l^2}$ is obtained (similiar (similarly for 60, 61 below) where l is total length of member.	54 *M is the bending moment due to the lateral load Q.
60	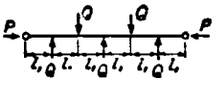 Both ends pinned	$P_k=\frac{\pi^2EI}{l^2}$	54
61	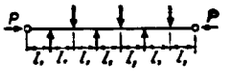 Both ends pinned. Load antisymmetrical.	$P_k=4\frac{\pi^2EI}{l^2}$	54
62	 Both ends pinned	$\frac{T^2}{4(EI)^2}+\frac{P}{EI}=\frac{\pi^2}{l^2}$ Assuming P = O, the buckling value T' is obtained in the case when the torsion moment T acts individually. If the given T is T', P becomes negative, P expresses the tensile force required to prevent buckling.	55
63	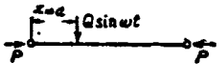 Both ends. pinned. Lateral periodic force applied.	$P_k=\frac{n^2\pi^2EI}{l^2}-\frac{\rho Al^2\omega^2}{n^2\pi^2}-\sqrt{\frac{2Q^2\omega^2l}{n^2\pi^2g}\left(\frac{n^2\pi^2EI}{l^2}-\frac{\rho Al^2\omega^2}{n^2\pi^2}\right)}$ Where l is total length of member. $\frac{n^2\pi^2EI}{l^2}$ Indicates the n Euler order load.	56
64	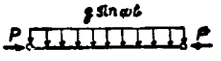 Both ends pinned. A lateral equally distributed periodic course is applied.	$P_k=\frac{(2n+1)^2\pi^2EI}{l^2}-\frac{\rho A\omega^2l^2}{(2n+1)^2\pi^2}-\sqrt{\frac{8q^2\omega^2l^2}{(2n+1)^4\pi^4g}\left(\frac{(2n+1)^2\pi^2EI}{l^2}-\frac{\rho A\omega^2l^2}{(2n+1)^2\pi^2}\right)}$ Where $\frac{(2n+1)^2\pi^2EI}{l^2}$ indicates the (2n + 1) Euler load	56

NUMBER	DIAGRAM & BOUNDARY CONDITIONS	FORMULA OR TABLE FOR RESULTS	REFERENCES, NOTES
65	Member vibrating in lateral direction. 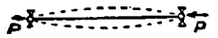 both ends pinned.	$P_{kf}=P_e-W\frac{l}{g}(2f)^2\left(1+\left[\frac{\pi}{\lambda}\right]^2\right)$ $\left(\frac{\pi}{\lambda}\right)^2$ Ignoring $P_{kf}\fallingdotseq P_e-W\frac{l}{g}(2f)^2$ where total weight W = gl, $f=\frac{\omega}{2\pi}$ vibration number	57 $\omega_1=\frac{\pi^2}{l^2}\sqrt{\frac{EI}{\mu}}\cdot\sqrt{1-\frac{P}{P_e}}$ Resonance when
66	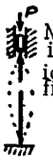 Member vibrating in lateral direction. Both ends fixed.	$P_{kf}=4\pi^2\frac{EI}{l^2}-0.778W\frac{l}{g}(2f)^2$ Where total weight W = gl, $f=\frac{\omega}{2\pi}$ vibration number	57
67	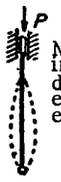 Member vibration in lateral direction. Upper end fixed. Lower end pinned.	$P_{kf}=2\pi^2\frac{EI}{l^2}-0.819W\frac{l}{g}(2f)^2$ where total weight W = gl, $f=\frac{\omega}{2\pi}$ vibration number	57
68	Member vibrating in lateral direction. Upper end free, lower end fixed.	$P_{kf}=\frac{1}{1+8\frac{l}{g}(2f)^2}\left(\frac{\pi^2}{4}\cdot\frac{EI}{l^2}-1.816W\frac{l}{g}(2f)^2\right)$ f when f is small $P_{kf}=\frac{1}{1+8\frac{l}{g}(2f)^2}\frac{\pi^2}{4}\frac{EI}{l^2}$ where total weitht W - gl, $f=\frac{\omega}{2\pi}$ vibration number	57 Assuming $y=A\cdot\left(1-\cos\frac{\pi z}{2l}\right)\cdot\sin$ The energy method is used. A is an arbitrary constant
69	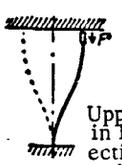 Upper end free in lateral direction. Lower end fixed	$P_{kf}=\frac{1}{1+8\frac{l}{g}(2f)^2}\left(\pi^2\frac{EI}{l^2}-3.10W\frac{l}{g}(2f)^2\right)$ f when f is small $P_{kf}=\frac{1}{1+8\frac{l}{g}(2f)^2}\pi^2\frac{EI}{l^2}$	57 Energy method
70	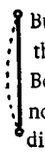 Buckling due to, thermal expansion Both ends pinned, no displacement in direction of axis	$\theta_k=\frac{\pi^2}{k}\left(\frac{i}{l}\right)^2$ k: linear expansion coefficient θ_k: buckling temperature	58

NUMBER	DIAGRAM & BOUNDARY CONDITIONS	FORMULA OR TABLE FOR RESULTS	REFERENCES, NOTES
71	Axial compression P proportional to time, gradually increases to $P(t)=V\cdot t$	Basic equation $\rho A\frac{\partial^2 y}{\partial t^2}+EI\frac{\partial^4 y}{\partial x^4}+P(t)\frac{\partial^2 y}{\partial x^2}=D$ $y=\Sigma a_n(t)\cdot\sin n\frac{\pi}{l}x$ If we solve, assuming $y=\frac{(2\pi)^3}{\sqrt{27}}\sum_{n=1,2,3}a_{0n}\cdot\left(\frac{3}{4\pi}k_n\right)\sqrt{1-\frac{t}{t_n}}\left[J_{\frac{1}{3}}\left\{k_n\right\}\cdot J_{\frac{1}{3}}\left\{k_n\sqrt[3]{1-\frac{t}{t_n}}\right\}+J_{-\frac{1}{3}}\left\{k_n\right\}J_{-\frac{1}{3}}\left\{k_n\sqrt[3]{1-\frac{t}{t_n}}\right\}\right]\cdot\sin n\frac{\pi}{l}x.$ here $k_n=\frac{2}{3}n^4\pi^4\frac{E^{\frac{1}{3}}}{\rho^{\frac{1}{2}}}\frac{1}{\lambda^2 vl}$ $P_n=V.t_n\quad P(t)=P_n\cdot\frac{t}{t_n}$ 但し $P_n=\left(n\frac{\pi}{l}\right)^2EI$ v: compressive stress velocity kg·cm⁻²/sec The effect of the axial compressive force P(t) with respect to 1 order, 2 order ... n order vebration from the above equation is on the load velocity Vp is determined from a_n/a_{0n}.	59
72	Slender strip sustaining a periodic external force $P\cos\omega_0 t$ in the direction of the long axis. 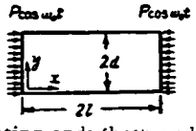 Rotating ends (both ends). In the case of a rectangular plate, and rotating around edge.	The lateral vibration equation becomes as follows, if we take into consideration Cox's hypothesis that the strain with respect for the axial forces for the plate in its entirety is uniform, and also take into account the effect of the plate shear. $D\frac{\partial^4 w}{\partial x^4}+\left\{P\cos\omega_0 t-\frac{AE}{4b}\int_0^{2b}\left(\frac{\partial w}{\partial x}\right)^2 dx+\frac{D}{2}\left(\frac{\partial^2 w}{\partial x^2}\right)^2\right\}\cdot\frac{\partial^2 w}{\partial x^2}+\rho\frac{\partial^2 w}{\partial t^2}=0$ Here w = deflection displacement, A = cross-section area, D = bending stiffness of plate, E = Young's modulus, = mass per unit area Here, substituting $w=\frac{2b}{n\pi}\phi(t)\sin\frac{n\pi}{2b}x$ By means of Galerkin's method, we determine the equation which satisfies approximately (t) $\frac{d^2\phi}{dt^2}+(p_0^2-\alpha_0^2\cos\omega_0 t)\phi+\beta\phi^3=0.$ Here $p_0^2=\frac{D}{\rho}\left(\frac{n\pi}{2b}\right)^2,\quad \alpha_0^2=\frac{P}{\rho},\quad \beta=\frac{AE}{4\rho}-\frac{3}{8}\frac{D}{\rho}\left(\frac{n\pi}{2b}\right)^2$ Furthermore, introducing $p^2=p_0^2+\frac{3}{4}\beta\phi_0^2-\cdots$ The above equation becomes approximately. $\frac{d^2\phi}{dt^2}+(p^2-\alpha_0^2\cos\omega_0 t)=0$ i e., This becomes Mathieu's differential equation	60 In the case of a rectangular plate, assuming $w=\frac{2b}{n\pi}\phi(t)\cdot\sin\frac{m\pi x}{2b}\cdot\sin\frac{n\pi y}{2d}$ と Equation (t) becomes exactly the same shape. Where the constant $p_0^2=\frac{D}{\rho}\cdot\left[\left(\frac{m\pi}{2b}\right)^2+\left(\frac{n\pi}{2a}\right)^2\right]^2$ $\alpha_0^2=\frac{P}{\rho}$ $\beta=\frac{1}{\rho}\frac{Eh}{32}\cdot\left[\left(\frac{m\pi}{2b}\right)^2+\left(\frac{n\pi}{2d}\right)^2\right]^2$ h = plate thickness

NUMBER	DIAGRAM & BOUNDARY CONDITIONS	FORMULA OR TABLE FOR RESULTS	REFERENCES, NOTES

/191

72

When the stability conditions, according to Vander Pol's paper* is defined from the following equation

$$\cos\frac{\pi p_1}{\omega_0}\cos\frac{\pi p_2}{\omega_0}-\frac{p_1^2+p_2^2}{2p_1p_2}\sin\frac{\pi p_1}{\omega_0}\sin\frac{\pi p_2}{\omega_0}=1$$

Here $p_1^2=p_0^2-\alpha_0^2, \quad p_2^2=p_0^2+\alpha_0^2$

The results of numerical computations are expressed in the graphs below.

where C_{e1}, S_{e1} are Mathieu's functions

$\beta=\frac{3}{4}\frac{\varphi_0^2}{p_0^2}$, φ_0=maximum amplitude

* Balth van der Pol : Phil. Mag. (1928)

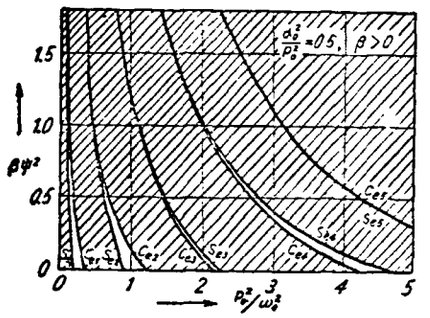

Figure 72.1

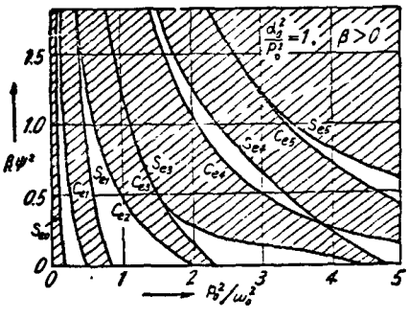

Figure 72.2

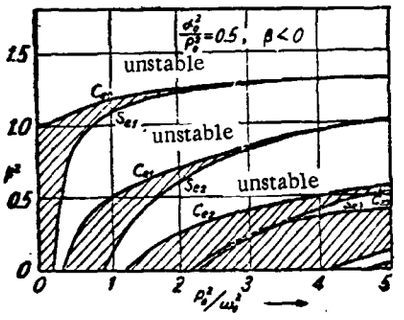

Figure 72.3

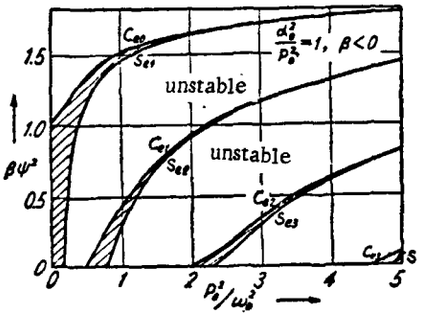

Figure 72.4

NUMBER	DIAGRAM & BOUNDARY CONDITIONS	FORMULA OR TABLE FOR RESULTS	REFERENCES, NOTES
73	Member with linear variationsiin cross-section 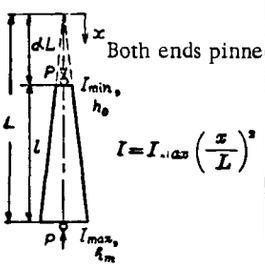 Both ends pinned $I=I_{max}\left(\frac{x}{L}\right)^2$ h is section height	$P_k=\mu\frac{\pi^2EI_{ax}}{l^2}$ $\mu=0.20+0.80\sqrt[3]{\left(\frac{I_{min}}{I_{max}}\right)^2}$ where $h_0/h_m\geqq 0.2$.	61 /192
		Buckling length l_k determined from the following equation $\gamma=\frac{l_k}{l}=\frac{2\pi}{(1-\alpha)\sqrt{1-4\left(\frac{\pi}{\log_e\alpha}\right)^2}}$ where $\alpha=\sqrt{\frac{I_{min}}{I_{max}}}$	62
		α^2: 0, 0.01, 0.1, 0.2, 0.3, 0.4 γ: 6.283, 1.950, 1.656, 1.444, 1.325, 1.243 α^2: 0.5, 0.6, 0.7, 0.8, 0.9, 1.0 γ: 1.181, 1.132, 1.091, 1.057, 1.027, 1.000	
		Approximation equation $\gamma_k=3.20-2.20\sqrt[3]{\left(\frac{h_{min}}{h_{max}}\right)^2}$ where $h_0/h_m\geqq 0.2$.	
74	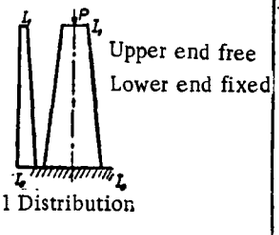 Upper end free Lower end fixed 1 Distribution	Assuming $P_k=\alpha\frac{EI_0}{l^2}$, $I_1=I_0(1-k)$ is shown in the table below $\alpha=1.510+0.960\frac{I_1}{I_0}$	63
		k: 0 | 0.5 | 1.0 α: $\frac{\pi^2}{4}=2.467$ | 2.067 | 1.510	
75	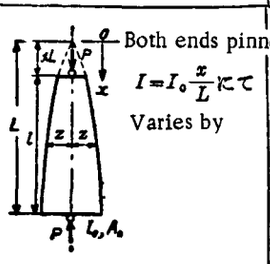 Both ends pinned $I=I_0\frac{x}{L}$ に て Varies by	$P_k=\frac{\varsigma_0^2(\kappa^2-1)}{4\kappa^2\pi^2}\frac{\pi^2EI_0}{l^2}$ where ς_0 は $J_1(\kappa\varsigma)Y_1(\kappa\varsigma)-J_1(\kappa\varsigma)Y_1(\varsigma)=0$ smallest route of this $\kappa^2=\frac{1}{\alpha}$ $\varsigma=\sqrt{4\alpha L^2\frac{P}{EI_0}}$	64
		κ^2: ∞, 20, 4.0, 2.25, 1.44, 1.00 ς_0: —, 0.964, 3.20, 6.32, 0.517, — μ: 0.372, 4.428, 0.584, 0.700, 0.841, 1.00	
		$\mu=\frac{\varsigma_0^2(\kappa^2-1)}{4\kappa^2\pi^2}$.	

NUMBER	DIAGRAM & BOUNDARY CONDITIONS	FORMULA OR TABLE FOR RESULTS	REFERENCES, NOTES
76	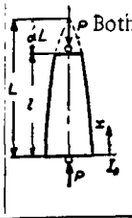 Both ends pinned. $I=I_0\cdot\left\{1-\left(\frac{x}{L}\right)^2\right\}^2$	$P_k=\mu\frac{\pi^2EI_0}{l^2}$ α: 0, 0.05, 0.1, 0.2 μ: 0.101, 0.360, 0.456, 0.595 α: 0.4, 0.6, 0.8, 1.0 μ: 0.896, 0.955, 0.987, 1.00	61 /193
77	Upper end free Lower end fixed. $I=I_0\left(\frac{x}{l}\right)^n$ $0<n<2$	$P_k=\mu\pi^2\frac{EI}{l^2}$ where $\mu\pi^2=\left\{\frac{(2-n)\pi_0}{2}\right\}^2$, π_0 is the first root of $J_{\frac{n-1}{2-n}}(x)=0$ n: 0, 1/3, 1/2, 1, 5/4, 4/3 $\frac{1}{\mu\pi^2}$: 0.405, 0.468, 0.5108, 0.691, 0.843, 0.912	63
78	Circular column having a sloping part in upper section Upper end has no lateral resistance. Both ends fixed.	$P_k=\frac{a^2b^2E}{4\alpha l^2}=\mu\frac{EI_0}{l^2}$ where λ is the first root of $\frac{(b-a)^2}{ab}\lambda-\left\{\lambda^2+\frac{(b-a)^2}{ab}\right\}\tan\lambda$ $\lambda-\frac{b-a}{b}\tan\lambda$ $=\lambda\tan\left\{\frac{(1-\alpha)a}{ab}\lambda\right\}$ is the first root of 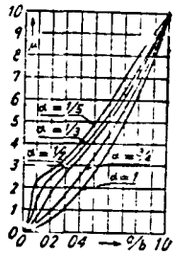	64
79	Circular column having sloping section in upper part. 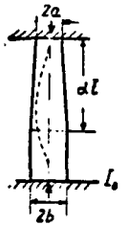 Both ends fixed	$P_k=\frac{1}{4}m\pi^2\frac{E}{l^2}=\mu\frac{EI_0}{l^2}$ where $m=\frac{\lambda ab}{\alpha}$ λ is the first root of $\lambda=\frac{\left[2-\left\{\frac{a^2+b^2}{ab}-\frac{(b-a)^2}{\alpha ab}\right\}\cos\lambda\cdot\cos\left\{\frac{(1-\alpha)a}{ab}\lambda\right\}-\left\{\frac{(1-\alpha)a^2+b(a+\alpha b)}{\alpha ab}-\frac{(a-b)^2}{a^2\lambda^2}\right\}\sin\lambda\cdot\sin\left\{\frac{(1-\alpha)a}{cb}\lambda\right\}\right]}{\left[\left\{\frac{1}{\alpha}+\frac{(1-\alpha)(a-b)^2}{\alpha ab\lambda^2}\right\}\sin\lambda\cdot\cos\left\{\frac{(1-\alpha)a}{\alpha b}\lambda\right\}+\left\{\frac{1}{\alpha}+\frac{(a-b)^2}{a^2\lambda^2}\right\}\cos\lambda\cdot\sin\left\{\frac{(1-\alpha)a}{\alpha b}\lambda\right\}\right]}$ indicated by chart on next page.	65

NUMBER	DIAGRAM & BOUNDARY COND	FORMULA OR TABLE FOR RESULTS	REFERENCES, NOTES
79		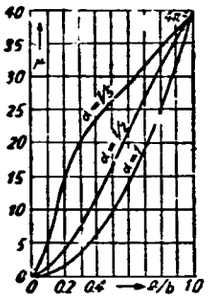	/194
80	Circular column having sloping portion 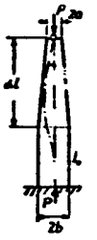 Upper end pinned Lower end fixed $I_0=\frac{\pi b^4}{4}$	$P_k=\frac{\pi^2\lambda^2 Eb}{4\alpha^2}\left(\frac{a-b}{l}\right)^2=\mu\frac{EI_0}{l^2}$ Assuming for $\kappa=\frac{b-a}{b}$ is first root of $\frac{1+\frac{\kappa}{\alpha}\lambda\tan\left(\frac{1-\alpha}{\alpha}\kappa\lambda\right)}{\frac{\kappa\lambda}{\alpha}-\tan\left(\frac{1-\alpha}{\alpha}\kappa\lambda\right)}$ $-\cot(\kappa\lambda)=\frac{1}{\lambda}$ indicated by graph to the right. 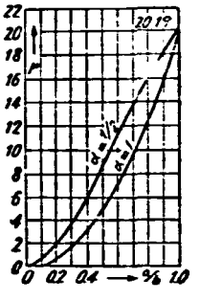	66
81	Circular column with sloping portion Lower end free. Upper end fixed. $I_0=\frac{\pi b^4}{4}$	$P_k=\frac{\pi\lambda^2 Eb^2}{4a^2}\left(\frac{a-b}{l}\right)^2=\mu\frac{EI_0}{l^2}$ where λ is $\tan\left\{\frac{(1-c)(b-a)}{ab}\lambda\right\}-\cot\left(\frac{a-b}{a}\right)\lambda=\frac{1}{\lambda}$ is the first root μ indicated in graph below 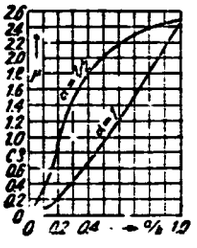	66

NUMBER	DIAGRAM & BOUNDARY CONDITIONS	FORMULA OR TABLE FOR RESULTS	REFERENCES, NOTES
82	Circular column having sloping portion 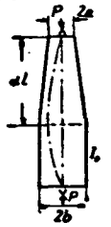 Both ends pinned. $I_0=\frac{\pi b^4}{4}$	$P_k=\frac{\pi\lambda^2 E b^2}{4a^2}\left(\frac{a-b}{l}\right)^2$ $=\mu\frac{EI_0}{l^2}$ λ is first root of $\cot\left\{\frac{(1-\alpha)(\beta-\alpha)}{\alpha\beta}\lambda\right\}+\cot\left(\frac{\beta-\alpha}{\alpha}\lambda\right)=-\frac{1}{\lambda}$ μ indicated below 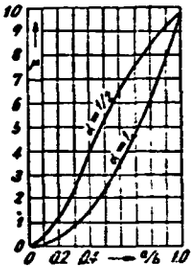 	66 /195
83	Linear variation of width, thickness constant, t 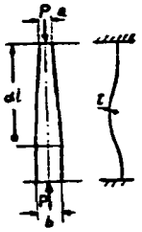 Both ends fixed $I_0=\frac{bt^3}{12}$	Buckling equation $\lambda^2=\frac{8/\pi}{\frac{a}{b}\left\{J_2\left(\sqrt{\frac{a}{b}}\lambda\right)Y_0(\lambda)-Y_2\left(\sqrt{\frac{a}{b}}\lambda\right)J_0(\lambda)\right\}-\left\{J_0\left(\sqrt{\frac{a}{b}}\lambda\right)Y_2(\lambda)-Y_0\left(\sqrt{\frac{a}{b}}\lambda\right)J_2(\lambda)\right\}}$ where $\lambda=2m\sqrt{t}$ $m=12\frac{P}{Et^3}\left(\frac{l}{b-a}\right)^2$ $P_k=\mu\frac{EI_0}{l^2}$ 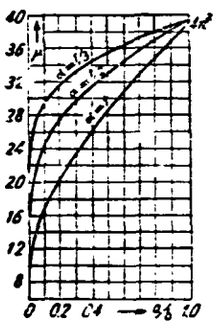 	65

NUMBER	DIAGRAM & BOUNDARY CONDITIONS	FORMULA OR TABLE FOR RESULTS	REFERENCES, NOTES
84	Linear variation of width, thickness constant, t 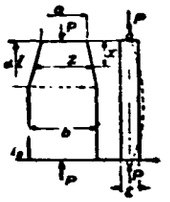 Both ends pinned	Buckling condition equation $$\frac{J_1\left(\sqrt{\frac{a}{b}}\lambda\right)Y_1(\lambda)-Y_1\left(\sqrt{\frac{a}{b}}\lambda\right)J_1(\lambda)}{J_1\left(\sqrt{\frac{a}{b}}\lambda\right)Y_0(\lambda)-Y_1\left(\sqrt{\frac{a}{b}}\lambda\right)J_0(\lambda)}=$$ $$-\tan\left\{\frac{(1-z)(b-a)}{2ab}\lambda\right\}.$$ Assuming its root to be $$P_k=\frac{\lambda^2Et^3}{48a^2b}\left(\frac{a-b}{l}\right)^2=\mu\frac{EI_0}{l^2}$$ μ indicated below 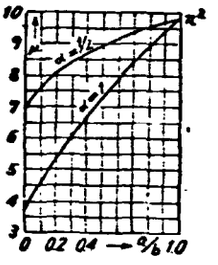	67 /196
85	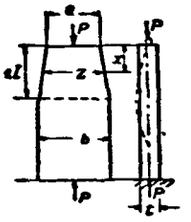 Upper end pinned, lower end fixed.	Buckling condition equation $$\frac{J_1\left(\sqrt{\frac{a}{b}}\lambda\right)Y_1(\lambda)-Y_1\left(\sqrt{\frac{a}{b}}\lambda\right)J_1(\lambda)}{J_1\left(\sqrt{\frac{a}{b}}\lambda\right)Y_0(\lambda)-Y_1\left(\sqrt{\frac{a}{b}}\lambda\right)J_1(\lambda)}$$ $$=\frac{\frac{a-b}{2ab}\lambda-\tan\left\{\frac{(1-z)(b-a)}{2ab}\lambda\right\}}{1+\frac{b-a}{2ab}\lambda\cdot\tan\left\{\frac{(1-z)(b-a)}{2ab}\lambda\right\}}.$$ Assuming the root to be $$P_k=\frac{\lambda^2Et^3}{48a^2b}\left(\frac{a-b}{l}\right)^2=\mu\frac{EI_0}{l^2}.$$ μ indicated in graph below 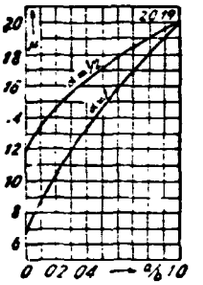	67

NUMBER	DIAGRAM & BOUNDARY CONDITIONS	FORMULA OR TABLE FOR RESULTS	REFERENCES, NOTES
86	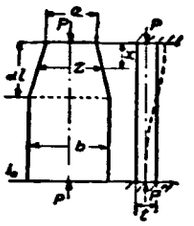 Both ends fixed. No lateral resistance in upper end.	Buckling condition equation $$\frac{J_0\left(\sqrt{\frac{a}{b}}\lambda\right)Y_0(\lambda)-Y_0\left(\sqrt{\frac{a}{b}}\lambda\right)J_0(\lambda)}{J_0\left(\sqrt{\frac{a}{b}}\lambda\right)Y_1(\lambda)-Y_0\left(\sqrt{\frac{a}{b}}\lambda\right)J_1(\lambda)}=\tan\left\{\frac{(1-\alpha)(b-a)}{2\alpha b}\lambda\right\}$$ Assuming the root of this to be $$P_k=\mu\frac{EI_0}{l^2}=\frac{\lambda^2Et^3}{48\alpha^2 b}\left(\frac{b-a}{l}\right)^2$$ is indicated by the graph on the right 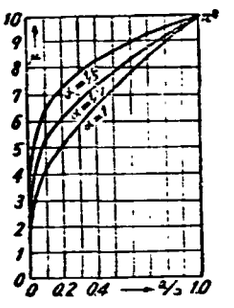	67 /197
87	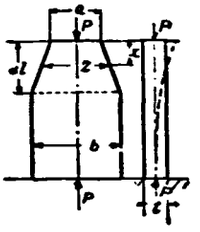 upper end free, lower end fixed.	Buckling condition equation $$\frac{J_1\left(\sqrt{\frac{a}{b}}\lambda\right)Y_0(\lambda)-Y_1\left(\sqrt{\frac{a}{b}}\lambda\right)J_0(\lambda)}{J_1\left(\sqrt{\frac{a}{b}}\lambda\right)Y_1(\lambda)-Y_1\left(\sqrt{\frac{a}{b}}\lambda\right)J_1(\lambda)}=\tan\left\{\frac{(1-\alpha)(b-a)}{2\alpha b}\lambda\right\}$$ $\alpha=1$ In the case of a slope over the entire length, $=1$, assuming $$\frac{J_1\left(\sqrt{\frac{a}{b}}\lambda\right)}{Y_1\left(\sqrt{\frac{a}{b}}\lambda\right)}=\frac{J_0(\lambda)}{Y_0(\lambda)}$$ $$P_k=\mu\frac{EI_0}{l^2}=\frac{\lambda^2Et^3}{48\alpha^2 b}\left(\frac{b-a}{l}\right)^2$$ indicated as below 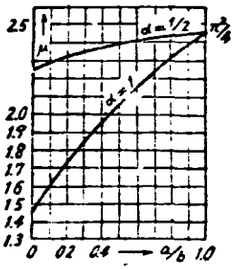	67

NUMBER	DIAGRAM & BOUNDARY CONDITIONS	FORMULA OR TABLE FOR RESULTS	REFERENCES, NOTES

88 Upper end is cross-section with varying indices and functions, plate thickness constant.

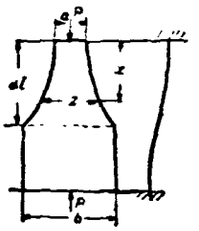

Both ends fixed, no lateral resistance in upper end.

$$z = ae^{\frac{n}{2i}\log\frac{x}{a}}$$

$$I = \beta z^{\tau}$$

$$I_0 = \beta b^{\tau}$$

$$P_k = \mu\frac{EI_0}{l^2}$$ μ is as indicated in the table and the graphs below.

/198

•	τ \ a/b	1/10	1/5	1/4	1/3	1/2	2/3	3/4	4/5	9/10
0.2	1	5.377	6.610	7.048	7.649	8.496	9.085	9.321	9.448	9.666
	2	3.201	4.184	4.071	5.545	7.053	8.252	8.737	9.004	9.470
	3	2.459	3.106	3.437	4.107	5.744	7.408	8.136	8.543	9.265
	4	0.756	2.614	2.861	3.305	4.701	6.585	7.532	8.079	9.050
0.5	1	4.615	5.681	6.106	6.722	7.730	8.558	8.915	9.124	—
	2	2.329	3.570	4.041	4.748	6.106	7.441	8.056	8.429	9.163
	3	0.672	2.135	2.715	3.498	4.917	6.461	7.286	7.794	8.829
	4	0.124	0.914	1.532	2.514	4.036	5.659	6 603	7.211	8.500
0.75	1	3.946	5.194	5.668	6.348	7.438	8.373	8.780	9.019	—
	2	1.340	2.677	3.249	4.114	5.668	7.115	7.818	8.234	9.058
	3	0.309	1.181	1.702	2.585	4.313	6.059	6.970	7.528	8.680
	4	0.055	0.428	0.768	1.503	3.248	5.165	6.216	6.886	8.311
1.00	1	3.054	4.378	4.914	5.678	6.974	8.102	8.552	8.833	—
	2	0.824	1.858	2.376	3.226	4.911	6.573	7.399	7.895	—
	3	0.176	0.716	1.081	1.781	3.434	5.353	6.399	7.057	8.428
	4	0.031	0.246	0.451	0.937	2.376	4.352	5.532	6.304	7.993

68
69

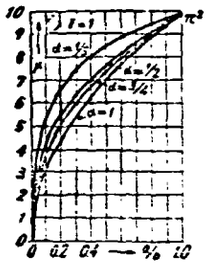

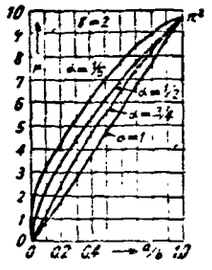

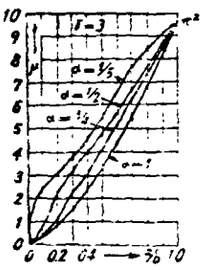

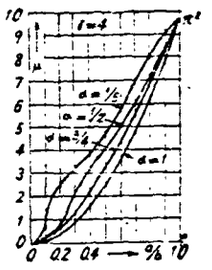

NUMBER	DIAGRAM & BOUNDARY CONDITIONS	FORMULA OR TABLE FOR RESULTS	REFERENCES, NOTES

8) Upper end is cross-sectioned with varying indices and functions, plate thickness constant.

/199

$$P_k = \mu \frac{EI_0}{l^2}$$ μ indicated by the table and graphs below.

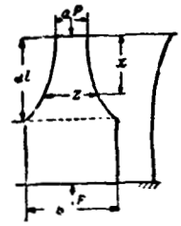

Upper end free, lower end fixed.

$$z = ae^{\frac{x}{al}\log\frac{b}{a}}$$

$$I = \beta z^{\tau}$$

$$I_0 = \beta b^{\tau}$$

α	τ \ a/b	1/10	1/5	1/4	1/3	1/2	2/3	3/4	4/5	9/10
0.2	1	2.435	2.448	2.454	2.455	2.461	2.464	2.465	2.466	2.465
	2	2.310	2.405	2.421	2.437	2.452	2.460	2.463	2.463	2.467
	3	1.447	2.287	2.352	2.402	2.440	2.456	2.459	2.462	2.462
	4	0.302	1.767	2.147	2.332	2.422	2.450	2.456	2.461	2.464
0.5	1	2.025	2.202	2.252	2.308	2.376	2.419	2.436	2.436	2.455
	2	1.052	1.699	1.872	2.054	2.250	2.355	2.394	2.411	2.442
	3	0.270	0.947	1.268	1.667	2.089	2.285	2.348	2.379	2.249
	4	0.049	0.371	0.646	1.154	1.871	2.202	2.297	2.343	2.415
0.75	1	1.480	1.805	1.906	2.033	2.204	2.318	2.360	2.385	2.430
	2	0.534	1.056	1.259	1.555	1.907	2.156	2.250	2.300	2.391
	3	0.122	0.471	0.680	1.022	1.586	1.882	2.133	2.213	2.351
	4	0.022	0.159	0.305	0.600	1.259	1.798	2.010	2.122	2.311
1.0	1	1.059	1.416	1.546	1.721	1.986	2.178	2.264	2.310	–
	2	0.318	0.686	0.855	1.111	1.546	1.904	2.062	2.149	2.316
	3	0.069	0.278	0.413	0.660	1.170	1.648	1.870	1.998	2.241
	4	0.012	0.097	0.176	0.360	0.855	1.410	1.688	1.850	2.166

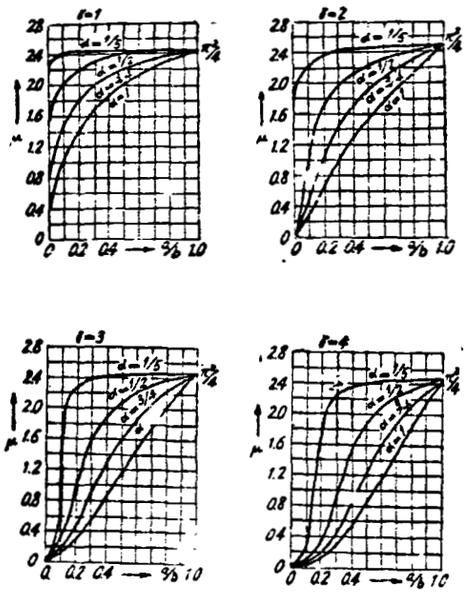

70
71

NUMBER	DIAGRAM & BOUNDARY CONDITIONS	FORMULA OR TABLE FOR RESULTS	REFERENCES, NOTES
90	Upper portion varies in index and function, thicknesses constant.	$P_k=\mu\frac{EI_0}{l^2}$ μ indicated by table and graphs below	/200

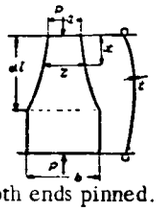

Both ends pinned.

Variations in cross-section based on following equation.

$$z=ae^{\frac{x}{al}\log\frac{b}{a}}$$

$$I=\beta x^{\tau} \quad 0\leqq x\leqq al$$
$$I_0=\beta b^{\tau} \quad al\leqq x\leqq l$$

α	τ \ a/b	1/10	1/5	1/4	1/3	1/2	2/3	3/4	4/5	9/10
0.2	1	9.322	9.573	9.621	9.700	9.773	9.817	9.833	9.846	9.860
	2	6.645	8.760	9.079	9.361	9.622	9.747	9.788	9.808	9.843
	3	1.814	6.177	7.563	8.691	9.411	9.666	9.739	9.773	9.829
	4	0.323	2.499	4.326	7.109	9.083	9.561	9.680	9.732	9.813
0.5	1	5.452	6.936	7.405	7.983	8.743	9.239	9.428	9.533	—
	2	1.641	3.613	4.471	5.678	7.466	8.529	8.990	9.170	9.551
	3	0.335	1.425	2.155	3.475	5.933	7.750	8.433	8.786	9.385
	4	0.057	0.474	0.887	1.884	4.472	6.914	7.881	8.376	9.[illegible]12
0.75	1	3.571	5.087	5.655	6.436	7.631	8.538	8.981	9.128	—
	2	0.873	2.121	2.755	3.781	5.655	7.272	7.994	8.401	9.171
	3	0.167	0.750	1.175	2.024	4.021	6.107	7.116	7.703	8.826
	4	0.027	0.237	0.454	1.036	2.755	5.058	6.289	7.030	8.482
1.00	1	2.715	4.115	4.688	5.514	6.885	8.021	8.529	8.800	—
	2	0.582	1.509	2.017	2.893	4.686	6.463	7.336	7.855	—
	3	0.105	0.496	0.798	1.434	3.111	5.163	6.281	6.976	8.402
	4	0.017	0.150	0.294	0.676	2.[illegible]7	4.087	5.35[illegible]	6.181	7.882

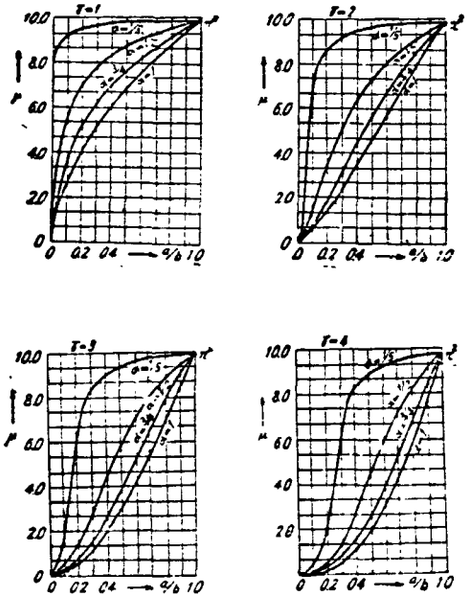

70
71

NUMBER	DIAGRAM & BOUNDARY CONDITIONS	FORMULA OR TABLE FOR RESULTS	REFERENCES, NOTES

91 Member with constant thickness, in which the upper part varies by an exponential function.

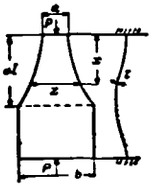

Both ends fixed.

$$s=ae^{\frac{b}{\tau}\log\frac{b}{a}}$$

$$I=\beta s^{\gamma}$$

$$I_0=\beta b^{\gamma}$$

$$P=P_k\frac{EI_0}{l^3}$$ μ is as shown in the table and figures below.

/201

α	γ \ a/b	1/10	1/5	1/4	1/3	1/2	2/3	3/4	4/5	9/10
0.2	1	27.39	30.74	31.41	32.92	35.13	36.95	37.68	31.10	38.83
	2	18.25	24.22	25.71	27.84	31.43	34.54	35.93	36.72	38.19
	3	5.032	16.82	20.66	23.96	28.28	32.30	34.24	35.37	37.52
	4	1.056	6.867	11.87	19.45	25.71	30.27	32.65	34.07	36.87
0.5	1	18.50	24.38	26.38	29.03	32.81	35.55	36.67	—	—
	2	5.768	12.06	14.98	19.35	26.38	31.70	33.92	35.17	—
	3	1.566	5.093	7.366	11.59	20.32	27.95	31.22	33.03	36.04
	4	0.351	2.054	3.406	6.478	14.98	24.27	28.54	30.94	35.39
1.0	1	1 1.30	18.80	19.03	22.27	27.66	32.14	—	—	—
	2	2.684	6.507	8.544	12.01	19.03	25.99	—	—	—
	3	0 540	2.314	3,594	6.204	12.86	20.89	25.28	28.01	—
	4	0.094	0.759	1.422	3.083	8.544	16.69	21.65	24.88	—

68
69

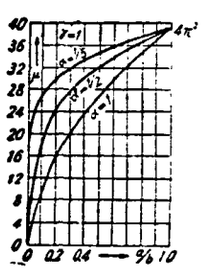

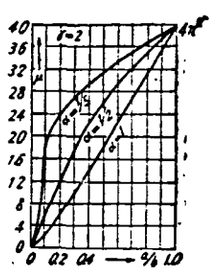

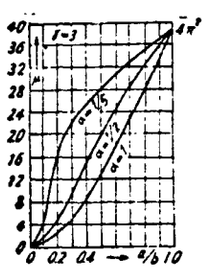

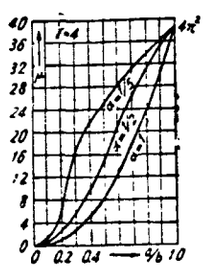

NUMBER	DIAGRAM & BOUNDARY CONDITIONS	FORMULA OR TABLE FOR RESULTS	REFERENCES, NOTES
92	Member of constant thickness in which the upper part varies by an exponential function	$P_k=\mu\frac{EI_0}{l^2}$ μ as shown in the table and figures below	/202

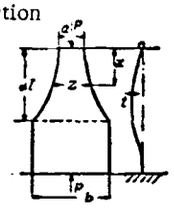

Upper end pinned, lower end fixed.

$z=a^{\frac{x}{al}\log\frac{b}{a}}$

$I=\beta z^\tau$

$I_0=\beta b^\tau$

α	τ \ a/b	1/10	1/5	1/4	1/3	1/2	2/3	3/4	4/5	9/10
0.2	1	17.746	18.872	19.139	19.429	19.764	19.963	20.031	20.071	20.135
	2	8.899	15.157	16.611	17.954	19.136	19.679	19.849	19.935	20.077
	3	2.180	7.910	11.001	14.863	18.172	19.317	19.633	19.781	20.016
	4	0.501	2.968	5.226	9.876	16.612	18.857	19.381	19.609	19.961
0.5	1	9.146	12.249	13.334	14.768	16.810	18.250	18.820	19.317	—
	2	2.833	5.889	7.342	9.583	13.334	16.219	17.403	18.042	19.193
	3	0.786	2.510	3.604	5.662	10.089	14.178	15.957	16.932	18.685
	4	0.174	1.209	1.695	3.175	7.344	12.191	14.506	15.807	18.168
1.0	1	5.729	8.552	9.695	11.360	14.135	16.435	17.462	18.044	—
	2	1.348	3.290	4.324	6.099	9.697	13.272	15.038	16.087	—
	3	0.270	1.161	1.808	3.134	6.532	10.651	12.906	14.312	—
	4	0.047	0.380	0.712	1.550	4.325	8.494	11.044	12.705	16.295

70

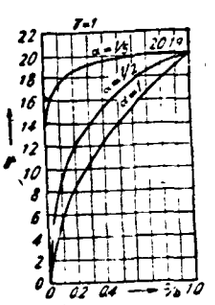

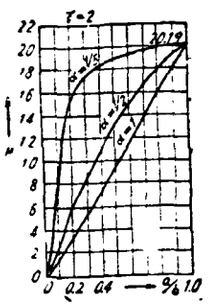

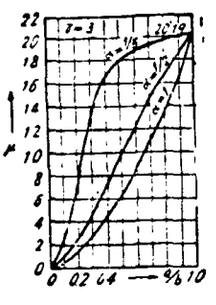

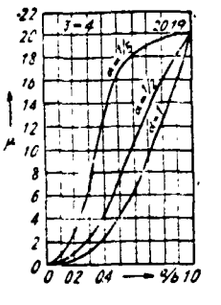

NUMBER	DIAGRAM & BOUNDARY CONDITIONS	FORMULA OR TABLE FOR RESULTS	REFERENCES, NOTES
93	Member of constant width but varying thickness 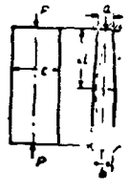 both ends fixed	$P_k=\frac{1}{12}m^2Ec\left(\frac{b-a}{l}\right)$ where $m=-\frac{1}{2}\lambda\sqrt{b}$, λ is initial root of following equation $\lambda^2=\frac{8/\pi}{\left[\frac{b}{a}\left\{J_2\left(\sqrt{\frac{b}{a}}\lambda\right)Y_0(\lambda)-Y_2\left(\sqrt{\frac{b}{a}}\lambda\right)J_0(\lambda)\right\}-\left\{J_0\left(\sqrt{\frac{b}{a}}\lambda\right)Y_2(\lambda)-Y_0\left(\sqrt{\frac{b}{a}}\lambda\right)J_2(\lambda)\right\}\right]}$ If $P_k=\mu\frac{EI_0}{l^2}$ μ will be as in the follwoing graph. 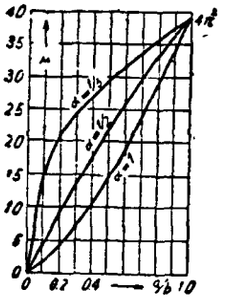	65 /203
94	Member of constant width and varying thickness 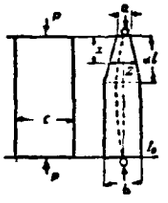 Both ends pinned	Buckling condition equation $\frac{J_2\left(\sqrt{\frac{b}{a}}\lambda\right)Y_0(\lambda)-Y_2\left(\sqrt{\frac{b}{a}}\lambda\right)J_0(\lambda)}{J_0\left(\sqrt{\frac{b}{a}}\lambda\right)Y_1(\lambda)-Y_2\left(\sqrt{\frac{b}{a}}\lambda\right)J_1(\lambda)}=\frac{2}{\lambda}+\cot\left\{\frac{(1-\alpha)(b-\alpha)}{2\alpha b}\right\}$. Assuming the initial root to be $P=\frac{\lambda^2EI_cb}{4l\alpha^2}\left(\frac{a-b}{l}\right)^2=\mu\frac{EI_0}{l^2}$. μ shown by the graph and table below a/a | a = 1 | 1/2 0 | — | 0 1/20 | — | 0.757 1/10 | 0.467 | 1.529 1/5 | 1.082 | 3.028 1/4 | 1.444 | 3.724 1/3 | 2.090 | 4.802 1/2 | 3.629 | 6.605 2/3 | 5 474 | 7.999 2/4 | 6.483 | 8.542 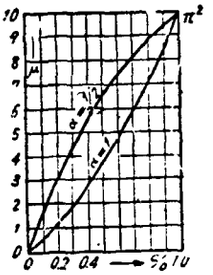	67

NUMBER	DIAGRAM & BOUNDARY CONDITIONS	FORMULA OR TABLE FOR RESULTS	REFERENCES, NOTES
95	Member of constant width and varying thickness 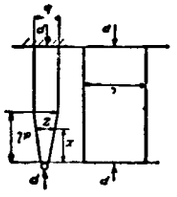 Upper end pinned. Lower end fixed.	Buckling condition equation $$\frac{J_1\left(\sqrt{\frac{b}{a}}\lambda\right)Y_0(\lambda)-Y_1\left(\sqrt{\frac{b}{a}}\lambda\right)J_0(\lambda)}{J_0\left(\sqrt{\frac{b}{a}}\lambda\right)Y_1(\lambda)-Y_1\left(\sqrt{\frac{b}{a}}\lambda\right)J_1(\lambda)}$$ $$=\frac{2}{\lambda}-\frac{1+\frac{b-a}{2ab}\lambda\cdot\tan\left\{\frac{(1-\alpha)(b-a)}{2ab}\lambda\right\}}{\frac{b-a}{2ab}\lambda-\tan\left\{\frac{(1-\alpha)(b-a)}{2ab}\lambda\right\}}.$$ Assuming the initial root to be $$P_k=\frac{\lambda^2 Ecb}{48\alpha^2}\left(\frac{a-b}{l}\right)^2=\mu\frac{EI}{l^2}.$$ μ as shown in the table and graph below α / a/b | 1 | 1/2 0 | 0 | 0 1/10 | 0.874 | 2.184 1/5 | 2.120 | 4.510 1/4 | 2.845 | 5.685 1/3 | 4.192 | 7.625 1/2 | 7.363 | 11.340 2/3 | 11.11 | 14.720 3/4 | 12.19 | 16.346 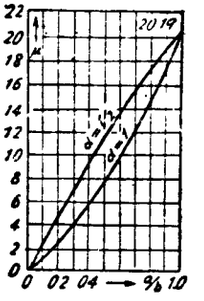	67
96	Member of constant width and varying thickness 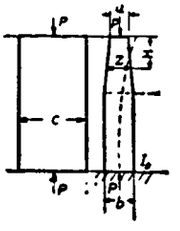	Buckling condition equation $$\frac{J_1\left(\sqrt{\frac{b}{a}}\lambda\right)Y_0(\lambda)-Y_1\left(\sqrt{\frac{b}{a}}\lambda\right)J_0(\lambda)}{J_1\left(\sqrt{\frac{b}{a}}\lambda\right)Y_1(\lambda)-Y_1\left(\sqrt{\frac{b}{a}}\lambda\right)J_1(\lambda)}$$ $$=\frac{2}{\lambda}-\tan\left\{\frac{(1-\alpha)(b-a)}{2ab}\lambda\right\}.$$ Assuming the initial root tobe $$P_k=\frac{\lambda^2 Ecb}{48\alpha^2}\left(\frac{a-b}{l}\right)^2=\mu\frac{EI_0}{l^2}.$$ μ as shown by the table and graph below α / a/b | 1 | 1/2 0 | — | 0 1/20 | — | 0.146 1/10 | 0.321 | 1.103 1/5 | 0.597 | 1.618 1/4 | 0.728 | 1.772 1/3 | 0.935 | 1.953 1/2 | 1.337 | 2.174 2/3 | 1.721 | 2.308 3/4 | 1.972 | 2.359 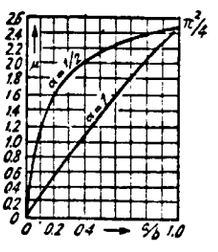	67

NUMBER	DIAGRAM & BOUNDARY CONDITIONS	FORMULA OR TABLE FOR RESULTS	REFERENCES, NOTES
			/205
97	Non-uniform plate cross-section where thickness and width of cross-section in upper part are inversely proportional 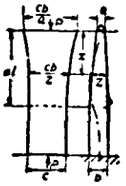 Upper end pinned. Lower end fixed.	$P_k=\frac{1}{12}m^2\frac{Ecb}{l^2}=\mu\frac{EI_0}{l^2}=\lambda$ when assuming $\frac{m\alpha}{b-\alpha}<\frac{1}{2}$ $\sqrt{1-4\left(\frac{m\alpha}{b-\alpha}\right)^2}=\lambda$ とおけば $\lambda\coth\left(\frac{\lambda}{2}\log\frac{b}{a}\right)+1$ $=\sqrt{1-\lambda^2}$ $\cdot\frac{1+\frac{b-\alpha}{2\alpha b}\sqrt{1-\lambda^2}\cdot\tan\left\{\frac{(1-\alpha)(b-\alpha)}{2\alpha b}\sqrt{1-\lambda^2}\right\}}{\frac{b-\alpha}{2\alpha b}\sqrt{1-\lambda^2}-\tan\left\{\frac{(1-\alpha)(b-\alpha)}{2\alpha b}\sqrt{1-\lambda^2}\right\}}$ when assuming $\frac{m\alpha}{b-\alpha}>\frac{1}{2}$ $\sqrt{1-4\left(\frac{m\alpha}{b-\alpha}\right)^2}=i\lambda$ とおけば When replacing $\lambda\cot\left(\frac{\lambda}{2}\log\frac{b}{a}\right)+1=($ $\sqrt{1-\lambda^2}$ を $\sqrt{1+\lambda^2}$ in the above equation by 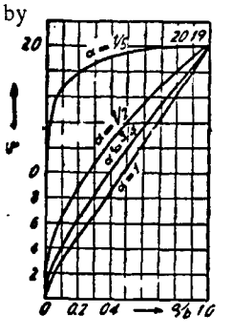	72
98	Member of non-uniform cross-section in which thickness of cross-section and width of upper parts are inversely proportional 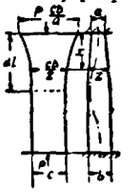 Both ends fixed.	$P_k=\frac{1}{12}m^2\frac{Ecb}{l^2}=\mu\frac{EI_0}{l^2}$ $\frac{m\alpha}{b-\alpha}<\frac{1}{2}$ if $\sqrt{1-4\left(\frac{m\alpha}{b-\alpha}\right)^2}=\lambda$ when $\left\{\lambda^2u(\lambda)+w(\lambda)\right\}\sinh\left(\frac{\lambda}{2}\log\frac{b}{a}\right)$ $=2\lambda\left\{2\sqrt{\frac{a}{b}}-v(\lambda)\cosh\left(\frac{\lambda}{2}\log\frac{b}{a}\right)\right\}.$ $\frac{m\alpha}{b-\alpha}>\frac{1}{2}$ if $\sqrt{1-4\left(\frac{m\alpha}{b-\alpha}\right)^2}=i\lambda$ when $\left\{\lambda^2u(\lambda)+w(\lambda)\right\}\sin\left(\frac{\lambda}{2}\log\frac{b}{a}\right)$ $=2\lambda\left\{v(\lambda)\cos\left(\frac{\lambda}{2}\log\frac{b}{a}\right)-2\sqrt{\frac{a}{b}}\right\}.$ where $u(\lambda)=\frac{1}{\sqrt{1\pm\lambda^2}}\sin\left\{\frac{(1-\alpha)(b-\alpha)}{2\alpha b}\sqrt{1\pm\lambda^2}\right\}$ $-\frac{b-\alpha}{\alpha b}\left\{\frac{(1-\alpha)(b-\alpha)}{2\alpha b}\sqrt{1\pm\lambda^2}\right\}.$	72

NUMBER	DIAGRAM & BOUNDARY CONDITIONS	FORMULA OR TABLE FOR RESULTS	REFERENCES, NOTES
98		$\psi(\lambda)=\frac{b-a}{2ab}\sqrt{1\pm\lambda^2}\sin\left\{\frac{(1-\alpha)(b-a)}{2ab}\sqrt{1\pm\lambda^2}\right\}$ $+\frac{b+a}{b}\cos\left\{\frac{(1-\alpha)(b-a)}{2ab}\sqrt{1\pm\lambda^2}\right\}$, $w(\lambda)=\frac{(1-2\alpha)(b-a)}{ab}\cos\left\{\frac{(1-\alpha)(b-a)}{2ab}\sqrt{1\pm\lambda^2}\right\}$ $-\left\{\frac{2}{\sqrt{1\pm\lambda^2}}+\frac{b-(1-2\alpha)a}{ab}\sqrt{1\pm\lambda^2}\right\}$ $\cdot\sin\left\{\frac{(1-\alpha)(b-a)}{2ab}\sqrt{1\pm\lambda^2}\right\}$. is negative when $+\frac{m\alpha}{b-a}<\frac{1}{2}$, is positive $\frac{m\alpha}{b-a}>\frac{1}{2}$. 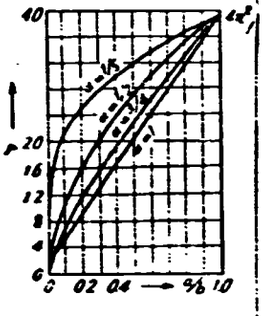	/206
99	Member of non-uniform cross-section in which the thickness and the width of the cross-section in the upper part are inversely proportional. 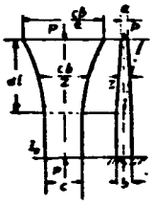 Upper end free lower end fixed.	$P=\frac{1}{12}m^2\frac{Ecb}{l^2}=\mu\frac{EI_0}{l^2}$ when $\frac{m\alpha}{b-a}<\frac{1}{2}$ if $\sqrt{1-4\left(\frac{m\alpha}{b-a}\right)^2}=\lambda$ The condition equation is $\lambda\coth\left(\frac{\lambda}{2}\log\frac{b}{a}\right)+1$ $=\sqrt{1-\lambda^2}\tan\left\{\frac{(1-\alpha)(b-a)}{2ab}\sqrt{1-\lambda^2}\right\}$. when $\frac{m\alpha}{b-a}>\frac{1}{2}$ if $\sqrt{1-4\left(\frac{m\alpha}{b-a}\right)^2}=i\lambda$ $\lambda\cot\left(\frac{\lambda}{2}\log\frac{b}{a}\right)+1$ $=\sqrt{1+\lambda^2}\tan\left\{\frac{(1-\alpha)(b-a)}{2ab}\sqrt{1+\lambda^2}\right\}$ as in the graph below 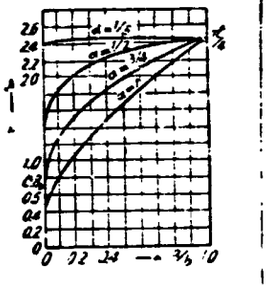	72

NUMBER	DIAGRAM & BOUNDARY CONDITIONS	FORMULA OR TABLE FOR RESULTS	REFERENCES, NOTES
100	Member of non-uniform cross-section in which the thickness and the width of the cross-section in the upper parts are inversely proportional. 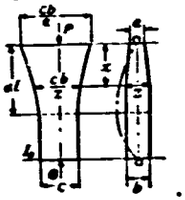 Both ends pinned.	when $P=\frac{1}{12}m^2\frac{Ecb}{l^2}=\mu\frac{EI_0}{l^2}$ $\frac{mx}{b-a}<\frac{1}{2}$ if $\sqrt{1-4\left(\frac{mx}{b-a}\right)^2}=\lambda$ $\lambda\coth\left(\frac{\lambda}{2}\log\frac{b}{a}\right)+1$ when $=-\sqrt{1-\lambda^2}\cot\left\{\frac{(l-x)(b-a)}{2xb}\sqrt{1-\lambda^2}\right\}$. $\frac{mx}{b-a}>\frac{1}{2}$ if $\sqrt{1-4\left(\frac{mx}{b-a}\right)^2}=i\lambda$ $\lambda\cot\left(\frac{\lambda}{2}\log\frac{b}{a}\right)+1$ $=-\sqrt{1+\lambda^2}\cot\left\{\frac{(l-x)(b-a)}{2xb}\sqrt{1+\lambda^2}\right\}$. μ is an shown in the graph below 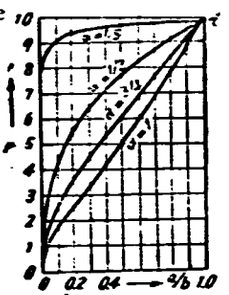	73 /207
101	Symmetrical member having linear sine members. $I=I_m\left(1-\frac{2x}{L}\right)^2$ 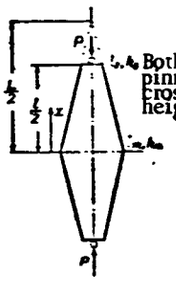 Both ends pinned, h_0 is cross-section height.	$P_c=\mu\frac{\pi^2EI_m}{l^2}$ h_0/h_m: 0 | 0.2 | 0.4 μ: 0.101 | 0.449 | 0.610 h_0/h_m: 0.6 | 0.8 | 1.0 i: 0.749 | 0.881 | 1.00 Approximation equation $\mu=0.34+0.66\sqrt{\frac{I_0}{I_m}}$ where $h_0/h_m\leqq 0.2$	74
102	$I=I_0\left(1-\frac{y}{L}\right)^n$ Upper end free. Lower end fixed.	$P_c=\mu\pi^2\frac{EI_0}{l^2}$ n: 1/2 | 1 | 2 $\mu\pi^2$: 1.959 | 1.446 | 0.25	75

NUMBER	DIAGRAM & BOUNDARY CONDITIONS	FORMULA OR TABLE FOR RESULTS	REFERENCES, NOTES
103	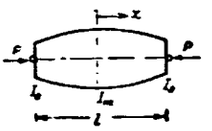 Both ends pinned. $I(x)=I_m - (I_m-I_0)\left(\frac{2x}{l}\right)^n$ where $0<\frac{I_0}{I_m}\leq 1$	$P_m=\mu_m\frac{EI_m}{l^2}$ μ_m is shown in Figure 103.1 $P_{k0}=\mu_0\frac{EI_0}{l^2}$ μ_0 is shown in Figure 103.2 $k=\frac{I_0}{I_m}$ 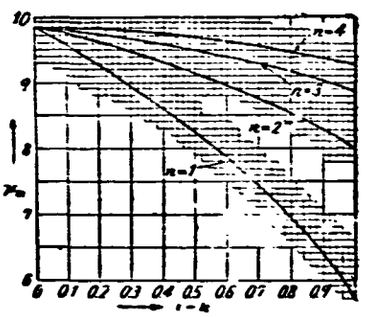 Figure 103.1 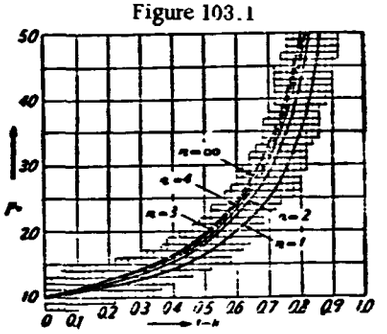 Figure 103.2	75 Differential equation solved by power series.
104	 Both ends pinned. $I=I_0\left(1-\frac{x^2}{\kappa^2}\right)^2$ where $\kappa^2=\frac{4}{l^2}\left(1-\sqrt{\frac{I_1}{I_0}}\right)$	$P_k=\mu\frac{EI_0}{l^2}$ where $\mu=\frac{l^2}{\kappa^2}\left(\frac{\kappa^2}{\log^2\frac{2\kappa+l}{2\kappa-l}}+1\right)$ $\varepsilon^2=\frac{P\kappa^4}{EI_0}$ L_1/L_0 | 0 | 0.1 | 0.2 | 0.3 | 0.4 | 0.5 μ | 4.0 | 7.60 | 8.15 | 8.52 | 8.81 | 9.05 L_1/L_0 | 0.6 | 0.7 | 0.8 | 0.9 | 1.0 | μ | 9.25 | 9.43 | 9.59 | 9.84 | π^2 |	76

105

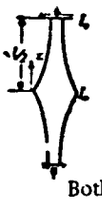

$$I=I_0\cdot\left(1-\frac{x^2}{\kappa^2}\right)^2\cdot$$

$$\frac{1}{\kappa^2}=\frac{4}{l^2}$$

$$\cdot\left(1-\sqrt{\frac{I_1}{I_0}}\right)\cdot$$

Both ends fixed.

$$P_k=\mu\frac{EI_0}{l^2}\cdot$$

where $\mu=\frac{l^2}{\kappa^2}\left[\frac{4\rho^2}{\left(\log\frac{2\kappa+l}{2\kappa-l}\right)^2}+1\right]\cdot$

$$\rho=\frac{\sqrt{a^2-\kappa^2}}{2\kappa}\cdot\log\frac{2\kappa+l}{2\kappa-l}\cdot\qquad a^2=\frac{P\cdot\kappa^2}{EI_0}\cdot$$

I_1/I_0	0.1	0.2	0.3	0.4	0.5
μ	18.27	22.50	25.62	28.24	30.54
I_1/I_0	0.6	0.7	0.8	0.9	1.0
μ	32.62	34.50	36.26	39.48	$4\pi^2$

76

106

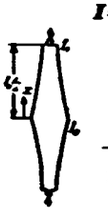

$$I=\frac{I_0}{\left(1+\frac{x}{\kappa}\right)^m}\cdot$$

where

$$\kappa=\frac{l}{2\left(\sqrt[m]{\frac{I_0}{I_1}}-1\right)}\cdot$$

Both ends pinned.

$$P_k=\mu\frac{EI_0}{l^2}\cdot$$

I_1/I_0 \ m	1	2	3	4
0.2	4.43	5.01	5.22	5.34
0.4	6.79	7.06	7.16	7.20
0.6	8.23	8.32	8.35	8.38
0.8	9.19	9.20	9.21	9.21

76

107

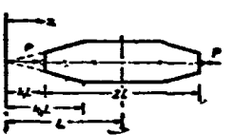

$$I=I_1\left(\frac{x}{k_2L}\right)^n,$$

$$0\leqq x\leqq k_2L.$$

Both ends pinned.

$$P_k=\mu\frac{EI_1}{(2l)^2}\cdot$$

ς_0 is the minimum root satisfying the

where $\mu=\varsigma_0^2(2-n)^2\frac{(1-k_1)^2}{k_2^2}\cdot$ buckling condition equation.

$k_1=0$ μ, ς_0 are as shown in the table below

k_2 \ n		1	4/3	3/2	5/3	7/4
1.0	μ	5.76	—	—	—	—
	ς_0	2.40	3.00	3.83	5.14	6.38
0.8	μ	7.02	5.06	4.25	3.21	2.49
	ς_0	2.12	2.70	3.30	4.30	5.20
0.6	μ	8.41	—	—	—	—
	ς_0	1.74	2.15	2.50	3.00	3.30
0.4	μ	9.30	—	—	—	—
	ς_0	1.22	1.45	1.55	1.70	1.80

77

The buckling condition equation is expressed by the Bessel function relating to ξ. Here, ξ is the following equation:

$$\varsigma=\frac{2}{2-n}\cdot\sqrt{\frac{P}{EI_1}}k_2L$$

$n=1$ when

$$P_k=\varsigma_0^2\frac{(1-k_1)^2}{k_2^2}\cdot\frac{EI_1}{(2l)^2}\cdot$$

ς_0 expressed in the following table:

k_2 \ k_1/k_2	0.1	0.2	0.4	0.6	0.8
1.0	2.80	3.29	4.66	7.32	
0.8	2.40	2.70	3 50	4.70	7.00
0.6	1.90	2.05	2.45	2.90	3.60
0.4	1.30	1.30	1.50	1.60	1.85

77

NUMBER	DIAGRAM & BOUNDARY CONDITIONS	FORMULA OR TABLE FOR RESULTS	REFERENCES, NOTES
108	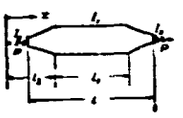 $I=I_2\left(\frac{x}{l_2}\right)^n$, $0\leqq x\leqq l_2$. At the end, $l=l_0$, both ends pinned.	$P_k=\mu\frac{EI_2}{l^2}$. μ shown in the table below	76 /210

I_1/I_0	n \ l_2/l	0	0.2	0.4	0.6	0.8
0.1	1	6.48	7.58	8.68	9.40	9.82
	2	5.40	6.67	8.08	9.24	9.79
	3	5.01	6.32	7.84	9.14	9.77
	4	4.81	6.11	7.68	9.01	9.77
0.2	1	7.01	7.99	8.91	9.63	9.83
	2	6.37	7.49	8.61	9.44	9.81
	3	6.14	7.31	8.49	9.39	9.81
	4	6.02	7.20	8.42	9.38	9.80
0.4	1	7.87	8.50	9.19	9.74	9.84
	2	7.61	8.42	9.15	9.63	9.84
	3	7.52	8.39	9.11	9.62	9.84
	4	7.48	8.33	9.10	9.62	9.84
0.6	1	8.61	9.12	9.55	9.76	9.85
	2	8.51	9.04	9.48	9.74	9.85
	3	8.50	9.02	9.46	9.74	9.85
	4	8.47	9.01	9.45	9.74	9.85
0.8	1	9.27	9.54	9.68	9.83	9.86
	2	9.24	9.50	9.70	9.82	9.86
	3	9.23	9.50	9.69	9.81	9.86
	4	9.23	9.49	9.69	9.81	9.86

109	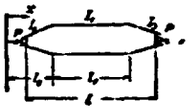 $I=I_2\left(\frac{x}{l_2}\right)^n$, $0\leqq x\leqq l_2$. $I=I_0$. Both ends pinned.	$P_k=\frac{\pi^2 EI_k}{l^2}$, $I_k\equiv\varkappa I_2$. The correction coefficient $\varkappa$ for the geometric moments of inetia is shown below.	76

I_0/I_2	n \ l_2/l	1	0.2	0.4	0.6	0.8	1.0
0.1	1	0.656	0.768	0.879	0.958	0.995	1.000
	2	0.547	0.676	0.819	0.937	0.992	1.000
	3	0.508	0.640	0.794	0.926	0.990	1.000
	4	0.487	0.619	0.778	0.920	0.990	1.000
0.2	1	0.710	0.809	0.903	0.976	0.995	1.000
	2	0.645	0.759	0.872	0.956	0.994	1.000
	3	0.622	0.740	0.860	0.951	0.994	1.000
	4	0.610	0.729	0.853	0.950	0.993	1.000
0.4	1	0.797	0.871	0.931	0.983	0.997	1.000
	2	0.771	0.853	0.927	0.976	0.997	1.000
	3	0.762	0.849	0.924	0.976	0.997	1.000
	4	0.758	0.844	0.922	0.975	0.997	1.000
0.6	1	0.871	0.924	0.968	0.987	0.998	1.000
	2	0.862	0.915	0.960	0.987	0.998	1.000
	3	0.861	0.914	0.959	0.987	0.998	1.000
	4	0.858	0.913	0.957	0.987	0.998	1.000
0.8	1	0.939	0.967	0.982	0.996	0.999	1.000
	2	0.936	0.962	0.982	0.995	0.999	1.000
	3	0.935	0.962	0.982	0.994	0.999	1.000
	4	0.935	0.961	0.982	0.994	0.999	1.000

NUMBER	DIAGRAM & BOUNDARY CONDITIONS	FORMULA OR TABLE FOR RESULTS	REFERENCES, NOTES
110	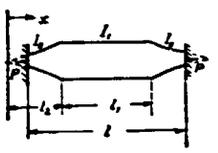 $I=I_1\left(\frac{x}{l_2}\right)^n$, $0 \leqq x \leqq l_2$. $I = I_2$ at ends. Both ends fixed.	$P_k=\mu\frac{EI_1}{l^2}$. μ shown by table below I_0/I_1 \ l_1/l | n | 0 | 0.2 | 0.4 | 0.6 | 0.8 0.1 | 1 | — | — | — | — | — 2 | 14.39 | 16.85 | 18.84 | 20.29 | 23.41 3 | — | — | — | — | — 4 | 13.30 | 15.96 | 18.18 | 19.60 | 22.39 0.2 | 1 | 20.36 | 22.36 | 23.42 | 25.44 | 29.00 2 | 18.94 | 21.25 | 22.91 | 24.29 | 27.67 3 | 18.48 | 20.88 | 22.64 | 23.96 | 27.24 4 | 18.23 | 20.71 | 22.49 | 23.80 | 27.03 0.4 | 1 | 26.16 | 27.80 | 28.96 | 30.20 | 33.08 2 | 25.54 | 27.35 | 28.52 | 29.69 | 32.59 3 | 25.32 | 27.20 | 28.40 | 29.52 | 32.44 4 | 25.23 | 27.13 | 28.33 | 29.46 | 32.35 0.6 | 1 | 31.04 | 32.20 | 32.92 | 33.80 | 35.80 2 | 30.79 | 32.02 | 32.77 | 33.63 | 35.64 3 | 30.72 | 31.96 | 32.72 | 33.56 | 35.60 4 | 30.68 | 31.94 | 32.69 | 33.54 | 35.56 0.8 | 1 | 35.40 | 36.00 | 36.36 | 36.84 | 37.84 2 | 35.35 | 35.97 | 36.34 | 36.80 | 37.81 3 | 33.32 | 35.96 | 36.32 | 36.80 | 37.80 4 | 35.33 | 35.96 | 36.32 | 36.78 | 37.80	76 /211
111	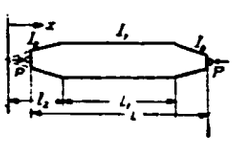 $I=I_1\left(\frac{x}{l_2}\right)$, $0 \leqq x \leqq l_2$. Both ends pinned.	$P_k=\mu\frac{EI_1}{l^2}$. μ shown in table below I_0/I_1 \ l_1/l | 0 | 0.01 | 0.1 | 0.2 | 0.4 | 0.6 | 0.8 0 | 5.87 | 5.78 | 6.48 | 7.01 | 7.86 | 8.61 | 9.27 0.2 | 7.04 | 7.11 | 7.58 | 7.99 | 8.59 | 9.12 | 9.53 0.4 | 8.35 | 8.40 | 8.63 | 8.90 | 9.19 | 9.55 | 9.68 0.6 | 9.36 | 9.40 | 9.46 | 9.73 | 9.70 | 9.76 | 9.82 0.8 | 9.80 | 9.80 | 9.82 | 9.82 | 9.83 | 9.85 | 9.86	78 e.g., rectangular plate of varying width.
112	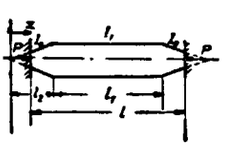 $I=I_1\left(\frac{x}{l_2}\right)$, $0 \leqq x \leqq l_2$. Both ends fixed.	$P_k=\mu\frac{EI_0}{l^2}$. μ shown in table below. I_0/I_1 \ l_1/l | 0.2 | 0.4 | 0.6 | 0.8 0 | 20.36 | 26.16 | 31.04 | 35.40 0.2 | 22.36 | 27.80 | 32.20 | 36.00 0.4 | 23.42 | 28.96 | 32.92 | 36.36 0.6 | 25.44 | 30.20 | 33.80 | 36.84 0.8 | 29.00 | 33.08 | 35.80 | 37.84	78

NUMBER	DIAGRAM & BOUNDARY CONDITIONS	FORMULA OR TABLE FOR RESULTS	REFERENCES, NOTES
	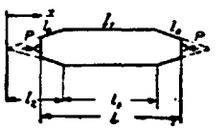 $I=I_1\left(\frac{x}{l_2}\right)^2$. Both ends pinned.	$P_E=\mu\frac{EI_1}{l^2}$. μ shown in table below	73 e.g., Built-up member consisting of 4 slender members. /212

I_0/I_1 / l_1/l	0	0.1	0.1	0.2	0.4	0.6	0.8
0	1.00	3.45	5.40	6.37	7.61	8.51	9.24
0.2	1.56	4.73	6.67	7.49	8.42	9.04	9.50
0.4	2.78	6.58	8.08	8.61	9.15	9.48	9.70
0.6	6.25	8.62	9.25	9.44	9.63	9.74	9.82
0.8	9.57	9.71	9.79	9.81	9.84	9.84	9.86

	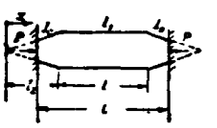 $I=I_1\left(\frac{x}{l_2}\right)^2$. Both ends fixed	$P_E=\mu\frac{EI_1}{l^2}$. μ shown in table below	78

I_0/I_1 / l_1/l	0.2	0.4	0.6	0.8
0	18.94	25.54	30.79	35.35
0.2	21.25	27.35	32.02	35.97
0.4	22.91	28.52	32.77	36.34
0.6	24.29	29.69	33.63	36.80
0.8	27.67	32.59	35.64	37.81

	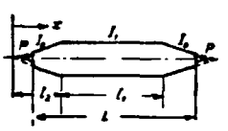 $I=I_1\left(\frac{x}{l_2}\right)^3$. Both ends pinned	$P_E=\mu\frac{EI_2}{l^2}$. μ shown in table below	78 e.g., rectangular plate with varying thickness.

I_0/I_1 / l_1/L	0.01	0.1	0.2	0.4	0.6	0.8
0	2.55	5.01	6.14	7.52	8.50	9.23
0.2	3.65	6.32	7.31	8.38	9.02	9.50
0.4	5.42	7.84	8.49	9.10	9.46	9.69
0.6	7.99	9.14	9.39	9.62	9.74	9.81
0.8	9.03	9.77	9.81	9.84	9.85	9.86

	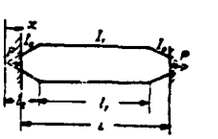 $I=I_1\left(\frac{x}{l_2}\right)^3$. Both ends fixed	$P=\mu\frac{EI_1}{l^2}$. μ shown in table below	78

I_0/I_1 / l_1/l	0.2	0.4	0.6	0.8
0	18.48	25.32	30.72	35.32
0.2	20.88	27.20	31.96	35.96
0.4	22.64	28.40	32.72	36.32
0.6	23.96	29.52	33.56	36.80
0.8	27.24	32.94	35.60	37.80

NUMBER	DIAGRAM & BOUNDARY CONDITIONS	FORMULA OR TABLE FOR RESULTS	REFERENCES, NOTES
117	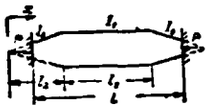 $I=I_1\left(\frac{x}{l_0}\right)^4$. Both ends pinned.	$P_k=\mu\frac{EI_1}{l^2}$. μ shown in table below	78 e g., Case where a member and is either pyramid or cone /213
118	$I=I_1\left(\frac{x}{l_0}\right)^4$. Both ends fixed.	$P=\mu\frac{EI_1}{l^2}$. μ shown in table below	78
119	True hexagonal plate 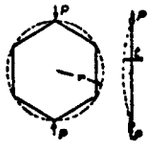 Both ends pinned	$P_k=0.3218\frac{Et^3}{r}$.	79
120	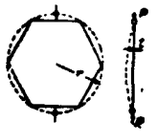 Both ends pinned.	$P_k=0.3767\frac{Et^3}{r}$.	79 The upper half is considered as divided into one isodeles triangle and one rectangle.
121	Both ends pinned.	$P_k=0.3059\frac{Ebt^3}{l^2}$.	80

l_1/l \ I_1/I_0	0.01	0.1	0.2	0.4	0.6	0.8
0	2.15	4.81	6.02	7.48	8.47	9.23
0.2	3.13	6.11	7.20	8.33	9.01	9.49
0.4	4.84	7.68	8.42	9.10	9.45	9.69
0.6	7.53	9.08	9.38	9.62	9.74	9.81
0.8	9.56	9.77	9.80	9.84	9.85	9.86

l_2/l \ I_1/I_0	0.2	0.4	0.6	0.8
0	18.23	25.23	30.68	35.33
0.2	20.71	27.13	31.94	35.96
0.4	22.49	28.33	32.69	36.32
0.6	23.80	29.46	33.54	36.78
0.8	27.03	32.35	35.56	37.80

NUMBER	DIAGRAM & BOUNDARY CONDITIONS	FORMULA OR TABLE FOR RESULTS	REFERENCES, NOTES
122	Upper end free, lower end fixed.	$P_k=0.1206\frac{Ebt^3}{l^2}$.	80 /214
123	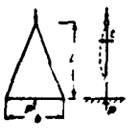 Upper end pinned, lower end fixed.	$P_k=0.5493\frac{Ebt^3}{l^2}$.	80
124	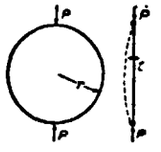 Upper end pinned.	$P_k=0.3754\frac{Et^3}{r}$.	81 Slightly larger than the test value. When r/t is large, is it applicable.
		$P_k=10\cdot\frac{Et^3}{0.07508+\frac{2r}{t}}$.	Test equation When r/t is small, it is used.
125	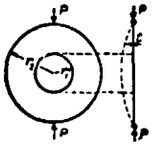 Both ends pinned.	$P_k=\frac{1}{6}m\frac{Et^3}{r_2}$.	81 When the whole diameter is not very large (when is not very large) this agrees with the experiment values. The differential equation is solved by series, these values are taken as far as the section term Here, where ◻ 0.95 only the first term was taken.

α	0	0.2	0.4	0.6
m	2.228	2.086	1.680	1.151
α	0.8	0.9	0.95	1.0
m	0.593	0.300	(0.10025)	0

$\alpha=r_1/r_2$.

m Approximation equation for m

$m^2-6.81\,m+10.264\,(1-\alpha^2)=0$.

NUMBER	DIAGRAM & BOUNDARY CONDITIONS	FORMULA OR TABLE FOR RESULTS	REFERENCES, NOTES
126	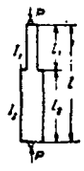 Both ends pinned.	The buckling lengthcoefficient, r, as the basisfor the maximum cross section. $r=\sqrt{\frac{\pi^2 EI_2}{l^2 P_k}}=\frac{\pi}{\alpha_1}, \quad l_k=rl.$ α_1 is which is the root of $\sqrt{\frac{I_1}{I_2}}\tan\left[\frac{1-\sqrt{\frac{l_1}{l}}}{\sqrt{\frac{l_2}{l}}}\alpha_1\right]=-\tan\left[\sqrt{\frac{l_1}{l}}\alpha_1\right]$ の根. r is as in the following table	82 Energy method

I_1/I_2 \ l_2/l	0.5	0.6	0.7	0.8	0.9	1.0	0.5
0.1	2.505	2.169	1.775	1.347	1.039	1.000	2.500
0.2	1.815	1.602	1.360	1.131	1.015	1.000	1.812
0.3	1.520	1.368	1.204	1.069	1.008	1.000	
0.4	1.351	1.240	1.127	1.041	1.005	1.000	1.350
0.5	1.241	1.160	1.082	1.027	1.003	1.000	
0.6	1.163	1.106	1.053	1.017	1.002	1.000	1.163
0.7	1.106	1.067	1.033	1.011	1.001	1.000	
0.8	1.062	1.037	1.019	1.006	1.001	1.000	1.062
0.9	1.028	1.017	1.008	1.003	1.000	1.000	
1.0	1.000	1.000	1.000	1.000	1.000	1.000	1.000

if $P_k=\alpha_2\pi^2\frac{EI_2}{l^2}$ x_2 is the root of

$$\frac{\tan\left[\sqrt{\frac{I_2}{I_1}}\left(1-\frac{l_1}{l}\right)\pi\sqrt{\alpha_2}\right]}{\tan\left[\frac{l_1}{l}\pi\sqrt{\alpha_2}\right]}=-\sqrt{\frac{I_2}{I_1}} \quad \text{etc.}$$

α_2 expressed by the table below

$\sqrt{I_1/I_2}$ \ l_1/l	0.9	0.8	0.7	0.6	0.5	0.4	0.3	0.2	0.1	0
1.0	1.00	1.00	1.00	1.00	1.00	1.00	1.00	1.00	1.00	–
0.95	1.00	1.00	1.00	1.00	1.00	1.00	1.00	0.98	0.78	0
0.90	1.00	1.00	1.00	0.99	0.98	0.97	0.91	0.75	0.24	0
0.85	1.00	0.99	0.98	0.96	0.93	0.86	0.72	0.51	0.12	0
0.80	0.99	0.97	0.95	0.91	0.83	0.72	0.52	0.26	0.07	0
0.75	0.98	0.95	0.90	0.83	0.73	0.57	0.38	0.18	0.05	0
0.70	0.97	0.92	0.85	0.76	0.62	0.46	0.26	0.14	0.04	0
0.65	0.95	0.89	0.79	0.68	0.54	0.33	0.23	0.11	0.03	0
0.60	0.93	0.85	0.74	0.61	0.47	0.32	0.19	0.09	0.02	0
0.55	0.91	0.81	0.69	0.55	0.41	0.28	0.16	0.08	0.02	0
0.50	0.89	0.77	0.64	0.50	0.37	0.25	0.15	0.06	0.02	0

$\sqrt{I_1/I_2}=1.0$ when $\alpha_2=1.000$.

NUMBER	DIAGRAM & BOUNDARY CONDITIONS	FORMULA OR TABLE FOR RESULTS	REFERENCES, NOTES
127	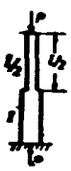 Upper end free. Lower end fixed.	$P_k=4\times(0.7189)^2\frac{EI}{l^2}$.	26
128	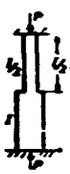 Both ends fixed.	$P_k=4\times(2.5421)^2\frac{EI}{l^2}$.	26
129	Upper end pinned. Lower end fixed.	$P_k=4\times(1.7742)^2\frac{EI}{l^2}$.	26
130	Upper end fixed. Lower end pinned.	$P_k=4\times(1.9341)^2\frac{EI}{l^2}$.	26
131	Upper end free. Lower end fixed	$P_k=4\times(1.5708)^2\frac{EI}{l^2}$.	26
132	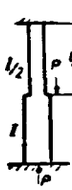 Both ends fixed.	$P_k=4\times(3.8133)^2\frac{EI}{l^2}$.	26

/216

NUMBER	DIAGRAM & BOUNDARY CONDITIONS	FORMULA OR TABLE FOR RESULTS	REFERENCES, NOTES
133	Upper end pinned Lower end fixed.	$P_k=4\times(2.9333)^2\frac{EI}{l^2}$.	26
134	Upper end fixed Lower end pinned	$P_k=4\times(2.5554)^2\frac{EI}{l^2}$.	26
135	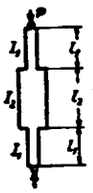 Both ends pinned.	$P_k=\alpha\frac{\pi^2EI_2}{l^2}$.	83

l_1/l \ $\sqrt{I_1/I_2}$	1.0	0.9	0.8	0.7	0.6	0.5	0.4	0.3	0.2	0.1	0
0	1.00	1.00	1.00	1.00	1.00	1.00	1.00	1.00	1.00	1.00	—
0.05	1.00	1.00	1.00	1.00	1.00	1.00	0.99	0.99	0.96	0.71	0
0.10	1.00	1.00	1.00	0.99	0.98	0.96	0.93	0.86	0.66	0.22	0
0.15	1.00	0.99	0.98	0.95	0.92	0.87	0.77	0.62	0.36	0.11	0
0.20	1.00	0.98	0.94	0.90	0.83	0.74	0.60	0.43	0.22	0.07	0
0.25	1.00	0.96	0.90	0 83	0.74	0.61	0.46	0.30	0.15	0.04	0
0.30	1.00	0.93	0.86	0.76	0.6	0.51	0.36	0.22	0.11	0.03	0
0.35	1.00	0.91	0.80	0.68	0.56	0.42	0.29	0.17	0.08	0.02	0
0.40	1.00	0.87	0.75	0.61	0.47	0.35	0.23	0.14	0.06	0.02	0
0.45	1.00	0.84	0.69	0.54	0.41	0.29	0.19	0.11	0.05	0.01	0
0.50	1.00	0.81	0.64	0.49	0.36	0.25	0.16	0.09	0.04	0.01	0

NUMBER	DIAGRAM & BOUNDARY CONDITIONS	FORMULA OR TABLE FOR RESULTS	REFERENCES, NOTES
136	Distribution of compressive force. Cross-section variable. Upper end free, lower end fixed. $p=p_0\left(1-\frac{x}{l}\right)^m$ $I=I_0\left(1-\frac{x}{l}\right)^n$	$P_k=\mu\frac{EI_0}{l^2}$. where $P=\int_0^l pdx$.	84

n \ m	0	1	2	3	4
0	7.84	5.78	3.67	1.0	—
1	16.1	13.0	9.87	6.59	2.25
2	27.3	23.1	18.9	14.7	10.2
3	41.3	36.1	30.9	25.7	20.2
4	—	52.1	45.8	39.5	33.0

/217

NUMBER	DIAGRAM & BOUNDARY CONDITIONS	FORMULA OR TABLE FOR RESULTS	REFERENCES, NOTES
137	Both ends pinned Cross-section variable. $I=I_0\left(1-2\frac{x}{l}\right)$ Distribution of compressive force $P=p_0\frac{l}{2}\left(1-2\frac{x}{l}\right)$ Symmetrical at center point	$\left(p_0\frac{l}{2}\right)_k=23.1\frac{EI_0}{l^2}$.	84 The load P_0 along the line of the axis is applied uniformly in the direction of the center (x = 0). /218
138	Both ends pinned. Cross-section variable. $I=I_0\left(1-4\frac{x^2}{l^2}\right)$ $p=p_0\frac{2x}{l}$ Distribution of compressive force $P=p_0\frac{l}{4}\left(1-4\frac{x^2}{l^2}\right)$ Symmetrical at center point	$P_k=\left(p_0\frac{l}{4}\right)_k=18.5\frac{EI_0}{l^2}$.	The load on the axis having a distribution expressed by $p=p_0\frac{2x}{l}$ is applied in the direction of the center.
139	Member in which there is a rapid change in the load and the cross-section in center. 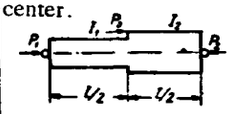 Both ends pinned. $\frac{P_2}{P_1}=k_1^2$, $\frac{I_2}{I_1}=k_2^2$ $P_1+P_0=P_2$	$(P_1)_k=\frac{\pi^2EI_1}{(rl)^2}$, r is buckling length coefficient r is shown in the table below, its apporximation formula is: $r=(0.63+0.13k_1^2)+(0.11+0.13k_1^2)k_2^2$.	85

k_1^2 \ k_2^2	1	1.5	2
0	0.729	0.781	0.832
0.2	0.784	0.855	0.922
0.4	0.840	0.926	1.008
0.6	0.896	0.994	1.088
0.8	0.951	1.064	1.168
1.0	1.000	1.129	1.240

k_1^2 \ k_2^2	1.00	1.25	1.50	1.75	2.00
1.00	1.00	1.06	1.12	1.18	1.24
1.25	0.95	1.01	1.06	1.11	1.16
1.50	0.91	0.97	1.02	1.07	1.12
1.75	0.89	0.94	0.99	1.04	1.08
2.00	0.87	0.92	0.96	1.01	1.05
∞	0.73	0.75	0.77	0.81	0.83

NUMBER	DIAGRAM & BOUNDARY CONDITIONS	FORMULA OR TABLE FOR RESULTS	REFERENCES, NOTES
140	Joined member consisting of members of 2 different materials 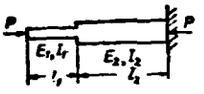 Left end free, right end fixed.	Approximation equation. $P_k=\frac{2}{\pi^2}\left[A+\sqrt{A^2-B}\right]$ Here $A=\frac{l_1^2}{E_1I_1}+\frac{l_2^2}{E_2I_2}+\frac{16\,l_1l_2}{\pi^2E_2I_2}$ $B=4\frac{l_1^2l_2^2}{E_1E_2I_1I_2}$ where $\frac{l_1^2}{E_1I_1}>\frac{l_2^2}{E_2I_2}$	63
141	Member with rapid changes in load and cross-section. 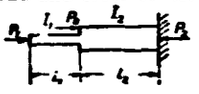 Left end free, right end fixed $P_1+P_0=P_2$	$(P_2)_k=\frac{\mu_0^2}{l_2^2}EI_2$. where μ_0 is first root of $k\tan k\mu\cdot\tan\mu=\frac{l_1}{l_2}\frac{I_2}{I_1}$ here $k=\frac{l_1}{l_2}\sqrt{\frac{P_1}{P_0}\frac{I_2}{I_1}}$.	26
142	Member in which load and cross-section change suddenly 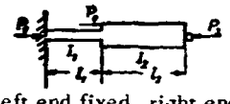 Left end fixed, right end pinned. $P_1+P_0=P_2$	$(P_2)_k=\frac{\mu_0^2}{l_2^2}EI_2$. where μ_0 is the first root of $k\mu\frac{l_2}{l_1}\left(\frac{l}{l_2}-\frac{P_0}{P_2}\right)\left(\tan k\mu\cdot\tan\mu-k\frac{l_2}{l_1}\frac{I_2}{I_1}\right)$ $=2\cdot\frac{P_0}{P_2}\frac{\tan\mu}{\cos k\mu}-\left(1+\frac{P_0^2}{P_1^2}\right)\tan\mu-k\cdot\frac{l_2}{l_1}\frac{I_2}{I_1}\tan k\mu$ Here: $k=\frac{l_1}{l_2}\sqrt{\frac{P_1}{P_2}\frac{I_2}{I_1}}$.	26
143	Member in which load and cross-section change suddenly. 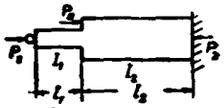 Left end pinned, right end fixed. $P_1+P_0=P_2$	$(P_2)_k=\mu_0\frac{EI_2}{l_2^2}$. Where μ_0 is first root of $\kappa\left(\frac{1}{2}-2\frac{P_0}{P_2}\frac{l_2}{l_1}\right)\left(\tan\mu\cdot\tan\mu-\frac{l_1}{l_2}\frac{I_2}{I_1}\right)$ $=\frac{1}{2}\left(\frac{P_0}{P_2}-\frac{P_2}{P_0}\right)\tan k\mu+\frac{1}{2}\frac{l_2}{l_1}\frac{P_0}{P_2}k\tan\mu$ $+\frac{1}{\cos\mu}\tan\left(k\frac{I_2}{I_1}\right)$ $k=\frac{l_1}{l_2}\sqrt{\frac{P_1}{P_0}\frac{I_2}{I_1}}$.	26
		In $(P_2)_k=m\pi^2\frac{EI_2}{(0.7\,l)^2}$. m is shown by the graph on the following page. Where $\kappa=\frac{P}{P_2}$.	86

/219

NUMBER	DIAGRAM & BOUNDARY CONDITIONS	FORMULA OR TABLE FOR RESULTS	REFERENCES, NOTES
143		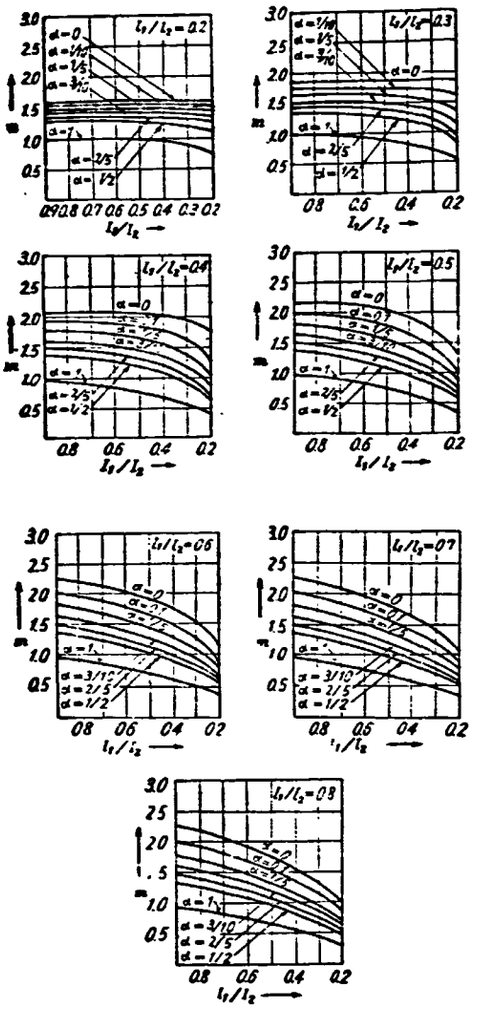	/220
144	Member in which load and cross-section change suddenly. 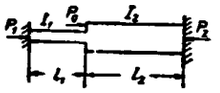 Both ends fixed $P_1+P_0=P_2$	$(P_2)_k=\mu_0^2\frac{EI_2}{l_0^2}$. where μ_0 is first root of $\mu\left(\frac{P_0}{P_1}-\frac{l}{l_0}\right)\left(\tan\mu+\frac{l_1}{l_2}\frac{I_2}{I_1}\tan k\mu\right)$ $+\left(\frac{l_2}{l_1}k+\frac{1}{k}\frac{l_1}{l_2}\right)\tan k\mu\tan\mu$ $=\frac{P_0^2+P_1^2+P_2^2}{2P_1P_2}-\frac{2}{\cos k\mu\cos\mu}-2\frac{I_2}{I_1}\frac{1}{\cos k\mu}$ $+2\frac{P_2}{P_0}\frac{1}{\cos\mu}$	26

NUMBER	DIAGRAM & BOUNDARY CONDITIONS	FORMULA OR TABLE FOR RESULTS	REFERENCES, NOTES
144		here $k=\frac{l_1}{l_2}\sqrt{\frac{P_1}{P_2}\frac{I_2}{I_1}}$.	
		$(P_2)_k=m\pi^2\frac{EI_2}{l^2}$. where $\alpha=P_1/P_2$ m shown in graphs below	87

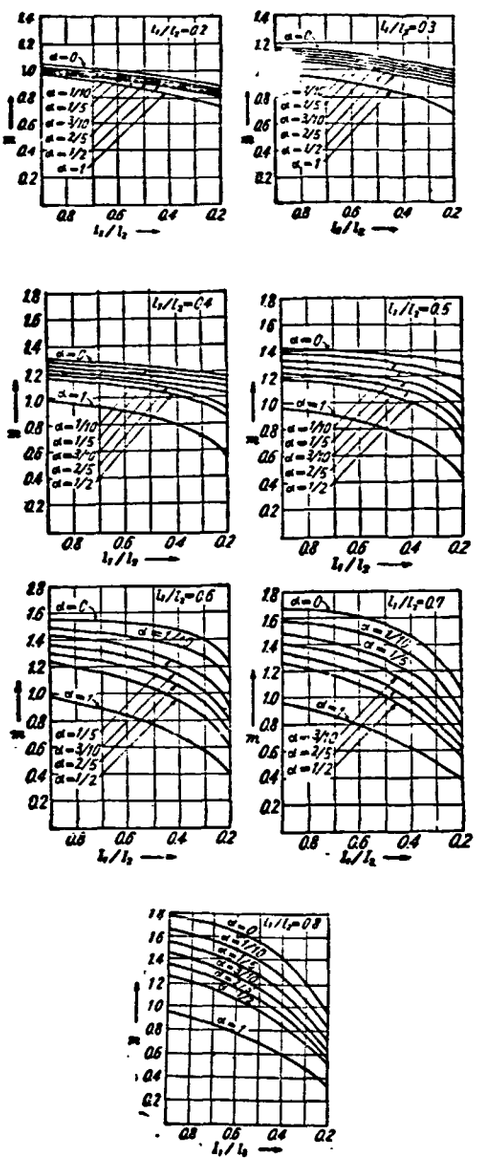

NUMBER	DIAGRAM & BOUNDARY CONDITIONS	FORMULA OR TABLE FOR RESULTS	REFERENCES, NOTES
145	Long spring under compression. 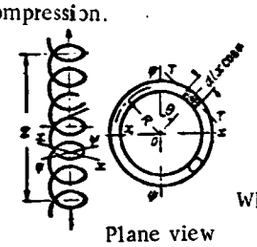 Plane view TT 面 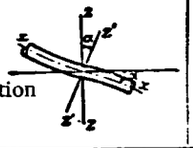 cross-section	Effective geometric moment of inertia $I'=I\cdot\frac{\sin\alpha}{1+\left(\frac{\kappa-1}{2}\right)\cdot\cos^2\alpha}$ $\kappa=\frac{EI}{GI_z}$ When α is small, with respect to a steel needle, $I'=I\frac{2\sin\alpha}{1+\kappa}$, $P=\frac{\sin\alpha}{1.125}I$. With respect to upper end free, lower end fixed. $P_k=\frac{\pi^2EI'}{4z^2}$. Below, in place of l, if l' is used, this is the same as the case of a solid column.	88 /222
146	Spring sustaining compression and torsion. 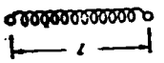 	l_0 = initial spring length, l = compressed spring length, n = number of windings $z=\frac{l}{l_0}$ I_2 = geometric moment of inertia parallel to principle axis I_1 = geometric moment of inertia perpendicular to this I_p = geometric moment of inertia bending stiffness $=\frac{M}{\Delta\varphi}=\varkappa_0 z$, $\Delta\varphi$ =deflection angle shear stiffness $=\frac{Q}{\Delta a}=\beta_0 z$, Δa =lateral displacement compression $=\frac{P}{\Delta b}=\tau_0 z$, Δb =contraction torsion stiffness $=\frac{M}{\Delta\chi}=\delta_0 z$, $\Delta\chi$ =torsion angle per unit length $\frac{1}{\alpha_0}=\frac{n}{l_0}\cdot\frac{\pi R}{EI_1}\left(1+2k\frac{m+1}{m}\cdot\frac{I_1}{I_2}\right)$, $\frac{1}{\beta_0}=\frac{n}{l_0}\cdot\frac{\pi R^2}{EI_2}$. k = cross-section auxiliary number (when circular, 1.000) (when square, 1.182) Buckling condition equation $\frac{\left(\frac{\delta}{\alpha}-\frac{P}{\beta}\right)^2}{\left(1-\frac{P}{\beta}\right)^2}\cdot\frac{W^2}{4\delta^2}+\frac{\frac{P}{\alpha}}{1-\frac{P}{\beta}}=\frac{\pi^2}{l^2}$. When $\beta=\infty$ $\frac{W^2}{4\alpha^2}+\frac{P}{\alpha}=\frac{\pi^2}{l^2}$. Moreover, when P = O $W_1=\frac{2\pi\alpha}{l}=\frac{2\pi\alpha_0}{l_0}$. When W = O $\frac{P}{\alpha\left(1-\frac{P}{\beta}\right)}=\frac{\pi^2}{l^2}$.	

Explanation of Boundary Conditions

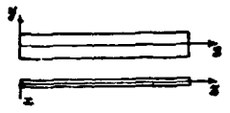

Simple support: Rotation possible around x, y axes at end, rotation impossible around z axis.

Couple: Rotation possible around x axis at ends, rotation around axes y, z impossible.

Fixed: Rotation impossible around axes x, y, z at ends.

NUMBER	DIAGRAM & BOUNDARY CONDITIONS	FORMULA OR TABLE FOR RESULTS	REFERENCE NOTES
147	Rectangular cross-section tie plate sustaining pure bending. Both ends have simple support. M acts on plane yz..	when $B_1=\frac{bh^3}{12}E$ (Bending stiffness around y axis) $C=\frac{b^3h}{3}\left(1-0.630\frac{b}{h}\right)G$ (Torsion stiffness around z axis) $M_k=\frac{\pi\sqrt{B_1C}}{l}$. Where b/h is small, considered not to be related to B_2 (bending stiffness around x axis).	90
148	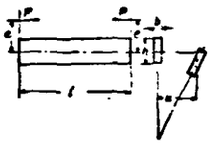 Both ends with simple support. P acts around plane yz.	(1) when e is large $M_k=\frac{\pi\sqrt{B_1C}}{l}\frac{1}{\sqrt{1+\frac{l}{\pi e}\sqrt{\frac{C}{B_1}}}}$. (2) When e is small $P_k=\frac{\pi^2B_1}{l^2}\frac{1}{1+\frac{\pi^2B_1}{l^2}\frac{e^2}{l^2}}$.	90
149	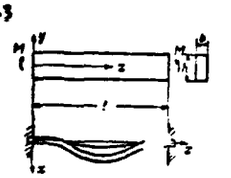 Both ends coupled	$M_k=\frac{2\pi\sqrt{B_1C}}{l}$.	90

NUMBER	DIAGRAM & BOUNDARY CONDITIONS	FORMULA OR TABLE FOR RESULTS	REFERENCES, NOTES
150	Cantilever beam sustaining concentrated load at member ends. 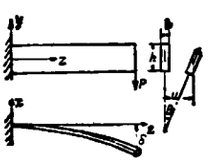 Left end fixed, right end free. P acts along the y axis at the free end.	$B_1=\frac{hb^3}{12}E,\quad C=\frac{hb^3}{3}\left(1-0.630\frac{b}{h}\right)G,$ $P_k=\frac{m\sqrt{B_1C}}{l^2}.$ Here b/h: $<\frac{1}{10}$ | $\frac{1}{10}$ | $\frac{1}{5}$ | $\frac{1}{3}$ m: 4.013 | 4.085 | 4.324 | 5.030 Assuming that a is the distance in the direction of y between the point of application of the load and the center of the cross-section the effect of the point of application is expressed by the following equation: $m=4.013\left(1-\frac{a}{l}\sqrt{\frac{B_1}{C}}\right).$ where y in the figure is positive	90 /224
151	Beam sustaining central concentrated load 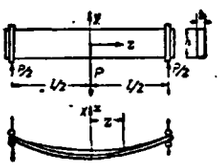 Both ends with simple support. P acts on plane yz.	$B_1=\frac{hb^3}{12}E,\quad C=\frac{hb^3}{3}\left(1-0.630\frac{b}{h}\right)G$ $P_k=\frac{16.93\sqrt{B_1C}}{l^2}.$ a The effect of a is approximately (a is the same as in the previous column (150). $P_k=\frac{16.93\sqrt{B_1C}}{l^2}\left(1-\frac{3.48a}{l}\sqrt{\frac{B_1}{C}}\right).$	90
152	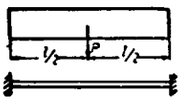 Both ends pinned.	$B_1=\frac{b^3h}{12}E,\quad C=\frac{b^3h}{3}\left(1-0.630\frac{b}{h}\right)G,$ $P_k=\frac{26.6\sqrt{B_1C}}{l^2}.$	90
153	Beam sustaining equally distributed load. 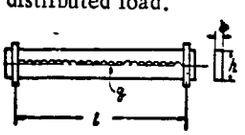 Both ends with simple support.	$B_1=\frac{b^3h}{12}E,\quad C=\frac{b^3h}{3}\left(1-0.630\frac{b}{h}\right)G,$ $(ql)_k=\frac{28.3\sqrt{B_1C}}{l^2}.$	90

NUMBER	DIAGRAM & BOUNDARY CONDITIONS	FORMULA OR TABLE FOR RESULTS	REFERENCES, NOTES
154	Cantilever beam with load in center 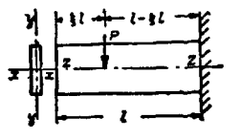 Left end free Right end fixed P acts on the centroid of the cross-section	$P_k=\frac{k\sqrt{B_1C}}{l^2}$. B_1 = bending stiffness around y axis Values of k	94

ξ	0	0.10	0.20	0.30	0.40	0.50	0.60	0.70
k	4.012	4.960	6.275	8.190	11.15	16.05	25.08	44.58

ξ	0.80	0.90	0.93	0.95	0.97	0.99	1.00
k	100.30	401.20	818.78	1604.80	4458.78	40120.11	∞

NUMBER	DIAGRAM & BOUNDARY CONDITIONS	FORMULA OR TABLE FOR RESULTS	REFERENCES, NOTES
155	Beam sustaining concentrated load in middle 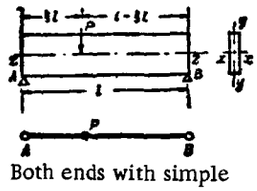 Both ends with simple support P acts on centroid of cross-section	$P_k=k\frac{\sqrt{B_1C}}{l^2}$. Values of k (From Ref 94)	90, 94

ξ	0.01	0.05	0.10	0.20	0.30	0.40	0.50
k	550.51	110.32	55.78	29.10	21.00	17.81	16.94

Values of k (From Ref. 90)

ξ	0.05	0.10	0.15	0.20	0.25	0.30	0.35
k	111.6	56.01	37.88	29.11	24.10	21.01	19.04

ξ	0.40	0.45	0.50
k	17.82	17.15	16.93

NUMBER	DIAGRAM & BOUNDARY CONDITIONS	FORMULA OR TABLE FOR RESULTS	REFERENCES, NOTES
156	 Both ends pinned P acts on centroid of cross-section	$P_k=k\frac{\sqrt{B_1C}}{l^2}$. Values of k	94

ξ	0.01	0.05	0.10	0.20	0.30	0.40	0.50
k	910.81	140.98	74.29	41.72	31.43	27.10	25.89

NUMBER	DIAGRAM & BOUNDARY CONDITIONS	FORMULA OR TABLE FOR RESULTS	REFERENCES, NOTES
157	 Both ends fixed	$P_k=\frac{k\sqrt{B_1C}}{l^2}$. Value of K ϵ: 0.01 | 0.05 | 0.10 | 0.20 | 0.30 | 0.40 | 0.50 k: 29100 | 1295 | 360.4 | 111.5 | 62.1 | 45.13 | 39.65	94
158	1 beam sustaining simple bending 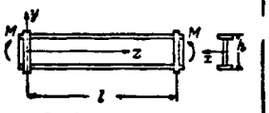 Both ends with simple support b = flange width t = flange average thickness h = height of beam t_1 = web of thickness	B_1 = bending stiffness around y axis which is approximately equal to 2D Where D= bending stiffness around y_1 axis of flange of 1 side $C=G\left(\frac{2}{3}bt^3+\frac{1}{3}ht_1^3\right)$. $M_k=\frac{m\sqrt{B_1C}}{l}$. l^2/a^2: 0.1 | 1.0 | 2.0 | 4.0 | 6.0 | 8.0 | 10 | 12 m: 31.4 | 10.36 | 7.66 | 5.85 | 5.11 | 1.70 | 4.43 | 4.24 l^2/a^2: 16 | 20 | 24 | 28 | 32 | 36 | 40 | 100 m: 4.00 | 3.83 | 3.73 | 3.66 | 3.59 | 3.55 | 3.51 | 3.29 ここに $\frac{l^2}{a^2}=\frac{2C}{D}\frac{l^2}{h^2}$.	90
159	Cantilever 1 beam sustaining contrated load at free end 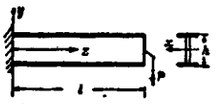 Left end fixed, right end free b = flange width t - flange average thickness h = beam height t_1 = web thickness P acts on centroid of cross-section	$P_k=\frac{m\sqrt{B_1C}}{l^2}$. Here B_1 = bending stiffness around y axis $C=G\left(\frac{2}{3}bt^3+\frac{1}{3}ht_1^3\right)$, $\frac{l^2}{a^2}=\frac{2C}{D}\frac{l^2}{h^2}$, $D\fallingdotseq\frac{1}{2}B_1$. Where D = bending stiffness around y axis of flange of 1 side l^2/a^2: 0.1 | 1 | 2 | 3 | 4 | 6 | 8 | 10 m: 44.3 | 15.7 | 12.2 | 10.7 | 9.76 | 8.69 | 8.03 | 7.58 l^2/a^2: 12 | 14 | 16 | 24 | 32 | 40 | >40 m: 7.20 | 6.96 | 6.73 | 6.19 | 5.87 | 5.64 | $\frac{4.01}{(1-a/l)^2}$ (NOTE) $\sigma_k=\frac{ml}{4a}E\frac{h^2}{l^2}\frac{B_1}{B_2}<$ proportional limit where B_2 = bending stiffness around x axis of beam	90

/226

NUMBER	DIAGRAM & BOUNDARY CONDITIONS	FORMULA OR TABLE FOR RESULTS	REFERENCES, NOTES
160	1 beam sustaining centrally concentrated load. 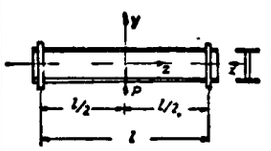 Both ends with simple support. b = flange width t = flange average thickness h = beam height t_1 = web thickness P acts on centroil of cross-section.	B_1 = bending stiffness around $C=G\left(\frac{2}{3}bt^3+\frac{1}{3}ht_1^3\right)$, $\frac{l^2}{a^2}=\frac{2C}{D}\frac{l^2}{h^2}$, $D\fallingdotseq\frac{B_1}{2}$. where, when D = bending stiffness around y axis of flange of 1 side 時 $P_k=\frac{m\sqrt{B_1C}}{l^2}$.	90
161	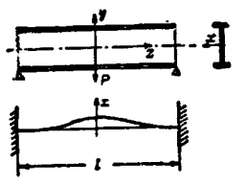 Both ends pinned. P acts on centroid cross-section.	$P_k=m\frac{\sqrt{B_1C}}{l^2}$. Here B_1 = Bending stiffness around y axis. $C=G\left(\frac{2}{3}bt^3+\frac{1}{3}ht_1^3\right)$.	90

l^2/a^2	0.4	4.0	8.0	16.0	24.0	32.0	48.0
m	86.4	31.9	25.6	21.8	20.3	19.6	18.8

l^2/a^2	64.0	80.0	96.0	160	240	320	400
m	18.3	18.1	17.9	17.5	17.4	17.2	17.2

(Note) $\sigma_k=\frac{m}{16}\frac{l}{a}E\frac{h^2}{l^2}\frac{B_1}{B_2}$ <proportional limit

where B_2 = bending stiffness around x axis of beam.

l^2/a^2	0.4	4.0	8	16	24	32
m	26.8	88.8	65.5	50.2	43.6	40.2

l^2/a^2	64	128	200	320
m	34.1	30.7	29.4	28.4

NUMBER	DIAGRAM & BOUNDARY CONDITIONS	FORMULA OR TABLE FOR RESULTS	REFERENCES, NOTES
162	1. Beam sustaining equally distributed load. 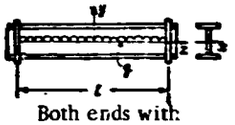 Both ends with simple support. b = flange width t = flange average thickness h = beam height t_1 = web thickness q = equally distributed load acting on plane yz on center line	B_1 = Bending stiffness around y axis $C = G\left(\frac{2}{3}bt^3 + \frac{1}{3}ht_1^3\right)$, $\frac{l^2}{a^2} = \frac{2C}{D}\frac{l^2}{h^2}$, $D \fallingdotseq \frac{B_1}{2}$. where D = bending stiffness around y axis of flange of one side $(ql)_k = \frac{m\sqrt{B_1 C}}{l^2}$.	90 /228

l^2/a^2	0.4	4.0	8.0	16	24	32	48
m	1.43	53.0	42.6	36.3	33.8	32.6	31.5

l^2/a^2	64	80	128	200	280	360	400
m	30.5	30.1	29.4	29.0	28.8	28.6	28.5

(NOTE) $\sigma_k = \frac{m}{32}\frac{l}{a}E\frac{h^2}{l^2}\frac{B_1}{B_2}$ ◁proportional limit

where B_2 = bending stiffness around x axis of beam

NUMBER	DIAGRAM & BOUNDARY CONDITIONS	FORMULA OR TABLE FOR RESULTS	REFERENCES, NOTES
163	Beam sustaining equally distributed load. 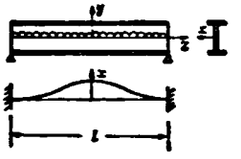 Both ends pinned.	$(ql)_k = \frac{m\sqrt{B_1 C}}{l^2}$. where. B_1 = bending stiffness around y axis. $C = G\left(\frac{2}{3}bt^3 + \frac{1}{3}ht_1^3\right)$, $\frac{l^2}{a^2} = \frac{2C}{D}\frac{l^2}{h^2}$.	90

l^2/a^2	0.4	4	8	16	32	96
m	488	161	119	91.3	73.0	58.0

l^2/a^2	128	200	400
m	55.8	53.5	51.2

NUMBER	DIAGRAM & BOUNDARY CONDITIONS	FORMULA OR TABLE FOR RESULTS	REFERENCES, NOTES
164	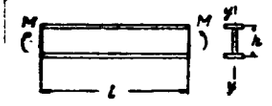 Both ends with simple support. 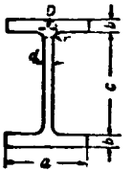 D = maximum radius of inscribed circle h = distance between flange centers	$M_k=\frac{\pi\sqrt{(EI_y)(GI_p)}}{l}\sqrt{1+\pi^2\frac{I_fEh^2}{2I_pGl^2}}$. I_y = geometric moment of inertia of entire cross-section with respect to y axis. I_f = geometric moment of inertia of 1 side flange with respect to y axis. GI_p = tortional strength of the cross-section In the diagram on the left $I_p=2I_{p1}+I_{p2}+2\alpha D^4$. here $I_{p1}=ab^3\left[\frac{1}{3}-0.21\frac{b}{a}\left(1-\frac{b^4}{12a^4}\right)\right]$, $I_{p2}=\frac{1}{3}cd^3$, $\alpha=\frac{t}{t_1}\left(0.15+0.1\frac{r}{b}\right)$, where $b<d$ when $t=b$, $d<b$ when $t=d$. $b<d$ when $t_1=d$, $d<b$ when $t_1=b$.	91
165	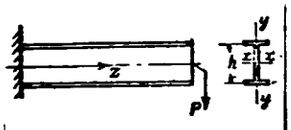 Left end fixed, Right end free. 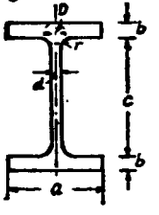 h = distance between flange centers. Load P acts on the center of gravity of the cross-section	$P_k=\frac{m\sqrt{(EI_y)(GI_p)}}{l^2}$ here $m\fallingdotseq 4.01+11.7\sqrt{\frac{I_fEh^2}{2I_pGl^2}}$. I_y = geometric moment of inertia of entire cross-section with respect to y axis. I_f = y geometric moment of inertia of flange of 1 side with respect to y axis. In the diagram to the left. $I_p=2I_{p1}+I_{p2}+2\alpha D^4$. Here $I_{p1}=ab^3\left[\frac{1}{3}-0.21\frac{b}{a}\left(1-\frac{b^4}{12a^4}\right)\right]$, $I_{p2}=\frac{1}{3}cd^3$, $\alpha=\frac{t}{t_1}\left(0.15+0.1\frac{r}{b}\right)$. $b<d$ when $t=b$, $d<b$ when $t=d$. $b<d$ when $t_1=d$, $d<b$ when $t_1=b$.	91
166	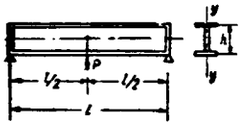 Both ends with free support.	$P_k=\frac{m\sqrt{(EI_y)(GI_p)}}{l^2}$. Here: $m\fallingdotseq 16.93+45\left(\frac{I_fEh^2}{2I_pGl}\right)^{0.8}$. I_y = geometric moment of inertia of entire cross-section with respect to y axis. I_f = geometric moment of inertia of entire cross-section with respect to y axis.	91

/229

NUMBER	DIAGRAM & BOUNDARY CONDITIONS	FORMULA OR TABLE FOR RESULTS	REFERENCES, NOTES
166	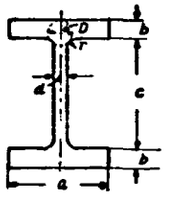	h = distance between flange centers. In the diagram on the left. $I_p=2I_{p1}+I_{p2}+2\alpha D^4$. Here $I_{p1}=ab^3\left[\frac{1}{3}-0.21\frac{b}{a}\left(1-\frac{b^4}{12a^4}\right)\right]$, $I_{p2}=\frac{1}{3}cd^3$, $\alpha=\frac{t}{t_1}\left(0.15+0.1\frac{r}{b}\right)$. $b<d$ when $t=b$, $d<b$ when $t=d$. $b<d$ when $t_1=d$, $d<b$ when $t_1=b$.	/230
167	1 beam in which center is constrained by press. 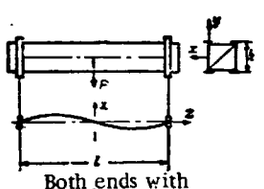 Both ends with simple support. b = flange width t = flange average thickness h = beam height t_1 = web thickness	B_1 = bending stiffness around y axis. $C\fallingdotseq G\left(\frac{2}{3}bt^3+\frac{1}{3}bt_1^3\right)$, $\frac{l^2}{a^2}=\frac{2C}{D}\frac{l^2}{h^2}$, $D\fallingdotseq\frac{B_1}{2}$. D = bending stiffness around y axis. of flange of 1 side, $P_k=\frac{m\sqrt{B_1C}}{l^2}$. l^2/a^2: 0.4 | 4.0 | 8.0 | 16.0 | 32.0 | 96.0 | 128 | 200 | 400 m: 466 | 154 | 114 | 86.4 | 69.2 | 54.5 | 52.4 | 49.8 | 47.4 (NOTE) $\sigma_k=\frac{m}{16}\frac{l}{a}E\frac{h^2}{l^2}\frac{B_1}{B_2}<$ Proportional Limit Where, B_2 = bending stiffness around x axis of beam.	90
168	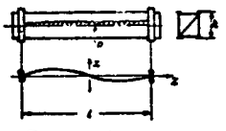 Both ends with simple support. b = flange width t = flange average thickness h = beam height t_1 = web thickness	B_1 = bending stiffness around y axis. $C=G\left(\frac{2}{3}bt^3+\frac{1}{3}bt_1^3\right)$, $\frac{l^2}{a^2}=\frac{2C}{D}\frac{l^2}{h^2}$. D = bending stiffness around y. axis of flange of 1 side. $(pl)_k=\frac{m\sqrt{B_1C}}{l^2}$. l^2/a^2: 0·4 | 4.0 | 8.0 | 16 | 64 | 96 | 128 | 200 m: 673 | 221 | 164 | 126 | 101 | 79.5 | 76.4 | 72.8 (NOTE) $\sigma_k=\frac{m}{32}\frac{l}{a}E\frac{h^2}{l^2}\frac{B_2}{B_1}<$ proportional limit where B_2 = stiffness around x axis of beam.	90

NUMBER	DIAGRAM & BOUNDARY CONDITIONS	FORMULA OR TABLE FOR RESULTS	REFERENCES, NOTES
169	Torsion vibration stability limit (sheet steel girder) of a reinforcing stiffener in the case when the wind force in the horizontal direction of a suspension bridge acts perpendicularly to the bridge axis. 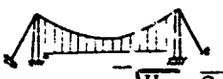	The critical wind velocity is approximately $V_k = \frac{120}{\nu}\frac{\sqrt{EJ \cdot GK}}{\mu C_d \rho b l^3}$ Where EJ = converted deflection stiffness of suspension bridge $= EI + \frac{l^2}{2\pi^2}H$ GK = converted deflection stiffness of suspension bridge $= GK + \pi^2\frac{b^2}{l^2}EJ$ $\mu = +\sqrt{1 + \frac{\sqrt{128\,S}}{4\pi^2 C_e}}$ V_k Critical wind speed C_d = Resistance coefficient b = Distance between 2 cables or width of reinforcing stiffener l = effective span EI = bending stiffness of total cross-section of reinforcing stiffener GK = torsion stiffness of entire cross-section of reinforcing stiffener H = horizontal tensil force of cable due to dead load S = slope of lift curve C_e = Lift coefficient φ = Note of incidence of reinforcing stiffener	95
170	Tie-plate of non-uniform cross-section sustaining simple bending. 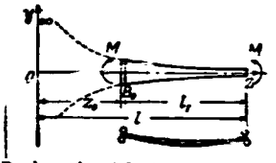 Both ends with simple support. $B = B_0 u^{-n}$ (Bending stiffness around y axis $C = C_0 u^{-n}$, $u = \frac{z}{l}$. Rectangular cross-section. $h >> b$ where h = height of beam b = width of beam	$B = E\frac{b^3 h}{12}$, $C = G\frac{hb^3}{3}$ Rectangular cross-section $(h >> b)$ $M_k = \mu\pi\sqrt{\frac{B_0 C_0}{l_1}}$. Here $\mu = \frac{1+n}{(1+u_0)(1-u_0^{1+n})}$. Where $u_0 = \frac{z_0}{l}$. μ is shown in the table below	92

u_0	n						
	0	1/4	1/3	1/2	1	1.5	3
0	1.000	1.250	1.333	1.500	2.000	2.500	4.000
1/8	1.016	1.191	1.264	1.395	1.802	2.235	3.557
1/4	1.067	1.251	1.261	1.372	1.701	2.055	3.213
3/8	1.164	1.276	1.329	1.416	1.693	1.990	2.967
1/2	1.333	1.438	1.474	1.547	1.779	2.025	2.844

NUMBER	DIAGRAM & BOUNDARY CONDITIONS	FORMULA OR TABLE FOR RESULTS	REFERENCES, NOTES
171	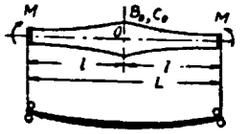 Both ends with simple support $B = B_0(1+bu)^{-n}$, $C = C_0(1+bu)^{-n}$, $u = \frac{z}{l}$. b, n or	$M_k = \mu\pi\frac{\sqrt{B_0 C_0}}{L}$. $\mu = \frac{b(1+n)}{(1+b)^{1+n}-1}$. μ is shown in the table below	92

b	n									
	0	1/4	1/3	1/2	1	1.5	2	3	6	9
0	1.000	1.000	1.000	1.000	1.000	1.000	1.000	4.000	1.000	1.000
0.2	1.000	0.977	0.969	0.954	0.909	0.866	0.824	0.745	0.542	0.385
0.4	1.000	0.956	0.942	0.914	0.833	0.758	0.688	0.563	0.293	0.143
0.6	1.000	0.938	0.918	0.879	0.769	0.670	0.581	0.432	0.163	0.055
0.8	1.000	0.922	0.897	0.848	0.714	0.598	0.497	0.337	0.093	0.022
1.0	1.000	0.907	0.877	0.820	0.667	0.537	0.429	0.267	0.055	0.001

/231

NUMBER	DIAGRAM & BOUNDARY CONDITIONS	FORMULA OR TABLE FOR RESULTS	REFERENCES, NOTES
172	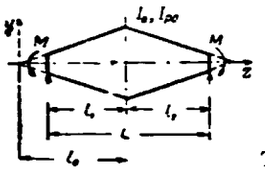 Both ends with simple support $I_y=I_0\left(\frac{z}{l_0}\right)$, $(b<<h)$. $I_{p0}=I_{p0}\left(\frac{z}{l_0}\right)$. $(l_0-l_1)\leqq z\leqq l_0$.	Assuming $M_k=\mu\pi\frac{\sqrt{EI_0GI_{p0}}}{L}$, $\xi=\frac{l_0-l_1}{l_0}$. The value of μ is an shown below: ξ: 0.00 0.01 0.05 0.10 0.20 0.40 0.60 0.80 1.00 μ: 0.000 0.215 0.317 0.391 0.497 0.655 0.789 0.903 1.000	93
173	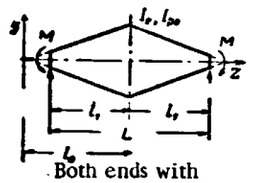 Both ends with simple support. $I_y=I_0\left(\frac{z}{l_0}\right)^2$, $(b<<h)$. $I_{p0}=I_{p0}\left(\frac{z}{l_0}\right)^2$. $(l_0-l_1)\leqq z\leqq l_0$.	Assuming $M_k=\mu\pi\frac{\sqrt{EI_0GI_{p0}}}{L}$, $\xi=\frac{l_0-l_1}{l_0}$. Values of μ shown in the table below ξ: 0.00 0.01 0.05 0.10 0.20 0.40 0.60 0.80 1.00 μ: 0.00 0.01 0.05 0.10 0.20 0.40 0.60 0.80 1.00	93
174	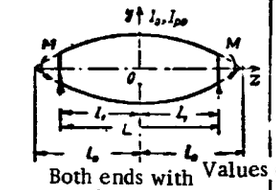 Both ends with simple support $I_y=I_0\left\{1-\left(\frac{z}{l_0}\right)^2\right\}$, $(b<<h)$, $I_{p0}=I_{p0}\left\{1-\left(\frac{z}{l_0}\right)^2\right\}$.	$M_k=\mu\pi\frac{\sqrt{EI_0GI_{p0}}}{L}$, $\mu=\frac{l_1}{l_0}\frac{1}{\tanh^{-1}\frac{l_1}{l_0}}$. Values of μ given below. l_1/l_0: 1.00 0.95 0.90 0.80 0.60 0.40 0.20 0.00 μ: 0 0.510 0.61[illegible] 0.729 0.863 0.943 0.981 1.00	93
175	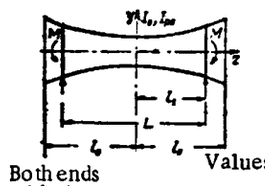 Both ends with simple support $I_y=I_0\left\{1+\left(\frac{z}{l_0}\right)^2\right\}$, $(b<<h)$. $I_{p0}=I_{p0}\left\{1+\left(\frac{z}{l_0}\right)^2\right\}$.	$M_k=\mu\pi\frac{\sqrt{EI_0GI_{p0}}}{L}$, $\mu=\frac{l_1}{l_0}\frac{1}{\tanh^{-1}\frac{l_1}{l_0}}$. Values of μ given below. l_1/l_0: 1.00 0.95 0.90 0.80 0.60 0.40 0.20 0.00 μ: 1.275 1.250 1.225 1.183 1.107 1.044 1.010 1	93

/232

NUMBER	DIAGRAM & BOUNDARY CONDITIONS	FORMULA OR TABLE FOR RESULTS	REFERENCES, NOTES
176	Cantilever beam of non-uniform cross-section sustaining lateral load. 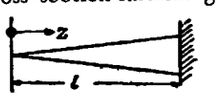 Left end free, right end fixed. b = width, h = height, $b<<h$ $I_y=I_0\frac{z}{l}$, $I_{yo}=I_{yo}\frac{z}{l}$ 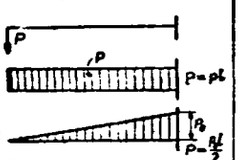 (d) Case when sustaining a concentrated load P at the front end.	$I_y=\frac{1}{12}b^3h$, $I_{yo}=\frac{1}{3}b^3h$, $P_k=\frac{\mu\sqrt{EI_0GI_{yo}}}{l^2}$. (a) $\mu=4.012$, (b) $\mu=12.852$, (c) $\mu=26.52$, (d) $l_k=3.51\sqrt[6]{\frac{EI_0GI_{yo}}{P^2}}$.	93
177	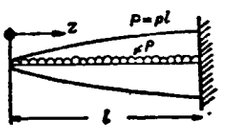 $I_y=I_0\left(\frac{z}{l}\right)^n$ $I_{yo}=I_{yo}\left(\frac{z}{l}\right)^n$	$I_y=\frac{1}{12}b^3h$, $I_{yo}=\frac{1}{3}b^3h$, $P_k=\mu\frac{\sqrt{EI_0GI_{yo}}}{l^2}$. (a) Case when sustaining a dead weight (P = dead weight at fixed ends). (b) When fully loaded with distributed load p (c) When sustaining dead weight (P = dead weight at fixed end). $n=\frac{1}{2}$ when $l_k=2.950\sqrt[6]{\frac{EI_0GI_{yo}}{P^2}}$.	93
	n | 1/4 | 1/3 | 1/2 | 3/4 (a) | 12.05 | — | 11.24 | 10.43 (b) | 3.614 | 3.78 | 3.213 | 2.811		
178	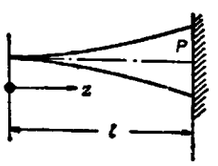 $I_y=I_0\left(\frac{z}{l}\right)^3$ $I_{yo}=I_{yo}\left(\frac{z}{l}\right)^3$ When sustaining dead weight (P = dead weight at fixed end).	$l_k=4.573\sqrt[6]{\frac{EI_0GI_{yo}}{P^2}}$.	93

/233

NUMBER	DIAGRAM & BOUNDARY CONDITIONS	FORMULA OR TABLE FOR RESULTS	REFERENCES, NOTES
			/234
179	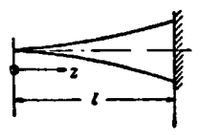 $I_y=I_0\left(\frac{z}{l}\right)^3$, $I_{ps}=I_{ps0}\left(\frac{z}{l}\right)^3$. (a) (b)	$I_y=\frac{b^3h}{12}$, $I_{ps}=\frac{b^3h}{3}$, $P_k=\mu\frac{\sqrt{EI_0GI_{ps0}}}{l^2}$. (a) $\mu=6.284$ (b) $\mu=11.493$	93
180	Symmetrical elliptical plate sustaining centrally concentrated load 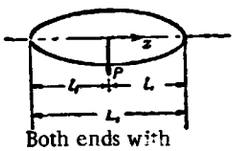 Both ends with simple support. $I_y=I_0\left(\frac{z}{l}\right)^{\frac{3}{2}}$, $I_{ps}=I_{ps0}\left(\frac{z}{l}\right)^{\frac{3}{2}}$. $0\leq z\leq l_1$.	$P_k=\frac{9.522\sqrt{EI_0GI_{ps0}}}{L^2}$.	93

NUMBER	DIAGRAM & BOUNDARY CONDITIONS	FORMULA OR TABLE FOR RESULTS	REFERENCES, NOTES
181		The allowable buckling unit stress is determined from the following equation: $f'=\frac{f}{\beta}$ where $f'=\frac{\sigma_c}{\nu}$: Allowable unit stress of eccentric compression member $f=\frac{\sigma_{c0}}{\nu}$: Allowable buckling unit stress of centrally compressed member. $\beta=\frac{\sigma_{c0}}{\sigma_c}$: Ratio of buckling unit stress of centrally compressive member and eccentrically compressed member. ν : Safety factor σ_c : Buckling unit stress of eccentrically compressed member σ_{c0} : Buckling unit stress of centrally compressed member The values of β are determined from the following equations with respect to each type member Structural steel members a. $\sigma_y=34$ kips/in^2, Slenderness ratio $\frac{l}{i}=20\sim80$, $\beta=\left(1+\frac{\kappa}{2}\right)+\frac{\sqrt{\kappa}}{10,000}\left(\frac{l}{i}\right)^2$ For $\frac{l}{i}=100\sim200$, $\beta=1+\frac{12,200\sqrt[3]{\kappa^2}}{(l/i)^2}$ $80<l/i<100$ integrals β_{80}, β_{100} is lineraly interpolated σ_y: yield point unit stress $\kappa=\frac{e}{s}$: eccentricity b. $\sigma_y=40$ kips/in^2 $\frac{l}{i}=20\sim75$, $\beta=\left(1+\frac{\kappa}{2}\right)+\frac{\sqrt{\kappa}}{9,000}\left(\frac{l}{i}\right)^2$ For $\frac{l}{i}=95\sim200$, $\beta=1+\frac{10,600\sqrt[3]{\kappa^2}}{(l/i)^2}$ $75<l/i<95$ integrals β_{75}, β_{95} are linearly interpolated c. $\sigma_y=50$ kips/in^2 $\frac{l}{i}=20\sim70$, $\beta=\left(1+\frac{\kappa}{2}\right)+\frac{\sqrt{\kappa}}{7,000}\left(\frac{l}{i}\right)^2$ For $\frac{l}{i}=90\sim200$, $\beta=1+\frac{8,400\sqrt[3]{\kappa^2}}{(l/i)^2}$ $70<l/i<90$ integrals β_{70}, β_{90} are linearly interpolated Where Depending on the configuration of the cross-section corrections are made for by multiplying by in the following Configuration of cross-section β 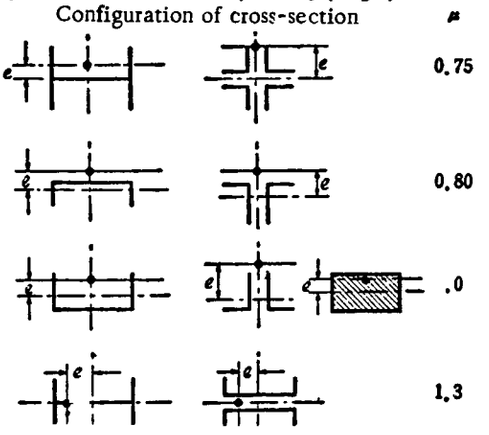 0.75 0.80 .0 1.3	96

/235

NUMBER	DIAGRAM & BOUNDARY CONDITIONS	FORMULA OR TABLE FOR RESULTS	REFERENCES, NOTES

/236

182

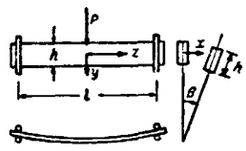

Arbitrary cross-section configuration.

Simple beam, the critical fiber bending unit stress σ_k for the beam flange is expressed by the following equation: 97

なる.

$$\sigma_k = \frac{I_y h^2}{I_z a^2} \cdot E \cdot \frac{a^2}{l^2} \cdot K$$

I_z, I_y: geometric moment of inertia with respect to the x, y axes

h: beam height

a: Coefficient expressing the bending and torsion stiffness of the beam

K: Constant determined by the conditions of action of the load

Simple beam (K table) (a) Simple beam

l/h	Centrally Concentrated Load			Equally distributed load		
	Top	Center	Bottom	Top	Center	Bottom
2	2.525	3.982	6.272	2.269	3.310	4.824
3	3.127	4.649	6.885	2.788	3.860	5.341
4	3.863	5.440	7.632	3.418	4.518	5.969
5	4.687	6.310	8.469	4.121	5.244	6.669
6	5.568	7.232	9.365	4.972	6.013	7.417
7	6.490	8.187	10.30	5.655	6.810	8.197
8	7.439	9.164	11.26	6.459	7.626	8.999
9	8.409	10.16	12.24	7.280	8.456	9.817
10	9.393	11.16	13.24	8.113	9.296	10.60
11	10.39	12.18	14.24	8.954	10.14	11.49
12	11.39	13.20	15.26	9.802	11.00	12.33
13	12.41	14.22	16.28	10.65	11.85	13.18
14	13.43	15.25	17.30	11.51	12.72	14.04

183

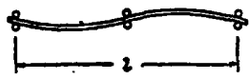

(b) Beam with Lateral Direction Constrained in Center. 97

l/h	Concentrated load	Equally distributed load		
		Top	Center	Bottom
2	5.411	3.499	3.917	4.381
3	6.287	4.142	4.560	5.018
4	7.301	4.911	5.329	5.780
5	8.476	5.[illegible]7	6.174	6.620
6	9.696	6.[illegible]1	7.069	7.589
7	10.94	7.579	7.995	8.432
8	12.22	8.[illegible]9	8.944	9.378
9	13.52	9.494	9.909	10.34
10	14.84	10.47	10.89	11.31
11	16.17	11.46	11.87	12.30
12	17.51	12.45	12.86	13.29
13	18.86	13.45	13.86	14.29
14	20.21	14.45	14.86	15.29

NUMBER	DIAGRAM & BOUNDARY CONDITIONS	FORMULA OR TABLE FOR RESULTS	REFERENCES NOTES

184

Practical System for Calculating Buckling Unit Stress of Simple Beams

(a) Equally Distributed Load (l_b/in^2)

Load Point	Type of Steel	Short Beam	Length, Short Critical Point		Long Beam
Top	C Stl	$33,000-0.0125\,\lambda^2$	800	25,000	$\frac{20,000,000}{\lambda}$
	Si Stl	$45,000-0.0321\,\lambda^2$	600	33,333	
	Ni Stl	$55,000-0.06\,\lambda^2$	500	40,000	
Center	C Stl	$33,000-0.00865\,\lambda^2$	960	25,000	$\frac{24,000,000}{\lambda}$
	Si Stl	$45,000-0.02251\,\lambda^2$	720	33,333	
	Ni Stl	$55,000-0.04167\,\lambda^2$	600	40,000	
Bottom	C Stl	$33,000-0.00656\,\lambda^2$	1,080	25,000	$\frac{27,000,000}{\lambda}$
	Si Stl	$45,000-0.01778\,\lambda^2$	810	33,333	
	Ni Stl	$55,000-0.03292\,\lambda^2$	675	40,000	

b) Centrally Concentrated Load

Load Point	Type of Steel	Short Beam	Long & Short Critical Points λ	σ_{cr}	Long Beams
Top	C Stl	$33,000-0.00945\,\lambda^2$	920	25,000	$\frac{23,000,000}{\lambda}$
	Si Stl	$45,000-0.0245\,\lambda^2$	690	33,333	
	Ni Stl	$55,000-0.04537\,\lambda^2$	575	40,000	
Center	C Stl	$33,000-0.00633\,\lambda^2$	1,120	25,000	$\frac{28,000,000}{\lambda}$
	Si Stl	$45,000-0.01653\,\lambda^2$	840	33,333	
	Ni Stl	$55,000-0.03061\,\lambda^2$	700	40,000	
Bottom	C Stl	$33,000-0.00433\,\lambda^2$	1,360	250000	$\frac{34,000,000}{\lambda}$
	Si Stl	$45,000-0.01121\,\lambda^2$	1,020	33,333	
	Ni Stl	$55,000-0.02076\,\lambda^2$	850	40,000	

l : span length $\quad \lambda : = \left(\frac{l}{b}\frac{h}{t}\right)$

h : beam height $\quad b$: flange width

t : flange thickness

/237

185

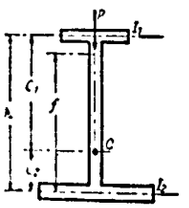

$I = I_1 + I_2$

Lateral buckling of 1 beam

○ Centrally concentrated load

Cross-section with 1 axis symmetrical

$$P_k = \frac{48\pi^2 E}{L^2(6+\pi^2)}\left[(hI_1 - fI) + \sqrt{(hI_1 - fI)^2 + \frac{6+\pi^2}{48}h^2 I_1 I_2 \pi^2}\right]$$

Case in which the tension side is constrained

$$P_k = EI\frac{\pi^2}{2L^2}h^2\frac{I_2\pi}{fI + \frac{hI_1}{2}\left(\frac{\pi^2}{4}-1\right)}$$

Cross-section with two axes symmetrical

$$P_k = EhI_0\frac{\pi^2}{L^2}\sqrt{\frac{48}{6+\pi^2}} \qquad I_0 = I_1 = I_2$$

Case in which the tension side is constrained

$$P_k = EI\frac{\pi^2}{L^2}h\frac{2\pi}{\frac{\pi^2}{4}+1}$$

○ Pure bending cross-section with one axis symmetrical

$$M_k = Eh\frac{\pi^2}{2L^2}\left[I_1 - I_2 + \sqrt{I^2 + 4CI\frac{L^2}{\pi^2 h^2}}\right]$$

C : Torsion stiffness

Case in which tension side is constrained

$$M_k = Eh\left(I_1\frac{\pi^2}{L^2} + \frac{C}{h^2}\right)$$

Cross-section with two symmetrical axes

$$M_k = E\frac{\pi^2}{L^2}\sqrt{I_0^2 h^2 + 2CI_0\frac{L^2}{\pi^2}}$$

38

NUMBER	DIAGRAM & BOUNDARY CONDITIONS	FORMULA OR TABLE FOR RESULTS	REFERENCES, NOTES
186	Cross-section configuration	St. Venant's torsion resistance J_T	99 96
	1. 円	$J_T=\frac{1}{2}\pi r^4$	
	2. Ellipse 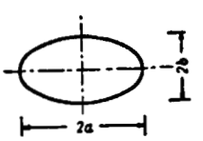	$J_T=\frac{\pi^3 a^3 b^3}{a^2+b^2}$	
	3. Square 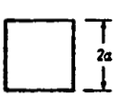	$J_T=2.250\,a^4$	
	4. Rectangle 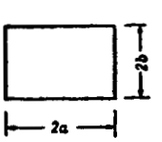	$J_T=ab^3\left[\frac{16}{3}-3.36\frac{b}{a}\left(1-\frac{b^4}{12a^4}\right)\right]$	
	5. Equilateral Triangle	$J_T=\frac{\sqrt{3}}{80}a^4$	
	6. Hollow Circle	$J_T=\frac{1}{2}\pi(r_0^4-r_i^4)$	
	7. Hollow Ellipse 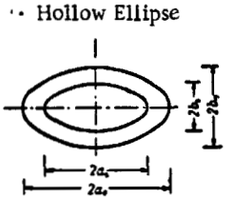	$J_T=\frac{\pi a_0^3 b_0^3}{a_0^2+b_0^2}(1-m^4)$ $m=\frac{a_i}{a_0}=\frac{b_i}{b_0}$	

/238

NUMBER	DIAGRAM & BOUNDARY CONDITIONS	FORMULA OR TABLE FOR RESULTS	REFERENCES, NOTES
8.	Closed cross-section of arbitrary thickness.	$J_T = 4A^2 \Big/ \oint \frac{ds}{t}$ When t is constant $J_T = 4A^2 \Big/ \frac{s}{t}$ A: Area described by centerline of wall s: Length of centerline of wall surface	/239
9.	Bulb angle cross-section 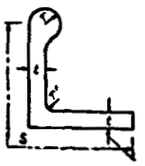	$J_T = \frac{1}{3} s t^3 \left\{ 1 + \frac{4.14 + 4.71 (r/t)^4}{s/t} \right\}$ r: Bulb radius. S: Length of expansion of centerline as far as center of bulb	
10.	I Cross-section 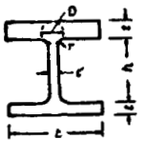	$J_T = 2 J_{T_1} + J_{T_2} + 2 \alpha D^4$ $J_{T_1} = \frac{1}{3} b t^3 \left[1 - 0.63 \frac{t}{b} \left(1 - \frac{t^4}{12 b^4} \right) \right]$ $J_{T_2} = \frac{1}{3} h t'^3$ $\alpha = \frac{t_1}{t_2} \left(0.15 + 0.1 \frac{r}{t} \right)$ Here $t < t'$ If $t_1 = t$, $t_2 = t'$ $t > t'$ $t_1 = t'$, $t_2 = t$	
11.	T Cross-Section 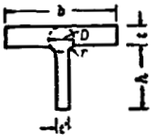	$J_T = J_{T_1} + J_{T_2} + \alpha D^4$ $J_{T_1} = \frac{1}{3} b t^3 \left[1 - 0.63 \frac{t}{b} \left(1 - \frac{t^4}{12 b^4} \right) \right]$ $J_{T_2} = \frac{1}{3} h t'^3 \left[1 - 0.315 \frac{t'}{h} \left(1 - \frac{t'^4}{192 h^4} \right) \right]$ $\alpha = \frac{t_1}{t_2} \left(0.15 + 0.10 \frac{r}{t} \right)$ t_1, t_2 same as 10	
12.	Angle 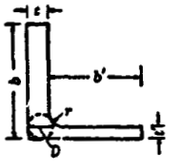	$J_T = J_{T_1} + J_{T_2} + \alpha D^4$ $J_{T_1} = \frac{1}{3} b t^3 \left[1 - 0.63 \frac{t}{b} \left(1 - \frac{t^4}{12 b^4} \right) \right]$ $J_{T_2} = \frac{1}{3} b' t'^3 \left[1 - 0.315 \frac{t'}{b'} \left(1 - \frac{t'^4}{192 b'^4} \right) \right]$ $\alpha = \frac{t}{t'} \left(0.07 + 0.076 \frac{r}{t} \right)$	
13.	[, Z cross-section 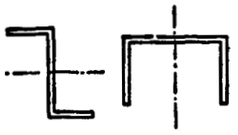	12 T Same as 12, total of J_T of all elements	

NUMBER	DIAGRAM & BOUNDARY CONDITIONS	FORMULA OR TABLE FOR RESULTS	REFERENCES, NOTES
187		Bending Torsion Resistance C_{BT} $C_{BT}=C_{BTu}+C_{BTn}$ C_{BTu}: Direct strain and torsion resistance of wall surface due to changes in the warp of the cross-section C_{BTn}: Direct strain bending and torsion resistance in direction of thickness caused by changes in the curvature of the wall surface.	/240
1 Shape s: Shear center o: Center of gravity 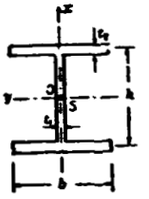		$C_{BTu}=\frac{1}{24}t_1h^2b^3$ (For o,s)	
2. Z shape 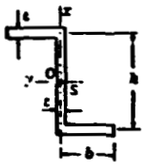		$C_{BTu}=\frac{tb^3h^2}{12}\cdot\frac{2+\rho}{1+2\rho}$ (For o,s) $\rho=\frac{b}{h}$	
3. Bulb attached Z shape 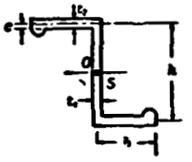		$C_{BTu}=\frac{t_1b^3h^2}{12}\left\{\frac{\rho(2+\rho)+2\beta(3+2\rho)+24\varepsilon\beta\{(1+\rho)+\varepsilon(1+2\rho)\}}{1+2\rho+3\beta}\right\}$ (For o,s) $\rho=\frac{bt_2}{ht_1}$ $\beta=\frac{A}{ht_1}$, $\varepsilon=\frac{e}{h}$ A: Bulb cross-section area	
4. Lip Z shape 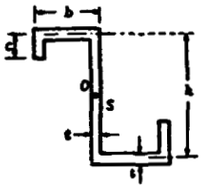		$C_{BTu}=\frac{tb^3h^2}{12}\left\{\frac{\rho(2+\rho)+2\varepsilon(3+2\rho+6\varepsilon(1+\rho)+4\varepsilon^2(1+2\rho)+2\varepsilon^3}{1+2\rho+2\varepsilon}\right\}$ (For o,s) $\rho=\frac{b}{h}$, $\varepsilon=\frac{c}{h}$	
5. Angles with equal sides 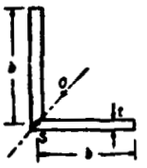		$C_{BTu}=\frac{A^2}{144}$ (For o,s) A: Total cross-section area	

NUMBERS	DIAGRAM & BOUNDARY CONDITIONS	FORMULA OR TABLE FOR RESULTS	REFERENCES, NOTES
187	6. Angle with unequal sides 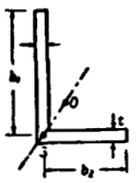	$C_{BT_s}=\frac{t^3}{36}(b_1^2+b_2^2)$ (For s)	/241
	7. Lip angle 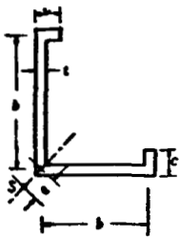	$C_{BT_s}=\frac{tb^2c^2}{6}\cdot\frac{4+3\epsilon}{1+3\epsilon-3\epsilon^2+\epsilon^3}$ (For heel) $\epsilon=\frac{c}{b}$ $\epsilon=\frac{b}{\sqrt{2}}\cdot\frac{3-2\epsilon}{1+3\epsilon-3\epsilon^2+\epsilon^3}$	
	8. Angle with bulb 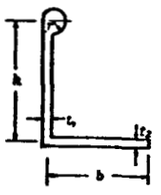	$C_{BT_s}=\frac{t_1^3h^3}{18}\left\{\frac{1}{2}\left[1+\left(\frac{t_2b}{t_1h}\right)^3\right]+4.5\,\pi\frac{(r/t)^4}{(h/t_1)}\right\}$ (For s)	
	9. $\bar{T}$ shape 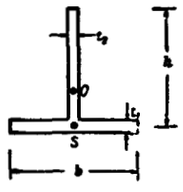	$C_{BT_s}=\frac{t_1^3b^3}{144}+\frac{t_2^3h^3}{36}$ (For s)	
	10. I Shape with one axis symmetrical 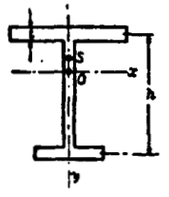	$C_{BT_s}=\frac{h^2I_1I_2}{I_1+I_2}$ I_1, I_2, geometric moment of inertia of upper and lower flanges with respect to the y axes.	

NUMBERS	DIAGRAM & BOUNDARY CONDITIONS	FORMULA OR TABLE FOR RESULTS	REFERENCES, NOTES

/242

187

11.

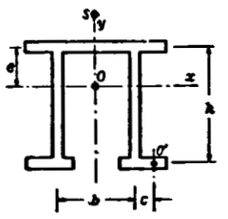

t = constant

O': flange center of gravity

$$C_{BT_0}=\frac{b^4}{4}\left\{I_z+e^2A\left(1-\frac{b^2A}{4I_y}\right)+2h^2I_F-2bch^2A_F+b^2heA\frac{I_F}{I_y}-4h^2\frac{I_F^2}{I_y}\right.$$

A: Total cross-section area

l_x, l_y: Geometric moment of inertia with respect to x, y axe

A_F: Cross-section area of lower flange

l_F: Geometric moment of inertia of lower flange with respect to web axis

C: Distance from center of flange from to web axis

12. ⊏ Cross-section

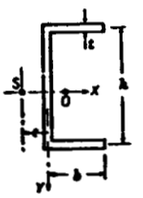

$$C_{BT_0}=\frac{th^2b^3}{12}\cdot\frac{2+3\rho}{1+6\rho}\quad\text{(For s)}$$

$$\rho=\frac{b}{h},\qquad e=b\frac{3\rho}{1+6\rho}$$

13. Lip ⊏, ⊑

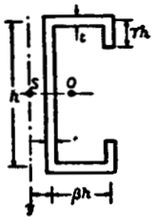

$$C_{BT_0}=A_c\cdot t\cdot h^3+C_c\cdot t^3\cdot h^3\quad\text{(For s)}$$ 101

Here,

$$A_c=\frac{\beta^3}{6}-\beta^2\left(\frac{\tau}{2}\mp\tau^2+\frac{2}{3}\tau^3\right)-t'\left\{\frac{\beta^2}{2}+\beta\left(\tau-\frac{4}{3}\tau^2\right)\right\}+t'^2\left(\frac{1}{12}+\frac{\beta}{2}+\frac{\tau}{2}\mp\tau^2+\frac{2}{3}\tau^3\right)$$

$$C_c=\frac{1}{6}\left(\frac{1}{24}+\frac{\beta^3}{3}+\frac{\tau}{4}\mp\frac{\tau^2}{2}+\frac{\tau^3}{3}+t'\beta^2+t'^2\beta\right)$$

$$t'=\left\{\frac{\beta^2}{8}+\beta\left(\frac{\tau}{4}-\frac{\tau^2}{3}\right)\right\}\Big/\left(\frac{1}{24}+\frac{\beta}{4}+\frac{\tau}{4}\mp\frac{\tau^2}{2}+\frac{\tau^3}{3}\right)$$

14.

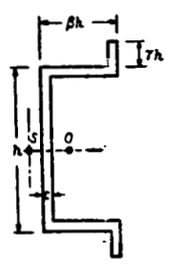

The ± in the above equation employs (-) with respect to form ⊏ and + for ⊑.

188

Thin-walled open tube

Position of shear center

99

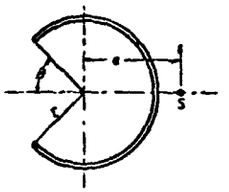

$$e=\frac{2a}{(\pi-\theta)+\sin\theta\cos\theta}[(\pi-\theta)\cos\theta+\sin\theta]$$

$\theta=0$ When $e=2a$

2. Semi-circle

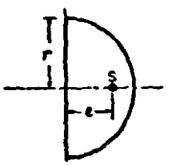

$$e=\left(\frac{8}{15\pi}\frac{3+4\nu}{1+\nu}\right)r$$

ν : Poisson ratio

3. Channel

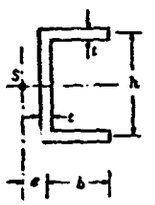

$$e=h\frac{I_{xy}}{I_y}$$

I_{xy} : Product of inertia of area

When t is uniform and small

$$e=\frac{h^2b^2t}{4I_y}=b\frac{3\left(\frac{b}{h}\right)}{1+6\left(\frac{b}{h}\right)}$$

4. Non-symmetric I shape

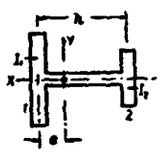

$$e=h\left(\frac{I'}{I_1+I_2}\right)$$

I_1, I_2 are the respective geometric moments of inertia of the flanges with respect to the x axis.

5. Beam having a common neutral axis, consisting of n elements.

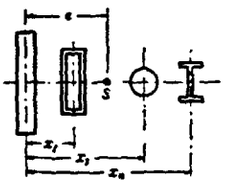

$$e=\frac{\sum_{r=1}^{n}E_rI_rx_r}{\sum_{r=1}^{n}E_rI_r}$$

I_r is the geometric moment of inertia around the neutral axis of the rth element.

188

6. Rectangular tube with effective wall surfaces only for the shear in 4 columns, each of which is symmetrical.

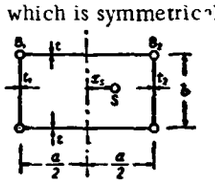

$$\frac{z_S}{a}=\frac{B_2-B_1}{2(B_2+B_1)}-\frac{2b\left(\frac{B_2}{t_2}-\frac{B_1}{t_1}\right)}{(B_2+B_1)\left(\frac{b}{t_1}+\frac{b}{t_2}+\frac{2a}{t}\right)}$$

$B_{1,2}$: Cross-section area of corner columns 1, 2.

7. Angle with unequal sides

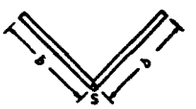

s is point of intersection of the centerlines of both sides.

8. Angle with unequal sides

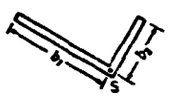

s is point of intersection of the centerline of both sides

9. I shape

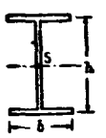

Matches centroid

10. T shape

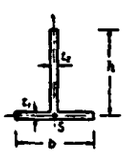

Point of intersection of centerlines of web and flange

11.

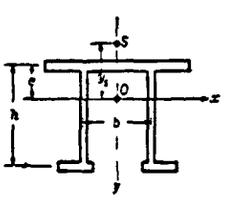

$$y_s=-e\left(1+\frac{b^2A}{4I_y}\right)+2h\frac{I_F}{I_y}$$

A: Total cross-section area

I_F: Geometric moment of inertia around web axis of lower flange

I_y: Geometric moment of inertia around axis

188

12. Cross-section

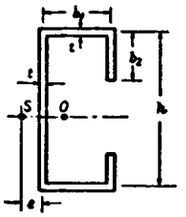

$$e = b_1 \frac{\left\{1+\frac{1}{2}b_1/b_2-\frac{4}{3}(b_1/h)^2\right\}}{\left\{1+b_1/b_2+\frac{1}{6}h/b_2-2(b_2/h)\left(1-\frac{2}{3}b_2/h\right)\right\}}$$

Position of shear centers of each cross-section dimension

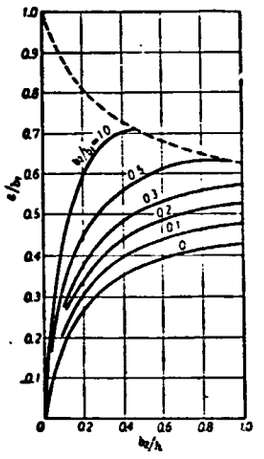

13. ⊐ Cross-section

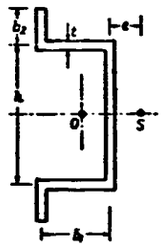

$$e = d_1 \frac{\left\{1+\frac{1}{2}b_1/b_2-\frac{4}{3}(b_1/h)^2\right\}}{\left\{1+b_1/b_2+\frac{1}{b}h/b_2+2(b_2/h)\left(1+\frac{2}{3}b_2/h\right)\right\}}$$

Position of shear of each type of cross-section dimension

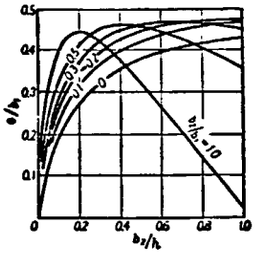

14. having concentrated members

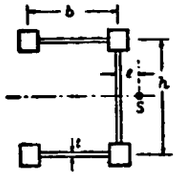

$$e = \frac{b(1+2n)}{\left\{2+\frac{1}{3}(h/b+4n)\right\}}$$

n: Variable relating to the cross-section area of the concentrated members

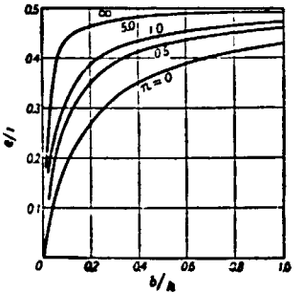

100

189

Wagner's theoretical equation taking member end conditions into consideration.

$$\sigma_w=\frac{P_w}{A}=\frac{k_d}{I_{SP}}\left(GJ_T+k_m\frac{\pi^2E}{L^2}C_{BT}\right)$$

GJ_T: St. Venant's torsion stiffness

EC_{BT}: Bending torsion stiffness

L: Member length

k_d, k_m: Coefficient determined by

1). Pin end $\varphi=0$, $\varphi''=0$ member end conditions

φ: Torsion angle of cross section

$k_d=1$, $k_m=1$

Corresponds to Wagner's theoretical equation

2) Fixed end $\varphi=0$, $\varphi'=0$

$k_d=1$

$k_m=4$

3) Spherical end

$$\varphi'=0,\ EC_{BT}\varphi'''+(P_{i_SP}{}^2-GJ_T)\varphi'-Pr_0{}^2\varphi'\frac{2}{L}=0$$

r_0: Distance between shear center and centroid

Strictly, denoting

$$T_0=\frac{L^2}{4}\frac{r_0{}^2}{i_{SP}{}^2}\frac{GJ_T}{EC_{BT}}$$

$$T_1=\frac{r_0{}^2}{i_{SP}{}^2}$$

From the following chart, the value of m^2 with respect to $\frac{T_0}{T_1}$.

$k_d = 1$, $k_m = \frac{4m^2}{\pi^2}$ is determined

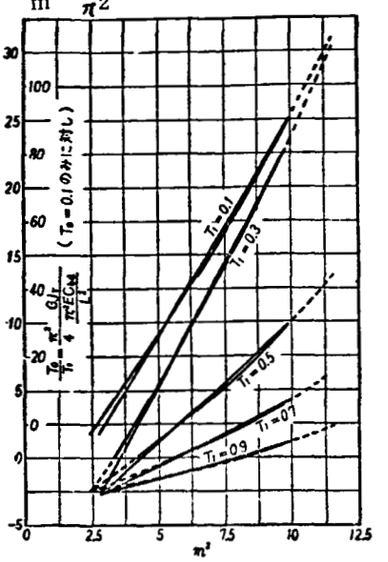

101

189

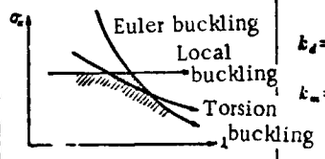

Approximately

$k_d = \frac{1}{1-0.72T_1}$ (See the following table)

$k_m = 1.12$

T_1	0.1	0.3	0.5	0.7	0.9	1
k_d	1.076	1.275	1.562	2.015	2.84	3.37

where

if $m > \pi$ $\quad kd = 1$

$k_m = 4$

190

Conditions under which torsion buckling actually occurs

Torsion buckling load is flexural buckling (Euler's buckling): actually occurs as long as it is smaller than the local buckling load. 101

Condition equation $K_m > \frac{6(1-\nu)d_0}{\frac{1}{kd} - \frac{k_m d_0}{b_0}}$

K_m: Local buckling coefficient

k_m, kd: Coefficient determined by member end conditions (re: Ref. 189).

$b_0 = \left(\frac{i}{b}\right)^2$;

i Geometric radius of gyration of cross-section

b: Plate width of basic wall surface of cross-section in which local buckling occurs.

d_0, d_a, r_1, d_1: Coefficients determined by cross-section configuration when determining J_T, C_{BT}

Member length $l = \left(\frac{b}{L}\right)^2$ Assuming condition equation

$$l_{min} = \frac{d_0}{\frac{2\pi^2(1+\nu)}{\frac{b_0}{kd} - k_m d_a}} \left(\frac{t}{b}\right)^2$$

$$l_{max} = \frac{K_m}{\frac{12(1-\nu^2)k_d}{\pi^2 k d_a} - \frac{d_0}{2(1+\nu)}} \left(\frac{t}{b}\right)^2$$

L: Member length

190

C, C Values of K_m of Cross-section

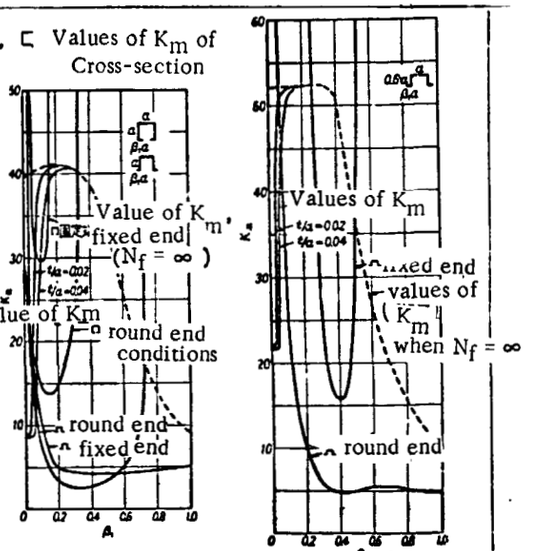

Condition equation when the lip width of the cross-section is adequately large.

Within proportional limits $K_1 > \dfrac{\frac{a_0}{2(1+\nu)}\left(\frac{t}{b}\right)}{\frac{1}{kd} - \frac{k_m d_e}{b_0}}$

Outside of proportional limit $K_m > \dfrac{6(1-\nu)d_e}{\frac{1}{k_d} - \frac{k_m d_e}{b_e}}$

$K_1 = \sqrt{\dfrac{K_m}{12(1-\nu^2)}\dfrac{\sigma_p}{E}}$ Local buckling coefficient

σ_p: Proportional limit unit stress

Condition equation for member length l_{min} same as in above equation

$$l_{max} = \frac{\frac{1+\nu_s(t/b)^3}{kd} \cdot K_1\left(\frac{t}{b}\right) - \frac{d_s}{2(1+\nu)}\left(\frac{t}{b}\right)^3}{k_m \pi^2 \left\{d_e + d_s\left(\frac{t}{b}\right)^2\right\}}$$

C, C Values of k_1 for cross-section

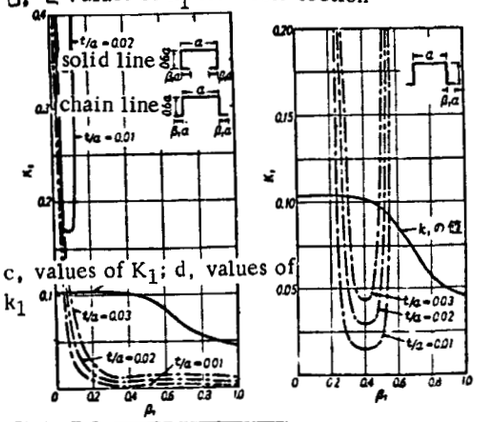

191

General formula for compound buckling considering bending and torsion — 102

a) Center compressed load

1) Cross-section with 2 symmetrical axes and symmetrical points

Wagner's equation $P_w=\frac{1}{i_{SP}^2}\left(GJ_T+\frac{\pi^2 EC_{BT}}{L^2}\right)$

2) Cross-section with 1 symmetrical axis

Case where x axis is symmetrical. When the y axis is symmetrical, Y is reread as X

$$\frac{1}{P_k}=\frac{1}{2}\left\{\frac{1}{P_{eY}}+\frac{1}{P_w}\pm\sqrt{\left(\frac{1}{P_{eY}}-\frac{1}{P_w}\right)^2+\frac{4}{P_{eY}P_w}\cdot\frac{x_0^2}{i_{SP}^2}}\right\}$$

P_{eY}: Euler's buckling value which is displaced in the direction of the x axis

P_w: Wagner's buckling value

x_0, y_0: Coordinates of center of gravity with respect to shear center

3) Arbitrary cross-section

Minimum value determined from the following three equations for P_k

$$\left(1-\frac{P_{eX}}{P_K}\right)\left(1-\frac{P_{eY}}{P_K}\right)\left(1-\frac{P_w}{P_K}\right)-\left(1-\frac{P_{eX}}{P_K}\right)\frac{x_0^2}{i_{SP}^2}-\left(1-\frac{P_{eY}}{P_K}\right)\frac{y_0^2}{i_{SP}^2}=0$$

b) When pure bending moment is acting

1) Cross-section with 2 symmetrical axes or point symmetry

$M_Y=0$ when

$$M_X=\pm\sqrt{P_{eX}\cdot P_w\cdot i_{SP}^2}$$

where

M_X, M_Y: Bending moments around X, Y axes

2) Cross-section with 1 symmetrical axis (X axis symmetrical)

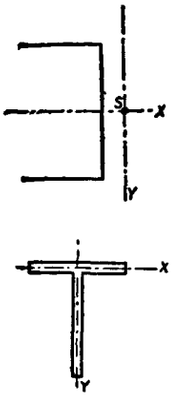

Case of ⊏ configuration $M_y = 0$

$$M_X=\pm\sqrt{P_{eX}\cdot P_w\cdot i_{SP}^2}$$

Case of T configuration $M_y = 0$

$$M_X=\frac{1}{2}\left\{P_{eX}\frac{k_X}{I_X}\pm\sqrt{P_{eX}^2\frac{k_X^2}{I_X^2}+4P_{eX}\cdot P_w\cdot i_{SP}^2}\right\}$$

$$k_X=\int y(x^2+y^2)dA-y_0 A i_{SP}^2$$

y_0: Distance from shear center to centroid in direction Y

A: Cross-section area

c) Case in which an eccentric compressive load is sustained.

Minimum value of P_K determined from following equation

$$i_{SP}^2\left(1-\frac{P_{eX}}{P_K}\right)\left(1-\frac{P_{eY}}{P_K}\right)\left(1-\frac{P_w}{P_K}\right)+\left(1-\frac{P_{eX}}{P_K}\right)\left(1-\frac{P_{eY}}{P_K}\right)\left(\frac{e_X k_Y}{I_Y}+\frac{e_Y k_X}{I_X}\right)-\left(1-\frac{P_{eY}}{P_K}\right)(e_X+x_0)^2-\left(1-\frac{P_{eY}}{P_K}\right)(e_Y+y_0)^2=0$$

e_X, e_Y: Eccentricity in direction, X, Y

191

1) Cross-section with two symmetrical axes, where $e_X = 0$

$$\frac{1}{P_K}=\frac{1}{2}\left\{\frac{1}{P_{eX}}+\frac{1}{P_w}\pm\sqrt{\left(\frac{1}{P_{eX}}-\frac{1}{P_w}\right)^2+\frac{4e_Y^2}{P_{eX}P_w i_{SP}^2}}\right\}$$

2) Cross-section with one symmetrical axis (y axis symmetrical) where $e_Y = 0$

$P_k = P_{ey}$ or smallest root from following equation

$$\frac{1}{P_K^2}-\left(\frac{1}{P_{eX}}+\frac{1}{P_w}+\frac{1}{P_w}\cdot\frac{e_Y k_Y}{i_{SP}^2 I_Y}\right)\frac{1}{P_K}+\left\{1+\frac{e_Y k_Y}{i_{SP}^2 I_Y}-\frac{(e_Y+y_0)^2}{i_{SP}^2}\right\}\frac{1}{P_{eX}P_w}=0$$

d) Torsional buckling in the case when a central compressive load and pure bending moment act on the member end

1) where the center of the buckled cross section and the center of the figure are identical, and the condition at the ends with respect to bending and torsion are the same. Simple support at the ends and free camber of the cross-section.

$$M_K{}'=i_{SP}^2(P_w-P_K)(P_e-P_K)$$

$$i_{SP}^2=\frac{1}{A}\int_A r^2 dA$$

A: Cross-section area
r: Distance from shear center to cross-section element
P_w: Wagner's buckling load
P_e: Flexural buckling load
P_k: Critical compressive load acting on end
M_k: Critical bending moment acting n end
$M_k = 0$, buckling occurring with minimum value among P_e, P_w
$P_k = 0$, $M_k l^2 = i_{SP}^2 . P_w . P_e$
The relationship between P_w, P_e, Mk, R_k is shown by the following graphs

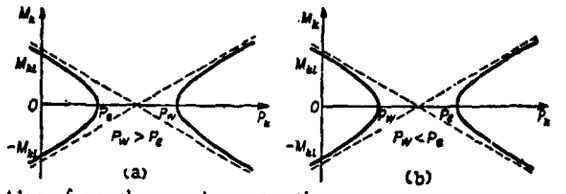

Also, from the previous equation

$$\left(\frac{M_K}{M_{K1}}\right)^2=\left(1-\frac{P_K}{P_w}\right)\left(1-\frac{P_K}{P_e}\right)$$

The relationship between each of the terms in the above equation is expressed by the following graph.

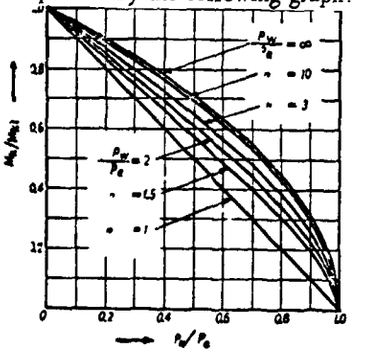

191

Both ends fixed

$$M_K^2 = \left(\frac{m^2 EC_{BT}}{l_0^2} + GJ_T - p_K i_{sp}^2\right)\left(\frac{m^2 EI}{l^2} - p_K\right) \qquad m = \pi$$

One end fixed, one end free.

$$m = 2.247$$

End conditions of bending and buckling not the same

a) With respect to bending, warping of cross-section free

With respect to torsion, fixed

$$M_K^2 = C i_{SP}^2 (P_w - P_K)(P_e - P_K)$$

Also $$\left(\frac{M_K}{M_{Ki}}\right)^2 = \left(1 - \frac{P_K}{P_e}\right)\left(1 - \frac{P_K}{P_w}\right)$$

C: Approximately a constant. In this case, 1.31

(b) Fixed with respect to bending

Warping of cross-section free with respect to torsion

a) Same results obtained as in case

2) Case when shear center does not coincide with centroid.

Case in which the end conditions are the same with respect to bending and torsion.

$$(M_K + P_K \cdot \zeta_s)^2 + i_{sm} \cdot M_K \cdot (P_K - Pe_c) - i_{SP}^2 (P_w - P_K)(Pe_c - P_K) = 0$$

Where bending moment is in the direction of the η axis

$$i_{sm} = \frac{1}{I_\eta} \int_A \zeta r^2 dA$$

$I_{e\zeta}$: Flexural buckling value in direction of

η, ζ: Indicate the x, y axes after deformation

ζ_3: Coordinates of shear center in direction of ζ axis

r: Distance from shear center of cross-section elements

Curves of $M_k : P_k$

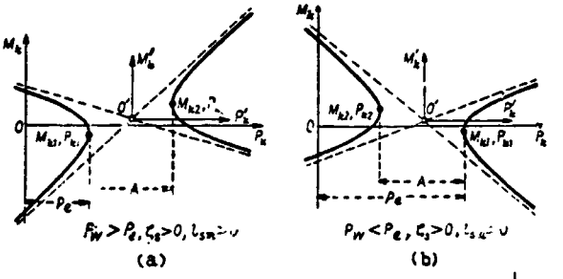

$M_K = 0$ When

$$\zeta_s^2 P_K \cdot i_{SP}^2 (P_w - P_K)(P_{ec} - P_K) = 0$$

$$P_K = \frac{P_w + P_{ec}}{2(1 - \zeta_s^2 / i_{SP}^2)} \pm \frac{\sqrt{(P_w - P_{ec})^2 - 4(1 - \zeta_s^2/i_{SP}^2) P_w P_{ec}}}{2(1 - \zeta_s^2/i_{SP}^2)}$$

$P_K = 0$ When

$$M^2 l - i_{sm} M_t P_{ec} - i_{SP}^2 P_w \cdot P_{ec} = 0$$

$$M_t l = \frac{i_{sm} \cdot P_w}{2} \pm \sqrt{\left(\frac{i_{sm} P_{ec}}{2}\right)^2 + i_{SP}^2 P_w P_{ec}}$$

192

Case in which the end conditions with respect to bending and torsion are not the same.

$$(M_E+C_2P_E)^2+C_1i_{sm}M_E(P_E-P_e)$$
$$-C_1i_{SP}^2(P_e-P)(P_e-P_E)=0$$

C_1, C_2 are constants determined by the end conditions

Pure torsion buckling

a) Anti-symmetrical shape

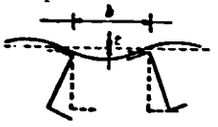

b) Symmetrical shape

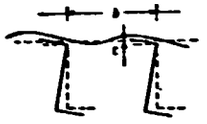

1) Z cross-section in which A_{PLT} is symmetrical with respect to the rivet line

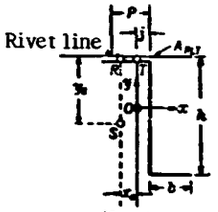

A_{PLT}: area of the effective cross-sectional area of the flat plate.

$$=\dot{\sigma}\cdot\frac{d\sigma_a}{d\sigma_e}$$

σ_a: Average unit stress of flat plate after buckling

σ_e: End fiber stress of flat plate after buckling

2) Z cross-section in which A_{PLT} is symmetrical with respect to the cross-section

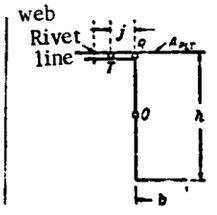

Torsional buckling of stiffeners attached to flat plates — 90

1) Pure Torsional buckling

Z cross-section, Point T are on a straight line during deformation, forming center rotation.

Two cases in which the pure torsion buckling unit stress around Point T are symmetrical and anti-symmetrical are expressed by the following equation

$$\sigma_T=\frac{GJ_T+\left(\frac{\pi}{\lambda}\right)^2E_tC_{BT}+\left(\frac{\lambda}{\pi}\right)^2K}{I_\rho}$$

λ: Half wave length of buckling curve

E_t: tangent modulus

E_tC_{BT}: Bending and torsion stiffnes of stiffener with respect to Point T

GJ_T: St. Venant's torsion stiffness of stiffener

I_ρ: Some os extreme geometric moments of stiffener and inertia and flat plate with respect to T"

K: Elasticity constraint modulus of plate with respect to stiffner, determined from the following equation, using (lb-in/in. radians)

$$\frac{1}{K}=\frac{1}{K_{\rho l}}+\frac{1}{K_{st}}+\frac{1}{K_r}$$

$K_{\rho l}$: Bending stiffness of a flat plate

Case of anti-symmetrical deformation

$$K_{\rho l}=\frac{Et^3}{3b}\left\{1+0.6\frac{\sigma_e-\sigma_\rho}{\sigma_\rho}\right\}$$

σ_p: Compression unit stress in case where flat plate buckles 1st

Case of symmetrical deformation $K_{\rho l}=\frac{Et^3}{b}$

K_{st}: Stiffener bending stiffness $=\frac{Et^3}{3(h+4\rho)}$

K_T: Bending stiffness of rivets

Z stiffener –

$$j=\frac{\rho}{2+2\rho}b$$

$$C_{BT}=\frac{t_1h^3}{3}\rho^2\left(\frac{1+\rho}{1+2\rho}\right)^2$$

NUMBERS	DIAGRAM I& BOUNDARY CONDITIONS	FORMULA FOR TABLE FOR RESULTS	REFERENCES, /253 NOTES
192	O: Center of gravity of effective cross-section area of stiffner and flat plate S: Shear center of above T: Center of rotation of pure torsion **R:** Hypothetical center of rotation of compound buckling consisting of bending and torsion	• I_{Pst} of stiffener $I_{Pst}=\frac{t_s h^3}{3}\frac{1+5\rho+6\rho^2+2\rho^3+7\rho^4}{1+2\rho}$ $J_T=\frac{t_s^3 h}{3}(1+2\rho)$ $\rho=\frac{b}{h}$. t_s: stiffener wall thickness When A_{PLT} is symmetrical with respect to the web (Case shown in Figure 2) $I_{SPR}=\frac{t_s h^3}{3}(1+2\rho)(1+\rho)$ $C_{BTR}=\frac{t_s h^3}{3}\rho^3\left\{1-\frac{3t_s d}{4(A_S+A_{PLT})}\right\}$ A_S; Stiffner cross-section area Since A_{PLT} is small, eliminating it $C_{BTR}=\frac{t_s h^3}{3(1+2\rho)}\rho^3\left(1+\frac{5}{4}\rho\right)$ 2) Compound buckling consisting of bending and torsion. The compound buckling in the case where stiffeners of arbitrary cross-section are attached is expressed by the minimum root of σ_k in the following equation $\sigma_k^2\left[1-\left(\frac{x_0}{i_{PR}}\right)^2\right]-\sigma_k\left[(\sigma_e+\sigma_R)+\frac{2x_0y_0}{(i_{PR})^2}\sigma_{xy}\right]$ $-\sigma_e\cdot\sigma_R-\left(\frac{y_0}{i_{PR}}\right)^2\sigma_{xy}^2=0$ σ_e: Euler's buckling unit stress σ_R: Torsional buckling unit stress around point R i_{PR}: Extreme radius of gyration of area with respect to $R=\left(\frac{I_{PR}}{A_S+A_{PLS}}\right)^{\frac{1}{2}}$ I_{PR}: Extreme geometric moment of inertia with respect to R A_S: Stiffener cross-section area $A_{PLS}=bt\cdot\frac{\sigma_e}{\sigma_c}$: Effective cross-section area of flat plate $\sigma_{xy}=\frac{\pi^2 E_i\cdot I_{xy}}{\lambda^2\cdot(A_S+A_{PLS})}$ I_{xy}: Product of inertia of area (A_S + A_{PLS}) with respect to x, y Approximately, assuming $x_0 = 0$,

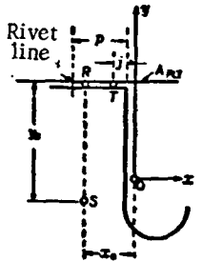

NUMBERS	DIAGRAM & BOUNDARY CONDITIONS	FORMULA OR TABLE FOR RESULTS	REFERENCES, NOTES /254
192		$\sigma_R^2-\sigma_R(\sigma_e+\sigma_R)+\sigma_e\sigma_R-\left(\frac{y_s}{i_{PR}}\right)^2\sigma_{xy}^2=0$ Also $\sigma_R=\frac{\sigma_e+\sigma_R\pm\left[(\sigma_e-\sigma_R)^2+4\left(\frac{S}{i_{PR}}\right)^2\sigma_{xy}^2\right]^{\frac{1}{2}}}{2}$ The σ_{min} determined from the above equation is expressed in the following diagram. 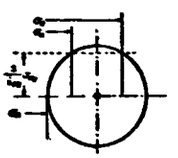	/254

REFERENCES

/255

CHAPTER 1: COMPRESSED MEMBERS

1. Bleich, F., *Stahlhochbauten I*, Springer, Berlin (1932), S. 131.
2. Jakkula, A. A. and H. K. Stephenson: "Steel Columns," A Survey and Appraisal of Part Works," Bulletin of the Agricultural and Mechanical College of Texas, No. 91 (1947-7-1), p. 14.
3. Salmon, E. H., "Columns," Oxford Technical Publications, London (1921), p. 228.
4. Salmon, E. H., Reference (3), p. 231.
5. Roark, R. J., "Formulas for Stress and Strain," McGraw-Hill (1938), p. 196.
6. Ježek, K., *Die Festigkeit von Druckstäben aus Stahl*, Springer, Wien (1937).
7. Municipal Architectural Building Code (May 28, 1946), Regulation No. 26 of the Ministry of Internal Affairs, Article No. 107.
8. Japan Architectural Standards, Architecture 3001.
9. Moisseiff, L. S. and F. Lienhard, "Theory of Elastic Stability Applied to Structural Design," Proc., A.S.C.E. (1940-1), pp. 31-70.
10. Balog, L., "Discussions," Proc., A.S.C.E. (1940-11) pp. 1713-1720.
11. Stahlbau-Kalender, Ernst u. Sohn, Berlin (1939), S. 224.
12. Gehler, W., *Erläuterungen zur Bemessung von Knickstäben nach DIN 4114 (2. Teil)*," Deutscher Normenausschuss e. V., Berlin, Deutscher Stahlbau-Verband, Berlin.
13. Japan Architectural Society, Structural Members from II (Sept. 1949), pp. 50-51.
14. State of California, California Administrative Code, Title 21, Public Works, Reprint (1948-9-1), p. 804.
15. Southwell, R. V., "An Introduction to the Theory of Elasticity," Oxford, 2nd ed., (1949), p. 438 .
16. Ratzersdorfer, J., *Die Knickfestigkeit von Stäben und Stabwerken*, Springer, Wien (1936), S. 66.
17. Schleussner, A., *Strenge Theorie der Knickung und Biegung*, L. Teil, Teubner (1937).
18. Salmon, E. H., Reference (3), p. 214.
19. Timoshenko, S., "Theory of Elastic Stability," McGraw-Hill L936), p. 20.
20. Van den Broek, "Limit Design," John Wiley and Sons, New York (1948), p. 73.
21. Van den Broek, Reference (20), pp. 83-111.

CHAPTER 2: LATERAL BUCKLING OF BEAMS

22. Chwalla, E., *Die Kipp-Stabilität gerader Träger mit doppelt-symmetrischem I-Querschnitt*, Julius Springer, Berlin (1939).
23. Timoshenko, S., Reference (19), p. 259.

MATERIALS

1. Members with Constant Cross-Section (See Chapter 1)

a. Central Compression

24. Kiichi, Yuasa, "Materials, Dynamics," Sankaido, Publishers (1939), p. 504.
25. Yuzo, Nakagawa, "Relationship Between the Stiffness of the Ends of Columns and Buckling Loads," Papers of the Mechanical Society, Vol. 4, No. 14.
26. Shunzo, Kin, "Statistical Theory of the Buckling Strength of Continuous Columns having Multiple Diameter Spans Having Either a Straight Multiple Lattice Span or Intermediate Stiffness Support," Journal of the Civil Engineering Society, Feb. 1940).
27. Ratzersdorfer, J., Reference (16) pages 26-27.
28. Puwein, M. G., *Die Knickfestigkeit des Rechteckrahmens*, Bautechnik (1940-1-19).
29. Engesser, *Zentralblatt der Bauver-waltung*, 11 (1893). S. 483. /256
30. Olsen: R. G., Stahlbau, 7 (1934), S. 13.
31. Koga, Kato, "Mechanical Investigation on the Mechanical Problems of Transmission Line," Journal of the Mechanics Society, Vol. 19, No. 11, (Nov. 1925).
32. Ratzersdorfer, J., Reference (16), p. 108-113.
33. Sievers, H., *Die Knickfestigkeit elastich eingespannter Stabe*, Stahlbau (1940-5-3).
34. Kiyoshi, Takefuji, "Problems Relating to the 85th Structural Dynamics Prize," Architectural World (1941).
35. Ratzersdorfer, J., Reference (6), p. 33.
36. Bleich, F., "Theory and Calculation of Steel Bridges," Corona Publishers, 1938, p. 197.
37. Makoto, Sugano, "On the General Calculation Method for Steel Structural and Wooden Structural Compression Methods by Means of a New Calculation Standard," Technology lecture at the Architectural Society (March 1948).
38. Shichiro, Sato, "Investigation of Calculations of the Buckling of a Circular Column which Does Not Follow Hooke's Law," Journal of the Mechanics Society, Vol. 49, No. 338 (July 1946).
39. Mutsuo, Kakuzen, "Method of Computations for Determining the Buckling Stress with Respect to Soft Steel and Cast Iron Bars," Journal of the Mechanics Society, Vol. 39, No. 198 (Oct., 1933).
40. Shizuo, Saka, Okushima Seiichi, "On the Ultimate Strength of Reinforced Concrete and the Critical Loads of Columns of the Same Length," Papers of the Mechanics Society, No. 15 (Nov., 1939).
41. Masatsugu, Kuranishi, Hayashi Shiguru, etal., "Planning Materials on Steel Machinery, Strength and Stiffness," (Nov., 1945), unpublished.

b. Eccentric Compression

42. Royen, N., "Knickfestigkeit exzentrisch beanspruchter Säulen aus Baustoff, der nur gegen Druck wiederstandsfähig ist," Bauingenieur (1937-7-23).
43. Timoshenko, S., "Buckling Theory," Corona Publishers, (1938), pp. 27-29.
44. Shizuo, Saka, "Design Formulas for Exccentrically Compressed Reinforced Concrete Columns, Based on Rupture Strength," Papers of the Mechanics Society, No. 32-36 (june 1947).

45. Shizuo, Saka, Okushima Seiichi, "On the Ultimate Strength of Reinforced Concrete and the Critical Loads of Columns of the Same Length," Papers of the Mechanics Society, No. 15 (Nov., 1939).

c. Combined Loads

46. Roark, R. J., Reference (5), p. 262.
47. Timoshenko, S., Reference (43), p. 75.
48. Ratzersdorfer, J., Reference (16), p. 148.
49. Ratzersdorfer, J., Reference (16), p. 143.
50. Ichiro, Ono, "Calculations of Rail Buckling," *Journal of the Civil Engineering Society*, Vol. 29, no. 7 (July 1943).
51. Takashi, Inada, "On the Lifting Buckling of Rails and the Deflection of Columns Sustaining Axial and Lateral Compression," *Journal of the Civil Engineering Society*, Vol. 25, No. 6 (June 1939).
52. Wagner, H. and G. Kimm, "Bauelemente des Flugzeuges," R. Oldenburg, Munchen and Berlin (1940), p. 239.
53. Ratzersdorfer, J., Reference (16), pp. 153-155.
54. Ratzersdorfer, J., Reference (16), pp. 78-81.
55. Roark, R. J., Reference (5), p. 263.
56. Kutaro, Ozawa, "Forced Vibration of Compression Members," *Journal of the Civil Engineering Society*, Vol. 19, No. 4 (April 1933).

d. Vibration and Thermal Stress

57. Puwein, M. G., "Die Verwindurung der Knicklast eines Stabes durch Querschwingungen," Bauingenieur (1939-1-13).
58. Ratzersdorfer, J., Reference (16), p. 31.

e. Dynamic Compression

59. Senri, Katsuda, "Theory of High Speed Buckling of Elastic Columns," Paper read at the Engineering Lectures of the Architectural Society (Nov., 1947). /257
60. Ryusuke, Inouye, "The Dynamic Stability and Non-linear Characteristics of Thin Plates and Columns Sustaining Periodic Axial Forces," Report of the Institute of Aeronautics, No. 229 (Nov., 1943).

2. VARIABLE CROSS-SECTION MEMBERS (See Chapter 1)

61. Minoru, Tanaka, "On the Strength of Column with Variable Cross-Section," *Journal of the Civil Engineering Society*, Vol. 15, No. 3 (March, 1929).
62. Bleich, F., Steel Frame Constructions," Corona Publishers, (1941), p. 182.
63. Keichi, Aichi, "General Formulas Giving the Load which is Supportable by a Long Strut with a Non-uniform Section," "The Strength of Combined Struts," *Journal of the Mechanical Society*, Vol. 22, No. 56 (Feb., 1919).
64. Geng, Nakagawa, "Buckling of Plates and Columns having No Lateral Resistance and a Fixed Inclination," *Journal of the Mechanical Society*, Vol. 42, No. 226 (May 1939).

65. Geng, Nakagawa, "Buckling of Plates and Columns Having a Slope Fixed at Both Ends," *Journal of the Mechanical Society*, Vol. 40, No. 248 (Dec., 1937).
66. Geng, Nakagawa, "Buckling of Circular Columns Having a Sloping Section," *Journal of the Mechanical Society*, Vol. 39, No. 235 (Dec. 1936).
67. Geng, Nakagawa, "Buckling of Rectangular Plates Having a Sloping Section," *Journal of the Mechanical Society*, Vol. 39, No. 236 (Dec. 1936).
68. Geng, Nakagawa, "Buckling of Columns Having an Exponential Function Gradually Varying Cross-section" Report No. 3), Papers of the Mechanical Society, Vol. 8, No. 23 (Aug., 1942).
69. Geng, Nakagawa, "Buckling of Columns Having an Exponential Function Gradually Varying Cross-section (Report No. 3)" *Journal of the Mechanical Society*, Vol. 45, No. 304 (Aug., 1942).
70. Geng, Nakagawa, "Buckling of Columns Having an Exponential Function Gradually Varying Cross-section (Report No. 2)," Papers of the Mechanical Society, Vol. 8, No. 32 (August, 1942).
71. Geng, Nakagawa,"Buckling of Columns Having an Exponential Function Gradually Varying Cross-section (Report No. 2)," Vol. 45, No. 304 (July 1942).
72. Geng, Nakagawa, "Buckling of a Plate in Which the Thickness and the Width of the Cross-section are Inversely Proportioned," *Journal of the Mechanics Society*, Vol. 41, No. 254 (May 1938).
73. Bleich, F., Reference (62), p. 180.
74. Ratzersdorfer, J., Reference (16), pp. 96-91.
75. Shuhei, Yokota, "Critical Loads of Compression Members Having Variable Cross-section, Solved by Expanding Basic Differential Equation to an Exponential Series," *Journal of the Civil Engineering Society*, Vol. 26, No. 10 (Oct., 1940).
76. Ratzersdorfer, J., Reference (16), pp. 96-102.
77. Daizo, Hiura, "Problems of the Stability of Columns Having Variable Cross-section at Their Ends," *Journal of the Civil Engineering Society*, Vol. 21, No. 5 (May 1935).
78. Roark, R. J., Reference (5), p. 266.
79. Shigemasa, Iwafuji, "The Buckling of Thin Regular Hexahedron Plates," *Journal of the Mechanical Society*, Vol. 37, No. 207 (July, 1934).
80. Shigemasa, Iwafuji, "Buckling of Thin Isoceles Triangular Plates," *Journal of the Mechanical Society*, Vol. 37, No. 207 (July, 1934).
81. Yuzo, Nakagawa, Fukuchi Seizo, "Buckling of Thin Circular Plates," *Journal of the Mechanical Society*, Vol. 36, No. 193 (May 1933).
82. Makoto, Sugano, Unpublished manuscript.
83. Makoto, Sugano, Unpublished manuscript.
84. Ratzersdorfer, J., Reference (16), pp. 116-117.
85. Bleich, F., Reference (36), p. 119.
86. Seiichi, Okushima, "A Study of the Buckling Load on a Stepped Column, (Industrial Crane Support) Having an Intermediate Load (Report No. 1)" *Journal of the Architectural Society*, Vol. 55, No. 676, (July 1941).
87. Seiichi, Okushima, "A Study of the Buckling Load on a Stepped Column, (Industrial Crane Support) Having an Intermediate Load (Report No. 2)" *Journal of the Architectural Society*, Vol. 55, No. 676, (July 1941).

3 3. HELICAL SPRINGS (See Chapter 1)

88. Eiji, Utsumi, "Buckling of a Long Helical Spring under the Compression Load," *Journal of the Mechanical Society*, Vol. 28, No. 101 (Sept. 1925).
89. Ziegler, H., "Das Knicken der gedrückten und tordierten Schraubenfeder," *Zeitschriit des Österreichischen Ingenieur und Architeketen Vereins* /258 (1939-4).

4. LATERAL BUCKLING OF BEAMS (See Chapter 2)

90. Timoshenko, S., Reference (43), pp. 164-184.
91. Roark, R. J., Reference (5).
92. Seiji, Kondo, "Problems in the Stability of a Beam Having a Gradually Varying Cross-section Sustaining a Homogeneous Bending Moment," *Journal of the Mechanical Society*, Vol. 46, No. 311 (Feb., 1943).
93. Keiji, Endo, "On Kipperscheinung of Girder Plates with Gradually Varying Cutting Edges," *Journal of the Civil Engineering Society*, Vol. 91, No. 8 (Aug., 1933).
94. Sakutaro, Nakamura, "On the Buckling Load of the Deep Beam," *Journal of the Civil Engineering Society*, Vol. 29, No. 12 (Dec., 1943).
95. Atsushi, Hirai, "On the Stability with Respect to the Torsional Vibration of a Suspension Bridge," *Journal of the Civil Engineering Society*, Vol. 28, No. 9 (Sept. 1942).

SUPPLEMENTARY REFERENCES

96. Bleich, F. "Buckling Strength of Metal Structures," McGraw-Hill (1952).
97. deVries, K., "Strength of Beams as determined by Lateral Buckling," Proc. A.S.C.E. (1946).
98. Winter, G., "Lateral Stability of Unsymmetrical I-Beams and Trusses in Bending," A.S.C.E. Trans. (1946).
99. The Roy Aero. Soci., "Structural Principles and Data," Sir Isaac Pitman & Sons, Ltd. (1952).
100. Haas, T., "Some Notes on the Shear Center of Thin-Walled Open Sections," J. Roy. Aero. Soci., (1953).
101. Masatsugu, Kuranishi, "Torsion and Bending Strength of a Thin-Walled Flat Profile Column Sustaining an Axial Compressive Load," Papers of the Mechanical Society, Collection No. 1, No. 5 (Nov., 1935).
102. Goodier, J. N., "Torsional and Flexural Buckling of Bars of Thin-Walled Open Section under Compressive and Bending Loads," *J. Appl. Mech.* (1942).
103. Kuranishi, Masatsugu, "Some Recent Investigations on the Elastic Stability of Bars," Report of Research Institute of Technology, Nihon Univ., No. 1 (1952).

3. FRAMES AND ARCHES /259

1. FRAMES (CONTINUOUS MEMBERS, BUILT-UP MEMBERS, TRUSSES, RIGID FRAMES)

3.1.1. HISTORICAL REMARKS

It is possible to construct basic equations for the case of handling the buckling of frames which consist of an assemblage of various components such as continuous members, trusses, built-up members, and rigid frames, on the basis of the properties of solid members in which bending and force in the direction of the axes occur together. In other words, exactly the same approaches are applied as in solid members. There is merely a requirement for an increase in the procedures for solving simultaneous equations for the case of assemblage of parts, and conceptually the approach is exactly the same as for solid members.

It is possible to find the free moment equations for members sustaining forces in the direction of the axis in Muller-Breslau's book [1] which is a basic application of this, while we must attribute to F. Bleich [2, 3] success in expanding this further, analyzing the stability of frames and applying this to actual practice. F. Bleich calculated the buckling values for compressive members having various trusses by means of a four-moment equation, and found approximation formula(s) for this. His proposal for such approximation formula(s) was first adopted for German specifications [4, 5] and it has come to be adopted in the specifications of various countries. Timoshenko [6] and Ratzersdorfer [7] have described in detail the basic theory and methods for application to problems in the stability of frames.

In the analysis of the buckling of continuous members, the three moments equations or four moments equations may be utilized or as in the case of a solid member, it is possible to obtain results by solving directly from the differential equations of the member, introducing boundary conditions. With regard to two-span continuous members, Kim Shunzo [8] found a numerical solution for the case of various member and support conditions and for the case in which the geometric moments of inertia between support points differs according to the span, from the matrices of the solutions of this differential equation.

J. Ratzersdorfer [7] has exemplified the solution of various cases for determining the buckling load of trusses and frames by means of a hypothetical work method. The derivation of a deflection angle equation for members sustaining an axial force has been carried out for general cases, by many authors. Dr. Saka was the first to write a paper on this subject in Japan [9], and it is one of the most important. Mizuhara also derived the deflection angle equations for a bar [10] in his discussion of the vibration of rigid frames, and indicated their application to determining the buckling load of multi-storied, rigid frames. [11]

Hans Sievers [12] has conducted research on the buckling of gate frames having angle braces or truss beams. Wilhelm Bultmann [13] obtained an accurate /260 solution directly from differential equations for the buckling of three pinned type gate frames having variable cross-section beams or columns, and indcates his results in a numerical table. Recent important work on the buckling of rectangular rigid frames includes the papers of Chwalla and Jokisch [14]. Lundquist has applied this to aircraft engineering and has presented a large number of papers [15] which include numerical tables to simplify the design calculations. The research of George Winter, Hsu, et al. [16] and Thomas C. Kavanaugh [17] also merits attention. In our country, the research of Hiruta [18] Tsuboi; Wakabayashi [19], Sugano [20], [21] and Fujimoto [22] has been reported recently to the Japan Architectural Society [16]. Moreover, the new German buckling standard (DIN 4114) also merits attention, [57].

3.1.2. METHODS OF STABILITY ANALYSIS

In the analysis of the stability of continuous members, trusses, built-up members, and rigid frames which consist of a combination of solid members, the bending and member ends deformation (deflection angle or displacement) are merely added to the analysis as unknown quantities, but basically the method is the same as for the analysis of stability of solid members. One may use exactly the same approach as for the buckling of solid members, taking into consideration the member end constraints and deformation. The methods which can be generally used for statically determinant stress may be employed by expanding them for such analyses.

It is possible to divide the methods into the following five types:

(1) Differential Equation Analysis

This is a precise method, in which the analysis is carried out by numerically solving the differential equations for a member and introducing boundary conditions. It is effective when the frame and the load conditions are simple. Although it is possible to obtain as mathematically precise a solution as one wants, it is difficult to employ for complexed frames.

(2) Strain Energy Method, Minimum Work Method, Hypothetical Work Method

As a basic principle, solutions are obtained by employing the state in which the secondary degree of change in the overall potential energy of the system is 0 in the case of buckling. Fitz's approximation method belongs to this system. These methods are convenient when utilized for rough calculations to determine special cases in which the strain energy variation is 0, by hypothesizing a deformation curve. J. Ratzersdorfer [7] gives examples of several cases based on a hypothetical work method, for determining the buckling of trusses and frame members.

(3) Simultaneous Equations, Solutions, Matrix Solutions

If one takes the stress (the axial force and bending moment) and the displacement (deflection angle and deformation) of a member as an unknown quantity in the equation, of a linear quadratic simultaneous equation of the same order as the unknown number is established on the basis of the ordinary hypothesis of literal displacement. Forms of such equations include the deflection angle method [9], [16], [20], the three moment method, four moment method, [2], [3] and Mises' equation. It is posible to determine the buckling condition equations by taking the determinants of these equations as 0.

(4) Convergence Method, Series Method

These are based on the theory for the solving of instability by the elimination of the constraints on the end of a member by means of sequential approximations, and can be classified into mathematical methods and graphical calcu- /261
lation methods. Lundquist's method [15], the fixed moment method [21] and Hoff's Method are examples of this.

(5) Mixed Method

The mixed method obtains a solution by combining the above methods. For example, using ordinary trial methods, in the case based on matrix and series solutions, one approaches an accurate solution by successive approximation, from the values of the first approximation to the second, etc., and the energy method is generally employed first in order to determine the first approximation values.

3.1.3. CLASSIFICATION OF FRAMES

In analyzing the stability of frames, it is convenient first to classify them as follows in terms of their properties.

(1) Hinged Frames

The member ends are all hinged. This type is sub-divided into the two following classifications:

(a) Cases in which variation in member length is considered.

(b) Cases in which variation in member length is not considered.

For stability analysis, it is possible to employ the solution for solid members, taking into consideration the displacement of the joint, without any extra modifications on the analysis.

(2) Rigid Frames

(a) Case in which the displacement of the joints is constrained. (Figure 3.1.1). In this case, it is possible to obtain a solution by only using the so-called joint equation. It is relatively simple as a method of

stability analysis, and the solution is easy. Since no displacement of the joints occurs, the deflection of the member and the displacement of the joint is 0, the unknown quantity is merely the deflection angles for each member end, and for this reason one can get along with a small number of equations.

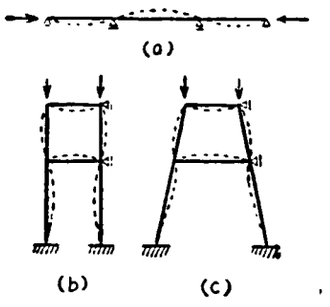

Figure 3.1.1

(b) Cases in which there is displacement of the joints (Figure 3.1.2). These cases can also be divided into those in which the variation in member length is considered, and cases in which such variation is not considered. In the former instance, considerable time and effort are required, so in most cases the solution is obtained ignoring the variation in member length. However, in cases such as ladder columns, variation in member length accumulates and has a large effect on the solution, and for this reason it must be heated. Moreover, in the case of ordinary rigid frame, there is no particular objection in practice to solve the equations ignoring variation in member length.

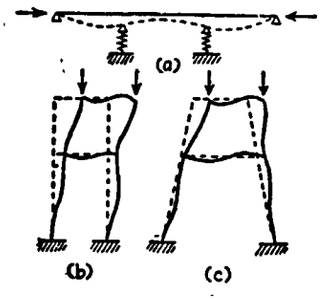

Figure 3.1.2

(3) Elastically Connected Frames

In this case, the parts are member ends, are neither hinged nor rigid connections, instead the connection is elastic. That is, they straddle angle θ in direct proportion to the bending moment M, varies.

$$\theta = \beta M.$$

In this case, by employing the proportion constant β (bending constant or spring constant) as a parameter, it is possible to obtain a solution based on the case of a rigid joint.

(4) Frames in General /262

For frames in general, a combination of the above three cases is used.

In the case of ordinary, continuous members, trusses, built-up members and rigid frames, one very frequently obtains a solution by assuming the case in which the displacement of the joint of a stiff jointed frame is constrained, or the case in which the joint varies, without taking into consideration variation in member length, as in (2a) and (2b) respectively above. In obtaining especially accurate solutions, the variation in member length is taken into account, and a solution is obtained as for an elastically jointed frame. Moreover, in any of the above cases, there are instances in which a support point of the structures are elastically supported. Figure (3.1.2 a) is an example of this, and in such cases, as in the case of elastically connected frames, one employs

the relation

$$\delta = k_1 R$$

in which the resultant R and the displacement δ are proportional, and then it is possible to obtain a solution using the proportional constant k_1 (bearing constant or spring constant) as a parameter.

3.1.4. HYPOTHESES IN STABILITY ANALYSIS

As with solid members, in analyzing the stability of frames such as continuous members, trusses and rigid frames, naturally the elasticity and non-elasticity regions pose a problem. However, within the non-elastic range, since the properties of the region beyond the proportional limit of the material; i.e., the characteristics of yield and elasticity have a large influence, the analysis is relatively difficult, and outside of experimental investigations, it is not handled very frequently.

The derivation of methods for the analysis of stability that are normally carried out is based on the following hypothesis. In applying these methods, one must remember that these assumptions are being made. Moreover, depending upon the type of frame, errors in these assumptions may accumulate, causing considerable differences from reality, so caution must be exercised.

(1) Buckling pertains to the buckling within the structure.

(2) The extension of a member due to normal stress is not considered.

(3) The extension of a member due to deformation is not considered.

(4) Depending on the conditions of the rigid connections, the scissor angles between the parts at the joints do not change.

(5) A state of equilibrium is maintained without external forces causing any curvature of the parts.

Among the methods for the analysis of the stability of such frames as continuous members, trusses, built-up members and rigid frames, we shall describe briefly the deflection angle method which is considered to be the most representative, and the analysis based on the fixed moment method. It must be borne in mind that the methods in the two sections below are derived on the basis of the assumptions mentioned above.

3.1.5. ANALYSIS BASED ON THE DEFLECTION ANGLE METHOD

(1) Basic equations. A member A, B which connects joints AB of a rigid frame which is elastically fixed at both ends undergoes the deformation indicated in Figure 3.1.3, and is assumed to be in a state of equilibrium. Using the following auxiliary numbers:

(3.1.1) /263

$$\left.\begin{aligned} s&=l_{AB}\sqrt{\frac{N_{AB}}{EI_{AB}}}\\ N_{AB}&=\frac{s^2}{l_{AB}^2}\cdot EI_{AB}. \end{aligned}\right\}$$

or

The following equation is established as a general equation for the deflection angle method for a member sustaining an axial force. [14], [16], [20]

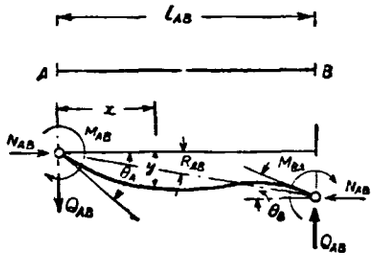

Figure 3.1.3

$$\left.\begin{aligned} M_{AB}&=EK_{AB}\left[\alpha_{AB}\theta_A+\beta_{AB}\theta_B-(\alpha_{AB}+\beta_{AB})R_{AB}\right],\\ M_{BA}&=EK_{AB}\left[\alpha_{AB}\theta_B+\beta_{AB}\theta_A-(\alpha_{AB}+\beta_{AB})R_{AB}\right], \end{aligned}\right\} \quad (3.1.2)$$

Here, when the member AB sustains a compressive force

$$\left.\begin{aligned} \alpha_{AB}&=\frac{z\sin z-z^2\cos z}{2(1-\cos z)-z\sin z},\\ \beta_{AB}&=\frac{z^2-z\sin z}{2(1-\cos z)-z\sin z}. \end{aligned}\right\} \quad (3.1.3)$$

When member AB sustains a tensile force, the circular function in the above equation becomes a hyperbolic function, becoming

$$\left.\begin{aligned} \alpha_{AB}&=\frac{z\sinh z-z^2\cosh z}{2(\cosh z-1)-z\sinh z},\\ \beta_{AB}&=\frac{z^2-z\sinh z}{2(\cosh z-1)-z\sinh z}. \end{aligned}\right\} \quad (3.1.4)$$

Since it is considered convenient in practice to have a table indicating the numerical values of α and β in equation (3.1.3) and (3.1.4), this table is given in Section 3.1.7.

When the end A is pinned, equation (3.1.2) becomes

$$\left.\begin{aligned} M_{AB}&=0,\\ M_{BA}&=EK_{AB}\gamma(\theta_B-R_{AB}). \end{aligned}\right\} \quad (3.1.5)$$

When end B is pinned, similarly, equation (3.1.2) becomes

$$\left.\begin{aligned} M_{AB}&=EK_{AB}\gamma(\theta_A-R_{AB}),\\ M_{BA}&=0. \end{aligned}\right\} \quad (3.1.6)$$

where

$$\gamma=\frac{\alpha_{AB}^2-\beta_{AB}^2}{\alpha_{AB}}. \tag{3.1.7}$$

the values of γ are also given in Section 3.1.7.

(2) Joint Equation. Generally, the joint equation is expressed by

$$\sum_X M_{AX}=0 \tag{3.1.8}$$

and for the values of M_{AX} in this equation, equation (3.1.2) or equations (3.1. /264
5), (3.1.6) may be substituted.

When no displacement of the joint occurs, since the deflection R = 0, equation (3.1.2) is expressed by

$$M_{AX}=EK_{AX}(\alpha_{AX}\theta_A+\beta_{AX}\theta_X) \tag{3.1.9}$$

Since equation (3.1.8) holds for each joint, a joint equation is obtained only for n number of joints. Since the unknown quantity with respect to this is only the deflection angle θ of each joint, it is possible to write n linear simultaneous equations having n unknowns. If we assume the determinant to be 0, this immediately becomes a buckling condition equation and using the numerical table in section 3.1.7, the buckling load is determined by trial method.

(3) Shear Equation. Using the symbols in Figure 3.1.3, the following shear equation [storey moment equation] is established for a member sustaining a compressive force.

$$Q\cdot l=M_{AB}+M_{BA}+EKz^2R_{AB}. \tag{3.1.10}$$

In the case of a member sustaining a tensile force, the third term becomes negative and the following equation

$$Q\cdot l=M_{AB}+M_{BA}-EKz^2R_{AB} \tag{3.1.11}$$

is obtained.

In a truss or irregular rigid frame consisting of members of differing lengths, it is convenient to employ the following shear equation, by dividing both sides of the above two equations by the member length l.

$$Q=\frac{1}{l}(M_{AB}+M_{BA}\pm EKz^2R_{AB}). \tag{3.1.12}$$

Here, in the double signs in the above equation, the upper one is for the case of a compressed member and the lower for the case of a tension member. This section, the sign will be used in the same way below.

Inserting equation (3.1.2) in equation (3.1.12)

$$Q=\frac{1}{l}EK_{AB}\left[(\alpha+\beta)(\theta_A+\theta_B)-\left\{2(\alpha+\beta)\mp z^2\right\}R_{AB}\right]. \tag{3.1.13}$$

when the other end is pinned, inserting equation (3.1.5)

$$Q=\frac{1}{l}EK_{AB}\left[\gamma\theta_B-(\gamma\mp z^2)R_{AB}\right]. \tag{3.1.14}$$

for the shear equation,

$$\sum_x Q_x=0 \tag{3.1.15}$$

is obtained.

In a rigid frame with a constant story height, and with a constant member length h for each column, if we insert equation (3.1.13) into the story moment equation

$$\sum_x Q_x\cdot h=0 \tag{3.1.16}$$

thus revising it /265

$$R_{AB}=\frac{\Sigma EK_{AB}(\alpha_{AB}+\beta_{AB})(\theta_A+\theta_B)}{\Sigma EK_{AB}\left[2(\alpha_{AB}+\beta_{AB})\mp z^2\right]}. \tag{3.1.17}$$

When the lower end is fixed, with $\theta_A = 0$

$$R_{AB}=\frac{\Sigma EK_{AB}(\alpha_{AB}+\beta_{AB})\theta_B}{\Sigma EK_{AB}\left[2(\alpha_{AB}+\beta_{AB})\mp z^2\right]}. \tag{3.1.18}$$

When the lower end is pinned, from equation (3.1.14)

$$R_{AB}=\frac{\Sigma EK_{AB}\gamma_{AB}\theta_B}{\Sigma EK_{AB}(\gamma_{AB}\mp z^2)}. \tag{3.1.19}$$

That is, it is possible to replace all deflection by deflection angle functions. Consequently, adding the story equation, or using equations (3.1.17), (3.1.18), (3.1.19) and a necessary and sufficient equation is obtained to derive the buckling condition equation and as in the previous case, by using the numerical table in Section 3.1.7, the buckling load can be determined by the trial method.

3.1.6. SOLUTION BY THE FIXED MOMENT METHOD

(1) Relationship between fixed moment method coefficients and deflection angle method coefficients. The following relationship obtains [21] between the coefficients for the deflection angle equation for a member sustaining an axial force, and the coefficients for the case in which the fixed moment method is used.

Member end stiffness $=\alpha k$. (3.1.20)

Joint stiffness $\rho=\sum \alpha k$. (3.1.21)

Distribution factor $\mu=\frac{\alpha k}{\rho}=\frac{\alpha k}{\sum \alpha k}$. (3.1.22)

Carry-over factor $c=\frac{\beta}{\alpha}$. (3.1.23)

The numerical tables for α, β and c are given in Section 3.1.7 and were included for the convenience of designers.

(2) Graphic solution paper. It is convenient to use the paper shown in Figure 3.1.4 in the graphic solution of the fixed moment method. The method of using this paper is exactly the same as in the method for solving by the fixed moment method, and the procedure should be carried out as follows:

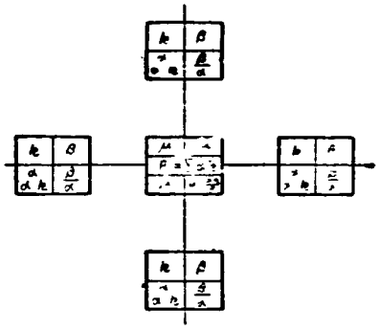

Figure 3.1.4

(3) Preparatory Calculations. The procedure for preparatory calculations by the graphic solution method is as follows. (See Figure 3.1.4).

(a) The stiffness ratio k of the member is introduced.

(b) α, β in the case when a load is assumed and it is sustained in the axial direction are introduced. For the beams of ordinary rigid frames, since there is no axial force, it is always the case that α= 4, β = 2.

(c) The carry-over factor c = β/α is computed and introduced.

(d) αк is calculated and introduced. /266

(e) The joint stiffness $\rho=\Sigma \alpha k$ is calculated and introduced.

(f) The distribution factor $\mu=\frac{\alpha k}{\Sigma \alpha k}$ is calculated and introduced.

(4) Sequence of Solution.

(a) When there is no displacement in a lateral direction (when the joints do not move).

In structures in which there is a load only on the joints, an arbitrary moment is added to an arbitrary joint, reaching a particular moment

and the constraints on each joint are eliminated. In this case, if the carryovers converge, the system becomes stable, and if they are dispersed, the system is not stable. The carryover method is exactly the same as in the case for the fixed moment method, but the stiffness, distribution factor and carryover factor are based respectively on equations (3.1.20), (3.1.21), (3.1.22), and (3.1.23).

(b) Case in which there is displacement in lateral direction (case when joints move.)

Except in the case when there is reinforcement by means of a rigid wall and a rigid floor, ordinary rigid frames buckle because their joints move in a lateral direction. In the solution for this case using the fixed moment method, is as follows:

First, one assumes a load close to the buckling load, and a rigid frame which sustains an axial force when such a load is received and then an arbitrary deflection is assigned to the frame. When the story shear in such a case is 0; i.e.,

$$\Sigma Q=\sum \frac{1}{l}\left(M_{AB}+M_{BA}\mp \frac{z}{\alpha_{AB}+\beta_{BA}} M_F\right)=0 \qquad (3.1.24)$$

The hypothetical load becomes the buckling load.

Here M_F is the bending moment when the upper and lower ends are given deflection while the joints remain rigid.

$$M_F=-EK_{AB}(\alpha_{AB}+\beta_{AB})R_{AB}=-EK_{AB}(\alpha_{AB}+\beta_{AB})\frac{d}{l}. \qquad (3.1.25)$$

The symbols are d = lateral displacement of joints
l = member length

In actual solutions, one follows a trial method, by assuming a load, finding the case in which $\Sigma Q \lesssim 0$ and narrowing its range, but since M_{AB}, M_{BA} are proportional to M_F irrespective of deflection R that should be given, and the absolute value of the displacement d, ΣQ should be determined, by giving a fixed moment M_F, in proportion to

$$\frac{EK_{AB}(\alpha_{AB}+\beta_{AB})}{l}$$

and then cancel it out.

3.1.7. AUXILIARY NUMERICAL VALUES

Since it is very convenient and practical in calculations to prepare a table of numerical values for the auxiliary terms α, β, and c used in the solution method based on the deflection angle (Section 3.1.5) and the solution based on the fixed moment method (Section 3.1.6), these are given in Tables 3.1.1-2 for /267

(1) Graph. Figure 3.1.5 is a graph of the results of calculations.*

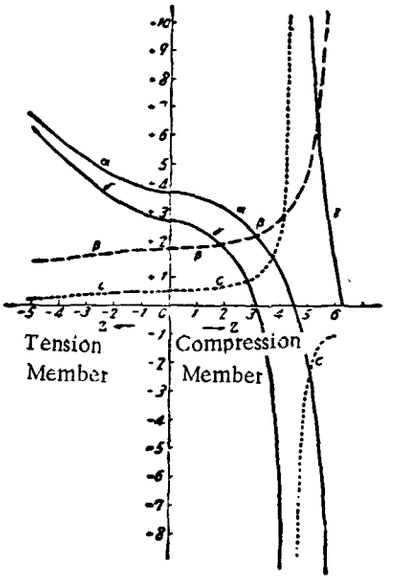

Figure 3.1.5

(2) Numerical values of auxiliary numbers for members sustaining compressive load:

$$\alpha=\frac{z\sin z-z^2\cos z}{2(1-\cos z)-z\sin z}, \tag{3.1.26}$$

$$\beta=\frac{z^2-z\sin z}{2(1-\cos z)-z\sin z}, \tag{3.1.27}$$

$$\gamma=\frac{\alpha^2-\beta^2}{\alpha}=\frac{z^2\sin z}{\sin z-z\cos z}, \tag{3.1.28}$$

$$c=\frac{\beta}{\alpha}=\frac{z-\sin z}{\sin z-z\cos z}. \tag{3.1.29}$$

Where $z=l\sqrt{\frac{N}{EI}}$.

(3) Numerical values of auxiliary numbers for members sustaining tensile force:

$$\alpha=\frac{z\sinh z-z^2\cosh z}{2(\cosh z-1)-z\sinh z}, \tag{3.1.30}$$

$$\beta=\frac{z^2-z\sinh z}{2(\cosh z-1)-z\sinh z}, \tag{3.1.31}$$

$$\gamma=\frac{\alpha^2-\beta^2}{\alpha}=\frac{z^2\sinh z}{z\cosh z-\sinh z}, \tag{3.1.32}$$

$$c=\frac{\beta}{\alpha}=\frac{z-\sinh z}{\sinh z-z\cosh z}. \tag{3.1.33}$$

where

$$z=l\sqrt{\frac{N}{EI}}.$$

*Please note: Where $z = 0$, $\alpha = 4$, $\beta = 2$, $\gamma = 3$, $c = 0.5$
Where $z = \pi$, $\alpha = \beta = 2.467$, $\gamma = 0$, $c = 1.0$
Where $z = 2\pi$, $\alpha = -\infty$, $\beta = \infty$, $\gamma = 0$, $c = -1.0$.

TABLE 3.1.1. TABLE OF COEFFICIENTS FOR A MEMBER SUSTAINING A COMPRESSIVE FORCE /268

ε	α	β	γ	c
0.00	4.000	2.000	3.000	0.5000
0.10	3.999	2.000	2.998	0.5002
0.20	3.995	2.001	2.992	0.5010
0.30	3.988	2.003	2.982	0.5023
0.40	3.979	2.005	2.968	0.5040
0.50	3.967	2.008	2.950	0.5063
0.60	3.952	2.012	2.927	0.5092
0.70	3.934	2.017	2.900	0.5126
0.80	3.914	2.022	2.[illegible]	0.5166
0.90	3.891	2.028	2.[illegible]	0.5211
1.00	3.865	2.034	2.[illegible]	0.5264
1.10	3.836	2.042	2.749	0.5323
1.20	3.804	2.050	2.699	0.5389
1.30	3.769	2.059	2.644	0.5463
1.40	3.732	2.070	2.584	0.5546
1.50	3.691	2.081	2.518	0.5637
1.60	3.647	2.093	2.446	0.5739
1.70	3.599	2.105	2.367	0.5851
1.80	3.548	2.120	2.282	0.5974
1.90	3.494	2.135	2.189	0.6111
2.00	3.436	2.152	2.088	0.6263
2.10	3.374	2.170	1.979	0.6430
2.20	3.309	2.189	1.860	0.6616
2.30	3.239	2.210	1.732	0.6823
2.40	3.166	2.233	1.594	0.7053
2.50	3.088	2.257	1.438	0.7310
2.60	3.005	2.283	1.270	0.7598
2.70	2.918	2.312	1.085	0.7923
2.80	2.825	2.342	0.8832	0.8291
2.90	2.728	2.376	0.6588	0.8709
3.00	2.624	2.411	0.4084	0.9189
3.10	2.515	2.450	0.1273	0.9744
(π)	(2.467)	(2.467)	(0.0000)	(1.0000)
3.20	2.399	2.492	−0.1906	1.039
3.30	2.276	2.538	−0.5540	1.115
3.40	2.146	2.588	−0.9744	1.206
3.50	2.006	2.642	−1.468	1.316
3.60	1.862	2.702	−2.059	1.451
3.70	1.706	2.767	−2.781	1.622
3.80	1.540	2.838	−3.691	1.843
3.90	1.363	2.917	−4.880	2.140
4.00	1.173	3.004	−6.516	2.560
4.10	0.9697	3.110	−8.940	3.197
4.20	0.7510	3.207	−12.95	4.271
4.30	0.5149	3.327	−20.98	+6.461
4.40	0.2592	3.462	−46.00	+13.36
4.50	−0.0191	3.614	+682.0	−188.7
4.60	−0.3234	3.787	+44.00	−11.71
4.70	−0.6580	3.984	+23.46	−6.053
4.80	−1.029	4.211	+16.21	−4.093
4.90	−1.443	4.475	12.44	−3.102
5.00	−1.909	4.785	10.08	−2.507
5.10	−2.439	5.151	8.440	−2.112
5.20	−3.052	5.592	7.196	−1.833
5.30	−3.769	6.130	6.200	−1.626
5.40	−4.625	6.798	5.364	−1.470
5.50	−5.673	7.647	4.638	−1.348
5.60	−6.9[illegible]	8.759	3.980	−1.253
5.70	−8.721	10.269	3.370	−1.177
5.80	−11.111	12.428	2.791	−1.119
5.90	−14.671	15.745	2.226	−1.073
6.00	−20.637	21.453	1.665	−1.040
6.10	−32.934	33.478	1.097	−1.017
6.20	−74.362	74.617	0.510	−1.003
(2π)	(−∞)	(∞)	(0.000)	(−1.000)

TABLE 3.1.2. TABLE OF COEFFICIENTS FOR A MEMBER SUSTAINING TENSILE FORCE

/269

s	α	β	τ	c
0.00	4.000	2.000	3.000	0.5000
0.10	4.001	2.000	3.002	0.4998
0.20	4.005	1.999	3.008	0.4990
0.30	4.012	1.997	3.018	0.4978
0.40	4.021	1.995	3.032	0.4961
0.50	4.033	1.992	3.050	0.4938
0.60	4.048	1.988	3.071	0.4912
0.70	4.065	1.984	3.093	0.4881
0.80	4.085	1.979	3.126	0.4845
0.90	4.107	1.974	3.158	0.4805
1.00	4.132	1.968	3.194	0.4762
1.10	4.159	1.961	3.232	0.4716
1.20	4.189	1.954	3.277	0.4665
1.30	4.221	1.946	3.323	0.4612
1.40	4.255	1.938	3.372	0.4556
1.50	4.292	1.931	3.421	0.4497
1.60	4.330	1.921	3.478	0.4436
1.70	4.372	1.912	3.536	0.4373
1.80	4.415	1.902	3.596	0.4308
1.90	4.460	1.892	3.656	0.4242
2.00	4.508	1.882	3.722	0.4174
2.10	4.557	1.871	3.789	0.4105
2.20	4.608	1.869	3.858	0.4036
2.30	4.661	1.849	3.928	0.3966
2.40	4.716	1.837	4.000	0.3896
2.50	4.773	1.826	4.076	0.3825
2.60	4.831	1.814	4.152	0.3755
2.70	4.891	1.802	4.228	0.3685
2.80	4.953	1.791	4.304	0.3615
2.90	5.016	1.779	4.384	0.3546
3.00	5.081	1.767	4.468	0.3477
3.10	5.147	1.754	4.548	0.3409
3.20	5.214	1.742	4.632	0.3341
3.30	5.283	1.730	4.716	0.3275
3.40	5.353	1.718	4.800	0.3210
3.50	5.424	1.706	4.888	0.3146
3.60	5.497	1.694	4.976	0.3086
3.70	5.570	1.683	5.060	0.3021
3.80	5.645	1.671	5.152	0.2950
3.90	5.720	1.659	5.240	0.2900
4.00	5.788	1.647	5.328	0.2842
5.00	6.608	1.541	6.248	0.2231

3.1.8. ABBREVIATED METHOD OF CALCULATION FOR A BUILT-UP COMPRESSION MEMBER

In actually designing a built-up compression member, various methods are employed. The method given in DIN E 4114 [5], is given below:

(1) Calculations for a solid web axis (See Figures 3.1.6-11).

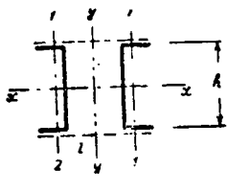

Figure 3.1.6

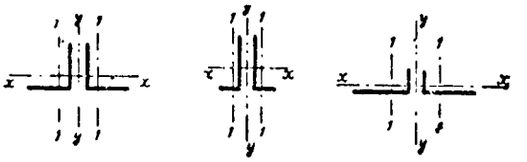

Figure 3.1.7

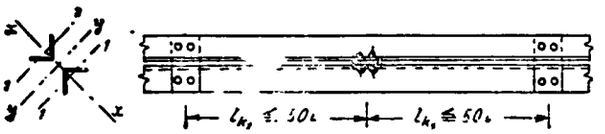

Figure 3.1.8

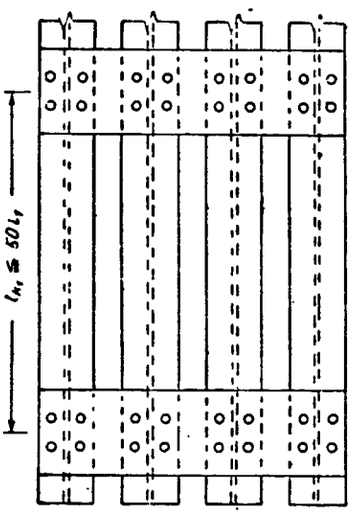

Figure 3.1.11

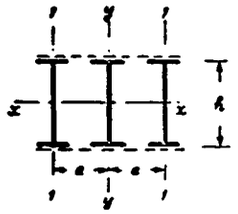

Figure 3.1.9

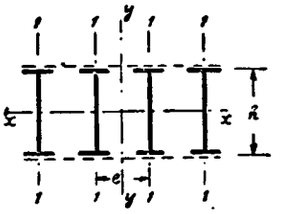

Figure 3.1.10

For buckling with respect to a solid web axis; i.e., buckling around x-x, calculations may be performed exactly as in the case of a solid member.

(2) Calculations with respect to an axis where no solid web is involved (Figures 3.1.6-12). The buckling with respect to an axis which is not a solid web; i.e., buckling around y-y, is calculated using the following hypothetical slenderness ratio λ_{yi}.

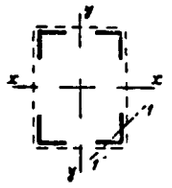

Figure 3.1.12

$$\lambda_{yi}=\sqrt{\lambda_y^2+\frac{n}{2}\lambda_1^2}\,. \qquad (3.1.34)$$

Here

λ_y = slenderness ratio of total member based on buckling length l_{ky} and geometric moment of inertia I_y with respect to the y-y axis (See Figure 3.1.6-11).

As in Figure 3.1.12, in the case of an axis where there is no solid web in both directions, the λ_y is taken for the axis giving the smallest geometric moment of inertia.

λ_1 = buckling length l_{k1}, geometric moment of inertia I_1. The I_1 here is taken as pertaining to the axis 1-1 of an individual member parallel to a non-solid web axis, when there is only one axis (Figures 3.1.6-11), and pertaining to the axis of an individual member given the smallest geometric moment of inertia when there are two non-solid web axes (Figure 3.1.12).

l_{k1} = buckling length of individual member, in lattice column. This is the length of the truss line, and in an open web column the center distance of the tie plates is taken.

n = number of individual members.

(3) Detailed Regulations on Structures. When using the above abbreviated calculation method, it is necessary to follow the following detailed regulations on structures. In actual built-up members, it is necessary not only to consider the stability of the overall built-up member itself, but to design it so that no local buckling will occur in the individual members or in the joining members. It can be said that the detailed regulations are extremely important in design.

(a) The slenderness ratio of λ_1 of an individual member is to be less than 50. /271

(b) In open web columns, tie plates are installed at both ends at intervals of 1/3 the buckling length.

(c) In lattice built-up compression members, tie plates are installed at the member ends.

(d) In members having a ⊣⊢ the tie plates are installed alternately (see Figure 3.1.8).

(e) Each tie plate is attached to each individual member by more than two rivets. The tie plate rivets on the member ends are to be one more than the number of rivets on the intermediate tie plates.

(f) Only when it is impossible to use rivets in the structure, bolts can be used for connecting the tie plates for lattices. In this case polished bolts are used.

(g) The distance between the centers of gravity of the individual members e (maximum distance when the number of individual members exceeds 2) is smaller than the cross-section height h in the direction y-y. When e is especially large, the allowable unit stress of the tie plate, lattice and connecting parts must be reduced to less than 80% of normal allowable stress (Figures 3.1.6, 3.1.9, and 3.1.10).

3.1. BUCKLING SHEAR

When a member begins to buckle, a shear force occurs in the compressed member. The connecting pieces of built-up members (tie plates and lattices) must be designed so that they are safe with respect to this shear force. Theoretically, there are methods for calculating from the deflection or bending moment of the member when the buckling deformation occurs, but the following methods are used as an abbreviated form of computation.

(1) German Structural Steel Buckling Standard (DIN E 4114). This is determined from Table 3.1.3 corresponding to the slenderness ratio λ_x and the total strength P of the frame work members.

Symbols $$P=\frac{A\cdot f_c}{\omega_x}. \qquad (3.1.35)$$

A = cross-section area of compression member,

f_c = allowable compression unit stress

ω_x = buckling modulus

Table 3.1.3 Q (Percent with Respect to P)

	λ	40 Less Than	80 〃	120 〃	150 〃	200 〃	250 〃
Commercial Steel	St. 37.12 St. 00.12	1	2	4	6	10	14
	St. 52	1	3	6	9	14	19

where when $\lambda > 40$, intermediate values are linearly interpolated.

(2) Japan Civil Engineering Society

$$Q=\frac{Pl}{4000\,y}. \qquad (3.1.36)$$

Symbols P = total strength of frame work members or compressive force kg

l = buckling length cm /272

y = distance cm from neutral axis of cross-section to end fiber.

(3) Japan Architectural Society

The design is carried out considering that the following shear force Q_k acts at right angles to the member axis.

$$Q_k = \frac{\omega_{ye} \cdot P}{70}$$

Symbols ω_{ye} = buckling modulus corresponding to λ_{ye}

P = compressive force

3.1.10. STIFFENING OF SUPPORT POINTS

The distance between support points in compression members forms the basis for calculating buckling strength. When the support points are removed from the member axis, and begin to move, they have a considerable influence on the buckling length, so in actual design, it is necessary to provide adequate stiffness in the joints so that movement of the joints is prevented. (See Figure 3.13.) In order to study the degree of stiffening in detail, it is necessary to follow accurate theoretical analyses; e.g., DIN E 4114 III b(5)).

However, these accurate analyses are extremely troublesome, so in normal abbreviated calculations, if it is safe after 1% of the compressive force is applied at right angles to the surface of the structure, there is no objection to considering that the joint is a non-moving point [5]. (Figures 3.1.13-15)

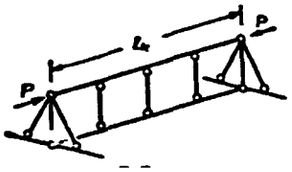

(a) When there are no stiffeners

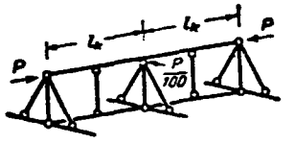

(b) With stiffeners

Figure 3.1.13

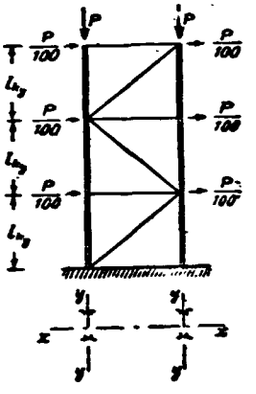

Figure 3.1.14

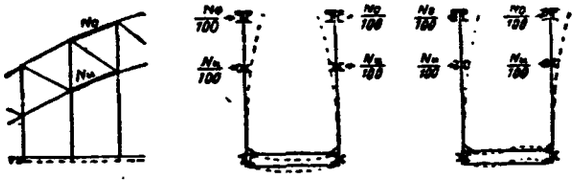

Figure 3.1.15

However, when these joints are in long, connected compression members with elastic supports, since considerable errors may arise, in such cases an accurate analysis is necessary.

Moreover, the lateral force is applied in order to check the stiffeners is applied not only to the stiffened portion, but to the column, the base, and all of the structures that support it. It is necessary to make sure that each part is safe with respect to this.

3.1.11. EXAMPLES OF THE CALCULATION OF BUCKLING LOAD (Supplement) /273

Below are given examples of the calculation of actual buckling load in frames, together with an explanation.

(1) Example 1 of Analysis by Deflection Angle Method. Case of column leg pin π type rigid frame.

(a) When there is no movement in the joints (Figure 3.1.16).

When there is no movement in the joints, since no deflection angle is formed, the buckling condition equation is established only from the moment equation. Using the symbols indicated,

$$M_{EA}=EK_{EA}\cdot 3\theta_E;\quad M_{EB}=EK_{EB}\gamma_{EB}\theta_E;$$

$$M_{EF}=EK_{EF}(4\theta_E+2\theta_F)=EK_{EF}\cdot 2\theta_E.$$

In this case, the moment equation $\sum M_{EF}=0$ becomes the buckling condition equation itself.

$$3K_{EA}+\gamma K_{EB}+2K_{EF}=0.$$

Here, if $\frac{K_{AE}}{K_{EB}}=k_1$, $\frac{K_{EF}}{K_{EB}}=k_2$

$$3k_1+\gamma+2k_2=0$$

Moreover, when $k_1 = k_2 = k$, this becomes $\gamma + 5k = 0$.

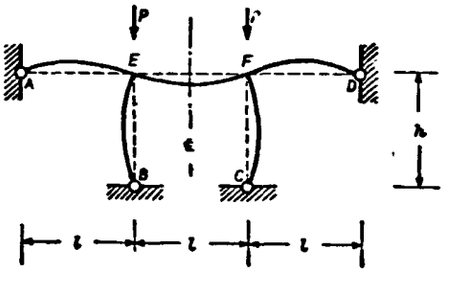

Figure 3.1.16

Solving this by the trial method or graphic formula, if

$$P_k=\frac{z^2EI}{h^2}=\frac{\mu EI}{h^2}$$

the values of z, μ are shown in the following table:

k	0	0.2	0.4	0.6	0.8	1.0	1.5	2.0	2.5	3.0	4.0	5.0	6.0	∞
z	π	3.41	3.59	3.72	3.83	3.91	4.04	4.13	4.19	4.23	4.29	4.32	4.34	4.49
μ	9.87	11.6	12.9	13.9	14.6	15.3	16.3	17.0	17.5	17.9	18.4	18.6	18.8	20.2

(b) When the joints do not move, (Figure 3.1.17). In this case, it is also necessary to complete the deflection equation.

$$M_{EA}=EK_{EA}\cdot 3\theta_E;$$

$$M_{EB}=EK_{EB}\cdot\gamma(\theta_E-R_{EB});$$

$$M_{EF}=EK_{EF}(4\theta_E+2\theta_F)=EK_{EF}\cdot 6\theta_E.$$

From the moment equation, $\sum M_{EE}=0$ より

$$(3k_1+6k_2+\gamma)\theta_E-\gamma R_{EB}=0.$$

From the deflection equation

$$Ql=M_{BE}+M_{EB}-F^{K_2}P_{EB}=0$$

$$\gamma\theta_E+(z^2-\gamma)R_{EB}=0$$

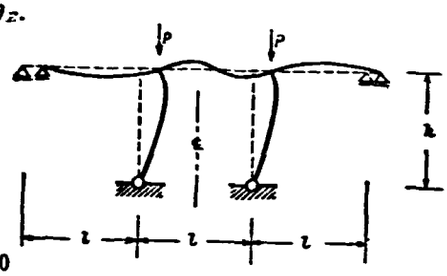

Figure 3.1.17

From these two equations, if θ_E and R_{EB} are eliminated, the buckling condition equation

$$\begin{vmatrix} 3k_1+6k_2+\gamma & \gamma \\ \gamma & z^2-\gamma \end{vmatrix}=0$$ /274

is obtained. When $k_1 = k_2 = k$, expanding the above equation

$$z^2(9k+\gamma)-9k\gamma=0$$

Solving this graphically, assuming

$$P_k=\frac{z^2EI}{h^2}=\frac{\mu EI}{h^2}$$

the results in the following table are obtained:

k	0	0.2	0.4	0.6	0.8	1.0	1.5	2.0	2.5	3.0	4.0	5.0	6.0	∞
z	0	1.04	1.24	1.33	1.38	1.42	1.46	1.49	1.50	1.52	1.53	1.54	1.54	$\pi/2$
μ	0	1.09	1.53	1.77	1.91	2.01	2.14	2.21	2.26	2.30	2.34	2.36	2.38	$\pi^2/4$

(2) Example 2 of Analysis by the Deflection Angle Method. Case of a type rigid frame with column legs fixed.

(a) Case in which the joints do not move (Figure 3.1.18). As in the above cases,

$$M_{EA}=EK_{EA}\cdot 3\theta_E;\ M_{EB}=EK_{EB}\cdot\alpha_{EB}\theta_E;$$

$$M_{EF}=EK_{EF}(4\theta_E+2\theta_F)=EK_{EF}\cdot 2\theta_E$$

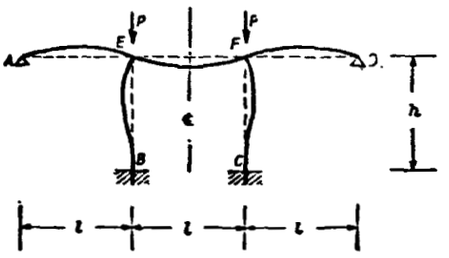

Figure 3.1.18

Therefore, if

$$\frac{E_{EA}}{E_{EB}}=k_1,\quad \frac{K_{EF}}{K_{EB}}=k_2$$

the buckling condition equation becomes

$$\alpha+3k_1+2k_2=0$$

When $k_1 = k_2 = k$,

$$\alpha+5k=0$$

If we solve this equation, assuming

$$P_k=\frac{z^2EI}{h^2}=\frac{\mu EI}{h^2}$$

The results in the following table are obtained:

k	0	0.2	0.4	0.6	0.8	1.0	1.5	2.0	2.5	3.0	4.0	5.0	6.0	∞
z	4.49	4.79	5.02	5.19	5.33	5.44	5.63	5.75	5.84	5.91	5.99	6.04	6.08	2π
μ	20.2	23.0	25.2	27.0	28.4	29.6	31.7	33.1	34.1	34.9	35.9	36.4	37.3	39.5

(b) Case in which the joints move (Figure 3.1.19).

$M_{EA}=EK_{EA}\cdot 3\theta_E$;

$M_{EF}=EK_{EF}(4\theta_E+2\theta_F)=EK_{EF}\cdot 6\theta_E$;

$M_{EB}=EK_{EB}\{\alpha\theta_E-(\alpha+\beta)R_{EB}\}$;

$M_{BE}=EK_{EB}\{\beta\theta_E-(\alpha+\beta)R_{EB}\}$.

From $\sum M_{EF}=0$ より

$$(3k_1+6k_2+\alpha)\theta_E-(\alpha+\beta)R_{EB}=0$$

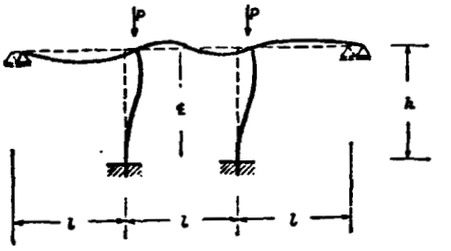

Figure 3.1.19

Also, from the equations $Ql=M_{BE}+M_{EB}+EKz^2R_{EB}=0$ /275

$$(\alpha+\beta)\theta_E-2(\alpha+\beta)R_{EB}+z^2R_{EB}=0$$

From these two equations, if we eliminate θ_E, R_{EB}, the following buckling condition equation is obtained

$$\begin{vmatrix} 3k_1+6k_2+\alpha & -(\alpha+\beta) \\ \alpha+\beta & z^2-2(\alpha+\beta) \end{vmatrix}=0$$

When $k_1 = k_2 = k$, expanding the above matrix

$$\Delta=(9k+\alpha)\{2(\alpha+\beta)-z^2\}-(\alpha+\beta)^2=0$$

is obtained. If we solve this equation, assuming

$$P_k=\frac{z^2EI}{h^2}=\frac{\mu EI}{h^2}$$

the following results are obtained:

k	0	0.2	0.4	0.6	0.8	1.0	1.5	2.0	2.5	3.0	4.0	5.0	6.0	∞
z	$\pi/2$	2.25	2.53	2.68	2.77	2.84	2.93	2.98	3.01	3.03	3.06	3.07	3.08	π
μ	2.47	5.04	6.40	7.19	7.70	8.04	8.57	8.87	9.05	9.18	9.35	9.44	9.51	9.87

(3) Example of Analysis by the Fixed Moment Method.

We shall attempt to determine by the buckling mode of a 2-span steel rigid frame shown in Figure 3.1.20.

(a) Case in which the joints do not move in lateral direction.

(i) Preparatory calculations.

The stiffness ratio calculations are exactly the same as for an ordinary rigid frame. Next, it is necessary to determine α, β but in this case, it is necessary to assume a load and to attempt to solve by the trial method, using α and β. Now, considering the case in which P = 260 t, from the relationship

$$z=l\sqrt{\frac{N}{EI}}=\sqrt{\frac{Nl^2}{EI}}$$

z is first determined and then the values of α and β corresponding to this are determined from Table 3.1.1. That is, the following computations and notations are used:

Member	N_i	I cm^4	l cm	z	α	β
AB	104	800	600	4.71	- 595	+4.007
FC	260	1,600	600	5.27	−3.554	+5.969
DE	156	1,200	600	4.72	−0.732	+4.029
BC	0	1,200	600	0	+4.000	+2.000
CD	"	1,600	900	0	+4.000	+2.000

The values of α, β in the above table are inserted in figure 3.1.4, next the carryover factor $c = \alpha/\beta$, k, the joint stiffness $\rho=\sum\alpha k$, and the distribution factor $\mu = \alpha k/\rho$ are calculated, resulting in that which is shown in Figure 3.1.21 below. /276

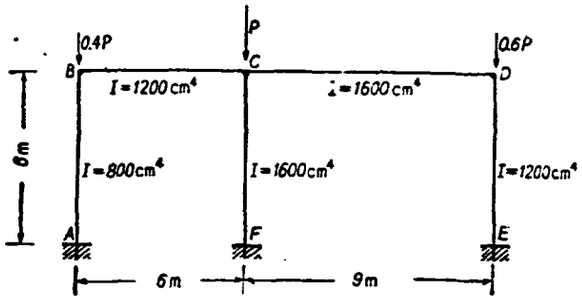

Figure 3.1.20

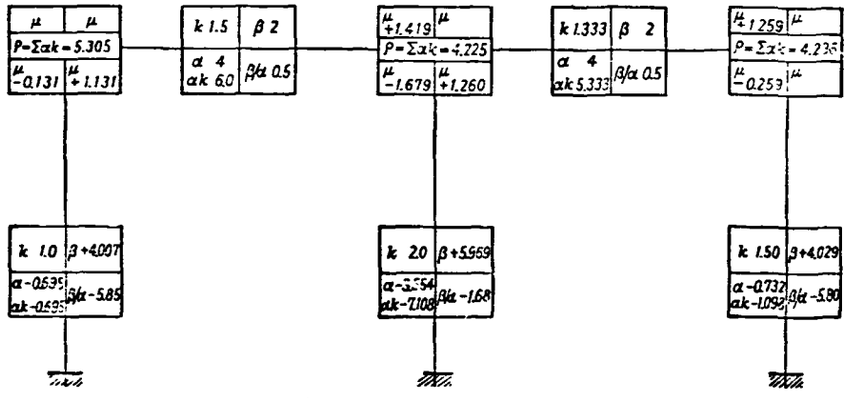

Figure 3.1.21

(ii) Graphical calculations.

Calculations are carried out in the same manner as the ordinary fixed moment method, using the distribution factor and carryover factor determined above. Figure 3.1.22 indicates the operation for this. It is clear that the unit moments applied to joint B, after one cycle, are reduced by 0.559 and converge. Consequently, in this case, it can be seen that this is safe with respect to P = 260 t.

(iii) Similarly, calculating for the case where P = 270 t, the unit moment applied to joint B after one cycle increases by 1.655 and disperses. (Graph is omitted here.) Consequently, in this case, it is unstable, and it is seen that the buckling load is between 260 t and 270 t. It can be seen that by gradually contracting this region, the P = 266 t is very close to the buckling load. The calculations in this case are performed as follows:

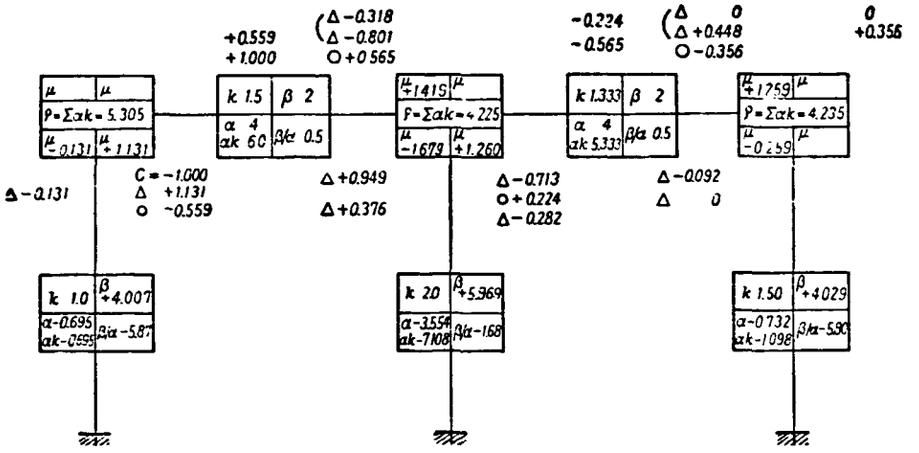

Figure 3.1.22

Member	z	α	β
AB	4.77	−0.918	+4.143
FC	5.34	−4.111	+6.397
DE	4.79	−0.992	+4.188
BC	0	+4.000	+2.000
CD	0	+4.000	+2.000

/277

The graphical calculations are as shown in Figure 3.1.23

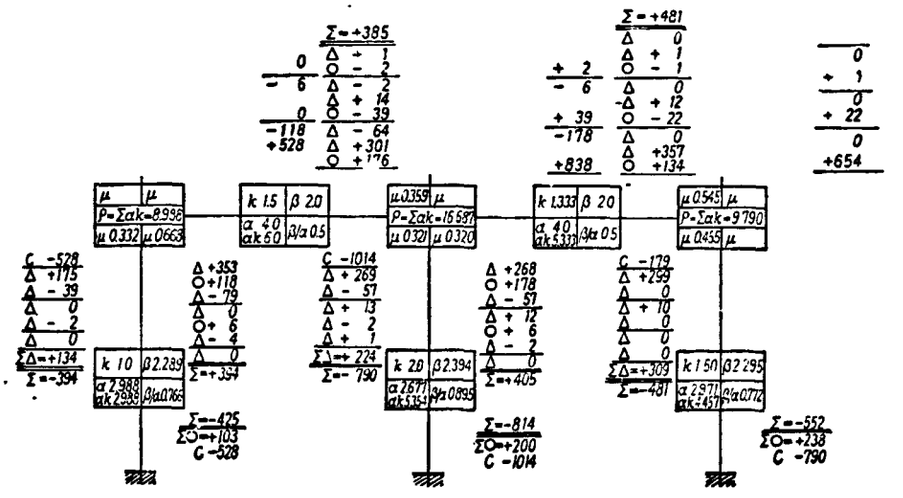

Figure 3.1.23

(b) Case in which the joints move in a lateral direction.

(i) Preparatory computations

The trial method is used even when the joints move in a lateral direction, but it can be seen that stability is reached in the vicinity of P = 80 t and that buckling occurs at P = 81 t. We shall give examples of the analysis for the case where P = 81 t.

First, as preliminary calculations, we determine α, β but this method is exactly the same as that used above.

Member	N_t	I cm^4	l cm	z	α	β
AB	32	800	600	2.62	2.988	2.289
FC	81	1,600	600	2.95	2.677	2.394
DE	49	1,200	600	2.64	2.971	2.295
BC	0	1,200	600	0	4.000	2.000
CD	0	1,600	900	0	4.000	2.000

Note: We assume E = 2,100 t/cm^2

We insert the values of α, β from the above table onto calculating paper, and then calculate and introduce the carryover factor $c=\frac{\beta}{\alpha}$, αk, $\rho=\sum \alpha k$, and $u=\frac{\alpha k}{\rho}$ (See Figure 3.1.24).

Next, we calculate the fixed end moment (α + β)k in the case when a unit deflection is applied to a column.

Member	k	$\alpha+\beta$	$(\alpha+\beta)k$
AB	1.0	5.277	5.277
FC	2.0	5.071	10.142
ED	1.5	5.266	7.898

/278

(ii) Graphic calculations

The graphical calculations for the case when the above unit deflection is given, are shown in Figure 3.1.24.

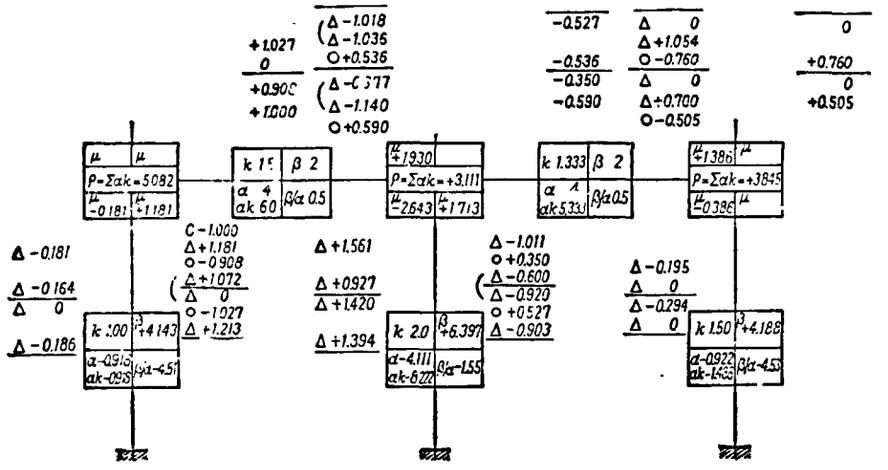

Figure 3.1.24

(iii) Determining the story-shearing force from these results

Member	$M_{upper,lower}$	$-M_{upper,lower}$	z	$\alpha+\beta$	M_F	Q
AB	−394	−425	2.62	5.277	−528	$+132/h$
FC	−814	−790	2.95	5.071	−1,014	$-136/h$
ED	−552	−480	2.64	5.266	−790	$-5/h$

$\Sigma Q=-9/h$

(iv) Similarly, solving for the case where P = 80 t

$$\Sigma Q=\Sigma\left[-\frac{1}{h}\left\{M_{AB}+M_{BA}-\frac{z^2}{\alpha+\beta}M_F\right\}\right]=+\frac{16}{h}$$

(v) Therefore, the buckling load is linearly extrapolated between (iii) and (iv) and becomes

$$P_t=80+\frac{16}{16+9}=80.6\,t$$

CONTINUOUS MEMBERS

NUMBER	GRAPH AND BOUNDARY CONDITIONS	EQUATION OR TABLE OF RESULTS	REFERENCES, NOTES
1	General Continuous Member 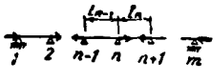	Buckling Condition Equation $\begin{vmatrix} \varphi(u_1), \Psi(u_2), \Phi(u_3) & & \\ \varphi(u_2), \Psi(u_3), \Phi(u_4) & & \\ \cdots\cdots\cdots & \cdots\cdots & \cdots\cdots \\ & \cdots\cdots & \cdots\cdots \end{vmatrix} = 0$ where $\varphi(u_n)=\frac{3}{u_n}\left(\frac{1}{\sin 2u_n}-\frac{1}{2u_n}\right)$, $\phi(u_n)=\frac{3}{2u_n}\left(\frac{1}{2u_n}-\frac{1}{\tan 2u_n}\right)$, $\Phi(u_n)=\frac{l_n}{l_{n-1}}\cdot\frac{I_{n-1}}{I_n}\cdot\cdots$, $\Psi(u_n)=2\left[\phi(u_n)+\frac{l_n}{l_{n-1}}\cdot\frac{I_{n-1}}{I_n}\cdot\psi(u_n)\right]$, $u_n=\frac{l_n}{2}\sqrt{\frac{P_n}{EI_n}}$.	23 /279
2	2-span continuous member 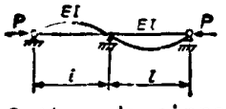 Both ends pinned	$P_k=\frac{\pi^2 EI}{l^2}$.	23
3	2-span continuous member Displaced constraints	$P_k=\frac{20.16\,EI}{l^2}=\frac{\pi^2 EI}{(0.7l)^2}$.	23
4	2-span continuous member 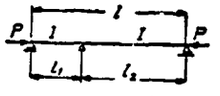 Both ends pinned, Support intermediate	Buckling condition equation $k^2 l_1 l_2 \sin kl - kl \sin kl_1 \cdot \sin kl_2 = 0$. where $k=\sqrt{\frac{P}{EI}}$.	24
	When $l_1=2l_2$ の時 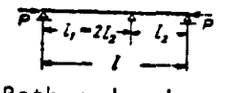 Both ends pinned Support intermediate	$P_k=33.4\frac{EI}{l^2}$.	

<table>
<tr><th>NUMBER</th><th>GRAPH AND BOUNDARY CONDITIONS</th><th>EQUATION OR TABLE OF RESULTS</th><th>REFERENCES, NOTES</th></tr>
<tr><td>5</td><td>3-span continuous member
 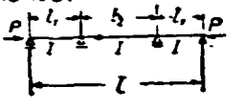

When
(1) $l_1=l_2=\frac{l}{3}$
When
(2) $l_1=\frac{l}{4}$, $l_2=\frac{l}{2}$</td><td>Buckling condition equation
$$\begin{cases}\lambda_2\cos\left(\lambda_1+\frac{\lambda_2}{2}\right)=\cos\frac{\lambda_2}{2}\cdot\sin\lambda_{1,2}\\ \lambda_1\lambda_2\sin\left(\lambda_1+\frac{\lambda_2}{2}\right)=(2\lambda_1+\lambda_2)\sin\lambda_1\cdot\sin\frac{\lambda_2}{2}.\end{cases}$$
Where
$$k=\sqrt{\frac{P}{EI}},\quad \lambda_1=kl_1,\quad \lambda_2=kl_2.$$
(1) $P_k=\pi^2\frac{EI}{l_1^2}=9\pi^2\frac{EI}{l^2}$.
(2) $P_k=80.76\frac{EI}{l^2}=8.184\pi^2\frac{EI}{l^2}$.</td><td>24</td></tr>
<tr><td>6</td><td>2-span continuous member
 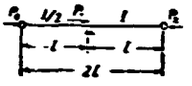
</td><td>$$(P_2)_k=\frac{x_0^2}{l^2}EI,\quad \alpha=\frac{P_1}{P_2}.$$
<table><tr><td>α</td><td>0.0</td><td>0.5</td><td>1.0</td><td>1.5</td><td>2.0</td><td>2.5</td></tr><tr><td>x_0</td><td>2.5974</td><td>2.9574</td><td>π</td><td>3.2404</td><td>3.2989</td><td>3.3326</td></tr></table><table><tr><td>α</td><td>3.0</td><td>4.0</td><td>9.0</td><td>19.0</td><td>∞</td></tr><tr><td>x_0</td><td>3.3630</td><td>3.3972</td><td>3.4561</td><td>3.4824</td><td>3.5059</td></tr></table></td><td>25</td></tr>
<tr><td>7</td><td>2-span continuous member
 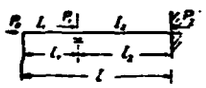

Left end free
Right end fixed</td><td>Buckling condition equation
$$\left(1+\frac{c_1}{\lambda_2-1}kx\tan kx\right)kx\tan x$$
$$=kx+(1-\beta_1)(\lambda_2-1)\left(\frac{1}{\cos x}-1\right)\tan kx.$$
Where
$$x=l_2\sqrt{\frac{P_2}{EI_2}},\quad kx=l_1\sqrt{\frac{P_0}{EI_1}},\quad k=(\lambda_2-1)\sqrt{\frac{1-\beta_1}{2c_1}}.$$
$$\beta_1=\frac{\alpha-1}{\alpha+1},\quad \alpha=\frac{P_1}{P_2},\quad c_1=\frac{I_1}{I_2},\quad \lambda_2=\frac{l}{l_2}.$$
Assuming this solution to be x_0
$$(P_2)_k=x_0^2\cdot\frac{EI_2}{l_2^2}.$$</td><td>25</td></tr>
</table>

/280

NUMBER	GRAPH AND BOUNDARY CONDITIONS	EQUATION OR TABLE OF RESULTS	REFERENCES, NOTES
8	2-span continuous member 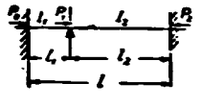 Both ends fixed	Buckling condition equation $\left(1+\frac{c_1}{\lambda_0-1}\right)kx\tan kx\cdot\tan x$ $+\sqrt{2c_1(1-\beta_1)}\left(1-\frac{\lambda_0-1}{2c_1}x^2\right)\tan kx$ $+\left(2-\frac{c_1}{\lambda_0-1}k^2x^2\right)\tan x=\frac{2}{\cos kx}(\tan x-x)$ $+\frac{\sqrt{2c_1(1-\beta_1)}}{\cos x}(\tan kx-kx)$ $+\left[2+(\lambda_0-1)(1-\beta_1)\right]x.$ The symbols are the same as in (7) in the previous column $(P_2)_k=x_0^2\cdot\frac{EI_2}{l_0^2}.$	25 /281
9	2-span continuous member 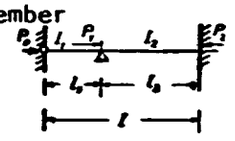 Left end pinned Right end fixed	Buckling condition equation $\tan kx\left[(\lambda_0-1)(1-\beta_1)\left(\frac{1}{\cos x}-1\right)-1\right]+kx$ $=k\tan x\left[\frac{\tan kx}{kx}\left\{\frac{x^2}{2}(\lambda_0-1)(1-\beta_1)-1\right\}+1\right].$ Symbols the same as in (7) Assuming the solution of this to be x_0 $(P_2)_k=x_0^2\cdot\frac{EI_2}{l_0^2}.$	25
10	2-span continuous member 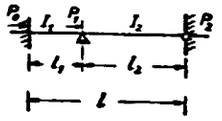 Right end fixed [sic] right end pinned	Buckling condition equation $2\frac{\tan x}{\cos kx}+kx\left(\frac{c_1}{\lambda_0-1}\frac{1}{x^2}-1\right)\sin kx\tan x$ $+\frac{x}{2}(\lambda_0-1)(1-\beta_1)$ $=\left\{2+\frac{1}{2}(\lambda_0-1)(1-\beta_1)\right\}\tan x+\frac{c_1k}{\lambda_0-1}\tan kx.$ Symbols the same as in (7) Assuming the solution of this to be x_0 $(P_2)_k=x_0^2\cdot\frac{EI_2}{l_0^2}.$	25

NUMBER	GRAPH AND BOUNDARY CONDITIONS	EQUATION OR TABLE OF RESULTS	REFERENCES, NOTES
11	2-span continuous member 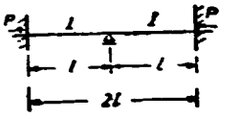 Both ends fixed	$P_k = \frac{(4.4934)^2}{l^2} EI.$	25 /282
12	2-span continuous member 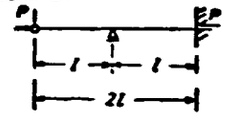 Left end fixed Right end pinned	$P_k = \frac{(3.5748)^2}{l^2} EI.$	25
13	2-span continuous member 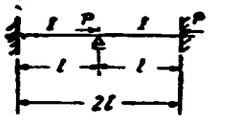 Both ends fixed	$P_k = \frac{(5.3280)^2}{l^2} EI.$	25
14	2-span continuous member 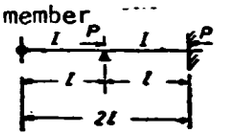 Left end pinned Right end fixed	$P_k = \frac{(5.1922)^2}{l^2} EI.$	25
15	2-span continuous member 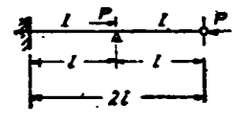 Left end fixed Right end pinned	$P_k = \frac{(3.8289)^2}{l^2} EI.$	25
16	3-span continuous member 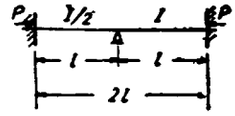 Energy method	$P_k = \frac{(3.7092)^2}{l^2} EI.$	25

NUMBER	GRAPH OR BOUNDARY CONDITIONS	EQUATION OR TABLE OF RESULTS	REFERENCES, NOTES
17	2-Span continuous member 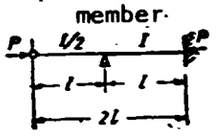 One end pinned, one end fixed	$P_k=\frac{(2.7927)^2}{l^2}EI.$	25
18	2-Span continuous member 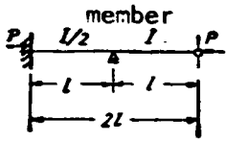 One end fixed, one end pinned	$P_k=(3.1571)^2\frac{EI}{l^2}.$	25
19	2-Span continuous member 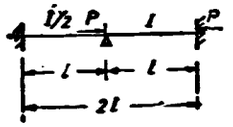 Both ends fixed	$P_k=(5.0182)^2\frac{EI}{l^2}.$	25
20	2-Span continuous member 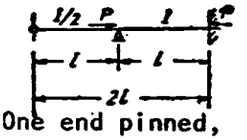 One end pinned, one end fixed	$P_k=(4.9131)^2\frac{EI}{l^2}.$	25
21	2-Span continuous member 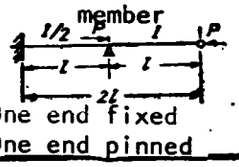 One end fixed One end pinned	$P_k=(3.5904)^2\frac{EI}{l^2}.$	25
22	4-Span continuous member 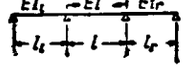	$P_k=\frac{\pi^2EI}{(\alpha l)^2}.$ $\alpha=0.5\left(1+\frac{1}{3}k_l+\frac{1}{3}k_r\right).$ Here $k_l=\frac{I}{I_l}\frac{l_l}{l}, \quad k_r=\frac{I}{I_r}\cdot\frac{l_r}{l}.$	26 (12) エネルギ法

/283

NUMBER	GRAPH AND BOUNDARY CONDITIONS	EQUATION OR TABLE OF RESULTS	REFERENCES, NOTES
23	Continuous member with overhang 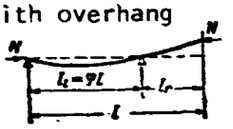	When $l_k = \gamma \cdot l$, r is as shown in the table below	27 /284

φ	0	0.1	0.2	0.25	0.3	0.4	0.5
γ	2.000	1.870	1.736	1.668	1.603	1.473	1.348

φ	0.6	0.7	0.75	0.8	0.9	1.0
γ	1.231	1.130	1.089	1.055	1.012	1.000

Between $0<\psi<0.5$, approximately

$$\gamma=2(1-0.65\varphi).$$

24	2-span continuous member 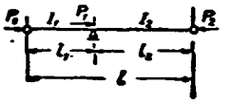 Both ends pinned	Buckling condition equation $$\left[1+\frac{1}{2}(\lambda_2-1)(1-\beta_1)\right]\frac{\tan kx\tan x}{x}$$ $$=k\tan x+\frac{1}{2}(\lambda_2-1)(1-\beta_1)\tan kx.$$ Where $$x=i_2\sqrt{\frac{P_2}{EI_2}},\qquad kx=l_1\sqrt{\frac{P_0}{EI_1}}.$$ $$k=(\lambda_2-1)\sqrt{\frac{1-\beta_1}{2c_1}},\qquad \beta_1=\frac{\alpha-1}{\alpha+1}.$$ $$\alpha=\frac{P_1}{P_0},\qquad c_1=\frac{I_1}{I_2},\qquad \lambda_2=\frac{l}{l_0}.$$ The solution under these conditions if x_0 is given is: $$(P_2)_k=x_0^2\cdot\frac{EI_2}{l_0^2}.$$	25
25	2-span continuous member 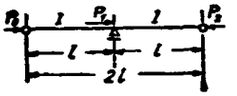 Both ends pinned	$$(P_2)_k=\frac{x_0^2}{l^2},\qquad \alpha=\frac{P_1}{P_0}.$$	25

α	0.0	0.5	1.0	1.5	2.0	2.5
x_0	π	3.3934	3.5014	3.5579	3.5834	3.6149

α	3.0	4.0	9.0	19.0	∞
x_0	3.6312	3.6643	3.6917	3.7089	3.7264

NUMBER	GRAPH AND BOUNDARY CONDITIONS	EQUATION OR TABLE OF RESULTS	REFERENCES, NOTES
26	2-span continuous member 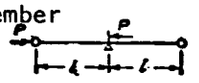 Both ends pinned	$P_k=13.91\frac{EI}{l^2}$.	28 Buckling deflection angle
27	2-span continuous member 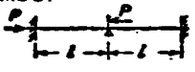 Both ends fixed	$P_k=28.4\frac{EI}{l^2}$.	28 As above
28	2-Span continuous member with movable intermediate support points 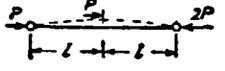 Both ends pinned	$P_k=1.638\frac{EI}{l^2}$.	28 As above
29	2-Span continuous member with movable intermediate support points 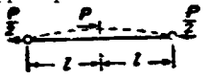 Both ends pinned	$P_k=2\pi^2\frac{EI}{l^2}$.	28 As above
30	2-Span continuous member with movable intermediate support points 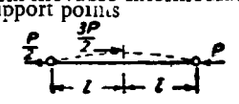 Both ends pinned	$P_k=7.044\frac{EI}{l^2}$.	28 As above
31	2-span continuous member 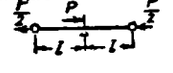 Both ends pinned	$P_k=30.9\frac{EI}{l^2}$.	29 Deflection angle method
32	2-span continuous member 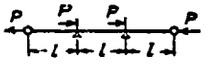 Both ends pinned	$P_k=14.06\frac{EI}{l^2}$.	29 As above

/285

NUMBER	GRAPH AND BOUNDARY CONDITIONS	EQUATION OR TABLE OF RESULTS	REFERENCES NOTES
33	4-span continuous member 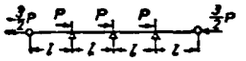 Both ends pinned	$P_k=9.07\frac{EI}{l^2}$.	29 Buckling Deflection Angle Method /286
34	5-span continuous member 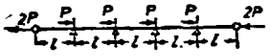 Both ends pinned	$P_k=6.55\frac{EI}{l^2}$.	29 As above
35	2-span continuous member 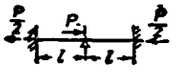 Both ends fixed	$P_k=62.9\frac{EI}{l^2}$.	29 As above
36	3-span continuous member 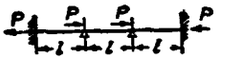 Both ends fixed	$P_k=27.88\frac{EI}{l^2}$.	29 As above
37	4-span continuous member 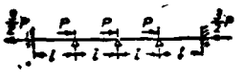 Both ends fixed	$P_k=16.76\frac{EI}{l^2}$.	29 As above
38	5-span continuous member 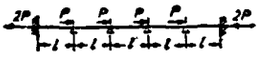 Both ends fixed	$P_k=11.49\frac{EI}{l^2}$.	29 As above

NUMBER	GRAPH AND BOUNDARY CONDITIONS	EQUATION OR TABLE OF RESULTS	REFERENCES, NOTES
39	Continuous member on elastic support points 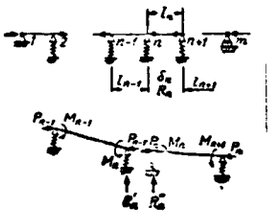	α: spring constant δ: deflection R: reaction From $R_n'+R_n''=R_n=\alpha_n\cdot\delta_n$ $$\alpha_n\delta_n=\left(\frac{P_{n-1}}{l_{n-1}}+\frac{P_n}{l_n}\right)\delta_n-\frac{P_{n-1}}{l_{n-1}}\delta_{n-1}+\frac{P_n}{l_n}\delta_{n+1}-\left(\frac{1}{l_{n-1}}+\frac{1}{l_n}\right)M_n. \quad (39\cdot1)$$ The three-moment equation for a continuous beam is $$M_{n-1}\phi(u_{n-1})+2M_n\left\{\Psi(u_{n-1})+\frac{l_n}{l_{n-1}}\cdot\frac{I_{n-1}}{I_n}\Psi(u_n)\right\}+M_{n+1}\cdot\frac{l_n}{l_{n-1}}\cdot\frac{I_{n-1}}{I_n}\varphi(u_n)=\frac{6EI_{n-1}}{l_{n-1}}\left\{\frac{\delta_n-\delta_{n-1}}{l_{n-1}}-\frac{\delta_{n+1}-\delta_n}{l_n}\right\}. \quad (39\cdot2)$$ where $$\phi(u_n)=\frac{3}{u_n}\left(\frac{1}{\sin 2u_n}-\frac{1}{2u_n}\right),$$ $$\Psi(u_n)=\frac{3}{2u_n}\left(\frac{1}{2u_n}-\frac{1}{\tan 2u_n}\right),$$ $$u_n=\frac{l_n}{2}\sqrt{\frac{P_n}{EI_n}}.$$ If equations (39.1, 39.2) are determined for each reaction point δ is eliminated, a simultaneous equation is obtained for M. Assuming the matrix for M to be Δ, the buckling load is obtained from Δ = 0.	23 /287
40	Continuous member on elastic support points 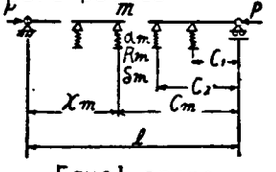 Equal spans α is constant	When the equal span continuous member shown in the figure to the left buckles with each support point as a point of bending. $$P_k=\frac{m^2\pi^2EI}{l^2}.$$ The necessary spring stiffness in this case is $$\alpha=\frac{mP_k}{\beta l}.$$ Where m: number of spans; α: spring constant; β: coefficient related to number of spans (See below table)	23

m	2	3	4	5	6
β	0.500	0.333	0.293	0.276	0.268

m	7	9	11
β	0.263	0.258	0.255

NUMBER	GRAPH AND BOUNDARY CONDITIONS	EQUATION OR TABLE OF RESULTS	REFERENCES, NOTES
41	Continuous member on elastic support point Degree of compressive force	$\left(\frac{q_0 \cdot l}{4}\right)_k = \frac{\pi^2 EI}{l_k^2}$. $\frac{\beta l^4}{16EI}$: 0 | 5 | 10 | 15 | 22.8 | 56.5 $\frac{l_k}{l}$: 0.696 | 0.524 | 0.443 | 0.369 | 0.363 | 0.324 $\frac{\beta l^4}{16EI}$: 100 | 162.8 | 200 | 300 | 500 | 1,000 $\frac{l_k}{l}$: 0.290 | 0.259 | 0.246 | 0.225 | 0.204 | 0.174 Here =basic coefficient *1 when assuming that the beam is on an elastic bed	23 *1 Assuming that each reaction point has an equal spring constant and assuming that the distance between support points is a, $\beta=\alpha/a$. Only when the buckling half wave length is considerably greater than the distance between support points is it possible to replace the elastic support point for the elasticity base corresponding to it. /288
42	Continuous rigid member based on elastic couplings 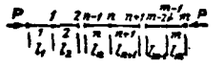 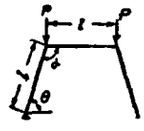 (a) 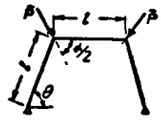 (b)	Generally $M_n = -D_n(R_{n+1} - R_n)$ *2. R_{n+1}, R_n : n+1 member, displacement angle of part of member n D_n : n joint stiffness of joint Buckling condition equation $\begin{vmatrix} Pl_1 - D_1 & D_1 & & \\ D_1 & Pl_2 - (D_1+D_2) & D_2 & \\ & \cdots\cdots\cdots & & \\ & & D_{m-1} & Pl_m - D_{m-1} \end{vmatrix} = 0.$ when $l_1 = l_2 = \cdots = l_m = l$ $D_1 = D_2 = \cdots = D_{m-1} = D$ $P_k = 2\left(1 - \cos\frac{\pi}{m}\right)\frac{D}{l}$. e.g., when (a): $P_k = \frac{D}{l} \cdot \frac{(1+2\cos\theta)^2 \sin\theta}{1+2\cos^3\theta}$. when (b) $P_k = \frac{D}{l} \cdot \frac{2(1+2\cos\theta)^2}{1+2\cos^3\theta} \sin\frac{\theta}{2}$.	30 *1 If is assumed that each part of the continuous column is a rigid body. The bending moment of the joints is assumed to be proportional to the difference in the displacement angle of the parts of 2 adjoining members.
BUILT-UP MEMBERS			
番号	図及び境界条件	結 果 の 式 又 は 表	文献・備考
43	Isoceles 2-member truss 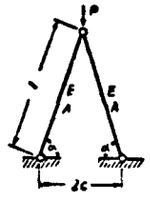	$P_k = 2EA\cos^2\alpha \sin\alpha$. or Smaller value in 2 EA $\sin^3\alpha$	31 Based on hypothetical work method

NUMBER	GRAPH AND BOUNDARY CONDITIONS	EQUATION OR TABLE OF RESULTS	REFERENCES, NOTES
44	Isoceles 3-member truss 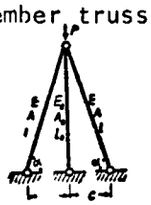	When $E_0A_0 = EA$ $$P_k = EA\left(1-\frac{a_0}{l_0}\right)(1+2\sin^3\alpha).$$ or the smaller side in $$EA\left(1-\frac{a}{l}\right)\frac{1+2\sin^3\alpha}{\sin^3\alpha}$$ where a, a_0 = length of l, l_0 when sustaining load P_k.	31 Based on hypothetical work method /289
45	+ truss 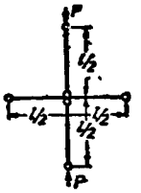	$l_k = 0.907\,l$.*1 The bending stiffness of the member is equal both vertically and horizontally. The same is true for the six columns below.	*1 The buckling inside and outside of the structure surface is taken into consideration and the smallest buckling value is taken. The same is true for (46), (47), (48), (49), (50), and (51).
46	+ truss	$l_k = 0.500\,l$.	32
47	+ truss 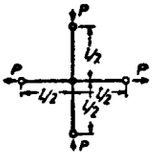	$l_k = 0.713\,l$.	32
48	+ truss 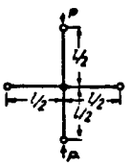	$l_k = 0.393\,l$.	32

NUMBER	GRAPH AND BOUNDARY CONDITIONS	EQUATION OR TABLE OF RESULTS	REFERENCES NOTES
49	X truss (member intersecting with tension member 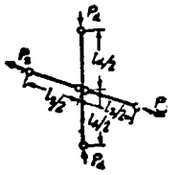	$\frac{l}{l_k}=\sqrt{1-\frac{1}{4}\frac{P_s}{P_d}\frac{l_d}{l_s}\left(3+\frac{\pi^2}{\varphi_d^2}\right)}$ and ≥ 0.5 $\fallingdotseq\sqrt{1-\frac{3}{4}\frac{P_s}{P_d}\frac{l_d}{l_s}}$. where $\varphi_d=\frac{l_d}{2}\sqrt{\frac{P_d}{EI_d}}$.	33
50	X truss (member intersecting with tension member) 	$l_k=l\sqrt{1-0.75\frac{P_s}{P_1}}$. P_s/P_1: 0 | 0.1 | 0.2 | 0.3 | 0.4 | 0.5 l/l_k: 1.000 | 0.959 | 0.916 | 0.871 | 0.824 | 0.774 P_s/P_1: 0.6 | 0.7 | 0.8 | 0.9 | 1.0 l/l_k: 0.722 | 0.668 | 0.611 | 0.554 | 0.500	33
51	X truss (member intersecting with tension member) 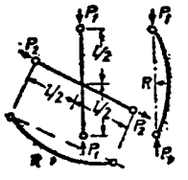	Buckling condition equation $\tanh\left(k\sqrt{\frac{P_s}{P_1}}\right)=\frac{P_s}{P_1}\sqrt{\frac{P_s}{P_1}}\left\{\left(\frac{P_1}{P_s}-1\right)k+\tan k\right\}$. P_s/P_1: 0 | 0.2 | 0.4 | 0.6 | 0.8 | 1.0 l_k/l: 0.713 | 0.644 | 0.571 | 0.500 | 0.500 | 0.500 where $k=\frac{\alpha l}{2}$, $\alpha=\sqrt{\frac{P_1}{EI}}$. when $P_s/P_1>0.5$, buckling inside structure plane	33
52	Truss type built-up member 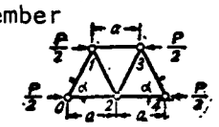 Chord member-A,E,a Diagonal member-A',E',a'	$I=\frac{1}{2}\left(\frac{a}{4}\tan\alpha\right)^2$. $L=\frac{3}{2}a$ とすれば For symmetrical buckling $P_k=\frac{36}{3+2\omega}\cdot\frac{EI}{L^2}$. For non-symmetrical buckling $P_k=\frac{72}{1+\omega}\cdot\frac{EI}{L^2}$. where $\omega=\frac{EA\,a'}{E'A'a}\cdot\frac{1}{\cos^2\alpha}$. when $\omega=0$, and the inclined member is completely rigid $P_k=12\frac{EI}{L^2}$ or $72\frac{EI}{L^2}$.	34 Based on hypothetical work method

/290

NUMBER	GRAPH AND BOUNDARY CONDITIONS	EQUATION OR TABLE OF RESULTS	REFERENCES NOTES
53	General truss type built-up member 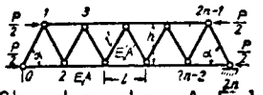 Chord member-A,E,I Diagonal member-A',E',I' $I=A\cdot\frac{h^2}{2}$ $L=\left(n-\frac{1}{2}\right)l$	a) When the diagonal member is extremely stiff, and the number of components is limited $P_k=k^2\pi^2\frac{EI}{L^2}$. where $k^2=\left(\frac{4n-2}{\pi}\tan\frac{\pi}{4n-2}\right)^2$, $L=\left(n-\frac{1}{2}\right)l$. k is as shown on table below b) When the diagonal member is weak and the number of components is large $P_k=\pi^2\frac{EI}{L^2}\cdot\frac{1}{1+\frac{\pi^2}{4n}\omega}$. where $\omega=\frac{EA'l'}{E'A'l}\cdot\frac{1}{\cos^2\alpha}$. c) When the diagonal member is weak and the number of components is limited. $P_k=E'A'\sin^2\alpha\cdot\cos\alpha\cdot\frac{1}{\cos^2\frac{\pi}{2n}}$ $\fallingdotseq E'A'\sin^2\alpha\cdot\cos\alpha\left(\frac{\pi^2}{1+4n^2}\right)$. d) In the general case $P_k=\frac{k^2}{1+\lambda\omega}\pi^2\frac{EI}{L^2}$. where $k^2=\left(\frac{4n-2}{\pi}\tan\frac{\pi}{4n-2}\right)^2$, $\lambda=\left(2\tan\frac{4}{4n-2}\cos\frac{\pi}{2n}\right)^2$, $\omega=\frac{EA}{E'A'}\cdot\frac{1}{2\cos^2\alpha}$. k^2, λ are shown in table below.	34 Based on hypothetical work method /291

n	2	3	4	5	10	∞
k^2	1.216	1.070	1.035	1.020	1.004	1.000

n	2	3	4	5	10	∞
k^2	1.216	1.070	1.035	1.020	1.004	1.000
λ	0.3667	0.3167	0.1778	0.1125	0.0269	0.0000

NUMBER	GRAPH AND BOUNDARY CONDITIONS	EQUATION OR TABLE OF RESULTS	REFERENCES NOTES
54	Rigid frame type built-up member 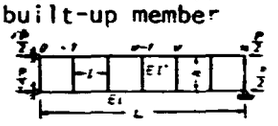	writing $\kappa=\frac{E'I'}{EI}\cdot\frac{l}{h}$ When n is large and κ is small if $\bar{I}=2I$ $P_k=\pi^2\frac{E\bar{I}}{L^2}+12\frac{E'I'}{hl}$.	34
55	Truss type built-up member 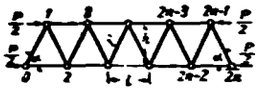 Chord member-E,A,I Diagona. member- E',A',l'	a) When the number of components is large $P_k=\pi^2\frac{E\bar{I}}{L^2}\left\{1-\frac{1}{12}\cdot\frac{\pi^2}{(2n-1)^2}\frac{Eh^2}{\bar{I}}(1+6\omega)\right\}$. Here $\omega=\frac{EA}{E'A'}\cdot\frac{l'}{l}\cdot\frac{1}{\cos^3\alpha}$. $\bar{I}=2\left(I+\frac{Ah^2}{4}\right)$, $I=A\cdot\frac{h^2}{2}$. $L=\left(n-\frac{1}{2}\right)L$ Approximately $P_k=\pi^2\frac{E\bar{I}}{L^2}$. b) When the number of components is large and the diagonal member is weak. $P_k=\pi^2\frac{EI}{L^2}\cdot\frac{1}{1+\frac{\pi^2}{4n^2}\cdot\frac{\omega}{1+\rho}}$. $\rho=\frac{4I}{Ah^2}$. when $\omega\to\infty$ $\frac{P_k}{2}=\pi^2\frac{EI}{(nl)^2}$ or $\frac{P_k}{2}=\pi^2\frac{EI}{((n-1)l)^2}$.	34

/292

NUMBER	GRAPH AND BOUNDARY CONDITIONS	EQUATION OR TABLE OF RESULTS	REFERENCES, NOTES
56	Truss type built-built-up member	When the connecting members are extremely stiff and the number of components is large $$P_k=\pi^2\frac{EI}{L^2}\left(I-\frac{1}{48}\cdot\frac{\pi^2}{n^2}\frac{Ah^2}{\bar{I}}\right).$$ where $$\bar{I}=2\left(I+A\frac{h^2}{4}\right).$$ Approximately $$P_k=\pi^2\frac{E\bar{I}}{L^2}.$$	34
57	Truss type built-built-up member & tubular col. 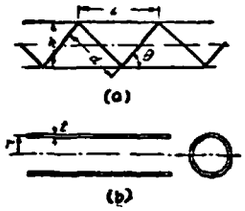 (a) (b)	Reduction of moment of inertia due to bending $$I=I_0\left(1-\frac{\beta}{R^2}\right).$$ $\frac{1}{R}$ = Curvature of buckled frame; I_0 = geometric moment of inertia of frame prior to buckling. a) Warren type combined member $$\beta^2=\frac{td^2}{2h^2}\cdot\frac{A_f}{A_d}-\frac{t^2}{16}\fallingdotseq\frac{L_d^2}{2h^2}\cdot\frac{A_f}{A_d}.$$ Where A_f: 弦材の断面積, A_d: 斜材の断面積. Buckling condition equation $$\frac{\beta^2}{a^2}=\frac{2}{3}.$$ $$\frac{1}{a^2}=\frac{P}{EI_0}\fallingdotseq\frac{\pi^2}{L^2}$$ Or condition of no buckling (L: column length) $$\frac{A_d}{A_f}\geq\frac{6\pi^2\cos\theta}{\lambda^2\sin^4\theta}.$$ b) Tubular column $$\beta^2=\frac{r^2(12r^2+t^2)}{2t^2(4r^2+t^2)}.$$ Condition of no buckling[*2] $$\frac{t^2}{r^2}\geq\frac{1}{2}\cdot\left\{\sqrt{16+30\pi^2\left(\frac{r}{L}\right)^2+\frac{9\pi^2}{16}\left(\frac{r}{L}\right)^4}-4+\frac{3\pi^2}{4}\left(\frac{r}{L}\right)^2\right\}.$$ when $\frac{r}{L}$ is small $$\frac{t}{r}\geq\frac{3\pi}{2}\left(\frac{r}{L}\right)\left\{1-\frac{3\pi^2}{16}\left(\frac{r}{L}\right)^2\right\}.\fallingdotseq\frac{3\pi}{2}\left(\frac{r}{L}\right).$$ Taking the influence of shear stress into account $$P_k=\frac{P_e}{1+\frac{nP_e}{2\pi rtG}},\quad P_e=\frac{\pi^2EI_0}{L^2}.$$ n: Correction coefficient of cross-section	35 *1 We assume as an approximation equation for the vicinity of the buckling critical point of the differential equation for the deflection curve to be $$\frac{d^2y}{dx^2}+\frac{y}{a^2}\cdot\left(1+\frac{\beta^2y^2}{a^4}\right)=0.$$ If this is solved, as a non-buckling condition $$\frac{\beta^2}{a^2}\leq\frac{2}{3}.$$ *2 More accurate. More accurately, the conditions for the non-occurence of buckling refers to the conditions under which unstable buckling does not occur; i e. the conditions under which no buckling will occur such that there is a decrease in external forces with respect to an increase in displacement.

NUMBER	GRAPH AND BOUNDARY CONDITIONS	EQUATION OR TABLE OF RESULTS	REFERENCES, NOTES
58	Truss type built-up member	Below are given the results of calculations which take into account the shear forces for a combination square column having the planes of structure shown in the figure to the left on the sides.	35 See note *2 on previous page in this column on "Conditions for the Non-occurrence of Buckling."

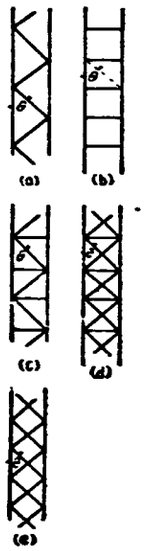

	Buckling Limit load	conditions where buckling does not occur: Buckling within plane of frame	Buckling in direction of diagonal
(a)	$\frac{\pi^2 E I_0}{L^2}\cdot\frac{1}{1+\frac{2\pi^2}{\lambda^2\sin^2\theta\cos\theta}\cdot\frac{A_f}{A_d}}$	$\frac{A_d}{A_f}\geqq\frac{6\pi^2\cos\theta}{\lambda^2\sin^4\theta}$	$\frac{A_d}{A_f}\geqq\frac{\pi^2\lambda_d^2\cos\theta}{2\lambda^2\sin^2\theta}$
(b)	$\frac{\pi^2 E I_0}{L^2}\cdot\frac{1}{1+\frac{\pi^2\lambda_h^2\cos\theta}{6\lambda^2\sin\theta}\cdot\frac{A_f}{A_h}+\frac{\pi^2\lambda_h^2}{12\lambda^2}}$	$\frac{A_h}{A_f}\geqq\frac{6\pi^2\cos\theta}{\lambda^2\sin\theta}$	$\frac{A_h}{A_f}\geqq\frac{\pi^2\lambda_h^2\cos\theta}{2\lambda^2\sin^2\theta}$
(c)	$\frac{\pi^2 E I_0}{L^2}\cdot\frac{1}{1+\frac{\pi^2}{\lambda^2\sin^2\theta\cos\theta}\cdot\frac{A_f}{A_d}}$	$\frac{1}{A_f}(A_h+A_d\sin^3\theta)\geqq\frac{6\pi^2\cos\theta}{\lambda^2\sin\theta}$	$\frac{A_d}{A_h}\left(\frac{A_h}{A_d\lambda_d^2}+\frac{2\sin\theta}{\lambda_d^2}\right)\geqq\frac{\pi^2\cos\theta}{\lambda^2\sin\theta}$
(d)	$\frac{\pi^2 E I_0}{L^2}\cdot\frac{1}{1+\frac{\pi^2}{\lambda^2\sin^2\theta\cos\theta}\cdot\frac{A_f}{A_d}}$	$\frac{1}{A_f}(A_h+2A_d\sin^3\theta)\geqq\frac{6\pi^2\cos\theta}{\lambda^2\sin\theta}$	$\frac{A_d}{A_f}\left(\frac{A_h}{A_d\lambda_d^2}+\frac{2\sin\theta}{\lambda_d^2}\right)\geqq\frac{\pi^2\cos\theta}{\lambda^2\sin\theta}$
(e)	$\frac{\pi^2 E I_0}{L^2}\cdot\frac{1}{1+\frac{\pi^2}{\lambda^2\sin^2\theta\cos\theta}\cdot\frac{A_f}{A_d}}$	$\frac{A_d}{A_f}\geqq\frac{3\pi^2\cos\theta}{\lambda^2\sin^4\theta}$	$\frac{A_d}{A_f}\geqq\frac{\pi^2\lambda_d^2\cos\theta}{4\lambda^2\sin\theta}$

Below are the results of calculations which take into account the shear forces for a combination triangular column having the plane of structure shown in the diagram on the sides.

	buckling limit load	conditions under which buckling does not occur
(a)	$\frac{\pi^2 E I_0}{L^2}\cdot\frac{1}{1+\frac{2\pi^2}{\lambda^2\sin^2\theta\cos\theta}\cdot\frac{A_f}{A_d}}$	$\frac{A_d}{A_f}\geqq\frac{9\pi^2\cos\theta}{\lambda^2\sin^4\theta}$
(b)	$\frac{\pi^2 E I_0}{L^2}\cdot\frac{1}{1+\frac{\pi^2\lambda_h^2\cos\theta}{6\lambda^2\sin\theta}\cdot\frac{A_f}{A_h}+\frac{\pi^2\lambda_h^2}{12\lambda^2}}$	$\frac{A_h}{A_f}\geqq\frac{9\pi^2\cos\theta}{\lambda^2\sin\theta}$
(c)	$\frac{\pi^2 E I_0}{L^2}\cdot\frac{1}{1+\frac{2\pi^2}{\lambda^2\sin^2\theta\cos\theta}\cdot\frac{A_f}{A_d}}$	$\frac{1}{A_f}(A_h+A_d\sin^3\theta)\geqq\frac{9\pi^2\cos\theta}{\lambda^2\sin\theta}$
(d)	$\frac{\pi^2 E I_0}{L^2}\cdot\frac{1}{1+\frac{\pi^2}{\lambda^2\sin^2\theta\cos\theta}\cdot\frac{A_f}{A_d}}$	$\frac{1}{A_f}(A_h+2A_d\sin^3\theta)\geqq\frac{9\pi^2\cos\theta}{\lambda^2\sin\theta}$
(e)	$\frac{\pi^2 E I_0}{L^2}\cdot\frac{1}{1+\frac{\pi^2}{\lambda^2\sin^2\theta\cos\theta}\cdot\frac{A_f}{A_d}}$	$\frac{A_d}{A_f}\geqq\frac{9\pi^2\cos\theta}{2\lambda^2\sin^4\theta}$

Here f, d, h are subscripts which indicate respectively chord member (flange), diagonal member and horizontal member

$\lambda, \lambda_h, \lambda_f$ slenderness ratios of columns and diagonal member, respectively.

The other symbols are the same as in the previous column (57).

NUMBER	GRAPH AND BOUNDARY CONDITIONS	EQUATION OR TABLE OF RESULTS	REFERENCES NOTES
59	Truss-type built-up member 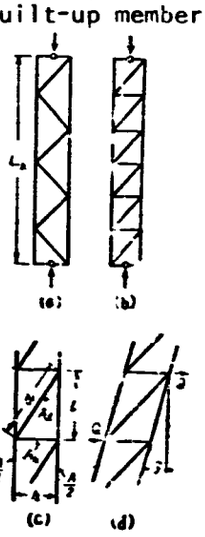 (a) (b) (c) (d)	Solution which takes into consideration shear force and bending. $\lambda^2_{id}=\lambda^2\left(1+\frac{P_k}{S}\right)^{*1}$ $P_k=\frac{\pi^2 EI}{l^2}$ $S=$ shearing strength $\frac{1}{S}=\frac{d^2}{lh^2EA_d}+\frac{h}{lEA_h}$ $\lambda^2_{id}=\lambda^2\left\{1+\frac{P_k}{E}\left(\frac{d^2}{A_d lh^2}+\frac{h}{A_h l}\right)\right\}$ Especially within the elasticity range. $\lambda^2_{id}=\lambda^2+\pi^2\left\{\frac{A}{A_d}\cdot\frac{d^2}{lh^2}+\frac{A}{A_h}\cdot\frac{h}{l}\right\}$	36 *1 The solution of the differential equation which takes into consideration the shear force and bending is the slenderness ratio of the entire column when the effect of the shear force is not taken into consideration. This is the same in (60) and (61) below.
60	Truss type built-up member (case in which the centerline of the lattice does not match the axis of the center of gravity of the flange) 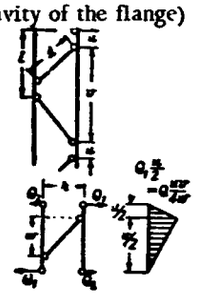	$\lambda^2_{id}=\lambda^2\left\{1+\frac{P_k}{E}\cdot\frac{d^2}{A_d lh^2}\left(\frac{e}{w}\right)^2\right\}+\left(\frac{v}{w}\right)^2\lambda_1^2$. here $\lambda_1=u/i_0$, i_0 = radius of rotation of flange A = flange cross-section area A_d = cross-section area of diagonal member Within the elasticity range $\lambda^2_{id}=\lambda^2+\pi^2\frac{A}{A_d}\frac{d^2}{lh^2}\left(\frac{l}{w}\right)^2+\left(\frac{v}{w}\right)^2\lambda_1^2$.	36
61	Truss type built-up member (case in which the centerline of the lattice does not match the axis of the center of gravity of the flange) 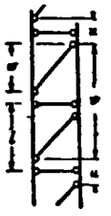	$\lambda^2_{id}=\lambda^2\left\{1+\frac{P_k}{E}\left(\frac{d^2}{A_d lh^2}+\frac{h}{A_h l}\right)\left(\frac{l}{w}\right)^2\right\}+\left(\frac{v}{w}\right)^2\lambda_1^2$. $\lambda_1=u/i_0$. Within the elasticity range $\lambda^2_{id}=\lambda^2+\pi^2\left(\frac{d^2}{A_d lh^2}+\frac{h}{A_h l}\right)\left(\frac{l}{w}\right)^2+\left(\frac{v}{w}\right)^2\lambda_1^2$.	36

NUMBER	GRAPH AND BOUNDARY CONDITIONS	EQUATION OR TABLE OF RESULTS	REFERENCE /296 NOTES
62	Compound lattice type built-up member 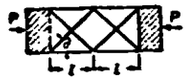 2 sections, both ends fixed 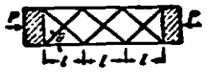 3 sections, both ends fixed 3 sections, both ends pinned at joints 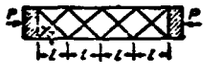 4 sections, both ends fixed 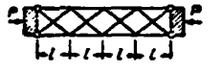 4 sections, both ends pinned at joints	i) 2 sections, both ends fixed Buckling conditions $Z=2\pi$ or $\frac{\sigma}{E}\cdot\frac{1+K\cos^2\theta}{K\sin^2\theta\cos\theta}=\frac{Z(1+\cos Z)-2\sin Z}{Z(1+\cos Z)}$. Here $K=\frac{A_d}{A_f}=\frac{\text{diagonal member cross-section area}}{\text{chord member cross-section area}}$ $Z=\frac{l}{k}=l\sqrt{\frac{P}{2EI_f}}=l\sqrt{\frac{\sigma}{E}}$. I_f=Geometric moment of inertia of flange σ=平均応力度$=\frac{P}{2A_f}$. Range of Z_k $2\pi>Z_k>\pi$ [1]. If $\left(l_k=\tau l,\ \tau=\frac{\pi}{Z_k}\right)$ ii) 3 sections a) Both ends fixed Buckling conditions $Z=2\pi$ $\frac{\sigma}{E}\frac{1+K\cos^2\theta}{K\sin^2\theta\cos\theta}=\frac{6Z\cos Z+3Z-9\sin Z}{2Z\cos Z+Z}$. Range of Z_k: $1{,}227\pi>Z_k>\frac{2\pi}{3}$ [2]. b) Both ends pinned at joints Buckling conditions $Z=\pi$ or $\frac{\sigma}{E}\frac{1+K\cos^2\theta}{K\sin^2\theta\cos\theta}=\frac{3(2Z\cos Z-Z-\sin Z)}{Z(2\cos Z-1)}$. Range of Z_k $\pi>Z_k>\frac{\pi}{3}$ [3]. iii) 4 sections a) Both ends fixed Buckling conditions $Z=2\pi$ or $\begin{vmatrix}(6-2\beta)\frac{Z\cos Z}{\sin Z}+(2-2\beta)\frac{Z}{\sin Z}-8 & 4\left(\frac{Z\cos Z}{\sin Z}-1\right)\\ 8\frac{Z\cos Z}{\sin Z}+(2+2\beta)\frac{Z}{\sin Z}-10 & (6-2\beta)\frac{Z\cos Z}{\sin Z}-6\end{vmatrix}=0.$ Range of Z_k $1{,}430\pi>Z_k>\frac{\pi}{2}$ [4]. b) Both ends pinned at joints Buckling conditions $Z=\pi$ or $\begin{vmatrix}\frac{4Z}{\sin Z}-(6-2\beta)\frac{Z\cos Z}{\sin Z}+2 & (3-\beta)\frac{Z}{\sin Z}-\frac{4Z\cos Z}{\sin Z}+1\\ (6-2\beta)\frac{Z}{\sin Z}-\frac{8Z\cos Z}{\sin Z}+2 & \frac{4Z}{\sin Z}-(6-2\beta)\frac{Z\cos Z}{\sin Z}+2\end{vmatrix}=0.$ Range of Z_k $\pi>Z_k>\frac{\pi}{4}$ [5]. Where $\beta=\frac{\sigma}{E}\cdot\frac{1+K\cos^2\theta}{K\sin^2\theta\cos\theta}$.	37 *1,2,3,4,5 As long as $K=\frac{A_d}{A_f}$ is not extremely small, Z_k has a value close to the upper limit value.

NUMBER	GRAPH AND BOUNDARY CONDITIONS	EQUATION OR TABLE OF RESULTS	REFERENCES, /297 NOTES
62	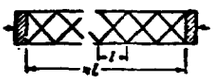 n sections, both ends fixed 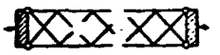 n sections, both ends pinned at joints	iv) n sections a) Both ends fixed Lower limit: $(Z_k)_{min}=\frac{2\pi}{n}$. Upper limit value:*6 Values of Z satisfying the relations below. $\begin{cases} n \text{ is an even number} & \cos\frac{2\pi}{n}=-\frac{Z\cos Z-\sin Z}{Z-\sin Z}, \\ n \text{ is an odd number} & \cos\frac{\pi}{n}=-\frac{Z\cos Z-\sin Z}{Z-\sin Z}. \end{cases}$ b) Both ends pinned at joints Lower limit value $(Z_k)_{min}=\frac{\pi}{n}$. Upper limit value*7: Values of Z which satisfy the relations below. $\begin{cases} n \text{ is an even number} & \cos\frac{\pi}{n}=-\frac{Z\cos Z-\sin Z}{Z-\sin Z}, \\ n \text{ is an odd number} & \cos\frac{2\pi}{n}=-\frac{Z\cos Z-\sin Z}{Z-\sin Z}. \end{cases}$	37 See *6 *7 in the remarks on the previous page.
63	Torsional buckling of I type built-up member. 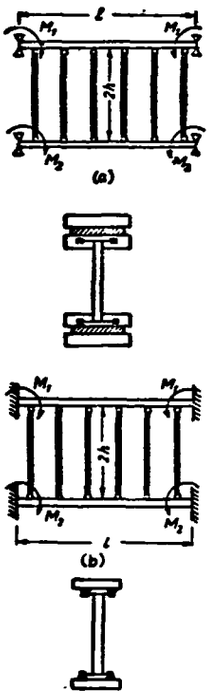	Table 63.1	38

$\frac{m_2}{m_1}$	Values of m_1		
	$b=0$	$b=1$	$b=100$
1	3.142	3.587	17.603
3/4	3.553	4.051	19.563
1/2	3.974	4.497	20.480
1/4	4.310	4.806	19.840
0	4.443	4.855	18.012
−1/4	4.310	4.619	15.793
−1/2	3.974	4.203	13.710
−3/4	3.553	3.736	11.936
−1	3.142	3.297	10.482

Table 63.2

$\frac{m_2}{m_1}$	Values of m_1		
	$b=0$	$b=1$	$b=100$
1	6.283	6.917	19.460
3/4	7.109	—	—
1/2	7.948	—	—
1/4	8.620	—	—
0	8.886	9.484	21.890
−1/4	8.620	—	—
−1/2	7.948	—	—
−3/4	7.109	—	—
−1	6.283	6.512	13.226

NUMBER	GRAPH AND BOUNDARY CONDITIONS	EQUATION OR TABLE OF RESULTS	REFERENCES, NOTES /298
63		Symbols $m_1=\frac{M_1 l}{\sqrt{AC}}$, $m_2=\frac{M_2 l}{\sqrt{AC}}$, $b=\frac{B_r l}{Ch}$. Here A=bending stiffness within lattice plane of chord member B=bending stiffness in direction at right angles to the lattice plane of the chord member B_r=some of the bending stiffness of each lattice in the direction at right angles to lattice surface C=torsional stiffness of chord member	
64	Lateral buckling rigid frame-type built-up member 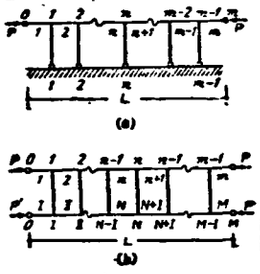 (a) (b)	Assumptions: (1)The chord member only resists the bending and the torsion outside of the structural plane. (2)The web members are rigidly joined to the chord members. (3)The support points 0, m can rotate only around the axis perpendicular to the movement in the direction of 0 m. (4)In case (b) in the diagram on the left, the upper chord member and lower chord member have equal cross-section. Where $P_e=\frac{\pi^2 EI}{L^2}$, $\mu=\frac{L^2}{h^2}\cdot\frac{GI_p}{EI}$. I_p: Torsional resistance moment of chord member I: Geometric moment of inertia of chord member The graphs below indicate the relationships of P_k/P_e and μ for cases (a) and (b). 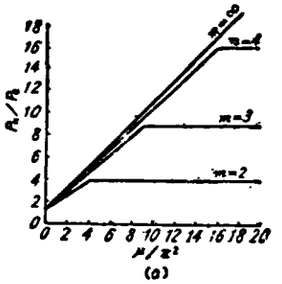 (a) 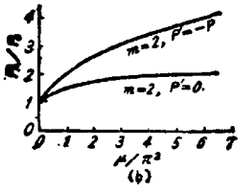 (b)	39

THREE-DIMENSIONAL TRUSSES

NUMBER	GRAPH AND BOUNDARY CONDITIONS	EQUATIONOR TABLE OF RESULTS	REFERENCES, NOTES /299
65	Equilateral three-dimensional truss 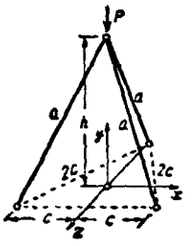	Case in which the ends of the three members of equal length form an equilateral triangle on one plane. Assuming $\cos\alpha=\frac{c}{a}$, $\cos\beta=\frac{h}{a}$. The smaller of $P_k=\frac{\sqrt{3}}{2}EA\frac{c}{l}\sin 2\beta$ or $2\sqrt{3}EA\frac{c}{l}\cdot\frac{\cos^3\beta}{\sin\beta}$ is taken. The symbols are based on case 44 above.	40 Based on the hypothetical work method.
66	Three-dimensional truss built-up member 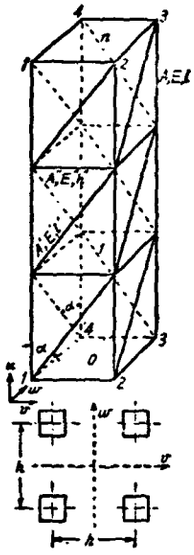	Notation: A,E,l = cross-section area, Young's modulus, member length of chord member; A',E',V = cross-section area, Young's modulus, member length of diagonal member; A",E",h" = cross-section area, Young's modulus, member length of horizontal member. a) Case in which the connecting members are very weak. $(A'\to 0,\ A''\to 0)$, $P_k=4\pi^2\frac{EI_w}{L^2}$ 又は $4\pi^2\frac{EI_v}{L^2}$. b) Case in which the number of components is very large and there are very stiff connecting members. Assuming $\left(\frac{1}{A'}\to 0,\ \frac{1}{A''}\to 0\right)$. $\bar{I}_w=4\left(I_w+A\frac{h^2}{4}\right)$, $\bar{I}_v=4\left(I_v+A\frac{h^2}{4}\right)$. As a first approximation $P_k=\pi^2\frac{E\bar{I}_w}{L^2}$ 又は $\pi^2\frac{E\bar{I}_v}{L^2}$. As a second approximation $P_k=\pi^2\frac{E\bar{I}_w}{L^2}\left(1-\frac{1}{6}\cdot\frac{\pi^2}{n^2}\cdot\frac{Ah^2}{\bar{I}_w}\right)$. or $P_k=\pi^2\frac{E\bar{I}_v}{L^2}\left(1-\frac{1}{6}\cdot\frac{\pi^2}{n^2}\cdot\frac{Ah^2}{\bar{I}_v}\right)$.	40 Based on the hypothetical work method.

NUMBER	GRAPH AND BOUNDARY CONDITIONS	EQUATION OR TABLE OF RESULTS	REFERENCES, NOTES
67	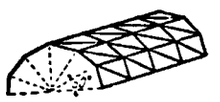 (i) 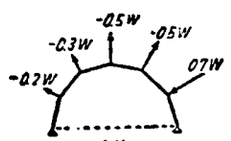 (ii)	(i) When an equally distributed perpendicular load P acts on each joint 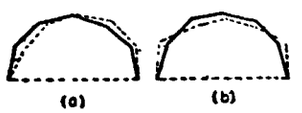 (a) (b) Form of buckling | (a) | (b) P_k Unit EA | 0.0124 | 0.0541 Maximum buckling unit stress *1 Unit EA | 0.0368 | 0.1606 A is the cross-section area of a member and is uniform (ii) Case in which a wind load W having a wind force corfficient such as that shown in the figure acts. 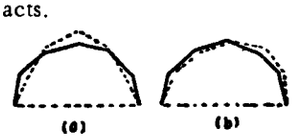 (a) (b) Form of buckling | (a) | (b) W_k Unit EA | 0.0386 | 0.155 Maximum buckling unit stress *1 Unit EA | 0.1337 | 0.5375	41 For 3-dimensional trusses, a general analysis was carried out based on the energy method, and the 3-dimensional trusses shown in the figures were used as examples of calculations. *1 The maximum buckling unit stress is the value of the stresses which occur within the members of the frame at the time of buckling, in steel, since the allowable unit stress normally considered is around 0,001 EA, it can be seen that there is little danger of buckling occurring if the design is carried out within the allowable values.
RIGID FRAMES			
68	Regular polygonal rigid frame sustaining a radial load 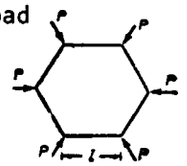	$n=3: \quad P_k \approx 2\sin\frac{\pi}{n}(1.23\pi)^2\frac{EI}{l^2}$, $n>3: \quad P_k=2\sin\frac{\pi}{n}\left(\frac{4\pi}{n}\right)^2\frac{EI}{l^2}$. where n is number of sides of regular polygon.	42

NUMBER	GRAPH AND BOUNDARY CONDITIONS	EQUATION OR TABLE OF RESULTS	REFERENCES, NOTES
69	Regular polygonal rigid frame 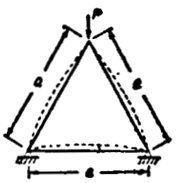 	Buckling condition $6\psi(u)+4\psi'(u)-\phi^2(u)=0.$ [a1] where $\begin{cases}\phi(u)=\frac{3}{u}\left(\frac{1}{\sin 2u}-\frac{1}{2u}\right),\\ \phi(u)=\frac{3}{u}\left(\frac{1}{2u}-\frac{1}{\tan 2u}\right),\\ u=\frac{a}{2}\sqrt{\frac{N}{EI}}\end{cases}$ where N is axial stress $N_k=25.25\frac{EI}{a^2}.$ $P_k=iN_k\sqrt{3}=43.73\frac{EI}{a^2}.$	43 *1 Derived from 3-moment equation of member in the moments with respect to buckling.
70	Buckling outside of structural plane of 3 rigidly connected members 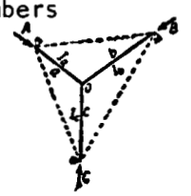 	Buckling condition $\frac{\omega_1 a}{\tan\omega_1 a}F_a+\frac{\omega_2 b}{\tan\omega_2 b}F_b+\frac{\omega_3 c}{\tan\omega_3 c}F_c=0.$ $\begin{cases}\omega_1=\sqrt{\frac{A}{EI_a}},\\ \omega_2=\sqrt{\frac{B}{EI_b}},\\ \omega_3=\sqrt{\frac{C}{EI_c}}.\end{cases}$ F_a, F_b, F_c are respectively the areas of BOC, COA, AOB.	44 Outside of the structural plane, the condition is considered in which point 0 also includes the tangential plane.
71	Gate type Rigid frame 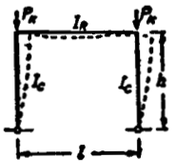 Column legs pinned	Buckling condition equation $kl\tan kl=6\frac{I_R h}{I_C l}=6\frac{K_R}{K_C}.$ where $k^2=\frac{P_k}{EI_C},\quad K_R=\frac{I_R}{l},\quad K_C=\frac{I_C}{h}.$ By graph, in $l_k=\gamma h$, γ is as shown in the table below.	42 45 46

K_R/K_C	0	0.5	1.0	1.5	2.0	2.5	3.0	4.0	∞
γ	∞	2.635	2.328	2.220	2.166	2.133	2.111	2.083	2.000

According to E. Chwalla, for approximation purposes, it is possible to assume the following.

$$l_k=2h\sqrt{1+0.38\left(\frac{K_C}{K_R}\right)}.$$

NUMBER	GRAPH AND BOUNDARY CONDITIONS	EQUATION OR TABLE OF RESULTS	REFERENCES, NOTES
72	Gate rigid frame 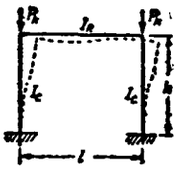 Column legs fixed	Buckling condition equation $$\frac{kh}{\tan kh}=-\frac{6hI_R}{lI_C}=-6\frac{K_R}{K_C}.$$ where $$k^2=\frac{P_k}{EI_C},\quad K_R=\frac{I_R}{l},\quad K_C=\frac{I_C}{h}.$$ Solving graphically, where $l_k=\gamma h$, γ becomes as shown in the table below.	42 46
73	Rectangular rigid frame, assymetrical buckling 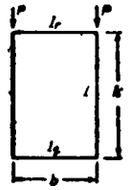 (a) 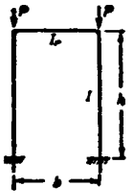 (b) 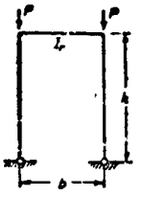 (c)	a) Buckling condition equation $$\tan^{-1}\frac{\gamma}{\pi}\cdot\frac{6K_q}{K}+\tan^{-1}\frac{\gamma}{\pi}\frac{6K_r}{K}=\frac{\pi}{\gamma}.$$ Notation $$K_q=\frac{I_q}{b},\quad K=\frac{I}{h},\quad K_r=\frac{I_r}{h},\quad P=\frac{\pi^2EI}{(\gamma h)^2}.$$ Abbreviated formula*1 $$\gamma=1+\frac{1}{6k}\left(\frac{I_r}{I_q}+1\right),$$ $$k=\frac{I_rh}{Ib}=\frac{K_r}{K}.$$ When γ is large, as a correction for the stiffness of the beam, $$\gamma=1+\frac{1+\frac{I_r}{I_q}}{6k+0.2\left(1+\frac{I_r}{I_q}\right)}.$$ b) Buckling condition equation $$-\frac{\pi}{\gamma}\cdot\cot\frac{\pi}{\gamma}=\frac{6K_r}{K}.$$*3 Abbreviated formula*3 $$\gamma=1+\frac{1}{6k},\quad k=\frac{I_rh}{Ib}=\frac{K_r}{K}.$$ This can be used as long as γ is not significantly greater than 1. When γ is large $$\gamma=1+\frac{1}{6k+0.2}.$$ c) Buckling condition equation $$\frac{\pi}{\gamma}\tan\frac{\pi}{\gamma}=\frac{6K_r}{K}.$$*4 Abbreviated formula*5 $$\gamma=2+\frac{1}{3k},\quad k=\frac{I_rh}{Ib}=\frac{K_r}{K}.$$ When γ is large, correcting on the basis of the stiffness of the beam $$\gamma=2+\frac{1}{3k+0.1}.$$	47 *1,3,5 Based on erg *1,3,5 Based on energy method. *2 It is assumed that $I_q=\infty$ in the buckling condition equation for case a). *4 It is assumed that $I_q=0$ in the buckling condition equation for case a).

K_R/K_C	0	0.5	1.0	1.5	2.0	2.5	3.0	4.0	...
γ	2.000	1.280	1.157	1.108	1.082	1.066	1.055	1.041	1.000

NUMBER	GRAPH AND BOUNDARY CONDITIONS	EQUATION OR TABLE OF RESULTS	REFERENCES, NOTES
74	Gate type Rigid frame 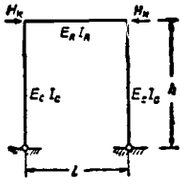	$H_k=\frac{\pi^2 E_c I_R}{l^2}\cdot\left(\frac{8+4c}{c}\right)$. where $c=\frac{E_C I_C}{h}\cdot\frac{l}{E_R I_R}$.	48
75	Gate type Rigid frame 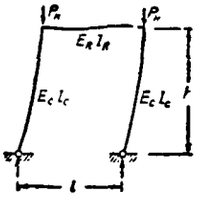	when $c<2.4$ $\quad l_k\fallingdotseq 2h\left(1+\frac{c^2}{6}\right)$. when $c>2.4$ $\quad l_k\fallingdotseq 2h\sqrt{1+0.4c}$. where $c=\frac{E_C I_C}{h}\cdot\frac{l}{E_R I_R}$.	48
76	Rectangular Rigid frame 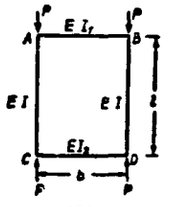 (a) 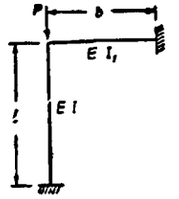 (b)	a) Buckling condition equation $\left[\frac{1}{\alpha}+\frac{l\phi(u)}{3EI}\right]\left[\frac{1}{\beta}+\frac{l\phi(u)}{3EI}\right]-\left[\frac{l\phi(u)}{6EI}\right]^2=0$.*1 Notation $u=\frac{l}{2}\sqrt{\frac{P}{EI}}$, $\alpha=\frac{2EI_1}{b}$, $\beta=\frac{2EI_2}{b}$. $\phi(u)=\frac{3}{u}\left(\frac{1}{\sin 2u}-\frac{1}{2u}\right)$, $\psi(u)=\frac{3}{2u}\left(\frac{1}{2u}-\frac{1}{\tan 2u}\right)$. when $\alpha=\beta$ $\frac{1}{\alpha}+\frac{l\psi(u)}{3EI}=-\frac{l\phi(u)}{6EI}$. P_k determined by the trial method. b) Buckling condition equation $\left[\frac{3EI}{\alpha l}+\psi(u)\right]\psi(u)=\frac{1}{4}\left[\phi(u)\right]^2$.*2	42 *1 The condition is determined under which M becomes ∞ from the deflection angle method formulas. *2 It is assumed that $\beta=\infty$ in the buckling conditions for case a).

NUMBER	GRAPH AND BOUNDARY CONDITIONS	EQUATION OR TABLE OF RESULTS	REFERENCES, NOTES
77	Rectangular rigid frame 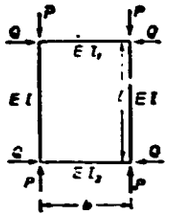	Buckling condition equation $$\left[\frac{1}{\alpha}+\frac{l\phi(u)}{3EI}\right]\left[\frac{1}{\beta}+\frac{l\phi(u)}{3EI}\right]-\left[\frac{l\phi(u)}{6EI}\right]^2=0.$$ $$u=\frac{l}{2}\sqrt{\frac{P}{EI}}.$$ $$\alpha=\frac{2EI_1}{b}\cdot\frac{u_1}{\tan u_1},\quad u_1=\frac{b}{2}\sqrt{\frac{Q}{EI_1}}.$$ $$\beta=\frac{2EI_2}{b}\cdot\frac{u_2}{\tan u_2},\quad u_2=\frac{b}{2}\sqrt{\frac{Q}{EI_2}}.$$ Determined by the trial method. $\phi(u)$, $\phi(u)$ same as in (76) above.	42 *1 Condition determined under which M is from the deflection angle method formulas
78	Inverted gate type rigid frame 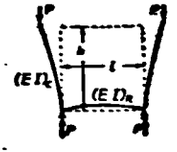	$$P_k=\alpha_0^2(EI)_C.$$ Here α_0 is the solution of the buckling condition. $$(\alpha h)\tan(\alpha h)=\frac{2}{\theta}$$ $$\theta=\frac{(EI)_C}{h}\cdot\frac{l}{(EI)_B}.$$ $$\alpha=\sqrt{\frac{P}{(EI)_C}}.$$	48
79	Gate type rigid frame with non-symmetrical buckling 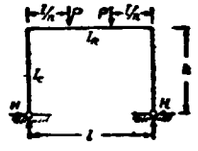	Buckling condition equation*1 $$\begin{cases}\frac{H^2}{P^2}(1-\varphi h\cot\varphi h)\cos\frac{\phi l}{2}+\cos\frac{\phi l}{2} \\ \quad -\cos\phi\left(\frac{1}{2}-\frac{1}{n}\right)+\frac{\phi hH}{P}\sin\frac{\phi l}{2}=0, \\ \varphi h\cot\varphi h-\frac{2Ph}{Hl}\left(1-\frac{\phi^2}{2}\cot\frac{\phi l}{2}\right) \\ \quad +\frac{Hh}{Pl}\left(2-\varphi h\cot\varphi h-\frac{\varphi^2h^2}{\sin^2\varphi h}\right)=0. \\ \varphi=\sqrt{\frac{P}{EI_C}},\quad \phi=\sqrt{\frac{H}{EI_B}}.\end{cases}$$ when $l=h$, $n=3$, $I_C=I_B=I$ の時 $$P_k=1.775\frac{EI}{h^2},\quad H_k=0.266\frac{EI}{h^2}.$$ when $l=3h$, $n=3$, $I_C=I_B=I$ の時 $$P_k=1.058\frac{EI}{h^2},\quad H_k=0.774\frac{EI}{h^2}.$$	49 *1 Condition under which the rigid frame sustains a symmetrical load & symmetrical deformation & changes to nonsymmetrical deformation.

NUMBER	GRAPH AND BOUNDARY CONDITIONS	EQUATION OR TABLE OF RESULTS	REFERENCES NOTES
80	Three-pin type gate rigid frame, case in which a load is sustained in corner sections 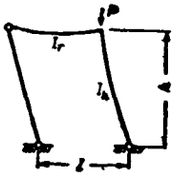	Buckling condition $Z\tan Z=3c$, $Z=\alpha h$, $\alpha^2=\frac{P_k}{EI_h}$. $c=\frac{h}{l}\frac{I_r}{I_h}=\frac{K_r}{K_h}$, $\gamma=\frac{\pi}{Z}$. $P_k=\frac{\pi^2 EI_h}{(\gamma h)^2}$. γ is shown in the graph on the right 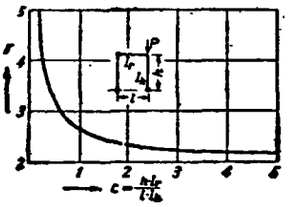 Elasticity range $c\geqq 2$ $\gamma\fallingdotseq 2\sqrt{1+\frac{0.70}{c}}$. $c\leqq 2$ $\gamma\fallingdotseq 2\sqrt{1+\frac{0.70}{c}+\frac{0.035}{c^2}}$. Plasticity range $\gamma\fallingdotseq\sqrt{2+2\sqrt{1+\frac{0.70\,A\lambda_{II}^2}{c}}}$. where $\lambda_{II}=\frac{h}{i}$, $A=\frac{\sigma_{kI}}{E\pi^2}$. using St 37 $\sigma_{kI}=2400$ kg/cm². St 52 $\sigma_{kI}=3600$ kg/cm²	50
81	Three-pin type gate rigid frame, case in which a load is sustained in the intermediate section of the column. 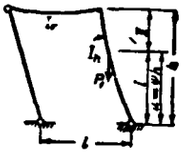	Buckling condition $Z\tan\psi Z\left(1-\psi+\frac{1}{3c}\right)=1$. where $\frac{u}{h}=\psi$, $Z=\alpha h$, $\alpha^2=\frac{(P_1)_k}{EI_h}$. Conversion is made to the buckling length γh for the case in which a load is sustained in the corner section, i.e., (80) above, and the buckling load is corrected by μ. $(P_1)_k=\frac{\pi^2 EI_h}{\mu(\gamma h)^2}$ とすると $\mu\fallingdotseq\frac{\mu_{c=\infty}\cdot c+0.70\psi}{c+0.70}$. here $\mu_{c=\infty}\fallingdotseq(2.55-2.00\psi+0.45\psi^2)\psi$. 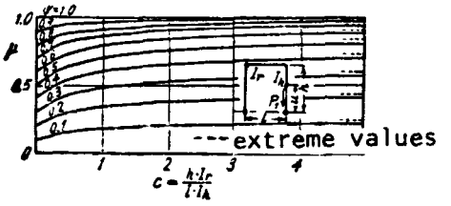 ---extreme values	50

NUMBER	GRAPH AND BOUNDARY CONDITIONS	EQUATION OR TABLE OF RESULTS	REFERENCES, NOTES
82	2-pin type gate rigid frame Case in which a load is sustained in intermediate part of column. 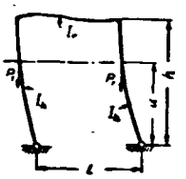	Conversion is made to the buckling length γh expressed in (80) and the buckling load is corrected by μ The buckling load is $(P_1)_k=\frac{\pi^2 EI_h}{\mu(\gamma h)^2}$. $\mu=\frac{\mu_{c=\infty}\cdot c+0.35\phi}{c+0.35}$, $\mu_{c=\infty}\fallingdotseq(2.55-2.00\phi+0.45\phi^2)\phi$. where $\phi=\frac{u}{h}$, $c=\frac{h}{l}\cdot\frac{I_0}{I_r}$. 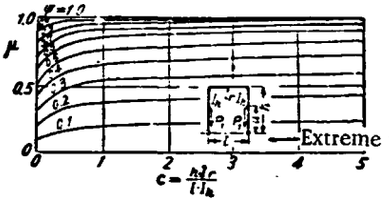 Extreme values	50
83	3-pin type gate rigid frame. Case in which the load acts simultaneous on the corner section and the intermediate section of the column. 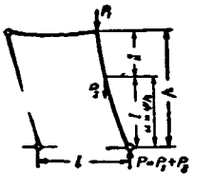	The buckling conditions are $\frac{Z\left\{\sqrt{m}\tan\phi Z+m\tan\left[(1-\phi)\sqrt{m}\,Z\right]\right\}}{\sqrt{m}-\tan\phi Z\tan\left[(1-\phi)\sqrt{m}\,Z\right]}=3c.$ $Z_2=\alpha h$, $u=\phi h$, $\frac{P}{EI_h}=\alpha^2$, $\frac{P_1}{EI_h}=\beta^2$, $m=\frac{P_1}{P}$, $\beta^2=m\alpha^2$, $\frac{P_2}{EI_h}=\alpha^2-\beta^2$. The buckling load is converted to case (80) and corrected by μ_1. $P_k=(P_1+P_2)_k=\frac{\pi^2 EI_h}{\mu_1(\gamma h)^2}$. P_1 is considered to act simultaneously with P of (80) with respect to buckling, so when converting to (80) P_2 is corrected, and it is possible to express this by the right side of the following equation. $\mu_1(P_1+P_2)=P_1+\mu_2 P_2$. Assuming $\phi=0.5$, for various values of m, 2 is as indicated below. 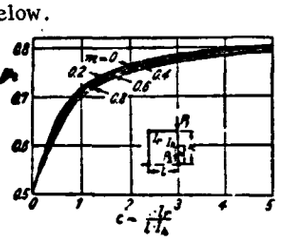	50

NUMBER	GRAPH AND BOUNDARY CONDITIONS	EQUATION OR TABLE OF RESULTS	REFERENCES, NOTES
84	Three-pin type gate type rigid frame 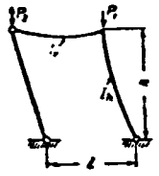	Buckling condition a) When P_2 is upwards $\frac{(1+m)Z^2\tan Z}{(1+m)Z-m\tan Z}=3c,$ $P_2=mP_1,\quad Z=\alpha h,\quad \alpha^2=\frac{P_1}{EI_h}.$ if $c=\infty$ $\quad \tan Z=\frac{1+m}{m}Z.$ b) When P_2 is downwards $\frac{(1-m)Z^2\tan Z}{(1-m)Z+m\tan Z}=3c$ If c = ∞ $\tan Z=-\frac{1-m}{m}Z.$ The value of $c=\infty(I_r=\infty)$ when $\tau_{c=\infty}$ is indicated in the table on the right where $(P_1)_k=\frac{EI_h\pi^2}{(\tau h)^2}.$ Values of $\gamma_c = \infty$	50
85	Two-pin type gate type rigid frame 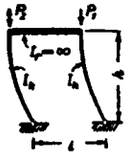	Buckling conditions when $I_r = \infty$ a) When P_2 is downwards $\tan\sqrt{m}Z+m\sqrt{m}\cdot\tan Z=(1+m)\sqrt{m}Z.$ b) When P_2 is upwards $\tanh\sqrt{m}Z-m\sqrt{m}\cdot\tan Z=(1-m)\sqrt{m}Z.$ in $(P_1)_k=\frac{\pi^2EI_h}{(\tau h)^2}$ The value of $c=\infty$ $(I_r=\infty)$ when $\tau_{c=\infty}$ is indicated in the table on the right where $m=\frac{P_2}{P_1},\quad Z=\alpha h,$ $\alpha^2=\frac{P_1}{EI_h}.$ The value of Tc = ∞	50

m	Direction of P_2	
	Downwards	Upwards
0	2.000	2.000
0.1	2.080	1.917
0.2	2.155	1.831
0.25	2.194	1.786
0.3	2.231	1.741
0.4	2.303	1.647
0.5	2.373	1.549
0.6	2.440	1.445
0.7	2.507	1.336
0.75	2.539	1.279
0.8	2.571	1.222
0.9	2.634	1.108
1.0	2.695	1.000

m	Direction of P_2	
	Downwards	Upwards
0	1.426	1.426
0.1	1.491	1.358
0.2	1.555	1.288
0.25	1.586	1.252
0.3	1.617	1.215
0.4	1.676	1.142
0.5	1.734	1.068
0.6	1.790	0.995
0.7	1.844	0.929
0.75	1.871	0.899
0.8	1.898	0.873
0.9	1.950	0.832
1.0	2.000	0.800

NUMBER	GRAPH AND BOUNDARY CONDITIONS	EQUATION OR TABLE OF RESULTS	REFERENCES, NOTES

/308

86	Two-pin gate type rigid frame symmetrical load 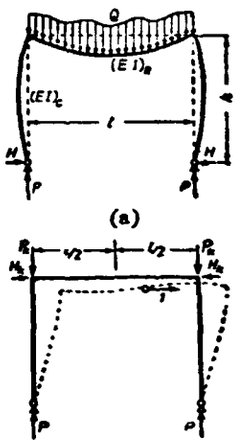 (a) (b)	It is assumed that the load is P_k in the case when a rigid frame undergoing symmetrical deformation due to a symmetrical load shifts toward the asymmetrical deformation indicated by the broken line in (b) in the diagram on the left. Moreover, (87), (88),(89),(90),(91), and (92) also indicate a buckling value P_k in the same sense. $P_k=\pi^2\frac{(EI)_c}{(2h)^2}\cdot\frac{1+\frac{e}{2}}{1+\frac{5}{3}\cdot\frac{e}{2}+\left(\frac{\pi^2}{12}+\frac{d}{4}\right)\left(\frac{e}{2}\right)^2}\cdot$ $Q_k=2P_k=\pi^2\frac{(EI)_c}{(2h)^2}\cdot\frac{96+48e}{48+40e+(\pi^2+3d)e^2}\cdot$ $H_k=P_k\cdot\frac{H}{P}.$ where $e=\frac{(EI)_c}{h}\frac{l}{(EI)_g},\quad d=\frac{Hl}{2Ph}=\frac{Hl}{Qh}.$	48 Consideration is given to the deformation of a rigid frame when a horizontal force 1 is applied to the center of a beam, the energy method is applied, the solution is compared with the solution for special cases in order to make corrections This is true in (87),(88),(89), (90),(91), and (92), below.
87	Rectangular rigid frame. Symmetrical load 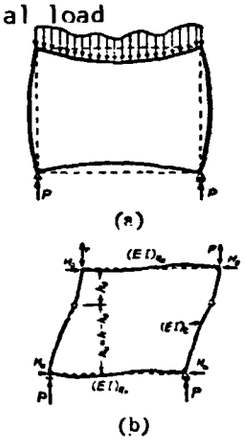 (a) (b)	Assuming an inflection point height h_u, the buckling load of a two-pin gate type rigid frame with heights h_o, h_u, is determined from (86), and when the case is determined in which the load is the same on the upper and lower ends, this is the buckling load.	48
88	Gate type rigid frame symmetrical load. 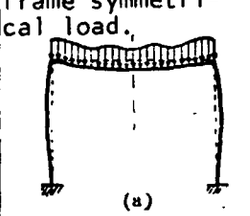 (a)	Assuming an inflection point height h_u, the buckling load of the 2-pin gate type rigid frame with a height h_o is determined by (86) and when the case is determined in which the buckling loads for a 2-column member with 1 end fixed and the other free are equal, this becomes the buckling load.	48

NUMBER	GRAPH AND BOUNDARY CONDITIONS	EQUATION OR TABLE OF RESULTS	REFERENCES, NOTES /309
88	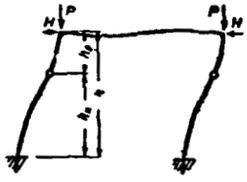 (b)		
89	Symmetrical angle type rigid frame. Symmetrical load. 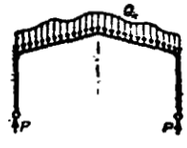 (a) 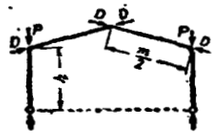 (b)	$P_k=\pi^2\cdot\frac{(EI)_C}{(2h)^2}\cdot$ $\cdot\frac{1+\frac{c}{2}}{1+\frac{5}{3}\cdot\frac{c}{2}+\left(\frac{\pi^2}{12}+\frac{d^2}{4}\right)\left(\frac{c}{2}\right)^2}\cdot$ $Q_k=2P_k=\pi^2\cdot\frac{(EI)_C}{(2h)^2}\cdot$ $\cdot\frac{96+48c}{48+40c+(\pi^2+3d)c^2}\cdot$ $D_k=P_k\cdot\frac{D}{P}\cdot$ where $c=\frac{(EI)_C}{h}\cdot\frac{m}{(EI)_D}$, $d=\frac{Dm}{2Ph}=\frac{Dm}{Qh}$. $(EI)_D$= bending stiffness of angle beam	48
90	Symmetrical angle rigid frames. Symmetrical load. 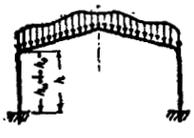	Assuming an inflection point height h_u, the buckling load for the case of a column leg pin [literal translation] wight a height h_o is obtained by (89) and when this and the case in which the buckling load of the two-column member of height h_u with one end fixed and the other end free are equal is found, this is the required buckling load.	48

NUMBER	GRAPH AND BOUNDARY CONDITIONS	EQUATION OR TABLE OF RESULTS	REFERENCES, NOTES
91	π-type rigid frame symmetrical load 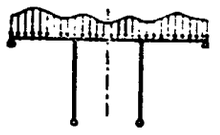 ( ) 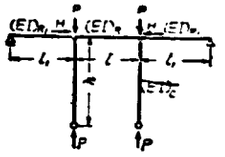 (b)	$P_k=\pi^2\frac{(EI)_c}{(2h)^2}\cdot\frac{1+\frac{c_m}{2}}{1+\frac{5}{3}\cdot\frac{c_m}{2}+\left(\frac{\pi^2}{12}+\frac{d}{4}\right)\left(\frac{c_m}{2}\right)^2}\cdot$ $Q_k=2P_k=\pi^2\frac{(EI)_c}{(2h)^2}\cdot\frac{96+48c_m}{48+40c_m+(\pi^2+3d)c_m^2}\cdot$ $H_k=P_k\frac{H}{P}.$ where $c_m=\frac{2c_1c}{2c_1+c},\quad c_1=\frac{(EI)_c}{h}\cdot\frac{l_1}{(EI)_{R1}},\quad c=\frac{(EI)_c}{h}\cdot\frac{l}{(EI)_R},$ $d=\frac{Hl}{2Ph}=\frac{Hl}{Qh}.$	48
92	π-type rigid frame symmetrical load 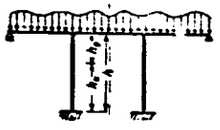	(91) is used to determine the buckling load for the case of pinned column base with a height h_0, assuming an inflection point height h_u. The required buckling load is determined when this, and the case in which the buckling loads of a 2-member column with a height h_u and one end fixed and one end free are equal, it is found.	48
93	Rectangular rigid frame having braces Asymmetrical buckling 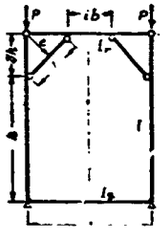	$\gamma=1+\frac{1}{6}(\nu_q+7\vartheta+i^2\nu_r)+\frac{I}{A}\cdot\frac{l}{h}\cdot\frac{1}{e^2}.$ ここに $\nu_q=\frac{I}{I_q}\cdot\frac{b}{h},\quad \nu_r=\frac{I}{I_r}\cdot\frac{b}{h}.$ $P_k=\frac{\pi^2EI}{(\gamma h)^2}$ A = cross-section area of brace.	47 Abbreviated solution by energy m Abbreviated solution by energy method. It is assumed that the brace does not undergo buckling. The same is true below.
94	Gate type rigid frame having braces. Asymmetrical buckling. 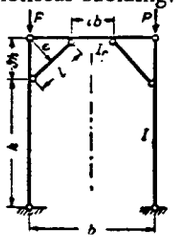	$\gamma=2+\frac{1}{3}(2\vartheta+i^2\nu)+2\frac{I}{A}\cdot\frac{l}{h}\cdot\frac{1}{e^2}.$ $\nu=\frac{I}{I_r}\cdot\frac{b}{h}.$ $P_k=\frac{\pi^2EI}{(\gamma h)^2}.$ A = cross-section area of brace.	47

95

Gate type rigid frame having braces

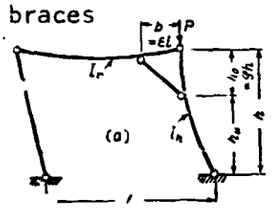

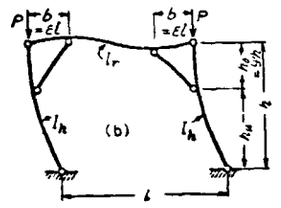

Case in which the load acts on the corner sections.
Buckling condition equation

$$\frac{\varphi^2 z_1^2(\tan\varphi z_1+\tan(1-\varphi)z_1)}{\varphi z_1(\tan\varphi z_1+\tan(1-\varphi)z_1)-\tan\varphi z_1\tan(1-\varphi)z_1}=k.$$

here

(a) 三ピン : $k=\frac{3c}{(1-\varepsilon)^2}$,

(b) 二ピン : $k=\frac{6c}{(1-2\varepsilon)^2}$.

$$c=\frac{hI_r}{lI_h},\quad z_1=\alpha h,\quad \varphi=\frac{h_0}{h},\quad \varepsilon=\frac{b}{l}.$$

$$\alpha^2=\frac{P_c}{EI_h}.$$

when $\tau=\frac{\pi}{z_1}$ is found in $l_k=\gamma h$, the following diagram is obtained.

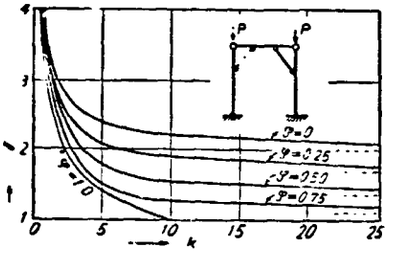

In the general case, using the values of k above, approximately

$1\leqq k\leqq 20$:

$$\tau\fallingdotseq 2(1-0.65\varphi)\sqrt{(1-0.23\varphi)+\frac{2.1+4.4\varphi}{k}}.$$

$k>20$:

$$\tau\fallingdotseq 2(1-0.65\varphi)\sqrt{1+\frac{2.1}{k}}.$$

$k=\infty$:

$\gamma_k=\infty$ is indicated in the table below

φ	0	0.1	0.2	0.25	0.3	0.4	0.5
$\gamma_{k=\infty}$	2.000	1.870	1.736	1.668	1.603	1.473	1.348

φ	0.6	0.7	0.75	0.8	0.9	1
$\gamma_{k=\infty}$	1.231	1.130	1.089	1.055	1.012	1.000

50

NUMBER	GRAPH AND BOUNDARY CONDITIONS	EQUATION OR TABLE OF RESULTS	REFERENCES, NOTES
96	Gate type rigid frame having braces. Case in which a load acts on the column in the lower section of the brace.	Buckling condition equation $\frac{z_1 \tan\phi z_1}{1-\left(1-\frac{2}{3}\varphi-\phi\right) z_1 \tan z_1} = k.$ here (a) 三ピン： $k=\frac{3c}{(1-\varepsilon)^2}$, (b) 二ピン： $k=\frac{6c}{(1-2\varepsilon)^2}$. $c=\frac{h I_r}{l I_h}$, $z_1=\alpha h$, $\alpha^2=\frac{P}{EI_h}$. ③ 隅角部に荷重をうける場合即ち前例 (95) の座屈長さ τh に換算し座屈荷重を μ で修正する. $P_k=\frac{\pi^2 EI_h}{\mu(\tau h)^2}$. when $\varphi=0.25$ μ is indicated in the diagram below	50

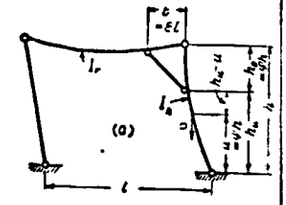

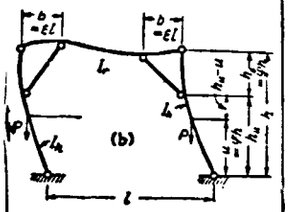

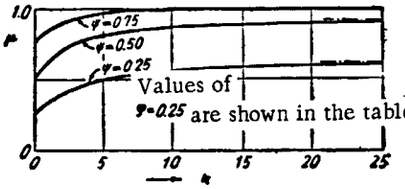

Values of $\varphi=0.25$ are shown in the table below

Values of $\mu_k = \infty$ are shown in the table below.

ϕ	φ 0.0	0.1	0.2	0.25	0.3	0.4	0.5	0.6	0.7	0.75	0.8	0.9
0.1	0.230	0.245	0.263	0.272	0.282	0.304	0.326	0.348	0.361	0.361	0.355	0.322
0.2	0.428	0.454	0.483	0.498	0.514	0.548	0.582	0.610	0.622	0.615	0.597	
0.25	0.515	0.544	0.576	0.593	0.611	0.648	0.683	0.711	0.716	0.703		
0.3	0.594	0.625	0.660	0.677	0.696	0.734	0.768	0.792	0.788			
0.4	0.729	0.761	0.796	0.814	0.831	0.860	0.890	0.898				
0.5	0.834	0.863	0.894	0.908	0.922	0.945	0.955					
0.6	0.910	0.934	0.956	0.966	0.973	0.983						
0.7	0.960	0.976	0.988	0.992	0.994							
0.75	0.976	0.988	0.995	0.998								
0.8	0.988	0.995	0.999									
0.9	0.999	0.999										
1.0	1.000											

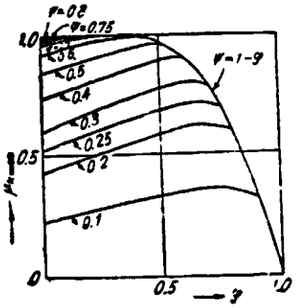

The values for buckling when $I_r = \infty$, consequently $k = \infty$, are obtained from the above table and the graph on the right. In the general case,

$$\mu \fallingdotseq \frac{\mu_k=\infty k+2.1\phi}{k+2.1}.$$

NUMBER	GRAPH AND BOUNDARY CONDITIONS	EQUATION OR TABLE OF RESULTS	REFERENCES, NOTES /313
97	2-beam span rigid frame having braces, asymmetrical buckling. 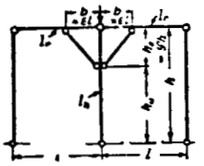	If the results for the gate rigid frame (95) having braces are applied appropriately, the buckling condition equation is $$\frac{\varphi^2 z_1^2[\tan\varphi z_1+\tan(1-\varphi)z_1]}{\varphi z_1[\tan\varphi z_1+\tan(1-\varphi)z_1]-\tan\varphi z_1\tan(1-\varphi)z_1}=k.$$ $$k=\frac{6c}{(1-c)^2}.$$ Here $$c=\frac{hI_r}{lI_h},\quad z_1=\alpha h,\quad \alpha^2=\frac{P}{EI_h}.$$	50
98	Rectangular rigid frame having brace beams, asymmetrical buckling. 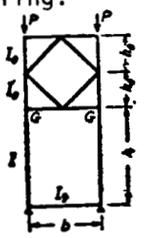	$$\tau=1+\frac{1}{6}\left(\nu_0+\frac{7}{4}\nu_0\right)+\frac{I}{h}\sum\frac{S^2l}{A}.$$ Here $$\nu_1=\frac{I}{I_1}\cdot\frac{h}{b},\quad \nu_0=\frac{I}{I_0}\cdot\frac{h_0}{h}.$$ $$P_k=\frac{\pi^2EI}{(\tau h)^2}.$$ S is the member stress of each member of the brace brams when a moment M = 1 is applied to the point G, 1 is the member length of each member, A is the cross-section area of each member.	47 Calculated by energy method.
99	Gate-type rigid frame having brace beams, asymmetrical buckling. 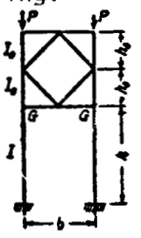	$$\tau=1+\frac{7}{24}\nu_0+\frac{I}{h}\sum\frac{S^2l}{A}.$$ Notation: completely the same as in (98)	47
100	Gate-type rigid frame having brace beams, asymmetrical buckling. 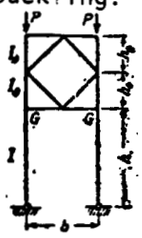	$$\tau=2+\frac{7}{12}\nu_0+\frac{2I}{h}\sum\frac{S^2l}{A}.$$ Notation: the same as in (98).	47

/313

NUMBER	GRAPH AND BOUNDARY CONDITIONS	EQUATION OR TABLE OF RESULTS	REFERENCES, NOTES
101	3-pin gate type rigid frame having lattice beams, asymmetrical buckling 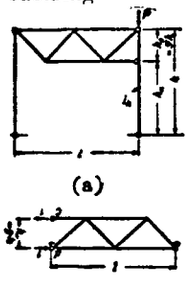 (a) (b)	The buckling condition equation is as follows if the results for the 3-pin gate type rigid frame (95) having braces are used appropriately. $\frac{\varphi^2 z_1^3[\tan\varphi z_1+\tan(1-\varphi)z_1]}{\varphi z_1[\tan\varphi z_1+\tan(1-\varphi)z_1]-\tan\varphi z_1\tan(1-\varphi)z_1}=k.$ here $k=\frac{\varphi^2 h^3}{I_h\sum\frac{N_1^2 l_1}{A_1}}.$ $\delta=\sum\frac{N_1^2 l_1}{A_1}$ is the multiple E of the relative displacements of points c, d, due to the couples $1\cdot h_0$ indicated in Figure (b) on the left. where N_1= stress of each member of lattice beam A_1= cross section area of each member of lattice beam l_1=length of each member of lattice beam	50 /314
102	2-pin gate type rigid frame having lattice beams, asymmetrical buckling 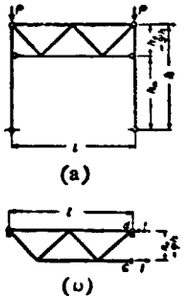 (a) (b)	The following equation is used for the k on the right side of the buckling condition equation (101) $k=\frac{2\varphi^2 h^3}{I_h\sum\frac{N_2^2 l_2}{A_2}}.$ here $\delta=\frac{1}{2}\sum\frac{N_2^2 l_2}{A_2}$ Is the factor of E for the relative idsplacement at points c and d in the figure to the left. N_2=stress at each part of a latice beam l_2= cross-section area of all the parts of a latice beam. A_2= the length of all parts of a latice beam.	50
103	Rectangular rigid frame having lattice beam, assymmetrical buckling 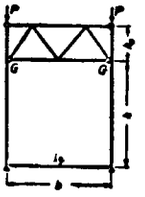	When the effect of the axial forces of the lattice are not considered $\tau=\frac{h_k}{h}=1+\frac{1}{6}(\nu_q+2\nu_0).$ When the effect of the axial forces of the lattice are considered $\tau=1+\frac{1}{6}(\nu_q+2\nu_0)+\frac{I}{h}\sum\frac{S^2 l}{A}.$ here $\nu_q=\frac{I}{I_q}\cdot\frac{h}{b},\quad \nu_0=\frac{I}{I_0}\cdot\frac{h_0}{h}.$ S is the stress of each member of the lattice beam when a moment M = 1 is applied at points G, 1 is the member length, A is the cross-section area of each member.	47 Abbreviated calculations by the energy method.

NUMBER	GRAPH AND BOUNDARY CONDITIONS	EQUATION OR TABLE OF RESULTS	REFERENCES, NOTES
104	Gate-type rigid frame having lattice beam, assymmetrical buckling 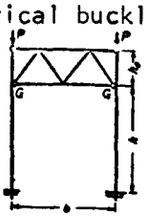	$\tau=1+\frac{1}{3}\nu_0+\frac{I}{h}\sum\frac{S^2l}{A}$. $P=\frac{\pi^2EI}{(\tau h)^2}$. Notation the same as in (103).	47 /315
105	Gate-type rigid frame having lattice beam, assymmetrical buckling 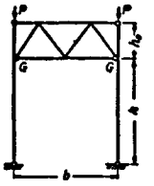	$\tau=2+\frac{2}{3}\nu_0+\frac{2I}{h}\sum\frac{S^2l}{A}$ Notation the same as in (103).	4
106	Two-story rigid frame, assymmetrical buckling 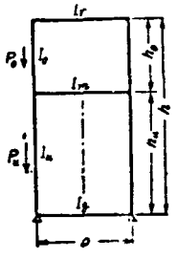	Buckling condition equation *1 $\frac{\pi}{\kappa_u}\left(\tan\left(\frac{\pi}{\kappa_u}\tan^{-1}\frac{6K_0}{K_u}\cdot\frac{\kappa_u}{\pi}\right)+\beta\tan\left(\frac{\pi}{\kappa_0}-\tan^{-1}\frac{6K_r}{K}\cdot\frac{\kappa_0}{\pi}\right)\right)=\frac{6K_m}{K_u}$. Notation $P_k=\frac{\pi^2EI}{(\kappa h)^2}$, $\frac{\kappa_0}{\kappa_u}=\alpha\frac{h_u}{h_0}$, $\alpha=\sqrt{\frac{I_0}{I_u}\cdot\frac{P_u}{P_0}}$, $\beta=\sqrt{\frac{I_0}{I_u}\cdot\frac{P_0}{P_u}}$. $K_0=\frac{I_0}{h_0}$, $K_r=\frac{I_r}{b}$, ... Abbreviated equation for buckling conditions *2 $\tau_u\left(1+\sqrt{\frac{I_0}{I_u}\cdot\frac{P_0}{P_u}}\right)=1+\frac{P_0}{P_u}\cdot\frac{h_0}{h_u}+\frac{\nu}{6}\left(\frac{I_m}{I_0}+\left(1+\sqrt{\frac{I_0}{I_u}\cdot\frac{P_0}{P_u}}\right)^2+\frac{I_0}{I_u}\cdot\frac{P_0}{P_u}\cdot\frac{I_m}{I_r}\right)$. $\tau_0=\tau_u\frac{h_u}{h_0}\sqrt{\frac{I_0}{I_u}\cdot\frac{P_u}{P_0}}$, $\nu=\frac{I_u}{I_m}\frac{b}{h_u}=\frac{K_u}{K_m}$, $P_k=\frac{\pi^2EI}{(\tau_u h_u)^2}$.	*1 The displacement curve is $y=f\sin\frac{\pi x}{\kappa h}$ This is the correct solution obtained from the continuity conditions and stability conditions of the members. *2 P_0, P_u are the compresive forces acting on the upper and lower columns respectively. The same is true below.

NUMBER	GRAPH AND BOUNDARY CONDITIONS	EQUATION OR TABLE OF RESULTS	REFERENCES, NOTES /316
107	Two-story rigid frame, assymmetrical buckling 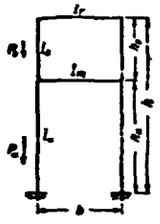	Buckling condition equation*1 $$\frac{\pi}{\kappa_u}\left(\beta\tan\left(\frac{\pi}{\kappa_0}-\tan^{-1}\frac{6K_r}{K_0}\cdot\frac{\kappa_0}{\pi}\right)-\cot\frac{\pi}{\kappa_u}\right)=\frac{6K_m}{K_u}.$$ Buckling condition abbreviated equation*2 $$\tau_u\left(1+\sqrt{\frac{I_0}{I_u}\cdot\frac{P_0}{P_u}}\right)=1+\frac{P_0}{P_u}\cdot\frac{h_0}{h_u}+\frac{\nu}{6}\left\{\left(1+\sqrt{\frac{I_0}{I_u}\cdot\frac{P_0}{P_u}}\right)^2+\frac{I_0}{I_u}\cdot\frac{P_0}{P_u}\cdot\frac{I_m}{I_r}\right\}.$$ Notation the same as in (106).	47 In the previous section (106) it is assumed $I_q = ,$ *1 The displacement curve is $y=f\sin\frac{\kappa z}{\kappa h}$ *2 Energy method
108	Two-story rigid frame, assymmetrical buckling 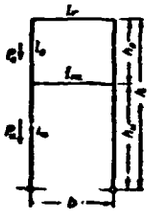	Buckling condition equation $$\frac{\pi}{\kappa_u}\left(\tan\frac{\pi}{\kappa_u}+\beta\tan\left(\frac{\pi}{\kappa_0}-\tan^{-1}\frac{6K_r}{K_0}\cdot\frac{\kappa_0}{\pi}\right)\right)=\frac{6K_m}{K_u}.$$ Abbreviated buckling equation $$\tau_u\left(\frac{1}{2}+\sqrt{\frac{I_0}{I_u}\cdot\frac{P_0}{P_u}}\right)=1+\frac{P_0}{P_u}\cdot\frac{h_0}{h_u}+\frac{\nu}{6}\left\{\left(1+\sqrt{\frac{I_0}{I_u}\cdot\frac{P_0}{P_u}}\right)^2+\frac{I_0}{I_u}\cdot\frac{P_0}{P_u}\cdot\frac{I_m}{I_r}\right\}$$ Notation the same as in (106).	47 It is assumed in (106) that $I_q = 0$
109	Two-story rigid frame, assymmetrical buckling 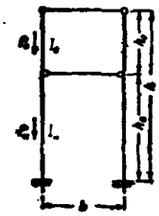	Buckling condition equation*1 $$\tan\frac{\pi}{\kappa_u}\tan\frac{\pi}{\kappa_0}=\frac{1}{\beta}.$$ $$\kappa_u h_u=\kappa(h_0+h_u)=\kappa h.$$ Notation as in (106). (a) When the compressive force $P_0 = P_u = P$, and the geometric moment of inertia $I_0 \neq I_u$ $$\tan\frac{\pi}{\kappa}\cdot\frac{h_u}{h}\tan\frac{\pi}{\kappa}\cdot\frac{h_0}{h}\sqrt{\frac{I_u}{I_0}}=\sqrt{\frac{I_u}{I_0}}.$$ $$P=\frac{\pi^2EI}{(\kappa h)^2}.$$ (b) When the compressive force $P_0 \neq P_u$, and the geometric moment of inertia $I_0 = I_u = I$ $$\tan h_u\sqrt{\frac{P_u}{EI}}\tan h_0\sqrt{\frac{P_0}{EI}}=\sqrt{\frac{P_u}{P_0}}.$$	47 *1 In (106) it is assumed $I_m = I_r = 0$.

NUMBER	GRAPH AND BOUNDARY CONDITIONS	EQUATION OR TABLE OF RESULTS	REFERENCES, NOTES /317
110	Single-span two-story rigid frame 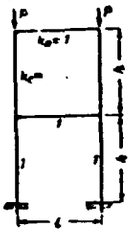	In $$P_k=m\frac{EI}{h^2}=\frac{\pi^2 EI}{(\gamma h)^2}.$$ m, γ have the values shown in the table below	51 Precisely calculated from the matrix of the equation in the buckling deflection angle method

	(a)	(b)	(c)
m	5.17	17.89	23.27
γ	1.382	0.743	0.651

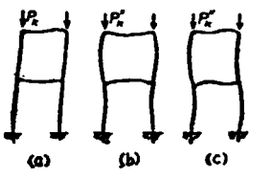

111	Single-span two-story rigid frame 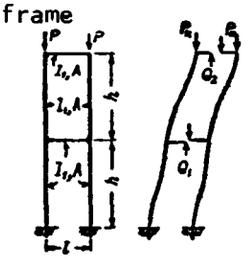	In $$\frac{P_k}{A}=\sigma_{k1}=\frac{\pi^2 E}{\lambda^2_{id}}.$$ λ_{id} has the values in the table below	52 Derived from the equations in the buckling deflection angle method

(a) When considering variation in member length

l	h	$h/2$	$h/4$	$h/8$
$\lambda_1=30$	42.06	38.89	43.64	62.02
40	55.75	50.33	52.60	69.75
50	69.49	62.01	62.21	77.20
60	83.26	73.82	72.20	84.94
70	97.05	85.71	82.48	93.08

(b) When disregarding variation in member length

l	h	$h/2$	$h/4$	$h/8$
$\lambda_1=30$	41.94	36.23	33.22	31.63
40	55.31	48.30	44.30	42.17
50	69.14	60.38	55.37	52.71
60	82.97	72.46	66.44	63.26
70	96.80	84.53	77.52	73.80

where $\lambda_1=h\Big/\sqrt{\frac{I_1}{A}}$.

NUMBER	GRAPH AND BOUNDARY CONDITIONS	EQUATION OR TABLE OF RESULTS	REFERENCES, NOTES /318
112	Single-span two-story rigid frame	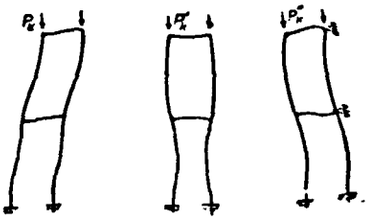 $P_k=6.76\frac{EI}{h^2}$, $P_k'=20.77\frac{EI}{h^2}$, $P_k''=28.05\frac{EI}{h^2}$.	52 Calculated from the matrices of the equation in the buckling deflection angle method
113	Two-span two-story rigid frame 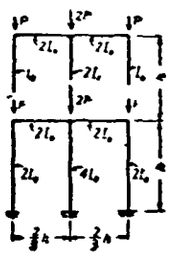	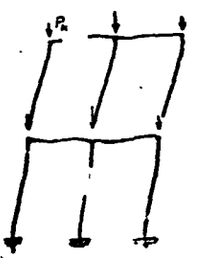 $P_k=7.09\frac{EI_0}{h^2}$, 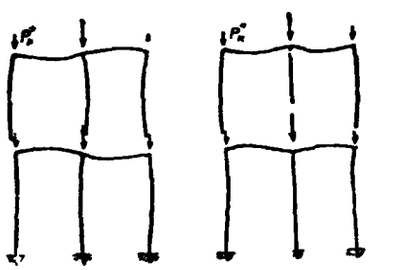 $P_k'=22.69\frac{EI_0}{h^2}$, $P_k''=26.79\frac{EI_0}{h^2}$, 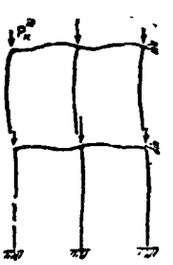 $P_k'''=29.34\frac{EI_0}{h^2}$.	52 Calculated from the equations in the buckling deflection angle method.

114	Single span, multiple story rigid frame, asymmetrical buckling 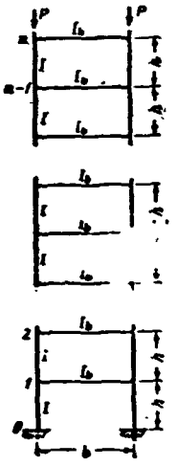	$\gamma=1+\frac{\nu}{6n}\left[4(n-1)+1\right]^{*2}$ $P_k=\frac{\pi^2 EI}{(\gamma h)^2}$ $\nu=\frac{I}{I_b}\cdot\frac{b}{h}=\frac{K}{K_b}$ $n=$ number of stories The above equation gives satisfactory approximate values *2 as long as is not significantly greater than 1 in spite of n. Moreover, if the effect of the axial forces is taken into consideration $\gamma=1+\frac{\nu}{6}\cdot\frac{4(n-1)+1}{n}+5.33n^2\left(\frac{h}{b}\right)^2\frac{1}{\lambda^2}\cdot^{*3}$ where $\lambda=\frac{h}{i}$. When the beam stiffness is small, consequently is large. The following equation is used which is a further correction to the above equation $\gamma=1+\frac{R}{6+0.2R}$ $R=\nu\frac{4(n-1)+1}{n}+32n^2\left(\frac{h}{b}\right)^2\frac{1}{\lambda^2}$.	47 *1 Calculated by energy method. *2 When n is large, this is Puwei's equation. Agrees with $\gamma=1+\frac{2}{3}\nu\cdot\cos^2\frac{\pi}{4n}$ *3 Puwein, with respect to the above equation $\gamma=1+\frac{2}{3}\nu\cdot\cos^2\frac{\pi}{4n}+6.5n^2\cdot\left(\frac{h}{b}\right)^2\cdot\frac{1}{\lambda^2}$.

VARIABLE CROSS-SECTIONS, RIGID FRAMES

No.	Graph & Boundary Conditions	Equation or Table of Results	References Notes
115	Gate type rigid frame having variable cross-section beams 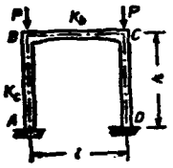	(a) When there is no displacement in lateral direction The buckling equation condition is $\frac{\alpha}{\alpha-b}=-\frac{K_b}{K_c}$. Where a, b deflection angle coefficient of the variable cross-section beam BC*1 α is the deflection angle coefficient in the buckling deflection angle equation (b) When there is displacement in the lateral direction The buckling equation condition is $\begin{vmatrix} \alpha+(a+b)\frac{K_b}{K_c} & -(\alpha+\beta) \\ -(\alpha+\beta) & 2(\alpha+\beta)-\alpha^2 \end{vmatrix}=0.$ Notation same as above.	53 Buckling deflection angle method *1 for the deflection angle coefficients a, b see the following reference (Kakumu Kazuo on the calculations of a frame having members with variable cross-sections, Architectural Magazine, 1931, Oct.).

NUMBER	GRAPH AND BOUNDARY CONDITIONS	EQUATION OR TABLE OF RESULTS	REFERENCES, NOTES
116	Gate type rigid frame having variable cross-section beam 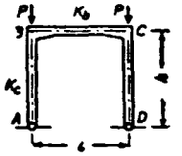 	(a) when there is no lateral displacement The buckling condition equation is $\frac{\tau}{a-b}=-\frac{K_b}{K_c}$. where $\tau=\frac{\alpha^2-\beta^2}{\alpha}$, α, β ; a, b are respectively, the buckling deflection angle coefficients and the deflection angle coefficients of the variable cross-section (b) When there is lateral displacement The buckling condition equation is $\begin{vmatrix} \tau+(a+b)\frac{K_b}{K_c} & -\tau \\ -\tau & \tau-s^2 \end{vmatrix}=0.$ Notation same as above.	53 Done by the buckling deflection angle method.
117	Gate type rigid frame having variable cross-section beam 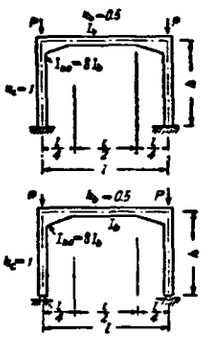 	In $P_k=\frac{\pi^2}{(\gamma h)^2}EI_c$ the values of γ are as shown in the table below. joint conditions / column base condition: no lateral displacement — lateral displacement column base fixed: 0.641 — 1.123 column base pinned: 0.898 — 2.254	53 Done by the buckling deflection angle method.
118	3-pin gate type rigid frame having variable cross-section beam When the geometric moment of inertia of the beams varies linearly 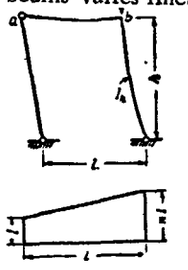 	Hypothetical geometric moment of inertia of beams. $I_r=\frac{I(n-1)^2}{3\left[\frac{(n-1)^2}{2}-(n-1)+\log_e n\right]}$ If one uses the above equation, this should be handled the same as in the case of a beam with a constant cross-section. See (80) above.	54

NUMBER	GRAPH AND BOUNDARY CONDITIONS	EQUATION OR TABLE OF RESULTS	REFERENCES, NOTES /321
119	3-pin gate type rigid frame having variable cross-section beams When the geometric moment of inertia of the beams varies parabolically 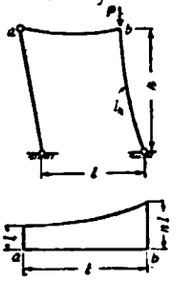	Hypothetical geometric moment of inertia of beams $$I_r = I \cdot \frac{5n}{2n+3}.$$ If the above equation is used, this can be treated the same as in the case of a beam of constant cross-section	54
120	3-pin gate type rigid frame having variable cross-section beams Case in which geometric moment of inertia of the beams varies suddenly 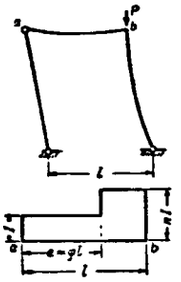	Hypothetical geometric moment of inertia of beam $$I_r = \frac{nI}{1+\varphi(n-1)}.$$ See (80) above.	54
121	3-pin gate type rigid frame having variable cross-section column Case in which the geometric moment of inertia of column varies parabolically 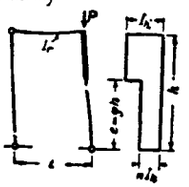	Buckling condition equation $$\frac{s\left[\sqrt{n}\tan\frac{\varphi z}{\sqrt{n}}+\tan(1-\varphi)z\right]}{1-\sqrt{n}\tan\frac{\varphi z}{\sqrt{n}}\cdot\tan(1-\varphi)z}=3c.$$ Here $$z=\alpha h, \quad \alpha^2=\frac{P}{EI_h}, \quad c=\frac{h\cdot I_r}{l\cdot I_h}.$$ $$P_k=\frac{\bar{n}\pi^2 EI_h}{(\tau h)^2}.$$ Where τh buckling length of the 3-pin rigid frame column (80) having a constant cross-section I_h and a load on the corners	54

NUMBER	GRAPH AND BOUNDARY CONDITIONS	EQUATION OR TABLE OF RESULTS	REFERENCES, NOTES /322
121		Values of $\bar{n}_{c=\infty}$ φ | $n=0.2$ | $n=0.4$ | $n=0.6$ | $n=0.8$ | $n=1.0$ 0.0 | 1.0000 | 1.0000 | 1.0000 | 1.0000 | 1.0000 0.1 | 0.9926 | 0.9976 | 0.9989 | 0.9996 | 1.0000 0.2 | 0.9543 | 0.9802 | 0.9913 | 0.9984 | 1.0000 0.3 | 0.8305 | 0.9358 | 0.9716 | 0.9894 | 1.0000 0.4 | 0.6782 | 0.8623 | 0.9366 | 0.9759 | 1.0000 0.5 | 0.5375 | 0.7700 | 0.8876 | 0.9560 | 1.0000 0.6 | 0.4277 | 0.6765 | 0.8293 | 0.9297 | 1.0000 0.7 | 0.3451 | 0.5903 | 0.7676 | 0.9009 | 1.0000 0.8 | 0.2832 | 0.5155 | 0.7071 | 0.8664 | 1.0000 0.9 | 0.2363 | 0.4526 | 0.6508 | 0.8828 | 1.0000 1.0 | 0.2000 | 0.4000 | 0.6000 | 0.8000 | 1.0000 c is all approximations derived from the following equation when a random value is used. $\bar{n}\fallingdotseq\frac{c+0.70}{\frac{c}{\bar{n}_{c=\infty}}+0.70}$.	
122	2-pin type gate rigid frame having variable cross-section columns Case in which the cross-section of the column changes suddenly 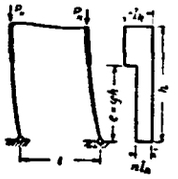	$P_k=\frac{\bar{n}\pi^2EI_h}{(rh)^2}$. $\bar{n}\fallingdotseq\frac{c+0.35}{\frac{c}{\bar{n}_{c=\infty}}+0.35}$. The numbers in the table in (121) are used for the values of $\bar{n}_c=\infty$. Notation the same as in (121).	54
123	3-pin gate type rigid frame having variable cross-section columns Case in which the cross-section of the column varies gradually 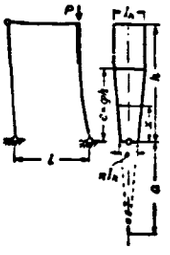	$I_x=I_h\left(\frac{a+x}{a+e}\right)^3$. The buckling condition equation is $\frac{(1-\sqrt{n})\sqrt{k^2+1}\left\{\sqrt{k^2+1}\tan\left(\frac{k}{2}\log_e\frac{1}{\sqrt{n}}\right)+\tan\left\{\frac{(1-\varphi)(1-\sqrt{n})\sqrt{k^2+1}}{2\varphi}\right\}\cdot\left\{\tan\left(\frac{k}{2}\log_e\frac{1}{\sqrt{n}}\right)+k\right\}\right\}}{2\varphi\left\{k-\tan\left(\frac{k}{2}\log_e\frac{1}{\sqrt{n}}\right)\cdot\left\{\sqrt{k^2+1}\tan\left\{\frac{(1-\varphi)(1-\sqrt{n})\cdot\sqrt{k^2+1}}{2\varphi}\right\}-1\right\}\right\}}=3c$ Here $k=\sqrt{4\beta^2-1}$. $\beta^2=\frac{P(a+e)^2}{EI_h}$, $\alpha^2=\frac{P_k}{EI_h}=\frac{k^2+1}{4(a+e)^2}$. $c=\frac{hI_r}{lI_h}$.	54

123

$$P_k=\frac{\bar{n}\pi^2EI_h}{(\gamma h)^2}. \quad *1$$

Values of $\bar{n}_{c=\infty}$

φ	$n=0.05$	$n=0.1$	$n=0.2$	$n=0.4$	$n=0.6$	$n=0.8$	$n=1.0$
0.0	1.000	1.000	1.000	1.000	1.000	1.000	1.000
0.2	0.990	0.992	0.994	0.997	0.998	0.999	1.000
0.4	0.918	0.937	0.956	0.976	0.987	0.995	1.000
0.5	0.051	0.885	0.920	0.955	0.975	0.989	1.000
0.6	0.770	0.819	0.872	0.927	0.960	0.982	1.000
0.8	0.605	0.676	0.759	0.853	0.915	0.962	1.000
1.0	0.47	0.547	0.647	0.771	0.862	0.936	1.000

When c takes arbitrary values

$$\bar{n}\fallingdotseq\frac{c+0.70}{\frac{c}{\bar{n}_{c=\infty}}+0.70}.$$

*1 γh is the buckling length of the columns of a three-pin type rigid frame (see (80)) having a constant cross-section I_n and a load on its corners.

124 Two pin-type box frame with distorted cross-section column.

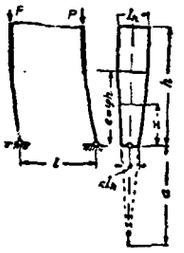

$$I_c=I_h\left(\frac{a+x}{a+e}\right)^3.$$

$$P_k=\frac{n\pi^2EI_h}{(\gamma h)^2}.$$

$$\bar{n}\fallingdotseq\frac{c+0.35}{\frac{c}{\bar{n}_{c=\infty}}+0.35}.$$

here

$$c=\frac{hI_c}{l\cdot I_h}.$$

Values of $\bar{n}_{c=\infty}$ are the numerical values in (123).

54

THREE DIMENSIONAL RIGID FRAMES

125 Cylindrical 3-dimensional frame

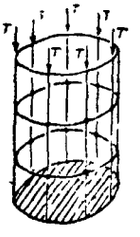

Buckling condition equation

$$\frac{kl}{\tan kl}=-12\eta+kl\,\varphi_n.$$

Here

$$k=\sqrt{T_k/EI},\quad \eta=(E_\eta I_0/l_0)/(EI/l).$$

$$\begin{cases}\varphi_1=0,\\ \varphi_n=\dfrac{kl\sin kl-12\eta\cos kl+kl\cos kl\cdot\varphi_{n-1}}{kl\cos kl+12\eta\sin kl-kl\sin kl\cdot\varphi_{n-1}}.\end{cases}$$

55 Calculations of buckling for rigid joint structures is carried out 2-dimensionally The numerical calculations are carried out assuming the deflection u occurs within the plane, and the story end is used as a parameter.

NUMBER	GRAPH AND BOUNDARY CONDITIONS	EQUATION OR TABLE OF RESULTS	REFERENCES, NOTES /324

125

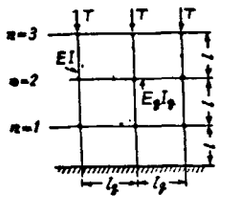

Upper end free,
Lower end fixed

Results of numerical calculations are as shown below.

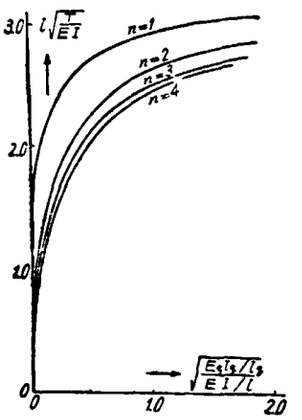

NUMBER	GRAPH AND BOUNDARY CONDITIONS	EQUATION OR TABLE OF RESULTS	REFERENCES, /325 NOTES
126	Two-span continuous member 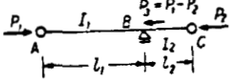 Both ends pinned	Buckling condition equation Notation: $K_1\gamma_1+K_2\gamma_2=0$ K_1 = Stiffness ratio of member AB K_2 = Stiffness ratio of member BC γ_1, γ_2 = buckling deflection angle method coefficients for member AB or member BC with other end pinned	Buckling deflection angle method 58
	Two-span continuous member 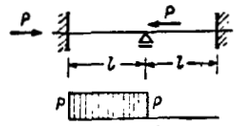 Diagram of axial force	When $l_1 = l_2$, $I_1 = I_2$, the buckling condition equation is $\gamma_1+\gamma_2=0$ $P_k=(3.73)^2\frac{EI}{l^2}=13.91\frac{EI}{l^2}$	Buckling deflection angle method 58
127	Two-span continuous member 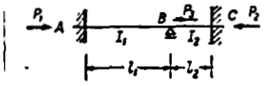 Both ends rotating	Buckling condition equation Notation: $K_1\alpha_1+K_2\alpha_2=0$ K_1, K_2 = Stiffness ratio of member AB or BC α_1, α_2 = Coefficients in the buckling deflection angle method for member AB or BC with the other end fixed.	58
	Two-span continuous member 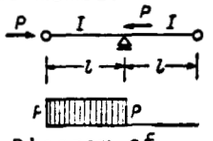 Diagram of axial force	The buckling condition equations when $I_1 = I_2$, $l_1 = l_2$ $\alpha_1+\alpha_2=0$ $P_k=(5.33)^2\frac{EI}{l^2}=28.4\frac{EI}{l^2}$	58
128	Two-span continuous member 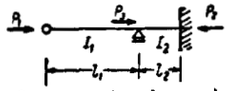 One end pinned Other end fixed	Buckling condition equation $K_1\gamma_1+K_2\alpha_2=0$ Notation: Same as in 126, 127	58
	Two-span continuous member 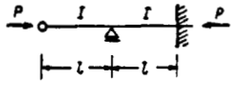	When $I_1 = I_2$, $l_1 = l_2$, the buckling condition equation is $\gamma_1+\alpha_2=0$ $P_k=\frac{(3.573)^2}{l^2}EI=\frac{12.77}{l^2}EI=\frac{\pi^2EI}{(0.879l)^2}$	58

NUMBER	GRAPH AND BOUNDARY CONDITIONS	EQUATION OR TABLE OF RESULTS	REFERENCES, NOTES /326
128	Two-span continuous member 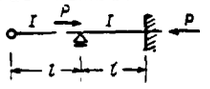	$P_k=\frac{(5.19)^2}{l^2}EI=\frac{26.94}{l^2}EI=\frac{\pi^2EI}{(0.605\,l)^2}$	58
	Two-span continuous member 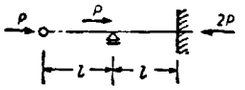 Graph of axial forces	$P_k=\frac{(3.165)^2}{l^2}EI=\frac{10.02}{l^2}EI=\frac{\pi^2EI}{(0.993\,l)^2}$	58
129	Multiple span continuous member (Equal spans with constant cross-sections) 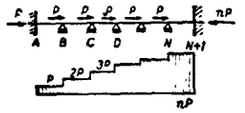 Axial forces	Buckling condition equation $\begin{vmatrix} \alpha_1+\alpha_2 & \beta_2 & 0 & 0 & \cdots & 0 & 0 & 0 \\ \beta_2 & \alpha_2+\alpha_3 & \beta_3 & 0 & \cdots & 0 & 0 & 0 \\ 0 & \beta_3 & \alpha_3+\alpha_4 & \beta_4 & \cdots & 0 & 0 & 0 \\ 0 & 0 & \beta_4 & \alpha_4+\alpha_5 & \cdots & 0 & 0 & 0 \\ \vdots & \vdots & \vdots & \vdots & & \vdots & \vdots & \vdots \\ 0 & 0 & 0 & 0 & \cdots & \beta_{n-2} & \alpha_{n-2}+\alpha_{n-1} & \beta_{n-1} \\ 0 & 0 & 0 & 0 & \cdots & 0 & \beta_{n-1} & \alpha_{n-1}+\alpha_n \end{vmatrix}=0$	58
	Three-span continuous member 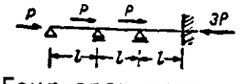	$P_k=\frac{(2.615)^2}{l^2}EI=6.84\frac{EI}{l^2}=\frac{\pi^2EI}{(1.20\,l)^2}$	58
	Four-span continuous member 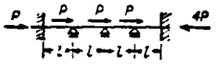	$P_k=\frac{(2.135)^2}{l^2}EI=4.56\frac{EI}{l^2}=\frac{\pi^2EI}{(1.47\,l)^2}$	58
	Five-span continuous member 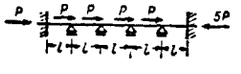	$P_k=\frac{(1.839)^2}{l^2}EI=3.38\frac{EI}{l^2}=\frac{\pi^2EI}{(1.71\,l)^2}$	58
130	Multiple span continuous member (Equal spans with constant cross-sections) axial forces	Buckling condition equation $\begin{vmatrix} r_1+\alpha_2 & \beta_2 & 0 & 0 & \cdots & 0 & 0 & 0 \\ \beta^2 & \alpha_2+\alpha_3 & \beta_3 & 0 & \cdots & 0 & 0 & 0 \\ 0 & \beta_3 & \alpha_3+\alpha_4 & \beta_4 & \cdots & 0 & 0 & 0 \\ \vdots & \vdots & \vdots & \vdots & & \vdots & \vdots & \\ 0 & 0 & 0 & 0 & \cdots & \beta_{n-2} & \alpha_{n-2}+\alpha_{n-1} & \beta_{n-1} \\ 0 & 0 & 0 & 0 & \cdots & 0 & \beta_{n-1} & \alpha_{n-1}+\alpha_n \end{vmatrix}=0$	Buckling deflection angle method 58

NUMBER	GRAPH AND BOUNDARY CONDITIONS	EQUATION OR TABLE OF RESULTS	REFERENCES, NOTES
130	Three span continuous member 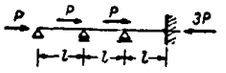	$P_k=(2.53)^2\frac{EI}{l^2}=6.40\frac{EI}{l^2}=\frac{\pi^2EI}{(1.24\,l)^2}$	Buckling deflection angle method 58
	Four-span continuous member 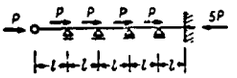	$P_k=\frac{(2.12)^2EI}{l^2}=4.49\frac{EI}{l^2}=\frac{\pi^2EI}{(1.48\,l)^2}$	Same as in 58
	Five-span continuous member 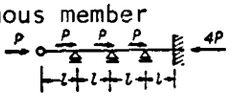	$P_c=\frac{(1.84)^2EI}{l^2}=3.38\frac{EI}{l^2}=\frac{EI}{(1.71\,l)^2}$	Same as in 58
	RIGID FRAMES		
131	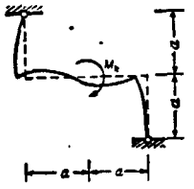	$M_k=1.142\frac{EI}{a}$	56
132	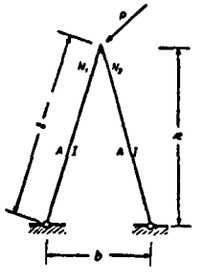	When $l_k=\gamma l$ $\gamma=0.80+0.05\left(1+\frac{N_2}{N_1}\right)^2$ except that $0.3\,h\leqq b\leqq 0.5\,h$	57
133	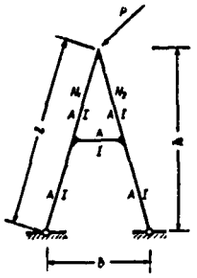	where $l_k=\gamma l$ $\gamma=0.44+0.12\left(1+\frac{N_2}{N_1}\right)+0.03\left(1+\frac{N_2}{N_1}\right)^2$ except that $0.3\,h\leqq b\leqq 0.5\,h$	57

NUMBER	GRAPH AND BOUNDARY CONDITIONS	EQUATION OR TABLE OF RESULTS	REFERENCES, NOTES /328
134	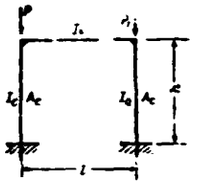	When it is assumed that $I_k = \gamma h$ $\gamma = \sqrt{\frac{1}{2}(1+m)}\sqrt{1+0.35(k+6\alpha)-0.017(k+6\alpha)^2}$ here $m=\frac{P_1}{P}\leqq 1,\quad k=\frac{K_c}{K_b}=\frac{I_c l}{I_b h}\leqq 10$ used when $\alpha=\frac{4I_c}{l^2A_c}\leqq 0.2$	57
135	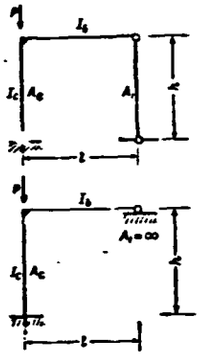	when $I_b=\gamma h$ $\gamma=\sqrt{1+(0.35)(2k-6\alpha)-(0.017)(2k+6\alpha)^2}$ here $k=\frac{K_c}{K_b}=\frac{I_c l}{I_b h}$ $\alpha=\frac{I_c}{l^2}\left(\frac{1}{A_c}+\frac{1}{A_1}\right)$	57
136	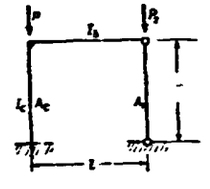	when $I_b=\gamma h \qquad P_2=nP,\ n\leqq 2$ $\gamma=\sqrt{1+0.86n}\sqrt{1+0.35(2k+6\alpha)-0.017(2k+6\alpha)^2}$ here $k=\frac{K_c}{K_b}=\frac{I_c l}{I_b h};\quad \alpha=\frac{I_c}{l^2}\left(\frac{1}{A_c}+\frac{1}{A_1}\right)$	57
137	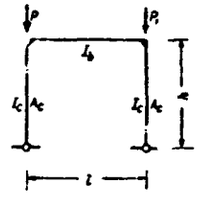	when $I_b=\gamma h$ $\gamma=\sqrt{\frac{1}{2}(1+m)}\sqrt{4+1.4(k+6\alpha)+0.02(k+6\alpha)^2}$ here used $m=\frac{P_1}{P}\leqq 1,\quad k=\frac{K_c}{K_b}=\frac{I_c l}{I_b h}\leqq 10$ when $\alpha=\frac{4I_c}{l^2A_c}\leqq 0.2$	57

NUMBER	GRAPH AND BOUNDARY CONDITIONS	EQUATION OR TABLE OF RESULTS	REFERENCES, NOTES /329
138	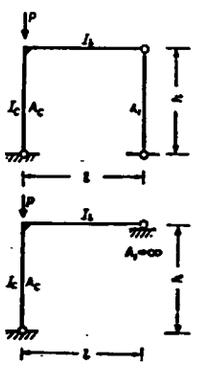	when $l_b=\tau h$ $\tau=\sqrt{4+1.4(2k+6\alpha)+0.02(2k+6\alpha)^2}$ here $k=\frac{K_c}{K_b}=\frac{I_c l}{I_b h}$ $\alpha=\frac{I_c}{l^2}\left(\frac{1}{A_c}+\frac{1}{A_1}\right)$	57
139	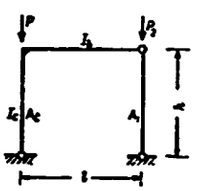	when $l_b=\tau l$ if $P_2=nP$, $n\leq 2$ $\tau=\sqrt{1+0.96n}\cdot\sqrt{4+1.4(2k+6\alpha)+0.02(2k+6\alpha)^2}$ here $k=\frac{K_c}{K_b}=\frac{I_c l}{I_b h}$; $\alpha=\frac{I_c}{l^2}\left(\frac{1}{A_c}+\frac{1}{A_1}\right)$	56
140	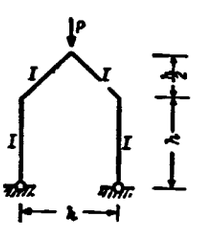	$P_k=3.210\frac{EI}{h^2}$	56
141	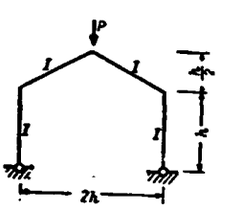	$P_k=2.577\frac{EI}{h^2}$	56
142	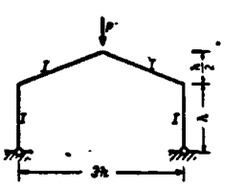	$P_k=2.033\frac{EI}{h^2}$	56

NUMBER	GRAPH AND BOUNDARY CONDITIONS	EQUATION OR TABLE OF RESULTS	REFERENCES, /330 NOTES
143	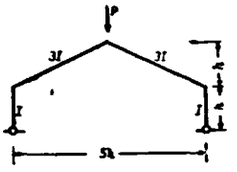	$P_k=1.085\frac{EI}{h^2}$	56
144	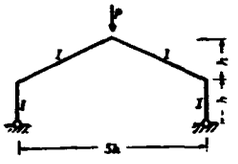	$P_k=2.547\frac{EI}{h^2}$	56
145	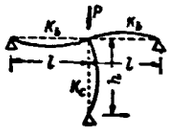	Assuming $\frac{K_b}{K_c}=k$ (stiffness ratio) if $P_k=\frac{\pi^2EI}{h^2}=\frac{mEI}{h^2}$	58

k	0	0.2	0.4	0.6	0.8	1.0	1.5	2.0	2.5	3.0	4.0	5.0	6.0	∞
z	π	3.43	3.65	3.79	3.89	3.97	4.10	4.18	4.23	4.26	4.31	4.34	4.36	4.49
m	π^2	11.8	13.3	14.4	15.2	15.8	16.8	17.5	17.9	18.2	18.6	18.8	19.0	20.2

146	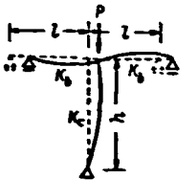	When $\frac{K_b}{K_c}=k$, $P_k=\frac{\pi^2EI}{h^2}=\frac{mEI}{h^2}$	58

k	0	0.2	0.4	0.6	0.8	1.0	1.5	2.0	2.5	3.0	4.0	5.0	6.0	∞
z	0	0.92	1.13	1.24	1.31	1.35	1.42	1.45	1.47	1.49	1.51	1.52	1.53	$\frac{\pi}{2}$
m	0	0.84	1.28	1.53	1.71	1.82	2.01	2.11	2.17	2.21	2.27	2.31	2.34	$\frac{\pi^2}{4}$

147	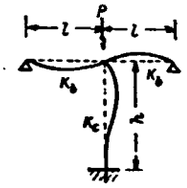	When $\frac{K_b}{K_c}=k$, $P_k=\frac{\pi^2EI}{h^2}=\frac{mEI}{h^2}$	58

k	0	0.2	0.4	0.6	0.8	1.0	1.5	2.0	2.5	3.0	4.0	5.0	6.0	∞
z	4.49	4.84	5.09	5.28	5.42	5.53	5.71	5.83	5.91	5.96	6.03	6.08	6.11	2π
m	20.2	23.4	25.9	27.8	29.3	30.5	32.6	33.9	34.9	35.5	36.3	36.9	37.3	39.5

148	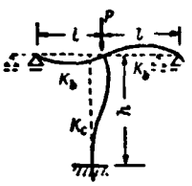	When $\frac{K_b}{K_c}=k$, $P_k=\frac{\pi^2EI}{h^2}=\frac{mEI}{h^2}$	58

k	0	0.2	0.4	0.6	0.8	1.0	1.5	2.0	2.5	3.0	4.0	5.0	6.0	∞
z	$\frac{\pi}{2}$	2.09	2.36	2.53	2.63	2.72	2.84	2.90	2.95	2.98	3.02	3.04	3.06	π
m	2.47	4.38	5.59	6.40	6.92	7.38	8.04	8.39	8.68	8.87	9.10	9.24	9.35	9.87

NUMBER	GRAPH AND BOUNDARY CONDITIONS	EQUATION OR TABLE OF RESULTS	REFERENCES, NOTES /331

149

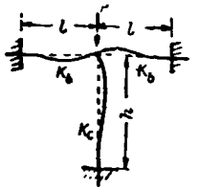

When it is assumed that $\frac{K_b}{K_c}=k,\ P_k=\frac{\pi^2 EI}{h^2}=\frac{mEI}{h^2}$ としたとき — 58

k	0	0.2	0.4	0.6	0.8	1.0	1.5	2.0	2.5	3.0	4.0	5.0	6.0	∞
z	4.49	4.93	5.22	5.42	5.56	5.66	5.85	5.92	5.96	6.03	6.09	6.12	6.14	2π
m	20.2	24.3	27.3	29.3	30.9	32.0	33.9	35.1	35.5	36.3	37.1	37.4	37.7	39.5

150

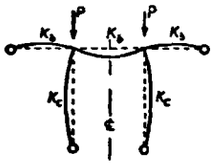

When it is assumed that $\frac{K_b}{K_c}=k,\ P_k=\frac{\pi^2 EI}{h^2}=\frac{mEI}{h^2}$ としたとき — 58

k	0	0.2	0.4	0.6	0.8	1.0	1.5	2.0	2.5	3.0	4.0	5.0	6.0	∞
z	π	3.41	3.59	3.72	3.83	3.91	4.04	4.13	4.19	4.23	4.29	4.32	4.34	4.49
m	9.87	11.6	12.9	13.9	14.6	15.3	16.3	17.0	17.5	17.9	18.4	18.6	18.8	20.2

151

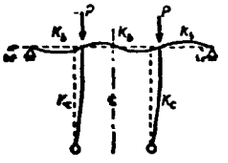

When it is assumed that $\frac{K_b}{K_c}=k,\ P_k=\frac{\pi^2 EI}{h^2}=\frac{mEI}{h^2}$ としたとき — 58

k	0	0.2	0.4	0.6	0.8	1.0	1.5	2.0	2.5	3.0	4.0	5.0	6.0	∞
z	0	1.04	1.24	1.33	1.38	1.42	1.46	1.49	1.50	1.52	1.53	1.54	1.54	$\frac{\pi}{2}$
m	0	1.09	1.53	1.77	1.91	2.01	2.14	2.21	2.26	2.30	2.34	2.36	2.38	$\frac{\pi^2}{4}$

152

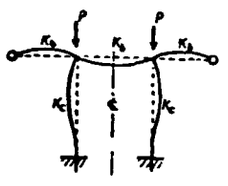

When it is assumed that $\frac{K_b}{K_c}=k,\ P_k=\frac{\pi^2 EI}{h^2}=\frac{mEI}{h^2}$ としたとき — 58

k	0	0.2	0.4	0.6	0.8	1.0	1.5	2.0	2.5	3.0	4.0	5.0	6.0	∞
z	4.49	4.79	5.02	5.19	5.33	5.44	5.63	5.75	5.84	5.91	5.99	6.04	6.08	2π
m	20.2	23.0	25.2	27.0	28.4	29.6	31.7	33.1	34.1	34.9	35.9	36.4	37.3	39.5

153

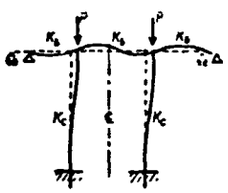

When it is assumed that $\frac{K_b}{K_c}=k,\ P_k=\frac{\pi^2 EI}{h^2}=\frac{mEI}{h^2}$ としたとき — 58

k	0	0.2	0.4	0.6	0.8	1.0	1.5	2.0	2.5	3.0	4.0	5.0	6.0	∞
z	$\frac{\pi}{2}$	2.25	2.53	2.68	2.77	2.84	2.93	2.98	3.01	3.03	3.06	3.07	3.08	π
m	2.47	5.04	6.40	7.19	7.70	8.04	8.57	8.87	9.05	9.18	9.35	9.44	9.51	π^2

154

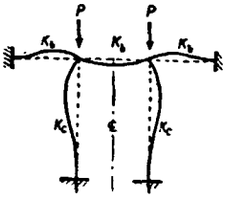

When it is assumed that $\frac{K_b}{K_c}=k,\ P_k=\frac{\pi^2 EI}{h^2}=\frac{mEI}{h^2}$ としたとき — 58

k	0	0.2	0.4	0.6	0.8	1.0	1.5	2.0	2.5	3.0	4.0	5.0	6.0	∞
z	4.49	4.84	5.09	5.28	5.42	5.53	5.71	5.83	5.91	5.96	6.03	6.08	6.11	2π
m	20.2	23.4	25.9	27.8	29.3	29.4	32.6	33.9	34.9	35.5	36.3	36.9	37.3	39.5

NUMBER	GRAPH AND BOUNDARY CONDITIONS	EQUATION OR TABLE OF RESULTS	REFERENCES, NOTES
155	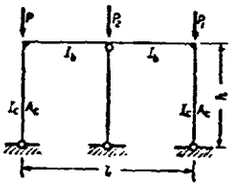	when $l_k = \gamma h$ $l_b = \tau h$ $P_1 = nP$; $n \leqq 2$ $\tau = \sqrt{1+0.48n}\sqrt{\frac{1}{2}(1+m)}\cdot\sqrt{4+1.4(k+6\alpha)+0.02(k+6\alpha)^2}$ here $m = \frac{P_1}{P} \leqq 1$, $k = \frac{K_c}{K_b} = \frac{I_c l}{I_b h} \leqq 10$ used when $\alpha = \frac{4I_c}{l^2 A_c} \leqq 0.2$	57
156	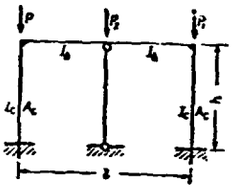	when $l_k = \gamma h$ $P_n = nP$; $n \leqq 2$ $\tau = \sqrt{1+0.43n}\sqrt{\frac{1}{2}(1+m)}\cdot\sqrt{1+0.35(k+6\alpha)-0.017(k+6\alpha)^2}$ here $m = \frac{P_1}{P} \leqq 1$; $k = \frac{K_c}{K_b} = \frac{I_c l}{I_b h} \leqq 10$ used when $\alpha = \frac{4I_c}{l^2 A_c} \leqq 0.2$	57
157	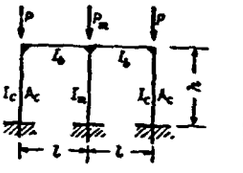	Assuming $l_b = \tau h$ $\tau = \frac{1+0.4k_n}{1+0.2k_n}\sqrt{\frac{2+p}{2+t}}$ here $k_n = k + \frac{9}{4}\alpha$; $k = \frac{K_c}{K_b} = \frac{I_c l}{I_b h}$ $p = \frac{P_n}{P}$; $t = \frac{I_n}{I_c}$; $\alpha = \frac{4I_c}{l^2 A_c}$ Range of application limited to cases where $\gamma \leq 3$.	57
158	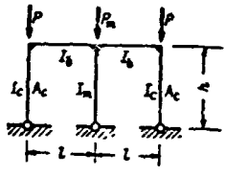	Assuming $l_b = \tau h$ $\tau = \frac{6+1.2k_n}{3+0.1k_n}\cdot\sqrt{\frac{2+p}{2+t}}$ Notation as in No. 157	57
159	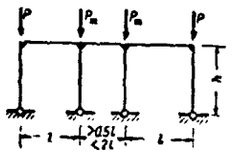	Assuming $l_b = \tau h$ $\tau = \frac{6+1.2k_n}{3+0.1k_n}\sqrt{\frac{1+p}{1+t}}$ Notation as in No. 157	57

NUMBER	GRAPH AND BOUNDARY CONDITIONS	EQUATION OR TABLE OF RESULTS	REFERENCES, NOTES
160	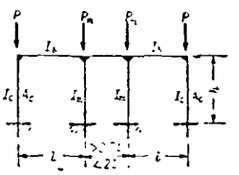	When $l_k = rh$ $r = \frac{1+0.4\,k_n}{1+0.2\,k_n}\sqrt{\frac{1+p}{1+t}}$ Notation as in No. 157	57
161	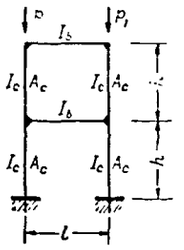	Assuming $l_k = rh$ $r = \sqrt{\frac{1}{2}(1+m)}\cdot\sqrt{1+12.5\alpha+0.89(1-\alpha)k-0.003(1-\alpha)k^2}$ Here $m = \frac{P_1}{P} \leqq 1$, $k = \frac{K_c}{K_b} = \frac{I_c l}{I_b h} \leqq 10$ used when $\alpha = \frac{4\,I_c}{l^2 A_c} \leqq 0.2$	

BIBLIOGRAPHY

1. Müller-Breslau, H., Die Neueren Methoden der Festigkeitslehre, 4 Aufl. Leipzig, 1918.
2. Bleich, F., Theorie and Berechnung der Eisernen Brücken, Springer, Berlin, 1924.
3. Bleich, F., Stahlhochbauten, Springer, Wien, 1932.
4. German Standards for the Calculation of Iron Frame Structures (DIN 1050).
5. German Standards (Proposal) Definitions of the Buckling of Steel for Structures (DIN 4114).
6. Timoshenko, S., Theory of Elastic Stability, McGraw-Hill, New York, 1934.
7. Ratzersdorfer, J., Die Knickfestigkeit von Stäben und Stabwerken, Springer, Wien, 1936.
8. Shunzo, Kin, "Computations and Theory of the Buckling Strength of Polygonal Span [literal] Continuous Columns having straight multiple lattice spans [literal translation] or Intermediate Stiffener Points," *Journal of Civil Engineering*, Feb., 1940.
9. Shizuo, Saka, "Theory of the Stability of Hinged Frames Based on the Deflection Angle Deflection Method," *Architectural Journal*, Nov., 1931.
10. Akira, Mizuhara, "On the Vibration of Multiple Story Rigid Frames Sustaining Axial Forces," Papers of the Architectural Society, No. 1, Mar. 1936.
11. Akira, Mizuhara, "The Buckling of Multiple Story Rigid Frames," Papers of the Architectural Society, No. 36, Dec. 1947.
12. Sievers, H., "Die Knickfestigkeit elastisch eingespannter Stäbe," *Der Stahlbau* (1940-3-3), pp. 48-52; (1940-6-7), pp. 61-63.
13. Bültmann, W., "Die Stabilität des Dreigelenkrechteckrahmens," *Der Stahlbau*, (1941-1-8), pp. 3-9; "Die Stabilität der Drei- und Zweigelenk-rechteckrahmen mit Eckstreben und mit Fachwerkriegeln," *Der Stahlbau* (1941-3-7), pp. 24-27.
14. Chwalla, E. and Jokisch, F., "Uber das ebene Knickproblem des Stockwerkrahmens," *Der Stahlbau*, Vol. 14, (1941-4-11), pp. 33-37; (1941-5-16), pp. 47-51.
15. Lundquist, "Stability of Structural Members under Axial Load," National Advisory Committee for Aero., Tech., Note.317 (1937). Lundquist and Kroll, "Tables of Stiffness and Carry over Factor for Structural Members under Axial Load," Natl. Adv. Committee for Aero., Tech., Note 65 (1938). There are many other papers on the subject.
16. Winter, G., Hsu, P. T., Koo, B. and Loh, M. H., "Buckling of Trusses and Rigid Frames," Cornell Univ., Engineering Experimental Station Bulletin No. 36 (1948-4).
17. Kavanagh, T. C., "Instability of Plane Truss Frameworks," Doctoral thesis submitted to the College of Engineering, New York University (1948-4-1), Theory of Buckling of Frameworks reproduced and distributed by the Column Research Council.
18. Shataro, Hiiuta, "Buckling of Frames Having Members with Variable Cross-section," Papers of the Architectural Society, No. 36, Dec. 1947.
19. Yoshikawa, Tsuboi, Minoru, Wakabayashi, "The Stability of Arches and Columns Consisting of Several Members Elastically Connected," Papers of the Architectural Society, No. 37, Apr. 1948.

20. Makoto, Sugano, "Basic Formulas for Calculating the Buckling of Rigid Frames by the Deflection Angle Method," Paper read to the Technology Table of the Japan Architectural Society at the Autumn Session, 1948.
21. Makoto, Sugano, "The Calculation of Buckling of Rigid Frames by the Fixed Moment Method," Research reports of The Japan Architectural Society, No. 1, Convention Issue, May 1949.
22. Morihisa, Fujimoto, "On the Buckling of Irregular Rigid Frames," Research report of the Japan Architectural Society, No. 1, Convention Issue, May 1949.

1. CONTINUOUS MEMBERS

23. Timoshenko, S. Theory of Elastic Stability, McGraw-Hill, New York, 1934.
24. Wittenbauel, Collection of Problems on Applied Dynamics.
25. Shunzo, Kin, ""Computations and Theory of the Buckling Strength of Polygonal Span [literal] Continuous Columns Having Straight Multiple Lattice Spans [literal translation] or Intermediate Stiffener Points," *Journal of Civil Engineering*, Feb., 1940.
26. Siever, H., "Die Knickfestigkeit elastish eingespannter Stäbe," *Der Stahlbau*, (1940-5-3), pp. 48-52; (1940-6-7), pp. 61-63.
27. Bültmann, W., "Die Stabilität des Dreigelenkrechteckrahmens," *Der Stahlbau* (1941-1-3), pp. 3-9. /335
28. Makoto, Sugano, "Calculating the Buckling of Continuous Columns by the Deflection Angle Method," Column Research Special Council Report (1948).
29. Makoto, Sugano, "Basic Formulas for Calculating the Buckling of Rigid Frames by the Deflection Angle Method," Paper read to the Technology Table of the Japan Architectural Society at the Autumn Session, 1948.
30. Yoshikatsu, Tsuboi, Minoru, Wakabayashi, "The Stability of Arches and Columns Consisting of Several Members Elastically Connected," Papers of the Architectural Society, No. 37, Apr. 1948.

2. TRUSSES

31. Ratzersdorfer, J., "Die Knickfestigkeit von Stäben und Stabwerken," Springer, Wien, 1936.
32. Makoto, Sugano, Papers explaining standards for calculating iron reinforced structures, Jan. 1941.
33. Bleich, F., Theorie and Berechnung der Eisernen Brucken, Springer, Berlin, 1924.

3. BUILT-UP MEMBERS

34. Ratzersdorfer, J., "Die Knickfestigkeit von Stäben und Stabwerken, Julius Springer, Wien, 1936.
35. Shuhei, Yokota, "Theoretical Research on the Buckling of Hollow Compressed Members," *Journal of the Civil Engineering Society*, March-April 1941.
36. Amstutz, E. and Stussi, F., "Die Knicklast gegliederter Stabe," *Schweizerische Bauzeitung*, (1941-8-30), pp. 97-101.
37. Masaru, Yasuya, "A Study of the Strength of Short Steel Columns Using Lacing Bars," Bulletin of the Engineering Department of Seoul University, Engineering Section, Vol. 1, No. 1, Jan. 1943.

38. Wienhold, J., "Uber Kipplasten eines Holm-Rippenrostes," Ingenieur-Archiv. Heft 6 (1938), pp. 411-419.
39. Yoshikatsu, Tsuboi and Minoru, Wakabayashi, "The Effect of Torsion Resistance of Chord Member in Lateral Buckling of Frames, Papers of the Japan Architectural Society, No. 38, Apr. 1949.

4. THREE-DIMENSIONAL TRUSSES

40. Ratzersdorfer, J., "Die Knickfestigkeit von Stäben und Stabwerken, Springer, Wien, 1936.
41. Kiyoshi, Takefuji, "The Buckling of Three-Dimensional Trusses," Papers of The Architectural Society, No. 13, Apr. 1939.

5. RIGID FRAMES

42. Timoshenko, S., Theory of Elastic Stability, McGraw-Hill, New York, 1934.
43. Kiyoshi, Takefuji, "The 90th Award of Prizes for Problems in Structural Dynamics." *Architectural World*, Apr. 1942.
44. Wittenbauel, Collection of Problems on Applied Dynamics.
45. Chwalla, E., "Erläuterungen zum Abschnitt A.I.C., S. 16; Erläuterungen zum Normblattentwurf DIN E 4114."
46. Makoto, Sugano, "The Buckling Load of Gate-type Rigid Frames," Column Research Special Council Report, Jan. 1949.
47. Sievers, H., "Die Knickfestigkeit elastisch eingespannter Stäbe," *Der Stahlbau* (1940-5-3), pp. 8-52; (1940-6-7), pp. 61-63.
48. Puwein, M. G., "Die Knickfestigkeit des Resteckrahmens," *Die Bautechnik*, (1940-1-19), pp. 32-35.
49. Chwalla, E., "Die Stabität lotrecht belasteter Rechsteckrahmen," *Der Bauingenieur* (1938-2-4), pp. 69-75.
50. Bültmann, W., "Die Stabilität des Dreigelenkrechteckrahmens," *Der Stahlbau* (1941-1-3), pp. 3-9; "Die Stabilität der Drei- und Zweigelenkrechteckrahmen mit Eckstreben und mit Fachwerkriegeln," *Der Stahlbau*
51. Makoto, Sugano, Unpublished M.S.
52. Chwalla, E. and Jokisch, F., "Uber das Ebene Knickproblem des Stockwerkrah-/336 mens," *Der Stahlbau*, Vol. 14 (1941-4-11), pp. 33-37; (1941-5-16), pp. 47-51.

6. RIGID FRAMES WITH VARIABLE CROSS-SECTION

53. Makoto, Sugano, "The Buckling of Gate-type Rigid Frames Having Beams of Variable Cross-Sections," Column Research Special Council Report, Jan. 1949.
54. Bultmann, W., "Die Stabilitat des Dreigelenkrechteckrahmens," *Der Stahlbau* (1941-1-3), pp. 3-9; "Die Stabilitat der Drei- und Zweigelenkrechteckrahmen mit Eckstreben and mit Fachwerkriegeln," *Der Stahlbau* (1941-3-7), pp. 24-27.

7. THREE-DIMENSIONAL RIGID FRAMES

55. Katsuo, Sezawa and Masami, Murakami, "The Buckling of Basket-shaped [literal translation] Columns Sustaining Axial Pressure," Tokyo University Aeronautics Research Institute Report, Vol. 13, Aug. 1938.

REFERENCES (SUPPLEMENT)

8. SUPPLEMENT

56. Morihisa, Fujimoto, "The Elastic Stability of Rigid Joint Frames," Papers of The Japan Architectural Society, No. 48, Mar. 1954.
57. "Berechnungsgrundlagen für Stabilitätsfälle im Stahlbau DIN 4114-Knickung, Kippung, Beulung," *Stahlbau-Handbuch* 1949/50.
58. Makoto, Sugano, Unpublished M.S.

CHAPTER 2

ARCH BRIDGES

3.2.1. INTRODUCTORY SURVEY

When using arches as bridges, the limit value of its horizontal reaction is an important point requiring consideration in designing arch bridges. For this reason, we will introduce here briefly some theoretical and experimental research on the subject. This paper will focus chiefly on vertical loads and will exclude consideration of extremely flat arches that approximate straight (linear) members. The types of arches that have been dealt with in this area up to the present time, include arch, parabolic, or sine-curve, three-hinged, two-hinged, and hingeless arches, and buckling within the arch plane when an equally distributed load acts on them. This has been the principle object of investigation.

F. Engesser (1903) determined the buckling values of flat, parabolic and circular three-hinged arches, R. Mayer (1921) did the same for flat, two-hinged and hingeless arches, while in 1925, J. Fritsche determined the buckling values for flat, parabolic three-hinged, two-hinged and hingeless arches. In 1930, the Germans enacted DIN 1075 which includes definitions for the buckling of arches.

E. Gaber (1933), who was dissatisfied with existing theoretical formulae, conducted experiments on a model with an effective span of 180 cm and attempted to compare his results with the above theoretical equations. As a result, he found that Fritsche's formulas, applied to flat arches, Mayer's equations for two-hinged arches, gave low values, while his own equations for hingeless arches were suitable for flat arches. He also concluded that the equations in DIN 1075 were suitable for hingeless arches with a relatively high rise. Gaber studied the case in which the moment of inertia of the arch cross-section is not constant, replacing it by a straight-pressure resistant member, having a constant moment of inertia, showing a deflection equal to such a case, and produced numerical tables indicating the converted buckling lengths.

W. Fuchssteiner (1935) studied the theoretical equations for three-hinged arches, compared them with the results of experiments, and demonstrated by experiment that the buckling force of a three-hinged arch, having a rise ratio (ratio of rise f to effective span l: f/l) greater than 1:3 was the same as that for a two-hinged arch of the same dimensions

F. Massi (1935) applied the Vianello-Engesser method to arches, proposed coefficients giving converted buckling lengths and found the relationship between the proper vibration numbers of arches from Stodola's method and the critical horizontal reactions.

Later C. F. Kollbrunner (1936) noticed that there were differences between DIN 1075 and the theoretical equations of Mayer and Fritsche and that Gaber

experimental methods were somewhat higher than Stüssi's theoretical value. In order to clarify these points, he conducted tests on a model with a 60 cm effective span and showed that Stüssi's equations have a rather high reliability.

In 1934, A. Lockschein used the Strömer-Adams method to numerically integrate differential equations for a bent beam and determined the buckling values. His study is a unique one in terms of practicality.

Later, when DIN E 4114 was being formulated, E. Chwalla, referring to the results of experiments by Gaber and Kollbrunner, made determinations for each type of arch with standards for the coefficients, giving the converted buckling lengths as functions of the rise ratio f/l.

B. Busch (1937) conducted experiments primarily on hingeless arches, de- /338
termined experimentally the effects of cross-section moment of inertia on the critical horizontal reaction, and obtained critical values. His results are almost identical with Gaber's coefficients.

Fr. Dischinger (1937) gives buckling values for parabolic arches, especially concrete arches. Comparing his formulas with Stüssi's results, the coefficients given by Stüssi as functions of the rise ratio are constants in Dischinger's work. However, in his work, the fact that he refers, for the first time, to two and three-hinged arches having stiffeners, is noteworthy in terms of applicability. In 1940, Dischinger published his theoretical work.

What has been described above pertains to cases in which there is a uniformly distributed load over the entire arch. E. Deutsch (1940) conducted experiments on cases where the equally distributed load on the left and right of the arch was assymmetrical, and found that the critical horizontal reaction in such a case was 50% lower than for an equally distributed load. He also treats cases in which the moment of inertia varies.

Hiura Daizo (1940) found a method for calculating the buckling of an arch by the deflection angle deflection method and showed through several examples, that his results approximated A. Lockschein's results rather closely.

The above concerns buckling within the arch plane, but in actuality, problems also arise in buckling in a vertical direction, and torsional buckling. However, research in this area apparently has not progressed very far. Timoshenko has provided one or two examples of solutions for elementary problems in the torsional buckling of circular arches, but they are not very practical for the design of bridges. Okamoto Shunzo recently has taken up problems in torsional buckling with reinforced concrete arches as his principal object of investigation (unpublished manuscript 1949). He has provided interesting research giving a theoretical explanation of the fact that the effective span of reinforced concrete arches is limited to, in practice, 30 to 10 times the actual width.

Next, we shall add further explanation on the research on bridges, but since it is useless to rely solely on theoretical equations at the present time, as far as bridge engineering is concerned with respect to the buckling of solid

web arches, experimental research has extremely important meaning.

3.2.2. BUCKLING OF SOLID WEB ARCHES DUE TO EQUALLY DISTRIBUTED LOADS

E. Gaber[1] conducted experiments on four types of arches having an effective span of 180 cm and a parabolic configuration: three-hinged arches, two-hinged arches, single-hinged arches and hingeless arches, using steel plate from St. 80 ($30 \times 4 = 120$ mm^2), and a Young's modulus of E = 2,072,500 kg/cm^2. Using the line connecting the support points on the right and left of the arches as a basis, he selected the values 1/3, 1/5, 1/7, 1/9, 1/12 for the ratio f/l between the height f of the center point of the arch and the effective span l, i.e., the rise ratio, and for arches having hinges at their crowns, he divided the arches into 9 equal coffers, and for those having no hinge at the crown, he divided them into 8 equal coffers and applied a load to each coffer point. The deflection stiffness EI of the members tested was 26,000-35,600 kg.cm^2.

According to his tests, the configuration of the buckling of the arches was as shown in the figure for three-hinged arches, and he found that there were three types of configuration. That is, in flat arches with a rise ratio f/l < 1/5, left-right symmetrical buckling such as that shown in figure 3.2.1 occurred but when f/l > 1/5, assymmetrical buckling such as that shown in figure 3.2.2 occurred, on one side the bending was upwards, and on the other side downwards. In the case of f/l = 1/5, there was a tendency for these three types of buckling to be manifested.

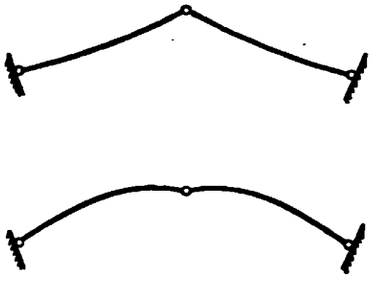

Figure 3.2.1
Left-right symmetrical buckling.

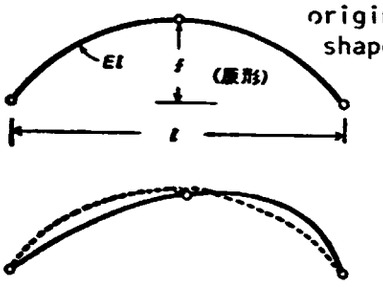

/339

Figure 3.2.2.
Left-right assymmetrical buckling.

Assymmetrical buckling occurs in two-hinged arches irrespective of the f/l and this is likewise true with hingeless arches.

In deriving the critical horizontal reaction H_k from the test values, Gaber used the following formula, for example, for the horizontal reaction H of a two-hinged arch

$$H \fallingdotseq \frac{5l}{8f} P\left[\left(\frac{a}{l}\right)^4 - 2\left(\frac{a}{l}\right)^3 + \left(\frac{a}{l}\right)\right].$$

Here H is the horizontal reaction in the case where the concentrated load P is at a distance a from the support point, and the above formula is none other than an approximation formula that is normally used in the designing of two-hinged

bridges of the arch type. In the case of seven concentrated loads, this becomes the following formula

$$H = 0.9869 \frac{l}{f} P.$$

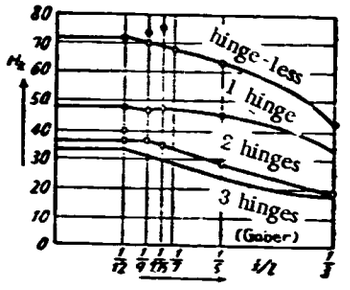

Figure 3.2.3

The results of calculating the critical horizontal reaction H_k of the four types of arches, using this method, are shown in Figure 3.2.3. As can be seen from the figure, the critical horizontal reaction H_k decreases as the rise ratio f/l increases for all four types of arches. Exceptional care is required for the test on flat arches such that f/l = 1/12 and Gaber provides the table (3.2.1) below for the numerical values or the critical horizontal reaction in such a case

TABLE 3.2.1 (GABER'S EXPERIMENTAL VALUES)

Number of Hinges	0	1	2	3
Critical horizontal reaction (kg)	$7.85\frac{\pi^2(EI)}{l^2}$ =71.70 kg	$5.27\frac{\pi^2(EI)}{l^2}$ =48.10 kg	$4.00\frac{\pi^2(EI)}{l^2}$ =36.60 kg	$3.58\frac{\pi^2(EI)}{l^2}$ =37.75 kg

The numerical values shown in Table 3.2.2 are obtained if one attempts to calculate the so-called converted buckling length L when a critical load is applied which is equivalent to the above maximum horizontal reaction, to a straight pressure resisting member having a deflection stiffness with the same constant EI. /340

TABLE 3.2.2

Number of hinges	0	1	2	3
L	$0.36\,l$	$0.43\,l$	$0.50\,l$	$0.53\,l$

Comparing Gaber's test values with the formulas of Engesser, Fritsche, and DIN 1075, as was mentioned in the previous section, there is a marked difference between them and the theoretical equations, indicating that the existing theoretical equations are valid only within a special range of rise ratios.

Fritz Stussi provides the following equation for the critical horizontal reaction H_k of a parabolic arch [2].

$$H_k = \alpha \frac{EI}{l^2}. \tag{3.2.1}$$

Here, l is the arch effective span, I is the moment of inertia of the rib I (constant), α is a constant with respect to the arch, and is calculated theoretically by Stüssi (See figure 3.2.4).

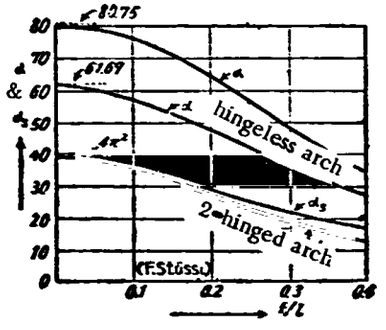

Figure 3.2.4

By comparing the previous equations and Euler's equation for a column with hinges at both ends having the same moment of inertia I, and finding the so-called converted buckling length L,

$$L = \frac{\pi l}{\sqrt{\alpha}} \tag{3.2.2}$$

Moreover, Stüssi gives the following formula for the proper vibration number (circular vibration number) p of the arch. The coefficient α_s in the numerical formula is as shown in Figure 3.2.4.

$$p = \frac{\alpha_s}{l^2}\sqrt{\frac{EI \cdot g}{w}}\sqrt{1-\frac{H}{H_k}}. \tag{3.2.3}$$

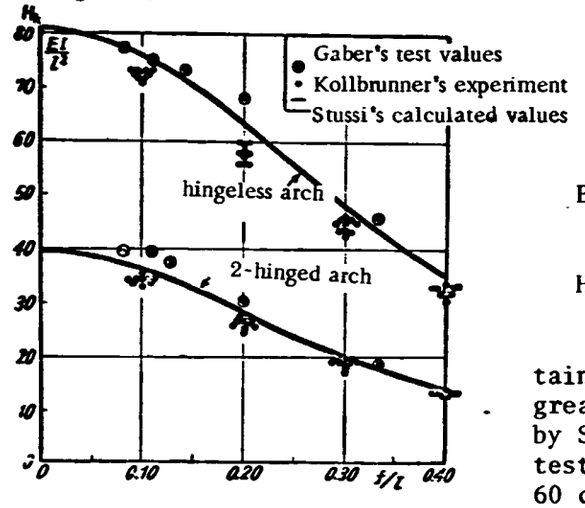

Figure 3.2.5

l: effective span
g: gravity acceleration
EI: deflection stiffness of ribs
w: equally distributed load
H: horizontal reaction due to w
H_k: critical horizontal reaction

The critical horizontal reaction obtained from Gaber's experiments is somewhat greater than the theoretical values obtained by Stüssi, so Kollbrunner [3], [4] repeated tests on an arch having an effective span of 60 cm using steel with a cross-section of 12 × 1 mm (cross-section area 0.12 cm^2), E = 2,200,000 kg/cm^2, and obtained the results shown in Figure 3.2.5.

There are two types of arches here, two-hinged arches and hingeless arches. /341 The rise ratio f/l has the following four types:

$$\frac{f}{l} = 0.10, \quad 0.20, \quad 0.30, \quad 0.40.$$

It also became clear that the proper vibration numbers agreed with Stüssi's theoretical values.

Tables 3.2.3 and 4 present in tabular form the coefficient in equation (3.2.1). Lockschein's numerical values are also included for comparison in the tables.

TABLE 3.2.3. NUMERICAL VALUES OF α AND β (PARABOLIC TWO-HINGED ARCH WITH CONSTANT CROSS-SECTION

f/l		0.05	0.1	0.2	0.3	0.4	0.5
α	(Stüssi)		36.0	28.0	20.0	13.5	
	(Lockschein)		35.6	28.4	19.4	13.7	9.6
β	(Stüssi)	—	1.02	1.08	1.17	1.28	—
	DIN E 4114	1.00	—	1.10	1.20	1.30	—

$H_k = \alpha \frac{EI}{l^2}$, $L = \beta \cdot s$. See Figure 3.2.6 for s

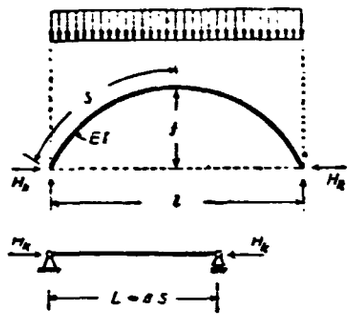

Figure 3.2.6

The converted buckling length L indicated in equation (3.2.2) can be rewritten as

$$L = \left(\frac{\pi}{\sqrt{\alpha}} \frac{l}{s}\right) s$$

if one uses the semi-arch length s in Figure 3.2.6. Now,

$$L = \beta \cdot s \qquad (3.2.4)$$

finding this coefficient data as a function of f/1, the numerical values shown in Table 3.2.3 and 3.2.4 in two-stages are obtained. Moreover, 1/s for a parabolic arch is

$$s = \frac{l^2}{32f}\left\{2t + \sinh 2t\right\}, \quad \sinh t = \frac{4f}{l}.$$

Consequently, for

$f/l =$ 0.1, 0.2, 0.3, 0.4,

$s/l =$ 0.513, 0.549, 0.602, 0.667.

TABLE 3.2.4. NUMERICAL VALUES OF α AND β (PARABOLIC HINGELESS ARCH WITH CONSTANT CROSS-SECTION

f/l		0.05	0.1	0.2	0.3	0.4
α	(Stüssi)	—	76.0	63.0	48.0	35.0
β	(Stüssi)	—	0.70	0.72	0.75	0.80
	DIN E 4114	0.70	—	0.75	0.80	0.85

$H_k = \alpha \frac{EI}{l^2}$, $L = \beta \cdot s$.

In the German bridge specification DIN E 4114, it is proposed that for numerical values of α, the bottom values of β in Tables 3.2.3 and 4 should be used. [4]. /342

B. Busch conducted research on the case in which the moment of inertia I of the rib section of a hingeless arch varied in different ways. The appratus he used for his experiments is shown in Figure 3.2.7.

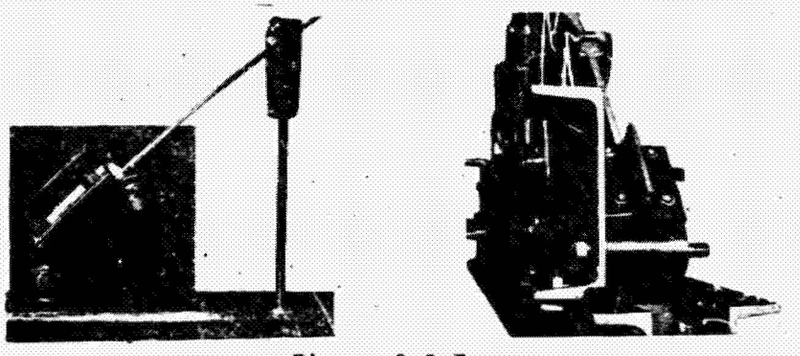

Figure 3.2.7

In the case of a constant parabolic arch in which I does not vary, it is possible to determine by the following formula the critical horizontal reaction H_k using Gaber-Kollbrunner's test values described above as a basis.

$$H_k = \frac{\pi^2 \cdot EI}{(\gamma l)^2}. \qquad (3.2.5)$$

EI: deflection stiffness of rib cross-section
l: arch effective span
γ: coefficient (see Table 3.2.5)

i.e., $$\gamma = \frac{\pi}{\sqrt{\alpha}}.$$

This was substituted for a column with both ends hinged and length γl, and the values of the coefficient γ are as shown in Table 3.2.5.

TABLE 3.2.5. NUMERICAL VALUES OF γ (HINGELESS PARABOLIC ARCH)

f/l	1/9	1/7.5	1/6	1/4.5	1/3
Gaber's experiments	0.36	0.365	0.37	0.39	0.46
Busch's experiments	0.36	0.37	0.38	0.40	

However, when the I of the rib-cross-section varies, it is not possible to shift the condition under which the rib cross-section changes to this substituted member without any modification. In such a case, it is permissible to replace it

a section member such that one end is rooted, the other end is hinged, and the column length is 1/2 of the total arc length of the arch length s. That is, as shown in Figure 3.2.8, one can clearly see that the condition of the buckling of the hingeless arch is quite similar to the buckling condition of the substituted member.

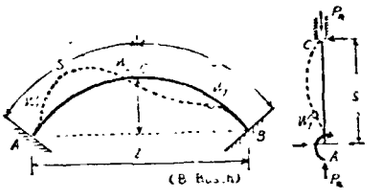

Figure 3.2.8

According to what has been shown in experiments, the critical value P_k of the substituted member with the length s shown in the figure, with one end rooted and the other end hinged, agrees well with the compressive force at point 1/4 of the arch [literal translation]. Consequently, in practice, the critical horizontal reaction H_k is given by the following equation if it is assumed that ψ_U is the diagonal angle at the point 1/4 of the arch. /343

$$\left.\begin{aligned} H_k &= P_k \cdot \cos\varphi_v = P_k \frac{1}{\sqrt{1+4(f/l)^2}}. \\ \text{where} \quad P_k &= \frac{20.19}{s^2} \times EI_s\mu. \end{aligned}\right\} \tag{3.2.6}$$

I_S is the moment of inertia of the cross-section of the crown. μ is a coefficient related to change in the moment of inertia. When I is a constant value, $\mu = 1$. Consequently, Busch gives the following equation for H_k corresponding to equation (3.2.5).

$$H_k = \frac{20.19}{s^2} \times \frac{EI}{\sqrt{1+4(f/l)^2}}. \tag{3.2.7}$$

Busch obtains the values of μ experimentally. As one example, taking the case in which the thickness h of the rib varies as a second order parabola, shown in Figure 3.2.9.

$$\left.\begin{aligned} h_k &= h_s\left\{1+(m-1)\frac{x^2}{s^2}\right\}. \\ \text{where} \quad m &= \frac{h_k}{h_s}. \end{aligned}\right\} \tag{3.2.8}$$

The value of μ in this case is as shown in Table 3.2.6.

TABLE 3.2.6. IN THE CASE WHEN THE RIB THICKNESS VARIES IN THE FORM OF A SECOND-ORDER PARABOLA. (BUSCH)

$m = h_k/h_s$	1.0	1.2	1.4	1.6	1.8
$n = I_k/I_s$	1.00	1.73	2.74	4.10	5.83
μ	1.00	1.19	1.39	1.60	1.83

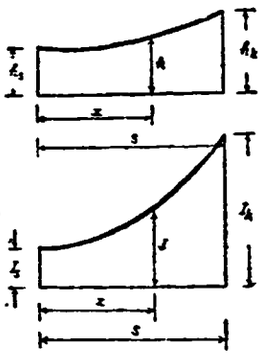

Figure 3.2.9

Taking the case in which the I of the rib cross-section varies in the form of a third-order parabola

$$I=I_s\left[1+\left\{8\frac{I_0}{I_s}-7-n\right\}\frac{x^2}{s^2}+\left\{6-8\frac{I_0}{I_s}+2n\right\}\frac{x^3}{s^3}\right]. \qquad (3.2.9)$$

where

$$I_0=I_s\frac{n}{\frac{n}{2}\frac{1}{\sqrt{1+4(f/l)^2}}+\frac{1}{2}\sqrt{\frac{1+16(f/l)^2}{1+4(f/l)^2}}},\qquad n=\frac{I_k}{I_s}$$

the state of this variation is close to Strassner's hypothesis* that the I/I cos ψ used in the arch solution method varies linearly. /344

The values of μ in this case are indicated in Table 3.2.7. Figure 3.2.10 illustrates the relationships in Table 3.2.7 three-dimensionally.

TABLE 3.2.7. μ IN THE CASE WHEN THE I OF THE CROSS-SECTION OF THE RIB VARIES IN THE FORM OF A THIRD-ORDER PARABOLA (BUSCH)

n	Rise Ratio f/l					
	1/12	1/10	1/8	1/6	1/4	1/3
1	0.99	0.99	0.98	0.98	0.96	0.95
2	1.32	1.31	1.31	1.31	1.31	1.31
4	1.64	1.64	1.64	1.64	1.66	1.68
6	1.84	1.84	1.84	1.84	1.87	1.90
8	1.99	1.99	2.00	2.00	2.03	2.07

TABLE 3.2.6 CASE WHEN CROSS-SECTION VARIES AS SECOND-ORDER PARABOLA

$m=h_k/h_s$	1.0	1.2	1.4	1.6	1.8
$n=I_k/I_s$	1.00	1.73	2.74	4.10	5.83
μ	1.00	1.19	1.39	1.60	1.83

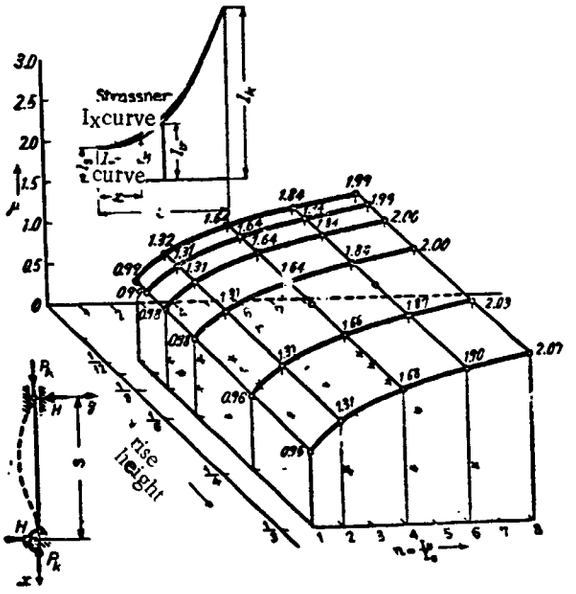

Figure 3.2.10. μ in case when I varies in the form of a third-order parabola (Busch)

*Strassner, "Neuere Methoden zur Statik der Rahmentragwerke und der elastichen Bogenträger," Bd. 2 (1927), p. 44.

3.2.3. BUCKLING OF SOLID WEB ARCH DUE TO ASYMMETRICALLY DISTRIBUTED LOAD.

The description given above is for the critical horizontal reaction in the case when an equally distributed load is applied throughout the span of an arch. However, what is particularly necessary in designing an arch bridge is the case in which an asymmetrical load is applied, as shown in Figure 3.2.11. Deutsch [6] conducted experiments on an arch with a cross-section 30 × 4 mm, effective span 180 cm, rise ratio f/l = 1/9, 1/7.5, 1/6, 1/4.5. He has made a valuable contribution to this field with his experiments.

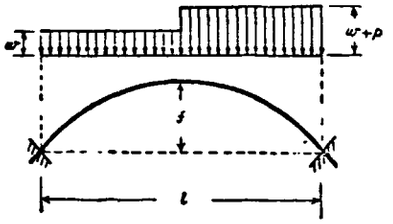

Figure 3.2.11

The configurations of the cross-sections used in the test, as shown in Figure 3.2.12, include 3 hingeless arches and 4 two-hinged arches. Attention is called to the fact that it is reported that in specimens no. 7 and 13, having a maximum cross-section in the vicinity of 1/4, the deformation at point 1/4 is large.

/345

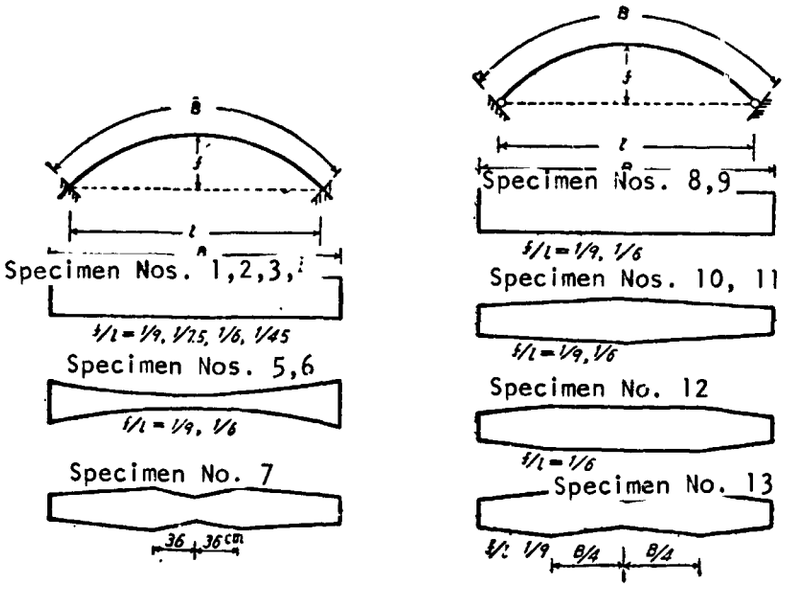

Figure 3.2.12. Types of arch model specimens (Deutsch).

As mentioned in the previous section, using H_k as the critical horizontal reaction due to the equally distributed load w, and denoting the critical horizontal reaction due to an asymmetrical load as shown in Figure 3.2.13 as H_{kr} we express this ratio by ϕ in the following equation

$$\phi=\frac{H_{kr}}{H_k} \quad \text{or} \quad H_{kr}=\phi \cdot H_k. \tag{3.2.10}$$

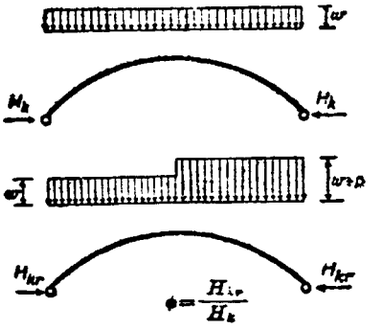

Figure 3.2.13

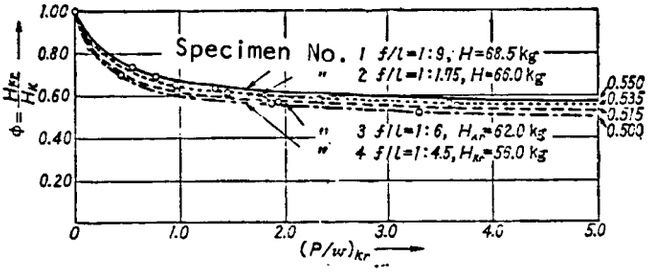

Figure 3.2.14. φ of hingeless arch when I = constant.

Generally, aside from hingeless arches and two-hinged arches, there is practically no effect on ϕ by the rate of variation of I or the differences in f/1, and as shown in Figure 3.2.15, when throughout the experiment $p/w \to \infty$, it is seen that $\phi = 0.5$.

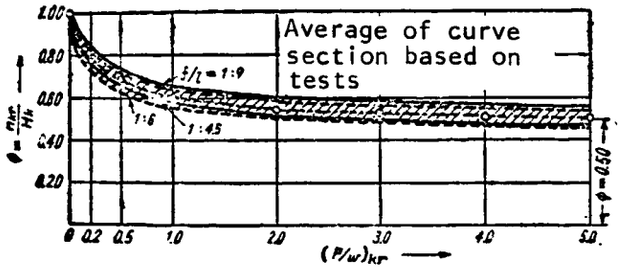

Figure 3.2.15. Average values of ϕ.

Consequently, if one ignores the fine points, it is possible, by means of equation (3.2.10) conveniently to handle the problem of the buckling of an arch with respect to an asymmetrical load in terms of the problem of the buckling of an arch due to an equally distributed load.

Deutsch processed his experimental values and gave the values of ϕ as functions of f/1 and p/w. These are shown in Figures 3.2.16 and 3.2.17.

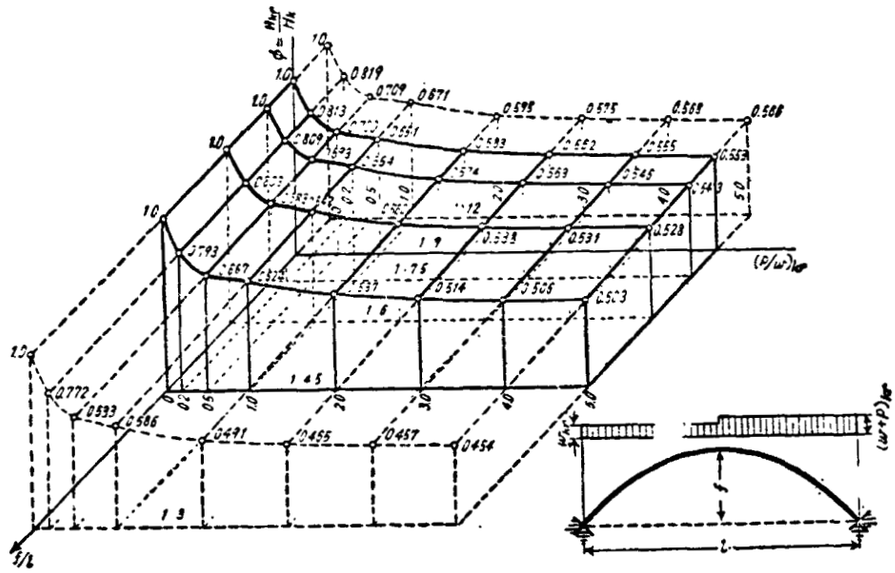

Figure 3.2.16. ϕ in the case of a hingeless arch (I = arbitrary) (Deutsch)

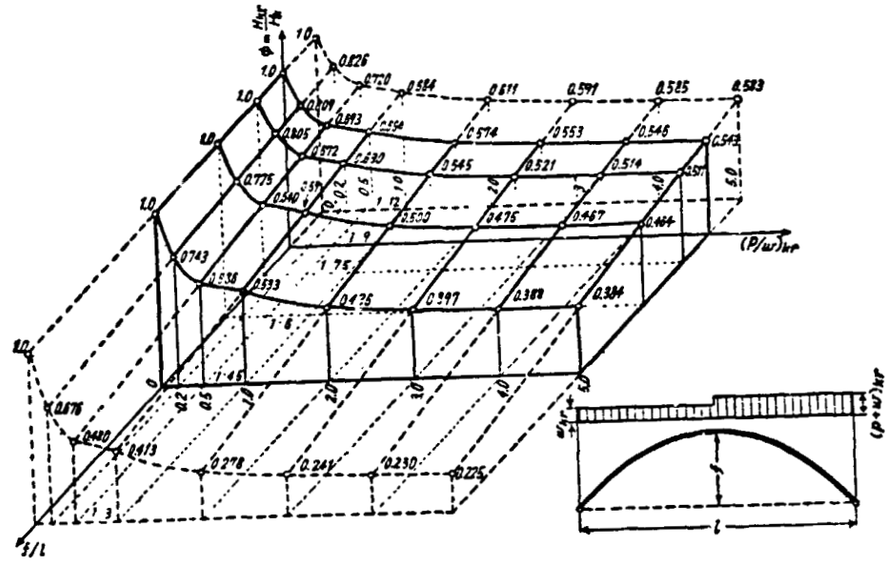

Figure 3.2.17. ϕ for a two-hinged arch (I = arbitrary)

In essence, the critical horizontal reaction H_{kr} or an arch due to an asymmetrical load is given by the following equation in practice.

(3.2.11) /347

Hingeless arch: $$H_{kr}=\phi\frac{20.19\,EI_s}{(B/2)^2}\mu\cdot\cos\varphi_u,$$

2-hinged arch: $$H_{kr}=\phi\frac{\pi^2 EI_s}{(B/2)^2}\mu\cdot\cos\varphi_u.$$

ϕ: rate of attenuation due to asymmetrical load,
B: total arc length of arch,
I_S: moment of inertia of crown cross-section,
μ: coefficient related to the change in configuration of the cross-section,
ψ_U: diagonal angle at point 1/4 of arch.

When the load is equally distributed throughout the arch span, if ϕ = 1.0 and I is constant throughout the span, u = 1. μ has already been discussed in the previous section (Tables 3.2.6 and 7). Deutsch gives the following in Figures 3.2.19, 20, 21 and 22.

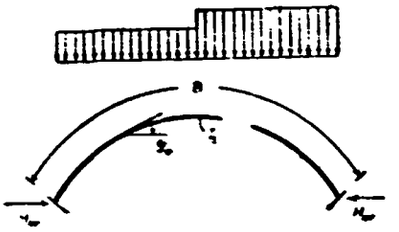

Figure 3.2.18

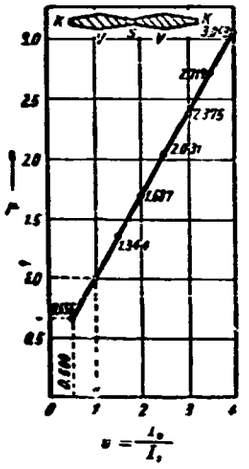

Figure 3.2.19. μ for hingeless arch.

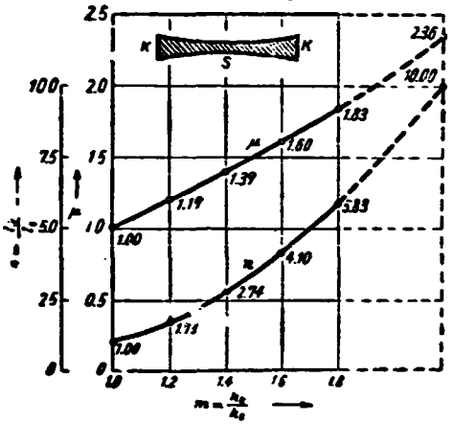

Figure 3.2.20. μ for hingeless arch.

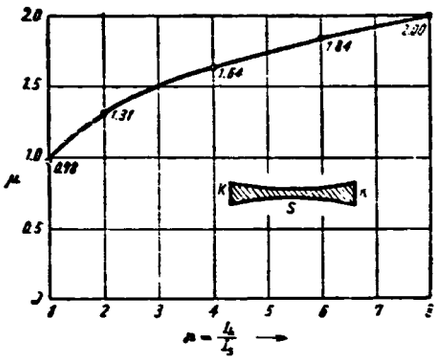

Figure 3.2.21

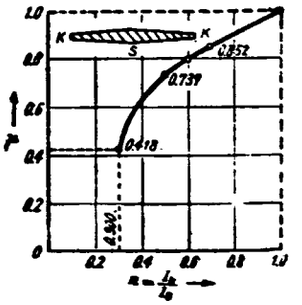

Figure 3.2.22

NOTATION

/349

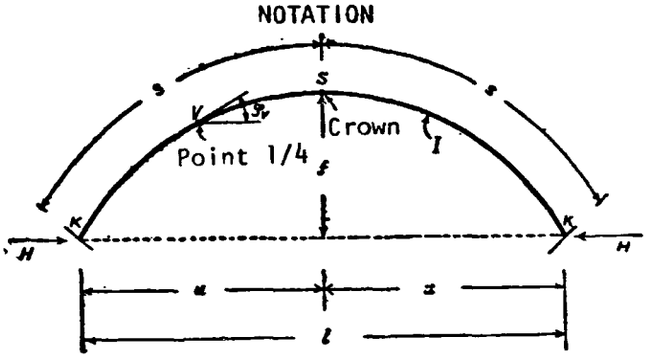

l: Arch effective span
s: Half of arch arc length
f: rise
ψ: Angle of inclination of arch axis
ψ_U: Angle of inclination at point 1/4 of arch
I: Geometric moment of inertia of rib cross-section
I_S: I at crown
I_k: I at rising point
I_U: I at point 1/4 of arch
A: Cross-section area at rib cross-section
H: Horizontal reaction
w: Equally distributed load over entire span (normally corresponding to dead load)———Vertical direction
p: Equally distributed load applied to half of span (normally indicates live load)———Vertical direction
L: Free buckling length
q: Equally distributed load in center direction of circular arch
r_0: Radius of circular arch
K: Rise point
V: Point 1/4
S: Crown

PARABOLIC ARCHES

Equally Distributed Load in Vertical Direction

No. 1

Parabolic 3-hinged arch

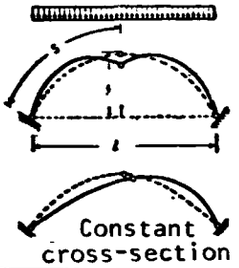

Constant cross-section

$L=\beta \cdot s.$

where L is converted buckling length

f/l		0.05	0.1	0.167	0.2	0.25	0.30	0.33	0.40
β	Gaber	–	1.05	1.11	–	1.17	–	1.15	–
	DIN E 4114	1.20	1.20	1.20	1.20	1.20	1.20	–	1.30

(NOTE) Symmetrical load when $f/l<0.295$, anti-symmetrical load when $f/l>0.295$

Ref.-Remarks: 1, 4

No. 2

Parabolic 2-hinged arch

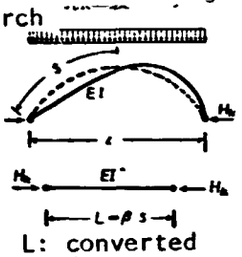

L: converted buckling length

Constant cross-section

$H_k=\alpha\frac{EI}{l^2}$ or $L=\beta \cdot s.$

f/l		0.05	0.1	0.2	0.3	0.4	0.5
α	Stüssi		36.0	28.0	20.0	13.5	
	Lockshein		35.6	28.4	19.4	13.7	9.6
β	Stüssi	–	1.02	1.08	1.17	1.28	–
	DIN E 4114	1.00	–	1.10	1.20	1.30	–

Ref.-Remarks: 2, 4

No. 3

Parabolic hingeless arch

I = constant ≡ I

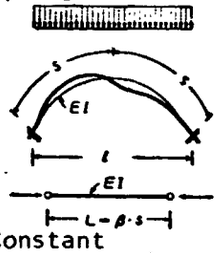

Constant cross-section

$H_k=\alpha\frac{EI}{l^2}$ or $L=\beta \cdot s.$

f/l		0.05	0.1	0.2	0.3	0.4
α	Stüssi	–	76.0	63.0	48.0	35.0
β	Stüssi	–	0.70	0.72	0.75	0.80
	DIN E 4114	0.70	–	0.75	0.80	0.85

Ref.-Remarks: 2, 4

No. 4

Parabolic 3-hinged arch

$I=\frac{I_s}{\cos\varphi}$

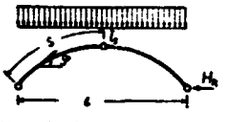

Variable cross-section

$H_k=\alpha\frac{EI_s}{l^2}$.

f/l		0.1	0.2	0.3	0.4
α	Symmetrical buckling	29.400	27.728	(25.332)	(22.596)
	Anti-symmetrical buckling	(37.200)	(31.582)	25.112	19.432

Ref.-Remarks: 7, Based on Dischinger

No.	Dia. & Bound. Cond.	Formulas or Tables of Results	Ref.-Remarks
5	Parabolic 2-hinged arch $I=\frac{I_s}{\cos\varphi}$ Variable cross-section	$H_k=\alpha\frac{EI_s}{l^2}$. f/l: 0.1 | 0.2 | 0.3 | 0.4 | 0.5 α: 37.2 | 31.6 | 25.1 | 19.4 | 15.0	8
6	Parabolic hingeless arch $I=\frac{I_s}{\cos\varphi}$ Variable cross-section	$H_k=\alpha\frac{EI_s}{l^2}$. f/l: 0.1 | 0.2 | 0.3 | 0.4 | 0.5 α: 78.2 | 71.0 | 61.3 | 51.1 | 41.9	8
7	Parabolic 2-hinged arch $I=\frac{I_s}{\cos^2\varphi}$ 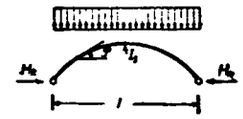 Variable cross-section	$H_k=\alpha\frac{EI_s}{l^2}$. f/l: 0.1 | 0.2 | 0.3 | 0.4 | 0.5 α: 38.4 | 37.4 | 33.8 | 31.6 | 29.4	8
8	Parabolic hingeless arch $I=\frac{I_s}{\cos^2\varphi}$ 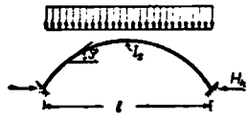 Variable cross-section	$H_k=\alpha\frac{EI_s}{l^2}$. f/l: 0.1 | 0.2 | 0.3 | 0.4 | 0.5 α: 82.2 | 85.6 | 89.4 | 92.7 | 95.5	8
9	Parabolic arch, End conditions arbitrary 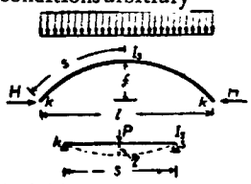 Variable cross-section	A determination is made of the moment of inertia I_i of the constant cross-section giving, under the same support conditions for the same load, a deflection which is exactly the same as the deflection of the center point occuring when the left or right half of the arch is converted to a straight axis and both ends are supported. Next, the critical horizontal reaction of the original arch having a constant I_i is regarded as the critical horizontal reaction of the original arch for convenience sake.	4 DIN E 4114
10	parabolic 3-hinged stiffened arch 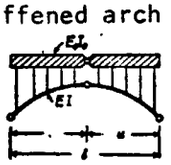	$H_k=7.437\frac{E_0I_0+EI}{u^2}$. $L=1.152\times u$. where L is free buckling length	7

No.	Dia. & Bound. Cond.	Formulas or Tables of Results	Ref.-Remarks
11	Parabolic 2-hinged stiffened arch (langor truss) 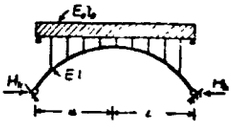	$H_k=9.87\frac{E_0I_0+EI}{u^2}$. $L=1.00\times u$. Where L is free buckling length	7
12	Parabolic hingeless arch 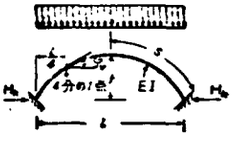 Constant cross-section	$H_k=\frac{\pi^2EI}{(\gamma l)^2}$. Numerical values of γ $H_k=P_k\cdot\cos\varphi_s=P_k\frac{1}{\sqrt{1+4\left(\frac{f}{l}\right)^2}}$. where $P_k=\frac{20.19}{s^2}EI$.	1 5
13	Parabolic hingeless arch, variable cross-section (varying linearly). $I=I_s\left[1+(n-1)\frac{x}{s}\right]$ $n=I_k/I_s$ 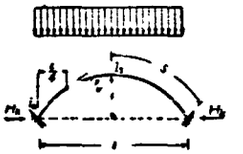 $H_k=P_k\cdot\cos\varphi_s$ P_k: axial pressure at point 1/4 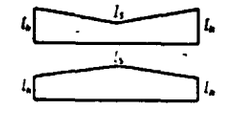	Variation in cross-section $I=I_s\left[1+(n-1)\frac{x}{s}\right]$. $n=\frac{I_k}{I_s}$. Axial pressure P_k at point 1/4 $P_k=20.34\frac{EI_s}{s^2}\left[1+(n-1)0.4904\right]$. $H_k=P_k\cdot\cos\varphi_s$. and $s=\frac{1}{2}\left[1+\frac{8}{3}\left(\frac{f}{l}\right)^2-\frac{32}{5}\left(\frac{f}{l}\right)^4\right]$.	5

Numerical values of γ

f/l		1/9	1/7.5	1/6	1/4.5	1/3
γ	Gaber	0.36	0.365	0.37	0.39	0.46
	Busch	0.36	0.37	0.38	0.40	

14

Parabolic hingeless arch
Variable cross-section

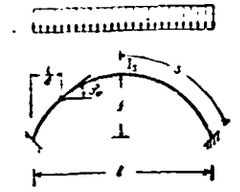

It is given that the rib height varies parabolically as shown below.

$$h_x = h_s\left[1+(m-1)\frac{x^2}{s^2}\right]$$

$$m = \frac{h_k}{h_s}$$

$$I = \frac{h_x^3}{h_s^3} I_s$$

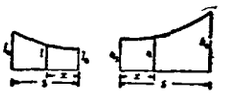

$$H_k = P_k \cdot \cos\varphi_v.$$

$$P_k = \frac{20.19\,EI_s}{s^2}\mu.$$

$m=\frac{h_s}{h_x}$	1.0	1.2	1.4	1.6	1.8
$n=\frac{I_k}{I_s}$	1.00	1.73	2.74	4.10	5.83
μ	1.00	1.19	1.39	1.60	1.83

5

15

Parabolic hingeless arch, variable cross-section

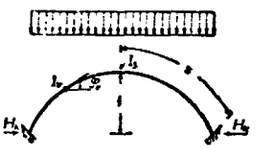

$$I = I_s\left[1+\left\{8\frac{I_v}{I_s}-7-n\right\}\frac{x^2}{s^2} + \left\{6-8\frac{I_v}{I_s}+2n\right\}\frac{x^3}{s^3}\right]$$

$$n = \frac{I_k}{I_s}$$

In the above equation an approximation is made on the basis of the assumption that $Is/I \cdot \cos\varphi$ will vary linearly.

$$H_k = P_k \cdot \cos\varphi_v.$$

$$P_k = \frac{20.19 \cdot EI_s}{s^2}\mu.$$

The M in the case when the I of the rib cross-section varies parabolically (illeg.) is shown in the table below

$n=I_k/I_s$	f/l					
	1/12	1/10	1/8	1/6	1/4	1/3
1	0.99	0.99	0.98	0.93	0.96	0.95
2	1.32	1.31	1.31	1.31	1.31	1.31
4	1.64	1.64	1.64	1.64	1.66	1.68
5	1.84	1.84	1.84	1.84	1.87	1.90
8	1.99	1.99	2.00	2.00	2.03	2.07

5

No.	Dia. & Bound. Cond.	Formulas or Tables of Results	Ref.-Remarks
16	Parabolic 2-hinged arch, asymmetric equally distributed load. 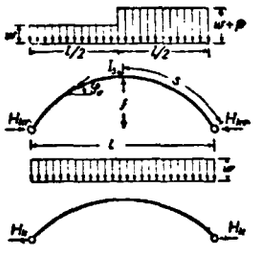 Variable cross-section	$H_{k'}=\phi \cdot H_k$. $H_k=\frac{\pi^2 EI_s}{s^2}\mu \cdot \cos\varphi_u$. $\phi=\alpha+\frac{1-\alpha}{e^{3m}}$. where $\alpha=0.70-1.44(f/l)$. $0 \leqq m \leqq 1$ . . . . $b=3.0-1.6m$, $1 \leqq m \leqq 5$ . . . . $b=1.5-0.1m$, $5 \leqq m \leqq \infty$ . . . . $b=1.0$, $m=(p/w)_k$.	6

f/l	$m=(p/w)_k$							
	0	0.2	0.5	1.0	2.0	3.0	4.0	5.0
1/12	1.000	0.826	0.720	0.684	0.611	0.591	0.585	0 583
1/9	1.000	0.809	0.693	0.654	0.574	0.553	0.546	0.543
1/7.5	1.000	0.805	0.672	0.630	0.545	0.521	0.514	0.511
1/6	1.000	0.776	0.640	0.590	0.500	0.475	0.467	0.464
1/4.5	1.000	0.743	0.586	0.533	0.426	0.397	0.388	0.384
1/3	1.000	0.676	0.480	0.413	0.278	0.241	0.230	0 225

17	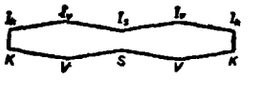 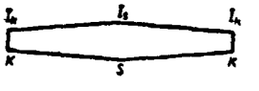	The coefficient μ refers to change in cross-section and in the case of a constant cross-section, μ = 1. I becomes a maximum at point 1/4 of the span, and the μ in the case of linear variation is as shown in the graph on the right. 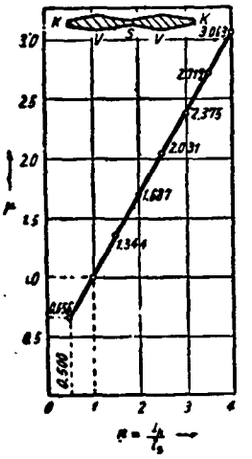 I becomes maximum at the crown, and the μ in the case of linear variation is as shown in the graph on the right. 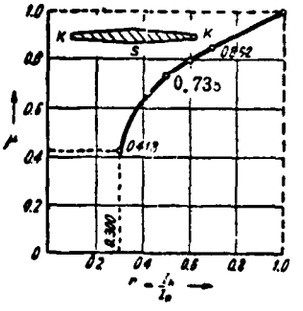	6

18

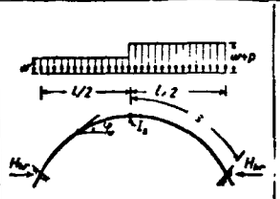

$$H_{kr}=\phi \cdot H_k.$$

$$H_k=\frac{20.19\,FI_s}{s^2}\mu\cos\varphi.$$

$$\phi=\alpha+\frac{1-\alpha}{e^{bm}}.$$

where $\alpha=0.60-0.45\,(f/l)$.

$0\leqq m\leqq 1$ . . . . $b=3.0-1.6\,m$,
$1\leqq m\leqq 5$ . . . . $b=1.5-0.1\,m$,
$5\leqq m\leqq \infty$ . . . . $b=1.0$,
$m=(p/w)_k$.

6

f/l	$m=(p/w)_k$							
	0	0.2	0.5	1.0	2.0	3.0	4.0	5.0
1/12	1.000	0.819	0.709	0.671	0.595	0.575	0.568	0.566
1/9	1.000	0.813	0.700	0.661	0.583	0.562	0.555	0.553
1/7.5	1.000	0.809	0.693	0.654	0.574	0.553	0.546	0.543
1/6	1.000	0.803	0.683	0.642	0.560	0.538	0.531	0.528
1/4.5	1.000	0.793	0.667	0.624	0.537	0.514	0.506	0.503
1/3	1.000	0.772	0.633	0.586	0.491	0.465	0.457	0.454

19

6

Case in which I varies as a second-order parabola

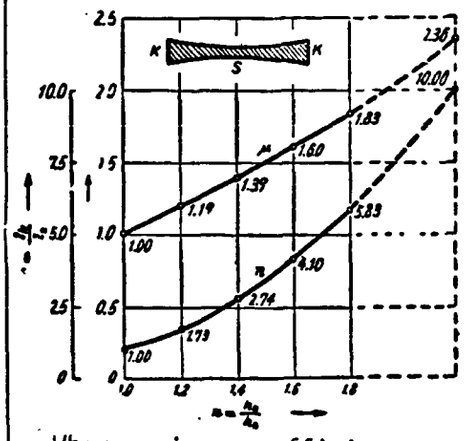

Case in which I varies as a third-order parabola

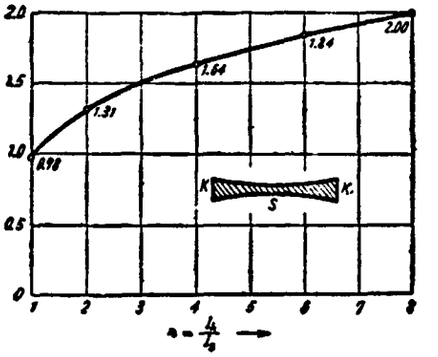

Where μ is a coefficient

SINE CURVE, FLAT ARCHES (NOT OF MUCH PRACTICAL VALUE)

No.	Dia. & Bound. Cond.	Formulas or Tables of Results	Ref.-Remarks
20	Flat 2-hinged arch, concentrated load 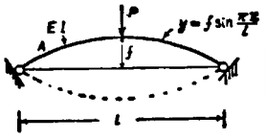 A: Cross-section area	The critical values in the case when the arch becomes unstable and buckles in a downward direction are obtained by the following equation. $u=1+\sqrt{\frac{4}{27}\frac{(1-m)^3}{m^3}}$. Here $m=\frac{4I}{Af^2}<1,\quad u=\frac{Pl^3}{48EI}\frac{1}{f}$.	9
21	Flat 2-hinged arch 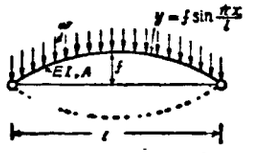 A: cross-section area	7 – The critical values in the case when the arch becomes unstable and buckles in a downward direction are obtained by the following equation. $u=1+\sqrt{\frac{5}{27}\frac{(1-m)^3}{m^3}}$. Here $m=\frac{4I}{Af^2}<1,\quad u=\frac{5}{384}\frac{wl^4}{EI}\frac{1}{f}$.	9
22	Flat 2-hinged arch 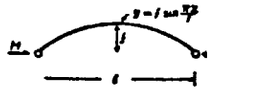 	$H_k=\frac{\pi^2EI}{l^2}\left(1+\frac{\pi^2i^2}{l^2}+\frac{\pi^2f^2}{8l^2}\right)$. where i: radius of gyration	10

TORSIONAL BUCKLING OF LANGER TRUSS (SUPPLEMENT)

番号	図及び境界条件	結果の式又は表	文献・備考
23	 Established deformation	I. Case in which the upper chord member has only a fixed position. when $f/l=0.16$ $\quad H_{cr}=\frac{EI_2}{l^2}\left(\frac{44.46}{1+0.0898\cdot r}\right)$ when $f/l=0.24$ $\quad H_{cr}=\frac{EI_2}{l^2}\left(\frac{67.80}{1+0.50\cdot r}\right)$ II. Case in which the upper chord member is fixed in a position and direction and is free with respect to torsion. when $f/l=0.16$ $\quad H_{cr}=\frac{EI_2}{l^2}\left(\frac{81.92}{1+0.0264\cdot r}\right)$ when $f/l=0.24$ $\quad H_{cr}=\frac{EI_2}{l_2}\left(\frac{67.92}{1+0.053\cdot r}\right)$ I_2 Geometric moment of inertia around vertical axis r Ratio of torsion stiffness to bending stiffness in lateral direction.	17

No.	Dia. & Bound. Cond.,	Formulas or Tables of Results	Ref.-Remarks
24	Circular 2-hinged arch 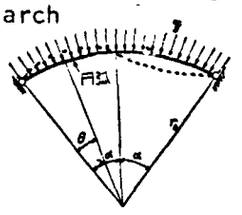 Constant cross-section	$q_k=\frac{EI}{r_0^3}\left(\frac{\pi^2}{\alpha^2}-1\right)$.	9 11
25	Circular hingeless arch 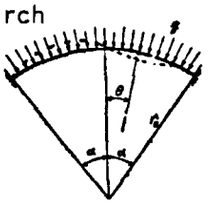 Constant cross-section	$q_k=\frac{EI}{r_0^3}(k^2-1)$. where k is given by the following equation $k\cdot\tan\alpha\cdot\cot k\alpha=1$. α: 30° 60° 90° 120° 150° 180° k: 8.621 4.375 3.000 2.364 2.066 2.000	9 12
26	Circular 2-hinged arch 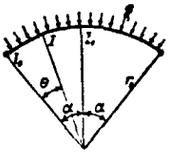 Variable cross-section $I=I_0\left\{1-\left(1-\frac{I_1}{I_0}\right)\frac{\theta}{\alpha}\right\}$	$q_k=\frac{m}{\alpha^2}\frac{EI_0}{r_0^3}$. Values of m α \ I_1/I_0: 0.1 0.2 0.4 0.6 0.8 1.0 0°: 4.67 5.41 6.68 7.80 8.85 π^2 30°: 4.54 5.20 6.48 7.58 8.62 9.60 60°: 4.16 4.82 5.94 6.94 7.89 8.77 90°: 3.53 4.08 5.02 5.86 6.66 7.40 (NOTE) The numerical values of $\alpha=0$ pertain to straight member with variable cross-section and the buckling configuration has a point of inflection in the center.	9
27	Circular 3-hinged arch 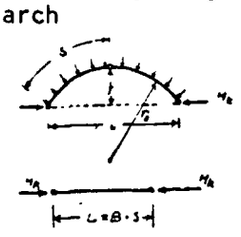 Constant cross-section	The free buckling length L is given by the following formula irrespective of f/l. $L=1.16\cdot s$.	13

No.	Dia. & Bound. Cond.	Formulas or Tables of Results	Ref.-Remarks
28	Circular tied arch (inside the surface) EI_1(outside the surface) 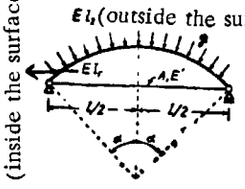 	[1] Buckling within plane containing centerline of beam $q_{k1}=q'_{k1}(1+\theta\cos^2\alpha)$. where $q'_{k1}=\frac{EI_1}{r^3}\left(\frac{\pi^2}{\alpha^2}-1\right)$. where $q'k_1$ is the buckling load of the circular two-hinged arch. [2] Buckling in directions outside of plane containing centerline of beam $q_{k2}=q'_{k2}(1+\theta\cos^2\alpha)$. where $q'_{k2}=\frac{EI_2}{r^3}\left(\frac{\pi^2}{\alpha^2}-1\right)^2\Big/\left(\frac{\pi^2}{\alpha^2}+\frac{EI_2}{c}\right)$. c: torsion stiffness of arch $\theta=\frac{EI_1\cdot\sin\alpha}{E'Ar^3}\Big/\left(1+\frac{\alpha}{2}\cos 2\alpha-\frac{3}{4}\sin 2\alpha\right)$. Values of Θ, $\Theta\cos^2\alpha$ unit $\frac{EI_1}{E'Ar^3}$	14
29	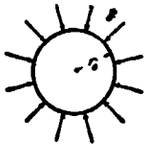	$q_k=\frac{3EI}{r_0^3}$.	M. Levy equation
30	Buckling inside plane of circle 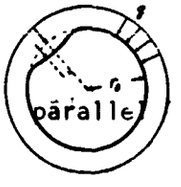 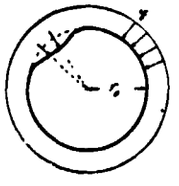 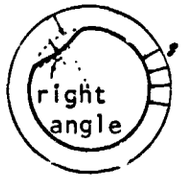 	[1] Case in which the direction of external pressure does not change even after deformation. $q_k=4\frac{EI}{r_0^3}$. [2] Case in which the external pressure is toward the center of the circle even after deformation. $q_k=4.5\frac{EI}{r_0^3}$. [3] Case in which the external pressure after deformation acts at right angles to the center axis of the circle. $q_k=3\frac{EI}{r_0^3}$.	1c

α°	15	16	18	20	22	25
θ	15.986	1235.5	771.77	506.62	346.18	207.83
$\theta\cos^2\alpha$	14925	1141.6	698.07	447.36	297.60	170.70

α°	30	35	40	45	50	60
θ	100.41	54.316	31.915	19.975	13.142	6.3735
$\theta\cos^2\alpha$	75.309	36.447	18.728	9.9874	5.4299	1.5934

31 Torsional buckling of circular arch

Simple support (the ends are free to rotate around the principal axes, but cannot rotate around the center axis).

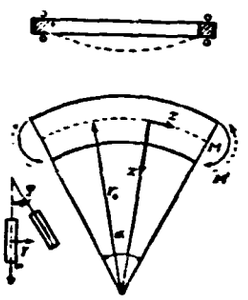

$$M_k = \frac{B+C}{2r_0} + \sqrt{\left(\frac{B-C}{2r_0}\right)^2 + \frac{BC}{r_0^2}\frac{\pi^2}{\alpha^2}},$$

$$M'_k = \frac{B+C}{2r_0} - \sqrt{\left(\frac{B-C}{2r_0}\right)^2 + \frac{BC}{r_0^2}\frac{\pi^2}{\alpha^2}}.$$

where

B: Bending stiffness in direction outside of paper, plane

C: Torsional stiffness

[note 1]

if $r_0 \to \infty$, $r_0\alpha = l$

$$M_k = +\frac{\pi\sqrt{BC}}{l}, \quad M'_k = -\frac{\pi\sqrt{BC}}{l}.$$

[note 2]

$\alpha = \pi$, $M'_k = 0$.

9

EQUALLY DISTRIBUTED LOAD q IN DIRECTION OF CENTER OF CIRCLE

No.	Dia. & BOund. Cond.	Formulas or Tables of Results	Re.-Remarks
32	Torsional buckling of circular arch Simple support	(1) Case in which the direction of load q does not change during buckling, and only laterally in a direction parallel to the original direction. $q_k r_0 = \frac{B}{r_0^2} \cdot \frac{(\pi^2-\alpha^2)^2}{\alpha^2\left(\pi^2+\alpha^2\frac{B}{C}\right)}$. If α is small and $\alpha r_0 = l$ $q_k r_0 = \frac{\pi^2 B}{l^2}$. [Euler's equation] where B: Bending stiffness toward outside of the plane of the page. C: Torsional stiffness (2) Case in which the direction of load q is always toward the center of the original curvature. $q_k r_0 = \frac{\pi^2 B}{r_0^2} \cdot \frac{\pi^2-\alpha^2}{\alpha^2\left(\pi^2+\alpha^2\frac{B}{C}\right)}$.	9

No.	Dia. & Bound. Cond.	Formulas or Tables of Results	Ref.-Remarks
33	Torsional buckling of circular arch 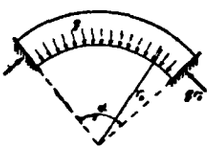 Both ends fixed	$q_k r_0 = m\frac{B}{r_0^2}$. B: Bending stiffness in direction outside of [indented] plane C: Torsional stiffness When $\alpha < \frac{\pi}{2}$ in place of the above formula, it is possible to use the following approximate formula. $q_k r_0 = \frac{B}{r_0^2}\frac{(4\pi^2-\alpha^2)^2}{\alpha^2\left(4\pi^2+\alpha^2\frac{B}{C}\right)}$. When $\alpha \to 0$, $\alpha r_0 = l$ $\quad q_k r_0 = \frac{4\pi^2 B}{l^2}$.	9

α	0.250π	0.500π	π	1.063π	1.10π	1.24π	1.50π	2π
m	60.1	12.6	1.85	1.54	1.40	1.00	0.69	0.50

DISTRIBUTED LOADS

No.	Bound. & Dia. Cond.	Formulas or Tables of Results	Ref.-Remarks
34	Torsional buckling of circular arch (Not hinged) 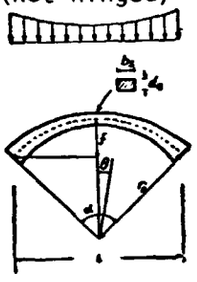 I_s: Moment of inertia of cross-section C_s: Same as above, torsion stiffness w_{sk}: Buckling limit load strength at crown Variation in cross-section $I = \frac{I_s}{1-0.3\frac{\sin\theta}{\sin\frac{\alpha}{2}}}$. Variation in distributed load : $w = \frac{H}{r}\sec^2\theta$.	Examples of calculations assuming $E = 2\times10^6$ kg/cm², $G = 1\times10^6$ kg/cm²	

$\frac{f}{l}$	l	f	r_0	b_s	d_s	I_s	G_s	$\frac{EI_s}{GC_s}$	$\frac{Hr_0^2}{EI_s}$	w_{sk}
Unit	m	m	m	m	m	m⁴	m⁴			t/m
$\frac{1}{4.65}$	60	13.99	39.16	3.5	1.2	4.28	1.57	5.46	0.585	83.5
	80	18.65	52.22	3.5	1.6	5.71	3.41	3.35	0.755	60.5
	100	23.32	65.27	3.5	2.0	7.15	6.00	2.38	0.872	44.8
$\alpha=100°$	120	27.98	78.32	3.5	2.4	8.57	9.28	1.85	0.951	33.9
	160	37.30	104.43	3.5	3.2	11.43	17.56	1.30	1.050	21.2
$\frac{1}{3.46}$	60	17.32	34.64	3.5	1.2	4.28	1.57	5.46	0.223	45.8
	80	23.09	46.19	3.5	1.6	5.71	3.41	3.35	0.265	30.7
$\alpha=120°$	100	28.87	57.74	3.5	2.0	7.15	6.00	2.38	0.312	23.2
	120	34.64	69.28	3.5	2.4	8.57	9.28	1.85	0.345	18.3
$\frac{1}{2.85}$	40	14.00	21.28	3.5	0.8	2.86	0.511	11.18	0.0336	19.9
	60	21.01	31.93	3.5	1.2	4.28	1.57	5.46	0.0574	15.0
	80	28.01	42.57	3.5	1.6	5.71	3.41	3.35	0.0778	11.5
$\alpha=140°$	100	35.01	53.21	3.5	2.0	7.15	6.00	2.38	0.0926	8.8
	120	42.01	63.85	3.5	2.4	8.57	9.28	1.85	0.104	6.8

REFERENCES CITED

CHAPTER 2. ARCH BRIDGES

1. Gaber, E., "Über die Knickischerheit vollwandigen Bogen," *Bautech*, 1934, pp. 646-651.
2. Stüssi, Fritz, "Aktuelle baustatische Probleme der Konstruktionpraxis," *Schweiz*, Bauzeitung, 1935, pp. 132-135.
3. Kollbrunner, C. F., "Versuche über die Knickischerheit und die Grundschwingungszahl vollwandiger Bogen," *Bautech*, 1936, pp. 186-188.
4. Knick and Beulvorschriften fur Baustahl---Erlauterungen zur Begründung des Normblattentwurfes von prof. E. Chwalla, *Bautech*, 1940 .
5. Busch, B., "Knicksicherheit vollwandiger Bögen," *Bauing*, 1937, pp. 812-820.
6. Deutsch, E., "Das Knicken von Bogenträgern bei unsymmetrischer Belastung," *Bauing*, 1940, pp. 353-360.
7. Dischinger, Fr., "Untersuchung über die Knickischerheit, die elastiche Verformung und des Kriechen des Betons ber Bogenbrücken," *Bauing*, 1937, pp. 487-520.
8. Hilman, L., "Nachrichten des Polytech. Inst. Leningrad., Bd. XXXIII.
9. Timoshenko, S. "Theory of Elastic Stability."
10. Marguerre, K., "Uber die Behandlung von Stabilitätsproblemen mit Hilfe der energetschen Methode," Z.A.M.M., Feb., 1938, pp. 57-73.
11. Hurlbrink, E., Schiffbau, Bd. 9, 1908, p. 517.
12. Nicolai, E. L., Z.A.M.M., Bd. 3, 1923, p. 227.
13. Nasarow, A., "Zur Frage der Knicksicherheit eines Bogens," *Bautech*, 1936, pp. 114-115.
14. Tokio, Uematsu, Masao, Tahara, Papers of the Japan Architectural Society, Vol. 8, No. 30. (February 1942) I-36.
15. Ratzersdorfer, J., "Über die stabilität des Kiesringes in seiner Ebene," Z.d. Österreichischen Ingenieur u. Architekten Vereines, (1938-5=27), pp. 146-148.
16. Shunzo, Okamoto, "On the Buckling of an Arch Bridge in the Side Direction," Sept. 24, 1949, unpublished.

REFERENCES CITED (SUPPLEMENT)

17. Godden, W. G., "The lateral buckling of tied arch," Proc. (1954), Paper No. 5965.

PART 4 PLATES

CHAPTER 1

HISTORY OF DEVELOPMENTS

It is a well known fact that when a thin flat plate sustains a compressive force, shear force, or stresses which are a combination of these, acting within its plane, the phenomenon of buckling occurs, lateral deflection arises and the plate is damaged. In structures consisting of flat plates and other parts, such as airplanes, ships and bridges, in those which were constructed of a light structure in order to reduce weight, the problem of the buckling of flat plates is one of the major factors in the design of these structures, and has been investigated extensively.

G. H. Bryan (1891) [10] was the first to theoretically define the occurrence of buckling when a rectangular flat plate receives a compressive load. He calculated buckling limit values for the case of peripherally rotating ends, and discussed the possibility of the occurrence of such buckling in the outer plating of ships. However, at that time, in the shipbuilding world, the concept of effective width was being discussed vaguely due to the fact that in thin plate structures the compressive stiffness decreases, as was found in results of the tests of the Destroyer Wolf but this was not treated as a problem related to buckling. Later, calculations were made of the buckling limit values by S. Timoshenko [11], Nizawa [12], G. I. Taylor [23] and others on the basis of various boundary conditions such as fixed boundaries. Moreover, as the occurrence of buckling on the decks of destroyers, tankers and other ships became noticed, the problem of buckling due to compressive forces received wider attention.

G. Schnadel [108] was the first to theoretically discuss the phenomenon in which the compressive stiffness decreases after the flat plate receives a compressive force and buckles. He found that when the buckling limit is exceeded, and a compressive load is applied, the compressive forces increase only on the end parts, the compressive force does not increase very much in the center part of the plate, and as a result, the effective stiffness decreases. As for this problem, research became greatly accelerated after stressed outer skin structures became applied to aircraft, and compressive force was applied also to outer skins, and through the tests of L. Schuman and G. Back [32], the theoretical studies of Th. v. Kármán and his colleagues [109], H. L. Cox [15] and K. Marguerre [112], the amount of theoretical research was increased greatly on problems of the effective width which expresses the decrease in effective stiffness after buckling and on the maximum loads that a plate can withstand when it sustains compression.

The problem of buckling due to the shear of a rectangular flat plate is extremely important in aircraft construction. H. Wagner indicated that buckling

occurs in the stressed skin of the aircraft due to the shear stresses which it sustains, and the calculations of the critical buckling point was carried out by S. Timoshenko [36], R. V. Southwell and S. W. Skan [37]. In aircraft structures, there are cases in which the outer skin must be very thin due to the need to reduce weight, and the buckling critical stress is lower than the stress used. The conditions under which the outer skin that is surrounded by longerons and frames assumes stresses when a load is applied exceeding such a buckling limit stress, have been discussed by H. Wagner [130] in terms of the theory of a tension field, and A. Kromm and K. Marguerre [133] and others have extended the research even further.

E. Clark showed that even in bridge girders sustaining primarily a bending load, when the thickness of the web near the neutral axis is reduced in order to reduce weight, the plate that is performed by the webs buckles due to the bending stresses and fails. This was further confirmed by M. Houboutte, F. E. /364
Turneau. Turneau, W. E. Lilly and others calculated the critical buckling point by considering that this type of buckling was due to the action of a principal compressive force arising in a direction inclined 45° to the beam axis due to the shear stresses that are present in the beam. Later S. Timoshenko [57] found the critical buckling values for rectangular plates that simultaneously undergo bending and shearing, and Lilly's method showed that such buckling was excessive with respect to safety. Moreover, H. Wagner [65], S. Timoshenko [57] and others determined the critical values for the case in which shear and compression are simultaneously sustained, and for the case in which bending and shear are sustained. H. Wagner [65], S. Timoshenko [57], E. Chwalla [67] and others have investigated problems of the forms of structures having deflection resistant members attached at right angles to beam axes. In beams sustaining bending, lateral buckling also occurs, but this problem is not treated here. Types of structures with thin anti-deflection plates are sometimes used in ships and airplanes. In these structures, molded members are arranged with respect to the rectangular plates sustaining compression, either in the direction of compression (called longerons, longitudinal anti-deflection members, or longitudinal reinforcers) in a direction at right angles to it. Lateral anti-deflection member), or at fixed intervals in both directions. Such longitudinal anti-deflection members sustain the compressive forces and at the same time restrict the buckling wave form that occurs. The lateral anti-deflection members, by restricting the buckling wave form, are also used to increase the critical buckling values. Various forms of buckling exist in the case in which such anti-deflection structures sustain compressive loads, and S. Timoshenko [36], A. J. Miles [146], and R. Barbré [147] and others have investigated the forms in which deflection buckling occurs in the anti-deflection members and flat plates simultaneously. Yamana [16] and others, in investigating this type of buckling, attempted to treat such anti-deflection structures as orthotropic plates. When the stiffness of the lateral anti deflection member is greater than the plate, as the compressive load increases, buckling first occurs only in the flat plates between the anti-deflection members, then the latter are also buckled and a maximum load for the anti-deflection structure is reached. In this case, after the buckling of the flat plates, the phenomenon of effective width is manifested in the flat plates, and only the portions adjacent to the anti-deflection members sustain a load, working together with the anti-deflection

members. Various forms of buckling of anti-deflection members occur depending upon the cross-section configuration, length, and other factors. These include the Euler buckling of anti-deflection members, bending and torsional buckling, local buckling of flanges and others. The fact that aside from the occurrence of these types of buckling, cases in which a maximum load is reached otherwise, are determined by the buckling of plates between rivets to which anti-deflection members are fixed (buckling between rivets) and by the reaching of a maximum load in the plates alone, has been discussed by many investigators with respect to aircraft, including E. E. Sechler [119], E. E. Lundquist [166], H. L. Cox [172] and others. Yoshiki [34] has studied the maximum loads which ships with longitudinal rib structures can withstand. S. Timoshenko [143], R. Barbre [147] and others have studied the required stiffness in problems of lateral anti-deflection members.

S. Timoshenko [1], H. Wagner [130] and others have discussed the fact that problems of anti-deflection thin plate structures sustaining shearing loads are of major importance to aircraft structures. In structures such that the plate first buckles, conditions after the buckling of the plate are treated as the problem of the tension field mentioned above, and when the interval between the anti-deflection members is relatively narrow, this may be treated as the buckling of orthotropic plates. With regard to wooden aircraft structures, treatment as isotropic plates becomes an important problem with regard to the properties of the wood itself and in connection with the use of plywood. Problems of isotropic plates are similarly applicable to corrugated structures.

In problems of the buckling of hollow four-angled columns, angle members, other open-type cross-section columns, i.e., so-called flat plate structures, consisting of thin plates, it is possible to treat the local buckling on the basis of the buckling of flat plates. S. Timoshenko [20], Kuranishi [184] and others discussed these problems.

CHAPTER 2

THE BUCKLING OF FLAT PLATES

4.2.1. CALCULATION OF THE CRITICAL BUCKLING POINT OF FLAT PLATES

G. H. Bryan [10] was the first to determine the critical buckling point of a flat plate, for the case of a rectangular plate with circumferentially rotating ends sustaining compressive loads. Bryan's method proceeds from equilibrium equations for infinitesimal displacement, and is a method of direct solution (called the static method) for determining the critical values from the conditions giving a deformation which is not 0, and in which the required boundary conditions are fulfilled. In addition, there is Nizawa's [12] vibration method for determining the critical values from the condition in which the vibration number is 0, considering infinitesimal deflection vibration, and Timoshenko's method [11], called the energy method, which utilizes the fact that in the state of equilibrium, the potential energy does not change with respect to a hypothetical displacement. In addition to the above, Galerkin's method, and Grammel's method can be used, which are sometimes used as a method of the approximate solution of eigen values. Attempts have also been made to achieve an approximate solution by using difference equations. Moreover, in order for buckling phenomena to be present, it is necessary for there to be at least more than two states of equilibrium under an identical external force state, and identical boundary conditions. For this reason, even though the infinitesimal deformation theory cannot be used to describe this adequately, it nevertheless may be used, as long as one is determining critical buckling points, and furthermore, as long as one is confining one's self to flat plates.*1

The equilibrium equation of infinitesimal deflection deformation in a flat plate is

$$D\nabla_1^4 w+N_x\frac{\partial^2 w}{\partial x^2}+N_y\frac{\partial^2 w}{\partial y^2}+2N_{xy}\frac{\partial^2 w}{\partial x\partial y}=0 \qquad (4.2.1)$$

Here, D = bending stiffness of plate $\left(=\frac{Et^3}{12(1-\nu^2)}\right)$

---

1 When an elastic body sustains a load and is in a state of equilibrium, given an infinitesimal deformation, one determines whether the equilibrium is stable, unstable, or neutral, the neutral state gives the critical point of buckling, (R. V. Southwell). In a flat plate, the initial state of equilibrium is reached by infinitesimal deformation from a state of non-equilibrium (in shells this is not necessarily infinitesimal), and even if the effects of the initial deformations are added, its effect may be disregarded.

* R. V. Southwell, "On the General Theory of Elastic Stability," Phil. Trans. Roy. Soc. Ser. A. 213 (1914), 187.

N_x, N_y = compressive force per unit width acting on the plate midplane in constant cross-sections x and y respectively.

N_{xy} = shear forces acting on the unit widths of the above.

$$\nabla_1^4=\left(\frac{\partial^2}{\partial x^2}+\frac{\partial^2}{\partial y^2}\right)^2.$$

Bryan makes the following hypothesis for deflection which satisfies the conditions

$w=0, \quad M_x=0$ (where x = 0 and x = a)

$w=0, \quad M_y=0$ (where y = 0 and y = b)

for the case where N_{xy} = 0 for four-sided rotating-ends.

i.e.

$$w=A_{mn}\sin\frac{m\pi x}{a}\sin\frac{n\pi x}{b} \qquad \text{(m, n both integers)} \tag{4.2.2}$$

This deflection is assumed to give the critical buckling value in which the condition (

$$D\left[\left(\frac{m\pi}{a}\right)^2+\left(\frac{n\pi}{b}\right)^2\right]^2=N_x\left(\frac{m\pi}{a}\right)^2+N_y\left(\frac{n\pi}{b}\right)^2 \tag{4.2.3}$$ /366

satisfies equation (4.2.1).

In the vibration method, the condition of vibration where the term for the force of inertia at the time of vibration is added to equation (4.2.1) is

$$D\nabla_1^4 w+N_x\frac{\partial^2 w}{\partial x^2}+N_y\frac{\partial^2 w}{\partial y^2}+2N_{xy}\frac{\partial^2 w}{\partial x\partial y}+\rho\frac{\partial^2 w}{\partial \zeta^2}=0 \tag{4.2.4}$$

where

ρ = mass of plate per unit surface area

ζ = time

and, by determining the vibration number which satisfies the boundary conditions, the critical value is obtained from the condition that the vibration number is 0. For example, for a rectangular plate with peripherally rotating ends, substituting

$$w=A_{mn}\sin\frac{m\pi x}{a}\cdot\sin\frac{n\pi y}{b}\cos(p\zeta+\varepsilon)$$

in equation (4.2.4) and making the condition p = 0 the same results are obtained as equation (4.2.3).

When it is difficult to obtain a solution by the direct method, using the energy method, sometimes an approximate solution is found. That is, assuming a deflection w which satisfies the boundary conditions, the critical value is determined by substitution in the following equation:

$$\delta\int_0^a\int_0^b\left[\frac{N_x}{2}\left(\frac{\partial w}{\partial x}\right)^2+N_{xy}\cdot\frac{\partial w}{\partial x}\cdot\frac{\partial w}{\partial y}+\frac{N_y}{2}\left(\frac{\partial w}{\partial y}\right)^2\right]dxdy \tag{4.2.5}$$

$$+D\,\delta\int_0^a\int_0^b\left[\frac{(\nabla_1^2 w)^2}{2}+(1-\nu)\left\{\frac{\partial^2 w}{\partial x^2}\cdot\frac{\partial^2 w}{\partial y^2}-\left(\frac{\partial^2 w}{\partial x\,\partial y}\right)^2\right\}\right]dxdy=0$$

Even better results are obtained if one expresses the deflection as the sum of several terms, and uses Ritz's method, adding unknown coefficients. Moreover, Timoshenko [20] also adds the variation of potential due to the moment and shear forces on the periphery, but under normal boundary conditions, since such variation is 0, it has been omitted here, but it must be added when necessary.

With regard to plates with a configuration other than rectangular, one may replace an operator ∇_1^4 for the curve coordinates for such a configuration. For example, for a circular plate sustaining a compressive force, N_r (per unit length) in the direction of the radius

$$D\left(\frac{\partial^2}{\partial r^2}+\frac{1}{r}\frac{\partial}{\partial r}+\frac{1}{r^2}\frac{\partial^2}{\partial\theta^2}\right)^2 w+N_r\left(\frac{\partial^2}{\partial r^2}+\frac{1}{r}\frac{\partial}{\partial r}+\frac{1}{r^2}\frac{\partial^2}{\partial\theta^2}\right)w=0 \tag{4.2.6}$$

becomes the condition of equilibrium.

4.2.2. THE BUCKLING OF RECTANGULAR FLAT PLATES

(1) Case in which Compression is Sustained. The critical value for a flat plate with peripherally rotating ends, sustaining a uniform compression from one direction (x), is found by assuming $N_y = 0$, in Bryan's equation (4.2.3) given above. Expressing the critical stress as σ_k,

$$\sigma=\frac{E\pi^2}{12(1-\nu^2)}\left(\frac{t}{b}\right)^2\left(\frac{bm}{an}+\frac{an}{bm}\right)^2 \tag{4.2.7}$$

Here, m and n indicate the number of half-waves of the buckling wave form in directions x and y. The case in which the number of waves in direction y n = 1, constantly gives a minimum value for σ_k but with regard to the value of m in direction x, the value of m which gives the minimum value of σ_k due to the aspect ratio of the plate a/b varies. That is, the minimum values of σ_k are given by m = 1 where /367

$$a/b\leqq\sqrt{2} \qquad \text{and by} \qquad \sqrt{2}\leqq a/b\leqq\sqrt{6}$$

Moreover, in the case where the aspect ratio a/b = 1.0, σ_k takes a minimum value

becoming

$$\sigma_k=4\cdot\frac{E\pi^2}{12(1-\nu^2)}\left(\frac{t}{b}\right)^2 \tag{4.2.8}$$

(See figure 4.2.2.) Moreover, where a/b > 3, this may be regarded as almost equal to the minimum value.

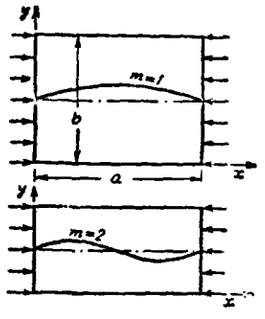

Figure 4.2.1

The solution which satisfies the condition that the edges are fixed, i.e.

$$w=0,\quad \frac{\partial w}{\partial x}=0 \qquad \text{(where x = 0 and x = a)}$$

$$w=0,\quad \frac{\partial w}{\partial y}=0 \qquad \text{(where y = 0 and y = b)}$$

and satisfies the equilibrium condition equation, is not easily found, so various methods of solution have been published. S. Timoshenko [11] has carried out approximation calculations by the energy method, while Nizawa [12], Yamana [16], employ the vibration method, Nizawa [13], O. H. Faxen [17], G. I. Taylor [23], Iguchi [26] obtain solutions by expanding to infinite series. Iguchi's solution is elegant in the sense that the coefficient which is included in the deflection equation varies according to the boundary conditions. i.e., in

$$w=\sum_m\sum_n A_{mn}\left\{\frac{c_m}{3}\left(\frac{x^3}{a^3}-\frac{x}{a}\right)-\frac{c_m'}{3}\left(\frac{x^3}{a^3}-\frac{3x^2}{a^2}+\frac{2x}{a}\right)+\frac{1}{m\pi}\sin\frac{m\pi x}{a}\right\}$$

$$\times\left\{\frac{d_n}{3}\left(\frac{y^3}{b^3}-\frac{y}{b}\right)-\frac{d_n'}{3}\left(\frac{y^3}{b^3}-\frac{3y^2}{b^2}+\frac{2y}{b}\right)+\frac{1}{n\pi}\sin\frac{n\pi y}{b}\right\}$$

(m, n = integers)

for four-side rotating ends, $c_m = c_m' = d_n = d_n' = 0$. If the end is fixed on four sides,

$$c_m=-1-2(-1)^m,\ c_m'=2+(-1)^m,\ d_n=-1-2(-1)^n,\ d_n'=2+(-1)^n,\ x=0$$

are fixed, and when the other three sides are rotating ends,

$$c_m=0,\ c_m'=\frac{3}{2},\ d_n=d_n'=0$$

Substituting w in the equilibrium equation and expanding to the series sin (mπx)/a sin (nπy)/b, the critical value is determined from the condition that the coefficients are 0.

S. Timoshenko [20], Nizawa and Nishimura [21], H. L. Cox [15], have solutions for the case in which the load edge to which a compressive force is applied has a rotating end and the edge parallel to the load is fixed. Conversely, K. Schleicher [22] and others have solutions for the case in which the load edge is fixed and the other edge has a rotating end. S. Timoshenko [20] has a solution for the case in which one side parallel to the load is free and the other three sides have rotating ends. A. J. Miles [146] provides a solution for the

case in which the load edge has a rotating end, while the other edges are elastically supported. Moreover, in the case in which the load edge has a rotating end, assuming the deflection

$$w=f(y)\sin\frac{m\pi x}{a}$$

Inserting in the equilibrium equation and determining f(y) /368

$$f(y)=C_1e^{-\alpha y}+C_2e^{\alpha y}+C_3\cos\beta y+C_4\sin\beta y$$

where

$$\alpha=\sqrt{\frac{m^2\pi^2}{a^2}+\sqrt{\frac{N_x}{D}\cdot\frac{m^2\pi^2}{a^2}}},\quad \beta=\sqrt{\frac{-m^2\pi^2}{a^2}+\sqrt{\frac{N_x}{D}\cdot\frac{m^2\pi^2}{a^2}}}$$

so, from the condition y = 0, y = b, the critical value is obtained by eliminating C_1, C_2, C_3, C_4.

In any of the above cases, the critical buckling stress σ_k can be expressed by the following equation. That is

$$\sigma_k=k\frac{\pi^2E}{12(1-\nu^2)}\left(\frac{t}{b}\right)^2=k\sigma_e \tag{4.2.9}$$

k is the number which is determined under the support conditions of the edge, and the aspect ratio a/b of the plate. Moreover, with the regard to the number of half-waves in the direction of compression, where a/b is small, 1 gives the minimum critical value, but as a/b increases, the number of half-waves giving the minimum critical value increases, as in the case of peripherally rotating ends. (See figure 4.2.2). Moreover, the critical buckling stress can be expressed by

$$\sigma_k=k'\frac{E}{1-\nu^2}\left(\frac{t}{b}\right)^2 \tag{4.2.10}$$

in place of equation (4.2.9) The k' in the equation is the same as the coefficient k.

With regard to experimental investigations of flat plates sustaining compression, there are the experiments of L. Schumann and G. Back [32] on sides parallel to the load, supported by V channels, using Duraluminum, Monel metal, uncast steel and nickel plates, Yamana's experiments using copper plates [16], in which the sides parallel to the load are fixed, and H. L. Cox's [15] experiments on Duraluminum plates. H. Wagner and R. Lahde [118] have conducted experiments on rectangular flat plates in which the sides parallel to the load are supported by anti-deflection members, in which super Duraluminum plates were /369 used. In addition, there have been experiments by H. L. Cox [33] and Yoshiki [34] using soft steel plates. For plates in which the edge parallel to the load is held down by knife edges, Yokoo [120] has conducted experiments using Duraluminum, super Duraluminum and non-cast steel plates and Yoshiki [35] has used soft steel plates. Moreover, in Yokoo's experiments, he includes plates supported by V channels. As for the load edges, except for the studies by

Yamana and Cox, aiming at fixed-edge conditions, most of the studies involved holding the rectangular plates on a flat surface.

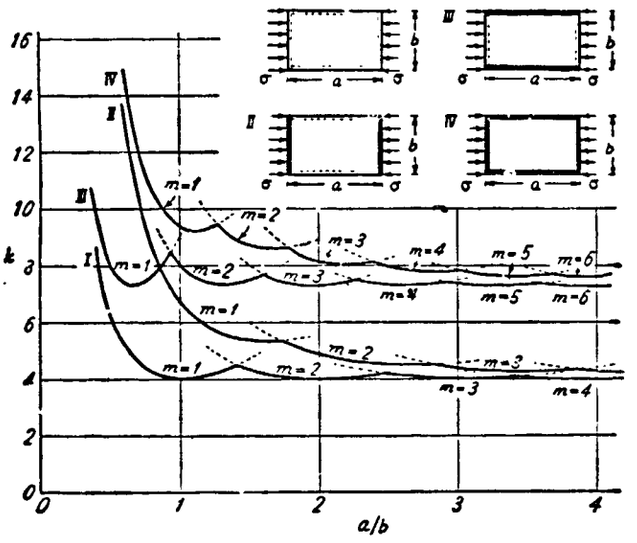

Figure 4.2.2

In experiments it is difficult to process the specimen so that it is completely flat and for this reason, there are many cases in which a clear critical point is not obtained. For this reason, there are few reports which discuss the value of the critical point, and it is said that Schumann's values are lower than those calculated by Bryan and that Cox's agree with the theoretical values in general for the case in which the edges are fixed. Yoshiki states that in determining the critical values by using the characteristics of the load-deflection curve after buckling, the values agree generally with those calculated as shown in Section 9 of the "Materials" below. [translator's note: "Materials" refers to the special section of charts and tables that follows the bibliography to this section on the buckling plates.]

Bryan has a solution for the peripherally rotating ends in the case when compressive forces N_x and N_y are received from two directions and there are solutions by Nizawa [13] and Iguchi [26] for other boundary conditions.

Adjusting Bryan's equation (4.2.3) for stress

$$\sigma_x m^2+\sigma_y n^2(a/b)^2=\sigma_c'\left\{m^2+n^2(a/b)^2\right\}^2 \qquad (4.2.11)$$

where

$$\sigma_c'=\frac{E\pi^2}{12(1-\nu^2)}\left(\frac{t}{a}\right)^2$$

However, the relationship between σ_x and σ_y giving the critical value is linear as is clear from equation (4.2.11). If the half-wave numbers m and n are varied,

various lines are obtained, but for the σ_x within the range

$$\sigma_c'\left\{1-4\,(a/b)^2\right\}<\sigma_x<\sigma_c'\left\{5+2(a/b)^2\right\} \tag{4.2.12}$$

m = 1, n = 1 give the minimum critical values and where σ_x is larger than this, the minimum values are given by m = 2, n = 1, and by m = 1, n = 2 where σ_k is small. (See Figure 4.2.3 and Timoshenko [6], p. 335.)

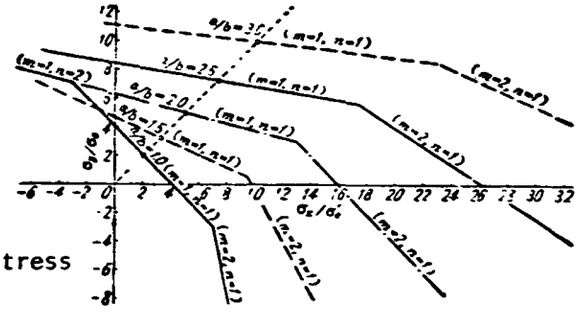

a = tensile stress

Figure 4.2.3

In the case where $\sigma = \sigma_y$

$$\sigma_r=\sigma_-=\sigma_c'\left\{m^2+n^2(a/b)^2\right\} \tag{4.2.13}$$

The minimum values are the case where m = 1, n = 1. (Point of intersection with straight line at 45° in Figure 4.2.3.) /370

S. Timoshenko [20] provides a solution for the critical values in the case of the buckling of a rectangular plate with peripherally rotating ends sustains a concentrated compressive load acting in the center of two opposing sides, using the energy method.

(2) The Case of Shear. The fact that when a rectangular plate sustains a shear force, it buckles, is known from E. Clark and M. Houbotte's experiments, according to which wrinkling occurs in the web of a beam sustaining bending and shearing. (See S. Timoshenko [6], p. 411.) S. Timoshenko [36] was the first to determine approximately by the energy method the buckling due purely to shearing force.

The equilibrium equation in the case where a shear is sustained is

$$D\nabla_1^4 w+2N_{xy}\frac{\partial^2 w}{\partial x\partial y}=0 \tag{4.2.14}$$

In the case of shear, since the direction of the buckles (wrinkles) has a slope with respect to the direction of the edges of the rectangle, a simple form of deflection cannot be obtained which satisfies the edge conditions, and even in the case of rotating edges, it is difficult to obtain a strict solution. R. V.

Southwell and S. W. Skan [37] give a close solution for an infinite tie plate, but the solution when the aspect ratio of the plate is finite is inevitably approximate.

In the case of rotating edges, E. Seydel [40] has a solution other than that of S. Timoshenko mentioned above, and in addition, for fixed edges, solutions have been given by Iguchi [42], H. L. Cox [44], Tomochika and Imai [45], Hidaka and Okubo [46].

The shear buckling limit stress τ_k is expressed by the following equation:

$$\tau_k = k\frac{\pi^2 E}{12(1-\nu^2)}\left(\frac{t}{b}\right)^2 = k\sigma_c \qquad (4.2.15)$$

The b indicates the length of the short side, k is the coefficient determined by the boundary conditions and the aspect ratio a/b. As a/b increases, the number of half-waves giving the lowest critical buckling value also increases, as in the case of compression.

F. Bollenrath [52], H. J. Gough and H. L. Cox [53], and E. Seydel [54] have conducted tests on buckling due to a shear load, but even in this case, since the initial deflection of the plate has a large influence on the results, no clear conclusions can be made concerning the relationship between the theoretical values and the experiment values. Bollenrath gives rather low experiment values, Gough and Cox claim that theirs agree, if one considers initial deflection, and when a/b is approximately equal to 1, they claim that their results agree well (H. L. Cox [2]).

(3) The Case in Which Plate Midplane Sustains Bending and Bending and Compressive Loading. S. Timoshenko [55], O. Stein [56] have provided solutions for the critical loading values when the rectangular plate sustains a bending load within the plane of the plate, under conditions of rotating edges. In this case, since the force N_x acting on the edges is a function of y, the equilibrium condition equation no longer is linear, so it is extremely difficult to obtain a close solution and one must rely on an approximate solution, indicating in place of N_x, the edge stress $\sigma_x = N_a/t$ as follows

$$\sigma_x = \sigma_1(1-\varphi \cdot y/b) \qquad (4.2.16)$$

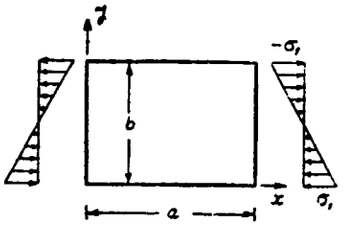

Figure 4.2.4

σ_1 indicates the compressive stress where y = 0, /371
at the edge x = a or x = 0 and depending on the value of ψ, equation (4.2.16) can express a uniform bending, or a combination of bending and compression. This means that when $\psi = 2$, this is uniform bending and where $\psi < 2$ a uniform compressive stress σ_1 (1 - 1/2ψ) and a bending moment fraction 1/12 $\psi b^2 t\sigma_1$ where the maximum value of the bending stress is 1/2$\psi\sigma_1$ are sustained. Moreover, it is clear that $\psi = 0$ indicates a simple compressive load. Timoshenko, using the energy

method, gives the critical value of the maximum compressive stress σ_1 with respect to various values, by the following equation

$$\sigma_{ii}=k\sigma, \tag{4.2.17}$$

In addition, K. Nölke [58] has found solutions for the case in which side a is fixed and side b is rotating, side y = b sustaining the tensile stress is fixed and the other three sides are rotating, in addition to the cases of rotating edges above. Saka's [59] solution is for the case in which the edge parallel to the load is free. Moreover, Saka [61] applies a difference equation to the case in which compression and bending is sustained, and claims that the accuracy of his solution is not inferior to Timoshenko's values, and the values from the energy method.

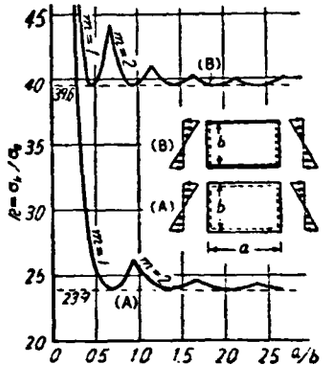

Figure 4.2.5

(4) The Case in Which a Combined Stress is Sustained. The combinations of stresses sustained by rectangular plates that are of practical value include bending and shear, bending and the compression, compression and shear. H. Wagner [65], E. Chwalla [67], and Iguchi [68] provide solutions for combinations of compression and shear, and cases of a combination of bending and shear are handled by S. Timoshenko [66], O. Stein [69], S. Way [70], Takefuji and Takeda [71] (See previous article on bending and compression.)

When combined stresses are sustained in such a manner, generally buckling occurs at lower stresses than the critical values in the case where the stresses operate singly. Denoting the critical stresses where the load acts singly, as σ_k* (or σ_{1k}*), and τ_k* and denoting the critical stress in the case of combined stresses by σ_k (σ_{1k}), τ_k, the following functions are obtained. In the case of bending and shear

$$\frac{\sigma_{1k}^*}{\sigma_{1k}}=f\left(\frac{\tau_k^*}{\tau_k}\right). \tag{4.2.18}$$

In the case of compression and shear /372

$$\frac{\sigma_k^*}{\sigma_k}=f'\left(\frac{\tau_k^*}{\tau_k}\right) \tag{4.2.19}$$

The form of the function is determined by the edge conditions, the aspect ratio of the plate a/b, etc. and proceeding from the critical values in which the stresses operate singly, there is a gradual reduction as the other stress components increase, and finally the other stress components reach the critical value in the case where they act singly. (See Figures 4.2.6 and 4.2.7).

Takefuji and Takeda discuss the relationship of the coefficients for the characteristics of buckling equations in the case where bending and shear are sustained.

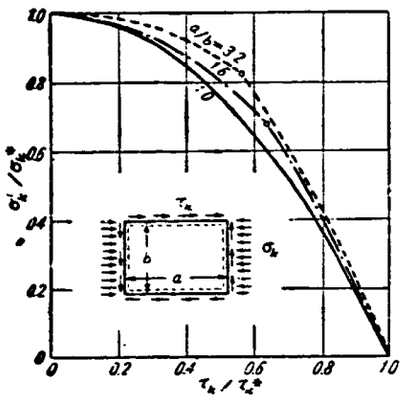

Figure 4.2.6

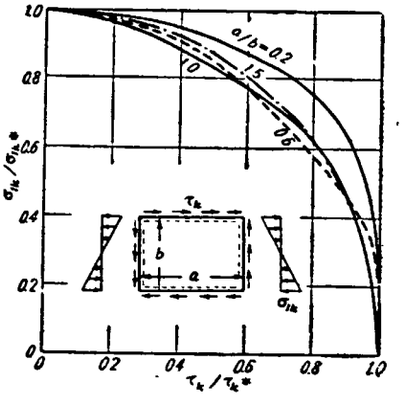

Figure 4.2.7

(5) Other Problems Related to Rectangular Plates. There are cases in which buckling occurs other than in the load conditions described above. For example, A. E. Green [72] and Ono [73] discuss the buckling of a rectangular plate due to torsion load.

When the thickness of the rectangular plate is not constant, since the stiffness of the plate D becomes a function of the coordinates, the equilibrium equation becomes

$$\nabla_1^2(D\nabla_1^2 w)-(1-\nu)\left(\frac{\partial^2 D}{\partial y^2}\cdot\frac{\partial^2 w}{\partial x^2}+\frac{\partial^2 D}{\partial x^2}\cdot\frac{\partial^2 w}{\partial y^2}-2\frac{\partial^2 D}{\partial x\partial y}\cdot\frac{\partial^2 w}{\partial x\partial y}\right) \qquad (4.2.20)$$

$$+N_x\frac{\partial^2 w}{\partial x^2}+N_y\frac{\partial^2 w}{\partial y^2}=0$$

and is no longer linear. D is a quadratic equation and for the form

$$D = cy^2$$

R. G. Olsson [74] has a solution. When the plate thickness gradually varies, one should determine solutions of (4.2.1) for each part of the plate thickness and then combine the conditions so that they are connected in connecting parts. Iida [75] has a solution for such a problem.

When the plate thickness is thin with respect to the dimensions of the plate (length or width) (i.e., when t/b is small), the buckling critical stress is lower than the proportional limit stress σ_p of the material and complete plastic buckling (buckling within the plastic region) occurs. However, as t/b becomes larger, the buckling critical stress becomes larger, and finally exceeds σ_p. When such a state is reached, since the values of E become small, this means that the critical values discussed up to this point in this article are too high. Timoshenko [76] determined a solution for four rotating edges, where he denotes the elasticity modulus under buckling stress by E_t, uses E_t for the direction in which the compression is sustained, and uses E without any additional notation. Since in a direction at right angles to this, not a

very high stress is formed. The equilibrium equation is

$$D\left(\alpha\frac{\partial^4 w}{\partial x^4}+2\sqrt{\alpha}\,\frac{\partial^4 w}{\partial x^2\partial y^2}+\frac{\partial^4 w}{\partial y^4}\right)+N_x\frac{\partial^2 w}{\partial x^2}=0 \tag{4.2.21}$$

where

$$\alpha=E_r/E$$

i.e.,

$$\sigma_k=\frac{\pi^2 D}{b^2 t}\left(\frac{b}{a}\sqrt{\alpha}+\frac{a}{b}\right)^2 \tag{4.2.22}$$

The minimum value of σ_k occurs at $a/b=\sqrt[4]{\alpha}$ and its minimum value is found to be

$$\sigma_{k\,min}=\frac{\pi^2 E}{3(1-\nu^2)}\sqrt{\alpha}\left(\frac{t}{b}\right)^2 \tag{4.2.23}$$

Moreover, E. Chwalla [77] gives, as a minimum value of σ_k /373

$$\sigma_{k\,min}=\frac{\pi^2 E}{3(1-\nu^2)}\alpha\left(\frac{t}{b}\right)^2 \tag{4.2.24}$$

calculating for the case in which both directions x and y have E_r. These two approaches can be considered as expressing the two extremes, but the actual numerical values give values that are not greatly different. In the case where a shearing stress is received, one may consider that both directions change and that this is isotropic.

When t/b increases further, and σ_k reaches the yield point stress σ_s, later, irrespective of the value of t/b, buckling is considered to occur at σ_s. Recently, problems of elastic buckling, in which the critical stress enters the plastic region, have been treated in discussion from the point of view of plastic deformation theory and plastic flow theory by E. Z. Stowell, G. H. Handelman, and W. Prager and C. E. Pearson [79].

Shibuya [80] and Inoue [81] handle the buckling in the case where a compressive load is applied, in the form of an impact to a rectangular plate, and it is shown that it is related to the characteristics of deflection vibration of a plate under the condition that a compressive load is sustained. Inoue utilizes the fact that during vibration, the compressive forces vary in different places and performs his calculations from that which is expressed approximately by Mathieu's differential equations, but it is considered that much more research is still needed in order to determine its characteristics.

4.2.3. BUCKLING OF CIRCULAR AND OTHER NON-RECTANGULAR FLAT PLATES

In determining the critical buckling points of flat plates with configurations of other than rectangular shapes, one may convert the equilibrium equation (4.2.1) into curve coordinates which express the configuration of the particular flat plate, and derive the critical buckling values from the equation and from the given boundary conditions. When it is difficult to obtain a solution of the equilibrium equation for the curved coordinates, one may, as with rectangular plates, obtain a solution by the energy method.

When a uniform compressive force is applied to the circumference of a flat circular plate, converting equation (4.2.1) to polar coordinates,

$$D\left(\frac{\partial^2}{\partial r^2}+\frac{1}{r}\frac{\partial}{\partial r}+\frac{1}{r^2}\frac{\partial^2}{\partial \theta^2}\right)^2 w+N_r\left(\frac{\partial^2}{\partial r^2}+\frac{1}{r}\frac{\partial}{\partial r}+\frac{1}{r^2}\frac{\partial^2}{\partial r^2}\right)w=0 \tag{4.2.25}$$

where N_r = compressive force acting per unit length of circumference

is obtained. When a uniform compressive force is received from the circumference, and when an axially symmetrical deformation does occur with respect to the center, a minimum critical buckling value is obtained and in this case the above equation becomes simplified, being expressed by

$$r^2\frac{d^2\phi}{dr^2}+r\frac{d\phi}{dr}-\phi=\frac{N_r}{D}r^2\phi \tag{4.2.26}$$

and its general solution is given by

$$\phi=C_1J_1(\alpha r)+C_2Y_1(\alpha r) \tag{4.2.27}$$

where $$\phi=\frac{dw}{dr}, \quad \alpha^2=\frac{N_r}{D}$$

A. Nadai [84] gives a critical buckling value N_K by including conditions of rotating and fixed ends at the circumference of the circle, and finding α. E. Meissner [87] provides a solution for the case in which there is a concentric hole in the circular plate, and the boundary of the hole is free from forces. /374
Wakafuji [89] provides a solution for the case in which the plate is fixed at the hole boundary, the outside boundary is free, and when the boundaries of the inner and outer circles are rotating ends. Kawamoto [88] provides a solution for the case in which a uniform pressure N_r is applied to the circumference of the hole.

Takahashi [92] provides a solution for the case in which when the thickness in the direction of the radius gradually varies, assuming that the deformation is similarly axially symmetrical, equation (4.2.26) can be derived from Sturm-Liouville's differential equation. Moreover, Nadai [84], Hayashi [91] discuss the occurrence of buckling due to non-uniformity of temperature distribution in a circular plate, and Hayashi finds the critical values for the case in which the circular plate is rotating.

When the deformation is not axially symmetrical, the solution of equation (4.2.25) becomes

$$w=[C_1J_\mu(\alpha r)+C_2r^\mu+C_3Y_\mu(\alpha r)+C_4r^{-\mu}]\sin\mu\theta \qquad (4.2.28)$$

where $\alpha^2=N_r/D$, μ = positive integer

In the case where the plate is fixed at the edges, the critical value is given by

$$J_{\mu+1}(\alpha a)=0$$

from the root λ_ν of

$$N_{\mu\nu}=\alpha^2D=\frac{\lambda_\nu^2D}{a^2}$$

In the above equation, μ indicates the number of node diameters and the number of ν indicate the number of node circles (including outside edge). Yamana [86] assumes a basic critical value $\mu = 0$, $\nu = 1$ and calculates the critical value with respect to the values of each μ, ν as multiples of it.

Aside from circles, Voinovsky-Krieger [93] obtain a solution by the energy method for the case in which, for an elliptical plate, with edges fixed, a uniform pressure is applied from the edges.

Yamamoto [99] uses the energy method to calculate for a plate having a form which is slightly deformed from a regular polygon expressed in the form

$$K(R^n\cos n\theta-1)+1-R^2=0 \qquad (4.2.29)$$

In addition, Shibuya [98] uses the difference method to handle problems in which a regular hexagonal plate sustains a shear load, and Sawada [97] finds a solution by the energy method for the case of a rectangular plate with four parallel sides. W. Burchard [96] found the critical values for the case in which a right triangular plate undergoes compression.

4.2.4. ORTHOTROPIC PLATES

Problems in orthotropic plates in which there is a difference in the elastic properties in two orthogonal directions have wide application to wrinkled plates and wooden thin plates (see Part 5 for a discussion on the details of Wrinkled Plates). In this case, equation (4.2.21) becomes

$$D_x\frac{\partial^4w}{\partial x^4}+2D_{xy}\frac{\partial^4w}{\partial x^2\partial y^2}+D_y\frac{\partial^4w}{\partial y^4}+N_x\frac{\partial^2w}{\partial x^2}+N_y\frac{\partial^2w}{\partial y^2}+2N_{xy}\frac{\partial^2w}{\partial x\partial y}=0 \qquad (4.2.30)$$

where D_X, D_y = bending stiffness in sections x, y

$4(GJ)_{xy}$ = torsion stiffness in xy cross-section

$$2D_{xy}=4(GJ)_{xy}+D_x\nu_y+D_y\nu_x$$

Yamana [100] in obtaining a solution for the case in which $N_y = 0$, $N_{xy} = 0$, with rotating edges, obtains /375

$$N_k\frac{b^2}{\pi^2}=D_x\left(\frac{nb}{a}\right)^2+2D_{xy}+D_y\left(\frac{a}{nb}\right)^2 \tag{4.2.31}$$

The minimum limit value is

$$N_{k\,min}=\left\{\sqrt{D_xD_y}+D_{xy}\right\}\frac{2\pi^2}{b^2} \tag{4.2.32}$$

The half-wave length at this time is given by

$$a/n=b\sqrt{D_x/D_y} \tag{4.2.33}$$

The critical stress τ_k of a rectangular plate with rotating edges, sustaining a shear load N_{xy}, according to E. Seydel [104] is

$$\tau_k=C_a(D_xD_y^3)^{\frac{1}{4}}(b/2)^2 \tag{4.2.34}$$

C_a is a coefficient which is determined by the parameter φ and α_a.

$$\vartheta=(D_xD_y)^{\frac{1}{2}}/D_{xy}$$

$$\alpha_a=(b/a)/(D_x/D_y)^{\frac{1}{4}}$$

Seydel [102] also gives values of C_a for the condition where edge a is fixed, in the case where $a = \infty$.

Hayashi [107] makes the following assumption for the deflection w for the case in which the direction of the principle axis of elasticity and the direction of load do not agree. By substituting the appropriate condition equations, he finds the stress function Φ as a function of w and obtains a method for determining the unknowns in the deflection equation from an energy equation. Moreover, the critical buckling value is given by f = 0. I.e.,

$$w=f\cos\frac{\pi y}{b}\cos\frac{\pi}{a}(x-my)$$

The appropriate condition equation is

$$\frac{1}{E_x}\frac{\partial^4\Phi}{\partial x^4}+\left(\frac{2}{F}+\frac{1}{G_{xy}}\right)\frac{\partial^4\Phi}{\partial x^2\partial y^2}+\frac{1}{E_y}\frac{\partial^4\Phi}{\partial y^4}-\frac{2}{H}\frac{\partial^2}{\partial x\partial y}(\nabla_1^2\Phi) \tag{4.2.35}$$
$$=\left(\frac{\partial^2w}{\partial x\partial y}\right)^2-\frac{\partial^2w}{\partial x^2}\frac{\partial^2w}{\partial y^2}$$

Moreover, when the direction of x and the direction of the principle axis of elasticity are 45°

$$\frac{1}{E_x}=\frac{1}{E_y}=\frac{1}{4}\left(\frac{1}{E_1}+\frac{1}{E_2}-\frac{2\nu_1}{E_1}+\frac{1}{G}\right),$$

$$\frac{1}{F}=\frac{1}{4}\left(\frac{1}{E_1}+\frac{1}{E_2}-\frac{2\nu_1}{E_1}-\frac{1}{G}\right),$$

$$\frac{1}{H}=\frac{1}{2}\left(\frac{1}{E_1}-\frac{1}{E_2}\right),$$

$$\frac{1}{G_{xy}}=\frac{1}{E_1}+\frac{1}{E_2}+\frac{2\nu_1}{E_1},$$

E_1, E_2, G, ν_1, ν_2 = Young's modulus, shear elasticity modulus and Poisson's ratio in the direction of the principle axis of elasticity.

CHAPTER 3 /376

PROBLEMS OF FLAT PLATE AFTER BUCKLING

4.3.1. EFFECTIVE WIDTH IN THE CASE OF A COMPRESSIVE LOAD

L. Schumann and G. Back [116] found, through experiments, that when a rectangular flat plate buckles after sustaining compression, the buckling load does not immediately become the maximum load which the flat plate can withstand. Moreover, G. Schnadel [108] carried out theoretical calculations and showed that a flat plate after buckling still bears the load and that at this time the distribution of the compressive stress is not uniform and that stresses may also occur in a direction at right angles to the compression. Later, Th. v. Kármán, E. E. Sechler and L. H. Donnell [109], judging from the fact that after the buckling of a plate, the compressive force is increased only in the portion that was immediately adjacent to the support end of the plate width, and that the compressive force hardly increased at all in the center of the plate width, considered as an approximation, that only the portion of a certain width close to the edge of the plate sustained a load under a uniform compressive stress, and that in the central portion, the compressive stress was 0. (See Figure 4.3.1.) They termed the width of the portion sustaining that stress as b_e as the effective width and investigated its properties. As a result, they determined that the effective width gradually decreases as the compressive stress at the edges increases. Moreover, the compressive stiffness of the plate decreases as the stress increases (See figure 4.3.2.)

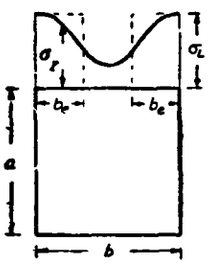

Figure 4.3.1

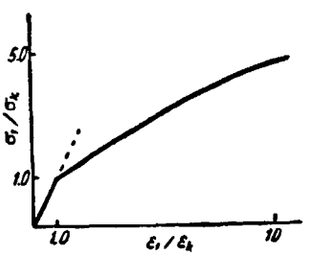

Figure 4.3.2

Later, a theoretical investigation was made of problems of effective width by H. L. Cox [110], Yamamoto and Kondo [111], K. Marguerre [112], K. Marguerre and E. Trefftz [113], and by Tsuruya [114]. Experiments on the effective width were also conducted by H. L. Cox [110], R. Lahde and H. Wagner [118], E. E. Sechler [119] and by Yokoo [120].

In order to investigate the effective width and other properties of the flat plate after buckling, the infinitesimal deformation theory cannot be used, and it is necessary to depend on the theory of finite deformation in which the deformation is quite large. When the deflection is large, it is necessary to

determine the strain component by taking into consideration the elongation of the center plane of the plate (the plane that passes through the center of the plate thickness). I.e., expressing the strain component of the center plane by

$$\left.\begin{aligned} \varepsilon_x &= \frac{\partial u}{\partial x} + \frac{1}{2}\left(\frac{\partial w}{\partial x}\right)^2, \\ \varepsilon_y &= \frac{\partial v}{\partial y} + \frac{1}{2}\left(\frac{\partial w}{\partial y}\right)^2, \\ \gamma_{xy} &= \frac{\partial u}{\partial y} + \frac{\partial v}{\partial x} + \frac{\partial w}{\partial x}\,\frac{\partial w}{\partial y}. \end{aligned}\right\} \qquad (4\ 3.1)$$

and determining the equilibrium equation

$$-D\nabla_1^4 w + \frac{\partial^2 U}{\partial y^2}\cdot\frac{\partial^2 w}{\partial x^2} + \frac{\partial^2 U}{\partial x^2}\cdot\frac{\partial^2 w}{\partial y^2} - 2\frac{\partial^2 U}{\partial x\,\partial y}\cdot\frac{\partial^2 w}{\partial x\,\partial y} = 0 \qquad (4.3.2)$$

/377

and the appropriate condition equation

$$\nabla_1^4 U + 12(1-\nu^2)\frac{D}{t^2}\left\{\frac{\partial^2 w}{\partial x^2}\,\frac{\partial^2 w}{\partial y^2} - \left(\frac{\partial^2 w}{\partial x\,\partial y}\right)^2\right\} = 0 \qquad (4.3.3)$$

where the non-linear simultaneous equation

$$N_x = -\frac{\partial^2 U}{\partial y^2}, \qquad N_y = -\frac{\partial^2 U}{\partial x^2} \qquad N_{xy} = -\frac{\partial^2 U}{\partial x\,\partial y}$$

is obtained.

It is difficult to solve thi· directly and various approximation methods have been proposed. Marguerre [113] first assumes a deflection w, and substitutes the strain energy equation

$$\begin{aligned} W = {} & \frac{Gt}{4(1-\nu)}\iint\left[-2\varepsilon_1 + 2\varepsilon_2 + 2(\hat{u}_x + \hat{v}_y) + w_x^2 + w_y^2\right]^2 dx\,dy \qquad (4.3.4) \\ & - \frac{Gt}{2}\iint\left[(-2\varepsilon_1 + 2\hat{u}_x + w_x^2)(2\varepsilon_2 + 2\hat{v}_y + w_y^2) - (\hat{u}_y + \hat{v}_x + w_x w_y)^2\right] dx\,dy \\ & + \frac{Gt^3}{12(1-\nu)}\iint(\nabla_1^2 w)^2\,dx\,dy - \frac{Gt^3}{6}\iint(w_{xx}w_{yy} - w_{xy}^2)\,dx\,dy \end{aligned}$$

where

$$u = -\varepsilon_1 x + \hat{u}, \qquad v = \varepsilon_2 y + \hat{v}$$

$$w_x = \frac{\partial w}{\partial x}, \qquad w_{xy} = \frac{\partial^2 w}{\partial x\,\partial y}, \qquad \hat{u}_x = \frac{\partial \hat{u}}{\partial x} \qquad \text{etc.}$$

and determines the relationship between the load, the deflection and compressive strength, from the fact that the variation in strain energy is 0 at the position of equilibrium and from the condition that the unknown f included in w, the average elongation in the direction at right angles ε_2, and the differential are 0.

Moreover, for the displacement u, v in directions x, y, from the condition that the variation for the varying components $\hat{u}$, $\hat{v}$ does not change, the following equation is derived as condition for determining $\hat{u}$, $\hat{v}$, and $\hat{u}$, $\hat{v}$ are determined as functions of w. I.e.,

$$\left.\begin{aligned} \nabla_1^2\hat{u}+\frac{1+\nu}{1-\nu}\frac{\partial}{\partial x}(\hat{u}_x+\hat{v}_y)+\frac{1}{1-\nu}\frac{\partial}{\partial x}(w_x^2+w_y^2)+w_xw_{yy}-w_yw_{xx}=0, \\ \nabla_1^2\hat{v}+\frac{1+\nu}{1-\nu}\frac{\partial}{\partial y}(\hat{u}_x+\hat{v}_y)+\frac{1}{1-\nu}\frac{\partial}{\partial y}(w_x^2+w_y^2)+w_yw_{xx}-w_xw_{yy}=0. \end{aligned}\right\} \quad (4.3.5)$$

The method of Tsuruya [114] is to assume w in the form of a series, substitute this in equation (4.3.2), consider the boundary conditions, and find U was a function of w. Then substituting these in the energy equations, he solves the problem from the hypothetical work principle. Cox [110] in determining the strain energy equations, performs his calculations taking the average value in the direction of length, without calculating precisely the term with respect to the elongation in the center plane, expressing this in the form

$$\frac{1}{2}Et\int_{-\frac{b}{2}}^{\frac{b}{2}}\left\{\varepsilon_1-\frac{1}{2a}\int_{-\frac{a}{2}}^{\frac{a}{2}}\left(\frac{\partial w}{\partial x}\right)^2dx\right\}^2dy \quad (4.3.6)$$

and obtains his solution from the hypothetical work principle. This is considered to be convenient for simple analysis. /378

As a result of these calculations, the effective width decreases with an increase in the compressive load of the flat plate after buckling (see Figure 4.3.3) and the effective compressive stiffness also gradually decreases in a similar manner. Of course, these effective widths, compressive stiffnesses and other values differ depending on the edge condition of the plate. It is apparent that the results close to those of Marguerre and Tsuruya agree well with experiments and Cox's results are quite good. The values for Kármán's effective width appear to be even closer. Moreover, the effective compressive stress immediately after buckling is 1/2 according to Marguerre and Tsuruya while Cox says that this is 1/3 but it is difficult to determine the appropriateness of these two from experiments owing to the presence of initial deflection in the plate used for the tests. Moreover, N. J. Hoff [168] states that in the case of a fixed edge parallel to the load, there is an agreement between the experiments of Lahde and Wagner and Cox's calculations and that the values of L. Schumann and G. Back [116] for the case of simple support come out somewhat smaller. E. E. Sechler has conducted experiments on the distribution of compressive stresses after buckling, and he shows that there is a difference between the case in which the edge is supported by a V channel and in which it is supported by an anti-deflection member (see Figure 4.3.4)

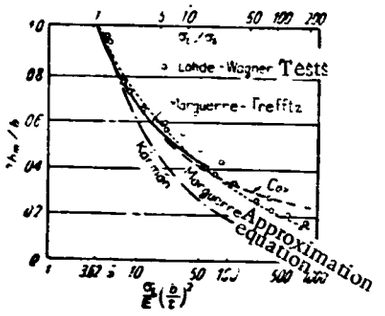

Figure 4.3.3

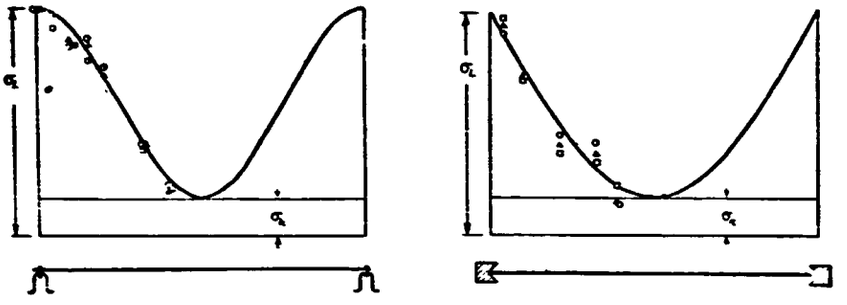

Figure 4.3.4

Hayashi [124] obtains a solution by the Galerkine method from the equilibrium equations for problems occurring after the buckling of orthotropic plates.

4.3.2. MAXIMUM LOAD OF RECTANGULAR FLAT PLATE SUSTAINING COMPRESSION A''D OTHER MATTERS

Research has been conducted by Th. v. Kármán and his colleagues [109], H. L. Cox [110], Yamamoto and Kondo [111] and S. Timoshenko [115] on the maximum load that can be withstood by a flat plate with respect to compressive load.

Kármán assumes that when the edge stress σ_L reaches the yield point stress σ_S of the material, the ultimate stress P_{ult} is reached, and determines this from his effective width theory in the form

$$P_{ult}=\frac{\pi}{\sqrt{3(1-\nu^2)}}\sqrt{E\sigma_s}\,t^2 \tag{4.3.7}$$

and compares this with the test results of L. Schumann and G. Back [116]. As a result, the values of equation (4.3.7) turn out to be 10 to 35% higher than the

experimental values. Cox gives the following

$$P_{ult}=Ee_m t\left(L\frac{t}{\sqrt{e_m}}+Mb\right), \tag{4.3.8}$$

where

L = 1.52 M = 0.09 (for rotating edges),

L = 2.18 M = 0.14 (for fixed edges),

assuming that this is the case in which the edge stress reaches a constant value e_m determined by the material. Yamamoto and Kondo determine this assuming that it is the case in which the maximum principle stress reaches a constant value and Timoshenko determines the ultimate load from the maximum value of the shear stress.

$$P_{ult}=bt\left\{0.434\,\sigma_s+2.04\,E\,(t/b)^2\right\} \tag{4.3.9}$$

Yokoo [120] gives an equation in which P_{ult} is proportional to t^2 from the test results on a rotating edge end. Yoshiki [122] similarly proposes an equation inserting the effect of b in Kármán's equation from the results of tests on soft steel plates

$$P_{ult}=1.77(a/b)^{-0.22}\sqrt{E\,\sigma_s}\,t^2 \tag{4.3.10}$$

and states that there is an agreement with the test results within an error of 10%.

The ratio between the ultimate load and the buckling load is greater, the smaller t/b and in the thickness of plates that are used for aircraft structures, a value of 10-20 is taken for this ratio, but as t/b increases, the ratio decreases, and at t/b ≒ 1/100, P_{ult}/P_k = 2-3 (case of soft-steel.) Furthermore, when t/b becomes larger and σ_k approaches σ_p or σ_s, the buckling load reaches the point where it is almost the same as the maximum load. Even in the case of the bending load, the same phenomena are observed. (See Yoshiki [63]).

One problem in the behavior of a flat plate after buckling is the degree to which the initial process of buckling can be allowed to continue in order for permanent deformation not to remain when a load has been removed after the flat plate has buckled in the elastic region. Shibuya [127] has made an analysis of the case of a column, assuming eccentricity, W. L. Howland and P. E. Sandorff [126] conducted tests on a flat plate and compared the results. That is, they assumed that the maximum stress due to bending and compression arises in the center of the plate, that permanent buckling deformation occurs at the point where the maximum strain reaches the yield point strain, and perform their calculations taking into account the effects of initial deflection. They are able to determine as well the degree of harmful deformation in accordance with the ratio between strengtheners and flat plates.

4.3.3. TENSION FIELD PROBLEMS

H. Wagner was the first to study the stress conditions after the buckling of a plate when a shearing load is applied to a flat plate attached between hinged frame structures [130, 131], and discusses this in terms of a theory of a tension field. He assumes that when buckling occurs in the flat plate, both the bending stiffness and compressive stiffness are 0, and that only the tensile stress σ is present in the direction of the buckling wrinkles. Assuming the direction of the wrinkles to be α, from the condition of equilibrium of the cross-section mn, (see Figure 4.3.5).

$$\sigma=\frac{2P}{d\cdot t\cdot\sin 2\alpha} \qquad (4.3.11)$$ /380

Assuming that the frame around the plate is a rigid body, α becomes 45° and

$$\sigma = 2\ P/d\cdot t$$

meaning that a tensile stress which is twice that of the shearing stress is operating when there is no buckling. When the frame is not a rigid body, it is necessary to determine the value of α taking into consideration displacement, but in ordinary aircraft structures, it is stated that this is about 40°. This means that a tension and bending load is applied vertically to the horizontal member due to this σ and that a compressive force of

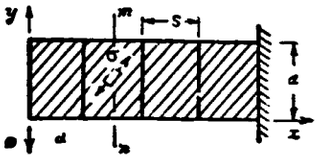

Figure 4.3.5

$$S=\sigma t b\sin^2\alpha \qquad (4.3.12)$$

is applied to the vertical reinforcing members. The force that is applied to the horizontal reinforcing members is

Horizontal component $q_x=\sigma t\sin\alpha\cos\alpha$ (per unit length) (4.3.13)

Vertical component $q_y=\sigma t\sin^2\alpha$ (" " ")

The tension field approach is to determine the stresses of each member ir this manner.

Later A. Kromm and K. Marguerre [133] proceeding from the equilibrium equation and compatibility condition equation [see equations (4.3.1) and (4.3.2)] and the strain energy equation analyze the stress condition after buckling in the case when a light compression and shear are applied, employing the hypothetical work principle and Galerkine's method. Assuming the deflection w to have the form

$$w=f\cos\frac{\pi y}{b}\cos\frac{\pi}{l}(x-my)$$

they determine the stress function F from the term w from the compatibility condition equation and from the hypothetical work principle f, l, m are determined from the strain energy equation. Moreover, assuming α to be the angle of inclination of the wrinkles, there is a relationship m = cot α, l sin α indicates

the pitch of the waves, and the calculations proceed with $\beta = b/(l \sin\alpha)$ as a parameter in place of l. As a result,

$$\left.\begin{aligned} p_1+\tau m &= \frac{\sigma_e}{2}(1+\beta^2)+E\frac{\pi^2 f^2}{16 b^2}\frac{1}{1+m^2}\left[\beta^2+\frac{m^2}{\beta^2(1+m^2)}\right] \\ p_2 &= \frac{\sigma_e}{4}(1-\beta^4)+E\frac{\pi^2 f^2}{16 b^2}\left(\frac{1}{1+m^2}\right)^2 \\ \frac{\tau}{m}+p_2 &= \frac{\sigma_e}{2}\left[(1+\beta^2)+2\right]-E\frac{\pi^2 f^2}{16 b^2}\cdot\frac{1}{\beta^2(1+m^2)} \end{aligned}\right\} \qquad (4.3.14)$$

where

p_1, p_2 τ = compressive stress and shear stress in directions x and y of the flat plate

$$\sigma_e = \frac{\pi^2 E}{12(1-\nu^2)}\left(\frac{t}{b}\right)^2$$

Denoting the cross-section area of the horizontal reinforcing area by A_1, and of the vertical reinforcing member by A_q, the magnitude of external force is

$$\left.\begin{aligned} P_x &= p_x(t\cdot b+A_1)=p_1 t b+p_1 A_1 \\ P_y &= p_y(t\cdot a+A_2)=p_2 t a+p_1 A_1 \end{aligned}\right\} \qquad (4.3.15)$$

Moreover, p_1, p_q, are respectively the compressive stress of the horizontal reinforcing member and vertical reinforcing member. Now, assuming $P_y = 0$, and the stiffness of the vertical reinforcing member to be 0, /381

$$p_2 = 0$$

is obtained and conversely, assuming the stiffness of the vertical member to be ∞

$$\varepsilon_2 = 0$$

is obtained and the calculations are carried out for the two above extreme conditions. When $p_2 = 0$, with β as a parameter

$$\left.\begin{aligned} \frac{p_1}{\sigma_e} &= \frac{1}{4}\left[t\beta^2(\beta^4-1)+2\beta^2-6t+8-\frac{2}{\beta^2}(t-1)\right], \\ \frac{p_1}{\sigma_e} &= \frac{1}{4}\left[3t\beta^2(\beta^4-1)+2\beta^2-6t+8-\frac{2}{\beta^2}(t-1)\right], \\ \frac{\tau}{\sigma_e} &= \frac{\sqrt{t-1}}{4}\left[\frac{(1+\beta^2)^2}{\beta^2}+4\right] \\ \frac{\tau}{\sigma_e} &= \frac{\sqrt{t-1}}{2}\left[\left(6+\beta^2+\frac{1}{\beta^2}\right)(1+\nu)+2t\beta^2(\beta^4-1)\right]. \end{aligned}\right\} \qquad (4.3.16)$$

where

$$t=1+m^2=\frac{1}{\sin^2\alpha} \qquad E\,\varepsilon_c=\sigma_c.$$

$\beta = 1$, $f = 0$ gives the critical buckling values. This is expressed in the form of a graph by finding p_1, p_1, etc. with respect to the external force P_x from the above equation and equation (4.3.15). (See Materials 94 [trans. note "Materials" refers to the section immediately following the bibliography to this section.]) The results for calculations in the case in which $\varepsilon_2 = 0$ are also given graphically. In addition to the above, the effective width ($b_m = b \cdot p_1/p_1$), the effective shear stiffness ($d\tau/d\gamma$), and the angle of the wrinkles α are also determined but it must be noted that as the load increases the wave length of the wrinkles decrease.

R. Lahde and H. Wagner [139] conducted extensive experiments, and as a result, it was found that with regard to the values based on Wagner's calculations, that in the ultimate condition reached after buckling, the values found were considerably different from those immediately after buckling, and that the compressive stress sustained by the vertical member showed quite low values owing to the effectiveness of the plate. It was found that soon after the buckling of the flat plate, Wagner's tension force theory no longer was completely valid, and such a state is termed the imperfect tension field. The experiments of Lahde and Wagner demonstrate the problems of this imperfect tension field.

In addition to the above, other research on problems of the behavior of a flat plate after shear and buckling include analysis for cases other than when the boundary configurations are rectangular, by E. Reissner [134] and by Kondo [135], and Takeuchi's analysis [140] using corrections for the case in which a bending load is applied.

CHAPTER 4

REINFORCING PLATES

4.4.1. BUCKLING OF REINFORCING PLATES SUSTAINING COMPRESSION

Problems in the buckling of rectangular plates having reinforcing members, receiving compressive loads can be handled in terms of orthotropic plates in the case when the space between reinforcing members is narrow. (See 4.2.4 concerning orthotropic plates). When the distance between reinforcing members is wide, the critical buckling load is determined from the condition that the equilibrium equation

$$D\nabla_1^4 w_i + N_x \frac{\partial^2 w_i}{\partial x^2} = 0 \tag{4.4.1}$$

For the case in which the flat plate between the reinforcing members receives compression, and the following boundary conditions are satisfied. That is, the critical values are determined from the condition that there is continuity between the deflection and the deflection angle of the flat plate on both sides at the position of the reinforcing members, and that the edge shear force and bending moment of the plate respectively form the distributed load and torsion moment of the reinforcing members. That is,

$$\left.\begin{aligned} &w_i = w_{i+1} = w_{is}, \\ &\frac{\partial w_i}{\partial y} = \frac{\partial w_{i+1}}{\partial y}, \\ &EI_i \frac{\partial^4 w_{is}}{\partial x^4} = -D_i\left\{\frac{\partial^2 w_i}{\partial y^2} + (2-\nu)\frac{\partial^2 w_i}{\partial x^2 \partial y}\right\} + D_{i+1}\left\{\frac{\partial^2 w_{i+1}}{\partial y^2} + (2-\nu)\frac{\partial^2 w_{i+1}}{\partial x^2 \partial y}\right\} \\ &\qquad\qquad - N_x A_i \frac{\partial^2 w_{is}}{\partial x^2}, \\ &GJ_i \frac{\partial^2 w_{is}}{\partial x^2 \partial y} = D_i\left(\frac{\partial^2 w_i}{\partial y^2} + \nu\frac{\partial^2 w_i}{\partial x^2}\right) - D_{i+1}\left(\frac{\partial^2 w_{i+1}}{\partial y^2} + \nu\frac{\partial^2 w_{i+1}}{\partial x^2}\right). \end{aligned}\right\} \tag{4.4.2}$$

where EI_i, GJ_i, A_i and w_{is} indicate the bending stiffness, torsional stiffness, cross-section area and deflection of the ith anti-deflection member.

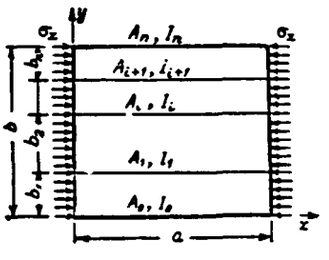

Figure 4.4.1

Actually it is very difficult to obtain a solution completely satisfying the conditions of equation (4.4.2). For this reason, very frequently a solution is obtained in which in the 4th part of equation (4.4.2) the torsion stiffness GJ_i of the anti-deflection member is ignored. R. Barbré [147] and H. Fröhlich [151] provide solutions for the case in which there is a reinforcing member between plates, L. Rendulic [144], and J. Miles [146] provide solutions in the case when there is a reinforcing member on the edge,

in which cases GJ_i are ignored.

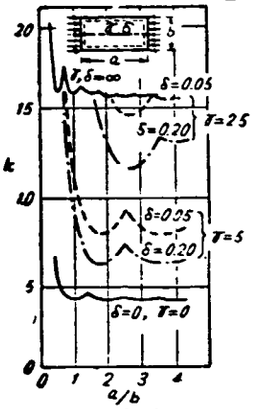

Figure 4.4.2

S. Timoshenko [143] presents a solution by the energy method. As an example, the case in which a plate with rotating edges has a single reinforcing member in the center is shown in Figure 4.4.2. A coefficient indicating the critical buckling values and the cross-section area and bending stiffness of the reinforcing member differ according to

$$\delta=A/(t\cdot b),\quad \gamma=EI/(b\cdot D) \qquad /383$$

And when these values are small, when the stiffness is adequately large and close to the critical value in the case in which there is no reinforcing member, they reach the point where they agree with the critical buckling values of a plate of half the width. R. Barbré [147] determines the minimum stiffness value γ_{min} necessary so that the position of the reinforcing member becomes a hinged straight line and the values are equal to the critical values of a plate of half the width, as shown in Figure 4.4.3.

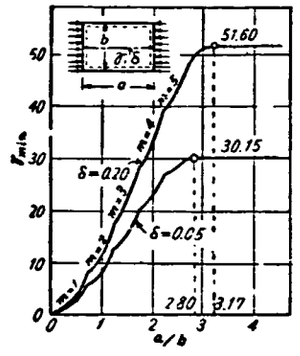

Figure 4.4.3.

S. Timoshenko [143] and R. Barbré [149] and others have analyzed and determined the critical values in a similar fashion for the case in which there is a reinforcing member in a direction at right angles to the load. In this case, since no compressive force is applied to the reinforcing member, the term A_i in the third part of equation (4.4.1) becomes unnecessary and only the bending stiffness of the reinforcing member has any influence on the critical values. When the position of the reinforcing member matches the position of the segment in mind, for the flat plate, except for that of the reinforcing member, the critical value is constant regardless of the stiffness of the reinforcing member, and when it does not agree, the critical value is greater, the greater the stiffness. Consequently, if reinforcing members are installed in order to raise the buckling limit of flat plates sustaining compression, this objective is not achieved if it is installed at the point where it matches the segmented straight line of the flat plate. At least it is necessary to restrict the wave forms of the wrinklings by installing more reinforcing members than the number of segmented lines. However, instead of installing lateral reinforcing members in this way, the installation of longitudinal reinforcing members is more effective since it is possible to reduce the width of buckling of the plate. In addition, it is further advantageous since the reinforcing members themselves sustain the compressive load. Of course, if the stiffness of the reinforcing member is less than γ_{min}, the increase in critical value is not marked.

H. Fröhlich [151] and the analyses by the energy method of Arima, Okuda [153] concern the case of reinforcing members installed laterally and longitudinally while W. Burchard [152] uses the difference method to calculate for the case in which there are reinforcing members on the diagonals of a square plate.

4.4.2. REINFORCING PLATES SUSTAINING SHEARING LOAD AND BENDING LOAD

S. Timoshenko [155] uses the energy method to determine the critical stress for the case of buckling where a reinforcing plate sustains a shearing force, when there are lateral reinforcing members on the webs. He also determines the minimum value of the bending stiffness of the reinforcing member necessary for the position of the reinforcing member to be on the segmented line. S. Way [156] performs similar calculations.

E. Chwalla [159] and M. Hampl [161] have determined the buckling values for the case in which longitudinal reinforcing members are attached to a rectangular plate sustaining a bending load. When the bending stiffness of the lateral reinforcing member is sufficiently great, and its position is a segmented line, the critical value becomes higher, and the number of half-waves also increases.

E. Chwalla [159] analyzes the critical values in the case in which longitudinal reinforcing members are installed on a rectangular plate sustaining compression and shear. It is difficult to solve the above problems by proceeding from equilibrium equations, so the energy method is primarily employed.

H. Schleicher [3] states that for the stiffness required to increase the critical values by installing many reinforcing members at set intervals on the web of a plate beam sustaining shear, it is appropriate to have a stiffness which is twice the values calculated by S. Timoshenko for a single reinforcing member. Chwalla states that for webs undergoing bending, since the length-width ratio giving the minimum buckling value is the small value of 0.667, it is effective to install lateral reinforcing members on the compression side.

4.4.3. MAXIMUM LOAD OF REINFORCING PLATES UNDERGOING COMPRESSION /384

When a reinforcing plate sustains a compressive load, and the bending stiffness of the longitudinal reinforcing member is greater than a certain degree ($> \gamma_{min}$), buckling first occurs in the flat plate panels between the reinforcing members, and the reinforcing members do not undergo deflection. The flat plate manifests the phenomenon of effective width after buckling, at the compressive stress is increased and a load acts upon only the reinforcing members at the areas immediately next to them. Under such a state, there are various approaches to the question concerning under what conditions the maximum load of the reinforcing plate in its entirety arises, when a load is applied. That is, the following are considered responsible for the maximum load being reached:

1) Deflection buckling of column formed in the effective width part of the reinforcing member and panel (Euler buckling),

2) Flexural torsional buckling of reinforcing member (Lundquist's primary buckling),

3) Local buckling of reinforcing member (Wrinkled buckling due to compression on free edge),

4) Buckling of flat plates between rivets attaching reinforcing members to flat plates (buckling between rivets),

5) Attainment of ultimate strength of material by reinforcing member or flat plate.

G. F. Wallace [163], E. E. Sechler [165] and H. L. Cox [172] discuss the collapse of a reinforcing member due to Euler buckling. The effective width of the plate is a function of the stress σ_{st} of the reinforcing member. However, the value for this differs according to the investigator, such as Kármán, Cox and Marguerre and there are considerable differences in how to determine the effective width using which values. The method for doing this is first of all to assume a σ_{st} during maximum load, determine the effective width corresponding to this, denoting it by b_m. One estimates the buckling stress of the column which consists of the reinforcing member and its effective width (or estimates the breaking stress from the Column curves), (H. B. Dickinson and J. R. Fischel [170] claim that it is necessary to determine this by experiment) and then repeat the estimation of values several times until they agree with the σ_{st} which was first assumed. When σ_{st} is thus found, the maximum load P_{ult} is determined by

$$P_{ult}=\sigma_{st}(A_{st}+b_m t)+\sigma_k(b-b_m)t \tag{4.4.3}$$

If the longitudinal reinforcing members are installed in a row and there are a large number of panels, one may employ addition by finding the load for each panel, by the above method. Yoshiki [176] discusses the cases in which when there is a difference in the dimensions of the reinforcing members, addition may be used and cases in which it is necessary to calculate taking the smaller values of σ_{st}. Cox determines σ_{st} by assuming that it is possible to approximate the load-deflection curve after buckling by a straight line

$$P_{ult}=(A_{st}\, b\cdot t/n)\,\sigma_{st}+\sigma_k\cdot b\cdot t\,(n-1)/n \tag{4.4.4}$$

where

$$\frac{1}{n}=\frac{\text{increment of average stress}}{\text{increment of }\sigma_{st}}=\frac{\delta\,\sigma_{mean}}{\delta\,\sigma_{st}}\ (=\text{effective width})$$

In addition, Wallace, Sechler, and N. J. Hoff [168] determine P_{ult} ignoring the load $\sigma_k(b - b_m)t$ sustained by the non-effective part of the panels, and Hoff states that since

$$P=Ee(A_{11}+b_m t) \tag{4.4.5}$$

The increase in load of the plate with respect to the increase in e is

$$\left(\frac{\partial P}{\partial e}\right)_{PL}=Et\left(b_m+e\frac{db_m}{de}\right) \tag{4.4.6}$$ /385

so consequently in reinforcing structures, it is necessary to use as an effective width

$$b'_m=b_m+e\frac{db_m}{de} \tag{4.4.7}$$

J. R. Fishel [171] gives the effective width in the case when the properties of the materials used in the reinforcing members and the flat plates differ, and Wallace, E. E. Lundquist and C. M. Fligg [166] give the effective width of plates on the outside of the reinforcing members. Yoshiki mentions that one can obtain good results which agree with experimental results by determining the maximum load from the yield due to the combination of bending stress and compressive stress after the buckling of a column consisting of the reinforcing member and the effective width. Cox has noted that the load becomes greater than the buckling of the reinforcing member, and attributes this to initial bending in a direction at right angles to the load. E. R. Reff [169] proposes experimental formulas for Z-shaped reinforcing members.

H. Wagner [187] was the first to discuss the occurrence of flexural and torsional buckling occurring under a compressive load, and later E. E. Lundquist and C. M. Fligg [166] describe a method of applying this to reinforcing plates. This occurs primarily in short reinforcing members with asymetrical thin-walled open cross-sections. It is considered that the load which causes such flexural and torsional buckling in reinforcing members including effective width gives the maximum load of the reinforcing plate overall.

Local buckling also occurs primarily in reinforcing members of open cross-section and in short reinforcing members. If one determines the minimum critical stress in cases in which buckling occurs on the free edge of a reinforcing member in terms of a rectangular plate with one edge free and the other edge supported, the load corresponding to this stress is obtained as the maximumum load due to this local buckling. In this case, the maximum load should be determined for the effective cross-section adding the effective width of the reinforcing member and the plate. N. J. Hoff [168], H. L. Cox [172] and others discuss this type of damage.

As for buckling between rivets, when plates which are fastened to reinforcing members buckle due to compression, in the intervals between the centers of the rivets, this buckling reaches a maximum overall load, according to W. L. Howland [177]. H. B. Dickinson and J. R. Fischel [170] claim that the maximum load is not reached even if buckling occurs between rivets, while E. E. Sechler [165] states that when buckling between rivets occurs, the effective width

rapidly decreases. A. Kromm [178] conducted experiments on the case in which Z-shaped, ⌐¬ - shaped and ⊔- shaped reinforcing members are attached to partially circular shells, and determined the effect of the distance between rivet centers on the stress at the time of rupture, and on the effective width.

CHAPTER 5

FLAT PLATE STRUCTURES

4.5.1. BUCKLING OF FLAT PLATE STRUCTURES UNDER COMPRESSION

As for problems of buckling due to the compression of flat plate structures (Faltwerk) built from combinations of flat plates, S. Timoshenko [181] was the first to state that the strength of a column is determined from the buckling stress of the flange part of the channel in the case of a column built of flat plates in channel form, which undergoes compression, and later, problems of buckling of columns with various types of cross-sections; i.e., angle, Z, Hut, hollow rectangle and hollow triangle, were treated by S. Timoshenko [182], E. E. Lundquist [183] and Kuranishi [184], [185]. In such problems, the sides of which the column is composed, are considered as flat plates and /386 the critical buckling values are determined in such a way as to satisfy the continuity conditions of the deflection, deflection angle, etc., between adjoining plates. Moreover, according to Kuranishi, in channel cross-sections, C-forms with very small end-wall surface widths and Hut cross-sections, in which the compressive stresses cannot maintain equilibrium around the centroids of the cross-sections, the buckling of the wall surface gives the maximum load for the column, and in columns with other types of cross-sections, when the average compressive stress σ_m reaches the value given by the following equation, this is the maximum load.

$$\sigma_m=\sqrt{\frac{k_m E\sigma_c}{12(1-\nu^2)}}\left(\frac{t}{b}\right) \qquad (4.5.1)$$

In the above equation, k_m is the coefficient determined by the cross-section configuration and if the back surface width in rectangular, C and Hut forms is constant, k_m is large when the side wall surface width is small. When the back and side-wall surfaces are constant, k_m is larger for a rectangle, than for C-forms or Hut forms.

When a column made of flat plates undergoes compression, the flat plates comprising the column walls described above, buckle, and the column collapses. In addition, Euler buckling is also present, according to which flexural buckling occurs throughout the column, causing collapse. This is not treated here, since it is determined by following what is stated in part 2. In columns made of flat plates, a compound buckling takes place in each cross-section of the column, causing twisting and bending with respect to the axis. This problem is treated by H. Wagner and W. Pretscher [187], and later by E. E. Lundquist and C. M. Fligg [188] and by R. Kappus [190].

According to Wagner, when columns having cross-sections other than circular undergo torsion, the line element in the direction of column length undergoes displacement in the direction of column length; consequently, a distribu-

tion of axial forces is formed in the lateral cross-section of the column. In Figure 4.5.1, the difference $\Delta\xi$ in displacement in the direction of the axis between point 2 in cross-section x is

$$\Delta\xi=\frac{\varphi}{z}\cdot r_i\Delta S=\frac{1}{2}\Delta F\,\eta \tag{4.5.2}$$

Consequently, the axial stress σ is

$$\sigma=E\frac{d\xi}{dx}=E\,v\frac{d^2\varphi}{dx^2} \tag{4.5.3}$$

where

ψ = torsion angle $\left(\theta=\frac{d\varphi}{dx}\right)$

Therefore, for the torsion moment, if one adds the component due to this axial force, in addition to the term corresponding to the shear stress,

$$M=-EC_{BT}\frac{d^3\varphi}{dx^3}+GJ_T\frac{d\varphi}{dx} \tag{4.5.4}$$

is obtained. Where

$C_{BT}=\int u^2\,dF$. (integration is carried out over entire cross-section)

u is the degree of longitudinal movement when θ = 1

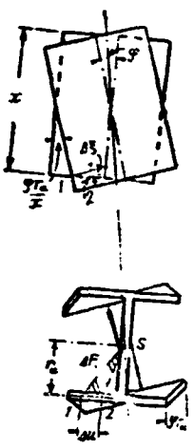

Figure 4.5.1

When a stress P is applied to the column, a horizontal component is formed due to the slope of the cross-section and this generates a torsion moment M' with respect to the shear center /387

$$M'=Pi_{SP}^2=P(i_x^2+e\cdot i_\eta) \tag{4.5.5}$$

$$i_{SP}^2=i_x^2+e\cdot i_\eta=\frac{1}{F}\int r^2dF+e\cdot\frac{1}{I}\int\eta\,r^2dF \tag{4.5.6}$$

e = eccentricity

η = distance from neutral axis.

Since the value of M' in equation (4.5.5) balances with M in equation (4.5.4), the following equation is obtained as an equilibrium condition.

$$EC_{BT}\frac{d^3\varphi}{dx^3}+(Pi_{SP}^2-GJ_T)\frac{d\varphi}{dx}=0 \tag{4.5.7}$$

Solving, under the conditions ψ = 0, ψ'' = 0 at the ends

$$P_k=\frac{1}{i_{SP}^2}\left(GJ_T+\frac{\pi^2}{l^2}EC_{BT}\right) \tag{4.5.8}$$

is obtained as the critical value of torsional and flexural buckling due to compression. When there is no eccentricity

$$\sigma_{kp}=\frac{GJ_T}{I_P}+\frac{\pi^2 EC_{BT}}{l^2 I_P} \tag{4.5.9}$$

is obtained as the critical stress.

Lundquist discusses Wagner's theory in greater detail and claims that Euler buckling is one special solution of this torsional and flexural buckling. He also calls this type of damage "primary column damage" and separates it from the wrinkling-type buckling of the flanges. There has been new research in the flexural and torsional buckling of flat plate structures by F. Bleich and J. N. Goodier (see Part 2, Chapter 3).

4.5.2. CONSIDERATIONS IN DESIGNING FLAT PLATE STRUCTURES

In designing structures whose principle members are flat plates, it is necessary both to investigate what should be the appropriate safety factor with respect to buckling, by calculating the critical buckling stresses σ_k for all possible types of buckling that may occur in a structure, and at the same time, to determine the safety characteristics with respect to ultimate strength, yield point and limit of fatigue. It is not possible to make a general statement concerning what the safety factors should be with respect to buckling in this case since the effects of various factors are involved, such as the purpose of the structure, load conditions and estimation of them, form of structure, precision of workmanship, presence or absence of original deflection, accuracy of calculations of critical buckling stress. A safety factor of 1.5 and 2.0 is taken for such structures as bridge girders, where relatively great stiffness is required, while there are extreme cases where a factor of less than 1.0 is required for shear buckling in the outer skin of aircraft.

The Architectural Society [191] makes a distinction between short-term and long-term loads, recommending a safety factor of 1.0 in the case of short-term loads for simple bending and shear, of 1.5 for uniform compression, and a factor of 1.5 times greater than that of short-term loads for all long-term loads. Generally, when σ_k is above the proportional limit, since the ratio of the buckling load to the maximum load is close to 1, it is necessary to use a large safety factor. When there is initial deflection, since it is generally the case that at loads lower than the critical load, lateral deflection occurs and no buckling phenomenon is clearly manifested, the stiffness also decreases. It is advisable to make a large safety factor estimate. Moreover, in the case of compressive loading, where there is initial deflection in a direction at right angles to the direction of load, or in the case of shear loads, there is a tendency in calculations for the critical values to increase due to the influence only of the initial deflection, but since there is a marked decrease in stiffness, and it is possible for buckling to occur rapidly at loads lower than those

observed in shells, it is not desirable to reduce the safety factor, taking into account the presence of the initial buckling. /388

In the event that the ratio of the length to the width of the flat plate section (e.g.) when $a/b \geq 3$ at the end rotating on four sides in the case of a compressive load, as, $a/b \geq 2$ with a torsional load, it is appropriate to consider that buckling will always develop under these load conditions at the minimum buckling load limit.

TABLE 4.5.1

Load	Edge Conditions	Minimum Actual Buckling Value (σ_k/σ)	Half-wave Length/Plate width (λ/b)
Simple Compression	Ends rotating on 4 sides	4.0	1.0
	a ends with sides free and rotating b ends with rotating sides	6.98	0.66
	a ends with sides free and rotating b ends with sides rotating	$0.982b^2/a^2+0.425$	minimum σ_k when $a/b=\infty$
	a sides free and fixed b side rotating ends	1.28	1.635
Shear	End with 4 sides rotating	5.335	1.25
	4 sides fixed	9.0	0.8
Simple bending	Ends with 4 sides rotating	23.9	0.667
	4 sides fixed	39.6	0.475

There are cases in which, when it is necessary to increase the critical buckling value when the length to width ratio of the plate is large instead of increasing the plate thickness, the objective is achieved by restricting the buckling wave forms produced, by using reinforcing members. For such a purpose, it is more effective to use longitudinal reinforcers (reinforcers parallel to the direction of load) for the compressive load, rather than use lateral reinforcers. Even when a bending load is sustained, longitudinal reinforcers should be used on the side of compressive stress (see E. Chwalla [5]). Also, for such purposes, it is effective to increase the required stiffness of the installed reinforcers to greater than γ_{min} and it is meaningless to put them in the positions of the segmented line in the case in which reinforcers are not used. For the flat plate panels that are thus separated by reinforcing members, if the method of attachment of the reinforcers is by a single row of bolts, or by welding, when the deflection of both sides of the reinforcer causes buckling in the form of asymmetrical wave forms, the critical value used should be that of the panels. (See buckling form I in "Materials 100"). A symmetrical form is used for the reinforcing member if said member has a large degree of stiffness with respect to torsion, if more than two rows of bolts are used (buckling form III in above reference). Simply stated, there

is no objection to considering this as a single rectangular plate with the condition of rotating ends for the former, and fixed ends for the latter.

In a flat plate sustaining a combination of stresses including compression, bending and shear, the equations for determining the safety factor for the σ_{vk} in the following equation or the yield point stress σ_s are given in DIN E 4114 [9]. Denoting the compressive or flexural buckling limit stress by σ_{1k} and the shear limit buckling stress by τ_k,

$$\sigma_{vk}=\sqrt{\sigma_1^2+3\tau^2}\Big/\sqrt{(\sigma_1/\sigma_{1k})^2+(\tau/\tau_k)^2} \qquad (4.5.10)$$

where σ_1 and τ indicate respectively the compressive, and bending and shear stresses used.

$$\text{safety factor}=\sigma_{vk}\ (\text{又は}\ \sigma_s)\Big/\sqrt{\sigma_1^2+3\tau^2} \qquad (4.5.11)$$

The safety factors determined by the above equations. However, when $\sigma_k < \sigma_{vk}$, σ_{vk} is calculated, or σ_s is calculated if $\sigma_{vk} \geqq \sigma_s$. Values of 1.4 to 1.6 are given for the safety factor with respect to the various conditions for bridge girders. /389

In the following Standards for Calculations of Steel Structures of the Architectural Society [191], the following basic formulae are given for designing the same type of web plates; that is, in the webs of plate beams, denoting plate thickness by t, web width by b, if t/b < 1/80 in places sustaining compression when t/b < 1/30, it is necessary to satisfy the following equation (4.5.12) for the maximum compressive stress σ, and shear stress τ occurring in the rectangular plates.

$$\left(\frac{\sigma}{f_1}\right)^2+\left(\frac{\tau}{f_2}\right)^2\leqq 1 \qquad (4.5.12)$$

Here $f_1=\dfrac{800f_c}{\mu\left(\frac{b}{t}\right)^2}k_1$ (allowable buckling stress of plate sustaining compression)

f_c = allowable compressive stress

$$\mu=1.5-\alpha/4,$$

$$\alpha=1-\frac{\sigma_{min}}{\sigma_{max}}$$ (simple bending α = 2) (simple compression α = 0)

$$k_1=\alpha^2+3\alpha^2+4 \qquad \left(\text{where } \beta=\frac{a}{b}\geq 1-\frac{\alpha}{6}\right)$$

$$=\frac{1}{4}\left(\frac{\beta}{1-\frac{\alpha}{6}}+\frac{1-\frac{\alpha}{6}}{\beta}\right)^2(\alpha^2+3\alpha^2+4) \quad \left(\text{where } \beta<1-\frac{\alpha}{6}\right).$$

and when $f_1 > \frac{2}{3}\frac{f_c}{\mu}$ the following f_1' is used in place of f_1.

$$f_1' = \frac{1.8 f_c}{f_c / f_1 + 1.2\mu},$$

$f_2 = \frac{800 f_c}{\left(\frac{b}{t}\right)^2 k_2}$ (allowable buckling strain of plate undergoing shear)

$k_2 = 5.4 + \frac{4}{\beta^2}$ (where $\beta \geq 1$)

$= \frac{5.4}{\beta^2} + 4$ (" $\beta < 1$).

L. S. Moisseiff [193] calculates the critical stress as follows, including cases when the proportional limit is exceeded. He gives a system for determining plate thickness so that a suitable safety coefficient is obtained for the critical stress.

$$\sigma_k \left(\text{ or } \tau_k \right) = k \frac{\pi^2 E \zeta}{12(1-\nu^2)} \left(\frac{t}{b}\right)^2 \tag{4.5.13}$$

$$\zeta = 0.5(\alpha + \sqrt{\alpha}), \quad \alpha = E_t / E$$

E_t is the value of E corresponding to the buckling stress after the proportional limit is exceeded. The stress used σ and the plate thickness are determined such that the safety factor becomes 2 with respect to the compression side flanges of plate beams and plates sustaining compression. Assuming σ and $\sigma = \sigma_\lambda / 2$ determining plate thickness for carbon steel, this is /390

$$\frac{b}{t} = 3620\sqrt{\frac{k\zeta}{\sigma}} \quad (\sigma : \text{lbs/in}^2) \tag{4.5.14}$$

And the required plate thickness is determined with respect to σ. Finding b/t for k = 4, which gives the minimum critical buckling value of ends with rotating edges, for compressive loads from the above equation, with a yield point stress σ_S = 36,000 lbs/in^2, this is 50 and when b/t is above this value, (plate thickness decreases with respect to width) since it becomes necessary to consider buckling, he says that the design should be carried out for a value below 50. He also gives the width/thickness ratio reaching the yield point in the same manner for compression members with free sides. In this case, the value of k is 0.43 and the sides are rotating ends and 1.28 when they are fixed ends. He also gives values of b/t for rolled members, riveted members and welded members. For rolled steel members and riveted flanges, he gives

$$\frac{b}{t} = 6000\sqrt{\frac{\zeta}{\sigma}} \tag{4.5.15}$$

For flanges of welded members

$$\frac{b}{t}=5400\sqrt{\frac{\zeta}{\sigma}} \tag{4.5.16}$$

For aluminum alloys, the coefficients of equations (4.5.14) and (4.5.15) are respectively 2,180 and 3,500.

Moisseiff also gives details on columns made of reinforced plates having reinforcing members in longitudinal and lateral directions, and on methods for designing webs of plate beams. His approach is to determine the number of panels, and consequently the number and distance between the centers of the reinforcers, so that the maximum allowable width/thickness ratio is obtained for the plate panels (50 in steel members) and to determine the dimensions of the reinforcers so that the buckling stress of the beams on columns, including all of the reinforcers thus determined, is equal to that of the panels. In this manner, he gives design formulas for columns and plate beams. If, in such a case, a safety factor of 1.5 is taken for the bending or shear buckling of webs of plate beams, or a factor of 1.4 for the combination of the two, this coincides with a safety factor of 2.0 for the buckling of flat plate panels and is sufficient.

/391

CHAPTER 6 (SUPPLEMENT)
BUCKLING OF SANDWICH PLATES

The increase in speed of aircraft has been accompanied by a necessity for reducing their weight. For this reason, an increase in the stiffness and strength has become necessary, and sandwich plates have come to be used for this purpose. Sandwich plates consist of a light, non-metallic plate called a core, covered on both sides with a thin metal sheeting called facing. By increasing the interval between the facings from the neutral axis, they aim at reducing weight and increasing bending stiffness. In addition, sandwich plates have the advantage of improving vibration characteristics due to their attenuation and are effective in insulation against sound and heat. Light weight and moisture resistance are required as core materials, for which purpose light wood (balsa, cryptomeri), extra materials (made from plant fibers), foam materials (foam rubber, sponge, etc.), honeycomb structures (glass fibers, paper), and aluminum corrugated materials, and aluminum foil are used. Thin metal plates are generally used as facings, and are attached by means of a special resonance glue (araldite, radax, etc.) to the core. Together with the rapid progress in the development of such adhesives, the uses of sandwich plates are rapidly expanding.

In terms of elastic stability, the buckling of sandwich plates are divided into two types. One is called overall buckling or quasi-Euler, when the facing and core buckle together, and wrinkling or, ripple type buckling, when wrinkles occur on the facing, when the core breaks up.

Overall buckling has been investigated over a long period of time, and since it is easy to simplify many of the problems with this type of buckling, various basic hypotheses are established which are considered to be valid in solving such problems. For example, (1) the core undergoes only shear deformations. (2) Some of the normal stresses and/or shear stresses are disregarded. (3) The bending stiffness of the facing is disregarded.

E. Reissner [194] treats sandwich plates as a combination of a facing which has no bending stiffness and a core which resists only shear deformation within the plane vertical to it and expansion and contraction in the direction of the plate thickness, and obtains the following differential equation of buckling.

$$\nabla_1^4 w=\left(1-\frac{thE_f}{2(1-\nu_f^2)G_c}\nabla_1^2\right)\left(N_{x0}\frac{\partial^2 w}{\partial x^2}+2S_0\frac{\partial^2 w}{\partial x\partial y}+N_{y0}\frac{\partial^2 w}{\partial y^2}\right),$$

Here, t = plate thickness of facing, h = total thickness, subscript "f" hyphen "c" core. This equation agrees with the equation for an isotropic plate, where $G_c \to \infty$ denoting the form of deflection by w = sin (mπx/a) sin

(nπy/b), for the buckling values when a rectangular plate having supported edges undergoes suppression in one direction, he obtained

$$N_0=\frac{\pi^2 D}{b^2}\cdot f(\lambda)=\frac{\pi^2 D}{b^2}\cdot\frac{(1+\lambda)^2}{\lambda[1+\mu(1+\lambda)]} \quad \text{Where } m=n=1)$$

$$\mu=\pi^2\frac{th}{b^2}\cdot\frac{E_f}{2(1-\nu_f^2)G} \qquad \lambda=\frac{b^2}{a^2}$$

for a plate of infinite length, $f(\lambda)=4/(1+\mu)^2$ for $\mu\ll 1$, $f(\lambda)=1/\mu$ for $\mu\gg 1$.

Also P. Seide and E. Z. Stowell [196] used the theory of C. Libove and S. B Batdorf [196], see below, for sandwich plates with supported edges, calculate seven physical constants on the basis of the same hypotheses as Reissner, obtain the same results as Reissner, and show that they agree well with the experiment values. In addition, they analyzed buckling in the plastic region applying plate theory, on the basis of E. Z. Stowell's plastic deformation theory [218], make corrections for the Poisson's ratio ν, give analyses for sandwich plates (ν = 13) with supported edges, and infinite length, in which the facing material is aluminum and uncast steel, and compare their results with the experimental values. The theoretical values are 8 to 25% higher than the experimental values. /392

More exact theory is required for cases not falling under the above hypotheses, i.e., cases in which there is a relatively thick facing on a core with large bending stiffness. A. C. Eringen [197], considering both facing and core to be isotropic, divides the strain energies into (1) bending elongation and shear energy of facing, (2) latent shear energy in core, (3) work performed by external forces, expands the deflection into a double series of a sine function and substitutes it, simultaneously treats overall buckling and wrinkle buckling, and for rectangular sandwich plates with supported edges, he gives graphs of the minimum buckling stress combining equations for the two types of buckling. S. V. Nardo [198] also gives the same type of calculations for the overall buckling of rectangular sandwich plates with the loaded end fixed (other end supported). Ideda [199] even considers the bending stiffness of the core, finds a relatively general form for the equilibrium equation, and obtains the same type of equations from energy calculations. As an example of its application, the minimun buckling value of a rectangular plate supported on four sides is given in the following form.

$$(P_{cr})_{min}=\frac{4\pi^2}{b^2}\left[\frac{D'}{1+2K}+D_c+2D_f\right].$$

Here D' = bending stiffness of plates, disregarding the bending stiffnesses of the facing and the core. This corresponds to the D in Reissner's equation.

$K=\frac{(\pi^2 t_c D')}{(b^2 h^2 G_c)}$, h = spacing between center planes of both cores. If in this equation one assumes $D_c = D_f = 0$, this matches Reissner's equation completely ($\lambda = 1$).

As mentioned above, Eringen and H. Neuber [200] provide a solution for ripple type buckling. J. N. Goodier and C. S. Hsu [201] found that with respect to sandwich plates having a special core (called an "antiplane core") having "antiplane stress" (such that with respect to deformations within the plane, the stiffness is 0, and the core only resists tensile stress and shear in the direction perpendicular to the plane), ripple type buckling could be handled in terms of problems of columns on an elastic base. At the same time, they showed that they were unable to give minimum values for sine function type ripple buckling of sandwich plates with both ends free or with rotating ends, and that asymmetrical buckling occurs with respect to the center plane of the core, such that deformation is limited to both ends, and the other parts remain flat. Syed Yusuff [202], investigated this in greater detail, divided ripple buckling into two types, obtaining a square root equation

$$\sigma_{cr}=\left(\frac{3}{2}E_f E_c \frac{t}{b}\right)^{\frac{1}{2}}$$

when the shearing force in the core is not taken under consideration, and when, in the same form as Goodier solution, that shearing force is considered, a cube root equation $\sigma_{cr} = 0.961(E_t E_c G_c)^{\frac{1}{3}}$ is obtained. This agrees, except for the constant coefficients with the equations of N. J. Hoff and S. E. Mautner [203], D. Williams [204] and E. Gough [205]. He showed that these solutions agreed well with the experimental values both for the wavelength and critical load.

Libove and Batdorf [196] treat a sandwich plate as a single isotropic plate and derive a basic equation, taking the effect of shear into account. The seven physical constants in the equation are determined experimentally. M. Stein and J. Mayers [206] have studied initial curvature.

In the Committee Report [207] on Airforce-Navy-Civil Aircraft design criteria of the U.S. Munitions Board Committee, sandwich plates are classified /393 into the following three types according to their structural materials:

(1) isotropic plates: in which the facing and core are isotropic within the plane

(2) orthotropic plates

(3) corrugated sandwich plates: facing attached to both faces of corrugated members.

Many papers [208, 209. 210, 211, 212] give design schemata for various edge and load conditions.

CHAPTER 7 (SUPPLEMENT)
PLASTIC BUCKLING OF RECTANGULAR PLATES

When the thickness t of a plate is thin in comparison with its width b, i.e., when t/b is small, the critical buckling stress is lower than the proportional limit stress σ_p, and so-called elastic buckling occurs, but as t/b becomes greater, the critical stress increases, the values found by the methods of calculation in Chapter 2 exceed the proportional limit, and the yield-point stress σ_s is also exceeded. When such a state is reached, the elasticity modulus at the critical value differs from Young's modulus, and the critical values found as the above elastic buckling, since low values were obtained. They give values that are excessively high and inconsistant. Buckling phenomena in such a state are referred to as plastic buckling.

A long time ago, E. Lamarle (1845), A. Considére (1889) and others found, with respect to the plastic buckling of columns, that within the range of applicability of Euler's formulae, the critical value reaches σ_p, and when critical values above this are given, calculations should be performed using somewhat lower values in place of Young's modulus E. In addition, the following theories were proposed: F. Engesser's tangent modulus theory (1889) (in which he claimed that in place of E, a tangent modulus E_t should be used, corresponding to the critical buckling stress), the conversion coefficient theories of F. Engesser (1895), T. von Kármán (1909), R. V. Southwell (1912) (according to which, when buckling and bending occurs, since the compressive strain on the convex sides decreases, the stress-strain relationship is given by Young's modulus, and since the compressive strain on the concave side increases, calculations should be performed using the tangent modulus corresponding to the compressive strain). Whereas theoretically, the conversion coefficient critical values (the critical values found using conversion coefficients in place of Young's modulus) appear satisfactory, in most cases the experiment results showed values close to the tangent modulus critical value (values found using tangent modulus).

In 1947, F. R. Shanley [213] performed calculations based on a simplification of the plastic portion, and as a result, he showed that even if the tangent modulus critical values are exceeded, a stable condition can be maintained, but the increment in bending with respect to the increment in load rapidly increases, the strain increases initinitely in the conversion coefficient critical values, and stability cannot be maintained. That is, the tangent modulus critical values are considered to be the lower limit of the critical buckling values, and that in actual structures, the critical values cannot be much higher than these.

With regard to the plastic buckling of rectangular flat plates, S. Timoshenko [214] and F. Bleich [215] studied cases in which compression is

sustained from one direct[illegible] Considering the decrease in bending st[illegible]ness due to decrease in the mo[illegible]us of elasticity only in the direction in which the load is sustained, they proposed a method of calculation which assumes no decrease in directions at right angles to this direction. That is, denoting by $\alpha_t (=E_t/E)$ the ratio of the tangent modulus E_t and Young's modulus, corresponding to the critical stress, the equilibrium equation was assumed to be given by

$$D\left(\alpha_t\frac{\partial^4 w}{\partial x^4}+2\sqrt{\alpha_t}\frac{\partial^4 w}{\partial x^2\partial y^2}+\frac{\partial^4 w}{\partial y^4}\right)+N_x\frac{\partial^2 w}{\partial x^2}=0 \qquad (4.7.1)$$

/394

the second term refers to the torsion stiffness. The decrease in stiffness in this term is assumed to be proportional to $\sqrt{\alpha_t}$. From this, the limits stress in the case of four side rotating ends is given by

$$\sigma_k=\frac{\pi^2 D}{b^2 t}\left(\frac{b}{a}\sqrt{\alpha_t}+\frac{a}{b}\right)^2 \qquad (4.7.2)$$

the minimum value begins at $a/b = \sqrt{\alpha_t}$, and its value becomes

$$\sigma_{k\min}=\frac{\pi^2 E}{3(1-\nu^2)}\sqrt{\alpha_t}\left(\frac{t}{b}\right)^2 \qquad (4.7.3)$$

Moreover, E. Chwalla [216], M. Roš and A. Eichinger [217] consider that in the plastic state, the material becomes isotropic and has the same modulus of elasticity in both directions. They obtained the following equilibrium equation.

$$D\alpha_r\left(\frac{\partial^4 w}{\partial x^4}+2\frac{\partial^4 w}{\partial x^2\partial y^2}+\frac{\partial^4 w}{\partial y^4}\right)+N_x\frac{\partial^2 w}{\partial x^2}=0 \qquad (4.7.4)$$

In this case, if the elastic buckling value is increased α_r times, the critical value of plastic buckling is obtained. Moreover, Chwalla uses a conversion factor E_r as the elasticity modulus, and $\alpha_r = E_r/E$.

After the initial development of the theory of plastic buckling, there was a gradual increase in the publication of new theories of plastic buckling starting around 1940, which took into account the stress-strain relationship based on plasticity theory. On the basis of Hencky's theory of plastic deformation, E. Z. Stowell [218] P. Bijlaard [219], E. Z. Stowell and R. A. Pride [220], and A. A. Ilyushin [221] publisned papers, and the theories of

G. H. Handelman and W. Prager [222] and C. E. Pearson [223] were published, which were based on Prandtl-Reuss's plastic flow theory.

Stowell's theory based on plastic deformation theory is as follows. Assuming that from the flat state an infinitesimal deflection w(x,y) occurs, the degree of change in strain is given by

$$\delta\varepsilon_x=-z\frac{\partial^2 w}{\partial x^2},\quad \delta\varepsilon_y=-z\frac{\partial^2 w}{\partial y^2},\quad \delta\gamma=-2z\frac{\partial^2 w}{\partial x\partial y} \tag{4.7.5}$$

in plastic deformation theory, with respect tc two-dimensional state of stress,

$$\frac{\sigma_x-\nu\sigma_y}{\varepsilon_x}=\frac{\sigma_y-\nu\sigma_x}{\varepsilon_y}=\frac{2(1+\nu)\tau}{\gamma}=\frac{\sigma_i}{\varepsilon_i}=E_s \tag{4.7.6}$$

where

$$\left.\begin{aligned}\sigma_i&=\sqrt{\sigma_x^2+\sigma_y^2-\sigma_x\sigma_y+3\tau^2}\\ \varepsilon_i&=\frac{2}{\sqrt{3}}\sqrt{\varepsilon_x^2+\varepsilon_y^2+\varepsilon_x\varepsilon_y+\frac{1}{4}\gamma^2}\end{aligned}\right\} \tag{4.7.7}$$

E_s = Secant coefficient

from the change in strain energy,

$$\sigma_i\delta\varepsilon_i=\sigma_x\delta\varepsilon_x+\sigma_y\delta\varepsilon_y+\tau\delta\gamma \tag{4.7.8}/395$$

taking $\nu = 0.5$ for the plastic deformation, and inserting the relationship $\frac{\delta\sigma_i}{\delta\varepsilon_i} = E_t$, from equation (4.7.6)

$$\left.\begin{aligned}\delta\sigma_x-\frac{1}{2}\delta\sigma_y&=E_s\delta\varepsilon_x-\frac{\varepsilon_x}{\varepsilon_i}(E_s-E_t)\delta\varepsilon_i\\ \delta\sigma_y-\frac{1}{2}\delta\sigma_x&=E_s\delta\varepsilon_y-\frac{\varepsilon_y}{\varepsilon_i}(E_s-E_t)\delta\varepsilon_i\\ \delta\tau&=\frac{1}{3}E_s\delta\gamma-\frac{\gamma}{3\varepsilon_i}(E_s-E_t)\delta\varepsilon_i\end{aligned}\right\} \tag{4.7.9}$$

using the relationship of equation (4.7.8.), (4.7.9)

$$\left.\begin{aligned}
\delta\sigma_x &= \frac{4}{3}E_s\left[\left(1-\frac{3}{4}\kappa\frac{\sigma_x^2}{\sigma_i^2}\right)\delta\varepsilon_x+\frac{1}{2}\left(1-\frac{3}{4}\kappa\frac{\sigma_x\sigma_y}{\sigma_i^2}\right)\delta\varepsilon_y\right.\\
&\quad\left.-\frac{3}{4}\kappa\frac{\sigma_x\tau}{\sigma_i^2}\delta\gamma\right]\\
\delta\sigma_y &= \frac{4}{3}E_s\left[\frac{1}{2}\left(1-\frac{3}{2}\kappa\frac{\sigma_x\sigma_y}{\sigma_i^2}\right)\delta\varepsilon_x+\left(1-\frac{3}{4}\kappa\frac{\sigma_y^2}{\sigma_i^2}\right)\delta\varepsilon_y\right.\\
&\quad\left.-\frac{3}{4}\kappa\frac{\sigma_y\tau}{\sigma_i^2}\delta\gamma\right]\\
\delta\tau &= -\frac{E_s\kappa}{\sigma_i^2}\left[\sigma_x\tau\delta\varepsilon_x+\sigma_y\tau\delta\varepsilon_y\right]+\frac{E_s}{3\sigma_i^2}\left[\sigma_i^2-3\kappa\tau^2\right]\delta\gamma
\end{aligned}\right\} \qquad (4.7.10)$$

where $$\kappa = 1-\frac{E_t}{E_s}$$

including the relationship (4.7.5) and (4.7.10), and considering relationships such as

$$\delta M_x = \int_{-\frac{t}{2}}^{\frac{t}{2}}\delta\sigma_x\cdot z\,dz$$

the following relationships are obtained for δM_x, δM_y, δM_{xy}.

$$\left.\begin{aligned}
\delta M_x &= -D'\left[\left(1-\frac{3}{4}\kappa\frac{\sigma_x^2}{\sigma_i^2}\right)\frac{\partial^2 w}{\partial x^2}+\frac{1}{2}\left(1-\frac{3}{2}\kappa\frac{\sigma_x\sigma_y}{\sigma_i^2}\right)\frac{\partial^2 w}{\partial y^2}-\frac{3}{2}\kappa\frac{\sigma_x\tau}{\sigma_i^2}\frac{\partial^2 w}{\partial x\partial y}\right]\\
\delta M_y &= -D'\left[\frac{1}{2}\left(1-\frac{3}{2}\kappa\frac{\sigma_x\sigma_y}{\sigma_i^2}\right)\frac{\partial^2 w}{\partial x^2}+\left(1-\frac{3}{4}\kappa\frac{\sigma_y^2}{\sigma_i^2}\right)\frac{\partial^2 w}{\partial y^2}-\frac{3}{2}\kappa\frac{\sigma_y\tau}{\sigma_i^2}\frac{\partial^2 w}{\partial x\partial y}\right]\\
\delta M_{xy} &= -\frac{D'}{2}\left[\left(1-\kappa\frac{3\tau^2}{\sigma_i^2}\right)\frac{\partial^2 w}{\partial x\partial y}-\frac{3}{2}\kappa\left(\frac{\sigma_x\tau}{\sigma_i^2}\frac{\partial^2 w}{\partial x^2}+\frac{\sigma_y\tau}{\sigma_i^2}\frac{\partial^2 w}{\partial y^2}\right)\right]
\end{aligned}\right\} \qquad (4.7.11)$$

where $$D' = \frac{E_s t^3}{9}$$

Substituting equation (4.7.11) in an equilibrium equation, and assuming in particular $\sigma_x = -\sigma$, $\sigma_y = \tau = 0$, the equilibrium equation becomes as follows.

$$D'\left[\left(1-\frac{3}{4}\kappa\right)\frac{\partial^4 w}{\partial x^4}+2\frac{\partial^4 w}{\partial x^2\partial y^2}+\frac{\partial^4 w}{\partial y^4}\right]+t\sigma\frac{\partial^2 w}{\partial x^2}=0 \qquad (4.7.12)$$

When in a slender flat plate the side parallel to the load is a rotating end, for the stability limit stress σ_c

$$\sigma_c=\sigma_E\frac{E_t}{E}\left(\frac{1}{2}+\frac{1}{2}\sqrt{\frac{1}{4}+\frac{3}{4}\frac{E_t}{E}}\right) \tag{4.7.13}$$

is obtained. σ_E is the elastic buckling limit stress. /396

Handelman-Prager, following Prandtl-Reuss plastic flow theory, proceeding from the relationships

$$\left.\begin{aligned} d\varepsilon_x&=\frac{1}{E}(d\sigma_x-\nu d\sigma_y)+\frac{1}{2E}(\lambda-1)(2\sigma_x-\sigma_y)\frac{d\sigma_i}{\sigma_i}\\ d\varepsilon_y&=\frac{1}{E}(-\nu d\sigma_x+d\sigma_y)+\frac{1}{2E}(\lambda-1)(-\sigma_x+2\sigma_y)\frac{d\sigma_i}{\sigma_i}\\ d\gamma&=\frac{2(1+\nu)}{E}d\tau+\frac{1}{2E}(\lambda-1)\cdot 6\tau\frac{d\sigma_i}{\sigma_i} \end{aligned}\right\} \tag{4.7.14}$$

where

$$\lambda=\lambda(\sigma_i)=\frac{E}{E_t(\sigma_i)}$$

$$\frac{d\sigma_i}{\sigma_i}=\frac{\{(2\sigma_x-\sigma_y)d\sigma_x+(-\sigma_x+2\sigma_y)d\sigma_y+6\tau d\tau\}}{2\sigma_i^2}$$

for the state of two-dimensional stress, found

$$\sigma_c=\sigma_E\cdot\frac{1}{2}\left[\left\{1-\frac{3}{4}\left(\sqrt{\frac{E}{E_t}}-1\right)\left(\sqrt{\frac{E}{E_t}}+3\right)\Big/\left(\sqrt{\frac{E}{E_t}}+1\right)^2\right\}^{\frac{1}{2}}+1\right] \tag{4.7.15}$$

as the stability limit stress when the long side parallel to the load is a rotating end. As a result, even considering the limit where $E_t = 0$,

$$\sigma_c=\frac{3}{4}\sigma_E$$

is obtained, when σ_E becomes large, σ_c has a rather large value, giving a value which differs considerably from reality. Pearson attempted to a further improvement by taking Shanley's approach into consideration. That is, simplifying the stress-strain relationship, and substituting the relationship

$$d\sigma_x=\frac{(\lambda+3)E}{(5-4\nu)\lambda-(1-2\nu)^2}d\varepsilon_x+\frac{2(2\nu+\lambda-1)E}{(5-4\nu)\lambda-(1-2\nu)^2}d\varepsilon_y$$

$$d\sigma_y=\frac{2(2\nu+\lambda-1)E}{(5-4\nu)\lambda-(1-2\nu)^2}d\varepsilon_x+\frac{4\lambda E}{(5-4\nu)\lambda-(1-2\nu)^2}d\varepsilon_y \qquad (4.7.16)$$

$$d\tau=\frac{E}{2(1+\nu)}d\gamma$$

into the moment equation, finding the balance condition equation, he derived

$$D_{11}\frac{\partial^4 w}{\partial x^4}+2D_{12}\frac{\partial^4 w}{\partial x^2\partial y^2}+D_{22}\frac{\partial^4 w}{\partial y^4}+\sigma t\frac{\partial^2 w}{\partial x^2}=0 \qquad (4.7.17)$$

where

$$D_{11}=\frac{(\lambda+3)(1-\nu^2)}{(5-4\nu)\lambda-(1-2\nu)^2}D$$

$$D_{22}=\frac{4\lambda(1-\nu^2)}{(5-4\nu)\lambda-(1-2\nu)^2}D$$

$$D_{12}=(1-\nu^2)\left[\frac{2(2\nu+\lambda-1)}{(5-4\nu)\lambda-(1-2\nu)^2}+\frac{1}{1+\nu}\right]\cdot D$$

using $\nu = 0.5$, for the stability limit stress for a slender rectangular plate

$$\sigma_s=\frac{1}{2}\left[\frac{1}{2}\left(1+3\frac{E_t}{E}\right)^{\frac{1}{2}}+1\right]\sigma_E \qquad (4.7.18)$$

was obtained. Pearson's results also give values agreeing roughly with the /397
experiment results when $E_t/E \doteqdot 1$, but when $E_t/E \doteq 0$, high values are given, as in Prager's results.

W. Prager [224] offers the following four factors to account for the fact that the results based on flow theory, which is considered more perfect than plastic theory, show values which are more divergent from the experiment results than those given by deformation theory. i) Effects of creep (Marin), ii) effects of dynamic phenomena (Marin), iii) effects of initial irregularity such as initial deflection, excentric load, etc., (Lin, Pearson, Cicala, Duberg-Wilder), iv) effects due to the fact that the assumptions of the relationship between stress and strain in flow theory differ from reality (Batdorf, Drucker). however, with regard to i), ii) there are inconsistencies even in the range in which these effects are no problem. S. B. Batdorf [225] proposes a slip theory for the stress-strain relationship in iv) and obtains results close to the deformation theory. However, in slip theory, determining the elasticity range poses problems, and although it is considered that in this part the increment of plastic strain is non-linear with respect to the increment in

stress, this differs markedly from the relationship between stress and strain in flow theory, where the relationship is linear, and it is difficult to say that it has then proven experimentally.

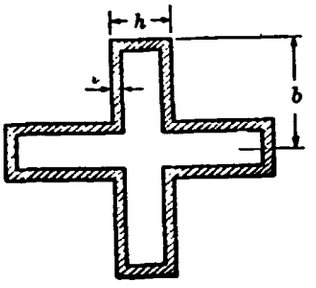

Figure 4.7.1.

With regard to the remaining problem, i.e. initial irregularities, E. T. Onat and D. C. Drucker [226] and J. F. Besseling [227] consider a cruciform column having a thin outer skin outside of the nucleus (Figure 4.7.1) where the inside nucleus functions to maintain shape, and the outside outer skin is used to support the load as a column. When the cruciform column undergoes compression, the outside skin part undergoes deformation according to the stress-strain relationship in flow theory, but owing to initial twisting in the cruciform column, the buckling load decreases, and the values of deformation theory are approached (Figure 4.7.2). Ammamoto [228] derived a theory of buckling from the strain-energy relationship on the basis of initial irregularities, considering a square sandwich plate in the center of a plate, a model with stiff plates attached to the outside of this, and that in the sandwich section only the outer skin reacts with respect to compressive force. The increment of strain-energy W(dε) due to the increment in stress is given by equation (4.7.19-20)

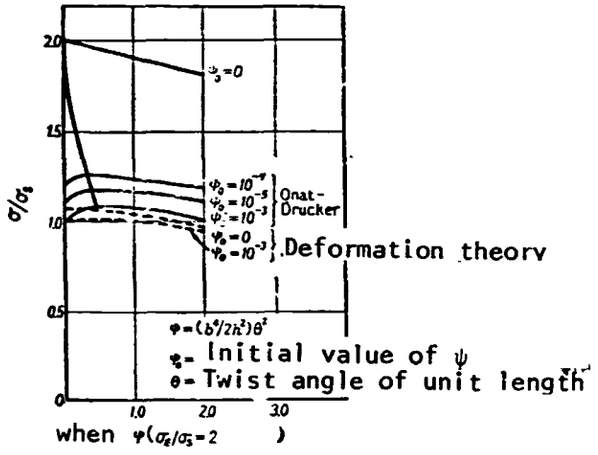

Figure 4.7.2.

$$W(d\varepsilon)=\frac{1}{2}(d\sigma_x\cdot d\varepsilon_x+d\sigma_y\cdot d\varepsilon_y+d\tau\cdot d\gamma) \tag{4.7.19}$$

$$=\frac{W_E(d\varepsilon)}{\Delta}+\frac{9(\lambda-1)}{4E\sigma_i^2\Delta}\{W_E(d\varepsilon)\cdot W_E(s)-\{W_E(d\varepsilon\cdot s)\}^2\} \tag{4.7.20}$$

where $W_E(d\varepsilon)$ is the increment in strain energy when complete elastic deformation occurs, and is given by /398

$$W_E(d\varepsilon)=\frac{1}{2}\frac{E}{1-\nu^2}\left[(d\varepsilon_x+d\varepsilon_y)^2+2(1-\nu)\left\{\left(\frac{d\gamma}{2}\right)^2-d\varepsilon_x\cdot d\varepsilon_y\right\}\right] \tag{4.7.21}$$

$$W_E(s)=\frac{1}{2}\cdot\frac{E}{1-\nu^2}[(s_{11}+s_{22})^2+2(1-\nu)(s_{12}^2-s_{11}\cdot s_{22})]$$

$$W_E(s\cdot d\varepsilon)=\frac{1}{2}\cdot\frac{E}{1-\nu^2}[(d\varepsilon_x+d\varepsilon_y)(s_{11}+s_{22}) \tag{4.7.22}$$

$$+(1-\nu)(d\gamma\cdot s_{12}-d\varepsilon_x\cdot s_{22}-d\varepsilon_y\cdot s_{11})]$$

$$\Delta=1+\frac{9(\lambda-1)}{4E\sigma_i^2}\cdot W_E(s) \tag{4.7.23}$$

$$=\lambda(\sigma_i)+\frac{1-2\nu}{2(1-\nu^2)}\left\{(1-\nu)-\frac{(\sigma_x+\sigma_y)^2}{2\sigma_i^2}\right\}(\lambda-1)$$

Moreover, if

$$s_{11}=\frac{1}{3}(2\sigma_x-\sigma_y),\quad s_{22}=\frac{1}{3}(2\sigma_y-\sigma_x),\quad s_{12}=\tau$$

However, since $W_E(d\varepsilon)$ is an expression of the elastic strain energy per unit volume .

$$W_E(d\varepsilon+\chi_s)=W_E(d\varepsilon)+2\chi W_E(d\varepsilon,\ s)+\chi^2W_E(s)\geqq 0$$

the χ where this equation is assumed to be zero has no true route, so

$$W_E(d\varepsilon)\cdot W_E(s)-\{W_E(d\varepsilon\cdot s)\}^2\geqq 0$$

$$\frac{d\varepsilon_x}{s_{11}}=\frac{d\varepsilon_y}{s_{22}}=\frac{\frac{1}{2}d\gamma}{s_{12}}$$

is the case in which there are equal signs in the above equation. In other words, the case in which the elastic strain is small and negligible can be seen from (4.7.14) that is, when the plastic strain is large, and the elastic strain is negligible, the equation which indicates the strain energy in (4.7.20) can be expressed approximately by

$$W(d\varepsilon)\fallingdotseq\frac{W_E(d\varepsilon)}{\Delta} \tag{4.7.24}$$

When the plastic strain is small and $\lambda \fallingdotseq 1$, the second term in equation (4.7.20) becomes almost zero, and even in this case equation (4.7.24) gives a lower approximation for (4.7.20). If the strain energy is given approximately by equation (4.7.24), it is possible to use this to find the stability limit stress of plastic buckling, exactly as in the case of elastic buckling. In this case it is as if one were considering that the value of the modulus of elasticity decreased to $1/\delta \fallingdotseq E_t(\sigma_i)/E$. Moreover, the tangent modulus E_t is a function of the converted stress σ_i when buckling occurs, but when the initial deflection is zero or small, it may be considered a function of the compression stress component σ. When the critical stress σ_{Et} (? illegible subscript) found by the tangent modulus using σ is taken, corresponding to the stability limit stress σ_{ct} is found by the following equation /399

$$\sigma_{cr}=\sigma_E \times \frac{E_t(\sigma_{kr})}{E} \tag{4.7.25}$$

When $\Delta(\sigma_i)$ in the vicinity of stress σ_{ct} rapidly decreases, as the compressive stress exceeds σ_{ct}, the bending stiffness of the plate rapidly decreases, and P_{ct} becomes the maximum compressive stress, i.e., the stability limit stress. This σ_{ct} is a low approximate value for the stability limit stress. When $\Delta(\sigma_i)$ does not rapidly change in this vicinity, the decrease in bending stiffness is not appreciable, due to change in excess load occurring on the convex side, σ_{ct} is exceeded and the plate can maintain its stability. In this case, this means that the value of cr found by using the value of Δ corresponding to the critical buckling value based on the conversion factor gives a low approximate value of the stability limits, i.e.

$$\sigma_{cr}=\frac{4\sigma_E}{(1+\sqrt{\Delta(\sigma_{kr})})^2} \fallingdotseq \frac{4\sigma_E}{\left(1+\sqrt{\dfrac{E}{E_t(\sigma_{kr})}}\right)^2} \tag{4.7.26}$$

the above is Yamamoto's theory. Yoshiki and Yamamoto [229] conducted experiments using aluminum plates and soft steel plates, and found that this theory agrees well with their experiment values (see Figures 4.7 3, 4.7.4).

Tests of plastic buckling of flat plates were conducted by C. F. Kollbrunner [230], G. J. Heimerl [231], Watanabe [233] and R. A. Pride [234] in addition to those by Yoshiki and Yamamoto, but none of them agree with the flow theory. Consequently, in designing flat plates that undergo plastic buckling, estimations are made following Yamamoto's theory, approximately employing $E_t(\sigma_i)$ or $4E\cdot E_t/(\sqrt{E}+\sqrt{E_t})^2$ in place of Young's modulus, or one may use the stability limit stress based on deformation theory. Apparently neither

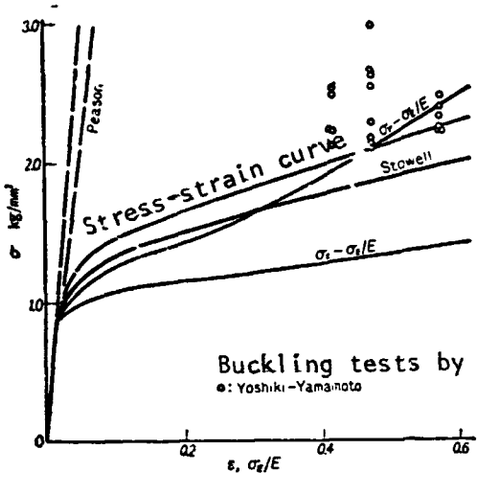

Figure 4.7.3.

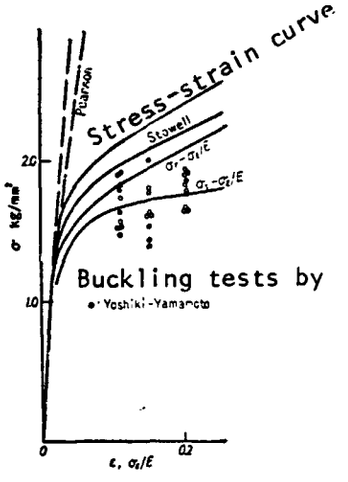

Figure 4.7.4.

deformation theory nor flow theory has been used for cases when the edge condition is elastic support. F. Bleich [237], proceeding from equation (4.7.1) gives results for cases in which two opposing sides parallel to the load have elastic support, and in which one side has elastic support, in which one side is free, and for others. Equation (4.7.1) is close to equation (4.7.12) based on deformation theory, and values calculated using E_t are close to experiment values, so it is considered that these results are close /400 to each other and can be used in actual calculations. Bleich's book gives many examples applied to H, channel, T, cruciform and hollow plate-flat plate structures.

P. P. Bijlaard [238] gives approximate calculations of plastic buckling due to combined shear and bending, or excentric compression.

Rectangular plates

Simple compression

/401

No.	Diagram and Bound. condition *1	Formulas or Tables of Results	Ref.-Remarks.
1	End with 4 sides rot. 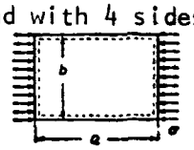	$\sigma_k = k\sigma_e$, *2 $k=\left(\frac{\beta}{m}+\frac{m}{\beta}\right)^2$, where $\beta=a/b$. $m=1$ for $(\beta \leqq \sqrt{2}$ $=2$ $(\sqrt{2} \leqq \beta \leqq \sqrt{6}$ 〃), $=3$ $(\sqrt{6} \leqq \beta \leqq \sqrt{12}$ 〃), $=4$ $(\sqrt{12} \leqq \beta \leqq \sqrt{20}$ 〃). for $\beta>4$ $k \fallingdotseq 4.00$.	10
2	End with 4 sides fixed 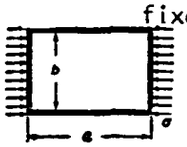	$\sigma_k = k\sigma_e$. value of k, Fig. in () are half number	15 17 18 19

a/b / Ref.	0.5	0.75	1.0	1.25	1.5
15	—	—	9.36	—	—
17	18.30 (1)	11.4 (1)	10.08 (1)	9.94 (2)	8.30 (2)
18	19.28 (1)	—	10.04 (1)	—	8.32 (2)
19	19.20 (1)	—	—	—	—

a/b / Ref.	1.75	2.0	2.75	3.0	3.5	∞
15	—	8.15	—	7.78	—	7.29
17	8.08 (3)	7.87 (3)	—	—	—	—
18	—	7.88 (3)	—	—	—	6.99
19	—	7.84 (3)	7.14 (4)	6.93 (4)	6.81 (5)	—

$k=\frac{4}{3}\left\{\frac{4a^2}{b^2(m^2+1)}+\frac{3m^2b^2}{4a^2}\cdot\frac{1+6/m^2+1/m^4}{1+1/m^2}\right\}$. 15

m is half wave number

$\sigma_k=(Lb^2/a^2+2.66+Ma^2/b^2)\sigma_e$. 16

m	1	2	3	4	5	$m>5$
L	4.00	8.37	15.0	23.6	34.4	$(\lambda/\pi)^2$, $\lambda=\frac{1}{2}(2m+1)\pi$
M	4.00	1.14	0.530	0.306	0.200	$\frac{16}{3}(\pi/\lambda)^2$

*1 Boundary conditions as follows: ---- rotating end, ▬ fixed end, — free end, -·-·- end with elastic support

*2 $\sigma_e=\frac{E\pi^2}{12(1-\nu^2)}\left(\frac{t}{b}\right)^2$. b = plate width, t = plate thickness, E = Young's modulus, ν = Poisson's ratio

No.	Diagram and Boundary Condition	Formulas or Tables of Results	Ref. Remarks
3	Side a fixed, side b rotating 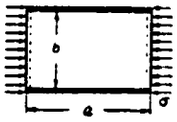	$\sigma_k = k\sigma_e$.	
		a/b: 0.4, 0.5, 0.6, 0.7 — k: 9.45, 7.69, 7.06, 7.00	20
		a/b: 0.8, 0.9, 1.0, 1.2 — k: 7.30, 7.83, 7.69, 7.06	
		$k = \frac{4}{3}\left(\frac{4a^2}{m^2b^2} + 2 + \frac{3m^2b^2}{4a^2}\right)$.	15
		a/b: 1.0, 2.0, 3.0, ∞ — k: 8.03 (2), 7.30 (3), 7.42 (5 or 4), 7.30	
		Figures in ( ) above = m, i.e. half wave no.	
		a/b: 0.5, 0.625, 0.667, 0.713, 1.0 — k: 7.75, 7.04, 6.98, 7.06, 8.63	29a
		$\frac{a}{b} = \beta \leqq 0.66$, $k = 2.366 + \frac{1}{\beta^2} + 5.3\beta^2$.	
		$\beta > 0.66$, $k = 6.97$.	30a
4	Side a rotating side b fixed 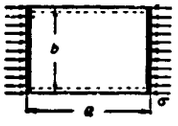	$\sigma_k = ' \sigma_e$.	22
		a/b: 0.4, 0.6, 0.8, 1.0, 1.2 — k: 27.12, 13.38, 8.73, 6.74, 5.84	
		a/b: 1.4, 1.6, 1.8, 2.0, 3.0 — k: 5.45, 5.34, 5.18, 4.85, 4.42	
5	Side a fixed other 3 sides rotating 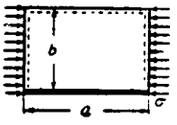	$\sigma_k = k\sigma_e$.	29b
		a/b: 0.728, 0.79, 0.889 — k: 5.47, 5.41, 5.51	
		minimum value of k = 5.41.	
		但し $a/b = 0.79$.	

No.	Diagram & Boundary Condition	Formulas or Tables of Results	Ref. Remarks
6	a, ends with sides free and rotating b, ends with sides rot	$\sigma_k = k\sigma_e$ a/b: 0.5 | 1.0 | 1.2 | 1.4 | 1.6 | 1.8 | 2.0 k: 4.40 | 1.44 | 1.14 | 0.952 | 0.835 | 0.755 | 0.698 a/b: 2.5 | 3.0 | 4.0 | 5.0 | 8.0 | 10.0 | ∞ [21] k: 0.610 | 0.546 | 0.516 | 0.506 | 0.470 | 0.465 | 0.425 $k = 0.42 + \frac{b^2}{a^2}$ (approximate equation)	20 21 29c 30b
7	a, ends with sides free and rotating b, ends with sides rotating	$\sigma_k = k\sigma_e$ a/b: 1.0 | 1.1 | 1.2 | 1.3 | 1.4 | 1.5 | 1.6 k: 1.70 | 1.56 | 1.47 | 1.41 | 1.36 | 1.34 | 1.33 a/b: 1.7 | 1.8 | 1.9 | 2.0 | 2.2 | 2.4 | 2.5 k: 1.33 | 1.34 | 1.36 | 1.38 | 1.45 | 1.47 | 1.59 (approxi te equation) $a/b = \beta \leqq 1.64$ $k = 0.559 + \frac{1}{\beta^2} + 0.13\beta^2$, $\beta > 1.64$ $k = 1.28$, minimum value of k = 1.28. where $a/b = 1.635$.	20 30c 29h
	Compression test on rectangular plates, sides supported by reinforcing members		
8	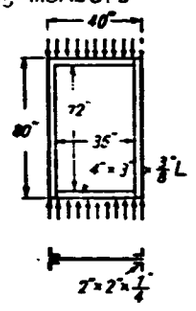	Test specimen a=80", b=40", t=1/4" soft steel a ... 2"×2"×1/4" angle steel b ... 4"×3"×3/8" ". Calculated values of P_k 26 ton Test values 29ton (31ton). (Determined by Cox's method)	33

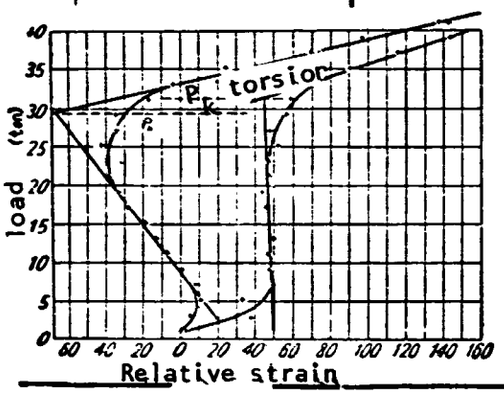

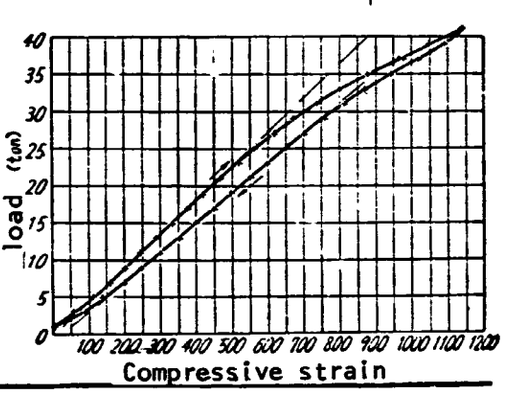

No.	Diagram & Bound.Cond.	Formulas or Tables of Results	Ref. Remarks
9	Ends with sides rotating, compression test 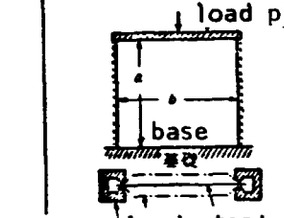	test specimen a=550mm, b=560~1818mm, t=2mm, 2.9mm, 4mm to 5mm. The critical buckling values generally agree with Bryan's calculated values. There is some disagreement due to the magnitude of initial deflection and configuration. The critical values are determined by Yoshiki's method (δ^2 method) 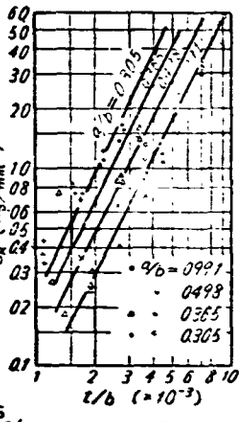 (straight lines indicate Bryan's calculated values) 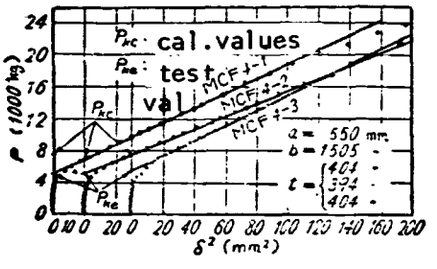	35 /404

= Compression in two directions

No.	Diagram & Bound Cond.	Formulas or Tables of Results	Ref. Remarks
10	End with 4 sides rotating 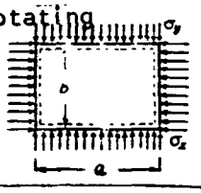	$$\sigma_{xk}\frac{m^2}{a^2}+\sigma_{yk}\frac{n^2}{b^2}=\frac{E\pi^2t^2}{12(1-\nu^2)}\left(\frac{m^2}{a^2}+\frac{n^2}{b^2}\right)^2.$$ m, n=x, y half wave of numbers in direction The values of m and n giving the minimum critical values are shown in Fig. 4.2.3 of previous text.	10
11	Ends with 4 sides fixed 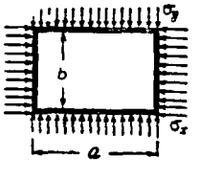	$$\sigma_{xk}+\frac{a^2}{b^2}\sigma_{yk}=1.34\,\sigma_e\left(3\frac{b^2}{a^2}+3\frac{a^2}{b^2}+2\right).$$ ($a\fallingdotseq b$, $\sigma_x\fallingdotseq\sigma_y$ The degree of approximation is satisfactory in this case. Case in which a=b (square shape) 13 14	31a

σ_y/σ_x	1	3/4	1/2	1/3	1/4
σ_{xk}/σ_e	5.61	6.41	7.48	8.40	8.80
σ_{yk}/σ_e	5.61	4.81	3.74	2.80	2.20

No.	Diagram & Boundary Conditions	Formulas or Tables of Results	Ref.	Remarks
11		σ_y/σ_x | 0 | −1/4 | −1/2 | −1 | −3/2 | −2 σ_{zk}/σ_z | 10.65 | 13.12 | 15.20 | 17.4 | 18.75 | 20.0 σ_{yk}/σ_z | 0 | −3.28 | −7.60 | −17.4 | −28.1 | −40.0 $a=b$, $\sigma_x=\sigma_y$ when $\sigma_{zk}=\sigma_{yk}=k\sigma_z$. $k=5.30$ $=5.304$ $=5.3036$.	23 17 26	
12	a, end with side fixed, b, end with sides rotating 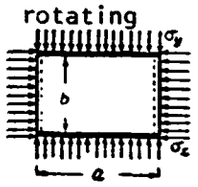 	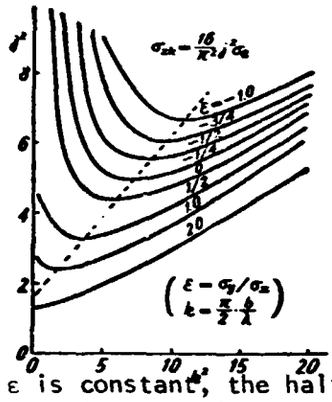 Where ε is constant, the half wave number becomes an integer, for k, j^2 is found from the graph. Case in which a=b (square) and ε=1.0 $\sigma_{zk}=3.8299\sigma_z$.	21 26	
13	Ends in which sides a,b are each fixed, the other sides are rotating 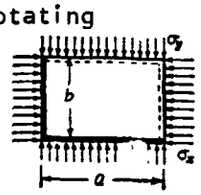 	$\sigma_{zk}=\frac{\pi^2}{20}\frac{D}{abt}\cdot\frac{41\left(\frac{b^2}{a^2}+\frac{a^2}{b^2}\right)+50}{\frac{b}{a}+\alpha\frac{a}{b}}$. where $\alpha=\sigma_y/\sigma_x$. Case in which a=b (square) $\sigma_{zk}=6.6\sigma_z\frac{1}{1+\alpha}$. Moreover when α=1 $\sigma_{zk}=3.3\sigma_z$ $=3.2316\sigma_z$.	27 26	

No.	D and B Conditions	Formulas or Tables of Results	Ref.-Remarks
14	Ends where one side b is fixed, other 3 sides rotating 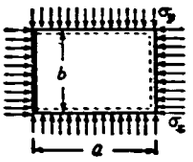	$\sigma_{xk}=\frac{\pi^2}{4}\frac{D}{abt}\cdot\frac{41\frac{b^2}{a^2}+16\frac{a^2}{b^2}+40}{5\frac{b}{a}+4\alpha\frac{a}{b}}$. where $\alpha=\sigma_y/\sigma_x$. Case in which a=b (square) $\sigma_{xk}=24.3\sigma_c\cdot\frac{1}{5+4\alpha}$. When $\alpha=1$ $\sigma_{xk}=2.69\sigma_c$ $=2.6627\sigma_e$.	28 /406 26
15	Ends with 3 sides fixed, one side rotating 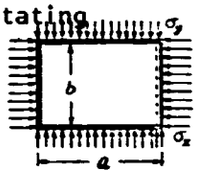	$a=b$ (rectangular) and when $\sigma_x=\sigma_y$ $\sigma_{xk}=4.3144\sigma_e$.	26

Compression due to concentrated load

No.	D and B Conditions	Formulas or Tables of Results	Ref.-Remarks
16	Ends with 4 sides rotating 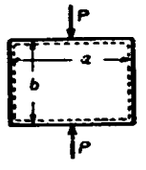	$P_k=\frac{\pi^2 D}{2b}\cdot\frac{1}{\beta^2\sum_{n=1,3,5,\ldots}\frac{1}{(\beta+n^2)^2}}$. where $\beta=a/b$, $D=\frac{Et^3}{12(1-\nu^2)}$. when $\beta>2$ $P_k\fallingdotseq\frac{\pi Et^3}{3(1-\nu^2)b}$.	20 31 D
17	Side a fixed, side b rotating 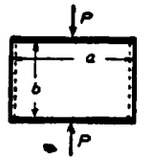	$P_k=\frac{\pi^2 D}{2b}\cdot\frac{1}{(2\beta)^2\sum_{n=1,3,5,\ldots}\frac{1}{\{(2\beta)^2+n^2\}^2}}$. where $\beta=a/b$, $D=\frac{Et^3}{12(1-\nu^2)}$. when $\beta\geqq 2$ $P_k\fallingdotseq\frac{2\pi Et^3}{3(1-\nu^2)b}$.	20

No.	Dia.&Bound.Cond.	Formulas or Tables of Results	Ref.-Remarks
18	Ends with 4 sides rotating 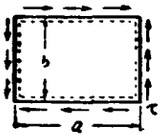	$\tau_k = k\sigma_c$. Table of k	36 41 42 40 39 51a 37

a/b / Ref.	0.2	0.3	0.4	0.5	0.6	0.8
36	145.5	65.7	38.8	26.5	19.1	12.2
41	137.5	63.3	37.4	25.4	18.8	12.3

a/b / Ref.	1.0	1.2	1.4	1.5	1.6	1.8
36	9.4	8.0	7.3	7.1	7.0	6.8
41	9.3	8.1	7.4	7.1	6.9	6.6
42	9.4	8.0	7.3	7.1	7.0	6.8

a/b / Ref.	2.0	2.5	3.0
36	6.6	6.3	6.1
41	6.3	6.0	5.8
42	6.6	6.3	6.1

$$\sigma_c = \frac{E\pi^2}{12(1-\nu^2)} \cdot \left(\frac{t}{b}\right)^2$$

By corrected values

a/b	k	References
1	9.35	40
2	6.48	39
3	6.04	51a
∞	5.35	37

Approximate equation 50a

$a/b \leq 1 \quad k = 4.00 + \frac{5.34}{\beta^2}$,

$a/b > 1 \quad k = 5.34 + \frac{4.00}{\beta^2}$.

where

$\beta = a/b$.

No.	Dia. & Bound. Cond.	Formulas or Tables of Results	Ref.-Rmarks
18	Edge with 4 fixed sides 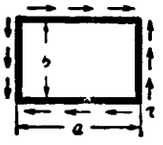	$\tau_k = k\sigma_c$. Table of k	42 43 44 47

Ref. \ a/b	0.4	0.5	0.67	1.0	1.5	2.0	2.5
42	67.81	43.84	25.65	14.53	11.40	10.96	10.85
43, 44	—	—	—	15.45	—	11.55	—
47	—	—	—	14.74	—	10.42	—

Correct values $a/b=\infty$, $k=8.98$. — 37

19	Ends with side a fixed, side b rotating 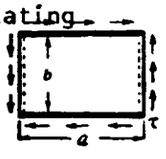	$\tau_k = k\sigma_c$.	42

a/b	0.33	0.4	0.5	0.67	1.0
k	55.53	40.00	26.80	17.50	12.28

a/b	1.5	2.0	2.5	3.0	∞
k	11.12	10.21	9.81	9.61	8.99*1

*1 37

20	End with side a rotating, side b fixed 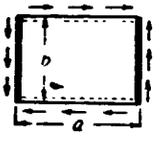	$\tau_k = k\sigma_c$.	42

a/b	0.33	0.4	0.5	0.67	1.0
k	86.49	61.31	40.84	25.02	12.28

a/b	1.5	2.0	2.5	3.0	∞
k	7.78	6.70	6.40	6.17	5.35*1

*1 37

21	One side a free, other 3 sides rotating ends 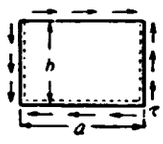	$\tau_k = k\sigma_c$.	48

a/b	0.5	0.8	1.0	1.5
k	59.04	10.12	3.83	2.30

a/b	2.0	3.0	4.0	5.0
k	1.72	1.45	1.45	1.21

where $\nu=0$

/409

No.	Dia.& Bound.Cond.	Formulas or Tables of Results	Ref.-Remarks
22	Strip having initial deflection, end sides rotating	$\tau_k=\alpha\tau_{k0}$. where $\tau_{k0}=5.35\sigma_e$ (critical value when there is no initial deflection)	49

$\frac{2\sqrt{3(1-\nu^2)}}{\rho t\pi^2}b^2$	0	1	2	3	4	5.5	7
$m^2=\left(\frac{\pi}{l}\right)^2$	0.63	0.83	(1.15)	(1.35)	1.6	(1.75)	1.85
α	1.000	1.116	(1.342)	(1.574)	1.785	(2.133)	2.348

The () in the table above indicate second approximation values, the others are third approximation values. It is assumed that the initial deflection forms a circular plane with a radius ρ in the direction of width. l indicates the half wave length in the direction of length

No.	Dia.& Bound.Cond.	Formulas or Tables of Results	Ref.-Remarks
23	Strip having initial deflection, end with sides fixed 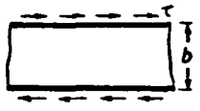	$\tau_k=\alpha\tau_{k0}$, $\tau_{k0}=8.98\sigma_e$.	49

$\frac{2\sqrt{3(1-\nu^2)}}{\rho t\pi^2}b^2$	0	1	2	3	4	5
$m^2=\left(\frac{\pi}{l}\right)^2$	1.48	1.55	1.75	1.95	2.1	2.2
α	1.664	1.714	1.855	2.035	2.245	2.471

No.	Dia.& Bound.Cond.	Formulas or Tables of Results	Ref.-Remarks
24	Test on rectangular plate, 2 sides fixed 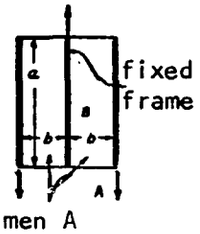 specimen A 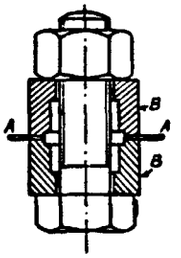	(A) Bollenrath 's experiment i) celluloid plate	52

	E kg/cm²	b cm	t cm	k' average
Test # 1–9	16,000	1.9~1.4	0.05	76,600
" 10–16	22,500	1.9~1.5	0.05	111,400
" 17–26	23,300	1.9~0.8	0.031	119,200
" 27–36	15,800	1.9~1.25	0.051	73,300

$S_k=k'\frac{t^3}{b^2}$ (S_k is buckling load per unit length)

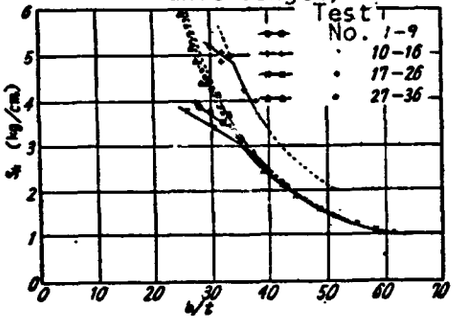

No.	Dia.& Bound.Cond.	Formulas or Tables of Results	Ref.-Remarks

24 Maximum Defl. (cm·10⁻²)

/410

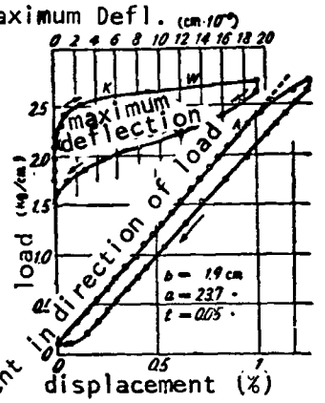

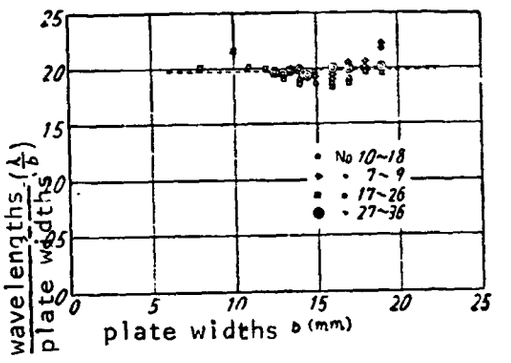

displacement

ii) duraluminum plate

b=3.50~1.00cm, t=0.03cm, 0.05cm.

E=748,000~775,000 kg/cm².

(av. 760,000 kg/cm²)

k=5.44~4.67.

$$S_k = k\frac{\pi^2 E}{12(1-\nu^2)}\frac{t^3}{b^2}.$$

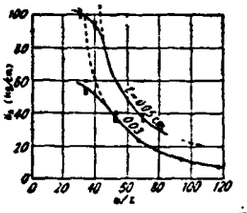

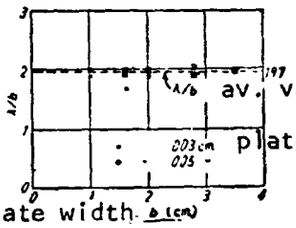

iii) brass plate

b=3.5~0.8cm, t=0.02cm.

E=943,000 kg/cm².

k=5.74~4.76.

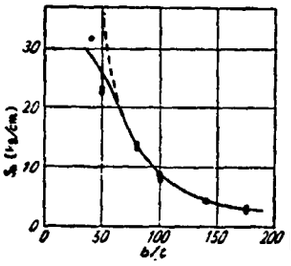

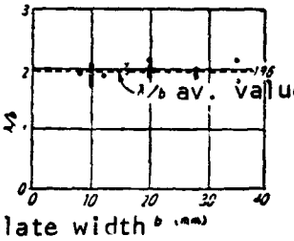

No.	Dia. & Bound.Cond.	Formulas or Tables of Results	Ref.-Remarks
24		(B) (experiments by Gough and Cox $a=20b$, $b=1/2''$, $3/4''$, $1''$, $1^1/_4''$, $1^1/_8''$. $t=0.0126''$.	53

a(in)		10	15	20	25	30
b(in)		1/2	3/4	1	$1^1/_4$	$1^1/_2$
S_k(ton)	cal.	16.0	10.3	8.2	6.5	5.4
	exp.	—	11.4	6.65	6.86	5.29

Experiment values are determined from the line δ with respect to $\frac{\delta}{S}$

25	Shear experiment on rectangular plate, load in direction of diagonal 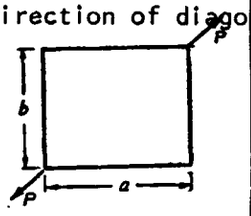	Duraluminum plate experiment $a=15$cm, 30cm, 45cm, $b=15$cm. $t=0.2$mm, 0.428mm. P_{kf} indicates the computed values of the critical buckling load 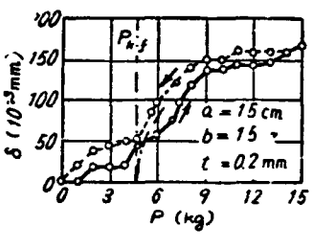 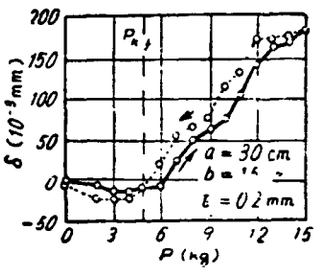 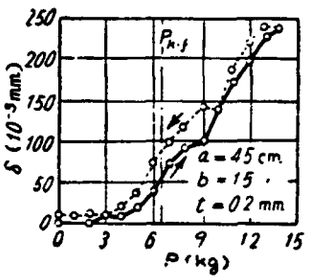 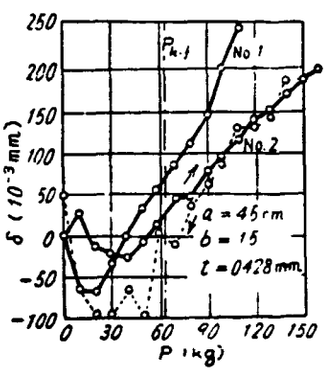	54

/411

No.	Dia. & Bound.Cond.	Formulas or Tables of Results	Ref.-Remarks
26	Ends with 4 sides rotating 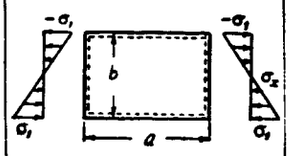	$\sigma_{ik}=k\sigma_c$.	55 56

a/b	0.3	0.4	0.5	0.6	0.67
k	37.4	29.1	25.5	24.1	23.9

a/b	0.8	0.9	1.0	1.2	1.5
k	24.4	25.6	25.5	24.1	24.1

German National Railroad provisional standard 62

$$\frac{a}{b}\leqq\frac{2}{3}\quad k=23.9+\left(\frac{2}{3}-\beta\right)^2+400\left(\frac{2}{3}-\beta\right)^4,$$

$$>\frac{2}{3}\quad =23.9.$$

E. Chwalla's approximation equation

$$\frac{a}{b}\leqq\frac{2}{3}\quad k=15.87+\frac{1.87}{\beta^2}+8.6\beta^2,$$

$$>\frac{2}{3}\quad =23.9.$$

where $\beta=\frac{a}{b}$.

No.	Dia. & Bound.Cond.	Formulas or Tables of Results	Ref.-Remarks
27	End with the side which sustains tension fixed, other 3 sides rotating 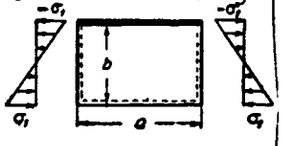	$\sigma_{ik}=k\sigma_c$.	58

a/b	0.4	0.5	0.6	0.67	0.7
k	29.5	26.0	24.6	24.6	24.6

a/b	0.8	0.9	1.0	1.2	1.6	2.1
k	25.2	26.5	26.0	24.6	25.2	24.6

No.	Dia. & Bound.Cond.	Formulas or Tables of Results	Ref.-Remarks
28	End with side a fixed, side b rotating 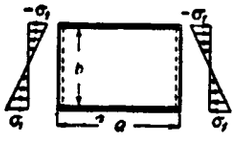	$\sigma_{ik}=k\sigma_c$.	58 60

a/b	0.3	0.35	0.4	0.47	0.5	0.6
k	47.3	43.0	40.7	39.6	39.7	41.8

a/b	0.7	0.8	1.0	1.2	1.5	2.0
k	43.0	40.7	39.7	40.7	39.7	39.7

No.	Dia. & Bound.Cond.	Formulas or Tables of Results	Ref.-Remarks
29	Simple bending experiment Guide a; compressive side free, free and fixed with respect to the rotation of tension sides deflection deformation not allowed Side b supported by double-angle steel	Sample a=200~50mm, b=40~100mm. t=0.5mm, 1.0mm, 1.5mm, 2.0mm. Soft steel buckling load M_k Experiment values somewhat lower than computed values (where a/b=0.6, large due to the effect of side b being fixed) Cal.values of M_k Tension side rotating a/b free fixed 0.6 0.8 1.0 1.5 2.0 3.0 Ultimate load M_{ult} $\frac{M_{ult}}{Et^3}=0.0147\left(\frac{a}{b}\right)^{-0.52}\left(\frac{b}{t}\right)^{0.9}$ Apparent maximum bending stress σ_1 $\sigma_1=\frac{6M_{ult}}{tb^2}=0.0882E\left(\frac{a}{b}\right)^{-0.52}\cdot\left(\frac{b}{t}\right)^{-1.1}$ (kg/mm²) Experiment formula (tension side rotating free)	63 /413

No. 30 — Dia. & Bound.Cond. With 4 sides rotating — Ref.-Remarks: 55, 57

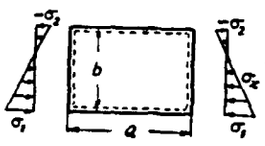

Formulas or Tables of Results

$$\sigma_x = \sigma_1 (1 - \varphi \cdot y/b),$$

$$\sigma_{1k} = k\,\sigma_c.$$

Table of k

φ \ a/b	0.4	0.5	0.6	0.667	0.75	0.8	0.9	1.0	1.5
2	29.1	25.6	24.1	23.9	24.1	24.4	25.6	25.6	24.1
4/3	18.7	—	12.9	—	11.5	11.2	—	11.0	11.5
1	15.1	—	9.7	—	8.4	8.1	—	7.8	8.4
4/5	13.3	—	8.3	—	7.1	6.9	—	6.6	7.1
2/3	10.8	—	7.1	—	6.1	6.0	—	5.8	6.1

where $\varphi = 2$ simple bending
$\varphi = 0$ simple compression
$\sigma_2 = \sigma_1 (1 - \varphi)$.

No. 31 — end with side a fixed, side b rotating ($\varphi = 1$) — Ref.-Remarks: 58

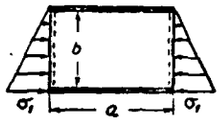

$$\sigma_{1k} = k\,\sigma_c$$

a/b	0.4	0.5	0.6	0.65	0.7
k	17.7	14.7	13.7	13.6	13.7

a/b	0.8	0.9	1.0	1.2	1.4
k	14.3	15.4	14.7	13.7	13.7

No. 32 — end with side a free and rotating, end with side b rotating ($\varphi = 1$) — Ref.-Remarks: 59

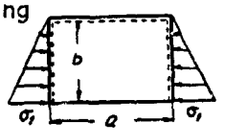

$$\sigma_{1k} = k\,\sigma_c.$$

a/b	0.4	0.5	0.6	0.8	1.0	1.5	2.0	3.0
k	9.86	6.58	4.80	3.02	2.18	1.36	1.08	0.86

No. 33 — end with side a free and rotating, end with side b rotating ($\varphi = 1$) — Ref.-Remarks: 59

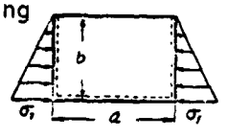

$$\sigma_{1k} = k\,\sigma_c.$$

a/b	0.8	1.0	1.5	2.0	3.0
k	6.72	5.02	3.36	2.80	2.40

Compression and shear

No.	Dia. & Bound. Cond.	Formulas or Tables of Results	Ref.-Remarks
34	Compression and shear in one direction with both sides rotating 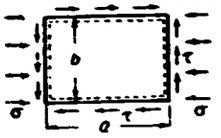	See Figure 4.2.6 (τ_k^* and σ_k^* indicate respectively the critical stresses in the case when they act individually)	65 68
35	Strip, compression and stress in one direction, side a fixed, a/b=∞ 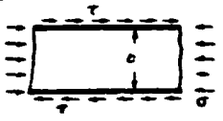	$\tau_k=k\sigma_e$ the negative sign of σ indicates tension stress 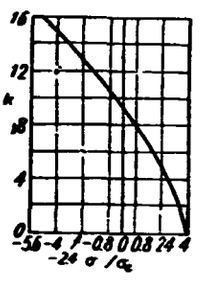	64
36	Compression and shear, end with 4 sides rotating 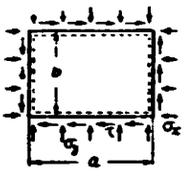	$\tau_k=\sigma_e\sqrt{\left\{2\sqrt{1-\frac{\sigma_y}{\sigma_e}}+2-\frac{\sigma_x}{\sigma_e}\right\}\cdot\left\{2\sqrt{1-\frac{\sigma_y}{\sigma_e}}+6-\frac{\sigma_x}{\sigma_e}\right\}}$. 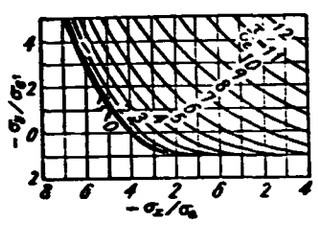	65
37	Compression and shear in 2 directions, 4 sides fixed 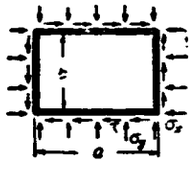	$\tau=\sigma_e\sqrt{\left\{\frac{4}{\sqrt{3}}\sqrt{4-\frac{\sigma_y}{\sigma_e}}+\frac{8}{3}-\frac{\sigma_x}{\sigma_e}\right\}\cdot\left\{\frac{4}{\sqrt{3}}\sqrt{4-\frac{\sigma_y}{\sigma_e}}+8-\frac{\sigma_x}{\sigma_e}\right\}}$. Assuming $\tau_k=k'\sigma_e$, $\sigma_k=k\sigma_e$ when a/b=1.0, $\sigma_x=\sigma_y=\sigma$ 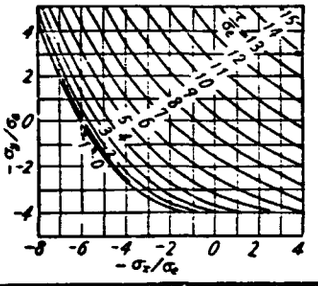	65

σ/τ	0	0.5	1.0	1.5	2.0	2.5	3.0	∞
k'	14.58	7.09	4.50	3.24	2.51	2.04	1 72	0
	0	3.55	4.50	4.86	5.02	5.10	5.16	5.30

69

/416

No.	Dia. & Bound. Cond.	Formulas or Tables of Results	Ref.-Remarks
38	End with 4 sides rotating 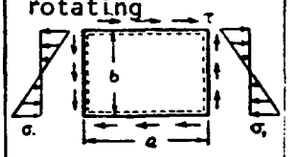	See Fig. 4.2.7 (σ_{1k}, τ_k indicate respectively the limit stresses $\tau_k=k'\sigma_1$, $\sigma_{1k}=k\sigma_1$ when they act individually)	66 69

$a/b=1.0$

k'	0	2	4	6	8	9	9.42
k	25.64	24.58	22.18	18.43	12.37	6.85	0

70

$a/b=4/5$

k'	0	4	8	10	11	12	12.26
k	24.5	22.84	17.72	13.25	10.01	4.61	0

$a/b=2/3$

k'	0	4	8	12	14	15	16.09
k	23.90	23.05	20.35	15.23	11.04	8.00	0

$a/b=1/2$

k'	0	4	8	12	16	20	24	26	26.9
k	25.64	25.40	24.30	22.55	19.94	16.13	10.26	5.44	0

Miscellaneous

No.	Dia. & Bound. Cond.	Formulas or Tables of Results	Ref.-Remarks
39	Torsion and tension of strip, edge side free 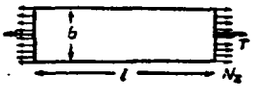	Critical torsion moment T_k $$T_k=G\frac{d\theta}{dx}bt^3\left(\frac{1}{3}-0.210\frac{t}{b}\right)+\frac{1}{360}Eb^3t\left(\frac{d\theta}{dx}\right)^3.$$ For a given N_x, μ is selected. and in graph below, $\frac{d\theta}{dx}\frac{b^3}{2\pi^2t}$ is found from $\frac{d\theta}{dx}$ are minimum values where 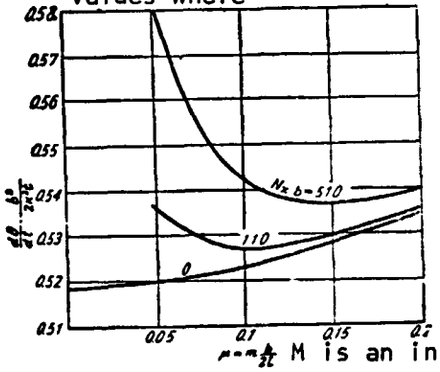 $\mu=m\frac{t}{b}$ M is an integer $$T_k=\frac{4Gt^3}{b}\left\{1+\frac{\pi^2}{24(1-\nu)}\left(\frac{b}{l}\right)^2\right\}.$$	72 73

No.	Dia. & Bound. Cond.	Formulas or Tables of Results	Ref.-Remarks
40	Torsion buckling test of strip, edge side free 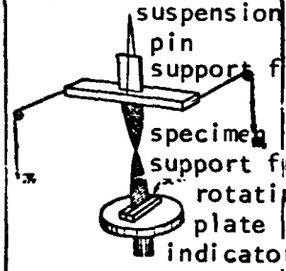 	Specimen Notation | b mm | t mm | l mm A +.O | 50 | 0.48 | 390,209 B △ | 12.3 | 0.3 | 251 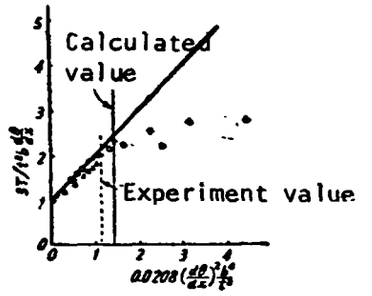 	72
41	Compression above proportional limit, end with 4 sides rotating	i) case in which one assumes a modulus of elasticity E_r only in the direction of compression $\sigma_k=\sigma_e\left(\frac{mb}{a}\sqrt{\alpha}+\frac{a}{mb}\right)^2$. $\alpha=E_r/E$. E_r = modulus of elasticity which has been reduced with respect to the stress above proportional limit when $a/b=\sqrt[4]{\alpha}$ σ_k becomes minimum value σ_{kmin} $\sigma_{kmin}=4\sigma_e\sqrt{\alpha}$. ii) Assuming an elasticity modulus E_r in both directions $\sigma_k=\sigma_e\alpha\left(\frac{mb}{a}+\frac{a}{mb}\right)^2$.	76 77
42	Compression in the case of only initial direction. End with with 4 sides rotating 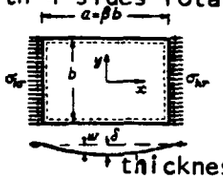 	Initial deflection $w_0=\delta\cos\frac{\pi x}{a}\cdot\cos\frac{\pi y}{b}$. i) From the condition that the principal stress is constant $\left(\frac{b}{t}\right)^2+\frac{\pi^2E(1+\nu\beta^2)}{2(\sigma_f-\sigma_{kr})(1-\beta^2)}\left(\frac{b}{t}\right)\left(\frac{\delta}{b}\right)-\frac{\pi^2E(1+\beta^2)^2}{12\sigma_{kr}(1-\nu^2)\beta^2}=0$. ii) From the condition that the principal strain is constant $\left(\frac{b}{t}\right)^2+\frac{\pi^2E}{2(\sigma_f-\sigma_{kr})}\left(\frac{b}{t}\right)\left(\frac{\delta}{b}\right)-\frac{\pi^2E(1+\beta^2)^2}{12\sigma_{kr}(1-\nu^2)\beta^2}=0$.	79

No.	Dia. & Bound.Cond.	Formulas or Tables of Results	Ref.-Remarks
42		iii) From the condition that the strain energy is constant $\left(\frac{\sigma_f^2}{\sigma_{kr}^2}-1\right)\left(1-\frac{\sigma_{kr}}{\sigma_k}\right)^2=k_1^2-k_1k_2+k_2^2+\left(1-\frac{\sigma_{kr}}{\sigma_k}\right)(2k_1+k_2).$ where $k_1=\frac{6(1+\nu\beta^2)}{(1+\beta^2)^2}\left(\frac{b}{t}\right)\left(\frac{\delta}{b}\right),$ $k_2=\frac{6(\nu+\beta^2)}{(1+\beta^2)^2}\left(\frac{b}{t}\right)\left(\frac{\delta}{b}\right),$ σ_f='yield-point stress, $\sigma_k=\sigma_e\left(\frac{m}{\beta}+\frac{\beta}{m}\right)^2$(critical stress when $\delta=0$) m='half-wave number σ_{kr}=' limit critical stress when the half-wave number is 1 From the condition that the principal strain is const. $E=2.1\times10^6$ kg/cm², $\nu=0.3$, $\sigma_f=2400$ kg/cm² Calculating for The critical value σ_{kr} is as shown in the graph below 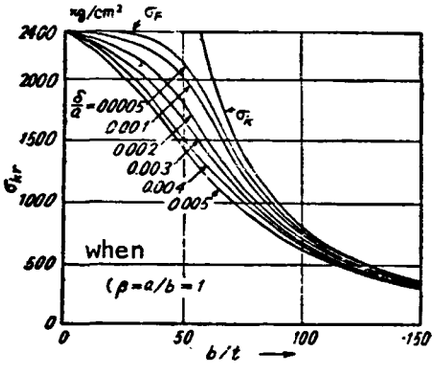 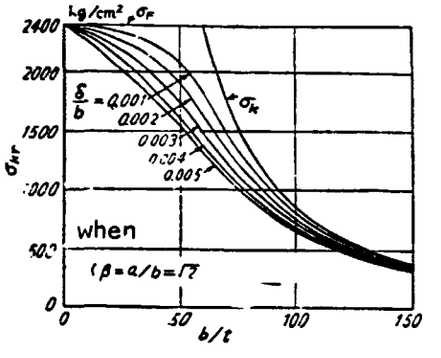 	/418

No.	Dia. & Bound. Cond.	Formulas or Tables of Results	Ref.-Remarks
42		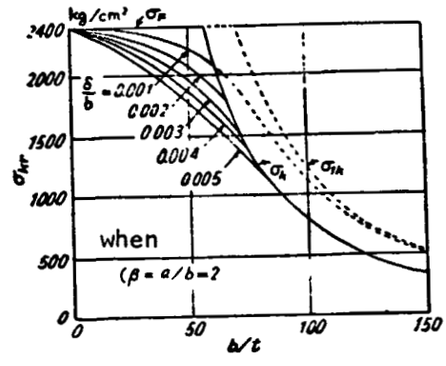	
43	Dynamic compressive stress, end with 4 sides rotating 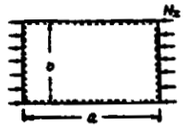	$N_x = N\cos\omega_0 t$. where the solution is for the case of a rectangular wave i.e. $0<t<\frac{\pi}{\omega_0}$, $N_x=N$. $\frac{\pi}{\omega_0}<t<\frac{2\pi}{\omega_0}$, $N_x=-N$. even where $N/P_k<1$, there are cases in which instability occurs (white region in graph) where $P_k=\pi^2 D\frac{1}{b^2}\left[\frac{bm}{cn}+\frac{cn}{bm}\right]^2$, $p_0=\frac{D}{\rho}\left[\left(\frac{m\pi}{a}\right)^2+\left(\frac{n\pi}{b}\right)^2\right]^2$, $\beta=\frac{1}{\rho}\frac{Et}{64}\left[\left(\frac{m\pi}{a}\right)^2+\left(\frac{n\pi}{b}\right)^2\right]$, $\psi^2=\frac{3}{4}\cdot\frac{\varphi_0^2}{p_0^2}$ $\phi_{(1)}$ is maximum amplitude 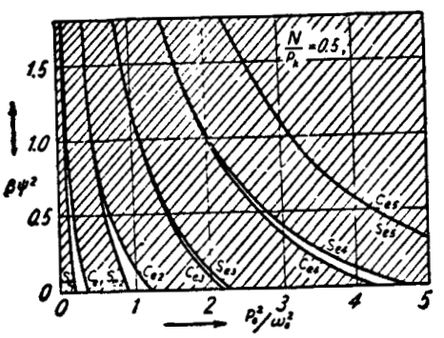	81

No.	Dia. & Bound. Cond.	Formulas or Tables of Results	Ref.-Remarks
43		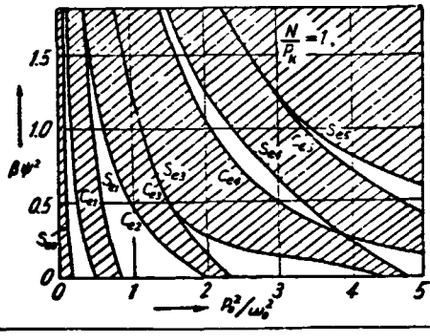	
44 pressure circular hole	Infinite plate sustaining internal pressure on 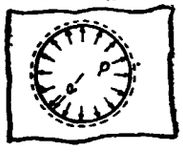	$p_k=\frac{D}{a^2t}\left[4m^2-(1+\nu)^2+2\sqrt{(m^2-1)\left\{4m^2-(1+\nu)^2\right\}}\right]$ where $m=$ anteger.number of segmented diameters (free at infinite distance)	82

Plate of Variable Thickness
Compression

No.	Dia. & Bound. Cond.	Formulas or Tables of Results	Ref.-Remarks
45	Compression of rectangular plates of variable thickness, and with sides rotating 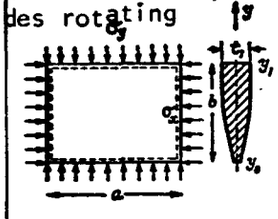	Buckling condition equation $J_p\left(\frac{\pi}{a}y_0\right)J_{-p}\left(\frac{\pi}{a}y_1\right)-J_p\left(\frac{\pi}{a}y_1\right)J_{-p}\left(\frac{\pi}{a}y_0\right)=0.$ where $p=\sqrt{\frac{1}{4}-\frac{\sigma_y t_1^2}{c}}$, $D=cy^2=\frac{Et_1^3}{12(1-\nu^2)y_1^3}y^3$, $2(1-\nu)c=(\sigma_x-\sigma_y)t.$ σ_k is found for the given y_0/y_1 from the graph on the right below in the case when i) $\frac{\sigma_y t_1}{c}=\frac{1}{4}$, p = 0, for $1\geq b/a\geq 0.7655$, and when ii) $\sigma_y=0$, $p=\frac{1}{2}$, for $1.220\geq b/a\geq 1.0$. when 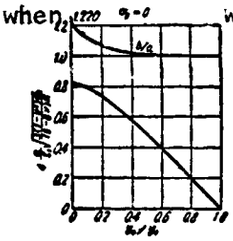 when 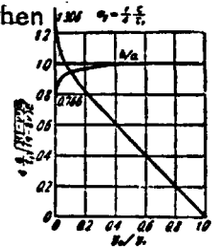	74

No.	Dia. & Bound. Cond.	Formulas or Tables of Results	Ref.-Remarks
46	One end with 4 sides rotating 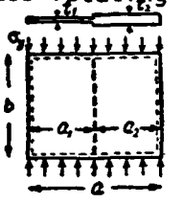	where $a=b,\ a_1=a_2=\frac{1}{2}a,\ t_2=1.5t_1$ $\sigma_{yk}=5.988\frac{\pi^2 D_1}{b^2 t_1}$, *1 $=2.661\frac{\pi^2 D_2}{b^2 t_2}$. *2	75
47	End with 4 sides rotating 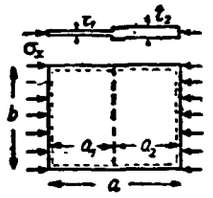	where $a=b,\ a_1=a_2=\frac{1}{2}a,\ t_2=1.5t_1$ $\sigma_{xk}=1.5114\frac{\pi^2 D_1}{a_1^2 t_1}$, $=0.4478\frac{\pi^2 D_2}{a_1^2 t_2}$.	75
48	Side b fixed, other 3 sides rotating 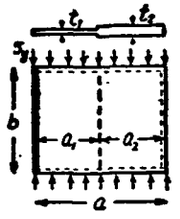	where $a=b,\ a_1=a_2=\frac{1}{2}a,\ t_2=1.5t_1$ $\sigma_{yk}=8.5118\frac{\pi^2 D_1}{b^2 t_1}$, $=3.7830\frac{\pi^2 D_2}{b^2 t_2}$.	75
49	Side b fixed, other 3 sides rotating 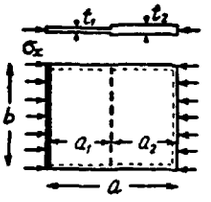	where $a=b,\ a_1=a_2=\frac{1}{2}a,\ t_2=1.5t_1$ $\sigma_{xk}=2.2547\frac{\pi^2 D_1}{a^2 t_1}$, $=0.6681\frac{\pi^2 D_2}{a_1^2 t_2}$.	75

*1 $D_1=\frac{E t_1^3}{12(1-\nu^2)}$

*2 $D_2=\frac{E t_2^3}{12(1-\nu^2)}$

No.	Dia.&Bound. Cond.	Formulas or Tables of Results	Ref.-Remarks
50	End with side b fixed, side a rotating 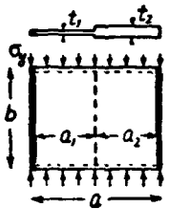	when $a=b,\ a_1=a_2=\frac{1}{2}a,\ t_2=1.5t_1$ $\sigma_{yk}=12.6805\frac{\pi^2 D_1}{b^2 t_1}$, $=5.6358\frac{\pi^2 D_2}{b^2 t_2}$.	75 /422
51	End with side b fixed, side a rotating 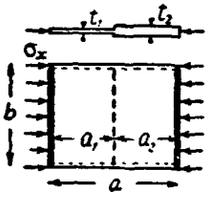	when $a=b,\ a_1=a_2=\frac{1}{2}a,\ t_2=1.5t_1$ $\sigma_{xk}=2.5819\frac{\pi^2 D_1}{a_1^2 t_1}$, $=0.7650\frac{\pi^2 D_2}{a_2^2 t_2}$.	75
52	One side of b free, other 3 sides rotating 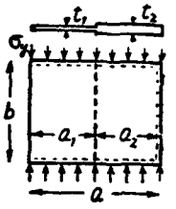	when $a=b,\ a_1=a_2=\frac{1}{2}a,\ t_2=1.5t_1$ $\sigma_{yk}=1.9811\frac{\pi^2 D_1}{b^2 t_1}$, $=0.8805\frac{\pi^2 D_2}{b^2 t_2}$.	75
53	One side of b free, other 3 sides fixed, sides a rotating 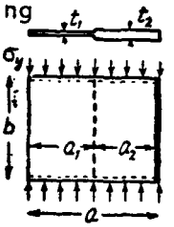	when $a=b,\ a_1=a_2=\frac{1}{2}a,\ t_2=1.5t_1$ $\sigma_{yk}=2.3485\frac{\pi^2 D_1}{b^2 t_1}$, $=1.0438\frac{\pi^2 D_2}{b^2 t_2}$.	75

/423

No.	Dia. & Bound. Cond.	Formulas or Tables of Results	Ref.-Remarks
54	End with side a rotating , sides b free 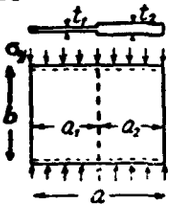	when $a=b,\ a_1=a_2=\frac{1}{2}a,\ t_2=1.5t_1$ $\sigma_{y1}=1.5045\frac{\pi^2 D_1}{b^2 t_1}$, $=0.6687\frac{\pi^2 D_2}{b^2 t_2}$.	75
55	End with 4 sides rotating, variable thickness part supported 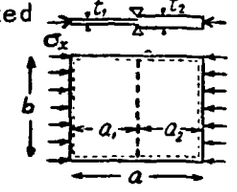	when $a=b,\ a_1=a_2=\frac{1}{2}a,\ t_2=1.5t_1$ $\sigma_x=2.2716\frac{\pi^2\mu_1}{a_1^2 t_1}$, $=0.6731\frac{\pi^2 D_2}{a_2^2 t_2}$.	75
56	End with side a rotating, side b free, variable thickness part supported 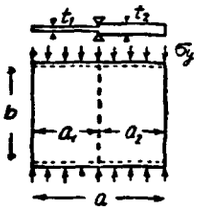	when $a=b,\ a_1=a_2=\frac{1}{2}a,\ t_2=1.5t_1$ $\sigma_y=3.9280\frac{\pi^2 D_1}{b^2 t_1}$, $=1.7458\frac{\pi^2 D_2}{b^2 t_2}$.	75

Circular Plates

Uniform external pressure

No.	Dia. & Bound. Cons	Formulas or Tables of Results	Ref-Remarks
57	Circular plate with uniform external pressure, end with circumference rotating 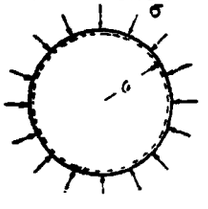	Case in which there are neither segmented circles nor segmented diameter where $\alpha^2=3.426\pi^2$, α is the lowest order route of $\alpha J_0(\alpha)-(1-\nu)J_1(\alpha)=0$	84 85 90

* $\sigma_c'=\frac{E\pi^2}{12(1-\nu^2)}\left(\frac{t}{a}\right)^2$

/424

No.	Dia. & Bound. Cond.	Formulas or Tables of Results	Ref.=Remarks
58	Circular plate with uniform external pressure, end with circumference rotating	i) case in which there is no segmented circle (pitch circle?) or segmented diameter $\sigma_k = 1.49\,\sigma_d'$. where $\alpha^2 = 1.49\pi^2$, α is the lowest order route of $J_1(\alpha)=0$ for; ii) case in which there is a pitch circle and segmented diameter $\sigma_k = \eta \times 1.49\,\sigma_d'$. 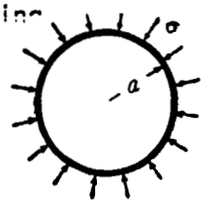 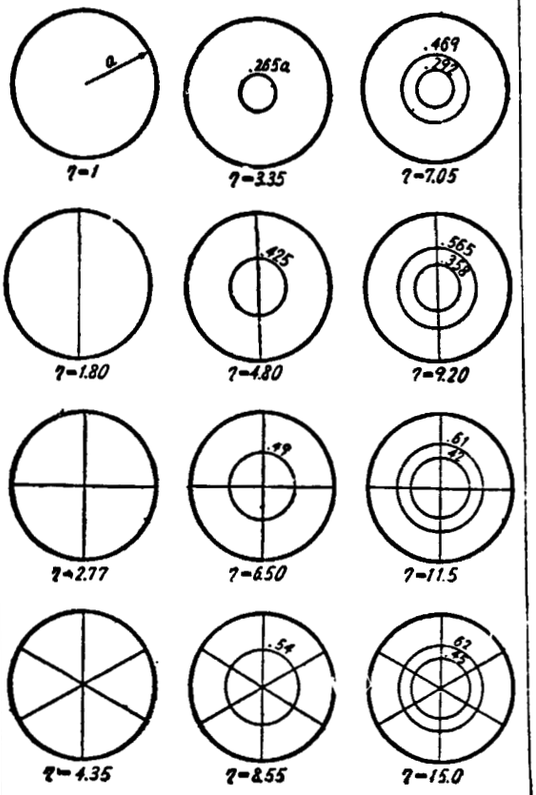	83 84 85 90 86
59	Perforated circular plate, uniform external pressure end with outside edge rotating, inside edge free 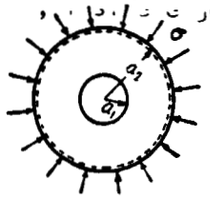	$\sigma_k = k\,\sigma_d'$	87

a_1/a_2	0	0.1	0.2	0.3	0..
k	0.426	0.402	0.365	0.328	0.280
a_1/a_2	0.5	0.6	0.7	0.8	0.9
k	0.256	0.231	0.219	0.207	0.195

No.	Dia. & Bound. Cond.	Formulas or Tables of Results	Ref.-Remarks
59		$\sigma_k=\alpha\frac{E}{1-\nu^2}\left(\frac{t}{a_2}\right)^2$. $\alpha=\frac{s^2-1}{12}\left\{\left(\frac{a_2}{a_1}\right)^2-1\right\}$. s is found from the following equation corresponding to the values of a_2/a_1 $\frac{(ms+1)J_{s-1}(\sqrt{s^2-1})-(ms-1)J_{s+1}(\sqrt{s^2-1})}{(ms+1)Y_{s-1}(\sqrt{s^2-1})-(ms-1)Y_{s+1}(\sqrt{s^2-1})}$ $=\frac{(ms+1)J_{s-1}(\sqrt{s^2-1}\cdot a_2/a_1)-(ms-1)J_{s+1}(\sqrt{s^2-1}\cdot a_2/a_1)}{(ms+1)Y_{s-1}(\sqrt{s^2-1}\cdot a_2/a_1)-(ms-1)Y_{s+1}(\sqrt{s^2-1}\cdot a_2/a_1)}$ where m=Poisson's ratio, case of symmetrical buckling	88
60	Perforated circular plate, uniform external pressure 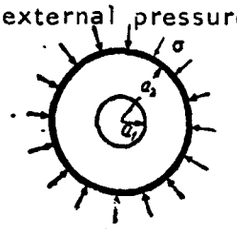 end with outside fixed, inside free	$\sigma_k=k\sigma_c'$ a_1/a_2: 0 | 0.1 | 0.2 | 0.3 | 0.4 | 0.5 k: 1.48 | 1.42 | 1.35 | 1.47 | 1.80 | 2.52 $\sigma_k=\alpha\frac{E}{1-\nu^2}\left(\frac{t}{a_2}\right)^2$, $\alpha=\frac{s^2-1}{12}\left\{\left(\frac{a_2}{a_1}\right)^2-1\right\}$ s is found from the following equation corresponding to the values a_2/a_1 $\frac{(ms+1)J_{s-1}(\sqrt{s^2-1})-(ms-1)J_{s+1}(\sqrt{s^2-1})}{(ms+1)Y_{s-1}(\sqrt{s^2-1})-(ms-1)Y_{s+1}(\sqrt{s^2-1})}$ $=\frac{J_s(\sqrt{s^2-1}\cdot a_2/a_1)}{Y_s(\sqrt{s^2-1}\cdot a_2/a_1)}$. Case in which m=Poisson's ratio, and symmetrical buckling is present 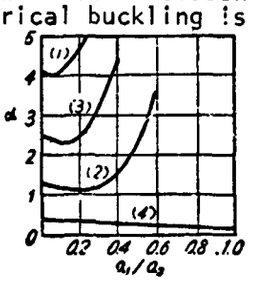 (1) outside edge fixed, 2nd order (2) " , lowest order (3) outside edge rotating, 2nd order (4) " , lowest order $\sigma_k=1.482\sigma_c$ (where $a_1/a_2=0.281$).	87 88 89

No.	Dia. & Bound. Cond.	Formulas or Tables of Results	Ref.-Remarks
61	Circular plate with hole, uniform external pressure, outside edge free, inside edge fixed 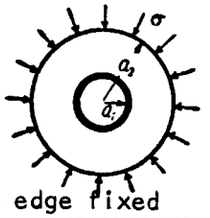	$\sigma_k=0.778\,\sigma_c'$. where $a_2/a_1=2.671$	89
62	Circular plate with hole, uniform external pressure, inside-outside edges both rotating, 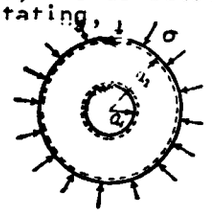	$\sigma_k=0.362\,\sigma_c'$. where $a_2/a_1=1.690$	89
63	Circular plate with hole, uniform external and internal pressure, outside edge rotating, inside edge free 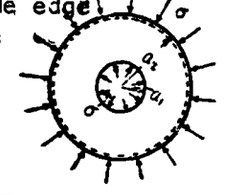	$\sigma_k=\alpha\frac{E}{1-\nu^2}\left(\frac{t}{a_2}\right)^2$. α given by following graph, s gives the number of segmented diameters 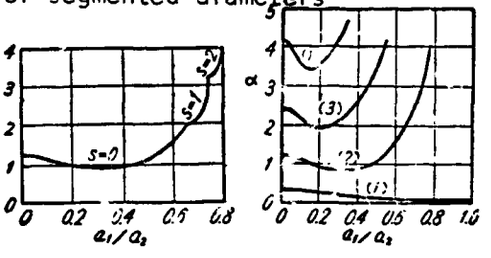 (1) outside edge fixed, 2nd order (2) " , lowest order (3) outside edge rotating, 2nd order (4) " , lowest order	88
64	as above, outside edge fixed, inside edge free 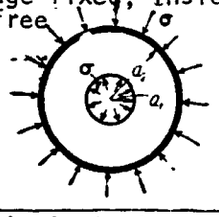		
65	eliptical plate, uniform external pressure, outside edge fixed, 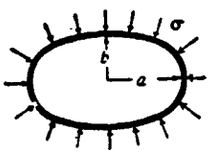	$\sigma_k=k\,\sigma_c$, where $\sigma_c=\frac{E\pi^2}{12(1-\nu^2)}\left(\frac{t}{b}\right)^2$.	93

a/b	1.0	1.1	1.2	1.3	1.4
k	1.30	1.38	1.29	1.24	1.20

a/b	1.5	2.0	3.0	4.0	5.0
k	1.17	1.12	1.12	1.13	1.14

Polygonal Plates

Compression

/427

No.	Dia. & Bound. Cond.	Formulas or Tables of Results	Ref.-Remarks
66	Equilateral triangular plate, uniform external pressure, end with edges rotating 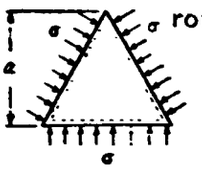	$\sigma_k=4.00\,\sigma_c'$. where $\sigma_c'=\frac{E\pi^2}{12(1-\nu^2)}\left(\frac{t}{a}\right)^2$.	94
67	Isosceles right triangular plate, uniform external pressure, end with edges rotating 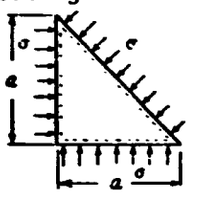	$\sigma_k=5.00\,\sigma_c'$. where $\sigma_c'=\frac{E\pi^2}{12(1-\nu^2)}\left(\frac{t}{a}\right)^2$.	95
68	Isosceles right traingal, compression in one direction, end with edges rotating 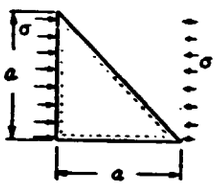	$\sigma_k=9.11\,\sigma_c'$. where $\sigma_c'=\frac{E\pi^2}{12(1-\nu^2)}\left(\frac{t}{a}\right)^2$.	96
69	Parallelogram plate, compression in two directions, 4 sides fixed 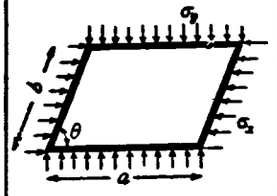	$\sigma_{mk}=\frac{4\left[m^4+(n/\beta)^4+\frac{2}{3}(mn/\beta)^2(1+\cos^2\theta)\right]}{\sin^2\theta\left[(\sin^2\theta+\lambda\cos^2\theta)m^2+\lambda(n/\beta)^2\right]}\sigma_c'$, or $\sigma_{mk}=\frac{42\left[1+1/\beta^4+\frac{4}{7}(1+2\cos^2\theta)/\beta^2\right]}{\sin^2\theta\left[\sin\theta+\lambda\cos^2\theta+\lambda\beta^2\right]}\sigma_c'$. where $\lambda=\sigma_x/\sigma_y$, $\beta=b/a$, m, n half-wave numbers in direction x,y $\sigma_c'=\frac{E\pi^2}{12(1-\nu^2)}\left(\frac{t}{a}\right)^2$.	97

No.	Dia. & Bound. Cond.	Formulas or Tables of Results	Ref.-Remarks
70	Regular polygonal plate with curved edge, external pressure, with sides fixed 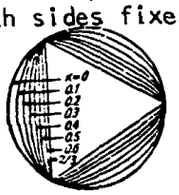 (1) 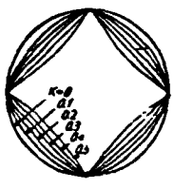 (2) (3)	uniform end $\sigma_k=\zeta\frac{D}{ta^2}$, where a = radius of base circle values of ζ	99

K	0.1	0.2	0.3	0.4	0.5	0.6	2/3
(1)	16.41	18.96	22.35	26.97	33.37	42.49	51.14
(2)	16.53	19.02	22.39	26.50	32.10	—	—
(3)	16.54	19.04	21.89	19.733 (K=0.1758)			

/428

Shear

No.	Dia. & Bound. Cond.	Formulas or Tables of Results	Ref.-Remarks
71	Regular hexagonal plate, shear load, end with edges rotating (1) 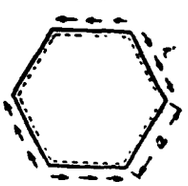 (2)	$\tau_k=k\frac{E\pi^2}{12(1-\nu^2)}\left(\frac{t}{a}\right)^2$. For (1) k=88.5, " (2) k=16.1.	98

Orthotropic plates

Compression

/429

No.	Dia. & Bound. Cond.	Formulas or Tables of Results	Ref.-Remarks
72	End with 4 sides rotating (case in which the principal axis of elasticity matches the direction of compression	$\sigma_k=\left\{D_x\left(\frac{mb}{a}\right)^2+2D_{xy}+D_y\left(\frac{a}{mb}\right)^2\right\}\frac{\pi^2}{b^2t}$. the minimum values of σ_k $\sigma_{k\min}=\left\{\sqrt{D_xD_y}+D_{xy}\right\}\frac{2\pi^2}{b^2t}$. the half-wave length in this case is $\lambda=\frac{a}{m}=b\sqrt[4]{D_x/D_y}$. 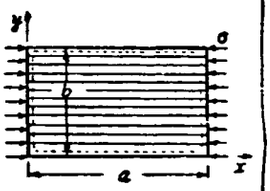	100 D_x, D_y = bending stiffness of of plate in sections x, y $4(GJ)_{xy}$ = torsion stiffness in direction x,y $2D_{xy}=4(GJ)_{xy}+\nu_yD_x+\nu_xD_y$
73	End with sides rotating, end with side b fixed (case in which singular principal axis matches direction of compression)	Case in which D_y is desregarded when $D_x >> D_y$ minimum values of σ_k $\sigma_k=\left\{2D_x\frac{b^2}{a^2}+D_{xy}\right\}\frac{2\pi^2}{b^2t}$. case where D_y is small $\sigma_k=\left\{4D_x\frac{b^2}{a^2}+2D_{xy}+\frac{3}{4}D_y\frac{a^2}{b^2}\right\}\frac{\pi^2}{b^2t}$. 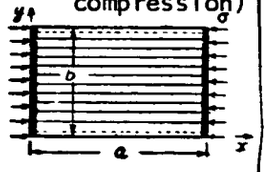	100
74	Compression in 2 directions end with 4 sides rotating (compression in direction of elastic principal axis) 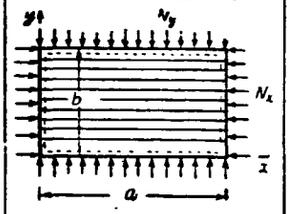	$N_{xk}\left(\frac{m\pi}{a}\right)^2+N_{yk}\left(\frac{n\pi}{b}\right)^2$ $=D\left(\frac{m\pi}{a}\right)^4+2D_{xy}\left(\frac{mn\pi^2}{ab}\right)^2+D_y\left(\frac{n\pi}{b}\right)^4$. Where m, n = number of half-wave in direction of x, y N_x, N_y = compression component per unit within direction x, y	100

No.	Dia. & Bound. Cond.	Formulas or Tables of Results	Ref.-Remarks
75	Uniform shear, end with 4 sides rotating	$\tau_z = C_\alpha (D\, D_y^3)^{1/4} / (b/2)^2$.	104 105
	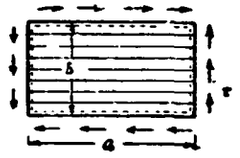	where C_α is given by the graph below by θ, α	
		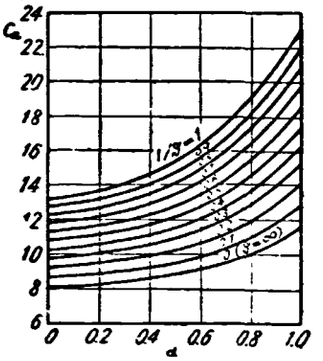	
		$\vartheta = (D_x D_y)^{1/2} / D_{xy}$	
		$\alpha = (b/a) / (D_x/D_y)^{1/4}$	
76	Orthotropic strip, uniform shear, end with sides rotating	Case in which i) $1 < \vartheta$ $(\vartheta = (D_x D_y)^{1/2} / D_{xy})$	102
	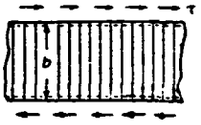	$\tau_z = C_\alpha (D_x D_y^3)^{1/4} / (b/2)^2$, half wavelength $l = C_\alpha' \sqrt[4]{D_x/D_y} \cdot (b/2)$,	

ϑ	1	2	3	5	10	20	40	∞
C_α	13.17	10.8	9.95	9.25	8.7	8.4	8.25	8.125
C_α'	2.49	2.28	2.16	2.13	2.08	2.05	2.05	2.05

or $C_\alpha = 8.125 + 5.64 \frac{1}{\vartheta} - 0.6 \frac{1}{\vartheta^2}$.

Case in which ii) $0 < \vartheta < 1$

$\tau_z = C_b (D_y \cdot D_{xy})^{1/2} / (b/2)^2$, half wavelength $l = C_b' \sqrt{D_{xy}/D_y} \cdot (b/2)$,

ϑ	0	0.2	0.5	1.0
C_b	11.71	11.8	12.2	13.17
C_b'	1.92	1.94	2.07	2.49

or $C_b = 11.71 + 2.155\,\vartheta^2 - 0.7\,\vartheta^4$.

Moreover, See materials (77) for C_a, C_b

No.	Dia. & Bound. Cond.	Formulas or Tables of Results	Ref.-Remarks
77	Orthotropic stric, uniform shear, end with edges fixed 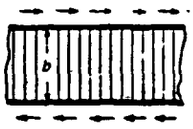	Case in which i) $1<\vartheta$ (ϑ same as in (75)) $\tau_k=C_a(D_xD_y^3)^{1/4}/(b/2)^2$, half wavelength $l=C_a'\sqrt{D_x/D_y}\cdot(b/2)$.	102
		ϑ | 1 | 2 | 3 | 5 | 10 | 20 | 40 | ∞	
		C_a | 22.15 | 18.75 | 17.55 | 16.5 | 15.85 | 15.45 | 15.25 | 15.065	
		C_a' | 1.66 | 1.54 | 1.48 | 1.44 | 1.41 | 1.39 | 1.38 | 1.36	
		Case in which ii) $0<\vartheta<1$ $\tau_k=C_b(D_y\cdot D_{xy})^{1/2}/(b/2)^2$, half wavelength $l=C_b'\sqrt{D_{xy}/D_y}\cdot(b/2)$.	
		ϑ | 0 | 0.2 | 0.5 | 1.0	
		C_b | 18.59 | 18.85 | 19.9 | 22.15	
		C_b' | 1.16 | 1.20 | 1.36 | 1.66	
		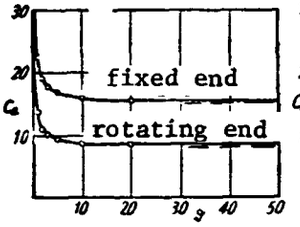 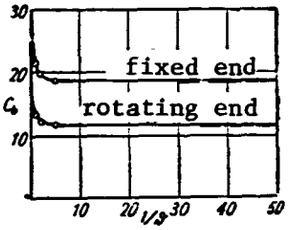	
78	Compression and shear load, end with 4 sides rotating, case where the principal axis of elasticity σ_y is 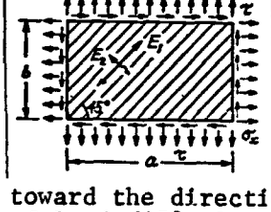 toward the direction of load (45° plate) E_1, E_2, G = Young's modulus and shear elasticity modulus in direction (1, 2,) of principal axis of elasticitv	Numerical examples Buckling of 45° tension orthotropic strip. $E_1=1200$ kg/mm², $E_2=60$ kg/mm², $G=125$ kg/mm², $\nu_1=0.150$, $\nu_2=\nu_1/2$, a = half wavelength in direction x, h = plate with $\mu=\pi/b$.	107
		angle θ	
		load | boundary conditions | a/b | in direction of wave | buckling load | other stresses at time of buckling	
	Compressive buckling	1) compr. $\sigma_{Mx}=-p_1$ ($\sigma_y=\tau=0$) | 1.034 | 69°28′ | $\sigma_{xk}=-0.248\cdot E_1\mu^2t^2$ | $\sigma_y=\tau=0$	
		2) compr. σ_y only $\sigma_y=-p_2$ ($\sigma_x=\tau=0$) | ∞ | 0° | $\sigma_{xk}=-0.0435\cdot E_1\mu^2t^2$ | $\sigma_x=\tau=0$	

No.	Dia. & Bound. Cond.	Formulas or Tables of Results	Ref.-Remarks

78

Shearing and buckling

Load boundary conditions		direction of wave	a/b	angle θ	Buckling load	Other stresses at time of buckling
3) Pure shear τ ($\sigma_x=\sigma_y=0$)	Positive shear $\tau>0$		1.296	49°51′	$\tau_k=0.232 \cdot E_1\mu^2t^2$	$\sigma_x=\sigma_y=0$
	reverse shear $\tau<0$		1.545	−49°41′	$\tau_k=-0.394 \cdot E_1\mu^2t^2$	$\sigma_x=\sigma_y=0$
4) Shear load τ with stiff edge $\varepsilon_L=\varepsilon_Q=0$	Positive shear $\tau>0$		0.870	47°20′	$\tau_k=0.563 \cdot E_1\mu^2t^2$	$\sigma_x=\sigma_y=-0.208 \cdot E_1\mu^2t^2$
	reverse shear $\tau<0$		∞	0°	$\tau_k=-0.117 \cdot E_1\mu^2t^2$	$\sigma_x=\sigma_y=0.0435 \cdot E_1\mu^2t^2$

/432

79 Corrugated square plate, shear test. elastic support by rivets around edges Shearing force is applied to plate by load in

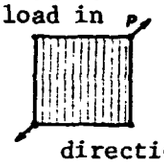

direction of the diagonal

Dimensions of test sample 90×90 cm, plate thickness 0.39 mm, wave-length 30.0 mm, wave height 9.15 mm in corrugated plate

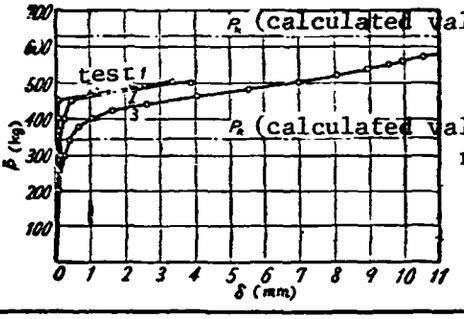

104

Condition After the Buckling of Rectangular Plates

Effective Width and Other Phenomenon due to Compression

No.	Dia. & Bound. Cond.	Formulas or Tables of Results	Ref.-Remarks

80 Ends with sides rotating, properties after buckling

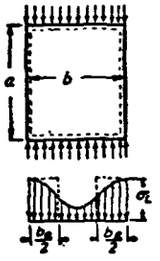

Effective width b_e after buckling

$$b_e=\frac{2\pi}{\sqrt{12(1-\nu^2)}}\sqrt{\frac{E}{\sigma_L}}\cdot t$$ 109

$$b_e=\frac{1.52}{\sqrt{e}}t+0.09b$$ 110

where e is compressive strain of plate edge

$$b_e=\left(e_k/e+\frac{1}{2}\varphi(\zeta)(1-e_k/e)\right)b$$ 112

as an approximation equation

$$b_e=b\sqrt[3]{e_k/e}\quad(e<20e_k)$$

$$b_e=\left(0.81\sqrt{\sigma_k/\sigma_L}+0.19\right)b$$

No.	Dia. & Bound. Cond.	Formulas or Tables of Results	Ref.-Remarks
80		Where e_k is compressive strain with respect to σ_k	
		$\varphi(\zeta)=\frac{4-6\zeta+18.6\zeta^2}{4-3\zeta+31.8\zeta^2}$	
		ζ is parameter indicating deformation when e/e_k is 25, about 0.06	
		$\sqrt{\frac{b_e}{b}}=0.571+0.429\sqrt{\frac{\sigma_k}{\sigma_L}}$	114
		$\fallingdotseq\frac{1}{2}\left(1+\sqrt{\sigma_k/\sigma_L}\right)$	
		where $\sigma_k=4\sigma_c$ (square) in any of the above cases, σ_L indicates the compressive stress on the plate edge $b_e\sigma_L=\int_0^b \sigma t dy$.	
	Same as above (approximation)	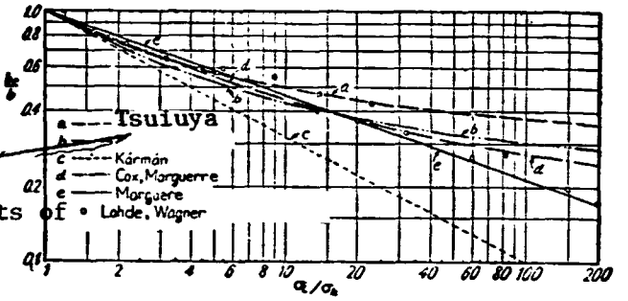	
		ii) ultimate load P_{ult} that the rectangular plate can stand	
		$P_{ult}=\frac{\pi}{\sqrt{3(1-\nu^2)}}\sqrt{E\sigma_s}\,t^2$	109
		$P_{ult}=Ee_{ml}\left(\frac{1.52}{\sqrt{e_m}}t+0.09b\right)$	110
		where e_m is the limit strain with respect to compression	
		$P_{ult}=bt\left\{0.434\sigma_s+2.04E\left(\frac{t}{b}\right)^n\right\}$	115
		σ_s is the yieldpoint stress	
		iii) compressive strain after buckling	
		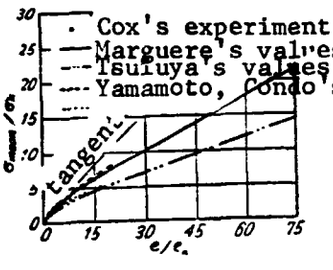	

No.	Dia. & Bound. Cond.	Formulas or Tables of Results	Ref.-Remarks
81	Ends with sides fixed 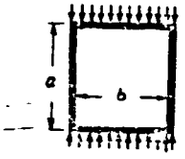	i) Effective width b_e $b_e = \frac{2.18}{\sqrt{e}}t + 0.14b.$ ii) Ultimate load P_{ult} $P_{ult} = Ee_m t\left(\frac{2.18}{\sqrt{e_m}}t + 0.14b\right)$	110 /434
82	Compression test or end with sides rotating (case in which the edge parallel to the load is supported by V channel) 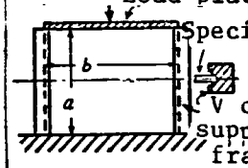	Specimen $a=24''$ constant $b=1\sim24''$ (10 types) $t=0.015\sim0.095''$ (6 types) $P_{ult}=K_1t^2-K_2t^2$ K_1 and K_2 are the coefficients based on the nature of the material, support conditions. etc. 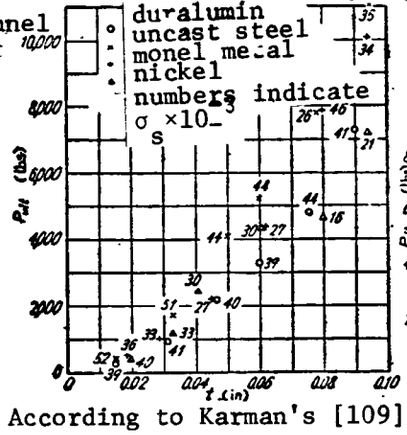 duraluminum plate 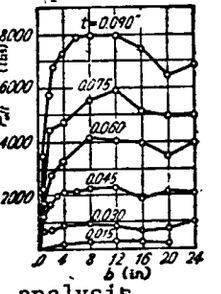 According to Karman's [109] analysis $P_{ult}=C\sqrt{E\sigma_s}\,t^2$ duraluminum $C=1.67\sim1.34$ uncast steel $1.71\sim1.24$ monel metal $1.43\sim1.15$ nickel $1.58\sim1.18$ (cal.value $C=1.90$) $b_e=0.8b\sqrt{\sigma_k/\sigma_s}$ (coefficient of calculated value 1.0) specimen plate width 0.042~2.44 mm, length 250 mm, width approximately 20~510 mm. duraluminum, super duraluminum, uncast steel $P_{ult}=2\times9.4\sigma_B t^2$ where σ_B is the ultimate tension strength	116 120

No.	Dia. & Bound. Cond.	Fromulas or Tables of Results	Ref.-Remarks
83	Experiment with end with sides rotating (case in which the edge parallel to the load is supported on knife edge) specimen	Specimen a=450 mm (—constant) b,t vary $P_{ult}=1350\,t^{1.8}$ duraluminum $=1000\,t^{1.8}$ " When the effective of the width b/t≈100, with an increase in b, P_{lt} increases, but above this even if the increases, P_{lt} does not increase Specimen a=550mm(-const.), b=56(1818 mm t=2 mm, 2.9 mm, 4 mm or 5 mm soft steel $P_{ult}=1.77\left(\frac{a}{b}\right)^{-0.22}\sqrt{E\sigma_s}\,t^2$. 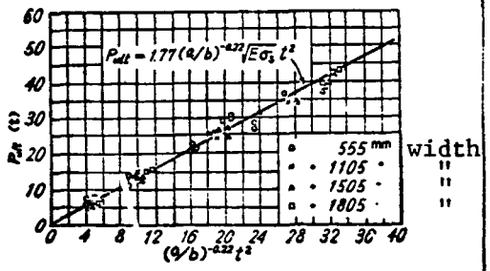 width " "	117 122
84	Experiment on fixed edge parallel to load	Specimen a=24" Fixed, b=12", 10", 8", 6", 4.4" t=0.037", 0.067" (duralmin) Effective width b_e at time of ultimate load $b_e=\frac{2.18t}{\sqrt{\varepsilon_m}}+0.14b$ 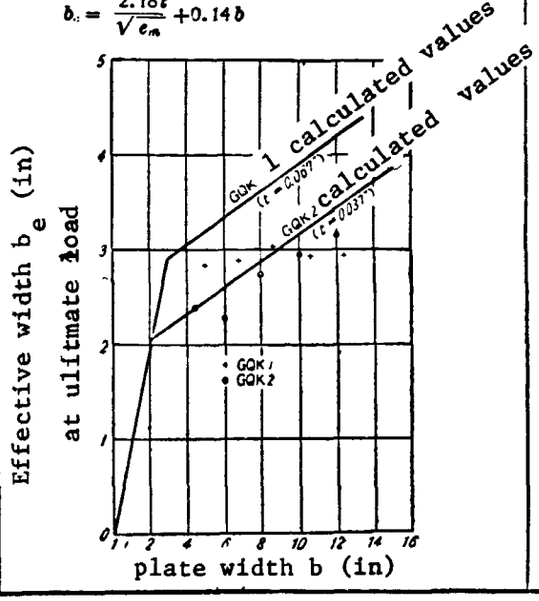 	110

No.	Dia & Bound. Cond..	Formulas or Tables of Results	Ref.-Remarks
85	Test in which the edge parallel to load is fixed with a reinforcing no. 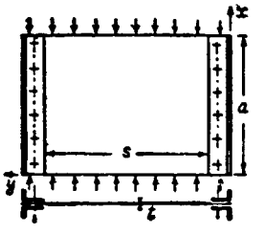	Sample a=600 mm, s=130 mm, t=0.1 mm, 0.2 mm, 0.4 mm, 0.6 mm, Material: duralmin i) Load P of plate after buckling $P=P_k\sqrt{\sigma_L/\sigma_k}$ $(\sigma_k<\sigma<3\sigma_k)$ $=\alpha P_k\sqrt{\sigma_L/\sigma_k}$ $(\sigma>3\sigma_k)$ α, shown below P_k is buckling load 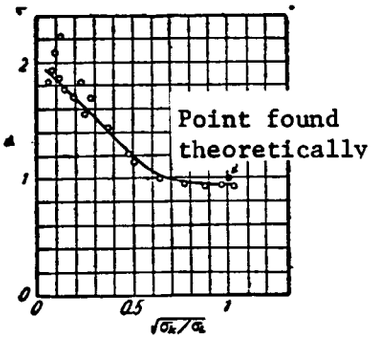 ii) Effective width b_e $\frac{b_e}{2s}=2.1\sqrt{\left(\frac{t}{s}\right)^2\frac{E}{\sigma_L}}-3.7\left(\frac{t}{s}\right)^2\frac{E}{\sigma_L}$ approximation equation (shown by broken line in graph below) 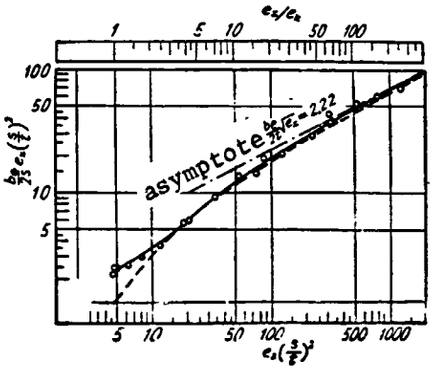	118

No.	Dia. & Bound. Cond.	Formulas or Tables of Results	Ref.-Remarks
85		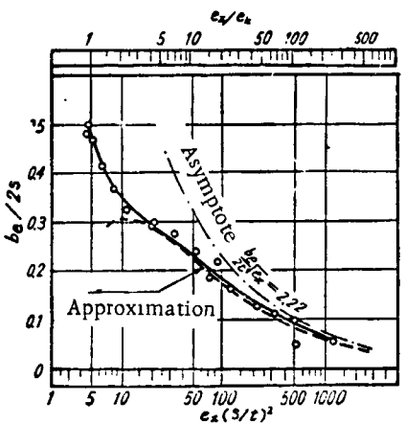 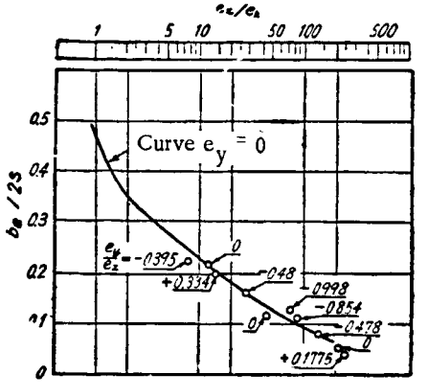 iii) Maximum stress σ_{max} (resultant stress of bending and comp) 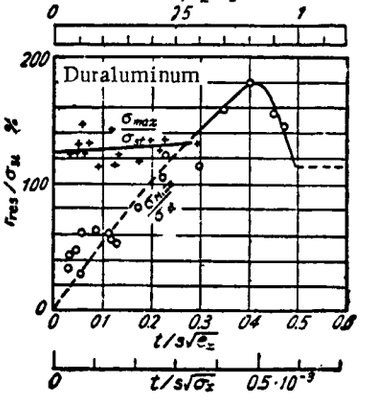 σ_{res}: Resultant stress, σ_{mitte} resultant stress σ_{st}: Compressive stress in center of plate of reinforcing member	/437

No.	Dia. & Bound. Cond.	Formulas or Tables or Results	Ref.-Remarks
85		iv) Distribution of stress in the direction of compression 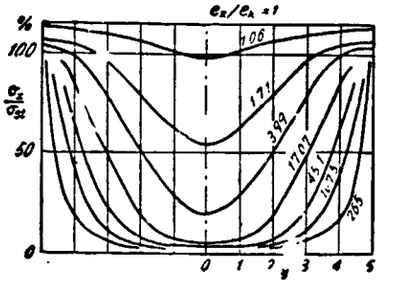 v) Average stress $-\sigma_y$ in direction at right angles to load 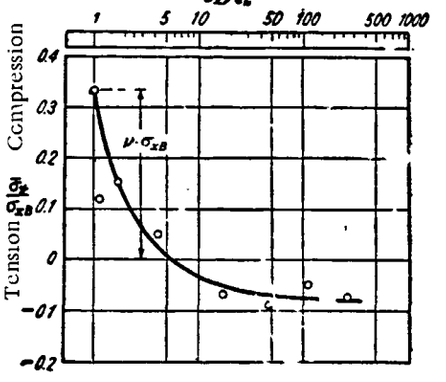 σ_{xB} is average stres to compression	/438
86	Test in which the edges are supported by reinforcing numbers (are measured by vibration method) 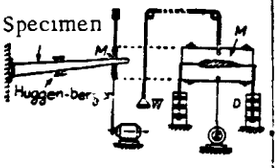 *M* : additional mass *D* : Damper *H* : Huggenberger strain guage	Experiment values of effective width 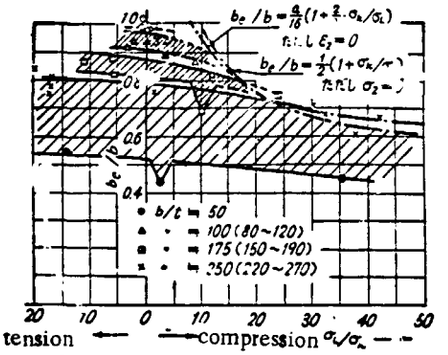 	121

No.	Dia. & Bound. Cond.	Formulas or Tables of Results	Ref.-Remarks
86		Effective width at time of breaking (based on test results on the compression of superduralu-minum plate) (Marguerre's approximation formula) where it is asumed that $\sigma_{Lult} = 25$ kg/mm^2 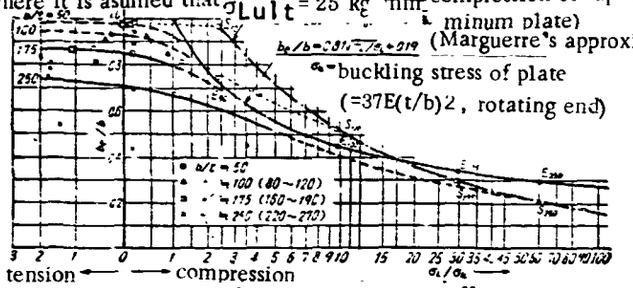 σ_k = buckling stress of plate (=37E(t/b)2, rotating end) values from experiments on effective width (including also tests on rectangular plate)	/439
87	End with 4 sides rotating, stiffener in center 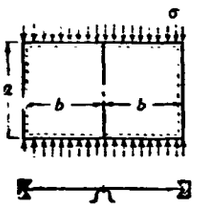	i) Effective width b_e $\frac{1}{2}b_e = C\,b\,\lambda$, (case with no stiffener, curve A) $\frac{1}{2}b_e = \left(\frac{0.50}{\lambda} + 1.82\lambda\right) b\,\lambda$ (case when supported by stiffener, curve B) where $\lambda = \sqrt{\frac{E}{\sigma_k}}\,\frac{t}{b}$. 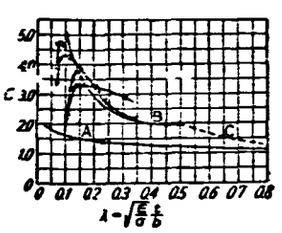 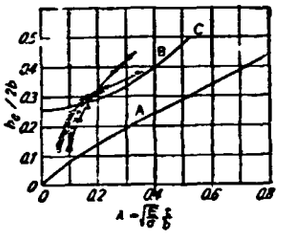 ii) ultimate load P_{ult} of plate $P_{ult} = C\sqrt{E\sigma_k}\,t^2$ (case with no stiffener, curve A) $C = \frac{0.50}{\lambda} + 1.81\lambda$ curve B, case in which supported by stiffener) In the portion where λ is small, the rapid decrease from B to A is due to buckling between rivets iii) distribution of compressive stress after buckling of plate Case in which 4 sides are supported $\sigma = \sigma_L - (\sigma_L - \sigma_k)\sin\frac{\pi y}{b}$. case in which support is by anti-deflection member $\sigma = \frac{1}{2}\left\{\sigma_{Lt} + \sigma_k + (\sigma_{Lt} - \sigma_k)\cos\frac{2\pi y}{b}\right\}$. (see Figure 4.3.4 in original text)	119

No.	Dia. & Bound. Cond.	Formulas or Tables of Results	Ref.-Remarks
88	Compression of rectangular plate having initial deflection	A) Case of end with sides fixed	128

i) Relationship of compressive load P and compressive strain e

$$\frac{P}{Ebt}=e-\beta_4(n)C^2\left[1-\left(\frac{f_0}{f}\right)^2\right],$$

$$C^2=\frac{e-e_n(1-f_0/f)}{(1-f_0/f)^2}=4\beta_3(n)\left(\frac{f}{a}\right)^2,$$

$$e_n=\frac{1}{1-\nu^2}\left[\beta_1(n)\left\{\left(\frac{b}{a}\right)^2+\left(\frac{a}{b}\right)^2\right\}+\beta_2(n)\right]\left(\frac{t}{b}\right)^2$$

n	1	2	3	4	5	6	7
β_1	3.51	5.92	8.42	12.06	16.45	21.62	26.84
β_2	2.01	1.90	1.88	1.97	2.09	2.24	2.37
β_3	0.45	0.55	0.70	0.83	0.96	1.08	1.20
β_4	0.55	0.65	0.69	0.74	0.77	0.79	0.81

ii) Effective width

$$b_e=\left[1-\frac{\beta_4(n)}{e}C\left\{1-\left(\frac{f_0}{f}\right)^2\right\}\right]b$$

f_0 is maximum value of initial deflection

f is maximum value of deflection

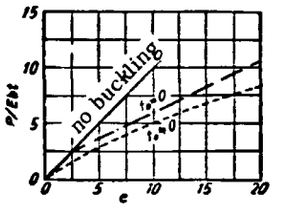

B) Case of end with sides rotating 129

$$\frac{P}{Ebt}=\frac{\pi^2}{16}\left(\frac{\delta}{a}\right)^2\left(1+2\frac{f_0}{\delta}\right)+e_k\left(1+\frac{f_0}{\delta}\right)^{-2}$$

where $\delta=f-f_0$

$$e=\frac{P}{Ebt}+\frac{\pi^2}{8}\left(\frac{f}{a}\right)^2\left\{1-\left(\frac{f_0}{f}\right)^2\right\}.$$

Example of deflection (calculated values shown by solid lines, dotted lines show experiment values)

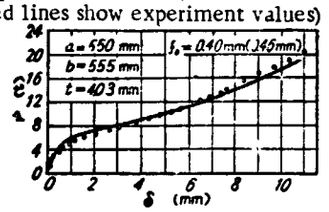

$$\frac{e_L}{e_k}=1+0.0216\left[\frac{e_{max}}{e_k}-1-6\cdot\frac{f_0}{t}\right]^2.$$ 126

where $e_{max}E=\sigma_{max}=\sigma_{direct}+\sigma_{bending}$.

No.	Dia. & Bound. Cond.	Formulas or Tables of Results	Ref.-Remarks
89	Residual deformation, rectangular plate sustaining compression	Maximum stress σ_{max} of flat plate. $$\sigma_{max}=\left(1+6.798\sqrt{\frac{\varepsilon_L}{\varepsilon_k}-1}\right)\sigma_k$$ at the point where $\sigma_{max}=\sigma_s$ is reached, residual deformation does not occur. σ_{max} above this, it is harmful for σ_{max} (or ε_{max}) to go above a specific value. The limit is given by the following equation $$\frac{\varepsilon_L}{\varepsilon_k}=1+0.0216\left(\frac{\varepsilon_{max}}{\varepsilon_k}-1\right)^2$$ 24 The graph below indicates cases in which harmful deformation occurs when $\varepsilon_{max}=0.0093$, for S.T. Alclad 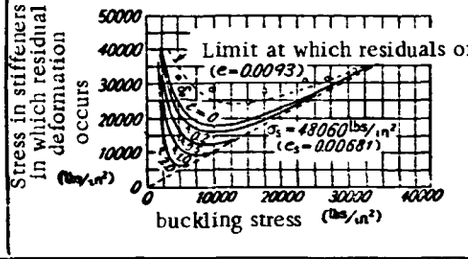	126
90	Orthotropic plate, end with 4 sides rotating	$$\frac{b_r}{b}=\frac{1+K}{3+K}+\frac{2}{3+K}\frac{\varepsilon_{zk}}{\varepsilon_z},$$ $$\frac{\sigma_z}{\sigma_{zk}}=\frac{2}{3+K}+\frac{1+K}{3+K}\frac{\varepsilon_z}{\varepsilon_{zk}},\quad K=\frac{a_y D_x}{a_x D_y}.$$ 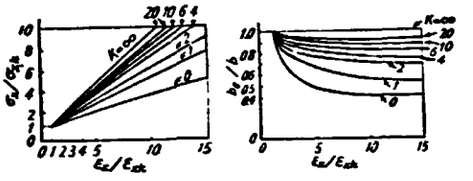	123
91	Orthotropic plate, case in which the principal axis of elasticity is inclined in the direction of load. 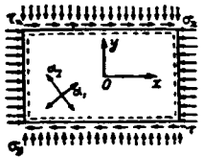	Condition after the shear buckling of a strip having stiffeners ($\varepsilon_L=\varepsilon_Q=0$)	124

$E_1=1200$, $E_2=600$, $G=125$ kg/mm², $\nu_1=0.150$, $\nu_2=0.075$.

m at time of buckling	a/b	$\theta°$	$\varphi°$	$\frac{\tau_z}{E_1\mu^2t^2}$	$\frac{\sigma_\cdot}{E_1\mu^2t^2}$	$\frac{\sigma_y}{E_1\mu^2t^2}$	$\frac{\tau}{\tau_k}$	$\frac{f}{t}$	$\frac{\tau}{\tau G_e}$
0.9218	0.870	47°20′	45°0′	0.5625	0.2033	0.2083	1.000	0	1.000
0.950	0.764	45°28′	44°50′	0.8235	0.3874	0.3969	1.464	0.665	0.963
1.000	0.559	45°	44°39′	2.381	1.593	1.650	4.233	1.469	0.876
1.020	0.451	44°26′	44°39′	5.289	4.020	4.150	9.403	2.039	0.834
1.030	0.381	44°9′	44°39′	10.015	8.106	8.343	17.805	2.534	0.811
1.035	0.340	44°1′	44°39′	15.638	13.058	13.415	27.801	2.913	0.798

$G_e=G/(1-k)=410$ kg/mm², $G_{xy}=G_{45°}=364$ kg/mm²

No.	Dia. & Bound. Cond.	Formulas or Tables of Results	Ref.-Remarks
92	Compression test on rectangular compound plate 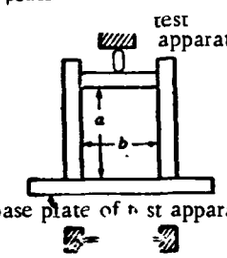 Relationship between direction of compression and principal axis of elasticity 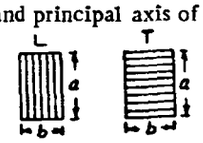 	Specimen, compound plate, plate thickness 2 mm a=80~500 mm, b=205 mm. i) relationship of rupture stress f and a/b 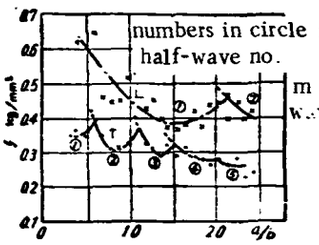 $f=P_{ult}/A$ (A = cross-section area) $P_{ult}=Ct^2\sqrt{E\sigma_t}$, $C=\sqrt{\frac{E}{\sigma_t}}\cdot\frac{t}{b}$. Comparing the values of C in the above equation, large values are indicated, where L = 13.9%, T = 14.2% ii) for the value m = 1 4 a/b giving the minimum critical buckling value Type of specimen / Value of a/b: Calculated / Through experiment L: 1.70 / 1.48 T: 0.59 / 0.43 Calculation formula $a/b=\frac{1}{2}\sqrt{D_x/D_y}$)	125 /442

TENSION FIELD

No.	Dia. & Bound. Cond.	Formulas or Tables or Results	Ref.-Remarks
93	Problem of the phenomena occurring after the shear buckling of a plate beam having reinforcing members on the sides. Tension field 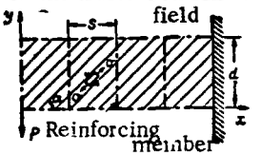 	Tension field after shear buckling of a plate Tension stress σ of plate $\sigma=\frac{2P}{d\cdot t\cdot\sin 2\alpha}\fallingdotseq\frac{2P}{d\cdot t}$ Compressive force V of perpendicular reinforcing member $V=P\frac{s}{d}\tan\alpha\fallingdotseq 0.9P\frac{s}{d}$	131 132

No.	Dia. & Bound. Cond.	Formulas or Tables of Results	Ref.-Remarks
93		Horizontal force H of vertical edge member (based on σ) $H=P\frac{\cot\alpha}{2}\fallingdotseq 0.6P.$ Adding directly that which is based on the load P $H=\pm Px/d-0.6P$ (+ upper edge member, - lower edge member) Change in angle γ due to shear $\gamma=2\cot\alpha(\varepsilon-\varepsilon_x)\fallingdotseq 2.8\frac{\sigma}{E}.$ $\tan^2\alpha=\frac{\frac{P}{d\cdot t}\frac{1}{\sin\alpha\cos\alpha}-\frac{P}{2A_H}\cot\alpha}{\frac{P}{d\cdot t}\frac{1}{\sin\alpha\cos\alpha}+\frac{P}{A_V}\frac{s}{d}\tan\alpha}$ From the above equation, it can be seen that $\alpha\simeq$ 40-42 °. if necessary, can be corrected. The collapse of the plate or buckling of the reinforcing member due to the σ found above gives the maximum load of the plate beam.	
94	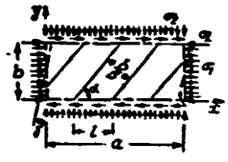	Average stress $\bar{\sigma}_x$ in direction x $\bar{\sigma}_x=\frac{\sigma_1 bt+\sigma_L A_L}{bt+A_L}.$ Average stress $\bar{\sigma}_y$ in direction y $\bar{\sigma}_y=-\frac{\sigma_x at+\sigma_V A_V}{at+A_V}=0$ σ_1, σ_2 are average stresses of plate in directions x, y A_L, A_V are the cross-section areas of the horizontal and vertical reinforcing σ_L, σ_V are the stresses of the horizontal & vertical reinforcing members i) $\sigma_2=0$ $(A_V/at=0)$ $\frac{\sigma_1}{4\sigma_e}=\frac{1}{4}\left\{\delta\lambda^2(\lambda^4-1)+2\lambda^2-6\delta+8-\frac{2}{\lambda^2}(\delta-1)\right\}.$ $\frac{\sigma_L}{4\sigma_e}=\frac{\sigma_1}{4\sigma_e}+\frac{\delta\lambda^2}{2}(\lambda^4-1)$ $\frac{\tau}{4\sigma_e}=\frac{\sqrt{\delta-1}}{2}\left\{6+\lambda^2+\frac{1}{\lambda^2}\right\}$ $\frac{\gamma E}{4\sigma_e}=\frac{\sqrt{\delta-1}}{2}\left\{\left(6+\lambda^2+\frac{1}{\lambda^2}\right)(1+\nu)+2\delta\lambda^2(\lambda^4-1)\right\}.$ ii) $\sigma_2=0$ $(A_V/at=\infty)$ $\frac{\sigma_2}{4\sigma_e}=\frac{1}{4}\times$ $\frac{(\lambda^4-1)2\delta\lambda^2\left\{\delta\left(1+\frac{1}{\lambda^2}\right)-1\right\}-4\nu\delta_1}{-2\delta\lambda^2\left\{\delta\left(1+\frac{1}{\lambda^2}\right)-1\right\}-1+\nu\left\{\delta\lambda^2+(\delta-1)\left(1+\frac{2}{\lambda^2}\right)\right\}}.$	133

No.	Dia. & Bound. Cond.	Formulas or Tables of Results	Ref.-Remarks
94		$\frac{\sigma_1}{4\sigma_c}=\hat{\sigma}_1+\frac{\sigma_2}{4\sigma_c}\left[\delta\lambda^2+(\delta-1)\left(1+\frac{2}{\lambda^2}\right)\right]$ $\frac{\sigma_L}{4\sigma_c}=\frac{\sigma_1}{4\sigma_c}+\frac{1}{2}\delta\lambda^2(\lambda^2-1)+(2\delta\lambda^2-\nu)\frac{\sigma_2}{4\sigma_c}$ $\frac{\tau}{4\sigma_c}=\hat{\tau}-\frac{\sigma_2}{4\sigma_c}\left(1+\frac{1}{\lambda^2}\right)\sqrt{\delta-1}$ $\frac{\tau E}{4\sigma_c}=\hat{\tau}+\frac{\sigma_2}{4\sigma_c}\left[4\delta\lambda^2-2(1+\nu)\left(1+\frac{1}{\lambda^2}\right)\right]\sqrt{\delta-1}$ $\left(\frac{f}{t}\right)^2=1.46\,\delta^2(\lambda^4-1)+5.85\,\delta^2\frac{\sigma_2}{4\sigma_c}.$ Where $\hat{\sigma}_1,\hat{\sigma}_2,\hat{\tau},\hat{\tau}$ etc indicate values corresponding to case 1). f indicates the maximum value of wrinkling $\delta=\frac{1}{\sin^2\alpha}$. When $\varepsilon_2=0$ the relations σ_1, σ_L, τ, τ are indicated by the following graph where $E\varepsilon_c=\sigma_c$) 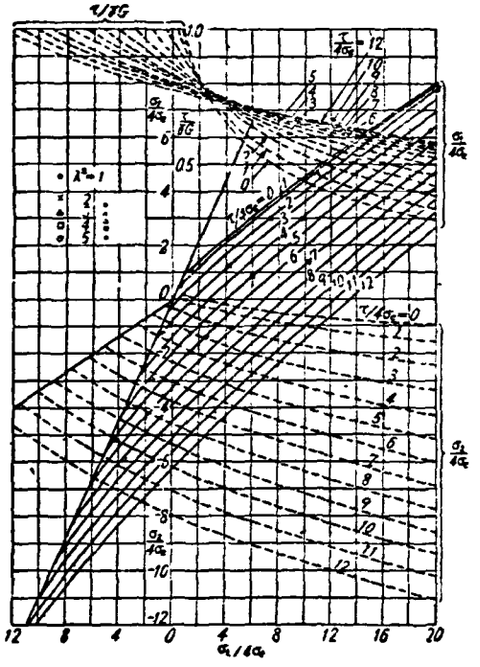 Relationships between σ_1, σ_2, τ, σ_L when $\varepsilon_2 = 0$	/444

No.	Dia. & Bound. Cond.	Formulas or Tables of Results	Ref.-Remarks
94		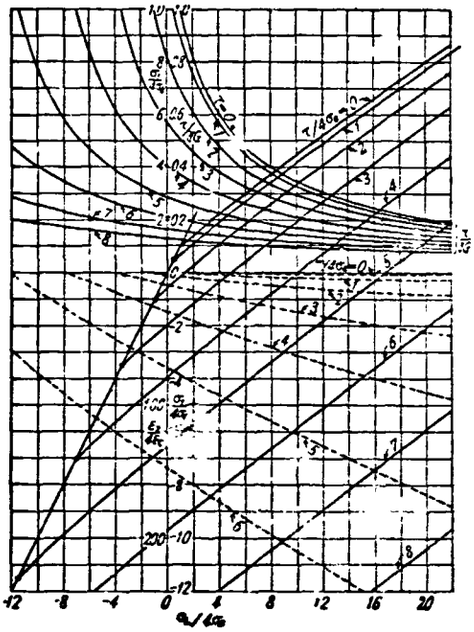 Relationship between σ_1, τ, ε_2 when $\sigma_1 = 0$ (dotted line indicates $\varepsilon_2/4\,\varepsilon_e$).	
95	Tension field test	Immediately after buckling of the plate, values are indicated which are intermediate between tension filed theory and beam theory disregarding the buckling of the plate. The values approach the tension field theory as the buckling develops. The graph below is a copulation from results of experiments. 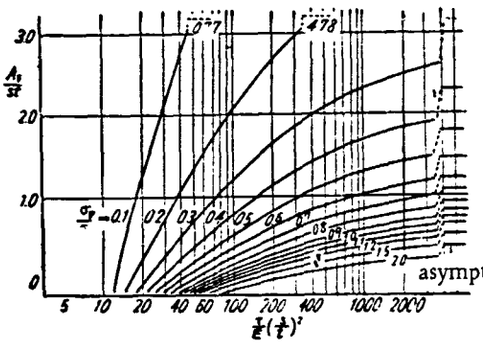 Relationship of cross-section area, stress and shear stress of vertical reinforcing members	139

No.	Dia. & Bound. Cond.	Formulas or Tables of Results	Ref.-Remarks
95		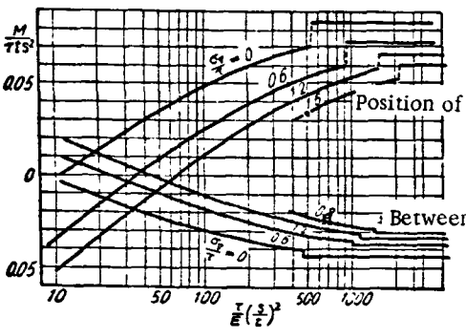 Position of reinforcing member; Between reinforcing members Maximum bending moment (M) of edge members 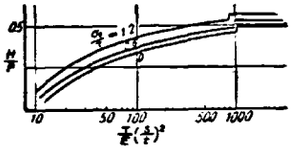 Additional compressive force (H) applied to lower edge member 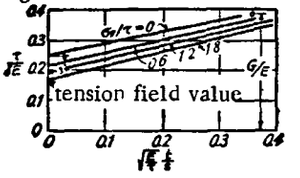 tension field value 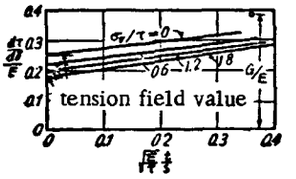 tension field value 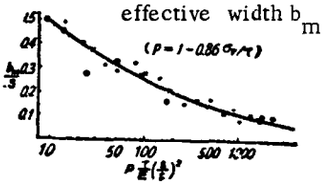 effective width b_m where effective width $b_m = \frac{s}{2}\frac{\sigma_{xs}-\sigma_{xm}}{\sigma_{xs}-\sigma_y}$. σ_{xs} is stress in direction x in tension field σ_{xm} average stress in direction x between vertical reinforcing members	

No.	Dia. & Bound. Cond.	Formulas or Tables of Results	Ref.-Remarks
96	Case where there is a diagonal vertical member 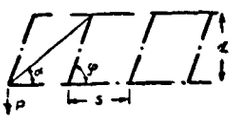	Tensile stress of plate σ $$\sigma=\frac{2P}{d\cdot t}\frac{1}{\sin 2\alpha}\frac{1}{1-\tan\alpha\cot\varphi}$$ Forces received by upper edge member (H_0), and lower edge member (H_u) $$H_0=\frac{P\cdot x}{d}-\frac{P}{2}(\cot\alpha+\cot\varphi)$$ $$H_u=-\frac{P\cdot x}{d}-\frac{P}{2}(\cot\alpha+\cot\varphi)$$ Forces received by vertical member $$V=\frac{P}{\sin\varphi}\frac{s}{d}\tan\alpha\frac{1}{1-\tan\alpha\cot\varphi}$$	131
97	Case in which there are upper and lower diagonal edge members 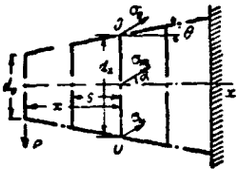	Tensile stress σ_m of plate intermediate between vertical members at a distance x from the end part $$\sigma_m=\frac{P}{t}\cdot\frac{d_0}{d_x^2}\frac{1}{\sin\alpha\cdot\cos\alpha}$$ At the upper and lower ends, respectively $$\sigma_0=\frac{\sigma_m}{(1-\cot\alpha\cdot\tan\theta)^2}$$ $$\sigma_u=\frac{\sigma_m}{(1+\cot\alpha\tan\theta)^2}$$ Compressive force V received by vertical member $$V=P\frac{s}{d_c}\tan\alpha$$	131
98	Case in which there are slanted upper and lower edge members 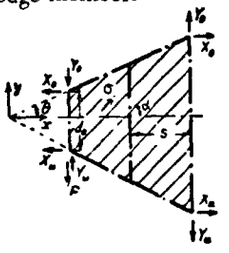	Plate stress σ (x, y) $$\sigma(x,y)=\frac{\sigma_m(\xi)}{(1-\cot\alpha\tan\theta)^2},\quad \xi=\frac{x-y\cot\alpha}{1-\tan\theta\cot\alpha}$$ Horizontal force X_0 received by upper edge member $$X_0=\frac{P}{2}\cot\theta\left[1-\frac{d_0\cot\alpha}{x(1-\cot\alpha\tan\theta)\log\mu}\right]$$ vertical force Y_0 $$Y_0=X_0\tan\theta$$ Horizontal force X_u and vertical force Y_u sustained by lower edge member $$X_u=-\frac{P}{2}\cot\theta\left[1-\frac{d_0\cot\alpha}{x(1+\cot\alpha\tan\theta)\log\mu}\right]$$ $$Y_u=X_0\tan\theta$$ Force V sustained by horizontal member $$V=ts\sin^2\alpha\,\sigma_m(x)\frac{x^2}{x^2-\frac{s^2}{4}}$$ Where $$\sigma_m(x)=\frac{Pd_0\cot\theta}{2tx^2\sin^2\alpha\cdot\log\mu}$$ $$\mu=\frac{1+\tan\theta\tan\alpha}{1-\tan\theta\tan\alpha}$$ x indicates the coordinates of each member	138

No.	Dia. & Bound. Cond.	Formulas or Tables of Results	Ref.-Remarks
99	General theory of tension field 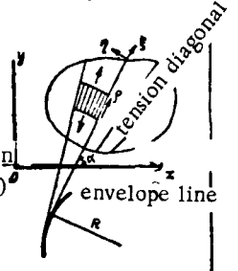 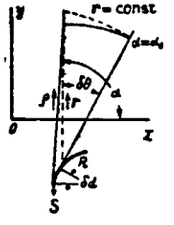 	General solution of displacement $\xi=\varphi(x)\log\rho+\Psi(x)$ $\eta=\varphi'(x)(1+\log\rho)+\Psi'(x)+\chi(x)\rho+\frac{R}{2\rho}\varphi(x)$ The critical values $\xi_1, \xi_2, \eta_1, \eta_2$ of ξ, η are determined from displacement at the boundary. moreover, from the relationship between the boundary displacement and the direction of the tension diagonal $\varphi(x)=\frac{\xi_1-\xi_2}{\log(\rho_1/\rho_2)}$, $\Psi(x)=\frac{\xi_2\tan\rho_1-\xi_1\log\rho_2}{\log(\rho_1/\rho_2)}$ $\chi(x)=\frac{\eta_1-\eta_2-\xi_1'-\xi_2'}{\rho_1-\rho_2}+\frac{\xi_1-\xi_2}{\log(\rho_1/\rho_2)}\cdot\left\{\frac{\rho_1'/\rho_1-\rho_2'/\rho_2}{\rho_1-\rho_2}+\frac{R(\alpha)}{2\rho_1\rho_2}\right\}$ Condition for the formation of wrinkling $\varepsilon>0,\quad -\varepsilon_\theta-\varepsilon/m>0$ where $\varepsilon=\frac{\partial\xi}{\partial\rho},\quad \varepsilon_\theta=\frac{\xi}{\rho}+\frac{1}{\rho}\frac{\partial\eta}{\partial\alpha}+\frac{R(\alpha)}{\rho}\frac{\partial\eta}{\partial\rho}$	135 /448

REINFORCING MEMBERS

Simple Compression

100	End with 4 sides rotating, single longitudinal reinforcing member 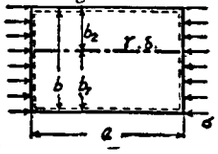 	when i) $b_1=b_2=b/2$ $\sigma_k=k\,\sigma_e$ where $\sigma_e=\frac{\pi^2 E}{12(1-\nu^2)}\left(\frac{t}{b}\right)^2$ Values of k (bending stiffness of reinforcing member assumed to be zero)	143

*2 γ / *1 β	5			10			15			20			25
	*3 δ 0.05	0.1	0.2	δ 0.05	0.1	0.2	δ 0.05	0.1	0.2	δ 0.05	0.1	0.2	0.05
0.6	16.5	16.5	16.5	16.5	16.5	16.5	16.5	16.5	16.5	16.5	16.5	16.5	16.5
0.8	15.4	14.5	13.0	16.8	16.8	16.8	16.8	16.8	16.8	16.8	16.8	16.8	16.8
1.0	12.0	11.1	9.72	16.0	16.0	15.8	16.0	16.0	16.0	16.0	16.0	16.0	16.0
1.2	9.83	9.06	7.88	15.3	14.2	12.4	16.5	16.5	16.5	16.5	16.5	16.5	16.5
1.4	8.62	7.91	6.82	12.9	12.0	10.3	16.1	15.7	13.6	16.1	16.1	16.1	16.1
1.6	8.01	7.38	6.32	11.4	10.5	9.05	14.7	13.6	11.8	16.1	16.1	14.4	16.1
1.8	7.84	7.19	6.16	10.6	9.70	8.35	13.2	12.2	10.5	15.9	14.7	12.6	16.2
2.0	7.96	7.29	6.24	10.2	9.35	8.03	12.4	11.4	9.80	14.9	13.4	11.6	16.0
2.2	8.28	7.58	6.50	10.2	9.30	7.99	12.0	11.0	9.45	13.9	12.7	10.9	15.8
2.4	8.79	8.06	6.91	10.4	9.49	8.15	11.9	10.9	9.37	13.5	12.4	10.6	15.1
2.6	9.27	8.50	7.28	10.8	9.86	8.48	12.1	11.1	9.53	13.5	12.4	10.6	14.8
2.8	8.62	7.91	6.31	11.4	10.4	8.94	12.5	11.5	9.85	13.7	12.6	10.8	14.8
3.0	8.31	7.62	6.53	12.0	11.1	9.52	13.1	12.0	10.3	14.1	13.0	11.1	15.2
3.2	8.01	7.38	6.32	11.4	10.5	9.05	13.9	12.7	10.9	14.8	13.5	11.6	15.6
3.6	7.84	7.19	6.16	10.6	9.70	8.35	13.2	12.2	10.5	15.9	14.7	12.6	16.2
4.0	7.96	7.29	6.24	10.2	9.35	8.03	12.4	11.4	9.8	14.6	13.4	11.6	16.0

*1 $\beta=\frac{a}{b}$, *2 $\delta=\frac{A}{bt}$, *3 $\gamma=\frac{EI}{Db}$.

A = cross-section area of reinforcing member

EI = bending stiffness of reinforcing member

No.	Dia. & Bound. Cond.	Formulas or Tables of Results	Ref.-Remarks
100		Buckling occurs under the values indicated above when $\gamma<\gamma_{min}$, the form of buckling is shown in II of the Figure below	/449

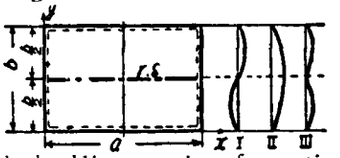

For the buckling equation of an anti-symmetrical shaped I when $\gamma>\gamma_{min}$ 149

$$k=4\left(\frac{2\beta}{m}+\frac{m}{2\beta}\right)^2.$$

For symmetrical shaped III 147

Buckling condition equation

$$-2(K_1^2+K_2^2)+\Phi_1\left(\frac{\tanh K_1}{K_1}-\frac{\tan K_2}{K_2}\right)=0$$

where

$$K_{\frac{1}{2}}=\sqrt{\nu_m(\sqrt{k_1}\pm\nu_m)},\quad k_1=k/4,$$

$$\nu_m=\frac{m\pi}{2\beta},\quad \Phi_1=\frac{1}{2}\tau\nu_m^4-\frac{1}{2}\pi^2k_1\delta\nu_m^2$$

$$\tau_{min}=\frac{2}{\pi^2}\frac{\left(\frac{2\beta}{m_1}+\frac{m_1}{2\beta}\right)\left(\frac{2\beta}{m}\right)^2}{\frac{\tanh K_1}{K_1}-\frac{\tan K_2}{K_2}}+\frac{4\beta^2}{m^2}\left(\frac{2\beta}{m_1}+\frac{m_1}{2\beta}\right)^2\delta$$

m_1 indicates the half-wave number giving the minimum critical value of a plate assuming that its end rotates around the edge and the position of the reinforcing member, m is the case in which there is no reinforcing member.

For example, when $0<\beta<\frac{\sqrt{2}}{2}$ $m_1=1$, $m=1$.

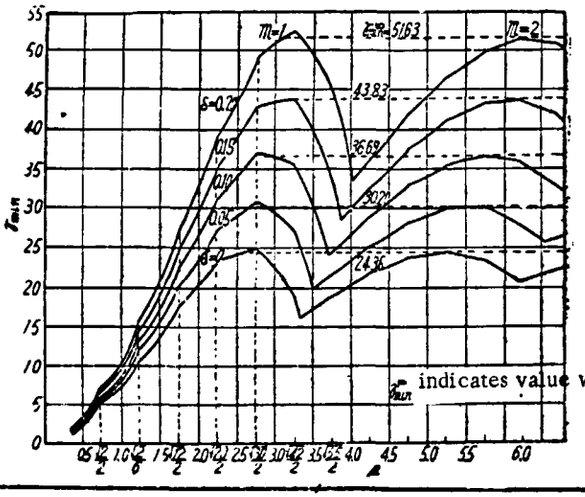

β_{∞} indicates value where

No.	Dia. & Bound. Cond.	Formulas or Tables of Results	Ref.-Remarks
100		When ii) $b_1=b/3$, $b_2=2b/3$	149

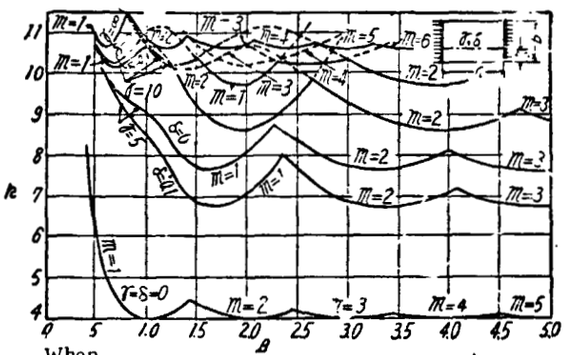

When

iii) $b_1=b/4$, $b=\frac{3}{4}b$

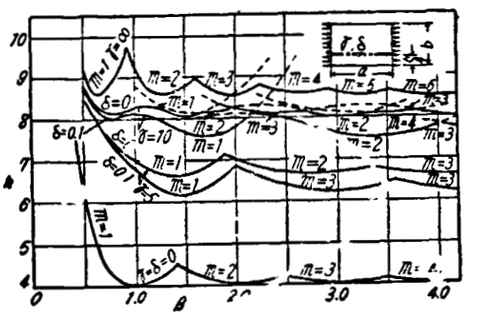

149

iv) Relationship between b_1 and k wher a=b

149

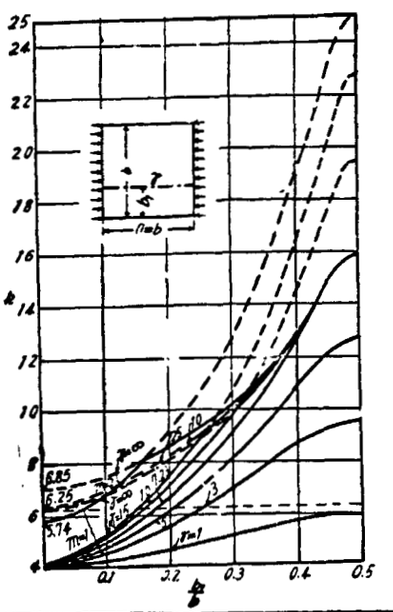

/450

No.	Dia.	Cond.	Formulas or Tables of Results	Ref.-Remarks

101 End wi
rotating. 2 longitudinal
reinforcing members

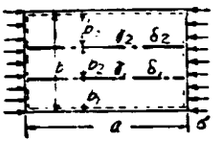

/451

when $b_1=b_2=\quad=\frac{b}{3}$, $r_1=r_2=r$, $\delta_1=\delta_2=\delta$

$$\sigma_k=\frac{(1+\beta^2)^2+3i}{\beta^2(1+3\delta)}\sigma_e \qquad 143$$

where $\sigma_e=\frac{\pi^2E}{12(1-\nu^2)}\left(\frac{t}{b}\right)^2$

$\sigma_k=k\,\sigma_e$

k is based on the graph below 149

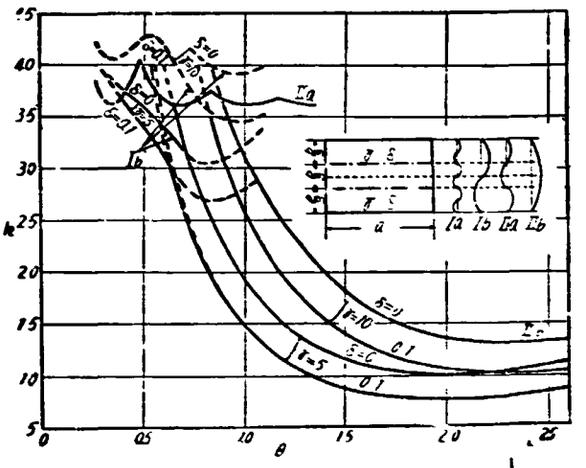

The shape of I_a does not pose any problem when the minimum value of k is 144. When $\gamma<\gamma_{min}$, 147
type II_b buckling occurs

$$\gamma_{min}=\frac{2\left(\frac{3\beta}{m_1}+\frac{m_1}{3\beta}\right)\left(\frac{3\beta}{m}\right)^2}{3\pi^2\,U_3}+\frac{9\beta^2}{m^2}\left(\frac{3\beta}{m_1}+\frac{m_1}{3\beta}\right)^2\delta$$

$$\eta_3=\frac{\sinh K_1}{K_1\left(4\cosh^2\frac{K_1}{2}-3\right)}-\frac{\sin K_2}{K_2\left(4\cos^2\frac{K_2}{2}-3\right)}$$

$$K_2=\pi\sqrt{\frac{m}{3\beta}\left(\frac{3\beta}{m_1}+\frac{m_1\pm m}{3\beta}\right)}$$

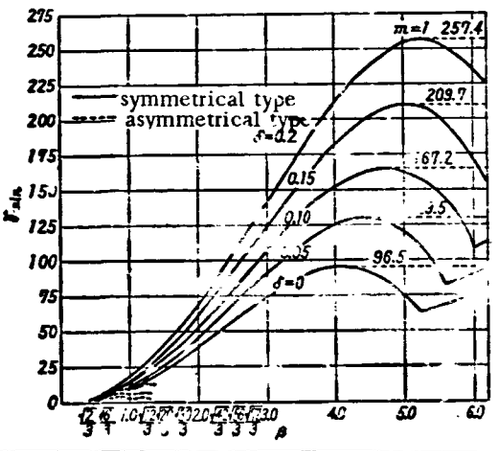

No.	Dia. & Bound. Comp.	Formulas or Tables of Results	Ref.	Remarks
102	End with 4 edges rotating, many longitudinal reinforcing members	Case in which there is equal spacing of reinforcing members $\sigma_k = \frac{(1+\beta^2)^2 + 2\sum_i \gamma_i \sin^2 \frac{\pi b_i}{b}}{\beta^2\left(1+2\sum_i \delta_i \sin^2 \frac{\pi b_i}{b}\right)} \cdot \sigma_c$	143	
103	End with sides A fixed, side B rotating, 1 longitudinal reinforcing member 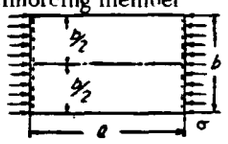	where $b_1 = b_2 = b/2$ $\sigma_k = k\,\sigma_{c_0} \qquad \sigma_c = \frac{\pi^2 E}{12(1-\nu^2)}\left(\frac{t}{b}\right)^2$ The values of k are given in the Figure below 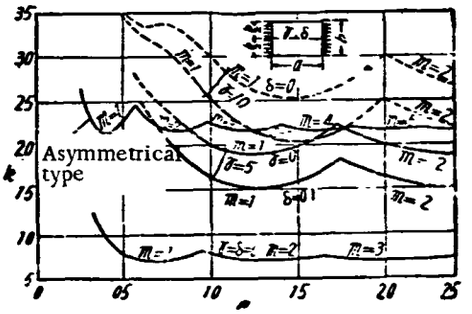 Minimum values of γ for asymmetrical type to be obtained 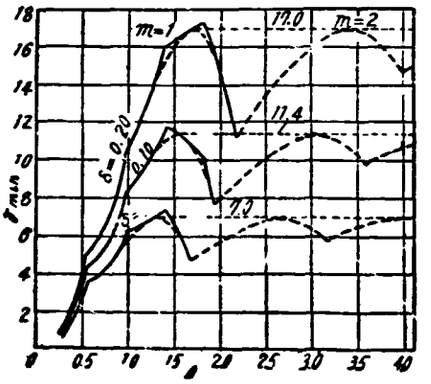	149	

No.	Dia. & Bound. Comp	Formulas or Tables of Results	Ref.-Remarks
104	Both sides (sides A) supported by reinforcing member 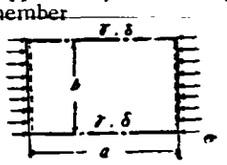	$\sigma_k = k\sigma_0$ Minimum value of k (when the reinforcing members on both sides are equal)	144 /453

δ \ τ	50	200	500	5000
0.5	3.87	3.97	3.99	4.00
2.5	3.83	3.97	3.99	4.00
5.0	—	3.96	3.99	4.00

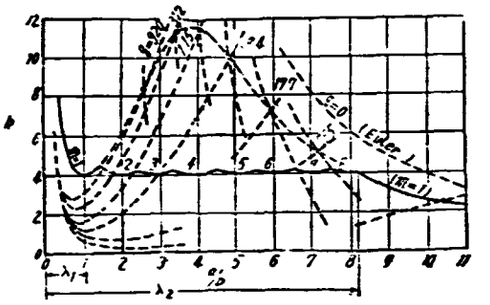

Approximation equation

$$k_{min} \fallingdotseq 4\left(1-\frac{1.5}{2\tau-8\delta}\right)$$

$$k = k_0\left\{1-\frac{4(k_0-\varphi^2-\nu)^2}{\pi^2 k_0(\varphi^2\tau-k_0\delta)}\right\}$$

$$k_0 = \left(\lambda_k+\frac{1}{\lambda_k}\right)^2$$

$$\varphi = \frac{mb}{a} = \frac{1}{\lambda},\quad \tau = \frac{EI}{bD},\quad \delta = \frac{A}{bt}$$

values of λ_k

δ \ τ	50	200	500	5000
0.5	1.035	1 008	1.003	1.000
2.5	1.060	1.028	1.003	1.000
5.0	—	1.008	1.003	1.000

$\sigma_k = \frac{\pi^2}{x^2}\cdot\sigma_e$ (x^2 minimum values are found from the diagram below, assuming m) 146

No.	Dia. & Bound. Comp.	Formulas or Tables of Results	Ref.-Remarks
104		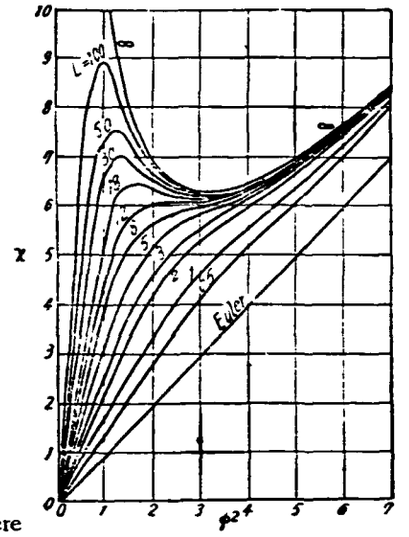 where $L=\tau-\delta(\tau^2/\varphi^4)$ $\varphi^2=m\times b/a$	/454
105	One side of sides A is supported by a reinforcing member, the other side has a rotating end 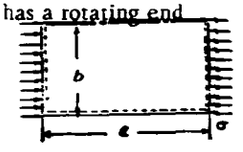	Conditions for elastically supported end $\frac{\partial^2 w}{\partial y^2}=C\frac{\partial w}{\partial y}$ i.e., when the bending moment is proportional to the angle of rotation $\sigma_k=k\sigma_c$	153

C \ a/b	1.0	1.3	1.5	1.8	2.0	2.3	2.5	2.7	3.0	4.0
2/b	1.49	1.13	1.01	0.92	0.90	0.89	0.90	0.93	0.98	0.[illegible]
8/b	1.58	1.25	1.16	1.11	1.12	1.18	1.23	1.22	1.16	1.12

$\sigma_k=k\sigma_c$ 145

Values of k indicated in graph

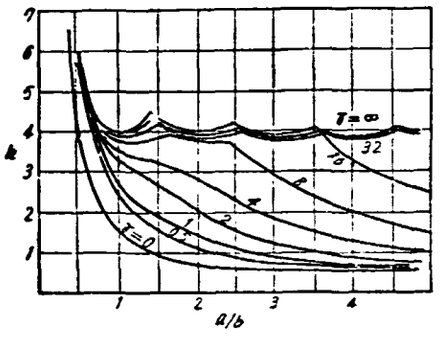

No.	Dia.& Bound. Comp.	Formulas or Tables of Results	Ref.-Remarks
105		$\sigma_k=\left(\frac{x}{\pi}\right)^2 \cdot \sigma_e$ Minimum values of x determined from graph below, assuming m 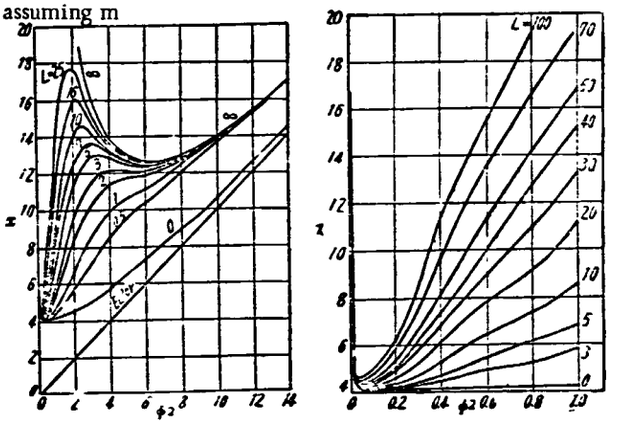 where $L=\tau-\delta(x^2/\varphi^4)$ $\varphi^2=m\pi b/a$ m is half-wave number	146
106	One side of sides A supported by reinforcing member, one side has fixed end, sides B are rotating 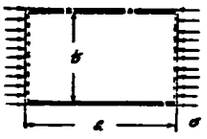	$\sigma_k=\left(\frac{x}{\pi}\right)^2\sigma_e$ Minimum value of x is determined from graph below, assuming m where $L=\tau-\delta(x^2/\varphi^4)$ $\varphi^2=m\pi b/a$ m is half-wave number 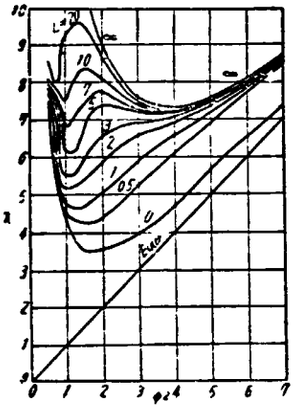	146

No.	Dia. & Bound. Comp.	Formulas or Tables of Results	Ref.-Remarks
107	End with 4 edges rotating, one lateral reinforcing member	When i) $a_1=a_2$	

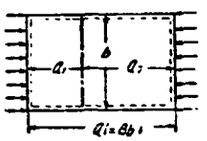

$$\sigma_k = k\,\sigma_e$$

$$k=\left(\frac{2m}{\beta}+\frac{\beta}{2m}\right)^2$$ 143 151

where $\tau > \tau_{min}$

Values of τ_{min}

Ref. \ β	0.5	0.6	0.7	0.8	0.9	1.0	1.2	1.41
143	12.6	7.18	4.39	2.80	1.82	1.26	0.433	0
151	12.75	7.24	4.42	2.82	1.84	1.19	0.435	——

$$k=\frac{(1+\beta^2)^2+2\tau\beta^2}{\beta^2}$$ 143

where $\tau < \tau_{min}$

When
ii) $a_1=a/3, \quad a_2=\frac{2}{3}a$

$$\sigma_k = k\,\sigma_e$$

Values of k given in the diagram and table 149

τ \ β	0.4	0.6	1.0	1.4	1.8
5	11.265	8.703	5.694	4.519	4.317
10	13.768	10.085	5.748	4.519	4.326
15	15.840	10.741	5.764	4.519	4.326

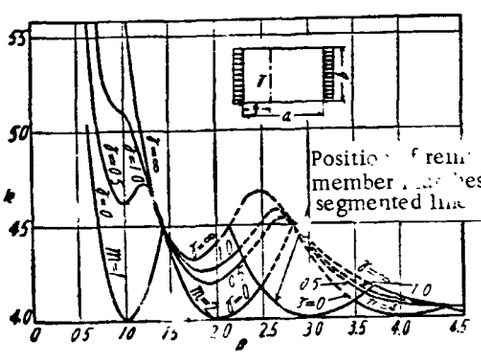

Positio[n] of reinforcing member [in]dicates the segmented line

when iii) $a_1=a/4, \quad a_2=3a/4$

$$\sigma_k = k\,\sigma_e$$ 149

τ \ β	0.4	0.6	1.0	1.4	1.8
5	10.287	7.474	5.317	4.515	4.458
10	11.907	8.655	5.402	4.516	4.472
15	13.210	9.226	5.429	4.516	4.477

No.	Dia. & Bound. Comp.	Formulas or Tables of Results	Ref.-Remarks
108	Ends with 4 edges rotating, two lateral reinforcing members, 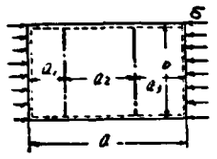 	i) when $\alpha_1=\alpha_2=\alpha/3$, $\tau_1=\tau_2=\tau$ $\sigma_k=k\,\sigma_c$ $k=\dfrac{(m^2+\beta^2)^2+3\tau\beta^2}{\beta^2}$. where $\tau<\tau_{min}$. $k=\left(\dfrac{3m}{\beta}+\dfrac{\beta}{3m}\right)^2$ where $\tau>\tau_{min}$. Values of τ_{min} β: 0.60 | 0.80 | 1.0 | 1.2 | 1.4 τ_{min}: 101 | 42.6 | 21.7 | 12.4 | 7.71 Diagram of k 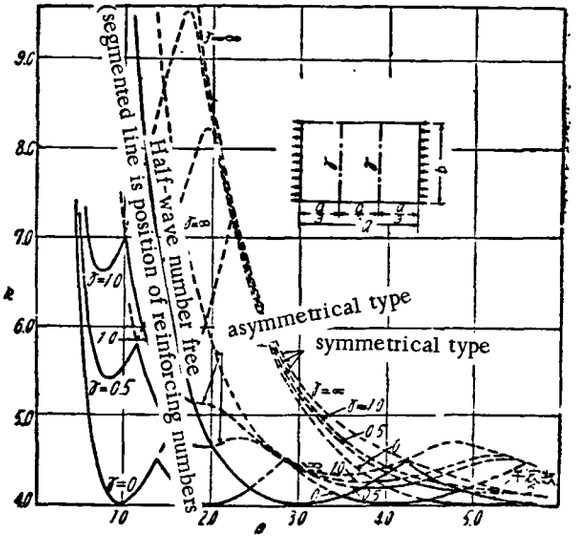 	143 149
109	End with 4 edges rotating, many lateral reinforcing members	Case in which reinforcing members are at equal distances $\sigma_k=\dfrac{(m^2+\beta^2)^2+(r+1)\tau\beta^2}{\beta^2 m^2}\cdot\sigma_c$ Where r is number of reinforcing members	143

No. Dia. & Bound Comp.	Formulas or Tables of Results	Ref.-Remarks
110 Ends with 4 edges rotating, and one reinforcing member each longitudinally and laterally 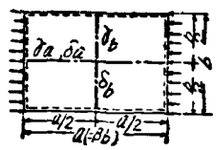	Case in which there is an anti-deflection member in the center of the plate A) Critical values when $\tau_a > \tau_{a\min}$, $\tau_b > \tau_{b\min}$ $\sigma_k = k\,\sigma_e$ $k = 4\left(\frac{m}{\beta} + n^2\frac{\beta}{m}\right)^2$ $\beta = a/b$ table of $\tau_{a\min}$ When i) $\beta = 1$	151 /458

δ_a \ ρ	0	1/4	1/2	3/4	1.0	1.5	2.0	3.0
0	7.00	5.10	4.27	3.66	3.22	2.60	2.18	1.67
0.20	10.20	7.65	6.39	5.50	4.83	3.90	3.28	2.47

ρ \ δ_a	0	0.05	0.10	0.15	0.20
1.0	3.22	3.62	4.02	4.42	4.83

When
ii) $0.5 \leqq \beta \leqq \sqrt{2}$

β	$\rho=1/2$		$\rho=1$		$\rho=2$	
	$\delta_a=0$	$=0.20$	$\delta_a=0$	$=0.20$	$\delta_a=0$	$=0.20$
0.5	2.65	3.71	2.34	3.39	2.03	3.00
1.0	4.27	6.39	3.22	4.83	2.18	3.28
$\sqrt{2}$	6.14	9.16	4.12	6.08	2.85	4.10

Where $\rho = \tau_b/\tau_a$

When
B) $\tau_a < \tau_{a\min}$, $\tau_b < \tau_{b\min}$

$$k = \frac{(1+\beta^2)^2}{\beta^2(1+2\delta_a)} + \frac{2(\tau_a+\tau_b\beta^2)}{\beta^2(1+2\delta_a)}$$

(Where m=1, n=1)

$$k = \frac{(1+4\beta^2)^2+32\tau_b\beta^2}{\beta^2}$$

(Where m=1, n=2)

$$k = \frac{(4+\beta^2)^2+32\tau_a}{4\beta^2(1+2\delta_a)}$$

(Where m=2, n=1)

No.	Dia. & Bound. Cond.	Formulas or Tables of Results	Ref.-Remarks
111	Case in which many reinforcing members are placed at equal intervals longitudinally and laterally 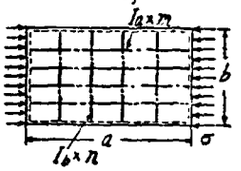 	i) End with 4 sides rotating $\sigma_k = \frac{\pi^2 aE}{bt}\left\{\frac{I_a(m+1)}{a^3}+\frac{I_b(n+1)}{b^3}\right\}$ ii) End with 4 sides fixed $\sigma_k = \frac{4\pi^2 aE}{bt}\left\{\frac{I_a(m+1)}{a^3}+\frac{I_b(n+1)}{b^3}\right\}$ iii) Ends with sides a fixed, sides b rotating $\sigma_k = \frac{16\pi^2 aE}{3bt}\left\{\frac{3I_a(m+1)}{16a^3}+\frac{I_b(n+1)}{b^3}\right\}$ iv) End wi th sides a rotating, sides b fixed $\sigma_k = \frac{4\pi^2 aE}{bt}\left\{\frac{I_a(m+1)}{a^3}+\frac{3I_b(n+1)}{16b^3}\right\}$	153
112	Square plate having diagonal reinforcing member, end with 4 edges rotating 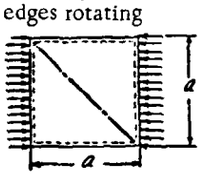 	$\sigma_k = 8.9\sigma_e$	154

SHEAR

No.	Dia. & Bound. Comp.	Formulas or Tables of Results	Ref.-Remarks
113	One lateral reinforcing member, ends with 4 sides rotating 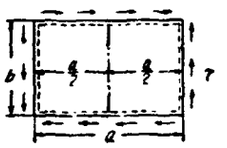 	$\tau_k = \frac{9\pi^2(1+\beta^2)^2}{32\beta^3}\sqrt{1+\frac{2\tau\beta^3}{(1+\beta^2)^2}}\,\sigma_e$ (when $\tau < \tau_{min}$) Values of τ_{min} β | 2.0 | 1.5 | 1.25 | 1.0 τ_{min} | 1.66 | 4.35 | 7.88 | 15 The case when $\tau > \tau_{min}$ matches the critical values when supported at position of reinforcing member	155 $\sigma_e = \frac{E\pi^2}{12(1-\nu^2)} \times \left(\frac{t}{b}\right)^2$ $\tau = \frac{E.I}{Db}$ $\beta = \frac{a}{b}$

/459

No.	Dia. & Bound. Cond.	Formulas or Tables of Results	Ref.-Remarks
114	Ends with 4 sides rotating, 2 reinforcing members	When $\tau_k = k\sigma_c$	156 /460

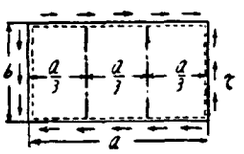

i) $\tau > \tau_{min}$

β	1.0	1.2	1.5	2.0	2.5	3.0
k	54.4	38.8	26.4	16.06	11.6	9.42
τ_{min}	40.0	27.6	16.9	7.2	3.5	2.0

ii) When $\tau < \tau_{min}$

$\beta = 1.0$

τ	0	10	20	30	40
k	11.55	32.75	41.6	48.5	54.4

$\beta = 1.2$

τ	24	30	36
k	36.7	40.1	43.2

$\beta = 1.5$

τ	0	7.5	15	22.5
k	8.09	19.43	25.2	29.5

$\beta = 2.0$

τ	0	4	10	20
k	6.74	13.07	18.2	23.8

$\beta = 2.5$

τ	0	2.5	5.0	7.5
k	6.21	10.3	13.1	15.1

$\beta = 3.0$

τ	0	0.6	1.2	1.8	2.4
k	6.04	7.29	8.39	9.21	9.59

No.	Dia. & Bound. Cond..	Formulas or Tables of Results	Ref.- Remarks
115	Strip having end with edges rotating, and many reinforcing members at equal intervals 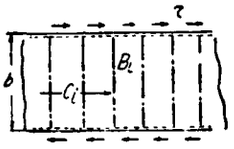	$\tau_k = k\,\sigma_c$ τ_1: 5, 10, 20, 30, 40, 50 k: 6.98, 7.70, 8.67, 9.36, 9.90, 10.4 τ_1: 60, 70, 80, 90, 100 k: 10.8, 11.1, 11.4, 11.7, 12.0 $\tau_1 = \frac{2\sum_i B_i \sin^2\frac{\pi c_i}{b}}{Db}$ B_1 is the bending stiffness of the reinforcing member at a distance c_i from one end	155 /461
116	Square plate having a diagonal reinforcing member, end with 4 edges rotating 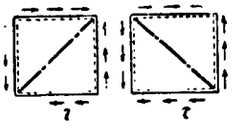	i) Case in which tension force acts on reinforcing $\tau_k = k\,\sigma_c$ $k = 11.75$ ii) Case in which compressive force acts on reinforcing member $\tau_k = 30.6\,\sigma_c$	157 157

BENDING

No.	Dia. & Bound. Cond.	Formulas or Tables of Results	Ref.-Remarks
117	Single longitudinal reinforcing member, in case of pure bending, end with 4 rotating edges 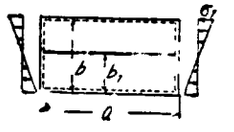	$\sigma_{1k} = k\,\sigma_c$ i) $a = 0.8\,b$, $b_1 = 0.75\,b$. when $\delta = 0.12$ where $\frac{i}{t} = \sqrt{\frac{\tau}{12(1-\nu^2)\delta}}$ 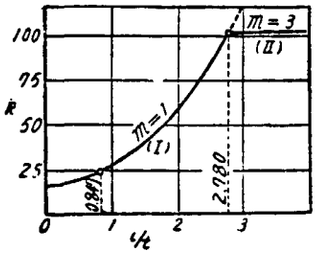	159 I is the shape of buckling together reinforcing member II is the shape forming a segmented line of the position of the reinforcing member

No.	Dia. & Bound. Cond.	Formulas or Tables of Results	Ref.-Remarks
117		When ii) $b_1=\frac{b}{2}$ $\sigma_{1k}=\sigma_e\frac{225\pi^2}{32}\frac{1+4\beta^2}{\beta^3}\times$ $\sqrt{\frac{(1+\beta^2)^2(1+9\beta^2)^2+2\gamma[(1+\beta^2)^2+(1+9\beta^2)^2]}{36(1+\beta^2)^2+54(1+9\beta^2)^2+5408\gamma}}$ $=k\sigma_e$ 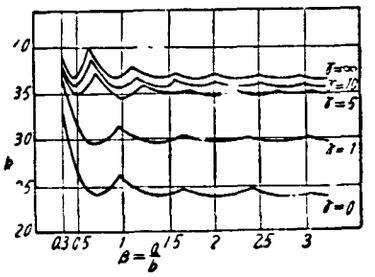 Table of k	161

β \ γ	0	1	5	10	∞
0.35	32.4	36.0	37.5	37.8	38.2
0.40	29.4	33.6	35.82	36.25	37.0
0.45	27.0	31.8	35.0	35.6	36.43
0.50	25.6	30.9	34.92	36.0	37.2
0.55	24.7	30.25	35.2	36.6	—
0.60	24.2	30.0	35.9	37.7	40.4
0.65	23.9	29.8	36.8	39.0	—
0.70	23.95	29.8	37.7	40.5	45.2
0.75	24.21	30.0	—	—	—
0.80	24.66	30.3	—	—	—
0.85	25.15	30.6	—	—	—
0.90	25.6	31.0	—	—	—
0.95	26.3	—	—	—	—
1.00	27.2	32.8	—	—	—

No.	Dia. & Bound. Cond.	Formulas or Tables of Results	Ref.-Remarks
118	Bending and compression reinforcing member on on one side of a, end with other 3 sides rotating 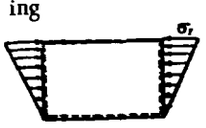	$\sigma_{cr}=k\sigma_c$ The values of k are given in the diagram 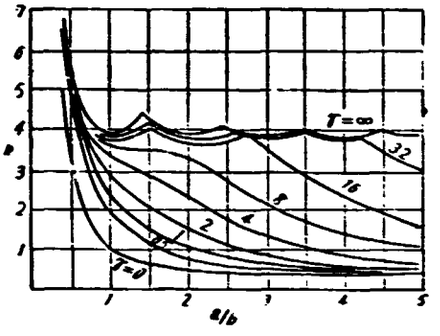	158

/463

COMPRESSION AND SHEAR

No.	Dia. & Bound. Cond.	Formalas or Tables of Results	Ref.-Remarks
119	End with 4 edges rotating one longitudinal reinforcing member 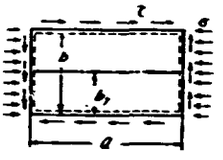	When $a/b=1.6$, $\delta=0.24$, $b_1=b/2$ 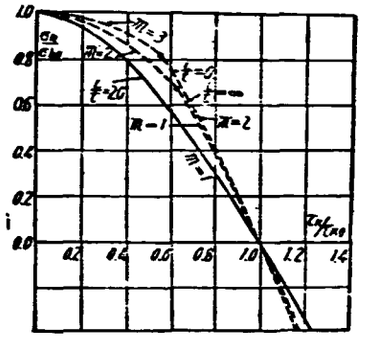 where σ_{cr0}, τ_{i0} respectively are the critical values when they act individually $\frac{i}{t}=\sqrt{\frac{\tau}{12(1-\nu^2)\beta}}$	159

ULTIMATE LOAD DUE TO COMPRESSION

No.	Dia. & Bound. Cond.	Formulas or Tables of Results	Ref.-Remarks
120	Reinforced rectangular plate under compression 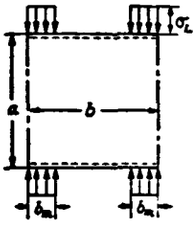	i) The assumption is made that the ultimate load is obtained from the Euler buckling of a column consisting of the effective widths of a reinforcing member and a flat plate $P_{ult}=\sigma_L(A_L+b_m t)$. If we posit σ_L, and assume that by finding the effective width b_m after the buckling of a flat plate, the effective width acts together with the reinforcing member, and then finds the value at which the buckling stress of a long column consisting of the above and the reinforcing member is equal to σ_m, P_{ult} is found from kthe above equation with respect to a single reinforcing member. When there are plates on both sides of the reinforcing member, B_m is taken for both sides.	

No.	Dia. & Bound. Cond.	Formulas or Tables of Results	Ref.-Remarks
120		For the ultimate load of the overall reinforced plate, there are some authors who would add the load $\sigma_L(b-2b_m)t$ acting on panels other than the effective section in the above equation, and others who would disregard this. For b_m, the following equations are used	
		a) $2b_m = 1.7t\sqrt{E/\sigma_L}$ With respect to interval between reinforcing members	163 164
		$= 1.6t\sqrt{E/\sigma_L}$ With respect to the outside portion of reinforcing members	166 175 175
		b) b_m is determined by the graph below	
		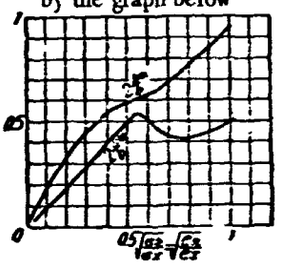 b_m' is taken as the effective width and the reinforcing member when calculating σ_L	
		c) $2b_m = b(0.50+1.82\lambda^2)$	165
		$\lambda = \sqrt{\frac{E}{\sigma_L}} \cdot \frac{t}{b}$	
		d) $2b_m = 2.52t\sqrt{E/\sigma_L}$	171
		When the proper materials in the reinforcing member and the flat plate are different	
		$2b_m = 2.52t\frac{\sigma_{PL}}{\sigma_L}\sqrt{\frac{E}{\sigma_L}}$	
		Where σ_{PL} is the compressive stress of a flat plate when a compressive strain is generated which equal to the strain of	
		e) the reinforcing member with respect to σ_L. b_m' is used for the effective width	168
		$b_m' = b_m + \varepsilon_L \frac{db_m}{d\varepsilon_L}$	
		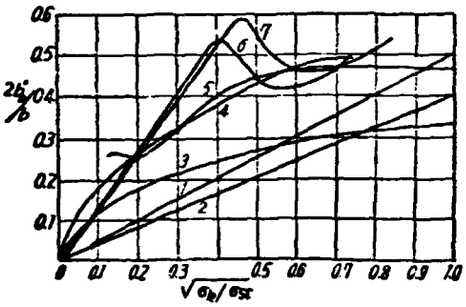	
		1. Karman's calculated values 2. As above (corrected values, from experiment values) 3. Cox (rotating end) 4. Cox (fixed end) 5. Marguerre 6. Wagner (free with indirection inside plane) 7. Wagner (fixed in direction inside plane)	

No.	Dia. & Bound. Cond.	Formulas or Tables of Results	Ref.-Remarks
120		The ultimate load is determined by finding the effective width b'_m with respect to σ_L, and determining the buckling stress of a reinforcing member to which the effective width is applied. Moreover, if a value is obtained in which there is no great difference between this ultimate load, and that which is found from the relationship $P=\sigma_L(A_L+b_m t)$ the value is considered to be P_{ult}. f) it is assumed that the load-contraction curve after the buckling of the flat plate is a straight line. The stress σ_{ult} in the case of ultimate load is $\sigma_{ult}=\left\{(H+1)\sigma_{ult}'-\frac{n-1}{n}\sigma_k'\right\}\Big/\left(H+\frac{1}{n}\right)$ where $H=2A_L/bt$ (it is assumed that there is a reinforcing member A_L in the center of the width b). $n=\frac{d\sigma_L}{d\sigma_m}$ (σ_m: average compressive stress) i.e. $\frac{1}{n}$ gives the coefficient of the effective width and $\sigma_{ult}'=(\sigma_k bt+A_L\sigma_{kL})/(bt+A_L)$. σ_{ult}' gives the ultimate stress in the case where $\sigma_k' \geqslant \sigma_{ult}'$. Moreover, σ_{kL} is the buckling stress of the reinforcing member and σ_k' is the buckling stress of the plate of half-widths. g) When the ultimate load is not very great in comparison with the buckling load of the flat plate, assuming the effective width to be a constant $\frac{1}{2}b$ the buckling of a column consisting of the effective width and the reinforcing member is found, and then the point of yield due to the resultant forces of the bending stress of the column and the compressor stress is considered to be the ultimate load. i.e. $P_{ult}=\hat{\varepsilon}E\left(A_L+\frac{1}{2}bt\right)+\frac{1}{2}\sigma_k bt$ For soft steel (from experiments) $\hat{\varepsilon}=0.167\frac{I}{A'_L l^2}\left(\frac{l}{2\eta}\right)^{1.6}$ where $\frac{I}{A_L' l^2}\left(\frac{l}{2\eta}\right)^{1.6}<6.6\times10^{-3}$ $=9.70\times10^{-4}+0.020\frac{I}{A_L' l^2}\left(\frac{l}{2\eta}\right)^{1.6}$ $\eta > 6.6\times10^{-3}$ where $A_L'=A_L+\frac{1}{2}bt$, η is the distance from the neutral axis of the cross-section A_L' to the edge of the reinforcing member, I is the geometric moment of inertia of A_L', l is the length of the reinforcing member.	172 176 /465

No.	Dia. & Bound. Cond.	Formulas or Tables of Results	Ref.-Remarks
120		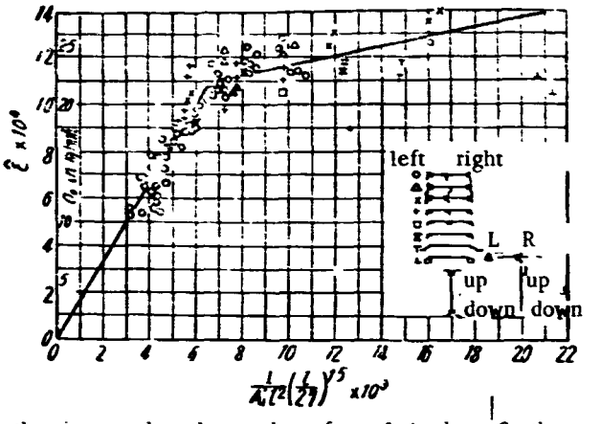	/466

In the above, when the number of panels is above 2, the sum of the loads found for the reinforcing members of each panel becomes the overall ultimate load.

b) $P_{ult}=P_0+Kb^{\frac{1}{2}}t$ 169

$K=125{,}000\,A_L^{\frac{1}{3}}$ (balanced Z type)

$=131{,}000\,A_L^{\frac{1}{3}}$ (unbalanced Z type)

P_0 is the extreme load of the reinforcing member when there is no flat plate

ii) based on the torsion bending load 166

$$\sigma_k'=\frac{\bar{G}J}{I_p}+\frac{C_{BT}}{I_p}\frac{n^2\pi^2\bar{E}}{L^2}+\frac{K_1E\,t^2}{6(1-\nu^2)d\,I_p}\frac{L^2}{n^2\pi^2}$$

where $\bar{E}=(E'C_{BT1}+E\,C_{BT})/C_{BT}$

$\bar{G}=\frac{1}{2}G(\alpha+\sqrt{\alpha})$

$\alpha=\bar{E}/E$

u is the degree of longitudinal movement when $\theta=\frac{d\varphi}{dx}=1$

$C_{BT}=\int u^2\,dA$

$E'=$ sine elasticity modulus

$K_1=2+\frac{\pi^2}{3}\left(\frac{nd}{L}\right)^2+\frac{\pi^4}{60}\left(\frac{nd}{L}\right)^4$

$d=$ center of reinforcing member

$n=$ integer

The smaller value between the bending rupture stress of the plate and σ_k is taken, and the ultimate load is determined by multiplying the area of the reinforcing member and the effective portion of the plate.

120

Moreover, for the effective width b_m, von Karman's equation is used for the side away from the attached rivets of the reinforcing member (refer to the figure below)

Details of reinforcing member

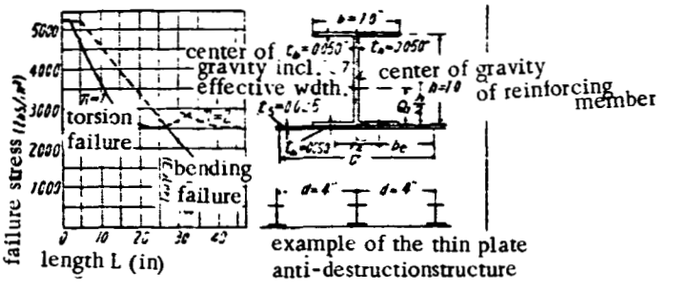

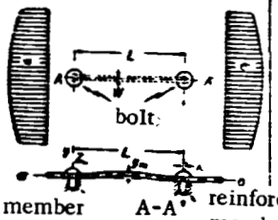

iii) Case considered to be due to the buckling of a plate between the centers of the bolts attached to reinforcing members

a) Maximum compressive stress σ_c of section between bolts (width w) | 177

$$\sigma_c = \frac{\pi^2 E t^2}{3 L^2}$$

stress of reinforcing member σ_{st}

$$\sigma_{st} = \lambda_t \frac{E}{L}$$

$$= \frac{E}{L^2}\left[\left(\frac{\sigma_t L^2}{2\pi E t} - \frac{\pi t}{6}\right)^2 + \frac{\pi^2 t^2}{3}\right]$$

λ_t = degree of contraction of section between bolts

σ_t = maximum stress sustained by the above

Determining σ_t in the case in which the σ_t is equal to the stress occurring in dangerous permanent deformation,

$P_{ult} = \sigma_{st}(A_L + b_m t)$. The values of σ_{st} when $\sigma_t = 2300$ lbs/in² are given in the following diagram

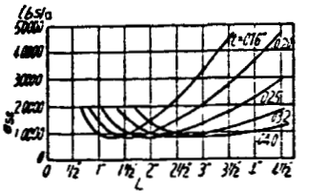

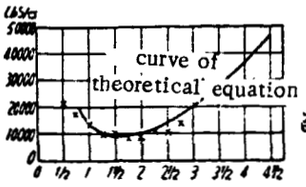

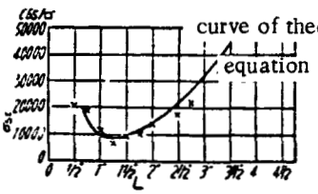

No.	Dia. & Bound. Cond.	Formulas or Tables of Results	Ref.-Remarks
120		b) Effect of center of rivet on ultimate load 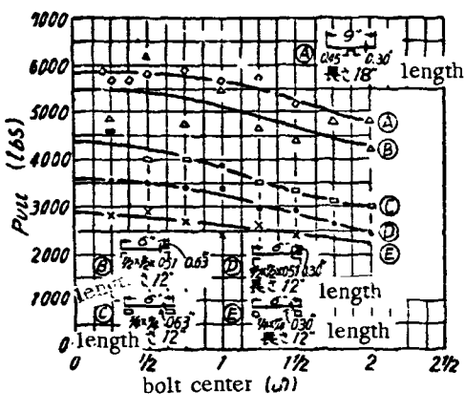 	177
		c) In order to make σ_{-t} and σ_t below the proportional limit σ_p $\frac{L}{t}=1.814\sqrt{\frac{E}{\sigma_p}}$, or $\frac{L}{t}=6.535\sqrt{\frac{E}{\sigma_p}}$	177
121	flat plate reinforced by corrugated plate 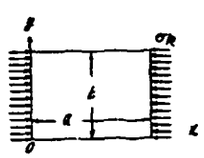 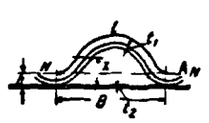	Buckling load P_k $P_k=\left(2\sqrt{D_x D_y}+2D_{xy}\right)\frac{\pi^2}{b^2}$. $\frac{n^2}{m^2}=\left(\frac{a}{b}\right)^2\sqrt{\frac{D_y}{D_x}}$ (m, n= number of half-waves x, y Considering the deformation of a flat plate $D_x=E\left(t_1\int z^2\sqrt{1+z'^2}\,dx-h^2\left(\int\sqrt{1+z'^2}\,dx+t_1\right.\right.$ $\left.\left.+Bt_2\sqrt{P'_k/P}\right)\right)\Big/B$ (P_k' is the buckling load of the plate only) $D_y=K\frac{Et_1^3}{12(1-\nu^2)}\left[\frac{B}{L}+\left(\frac{t_1}{t_2}\right)^3\right]$ $D_{xy}=\frac{Et_1}{1-\nu^2}\frac{2(\varepsilon_{max}/2)^3}{1-\nu}\frac{t_1/t_2}{1.218\,t_1/t_2+1}+2D_{xy}'$. D_{xy}' is the value of the currugated plate only	174

Local Buckling

No.	Dia. & Bound. Cond.	Formulas or Tables of Results	Ref.-Remarks
122	Channel compression 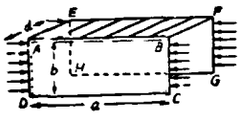	$\sigma_k = k\sigma_e$ $\mu b = 2$ a/b | 1.0 | 1.3 | 1.5 | 1.6 | 1.8 | 2.0 k | 1.50 | 1.13 | 1.01 | 0.97 | 0.92 | 0.896 a/b | 2.3 | 2.5 | 2.7 | 2.9 | 3.0 | 4.0 k | 0.89 | 0.905 | 0.928 | 0.958 | 0.976 | 0.90 $\mu b = 8$ a/b | 1.0 | 1.3 | 1.5 | 1.8 | 2.0 k | 1.58 | 1.25 | 1.16 | 1.11 | 1.12 a/b | 2.3 | 2.5 | 2.7 | 3.0 | 4.0 k | 1.18 | 1.23 | 1.22 | 1.16 | 1.12 $\mu b = \frac{D'}{D}\frac{2b}{d}$ D is side plate (B C and F G) D' is bending stiffness of top plate (B F) n Form of buckling 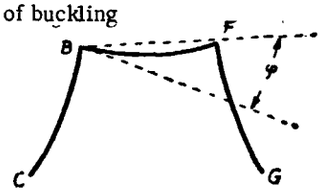	181 182 In this section we are dealing with the compound flexural torsional buckling consisting of local buckling causing ripples on the flanges and webs together with bending and torsion. In addition to this there is Euler buckling and torsion buckling due to bending but see Part 2 for this.
123	Compression of channel type and Z type	Buckling of flange $\sigma_{kF} = k_F \frac{\pi^2 E}{12(1-\nu^2)}\left(\frac{t_F}{b_F}\right)^2$ Buckling of web $\sigma_{kw} = k_W \frac{\pi^2 E}{12(1-\nu^2)}\left(\frac{t_w}{b_W}\right)^2$	183

No.	Dia. & Bound. Cond.	Formulas or Tables of Results	Ref.-Remarks
123		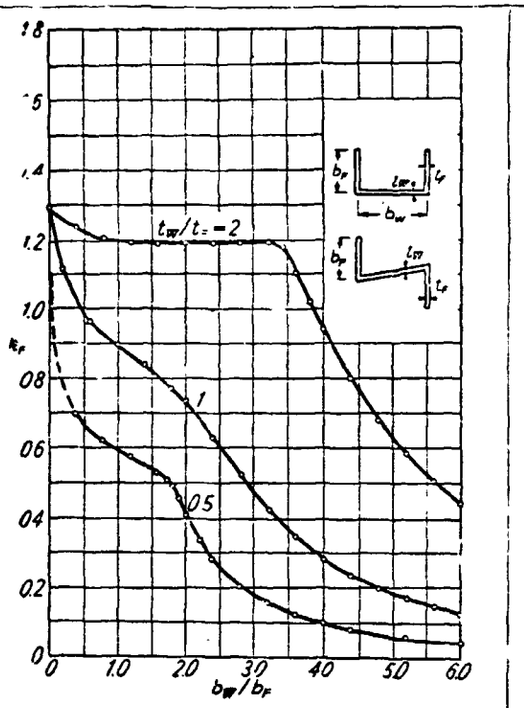 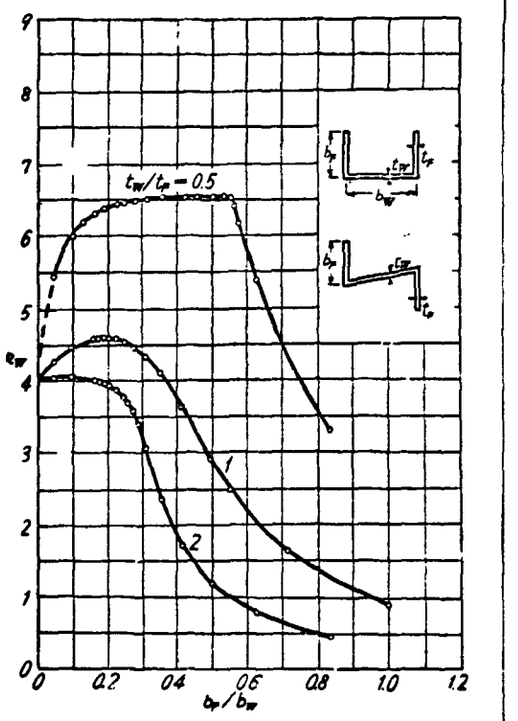	/470

No.	Dia. & Bound. Cond.	Formulas or Tables or Results	Ref.-Remarks
123		With respect to the critical stress above the proportional limit, assuming an effective elasticity modulus $\overline{E}$ $\alpha = \overline{E}/E$ From $\eta = \frac{\alpha + 3\sqrt{\alpha}}{4}$ If (η is the experiment value, it is used). if $\sigma_k = \eta k \sigma_e$ is assumed The maximum load occurs at the same time as σ_k is reached.	/471
124	Compression of channel cross-section 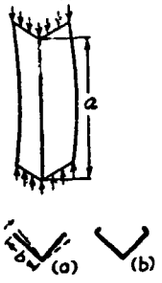 	$\sigma_k = k\sigma_e$ a/b: 0.5 | 1.0 | 1.2 | 1.4 | 1.6 | 1.8 k: 4.40 | 1.44 | 1.14 | 0.952 | 0.835 | 0.755 a/b: 2.0 | 2.5 | 3.0 | 4.0 | 5.0 k: 0.698 | 0.610 | 0.546 | 0.516 | 0.506 In the case of Figure b [], this is based on the channel cross-section value. When there is eccentricity e $\sigma_k = \frac{b(0.456 + b^2/a^2)}{b + 4e}\sigma_e$	182
125	Compression of equilateral channel cross-section having small flanges 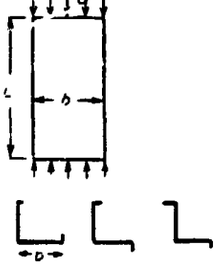 	$\sigma_k = k_m \frac{E}{12(1-\nu^2)}\left(\frac{t}{b}\right)^2$ The values of k_m are given in the graph below 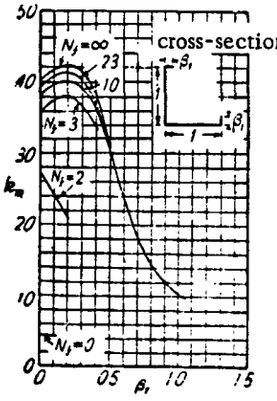 	184 185

No.	Dia. & Bound. Cond.	Formulas or Tables of Results	Ref.-Remarks
125		where $N_f=(1-\nu^2)\left(\frac{b}{t}\right)^2 \frac{\beta_1^2(\beta_1+4\beta_2+m)}{\beta_2(\beta_1+\beta_2+m)}$ $-3.582\frac{\beta_1}{\beta_2}$. $\alpha_m=\frac{B_m}{b}$, $\beta_n=\frac{b_n}{b}$. α_m given in the table below	/472

l/b_2	6.28	3.14	1.57	1.046	0.785
α_m	0.480	0.427	0.295	0.196	0.139

moreover, l is the half-wavelength, n is the number of sides (considering the end plane a[illegible] b is the standard width

126	Compression of C shape and Hut cross-section 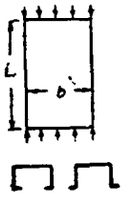	$\sigma_k=k_m\frac{E}{12(1-\nu^2)}\left(\frac{t}{b}\right)^2$ (When N_f and others involve the case of equilateral channel cross-sections with small flanges attached, same as in materials [125] 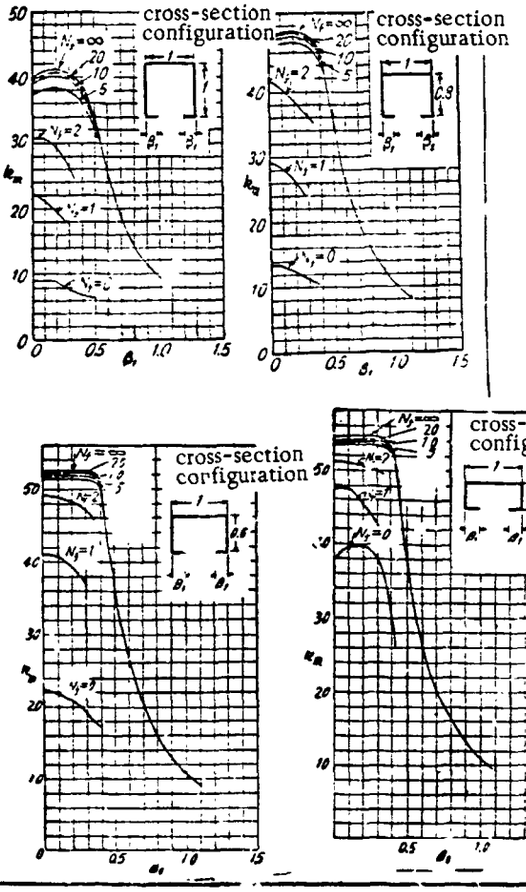	184 185

No.	Dia. & Bound. Cond.	Formulas or Tables of Results	Ref.-Remarks
125		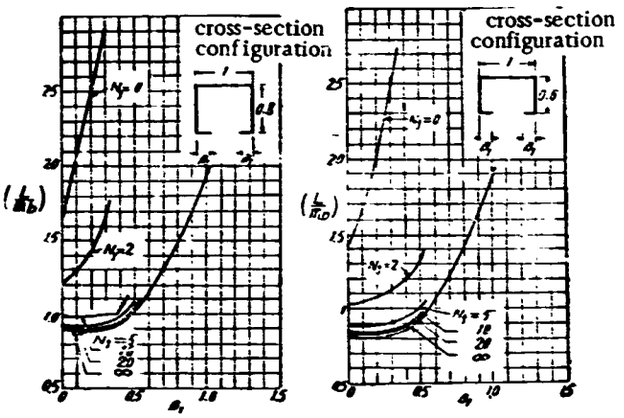 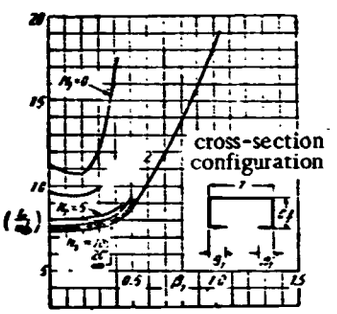 Stress at time of maximum load $\sigma_{cr,t}=\sqrt{\frac{k_m E \sigma_P}{12(1-\nu^2)}}\left(\frac{t}{b}\right)$. $(\sigma_k<\sigma_P)$ $\sigma_{cr,t}=\frac{k_m E}{12(1-\nu^2)}\left(\frac{t}{b}\right)^2$. $(\sigma_k>\sigma_P)$	/473
127	Compression of hollow square cross-section 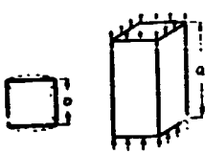	Based on the condition of an end with sides rotating $\sigma_k=(mb/a+a/mb)^2\sigma_e$	182

No.	Dia. & Bound. Cond..	Formulas or Tables of Results	Ref.-Remarks
123	Compression of hollow rectangular cross-section 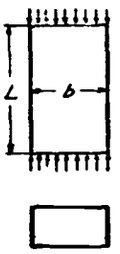	$\sigma_k = k_m \frac{E}{12(1-\nu^2)} \left(\frac{t}{b}\right)^2$. 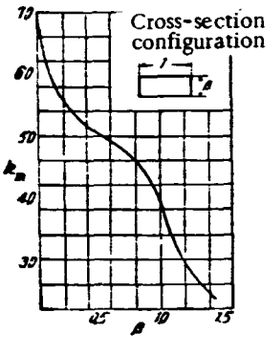	184
129	Compression of hollow open web cross-section 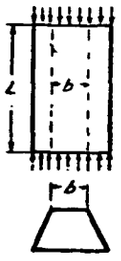	$\sigma_k = k_m \frac{E}{12(1-\nu^2)} \left(\frac{t}{b}\right)^2$. 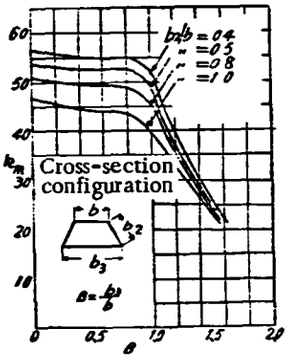	184
130	Compression of hollow triangular cross-section 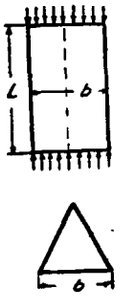	$\sigma_k = k_m \frac{E}{12(1-\nu^2)} \left(\frac{t}{b}\right)^2$. 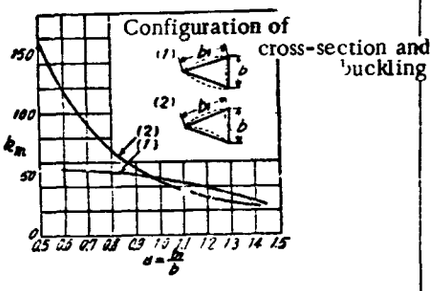	184

No.	Dia. & Bound. Cond.	Formulas or Tables of Results	Ref.-Remarks
131	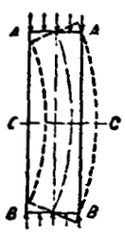 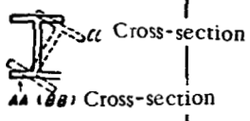 Cross-section Cross-section	Equilibrium condition $\frac{d^2\varphi}{dx^2} EC_{BT} + \frac{d\varphi}{dx}(P \cdot i_{SP}^2 - GJ_T) = 0.$ Critical buckling load $P_k = \frac{1}{i_{SP}^2}\left(GJ_T + \frac{\pi^2}{l^2} EC_{BT}\right).$ where $C_{BT} = \int u^2 \, dF.$ u is degree of longitudinal movement when $\frac{d\varphi}{dx} = 1$ φ : twist angle $i_{SP}^2 = \frac{1}{F}\int r^2 dF + e \cdot \frac{1}{I}\int \eta r^2 dF.$ r : distance from center of rotation η : distance from neutral axis e : degree of eccentricity of load GJ_T : torsion stiffness of cross-section F : cross-section area experiment on duraluminum column 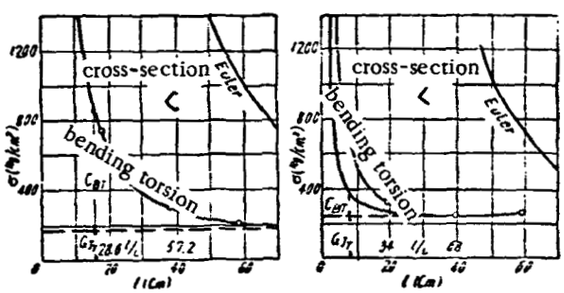 	187
		$C_{BT} = C_B + C_T.$ $C_B = \int u^2 t \, ds.$ $C_T = \frac{1}{12}\int t^3 \, ds.$ t = thickness s : length along center line in cross-section generally $C_{BT} = (C_{BT})_{\substack{P=0 \\ Q=0}} + I_x \cdot P^2 + I_y \cdot Q^2.$ I_x, I_y are respectively the geometric moments of inertia around the principal axes x and y of the cross-section, P, Q are the coordinates z and y of the center point with respect to the rotating component of the degree of movement of one end wi th respect to the other ends (with shear center as origin).	188

No.	Dia. & Bound. Cond.	Formulas or Tables of Results	Ref.-Remarks
131		Determining the conditions giving the minimum failure stress from this $P=0,\quad Q=0$ (rotationg axis is shear center) $P=0,\quad Q=\infty$ / $P=\infty,\quad Q=0$ case in which the axis of rotation is at some point of infinite distance on the principal axis these conditions determined from any of the above. In the case of a I cross-section column $\sigma_k=KG\frac{t_h^2}{h^2}+K_{BT}\frac{\pi^2 E t_b^2}{12 L_0^2}$. $K=\frac{4+8\frac{b}{h}\left(\frac{t_b}{t_h}\right)^3}{1+\left(2\frac{b}{h}\frac{t_b}{t_h}\right)\left(3+\left(\frac{b}{h}\right)^2\right)+12\left(1+2\frac{b}{h}\frac{t_b}{t_h}\right)\left(\left(\frac{P}{h}\right)^2+\left(\frac{Q}{h}\right)^2\right)}$ $K_B=\frac{6\left(\frac{b}{t_h}\right)^2\frac{t_b}{h}+12\left(\frac{P}{t_h}\right)^2\left(1+6\frac{b}{h}\frac{t_b}{t_h}\right)+24\left(\frac{b}{h}\right)^2\left(\frac{Q}{t_h}\right)^2\frac{t_b}{t_h}}{1+\left(2\frac{b}{h}\frac{t_b}{t_h}\right)\left(3+\left(\frac{b}{h}\right)^2\right)+12\left(1+2\frac{b}{h}\frac{t_b}{t_h}\right)\left(\left(\frac{P}{h}\right)^2+\left(\frac{Q}{h}\right)^2\right)}$ $K_T=\frac{1+2\left(\frac{b}{h}\right)^2\left(\frac{t_b}{t_h}\right)^3+12\left(2\frac{b}{h}\left(\frac{t_b}{t_h}\right)^2\left(\frac{P}{h}\right)^2+\left(\frac{Q}{h}\right)^2\right)}{1+\left(2\frac{b}{h}\frac{t_b}{t_h}\right)\left(3+\left(\frac{b}{h}\right)^2\right)+12\left(1+2\frac{b}{h}\frac{t_b}{t_h}\right)\left(\left(\frac{P}{h}\right)^2+\left(\frac{Q}{h}\right)^2\right)}$ when $K_{BT}=K_B+K_T$. $\frac{b}{h}<\sqrt[3]{\frac{t_h}{t_b}}$, minimum failure occurs due to the bend ing of the axis parallel to the web.	/476

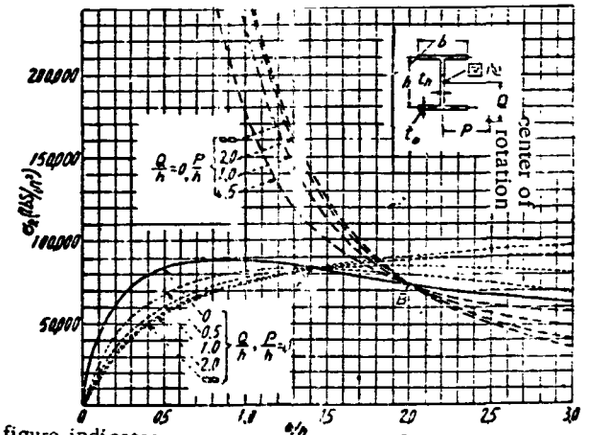

(the figure indicates the cases in which $b=2''$, $t_b=t_h=0.1''$, $E=10^7$ lbs/in²)

No. Dia. & Bound. Cond.	Formulas or Tables of Results	Ref.-Remarks
131	$\sigma_k = \frac{GJ}{I_p} + \frac{C_{BT}\pi^2 E}{I_p L_0^2}$ I_p = polar geometric moment of inertia L_0 = effective length When applied to duraluminum angle or channel type member, it is as given in the following graphs 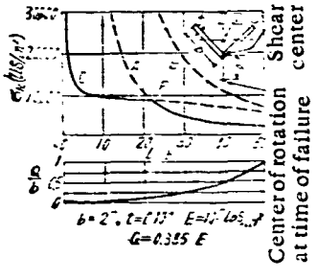 C : bending torsion failure. F : case in which the shear center is the center of rotation. A, B ; bending around axes 1-1 and 2-2 respectively (Euler buckling), when $Q \to \infty$ $C \to B$.	189 /477
	According to Kappus, since a distribution of the torsion moment in the direction of the axis occurs due to a displacement in the direction of the axis caused by torsion, the equilibrium equation $\frac{d^4\varphi}{dx^4} - EC_{BT} + \frac{d^2\varphi}{dx^2}\left(\sigma_m \tilde{J}_p - GJ_T\right) = 0$ the critical stress is $\sigma_{mk} = \left(GJ_T + \frac{\pi^2}{l^2} EC_{BT}\right) \Big/ \tilde{J}_p$ where $\tilde{J}_p = \int \tilde{r}^2 dF$. $\tilde{r}$ is the distance from the center of rotation D $\sigma_m = P/F$. (average compressive stress) The center point D of rotation is determined from energy equations.	190

No.	Dia. & Bound. Cond.	Formulas or Tables of Results	Ref.-Remarks
131		in an I shaped cross-section (E/G = 2.6)	

$$\sigma_{mk}=\frac{\pi^2}{l^2}E\frac{h^2b^2+0.312(h+2b)t^2l^2}{4b^3+12bh^2+2h^3}.$$

where h: web height, b: flange width

in a channel cross-section

$$\sigma_{mk}=\sigma_z+\frac{\rho_z^2}{\sigma_z}$$

$$\sigma_B=\frac{\pi^2E}{l^2}\times$$

$$\frac{h^2b^2(2h^2+15hb+26b^2)+\frac{4}{\pi^2}\left(\frac{l}{b}\right)^2(h+2b)^3t^2l^2}{(h+2b)\left\{\pi^2(h+6b)(h+2b)+4b^2(2h+b)\right\}}$$

$$\rho_z=\frac{\pi^2E}{l^2}\times$$

$$\frac{2h^2b^2(h+3b)}{(h+2b)\left[3\left\{\pi^2(h+6b)(h+2b)+4b^2(2h+b)\right\}\right]^{1/2}}$$

Where h: web height, b: flange width

When h/b = 1.0, comparing with Wagner's result σ_W, the following graph is obtained.

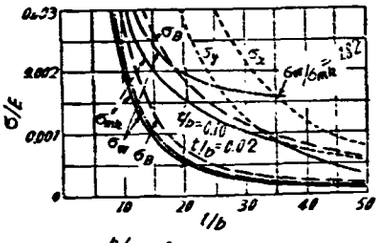

when $h/b = 1$

and $$\sigma_z=\frac{\pi^2E}{l^2}\frac{h^2(h+6b)}{12(h+2b)},$$

$$\sigma_y=\frac{\pi^2E}{l^2}\frac{b^2(2h+b)}{3(h+2b)^2}.$$

σ_B is Bleich's calculated values.

No.	Dia. & Bound. Cond.	Formulas or Tables of Results	Ref.-Remarks
132	End with 4 sides rotating 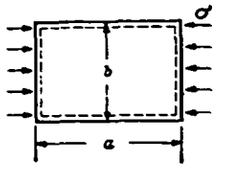	$\sigma_f^* = E_f \frac{\pi^2 D}{b^2 H} K$ Here (a) tension stiffness $H = E_f(t-t_c)+E_c t_c \fallingdotseq E_f(t-t_c)$ (b) bending stiffness $D = \frac{E_f}{12(1-\nu_f^2)}\left\{t^3 - \rho t_c^3 - \frac{3\rho t_c (t_{f_1}-t_{f_2})^2}{1-\rho\frac{t_c}{t}}\right\}$ $\rho = 1-\frac{E_c(1-\nu_f^2)}{E_f(1-\nu_c^2)}$, if both facing thicknesses are equal $t_{f_1} = t_{f_2}$. (1) when the core stiffness can be omitted $D = \frac{E_f}{12(1-\nu_f^2)}\left\{3t_{f_1}t_{f_2}\frac{(t+t_c)^2}{t-t_c} + t_{f_1}^3 + t_{f_2}^3\right\}$, when $D = \frac{E_f}{12(1-\nu_f^2)}[t^3 - t_c^3]$, $t_{f_1} = t_{f_2}$ (2) When the facing stiffness can be omitted $D = \frac{E_f t_{f_1} t_{f_2}(t+t_c)^2}{4(1-\nu_f^2)(t-t_c)}$, $D = \frac{E_f}{8(1-\nu_f^2)} t_f (t+t_c)^2$, $t_{f_1} = t_{f_2}$ (3) When the facing is very thin, and the quadruple of it can be omitted, $D = \frac{E_f}{2(1-\nu_f^2)} t t_f$ (c) Shear stiffness in direction of plate thickness $U = t_c G_c = \frac{1}{2}(t+t_c)G_c = \frac{(t+t_c)^2}{4t_c}G_c = \frac{t}{2t_c}(t+t_c)G_c$, When $t_f \ll t$, these all give the same value.	207 208

• σ_f = -overall buckling stress.
t = total plate thickness, t_f = facing thickness, t_c = core thickness
h= distance between centers of facing (approximatly, sandwich plate thickness). Subscript "f" is facing, "c" is core (as in E_f, G_c).

No.	Dia. & Bound. Cond.	Formulas or Tables of Results	Ref.-Remarks
132		(d) $K=K_f+K_m$ K_m (for a sandwich plate of normal construction) 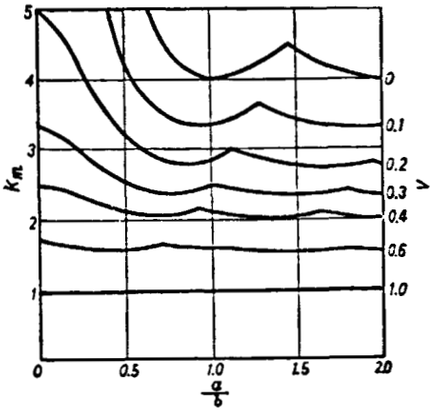	/480
133	Ends with sides a fixed, sides b rotating. 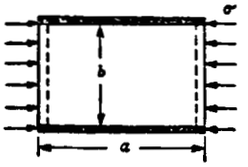	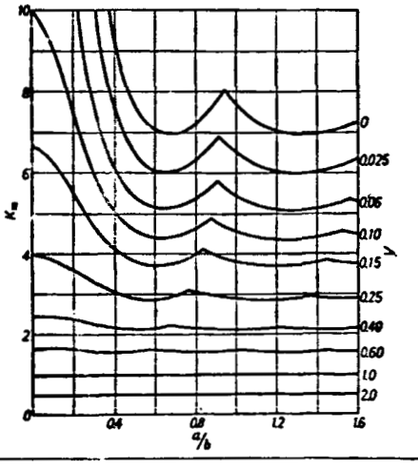	207 208
134	Ends with sides b fixed, sides a rotating. 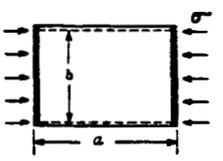	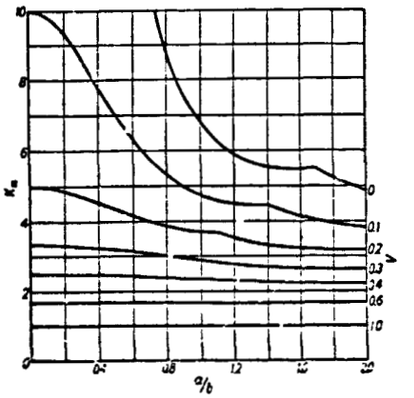	207 208

No.	Dia. & Bound. Cond.	Formulas or Tables of Results	Ref.-Remarks
135	Ends with 4 sides fixed 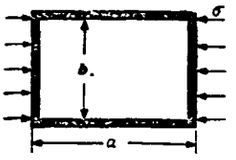	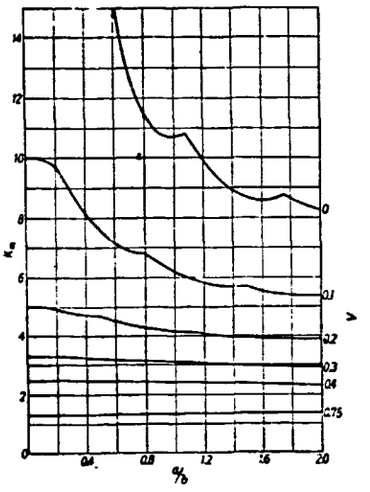	208

SIMPLE COMPRESSION (ripple type buckling)

No.	Dia. & Bound. Comp.	Formulas or Tables of Results	Ref.-Remarks
136	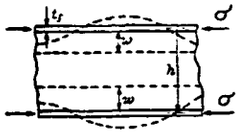	case of sine type buckling $\frac{h}{2} < w \begin{cases} \sigma_{cr} = \left(\frac{2}{3} E_f E_c \frac{t_f}{h}\right)^{\frac{1}{2}} \\ \lambda = 2\pi t \left(\frac{2}{3} \frac{E_f}{E_c} \frac{h}{t_f}\right)^{\frac{1}{4}} \end{cases}$ $\frac{h}{2} > w \begin{cases} \sigma_{cr} = 0.961 (E_f E_c G_c)^{\frac{1}{3}} \\ \lambda = 2.614 t_f \left(\frac{E_f^2}{E_c G_c}\right)^{\frac{1}{3}} \end{cases}$ $\frac{h}{2} = w \quad \{\sigma_{cr} = 0.82 (E_f E_c G_c)^{\frac{1}{3}}$ here λ = half-wavelength of ripple w = width of contour $= 0.721\, t (E_f E_c / G_c^2)^{\frac{1}{3}}$	202
137	Free end and supported end.	Cases of buckling other than of the sine type $P_{cr} = \frac{\overline{E}_f E_c t_f^3}{G_c h^2} \cdot S$ (per unit width) $f = \frac{G_c^2 h^3}{2 \overline{E}_f E_c t_f^3}$ the relationship between s and f is given by the following graph.	201

No.	Dia. & Bound. Cond.	Formulas or Tables of Results	Ref.-Remarks
137		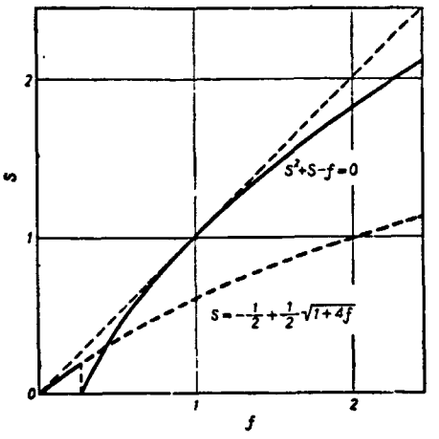	/482

SHEAR

No.	Dia. & Bound. Cond.	Formulas or Tables of Results	Ref.-Remarks
138	Ends with 4 sides rotating 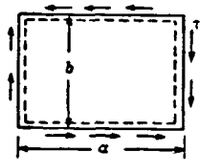	$\tau_f=\frac{\pi^2 G_f D}{b^2 N}K$ here, N = shear stiffness (in plane x, y) $=G_f(t-t_c)+G_c t_c$ $\fallingdotseq G_f(t-t_c)$ $K=\frac{4}{3}\frac{4+3\frac{b^2}{a^2}}{1+\frac{1}{3}\left(13+9\frac{b^2}{a^2}\right)V}$ when $0\leqq V\leqq\frac{1}{1+\frac{b^2}{a^2}}$ $K=\frac{1}{V}$ when $V>\frac{1}{1+\frac{b^2}{a^2}}$ where $V=\frac{\pi^2 D}{b^2 U}$, $\frac{b}{a}\leqq 1$	207 208 212
139	Edge with 4 sides fixed 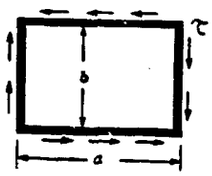	$\tau_f=\frac{\pi^2 G_f D}{b^2 N}K$ Here $K=\frac{1}{3}\frac{27+17\frac{b^2}{a^2}}{1+\frac{1}{3}\left(23+13\frac{b^2}{a^2}\right)V}$ when $0\leqq V\leqq\frac{3}{4\left(1+\frac{b^2}{a^2}\right)}$ $K=\frac{1}{V}$ when $V>\frac{3}{4\left(1+\frac{b^2}{a^2}\right)}$ where $V=\frac{\pi^2 D}{b^2 U}$, $\frac{b}{a}\leqq 1$.	207 208 212

SANDWICH PLATES WITH FACING ISOTROPIC, CORE ORTHOTROPIC (supplement)
Simple Compression

/483

No.	Dia. & Bound. Cond.	Formulas or Tables of Results	Ref.-Remarks
140	End with 4 sides rotating	$\sigma_f = E_f \frac{\pi^2 D}{b^2 H} K$	210 207

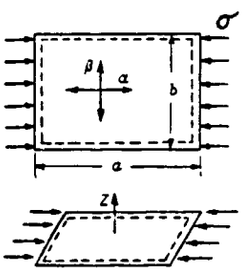

Here

$$H = E_f(t - t_c)$$

$$D = \frac{E_f}{12(1-\nu_f^2)}\left[3 t_{f_1} t_{f_2} \frac{(t+t_c)^2}{t-t_c} + t_{f_1}^3 + t_{f_2}^3\right]$$

$$K = K_f + K_m$$

$$K_f = \frac{E_f}{1-\nu_f^2} \frac{t_{f_1}^3 + t_{f_2}^3}{12 D}\left[c_1 + 2c_2 + c_3\right]$$

$$K_m = \frac{c_1 + 2c_2 + c_3 + VA\left[\frac{r}{c_4} + 1\right]}{1 + V\frac{r}{c_4}\left[c_1 + \frac{c_2}{3}\right] + V\left[c_3 + \frac{c_2}{3}\right] + V^2 \frac{rA}{c_4}}$$

$$A = c_1 c_3 - c_2^2 + \frac{c_2}{3}\left[c_1 + 2c_2 + c_3\right]$$

$$V = \frac{t_c t_{f_1} t_{f_2}}{t - t_c} \frac{\pi^2}{b^2} \frac{E_f}{(1-\nu_f^2) G_{c\alpha_2}}$$

$$r = \frac{G_{c\alpha_2}}{G_{c\beta_2}}$$

$$c_1 = c_4 = \frac{a^2}{m^2 b^2}, \quad c_2 = 1, \quad c_3 = \frac{m^2 b^2}{a^2}$$

m = number of half-wavelengths giving minimum buckling value

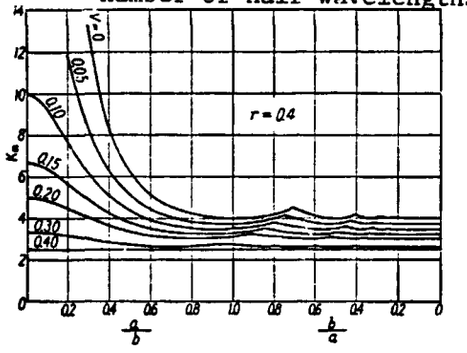

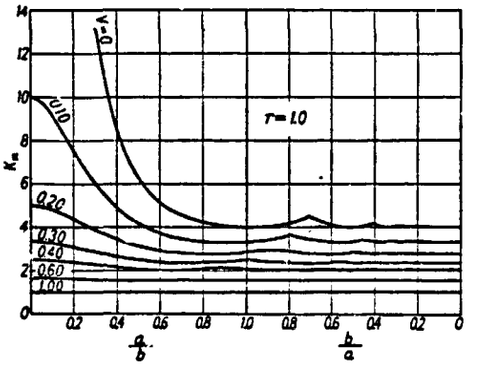

No.	Dia. & Bound. Cond.	Formulas or Tables of Results	Ref.-Remarks
140		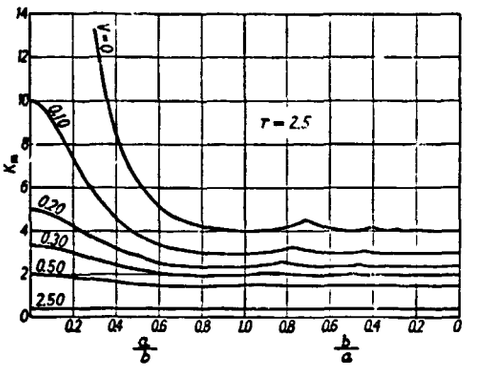	/484
141	End with sides a fixed, sides b rotating. 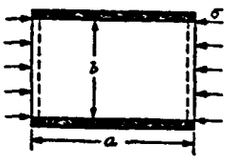	$c_1=\frac{16}{3}\frac{a^2}{\pi^2 b^2}$, $c_2=\frac{4}{3}$, $c_3=\frac{\pi^2 b^2}{a^2}$, $c_4=\frac{4}{3}\frac{a^2}{\pi^2 b^2}$ 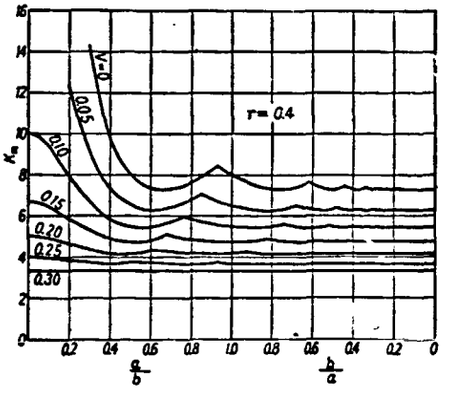 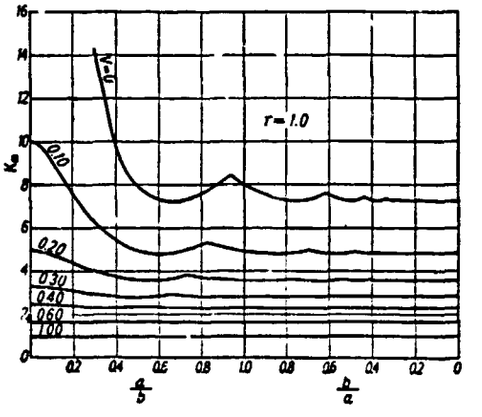	210 207

No.	Dia. & Bound. Cond.	Formulas or Tables of Results	Ref.-Remarks
141		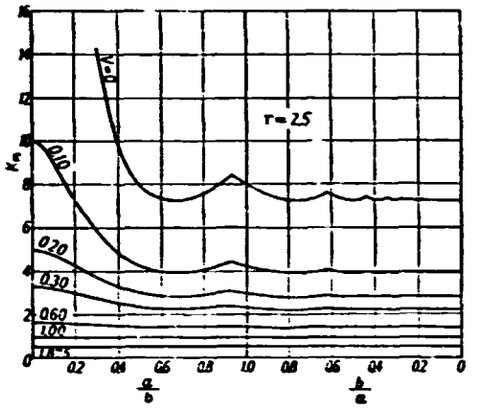	
142	Ends with sides b fixed, sides a rotating. 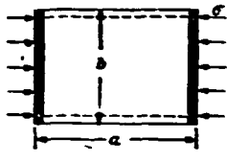	$c_1=c_4=\frac{3}{4}\frac{a^2}{b^2}$ $(\pi=1)$ $c_1=c_4=\frac{1}{\pi^2+1}\frac{a^2}{b^2}$ $(\pi>1)$ $c_2=1,\quad c_3=\frac{\pi^4+6\pi^2+1}{\pi^2+1}\frac{b^2}{a^2}$ 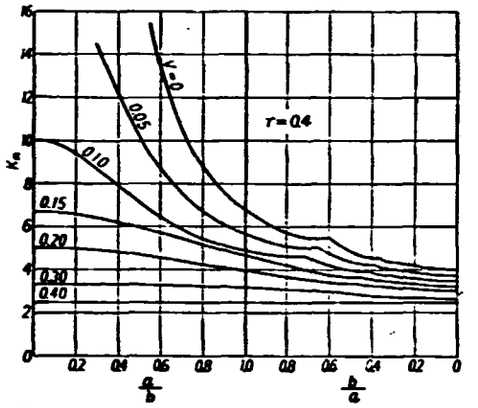 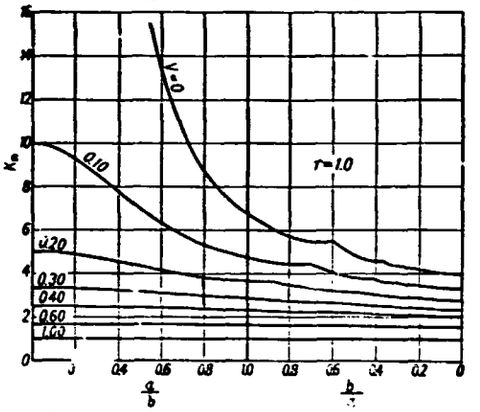	210 207

/485

No.	Dia. & Bound. Cond.	Formulas or Tables of Results	Ref.	Remarks
142		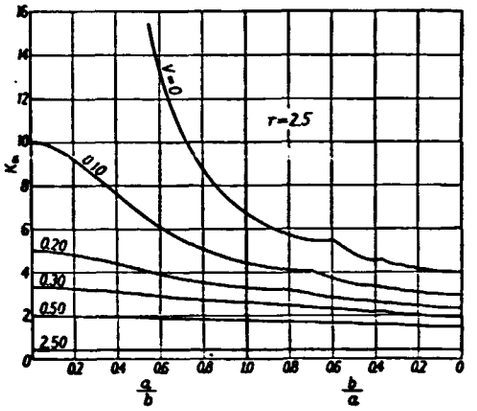		/486
143	Ends with 4 sides fixed. 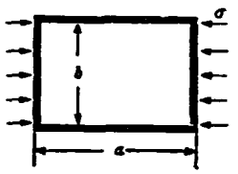	$c_1=4\,c_4=4\frac{a^2}{b^2}$ $(n=1)$ $c_1=4\,c_4=\frac{16}{3(n^2+1)}\frac{a^2}{b^2}$ $(n>1)$ $c_2=\frac{4}{3}$, $c_3=\frac{n^4+6n^2+1}{n^2+1}\frac{b^2}{a^2}$ 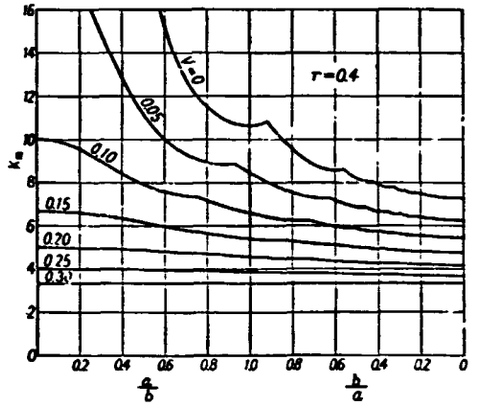 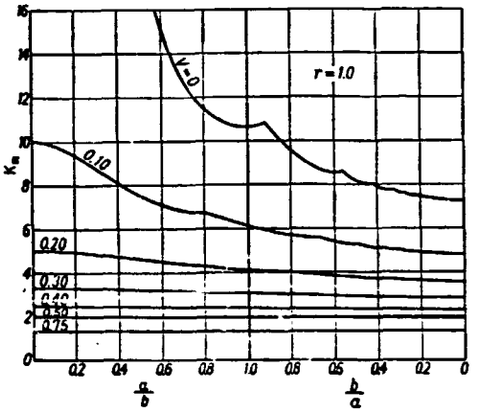	210 207	

No.	Dia. & Bound. Cond.	Formulas or Tables of Results	Ref.-Remarks
143		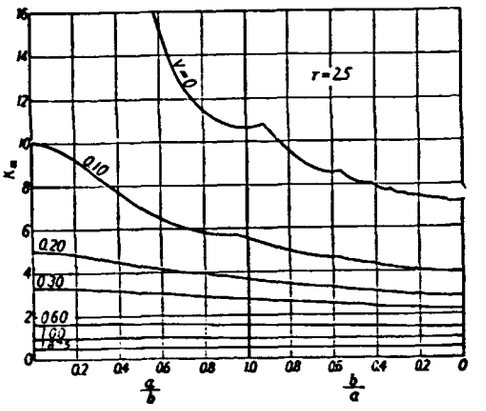	/487

ORTHOTROPIC SANDWICH PLATES (supplement)

Simple Compression

No.	Dia. & Bound. Cond.	Formulas or Tables of Results	Ref.-Remarks
144	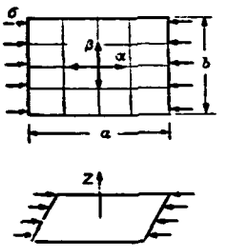	$\sigma_f=E_{f\alpha}\frac{\pi^2\sqrt{D_\alpha D_\beta}}{b^2H_\alpha}K$ Here, (a) $H_\alpha=E_{f\alpha}(t-t_c)+E_{c\alpha}t_c\fallingdotseq E_{f\alpha}(t-t_c)$ $H_\beta=E_{f\beta}(t-t_c)+E_{c\beta}t_c\fallingdotseq E_{f\beta}(t-t_c)$ (b) $D_\alpha=\frac{E_{f\alpha}}{12\lambda_f}\left\{t^3-\rho_\alpha t_c^3-\frac{3\rho_\alpha t_c(t_{f_1}-t_{f_2})^2}{1-\rho_\alpha\frac{t_c}{t}}\right\}$ $D_\beta=\frac{E_{f\beta}}{12\lambda_f}\left\{t^3-\rho_\beta t_c^3-\frac{3\rho_\beta t_c(t_{f_1}-t_{f_2})^2}{1-\rho_\beta\frac{t_c}{t}}\right\}$ $\rho_\alpha=1-\frac{E_{c\alpha}}{E_{f\alpha}}\frac{\lambda_f}{\lambda_c}$ $\rho_\beta=1-\frac{E_{c\beta}}{E_{f\beta}}\frac{\lambda_f}{\lambda_c}$ $\lambda=1-\nu_{\alpha\beta}\nu_{\beta\alpha}$ (1) when the core stiffness can be omitted $D_\alpha=\frac{E_{f\alpha}}{12\lambda_f}\left\{3t_{f_1}t_{f_2}\frac{(t+t_c)^2}{t-t_c}+t_{f_1}^3+t_{f_2}^3\right\}$ $D_\beta=\frac{E_{f\beta}}{12\lambda_f}\left\{3t_{f_1}t_{f_2}\frac{(t+t_c)^2}{t-t_c}+t_{f_1}^3+t_{f_2}^3\right\}$ when $t_{f_1}=t_{f_2}$ $D_\alpha=\frac{E_{f\alpha}}{12\lambda_f}[t^3-t_c^3]$ $D_\beta=\frac{E_{f\beta}}{12\lambda_f}[t^3-t_c^3]$	207 196

No.	Dia. & Bound. Cond.	Formulas or Tables of Results	Ref.- Remarks
144		(2) When the facing stiffness can be omitted, /488 $D_\alpha \simeq \frac{E_{f\alpha} t_{f_1} t_{f_2} (t+t_c)^2}{4\lambda_f (t-t_c)}$ $D_\beta = \frac{E_{f\beta} t_{f_1} t_{f_2} (t+t_c)^2}{4\lambda_f (t-t_c)}$ $t_{f_1}=t_{f_2}$ のときには, $D_\alpha = \frac{E_{f\alpha}}{8\lambda_f} t_f (t+t_c)^2$ $D_\beta = \frac{E_{f\beta}}{8\lambda_f} t_f (t+t_c)^2$ (3) When the core is extremely thin, and the quadruple of it can be omitted, $D_\alpha = \frac{E_{f\alpha}}{2\lambda_f} t t_c t_f$ $D_\beta = \frac{E_{f\beta}}{2\lambda_f} t t_c t_f$	
		(c) $D_{\alpha\beta}$= torsion stiffness $= \frac{G_{f\alpha\beta}}{12}\left\{t^3 - \rho_{\alpha\beta} t_c^3 - \frac{3\rho_{\alpha\beta} t_c (t_{f_1}-t_{f_2})^2}{1-\rho_{\alpha\beta}\frac{t_c}{t}}\right\}$ $\rho_{\alpha\beta} = 1 - \frac{G_{c\alpha\beta}}{G_{f\alpha\beta}}$ (1) When the core stiffness can be omitted, $D_{\alpha\beta} = \frac{G_{f\alpha\beta}}{12}\left\{3 t_{f_1} t_{f_2} \frac{(t+t_c)^2}{t-t_c} + t_{f_1}^3 + t_{f_2}^3\right\}$ $D_{\alpha\beta} = \frac{G_{f\alpha\beta}}{12}(t^3 - t_c^3)$ $t_{f_1}=t_{f_2}$ のとき (2) When the facing stiffness can be omitted, $D_{\alpha\beta} = \frac{G_{f\alpha\beta} t_{f_1} t_{f_2} (t+t_c)^2}{4(t-t_c)}$ $D_{\alpha\beta} = \frac{1}{8} G_{f\alpha\beta} t_f (t+t_c)^2$ $t_{f_1}=t_{f_2}$ のとき (3) When the facing is extremely thin, and the quadruple of it can be omitted $D_{\alpha\beta} = \frac{1}{2} G_{f\alpha\beta} t t_c t_f$	
		(d) U= shear stiffness in direction of plate thickness $U_{\alpha z} = t_c G_{c\alpha z} = \frac{1}{2}(t+t_c) G_{c\alpha z}$ $= \frac{(t+t_c)^2}{4t_c} G_{c\alpha z} = \frac{t}{2t_c}(t+t_c) G_{c\alpha z}$ $U_{\beta z} = t_c G_{c\beta z} = \frac{1}{2}(t+t_c) G_{c\beta z}$ $= \frac{(t+t_c)^2}{4t_c} G_{c\beta z} = \frac{t}{2t_c}(t+t_c) G_{c\beta z}$	
		(e) N= shear stiffness (in plane xy) $N_{\alpha\beta} = G_{f\alpha\beta}(t-t_c) + G_{c\alpha\beta} t_c$ $\fallingdotseq G_{f\alpha\beta}(t-t_c)$	

No.	Dia. & Bound. Cond.	Formulas or Tables of Results	Ref.-Remarks
144		(f) $K=K_f+K_m$ $K_f=\frac{E_{fs}}{k_f}\frac{t_{f_1}^3+t_{f_2}^3}{12\sqrt{D_\alpha D_\beta}}\left(B_1C_1+2B_2C_2+\frac{C_3}{B_1}\right)$ $K_m=\frac{B_1C_1+2B_2C_2+\frac{B_3}{B_1}+A\left(\frac{V_\alpha}{C_4}+V_\beta\right)}{1+(B_1C_1+B_2C_2)\frac{V_\alpha}{C_4}+\left(\frac{C_3}{B_1}+B_2C_2\right)V_\beta+\frac{V_\alpha V_\beta}{C_4}A}$ Here $A=C_1C_3-B_2^2C_2^2+B_2C_2\left(B_1C_1+2B_2C_2+\frac{C_3}{B_1}\right)$ $B_1=\sqrt{\frac{D_\beta}{D_\alpha}}$ $B_2=\frac{D_{\alpha\beta}+2D_{\alpha\beta}}{\sqrt{D_\alpha D_\beta}}=2B_1+B_1\nu_{f\beta\alpha}$ $B_3=\frac{D_{\alpha\beta}}{\sqrt{D_\alpha D_\beta}}$ $V_\alpha=\frac{\pi^4}{b^3}\frac{\sqrt{D_\alpha D_\beta}}{U_{\alpha_n}}$ $V_\beta=\frac{\pi^4}{b^3}\frac{\sqrt{D_\alpha D_\beta}}{U_{\beta_n}}$ C_1, C_2, C_3 and C_4 are given as follows corresponding to the boundary conditions.	/489
	End with 4 sides rotating 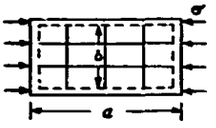	$C_1=C_4=\frac{a^2}{\pi^2b^2}$, $C_2=1$, $C_3=\frac{\pi^2b^2}{a^2}$	207 196
145	End with sides a fixed, sides b rotating 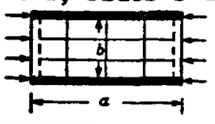	$C_1=\frac{16a^2}{3\pi^2b^2}$, $C_2=\frac{4}{3}$, $C_3=\frac{\pi^2b^2}{a^2}$, $C_4=\frac{4}{3}\frac{a^2}{\pi^2b^2}$	207 196
146	End with side b fixed, side a rotating 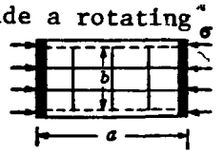	when $C_1=C_4=\frac{3}{4}\frac{a^2}{b^2}$, $n=1$ when $C_1=C_4=\frac{1}{n^2+1}\frac{a^2}{b^2}$, $n>1$ $C_2=1$, $C_3=\frac{n^4+6n^2+1}{n^2+1}\frac{b^2}{a^2}$	207 196
147	End with 4 sides fixed 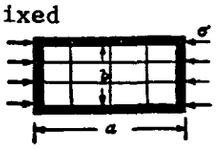	when $C_1=4$, $C_4=4\frac{a^2}{b^2}$ $n=1$ when $C_1=4$, $C_4=\frac{16}{3(n^2+1)}\frac{a^2}{b^2}$ $n<1$ $C_2=\frac{4}{3}$, $C_3=\frac{n^4+6n+1}{n^2+1}\frac{b^2}{a^2}$	207 196

No.	Dia. & Bound. Cond.	Formulas or Tables of Results	Ref.-Remarks
148	End with 4 sides rotating 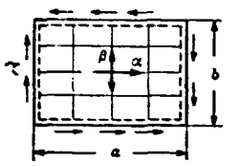	$\tau_f = \frac{4 G_{f\alpha\beta}}{a^2 N_{\alpha\beta}} \frac{(D_\beta^3 D_\alpha)^{\frac{1}{4}}}{1+4\left(\frac{K_m(V=0)}{K_m}-1\right)} j$ (approximate equation) K_m = calculated as n = 1 from equation in "M materials" 144. $K_m(V=0)$= same as above where $V_\alpha = V_\beta = 0$, where $\frac{1}{r} = \frac{b}{a}\left(\frac{D_\alpha}{D_\beta}\right)^{\frac{1}{4}}$ and $B_1 = \frac{D_\beta \nu_{f\beta\alpha} + 2 D_{\alpha\beta}}{\sqrt{D_\alpha D_\beta}}$ j determined by the graph below. 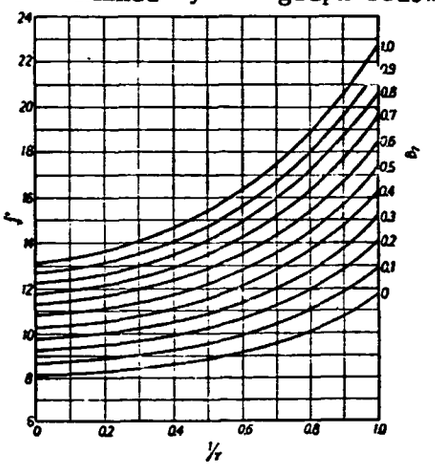	207 211
149	End with 4 sides fixed 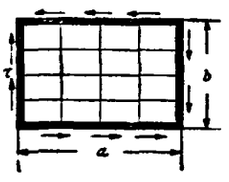	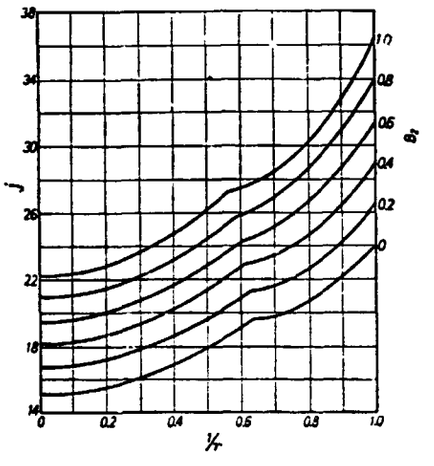	207 212

Simple compression

No.	Dia. & Bound. Cond.	Formulas or Tables of Results	Ref.-Remarks
150	End with 4 sides rotating	$\sigma_f = \frac{\pi^2 D_f E_f}{b^2 H} K$	207

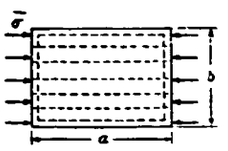

Here,

(a) tension stiffness

$$H = 2 t_f E_f + t_0 \left\{ 1 + \frac{h_c}{m} \frac{1-\cos\theta}{\sin\theta} \right\} E_c$$

(b) bending stiffness

$$D_f = \frac{t_f h^2 E_f}{2(1-\nu_f^2)}$$

$$D_c = \frac{E_c}{(1-\nu_c^2)} \left\{ \frac{1}{4} \left(1 - \frac{t_0 + h_c \cos\theta}{m \sin\theta} \right) h_c^2 t_0 + \frac{t_0 (h_c + t_0)^2}{12 m \sin\theta} \right\}$$

(c) shear stiffness in direction of plate thickness

$$U = \psi h \frac{E_c}{1-\nu_c^2} \left(\frac{t_0}{h_c} \right)^3$$

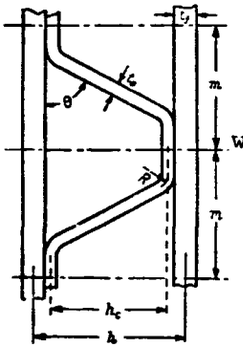

The values of ϕ are determined from the graph with respect $\frac{t_0}{t_f}$, $\frac{h_c}{t_0}$ to various and θ.

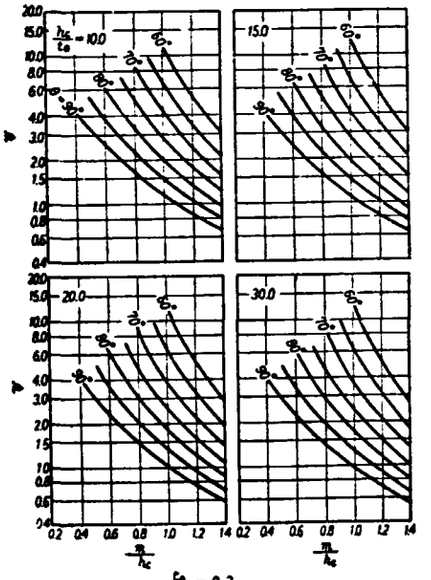

when $\frac{t_0}{t_f} = 0.3$

No.	Dia. & Bound. Cond.	Formulas or Tables of Results	Ref.-Remarks
150		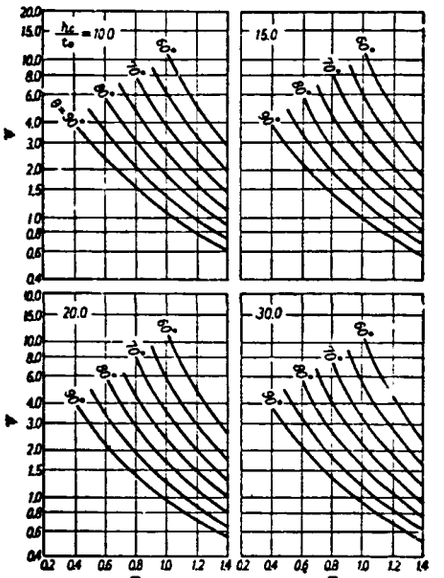 when $\frac{r_o}{r_f} = 0.5$ 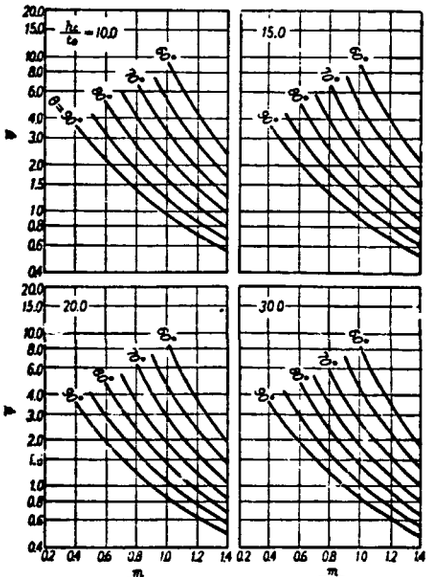 when $\frac{r_o}{r_f} = 0.8$	/492

No.	Dia. & Bound. Cond.	Formulas or Tables of Results	Ref.-Remarks
150		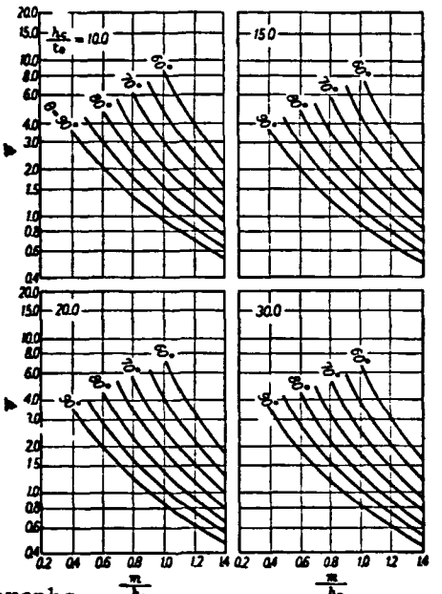	/493

(d) K is given by the graphs below in accordance with the boundary conditions with $\nu=\frac{\pi^2 D_f}{b^2 U}$, $\frac{b}{a}$ and $\frac{D_c}{D_f}$ as parameters. when $\frac{t_c}{t_f}=1.0$

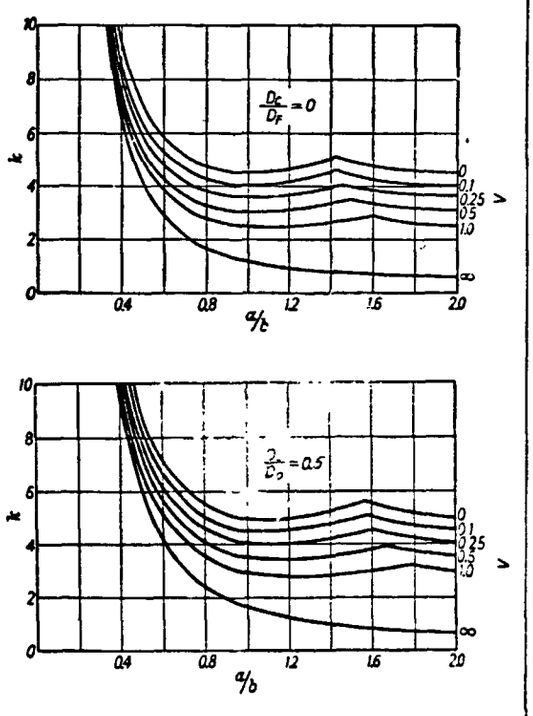

No.	Dia. & Bound. Cond.	Formulas or Tables of Results	Ref.-Remarks
150		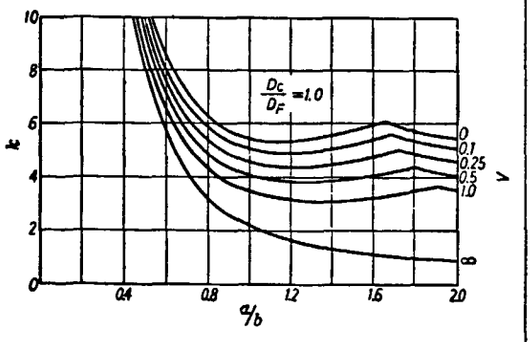 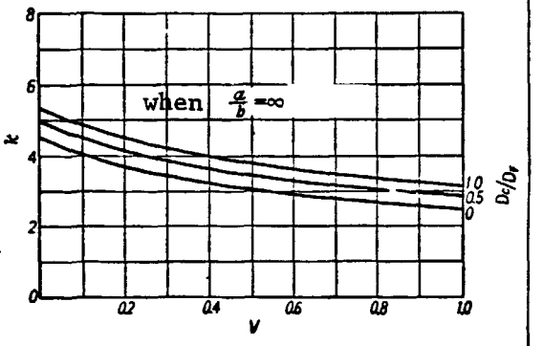	/494
151	Ends with sides a fixed, side b rotating 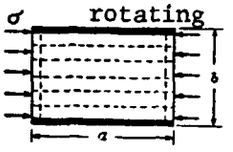	see Materials 150 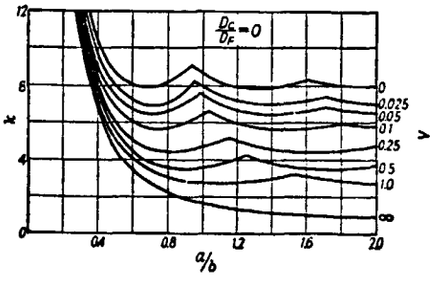 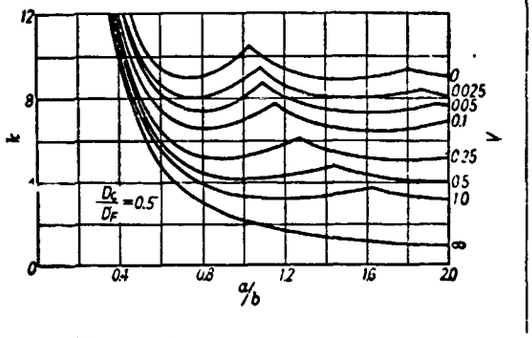	207

No.	Dia. & Bound. Cond.	Formulas or Tables of Results	Ref.-Remarks
151		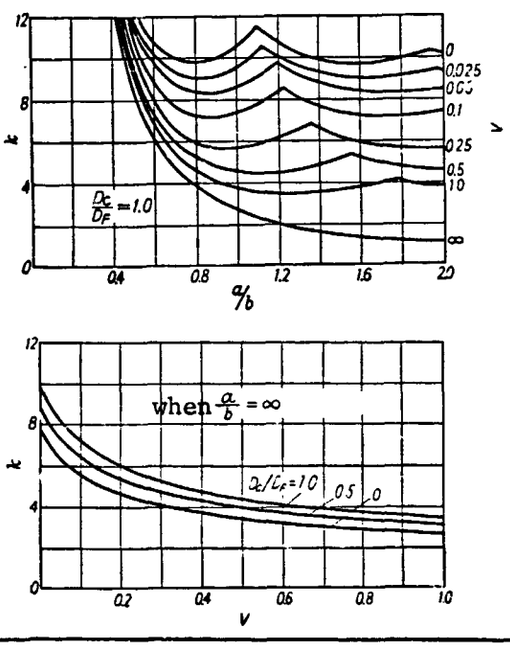	

PLASTIC BUCKLING OF RECTANGULAR PLATES
Compression

No.	Dia. & Bound. Cond.	Formulas or Tables of Results	Ref.-Remarks
152	End with 4 sides rotating 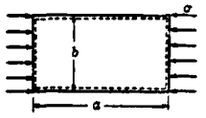	i) Based on deformation theory $\sigma_c=\eta(\sigma_c)\cdot\sigma_E$ * $\eta=\frac{E_s}{E}\left(\frac{1}{2}+\frac{1}{2}\sqrt{\frac{1}{4}+\frac{3}{4}\frac{E_t}{E_s}}\right)$ where $\nu=\frac{1}{2}$ $\eta=0.455(\sqrt{AD}+B+2F)$ where $A=\frac{\psi_1}{\psi_4}$, $B=\frac{\psi_2}{\psi_4}$ $D=\frac{\psi_3}{\psi_4}$, $F=\frac{1}{(2+2\nu+3\varepsilon)}$ $\psi_1=(1-2\beta)^2E+3(1+\varepsilon)E_t$ $\psi_2=(2-\beta)(1-2\beta)E-[(2-\beta)(1-2\beta)-4\nu\zeta-3\varepsilon\beta]E_t$ $\psi_3=(2-\beta)^2E+3(1+\varepsilon)\beta^2E_t$	218 219

* σ_E: critical buckling stress based on elasticity calculations
E_t: tangent modulus
E_s. secant modulus

No.	Dia. & Bound. Cond.	Formulas or Tables of Results	Ref.-Remarks
152		$\psi_1=[(5-4\nu)(1+\beta^2)+2(5\nu-4)\beta+3\epsilon\zeta^2]E$ $-(1-2\nu)[(1-2\nu)\zeta^2-3(1+\epsilon)\beta]E_t$	
		$\epsilon=\frac{E}{E_s}-1$	
		$\zeta=\beta^2-\beta+1$	
		$\beta=$ principal stress ratio (in this case $\beta=0$) take graph of η	
		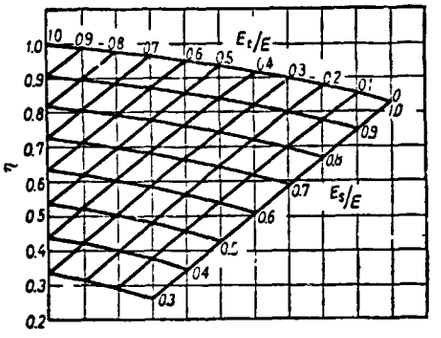	235
		$\eta=\frac{E_s(1-\nu^2)}{E(1-\mu^2)}\left(\frac{1}{2}+\frac{1}{2}\sqrt{\mu^2+(1-\mu^2)\frac{E_t}{E_s}}\right)$	220
		where $\mu=\frac{1}{2}-\left(\frac{1}{2}-\nu\right)\frac{E_s}{E}$	
		ii) Based on flow theory	
		$\eta=\left\{\frac{1}{2}\left(1+3\frac{E_t}{E}\right)^{\frac{1}{2}}+1\right\}$	223
		where $\nu=\frac{1}{2}$	
		$\eta=\frac{E_t}{E}$ case in which in the vicinity of σ_c, E_t decreases rapidly	228
		$\eta=\frac{4E}{\left(1+\sqrt{\frac{E}{E_t}}\right)^2}$ case in which the decrease in E_t in the vicinity of σ_c is slight.	
153	End where one side is rotating parallel to the load, other side free 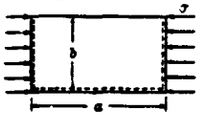	i) Based on deformation theory	
		$\eta=\frac{E_s}{E}$	218
		where $\nu=\frac{1}{2}$	
		$\eta=2.6F$ (see Materials for F)	219
		$\eta=\frac{E_s(1-\nu^2)}{E(1-\mu^2)}$	220

No.	Graph & Boundary Cond.	Formula or Table Results	Notes, Ref.
154	Two edges parallel to load clamped, Edge b rotating	i) Based on deformation theory $\eta=\frac{E_s}{E}\left(0.353+0.647\sqrt{\frac{1}{4}+\frac{3}{4}\frac{E_t}{E_s}}\right)$	218
		where $\nu=\frac{1}{2}$	
		$\eta=0.508\sqrt{AD}+0.312(B+2F)$	219
		(See Materials 152 for A, B, D, F)	
		ii) Based on flow theory $\eta=\frac{E_t}{E}$	
		Case in which E_t decreases rapidly in the vicinity of σ_c $\eta=\frac{4E}{\left(\sqrt{1+\frac{E}{E_t}}\right)^2}$	228
		Case in which decreases in E_t is slight in vicinity σ_c	
155	End with one side parallel to load clamped, other side free, sides b rotating. 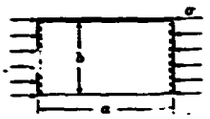	i) Based on deformation theory $\eta=\frac{E_s}{E}\left(0.330+0.670\sqrt{\frac{1}{4}+\frac{3}{4}\frac{E_t}{E_s}}\right)$	218
		where $\nu=\frac{1}{2}$	
		$\eta=0.473\left(\sqrt{AD}+2.97F-0.405B\right)$	219
		(See Materials for A, B, D, F)	
156	Side a with elastic support Side b rotating 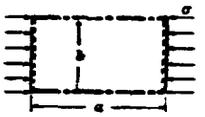	Solution of equation (4.7.1) of initial theory $\sigma_c=\frac{E\pi^2}{12(1-\nu^2)}\alpha\mu^2\left(\frac{n}{\beta}\right)^2\left(\frac{t}{b}\right)^2$ $\beta=a/b$	237
		where $\frac{b}{2}\kappa_1=\frac{n\pi}{2\beta}\sqrt[4]{\alpha}\sqrt{\mu+1}$	
		$\frac{b}{2}\kappa_2=\frac{n\pi}{2\beta}\sqrt[4]{\alpha}\sqrt{\mu-1}$	
		μ, n given by the root of the following equation. $\sqrt{\mu+1}\tanh\left(\frac{\pi}{2}\sqrt{\mu+1}\frac{n\sqrt[4]{\alpha}}{\beta}\right)+\sqrt{\mu-1}\tan\left(\frac{\pi}{2}\sqrt{\mu-1}\frac{n\sqrt[4]{\alpha}}{\beta}\right)+\pi\zeta_\mu\frac{n\sqrt[4]{\alpha}}{\beta}=0$ (a)	
		$\zeta=\frac{2}{b}\frac{D}{\bar{\varphi}}$, $M_y=-\bar{\zeta}\bar{\varphi}$	
		$\bar{\varphi}$ = rotation angle of side a	
		Approximate solution of equation (error within 1%) $\mu^2=1+p\left(\frac{\beta}{n\sqrt[4]{\alpha}}\right)^2+q\left(\frac{\beta}{n\sqrt[4]{\alpha}}\right)^4$ (b)	
		p, q functions of ζ and are given by the following graph.	

No.	Graph & Boundary Cond.	Formula or Table of Results	Notes, Ref.
156		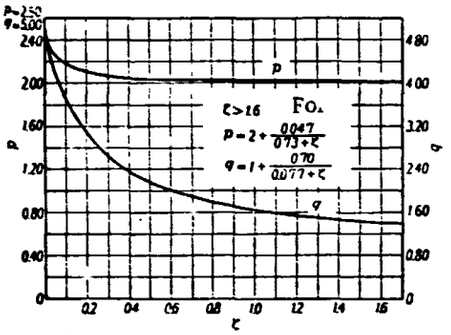 In a slender plate β large, the minimum value of σ_c is given by the following equation. $\sigma_{c\,min}=\frac{\pi^2 E\sqrt{\alpha}}{12(1-\nu^2)}\left(\frac{t}{b}\right)^2(p+2\sqrt{q})$ In this case, the half-wave length is given by by the following equation. $\beta_0=n\sqrt[4]{\frac{\alpha}{q}}$	/498
157	End with side a having elastic support and free, end with side b rotating 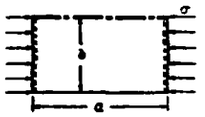	Solution of equation (4.7.1) of initial theory $\sigma_c=\frac{\pi^2 E\sqrt{\alpha}}{12(1-\nu^2)}\left(\frac{t}{b}\right)^2\left[\left(\frac{n\sqrt{\alpha}}{\beta}\right)^2+p+q\left(\frac{\beta}{n\sqrt{\alpha}}\right)^2\right]$ p, q shown in graph below. The result of this is an approximate solution to the following buckling condition equation. $\frac{2\gamma t}{\cosh\kappa_1 b\cos\kappa_2 b}+\gamma^2+t^2-\frac{\gamma^2\kappa_1^2-t^2\kappa_2^2}{\kappa_1\kappa_2}\times\tanh\kappa_1 b\tan\kappa_2 b+h\left(t^2\tanh\kappa_1 b-\gamma^2\frac{\kappa_1}{\kappa_2}\tan\kappa_2 b\right)=0$ 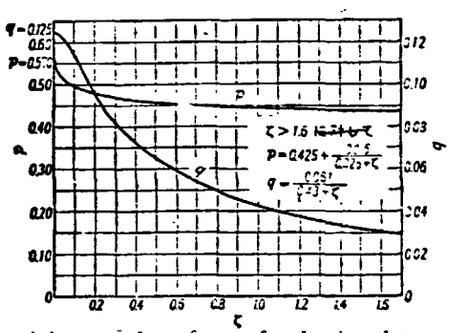 The minimum value of σ_c of a slender plate and its half-wave length are given respectively by the following equations: $\sigma_{c\,min}=\frac{\pi^2 E\sqrt{\alpha}}{12(1-\nu^2)}\left(\frac{t}{b}\right)^2(p+2\sqrt{q})$ $\beta_0=n\sqrt[4]{\frac{\alpha}{q}}$	237

No.	Graph & Boundary Cond.	Formula or Table Results	Notes, Ref.
158	End with 4 sides rotating 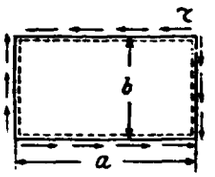 	$\tau_c = \eta(\tau_c)\tau_E$ i) Based on deformation theory Slender rectangular plate $\eta = 0.16$ $\times\{\alpha^{-1}\{\sqrt{A\{A(1+\alpha^4)+2(B+2F)\alpha^2\}}$ $+3A\alpha^2+B+2F\}\}$	/499 219
		Graph of η 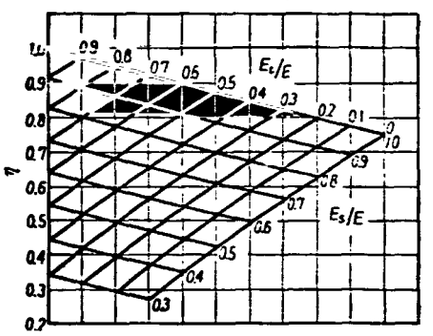 	235
		Square plate $\eta = 6.71(A+B+2F)$ $\times\sqrt{\frac{41A+9(B+2F)}{8249A+2601(B+2F)}}$	219
		Graph of η 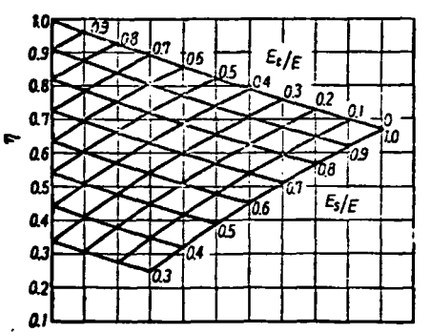 	235
		(See Materials 152 for A, B, F where β = 1) ii) Based on flow theory $\eta = \frac{E_t(\sqrt{3}\tau)}{E}$ Case in which E_t decreases rapidly in vicinity of τ_c $\eta = \frac{4E}{\left(1+\frac{E}{E_t}\sqrt{3}\tau\right)^2}$ Case in which the decrease in E_t is slight in vicinity of τ_c	228

REFERENCES CITED

/500

(A) GENERAL

1. Timoshenko, S., "Stability and Strength of Thin-Walled Construction," *Verhandl*, 3 te int. kongress f. tech. Mech., Stockholm, 1930, pp. 3-15.
2. Cox, H. L., "Summary of the Present State of Knowledge, Regarding Sheet Metal Construction," R. & M., A. R. C., No. 1553, 1933, pp. 423-442.
3. Schleicher, F., "Stabilitätsprobleme vollwandiger Stahltragwerke, Übersicht und Ausblich," *Bauing.*, 15, 1934, pp. 505-512.
4. Heck, O. S. and Ebner, H., "Formulae and Methods of Calculation of the Strength of Plate and Shell Structures in Aeroplane Construction," J. Roy. Aero. Soc., 40, 1936, pp. 769-788.
5. Chwalla, E., "Design of Horizontally Stiffened Web Plates of Plated Girders," 2 te Kongress int. Verein. f. Brükenb. u. Hochb., 1936, pp. 943-971.
6. Timoshenko, "Theory of Elastic Stability, 1936.
7. Hartmann, F., Knickung-Kippung-Beulung, 1937.
8. Roark, R. J., Formulas for Stress and Strain, 1938.
9. Chwalla, E., Erläuterungen zür Begründung des Normblattentwurfes. Knick- und Beulvorschriften für Stahlbau (DIN E 4114), 1940.

(B) WORKS CONCERNING THE CRITICAL BUCKLING OF RECTANGULAR PLATES UNDER COMPRESSION

10. Bryan, G. H., "On the Stability of a Plane Plate under Thrust in its Own Plane with Application to the 'Buckling of the Side of a Ship,'" Proc. London Math. Soc., 22, 1891, pp. 54-67.
11. Timoshenko, S., "Sur la stabilité des systemes élastique." Ann. des Ponts et Chauss., 15, 1913, pp. 496-566.
12. Sezawa, K., "The Stability of Thin Plates," Papers of the Shipbuilding Society, No. 38, 1926, pp. 79-108.
13. Sezawa, K. "On the Buckling under Edge Thrusts of a Rectangular Plate Clamped at Four Edges," Aeronautical Research Institute Report 6, 1931, pp. 45-59.
14. Sezawa, K., "The Vibration and Stability of a Rectangular Plate under Edge Thrusts Clamped at Four Edges," Papers of the Shipbuilding Society No. 49, 1932, pp. 87-93.
15. Cox, H. L., "The Buckling of Thin Plate in Compression," R. & M., A. R. C., No. 1554, 1933.
16. Yamana, M., "On the Elastic Stability of Aeroplane Structures," Engineering Bulletin, Tokyo University, 20, 1933, pp. 163-244.
17. Faxen, O. H., "Knickfestigkeit rechteckiger Platten," Z. A. M. M., 15, 1935, pp. 268-277.
18. Sezawa, K. and Watanabe, W., "Buckling of a Rectangular Plate with Four Clamped Edges Reexamined with an Improved Theory," Aeronautical Research Institute Report 11, 1936, pp. 407-418.

19. Maulbetch, J. L., "Buckling of Compressed Rectangular Plate with Built-in Edges," J. Appl. Mech., 4, 1937, A 59-62.
20. Timoshenko, S., "Einige Stabilitätsprobleme der Elastizitäts-theorie," Z. f. Math. u. Phys., 58, 1910, p. 337.
21. Sezawa, K. and Nishimura, G., "On the Buckling of a Long Elastic Plate under Edge Thrusts," Papers of the Shipbuilding Society, No. 47, 1931, pp. 129-146.
22. Schleicher, F., "Die Knickspannungen von eingespannten rechteckigen Platten," Mitt. Forsh-Anst. Gutehoffnungshütte, 1, 1931, pp. 186-193.
23. Taylor, G. I., "The Buckling Load for a Rectangular Plate with Four Clamped Edges," Z.A.M.M., 13, 1933, pp. 147-152.
24. Trefftz,E ., "Die Bestimmung der Knicklast gedrückter, rechteckiger Platten," Z.A.M.M., 15, 1935, pp. 339-344. /501
25. Sattler, K., "Beitrag zur Knick Theorie dünnen Platten," Mitt. aus d. Forschungsanstalten v. G.O.A., M.A.N., 10, 1935, p. 257.
26. Iguchi, S., "Allgemeine Lösung der Knickungsaufgabe fur rechteckige Platten," Ing. Arch., 7, 1936, pp. 207-215.
27. Iwafuji, S. and Ita, "Buckling of Rectangular Plates Having Two Adjoining Clamped Edges with Other Two Edges Having Free Support," *Journal of the Mechanical Society*, 1948, Final Lecture Edition.
28. Iwafuji, S., "Buckling of Rectangular Plate with One Edge Clamped, Three Edges with Free Supports," *Journal of the Mechanical Society*, 1947, Final Lecture Edition, p. 248.
29. Hartmann, P., See Reference [7] (a) p. 163, (b) p. 166, (c) p. 170.
30. Chwalla, E., See Reference [9] (a), (b), (c) also p. 9.
31. Timoshenko, S., See Reference [6] (a) p. 364, (b) p. 365.
32. Schumann, L. and Back, G., "Strength of Rectangular Flat Plates under Edge Compression," N.A.C.A. Tech. Rep. No. 356, 1930.
33. Cox, H. L. and Clenshaw, W. J., "The Strength of Ships' Plating," Inst. Engs. and Shipb. Scotland, 81, 1937-8, p. 19.
34. Yoshiki, M., "On the Buckling and Collapsing Strength of Ship's Hull Parts under Compressive Load," Papers of the Shipbuilding Society, No. 75, 1953 pp. 85-109.
"On the Buckling and Collapsing Strength of Ship's Hull Parts under Compressive Load," Japan Sci. Review, Ser. 1, 1, 1949, pp. 148-153.
35. Yoshiki, M., "Proposal for a Method for Determining the Buckling Limit of Rectangular Flat Plates under Compression," *Journal of Applied Dynamics*, 1, 1948, pp. 193-199.

(C) WORKS CONCERNING THE CRITICAL BUCKLING OF RECTANGULAR PLATES UNDER SHEAR

36. Timoshenko, S., "Über die Stäbilitat versteifter Platten," *Eisenbau*, 12, 1921, pp. 147-163.
37. Southwell, R. V. and Skan, S. W., "On the Stability under Shearing Forces of a Flat Elastic Strip," Proc. Roy. Soc. London, A. 105, 1924, pp. 582-607.
38. Timoshenko, S., See Ref. [1].

39. Bergmann, S. and Reissner, H. "Neuere Probleme aus der Flugzeugstatik. Über die Knickung von rechteckigen Platten bei Schubbeanspruchung," Z.F.M., 23, 1932, pp. 6-12.
40. Seydel, E., "Über das Ausbeulen von rechteckige isotroper oder orthogonal-anithotropen Platten bei Schubbeanspruchung." Ing. Arch., 4, 1933, pp. 169-191.
41. Stein, O., "Die Stabilität der Blechträgerstehbleche im Zweiachsigen Spannungszustand," Stahlbau, 7, 1934, pp. 57-60.
42. Iguchi, S., "Die Knickung der rechteckigen Platte durch Schubkräfte," Ing. Arch., 9, 1938, pp. 1-12.
"Die Knickung der vierseitig eingespannten rechteckigen Platten durch Schubkräfte," Proc. Phys. Math. Soc. Japan, 20, 1938, pp. 814-832.
43. Bollenrath, F., "Wrinkling Phenomena of Thin Flat Plates Subjected to Shear Stresses," N.A.C.A. Tech. Memo, No. 601, 1931.
44. Cox, H. L., See Reference [2].
45. Tomochika, S., and Imai, K., "On the Elastic Stability of Square Flat Plates under Shearing Forces on Four Sides," *Sea and Air*, 18, 1938, pp. 142-152.
46. Hidaka, K. and Okubo, T., "Distortion of Elastic Plate under Shearing Forces on Four Sides," *Sea and Air*, 18, 1938, pp. 153-157.
47. Moheit, W., "Schubbeulung rechteckiger Platten mit eingespanten Rändern," *Stahlbau*, 13, 1940, pp. 39-44.
48. Tsuboi, Y., "Shear Buckling of a Rectangular Plate with One Edge Free and Three Sides Supported," Unpublished M.S.
49. Leggett, D. M. A., "The Elastic Stability of a Long and Slightly Bent Rectangular Plate under Uniform Shear," Proc. Roy. Soc. London, A. 162, 1937, pp. 62-83.
50. Chwalla, E., See Reference [9], p. 11. /502
51. Hartmann, F., See Reference [7], p. 192.
52. Bollenrath, F., "Ausbeulerscheinungen an ebenen, auf Schub beanspruchten Platten," Lufo., 6, 1929, pp. 1-17.
53. Gough, H. J. and Cox, H. L., "Some Tests on the Stability of Thin Strip Material under Shearing Forces in the Plane of the Strip," Proc. Roy. Soc. London, A 137, 1932, pp. 145-157.
54. Seydel, E., "Ausbeul-Schublast rechteckiger Platten," (Zahlenbeispiele u. Versuchsergebnisse), Z.F.M., 24, 1933, pp. 78-83.

(D) WORKS CONCERNING THE CRITICAL BUCKLING OF RECTANGULAR PLATES UNDER SIMPLE BENDING, AND COMPRESSION AND BENDING

55. Timoshenko, S., See Reference [36].
56. Stein, O., See Reference [41].
57. Timoshenko, S., "The Stability of the Webs of Plate Girders," Engg., 138, 1934, pp. 207-209.
58. Nölke, K., "Biegungsbeulung der Rechteckplatte," Ing. Arch., 8, 1937, p. 403.
59. Ban, S., "Knickung der rechteckigen Platten bei veränderlicher Randbelastung," Abh. 4 te int. Kongr. Brückb. u. Hochb., 3, 1935, pp. 1-18.
60. Nolke, K., "Biegungs-Beulung der Rechteckplatte mit eingespanter Längsrändern," Baulng., 17, 1936, p. 111.

61. Saka, S., "On the Buckling of Rectangular Plates Undergoing Side Pressures on Opposing Sides," *Journal of the Architectural Society*, 49, 1935, pp. 559-577.
62. Chwalla, E., See Reference [9], p. 10.
63. Yoshiki, M., "On the Strength of Thin Plate Webs under Simple Bending," Papers of the Shipbuilding Society, No. 70, 1942, pp. 183-223.

(E) WORKS CONCERNING THE CRITICAL BUCKLING OF RECTANGULAR PLATES UNDER COMBINED STRESSES

64. Southwell, R. V. and Skan, S. W., See Reference [37].
65. Wagner, H., "Über Konstruktions- und Berechnungs-fragen des Blechbaues," Jb. wiss. Ges. Luftf., 1928, pp. 113-125.
66. Timoshenko, S., See Reference[57].
67. Chwalla, E., "Beitrag zur Stabilitätstheorie des Stegbleches vollwandiger Träger," Stahlbau 9, 1936, p. 161.
68. Iguchi, S., See Reference [42].
69. Stein, O., See Reference [41].
70. Way, S., "Stability of Rectangular Plates under Shearing and Bending Forces," *J. Appl. Mech.*, 3, 1936, No. 4.
71. Takefuji, K. and Takeda, A., "Investigation of the Buckling of Rectangular Web Plates--Characteristics of General Equations," Papers of the Architectural Society, No. 22, 1941, pp. 77-86.

(F) ON BUCKLING AND OTHER PROBLEMS IN RECTANGULAR PLATES

72. Green, A. E., "The Equilibrium on Elastic Stability of a Thin Twisted Strip," Proc. Roy. Soc. London, A. 154, 1936, pp. 430-455; "The Elastic Stability of a Thin Twisted Strip II," Proc. Roy. Soc. London, A. 161, 1937, pp. 197-222.
73. Ono, M., "On the Torsion of Rectangular Plates," *Journal of the Mechanical Society*, 37, 1934, p. 379.
74. Olsson, R. G., "Beitrag zur Knickung der Rechteckplatte von quadratisch veränderlicher Steifigkeit," Ing. Arch., 10, 1939, pp. 175-181.
75. Kurata, M., "A Study on the Problems of Buckling of Composite Rectangular Plates," Construction Engineering, 1, 1947, pp. 19-33, 2, 1948, pp. 27-37. M. Kurata, "A Study on the Problems of Buckling of the Composite Rectangular Plates," Engineering Bulletin of Hokkaido University, 8, 1950, pp. 151-336.
76. Timoshenko, S., See Reference [6], p. 387.
77. Chwalla, E., See Reference [6], p. 389. /503
78. Stowell, E. Z., "A Unified Theory of Plastic Buckling of Columns and Plates," N.A.C. A. Tech. Note, No. 1556, 1948; Handelman, G. H. and Prager, W., "Plastic Buckling of a Rectangular Plate under Edge Thrusts," N.A.C.A. Tech. Note, No. 1530, 1948; Pearson C. E., "Bifurcation Criterion and Plastic Buckling of Plates and Columns," *J. Aero Sci.*, 17, 1950, pp. 417-424, 455.
79. Zezek, K., "Die Festigkeit leicht gekrümmter, auf Druck belasteter Rechteckplatten aus Stahl," Bauing., 19, 1938, pp. 548-552.
80. Shibuya, I., "Buckling and Dynamic Loading of Thin Plates," *Journal of the Aeronautic Society*, 9, 1942, pp. 802-808.

81. Inoue, T., "On the Dynamic Stability and Nonlinear Characteristics of Thin Plates and Columns under Periodic Axial Forces," Papers of the Aeronautical Research Institute, No. 229, 1944, pp. 265-285.
82. Kawashima, Y., "Buckling of Thin Plates Due to Internal Pressure in Rivet Holes," *Journal of the Aeronautical Society*, 9, 1942, pp. 1048-1056.

(G) WORKS CONCERNING THE CRITICAL BUCKLING OF CIRCULAR AND OTHER NON-RECTANGULAR FLAT PLATES

83. Bryan, G. H., See Reference [10].
84. Nadai, A., "Über das Ausbeulen von kreisförmigen Platten," Z.V.D.I., 59, 1915, pp. 169-174.
85. Sezawa, K., See Reference [12].
86. Yamana, M., See Reference [16].
87. Meissner, E., "Über des Knicken kreis-ringförmiger Scheiben," Schweiss Bauz., 101, 1933, p. 87.
88. Kawamoto, N., "The Stability of Thin Circular Plates having Circular Holes in the Center," *Journal of the Mechanical Society*, No. 39, 1936, pp. 449-450.
89. Iwafuji, S., "The Stability of Thin Circular Plates having Circular Holes in the Middle," *Journal of the Mechanical Society*, No. 42, 1939, pp. 663-664.
90. Iwafuji, S., Ita, T. and Suzuki, M., "Approximation Calculations of the Buckling Load of Thin Circular Plates," *Journal of the Mechanical Society*, 50th Anniversary Edition, 15, 1939, pp. 1-64.
91. Hayashi, S., "On the Tensioning of Circular Saws (Problems in the Thermal Elastic Buckling of Rotating Circular Plates)," *Applied Physics*, 17, 1948, pp. 251-257.
92. Takahashi, R., "On the Buckling of Circular Plates with Gradually Changing Thickness in the Direction of the Radius," *Journal of the Mechanical Society*, 49, 1946, pp. 355-357.
93. Voinovsky-Krieger,S., "The Stability of a Clamped Elliptic Plate under Uniform Compression," *J. Appl. Mech.*, 4, 1934, No. 4.
94. Voinovsky-Krieger, S., "Berechnung der ringsum frei aufliegenden gleichseitigen Dreiecksplatten," Ing. Arch., 4, 1933, pp. 254-262.
95. Wakasugi, S., "Buckling of Right Isoceles Triangular Plate with Rotating Edges," Papers of the Mechanical Society, 19, 1953, pp. 59-65; Wakasugi, S., "Buckling of Right Isoceles Triangular Plate under Uniform Compressive Forces," Papers of the Mechanical Society, 21, 1955, pp. 424-480, Hanover (1936).
96. Burchard, W., "Beulspannungen der quadratichen Platte mit Schrägsteife unter Druck bzw. Schub," Ing. Arch., 8, 1937, pp. 332-348.
97. Sawada, M., "Approximation for Rectangular Plate with Four Parallel Sides," *Journal of Mechanical Society*, 33, 1935, pp. 169.
98. Shibuya, I., "Application of Oblique Axes to Thin Plate Stability Theory," *Journal of the Aeronautical Society*, 6, 1939, pp. 45-49.
99. Yamamoto, M., "Buckling of Curved Polygonal Plates with Sides Clamped," Papers of the Mechanical Society, 13, 1947, pp. 8-16.

(H) WORKS CONCERNING THE BUCKLING OF ORTHOTROPIC PLATES

100. Yamana, M., See Ref. [16].
101. Bergmann, S. and Reissner, H., "Neuere Probleme aus der Flugzeugstatik. Uber die Knickung von Wellblechstreifen bei Schubbeanspruchung," Z.F.M., 18, 1929, pp. 475-481.
102. Seydel, E., "Beitrag zur Frage des Ausbeulens von versteiften Platten bei Schubbeanspruchung," Lufo., 8, 1930, pp. 71-90.
103. Seydel, E., "Schubknickversuche mit wellblechtafeln," 230. D.V.L. Bericht, D.V.L. Jb. (1931), pp. 233-245.
104. Seydel, "Ausbeul-Schublast rechteckiger Platten," Z.F.M., 24, 1933, pp. 78-83. /504
105. Seydel, E., See Ref. [40].
106. Green, A. E., "Elastic Stability of a Corrugated Plate under a Shearing Force," Proc. Cambridge Phil. Soc., 33, 1937, pp. 459-473.
107. Hayashi, S., "The Buckling of Orthotropic Plates in Which the Principal Axis of Elasticity is Diagonal to the Boundary Line," *Journal of the Aeronautical Society*, Final Lecture Series, 1944.

(I) WORKS CONCERNING THE EFFECTIVE WIDTH AND ULTIMATE LOAD OF RECTANGULAR PLATES UNDER COMPRESSION

108. Schnadel, G., "Über die Knickung von Platten" Jb. Schiffbt. Ges. 30, 1929, pp. 170-194; "Die Uberschreitung der Knickgrenze bei dünnen Platten," Verh. 3te int. Kongr. f. tech. Mech., Stockholm 3, 1930, pp. 73-81.
109. Kármán, Th. v., Sechler, E. E., and Donnell, L. H., "The Strength of Thin Plate in Compression," Trans. A.S.M.E. 54, 1932, pp. 53-56.
110. Cox, H. L., See Reference [15].
111. Yamomoto, M., Kondo, K., "Buckling and Failure of Rectangular Thin Plates under Compression," *Journal of the Aeronautical Society*, 2, 1935, pp. 323-344, 998-999.
112. Marguerre, K., "Die Mittragende Breite der gedrückten Platte," Lufo., 14, 1937, pp. 121-128.
113. Marguerre, K.- and Trefftz, E., "Über die Trägfäigkeit eines längsbelasteten Plattenstreifens nach Überschreiten der Beullast," Z.A.M.M., 17, 1937, pp. 85-100.
114. Tsuruya, M., "Large Deflection of Flat Plates, Compressed Plates and Their Effective Width," *Journal of the Aeronautical Society*, 6, 1939, pp. 589-607.
115. Timoshenko, S., See Reference [6], pp. 390-395.
116. Schumann, L. and Back, G., "Strength of Rectangular Flat Plates under Edge Compression," N.A.C.A. Tech. Rep., No. 356, 1930.
117. Naval Aeronautical Engineering Laboratory, "Comparision of the Compressive Strength of Super Duraluminum Flat Plates and Ordinary Duraluminum Flat Plates," Reports of the Aeronautical Engineering Laboratory, 1934, unpublished.
118. Lahde, R. and Wagner, H., "Versuche zur Ermittlung der mittragende Breite von verbeulten Blechen," Lufo., 13, 1936, pp. 214-223.
119. Sechler, E. E., "Stress Distribution in Stiffened Panels under Compression," *J. Aero Sci.*, 4, 1936-7, pp. 320-323.

120. Yokoo, T., "The Effective Width of Flat Plates and Curved Plates," *Journal of the Aeronautical Society*, 8, 1941, p. 200-203.
121. Yamana, M., and Matsuhira, K., Ishakawa, J., and Tamaru, Y., "Measurement of the Distribution of Stresses of Semi-monocoke Main Wing Outer Plates by Vibration Tests (Primarily Measurement of Effective Width of Outer Plates)," *Journal of the Aeronautical Society*, 5, 1938, pp. 789-803.
122. Yoshiki, M., See Reference [34].
123. Hyashi, S., "Deflection Equations for Orthotropic Plates and Efficiency After the Compressive Buckling of Rectangular Plates," *Journal of the Aeronautical Society*, 9, 1942, pp. 255-261.
124. Hyashi, S., See Reference [107].
125. Inoue, M., Sugahara, Y., Watanabe, M. and Sakahigashi, Y., "On the Compressive Strength of Plywood Plates," *Journal of the Aeronautical Society*, 9, 1942, pp. 1057-1074.
126. Howland, W. L. and Sandorf, P. E., "Permanent Buckling Stress of Thin-Sheet Panels under Compression," *J. Aero. Sci.*, 8, 1940-1, pp. 261-269.
127. Shibuya, I., "Permanent Buckling Deformation Theory (Preliminary Report)," *Journal of the Aeronautical Society*, 10, 1943, pp. 416-420.
128. Watanabe, K., "On the Efficiency of a Thin Plate Having Initial Strain With Respect to Compressive Force," Reports of the Shipbuilding Society, No. 61, 1937, pp. 235-242.
129. Yoshiki, M., See Reference [35].

(J) PAPERS CONCERNING TENSION FIELD THEORY

130. Wagner, H., See Reference [65]. /505
131. Wagner, H., "Ebene Blechwandträger mit sehr dünnen Stegblech," Z.F.M., 20, 1929, pp. 200-207, 227-233, 256-262, 279-284, 306-314.
132. Timoshenko, S., See Reference [1].
133. Kromm, A. and Marguerre, K., "Verhalten eines von Schub- und Druckkräften beanspuchten Plattensteifens oberharb der Beullast," Lufo., 14, 1937, pp. 627-639.
134. Reissner, E., "On Tension Field Theory," Proc. 5th Int. Congr. Appl. Mech. Cambridge, Mass., 1938, pp. 88-92.
135. Kondo, K., "General Solutions for Flat Plane Tension Field," *Journal of the Aeronautical Society*, 5, 1938, pp. 887-901.
136. Shibuya, I., "On the Effective Shearing Stiffness in Tension Shell Structures," *Journal of the Aeronautical Society*, 8, 1941, pp. 661-678.
137. Tsuboi, Y. and (?Thaimi?), "One Solution of Imperfect Tension Field," Papers of the Architectural Society, 37, 1948, pp. 18-21.
138. Schmieden, C., "Ebene Blechwandtrager mit nicht-parallelen Holmen," Lufo. 13, 1936, pp. 391-393.
139. Lahde, R. and Wagner, H., "Versuche zur Ermittlung des Spannungszustand in Zugfeldern," Lufo., 13, 1936, pp. 262-268.
140. Takeuchi, M., "On the Design of Monocoque Structure Main Wings," *Journal of the Aeronautical Society*, 5, 1938, pp. 542-556.
141. Kondo, K., "The Geometry of the Perfect Tension Field," *Applied Dynamics*, 2, 1954, pp. 3-4.
142. Kondo, K., "The Geometry of the Perfect Tension Field. I, II," *Applied Dynamics*, 3, 1950, pp. 12-15.

(K) PAPERS CONCERNING THE CRITICAL BUCKLING OF REINFORCED PLATES UNDER COMPRESSION

143. Timoshenko, S., See Reference [36].
144. Rendulic, L., "Über die Stabilität von Stäben, welche aus einen mit Randwinkeln verstärkten Blech bestehen," Ing. Arch., 3, 1932, pp. 447-455.
145. Ban, S., See Reference [59].
146. Miles, J., "Stability of Rectangular Plates Elastically Supported at the Edges," *J. Appl. Mech.*, 3, 1936.
147. Barbré, R., "Bealspannungen von Rechteckplatten mit Längssteifen bei gleichmässiger Druckbeanspruchung," Bauing, 17, 1936, pp. 268-273.
148. Chwalla, E., See Reference [5].
149. Barbré, R., "Stabilität gleichmässig gedrückter Rechteckplatten mit Längs- oder Quersteifen," Ing. Arch., 8, 1937, pp. 117-150.
150. Schleicher, F. and Barbré, R., "Stabilität versteifter Rechteckplatten mit anfanglicher Ausbiegung," Bauing., 19, 1938, p. 665.
151. Fröhlich, H., "Stabilität der gleichmässig gedrückter Rechteckplatte mit Steifenkruez," Bauing., 18, 1937, pp. 673-682.
152. Burchard, W., See Reference [96].
153. Okuda, O., and Arima, K., "The Strength and Proper Vibration Numbers of Rectangular Thin Plates Having Longitudinal and Lateral Anti-deflection Members," *Journal of the Shipbuilding Society*, No. 58, 1936, 59, No. 59, 1936, p. 163.
154. Timoshenko, S., See Reference [1].

(L) PAPERS CONCERNING THE CRITICAL BUCKLING OF REINFORCED PLATES UNDERGOING SHEAR AND OTHER TYPES OF LOAD

155. Timoshenko, S., See Reference [36].
156. Way, S., See Reference [70].
157. Burchard, W., See Reference [96].
158. Ban, S., See Reference [59].
159. Chwalla, E., See Reference [5].
160. Chwalla, E., See Reference [67].
161. Hampl, M., "Ein Beitrag zur Stabilität des horizontal aussteiften Stegbleches," Stahlbau, 10, 1937, p. 16. /506

(M) PAPERS CONCERNING THE ULTIMATE LOADS OF REINFORCED PLATES UNDERGOING COMPRESSION

162. Rossell, H. E., "Strength of Plating in Compression," Trans. Soc. N.A. & M.E., 43, 1935, pp. 121-126.
163. Wallace, G. F., "Note on the Strength of Stressed Skin Fuselages," J. Roy. Aero Soc., 40, 1936, pp. 304-312.
164. Heck, O.S. and Ebner, H., See Reference [4].
165. Sechler, E. E., See Reference [119].
166. Lundquist, E. E. and Fligg, C. M., "A Theory of Primary Failure of Straight Centrally Loaded Column," N.A.C.A. Tech. Rep., No. 582, 1937.
167. Ebner, H., "Theorie und Versuche zur Festigkeit von Schalenrümpfen," Lufo. 14, 1937, pp. 93-115.

168. Hoff, N. J., "Instability of Monocoque Structur·s in Pure Bending," J. Roy. Aero. Soc., 42, 1938, pp. 291-346.
169. Reff, E. R., "Empirical Formulae for Allowable Compression Loads in Stiffened Sheet Panels," *J. Aero. Sci.*, 6, 1938-9, pp. 505-510.
170. Dickinson, H. B., and Fischel, J. R., "Measurement of Stiffener Stresses and Effective Widths in Stiffened Panels, J. *Aero Sci.*, 6, 1938-9, pp. 249-254.
171. Fishel, J. R., "Effective Width in Stiffened Panels under Compression," *J. Aero Sci.*, 7, 1939-40, pp. 213-216.
172. Cox, H. L., "Stress Analysis of Thin Metal Construction," J. Roy Aero. Soc., 44, 1940, pp. 231-272.
173. Shibuya, I., Seki, H., "On the Stability Strength of Reinforcing Members and Plates in Tin Plate Structures," *Journal of the Aeronautical Society*, 9, 1942, pp. 403-415.
174. Shibuya, I., "Compressive Failure and Stiffness of Corrugated Plates Combined with Outer Plating," *Journal of the Aeronautical Society*, 11, 1944, pp. 292-302.
175. Lahde, R. and Wagner, H., See Reference [118].
176. Yoshiki, M., See Reference [34].
177. Howland, W. L., "Effect of Rivet Spacing on Stiffened Thin Sheet Under Compression," *J. Aero. Sci.*, 3, 1935-6, pp. 434-439.
178. Kromm, A., "Einfluss der Nietteilung auf die Druckfestigkeit verstieften Schalen aus Duralmin," Lufo., 14, 1937, pp. 116-120
179. Shibuya, I., "On the Effects of the Dimensions of Thin Plates on the Spacing of Rivets," *Journal of the Aeronautical Society*, 8, 1942, pp. 1061.
180. Kubo, T., "Investigation of the Buckling of Plates Attached with Rivets," *Applied Dynamics*, 3, 1950, pp. 13-24.

(N) PAPERS CONCERNING FLAT PLATE STRUCTURES

181. Timoshenko, S., See Reference [20].
182. Timoshenko, S., See Reference [1].
183. Lundquist, E. E., "Local Instability of Centrally Loaded Columns of Channel Section and Z-section," N.A.C.A. Tech. Note, No. 722 (1939).
184. Kuranishi, M., "Bending Strength of the Walls of Thin Flat Wall Profile Columns under Axial Compressive Load," *Journal of the Aeronautical Society*, 2, 1935, pp. 55-86, 259-284, 485-506.
185. Kuranishi, M., "Concerning the Bending Strength and Minimum Weight Conditions for Various Types of Thin Walled Flat Profile Columns under Axial Compression," *Journal of the Shipbuilding Society*, No. 56, 1935, pp 127-142.
186. Sillman, J. C., "Elastic Stability Design Charts for Duralmin Channels in Compression," *J. Aero. Sci.*, 8, 1940-1, pp. 32-34.
187. Wagner, H., and Pretscher, W., "Verhandlung und Knickung von offenen Profilen," Lufo., 11, 1934, pp 174-180.
188. Lundquist, E., E. and Fligg, C. M., See Reference [166]. /507
189. Lundquist, E. E., "On the Strength of Columns that Fail by Twisting," *J. Aero. Sci.*, 4, 1936-7, pp. 249-253.
190. Kappus, K., "Drillknicken zentrisch gedruckter Stäbe mit offenen Profil," Lufo., 14, 1937, pp. 444-459

191. Journal of Japan Architectural Society: Standards for the Calculation of Steel Structures, with Explanations, 1954, p. 84.
192. Journal of Japan Architectural Society, See Reference [191], pp. 81-82.
193. Moisseiff, L. S. and Lienhard, F., "Theory of Elastic Stability Applied to Structural Design," Proc. Amer. Soc. Civil Engr., 66, 1940, pp. 31-70.

REFERENCES CITED (SUPPLEMENT)

(O) PAPERS CONCERNING THE BUCKLING OF SANDWICH PLATES

194. Reissner, E., "Finite Deflection of Sandwitch Plate," *J. Aero. Sci.*, 15, 1948, p. 435.
195. Seide, P. and Stowell, E. Z., "Elastic and Plastic Buckling of Simply Supported Solid Core Sandwitch Plates in Compression," N.A.C.A. Rep. No. 967, 1950, pp. 357-366.
196. Libove, C. and Batdorf, S. B., "A General Small-Deflection Theory for Flat Sandwitch Plates," N.A.C.A. Rept. No. 899, 1948.
197. Eringen, A. C., "Bending and Buckling of Rectangular Sandwitch Plates," U.S. National Congress of Appl. Mech., Chicago, 1951, pp. 381-390.
198. Nardo, S. V., "An Exact Solution for the Buckling of Flat Sandwitch Panels with Loaded Edges Clamped," *J. Aero. Sci.*, 20, 1953, pp. 605-12.
199. Ikeda, T., "The Theory of the Bending of Flat Isotropic Sandwich Plates and Examples of its Application," *Journal of the Aeronautical Society*, 3, 1955, pp. 289-294.
200. Neuber, H., "Theorie der Druckstabilität der Sandwitch-Platte," Z.A.M.M., 32, 1952, pp. 325-337; 33, 1953, pp. 10-26.
201. Goodier, J. N. and Hsu, C. S., "Nonsinusoidal Buckling Modes of Sandwitch Plates," *J. Aero. Sci.*, 21, 1954, pp. 525-532.
202. Yusuff, S., "Theory of Wrinkling in Sandwitch Construction," J. Roy. Aero. Soc., 59, 1955, pp. 30-36.
203. Hoff, N. J. and Mautner, S. E., "The Buckling of Sandwitch Type Panels," *J. Aero. Sci.*, 12, 1945, p. 285.
204. Williams, D., "Sandwitch Construction-A Practical Approach for the Use of Designers," Roy. Aircraft Establishment, Rep. Structure 2, 1947.

205. Gough, E. and deBruyne, "The Instability of Thin Sheet by a Supporting Medium," J. Roy. Aero. Soc., 44, 1940, p. 12.
206. Stein, M. and Mayers, J., "A Small Deflection Theory for Curved Sandwitch Plates," N.A.C.A. Tech. Note No. 2017, 1950.
207. Munitions Board Committee, "Sandwitch Construction for Aircraft," Part I, II A.N.C. Bulletin 23, Sec. Edition, 1955.
208. Ericksen, W. S. and March, H. W., "Effects of Shear Deformation in the Core of a Flat Rectangular Sandwitch Panel, Compressive Buckling of Sandwitch Panels Having Facings of Unequal Thickness," Forest Products Lab. Rep. No. 1583-B, 1950.
209. Kuenzi, E. W., "Stability of a Few Flat Sandwitch Panels Subjected to Shear," Forest Products Lab., Rep. No. 1560, 1947.

210. Norri, C. B., "Compressive Buckling Design Curves for Sandwitch Panels with Isotropic Facings and Orthotropic Cores," Forest Products Lab., Rep. No. 1854, 1956.
211. Seydel, E., "Ausbeul-Schublast Rechteckiger Platten (Zahlenbeispiele u. Versuchsergebnisse)," Zeits. f. Flugtechnik und Luftschiffahrt, 24, 1933, pp. 78-88. /508
212. Smith, R. C. T., "The Buckling of Plywood Plates in Shear," Rept. SM.51 of the Council for Sci. and Industrial Res. Div. of Aeronautics, Commonwealth of Australia.

(P) PAPERS CONCERNING THE ELASTIC BUCKLING OF RECTANGULAR PLATES

213. Shanley, F. R., "Inelastic Column Theory," *J. Aero. Sci.*, 14, 1947, pp. 261-268.
214. Timoshenko, S., See Reference [6], pp. 386-387.
215. Bleich, F., "Theorie der Eisernen Brücken," 1924, p. 216.
216. Chwalla, E., See Reference [77].
217. Ros, M and Eichinger, A., See Reference [6], p. 389.
218. Stowell, E. Z., "A Unified Theory of Plastic Buckling of Columns and Plates," N.A.C.A. Tech. Note No. 1556, 1948.
219. Bijlaard, P. P., "Theory and Tests on the Plastic Stability of Plates and Shells," *J. Aero. Sci.*, 16, 1949, pp. 529-541; "On the Plastic Buckling of Plates," *J. Aero. Sci.*, 17, 1950, p. 493; "Taking Account of the Compressibility of the Material in the Plastic Buckling of Plates," *J. Aero. Sci.*, 19, 1952, p. 493.
220. Stowell, E. Z. and Pride, R. A., "The Effect of Compressibility of the Material on Plastic Buckling," *J. Aero. Sci.*, 18, 1951, p. 773.
221. Ilyushin, A. A., "The Elasto-Plastic Stability of Plate," N.A.C.A. Tech. Memo. No. 1188, 1947.
222. Handelman, C. H. and Prager, W., "Plastic Buckling of a Rectangular Plate under Edge Thrusts," N.A.C.A. Tech. Note No. 1530, 1948.
223. Pearson, C. E., "Bifurcation Criterion and Plastic Buckling of Plates and Columns," *J. Aero. Sci.*, 17, 1950, pp. 417-424.
224. Prager, W., "Recent Contribution to the Theory of Plasticity," *Appl. Mech. Rev.*, 1951.
225. Batdorf, S. B., "Theories of Plastic Buckling," *J. Aero. Sci.*, 16, 1949, pp. 405-408.
226. Onat, E. T. and Drucker, D. C., "Inelastic Instability and Incremental Theory of Plasticity," *J. Aero. Sci.*, 20, 1953, pp. 181-186.
227. Besseling, J. F., "Analysis of the Plastic Collapse of Cruciform Column with Initial Twist, Loaded in Compression," *J. Aero. Sci.*, 23, 1956, p. 49.
228. Yamamoto, Y., "A General Theory of Plastic Buckling of Plate," Papers of the Shipbuilding Society, No. 96, 1955, pp. 71-77; Yamamoto, Y., "Buckling Accompanying the Elastic Deformation of Columns and Plates Having Initial Deflection," Papers of the Shipbuilding Society, No. 97, 1955, pp. 57-68.
229. Yoshiki, M. and Yamamoto, Y., "Buckling of Rectangular Plates Compressed Beyond Elastic Limit," Int. Shipb. Progress, 3, 1956, pp. 634-640.

230. Kollbrunner, C. F., "Das Ausbeulen der auf einseitigen, gleichmassig verteilten Druck beanspruchten Platten im elastichen und plastischen Bereich," Mitteilungen Inst. fur Baustatik, Zurich, 4, 1935, 17, 1946.
231. Heimerl, G. J., "Determination of Plate Compressive Strength," N.A.C.A. Tech. Note, No. 1980, 1947.
232. Pride, R. A. and Heimerl, C. H., "Plastic Buckling of Simply Supported Compressed Plates," N.A.C.A. Tech. Note, No. 1817, 1949.
233. Watanabe, M., "The Buckling of Plates in a State Exceeding the Elastic Limit," *Journal of the Shipbuilding Society*, No. 81, 1949, pp. 71-82.
234. Pride, R. A., "Plastic Buckling of a Simply Supported Plate in Compression," *J. Aero. Sci.*, 19, 1952, pp. 69-70.
235. Krivetsky, A., "Plastic Coefficients for the Plastic Buckling of Plates and Shells," *J. Aero. Sci.*, 22, 1955, pp. 432-435.
236. Sechler, E. E., "Inelastic Buckling from a Designer's Viewpoint," *J. Aero. Sci.*, 23, 1956, pp. 500-506.
237. Bleich. F., "Buckling Strength of Metal Structures," New York, 1952, pp. 315-330.
238. Bijlaard, P. P., "Plastic Buckling of Simply Supported Plates Subjected to Combined Shear and Bending or Eccentric Compression in Their Plane," *J. Aero Sci.*, 24, 1957, pp. 291-303.

PART 5 SHELLS /509

CHAPTER 1

INTRODUCTION

5.1.1. SHELL STRUCTURES

Objects having the shape of curved plates, cylinders, spherical shells, elliptical shells and conical shells are called shells in general. For example, these include gas tanks, oil tanks, pipes, boilers, spherical shells, corrugated plates, machine structures, aircraft structures, architectural shells, railroad cars, automobile bodies, ship hulls, etc. Cylinders and curved plates are the most frequently used shells.

Shells can be classified, in terms of their functions, into cases where they are required as structures having curvature and into cases in which they are used as structures which are convenient in terms of strength and rigidity, when selection of the type of structure is open. Generally, shells are lighter and stronger than trusses, rigid frames, or flat plates, and since they normally are used for thin-walled structures, the occurrence of buckling is possible. This buckling occurs more rapidly than in plates, and the shells have the tendency of immediately losing their strength. Consequently, the investigation of buckling phenomenon is a particular problem in the design of shell structures.

Problems in the elastic stability of shells include calculating the buckling load for structural elements, problems in the analysis of stress when part of the structure has buckled, and problems in calculating the ultimate breaking load. In addition to this, there are problems of stiffness. Shell structures are frequently reinforced by reinforcing members and in this case, since generally the breaking of the reinforcing member determines the ultimate strength of the overall structure, a large number of data concerning the buckling of columns, beam columns, arches, rigid frames and flat plates, as reinforcing members is necessary.

5.1.2. FORMS OF BUCKLING THAT MAY OCCUR IN SHELLS.

Generally, in shells, there are few cases in which, as in columns and plates, buckling occurs in the form of infinitesimal deformations and generally they have the property that the buckling phenomenon occurs rapidly together with finite deformation. The effects of initial deformation are particularly marked in thin shells.

(1) Buckling occurs due to compression, bending, torsion, external pressure and combined loads of these in cylinders, curved plates, elliptical cylinders,

and conical shells. In curved plates, buckling also occurs due to shearing forces.

(2) In spherical shells and elliptical shells, there is a possibility of buckling occurring due to external pressure and in flat elliptical shells, buckling may also occur due to internal pressure.

(3) In blocks, -type shells, buckling occurs due to compression, bending, torsion and external pressure.

(4) In reinforced structures, the types of buckling that can occur are outer plate buckling, buckling of longitudinal reinforcing members, buckling of riveted members, buckling between rivets in outer plates and reinforcing members, simultaneous buckling of outer plate and reinforcing member (local and overall), and buckling of reinforcing members after buckling of outer plates.

The forms of buckling enumerated above are shown representatively in Figure 5.1.1.

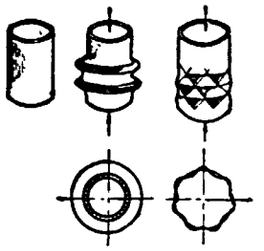

(a) Compressive buckling of cylinders

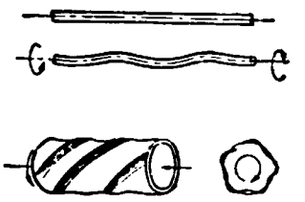

(b) Torsional buckling of cylinders

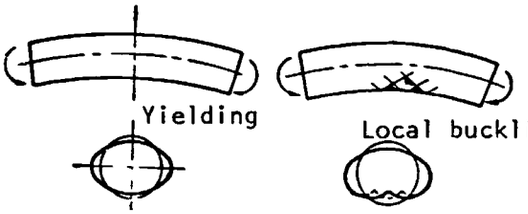

(c) Bending buckling of cylinders

(d) Buckling due to external pressure on cylinder

(e) Compressive buckling and shear buckling of curved plate

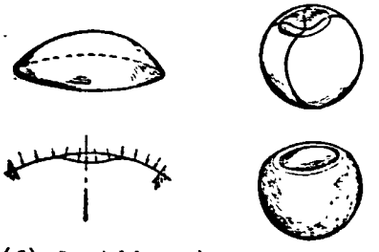

(f) Buckling due to external pressure on spherical shell

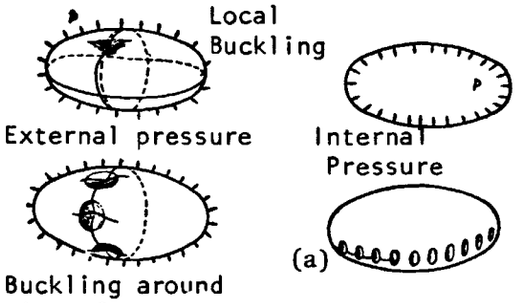

(g) Buckling due to external pressure and internal pressure on elliptical shells

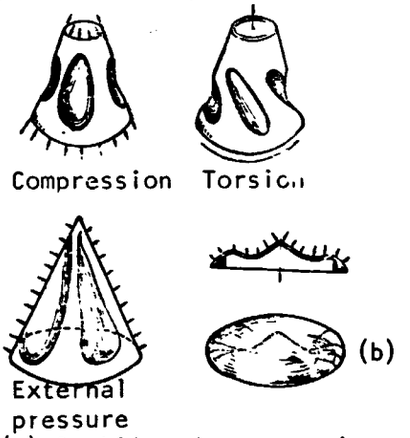

(h) Buckling due to various loads on conical shells

FIGURE 5.1.1

/511

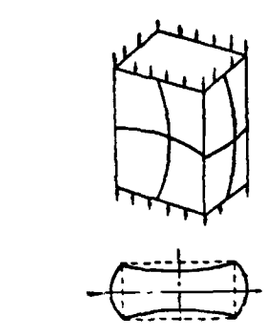

Compressive buckling

(i) Buckling of box-type shell

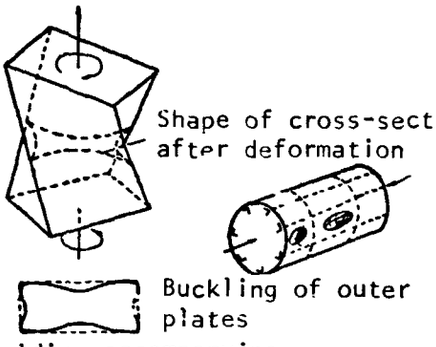

Yielding accompanying reduction in size of cross-section due to twisting

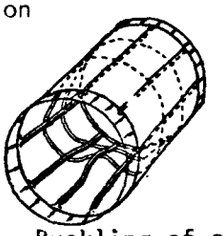

Buckling of outer plate reinforcing members

(j) Compressive buckling of reinforced shell

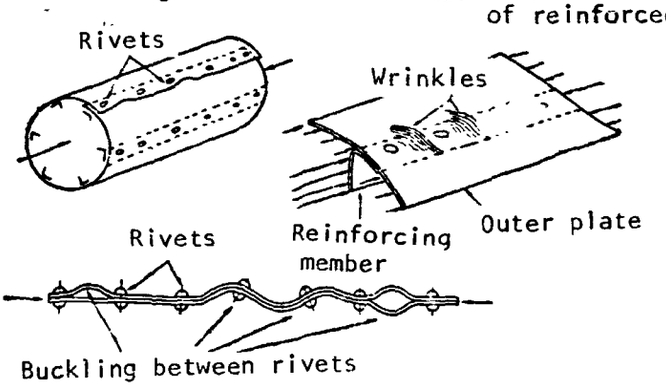

(k) Buckling between rivets in riveted section

CHAPTER 2

BUCKLING THEORY OF SHELLS

5.2.1. GENERAL DESCRIPTION OF HISTORY [1-39]

The history of the theory of buckling with relation to shells can be considered to be divided into two main areas; the infinitesimal deformation theory that was first developed, and the finite deformation theory that was later constructed. Shells involve problems as single bodies, and as reinforced constructions. The amount of research in these fields is extremely great, due to the extensive application of this theory in mechanical structures, architectural structures, ship structures and aircraft structures.

R. Lorenz [1] was the first to attempt an analysis of the buckling phenomena of cylinders under compressive force in terms of finite deformation theory. As can be seen from the table of references, the theory of buckling for cylindrical and spherical shells under compressive forces and external pressure was established by S. Timoshenko (1910) [2], R. v. Southwell (1913) [4], R. v. Mises (1914) [5], R. Zoelly (1915) [6]. In this method of analysis, the buckling load is determined as the case in which, when a load is sustained and a /512
state of equilibrium changes from a balanced equilibrium to another equilibrium causing an infinitesimal added displacement which can be under an identical load. The difference equation which expresses the second state of equilibrium is linear with respect to the infinitesimal added displacement. Consequently, this is called infinitesimal deformation theory. Afterward, buckling phenomena due to various types of load were investigated for shells of varying types, in accordance with this theory. In addition to the above, others who have studied the compressive buckling of cylinders include W. R. Dean (1925) [7], L. Föppl (1926) [71], J. W. Geckeler (1928) [73], A. Robertson (1929) [72], W. Flügge (1932) [75], K. v. Sanden-F. Tölke (1932) [74], R. Lorenz (1911) [105], R. v. Southwell (1915) [106], R. v. Mises (1914) [110], Tokugawa Takesada (1925) [112, 113] have investigated internal pressure. A. G. Greenhill (1883) [85], E. Schwerin (1925) [86], Sezawa-Kubo (1931) [87], Sezawa (1933) [89], Yamana (1933) [124], K. v. Sanden-F. Tölke (1932) [88] have studied buckling under torsion, flexural buckling has been the subject of studies by L. G. Brazier (1927) [96], R. W. Mossman-R. G. Robinson (1933) [99], W. Flügge (1932) [98], E. E. Lundquist (1933) [101], L. H. Donnell (1934) [103], and compressive loads have been studied by R. v. Mises (1929) [120, 121], K. v. Sanden-F. Tölke (1932) [122], W. Flügge (1932) [123], Yamana (1933) [124], D. F. Windenburg-C. Trilling (1934) [126].

Similar investigations have been carried out for cylinders and curved plates. S. C. Redshaw (1933) [41], S. Timoshenko (1936) [43], J. S. Newell (1931-32) [40] have studied compressive buckling; H. Wagner-W. Ballerstedt (1936), D. M. A. Leggett (1937) [54], and A. Kromm (1938) [57] have investigated shear buckling.

With regard to spherical shells, there have been studies on buckling due to external pressure by R. Zoelly (1915) [135], E. Schwerin (1922) [136], A. Van der Neut (1932), T. Tokugawa (1936) [137].

In reinforced structures, when the spacing between lateral and longitudinal reinforcing members is relatively close, it is possible for the reinforcing members and the outer plates simultaneously to undergo buckling over a wide area. Such cases can be handled as a shell having orthotropic outside plates. Plywood cylinders are also essentially orthotropic external plates. The buckling of curved plates and cylinders having such orthotropic outer plates has been studied by Yamana (1933) [146], D. D. Dschou (1934) [147], Shibuya (1937) [148], Inoue (1942) [159], and Hayashi (1949) [155], [160]. Hayashi (1949) [160, 164] has investigated flexural and torsional buckling, while Shibuya (1937) [132] studied the compression of elliptical cylinders and O. S. Heck (1937) [161] investigated bending.

In plates and shells, considerable deformation occurs, depending on the buckling, and there are many cases in which the displacement extends from the range of infinitesimal deformation into the range of finite information; i.e., from one to ten times the plate thickness, so it became necessary to establish the so-called finite deformation theory which could handle problems within this range. From this point of view, E. Trefftz [11] established a finite deformation theory in 1930, and discussed problems of elastic stability in terms of it. This constituted the first research in the second theory mentioned above. In 1937, E. Trefftz-K. Marguerre [13, 14] succeeded in applying the theory to problems in effective width after the compressive buckling of rectangular plates, and A. Kromm (1938) [57] applied it to the shear buckling of curved plates. E. Trefftz (1935) obtained equilibrium equation for finitely deformed shells. L. H. Donnell (1934) [10] found equilibrium equations for cylindrical shells and K. Marguerre (1938) [15] derived equations for arc plates.

The major problem in shells at that time was that the discrepancy between /513
theoretical values and experimental values for compressive buckling was greater, the smaller the ratio of diameter to plate thickness in cylinders and the experiment values were widely scattered. In L. H. Donnell's [10] research, which considered the reason for this discrepancy to be due to the original deformation of the shell, since it was necessary to posit a rather large original deformation in order to explain this, he was unable to avoid further theoretical problems at the point where he could not explain the scattering of the experiment values. In 1938, K. Marguerre [19] published his investigations in the case of a beam having two moving rotating ends and an extremely small initial curvature, and C. B. Biezeno [20] published his study of the case in which a spherical shell having extremely small initial curvature underwent a concentrated load. In each case, marked instability phenomena was shown and it was demonstrated that they were accompanied by finite deformation. In 1940, Th. v. Kármán-H. S. Tsien [22], who were greatly stimulated by these studies, first made an analysis of spherical shells under external pressure, taking the finite deformation of shells into account, and established a new theory which made clear the possibilities of a new buckling mechanism, which differed completely from that which was based on classical infinitesimal deformation theory. This mechanism was strikingly similar to that of K. Marguerre [19] and C. B. Biezeno [20] mentioned above.

They showed that the number of buckling waves at the beginning of a buckling of a cylinder was large, and that it decreased as the deformation increases, that a state of deformation which was stable for stress lower than classical buckling stresses existed, and that stress was extremely close to the values obtained by experiment. In this manner, they were able to explain many facts from experiments. In the above theory, if the classical buckling value is not reached at least once, the lower state of stable stress will not be reached. Karman and Tsien found that in experiments, with regard to the fact that buckling occurs at stresses much lower than the classical buckling values, actually, when the load increases to a point within the theoretical curves, it jumps to the lower stable state of stress, as in the experiments, due to some external vibration and impact. They called this the jump theory. Kuranishi Masatsugu called this "jump transition theory." Since there are problems involved in making explanations by their theory, Hayashi Shigeru and Imanaka Keisaburo [28], in order to correct the theory found that a very small initial deflection causes a marked decrease in the compressive buckling load, and showed that it was possible to explain roughly the facts of the experiment by taking this initial deflection into consideration. Later, L. H. Donnell [29] obtained the same results by calculating the effects of the same type of initial deflection.

Since there were still deficiencies in Kármán-Tsien's jump theory for spherical shells, Tsien (1942) made a detailed analysis of changes accompanying energy buckling in positions throughout the system. Assuming that the jump began from a state having an energy which was equal to the energy in the state after jumping, he calculated the pressure of that state and with respect to the state after jumping and showed that this could be compared favorably with the test values. However, it is necessary for some energy to be supplied externally in order for one of the two states of equivalent energy to jump to the other, and there are still problems with regard to this point. It is believed that such defects can be attributed to the fact that the above research concerns only static state of equilibrium. Even considering that buckling phenomena in cylinders and shells occurs suddenly, it becomes necessary to treat these phenomena as dynamic buckling phenomena. No research has yet been conducted on the dynamic buckling of shells.

R. Kappus [21] expanded E. Trefftz's [11, 12] finite deformation theory and determined a buckling condition equation based on energy.

The same kind of finite deformation buckling phenomena as occurs in cylinders is anticipated with regard to shells of various configurations. In shells having a double curvature, there is a possibility of local buckling waves to occur, but these problems have not yet been investigated. /514

W. A. Wenzek (1938) [63], A. Kromm (1937) [62], H. Ebner (1937) [61], E. Schapitz (1937) [109], Th. v. Kármán, L. G. Dunn, H. S. Tsien (1940) [82], and Kawano (1946) [64] have investigated the properties of the case after shear buckling, and of effective width after the compressive buckling of cylindrically curved plates, as a problem in structural dynamics. H. Ebner-H. Köller (1937) [31], H. Ebner (1937) [30], H. Ebner-H. Köller (1938) [32], E. Schapitz-G. Krümmling (1937) [33], E. Schapitz, H. Feller, H. Köller (1938) [34], have

studied the problems in the buckling of reinforced structures, the distribution of stress after the buckling of side plates, and the ultimate breaking strength. When a shell has a flat plate section, effective width theory after the buckling of the plate is useful, and for the ultimate strength of reinforcing members, the buckling strength of a solid member supported by elastic supports using external plates becomes a problem. Buckling theory for such reinforced structures was first developed after an adequate investigation of the unit structural elements of which these reinforced structures are made.

Although it is normal for the outer plates of reinforced shells to buckle first, at the present time, it is possible to determine the distribution of stress after the buckling of external plates by calculations. In ordinary structures, the overall strength of the structure generally is lost when the reinforcing members buckle and if it is possible to determine the buckling load of the reinforcing members having external plates after buckling, it is possible to calculate the strength. In reinforced shells undergoing fewer bending loads, if one determines the effective width after the buckling of the outer plates, it is possible to calculate the buckling strength of the reinforcing member with some degree of accuracy, and to estimate the breaking-bending moment. However, in cases where combined loads are sustained, or the configuration of the reinforcing members undergoes complex types of buckling, since problems in determining the buckling strength of the reinforcing member, and the maximum load that can be withstood must be dealt with in terms of difficult non-linear problems, theoretical investigations have not yet been made on this. In such cases, at the present time, the only approach is to make estimations based on test data [30].

Practically no work has been done up to the present time on problems of the buckling of shell structures within the plastic range. For this reason, further investigation is required, as in the case mentioned above. The sandwich construction method makes it possible to increase the conventional allowable stress of thin-walled structures and the local stiffness so it is now used extensively in aircraft structures. It is also expected that sandwich construction methods will also be applied extensively to automobiles, railroad cars, ships and architecture. We have also collected references on this in this section.

5.2.2. ANALYTICAL THEORY

In the course of the above developments, Zoelly's [6] general theory of the buckling of shells is an important first step, and the infinitesimal deformation theory of Love [9], Southwell [4], Flugge [35], and Donnell [10] is generally applied to buckling phenomena in shells. It is important since it has gained considerable success, and the later finite deformation theory will form the basis of future developments in the sense described above, and for this reason, much is expected of it in the future. Below we shall explain this theory.

Denoting the deformation energy of a shell in a state of equilibrium with a particular load as A, and the external force potential as V, the conditions

for equilibrium are

$$\delta(A+V)=0 \tag{5.2.1}$$

The condition for stability to obtain is

$$\delta^2(A+V)>0 \tag{5.2.2}$$

Here

$$A=\int a\,df$$

$$a=\frac{Et}{2(1-\nu^2)}\left[(\varepsilon_1+\varepsilon_2)^2-2(1-\nu)\left(\varepsilon_1\varepsilon_2-\frac{\gamma^2}{4}\right)\right] \qquad \text{/515}$$

$$+\frac{Et^3}{24(1-\nu^2)}\left[(\kappa_1+\kappa_2)^2-2(1-\nu)(\kappa_1\kappa_2-\tau^2)\right]$$

ε_1, ε_2; γ = elongation strain in two intersecting directions in the center plane of shell element and shear strain between these two directions

κ_1, κ_2; τ = curvature and twist in center plane as above

E, ν = Young's modulus, Poisson's ratio (isotropic materials)

f, t = surface area of shell, plate thickness of shell.

We consider a hypothetical displacement measured from the state of equilibrium expressed by these ε_1, ε_2, ω, κ_1, κ_2, τ.. The new state of deformation is assumed to be expressed by $\varepsilon_1 + \Delta\varepsilon_1$, $\varepsilon_2 + \Delta\varepsilon_2$ .... Here, we assume that $\Delta\varepsilon_1$, $\Delta\varepsilon_2$... are infinitesimally small. Moreover, assuming

$$\Delta\varepsilon_1=(\Delta\varepsilon_1)_I+(\Delta\varepsilon_1)_{II}+(\Delta\varepsilon_1)_{III}+\cdots$$

we express the other degrees of change similarly. Here we assume that $(\Delta\varepsilon_1)_I$ is the infinitely small change in the first position of elongation strain, $(\Delta\varepsilon_1)_{II}$ is the infinitely small change in position 2. In order to investigate stability, since it is not necessary to have an infinitely smaller quantity of a higher order than the infinitely small second position, we can write

$$\Delta\varepsilon_1=(\Delta\varepsilon_1)_I+(\Delta\varepsilon_1)_{II}$$

The deformation energy of the shell accompanying this change is

$$A+\delta A+\delta^2 A$$

$$=\int df\left\{\frac{Et}{2(1-\nu^2)}\left[(\varepsilon_1+\Delta\varepsilon_1+\Delta\varepsilon_2)^2-2(1-\nu)\left((\varepsilon_1+\Delta\varepsilon_1)(\varepsilon_2+\Delta\varepsilon_2)-\frac{1}{4}(\gamma+\Delta\gamma)^2\right)\right]\right.$$

$$\left.+\frac{Et^3}{24(1-\nu^2)}\left[(\kappa_1+\Delta\kappa_1+\kappa_2+\Delta\kappa_2)^2-2(1-\nu)\left((\kappa_1+\Delta\kappa_1)(\kappa_2+\Delta\kappa_2)-(\tau+\Delta\tau)^2\right)\right]\right\}$$

In order to determine the stability, $\delta^2 A$ is necessary. We express this by the following:

$$\delta^2 A=J_1+J_2+J_3$$

Here (5.2.3)

$$\left.\begin{aligned} J_1&=\int\left[N_1(\Delta\varepsilon_1)_{II}+N_2(\Delta\varepsilon_2)_{II}+N_{12}(\Delta\gamma)_{II}+M_1(\Delta\kappa_1)_{II}+M_2(\Delta\kappa_2)_{II}+2M_{12}(\Delta\tau)_{II}\right]df\\ J_2&=\int\frac{E}{2(1-\nu^2)}\left[\left((\Delta\varepsilon_1)_I+(\Delta\varepsilon_2)_I\right)^2-2(1-\nu)\left((\Delta\varepsilon_1)_I(\Delta\varepsilon_2)_I-\frac{1}{4}(\Delta\gamma)_I^2\right)\right]df\\ J&=\int\frac{Et^2}{24(1-\nu^2)}\left[\left((\Delta\kappa_1)_I+(\Delta\kappa_2)_I\right)^2-2(1-\nu)\left((\Delta\kappa_1)_I(\Delta\kappa_2)_I-(\Delta\tau)_I^2\right)\right]df \end{aligned}\right\}$$

N_1, N_2, N_{12} are the internal force components. M_1, M_2, M_{12} are the moment components. Below we shall consider cases that are particularly important in practice. That is, we shall assume that in the state of equilibrium which we are considering, bending has no effect.

/516

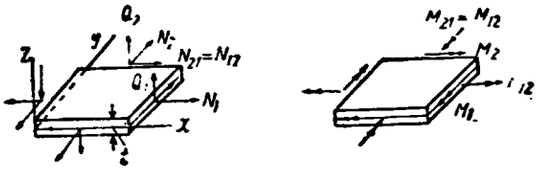

Figure 5.2.1

$$\kappa_1=\kappa_2=\tau=0,\qquad M_1=M_2=M_{12}=0$$

In this case, J_1 becomes

$$J_1=\int\left[N_1(\Delta\varepsilon_1)_{II}+N_2(\Delta\varepsilon_2)_{II}+N_{12}(\Delta\gamma)_{II}\right]df$$

Now, if when the hypothetical displacement is given

$$\delta^2V+J_1+J_2+J_3<0 \qquad (5.2.4)$$

this is unstable. J_2 is called the extension term due to extension of the center plane, and J_3 is called the bending term since it is the term originating from bending, and twisting. The J_2, J_3 on the left side of equation (5.2.4) are quantities unrelated to the state of stress of the shell or the external load, they are merely quantities that are due to the deformation and material constants of the shell. δ^2V and J_1 are related to the external load. We proceed from a given state of equilbrium and consider the load condition in which all loads are multipled by λ. In this case, a new state of equilibrium is obtained in which the stress also is multipled by the same degree λ. If this new state of equilibrium is unstable,

$$\lambda\left(\delta^2V+J_1\right)+J_2+J_3<0 \qquad (5.2.5)$$

here, we assume in the above two cases an equivalent hypothetical deformation. In this case, J_1, J_2, J_3 are the same as in the first case.

Since if J_2 and J_3 are not 0, they are always a positive value, for some small value of λ we obtain $\lambda(\delta^2V + J_1) + J_2 + J_3 > 0$, and we see that the shell must be in stable equilibrium. In this manner, when the shell undergoes an arbitrary load, in a sufficiently small state of this load, it is always possible for stable equilibrium. On the other hand, in the case of a sufficiently large positive or negative value of λ, the unequal equation (5.2.5) obtains and the equilibrium becomes unstable.

Next, depending on whether or not J_2 is 0, it is possible to classify the stability problem into the following two types. The first one is of the shape

$$J_2 = 0$$

and in this case, at each place on the center plane

$$(\Delta\varepsilon_1)_I=(\Delta\varepsilon_2)_I=(\Delta\gamma)_I=0$$

obtains, so since the center plane of the shell does not undergo expansion or contraction or shearing deformation in the first approximation, this is called the inextensional deformation. The infinitely small $(\Delta\varepsilon_1)_{II}$, $(\Delta\varepsilon_2)_{II}$, $(\Delta\omega)_{II}$ in the second position generally do not disappear. As a first approximation, the shell is unextended, and has a form in which only the curvature changes.

Employing the above considerations when this inextensional deformation $J_2 =$ 0, the buckling load of the shell in this case is proportional to t^3. Since the thickness of the shell enters in the form of t^3, in the case of inextensional deformation, the shape of the buckling wave of the shell is not related to the thickness of the shell. Moreover, the maximum strain ε_0 at the time of buckling is proportional to t^2 so, depending on the configuration of the shell, if the plate thickness is adequately thin, we can conclude that there is a possibility of the occurrence of this type of buckling within the elasticity range. /517

Above we have explained the characteristics of inextensional deformation, but in any problem of the equilibrium of shells, there is a problem as to whether or not it is possible for any other type of additional displacement without extension to occur. The condition for inextensional deformation to be possible is related to the configuration of the shell and the boundary conditions. In the case of a flat plate, the buckling is possible only by virtue of the deflection term and a good example is $J_2 = 0$. Actually, denoting the displacement in the direction perpendicular to the plate at a point on the center plane of a plate as w, the strain in the center plate due only to w becomes

$$\Delta\varepsilon_1=\frac{1}{2}\left(\frac{\partial w}{\partial x}\right)^2,\qquad \Delta\varepsilon_2=\frac{1}{2}\left(\frac{\partial w}{\partial y}\right)^2,\qquad \Delta\gamma=\frac{\partial w}{\partial x}\frac{\partial w}{\partial y}$$

so

$$(\Delta\varepsilon_1)_I=(\Delta\varepsilon_2)_I=(\Delta\gamma)_I=0$$

The center plane, in the case of such deformation, as a first approximation is not extended. However, the infinitely small extensional strain in the second position is not 0 and has the following values

$$(\Delta\varepsilon_x)_{II}=\frac{1}{2}\left(\frac{\partial w}{\partial x}\right)^2,\quad (\Delta\varepsilon_z)_{II}=\frac{1}{2}\left(\frac{\partial w}{\partial y}\right)^2,\quad (\Delta\gamma)_{II}=\frac{\partial w}{\partial x}\frac{\partial w}{\partial y}$$

Also in the case of a cylinder, which is adequately long and which undergoes external pressure inextensional deformation is possible, and the pressure at the time of buckling is proportional to t^3.

Moreover, there are cases in which additional inextensional displacement (additional displacement at the time of buckling) may not occur owing to the configuration of the shell or the boundary conditions, and this belongs to the second type. Such a state of equilibrium is much more stable than in the case of inextensional deformation, and the buckling load is considerably great. This is because the positive term J_2 is added to the left side of the inequality equation. When the term J_2 is present, generally J_2 is much greater than J_3. The form of buckling of a cylinder undergoing compression or undergoing twisting belongs to this extended type of deformation.

The above is a discussion of the types of buckling of shells, and now we shall consider infinitesimal deformation theory and finite deformation theory as means of determining buckling load.

Equilibrium equation based on the theory of infinitesimal deformation of cylindrical shells.

Figure 5.2.2

In the state in which a cylindrical shell undergoes tension and shearing load (P, S) and the cylinder is in a state of balance, we assume that an additional displacement (u, v, w) occurs in the center plane and a new state of equilibrium is entered. Assuming the displacement component, internal force component and moment component as shown in the figure,

strain component $\varepsilon_x=\frac{\partial u}{\partial x},\quad \varepsilon_y=\frac{\partial v}{\partial y}+\frac{w}{r},\quad \gamma_{xy}=\frac{\partial u}{\partial y}+\frac{\partial v}{\partial x}$ /518

curvature, twist $\kappa_x=\frac{\partial^2 w}{\partial x^2},\quad \kappa_y=\frac{\partial^2 w}{\partial y^2},\quad \tau=\frac{\partial^2 w}{\partial x\partial y}$

internal force component $N_x=\frac{Et}{1-\nu^2}(\varepsilon_x+\nu\varepsilon_y),\quad N_y=\frac{Et}{1-\nu^2}(\varepsilon_y+\nu\varepsilon_x)$

$$N_{xy}=N_{yx}=G\,t\,\gamma_{xy}$$

moment component $M_x=D(\kappa_x+\nu\kappa_y)$, $M_y=D(\kappa_y+\nu\kappa_x)$,

$$M_{xy}=M_{yx}=D(1-\nu)\tau \qquad D=\frac{E\,t^3}{12(1-\nu^2)}$$

The equilibrium equation for the new state of equilibrium is expressed by

$$\begin{cases} \dfrac{\partial N_x}{\partial x}+\dfrac{\partial N_{xy}}{\partial y}=0, \quad \dfrac{\partial N_{xy}}{\partial x}+\dfrac{\partial N_y}{\partial y}=0 \\ \dfrac{\partial Q_x}{\partial x}+\dfrac{\partial Q_y}{\partial y}+\dfrac{N_y}{r}-P\dfrac{\partial^2 w}{\partial x^2}-2S\dfrac{\partial^2 w}{\partial x\partial y}=0 \\ \dfrac{\partial M_x}{\partial x}+\dfrac{\partial M_{yx}}{\partial y}-Q_x=0 \\ \dfrac{\partial M_{yx}}{\partial x}+\dfrac{\partial M_y}{\partial y}-Q_y=0 \end{cases}$$

Here, P, S are the uniformly distributed internal force of tension and internal force of shear acting in the initial state of equilibrium. This changes in the case of added displacement (infinitesimally small displacement) but since it is slight, it can be regarded as unchanging.

In the displacement equation

$$\begin{cases} \dfrac{\partial^2 u}{\partial x^2}+\dfrac{1-\nu}{2}\dfrac{\partial^2 u}{\partial y^2}+\dfrac{1+\nu}{2}\dfrac{\partial^2 v}{\partial x\partial y}+\dfrac{\nu}{r}\dfrac{\partial w}{\partial x}=0 \\ \dfrac{\partial^2 v}{\partial y^2}+\dfrac{1-\nu}{2}\dfrac{\partial^2 v}{\partial x^2}+\dfrac{1+\nu}{2}\dfrac{\partial^2 u}{\partial x\partial y}+\dfrac{1}{r}\dfrac{\partial w}{\partial y}=0 \\ D\nabla^4 w+\dfrac{E\,t}{(1-\nu^2)}\cdot\dfrac{1}{r}\left(\dfrac{\partial v}{\partial y}+\dfrac{w}{r}+\nu\dfrac{\partial u}{\partial x}\right)-P\dfrac{\partial^2 w}{\partial x^2}-2S\dfrac{\partial^2 w}{\partial x\partial y}=0 \end{cases}$$

Moreover, as Love found, it is possible to introduce a higher order term, but as the result of examining the effects of the magnitude of u, v, w which are the components of displacement with respect to the buckling deformation of a shell surface by Donnell [10, 90] and of high order terms, u, v both are quantities about equal to $\sqrt{\frac{t}{r}}w$

so the high order terms omitted from the above equation, as long as they are viewed in terms of infinitesimal deformation theory, do not have any substantial effect. Moreover,

$$\nabla^2=\partial^2/\partial x^2+\partial^2/\partial y^2$$

Eliminating v and u from the above equation

$$\begin{cases} r\nabla^4 u=-\nu\dfrac{\partial^3 w}{\partial x^3}+\dfrac{\partial^3 w}{\partial x\partial y^2} \\ r\nabla^4 v=-(2+\nu)\dfrac{\partial^3 w}{\partial x^2\partial y}-\dfrac{\partial^3 w}{\partial y^3} \end{cases}$$

is obtained. Inserting this in the third equation, the equation for w only, /519

$$D\nabla^4 w+\frac{Et}{r^2}\frac{\partial^4 w}{\partial x^4}-r^4\left(P\frac{\partial^2 w}{\partial x^2}+2S\frac{\partial^2 w}{\partial x\partial y}\right)=0$$

is obtained.

Assuming that in the problem of buckling, when the added displacements from the initial state (u, v, w) when there is a uniform P, S, occurs, the change in this state of internal forces is small even if it occurs, and assuming a constant everywhere, we determine the (u, v, w) which satisfy the boundary conditions and equilibrium equation. The method is widely used in which the buckling wave form (u, v, w) satisfying the boundary conditions is appropriately positive, inserted into the equilibrium equation, the matrix is assumed to be 0, and P, S are found that will satisfy this. This is the eigen value, is normally handled in terms of solving a complicated function equation, and considerable effort is required in order to solve it.

Similarly, for spherical shells and parabolic shells, an equilibrium equation is derived for infinitesimal deformation.

EQUILIBRIUM EQUATIONS FOR CYLINDRICAL SHELLS BASED ON FINITE DEFORMATION THEORY [10, 11, 21, 24]

When a cylindrical shell undergoes finite deformation, and reaches a state of equilibrium, it is necessary to consider a higher order term. For the strain component in the midplane,

$$\varepsilon_x=\frac{\partial u}{\partial x}+\frac{1}{2}\left(\frac{\partial w}{\partial x}\right)^2,$$

$$\varepsilon_y=\frac{\partial v}{\partial y}+\frac{1}{2}\left(\frac{\partial w}{\partial y}\right)^2+\frac{w}{r},$$

$$\gamma_{xy}=\frac{\partial u}{\partial y}+\frac{\partial v}{\partial x}+\frac{\partial w}{\partial x}\frac{\partial w}{\partial y}.$$

Similarly, the change in curvature and twist,

$$\kappa_x=-\frac{\partial^2 w}{\partial x^2},\quad \kappa_y=-\frac{\partial^2 w}{\partial y^2},\quad \tau=-\frac{\partial^2 w}{\partial x\partial y}$$

The stress-strain relationship in the midplane is

$$\sigma_x=\frac{E}{1-\nu^2}(\varepsilon_x+\nu\varepsilon_y),\quad \sigma_y=\frac{E}{1-\nu^2}(\varepsilon_y+\nu\varepsilon_x),\quad \tau_{xy}=\frac{E}{2(1+\nu)}\gamma_{xy}$$

The equilibrium condition for an element of force paraliel to the shell surface can be considered to be approximately

$$\frac{\partial\sigma_x}{\partial x}+\frac{\partial\tau_{xy}}{\partial y}=0,\qquad \frac{\partial\tau_{xy}}{\partial x}+\frac{\partial\sigma_y}{\partial y}=0$$

From this it is possible to assume the presence of one stress function F(xy).

$$\sigma_x=\frac{\partial^2 F}{\partial y^2},\qquad \tau_{xy}=-\frac{\partial^2 F}{\partial x\partial y},\qquad \sigma_y=\frac{\partial^2 F}{\partial x^2}$$

The stress component is expressed by using this stress function F(xy) and eliminating u, v from the expression based on the displacement components, the relation between F(xy) and w is obtained as a compatability condition.

$$\left(\frac{\partial^2}{\partial x^2}+\frac{\partial^2}{\partial y^2}\right)^2 F=\nabla^4 F=E\left[\left(\frac{\partial^2 w}{\partial x\partial y}\right)^2-\frac{\partial^2 w}{\partial x^2}\frac{\partial^2 w}{\partial y^2}+\frac{1}{r}\frac{\partial^2 w}{\partial x^2}\right] \qquad (A)$$

Next, the strain energy with respect to a section (a × b) of the cylinder /520

$$W_1=\frac{t}{2E}\int_0^a\int_0^b\left[(\sigma_x+\sigma_y)^2-2(1+\nu)(\sigma_x\sigma_y-\tau_{xy}^2)\right]dx\,dy$$

$$+\frac{Et^3}{24(1-\nu^2)}\int_0^a\int_0^b\left[\left(\frac{\partial^2 w}{\partial x^2}+\frac{\partial^2 w}{\partial y^2}\right)^2-2(1-\nu)\left\{\frac{\partial^2 w}{\partial x^2}\frac{\partial^2 w}{\partial y^2}-\left(\frac{\partial^2 w}{\partial x\partial y}\right)^2\right\}\right]dx\,dy$$

the potential energy of the external force is

$$W_2=-\int_0^b (N_x)_{x=a}\,dy\int_0^a\frac{\partial u}{\partial x}dx-\int_0^a (N_{xy})_{x=a}\,dy\int_0^a\frac{\partial v}{\partial x}dx$$

Consequently, the equilibrium equation is found by assuming 0 for the variation of $W_1 + W_2$. Donnell found the following equation by this method.

$$\frac{Et^3}{12(1-\nu^2)}\nabla^8 w+\frac{Et}{r^2}\frac{\partial^4 w}{\partial x^4}=\nabla^4\left\{p+t\left(\sigma_x\frac{\partial^2 w}{\partial x^2}+2\tau_{xy}\frac{\partial^2 w}{\partial x\partial y}+\sigma_y\frac{\partial^2 w}{\partial y^2}\right)\right\}$$

p is internal pressure. Using the stress function F

$$\frac{Et^3}{12(1-\nu^2)}\nabla^8 w+\frac{E}{r^2}\frac{\partial^4 w}{\partial x^4}=\nabla^4\left[\frac{p}{t}+\frac{\partial^2 E}{\partial y^2}\frac{\partial^2 w}{\partial x^2}-2\frac{\partial^2 F}{\partial x\partial y}\frac{\partial^2 w}{\partial x\partial y}+\frac{\partial^2 F}{\partial x^2}\frac{\partial^2 w}{\partial y^2}\right] \qquad (B)$$

The problem is to determine exaction F,w from (A) (B) under the given boundary conditions, or as a second method, to first posit an appropriate w(xy) that will satisfy the boundary conditions which include an unknown factor and then find the stress function F from (A). Then, calculating the change in energy $W_1 + W_2$, the unknown factor is determined which is included in w so that this is reduced to a minimum. Kármán-Tsien [24] by means of this second method, established a new theory, by calculating the buckling of a cylinder under compression.

E. Trefftz (1933) [12] proceeded from the finite deformation theory of elasticity and derived finite deformation equilibrium conditions for shells from Castigliano's energy principle, hypothesizing a normal stress distribution in the direction of the plate thickness in 1935. This hypothesis is not strictly compatible with the normal conservation law. This is an equation

having the same structure as that which was derived by W. Flügge (1934) [35] assuming the normal conservation law, at least to the extent of an approximation which excludes the term of the square of t/r. In 1934, L. H. Donnell [10] derived the equation described above and in 1938, K. Marguerre [15] derived the similar strict equation for a cylindrical shell. In 1939, R. Kappus (1939) [21] generalized the Trefftz-Marguerre theory and found a general equation for energy. These strict theories are complicated and at the present time are not of practical use. Donnell's [10] equation is not highly accurate, but it is easy to use in practice. Moreover, according to R. Kappus [21] method, since the energy expression is strictly determined, it has a powerful basis when the energy method is applied. Generally, in most cases it is difficult to employ the equilibrium conditions for a neutral state of equilibrium, since this becomes non-linear and the necessity frequently arises to make simplifications of the treatment, by making appropriate simplifications according to the shell configuration.

The reader is referred to the literature for details on finite deformation theory.

CHAPTER 3 /521

BUCKLING PHENOMENA AND BUCKLING LOAD FOR VARIOUS TYPES OF SHELLS

5.3.1. BUCKLING OF CYLINDERS

Compressive Buckling. Research on the compressive buckling of cylinders began as described in the previous chapter with R. Lorenz (1908). Extensive research has also been carried out by the following: S. Timoshenko (1910), R. Lorenz (1911), R. v. Southwell (1914), W. R. Dean (1925), L. Föppl (1926), A. Robertson (1927), J. W. Geckeler (1928), K. v. Sanden-F. Tölke (1932), W. Flügge (1932), E. E. Lundquist (1933), L. H. Donnell (1934), W. Kaufmann (1935-37), K. Marguerre (1938), Th. v. Kármán, L. G. Dunn and H. S. Tsien (1940), Th. v. Kármán-H. S. Tsien (1941) and L. H. Donnell-C. C. Wan (1950).

According to compression tests [72, 76] of cylinders with simple supports at both ends or with both ends fixed, the forms of breakage can be classified into the following three types depending on the value of the radius to plate thickness ratio r/t of the cylinder.

(1) Breakage of material.

(2) Axially symmetrical deformation buckling (A).

(3) Asymmetrical deformation buckling (B, C).

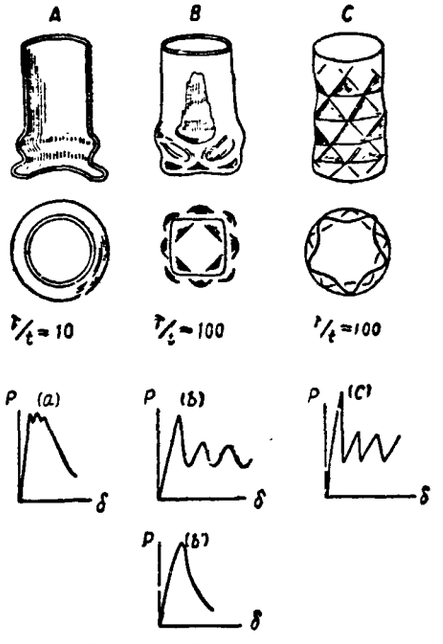

Figure 5.3.1

If r/t is sufficiently small, breakage occurs at the breaking strength of the material and when r/t is within a small range, axially symmetrical deformation or asymettrical deformation occurs due to compressive stress in the plastic region, and in thin-walled cylinders where r/t is large, asymmetrical buckling occurs within the elastic region.

In the case of axially symmetrical wave forms, almost all of the cylinder planes are displaced in the outwards direction. In asymmetrical buckling, the same degree of displacement occurs outwards and inwards in the case of the plastic region, and in the case of buckling in the elastic region, displacement inwards is predominant. Moreover, these wave forms are hardly effected by the boundary conditions at both ends when

the length of the cylinder l is 1.5 times greater than the radius.

The experimental curves for the compressive load P and contraction δ are of the types (a), (b), (b'), (c). In Robertson's experiments (1929) [72], in almost all cases, buckling occurs in the plastic region, but in both the cases of A and B, the P-δ curve is usually of the type (a) and (b'). In the case of type B deformation, there are examples in which P-δ curve type (b) occurs. This (b) is seen in the case when the wave form around the edge of the cylinder is symmetrically formed. When, on the other hand, asymmetrical locally concentrated wave forms appear, they take the shape of (b') and then, since the distribution of stresses is affected by the compressive bending which deviates from the neutral axis in the direction opposite to the wave crest, the cylinder undergoes breakage locally. The P-δ curve assumes a sharpened form. In the case of a thin wall and buckling occurring in the elastic region, the number of waves occurring in the direction of the circumference is relatively large (n = 10-20). Consequently, the occurrence of wave forms extends around the circumference, /522
and has a tendency to occur rather evenly. When the wave forms occur, they emit a loud noise. Moreover, more than in the case of the plastic region, the P-δ curve manifests a sharp saw-tooth curve shape and each time that a wave is formed, a crest is also formed. Also in the case of impact compression, a similar P-δ curve is manifested, but in this case, the value of P where the first peak appears is much greater than the value of the peaks after the second one. (Unpublished reports of experiments by Majima and Hanada.)

R. Lorenz (1908) [66] was the first to analyze axially symmetrical compressive buckling, and he derives an equilibrium equation corresponding to the displacement w in an outside direction in the elastic region.

$$D\frac{d^4w}{dx^4}+P_k\frac{d^2w}{dx^2}+\frac{Et}{r^2}w=0 \qquad P_k=\sigma_k t= \text{ limit width compressive force} \tag{5.3.1}$$

assuming w = C sin nπx/l for the half-wave length and buckling stress he obtained

$$\frac{\lambda}{2}=\frac{\pi}{\sqrt[4]{12(1-\nu^2)}}\cdot\sqrt{rt}\sim 1.715\sqrt{rt},\ (\nu=0.3),\quad \sigma_k=\frac{E}{\sqrt{3(1-\nu^2)}}\cdot\frac{t}{r} \tag{5.3.2}$$

but the posited wave form has the same shape both inwards and outwards and he was unable to explain by experiment the outwards displacement. Moreover, the stresses themselves did not agree with the experiments. S. Timoshenko [67] made the same calculations. L. Föppl [71] suggested that the disagreement was due to the fact that the end conditions of the actual cylinder differed from theory (1926). That is, depending on the compression, the cylinder bulges in a lateral direction, but owing to friction with the test apparatus, the ends are not displaced and the cylinder plane at the end undergoes considerable bending. Taking this into consideration, J. W. Geckeler (1927) solved (1) but he was unable to make a correct explanation. Discovering that this form of buckling occurs within the plastic region, Geckeler [73] in 1928 employed the same Knickmodul K as in Engesser-Kármán's plastic region buckling of a column, and using E for the circumferential direction, he derived an equilibrium equation

$$\left.\begin{aligned} &\frac{d^4w}{dx^4}+\frac{12(1-\nu^2)P}{t^3K}\frac{d^2w}{dx^2}+\frac{12(1-\nu^2)E}{t^2r^2K}w=0 \\ &\text{here}\qquad K=\frac{4EE'}{(\sqrt{E}+\sqrt{E'})^2},\quad E'=\left(\frac{d\sigma}{d\varepsilon}\right)_{\sigma},\quad P=\sigma_k t \end{aligned}\right\} \tag{5.3.3}$$

In solving this, he obtained, for the buckling load

$$W_k=\frac{2\pi t^2}{\sqrt{3(1-\nu^2)}}\cdot\sqrt{EK}, \tag{5.3.4}$$

For the buckling stress, the E in equation (5.3.2) appears in the form $\sqrt{EK}$.

The W_k-r/t for soft steel is as shown in the figure in Materials 17. [This refers to the materials following part 5.] Where there is an extremely small r/t, breakage occurs at the compressive breaking strength of the material.

Since the deformation is considered to be of a sine wave shape, there are still discrepancies with the experiments, but equation (5.3.4) at least becomes one measure of convenience. Shibuya and Kuranishi provide analyses of this type of elastic buckling.

R. Lorenz (1911) [68], R. v. Southwell (1914) [69], S. Timoshenko (1911) [67] have calculated asymmetrical buckling in the elastic region. On the basis /523 of the equilibrium equations for a shell surface in infinitesimal deformation theory, assuming the added displacement at the time of buckling to be

$$u=A\sin\frac{ny}{r}\cos\frac{m\pi x}{l},\quad v=B\cos\frac{ny}{r}\sin\frac{m\pi x}{l},\quad w=C\sin\frac{ny}{r}\sin\frac{m\pi x}{l}$$

(1) When r/t is quite large, and the wave length in the direction of the axis is short, i.e., when $m\pi r/l$ is large

$$\sigma_k=\frac{E}{\sqrt{3(1-\nu^2)}}\cdot\frac{1}{r};\quad n=\sqrt[4]{\frac{3}{4}(1-\nu^2)}\sqrt{\frac{r}{t}}=0.91\sqrt{\frac{r}{t}},$$

Half-wave length in direction of circumference = $\frac{\pi r}{n}=3.45\sqrt{rt}$.

(2) In particular, in the case of a short cylinder,

$$\sigma_k=\frac{\pi^2E}{12(1-\nu^2)}\cdot\frac{t^2}{l^2}=\text{Euler-buckling stress}$$

(3) In a long cylinder where there are relatively long longitudinal waves produced

$$\sigma_k=\frac{E}{\sqrt{3(1-\nu^2)}}\cdot\frac{n^2-1}{n^2+1}\cdot\frac{t}{r},\ \text{when } n=2\quad \sigma_k=\frac{3}{5}\cdot\frac{E}{\sqrt{3(1-\nu^2)}}\cdot\frac{t}{r}$$

were obtained. W. Flügge obtained a graph of σ_k-1/mr with n as a parameter for a cylinder with a defined t/r.

E. E. Lundquist (1933) [76], L. H. Donnell (1934) [77] conducted compression tests on thin-walled cylinders in relation to problems in the design of aircraft structures (see Materials 19).

According to the results of these experiments, as shown by infinitesimal deformation buckling theory, the buckling wave forms display relatively small waves. Normally the wave length in the direction of the axis and the circumference are about the same. The number of waves is about 80 to 50% of that in the theory. The waves that are first produced increase in size with the load and the number of waves decreases. Moreover, the displacement was overwhelmingly inwards. The experiment points of r/t with respect to the buckling stress σ_k are extremely scattered as shown in Donnell's paper [77] (See Materials 19). They appear to be 20 to 60% of the theoretical values, and this discrepancy is more marked the greater the r/t in thin-walled cylinders.

Donnell (1934) attempted to explain the discrepancy between the above results, by considering that the cause for this discrepancy was due to the initial deformation at the time of manufacture of the cylinder, and he analyzed its effects; however, even though this will explain the decrease in the buckling stress, the problem still remains concerning the scattering of the test points.

It gradually became clear that this deformation accompanied finite deformation and the development of finite deformation elasticity theory was thus stimulated. From this point of view, Kármán-Tsien (1938) analyzed the problems of the buckling of spherical shells [138] and the compressive buckling of cylinders and established a new theory. In the case of a spherical shell supported around the circumference, and sustaining pressure, the relationship between the pressure /524
p and the central deflection δ is as shown by O A B C D in Figure 5.3.2. This relationship gradually takes the form of the upper curve, as the plate thickness increases. Such a buckling phenomenon accompanying finite deformation can also occur in the case of the compression of a cylinder, and in the conventional theory, the equilibrium equation was determined for the shape prior to deformation. Moreover, it was assumed that there was a basic defect in assuming infinitesimal deformation. As a special case, they proceeded from a more rational deformation equation which included the conventional theory and expressed the facts of the experiments. That is, considering that displacement inwards is strongly manifested, for the displacement they considered

$$\frac{w_1}{r}=\cos^2\frac{(mx+ny)}{2r}\cos^2\frac{(mx-ny)}{2r}.$$

and they also considered for convenience, the conventional wave form with respect to deflection in infinitesimal deformation

$$\frac{w_2}{r}=\cos\frac{mx}{r}\cos\frac{ny}{r}.$$

and ultimately posited the following equation:

$$\frac{w}{r}=\left(f_0+\frac{f_1}{4}\right)+\frac{f_1}{2}\left(\cos\frac{mx}{r}\cos\frac{ny}{r}+\frac{1}{4}\cos\frac{2mx}{r}+\frac{1}{4}\cos\frac{2ny}{r}\right)$$
$$+\frac{f_2}{4}\left(\cos\frac{2mx}{r}+\cos\frac{2ny}{r}\right).$$

f_0, f_1, f_2 are unknown quantities. f_0 is the term used in order to take into consideration expansion in the direction of the radius due to compression. n is the number of waves in the direction of the circumference. If the length is greater than 1.5 times the radius, there is practically no effect from the ends, and may be excluded here. Assuming $f_0 = f_2 = 0$, this becomes the expression w_1/r, and assuming

$$(f_1/4+f_2/4)=0,\ f_0+\frac{f_1}{4}=0$$

w_2/r appears. In values other than these parameters, these appear intermediate between these two extreme ends. Positing the above buckling deformation, inserting them in the above compatability conditions of the finite deformation theory, determining the stress function F(xy) and calculating the stress component and displacement component, the energy $W_1 + W_2$ within the region of one wave length is found as a function of f_0, f_1, f_2. Moreover, from the equation $\partial/\partial f_0(W_1 + W_2) = 0$, f_0 is expressed as $f_1 f_2 \sigma$ (σ is the average compressive stress), assuming $W_1 + W_2 = fn\ (f_1 f_2 \sigma)$, partially differentiating this by f_1, f_2, the equilibrium condition is determined. As a numerical example, the following results were obtained using the case where $\mu = m/n$ was 1.0 and 0.5 (the ratio of the wave length in the direction of the circumference of the wave to the wave length in the longitduinal direction). Kármán and Tsien state that they calculated the case where $\mu = 1.0$ and 0.5 on the basis of experiments and derived $\mu = 1.0$ from infinitesimal deformation theory also. However, the case of 0.5 is still theoretically undetermined.

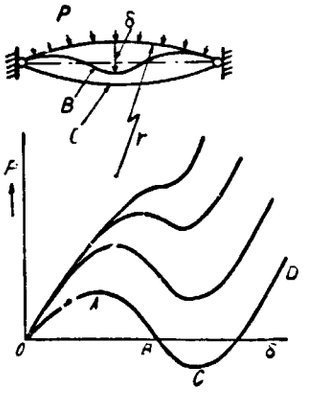

Figure 5.3.2

For a cylinder where r/t = 1000, the curve for σ r/Et and $\xi = f_1 r/t$ or ε r/t in the case where $\mu = 1.0$, case in which the wave length is equal in the axial direction and in the direction of the circumference is as shown in the diagram in Materials 22 describing $\eta = n^2 t/r$ as a parameter. Also n is considered as the parameter, if its envelope line is determined, the latter gives the relationship between the deformation and the $\sigma r/Et$ that should actually occur. The wave form suddenly develops from the classical value $\sigma r/Et = 0.6$, the contraction at the ends decreases and the load decreases. Consequently, this buckling process is extremely unstable. Moreover, the curve passes through the minimum point $\sigma r/Et$ and then rises again During this time the number of waves in the direction of the circumference is 26 in the initial period of buckling when r/t = 1000 and then it gradually decreases, becomes 13 at the minimum point and then decreases further. Moreover, the wave form becomes large. Such a property of change in wave

/525

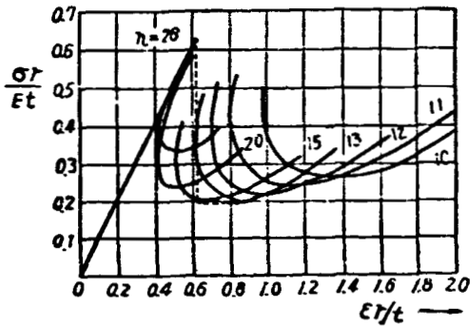

Case when r/t = 1,000, μ = 1.00
Curve of σr/Et to εr/t
The parameter n is the wave number in the direction of the circumference

Figure 5.3.3

form is very often seen in experiments. The lower minimum point stress is

$$\sigma = 0.794 E \frac{t}{r}$$

This stress is extremely close to the experiment values of Lundquist and Donnell. Kármán and Tsien explain that it jumps from the ultimate load point to this value. It is for this reason that they propose their "jump theory." They also assume that this jump could occur before the ultimate load point; i.e., the classical buckling stress is reached when there is a shock from the outside. Even when μ = 0.5, they showed that the same phenomenon could occur, but in this case they obtained the result that the load dropped as far as a value of 0. In the process in which the load increases, the jump can occur suddenly due to some stimulus and they say that this is affected by the rigidity of the test apparatus.

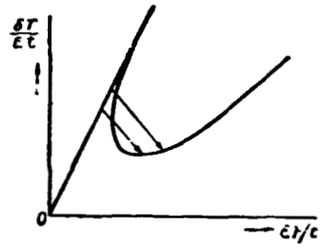

Figure 5.3.4

Ikeda indicated that Kármán-Tsien's jump theory contradicted the experimental evidence and with respect to this, Hayashi and Imanaka [28] investigated the effects of initial deflection, found that when there was initial deflection, this sharp peak became round, the difference between the ultimate stress and the minimum point decreased, and that the effect was extremely marked. They concluded that the experiment curves appeared to be very close to the curves in the case of such initial deformation, without taking Kármán-Tsien's ideal form into account. In their analysis, they posited a periodic deformation as an initial deformation and assumed that the additional deflection caused by compression increased in exactly the same form. This can be posited on the basis of the detailed results of measurements of the deformation of a cylindrical plane undergoing a compression that was carried out by Shibuya.

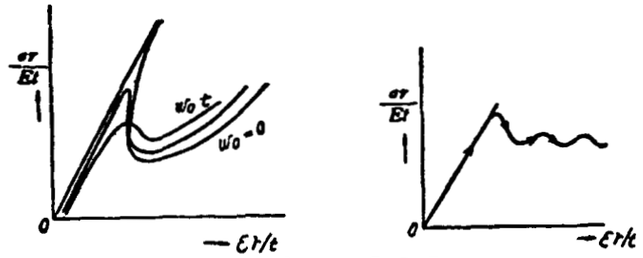

Figure 5.3.5

As described above, in experiments wave forms are not formed all at once throughout the entire cylinder plane, but occur locally, and when the waves that occur in one part reach a certain magnitude, it is observed that new buckling occurs in other parts. This expresses the peak of the σ-ε curve which is gradually formed. By means of the above, some explanation was provided for the discrepancy between the explanation of the phenomena of compressive buckling of a cylinder, the theory of buckling stress and experimental results. It was found that the experiment values which were about 1/2 of the classical theoretical values, indicated a lower stress of /526

$$\sigma_k = 0.194 E\frac{t}{r} \approx 0.2 E\frac{t}{r}$$

from an analysis based on the above finite deformation theory. In practice, it is more rational to employ this value than the $\sigma_k = 0.6\ E(t/r)$ which is the classical theoretical value.

Later, L. H. Donnell and C. C. Wan [84] performed the same calculations as Hayashi and Imanaka [28] for the effects of initial deflection and the yield of the plane of a cylindrical shell. As shown in the Materials 23, they posited an initial deflection, assumed that the additional deflection also occurred in the same form as this, and by the energy method, they determined the relationship between the average compressive stress of the cylinder and the average compressive strain. Their results are practically no different from those of Hayashi and Imanaka [28]. These authors have also compiled the results of many experiments that have been performed up to the present time.

In a short cylinder ($l \leq 1.5r$) the effect of boundary conditions becomes involved and when Hayashi and Murakami [158] analyzed two or three cases of this, they found that the effects were great. They obtained the result that the minimum stress value; i.e., the lower stable stress value decreased significantly more than in the case of a perfect cylinder. Experimental values have been obtained for buckling within the plastic region in a cylinder, and in the analysis of these, in addition to Geckeler's analysis described above, Shebuya and Kuranishi [39] considered the case of symmetrical buckling. Kuranishi's results explain well A. Robertson's experiment.

Torsional Buckling of a Cylinder. A. G. Greenhill (1883) was the first to study the torsion buckling of a slender axis, and analysis of the torsion buckling of cylinders have been carried out by E. Schwerin (1924), K. Sezawa-K. Kubo (1931), K. Sezawa (1933, K. v. Sanden-F. Tölke (1932), L. H. Donnell (1933), W. Flügge (1934), A. H. Stang, W. Ramberg and G. Back (1937) and J. E. Younger. Experimental research has been carried out by K. Sezawa-K. Kubo (1931), L. H. Donnell (1933), E. E. Lundquist (1932), W. Ballerstedt-H. Wagner (1936), A. H. Stang and W. Ramberg and G. Back (1937).

In the case where the axis is slender, and the plate thickness to radius ratio is small, the buckling waves do not occur on the wall of the cylinder axis, the cross-section shape remains circular, and the overall axis is twisted and buckles in the shape of a morning glory vine. This torsional buckling moment is a minimum when the torsion wave forms one perfect wave length over the

wave length l and its value agrees with that which Greenhill [85] determined for a true thin rod and is given as

$$T_1=\frac{\pi EJ}{l}$$

J is the polar moment of inertia of area.

In thin-walled cylinders, buckling waves may occur on the walls in the elastic region (refer to the configurations of buckling in Chapter 1). L. H. Donnell [90] investigated buckling wave forms, and denoting the additional displacement at the time of buckling in the basic equations for infinitesimal deformation in chapter 2 by

$$u=\sum U_n \sin 2\left(\frac{ny}{d}-\frac{\lambda_n x}{l}\right), \quad v=\sum V_n \sin 2\left(\frac{ny}{d}-\frac{\lambda_n x}{l}\right),$$

$$w=\sum W_n \cos 2\left(\frac{ny}{d}-\frac{\lambda_n x}{l}\right).$$

he obtained general results by solving differential equations carrying out simplification with respect to deformation, by taking into consideration the boundary conditions (rotating ends and fixed ends) of both ends of the cylinder. Since the experiment values fall within 60 to 70% of the theory, in design formulas, the equation which uses the 60% figure can be employed. In a relatively long cylinder, irrespective of the boundary conditions at both ends, /527

$$\tau_2=0.272\frac{E}{(1-\nu^2)^{\frac{3}{4}}}\left(\frac{t}{r}\right)^{\frac{3}{2}}$$

is obtained and this result matches with the result found by E. Schwerin [86].

In a relatively short cylinder, $1/r < 5$, the experimental equation of W. Ballerstedt-H. Wagner [93]

$$\tau_1=0.1E\frac{t}{r}+k\cdot E\left(\frac{t}{l}\right)^2$$

where k = 5.0 with both ends rotating
9.1 with fixed ends

is useful [Materials 26].

A. H. Stang, W. Ramberg and G. Back [95] have studied the buckling accompanying plastic deformation and have provided experimental equations and charts. In short cylinders, after buckling, if the shape of the ends is unchanged, the simple part becomes constricted and the cylinder assumes the shape of an hour glass. Sezawa, Kubo [87] have conducted detailed experiments on rubber cylinders, for this type of deformation. Hayashi, and Shimano (lectures at the Applied Japan Dynamics Society, 1948) have analyzed and discussed the torsion stiffness and stress distribution after buckling. According to their analysis, the torsion stiffness decreases to about 70% of that before buckling, immediately after buckling.

Flexural Buckling of Cylinders. L. G. Brazier (1927) was the first to analyze the pure flexural buckling of cylinders. In addition, there have been studies by S. Timoshenko (1930), W. Flügge (1932), R. W Mossman and Robinson (1933), E. Chwalla, E. E. Lundquist, J. E. Younger (1933), L. H. Dornell (1934). The case of compound loads is discussed later.

When a pure bending moment M is applied to an infinitely long cylinder, a curvature κ occurs in the direction of the axis. Now, if in the two cross-sections a portion infinitesimally long is cut out, the bending stress acting on the cross-section has a component in the direction toward the neutral axis, and owing to this, the shape of the cross-section becomes flat. Consequently, the flexural stiffness decreases. When the stiffness decreases, the curvature increases, the flattening progresses and finally when the flattening has progressed to a certain configuration, a maximum resistance is indicated after which, if the curvature increases further, unless there is a small bending moment, the equilibrium no longer can be maintained. In this manner, a peak can occur in the M-κ curve. The bending moment above this maximum value cannot be accepted. This phenomenon is called the bending yield of a cylinder.

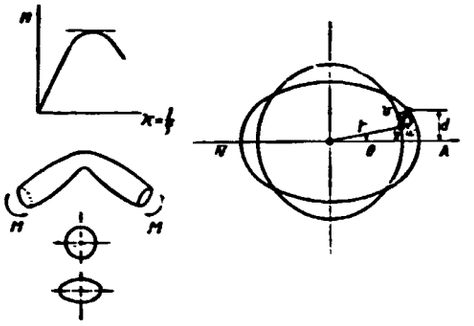

Figure 5.3.6

L. G. Brazier [96] determined the maximum bending moment in the following manner. Considering the unit length of the cylinder, if the strain energy W_1 due to expansion and contraction in the direction of the axis due to the external moment when a displacement (v, w) is formed at a point on the cross-section and the strain energy W_2 due to change in curvature in the direction of the circumference are determined

/528

$$U_1=\frac{1}{2}\alpha_1\kappa_1^2\oint d^2dy, \qquad U_2=\frac{1}{2}D_2\oint\kappa_2^2dy$$

α_1 = Tensile stiffness in direction of axis of outer plate.

D_2 = Bending stiffness in direction of circumference of outer plate

k_1 = Curvature in direction of axis due to bending moment M

k_2 = Change in curvature in direction of circumference due to deformation v, w

d = Distance from neutral axis NA at point after deformation.

The strain energy is $U = U_1 + U_2$

The bending moment, from Castigliano's theorem is given as

$$M=\frac{dU}{d\kappa_1}$$

Since normally it is possible to assume inextensional deformation with respect to the deformation of the circumference, on the basis of this assumption, determining the relationship between M and κ_1 in the above equation

$$M=\pi r^2\alpha_1\left(\kappa_1-\frac{1}{8}\cdot\frac{\alpha_1 r^4}{D_2}\kappa_1^3\right)$$

Therefore

$$M_{max}=\frac{4\sqrt{6}}{9}\pi r\sqrt{D_2\alpha_1},$$

This is the result obtained by Hayashi [165] for a general orthotropic cylinder. Moreover, w_{max} = 2/9r.

The maximum compressive internal force (per unit width) N_1 due to bending at the most remote point from the neutral axis is

$$N_1=\alpha_1\kappa_1 r=\sqrt{\frac{8}{3}}\cdot\frac{\sqrt{D_2\alpha_1}}{r}$$

In an isotropic cylinder with uniform thickness, since it is

$$D_2=\frac{Et^3}{12(1-\nu^2)},\quad \alpha_1=\frac{Et}{1-\nu^2}$$

$$M_{max}=\frac{2\sqrt{2}}{9}\cdot\frac{\pi}{1-\nu^2}Ert^2,\qquad \sigma_{max}=\frac{2\sqrt{2}}{9(1-\nu^2)}E\frac{t}{r}$$

when ν = 0.3, this is

$$M_{max}=1.086\,Ert^2\qquad\qquad \sigma_{max}=0.346\,E\frac{t}{r}$$

and this agrees with the results obtained by Brazier.

In a comparison [96] with experiment results, the maximum experiment values are close to the above values for M_{max}. However, normally before such buckling due to flattening can occur, local buckling occurs on the compression side at a particular load. Consequently, in thin-walled cylinders, it is possible to estimate approximately the maximum bending moment in the case when breakage to a thin-walled cylinder occurs due to such local buckling as the value at which the bending stress reaches the lower extreme value stress of the cylinder undergoing pure compression σ_k = 0.2 E(t/r) (Kármán-Tsien's theoretical value). According to this,

$$M_{max}=Z\sigma_k=\pi tr^2\sigma_k=0.2\pi Ert^2\quad\text{(For thin-wall } Z\fallingdotseq\pi r^2t\text{)}$$

is obtained. Actually, since the local buckling stress is larger than the buckling stress 0.2 E t/r at the time of pure compression, the value of this M_{max} should appear on the safe side.

As can be seen from Materials 29, in L. H. Donnell's [103] experiments, /529
the buckling stress with respect to various r/t is extremely scattered, and the scattering of such experiment points indicates that the buckling, as in the case of compressive buckling of a cylinder, occurs together with finite deformation. The fact that the maximum bending stress at the time of buckling determined by beam theory from the bending moment, comes close to the pure compression buckling stress 0.2E r/t indicates that the estimation of M_{max} described above is quite valid. The yield buckling due to flattening occurs in the case of relatively thin rubber tubing.

Cylinder Under External Pressure. When an external pressure p acts on a long cylinder, a compressive stress p r/t is sustained in the direction of the circumference. When p is gradually increased, the cylindrical shape is lost and buckling occurs due to this compressive stress. Such problems have been investigated over a long period of time, and there has been research by H. Bryan (1888), R. Lorenz (1911), R. v. Southwell (1913), G. Cook (1913), R. v. Mises (1914), K. v. Sanden-K. Günther (1920, 1921), Tokugawa (1925, 1931, 1932, 1936, 1940), H. M. Westergaard (1934) and W. Flügge (1934).

When the cylinder is extremely long, since axially symmetrical deformation occurs, this becomes the same form as the expression of buckling pressure due to external pressure on the circumference. In this case, inextensional deformation becomes possible (See Materials 31).

When the length is finite and the deflection at both ends is suppressed, the boundary conditions for both ends become involved, so inextensional deformation becomes unallowable. In this case, for the displacement at a point on the shell center plane, it is convenient to assume a periodic wave form on axis (x) and in the direction of the circumference (ψ).

$$u=U\cos n\varphi\cos\frac{m\pi x}{l},\qquad v=V\sin n\varphi\sin\frac{m\pi x}{l},\qquad w=W\cos n\varphi\sin\frac{m\pi x}{l}$$

This satisfies the condition that both ends be rotating ends and that the force in the direction of the axis is 0. By substituting this displacement in the equilibrium condition equations after buckling, it is possible to determine the relationship between the buckling pressure p_k from the buckling conditions obtained assuming that the matrix of the coefficients U, V, W is 0, and m, nπr/l. This is the equation obtained by Tokugawa [112, 119] given in Materials 32.

In exactly the same manner, R. v. Mises [120], W. Flügge [117] and Tokugawa [113, 114, 119] analyzed the case in which an external pressure acts on the total surface of a cylinder closed at both ends. R. v. Mises derived the formula shown in Materials 33 and D. F. Windenburg and C. Trilling [126] calculated the end which should be made a minimum with respect to the t/2r, l/2r giving the p_k in this equation, and obtain the charts indicated in Materials 33.

W. Flügge conducted an analysis of the case in which the compressive stress σ in the direction of the axis simultaneously acts with external pressure p,

and obtained the charts shown in Materials 35. This is a numerical example of the case when $\gamma = t^2/(12r^2) = 1 \times 10^{-5}$, $\nu = 1/6$. From this chart, it can be seen that the buckling value must be decreased in the case when the presence of compressive stress in the direction of the axis or of external pressure acts independently. According to experiments by D. F. Windenburg and C. Trilling [126] and by Tokugawa [114], the wave number in the direction of the circumference agrees with the theory. However, as for the stress at the time of buckling the theory explains the general tendency, but the experiment points are scattered at a lower value than in the theory. According to Tokugawa's experiments [119, 38], the experiment values seem to be about 60% of that of the theory.

The scattering of the experiment points predicts that the buckling phenomenon accompanies finite deformation and occurs suddenly. However, no research has yet been conducted which takes finite deformation into account.

Compression and Bending. This is equivalent to the case in which an eccentric compressive load acts on a cylinder, and with regard to this, W. Flügge [123] made calculations of the buckling displacement using the equations of infinitesimal deformation. /530

$$u=\cos\frac{m\pi x}{l}\sum_{0}^{\infty}A_n\cos n\theta, \qquad v=\sin\frac{m\pi x}{l}\sum_{0}^{\infty}B_n\sin n\theta,$$

$$w=\sin\frac{m\pi x}{l}\sum_{0}^{\infty}C_n\cos n\theta$$

The solid line in the graph in Materials 36 indicate his results. The chain lines are approximations in which the maximum stress is made to be equal to the classical buckling value at the time of pure compression, and as explained in the article on pure bending, it is valid to make this equal to the lower limit value $\sigma_k = 0.2\ E\ t/r$ taking finite deformation into consideration.

Ikeda [129] analyzed the case in which bending and external or internal pressure is sustained, using the same method as L. G. Brazier, and compares his results with experiments. In the case of external pressure and bending, the results match favorably with the experiments, but in the case of internal pressure and bending, an extreme discrepancy is shown. In theory, a yield buckling due to flattening is assumed, treating an adequately long case, but in the experiments, local buckling occurs on the compression side. The limitations of infinitesimal deformation theory can also be seen here. Analysis by finite deformation theory remains to be carried out.

Yoshimura and Mori [130] have analyzed the case of torsion and external or internal pressure, and have found an approximate equation. According to comparisons with experiments, when the external pressure p_k is small, they agree with the theory, but when the pressure is increased, the experiment values reach about 85% of that of the theory. A. Kromm [130] has investigated the buckling strength of reinforced shells under torsion and internal pressure but since the original report is unavailable, its contents are not known.

Torsion and Compression or Tension. F. J. Bridget, C. C. Jerome and A. B. Vosseller [125] have conducted extensive experiments on this case. Denoting the torsion moment by T, the compressive stress by σ and denoting the buckling values when these act independently by T_0, σ_0, the curve $(T_k/T_0 - \sigma_k/\sigma_0)$ corresponding to the buckling values T_k, σ_k when they act simultaneously is given in the graph in Materials 39. It can be seen that the third order parabola in Materials 41 is extremely close to this. According to experiments by W. Ballerstedt and H. Wagner for this, the results are closer to a second order parabola, Materials 40, for torsion and compression. The experiment values within the torsion and tension range are expressed by

$$\frac{T_k}{T_0} = \frac{\tau_k}{\tau_0} = 1 + \frac{1}{2}\frac{\sigma_k}{\sigma_0}$$

Yamana [124] derived basic equations for compound loads from the point of view of infinitesimal deformation.

5.3.2. CURVED PLATES

In most cases, curved plates refer to parts of cylinders and are called partial cylinders, cylindrical curved plates or cylindrical plates. Here, we shall mean the plates of cylinders, when talking about curved plates. As far as the characteristics of these curved plates are concerned, they have the property of a "flat plate" from the fact that they have four sides, and the property of a "cylinder" from the fact that they have the curvature arc. Generally the sectional outer plates in reinforced members are most frequently considered as curve plates.

The compressive buckling of curved plates has been investigated by J. S. Newell (1931-32), S. C. Redshaw (1933), S. Timoshenko (1936), H. Ebner (1937), W. A. Wenzek (1938), Shibuya (1940), Kawano (1941) and Yokoo (1941) and Kuranishi (1948). /531

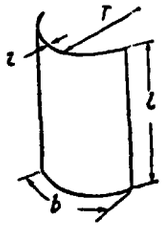

Figure 5.3.7

J. S. Newell's experimental equations and the analytical equations of R. C. Redshaw and S. Timoshenko each consist of terms for flat plates and terms for the curvature in cylinders. Both Timoshenko and Redshaw determine their buckling stress equations from the same kind of infinitesimal deformation theory as in the case of cylinders. Kawano [64] investigated these phenomena in terms of finite deformation theory on the basis of the basic equations established by K. Marguerre [15]. It became clear that the same marked instability phenomena occur as in the case of cylinders.

The shear buckling of curved plates has been investigated by H. Wagner (1928), G. M. Smith (1930), D. M. A. Leggett (1937), H. Ebner (1937), A. Zahorski (1937), A. Kromm (1938). H. Wagner [52] developed a famous experimental equation while A. Kromm [57] carried out a detailed analysis in terms of finite deformation theory and obtained the charts shown in Materials 7. As can

be seen from the charts, the theory well explains Wagner's experimental equations.

Moreover, H. Ebner [55] following the formulas of Timoshenko and Redshaw for compression, formulated the equations such as those shown in Materials 9, in which he reasons that the same kind of expressions might be usable formally even in the case of shear. These can also be used as experimental equations.

Buckling due to external pressure of curved plates. When the curved plate is sufficiently long, buckling due to external pressure in the case in which the two straight edges are considered to be rotating edges or fixed edges can involve inextensional deformation and the same type of results are obtained as in the case of a bent beam. This has been studied by E. Hurbrink (1908) [58], E. U. Nicolai [59] (1923) and S. Timoshenko (1936).

Inextensional deformation does not occur when the plate is of finite length and the boundary conditions of both ends are included, so the buckling pressure increases further, but no research has been done on this yet.

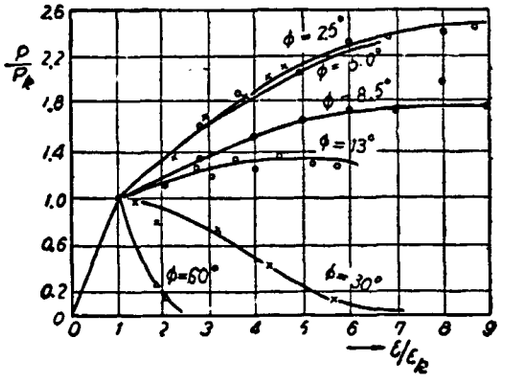

Relationship between compressive load P of curved plate and end strain ε
ϕ = center angle = b/r
b = length of arc of curved plate, r = radius
P_k = compressive force at time of buckling) actually
ε_k = buckling strain) measured *
*Wenzek's experiments
Figure 5.3.8

Effective Width of Curved Plate. It is convenient to express the forces sustained in terms of the concept of effective width, as in the case of flat plates, when dealing with curved plates after compressive buckling. (See Section on Effective Width of Plates.) With regard to this, W. A. Wenzek [63] has conducted experiments and published experimental equations, Kawano [64] has made an analysis and H. Ebner [61] has constructed design formulas.

H. Ebner's approach is to consider that when a curved plate is compressed, buckling occurs due to buckling stress ($\sigma_R \fallingdotseq 0.3\ E\ t/r$) and then it loses its curvature effect as a curved plate, becoming a "flat plate" and this acts on the edge reinforcing members. Consequently, the effective width of the edge reinforcing members with respect to a given stress σ_L is given by

$$b_m = \bar{b}_m + \frac{\sigma_R}{\sigma_L}(b - \bar{b}_m)$$

In σ_L, σ_R is used to cause the buckling of the curved plate and functions as a "flat plate" with respect to the pressure difference $\sigma_L - \sigma_R$. $\bar{b}_m$ is the effective width with respect to $\sigma_L - \sigma_R$; e.g., according to Marguerre's equation [14] it is given by /532

$$\bar{b}_m = \sqrt{\frac{\sigma_R}{\sigma_L - \sigma_R}} \cdot b$$

This method of Ebner's has been compared with the results of strength tests on tension shell constructions and found to be generally valid.

5.3.3. BUCKLING OF ELLIPTICAL CYLINDERS

Compressive Buckling. Shibuya (1940) [132] determined buckling condition equations from infinitesimal deformation theory for the compressive buckling of elliptical cylinders, and compared them with experiments and the experiment values turned out to be 50% of the theoretical ones.

O. S. Heck (1937) [161] has conducted investigations of flexural buckling, (Materials 66). He analyzed orthotropic elliptical plates in terms of infinitesimal deformation theory.

5.3.4. BUCKLING OF SPHERICAL SHELLS

In 1915, R. Zoelly [135] studied the buckling of spherical shells under external pressure, and, later, also on the basis of classical theory, research was conducted by E. Schwerin (1922) [136], Tokugawa (1939) [137] (1940) [139]. In 1938, C. B. Biezeno [133] made analysis in terms of finite deformation, in which he explained the marked instability phenomena occuring in the case in which a partial spherical shell having initial curvature undergoes concentrated forces. Th. v. Kármán-H. S. Tsien (1939) [138] analyzed the case in which a uniformed pressure is sustained, using the same method, and established their "jump theory" which essentially gives the same results as those of C. B. Biezeno.

R. Zoelly [135], using infinitesimal deformation theory, assumed axially symmetrical concave-convex wave forms and for the buckling pressure, obtains

$$p=\frac{4E}{M}\left(\frac{t}{d}\right)+\frac{4E}{3(1-\nu^2)}N\left(\frac{t}{d}\right)^2,$$

t: plate thickness
d: diameter
n: number of wrinkles

$$N=4n^2+2n-1$$

This equation is composed of an expansion term and a bending term, as in the case of flat plates and cyllindrical curved plates. The former decreases as n increases while the latter increases. The n giving the minimum value, p_k where from

$$\partial p_k/\partial n=0 \qquad N=\sqrt{3(1-\nu^2)}\,(d/t)$$

is

$$p_{k\,min}=\frac{2E}{\sqrt{3(1-\nu^2)}}\cdot\left(\frac{t}{r}\right)^2,$$

The compressive stress along the shell surface, which is generated by this pressure, is

$$\sigma_t = \frac{P_{max} r}{2t} = \frac{E}{\sqrt{3(1-\nu^2)}} \frac{t}{r}$$

This is the same equation as the classical compressive buckling stress equation for a cylinder of radius r, and thickness t. Later, E. Schwerin [136] obtained the same results. The experiment values were 30% of the theoretical values, showing a wide discrepancy. In this regard, Tokugawa (1939) [137] derived an elegant approximation equation from the fact that the wave forms that occur on the spherical shell surface are regular polygons.

On the other hand, C. B. Biezeno (1938) investigated the deformation characteristics of the case of partial spherical shell having a small curvature supported on the edges at a concentrated load acting on the center and obtained the results given in Materials 43. The configuration of the partial spherical shell is determined by $\lambda \equiv r_a^4/R^2t^2$, R radius, t thickness, r_a radius of section. He determined the relationship between the load P and the deflection u_0 in direction P for various values of λ and constructed the graph shown in Materials 43. On the y axis $\mu \equiv PR/Et^3$ is used, while the x axis $\nu \equiv u_0/x_0$ ($x_0 = r_a^2/2$ R) is used. The subscripts for the parameters C of each curve indicate the values of λ, e.g., C_{20} means that $\lambda = 20$. When λ is small, the wall thickness is large, and when it is large, the wall is thin. When $\lambda = 50$, the μ-ν curve is S-shaped but up to $\lambda = 20$, this S curve does not occur. When λ is above 50, the position of the minimum point sags downward, when $\lambda = 100$, only the part $\mu < 0$ is obtained and when λ is large, there is a further downward drop. When this is not a negative P, this means that such a state of deformation cannot occur. As the deformation progresses and becomes greater than at the negative minimum point, P = 0 is obtained, but this indicates that the previous convex surface "turns outside in" to a concave surface. When the load is increased further, this becomes exactly like the case in which a rice bowl is supported by the edges and its bottom is pushed by the tips of chopsticks [sic] and then the μ-ν curve comes to have the positive slope. /533

Thus there is a portion with a negative slope in the interval from the first maximum point to the next minimum point in the μ-ν curve for λ where $\lambda > 20$ (and this part indicates an unstable state of equilibrium). If the load is made to reach the maximum point and maintained there, the displacement jumps from the maximum point to the point which corresponds to the load on the 2nd stability curve parallel to the abscissa in the graph. Consequently, the state of equilibrium at the maximum point is unstable, and the displacement, when the jump occurs, is a finite quantity. Such a phenomenon is called Durschlag, or Oilcanning, and is referred to as "jump transition." (Tobiutsuri in Japan).

When such a great displacement is not allowed, the value of the μ of the first peak of the μ-ν curve corresponds to the maximum load allowable for a given spherical shell. Denoting this by μ_k, the graph in Materials 43.1 is obtained from a μ_k - λ curve. K. Marguerre (1938) [19] discovered that also in the case of a curved beam having a small curvature and under concentrated force, a strikingly similar phenomenon occurs.

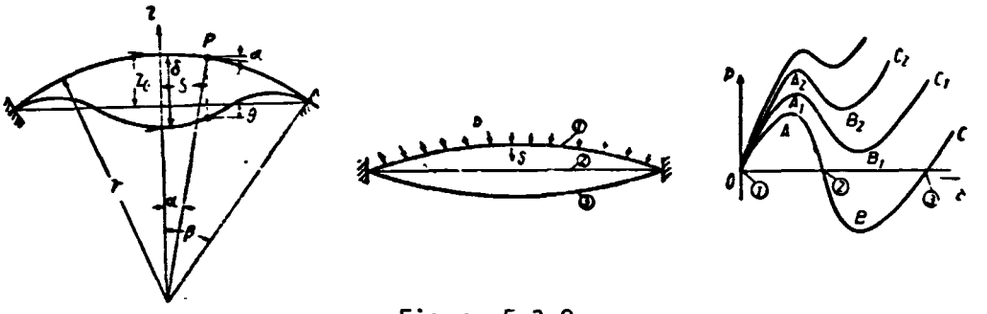

Figure 5.3.9

Th. v. Kármán-H. S. Tsien (1939) [138] analyzed the case of external pressure from exactly the same point of view as Biezeno and Marguerre. First they determined the expression for the total positional energy change W by combining the change in positional energy when the shell undergoes uniform compression from external pressure and the additional change in energy when local buckling occurs. Then substituting the axially symmetrical dent "deformation" approximation expression as the deformation entering the equation, they obtained the following results, by determining the unknown coefficients from the minimum condition W using the Ritz method. /534

$$\frac{\sigma}{E}=\frac{2}{5}\beta^2-\frac{6}{5}\frac{\delta}{r}+\frac{1}{\beta^2}\left(\frac{32}{35}\cdot\frac{\delta^2}{r^2}+\frac{4}{3}\frac{t^2}{r^2}\right)$$

Here σ is the average compressive stress inside the shell plane, δ is the maximum degree of "dent" displacement in the center, r, t are spherical shell radius and thickness, 2β is the center angle of buckling wave. Determining the β where σ is reduced to a minimum.

$$\beta=\sqrt[4]{\frac{16}{7}\left(\frac{\delta}{r}\right)^2+\frac{10}{3}\left(\frac{t}{r}\right)^2}$$

β with respect to this σ is

$$\frac{\sigma r}{Et}=\frac{4}{5}\left[\sqrt{\frac{16}{7}\left(\frac{\delta}{t}\right)^2+\frac{10}{3}}-\frac{3}{2}\frac{\delta}{t}\right]$$

This gives the relationship between the average compressive stress σ and the maximum deflection δ. "Consideration of Finite Deformation" in Materials 46 is based on this formulation. When $\delta/t = 0$, $\sigma = 1.4606\ Et/r$ and $\beta = 1.8257\sqrt{t/r}$. This expresses the stress at the time of buckling and the center angle and the stress at time of buckling is much higher than the classical theoretical value $0.606\ Et/r$. From the above equation

when $\delta/t\cong 10$ $\sigma_{min}=0.18258\,Et/r$

is obtained. The β for this is

$\beta=3.8218\sqrt{t/r}$

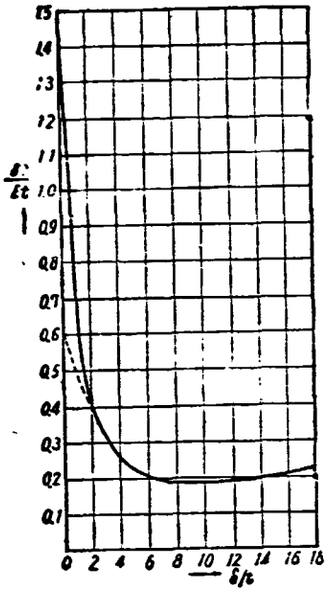

Figure 5.3.10

In experiments by E. E. Sechler-W. Bollay σ = 2480 lbs. per sq. in. was obtained as the stress at time of buckling when an external pressure was applied to a thin walled copper hemispherical shell with r = 18 in., t = 0.020 in., E = 14.5 × 10^6 lbs. per sq. in. Since this is expressed by σ = 0.154 Et/r, t is close to the minimum value σ_{min} based on the above theory. Moreover, whereas in the experiments β = 8°, $\delta/t \cong 12.5$, in this theory β = 7.4°, $\delta/t \cong$ 10, so the theory gives a good explanation of the experimental values. In classical theory β = 3.3° and δ/t is not determined. From these facts, Kármán and Tsien explained that a "lower buckling load" appears. However, the fact that the "upper buckling load" appears in this theory is much higher than the classical theory indicates that the positive buckling wave form is inappropriate for the initial buckling. Since in this period it is easier for the classical theory wave forms to appear, the classical theoretical values were assumed to be lower. Moreover, if the deformation is not large, since the posited concave wave forms express very well the actual wave forms, they assumed that a good fit with the above experiment is obtained, and as shown in Materials 46, they explained that actually a course is followed such as the dotted line which smoothly connects the classical buckling values with the lower buckling points obtained above. By this explanation, when the load is increased, the lower buckling load cannot be reached without once passing through the classical theoretical values. Thus in the experiments, almost all values obtained were close to this lower buckling load, and as an explanation of this, both authors state that in the process of increase in load, due to some external impact or vibration or the elasticity of the loading apparatus itself, a sudden jump is made to the lower buckling point, and since this is a very short period of time, in conventional experimental methods, values close to the lower buckling value are measured. /535

The latter author, H. S. Tsien[1] calculated the positional energy values of the entire system, and when he investigated the points indicating the same positional energy in the course of buckling ($\sigma r/Et$~δ/t) for the two extreme cases of a rigid testing machine and dead weight testing, he found that such a state was present before the upper buckling value is reached. He thus explained that as long as there is some external stimulus, jump can occur. In later tests, he measured the pressure at the beginning and ending of buckling, found that the

[1]H. S. Tsien, "A Theory for the Buckling of Thin Shells," *Jour. Aero. Sci.*, Vol. 9, No. 10 (Aug. 1942), pp. 373-384.

pressure at the beginning was higher than at the end, and when he compared the pressure appearing at the beginning which he estimated from observation of the energy, and the pressure at the time of equilibrium, after buckling, having an energy equal to this, with the above experiment values, he reported that they agree extremely well.

Although the comparison with pressure after buckling is interesting, as in this explanation, the shifts between these two states, which are equivalent to the positional energy, cannot occur freely. Some kind of externally supplied energy is required, and this point remains unexplained. Since in this regard it has been found recently that the effects of initial deformation are pronounced in the case of cylinders, it would be desirable to take this into consideration, make precise measurements on an actual specimen, determine the initial deformation, make an analysis of it and compare it with experiments. Since the initial deformation makes the sharp peak of the curve $\sigma r/Et$-δ/t flat, it is anticipated that in experiments, due to such a reason, either the upper buckling load will disappear or become extremely low, and turn out to be roughly equal to the lower buckling load.

In actual designs, using

$$\sigma_k = 0.18 Et/r$$

for the lower buckling load, this should be on the safe side.

5.3.5. ELLIPTICAL SHELLS

J. W. Geckeler (1928) [140] investigated buckling due to internal pressure in elliptical shells. In rotating elliptical shells formed by rotating an elliptical shell around the short axis, denoting the radius in the equatorial plane by r and the minimum radius of curvature of the meridian by ρ, when $\rho < r/2$, a compressive stress is formed due to internal pressure, in the direction along a circular cross-section parallel to the equatorial plane, and is maximum at the equator, being

$$N_k = \frac{rp}{2}\left(2 - \frac{r}{\rho}\right) \quad (N_k < 0 \text{ when } 2 < \frac{r}{\rho})$$

When the internal pressure p increases, buckling can occur along the equator due to this internal force. The equator assumes exactly the same state as a circle under compression, but the points having elastic support differ. Geckeler considered the action of elastic support only occurs due to the elongation and contraction of the equator, but did not consider the support action coming from other parts of the shell connected to the equatorial zone. The modulus of elastic support due to expansion and contraction of the equator is given by $\beta = Et/r^2$. The thickness of the shell t is assumed to be uniform. He obtained /536

$$N_k = 2\sqrt{B\beta}\left(1 - \frac{1}{2r^2}\sqrt{\frac{B}{\beta}}\right)$$

as the buckling internal force of the circular zone having a unit width undergoing this support action. B is the bending stiffness of the equatorial zone having a unit width. The second term in parentheses is small and may be omitted, for the buckling internal pressure $N_k = 2\sqrt{B\beta}$, he obtained

$$p_k = \frac{2}{\sqrt{3(1-\nu^2)}} \cdot \frac{1}{2-\frac{r}{\rho}} \cdot \frac{Et^2}{r^2}$$

In this case he finds the length λ of one wave and the wave number. (See Materials 48). This equation for buckling internal pressure and wave number reportedly agrees well with experiments (see *Handbuch der Physik VI, Mechanik der Elastischen Körper*, 1928, Springer, S. 304-305).

5.3.6. CONICAL SHELLS

Investigation of the buckling of conical shells has been done by A. Pfluger (1937) [141] and Tokugawa (1940) [142].

Pfluger, using infinitesimal deformation theory, formulated charts for the buckling load for the buckling of conical shells whose wall thickness is proportional to the distance from the peak, and which undergo surface pressure and distributed load in the direction of the axis (see Materials 49, 50).

Tokugawa Takesada found practical equations for external buckling pressure, from actual observations of wave forms, from many results of experiments in the case in which a uniform external load is sustained. (See Materials 51.) Reference [38] provides a detailed comparison with experiment results. The buckling waves that are formed are accompanied by finite deformation and should be investigated from this point of view.

5.3.7. REINFORCED CURVED PLATES

Reinforced curved plates include those roughly supported by large reinforcing members and those which can be treated as orthotropic plates, in which the spacing between reinforcing members is rather close. We shall consider the latter here. Veneer and plywood plates are anisotropic and are essentially made of anisotropic materials. Plates having closely spaced reinforcements are artificial orthotropic plates made of isotropic materials. We shall consider cases in which buckling occurs in reinforced plates at the same time that all reinforcing members buckle with the outer plates.

Figure 5.3.11

Tension shear and elasticity constants for bending and torsion serve as quantities expressing orthotropy. Two orthogonal directions are present, such that owing to simple internal tensile forces or moments, elongation and curvature occur only in the same direction as these. This is called the principal direction(s) of elasticity. Denoting these directions

as 1, 2, we shall use the subscripts 1, 2 to refer to quantities related to these directions. We denote the internal force per unit width in these directions as N_1, N_2 and the internal shear forces between them as N_{12}, N_{21}; also, we shall use M_1, M_2, M_{12}, M_{21} to express the bending moments and torsion moments for a unit width of the plate. Corresponding to these, if we express the plane strain by ε_1, ε_2, γ, and the curvature and twist by κ_1, κ_2, τ, generally the following relationship is attained.

$$\begin{cases} N_1=\alpha_1(\varepsilon_1+\nu_2\varepsilon_2) & M_1=D_1(\kappa_1+\mu_2\kappa_2) \\ N_2=\alpha_2(\varepsilon_2+\nu_1\varepsilon_1) & M_2=D_2(\kappa_2+\mu_1\kappa_1) \\ N_{12}=N_{21}=\beta\gamma & M_{12}=M_{21}=\frac{R}{2}\tau \end{cases}$$

$$\alpha_1\nu_2=\alpha_2\nu_1, \qquad D_1\mu_2=D_2\mu_1$$

Here /537

α_1, α_2; β = Extension stiffness $\alpha_1\alpha_2$ with respect to forces inside the center plane, and shear stiffness β

$\nu_1(\nu_2)$ = Shrinkage strain generated in directions 2(1) in accordance with the unit elongation strain in direction 1(2).... Poisson's ratio with respect to plane internal forces.

D_1D_2; R = Bending stiffness D_1D_2 and torsional stiffness R.

μ_1,μ_2 = Poisson's ratios for bending (generally these do not match ν_1, ν_2).

For example, in the case of a uniform material and uniform thickness, μ_1 and μ_2 respectively agree with ν_1 and ν_2 expressed by

$$\alpha_1=\frac{E_1t}{1-\nu_1\nu_2}, \qquad D_1=\frac{E_1t^3}{12(1-\nu_1\nu_2)}$$

$$\alpha_2=\frac{E_2t}{1-\nu_1\nu_2}, \qquad D_2=\frac{E_2t^3}{12(1-\nu_1\nu_2)}$$

$$\beta=Gt \qquad R=\frac{1}{3}Gt^3$$

E_1, E_2 are the elasticity moduli in directions 1, 2; G is the shear elasticity modulus between them. Moreover, in the case of reinforcement on only one side of the outer plate with a reinforcing member, the center plane does not exist, and the elasticity is asymmetrical; but if the eccentricity is not very large, one may treat this as an approximately symmetrical orthotropic plate.

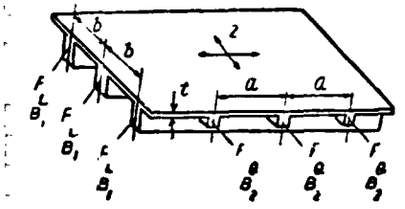

Figure 5.3.12

In ordinary reinforced plates such as that shown in Figure 5.3.12, it is possible to use

$$a_1 \fallingdotseq \frac{1}{b}(Et+E_LF_L) \qquad D_1=\frac{Et^3}{12}+\frac{B_1}{b}$$

$$a_2 \fallingdotseq \frac{1}{a}(Et+E_QF_Q) \qquad D_2=\frac{Et^3}{12}+\frac{B_2}{a}$$

$$\beta \fallingdotseq Gt+\beta_s \qquad R=\frac{1}{3}Gt^3+R_s$$

β_S, R_S are contributing terms respectively for the shear stiffness and torsion stiffness given by the reinforcing members. E_LF_L, E_QF_Q are the tension stiffnesses of the longitudinal and lateral reinforcing members and B_1, B_2 are their respective bending stiffnesses.

Compressive Buckling of Reinforced Curved Plates. Yamana (1933) [146], D. D. Dschou (1935) [147] and Shibuya (1940) [148] have studied the compressive buckling of curved plates having such orthotropy. The method of determining the buckling load is the same as in isotropic plates. Dschou obtained the results shown in Materials 52 from buckling condition equations. Yamana finds a basic equilibrium equation for general loading. Shibuya treated the case of circumferentially rotating edges, and the case of a fixed straight edge with the other edges rotating.

Normally, when the spacing between reinforcing members is large, first the outer plates buckle, then the reinforcing members buckle and the strength is lost. These cases will be surveyed in Chapters 4 and 5.

5.3.8. BUCKLING OF REINFORCED CYLINDERS /538

We shall also consider here buckling in the cases in which the shell surface can be treated as orthotropic plates. That is, we are dealing with cases in which both the outer plates and reinforcing members undergo total buckling simultaneously.

Compression of Reinforced Cylinders. This has been studied by Yamana (1933) [153], D. D. Dschou (1935) [154], Shibuya (1940) [148], Hayashi (1949) [155] and J. L. Taylor (1950) [156]. Dschou obtained

$$P_k=\frac{2E}{r}\sqrt{\frac{I_xI_y}{\frac{I_x}{t_x}+\frac{I_y}{t_y}\cdot\frac{t_x}{t}}}$$

for the unit width for the compressive buckling load of a cylinder reinforced longitudinally and laterally. Taking the axes x, y in the axial and circumferential directions, it is assumed that the principle directions of elasticity are taken in these directions. I_x and I_y are the average moments of inertia of the cross-section consisting of reinforcers and outer plates for the unit widths of the x and y cross-sections respectively; t_x, t_y are the average thicknesses of planes x, y and t is the outer plate thickness

Dschou obtains

$$P_k=\sigma_{ok}\sqrt{t\,t_x} \quad \text{or} \quad P_k=\sigma_{ok}\sqrt{t\,t_y}$$

for the unit width compressive buckling loads in the case of supports only in the direction of x (cylinder axis) or the circumference, but this is considered inappropriate. This is because, in cases in which there is a difference which depends on the reinforcement, not only the average plate thickness, but the bending stiffness becomes extremely high. Since there is no relationship between the bending stiffness and the tension stiffness, in the formula for p_k it is nece sary to include the bending stiffness in addition to the t_x or t_y which are related to the tension stiffness. Dschou's formula is a bold attempt at simplification and the reader should be warned of this.

In this regard, this may be handled as an outer plate having orthotropic characteristics. On this point, the formulas of Shibuya and Hayashi are superior. For example, Hayashi obtains

$$P_k=\frac{2}{r}\sqrt{D_2\alpha_1}\cdot K$$

for the case in which the principle directions of elasticity agree with the directions 1, 2 of the cylinder axis and the circumference. Here

$$K^2=\frac{(1+D_3/k^2D_2)(1-\nu_1\nu_2)}{1+(\alpha_1/2\beta k^2)(1-\nu_1\nu_2-2\nu_1\beta/\alpha_1)}, \quad D_3=D_1\mu_2+R/2.$$

$k=\frac{n}{m}=\frac{l}{b}=$ wave length ratio of axial and circumferential directions of buckling wave

The wave-length ratio is determined is as follows

$$C_1k^4+C_2k^2-C_3=0,$$

Here

$$C_1=2\frac{\beta D_3}{\alpha_1 D_2}-\left(1-\nu_1\nu_2-2\frac{\nu_1\beta}{\alpha_1}\right), \qquad C_2=\frac{2\beta D_3}{\alpha_1 D_2}\left(1-\frac{\alpha_1 D_2}{\alpha_2 D_1}\right),$$

$$C_3=\frac{D_1}{D_2}\left[2\frac{\beta D_3}{\alpha_2 D_1}-\left(1-\nu_1\nu_2-2\frac{\nu_1\beta}{\alpha_1}\right)\right].$$

Now we shall describe the results obtained from the above equations for the following two cases. /539

(1) Cylinder made of corrugated plates (direction of waves parallel to cylinder axis). In this case, since Yamana's relation $\alpha_1/\alpha_2 = D_1/D_2$ obtains the above equation is simplified to

$$k=\sqrt[4]{\frac{D_1}{D_2}}, \qquad \sigma_k=\frac{2}{r}\sqrt{\frac{D_2\alpha_1}{1+\frac{\alpha_1}{2\beta}\sqrt{\frac{D_2}{D_1}}}}$$

This gives the envelope of the family of curves calculated by Yamana for some numerical examples. Shibuya also obtains a similar expression. The experiment values appear as 30 to 60% of those in the above equation. Hayashi and Murakaimi [158] performed numerical calculations for the specimen tested by Yamana from the point of view of finite deformation theory, and when they found the lower buckling load, they obtained almost the same results as in Yamana's experiment.

(2) In the case of a cylinder of homogeneous material and uniform thickness (t)

Here

$$\left.\begin{aligned} k&=\sqrt[4]{\frac{E_1}{E_2}}, \qquad \sigma_k=\frac{P_k}{t}=C\cdot\sqrt{\frac{E_1E_2}{3(1-\nu_1\nu_2)}}\cdot\frac{t}{r}\\ C^2&=\frac{\sqrt{E_1E_2}+2G(1-\nu_1\nu_2)+E_1\nu_2}{\sqrt{E_1E_2}+(E_1E_2/2G)-E_1\nu_2}\end{aligned}\right\}$$

In this case, even if the principal direction of the outer plate is replaced, it is interesting that the buckling stress does not change.

(3) In the case of an isotropic plate

$$k=1, \qquad \sigma_k=\frac{E}{\sqrt{3(1-\nu_2)}}\cdot\frac{t}{r}$$

is obtained. It should be noted that in this case k = 1, i.e., the aspect ratio of the buckling wave is 1 and the wave lengths in the direction of the circumference are equal.

In actual practice, the most important case is that of a short cylinder supported only in the direction of the axis. For example, the section between the two ribs (frame) of a reinforced tension shell structure is an example of this. In a short cylinder, many buckling waves can occur only in the direction of the circumference. Dschou obtains the following equation for such a case.

$$\sigma_k=\frac{P_k}{t_x}=\sigma_E+\sigma_R\sqrt{\frac{t}{t_x}}$$

Consequently

$$P_k=\sigma_k t_x=\sigma_E t_x+\sigma_R\sqrt{t t_x}$$

Here

$$\sigma_E=\pi^2EI_x/(t_xl^2), \qquad \sigma_R=\frac{E}{\sqrt{3(1-\nu^2)}}\cdot\frac{t}{r}$$

and σ_E expresses the Euler's buckling stress of a reinforced plate of length l.

From the above equations it is possible to compare methods of reinforcement. In a sufficiently long reinforced shell, it is necessary to have reinforcement simultaneously in both directions in order to increase the buckling load, while

in short shells, longitudinal reinforcing members have a substantitive effect and the use of only lateral reinforcers is ineffective. The fact that the above formulas are applicable, indicates that this is the case in which, prior to the σ_k and P_k in both the reinforcing members and outer plates, the hypothesis that /540
local buckling does not occur, obtains. Although no general statement can be made regarding taking finite deformation characteristics into consideration, it is suitable to use about 20% of the above equation.

Torsional Buckling of Reinforced Cylinders. In 1949, Hayashi [161], in order to determine the torsional buckling load of a wooden plywood cylinder, posited the same form as in Donnell's formula for an isotropic cylinder, for the additional displacement during buckling, in a cylinder having orthotropic plates on the basis of infinitesimal deformation theory. He obtains results by advancing the analysis and expanding Donnell's results for isotropic cylinders to include general orthotropic cylinders. This is given by the following formulas in which S_k denotes the circumferential unit with shear load. When assuming

$$B=\frac{S_k}{\alpha_1(1-\nu_1\nu_2)}\cdot\sqrt{\frac{\alpha_1(1-\nu_1\nu_2)l^2}{12D_2}},\qquad J=\sqrt{\frac{12D_2l^4}{\alpha_1(1-\nu_1\nu_2)d^2}}$$

d = diameter, l = length. The principal directions 1, 2 match the axial and circumferential directions

(1) For short cylinders

With both ends rotating: $B=1.18\sqrt[4]{J}$ $n=2.31J^{-\frac{1}{4}}$ $(J<5.5)$

With both ends fixed: $B=1.29\sqrt[4]{J}$ $n=2.62J^{-\frac{1}{4}}$ $(J<7.8)$

(2) For long cylinders

Case of both ends rotating $J > 5.5$ $B=0.77\sqrt{J}$

Case of both ends fixed $J > 7.8$ $n=2$

In a cylinder of homogeneous material and uniform plate thickness, with $S_k/t = \tau_k$, this is expressed by

$$B=\frac{\tau_k l}{E_1 t}\sqrt{\frac{E_1(1-\nu_1\nu_2)}{E_2}},\qquad J=\frac{l^2t}{d^2}\sqrt{\frac{E_2}{E_1(1-\nu_1\nu_2)}}$$

The shear stress at the time of torsional buckling of a long cylinder is given by

$$\tau_k=0.272\sqrt[8]{E_1E_2^3}\left(\frac{t}{r}\right)^{\frac{3}{4}}\qquad n=2$$

To increase τ_k, it is effective to increase the circumferential modulus of elasticity E_2. When $E_1 > E_2$, usually the torsional buckling waves are inclined 10 to 20° in the direction of the axis, and especially when n = 2, the degree of deflection of the cylinder plane and the direction of the circumference is great. In order to reduce this deformation, the bending stiffness should be increased in the direction of the circumference and from this fact, E_2 has a greater effect on τ_k.

TABLE 5.1.3. COMPARISON WITH INOUE'S TEST RESULTS

/541

Material	Direction of surface grain	No.	Water content %	G kg/mm²	τ_B kg/mm²	τ_c kg/mm² Experiment	τ_c kg/mm² 60% of theory	n Theory
Linden Plywood	//	1	8.2	60	0.14	0.112	condition at both ends	
		2	8.2	70	0.14	0.112	supported 0.143	7
		3	7.9	95	0.18	0.144	fixed 0.157	8
		average	8.1	75	0.15	0.123		
	⊥	1	8.1	50	0.31	0.31		
		2	9.0	60	0.39	0.39	supported 0.231	4
		3	7.7	80	0.39	0.39	fixed 0.256	5
		average	8.3	65	0.36	0.36		
	regular 45°	1	9.0	200	0.18	0.162		
		2	9.0	240	0.21	0.189		
		average	9.0	220	0.20	0.176		
	reverse 45°	1	8.7	190	0.39	0.351		
		2	8.1	210	0.36	0.324		
		average	8.4	200	0.38	0.338		
Birch Plywood	//	1	7.5	120	0.26	0.208		
		2	8.0	90	0.29	0.232		
		3	7.8	80	0.24	0.192	supported 0.200	7
		4	7.7	100	0.23	0.184	fixed 0.219	9
		average	7.7	100	0.25	0.204		
	⊥	1	7.7	120	0.73	0.73	supported 0.332	4
		2	8.0	120	0.71	0.71	fixed 0.368	5
		average	7.9	120	0.72	0.72		
	regular 45°	1	8.0	380	0.50	0.450		
		2	8.1	260	0.43	0.387		
		average	8.0	320	0.47	0.419		
	reverse 45°	1	7.5	240	0.78	0.702		

E_1=731 kg/mm²
E_2=118 "
ν_1=0.500
ν_2=0.081

E_1=1093 kg/mm²
E_2=159 "
ν_1=0.500
ν_2=0.073

Remarks: (1) In the experiments, the torsion buckling moments were as foll for the breaking torsion moments:
With surface grain // 80%, hence the experiment value = 0.80 τ_B
" " " ⊥ 100%, " " " " = 1.00 τ_B
" " " 45° 90%, " " " " = 0.90 τ_B

(2) A surface grain direction // is parallel to the cylinder axis ⊥ is perpendicular to it. "Regular 45°" means that the direction of tensile stresses of the outer plate occurring to torsion matches that of the wood surface grain. "Reverse 45°" means that the torsion load in the case when these are orthogonal.

We shall compare the above equations with Inoue's results (1942) [160] of tests of the torsion of wooden cylinders. (See Table 5.3.1.) The specimens were a three-sheet wooden (?) plywood cylinder and a birch plywood cylinder. Their respective average moduli of elasticity E_1, E_2 and Poisson's ratios ν_1 ν_2 indicate values determined by experiment. It can be said that in this case, there is a relatively good agreement between the experiment values and the shear stress during buckling, which was 60% of that provided in the theory.

Flexural Buckling of Reinforced Cylinders. Research on this includes Inoue's [164] bending tests on plywood cylinders in 1942 and Hayashi's analysis [165] which was conducted in order to explain them. Hayashi determined the buckling and bending moment due to yield in a general orthotropic cylinder in which the principal directions of elasticity matched the direction of the cylinder axis and circumference. The equations discussed under isotropic cylinders are the results obtained by Hayashi for the general case. The yield buckling- /542
bending moment is given by

$$M_k=\frac{4\sqrt{6}}{9}\pi r\sqrt{D_2\alpha_1}$$

The maximum bending internal force for M_k is

$$N_1=\sqrt{\frac{8}{3}}\frac{\sqrt{D_2\alpha_1}}{r}$$

(internal force for unit width in direction of circumference)

As can be seen from these results, in order to increase the yield moment, the curvature should be increased and, in addition, for anisotropy, it can be seen that the bending thickness D_2 and the tension stiffness α_1 in the direction of the axis should be increased.

In a cylinder of homogeneous material of uniform thickness, this is

$$M_k=\frac{2\sqrt{2}}{9}\cdot\frac{\pi\sqrt{E_1E_2}}{1-\nu_1\nu_2}\cdot rt^2,\qquad \sigma_k=\frac{N_1}{t}=\frac{2\sqrt{2}}{9}\cdot\frac{\sqrt{E_1E_2}}{1-\nu_1\nu_2}\frac{t}{r}$$

and even if the principle direction of elasticity is changed, the value for yield moment or maximum internal force will not change. The comparison [165] of the above equations with results of Inoue's bending experiments [164] is rather good.

Local Buckling in Reinforced Cylinders. The above cases concern the simultaneous buckling of structural elements composing the outer plates of reinforced cylinders. Diametrically opposite to this is the case of local buckling which occurs very frequently in practice. In cylinders which are reinforced by strong reinforcements placed at large intervals, buckling will occur first in the outside plates if, for example, the cylinder is subjected to bending.

In 1936 and 1937, E. Schapitz [169, 170] constructed an analytical theory for the state after only the outer plate undergoes torsion and that is subjected

to shear buckling; i.e., for an imperfect tension field.

N. T. Hoff [163] proved and then confirmed by experiment that when a tension shell structure undergoes a pure bending moment, the yield buckling due to flattening, posited by Brazier does not occur, and that local buckling occurs on the compression side.

5.3.9. REINFORCED ELLIPTICAL CYLINDERS

In 1940, Shibuya investigated compressive buckling [148] and in 1936, O. S. Heck [162] studied flexural buckling, for the case in which an outer plate can be treated as an orthotropic plate, and in which the principal directions of elasticity match the direction of the axis and the circumference. Shibuya derived an equilibrium equation.

O. S. Heck determined the yield moment due to bending by following the Brazier approach. The maximum bending stress σ_k found from the yield moment by beam theory, differs depending on whether the bending is around the long or short axis. Whereas the calculated stress around the long axis agrees well with experiments, the agreement is poor for bending around the short axis, except when the eccentricity is extremely small. Heck derived an experimental formula for this case.

5.3.10. CORRUGATED MEMBERS

In determining what configuration should be used when employing corrugated members, it is necessary to make sure that buckling will not occur with respect to a given type of load. In particular, since there are many cases in which local buckling can cause total collapse, caution is required. /543

For example, in the case of a member under compression which has in its cross-section configuration a flat section and a curved section, if a large width (b) is taken for the flat section, due to the compression, the flat section will buckle first, and before the curved section displays adequate strength total collapse will be caused. The buckling stress σ_k in the case of compression in the direction of the length of a strip with two rotating ends is

$$\sigma_k = \frac{\pi^2 E}{3(1-\nu^2)}\left(\frac{t}{b}\right)^2$$

so in order to prevent buckling from occurring up to the yield point $\sigma_{y.p}$, b/t should be selected so that from $\sigma_k > \sigma_{y.p}$

$$\frac{b}{t} < \frac{\pi}{\sqrt{3(1-\nu^2)}} \cdot \sqrt{\frac{E}{\sigma_{y.p}}}$$

As for the flat section functioning as part of a frame, the two sides in the direction of length are elastically supported from the rotating end for stiffness, but it is safe to use the above formula.

The stress under which the curved section undergoes compressive buckling is

$$\sigma=0.2E\frac{t}{r}$$

and in order to prevent this from occurring up to the yield point,

$$\frac{r}{t}<0.2\frac{E}{\sigma_{0.2}}$$

should be used.

In cross-sections having flat plate or curved parts, in addition to determining the dimensions with consideration for each part individually, it is necessary to take measures to improve the stability for the overall cross-section (see Materials 73).

With regard to the compressive strength of corrugated plates, there are studies by Shibuya (1942) [175] and O. Nissen (1937) [176] and U.S. Standards. In corrugated plates, since the bending stiffness with respect to the direction of the waves is much higher than for the bending stiffness at the direction of right angles to the wave direction, the buckling which occurs when the four sides of the corrugated plates are supported by rotating edges, and a compressive load is applied in the direction of the wave crest, shows the characteristics almost of a column. In the compression of corrugated plates whose length is short with respect to width, only the boundary conditions of the compressed side have any influence. The conditions of the two sides parallel to the load have no effect, so the plate behaves like a column with a wave-form cross-section. Usually the wave crests break and buckling occurs.

In reinforced plates with flat plates attached to corrugated plates, the phenomenon occurs according to which, due to local buckling of the flat plate section, buckling is induced in the corrugated plates. This type of effect is especially great when the thickness of the flat plate is large. According to experiments by H. Ebner [177], as shown in Materials 69, it is not useful to increase the flat plate thickness in order to increase the overall compressive strength of the reinforced plate. Rather, it is more effective to increase the thickness of the corrugated plate. As for the shape of the waves, semi-circular form is superior to sine wave forms that can be formed by section. From compression tests on flat plates, reinforced by frames, it can be seen that it is more effective to reduce the thickness of the outer plates and use strong reinforcing members.

5.3.11. TORSION YIELD PHENOMENA IN SHELLS WITH CLOSED CROSS-SECTIONS /544

This phenomenon was discovered by Ikeda (1940) [143] when a non-circular thin-walled hollow cylinder undergoes torsion, the shear stress generated in the cross-section has a component in the normal direction with respect to the contour of the shell cross-section and for this reason, deformation of the cross-section occurs so that the cross-section area F is reduced. Consequently, the torsion stiffness decreases slightly, the decrease in stiffness with respect to the

increase in torsion moment increases, and finally the maximum resistable torsion moment is reached. This is strikingly similar to yielding due to the bending of a cylinder and can be termed "the torsion yield phenomenon." The maximum torsion moment $(M_t)_k$ at the time of yield is given by

$$(M_t)_k=\frac{4}{3}\sqrt{\frac{GK}{3\oint\frac{1}{t}ds}\cdot F^2}$$

appropriately positing deformation of the cross-section contour. Here G: elasticity modulus; t: plate thickness; s: distance along cross-section and F: area bounded by cross-section.

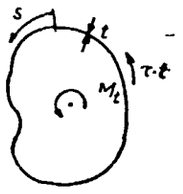

Figure 5.3.13

Denoting the strain energy due to change in configuration of cross-section by V, the degree of change (decrease) in the area bounded by the cross-section by f, K is determined as a coefficient when

$$V=K\cdot f^2$$

K can be easily calculated if one assumes displacement of the cross-section.

(i) For an equilateral triangular hollow cylinder, length of one edge a)

$$(M_t)_k\fallingdotseq\frac{0.152}{\sqrt{1-\nu}}Gat^2$$

Writing $(M_t)_k = \eta Gat^2$ and comparing with a celluloid triangular cylinder, there is a good match since

$$\eta_{theory} = 0.176 \qquad \eta_{experiment} = 0.20$$

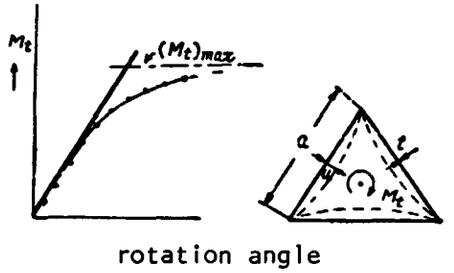

Figure 5.3.14

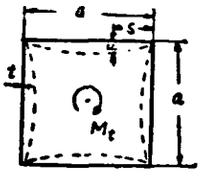

Figure 5.3.15

$\eta=\frac{0.152}{\sqrt{1-\nu}}$ in the above equation is the deformation of the cross-section, and one posits for each side the equation for beam deflection due to uniformly distributed load.

$$u=\frac{16c}{5}\left(\frac{s^4}{a^4}-2\frac{s^3}{a^3}+\frac{s}{a}\right)$$

(ii) For a square hollow cylinder

(a) $(M_t)_k=\frac{0.61}{\sqrt{1-\nu}}Ga t^2$ (When the connection in the four corners rotates)

(b) $(M_t)_k=\frac{1.49}{\sqrt{1-\nu}}Ga t^2$ (When the connection in the four corners is rigid)

The experiment results show that the case in which the connection is not rigid /545 is closer to reality.

In 1941, Shibuya [145] in his paper "On the Limits of Instability Phenomena Caused by the Torsion of a Thin-walled Angular Cylinder," discovered the following two types of failure.

(1) Cases in which failure occurs when a decrease in stiffness arises due to maximum torsion moment.

(2) Failure due to the compressive failure of a reinforcing member when a tension field is formed after the shear buckling of the plane.

Assuming $\kappa=0.409\sqrt{a/t}$, $p^*=\frac{\pi^2E}{3(1-\nu^2)}\left(\frac{t}{a}\right)^2$ failure type (1) occurs when $\kappa < 3.2$, and type (2) occurs at $\kappa > 3.2$. He concludes that the limit point of (1) and (2) is $\kappa = 3.2$, consequently $a/t = 62$.

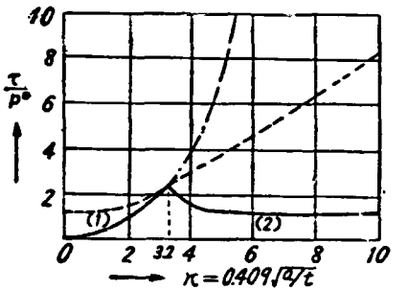

Figure 5.3.16

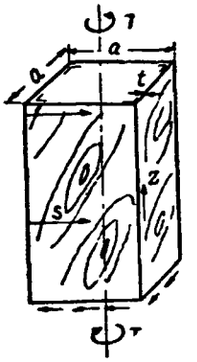

Figure 5.3.17

CHAPTER 4

STRESS CONDITIONS AFTER THE BUCKLING OF OUTER PLATES IN REINFORCED SHELLS

In the thin-walled reinforced structures, the strength and rigidity is determined by the means by which the outer plates and reinforcements are combined. Depending on the method of combination, there are three types of buckling: (1) Buckling occurs first in the outer plates, (2) Buckling occurs simultaneously in reinforcement and outer plates, and (3) Buckling first occurs in reinforcement. Type (3) is the most undesirable in structures, meaning that the structure is, in essence, not reinforced. In terms of strength, type (1) is the most tolerable. In terms of rigidity, normally (1) or (2) is most desirable in shells having curved plate sections. Of course, the selection of structure type differs according to whether selection is made in terms of strength, rigidity or strength and rigidity and in each case estimation of strength is necessary. In estimating the strength of reinforced structures, investigation of the state of stress after buckling of outer plates is indispensible. By determining the stress conditions, it also becomes possible to calculate the rigidity.

Below we shall consider the distribution of stress after the buckling of outer plates primarily in terms of structures of type (1).

5.4.1. EFFECTIVE WIDTH OF FLAT OUTER PLATES

In the cases when the outer plates of reinforced structures are flat, the concept of effective width has been employed in considering the effects on an outer plate of compressive force after it has buckled. The outer plate which /546
has cooperated with the reinforcement up to the time of buckling, loses its cooperation after buckling. Now, if there are reinforced plates under compression and it is assumed that the outer plates buckle first, the stress distribution will change as shown in Figure 5.4.1. That is, the stress of the outer plate at the edge is equal to the stress σ_L of the reinforcement, and in the center it is not much different from the outer plate buckling stress σ_K, showing the distribution in the figure. The force received by the outer plate in this case, is

$$\int_{-b/2}^{b/2} \sigma_x t\, dy$$

If we denote by b_m the width at which it is possible to consider that this cooperates with the reinforcement at a stress σ_L which is the same as that of the reinforcement

$$\sigma_L b_m t = \int_{-b/2}^{b/2} \sigma_x t\, dy$$

Thus,

$$b_m=\frac{\int_{-b/2}^{b/2}\sigma_x\,dy}{\sigma_L}$$

Denoting the average stress sustained by this plate as σ_m, this is expressed by

$$b_m=\frac{\sigma_m}{\sigma_L}b \tag{5.4.1}$$

In this manner, Kármán posits that a plate (original width b_b) under a load above that of buckling, has the same durability as the durability of a narrow plate of width b_m such that its buckling stress σ_{km} is exactly equal to that of the stress of the reinforcement σ_L.

$$\sigma_{km}=kE\left(\frac{t}{b_m}\right)^2=\sigma_L$$

From this, the effective width (Mittragende Breite) is obtained.

$$b_m=\sqrt{\frac{kE}{\sigma_L}}\cdot t=\sqrt{\frac{\sigma_k}{\sigma_L}}b \quad \text{Kármán's equation} \tag{5.4.2}$$

The average stress is

$$\sigma_m=\frac{b_m}{b}\sigma_L=\sqrt{\sigma_k\sigma_L} \tag{5.4.3}$$

E. Trefftz and K. Marguerre [13, 14] made detailed calculations according to finite deformation elasticity theory and established a theory of effective width. As a result, on the basis of the hypothesis that the four edges of a rectangular plate are displaced while maintaining their linear shape, they improved on the coefficients α and β in Cox's equation.

(5.4.4)

$$\frac{b_m}{b}=\alpha\sqrt{\frac{\sigma_k}{\sigma_L}}+\beta \cdot \text{ Cox's equation}$$

supported edge	$\alpha = 0.80$	$\beta = 0.09$
fixed edge	$\alpha = 0.82$	$\beta = 0.14$

and obtained

$$\frac{b_m}{b}=0.81\sqrt{\frac{\sigma_k}{\sigma_L}}+0.19 \tag{5.4.5}$$

Moreover, as a simple approximation, they obtained

$$\frac{b_m}{b}=\sqrt[3]{\frac{\sigma_k}{\sigma_L}}$$

If, when the buckling stress σ_K of the outer plate is determined by this equation, the unit stress σ_L at the edge of the outer plate is given, it is possible to calculate the effective width of the outer plate in that state. /547

Figure 5.4.2

In experimentally determining the effective width, if the stress σ_L of the reinforcement having a compressive force P and a reinforced plate having n plate fields is measured, the following equation can be used to find the effective width b_m for the load.

$$b_m=(P-\sigma_L \Sigma F_L)/(n t \sigma_L) \tag{5.4.7}$$

Here F_L is the cross-section area of one reinforcement. Also, in the case of curved plates and the outer plates of reinforced shells, the effective width can be similarly defined and employed to simplify structural design.

5.4.2. THE EFFECTIVE WIDTH OF CURVED PLATES

Experiments on the effective width of curved plates after compressive buckling were carried out by Wenzek [46] and J. S. Newell [40]. Newell conducted an experiment by clamping the long edges of a curved plate on V channels and pressing flat the upper and lower ends. In this method of support, the displacement does not occur in the direction of the radius, but can occur in the direction of the circumference and does not correspond with the actual conditions of a curved plate between two longitudinal reinforcements in actual tension shell structures. Wenzek connected three curved plates to three strong frames and conducted a flat press test. His approach was closer to reality than Newell's method, but there was a tendency for the connection with the frame to be too strong. According to Wenzek's tests, the relationship between the load P supported by the curved plate and the strain ε is as shown in the graph and marked differences are manifested depending on the size of the center angle.

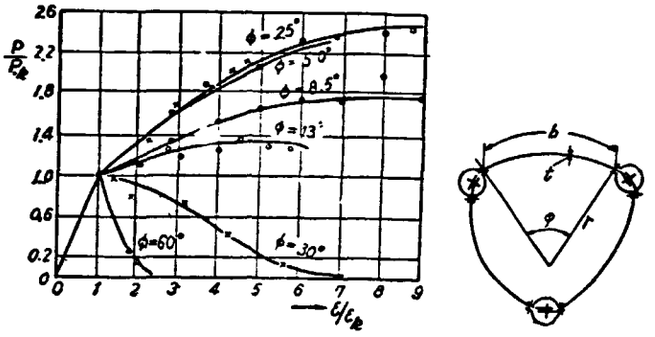

Figure 5.4.3.

As a test formula, he obtained

(5.4.8)

$$\left.\begin{aligned}\frac{b_m}{b}&=\sqrt{\frac{\sigma_k}{\sigma_L}}-\varphi\left(1-\frac{\sigma_k}{\sigma_L}\right)\\ \sigma_k&=5E\left(\frac{t}{b}\right)^2+0.3E\frac{t}{r}\end{aligned}\right\}$$

Here

According to Ebner (1937) [45, 171], as a result of applying this to the outer plates of actual structures, it was too far on the safe side. Ebner proposes the following method. A curved plate field owing to its "curvature" has a load resistance unrelated to the longitudinal reinforcing strength. The load that can be withstood due to the curvature is

$$P_R=\sigma_R bt, \qquad \sigma_R=(0.2\sim0.3)E\frac{t}{r}$$

When only this force is received, the plate buckles, loses its curvature, and then is assumed to behave as a "flat plate". Its effect as a "flat plate" exists with respect to an extreme fiber stress (σ_L - σ_R) in which σ_R is subtracted from the stress σ_L of the reinforcement. Denoting the effective width for this by $\bar{b}_m$. If the load as a "flat plate" is considered to be /548

$$P_P=(\sigma_L-\sigma_R)\bar{b}_m t$$

the overall load is

$$P_R+P_P=\sigma_R bt+(\sigma_L-\sigma_R)\bar{b}_m t=\sigma_L b_m t$$

For the effective width b_m of the curved plate from this

$$b_m=\bar{b}_m+\frac{\sigma_R}{\sigma_L}(b-\bar{b}_m) \tag{5.4.9}$$

Calculating with Marguerre's formula for the case in which the edges are supported and free to rotate

(5.4.10)

$$\bar{b}_m=\sqrt[3]{\frac{\sigma_P}{\sigma_L-\sigma_R}}b, \qquad \sigma_P=3.6E\left(\frac{t}{b}\right)^2 \quad \text{(buckling stress as a flat plate)}$$

In order to corroborate this formula, the D.V.L. (German Aeronautical Institute) conducted compression tests on reinforced curved plates. They attached a square timber so that a uniform load was applied to the upper plate and to the reinforcement. They measured the stress of each reinforcement with respect to the total load and found the effective width.

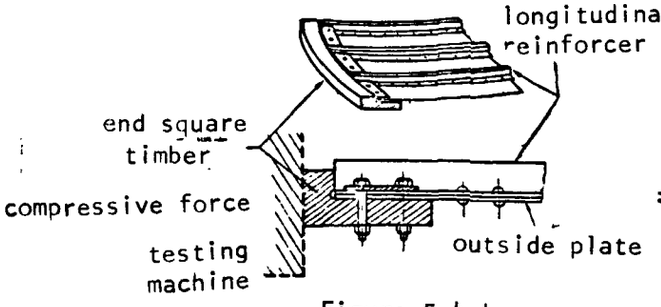

Figure 5.4.4.

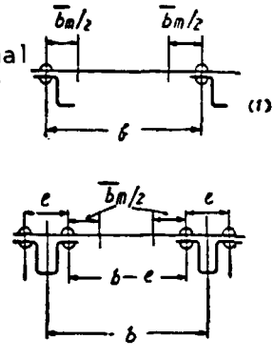

Figure 5.4.5

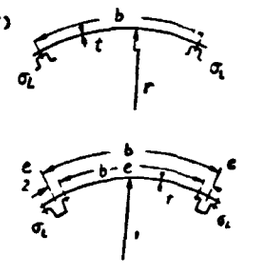

Figure 5.4.6

They found it was possible to use the following equations for calculations. As a result, in partial cylinders having an open profile

$$\bar{b}_m=1.63\sqrt{\frac{E}{\sigma_L-\sigma_R}}t+0.14b \tag{5.4.11}$$

In those having closed profiles

$$\bar{b}_m=2.15\sqrt{\frac{E}{\sigma_L-\sigma_R}}t+0.14(b-e) \tag{5.4.12}$$

$\bar{b}$ is the spacing between reinforcements, e is the distance between two rows of rivets in the reinforcements. Each one has half the value of b_m, is measured outwards from the row of rivets. The portion of plate between each row of rivets was considered completely effective and added to the cross-section area of the reinforcements.

In a comparison of the values of $\bar{b}_m$ obtained by experiment with those calculated from the above formulas, immediately after buckling, a good agreement was found between them in a strongly curved partial shell (r = 200 mm, t = 0.4 mm, b = 140 mm and r = 200, t = 0.4, b = 140, e = 22). When the curvature becomes small, the calculated values in the open profile shell become higher than the measured value, but, conversely, lower in the open profile shells. This indicates that the plate field is well supported by the closed profile. /549

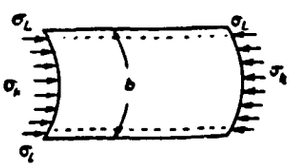

Figure 5.4.7 (a)

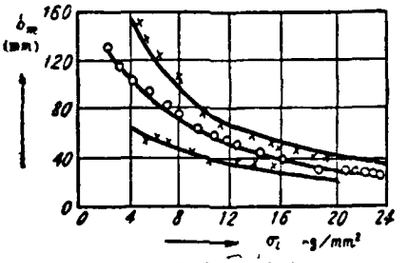

Figure 5.4.7 (b)

Since the outer plate has a thickness of 0.4 mm, the curve for the test values shows a bend near σ_L = 1,000 kg/cm^2, slightly ahead of this in open profile, slightly behind in closed profile. This is due to the fact that buckling of the outer plate occurs between rivets with a pitch of 20 mm in this vicinity. That is, when

$$\sigma_k = \frac{\pi^2 E}{3(1-\nu^2)} \cdot \left(\frac{t}{l}\right)^2, \quad E = 7400 \text{ kg/mm}^2$$
$$t = 0.4, l = 20 \text{ mm}$$

σ_k = 1070 kg/cm^2. The bending strength of the plate after buckling between rivets scarcely increases at all. Actually, if a load is applied over this stress, the curve for effective width (reinforcing stress) forms a quadratic hyperbola. According to H. Ebner [171].

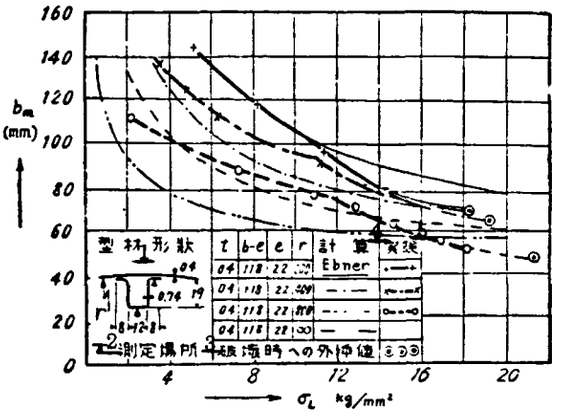

Figure 5.4.8 (a)

KEY for Figures 5.4.8 (a) and 5.4.8 (b):
1, profile shape; 2, place of measurement; 3, values extrapolated to time of failure; 4, calculations; 5, experiments.

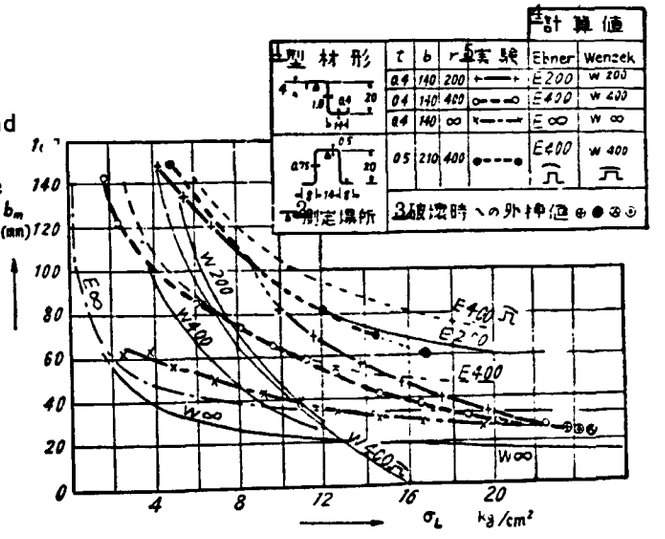

Figure 5.4.8 (b)

The following results were obtained from this experiment. The above formulas (5.4.11) and (5.4.12) for the effective width of reinforced plates having a curvature can be used within the range where buckling of outside plates between rivets does not occur. In open profiles they are somewhat higher, and somewhat lower in closed profiles. Within this range it can be seen that the effective width of the outer plate is higher, the greater the curvature.

After buckling occurs in the outer plates between rivets, the effective width of the curved plate decreases to far below that which is indicated by the calculated values. In the vicinity of the failure state, it drops to almost the values of a flat plate.

5.4.3. ANALYSIS OF STRESS AFTER THE BUCKLING OF THE OUTER PLATES OF REINFORCED SHELLS UNDER THE BENDING MOMENT /550

The stress conditions after the buckling of the outer plate of the reinforced shell under bending, are determined from the properties of the curved plate after compressive buckling. There are two methods for this: (1) detailed method. First, as a first approximation, the linear distributed stress c_0 is found, assuming that the outer plate functions perfectly even on the compression side, and by means of this the part of the compression side that buckles is determined Then the effective width b_{m1} of the plate field that has buckled at each reinforced position is calculated as in the preceding article. In the first approximation, the stress σ_{L0} is used in the part where the outer plate "cooperates" completely. In this manner, a new effective cross-section area which partly cooperates on the compression side is found, a new neutral axis is determined by this and the moment of inertia, which is taken in relation to this

$$J_i = \sum (F_L + b_{mi}t)_i y_i^2$$

is calculated. By using this, an improved linear stress distribution σ_1 is obtained. This further gives an accurate b_{m2} and J_2. It is possible to continue this procedure and obtain an even better stress distribution. Satisfactory values can be obtained if these repeated calculations are carried out one or two times.

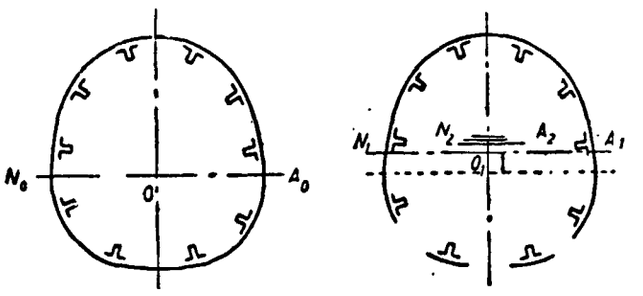

Figure 5.4.9

5.4.4. EFFECTS OF RIVET PITCH ON COMPRESSIVE STRENGTH OF REINFORCED SHELLS

A. Kromm [172] obtained the following results when he studied the effects of rivet pitch on the compressive strength of Duralumin reinforced partial cylinders. The shapes of the reinforcers were $\overline{\Gamma}, \overline{\Pi}, \overline{U}$, the radius of curvature was 400 mm and the plate width 720 mm. /501

(a) Figure 5.4.12 was obtained when he performed compression tests, varying the rivet pitch within 20-70 mm. It can be seen from this diagram that the bending strength of the outer plate decreases when the pitch is increased.

(b) Figure 5.4.13 shows the relationship of effective width stringer stress in the cases when p = 20 mm and 70 mm in reinforced shells having profiles. Buckling between rivets occurs when the reinforcement stress is close to 800 kg/cm^2 for the case when p = 20 mm. After this, the effective width of the plate section suddenly decreases. In cases where rivets p = 70 mm, a smooth curve is shown, but the effective width appears small. Almost identical curves are shown in shells having other forms of reinforcing members.

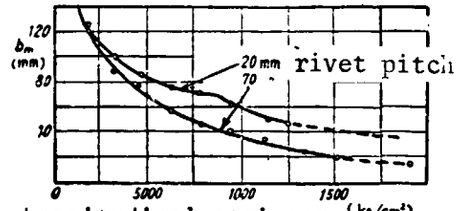

Longitudinal stringer stress σ_L

Figure 5.4.13

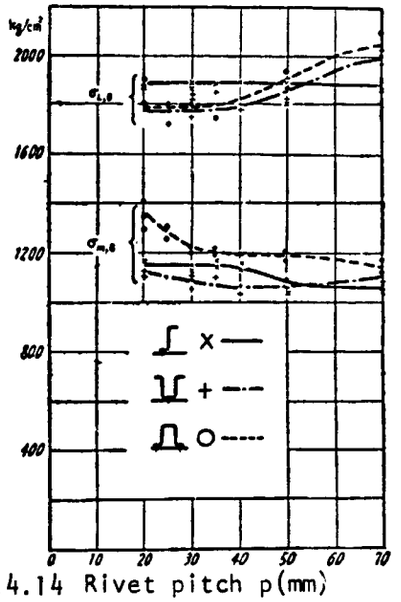

Figure 5.4.14 Rivet pitch p(mm)

(c) Figure 5.4.14 describes the average breaking stress of each shell. σ_{mB} and the breaking stress $\sigma_{L,B}$ of the reinforcing members with respect to the pitch p. In Z-members, $\sigma_{L,B}$ hardly changes at all because of the pitch. σ_{mB} decreases slightly when the pitch is increased, but no great difference is seen. On the other hand, in both channel profiles, $\sigma_{L,B}$ increases along with p and σ_{mB} decreases. This means that when this pitch is small, the buckling wave forms formed on the outer plate bear heavily on the reinforcing member, causing it to buckle, so when p is small $\sigma_{L,B}$ is smaller than when p is large. When p is large, the buckling wave forms of the outer plate do not exert much influence. This is true for the same reason in the case of open channels.

(d) Table 5.4.1 gives the results of compression tests only on reinforcing members without outer plates.

(2) A simpler but less accurate method than the above, is to d .ermine directly the new reinforcement stresses.

$$\sigma_{L1}=\frac{F_L+bt}{F_L+b_{m1}t}\sigma_{L0}, \qquad \sigma_{L2}=\frac{F_L+bt}{F_L+b_{m2}t} \quad \text{etc.}$$

From the reinforcement stress σ_{L0} and the effective width b_{m1}, b_{m2} .... for the case in which it is assumed that the cross-section works perfectly. By using this method, it is possible to admit the troublesome determination of the neutral axis and calculation of the moments of inertia. Although it is simple, the linear stress distribution on the compression side cannot be obtained immediately.

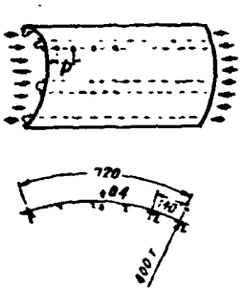

Figure 5.4.10
Flat Compression Test

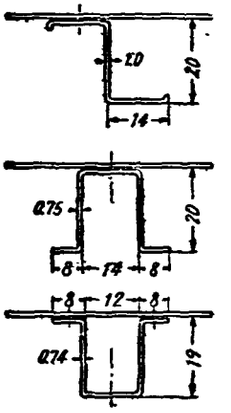

Figure 5.4.11

P_G total bending strength of shell
P_L bending strength of stringer
P_M bending strength of outer skin

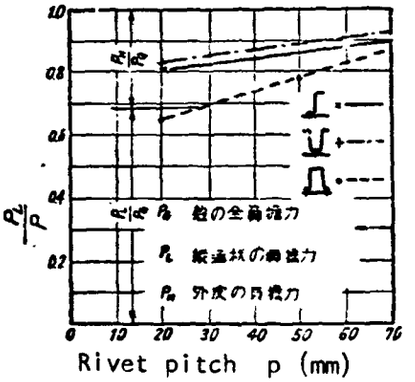

Figure 5.4.12

TABLE 5.4.1

Cross-section	Dimensions			Bending Strength	Breaking Stress
	Length (mm)	Thickness (mm)	Cross-section area cm^2	(kg)	(kg/cm^2)
	396	1.03	0.48	700	1460
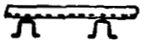	396	0.82	2×0.56=1.12	2700	2410
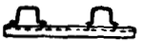	396	0.735	2×0.45=0.90	2300	2550

5.4.5. IMPERFECT TENSION FIELD IN CURVE PLATE SECTION AFTER SHEAR BUCKLING. /552

This problem has been investigated by E. Schapitz (1936) [169], (1937) [170]; and in 1937 by H. Ebner [171]. The reader is referred to the original articles for details.

CHAPTER 5

BREAKING STRENGTH OF REINFORCED SHELLS (WITH PARTICULAR REFERENCE TO FLEXURAL BREAKING STRENGTH)

5.5.1. EFFECTS OF OUTER PLATES ON BREAKING STRENGTH

The bending strength of a shell having a plate field and reinforcing members which resist buckling is determined by the compressive buckling stress σ_k. Shells having a plate field where the buckling has already occurred, lose their special shell-effect and change into a single-frame structure consisting of longitudinal reinforcements and ribs. In this case, when the ribs are sufficiently rigid, the bending strength becomes 0 when the longitudinal reinforcements fail. Consequently, it is the buckling strength of the longitudinal reinforcements that determine the flexural breaking moment of such shells. Failure of longitudinal members can occur in various forms, depending on length and cross-section. When the length and plate thickness of the longitudinal members is large, between the ribs, open profiles undergo Euler's buckling exactly like that in Euler's supports, perpendicular to the outer plates (flexural buckling). Buckling of open section profile supports is accompanied by twisting (torsional buckling). Local buckling occurs in both closed and open, short, very thin profiles. When there are no outer plates, it is possible to calculate the three-modes of buckling for only these profiles, but when outer plates are added, complex effects are exerted with respect to buckling phenomenon.

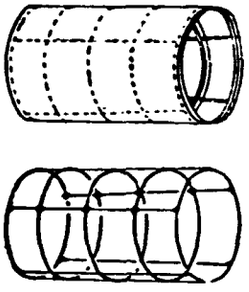

Figure 5.5.1

It is possible to determine the compressive buckling stress in the following manner for the case of flexural buckling of reinforcing members between ribs. The outer plates act, with respect to this flexural buckling, to increase the stiffness of the reinforcements. The effective width b_e of the plates with respect to this is not equal to the effective width b_m described above. It is given by the longitudinal stiffness at the moment of buckling.

$$EF_e = \frac{\partial (t\, b_m \sigma_L)}{\partial \epsilon} = Et\left(b_m + \sigma_L \frac{\partial b_m}{\partial \sigma_L}\right) = Et b_e \qquad (5.5.1)$$

Since $\partial b_m/\partial \sigma_L < 0$, $b_e < b_m$.

When using the Cox-Marguerre formula for a flat plate, for the effective width, when the curvature is small

$$\frac{b_m}{b}=0.81\sqrt{\frac{\varepsilon_k}{\varepsilon_L}}+0.19 \qquad \varepsilon_k=3.51E\left(\frac{t}{b}\right)^2 \tag{5.5.2}$$

This is

$$\frac{b_e}{b}=\frac{0.81}{2}\sqrt{\frac{\varepsilon_k}{\varepsilon_L}}+0.19 \tag{5.5.3}$$

in Marguerre's equation

$$\frac{b_m}{b}=\sqrt[3]{\frac{\varepsilon_k}{\varepsilon_L}} \qquad b_e=\frac{2}{3}\sqrt[3]{\frac{\varepsilon_k}{\varepsilon_L}}b=\frac{2}{3}b_m$$

and in Kármán's equation /553

$$b_e=\frac{1}{2}\sqrt{\frac{\varepsilon_k}{\varepsilon_L}}b=\frac{1}{2}b_m$$

The compressive buckling stress of the column consisting of this $b_e t$ and reinforcement is determined as follows by calculating the radius of rotation around the neutral axis.

$$\sigma_L=\sigma_{y.p.}-\frac{\sigma_{y.p.}^2}{4\pi^2 E_L}\left(\frac{l}{i}\right)^2 \tag{5.5.4}$$

The strain is determined from

$$\varepsilon_L=\varepsilon_{y.p.}-\frac{\varepsilon_{y.p.}^2}{4\pi^2}\left(\frac{l}{i}\right)^2$$

In this case, the required breaking load is as follows, denoting the effective total area of this state (ε_L or σ_{rL}) by F_e.

$$P_{break} = \sigma_L F_e \tag{5.5.5}$$

where F_e = (some of cross-section areas of reinforcements) + $nb_m t$
n = number of effective plate fields
b_m = effective width with respect to σ_L

When the plate field is curved plates, the formula for curved plates may be used as the effective width formula when determining the effective stiffness $Eb_e t$. This method of calculation is considered appropriate for closed Π profile and open π profile members. When the curvature is large, H. Ebner's equation [171] can be used for the effective stiffness of the shell outer plates.

5.5.2. ON BOUNDARY CONDITIONS WHEN USING TESTS ON PARTIAL STRUCTURES IN LIEU OF STRENGTH TESTS ON COMPLETE STRUCTURES

When one wishes to determine the buckling strength of large structures, it is frequently impossible to construct test specimens of the same size owing to the expense involved. In such cases, two approaches are conceivable: One is to employ a partial structure made to exactly the same dimensions as one part of the original, or to use a scale model which is identical in terms of geometry and elastic dynamics. This becomes a problem when the strength cannot be determined by analysis.

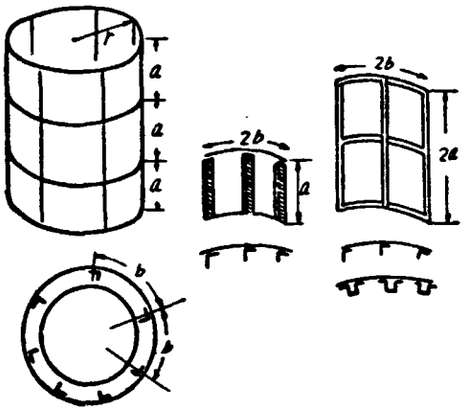

Figure 5.5.3

In the latter case, especially in reinforced structures, it is difficult to reduce the rivet size according to scale, or it is very difficult to reduce the plate thickness according to scale.

In the case of the former, where a partial structure is tested, it is necessary to make the loads acting on that partial structure and the deformation that arises from them, exactly the same as the loads and deformations occurring in the complete structures. In combined plates with easily-twisting ribs and longitudinal members, it is important to realize the correct effects of the buckling wave forms on the longitudinal members and ribs in terms of partial structures. At least it is necessary to test with a partial shell having (2a × 2 b) taking four basic sections (a × b) In the case of reinforcements with a closed cross-section ⊓ it is possible to test the strength using a partial shell with (a × 2b) with the width in two sections. /554

5.5.3. METHODS FOR DETERMINING BREAKING MOMENT

The total cylinder breaking moment can be calculated if breaking tests on partial shells (one part of reinforced cylinder) are used to determine the breaking stress. There are two methods for doing this.

(1) First Method: Assuming that the entire cross-section cooperates, the average compressive stress σ_{mB} of the partial shell at the time of breaking is calculated. This is multiplied by the resisting moment W of the cross-section of the entire shell as completely effective. That is, for the bending moment

$$M_B = \sigma_{mB} W$$

TABLE 5.5.1. RESULTS OF TESTS ON CYLINDERS IN D.V.L. COMPARISON WITH THEORY
(H. Ebner Lufo. 1, 4-3, 1937, S. 111)

	Bending Moment At Time of Buckling of Outer Plate kg•cm	Average Breaking Stress σ_{mB} of Partial Shell	σ_{LB} of reinforcement	Breaking moment of entire tension shell: Method of calculation $M_B=\sigma_{mB}W$ kg•cm	$M_B=\sigma_{LB}W'$ kg•cm	Method of measurement: Pure Bending	Shear Bending
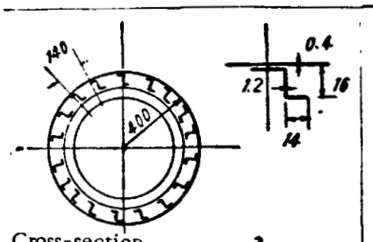 Cross-section area $F = 18.7\ cm^2$ $W = 367,\ W' = 255\ cm^3$	62700	−950	−1500	350000	380000	347000	380000 (Q= 1450kg)
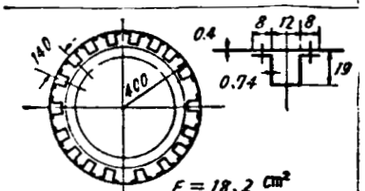 $F = 18.2\ cm^2$ $W = 356,\ W' = 279\ cm^3$	66800	−1320	−1820	484000	508000	487000	497000 (Q= 1870kg)
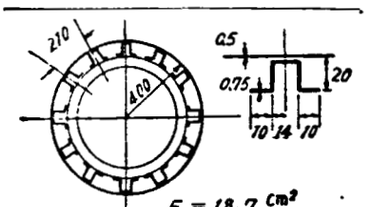 $F = 18.7\ cm^2$ $W = 367,\ W' = 243\ cm^3$	89000	−850	−1650	340000	405000	397000	407000 (Q= 1530kg)

(2) Second Method: This method uses the effective width. The breaking stress σ_{LB} of the reinforcement that exists at the instant of failure of the partial shell is calculated. Then this is multiplied by the overall tension shell resistance moment W' which considers the various effective widths at the position of each member in the case of bending. That is, the flexural breaking moment is /555

$$M_B = \sigma_{LB} W'$$

Instead of calculating the breaking stress σ_{LB} using the effective width, since it is possible to measure the stresses in the reinforcements in partial shell tests, right up to the time of breaking, that which occurs at the time of breaking can be extrapolated.

The values determined by Method One are lower than those found by Method Two. This is because only the effects of the effective widths of the extremely narrow section at the extreme outside fiber of the bent entire shell are involved. Consequently, Method One is much simpler since it is on the safe side, and since the troublesome calculation of the resistant moment W' can be omitted.

Table 5.5.1 compares tests and calculations by the above method in the D.V.L. The agreement with Method Two is extremely good.

CHAPTER 6

SIMILARITY LAWS FOR STRENGTH TESTS SCALE MODELS FOR OBTAINING THE NECESSARY DATA FOR THE DESIGN OF TENSION SHELL STRUCTURES

In the design of actual structures, theoretically analyzable cases are limited to extremely simple structures. Consequently, the designer must first substitute a standard "simplified structure" for the actual structure before applying the theoretical methods. However, depending on the type of substitution, since holes may develop in the stressed outer skin of the actual structure or other discontinuities may occur, in the case of complex structures, the strength and rigidity cannot be estimated with sufficient accuracy. In this case, the designer either increases the weight to be sure it is on the safe side or determines the strength and rigidity by tests. When it is impossible to conduct such full-scale tests, owing to cost or equipment limitations, it is necessary to estimate the strength and rigidity of the structure by:

(1) Partial Structure Test or

(2) Tests on small scale models.

In tests on partial structures, it is necessary to have the same deformation and load conditions as the total structure, with respect to the boundary conditions and dimensions.

When scale models are used, care must be exercised with regard to the similarity. Below we shall examine similarity laws for such cases. We assume that the models below are constructed to correct sale.

We denote the load acting on an actual object by P, the similar forces acting in the same direction in the corresponding plane in the scale model by P_m and the respective lengths as 1, l_m.

(1) Similarity of deformation in model and real object. We shall consider the real problem of determining displacement due to the load on an actual object using a small model. The model is geometrically similar to the actual object, but we assume that it is made of materials whose density, yield point and elasticity modulus differ from the real object.

The displacement δ at some point in the structure is expressed by /556

$$\delta=\varphi(P, l, E, G, \rho, g, \theta, \alpha) \tag{5.6.1}$$

P: working load, 1: representative length, E: Young's modulus, G: shear elasticity modulus, ρ: density, g: gravity acceleration, θ: temperature, α: linear expansion coefficient. Deflection assumed to be a function of these.

Considered to be within elasticity limits. Consequently,

$$\delta = \sum P^a l^b E^c G^d \rho^e g^f \theta^g \alpha^m$$

Since the dimensions must agree on both sides

$$\delta = l \cdot F\left[\left(\frac{El^2}{P}\right), \left(\frac{Gl^2}{P}\right), \left(\frac{\rho g l^3}{P}\right), (\alpha\theta)\right] \tag{5.6.2}$$

Consequently the comparison of the actual object with the model is

$$\frac{\delta}{\delta_m} = \frac{l \cdot F\left[\left(\frac{El^2}{P}\right), \left(\frac{Gl^2}{P}\right), \left(\frac{\rho g l^3}{P}\right), (\alpha\theta)\right]}{l_m \cdot F\left[\left(\frac{El^2}{P}\right)_m, \left(\frac{Gl^2}{P}\right)_m, \left(\frac{\rho g l^3}{P}\right)_m, (\alpha\theta_m)\right]} \tag{5.6.3}$$

Therefore, if

$$Gl^2/P = G_m l_m^2/P_m \tag{5.6.4}$$

$$El^2/P = E_m l_m^2/P_m \tag{5.6.5}$$

$$\rho g l^3/P = \rho_m g_m l_m^3/P_m \tag{5.6.6}$$

$$\alpha\theta = \alpha_m \theta_m \tag{5.6.7}$$

The values of the function F in the model and actual object become equal and

$$\frac{\delta}{\delta_m} = \frac{l}{l_m} \tag{5.6.8}$$

is obtained.

Next, we shall consider the conditions for the similarity law to obtain for equations (5.6.4), (5.6.5), (5.6.6), (5.6.7). First we require that $E/G = (E/G)_m$ from equations (5.6.4) and (5.6.5). In cases in which it is possible to eliminate the effects of shear deformation as in the case of a beam under lateral load, condition (5.6.5) may be omitted. Similarly, when the stress is primarily shear, equation (5.6.4) can be omitted. When both the normal stress and shear stress are important, it is necessary for E/G to be constant. In steel and Duralumin as can be seen from $E/G = 2(1 + \nu)$ (ν + Poisson's ratio) Since they have roughly the same values, the condition is satisfied. Assuming this is satisfied, from equation (5.6.4), since

$$P = P_m \left(\frac{l}{l_m}\right)^2 \frac{E}{E_m} \tag{5.6.9}$$

is obtained, if the load of the actual object acts by the same method as the model, and has a magnitude which is $(E/E_m)(1/l_m)^2$ times greater. The deflection that occurs is $1/l_m$ times that of the model

Next, considering equation (5.6.6) assuming conditions (5.6.4) and (5.6.5) are satisfied, from equations (5.6.6) and (5.6.4)

$$\rho gl/E=\rho_m g_m l_m/E_m$$

when $g = g_m$ /557

$$\frac{\rho}{E}=\frac{\rho_m}{E_m}\cdot\frac{l_m}{l} \tag{5.6.10}$$

when the model and actual object are made from the same material, and the deflection due to the weight of the structure is included in δ, this relation indicates that by appropriately distributing the additional mass, the model density may be artificially added to the ratio $1/1_m$.

Since usually the force and deformation are proportional, it is possible to accumulate the deformation due to the structural weight and the deformation due to load. Consequently, each can be handled independently. Thus, when only considering deformation due to load, condition (5.6.6) becomes unnecessary.

If the model load is greater, the closer it is to the breaking load of the structure, of course the proportional relationship between load and displacement is not established. However, the purpose of comparing the displacement in the model and real object is to determine the rigidity of the actual object and since the point is reached where a large load is used, this point is no obstacle. That is, in comparing rigidities, actually equation (5.6.6) may be omitted and the rigidity may be found from equation (5.6.8) or (5.6.9).

Linear Rigidity and Rotating Rigidity: Defining these as P/δ and $Pl/(\delta/l)$ respectively,

$$\frac{P}{\delta}\Big/\frac{P_m}{\delta_m}=\frac{E}{E_m}\,\frac{l}{l_m} \tag{5.6.11}$$

$$\left(\frac{Pl}{\delta/l}\right)\Big/\left(\frac{P_m l_m}{\delta_m/l_m}\right)=\frac{E}{E_m}\left(\frac{l}{l_m}\right)^3 \tag{5.6.12}$$

When the materials are the same, the linear rigidity is proportional to $1/1_m$ and the rotating rigidity is proportional to $(1/1_m^3)$.

Proper Vibration Number f: In vibration causing linear displacement, the vibration number varies in proportion to: $\sqrt{\text{rigidity/inertia}}$, so

$$f=k\sqrt{\frac{P/\delta}{\rho l^2}},\qquad \frac{f}{f_m}=\frac{1}{l}\sqrt{\frac{E}{\rho}}\Big/\left(\frac{1}{l}\sqrt{\frac{E}{\rho}}\right)_m \tag{5.6.13}$$

When the materials are the same, this becomes $f/f_m = 1_m/1$ and the proper vibration number is inversely proportionate to the length.

(2) Cases in which models are used for studying strength

In addition to the quantities E, G, ρ, g which effect the breaking load P_f of a structure, there is also the yield point or yield strength σ. Hence, the following results are obtained from dimensional analysis as above.

$$\text{Breaking load} \qquad P_f=(l^2E)f_n\left[\frac{G}{E},\ \frac{l\rho g}{E},\ \frac{\sigma}{E}\right] \tag{5.6.14}$$

Consequently, in this case it is necessary for G/E, σ/E to be equal in the model and actual structure, and the conditions in equations (5.6.10) must be satsified. When the structural weight is smaller than the working load, equation (5.6.10) becomes unnecessary.

Failure due to Direct Stress: When the structural weight can be disregarded and the failure is unrelated to G, E, as in a tie-rod, due to tensile force /558

$$P_f=k\cdot l^2\sigma$$

Consequently

$$P_f=\left(\frac{l}{l_m}\right)^2\frac{\sigma}{\sigma_m}P_m$$

Failure due to Elastic Instability: When failure occurs due to pure elastic instability, the important factor is the modulus of elasticity, and the effect of ρ and σ may be disregarded. Hence

$$P_f=lE.F\left(\frac{G}{E}\right) \tag{5.5.17}$$

Thus the form of failure includes expansion-contraction and slip deformation, and if related to E,G, it is necessary to have G/E the same in both model and actual structure. In this case

$$P_f=\frac{E}{E_m}\left(\frac{l}{l_m}\right)^2P_{fm} \tag{5.6.18}$$

and this agrees with Euler's formula $P_f = \pi^2EI/1^2 = kEl^2$. When the materials are the same.

$$\frac{\sqrt{P_f}}{l}=\frac{\sqrt{P_{fm}}}{l_m} \tag{5.6.19}$$

H. Wagner calls this quantity Kennwert. The relationship in equation (5.6.19) is convenient for determining the buckling stress σ_k in a compression support. If we describe the curve $\sigma_k \sim \sqrt{P_k/l}$, this relationship is linear within the column range, as can be seen from Euler's formula; that is, denoting by A the cross-section area of the column and by EI, the bending stiffness within the plane in which buckling deflection occurs.

$$\sigma_k = \frac{\pi \sqrt{EI}}{A} \cdot \frac{\sqrt{P_k}}{l} \qquad (5.6.20)$$

is obtained. In the range where l is small and $\sqrt{P_k/l}$ is large, from Euler's formula [misprinted word, untranslatable] enters the short column range, and near the yield,point, this curve becomes flat.

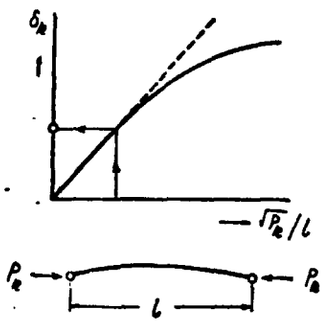

Figure 5.6.1

According to equation (5.6.19), in the case of a geometrically similar column, since the $\sqrt{P_k/l}$ agree in the model and in the actual structure, it can be seen that the buckling stress does not change. If this curve is determined experimentally for each model column with patterns having various cross-section dimension ratios, it is possible to directly determine the column with cross-sections having the lightest dimension ratios with respect to a given load P and load l by using the graphs that are constructed. That is, one may find a column with dimension ratios indicating the largest buckling stress σ_k with respect to the values obtained by calculating $\sqrt{P/l}$. In the usual σ_k slenderness ratio l/i curve, this cannot be determined as easily as with a graph.

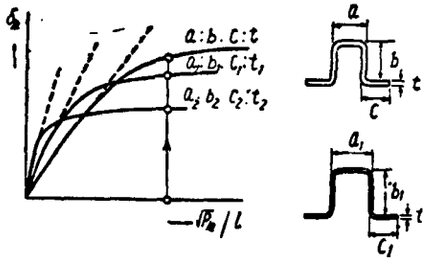

Figure 5.6.2

The above concerns axial loads, but in the case of buckling due to the bending or torsion moments of a cylinder, since the moment M_k at the time of buckling has the dimension $P_k l$, it can be derived from the above equation. It is expressed by

$$M_k = E r^3 \cdot F\left(\frac{t}{r}, \frac{l}{r}\right)$$

when (5.6.21) /559

$$\left.\begin{aligned} \frac{t}{r} &= \left(\frac{t}{r}\right)_m, \quad \frac{l}{r} = \left(\frac{l}{r}\right)_m \\ \frac{M_k}{Er^3} &= \left(\frac{M_k}{Er^3}\right)_m \end{aligned}\right\}$$

This is, proportional to the cube of the linear dimensions.

Secondary Failure: When failure occurs due to a combination of direct stress and secondary stress; e.g., in the failure of a cylinder after buckling, the values of σ/E must be the same in the model and in the actual structure. If the failure also depends on G/E, G/E is taken as the same for both.

When the same materials are used in the model and in the full scale and the effects of weight can be disregarded, for all forms of failure

$$P_f=\left(\frac{l}{l_m}\right)^3 P_{fm} \tag{5.6.22}$$

obtains.

Compression

No.	Graph & Bound. Cond.	Formula or Table of Results	Notes, Ref.
1	Flat press, ends with 2 straight sides rotating	As an experimental formula for compressive buckling strength $\sigma_k=\sigma_{KB}+0.18E\frac{t}{r}$. σ_{KB} is the buckling strength for a flat plate of the same width. The test results with $K=\sigma_k/\sigma_{KB}$ are given in the graph below. 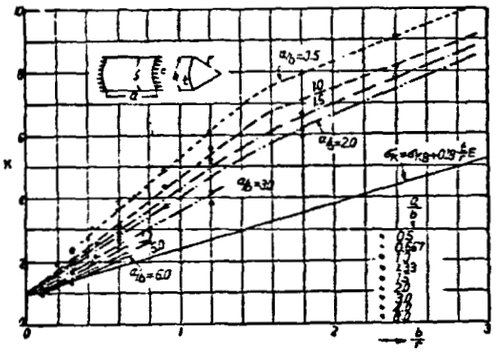 When $b/r=2\pi$, this agrees generally with the tube strength $0.18\,E\frac{t}{r}$. Note that in the vicinity $b/r=0$, there is a relatively flat section	39 (39), These data were taken from (40).
2	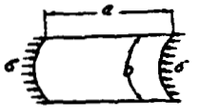 Straight sides rotating ends	Compressive buckling stress of curved plate $\sigma_k=\frac{1}{6}\frac{E}{1-\nu^2}\left\{\sqrt{12(1-\nu^2)\left(\frac{t}{r}\right)^2+\left(\frac{\pi t}{b}\right)^4}+\left(\frac{\pi t}{b}\right)^2\right\}$. when $\frac{b}{r}<\frac{1}{2}$ and $a\fallingdotseq b$ $\sigma_k=0.6E\left(\frac{t}{r}\right)$. r is radius of curvature, t is plate thickness.	41 Redshaw's formula Calculated values
3	End with 4 sides rotating	when $b\gtrsim 2\pi\sqrt[4]{\frac{r^2t^2}{12(1-\nu^2)}}=3.44\sqrt{rt}$ $(\nu=0.3)$ $\sigma_k=\frac{E}{\sqrt{3(1-\nu^2)}}\frac{t}{r}\equiv\sigma_R$ (Compressive buckling stress of tube). In a short arc plate $\sigma_k=\frac{E\pi^2}{3(1-\nu^2)}\left(\frac{t}{b}\right)^2+\frac{E}{4\pi^2}\left(\frac{b}{r}\right)^2$. The first term is the buckling stress $(\equiv \sigma_P)$ in the case of a flat plate with ends with 4 sides rotating. The second term is expresed by σ_R and σ_P and is determined as follows.	43 Timoshenko's equations

No.	Graph & Boundary Cond.	Formula or Table of Results	Notes, Ref.
4		Timoshenko's equations $\sigma_k=\sigma_P+\frac{\sigma_R^2}{4\sigma_P}$ when $\sigma_R\leqq 2\sigma_P$ $\sigma_k=\sigma_R$ when $\sigma_R\geqq 2\sigma_P$ Rewriting Redshaw's equations $\sigma_k=\sqrt{\sigma_R^2+\left(\frac{\sigma_P}{2}\right)^2}+\frac{\sigma_P}{2}$. Timoshenko's values here smaller than those of Redshaw in particular, when $\sigma_R\fallingdotseq 2\sigma_P$, the difference between the two is great, being 20% and when it is desirable to take into consideration the initial deflection of finite deformation, in both equations $\sigma_R=0.2E\frac{t}{r}$ may be used. Here $\sigma_P=\frac{\pi^2E}{3(1-\nu^2)}\cdot\frac{t^2}{b^2}$.	45 Ebner's expression Materials 2 and 3 (omitted text) may be rewritten
5	Flat press, both straight line edges reinforced	Experimental equation for the results of experiments on the compressive buckling of steel curved plates $\sigma_k=5E\left(\frac{t}{b}\right)^2+0.3E\frac{t}{r}$. This equation expresses well the test results on the right 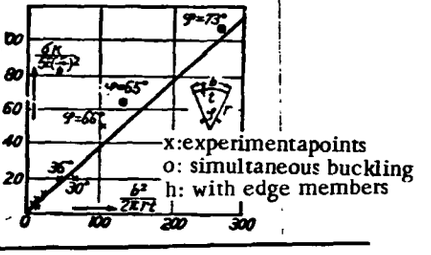 	46

SHEAR

No	Graph & Boundary Cond.	Formula or Table of Results	Notes, Ref.
6	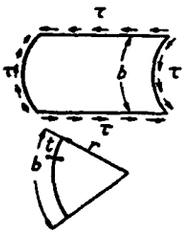 	The shear buckling stress of a curved plate can be expressed by the following equations of Wagner's. $\tau_k=0.1E\frac{t}{r}+5.0E\left(\frac{t}{b}\right)^2$ ..... (end with straight sides rotating) $\tau_k=0.1E\frac{t}{r}+7.5E\left(\frac{t}{b}\right)^2$ ..... (straight sides fixed)	52 These are experimental equations.

No.	Graph & Boundary Cond.	Formula or Table of Results	Notes, Ref
7	Rotating sides in a straight edge which is rigid with respect to bending, i.e. in a straight edge when no displacement occurs in the direction of the circumference along the curved plate surface. (In the case when $y=\pm\frac{b}{2}$ $v=0$ for the graph in Materials 8, b is plate width)	Leggett obtained the thin solid line in the following graph for the case in which the straight edge and all the rotating edges were stiff with respect to bending in the curved plate plane. 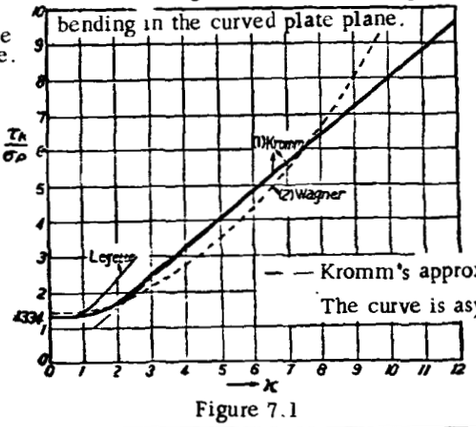 Figure 7.1	4 55 52
8	Rotating edge, soft with respect to bending 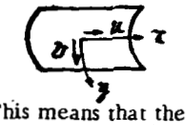 This means that the perpendicular stress on the edge is zero. $\left(y=\pm\frac{b}{2} \quad \sigma_y=0\right)$	Kromm obtained the curves in Figure 7.1 under the conditions on the left, and these can be expressed approximately as $\tau_k=\sigma_p\times 0.80\sqrt[4]{12(1-\nu^2)}\cdot\frac{b}{\pi t}\sqrt{\frac{\tau}{t}}=0.80\kappa\sigma_p$ $\kappa\equiv\sqrt[4]{12(1-\nu^2)}\cdot\frac{b}{\pi t}\sqrt{\frac{\tau}{t}}$, $\sigma_p=\frac{\pi^2 E}{3(1-\nu^2)}\left(\frac{t}{b}\right)^2$. this equation can be used up to $\kappa<8$	See Figure 7.1.
9	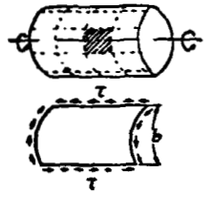	From the form of the equation of buckling stress in the case of compression, considering an expression which is formally identical to the case of shear, we obtain the experimental equation. That is according to Timoshenko $\tau_k=\tau_p+\frac{\tau_E^2}{4\tau_p}$ $\tau_E\leqq 2\tau_p$. $\tau_k=\tau_E$ $\tau_E\geqq 2\tau_p$. According to Redshaw $\tau_k=\sqrt{\tau_E^2+\left(\frac{\tau_p}{2}\right)^2}+\frac{\tau_p}{2}$. Here τ_E = shear buckling stress of unreinforced cylinder (e.g. Ballerstedt-Wagner's equation*), $\tau_p=4.85E\left(\frac{t}{b}\right)^2$ (τ_k of strip where width is b, simple support) $=8.15E\left(\frac{t}{b}\right)^2$ (" fixed). This agrees with the experiments. Compared with the experiments, Timoshenko's equation is 10% lower and Redshaw's equation is 10% higher. These equations can also be used for the torsion (shear) buckling of reinforced cylinder plates.	55 *See Materials 6.

SURFACE PRESSURE

No	Graph & Boundary Cond.	Formula or Table of Results	Notes, Ref.
10	Cylinder curve plate under surface pressure 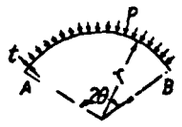 Deformation	Buckling surface pressure piece of p_k of cylinder under surface pressure a) end with side free, straight side rotating $p_k=\frac{Et^3\left(\frac{\pi^2}{\theta^2}-1\right)}{12r^3(1-\nu^2)}$. b) curved side free, straight side fixed $p_k=\frac{Et^3(\beta^2-1)}{12r^3(1-\nu^2)}$. β is given in a table below and is the solution of $\beta\tan\theta\cdot\cot\beta\theta=1$	58 59

θ	30°	60°	90°	120°	150°	180°
β	8.621	4.375	3	2.364	2.066	2

AFTER COMPRESSIVE BUCKLING

No.	Graph and Bound Cond.	Formula or Table of Results	Notes, Ref.
11	(1) 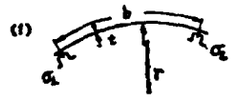 (2)	For the effective width after the compressive buckling of a curved plate $b_m=\bar{b}_m+\frac{\sigma_R}{\sigma_L}(b-\bar{b}_m)$. $\sigma_R=0.3E\frac{t}{r}$, σ_L = stress of reinforcement $\bar{b}_m$ indicates the effective width of a flat plate having extreme fiber stress σ_L -- σ_R i) Marguerre's equation $\bar{b}_m=\sqrt[3]{\frac{\sigma_k}{\sigma_L-\sigma_R}}\cdot b$, $\sigma_k=3.6E\left(\frac{t}{r}\right)^2$. ii) in a open cross-section profile $\bar{b}_m=1.63\sqrt{\frac{E}{\sigma_L-\sigma_R}}\cdot t+0.14b$. iii) in a closed section profile $\bar{b}_m=2.15\sqrt{\frac{E}{\sigma_L-\sigma_R}}\cdot t+0.14(b-e)$.	61
12	fixed 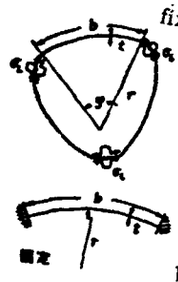	Effective width after the compressive buckling of a curved plate as an experimental equation for the effective width of a curved plate when Wenzek's equation is used $\frac{b_m}{b}=\sqrt{\frac{\sigma_k}{\sigma_L}}-\varphi\left(1-\frac{\sigma_k}{\sigma_L}\right)$. fixed $\sigma_k=5E\left(\frac{t}{b}\right)^2$ $+0.3E\frac{t}{r}$ (= Buckling stress of curved plate with two sides fixed) σ_L = stress of reinforced member. 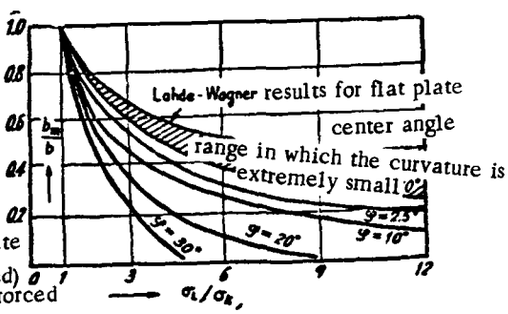	63

No.	Graph & Boundary Cond.	Formula or Table of Results	Notes, Ref.
13	Sides rotating around circumference 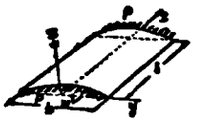	Initial configuration for the effective width of a curved plate having $W=F\cos\frac{\pi y}{b}$, the graph below is obtained while the energy method (finite displacement) 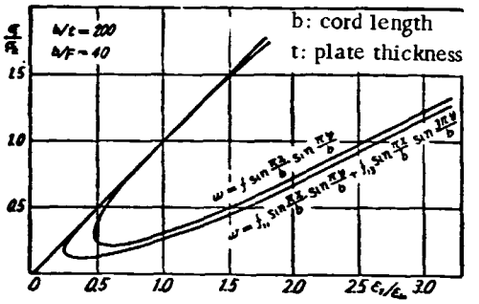 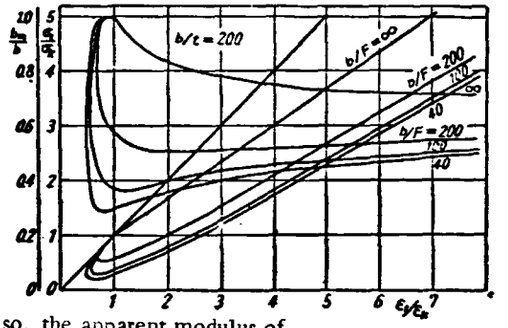 Also, the apparent modulus of elasticity after buckling becomes $\frac{1}{3}E$ σ_k = compressive buckling stress, ε_k = compressive buckling strain, σ_1 average stress for plate width.	64

PROFILES (BENDING)

No.	Graph & Boundary Cond.	Formula or Table of Results	Notes, Ref.
14	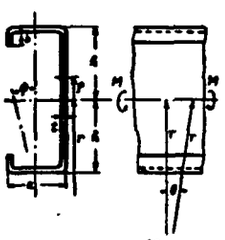 at both ends $\phi=\frac{d^2\phi}{dx^2}=0$ bending moment M.	$M_k=\frac{(C+B_1)}{2r}+\frac{\pi\sqrt{B_2C}}{l}\sqrt{\frac{l^2}{\pi^2CB_1}\frac{(C-B_1)^2}{4r^2}+1-\frac{k\pi^2}{l^2}}$. B_1 = bending stiffness, l = length, C = torsion stiffness Here k is calculated from $ck=-r^2\frac{Et}{1-\nu^2}\oint\rho a_0 ds$ Denoting the shear stress acting on the cross-section by τ , $\tau=-\frac{Et}{1-\nu^2}\varphi,\quad \theta=\sum_{n=1}^{n}a_n\frac{d\phi}{d\theta^n}$. ϕ = bending angle, θ = supplementary stress function.	65

No.	Graph & Boundary Cond.	Formula or Table of Results	Notes, Ref.
15	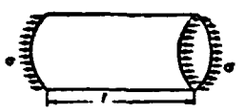 Flat press	is the solution for $\sigma_k = \frac{E}{\sqrt{3(1-\nu^2)}} \cdot \frac{t}{r}$ a long cylinder, and can be used with respect to a cylinder which has a larger length than $= 1.72\sqrt{rt}$ The test results appear to be 40-60% of that of the theoretical values, approximately $\sigma_k = 0.2 \sim 0.3 E \frac{t}{r}$. in a short cylinder $(l \leqq 1.72\sqrt{rt})$ $\sigma_k = \frac{E\pi^2}{12(1-\nu^2)} \left(\frac{t}{l}\right)^2$. but this is the Euler buckling stress of a strip of length 1.	66 72
16	Flat pressed	This shows the results of the compressive buckling stress on soft steel and nickel chromium steel cylinders with axial compression and eccentricity. Here, only the case of axial compression is indicated. 	72

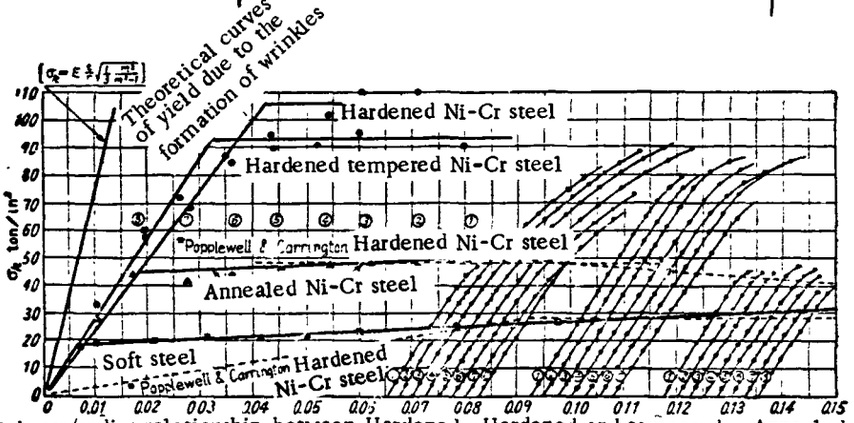

Plate thickness/radius relationship between t/r and buckling stress σ_k (t/in²)

Hardened and tempered Annealed

= Stress-strain graph of nickel-chromium steel tube

No.	Graph & Boundary Cond.	Formula or Table of Results	Notes, Ref.
17	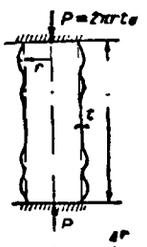 Level compression	The following equations obtained for the plastic buckling due to the longitudinal compression of a cylinder $\sigma_k = \frac{\sqrt{EK}}{\sqrt{3(1-\nu^2)}} \frac{t}{r} \sim \frac{Et}{r\sqrt{3(1-\nu^2)}} \frac{2}{1+\sqrt{E \cdot \frac{d\varepsilon}{d\sigma}}}$. Here $K = \frac{4EE'}{(\sqrt{E}+\sqrt{E'})^2}$ is Engesser-Karman's equivalent modulus of elasticity in the plastic range, and in the elastic range, K = 1, which agrees with the classical theory described above. This agrees approximately with the test results. $E' = \frac{d\sigma}{d\varepsilon}$. the convergence phenomena of the diameter in the boundary end section is not effected by σ_k as long as $l > 4.8\sqrt{rt}$. 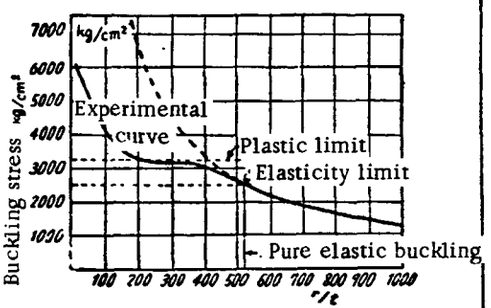 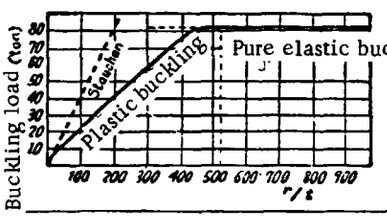	See References (47) and (48) for K
18	Both ends with rotating edges axial compression	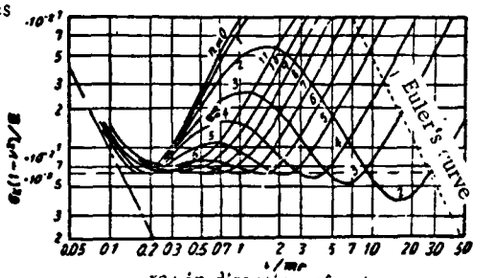 wave numbers m: in direction of axis n: in direction of circumference The above graph are the results of calculating the numerical values for the case, when $\alpha = \frac{1}{12}\left(\frac{t}{r}\right)^2 = 10^{-6}$, $\nu = \frac{1}{6}$	75

No.	Graph & Boundary Cond.	Formula or Table of Results	Notes, Ref.
19	Compression in direction of axis	allowable compressive stress of cylinder taking intial deformation into consideration: $\sigma_{ult}=E\frac{0.6\frac{t}{r}-10^{-3}\frac{r}{t}}{1+0.004\frac{E}{\sigma_{yp}}}$ σ_{ult} : allowable stress For brass and steel: $\frac{E}{\sigma_{yp}}=545.$ Duralumin: $\frac{E}{\sigma_{yp}}=265.$ $\frac{r}{t}=300\sim1500$ The above equation was constructed so that it agrees with the experiments 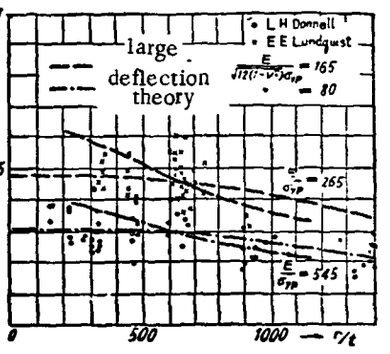	77
20		$P_k=\sigma_k\cdot t.$ In the elasticity range $\sigma_{k\,elast}=\frac{E\cdot t}{r\sqrt{3(1-\nu^2)}}.$ In the plastic range $\sigma_k=\sigma_0(1-\alpha\lambda),\quad \lambda=\frac{l}{i}$ $\sigma_k=\sigma_0\left[1+\frac{\sigma_0}{2Ek}-\sqrt{\frac{\sigma_0}{Ek}\left(1+\frac{\sigma_0}{4Ek}\right)}\right].$ Here $k=\frac{t^2}{3(1-\nu^2)\pi^2\alpha^2r^2}.$ also σ_0,α are the constants given from the materials (according to Tetmajer). Below a comparison is shown with Geckeler's equations**. 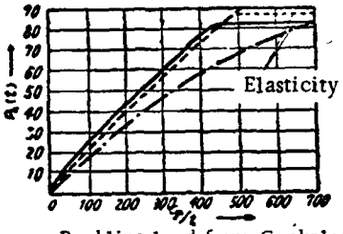 图中 —— Buckling load from Geckeler (martinsite steel) ---- } Buckling load from equations -.-.- } (medium hardened steel, ingot steel) medium hardened steel: $\sigma_0=3350\,kg/cm^2$, $\alpha=0.00188$, $E=2.25\cdot10^6 kg/cm^2$. ingot steel: $\sigma_0=3100\,kg/cm^2$, $\alpha=0.00368$, $E=2.15\cdot10^6 kg/cm^2$.	79

* L.v.Tetmajer 's equation

** Geckeler's equation $P_k=\frac{2\pi t^2}{\sqrt{3(1-\nu^2)}}\sqrt{EK}$.

Here K: Karman's equivalent elasticity modulus $\equiv\frac{4E'E}{(\sqrt{E'}+\sqrt{E})^2}$.

No.	Graph & Boundary Cond.	Formula or Table of Results	Notes, Ref.
21	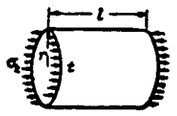 Flat press	Test results carried out by N. Nojima and S. Kanemitsu under the direction of E. E. Sechler. 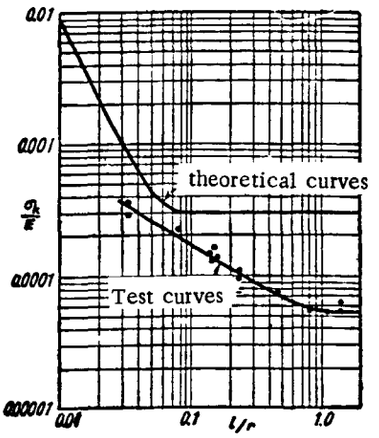 Figure 21.1. Effect of length of cylindrical shell with r/t = 200 on σ_t The point at which σ_t becomes unrelated to l/r is 0 1 in classical theory, but in the test results it is shown to be close to 1.5.	82 /569
22	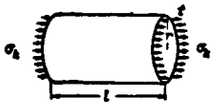 Flat press	For the lower equilibrium stress based on finite deformation theory $\sigma_t = 0.194\, E\frac{t}{r}$ 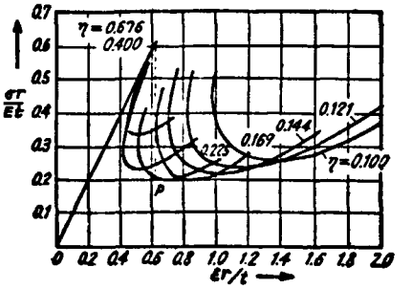 In the above graph μ=1.00, r/t=1000. It is assumed that the length is sufficiently long, $\eta = n^2\frac{t}{r}$, $\mu = \frac{m}{n}$. m: number of waves in direction of axis, n: number of waves in direction of circumference	83 Results of analysis

No.	Graph & Boundary Cond.	Formula or Table of Results	Notes, Ref.
23	$\frac{3}{4}d \leqq l \leqq (10-20)\cdot d$ $d = 2r$ Flat press 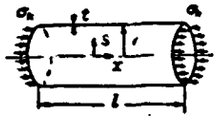	In the compressive buckling stress of the cylinder, we assume that the reason why the test results are much higher than the theoretical values is due to the effects of the initial deflection. From the point of view of finite deformation theory, we have compiled the results of many experiments and compared them below It is assumed that the form of initial buckling is as follows. $w_0 = a_0 t \cdot \left(\cos\frac{mnx}{r}\cos\frac{ns}{r} + b\cos\frac{2mnx}{r} + c\cos\frac{2ns}{r} + d\right)$. Here $a_0 = Ur^2/(m^{1.6}n^2 \cdot t^2)$. U : "unevenness factor" n= wave number in direction of circumference, $m = \frac{\text{wavelength in direction of circumference}}{\text{wavelength in direction of axis}}$ Moreover, we have assumed that the additional deflection occurs in a exactly the same form as w_0, and use the energy method (the five parameters m, n, b, c, d are also included) below we indicate the results of numerical computations σ_{cl}, ε_{cl} indicate buckling values based on classical infinitesimal deformation theory.	84 From L.H. Donnell, C.C. Wan /570

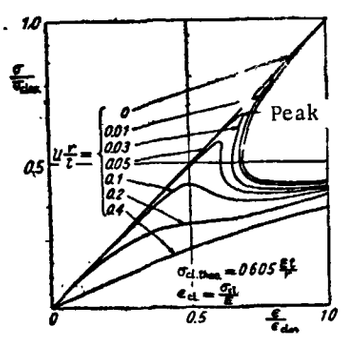

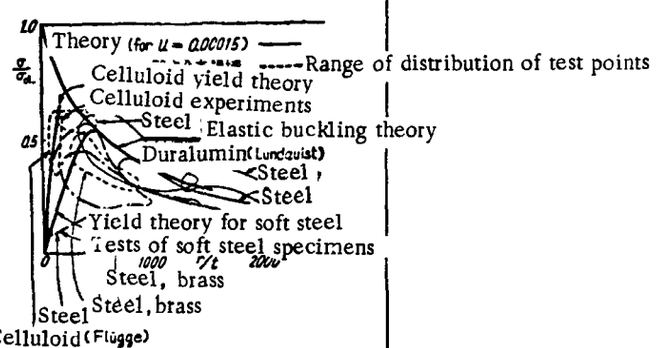

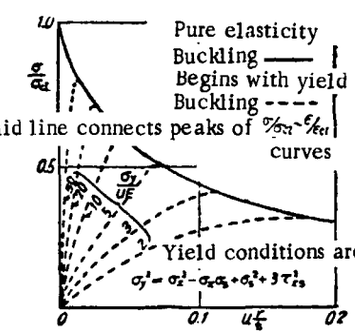

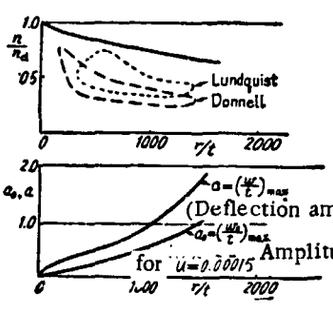

n_{cl} = n(classical theoretical value) = $0.87\sqrt{r/t}$

Twisting

No.	Graph & Boundary Cond.	Formula or Table of Results	Notes, Ref.
24	End with both ends rotating 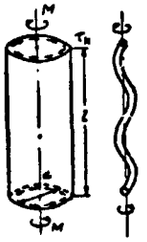	Torsional buckling in which the configuration of the cross-section does not change Torsion moment at time of buckling $T_k = \frac{\pi EJ}{l}$ l: length J: polar moment of inertial of cross-section	85 /571
25	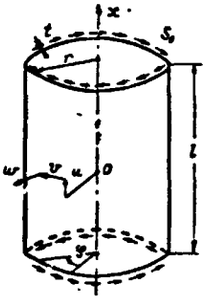	Both end conditions: Fixed / Rotating Ends l/r: Fixed 0, 1, 2, 3, ∞; Rotating Ends 0, 1, 2, 3, ∞ $S_0 l^2/D$: 22.2, 24.8, 32.4, 60.8, —; 13.2, 16.6, 28.8, 60.8, — $S_0 r^2/D$: —, 24.8, 8.1, 6.75, 6.75; —, 16.6, 7.2, 6.75, 6.75 n: —, 2, 2, 2, 2; —, 2, 2, 2, 2 θ: 38°, —, —, —, 27° 30′; 43°, —, —, —, 27° 30′ $S_0 = \tau_k t$, $D = \frac{Et^3}{12(1-\nu^2)}$, n = number of wrinkles θ = angle of wrinkles with respect to axis	87
26	a) end rotating around end circumference (maintains cross-section) 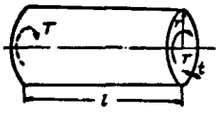	Torsional buckling of thin walled tube $\tau_k = \frac{T_k}{2\pi r t^2}$, $\tau_k = \frac{E}{1-\nu^2}\left(\frac{t}{l}\right)^2\left[2.8+\sqrt{2.5+0.495\alpha^{\frac{3}{2}}}\right]$ Here $\alpha = \sqrt{1-\nu^2}\,\frac{l^2}{tr}$. The experiment results are 60 to 70% of the above theoretical equation. For a design formula, 60% of the theoretical equation is used, and the equations below are used with $\nu = 0.3$. $\tau_k = E\left(\frac{t}{l}\right)^2\left[1.8+\sqrt{1.2-0.201\left(\frac{l}{\sqrt{tr}}\right)^3}\right]$. The above equation is limited to the case where $\frac{l}{r} < 6.6\sqrt{1-\nu^2}\cdot\sqrt{\frac{r}{t}}$ when l/r is greater than this $\tau_k = 0.272\frac{E}{(1-\nu^2)^{3/4}}\left(\frac{t}{r}\right)^{\frac{3}{2}}\cdot\left(1+0.45\frac{t}{r}\right)$.	50

No	Graph & Boundary Cond	Formula or Table of Results	Notes, Ref.
26		According to experiments, for $l/r < 5$ (Bailerstedt u. Wagner)	/572
	2) Theoretical curve 3) Steel 4) Brass 5) Donnell's experiments 6) Duralumin 7) Rubber 8) Celluloid 9) Duralumin 10) Brass 11) Steel Gough and Cox 11) Average of 83 experiments 12) Standard 13) Ultimate load 14) Maximum load 15) Bollenrath -- when wrinkles occur 16) Buckling load calculated assuming no original eccentricity	$\tau_k = 0.1E\frac{t}{r} + 5E\left(\frac{t}{l}\right)^2.$	93
		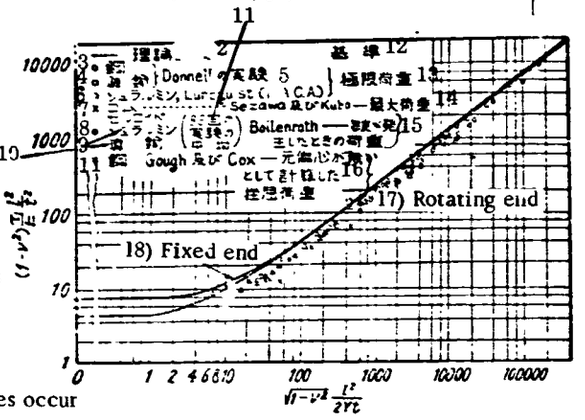	
		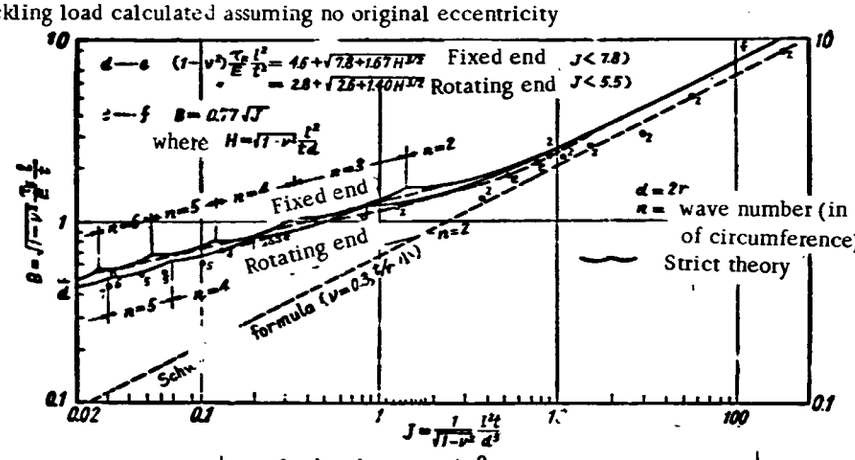	
		In the above graph ° experiment points for steels tubes (fixed end). The numbers indicate the values of n observed.	
	b) End section circumference fixed	$\tau_k = \frac{E}{1-\nu^2}\left(\frac{t}{l}\right)^2\left[4.6+\sqrt{7.8+0.590\alpha^{\frac{3}{2}}}\right]$ $\alpha = \sqrt{1-\nu^2}\cdot\frac{l^2}{tr}.$	90
		The experiment results are 60 to 70% of the above theoretical equations Using 60% for the design formulas, when, $\frac{l}{r} < 7.9\sqrt[4]{1-\nu^2}\cdot\sqrt{\frac{r}{t}}.$ $\tau_k = E\left(\frac{t}{l}\right)^2\left[3.0+\sqrt{3.4+0.240\left(\frac{l}{\sqrt{tr}}\right)^3}\right].$	

No.	Graph & Boundary Cond.	Formula or Table of Results	Notes, Ref.
26		When $\frac{l}{r} > 7.9\sqrt[4]{1-\nu^2}\sqrt{\frac{r}{t}}$	/573
		$\tau_k = 0.272\frac{E}{(1-\nu^2)^{3/4}}\left(\frac{t}{r}\right)^{\frac{5}{2}}$. according to tests when	86
		$\frac{l}{r} < 5$	
		$\tau_k = 0.1E\frac{t}{r} + 9.1E\left(\frac{t}{l}\right)^2$.	93
		and as a test formula $\tau_k = KE\left(\frac{t}{r}\right)^{2.85}$. here K takes the values in the table below according to l/r.	

l/r	0.2	0.25	0.30	0.40	0.50	0.7
K	3.30	2.75	2.45	2.02	1.78	1.45

l/r	1.0	1.5	2.0	3	4	5
K	1.27	1.06	0.94	0.78	0.68	0.61

27	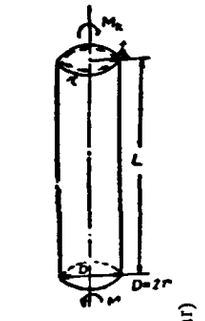 Deformation 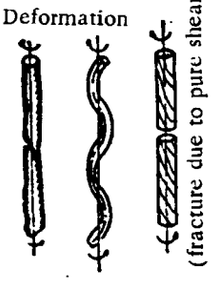 (fracture due to pure shear)	Below we show the results of torsion buckling tests on cylinders, for 63 chrome molybdenum steel and 102 17ST aluminum alloy cylinders.	95
		The types of buckling are generally classified as follows. (1) buckling with two wrinkle forms. (2) deformation in helical shape around cylinder axis. (3) accompanied by plastic deformation. (1),(2) occur within the elasticity region, and theoretical research has already been conducted on them for example, see Materials (26)	
		(1) $\tau_k = \frac{0.656E}{1-\nu^2}\left(\frac{t}{D}\right)^{\frac{5}{2}}\left\{1+2.4\frac{t}{D}+\cdots\right\}$: Long column	
		(2) $\tau_k = \frac{\pi E}{1-\nu}\frac{2r}{L}\left\{1-\frac{t}{D}+\frac{1}{3}\left(\frac{t}{D}\right)^2+\cdots\right\}$	
		Here an experimental equation and chart have been produced on the basis of a detailed investigation of case (3). M_k is the torsion moment at the time of buckling.	
		(1) Chromium, molybdenum steel (Figure 27.1) $\frac{M_k}{D^3\sigma_{y.p.}} = \frac{3.11\times10^7}{\sigma_{y.p.}}\left(\frac{t}{D}\right)^{\frac{5}{2}}\left(1+0.4\frac{t}{D}\right)^*$ where $0 \leq \frac{t}{D} \leq 0.024$.*	*elasticity region based on Schwerin

No.	Graph & Boundary Cond.	Formula or Table of Results	Notes, Ref.
27		$\frac{M_t}{D^3\sigma_{y.p.}} = 0.908\left(\frac{t}{D}\right)\left(1-2\frac{t}{D}+2\frac{t^2}{D^2}\right)$ $\cdot\left[15.27\frac{t}{D}\left(\frac{\sigma_{ult}}{\sigma_{y.p.}}-1\right)+0.981\right]$, where $0.015 < \frac{t}{D} < 0.072$. $\frac{M_t}{D^3\sigma_{y.p.}} = 0.908\frac{t}{D}\left(1-2\frac{t}{D}+2\frac{t^2}{D^2}\right)\frac{\sigma_{ult}}{\sigma_{y.p.}}$, where $0.068 < \frac{t}{D} < 0.100$. (2) Aluminum alloy (Figure 27.2) $\frac{M_t}{D^3\sigma_{ult}} = \frac{1.2\times10^7}{\sigma_{ult}}\left(\frac{t}{D}\right)^{\frac{5}{3}}\left(1+0.4\frac{t}{D}\right)$,* where $0 \leq \frac{t}{D} \leq 0.02$. $\frac{M_t}{D^3\sigma_{ult}} = 0.394\left(\frac{t}{D}\right)\left(1+15.9\frac{t}{D}-33.7\frac{t^2}{D^2}\right)$, where $0.02 < \frac{t}{D} < 0.088$. $\frac{M_t}{D^3\sigma_{ult}} = 1.005\left(\frac{t}{D}\right)\left(1-2\frac{t}{D}+2\frac{t^2}{D^2}\right)$, where $0.088 < \frac{t}{D} < 0.12$.	* Elasticity region based on Schwerin

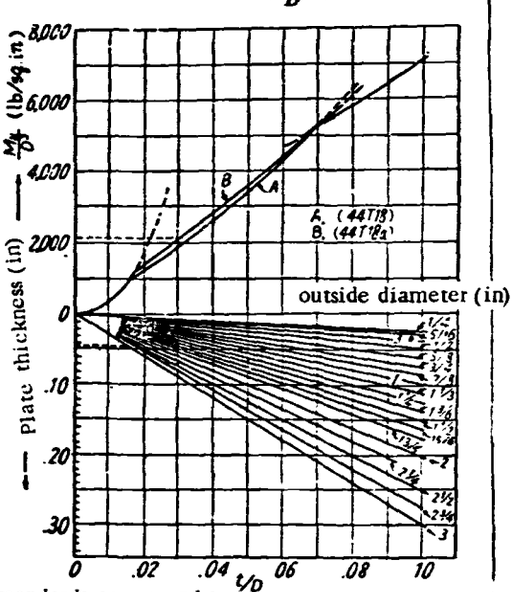

*Naval standards correspond to
44T18 (σ_{ult} = 95,000 lb/in², $\sigma_{y.p.}$ = 60,000 lb/in²)
44T18a (σ_{ult} = 95,000 lb/in, $\sigma_{y.p.}$ = 75,000 lb/in²)

design chart for the torsional strength of 19-60 inch chromium-molybdenum steel Figure 27.1

No.	Graph & Boundary Cond.	Formula or Table of Results	Notes, Ref.
27		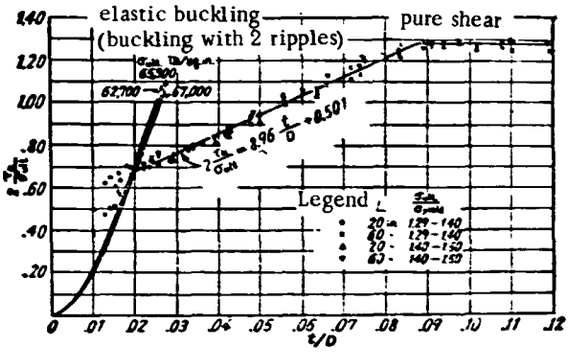 Figure 27.2. Results of Tests on 17ST aluminum alloy tube. 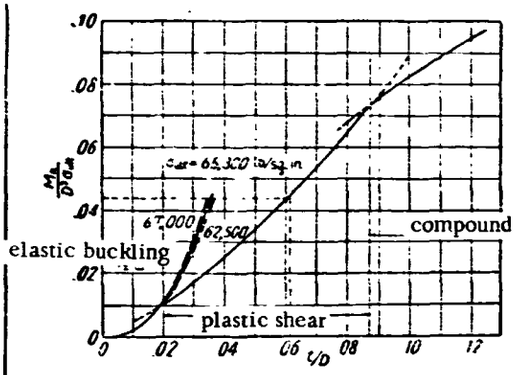 Figure 27.3. Design chart for the torsion strength of 17ST aluminum alloy tube.	/575

Bending

No.	Graph & Boundary Cond.	Formula or Table of Results	Notes, Ref.
28	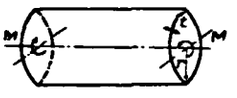	$M_x=\alpha\frac{E}{1-\nu^2}rt^2.$ In the case of a long tube $\alpha=\frac{2\sqrt{2}\pi}{9}=0.99.$ Average values of test results $\alpha=1.14$, Minimum values of test results $\alpha=0.72$. The effect of length may be disregarded except in the case of extremely short tubes.	96

No.	Graph & Boundary Cond.	Formula or Table of Results	Notes, Ref.
29	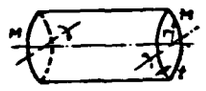	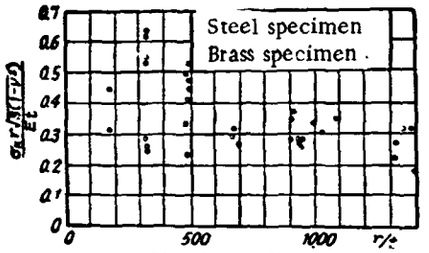 Simple bending test The bending stress σ_k at the time of buckling in the diagram has the value determined by beam from the moment M_k at the time of buckling $\sigma_k = \frac{M_k}{Z} = \frac{32}{\pi} \cdot \frac{D}{D^4 - d^4} \cdot M_k$ $D = 2r + t, \quad d = 2r - t.$	103 /576
30	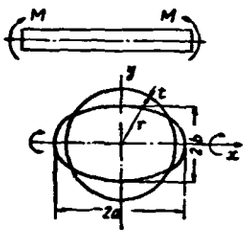 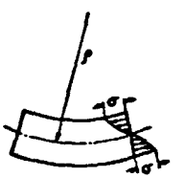 Boundary conditions not considered	Yield due to bending of thin tube The solution is carried out by the energy method, assuming that the cross-section is deformed in the shape of an elipse, and that the circumferential length does not change, taking into consideration accuracy up to a high order infinitesimal term. Attention is called to the fact that this indicates that this occurs in a state of deformation in which M_k ($\equiv M_{max}$) and σ_{max} differ. $M_{max} = M_k = 0.378 \pi E r t^2,$ $\sigma_{max} = 0.51 \, E t/r.$ Here is the maximum σ fiber stress 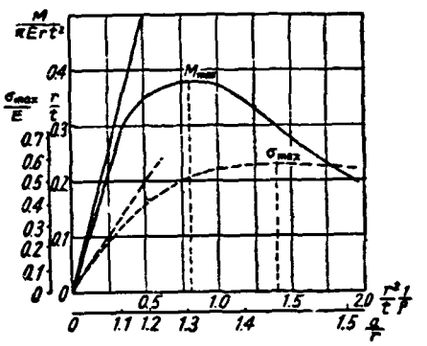	100

Surface pressure

No.	Graph & Boundary Cond.	Formula or Table of Results	Notes, Ref.
31	External pressure p 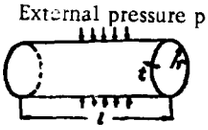 End conditions not considered. Case in which external pressure is received, but there is not axial force.	Buckling due to external pressure $l > 4.90 r\sqrt{\frac{r}{t}}$ $p_k = \frac{E}{4(1-\nu^2)}\left(\frac{t}{r}\right)^3$ * In the case of a short tube, when the member end maintains its circular shape, or a long tube is reinforced so that for each l it maintains its circular form, as an approximation $p_k = 0.807\frac{E t^2}{lr}\sqrt[4]{\left(\frac{1}{1-\nu^2}\right)^3\frac{t^2}{r^2}}$.	104 *this corresponds to the special case in R v. Mises results
32	Ditto	Collapsing pressure $p_k = \frac{E\frac{t}{2r}}{n^2-1+\frac{\alpha^2}{2}}$ $\cdot\left\{\frac{2\alpha^4}{(n^2+\alpha^2)^2}+\frac{2}{3}\frac{1}{(1-\nu^2)}\left(\frac{t}{2r}\right)^2\left\{(n^2+\alpha^2)-\frac{n^2(2n^2-1)}{(n^2+\alpha^2)^2}\right\}\right\}$. $\alpha = \frac{\pi r}{l}$, n = number of wrinkles (number of complete waves in direction of circumference, with half waves) n is determined from $\frac{\partial p_k}{\partial n}=0$ assuming $2r \ll l$, $\nu = 0.3$ $p_k = 2.4E\left(\frac{2r}{l}\right)\left(\frac{t}{2r}\right)^{2.5}$.	112 9
33	Uniform external pressure on entire surface 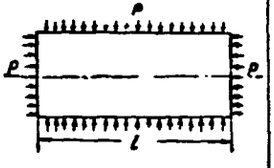 Case of a cylinder closed at both ends	Assuming that the member end maintains its circular shape $p_k = \frac{E\left(\frac{t}{r}\right)}{\frac{1}{2}\left(\frac{\pi r}{nl}\right)^2}$ $\cdot\left\{\frac{1}{\left\{1+\left(\frac{nl}{\pi r}\right)^2\right\}^2}+\frac{n^2t^2}{12r^2(1-\nu^2)}\left\{1+\left(\frac{\pi r}{nl}\right)^2\right\}^2\right\}$ Assuming n = 1, 2, ... in order to determine p_k with respect to a given t/r, if we describe the family of curves where $\frac{1}{l}$ is the abscissa and p_k is the ordinate, the minimum value of this one family of curves gives the required p_k with respect to 1/r. For a given t/2r, 1/2r, the p_k in the above equation should be reduced to a minimum, and the value of n that should be used in calculating p_k is shown in the following chart.	120

No.	Graph & Boundary Cond.	Formula or Table of Results	Notes, Ref
33		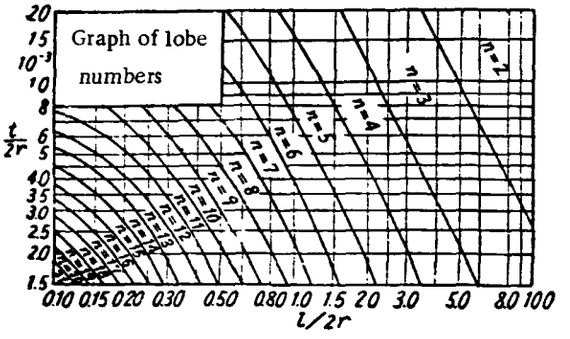	/578
34	Case where there is external pressure but no axial pressure The chart on the upper right was constructed by Timoshenko. The lower right graph is a graph of $p_k \cong 1/2r$ with t/2r found from R. v Mises' equation as parameters, for a steel cylinder where $E = 3.10^7$ p.s.i. $\sigma_{y,p,} = 2.6 \times 10^4$ p.s.i. (see ref. ce 115).	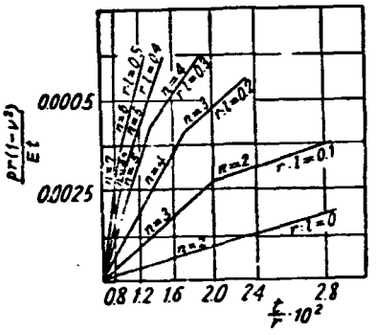 If the above results are expressed in a different form, the following graph is obtained 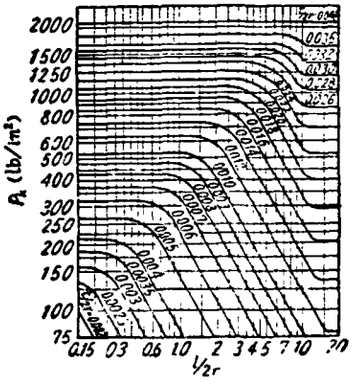	120

No.	Graph & Boundary Cond.	Formula or Table of Results	Notes, Ref.
35	External pressure and axial force 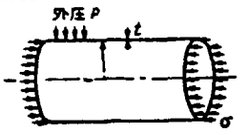 Ends with both ends rotating	Buckling due to combined load p, σ $\frac{pr(1-\nu^2)}{Et}=\phi_1, \quad \frac{\sigma(1-\nu^2)}{E}=-\phi_2.$ $\lambda=\frac{m\pi r}{2}$, Number of half-waves in direction of axis = m, outer pressure = p, number of waves in direction of circumference = 2n, compressive stress = σ. 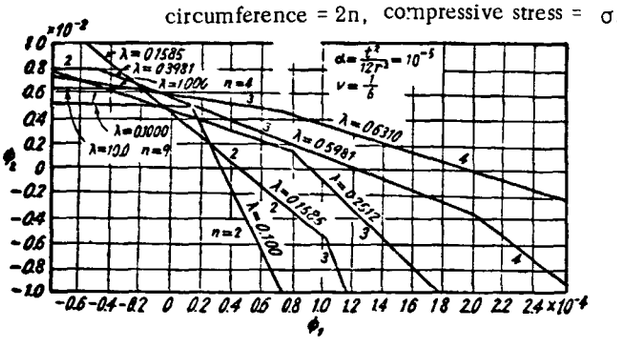 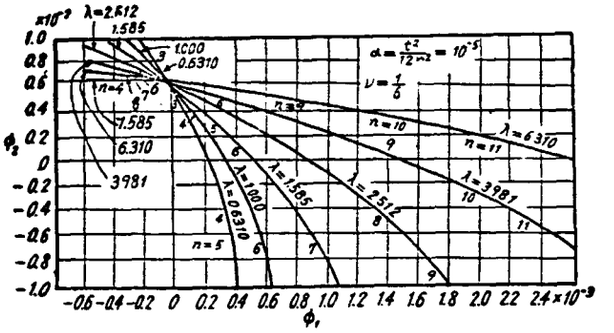	123 121 Materials 33 is a special case of this /579

COMPRESSION AND BENDING

No	Graph & Boundary Cond.	Formula or Table of Results	Notes, Ref.
36	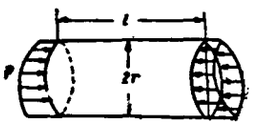 $p=p_0+p_1\cos\varphi$ p is the distributed load for the unit within the direction of the circumference 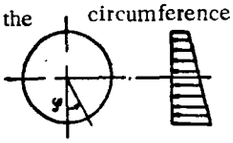 p_0, p_1 are positive in the case of compression	Approximation equation $\frac{1}{t}(p_0+p_1)_k=\frac{Et}{r\sqrt{3(1-\nu^2)}}$. The solid lines are accurate calculation results, the broken line is based on the above formula 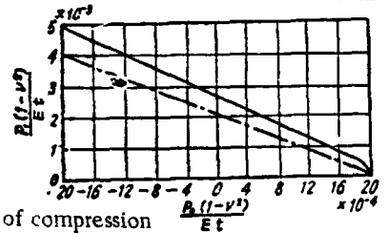	123

BENDING AND EXTERNAL, AND INTERNAL PRESSURE

No.	Graph & Boundary Cond.	Formula or Table of Results	Notes, Ref.
37	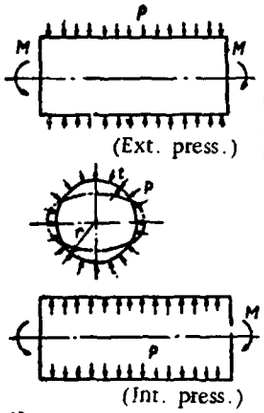 Calculations made for the case of an infinitely long cylinder.	Buckling of a cylinder under external or internal pressure and bending moment i) . External pressure, Assuming $(M_k)_{r=\infty}=\frac{2\sqrt{2}\,E\pi t^2}{9\sqrt{1-\nu^2}}$, *2 $(p_k)_{M=0}=\frac{E}{4(1-\nu^2)}\frac{t^3}{r^3}$. *3 $\frac{M^2_k}{(M_k)^2_{r=\infty}}+\frac{p_k}{(p_k)_{M=0}}=1.$ ii) Internal pressure, as an experimental equation $\frac{M_k}{(M_k)_{r=\infty}}=0.65+0.835\frac{\left(1-\frac{p_k}{(p_k)_{M=0}}\right)^{\frac{1}{2}}\left(4.8-\frac{2p_k}{(p_k)_{M=0}}\right)}{\left(3.25-\frac{p_k}{(p_k)_{M=0}}\right)\left(6.5-\frac{2p_k}{(p_k)_{M=0}}\right)}$. also, when p is relatively large $\frac{M_k}{(M_k)_{r=\infty}}=1.49+0.56\sqrt{1-\nu^2}\frac{r^2}{t^2}\frac{p_k}{E}$. 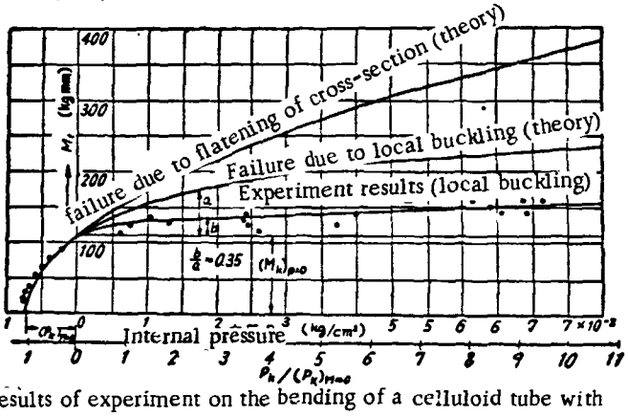 Results of experiment on the bending of a celluloid tube with t = 0.124 mm, r = 15.3 mm under internal or external pressure, comparison of calculated curves and experiment curves. Ordinat is M_k: abscissa is p_k or $p_k/(p_k)_{M=0}$	129 *1 L.G.Brazier *2 H. Bryan

/580

TORSION AND EXTERNAL PRESSURE

No.	Graph & Boundary Cond.	Formula or Table of Results	Notes, Ref.
38	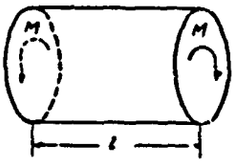	Torsion moment and internal or external pressure 1) case where l is comparatively large . A three-dimensional linear differential equation was derived from the basic equation for a cylindrical shell, and solving this, the following equation was obtained, if high order infinitesimal quantities are disregarded $\phi=\frac{K}{S}$.	130

No.	Graph & Boundary Cond.	Formula or Table of Results	Notes, Ref
38	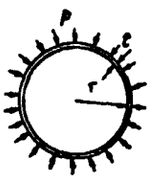	Here	130 /581

$$P=\lambda^6(1-\nu^2)+\alpha\Big[2\lambda^6(1-\nu^2)+(\lambda^2+n^2)^4+(3+\nu)\lambda^2n^2$$

$$-(2+\nu)(3+\nu)\lambda^4n^2-(7+\nu)\lambda^2n^4-2n^6+n^8\Big]$$

$$-\varphi\Big[\lambda^8+1.5\nu\lambda^4+3\lambda^6n^2-25\lambda^2n^2+3\lambda^2n-n^6+n^8\Big].$$

$$S=2\lambda n^6-2\lambda n^3+4\lambda^3n^3-2\lambda^3n+2\lambda^5n.$$

$$\alpha=\frac{t^2}{12r^2},\quad \phi=\frac{M_x(1-\nu^2)}{2\pi rEt},\quad \varphi=\frac{2r(1-\nu^2)}{Et}.$$

n - positive integer (number of waves in direction of circumference due to buckling), $1/\lambda$ = wavelength in direction of axis.

when $l>>r$, for $n=1$

$$M_x=\frac{2\pi^2r^3Et}{l}-\frac{5.5}{2}pr^2l.$$

$n\geq 2$

$$M_x=\frac{1}{3}\sqrt{\frac{2}{3}(n^2-1)}$$

$$\cdot\frac{\pi E}{(1-\nu^2)^{3/4}}\sqrt{rt^3}\left[1-\frac{12}{n^2-1}\frac{pr^2(1-\nu^2)}{Et^2}\right]^{\frac{3}{4}}.$$

The boundary conditions are not taken into consideration here, since in Donnell's calculations, there is only a slight difference between fixed and supported boundaries.

The shear stress is

$$\tau_x=\frac{1}{6}\sqrt{\frac{2}{3}(n^2-1)}$$

$$\cdot\frac{E}{(1-\nu^2)^{3/4}}\left(\frac{t}{r}\right)^{\frac{3}{2}}\left[1-\frac{12}{n^2-1}\frac{pr^2(1-\nu^2)}{Et^2}\right]^{\frac{3}{4}}.$$

2) when l is small

In the above equation, if calculations are performed up to term λ^2, the buckling condition equation is

$$\phi=\frac{R}{S}$$

$$=\frac{\lambda^4(1-\nu)+\alpha[(n^2-1)^2n^4+(n^2-1)\lambda^2(4n^2-3-\nu)]}{2\lambda n^3(n^2-1)}$$

$$\frac{-\varphi[n^4(n^2-1)+\lambda^2n^2(3n^2-2.5)]}{},$$

from $\frac{\partial\phi}{\partial\lambda}=0$

$$\lambda^2=\frac{n^2(n^2-1)}{6(1-\nu^2)}\left[\varphi\frac{3n^2-2.5}{n^2-1}-\alpha(4n^2-3-\nu)\right.$$

$$\left.\pm\sqrt{\left\{\alpha(4n^2-3-\nu)-\varphi\frac{3n^2-2.5}{n^2-1}\right\}^2+12(1-\nu^2)\left(\alpha-\frac{\varphi}{n^2-1}\right)}\right].$$

No	Graph & Boundary Cond.	Formula or Table of Results	Notes, Ref.
38		3) As an experimental formula $\left(\frac{M_k}{M_{k0}}\right)^{\frac{6}{5}}+\frac{p_k}{p_{k0}}=1.$ Here M_{k0}, p_{k0} express the critical torsion moment and external pressure when in the cylinder p = 0 and M = 0, and in particular, when l is large $M_{k0}=\frac{1}{3}\sqrt{\frac{2}{3}(n^2-1)}\ \frac{\pi E}{(1-\nu^2)^{3/4}}\sqrt{2rt^5},$ $p_{k0}=\frac{n^2-1}{12}\ \frac{Et^3}{r^3(1-\nu^2)}$ The experiment results agree with the theory when p_k is small, but when p_k is large, the experiment values are 85% of the theoretical values	/582

TORSION AND COMPRESSION

No.	Graph & Boundary Cond.	Formula or Table of Results	Notes, Ref.
39	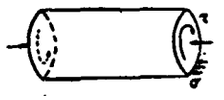 Torsion moment = T compressive stress = σ	Experiment results are indicated The solid line in the graph indicates the average curve of the experiment values $\sigma_0=(\sigma_k)_{T=0},$ $T_0=(T_k)_{\sigma=0}.$ 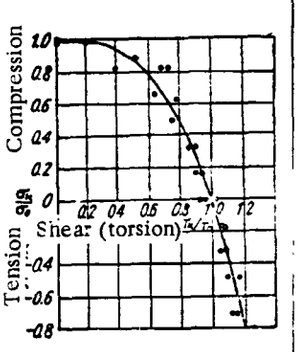	125
40	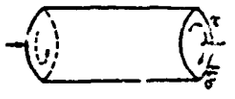	$\frac{\tau_k^2}{(\tau_k)^2_{\sigma=0}}+\frac{\sigma_k}{(\sigma_k)_{\sigma=0}}=1.$	131
41	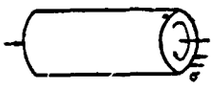	The experiment results are $\left(\frac{\tau_k}{(\tau_k)_{\sigma=0}}\right)^2+\frac{\sigma_k}{(\sigma_k)_{\tau=0}}=1.$	127

ELLIPTICAL CYLINDERS

COMPRESSION

/583

No.	Graph & Boundary Cond.	Formula or Table of Results	Notes, Ref.
42	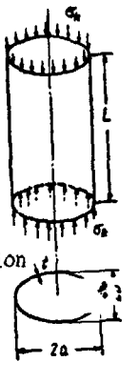 Cross-section Flat press	For the compressive buckling of a thin walled eliiptical cylinder Generally $Q=m^2\beta^2\left\{1+\frac{b^2}{a^4}\frac{3(1-\nu^2)}{t^2}\frac{1}{c_{00}}\right\}$. Here $Q\equiv\frac{P_k c^2}{D\pi^2 z^2}$, $\beta\equiv\frac{c}{2l}$, $d\equiv\frac{\pi a}{c}$. c: semi-circular length of elipse m: half-wave number in direction of axis c_{00}: polynomial related to $m\beta$ $m\beta$ is determined such that Q beomes Min e g : $a/b=1.5$. $\sigma_k=0.706\frac{Et}{\sqrt{3(1-\nu^2)}}$ Below is a graphical representation of a comparison of this with the experiment results. The comparison of calculations and experiment is as follows . 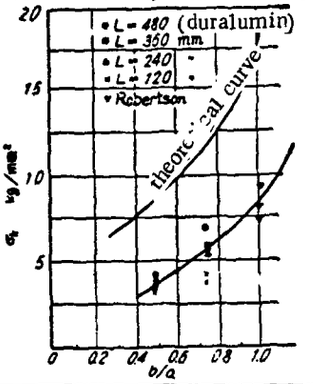	132

SPHERICAL SHELLS

Spherical shells under concentrated force

No.	Graph & Boundary Cond.	Formula or Table of Results	Notes, Ref.
43	End with circumference rotating 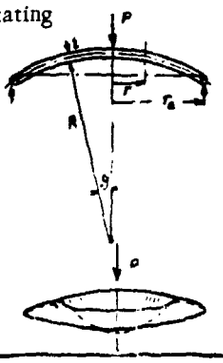	Jump of circular plate having small curvature (based on unit load P) (1) $\mu_k=\sqrt{0.152(\lambda+74.9)}-2.88$. $(20<\lambda<100)$. (2) $\mu_k=\sqrt{0.093(\lambda+11.5)}-0.94$. $(100<\lambda<500)$. Here $\mu_k\equiv\frac{Rl'_k}{Et^2}$, $\lambda\equiv\frac{r_a^4}{R^2\cdot t^2}$. This equation is shown in Figure 43.1. P_k is the maximum value on the positive side of P in Figure 43.2. As can be seen from Figure 43.2, in(1) it is always the case that $P>0$, but in (2) the equilibrium range $P<0$ occurs	133 When $0<\lambda<20$, the jump phenomenon does not occur in stable equilibrium

No.	Graph & Boundary Cond.	Formula or Table of Results	Notes, Ref.
43	w_0 = center deflection $w_0 = \frac{r_0^4}{2R}$	Moreover, when $\lambda \approx 300$, the second maximum point is generated, and where $\lambda = 330$, an isolated equilibrium point appears. 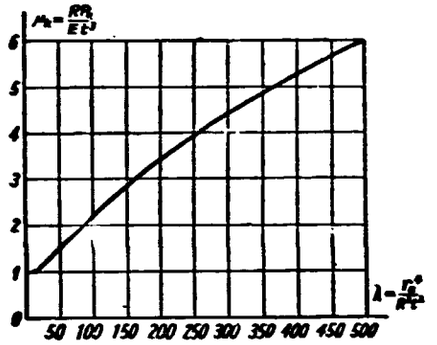 Figure 43.1 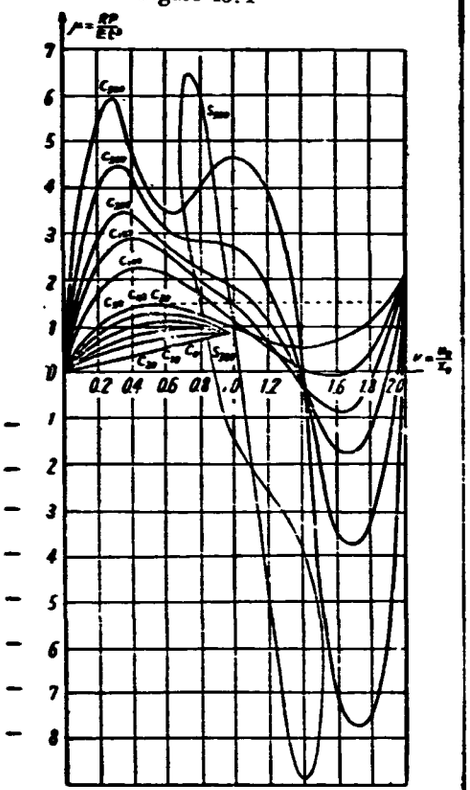 Figure 43.2 (NOTE) C_{100} refers to the curve $\lambda = 100$, and C_{20} refers to the curve $\lambda = 20$. Moreover, S_{500} indicates the isolated spiral $\lambda = 500$.	

SPHERICAL SHELLS

External Pressure

/585

No.	Graph & Boundary Cond.	Formula or Table of Results	Notes, Ref.
44		Buckling due to surface pressure of thin walled spherical shells (classical theory) $p_k=\frac{2Et^2}{r^2\sqrt{3(1-\nu^2)}}$.	135 According to R. Zoelly
45	As above	1) $p_k=17.95E\left(\frac{t}{d}\right)^{2.5}$. 2) $p_k=14.82E\left(\frac{t}{d}\right)^{2.5}$ $\left(\frac{t}{d}>0.0045\right)$. 3) $p_k=0.0122E\left(\frac{t}{d}\right)^{2.39}$ $\left(\frac{t}{d}<0.0045\right)$. • experiment values 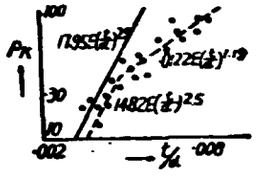	137 t, plate thickness d, diameter
46	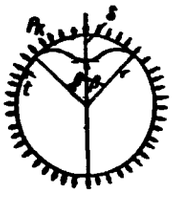 p= external pressure $\sigma=p$ compression inside shell stress $=\frac{pr}{2t}$ due to p	Karman provides the following approximation equation based on finite displacement theory. $p_{k\min}=0.36516E\left(\frac{t}{r}\right)^2$ 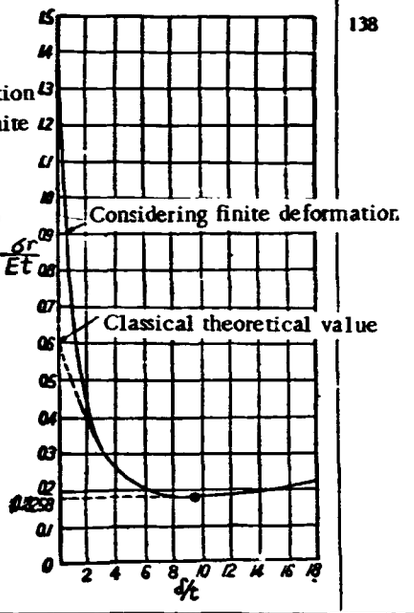	138
47	As above	For an approximate collapsing pressure $p_k=16.70E\left(\frac{t}{d}\right)^{2.5}$.	139

ELLIPTICAL SHELLS

Internal Pressure

/586

No.	Graph & Boundary Cond.	Formula or Table of Results	Notes, Ref.
48	Buckling due to internal pressure on a rotating elliptical shell 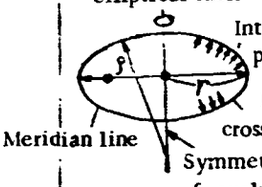 when $\left(\rho < \frac{r}{2}\right)$ Form of buckling equator	$N_k = \frac{r}{2} p\left(2 - \frac{r}{\rho}\right)$ N : case in which the plate thickness is multiplied by the compressive stress in the direction along the equator when $\rho < \frac{r}{2}$ $N<0$ becomes the internal compressive force p: uniform internal pressure, r: radius of equator ρ: minimum radius of curvature of meridian The pressure at the time of buckling of a revolving elliptical sheli due to the above internal compressive force is $p_k = \frac{2}{\sqrt{3(1-\nu^2)}} \frac{1}{2-\frac{r}{\rho}} \frac{Et^2}{r^2}$. The wavelength of the buckling waves that form around the equator $\lambda = 2\pi \sqrt[4]{\frac{1}{12(1-\nu^2)}} \cdot \sqrt{rt}$. The number of waves is $n = \frac{2\pi r}{\lambda} = \sqrt[4]{12(1-\nu^2)} \cdot \sqrt{\frac{r}{t}} = 1.83\sqrt{\frac{r}{t}}$. This p_k, n agree well with experiments.	140

CONICAL SHELLS

Distributed Loads

No.	Graph & Boundary Cond.	Formula or Table of Results	Notes, Ref.
49	 $t = t_2 \frac{r}{r_2}$ Buckling due to downward uniformly distributed load	A. Pfluger expanded the general theory on the basis of the energy method, for the buckling of a conical shell due to the pressure q that is sustained in the case when the thickness t is expressed as a function of s, performed calculations for the case when the wall thickness varied uniformly $\left(t = t_1 \frac{r}{r_1}\right)$ and obtained the following results (assuming n = 2) *1. $q_k = q_1 \frac{E}{1-\mu^2} \frac{t_2}{r_2}$, $k_2 = \frac{t_2^2}{12 r_2^2}$. μ: Poisson's ratio	141 The buckling wave forms are $u = A\rho^n \cdot \cos\lambda\varphi$ $v = B\rho^n \cdot \sin\lambda\varphi$ $w = C\rho^n \cdot \cos\lambda\varphi$ *1 the hypothesis n = 2 gives the buckling wave form with respect to the minimum buckling pressure.

No.	Graph & Boundary Cond.	Formula or Table of Results	Notes, Ref.
49		Here, q_1 is a constant as shown in the graph below 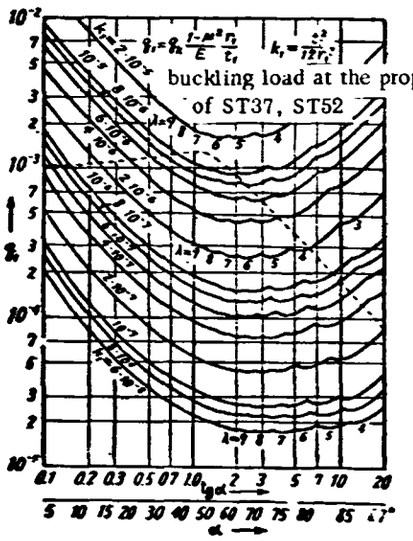 	/587
50	Uniform pressure 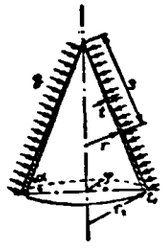 $t=t_1\frac{r}{r_1}$, $k_1=\frac{t_1^2}{12r_1^2}$, $q_k=q_1\frac{E}{1-\mu^2}\frac{t_1}{r_1}$. $(n=2)$	—Buckling due to uniform vertical pressure $\left(t=t_1\frac{r}{r_1},\ n=2,\ \mu=\text{Poisson's ratio}\right)$ 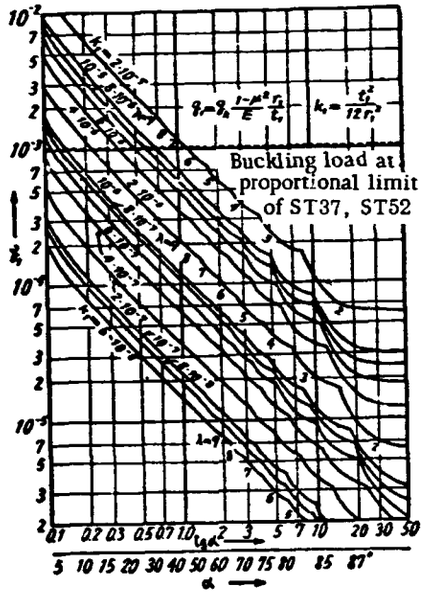 $\alpha=50.6°$ 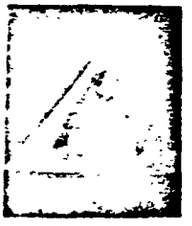 $\alpha=60.5°$	141

No.	Graph & Boundary Cond.	Formula or Table of Results	Notes, Ref.
51	External pressure P 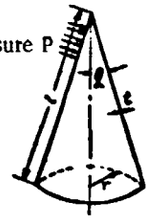	As an approximate solution $$p_k = 2.4E\left(\frac{r}{l}\right)\left(\frac{t}{r}\right)^{2.5}$$	142

/588

REINFORCED CURVED PLATES

Compression

No.	Graph & Boundary Cond.	Formula or Table of Results	Notes, Ref.
52	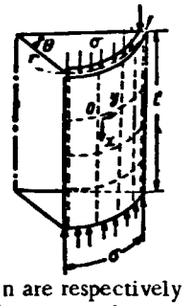 m, n are respectively the half-wave numbers in the direction of the axis and the circumference $t_x = t + \frac{F_x}{d_x}$ $t_y = t + \frac{F_y}{d_y}$ I_x, I_y = the I of the composite cross-section formed by adding one part of the surrounding wall to the cross-section of the stringer or rib. EI_{xy}, EI_{yx} = average torsion stiffness per unit width of strip taken in either the direction of the axis or the circumference of the shell. t = thickness of outer plate F_x, F_y = cross-section area of stringer or rib d_x, d_y = spacing between stringers or ribs	As in the case of a reinforced cylinder, $$\sigma_{k0} = \frac{2E}{rt_x}\sqrt{\frac{I_x I_y}{\frac{I_x}{t_x}+\frac{I_y}{t}\frac{t_x}{t_y}}}.$$ Where σ_{k0} indicates the buckling stress in the case where l, b are rather large, and are unrelated to the formation of wave forms. That is, it is used in the case where the half-wave numbers m, n >>1. The equation which analyses this in detail is $$\frac{1}{\lambda^2} = \sqrt{\left\{\left(\frac{I_x}{r^2 t_x}\right)+\beta^2\left(\frac{I_{xy}+I_{yx}}{r^2 t_x}\right)+\beta^4\left(\frac{I_y}{r^2 t_x}\right)\right\}\left\{\left(\frac{t_x}{t_y}\right)+2\beta^2\frac{t_x}{t}+\beta^4\right\}},$$ $$\beta = \frac{t_y I_x - \frac{t}{2}(I_{xy}+I_{yx})}{t_x I_y - \frac{t}{2}(I_{xy}+I_{yx})} = \frac{n}{\lambda} = \frac{\left(\frac{l}{m}\right)}{\left(\frac{\pi r}{n}\right)},$$ $$\lambda = \frac{m\pi r}{l}.$$ If the dimensions of each part of the curved plate are given, m, n are determined (1) when reinforced only in longitudinal direction $m \leq 1$, $n > 2$. $$\sigma_k = \sigma_c + \gamma\frac{E}{t}\sqrt{\frac{I_y}{t_x}}, \quad \sigma_c = \frac{\pi^2 E I_x}{t_x l^2}.$$ γ in the table below -- generally it is possible to write When reinforced only in the direction of the circumference when $$\sigma_k = \sigma_c\left(1+\frac{\sigma_{k0}^2}{4\sigma_c^2}\right).$$ (2) $m > 1$, $n \leq 1$ $$\sigma_k = \mu\sqrt{\sigma_1^2+\sigma_2^2}+\frac{\pi^2 E(I_{xy}+I_{yx})}{t_x(r\theta)^2}.$$ In the above equation $$\sigma_1 = \frac{2E}{t_x r}\sqrt{\frac{I_x I_y}{\frac{I_x}{t_x}+\frac{I_y}{t_y}}}, \quad \sigma_2 = \frac{2\pi^2 E}{t_x(r\theta)^2}\sqrt{I_x I_y}.$$	147

No	Graph & Boundary Cond.	Formula or Table of Results	Notes, Ref.
52		μ is given in the graphs below 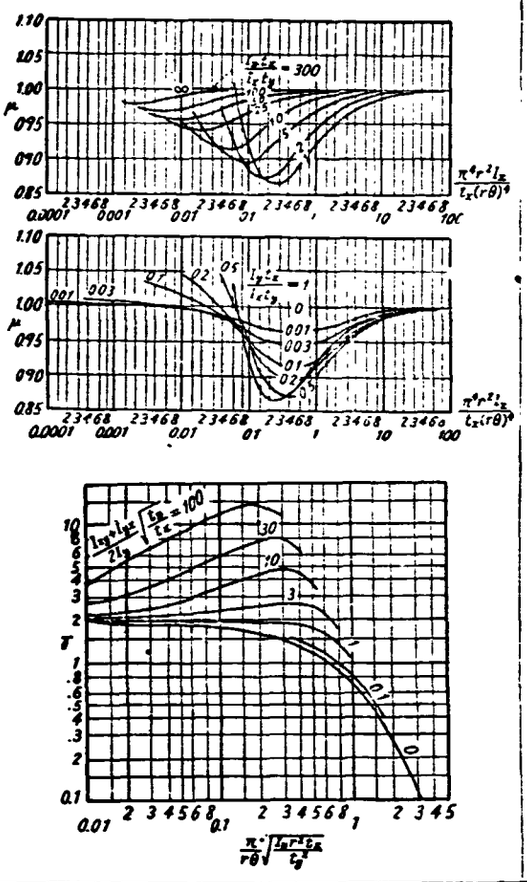	/589
53	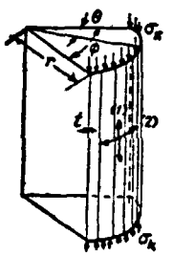 End revolving around circumference	$\frac{\sigma_z}{D_1}=\frac{2}{r}\sqrt{\frac{1}{D_1}\left(a_2+D_2\frac{n^2}{r^2}\right)}+\frac{n^2}{r^2D_1}(2D_2+\nu D_2)$. a_1, a_2 : elongation stiffness, D_1, D_2 : bending stiffness $D_2=D_1\nu_2+R/2$. R : torsion stiffness 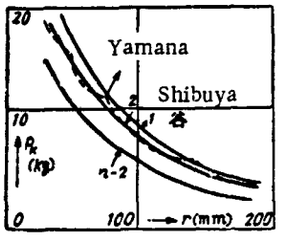	148

No.	Graph & Boundary Cond.	Formula or Table of Results	Notes, Ref.
54	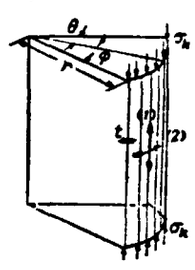 Straight side fixed, other side rotating end	$\frac{\sigma_k}{D_2}=\frac{2}{r}\sqrt{\frac{1}{D_1}\left(a_2+\frac{8}{3r^2}\left(\frac{\pi}{\phi}\right)^4 D_2\right)}+\frac{4}{3r^2 D_1}\left(\frac{\pi}{\phi}\right)^2\left\{2D_3+\nu D_2\right\}.$	/590

SHEAR (tension field)

No.	Graph & Boundary Cond.	Formula or Table of Results	Notes, Ref.
55	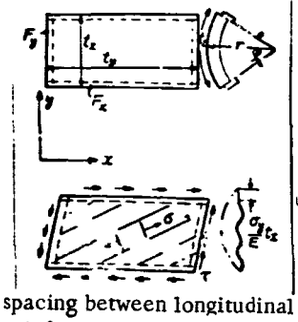 t_x = spacing between longitudinal reinforcements t_y = spacing between ribs t = outer plate thickness F_x, F_y = cross-section area of stringers and ribs respectively τ = shear stresss τ_k = shear buckling stress ($\tau > \tau_k$) of one section of curved plate σ = main tensile force of plate field $\alpha=\sigma$ angle formed by σ and stringer	Shear tension field of curved plate When the spacing between the longitudinal reinforcements is small ($t_x < \frac{R}{3}$) $\zeta=\frac{\tau-\tau_k}{\tau}\cdot\frac{t\cdot t_x}{F_x}$, (55.1) $\eta=\frac{\tau-\tau_k}{\tau}\cdot\frac{t\cdot t_y}{F_y}$. (55.2) with f: deflection of longitudinal reinforcement $\frac{t_x}{r}\sqrt{\frac{E}{\tau}}\sqrt{1+\frac{12f\cdot r}{t_x^2}}$ $=\sqrt{24\tan\alpha\left(\frac{\cos 2\alpha}{\sin^4\alpha}+a\right)}$. (55.3) $a=\zeta\cot^4\alpha-\eta$ (55.4) or $\cot\alpha=\sqrt[4]{\frac{a+\eta}{\zeta}}$ $=\sqrt[4]{\frac{F_x}{t\cdot t_x}\left(\frac{\tau}{\tau-\tau_k}a+\frac{t\cdot t_y}{F_x}\right)}$. (55.5) From these two equations a is anticipated and α is determined by the trial method. In this case, the right side of equation (55.3) is calculated, and cot α is determined from Figure 55.1 in combination with the anticipated a, and is made to agree with the cot α calculated from equation (55.5). Calculations may be performed first assuming f = 0. In the case of a continuous beam supported by reinforcements spaced equally, the average value of f is $f=\frac{1}{2}\cdot\frac{\sigma_y\cdot t\cdot\varphi\cdot t_y^4}{720EI_x}$, $\sigma_x=\sigma\sin\alpha\cos\alpha$. t: plate thickness If α is known, the principal tension of the tension field and the tension and stiffness of the reinforcement in the direction of the axis is	151

No.	Graph & Boundary Cond.	Formula or Table of Results	Notes, Ref.
55		$\sigma = \frac{\tau}{\sin\alpha\cos\alpha}, \quad \varepsilon_z = \frac{\sigma_z}{E} = -\frac{\tau}{E} c\cot\alpha.$ $\frac{\tau}{G} = \gamma = 2\cot\alpha(\varepsilon - \varepsilon_z).$ If σ_x of the reinforcement is first known, (when the stringer is curved, the stress is taken from the plate surface), in place of the above equations (55.4), (55.5), $a = \frac{\sigma_x}{\tau}\cot^3\alpha - \eta,$ $\cot\alpha = \sqrt[3]{\frac{\tau}{\sigma_x}(a+\eta)} = \sqrt[3]{\frac{\tau}{\sigma_x}\left(a + \frac{t \cdot t_y}{F_y}\frac{\tau - \tau_z}{\tau}\right)}$ are used. 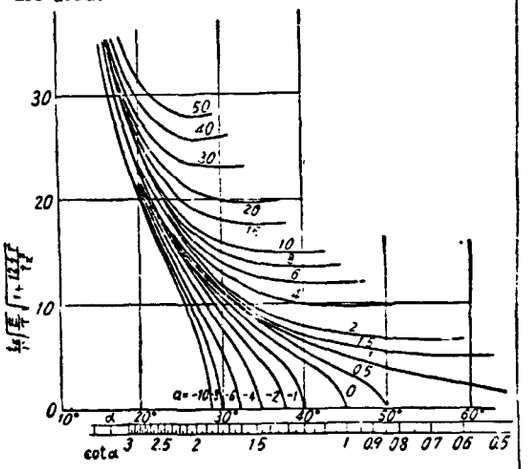 Figure 55.1	/591

REINFORCED CYLINDERS

Compression

No.	Graph. & Boundary Cond.	Formula or Table of Results	Notes, Ref.
56	t (thickness of outer plate) 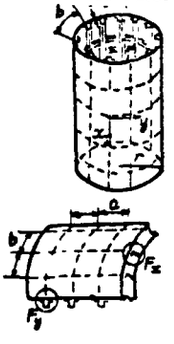	$P_k = \sigma_{ck} t = \frac{2E}{r}\sqrt{\frac{I_x I_y}{\frac{I_x}{t_x} + \frac{I_y}{t_y}\frac{t_x}{t}}}.$ Here t_x, t_y = average plate thickness of cross-sections x and y (for example, for t_x, in the case of a stringer cross-section F_L, and a facing b, it is assumed $t_x = t + F_x/b$. t is outer plate thickness) In the case when reinforcement is only in the directions x and y $\sigma_x = \frac{E}{\sqrt{3(1-\nu^2)}}\frac{t}{r}\sqrt{\frac{t}{t_x}} \equiv \sigma_{ck}\sqrt{\frac{t}{t_x}},$ $\sigma_t = \frac{E}{\sqrt{3(1-\nu^2)}}\frac{t}{r}\sqrt{\frac{t_y}{t}} \equiv \sigma_{ck}\sqrt{\frac{t_y}{t}}.$	147

No	Graph & Boundary Cond.	Formula or Table of Results	Notes, Ref.
56		Where EI_x, EI_y = bending stiffness in direction of the axis and the circumference for the unit width in the direction of the circumference and axis σ_{cl} = buckling stress of unreinforced cylinder $= \frac{E}{\sqrt{3(1-\nu^2)}} \frac{t}{r}$ In deriving the above equation, it is assumed that a considerable number of wrinkles are formed in directions x, y. It should also be noticed that in this case it is assumed that these simplifications $\frac{t}{t_x} \approx \sqrt{\frac{t_y}{t_x}} \fallingdotseq 1$ are allowed. In sufficiently long and wide reinforced shells, the buckling units stress is increased by reinforcements in the both lateral and longitudinal directions, but in short columnar shells, only reinforcement in direction x is essential.	/592
57	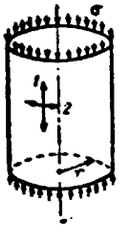	For an orthotropic cylinder *1 assuming axially symmetrical deformation and buckling, with uniform plate thickness and uniform material $\sigma_k = \frac{t}{r} \sqrt{\frac{E_1 E_2}{3(1-\nu_1\nu_2)}}$ In the general case $p_k = \frac{2}{r} \sqrt{D_1 \alpha_2 (1-\nu_{12}\nu_{21})} \fallingdotseq \frac{2}{r} \sqrt{D_1 \alpha_2}$. p_k : compressive stress per unit width	148 155

TORSION

No.	Graph & Boundary Cond.	Formula or Table of Results	Notes, Ref.
58	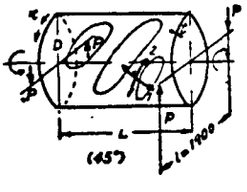	The results of experiments on the torsion strength of plywood cylinders are given. The tests were conducted on linden and Birch plywood cylinders where $D \fallingdotseq 500$ mm, $L \fallingdotseq 580$ mm, $t \fallingdotseq 1.5 \sim 2$ mm , (⊥ , //, 45° tension). Those with // and 45° directions formed large wrinkles, and the load did not increase when P_k was reached. In those with ⊥ no wrinkles were formed up to the end, cracks appeared in the direction of the circumference, and failure occurred. The buckling load P_k is about 75% of the maximum load P_{max} even when at its lowest value.	160

No.	Graph & Boundary Cond.	Formula or Table of Results	Notes. Ref
58			160

Grain

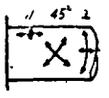

The 45° brace is installed so that the wood grain of each half of the plate has respectively a right and a left winding.

Specimen No.	1	2	3	4	9	10	5	6	7	8
Material	Linden plywood						Birch plywood			
Thickness (mm)	1.87	1.84	1.92	2.02	1.42	1.31	2.08	2.15	2.11	2.10
Direction of grain	//	45°	45°	⊥	45°	//	//	⊥	45°	45°
Diameter (mm)	498	493	496	495	494	496	501	497.5	496.5	495
P_k (kg)	60	82	72	128	34	—	124	214	164	160
P_{max} (kg)	80	86	82	128	38	37	140	214	174	178
P_k/P_{max}	75	95	88	100	89	—	95	100	95	90
G	68	183	193	—	—	-	112	105	196	199

Here $M_t=P\cdot l$, θ : rotation angle, I_p : polar moment of inertial

The shear elasticity modulus was calculated from $G=\frac{M_t\cdot L}{\theta\cdot I_p}$

Similar tests were made for specimens with dimension $D\fallingdotseq 220$ mm, $t\fallingdotseq 1$ mm and the results shown in the following table were obtained.

Buckling waveform

(//) birch plywood, 1 mm

(45°) linden plywood, 2 mm

Material	Direction of grain	No.	Shear breaking stress	Modulus of stiffness kg/mm²	Moisture %
Linden plywood	//	1	0.14	60	8.2%
		2	0.14	70	8.2
		3	0.18	95	7.9
		average	0.15	75	8.1
	⊥	1	0.31	50	8.1
		2	0.39	60	9.0
		3	0.39	80	7.7
		average	0.36	65	8.3
	Normal 45°	1	0.18	200	9.0
		2	0.21	240	9.0
		average	0.20	220	9.0
	Reverse 45°	1	0.39	190	8.7
		2	0.36	210	8.1
		average	0.38	200	8.4
Birch plywood	//	1	0.26	120	7.5
		2	0.29	90	8.0
		3	0.24	80	7.8
		4	0.23	100	7.7
		average	0.25	100	7.7
	⊥	1	0.73	120	7.7
		2	0.71	120	8.0
		average	0.72	120	7.9
	Normal 45°	1	0.50	380	8.0
		2	0.43	260	8.1
		average	0.47	320	8.0
	Reverse 45°	1	0.78	240	7.5

No.	Graph & Boundary Cond.	Formula or Table of Results	Not., Ref.

58

Material	Direction of grain	No.	Shear failure stress	Stiffness coefficient kg/mm²	Water content
CBK glued linden plywood	//	1	0.71	160	7.7
		2	0.58	140	7.7
		Average	0.65	150	7.7
	⊥	1	0.34	190	8.1
	Normal 45°	1	0.55	270	7.0
		2	0.65	350	7.8
		Average	0.60	310	7.4
	Reverse 45°	1	0.80	320	6.9
		2	0.83	220	8.0
		Average	0.82	270	7.5

"normal" 45° indicates that the direction of the grain on the surface (45° with respect to axis) and the direction of the tensile stress occurring on the outer plate due to torsion match, while when they cross each other this is called "reverse" 45°.

59

Torsional buckling
Case in which the principal directions of elasticity of the outer plate 1,2 match respectively the direction of the axis and the circumference of the cylinder.

Hayashi, using infinitesimal deformation theory, expanded Donnell's results for an isotropic cylinder, for the torsional buckling of an orthoropic cylinder. [161]

The shear buckling load S_k per unit width distributed along the circumference

$$B \equiv \frac{S_k}{a_1(1-\nu_1\nu_2)} \sqrt{\frac{a_1(1-\nu_1\nu_2)l^2}{12D_2}}, \qquad J \equiv \sqrt{\frac{12D_2 l^4}{a_1(1-\nu_1\nu_2)t^4}}.$$

The buckling waveform is assumed to be of the same shape as in Donnell's equations

a_1, a_2 : elongation stiffness in directions 1,2 respectively
D_1, D_2 : bending stiffness

i) for a short cylinder

End revolving around both ends: $B=1.18\sqrt[4]{J}$, $n=2.31J^{-\frac{1}{6}}$ $(J<5.5)$.

End fixed at both ends: $B=1.29\sqrt[4]{J}$, $n=2.62J^{-\frac{1}{6}}$ $(J<7.8)$.

ii) for a long cylinder

end revolving around both ends / both ends fixed: $B=0.77\sqrt{J}$ $(J>5.5)$, $n=2$.

n: number of waves in direction of circumference

In particular, in a cylinder of uniform material and uniform thickness t, is expressed by

$$S_k=t\cdot\tau_k, \quad B=\frac{\tau_k l}{\sqrt{E_1 t}}\sqrt{\frac{E_1(1-\nu_1\nu_2)}{E_2}}, \quad J=\frac{l^2 t}{d^2}\sqrt{\frac{E_2}{E_1(1-\nu_1\nu_2)}}.$$

The torsional buckling shear stress τ_k for a long cylinder is

$d=2r$

$$\tau_k=0.272\sqrt[4]{E_1 E_2^3}\left(\frac{t}{r}\right)^{\frac{3}{2}}, \quad n=2.$$

No.	Graph & Boundary Cond.	Formula or Table of Results	Notes, Ref.
60	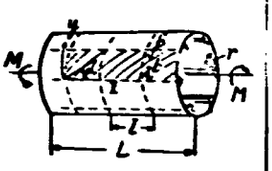	Comparison of the results of E. Schapitz and Heck-Ebner for an imperfect tension field.	159 169 170

	Perfect tension field	Imperfect tension field	Heck–Ebner
τ	$\frac{T}{2\pi r^2 t} = \vartheta \cdot \tau_k$ (τ_k = shear buckling stress)		
Donnel's τ_k	$\tau_k = 0.8\,5\,E\,(t/r)^{3/4}\cdot(r/l)^{1/2}$		
Rib stress σ_y	$\sigma_y = -\frac{tl}{F_y}\cdot\tau_k(\vartheta\tan\alpha - 1)$		$\sigma_y = -\frac{tl}{F_y}\tau_k\tan\alpha(\vartheta-1)$
Stringer lateral load	$p = \varphi t\,\tau_k(\vartheta\tan\alpha - 1)$		$p = \varphi t\,\tau_k\tan\alpha(\vartheta-1)$
Stringer bending stress	$\sigma_b(x) = \frac{\varphi t l^2}{2W_L}\tau_k(\vartheta\tan\alpha-1)\left(\frac{1}{6} - \frac{x}{l} + \frac{x^2}{l^2}\right)$		$\sigma_b(x) = \frac{\varphi t l^2}{2W_L}\tau_k\tan\alpha(\vartheta-1)\left(\frac{1}{6} - \frac{x}{l} + \frac{x^2}{l^2}\right)$
Stringer deflection	$\bar{f} = \frac{\varphi t l^4}{720 E I_L}\tau_k(\vartheta\tan\alpha - 1)$		$\bar{f} = \frac{\varphi t l^4}{720 E I_L}\tau_k\tan\alpha(\vartheta-1)$
Normal stress σ_x	$\sigma_x = \tau_k(\vartheta\cot\alpha - 1)$	$\sigma_x = \tau_k(\vartheta\cot\alpha-1)\left[1 - \sin^{\frac{\delta}{1+\delta}}\left(\frac{xy}{b_1}\right)\right]$ $-\sigma_b(x)\frac{\delta}{1+\delta}(1-R)\sin^{\frac{\delta}{1+\delta}}\left(\frac{xy}{b_1}\right)$	$\sigma_x = \tau_k\cot\alpha(\vartheta-1)$
Principal stress σ_1	$\sigma_1 = \tau_k\left(\frac{\vartheta}{\sin\alpha\cos\alpha} - 1\right)$	$\sigma_1 = \sigma_x + \tau_k\tan\alpha$	$\sigma_1 = \tau_k\frac{(\vartheta-1)}{\sin\alpha\cos\alpha}$
Principal stress σ_2	$\sigma_2 = -\tau_k$	$\sigma_2 = \sigma_x - \tau_k\cot\alpha$	$\sigma_2 = 0$
Compressive stress σ_x of stringer	$\sigma_x = -\delta\tau_k(\vartheta\cot\alpha - 1)$	$\sigma_x = -\delta R\tau_k(\vartheta\cot\alpha - 1)$ $-\frac{\delta}{1+\delta}(1-R)\sigma_b(x)$	$\sigma_x = -\delta\tau_k\cot\alpha(\vartheta-1)$
Principal axis angle α $\tan^2\alpha = \frac{Z}{N}$	$Z = (1+\delta)(\vartheta\cot\alpha - 1) + \vartheta\tan\alpha$, $N = \vartheta(\cot\alpha + \tan\alpha) - 1 + (1+\lambda)(\vartheta\tan\alpha - 1)$ $+\frac{E}{\tau_k}\left(\frac{\varphi^2}{24} + \frac{\Delta r}{r}\right)$	$Z = R(1+\delta)(\vartheta\cot\alpha - 1) + \vartheta\tan\alpha$ $N = R(\vartheta\cot\alpha - 1) + \vartheta\tan\alpha$ $-(1+\lambda)(\vartheta\tan\alpha - 1)$ $-\frac{E}{\tau_k}\left(\zeta_y - \frac{\Delta r}{r}\right)$	$Z = (\vartheta-1)(\tan\alpha + \cot\alpha(1+\delta))$ $N = (\vartheta-1)(\cot\alpha + \tan\alpha(1+\gamma+\lambda))$ $+\frac{E}{\tau_k}\left(\frac{\varphi^2}{24} + \frac{\Delta r}{r}\right)$
Twist angle ψ	$\psi = \frac{2L}{r}\cdot\frac{\tau_k}{E}\sqrt{Z\cdot N}$		

$$J(\omega) = \frac{2}{\pi}\int_0^{\frac{\pi}{2}} \sin^{\frac{1}{\omega}} x\,dx, \qquad x = \frac{xy}{b_1}.$$

$$R = \frac{1 - J(\omega)}{1 + \delta J(\omega)}, \qquad \delta = \frac{b_1 t}{F_L}, \qquad \gamma = \frac{a}{F_y}, \qquad \varkappa = \frac{t\varphi l^4}{720\,r\cdot I_L}, \qquad \zeta_y = \frac{b - b_1}{b_1}.$$

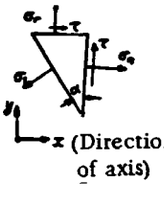

Δr = contraction in direction of radius at point of intersection of rib and stringer

F_x, F_y = cross-section areas of stringer and rib respectively

I_L = geometric moment of inertial of stringer

W_L = cross-section coefficient of stringer

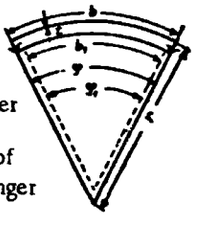

No.	Graph & Boundary Cond.	Formula or Table of Results	Notes, Ref.
61	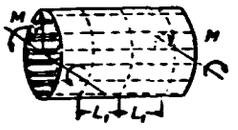 It is assumed that the frames at both ends are perfectly rigid bodies	It was shown by L. G. Brazier, that when an unsupported cylinder undergoes bending, the bending stiffness decreases and instability occurs owing to flattening of the cross-section, but such unstable forms do not occur in the case of a reinforced cylinder such as that shown on the left, and it was proved quantitatively by using the energy method that simultaneous buckling and local buckling occur on the compression side in the column and the stringers. The local buckling load of a stringer under maximum stress on the compression side is $P_k=\pi^2 E_{str} \cdot I_{str}/(2L_1)^2$.	163
		E_{str}: modulus of elasticity of stringer E_r : elasticity modulus of frame I_{str}*1: modulus moment of inertia of stringer I_r: moment of inertia of frame, L_1: spacing between adjoining frames λ : equivalent length coefficient $\Lambda \equiv \left(\frac{r}{L_1}\right)^2 \left(\frac{r}{d}\right) \frac{E_{str} \cdot I_{str}}{E_r I_r}$. d is spacing between stringers	*1 $I_{str}=I_{str\text{-}r}+\frac{1}{4}I_{str\text{-}t}$ $I_{str\text{-}r}$: moment of inertia with respect to bending in the direction of the stringer radius. $I_{str\text{-}t}$: moment of inertia with respect to the bending in the direction of the tangent
		The relationship between λ and Λ is shown in the graph below. m is the number of intermediate frames. According to the graph, local buckling is expected at the point where $\Lambda < 1$, and it can be seen that where $\Lambda < 0.1$, it is difficult for local buckling to occur.	
		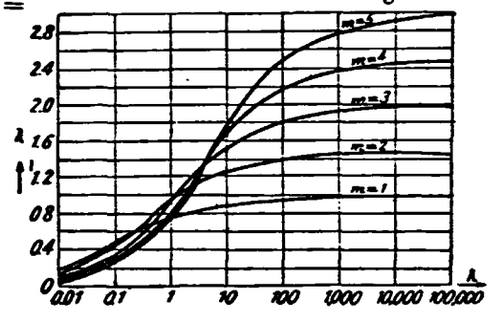	
	Deformation of cross-section 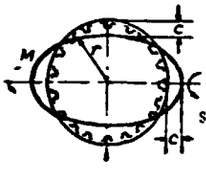	Tests were conducted on the specimens indicated below with the given dimensions. In the first specimen, a flatness ratio was indicated that was 25% higher *2 than the theoretical values, and in the second specimen, a local buckling stress was found which was 33% higher than the theoretical values.	*2 flatness ratio $\equiv \frac{\delta}{r}$ see figure on the left
		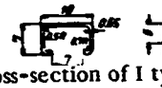 Cross-section of I type stringer circular frame 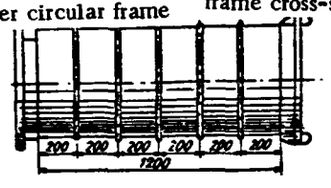 II type circular frame cross-section 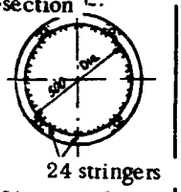 (mm unit) 24 stringers	
		(in the figure the outer plate thickness = 0.2 mm rivet pitch = 25 mm, circular frame riveted to stringer by 2.5 (illegible symbol) rivets outer wall riveted only to stringers rivet diameter = 2.5 mm.	

No.	Graph & Boundary Cond.	Formula or Table of Results	Notes, Ref.
62	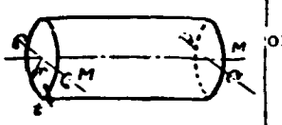	Experiment results are given for M_k. M_k is about 80% of $M_{failure}$ (// when the direction of the surface grain is parallel to the cylinder axis) M_k is about 30% of $M_{failure}$ ($\perp$ perpendicular to the above) Experiments were conducted for specimen 1) specimen with aircraft fabric glued on it (fabric thickness = 0.7 mm) 2) specimen with one layer of CBK glued on it (CBK thickness = 0.2 mm)	164

Specimen No.	Material	Diameter mm	Plate thickness	R/t	Bending stress σ_t (kg/mm²)	Direction of grain
1	birch	500	2.1	119	1.00	//
2	birch	498	2.07	120	1.11	$\perp$
3	linden	497	19.7	126	0.46	$\perp$
4	linden	499	1.82	137	0.40	//
5	linden	496	1.52	163	0.58	$\perp$
6	linden	498	1.45	171.5	0.54	//
7	linden	496	plate 1.55 airplane fabric 0.7	160	1.23	$\perp$
8	linden	497	plate 1.55 airplane fabric 0.7	160.5	1.09	//
9	linden	494	1.05	235	0.44	//
10	linden	497	1.12	222	0.33	$\perp$
11	birch	220	1.05		0.75	//
12	linden	220	1.0		0.52	//
13		220	plate 1.0 CBK 0.2		1.41	//

63	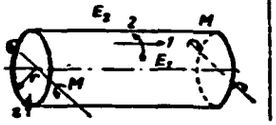	— flexural buckling of orthotropic cylinder of uniform thickness $M_k = \frac{2\sqrt{2}}{9} \pi \frac{\sqrt{E_1 E_2}}{1-\nu_1\nu_2} rt^2$ Here E_1, E_2 : modulii of elasticity in principal directions of elasticity M_k has the same value even if the principal directions of elasticity are switched .	165

When the principal directions of elasticity 1, 2 are respectively parallel to the cylinder axis and the circumference, the elasticity modulus of directions 1, 2 is denoted by E_1 , E_2 .

No	Graph & Boundary Cond.	Formula or Table of Results	Notes, Ref.
64	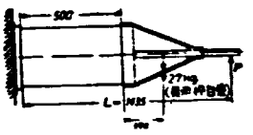 The load causes the couples P, P to act on the center of gravity of the dead weight of the load frame and the right end bending moment M = 1435P - 27 x (500 + 394) = 1435P - 24138 mmkg. Shear load V = P - 27 kg. (compression side) (load frame dead weight) 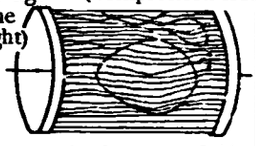 (in the case of //) The buckling waveform is not much different from that of pure bending, similarly, concave wrinkles occur in the vicinity of the attachment on the compression side.	Shear bending test of plywood cylinder as for P_k, when the grain direction of the surface is toward the cylinder axis, it is very close to $P_{failure}$ in the case of //, and about 60-80% of this in the case of ⊥ The experiment results are given below. In the table f is the bending stress determined by pure bending theory formulae from the maximum bending moment M	167

Specimen	Material	Thickness t (mm)	Diameter $2r$ (mm)	r/t	Direction of surface grain	Maximum M. (mmkg)	Shear load P (kg)	Bending stress f (kg/mm²)
1	linden	1.12	495	221	//	82062	47	0.38
2	linden	1.1	497	226	⊥	75362	42	0.35
3	linden	1.2	497	207	⊥	76362	43	0.33
4	linden	1.5	496	165	//	155161	97	0.54
5	linden	1.4	495	177	⊥	145062	91	0.54
6	linden	1.85	500	135	//	219862	143	0.61
7	linden	1.95	496	127	⊥	200062	129	0.53
8	linden	1.9	497	131	⊥	274362	181	0.75
9	birch	2.15	500	116	//	473862	320	1.13
10	birch	2.05	497	121	⊥	502862	340	1.28

COMPRESSION AND EXTERNAL PRESSURE

No.	Graph & Boundary Cond.	Formula or Table of Results	Notes, Ref.
65	External pressure 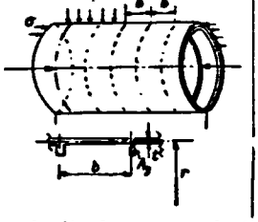 (longitudinal cross-section)	When EI_y is the bending stiffness of one frame including one part of the cylinder wall, the effective thickness: $t_e = t + \frac{A_y}{b}$, A_y is cross-section area of frame. $\phi_1 = \frac{pr(1-\nu^2)}{Et}$, $-\phi_2 = \frac{\sigma(1-\nu^2)}{Et}$ Calculating from the buckling condition equation, the following results are obtained. 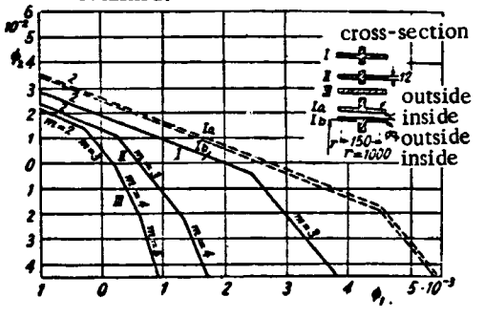	166

Bending

No.	Graph & Boundary Cond.	Formula or Table of Results	Notes, Ref.
66	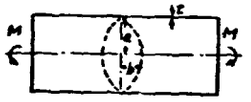	Flexural failure and rigidity of thin walled elliptical cylinder. When a thin-walled elliptical cylinder undergoes pure bending, as the curvature increases in the same manner as a circular cylinder, the bending stiffness decreases along with the flatness ratio of the cross-section. Generally, in thin walled cylinders, local buckling occurs by the time that the yield is reached, and the buckling stress due to yield is expressed by the following equations.	599 162

i) bending around long axis : $\sigma_k = C_g \frac{E}{\sqrt{1-\nu^2}} \frac{t}{\rho_g} \sqrt{\frac{t}{t_m}}$.

ii) bending around short axis : $\sigma_k = C_k \frac{E}{\sqrt{1-\nu^2}} \frac{t}{\rho_k} \sqrt{\frac{t}{t_m}}$.

Moreover, the critical moments are as follows for the above two equations.

i) $M_k = Z_g \sigma_{k_g} \qquad Z_g = \frac{\pi}{4} b(b+3a) t_m$,

ii) $M_k = Z_k \sigma_{k_g} \qquad Z_k = \frac{\pi}{4} a(a+3b) t_m$.

Here C_g , C_k are values which change according to $k^2 = \frac{a^2-b^2}{a^2}$ as shown in the graph below.

※ $t_m = t + \frac{F}{u}$ { F is the cross-section area of the reinforcing member in the direction of length, u: circumferential length.

$\rho_g = \frac{a^2}{b}, \quad \rho_k = \frac{b^2}{a}$.

As can be seen from the graph on the right, from the results of experiments, when $k^2 \geqq 0.25$, local buckling occurs on the compression side, and $k^2 = 0.25$ is the limiting point. The experiment results are shown in the table below

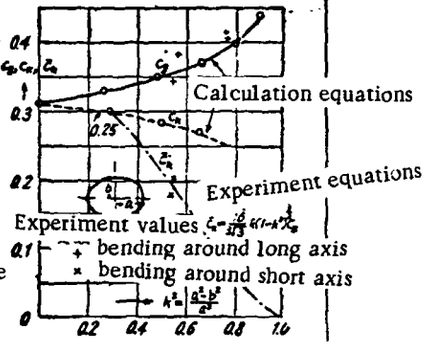

Specimen No.	Dimensions a (cm)	b (cm)	l (cm)	t (cm)	Bending around long axis: e_g cm	w_g cm³	$M_{g,k}$ cm/kg	σ_{gk} kg-cm²	C_g	Bending around short axis: e_k cm	w_k cm³	$M_{k,k}$ kg-cm	$\sigma_{k,k}$ kg/cm²	C_k
1	22.5	15	78	0.050	33.75	48.5	19600 21200	405 437	0.347 0.375	10	59.5	42500 47300	713 794	0·181 0.202
2	30	15	127	0.051	60	63.1	17350 16900	275 268	0.411 0.401	7.5	90.1	53700 52200	595 580	0.111 0.108

WAVEFORM PROFILES

No.	Graph & Boundary Cond.	Formula or Table of Results	Notes, Ref.
67	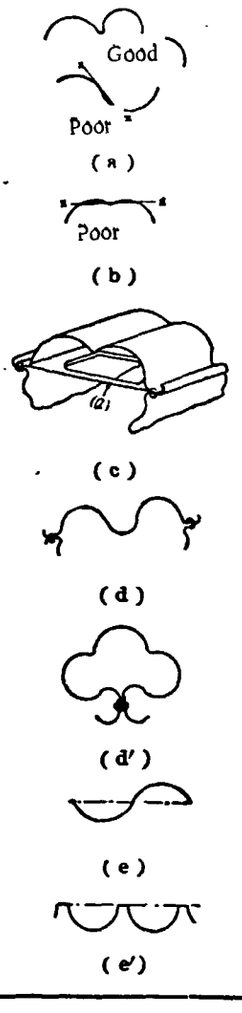	In order to increase the buckling stress of waveform profiles the following cautions are necessary. In particular, this is true when high-tension steel plate is used and high tension is required, for such materials as girder coamings. i) the linear section should not be more than 18 times greater than the plate thickness. ii) the radius of curvature should not exceed 30 times the plate thickness at any point. iii) at points where sections wi th large radii of curvature adjoin each other, caution should be taken so that they do not become flat. consequently, it is possible to insert sections with small radii of curvature between the sections with large radii as shown in (a) on the left. iv) as shown in Figure (b) when one should avoid inserting anything thing that is nearly flat with a small radius of curvature between the parts having large radii of curvature. v) when the coaming radius/thickness ratio exceed 30, there is a tendency for flattening to occur because of the load. Therefore as shown in Figure (c) plate a should be inserted as a tension member. vi) one should avoid having the end of the plate b a high tension part Otherwise, local buckling will occur only in the end part, and there is danger that this will extend over the entire part. Therefore, one may either attach a small diameter piece as in (d) or make sure that the end comes in the low stress part as shown in (d'). vii) comparing the waveforms in (e) and (e') since the wall buckling stress in (e') becomes several times greater than that in (e), (e') is more effective. With regard to attachment, similarly (e') is more effective	172 173 From Brazier /600

COMPRESSION

No	Graph & Boundary Cond.	Formula or Table of Results	Notes, Ref.
68	Flat press	Buckling strength of corrugated plate 1) there are no theoretical values for the buckling stress of the wall surface when under compressive force. ii) from the results on light alloy corrugated plates 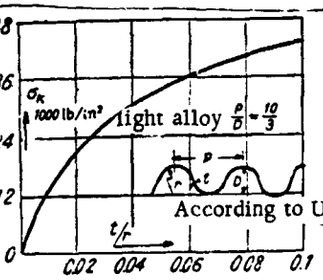 According to U.S. standards Figure 68.1.	174

No.	Graph & Boundary Cond.	Formula or Table of Results	Notes, Ref.
68		" when the wall surface buckling strength is adjusted for t/R, this becomes as shown in Figures 68.1, 68.2.	/601

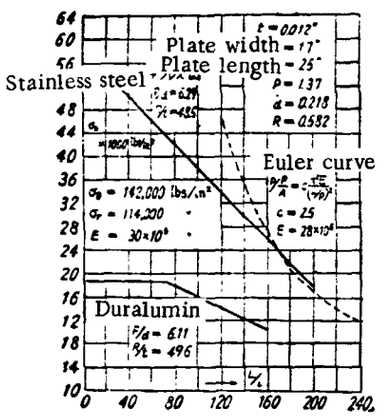

Figure 68.2

According to these, for $\sigma_k = K.\sigma_{kB}$ the value of K is almost equal to 1 (where σ_{kB} is the buckling strength of a flat plate of the same width)

iii) the compressive buckling strength for a corrugated plate column, is the buckling strength equation for a short column

$$\sigma_k = \sigma_{kk}\left(\frac{l'/l}{\pi\sqrt{E/\sigma_{kk}}}\right)^m$$

Here $l' = l/\sqrt{c}$ = buckling length

The above equation indicates the straight line equation where m is a constant, and is 2 in Johnson's equation and 1 in Euler's equation

In the above equation, if the above values are used for the vallu value of σ_{kk}, Figure 68.3 is obtained. The straight line formula is used in the U.S., which is

$$\sigma_k = \sigma_D\left(1-\alpha\frac{l}{i}\right),\ \alpha \text{ is a constant,}$$

e.g.
α=0.00368 soft steel
=0.00185 hard steel

including the values in the above graph in this σ_d, it alright to consider that a = 0.

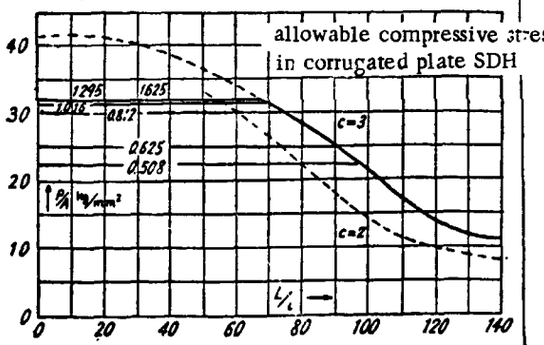

Figure 68.3

No.	Graph & Boundary Cond.	Formula or Table of Results	Notes, Ref.
68		iv) the compressive buckling strength for a corrugate plate is found from the equation for an orthotropic plate.	/602

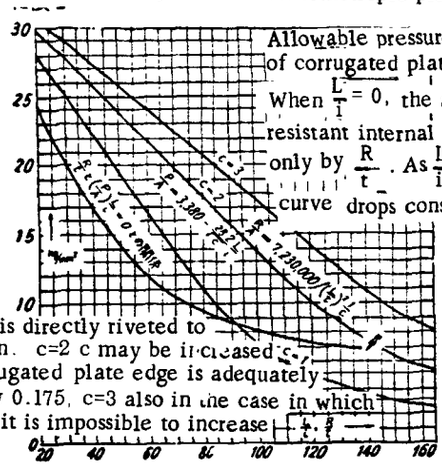

Allowable pressure resisting stress of corrugated plate

When $\frac{L}{i} = 0$, the allowable pressure resistant internal stress is determined only by $\frac{R}{t}$. As $\frac{L}{i}$ becomes larger, this curve drops considerably.

c=1 case in which the corrugated is directly riveted to the members around the partitian. c=2 c may be increased to 1.5 in the case when the corrugated plate edge is adequately supported and the width is below 0.175, c=3 also in the case in which both ends are considered fixed, it is impossible to increase this above 3

Figure 89.4

69			177

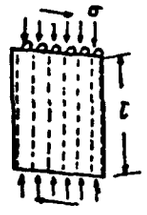

Semi-circular

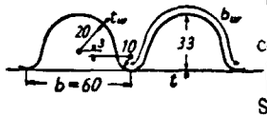

Sine wave shape

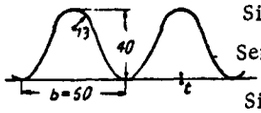

$t_m = t + t_w \frac{\sigma_w}{b}$

$G' = G \frac{t + t_w b / b_w}{t + t_w b_w / b}$

(equivalent shear elasticitymodulus)

The results of tests by H. Ebner on the compressive strength of flat plates reinforced by channels, and flat plates reinforced by corrugated plates (l = 500mm)

Shape of corrugated plate	Average plate thickness t_m (mm)	t (mm)	Corrugated plate thickness t_w	Buckling stress of outer skin σ_k (kg/cm²)	Breaking stress of corrugated plate $\sigma_{w,B}$ (kg/cm²)	Average breaking stress $\sigma_{m,B}$ (kg/cm²)	$\frac{G'}{G}$
Sine wave	1.69	0.60	0.59	400	1800	1550	0.54
Semi-circle	1.58	0.60	0.60	430	1950	1650	0.60
Sine wave	2.26	0.83	0.79	820	2300	2040	0.54
Semi-circle	2.16	0.80	0.81	840	2600	2260	0.60
Sine wave	3.70	1.50	1.19	1900	2500	2430	0.57
Semi-circle	3.61	1.61	1.20	2200	2600	2520	0.64
	1.75	0.50	0.81	520	3000	2470	0.53
Semi-circle	2.24	0.49	1.03	560	3100	2630	0.50
	2.72	0.74	1.20	670	3000	2550	0.53

/603

No.	Graph & Boundary Cond.	Formula or Table of Results	Notes, Ref.

70

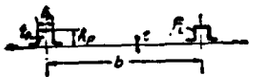

$$t_m = t + \frac{F_L}{b}$$

$$G' = G\frac{t}{t_m}$$

Channel type

$\frac{h_p}{b_p}$	h_p (mm)	Average plate thickness t_m (mm)	Plate thickness t (mm)	Spacing b (mm)	Buckling stress of outer skin σ_K (kg/cm²)	Breaking stress of reinforcement $\sigma_{L,B}$ (kg/cm²)	Average breaking stress $\sigma_{m,B}$ (kg/cm²)	$\frac{G'}{G}$
$\frac{30}{20}$	1.5	1.82	0.82	140	700	2450	1950	0.45
$\frac{20}{18}$	1.5	2.28	1.51	105	1700	2330	1930	0.66
$\frac{33}{23}$	1.5	2.20	0.50	105	190	2750	2400	0.22
$\frac{40}{30}$	1.5	2.70	1.20	140	800	2200	1880	0.44
$\frac{35}{25}$	1.5	2.73	1.03	105	720	2400	2020	0.38

Corrugated plate reinforcements are more effective for increasing the shear stiffness and compressive stiffness. This is because channel reinforced plates have a low shear stiffness.

CURVED PLATES (Supplement)

Compression

/604

No.	Graph & Boundary Cond.	Formula or Table of Results	Notes, Ref.
71	Curved plate Compression (with internal pressure) 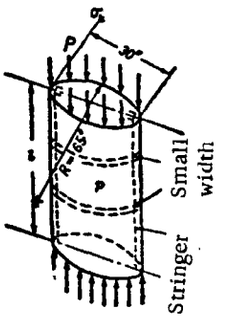 small width thickness $\frac{1}{8}$ in. curved plate thickness $\frac{81}{1,000}$ in. radius of curvature of curved plate 65 in	(experiment results) These are the results of compressive buckling tests in the case of pressure on the inside, for the two cases l = 50 3/4 in. small width spacing 10 in. l = 90 3/4 in. small width spacing 30 in. σ_b: compressive buckling stress (kips/sq.in.) P = compressive load p: internal pressure (lb/sq.in.) 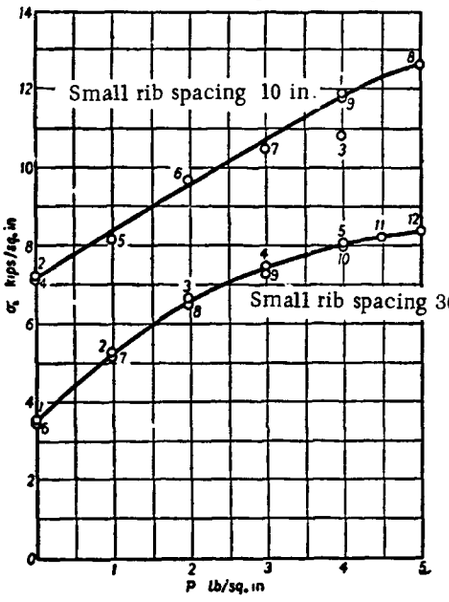 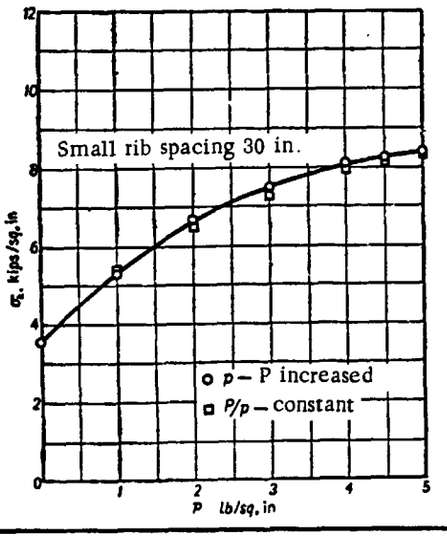 	191

No.	Graph & Boundary Cond.	Formula or Table of Results	Notes, Ref.
		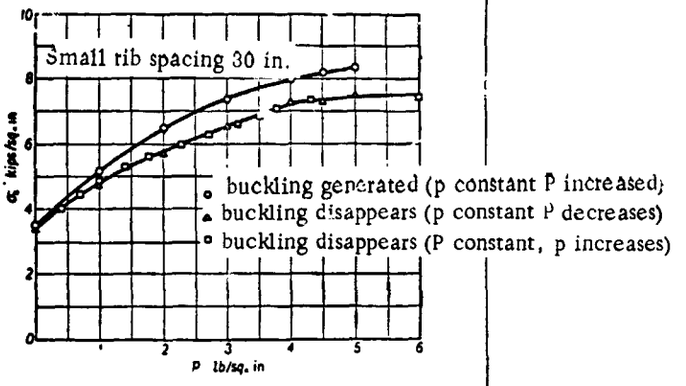	191 /605
72	Curved plate Compression	Experimental equation for magnesium alloy where the ratio of the diameter to the thickness is between 86 to 515 $\sigma_b = 0.42 E_s \left(\frac{t}{r}\right)$ E_s: secant modulus t: thickness r: radius	194
73	Curved plates Compression	range where i) $\frac{b^2}{rt} < 1$ Flat plate equation used $\sigma_b = \frac{k_c \pi^2 E}{12(1-\nu_e^2)} \left(\frac{t}{b}\right)^2$ See section on flat plates for k_c. ii) $1 < \frac{b^2}{rt} < 100$ $\sigma_b = \frac{k_c \pi^2 E}{12(1-\nu_e^2)} \left(\frac{t}{b}\right)^2$	219

No	Graph & Boundary Cond.	Formula or Table of Results	Notes, Ref.
		k_c based on following graphs.	/606

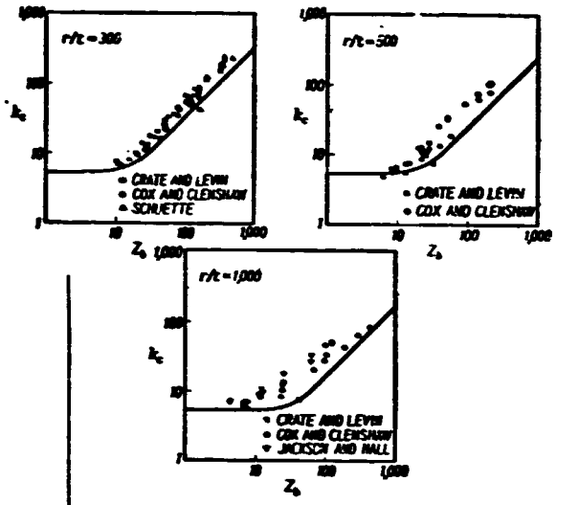

Where $Z_b=\frac{b^2}{rt}\sqrt{1-\nu_e^2}$

iii) $100<\frac{b^2}{rt}$

$$\sigma_b=\eta CE\frac{t}{r}$$

Where

$$\eta=\frac{E_s}{E}\left[\frac{E_t(1-\nu_e^2)}{E_s(1-\nu^2)}\right]^{\frac{1}{2}}$$

For C, the case of cylinder is used.

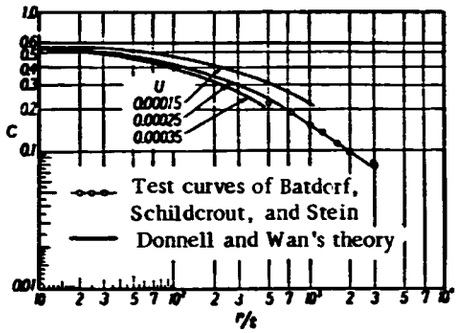

E_s=Secant modulus

E_t=Tangent modulus

$$\nu=\nu_p-(\nu_p-\nu_e)\frac{E_s}{E}$$

ν_e=0.3 (elastic region)

ν_p=0.5 (plastic region)

U= (Unevenness factor)

No.	Graph & Boundary Cond.	Formula or Table of Results	Notes, Ref.
74	Curved plate Shear 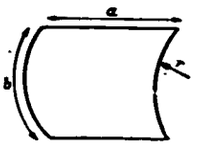 Four sides riveted	Test formulas of Kuhn and Levin $\frac{r}{t}>300$, $a \geqq b$ and $r>b$ i) $\frac{r}{t}>300$ $\tau_b=0.1E\frac{t}{r}\left[1.15+45\left(\frac{100t}{r}\right)^4\right]+6.4E\left(\frac{t}{b}\right)^2\left[1+0.8\left(\frac{b}{a}\right)^2\right]$ ii) $\frac{r}{t}>600$ $\tau_b=0.115E\frac{t}{r}+6.4E\left(\frac{t}{b}\right)^2\left[1+0.8\left(\frac{b}{a}\right)^2\right]$	193
75	Curved plate Shear l is considered sufficiently long 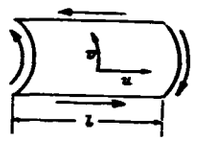 	$\tau_b=K\frac{\pi^2D}{l^2t}$ (Batdorf) (Schildcrout) (Stein) τ_b = shear buckling stress K = coefficient $D=\frac{Et^3}{12(1-\nu^2)}$ bending stiffness 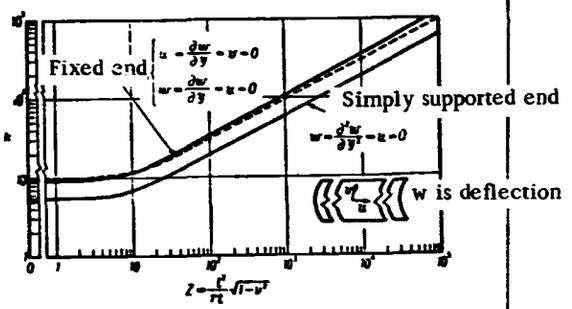 Comparison with other analyses 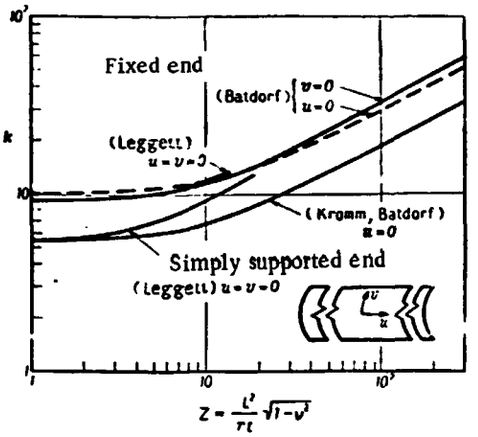 	179

No.	Graph & Boundary Cond.	Formula or Table of Results	Notes, Ref.
76	Curved plate Shear Simply supported end when $b > a$ 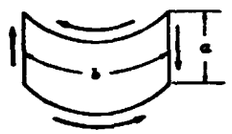	$\tau_b = K\frac{\pi^2 D}{a^2 t}$ (Batdorf) (Stein, Schildcrout) τ_b: shear buckling stress K: coefficient $D = \frac{Et^3}{12(1-\nu^2)}$ bending stiffness 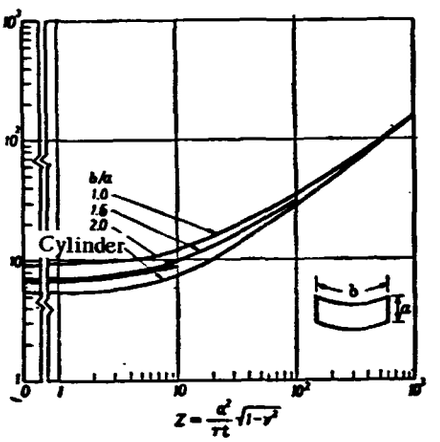 	179
77	Curved plate Shear Simply supported end when $a > b$ 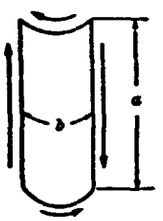	$\tau_b = K\frac{\pi^2 D}{b^2 t}$ (Batdorf) (Stein, Schildcrout) τ_b :shear buckling stress K: coefficient $D = \frac{Et^3}{12(-\nu^2)}$ bending stiffness 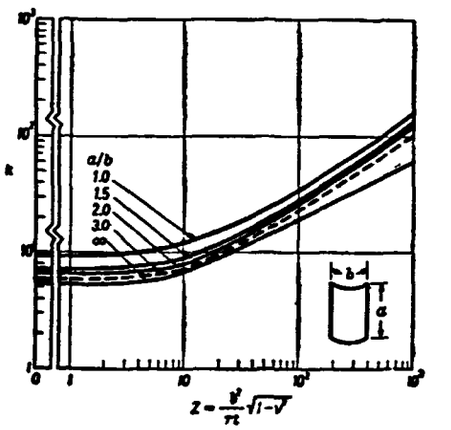 	179

/608

No.	Graph & Boundary Cond.	Formula or Table of Results	Notes, Ref.
78	Curved plate Shear	i) case where the radius of curvature is large. Flat plate equations used. ii) (Transition-length) $\tau_b = \frac{K_s \pi^2 E}{12(1-\nu_e^2)}\left(\frac{t}{b}\right)^2$ K_s is found from the graph below. Where $Z_b = \frac{b^2}{rt}\sqrt{1-\nu_e^2}$ 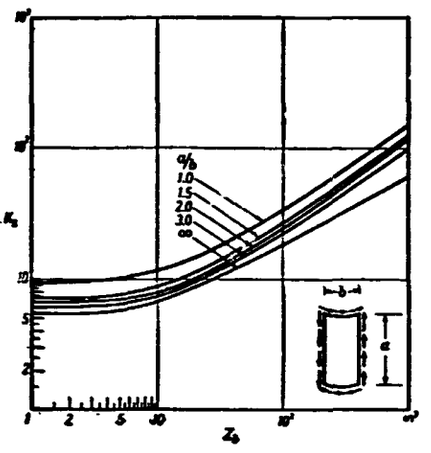 (a) long curb long curved plate (simple support) 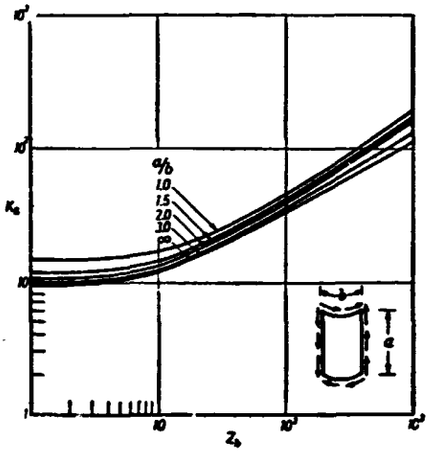 (b) long curved plate (fixed sides)	219 /609

No.	Graph & Boundary Cond.	Formula or Table of Results	Notes, Ref.

/610

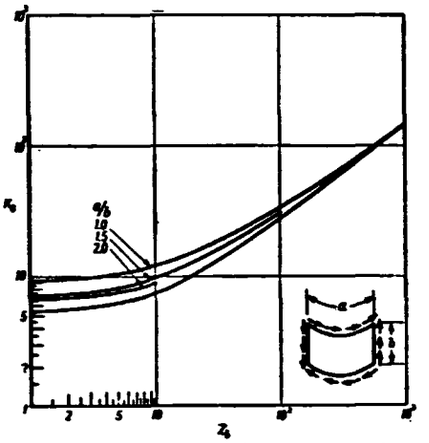

(c) wide curved plate (simple support)

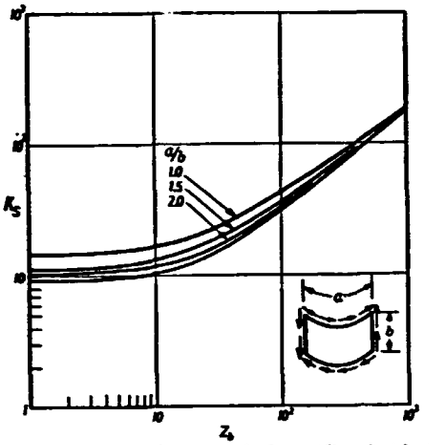

(d) wide curved plate (fixed sides)

iii) $\frac{b^2}{rt} > 30$

$\tau_b = 0.37(Z_b)^{\frac{1}{4}}\tau_b$ flat p'ate; τ_k flat plate is the shear buckling st-ess of a flat plate .

Comparison of theoretical values and experiment values

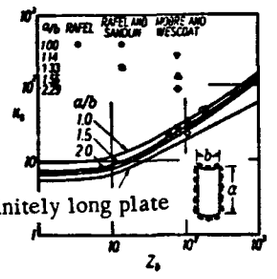

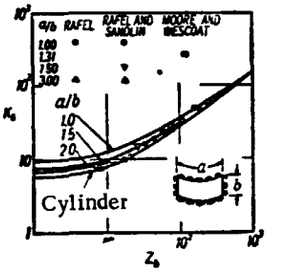

No	Graph & Boundary Cond.	Formula or Table of Results	Notes, Ref.
		The theoretical values are based on Batdorf-Stein-Schildcrout.	/611

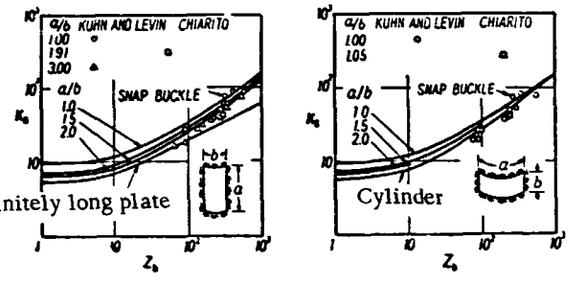

COMBINED LOADS

(Compression and Shear)

No.	Graph & Boundary Cond.	Formula or Table of Results	Notes, Ref.
79	Curved plate Compression and Shear 1 is considered sufficiently long 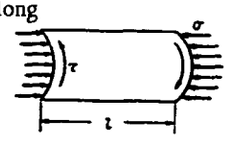	$\left(\frac{\tau_b}{(\tau_b)_{\sigma=0}}\right)^2+\frac{\sigma_b}{(\sigma_b)_{\tau=0}}=1$ (Batdorf) (Schildcrout Stein)	179

COMPRESSION AND INTFRNAL PRESSURE

No.	Graph & Boundary Cond.	Formula or Table of Results	Notes, Ref.
80	Curved plate Compression and Internal pressure	$R_c^2+R_p=1$ $R_c=\frac{\text{Acting compressive stress}}{\text{Buckling stress in the case of compression only}}$ $R_p=\frac{\text{Acting internal pressure}}{\text{Pressure at time of buckling when only external pressure is acting}}$	219

(AXIAL STRESS AND SHEAR)

No.	Graph & Boundary Cond.	Formula or Table of Results	Notes, Ref.
81	Curved plate Axial stress and shear	for $\left.\begin{array}{l}10<Z_b<100\\1<\frac{a}{b}<3\end{array}\right\}$ $R_s^2+R_X=1$ when $R_s=\frac{\text{Shear stress}}{\text{Buckling stress in the case of shear only}}$ $R_X=\frac{\text{Tensile or compressive stress}}{\text{Buckling stress in the case when there is only tension or compression}}$ $Z_b=\frac{b^2}{rt}\sqrt{1-\nu_e^2}$	219

SHEAR AND INTERNAL PRESSURE

No.	Graph & Boundary Cond.	Formula or Table of Results	Notes, Ref.
82	Curved plate Shear and Internal Pressure	$R_s^2+R_p=1$ $R_s=\dfrac{\text{Shear buckling stress}}{\text{Buckling stress when in the case of shear only}}$ $R_p=\dfrac{\text{Internal pressure}}{\text{Buckling stress in the case when only the external pressure acts}}$	219

EFFECTIVE WIDTH

No.	Graph & Boundary Cond.	Formula or Table of Results	Notes, Ref.
83	Curved plate Effective width Experiment equations	i) for cases in which $\frac{2b_e}{b}>0.45$ when $0\leqq Z_b\leqq 31$ $\dfrac{2b_e}{b}=K_c^{\frac{1}{2}}\dfrac{t}{b}\left(\dfrac{E}{\sigma_e}\right)^{\frac{1}{2}}$ From (Ramberg-Levy-Fienup ii) for the case in which $\frac{2b_e}{b}<0.45$ when $0\leqq Z_b\leqq 125$ $\dfrac{2b_e}{b}=K_p^{0.43}\left[\dfrac{t}{b}\left(\dfrac{E}{\sigma_e}\right)^{\frac{1}{2}}\right]^{0.86}$ ..... From (Jackson-Hall 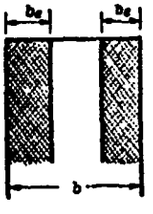 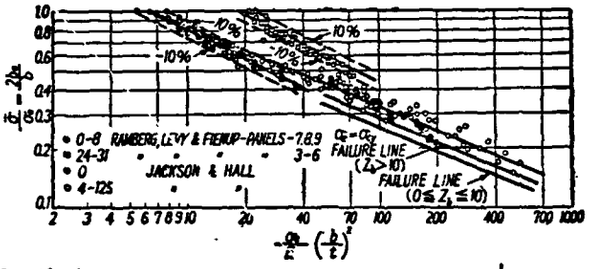 (Notation) $K_c=\dfrac{\pi^2 k_c}{12(1-\nu^2)}$ (k_c Compressive stress coefficient of flat plate) $K_p=6.3$ $b=$ plate width $b_e=$ effective width measured from end $\sigma_e=$ axial stress at end section $Z_b=$ (Curved plate parameter) $=\dfrac{b^2}{rt}\sqrt{1-\nu^2}$ $\bar{\sigma}=$ average axial stress $\sigma_{cy}=$ compressive yield stress	220

PROFILES, REINFORCED PLATES (supplement)

Compression

No.	Graph & Boundary Cond.	Formula or Table of Results	Notes, Ref.
84	Profiles, hollow cruciform cross-section Compression 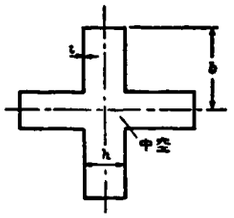 	$\sigma_b^e = \frac{3Gh^2}{b^2}$ $(h \ll b)$ σ_b^e: buckling stress within elasticity limit	190
85	Compression in open cross-section stringer attached to plate 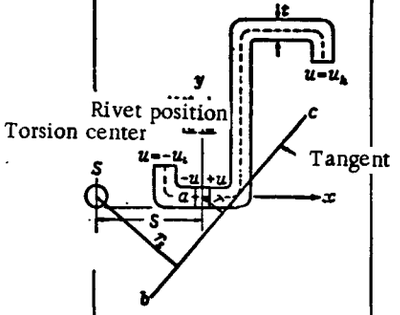 	$\frac{\sigma_b}{E} = \frac{\left(0.385 J_T + 0.385 B_1 + 9.87 \frac{C_1}{L^2}\right)}{J_{P_0} + 2M_y S + (A+a)S^2} + \frac{\frac{19.74R}{L^2} S + \left(0.385 B_2 + 9.87 \frac{I}{L^2}\right) \times S^2}{J_{P_0} + 2M_y S + (A+a)S^2}$ where $J_T = \frac{1}{3}\int_{u=-u_1}^{u=u_2} t^3 du$ $J_{P_0} = \int_{u=-u_1}^{u=u_2} (x^2+y^2) t du$ In Figure A $\begin{cases} B_1 = bh^3\left[0.0952 + 0.289\left(\frac{L}{b}\right)^2\right] \\ B_2 = 2.35\left(\frac{bh^3}{L^2}\right) \end{cases}$ In Figure B $\begin{cases} B_1 = bh^3\left[0.238 + 0.119\left(\frac{L}{b}\right)^2 + 0.119\left(\frac{b}{L}\right)^2\right] \\ B_2 = \frac{bh^3}{L^2}\left[1.175 + 2.35\left(\frac{L}{b}\right)^2 + 1.175\left(\frac{L}{b}\right)^4\right] \end{cases}$	199

No.	Graph & Boundary Cond.	Formula or Table of Results	Notes, Ref.
		A 図 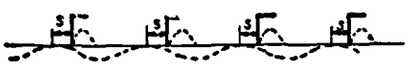 B 図 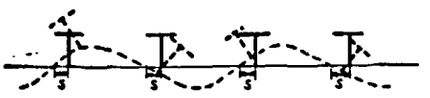	199 /614

b :stringer spacing

h : plate thickness

s :distance from twist center S to rivet position

L : effective length of panel

$$C_0=\int_{u=-s}^{u=b} W^2 t\,du-\frac{1}{A+a}\left(\int_{u=-s}^{u=b} W t\,du\right)^2$$

$$W=\int_0^u r\,du$$

A = cross-section area of stringer $=\int_{u=-s}^{u=b} t\,du$

a=- cross-section area of plate for stringers:

i) **for unbuckled sheet in a wide panel** $a=bh$

ii) **for buckled sheet in a wide panel** $a=\frac{bh}{2}$

$$M_y=\int_{u=-s}^{u=b} x\cdot t\,du$$

$$R=\int_{u=-s}^{u=b} W y t\,du-\frac{1}{A+a}\left(\int_{u=-s}^{u=b} W t\,du\right)\left(\int_{u=-s}^{u=b} y t\,du\right)$$

$$I=\int_{u=-s}^{u=b} y^2 t\,du-\frac{1}{A+a}\left(\int_{u=-s}^{u=b} y t\,du\right)^2$$

S (see above) found from the route of the following equation

$$\left(\frac{S}{L}\right)^3\left[9.87\,R(A+a)-M_y(0.385\,B_s L^2+9.87\,I)\right]$$
$$+\left(\frac{S}{L}\right)\left[(A+a)(0.385\,J_T L+0.385\,B_s L+9.87\frac{C_0}{L})-r_{P_0}\left(0.385\,B_s L+9.87\frac{I}{L}\right)\right]$$
$$+\left[M_y\left(0.385\,j_T+0.385\,B_s+9.87\,\frac{C_0}{L^2}\right)-\frac{9.87\,R}{L^2}J_{P_0}\right]=0$$

第 1 図

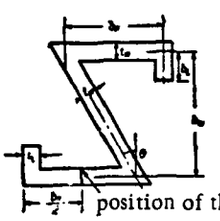

position of the rivet

In particular, the constants for panels having Z stringers is found as follows for Figures 1 and 2

(1) equal flange and equal rib stringers (Figure 1)

$$J_T=\frac{1}{3}\left[t_W^3(2\,b_F+b_W)+t_L^3(2\,b_L)\right]$$

$$A=2\,b_L t_L+t_W\left(2\,b_F+\frac{b_W}{\cos\theta}\right)$$

No.	Graph & Boundary Cond.	Formula or Table of Results	Notes, Ref.
		$C_0=\frac{1}{12}\left\{t_W\left(\frac{b_F^3 b_W^3}{\cos\theta}+b_W^3 b_F^3\right)+t_L(3\,b_W^2 b_F^2 b_L+10\,b_F^3 b_L^2+9\,b_W b_F^2 b_L^2-12\,b_F b_W b_L^2\tan\theta-6\,b_W^2 b_L^2 b_F\tan\theta+4\,b_W^2 b_L^3\tan^2\theta\right\}$	199
		$-\frac{1}{A+a}\left\{\frac{t_W}{4}\left(\frac{b_F b_W^2}{\cos\theta}\right)+t_L\left(\frac{b_W b_L^2}{2}\tan\theta-b_L^2 b_F-\frac{b_W b_L b_F}{2}\right)\right\}^2$	
		$R=\frac{1}{6}\left\{t_L(2\,b_L^3 b_F-3\,b_L^2 b_F b_W-3\,b_W^2 b_F b_L+3\,b_L^2 b_W^2\tan\theta-2\,b_L^3 b_W\tan\theta)+t_W\left(\frac{b_F b_W^3}{\cos\theta}\right)\right\}-\frac{1}{A+a}\left\{\frac{t_W}{4}\left(\frac{b_F b_W^3}{\cos\theta}\right)+t_L\left(\frac{b_W b_L^2}{2}\tan\theta-b_L^2 b_F-\frac{b_W b_L b_F}{2}\right)\right\}\times\left\{t_L b_W b_L+t_W\left(\frac{b_W^2}{2\cos\theta}+b_W b_F\right)\right\}$	
		$I=t_L\left(\frac{2}{3}b_L^3+b_W^2 b_L-b_W b_L^2\right)+t_W\left(\frac{b_W^3}{3\cos\theta}+b_W^2 b_F\right)-\frac{1}{A+a}\left\{t_L b_W b_L+t_W\left(\frac{b_W^2}{2\cos\theta}+b_W b_F\right)\right\}^2$	
		$M_y=t_L(b_F b_L-b_W b_L\tan\theta)+t_W\left(b_F^2+\frac{b_F b_W}{2\cos\theta}-b_W b_F\tan\theta-\frac{b_W^2}{2}\frac{\tan\theta}{\cos\theta}\right)$	
		$J_{P_0}=t_L\left\{\frac{5\,b_F^2 b_L}{2}+b_W^2 b_L\tan^2\theta-3\,b_F b_L b_W\tan\theta+\frac{2\,b_F^3}{3}+b_W^2 b_L-b_W b_L^2\right\}+t_W\left\{\frac{7\,b_F^3}{6}+\frac{b_F^2 b_W}{4\cos\theta}+\frac{b_W^3\tan^2\theta}{3\cos\theta}-\frac{b_F b_W^2\tan\theta}{2\cos\theta}+b_W^2 b_F\tan^2\theta-2\,b_W b_F^2\tan\theta+\frac{b_W^3}{3\cos\theta}+b_W^2 b_F\right\}$	
2	(2) Stringer with unequal flanges and no ribs (Figure 2)		
		$J_T=\frac{t_W^3}{3}(b_A+b_W+b_F)$	
		$A=t_W(b_A+b_W+b_F)$	
		$C_0=\frac{t_W}{12}\{b_A^2 b_W^3+3\,b_A^2 b_F b_W^2-6\,b_A b_W^2 b_F^2+4\,b_W^3 b_F^3\}-\frac{t_W^2}{A+a}\left\{\frac{b_A b_W^2}{4}+\frac{b_A b_W b_F}{2}-\frac{b_W b_F^2}{2}\right\}^2$	
		$R=\frac{t_W}{6}\{b_A b_W^3+3\,b_A b_W^2 b_F-3\,b_W^2 b_F^2\}-\frac{t_W^2}{A+a}\left\{\frac{b_A b_W^2}{4}+\frac{b_A b_W b_F}{2}-\frac{b_W b_F^2}{2}\right\}\times\left\{\frac{b_W^2}{2}+b_W b_F\right\}$	

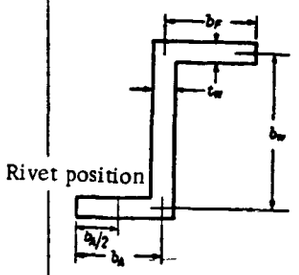

/615

No.	Graph & Boundary Cond.	Formula or Table of Results	Notes, Ref.
		$I = t_W\left[\frac{b_W^3}{3} + b_W^2 b_F\right] + \frac{t_W'}{A+a}\left[\frac{b_W^3}{2} + b_W b_F\right]^2$ $J_{P_0} = t_W\left[\frac{b_A^3}{12} + \frac{b_W^3}{3} + \frac{b_A^2 b_W}{4} + \frac{b_A b_F^2}{2} + \frac{b_A^2 b_F}{4} + b_W^2 b_F + \frac{b_F^3}{3}\right]$ $M_y = \frac{t_W}{2}(b_F^2 + b_A b_F + b_A b_W)$	/616
86	Hatcross-section stringer Compression 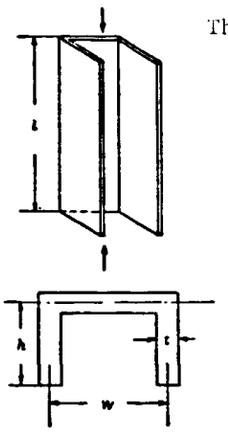 	lateral buckling occurs when $\frac{h}{W} > 5$ and The effect of t is neglected (if $\left(\frac{h}{W} > 5\right.$, t may be neglected). $\frac{\sigma_b}{E} = \frac{1}{2D+1}\left\{\frac{1}{2.6} - \frac{1}{6.76\left\{\frac{\pi^2}{12S^2}(1+2R) + \frac{1}{5.2}\left(\frac{1}{R}+2\right)\right\}}\right\}$ $D = \frac{8}{105}\left(\frac{C^2}{R^2}\right) + \frac{4}{35}CR^2 + \frac{1}{7}R$ $C = \frac{1}{R} + \frac{1}{(1+2R)}$ $R = \frac{h}{W}$ height-width ratio $S = \frac{l}{W}$ length-width ratio	200

CYLINDERS (supplement)

Compression Cylinder

/217

No.	Graph & Boundary Cond.	Formula or Table of Results	Notes, Ref.
87	Compression in direction of axis Simply supported ends 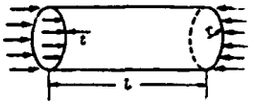	$\sigma_k = K\frac{\pi^2 D}{l^2 t}$ (Batdorf) σ_k = compressive buckling stress in direction of axis K = coefficient $D = \frac{Et^3}{12(1-\nu^2)}$ bending stiffness or the following expression may also be used $\sigma_k = \frac{1}{\nu\, 3(1-\nu^2)} \cdot \frac{Et}{r}$ when $3 < Z < 6\left(\frac{r}{t}\right)^2 (1-\nu^2)$, $K = 0.702\, Z$. 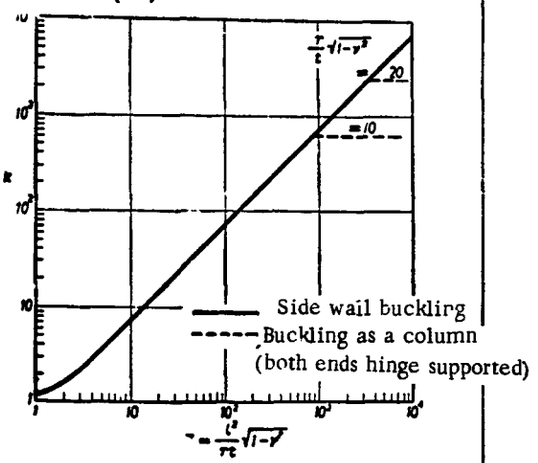	179
88	Cylinder Compression 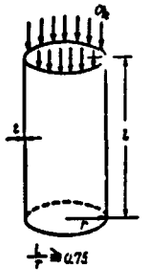	Experiment formulas $\sigma_k = K\frac{\pi^2 D}{l^2 t}$ (Batdrof, Schildcrout, Stein) σ_k = compressive buckling stress K = coefficient $D = \frac{Et^3}{12(1-\nu^2)}$ bending stiffness 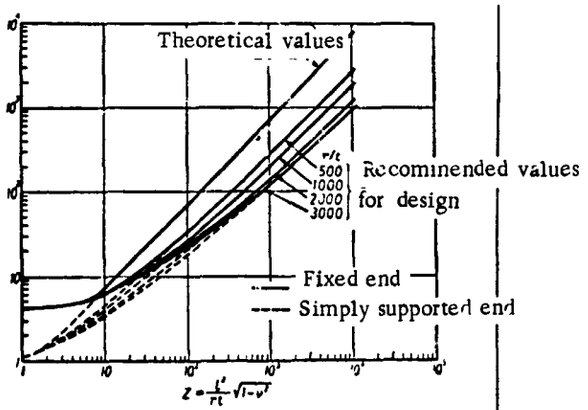	180

No.	Graph & Boundary Cond.	Formula or Table of Results	Notes, Ref.
		Comparison with experiments	180

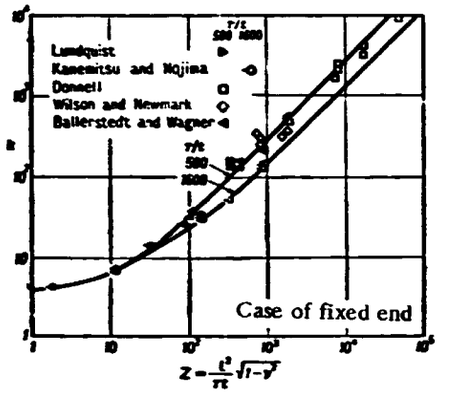

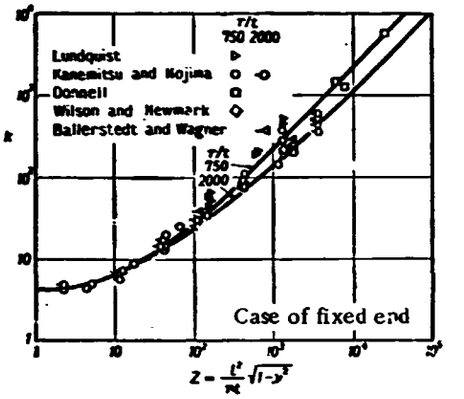

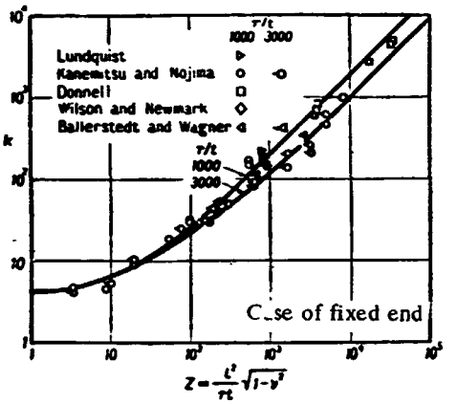

/618

No.	Graph & Boundary Cond.	Formula or Table of Results	Notes, Ref.
		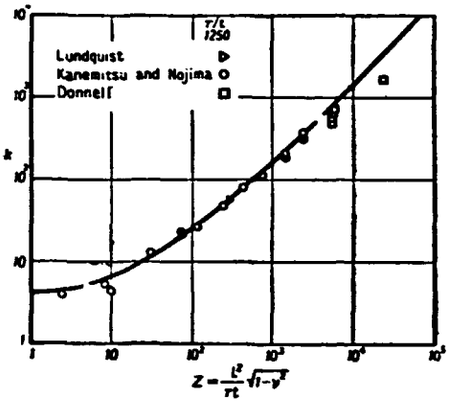	180 /619
		If Z is large, where $K=1.15CZ$	
		$\sigma_k=CE\frac{t}{r}\quad\left(\frac{l}{r}\geqq 0.75\right)$	
		C: coefficient	
		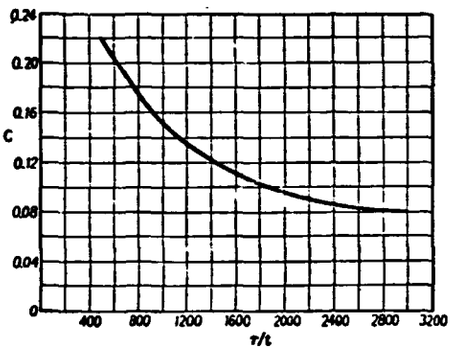	
89	Cylinder Compression 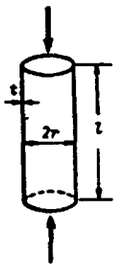	equations (experiment equations) of Kanemitsu and Nojima $500<\frac{r}{t}<3,000$ $0.10<\frac{l}{r}<2.5$ } Range $\frac{\sigma_k}{E}=9\left(\frac{t}{r}\right)^{1.6}+0.16\left(\frac{t}{l}\right)^{1.3}$ The above equations are more suitable than those of Ballerstedt and Wagner.	203

No.	Graph & Boundary Cond.	Formula or Table of Results	Notes, Ref.
90	Cylinder Compression 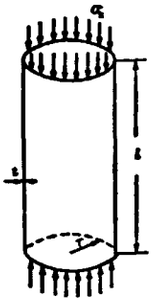	Equation of Ballerstedt and Wagner $\frac{\sigma_k}{E}=3.3\left(\frac{t}{l}\right)^2+0.2\left(\frac{t}{r}\right)$. Accuracy less than in equations of Kanemitsu and Nojima	180 /620
91	Cylinder Axial compression (plastic buckling) 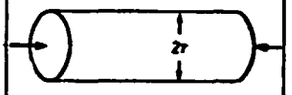 t = plate thickness $2r$ = average radius	$\sigma_k=\frac{k\pi^2\eta E}{12(1-\nu^2)}\left(\frac{t}{2r}\right)^2$ k = buckling at coefficient (for buckling within elastic range) η = modulus of plasticity; η = 1 within elasticity range 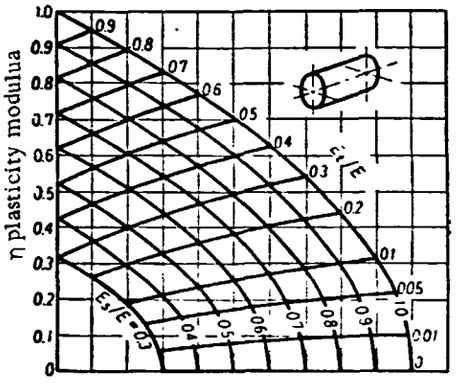	182
92	Cylinder Compression Local buckling 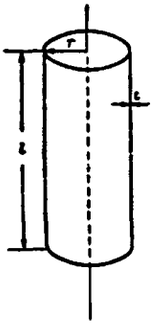	In a not very short cylinder, local buckling occurs. Its values differe according to the absolute values of t/r, r, and t, and according to l. In this paper, we consider the case where t/r is a constant value. Deformation W is expressed as follows $W=W_0+W_1\cos\frac{\pi x}{l_x}\cos\frac{\pi y}{l_y}+\frac{W_2}{2}\left(\cos\frac{2\pi x}{l_x}+\cos\frac{2\pi y}{l_y}\right)$ Total deformation energy W* is $W'=2\pi rl\cdot\frac{1}{2}Et\alpha\left\{\frac{3\pi r}{lnk}\left\{\frac{Q}{\pi^2}+(Gg_1^2+Hg_2^2)+q^2\right\}\right\}$ where $g_1=\frac{W_1\pi^2}{r}$ $g_2=\frac{W_2\pi^2}{r}$	183

No.	Graph & Boundary Cond.	Formula or Table of Results	Notes, Ref.
		$q=\frac{\sigma}{E\sqrt{\alpha}}$, $\alpha=\frac{t^2}{12(1-\nu^2)r^2}$	183 /621
		$\eta=n^2\cdot\sqrt{\alpha}$	
		$Q=Ag_1^4+Bg_1^2g_2^2+Cg_2^4-Dg_1^2g_2+Cg_1^2+Fg_2^2$	
		$A=k^4+\frac{1}{128}$	
		$B=k^4\left\{\frac{1}{(k^2+1)^2}+\frac{1}{4(9k^2+1)^2}+\frac{1}{4(k^2+9)^2}\right\}$	
		$C=\frac{k^4}{4(k^2+1)^2}$	
		$D=\frac{k^4}{(k^2+1)^2}+\frac{1}{16}$	
		$F=\frac{1}{6}$, $G=\frac{(k^2+1)^2}{4}$	
		$H=2(k^4+1)$	
		σ = average compressive stress in direction of axis	
		k = aspect ratio $\frac{l_y}{l_x}$ of buckling lobe	
		n = wave numbers in direction of circumference	
		With k and $\eta(n)$ as parameters, assuming	
		$\frac{\partial W'}{\partial g_1}=0$, $\frac{\partial W'}{\partial g_2}=0$	
		Before and after buckling it is possibel to find the compressive strain where the same amount of deformation energy becomes a minimum. in this case, the stress corresponding to strain becomes the buckling stress. The wave number m in the direction of the axis becomes a minimum of m = 1.5 in the case of local buckling.	
93	Cylinder (long cylinder) Compression Axial symmetrical buckling	Gerard's theoretical equation	207
		$\sigma_k=\frac{E_s}{\sqrt{3(1-\nu^2)}}\sqrt{\frac{E_t}{E_s}}\left(\frac{t}{R}\right)$	
		E_s=secant modulus	
		E_t=tangent modulus	
		t = thickness	
		R = cylinder radius	
	i) buckling in elasticity range: $(\sigma_k)_e$		
	Assuming	$E_s=E$, $\frac{E_t}{E_s}=1$, $\nu=\nu_e=0.3$	
		$(\sigma_k)_e=\frac{E}{\sqrt{3(1-\nu_e^2)}}\frac{t}{R}=0.6E\frac{t}{R}$	
	ii) buckling in plasticity range; σ_k		
	Assuming	$\sigma_k=\eta_c(\sigma_k)_e$	
		$\eta_c=\left(\frac{1-\nu_e^2}{1-\nu_t}\right)^{\frac{1}{2}}\frac{E_s}{E}\left(\frac{E_t}{E_s}\right)^{\frac{1}{2}}$	
		Therefore, generally	
		$\sigma_k=0.6\eta_cE\frac{t}{R}$	

No.	Graph & Boundary Cond.	Formula or Table of Results	Notes, Ref.
		Comparison with experiments 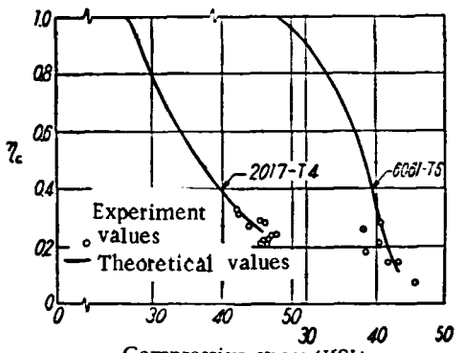 Compressive stress (KSI) Where the theoretical value is assumed to be $\nu_e = 0.3$.	212 /622
94	Cylinder Compression From **Fung-Sechler**	**Kanemitsu-Nojima**'s experimental equations are expressed by a separate method. $\sigma_b = K_c E\left(\frac{t}{r}\right)$ Where $K_c = \left(\frac{r}{t}\right)\left[9\left(\frac{t}{r}\right)^{1.6} + 0.16\left(\frac{t}{l}\right)^{1.8}\right]$ If this is written in the form of a graph, it has the following representation. 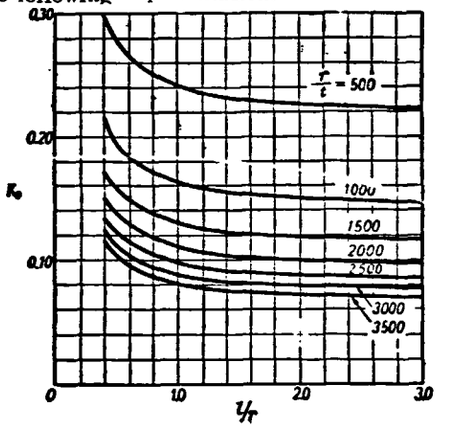 	212
95	Cylinder Compression 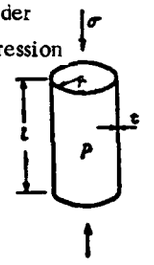 	i) short cylinder $\left(\frac{l}{rt} < 1\right)$ the equation for a flat plate is used $\sigma_b = \eta \frac{K_c \pi^2 E}{12(1-\nu_e^2)}\left(\frac{t}{l}\right)^2$ See section of Flat Plates for η, K_c. ii) **(Transition-length range)** $\left(1 < \frac{l}{rt} < 100\right)$	219

No.	Graph & Boundary Cond.	Formula or Table of Results	Notes, Ref
		In the elasticity range, this is found by the following equation $\sigma_k = \eta \frac{K_c \pi^2 E}{12(1-\nu_e^2)} \left(\frac{t}{l}\right)^2$ K_c is found from the following graphs 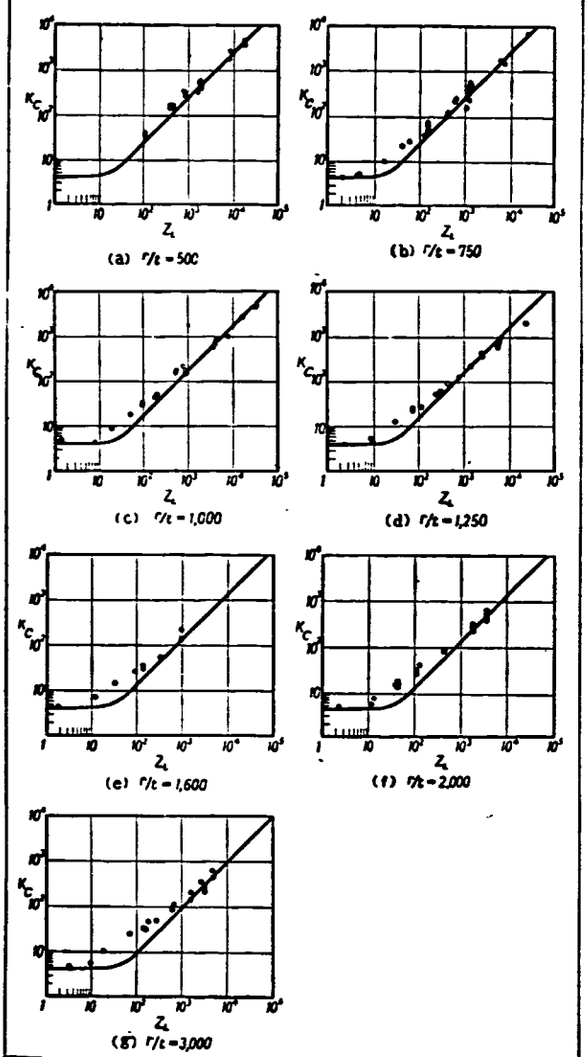 (a) $r/t = 500$ (b) $r/t = 750$ (c) $r/t = 1{,}000$ (d) $r/t = 1{,}250$ (e) $r/t = 1{,}500$ (f) $r/t = 2{,}000$ (g) $r/t = 3{,}000$ Where $Z_L = \frac{l^2}{rt}\sqrt{1-\nu_e^2}$ iii) long cylinder $\left(\frac{l^2}{rt} > 100\right)$ $\sigma_k = \eta C E \frac{t}{r}$ C is found in the bottom graph on p. 606. (notation) $\eta =$ (Plasticity reduction factor)	/623

No	Graph & Boundary Cond	Formula or Table of Results	Notes, Ref.
		$=\frac{E_s}{E}\left[\frac{E_t}{E_s}\frac{(1-\nu_e^2)}{(1-\nu^2)}\right]^{\frac{1}{2}}$ E_s=Secant modulus E_t=Tangent modulus E= Young's modulus ν = Poisson's ratio $=\nu_p-(\nu_p-\nu_e)\frac{E_s}{E}$ ν_e= Poisson's ratio (elastic range) = 0.3 ν_p= Poisson's ratio (plastic range) = 0 5 U= (Unevenness factor)	/624

TORSION

No.	Graph & Boundary Cond.	Formula or Table of Results	Notes, Ref
96	Cylinder Torsion Case of simply supported ends and fixed ends	$\tau_b=K\frac{\pi^2 D}{l^2 t}$ (Batdorf) (Stein, Schildcrout) τ_b= shear buckling stress K= coefficient $D=\frac{Et^3}{12(1-\nu^2)}$ Bending stiffness 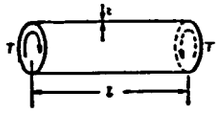 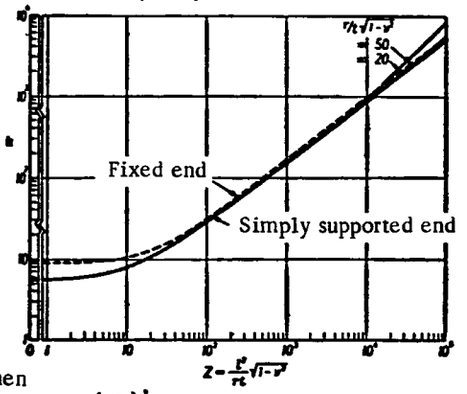 when $50<Z<10\left(\frac{r}{t}\right)^2(1-\nu^2)$ $K=0.85Z^{\frac{2}{3}}$ Comparison with experiments 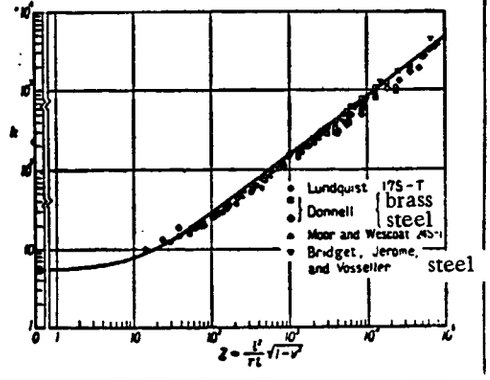	179

No.	Graph & Boundary Cond.	Formula or Table of Results	Notes, Ref
97	Cylinder Torsion	when i) $\frac{l}{r}<6.5\left(\frac{r}{t}\right)^{\frac{1}{2}}$ $\tau_k=0.815E\left(\frac{r}{l}\right)^{\frac{1}{2}}\left(\frac{t}{r}\right)^{\frac{3}{4}}$ ii) in other cases $\tau_k=0.29E\left(\frac{t}{r}\right)^{\frac{3}{4}}$	181
98	Cylinder (extremely long Torsion cylinder) Two-lobe buckling	Gerard's theoretical equation when the length is sufficiently long, the boundary conditions at the both ends no longer have any effect, and two-lobe buckling occurs. $\tau_k=0.272(1-\nu^2)^{-\frac{3}{4}}E_s\left(\frac{t}{R}\right)^{\frac{3}{4}}$ E_s = secant modulus t = thickness R = cylinder radius i) buckling in elastic range $(\tau_k)_e$ when $\left(\frac{l}{R}\right)^2\left(\frac{t}{R}\right)>\alpha$ 但し $\alpha=\begin{cases}42 & \text{when both ends supported}\\ 60 & \text{when both ends fixed}\end{cases}$ Assuming $\left.\begin{matrix}E_s=E\\ \nu=\nu_e\end{matrix}\right\}$ $(\tau_k)_e=0.272(1-\nu_e^2)^{-\frac{3}{4}}E\left(\frac{t}{R}\right)^{\frac{3}{4}}$ ii) buckling in plastic range τ_k : assuming $\tau_k=\eta_s\cdot(\tau_k)_e$ $\eta_s=\left(\frac{1-\nu_e^2}{1-\nu^2}\right)^{\frac{3}{4}}\frac{E_s}{E}=\left(\frac{1-\nu_e^2}{1-\nu^2}\right)^{\frac{3}{4}}\frac{G_s}{G}$ Therefore, generally $\tau_k=0.272(1-\nu_e^2)^{-\frac{3}{4}}\eta_s E\left(\frac{t}{R}\right)^{\frac{3}{4}}$ Comparison with experiments 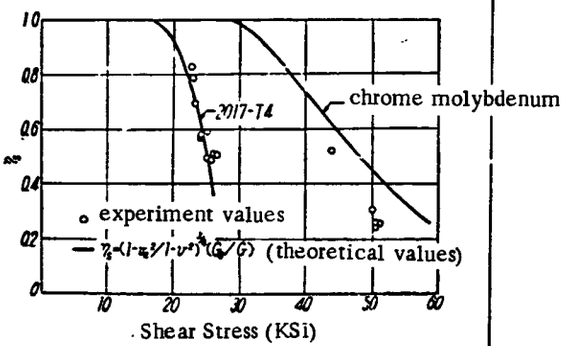 	209
99	Cylinder Torsion	when $50\frac{t}{R}<\left(\frac{l}{R}\right)^2<10\frac{R}{t}$ $\tau_k=0.747E\left(\frac{t}{R}\right)^{\frac{3}{4}}\left(\frac{R}{l}\right)^{\frac{1}{2}}$ (Batdorf)	208

/625

No.	Graph & Boundary Cond.	Formula or Table of Results	Notes, Ref.
100	Cylinder Torsion Plastic buckling 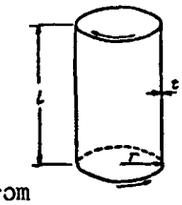 From **Lee-Ades**	In problems of buckling in the elastic range, the effects of large deflection and imperfection are important. In the plastic range, these do not have so much significance, but even so in the region close to the elastic range, they indicate an effect which should be considered We shall describe these effects in the plastic range (a) Case of a perfect cylinder $3.5910\,H\left(\frac{l}{t}\right)^2\left(\frac{3(\tau_k)_0}{E_s}\right)=3.2704\,H^4$ $\times\left[37.3063\,J^4+7.0422\left(1+\frac{1}{\xi_{k0}}\right)J^2+2\right]$ $+0.08213H^8\left\{\frac{1}{0.0276H^4+0.1660(3\xi_{k0}-1)H^2+1}\right.$ $\left.+\frac{1}{0.9608H^4+0.9802(3\xi_{k0}-1)H^2+1}\right\}$ (1) $(\tau_k)_{plastic}=\eta(\tau_k)_{elastic}$ (2) $\eta=\left\{1-(0.06+0.114H-0.006H^2)\right.$ $\left.\times\left(1-\xi_{k0}^{-\frac{1.6}{H}}\right)\right\}\left(\frac{E_s}{E}\right)$ (3) First, in equation (1) assuming we find $\xi_{k0}=1$, $E_s=E$ $(\tau_k)_0=(\tau_k)_{elastic}$ These equations are derived assuming that through the elasticity and plastic ranges the Poisson's ratio is 1/2, some errors will creep in for other Poisson's ratios. η is given approximately by equation (3), and this is sufficient for actual practice. The precise calculation η is extremely laborous The error in equation (3) and in a strict equation is below 1% in ordinary metal cylinders. Moreover, the values of η that can be used are from $0.5\left(\frac{E_s}{E}\right)$ to $\left(\frac{E_s}{E}\right)$ Below are shown the results for aluminum alloy (assuming N = 10) 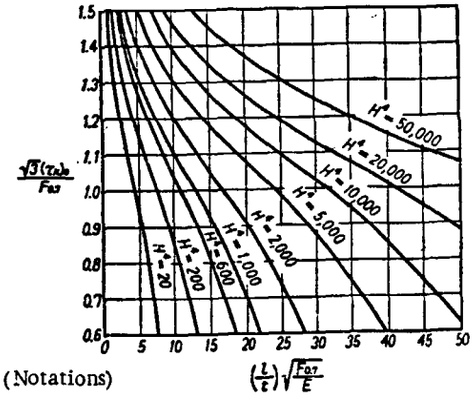 (Notations) $\left(\frac{l}{t}\right)\sqrt{\frac{F_{0.7}}{E}}$ $H=\left[\frac{l^2}{rt}\right]^{\frac{1}{4}}$ $J=\frac{1}{H}$	

No.	Graph & Boundary Cond.	Formula or Table of Results	Notes, Ref.
		$\xi_{k_0}=\left(\frac{E_s}{E_t}\right)_{\tau=(\tau_k)_0}=\frac{1+\frac{3}{7}N\left(\frac{\sqrt{3}\,\tau_{xs}}{F_{0.7}}\right)^{N-1}}{1+\frac{3}{7}\left(\frac{\sqrt{3}\,\tau_{xs}}{F_{0.7}}\right)^{N-1}}$	/627
		$(\tau_k)_0$= shear buckling stress of perfect cylinder N= configuration coefficient (experimentally) τ_{xs}= average shear stress $F_{0.7}$= stress value determined by secant with slope 0.7 (experimentally determined) E_s=Secant modulus E_t=Tangent modulus E= Young's modulus	
		(b) in the case of imperfection, in the plastic range, this is expressed approximately as follows $\frac{(\tau_k)_V}{(\tau_k)_0}=1-\frac{2}{3}\left[\frac{V}{\xi_{k_0}^{1/2}\left(\frac{l^2}{rt}\right)^{0.3}}\right]^{0.6}$ (4)	
		In the elastic range, this is based on the following equation $\frac{(\tau_k)_V}{(\tau_k)_0}=1-\frac{3}{4}\left[\frac{V}{\left(\frac{l^2}{rt}\right)^{0.3}}\right]^{0.6}$ (5)	
		The imperfection factor V, for the half-wave lengths l_x, l_s of the surface $V=2U_0\left\{\left[\frac{l_x\cdot l_s}{l_x+l_s}\right]\left(\frac{1}{t}\right)\right\}^2$ (6)	
		In particular, in the case of pure torsion $l_x\cong l$ $l_s=ml_x\cong ml$ According to Donnell and Wan, when , for a cylinder $U_0=1.5\sim3.0\times10^{-6}$ (machine processed) $=3.0\sim5.0\times10^{-6}$ (rolled well-flattened plate) $=5.0\sim10.0\times10^{-6}$ (rolled, unflattened plate) The graphs below are for the buckling stress with respect to various imperfections.	
		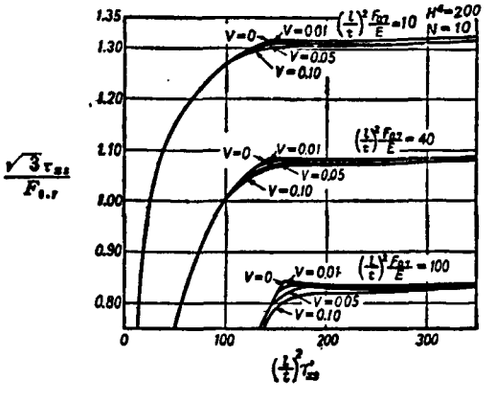	

No.	Graph & Boundary Cond.	Formula or Table of Results	Notes, Ref.

/628

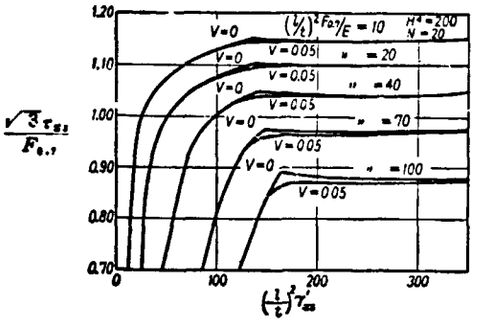

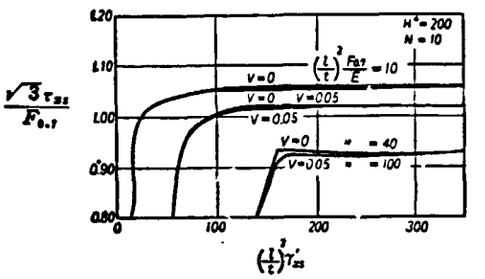

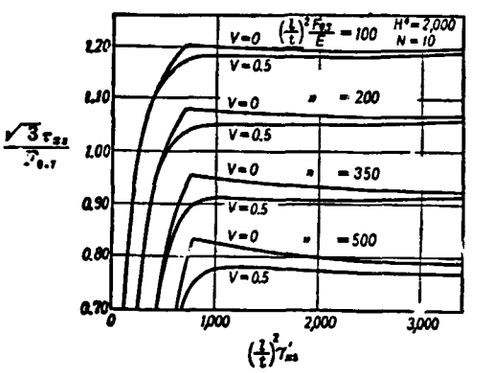

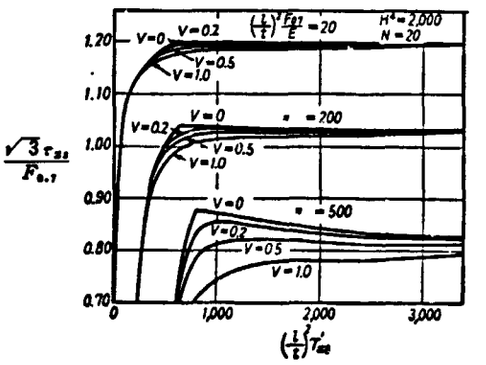

No.	Graph & Boundary Cond.	Formula or Table of Results	Notes, Ref.

/629

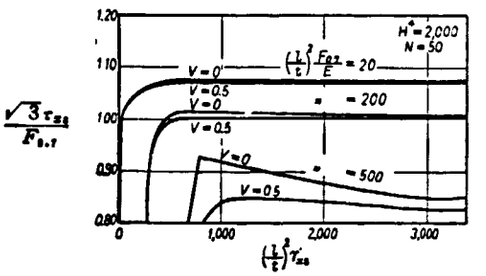

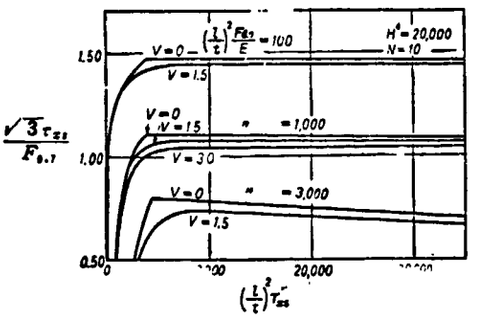

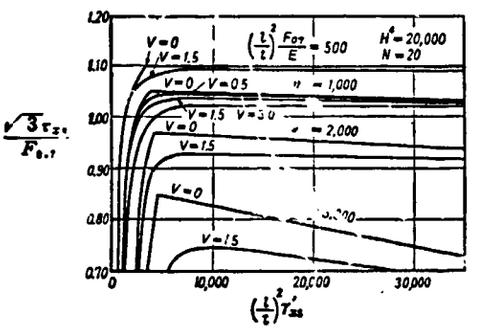

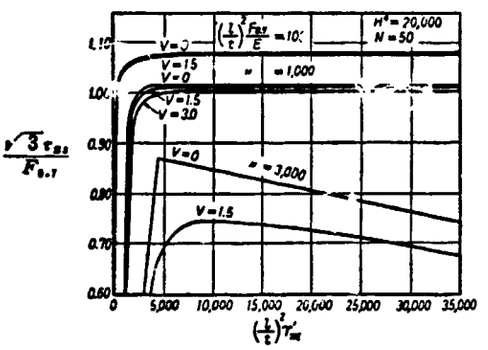

No.	Graph & Boundary Cond.	Formula or Table of Results	Notes, Ref.
		(Notation) $\tau'_{ss}=\dfrac{\text{Overall torsion angle of one end with respect to the other end of a cylinder}}{\left(\frac{l}{r}\right)}$ /630 $(\tau_k)_T=$ shear buckling stress of imperfect cylinder $V=$ (Imperfection factor) $U_0=$ (Unevenness factor) $l_m=$ half-wave lergth in direction of length $l_n=$ half-wave length in direction of circumference $\delta=$ (Second unevenness factor) $m=$ wavelength ratio Here, U_0 and δ are determined experimentally (c) Strict solution The above were solved by the energy method, but they include several simplifications and approximations. In order to check the above results, we analyze the case of an extremely long cylinder which buckles due to torsion. Timoshenko* by a method he used in the elasticity region, derived a basic equation for the plastic region. He obtained differential equations for 3 displacements from the relationship between the membrame force and the equilibrium and displacement of the bending moment. The buckling stress becomes as follows, using Timoshenko's surface displacement $\tau_k=\dfrac{E_t}{12}\cdot\dfrac{3\xi\lambda_m^4+1.33\left(\frac{t}{r}\right)^2[(27\xi^2+10.5)\lambda_m^2+36\xi]}{(9\xi-2)\lambda_m^2+12\lambda_m}$ (7) Where λ_m is the ratio of the wavelength in the direction of the the circumference to the wavelength in direction of length at the time of buckling. $3\xi(9\xi-2)\lambda^4+\left[108\xi-1.33\left(\frac{t}{r}\right)^2(9\xi-2)(27\xi^2+10.5)\right]\lambda^4$ $+192\left[\frac{1}{12}\left(\frac{t}{r}\right)^2(27\xi^2+10.5)-9\xi(9\xi-2)\right]\lambda^2$ $-6,912\xi=0$ (8) This is given by the minimum positive route of the following equation. $\frac{E_t}{E_t}\xi$ is the of (τ_k) during buckling.	* See Timoshenko's "Theory of Elastic Stability" pp. 480-490 for his method.
		(d) Comparison with experiment Steel cylinder Tensile strength 9×10^4 psi Young's modulus 2.9×10^7 psi Yieldpoint 7×10^4 psi $F_{0.7}=6.77\times10^4$ psi $N=17.6$	

No.	Graph & Boundary Cond.	Formula or Table of Results	Notes, Ref.

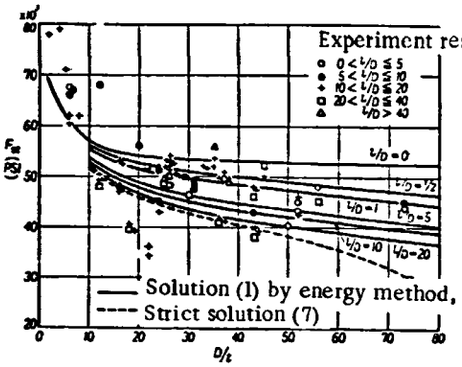

/631

where $F_{st}=\dfrac{(M_t)_k D}{2 I_0}$

$(M_t)_k={}'\tau_k)_0 \cdot 2\pi r^2 t$ Torsion moment during buckling

$D=$ Outer diameter

$I_0=$ Polar moment of inertia of area

(e) Comparison with experiments

Aluminum alloy cylinder

No.	$\frac{D}{t}$	$\frac{l}{D}$	$F_{s.t}$ psi	$(\tau_k)_e$ psi	$(\tau_k)_0$ psi	$\frac{(\tau_k)_e}{(\tau_k)_0}$	$\frac{(\tau_k)_e}{(\tau_k)_0}$ Experimental
1	9.9	6.41	73,050	53,400	54,000	0.999 1	0.982
2	15.1	6.94	〃	50,000	50,900	0.998 5	0.982
3	20.0	7.21	〃	43,600	48,200	0.997 8	0.904
4	20.1	6.55	〃	44,800	48,100	0.997 9	0.932
5	24.9	6.69	〃	41,900	46,400	0.997 1	0.904
6	30.1	6.78	〃	41,700	44,400	0.996 1	0.938
7	40.2	6.91	〃	38,600	40,500	0.993 2	0.958
8	48.9	6.98	〃	36,200	37,300	0.988 7	0.971
9	57.4	7.03	〃	33,100	33,700	0.982 2	0.982
10	80.6	7.09	〃	20,600	23,800	0.968 0	0.866
11	80.6	5.70	40,500	19,100	21,300	0.986 7	0.897
12	58.8	5.70	38,000	18,600	22,600	0.993 5	0.823
13	58.8	17.0	〃	17,400	19,800	0.985 3	0.878
14	39.4	5.70	38,500	22,700	25,100	0.996 5	0.904
15	39.4	17.0	〃	22,300	22,800	0.993 3	0.978
16	39.4	27.6	〃	22,000	21,600	0.990 6	1.018
17	19.8	5.70	39,800	25,400	29,000	0.998 3	0.876
18	19.8	17.1	〃	25,100	27,000	0.997 4	0.929
19	19.8	27.7	〃	25,900	26,200	0.996 8	0.988
20	10.0	17.1	39,700	28,600	30,500	0.998 8	0.937
21	80.6	11.5	40,700	15,400	17,600	0.971 3	0.875
22	60.6	11.5	40,000	20,200	21,200	0.987 5	0.952
23	40.4	11.5	41,500	23,900	24,800	0.994 1	0.963
24	20.1	11.5	38,600	24,500	27,200	0.997 9	0.901
						Average	0.930

No.	Graph & Boundary Cond.	Formula or Table of Results	Notes, Ref.
		No. 1 ～10 は 75S-T6 No. 11～24 は 61S-T6 $F_{0.7}$ is taken such that a residual stress of 0.2% occurs, $N=10$, $\tau_{z1}=73,050$ psi were used.	
101	Cylinder Torsion Plastic Buckling	(a) Long cylinder when $\left(\frac{l}{r}\right)^2>10\frac{r}{t}$ $\tau_b=0.272(1-\nu_e^2)^{-\frac{3}{4}}\cdot\eta_s E\left(\frac{t}{r}\right)^{\frac{3}{2}}$ $\eta_s=\left[\frac{1-\nu_e^2}{1-\nu^2}\right]^{\frac{3}{4}}\cdot\frac{E_s}{E}$ when (b) $50\frac{t}{r}<\left(\frac{l}{r}\right)^2<10\frac{r}{t}$ $\tau_b=0.701(1-\nu_e^2)^{-\frac{3}{8}}\cdot\eta_s E\left(\frac{t}{r}\right)^{\frac{3}{4}}\cdot\left(\frac{r}{l}\right)^{\frac{1}{2}}$ $\eta_s=\left[\frac{1-\nu_e^2}{1-\nu^2}\right]^{\frac{3}{8}}\cdot\frac{E_s}{E}$ (notation) η_s=塑性係数 (Plasticity reduction factor) E_s=Secant modulus ν_e= Poisson's ratio (value in elastic range) = 0.3 ν = Poisson's ratio	210 Gerard
102	Cylinder Torsion Plastic buckling Both ends simply supported	(hypotheses) 1. For the strain and curvature used to express displacement, thin shell theory was employed within the elastic range. 2. The secant shear modulus in the plastic range is defined as $\frac{\text{octahedral shear stress}}{\text{octahedral shear strain}}$... 3 Henchy-Nadai's stress-strain law is used, Moreover, it is assumed that the Poisson's ratio (ν) is 1/2. 4 In the infinitesimal buckling of the a entire cross-section, it is assumed that this is within the plastic range. $\tau_b=\frac{\pi^2 E_s t^2}{9l^2}$ 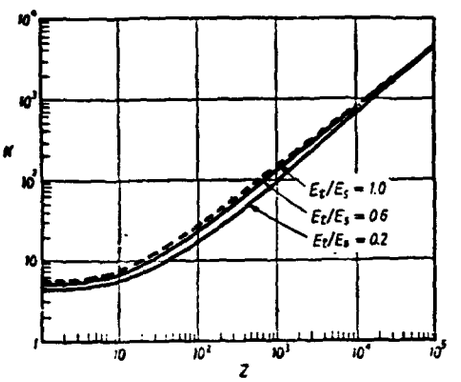 	216 From Radhakrishnan

No.	Graph & Boundary Cond.	Formula or Table of Results	Notes, Ref.
		(Notation) E_s = Secant modulus E_t = Tangent modulus $Z=\frac{\sqrt{3}}{2}\left(\frac{l^2}{rt}\right)$ Moreover, for the equilibrium equations, Donnell's equations were used, and solved by Galerkin's method.	/633
103	Cylinder Torsion	i) Short cylinder when $\left\{\frac{l}{r}<10\left(\frac{t}{r}\right)^{\frac{1}{2}}\right\}$ using the equation for a flat plate, $\tau_b=\eta\frac{K_s\pi^2E}{12(1-\nu_e^2)}\left(\frac{t}{l}\right)^2$ η, K_s employ the case of the shear of a flat plate ii) cylinder in i (Transition-length range) when $\left\{10\left(\frac{t}{r}\right)^{\frac{1}{2}}<\frac{l}{r}<3\left(\frac{r}{t}\right)^{\frac{1}{2}}\right\}$ (1) Case of simple support $\tau_b=\eta\frac{K_t\pi^2E}{12(1-\nu_e^2)}\left(\frac{t}{l}\right)^2$ K_t determined by the following graph. 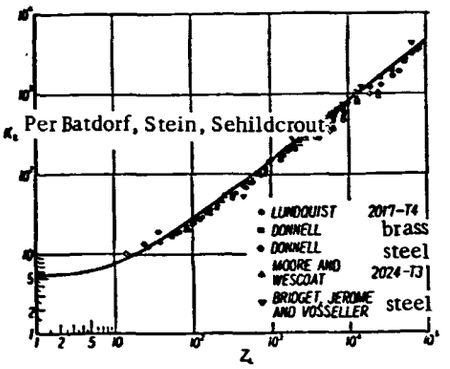 Per Batdorf, Stein, Sehildcrout where $Z_L=\frac{l^2}{rt}\sqrt{1-\nu_e^2}$ $\eta=\frac{E_s}{E}\left(\frac{1-\nu_e^2}{1-\nu^2}\right)^{\frac{3}{4}}$ (2) Linear equations may be used in the case of simple support. $\tau_b=\eta\frac{0.85\pi^2E}{12(1-\nu_e^2)^{\frac{3}{8}}}\left(\frac{t}{r}\right)^{\frac{5}{4}}\left(\frac{r}{l}\right)^{\frac{1}{2}}$ (3) In the case of fixed ends $\tau_b=\eta\frac{0.93\pi^2E}{12(1-\nu_e^2)^{\frac{3}{8}}}\left(\frac{t}{r}\right)^{\frac{5}{4}}\left(\frac{r}{l}\right)^{\frac{1}{2}}$ η is, in the case (2), (3) $\eta=\frac{E_s}{E}\left(\frac{1-\nu_e^2}{1-\nu^2}\right)^{\frac{3}{4}}$ iii) Long cylinder when $\left\{\frac{l}{r}>3\left(\frac{r}{t}\right)^{\frac{1}{2}}\right\}$ $\tau_b=\eta\frac{0.272E}{(1-\nu_e^2)^{\frac{3}{4}}}\left(\frac{t}{r}\right)^{\frac{3}{2}}$ where $\eta=\frac{E_s}{E}\left(\frac{1-\nu_e^2}{1-\nu^2}\right)^{\frac{3}{4}}$	219

No.	Graph & Boundary Cond.	Formula or Table of Results	Notes, Ref.
104	Cylinder Uniform external pressure only on side wall Simply supported end 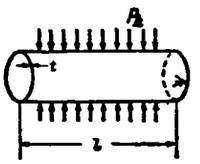	$\sigma_k = K\frac{\pi^2 D}{l^2 t}$ (Batdorf) σ_k Buckling stress in direction of circumference $= p_k r/t$ K = coefficient $D = \frac{Et^3}{12(1-\nu^2)}$ bending stiffness 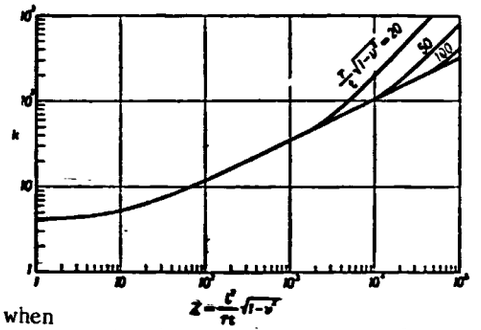 when $100 < Z < 5\left(\frac{r}{t}\right)^2(1-\nu^2)$ $K = 1.04Z^{\frac{1}{2}}$ Comparison with experiments 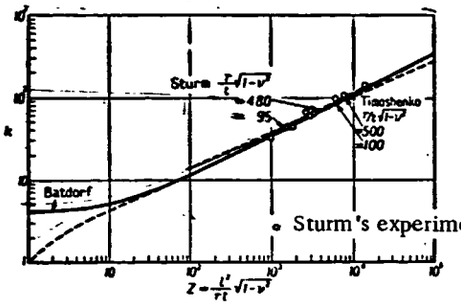 o Sturm's experiment results	179 719
105	Cylinder (cylinder closed at both ends) Uniform external pressure over entire surface, ends simply supported 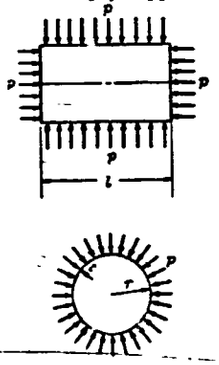	$p_k = C_p\frac{\pi^2 D}{l^2 r}$ (Batdorf) p_k = buckling pressure C_p = coefficient $D = \frac{Et^3}{12(1-\nu^2)}$ bending stiffness 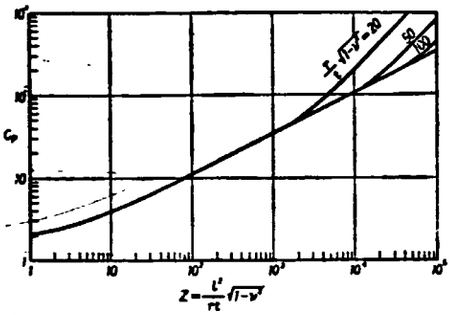	179

No.	Graph & Boundary Cond.	Formula or Table of Results	Notes, Ref.
		Comparison with experiment 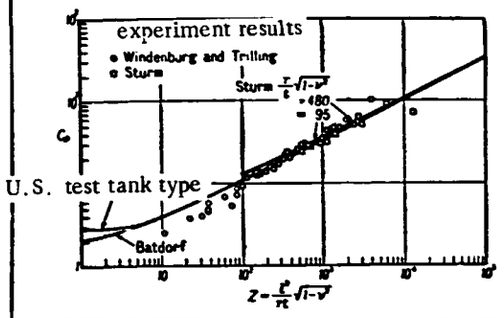 	/635
106	Thin-walled cylinder Water pressure Both ends fixed 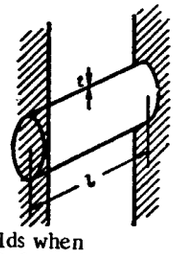 Holds when $m^2 > 1$	$p_k = \frac{1}{\left(\frac{3m^2}{4r} + \frac{r\delta^2}{2} - \frac{3}{4r}\right)} \left\{ \frac{Et^3}{24(1-\nu^2)} \right.$ $\left. \times \left(8\delta^4 + \frac{3m^4}{2r^4} + \frac{4\delta^2 m^2}{r^2} + \frac{4Et\delta^4}{\left\{ 4\delta^2 + \left(\frac{m^2}{r^2}\right) \right\}^2 r^2} \right) \right]$ $\delta = \frac{\pi}{l}$, r = average radius, t = thickness m : wave number in direction of circumference	184
107	Thin-walled cylinder Water pressure Both ends supported	$p = \frac{\frac{Et^3}{48(1-\nu^2)} \left(\delta^2 + \frac{m^2}{r^2}\right)^2 + \frac{Et\delta^4}{4\left\{\delta^2 + \left(\frac{m^2}{r^2}\right)\right\}^2 r^2}}{\left(\frac{m^2}{4r} + \frac{r\delta^2}{8} - \frac{1}{4r}\right)}$ $\delta = \frac{\pi}{l}$ m: wave number in direction of circumference	184
108	Thin-walled cylinder External pressure (water) (considering end conditions) Both ends fixed 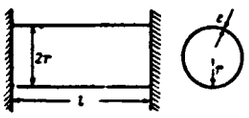	$p_k = \frac{1.382\left(\frac{t}{r}\right)^2 + 0.76\left(\frac{t}{r}\right)^{\frac{5}{2}}\left(\frac{r}{l}\right)}{\left(\frac{l}{r}\right)\left(\frac{r}{t}\right)^{\frac{1}{2}}} \cdot E$	185

No.	Graph & Boundary Cond	Formula or Table of Results	Notes, Ref.
109	Thin walled cylinders External pressure (water pressure) (total surface) 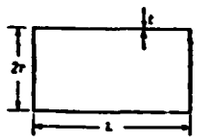	$$p_k = \frac{0.92E\left(\frac{t}{r}\right)^2}{\left(\frac{l}{r}\right)\left(\frac{r}{t}\right)^{\frac{1}{2}} - 0.636}$$	185 /636
110	Cylinder External pressure Plastic buckling 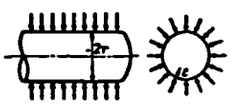	$$\sigma_k = \frac{k\pi^2\eta E}{12(1-\nu^2)} \cdot \left(\frac{t}{2r}\right)^2$$ η = plasticity modulus ($\eta = 1$ in buckling in elasticity region) k = buckling modulus 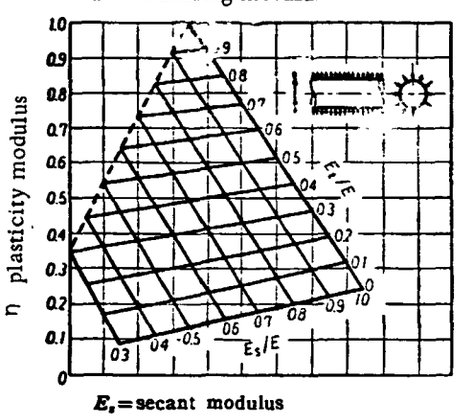 E_s = secant modulus E_t = tangent modulus	182
111	Cylinder External pressure) (side only) Simple support	Donnell's equation is solved adding the transverse shearing force term. $$\varphi = \frac{1-\nu^2}{\pi^2(1+\beta^2)^2} + \alpha\left\{\frac{\pi^2(1+\beta^2)^2}{\beta^4} - 1 - \frac{1+\nu}{1+\beta^2}\right\} \quad (1)$$ where $$\varphi = \frac{(1-\nu^2)p_k \cdot r}{Et}, \quad \alpha = \frac{1}{12}\left(\frac{t}{r}\right)^2, \quad \beta = \frac{nl}{\pi r}$$ assuming also $$W = W_{mn}\sin\left(\frac{m\pi x}{l}\right)\sin\left(\frac{ny}{r}\right), \quad m=1$$	214 Gerard

No.	Graph & Boundary Cond.	Formula or Table of Results	Notes, Ref.

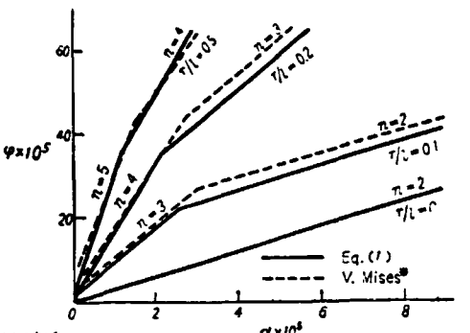

/637

Special case

1) Infinitely long cylinder $\left(\frac{r}{l} \to 0\right)$

in ths in this case, the above equation becomes as follows

$$p_k = \frac{E}{4(1-\nu^2)}\left(\frac{t}{r}\right)^3 \qquad (2)$$

according to Ling's equation

2) Length is finite, but radius is infinitely large

$\left(\frac{t}{r} \to 0,\ \frac{t}{r} \to 0\right)$

in this case, the above equation becomes the equation for a flat plate

* See reference V. D.I.Bd. No. 19 (1914) or Timoshenko "Theory of Elastic Stability" for V. Mises's solution in the graph on the left.

---

112 Cylinder
External pressure
(total surface)

i) $\frac{l^2}{rt} < 100$ の時

$$\sigma_k = \frac{K_p \pi^2 E}{12(1-\nu_e^2)}\left(\frac{t}{l}\right)^2$$

Where K_p as in the following graph.

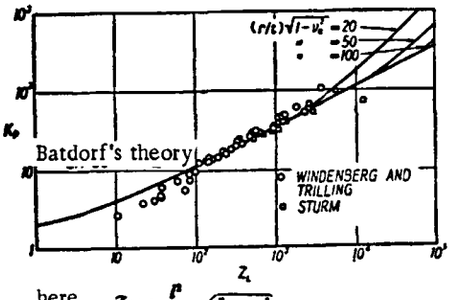

here $Z_L = \frac{l^2}{rt}\sqrt{1-\nu_e^2}$

ii) long cylinder $\left(100\frac{t}{r} < \left(\frac{l}{r}\right)^2 < 5\frac{r}{t}\right)$

either the equation for case i) is used, or the following is used.

$$\sigma_k = 0.93E\left(\frac{t}{r}\right)^{\frac{5}{2}}\left(\frac{r}{l}\right)$$

iii) very long cylinder $\left(\left(\frac{l}{r}\right)^2 > 5\frac{r}{t}\right)$

$$\sigma_k = \eta\frac{0.25E}{(1-\nu_e^2)}\left(\frac{t}{r}\right)^2$$

where $\eta = \frac{E_s}{E}\frac{(1-\nu_e^2)}{(1-\nu^2)}\left(\frac{1}{4}+\frac{3}{4}\frac{E_t}{E_s}\right)$

No.	Graph & Boundary Cond.	Formula or Table of Results	Notes, Ref.
113	Cylinder External pressure Plastic buckling 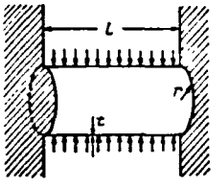 	(a) Long cylinder $\left(\frac{l}{r}\right)^2 > 5\frac{r}{t}$ $\sigma_k = \frac{\eta_y E}{3(1-\nu^2)}\left(\frac{t}{r}\right)^2$ $\eta_y = \left[\frac{1-\nu_e^2}{1-\nu^2}\right]\frac{E_s}{E}\left(\frac{1}{4}+\frac{3}{4}\frac{E_t}{E_s}\right)$ (b) $100\frac{t}{r} < \left(\frac{l}{r}\right)^2 < 5\frac{r}{t}$ $\sigma_k = 0.855\left[\frac{\eta_y E}{(1-\nu_e^2)\nu^4}\right]\left(\frac{t}{l}\right)\left(\frac{t}{r}\right)^{\frac{1}{2}}$ $\eta_y = \left[\frac{1-\nu_e^2}{1-\nu^2}\right]^{\frac{3}{4}} \cdot \frac{E_t}{E}\left(\frac{E_t}{E_s}\right)^{\frac{1}{4}}\left(\frac{1}{4}+\frac{3}{4}\frac{E_t}{E_s}\right)^{\frac{1}{2}}$ (notation) $\eta_y =$ (Plasticity reduction factor) E_t = Tangent modulus E_s = Secant modulus ν_e = Poisson's ratio (value of elasticity range) ≒ 0.3 ν = Poissons' ratio	210 Gerard
114	Cylinder External pressure (only in direction of circumference) **(Radial pressure)**	i) $\frac{l^2}{rt} < 100$ の時 $\sigma_k = \frac{K_y \pi^2 E}{12(1-\nu_e^2)}\left(\frac{t}{l}\right)^2$ Where K_y as shown below. 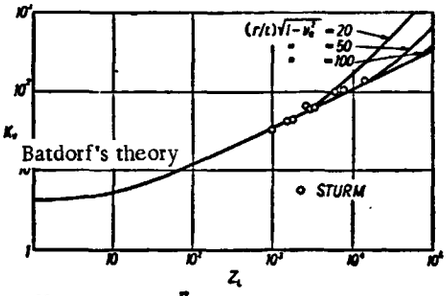 Here $Z_L = \frac{l^2}{rt}\sqrt{1-\nu_e^2}$ ii) Long cylinder $\left(100\frac{t}{r} < \left(\frac{l}{r}\right)^2 < 5\frac{r}{t}\right)$ either the equation in case i) described above, or the following equation is used. $\sigma_k = 0.93E\left(\frac{t}{r}\right)^{\frac{3}{2}}\left(\frac{r}{l}\right)$ iii) very long cylinder $\left(\left(\frac{l}{r}\right)^2 > 5\frac{r}{t}\right)$ $\sigma_k = \eta\frac{0.25E}{(1-\nu_e^2)}\left(\frac{t}{r}\right)^2$ Where $\eta = \frac{E_s}{E}\frac{(1-\nu_e^2)}{(1-\nu^2)}\left(\frac{1}{4}+\frac{3}{4}\frac{E_t}{E_s}\right)$	219

/638

BENDING

No.	Graph & Boundary Cond.	Formula or Table of Results	Notes, Ref.
115	Cylinder Bending	Experiment equation σ_b = maximum bending stress at time of buckling elastic region $\sigma_b = 0.36\frac{Et}{r}$ plastic region $\sigma_b = 0.36\frac{E_s t}{r}$ experiment results (17S-T aluminum alloy) 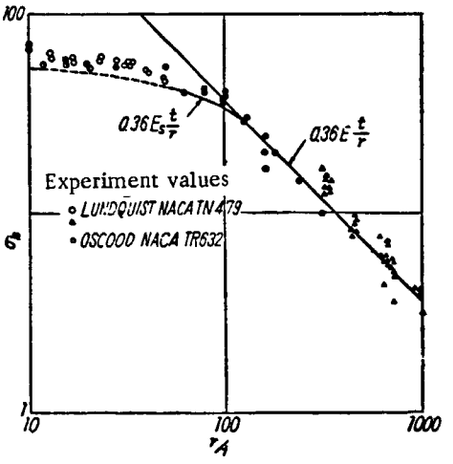 The experiment values are from **Lundquist** : NACA TN 479 and **Osgood** : NACA TR632	204
116	Cylinder Bending	Below is a comparison of the results of Lundquist and Donnell's experiments with Donnell's linear thoery. 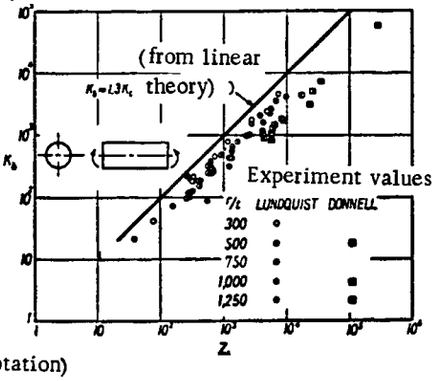 (notation) $Z_L = \frac{l^2}{rt}\sqrt{1-\nu_e^2}$ ν_e = Poisson's ratio (elastic region) = 0.3 $K_b = \frac{\sigma_b \cdot 12(1-\nu_e^2)l^2}{\pi^2 Et^2}$ (this σ_k is the pure flexural buckling stress)	219

No.	Graph & Boundary Cond.	Formula or Table of Results	Notes, Ref.
		$K_c = \frac{\sigma_k \cdot 12(1-\nu_e^2) l^2}{\pi^2 E t^2}$	/640
		(This σ_k is pure compressive buckling stress)	
		In the graph, $K_b = 1.3\ K_c$ is the result obtained by Flugge solving by the linear theory. That is, the maximum bending stress at the time of buckling due to bending is 30% higher than the buckling stress dut to due to pure compression.	

THERMAL BUCKLING

No	Graph & Boundary Cond.	Formula or Table of Results	Notes, Ref.
117	Cylinder Thermal buckling (uniform heating) Both ends fixed (no constraint in direction of axis) From Zuk	Galerkin's method is used in Donnell's equation buckling temperature $T_k = \frac{\pi^4 r^2 l^2 (6 l^4 + 32 l^4 \lambda^2) + 384 l^4 \lambda^4}{12(1-\nu^2)\pi^2 \alpha r^2 l^4 \lambda^2 (7 l^4 - 16 l^2 \lambda^2)}$ T_k = radius r = wall thickness t = length l = linear expansion α = coefficient λ = half wavelength in direction of circumference If the graph of $T_k - \lambda$ is described (during buckling) by inserting the estimated values of λ in the above equation, the minimum value of T_k can be determined. This is the buckling temperature.	213

COMBINED LOADS

(compression and torsion)

No.	Graph & Boundary Cond.	Formula or Table of Results	Notes, Ref.
118	Cylinder Torsion and compression 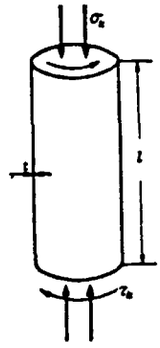 	$K_s = \frac{\tau_k l^2 t}{\pi^2 D}$ (Batdorf, Stein, Schildcrout) $K_x = \frac{\sigma_k l^2 t}{\pi^2 D}$ $D = \frac{E t^3}{12(1-\nu^2)}$; bending stiffness 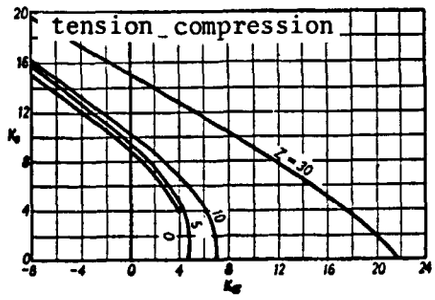 	179

No.	Graph & Boundary Cond.	Formula or Table of Results	Notes, Ref.
		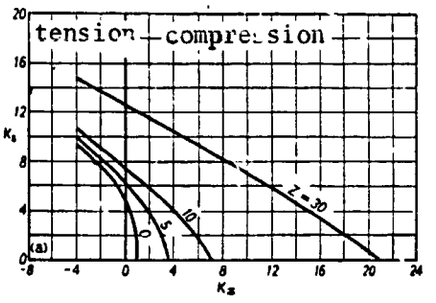 where $Z=\frac{l^2}{rt}\sqrt{1-\nu^2}$	179 /641
119	Cylinder Torsion and Compression 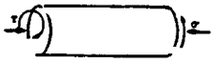	$\left(\frac{\tau_k}{(\tau_k)_{\sigma=0}}\right)^{1.5}+\frac{\sigma_k}{(\sigma_k)_{\tau=0}}=1$ Comparison with experiments 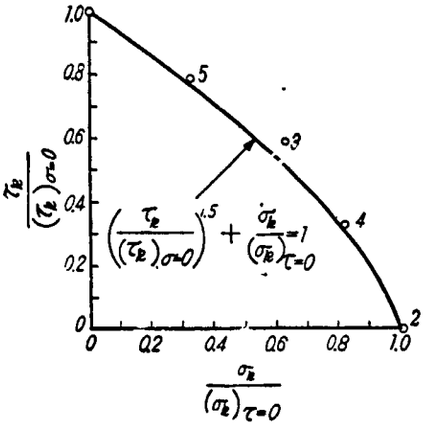	205
120	Cylinder Axial compression and torsion	$R_\sigma+R_\tau^2=1$ (Range of application) i) using the theoretical σ_k, τ_k, when $Z_L\left(=\frac{l^2}{rt}\sqrt{1-\nu_\sigma^2}\right)<1$ end with simple support when $Z_L<5$ Fixed end ii) using the experiment σ_k, τ_k when $<Z_L<7.7\left(\frac{r}{t}\right)^4$ simply supported end when $5<Z_L<7.7\left(\frac{r}{t}\right)^4$ Fixed end	219

No.	Graph & Boundary Cond.	Formula or Table of Results	Notes, Ref.
		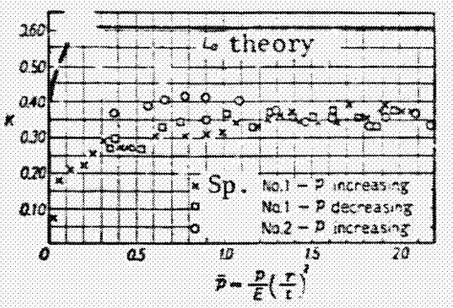	/644
		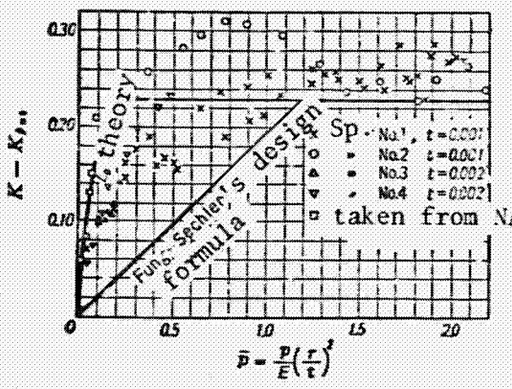 taken from NACATR 1027 Where, Fung-Sechler's specimen is a 24S-H alluminum alloy with l = 11", inside diameter 3.5". There are three thicknesses of 0.001", 0.002" and 0.003".	
	Explanation of photographs 1) shape of buckling when internal pressure is zero $t=0.001"$ $\bar{\sigma}_b=0.063$	Experiment photographs (1)	

No.	Graph & Boundary Cond.	Formula or Table of Results	Notes, Ref.
	2) form of buckling when internal pressure is small $t = 0.001''$ $\bar{p} = 0.309$ $\bar{\sigma}_k = 0.283$	(2)	212 /645
	3) case in which the internal pressure has increased somewhat $t = 0.001''$ $\bar{p} = 0.510$ $\bar{\sigma}_k = 0.269$	(3)	
	4) form of buckling when the internal pressure has become quite large $t = 0.001''$ $\bar{p} = 1.07$ $\bar{\sigma}_k = 0.340$	(4)	

No.	Graph & Boundary Cond.	Formula or Table of Results	Notes, Ref.
	5) form of buckling under high internal pressure $t = 0.001''$ $\bar{p} = 1.89$ $\bar{\sigma}_k = 0.382$	(5) where $\bar{\sigma}_k = \frac{\sigma_k}{E} \cdot \frac{r}{t}$	212 /646
122	Cylinder Compression and internal pressure 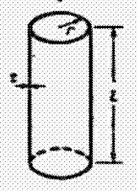 Solution from Lo-Crate-Schwartz	Flugge assumed that the presence of absence of internal pressure was independent of the compressive buckling stress. However, the Lo-Crate and Schwartz established through experiments that this conclusion of Flugge's was incorrect, and employing finite deformation theory, they found the theoretical values and compared them with those found by experiment. 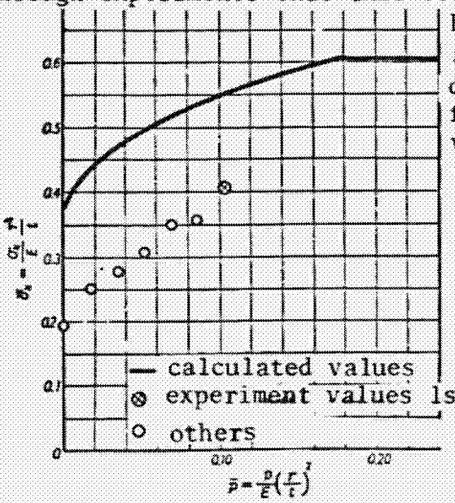 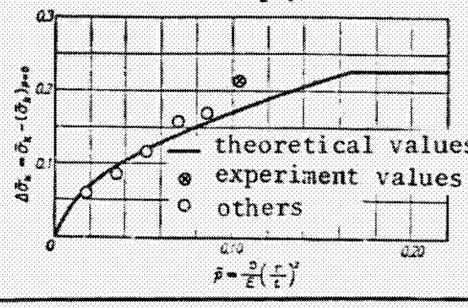 	215

No.	Graph & Boundary Cond.	Formula or Table of Results	Notes, Ref.
		(Specimen)	/647
		1 = 32" inside diameter = 15"	
		t = 0.0249"	
		24S-T aluminum alloy cylinder	
		(Notation)	
		$\bar{p}=\frac{p}{E}\left(\frac{r}{t}\right)^2$	
		$\bar{\sigma}_k=\frac{\sigma_k}{E}\frac{t}{r}$	
		p = internal pressure	
		σ_k = compressive buckling stress	
		E = Young's modulus	
		(Remarks)	
		$\bar{p}$ = 0.169, $\bar{\sigma}_k$ = 0.605 and this agrees with infinitesimal deformation theory. The fact that the theoretical and experimental values do not match can be explained by the following.	
		1) irregularities in producing the test specimen	
		2) non-homogeneity of materials	
		3) absorption of energy by load apparatus	

(COMPRESSION AND EXTERNAL PRESSURE)

No.	Graph & Boundary Cond.	Formula or Table of Results	Notes, Ref.
123	Cylinder External pressure (side wall) and axial compression Both ends simple support Plastic buckling	(Assumptions) 1. For the strain and curvature used to express displacement, thin shell theory in the elastic region is used. 2. The secant shear modulus in the plastic region is defined as $\frac{\text{octahedral shear stress}}{\text{octahedral shear strain}}$ 3. Henchy-Nadai's stress-strain law used. Moreover, it is assumed that the Poisson's ratio (ν) = 1/2. 4. It is assumed that the total cross-section is in the plastic region during infinitesimal buckling. $K_x=\frac{\sigma_x l^2}{\pi^2 E_s t^2}$ axial stress coefficient $K_y=\frac{9\sigma_y l^2}{\pi^2 E_s t^2}$ circumferential stress coefficient	216

No.	Graph & Boundary Cond.	Formula of table of Results	Notes, Ref.

σ_x, σ_y are the stress in the direction of the axis and the circumference during buckling. /648

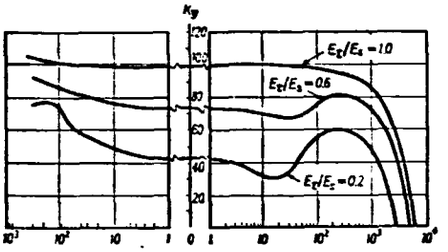

tension K_x Compression K_x

This graph indicates the values of K_x, K_y.... during buckling for the three values of $\frac{E_t}{E_s}=0.2$ when Z = 9,000.

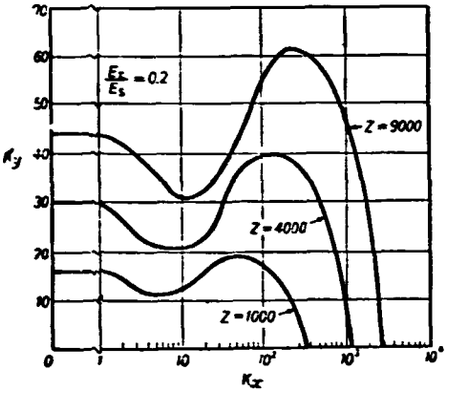

This graph indicates the K_x, K_y during buckling with respect to the three values of Z when E_t/E_s = = 0.2, moreover, the vertical displacement of the shell is

$$W = W_0 \sin\left(\frac{m\pi x}{l}\right) \sin\left(\frac{\pi y}{\lambda}\right)$$

(Notation)

No.	Graph & Boundary Cond.	Formula or Table of Results	Notes, Ref.
		E_s = Secant modulus E_t = Tangent modulus $Z=\frac{\sqrt{3}}{2}\left(\frac{l^2}{rt}\right)$ m = half wave number in direction of axis λ = half wave number in direction of circumference	

INTERNAL PRESSURE AND TORSION

No.	Graph & Boundary Cond.	Formula or Table of Results	Notes,Ref.
124	Cylinder Internal pressure and torsion	Experiment equation $\left(30\frac{t}{d}<\left(\frac{l}{d}\right)^2<5\frac{d}{t}\right)$ $\left(\frac{\tau_k}{(\tau_k)_{p=0}}\right)^2+\frac{p}{(p_k)_{\tau=0}}=1$ (Crate, Batdorf, Baab) when there is internal pressure, τ_k becomes higher.	186
125	Cylinder Torsion and internal pressure	$R_t^2 + R_p = 1$ $R_t = \frac{\text{Acting torsion moment}}{\text{Buckling moment when only torsion is acting}}$ $R_p = \frac{\text{Acting internal pressure}}{\text{Stress at time of buckling when only external pressure is acting}}$	219

/649

BENDING AND TORSION

No.	Graph & Boundary Cond.	Formula or table of Results	Notes,Ref.
126	Cylinder Bending and Torsion	$R_b^{1.5} + R_t^2 = 1$ (Range of Use) All $Z_L\left(=\frac{l^2}{rt}\sqrt{1-\nu_e^2}\right)$ All ends constrained	

No.	Graph & Boundary Cond.	Formula or Table of Results	Notes,Ref.
		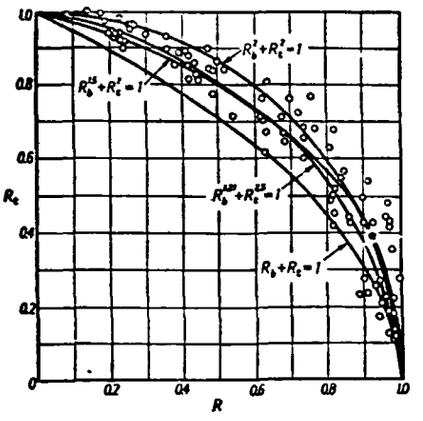	

TENSION AND TORSION

No.	Graph & Boundary Cond.	Formula or Table of Results	Notes,Ref.
127	Cylinder Tension and torsion	$0.4\,R_c + R_t = 1$ (range of use) Using the theoretical value τ_k $\left.\begin{aligned} -1 < R_c < 0 \\ 30 < Z_L < 7.7\left(\frac{r}{t}\right)^2 \end{aligned}\right\}$ where $Z_L = \frac{l^2}{rt}\sqrt{1-\nu_e^2}$	219 end conditions: simple support and fixed

COMPRESSION AND BENDING

No.	Graph & Boundary Cond.	Formula or Table of Results	Notes, Ref.
128	Cylinder Axial compression and bending	$R_c + R_b = 1$ $R_c = \frac{\text{compressive stress}}{\text{Buckling stress in the case only of compression}}$ $R_b = \frac{\text{bending stress}}{\text{Buckling stress in case of only bending}}$ (Range of application) Used for all Z_L $(= \frac{l^2}{rt}\sqrt{1-\nu_e^2})$ all ends constrained	219 /650

SHEAR AND BENDING

No.	Graph & Boundary Cond.	Formula or Table of Results	Notes, Ref.
129	Cylinder Shear and Bending	$R_b + R_s^2 = 1$ Where R_s uses the values 1.25 times greater than the theoretical buckling stress τ_k in the case of torsion alone. This is because the effects of the shear deformation of the cross-section are taken into account. R_s is the ratio between the maximum shear stress due to shearing load and $1.25\tau_k$. The multiple 1.25 appears on the safe side when compared with the experiment results.	219
	(INTERNAL PRESSURE, BENDING AND TORSION)		
130	Cylinder Internal pressure, Bending, torsion	$R_b^2+R_s^2=R_p(1-R_b^2)+1$ $\begin{cases} R_b=\frac{\sigma}{(\sigma_k)_p}, & R_s=\frac{\tau}{(\tau_k)_0} \\ R_p=\frac{p}{p_k} \end{cases}$ σ: maximum external skin compressive stress considering bending and internal pressure $(\sigma_k)_p$: compressive buckling stress when effects of bending and internal are considered τ: shearing stress in direction of circumference $(\tau_k)_0$: shear buckling stress when only the torsion moment is acting p: internal pressure p_k: Buckling pressure 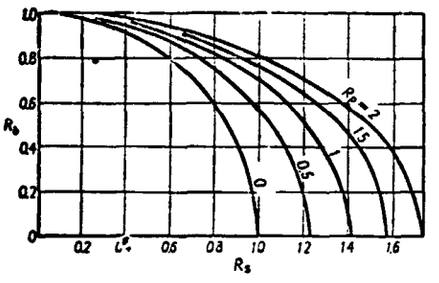 	187

COMPRESSION, BENDING AND TORSION

No.	Graph & Boundary Cond.	Formula or Table of Results	Notes, Ref.
131	Cylinder Compression, bending and torsion	$R_c + R_b + R_t^2 = 1$ $R_c = \frac{\text{compressive stress}}{\text{buckling stress when only compression is acting}}$ $R_b = \frac{\text{bending stress}}{\text{buckling stress when only bending is acting}}$ $R_t = \frac{\text{stress due to torsion}}{\text{buckling stress when only torsion is acting}}$	219 /651

COMPARISON OF THEORY AND EXPERIMENT

No.	Graph & Boundary Cond.	Formula or Table of Results	Notes, Ref.
132	Cylinder Comparison of linear buckling theory and experiment values	(a) axial compression: K_c (b) torsion: K_t (c) external radial pressure: K_y	219

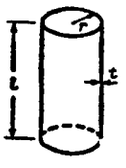

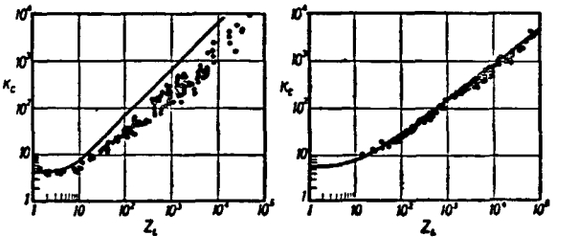

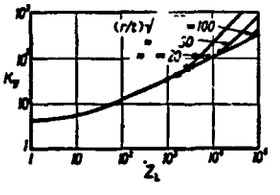

(Notation)

$$K_c = \frac{\sigma_b \cdot 12(1-\nu_e^2)l^2}{\pi^2 E t^2}$$

$$K_t = \frac{\tau_b \cdot 12(1-\nu_e^2)l^2}{\pi^2 E t^2}$$

$$K_y = \frac{\sigma_y \cdot 12(1-\nu_e^2)l^2}{\pi^2 E t^2} \quad \text{where} \quad \sigma_y = \frac{pr}{t}$$

No.	Graph & Boundary Cond.	Formula or Table of Results	Ref,Notes
		$Z_L=\frac{l^2}{rt}\sqrt{1-\nu_e^2}$ ν_e = Poisson's ratio (elastic region)=0.3	

ELLIPTICAL CYLINDERS (supplement)
Bending

No.	Graph & Boundary Cond.	Formula or Table of Results	Notes,Ref.
133	Elliptical cylinders Bending 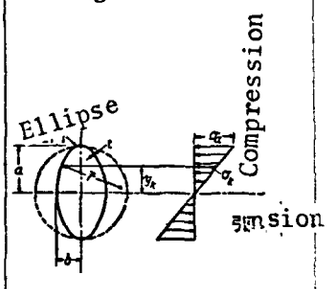 y_k = distance from NA (y coordinate) of point where buckling occurs on cross-section $\bar{r} = y_k$ radius of curvature of point $\frac{y_k}{a}$ may also be written $(y/a)_k$.	Method of calculating flexural buckling stress (1) $S_a = \pi a^2 t$ is found. The cross-section of the circular cross-section covered by the ellipse (2) $S_e = (S_e/S_a)S_a$ found from the graph below. 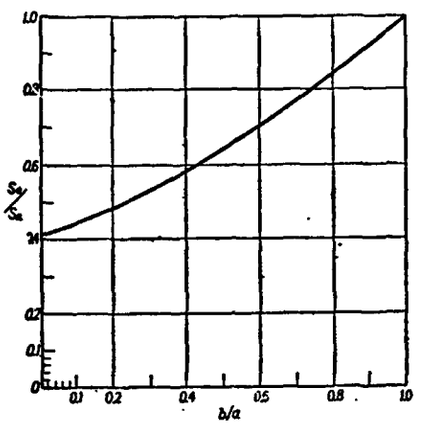 (3) $\left(\frac{\bar{y}}{a}\right)_k$ and $\frac{\bar{r}}{a}$ found from the graph below. 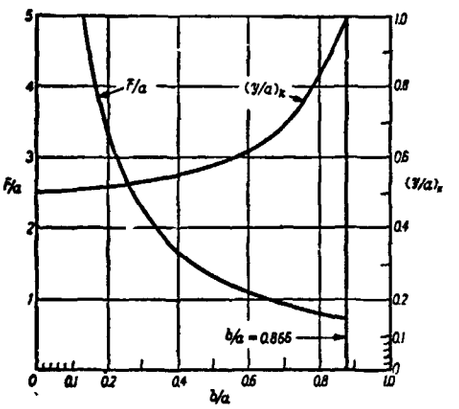 	219 /652

No.	Graph & Boundary Cond.	Formula or Table of Results	Notes, Ref.

WHERE

$\bar{r}$ = buckling curvature radius

when $\frac{b}{a} > 0.866$, the buckling occurs on the long axis end and $\bar{r} = a$.

$\left(\frac{y}{a}\right)_k$ is a non-dimensional quantity in expressing the position where buckling occurs.

(4) Distress occurring at the position of buckling curvature is found in the following equation.

$$\sigma_{yk} = M\left(\frac{y}{a}\right)_k \left(\frac{1}{S_x}\right)$$

where M = bending moment /653

(5) for a long elliptical cylinder, the buckling stress at the buckling curvature is determined from the following equation.

$$\sigma_k = C_b E \frac{t}{\bar{r}}$$

C_b found from the graph below.

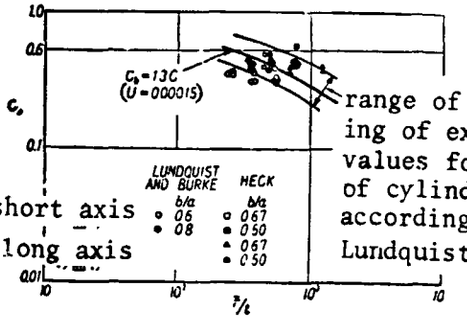

range of scattering of experiment values for bending of cylinder according to Lundquist

bending around short axis

bending around long axis

This indicates the results of experiments on aluminum alloy elliptical cylinders by Lundquist-Burke and Heck. The experiment values collect in the vicinity of the experiment values for a cylinder.

Comparison of experiment values $\left(250 < \frac{\bar{r}}{t} < 750\right)$ and

$\frac{\bar{r}}{t} = 500$ experiment equation

No.	Graph & Boundary Cond.	Formula or Table of Results	Notes, Ref.

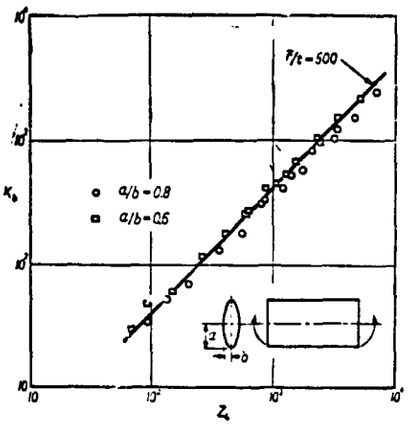

(Notation)

$$K_b = \frac{\sigma_b \cdot 12(1-\nu_e^2)r^2}{\pi^2 E t^2}$$

$$Z_L = \frac{l^2}{rt}\sqrt{1-\nu_e^2}$$

ν_e = Poisson's ratio (elasticity region) = 0.3

Method of determining the place and magnitude of the/654 buckling curvature radius

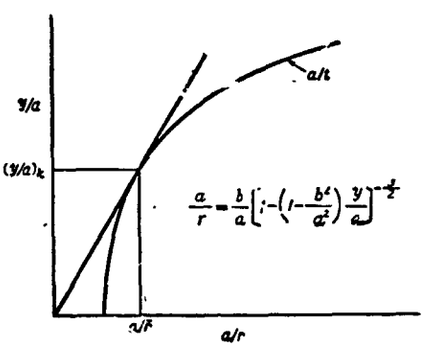

SPHERICAL SHELLS (supplement)

External Pressure

No.	Graph & Boundary Cond.	Formula or Table of Results	Notes, Ref.
134		H. S. Tsien used the energy method. Compared with the theory, his approach is better than that in that he takes jump-over into consideration.	201

No.	Graph & Boundary Cond.	Formula or Table of Results	Notes, Ref.

Spherical shells
External pressure

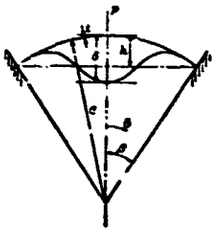

Moreover, the external pressure is constant before and after buckling. In order for buckling to occur, it is first necessary for the potential energies before and after buckling to be equal. Expressing the total potential energy W as dimensionless

$$W'=\frac{W_e}{\pi E t^3}=\frac{23-9\nu}{126(1-\nu)\alpha}y^4-\frac{(3-\nu)}{9(1-\nu)}y^3$$
$$+\left\{\frac{7-2\nu}{45(1-\nu)}\alpha-\frac{2}{3}z+\frac{8}{9(1-\nu^2)\alpha}\right\}y^2-(1-\nu)\alpha x^2$$

where

$$\begin{cases} z=\dfrac{pa^2}{2Et^2} \\ y=\dfrac{\delta}{t} \\ \alpha=\dfrac{a\beta^2}{t} \end{cases}$$

Therefore, assuming that W' are equal where y = 0 and y = y,

$$\frac{23-9\nu}{42(1-\nu)\alpha}y^2-\frac{3-\nu}{3(1-\nu)}y+\left\{\frac{7-2\nu}{15(1-\nu)}-2z\right.$$
$$\left.+\frac{8}{3(1-\nu^2)\alpha}\right\}=0 \qquad (1)$$

Moreover, denoting the state of equilibrium after buckling by y_e, this is expressed as follows.

$$y_e=\frac{1}{23-9\nu}\left[\frac{21(3-\nu)}{4}\alpha+\sqrt{\frac{7}{80}(259-146\nu+27\nu^2)\alpha^2+42(1-\nu)(23-9\nu)\alpha x-56\frac{(23-9\nu)}{1+\nu}}\right] \qquad (2)$$

From (1), (2), the relation between α and x becomes as follows.

assuming $\left(\nu=\frac{1}{3}\right)$.

$$9\alpha^2x^2-\left(\frac{29}{10}\alpha^2+27\right)\alpha x+\left(\frac{19}{1200}\alpha^4+\frac{87}{20}x^2+\frac{81}{4}\right)=0$$

this is, for minimum value of the curve on this graph indicates the buckling load.

No.	Graph & Boundary Cond.	Formula or Table of Results	Notes, Ref.

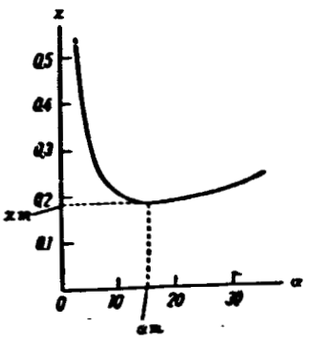

Below we give a comparison of the results of these two people [Tr. note: not mentioned previously], the theoretical values and Tsien's theory.

	Experiment values	Theoretical values Yoshimura-Uemcura	Tsien
z_m	0.154	0.1835	0.1581
y_m	12.5	14.0	16.6
α_m	14.7	15.0	19.0

No.	Graph & Boundary Cond.	Formula or Table of Results	Notes, Ref.
135	Spherical shell external pressure	Special research has been devoted to the phenomenon of Durchschlag (Oilcanning). That is, the process of buckling is considered, taking into account the energy barrier from the point of view of static energy, and the drop in buckling load in the experiments is expalined by introducing the concept of initial deflection caused by jumping over the energy barrier.	202 /656

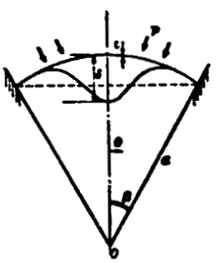

1) Upper buckling pressure x_a

x_a determined by the following equation.

$$x_a = 21(3-\nu)\{80(23-9\nu)+(7-\nu)(1-\nu^2)\alpha^2\}\alpha \times \frac{(1+\nu)\sqrt{\frac{7D^2}{15}}}{18(1-\nu^2)(23-9\nu)^2\alpha^2}$$

No.	Graph & Boundary Cond.	Formula or Table of Results	Notes, Ref.
		Where $D \equiv (301-194\nu+33\nu^2)\alpha^2 - \frac{160(23-9\nu)}{1+\nu}$ $\alpha = \frac{a\beta^2}{t}$ $z = \frac{pa^2}{2Et^2}$ $y = \frac{\delta}{t}$ This x_a becomes minimum in the case of $\alpha = \alpha_0$ given by the following equation. $\sqrt{(301-194\nu+33\nu^2)\alpha_0^2 - \frac{160(23-9\nu)}{1+\nu}} = \frac{3\sqrt{105}(3-\nu)\alpha_0\{80(23-9\nu)-(7-\nu)(1-\nu^2)\alpha_0^2\}}{(1+\nu)(301-194\nu+33\nu^2)\alpha^2+320(23-9\nu)}$ Moreover, oilcanning occurs in the following case $\alpha^2 > \alpha_0^2 = \frac{160(23-9\nu)}{(1+\nu)(301-194\nu+33\nu^2)}$ 2) Lower buckling pressure x_c $x_c = \frac{7(3-\nu)\{80(23-9\nu)+(7-\nu)(1-\nu^2)\alpha^2\}\alpha}{60(1-\nu)^2(23-9\nu)^2\alpha}$	
		Next, considering the buckling under external pressure under a spherical shell having initial deflection, the buckling load is given by the following equation. $x_{\substack{\max \\ \min}} = \frac{4,725\{7(3-\nu)\alpha-2(23-9\nu)y_0\}D_1 \pm \nu\sqrt{D_2}}{233,500(1-\nu)(23-9\nu)^2\alpha^2}$ where $D_1 = (7-\nu)(1-\nu)\alpha^2 + \frac{80(23-9\nu)}{1+\nu}$ $D_2 = 20(23-9\nu)^2y_0^2 - 140(3-\nu)(23-9\nu)y_0\alpha + 7\left[(301-194\nu+33\nu^2)\alpha^2 - \frac{160(23-9\nu)}{1+\nu}\right]$ subscript "0" expresses the initial state.	

No.	Graph & Boundary Cond.	Formula or Table of Results	Notes, Ref.
		$\alpha = \frac{a\beta^2}{t}$ $z = \frac{pa^2}{2Et^2}$ $y = \frac{\delta}{t}$	

N	Graph & Boundary Cond.	Formula or Table of Results	Notes, Ref.
136	Thin-walled spherical cylinder shell External pressure 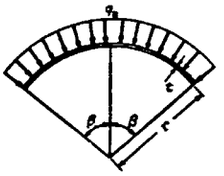 Solution by Beiss	$\begin{cases} \rho = 2C\frac{\beta^2 r}{t} \\ Q_k = 2\frac{Cq_k r^2}{Et^2} \end{cases}$ Where ρ = geometric parameter Q_k = loading parameter $C = \sqrt{\frac{3(1-\nu^2)}{2}}$ E = Young's modulus q_k = buckling external pressure ν = Poisson's ratio 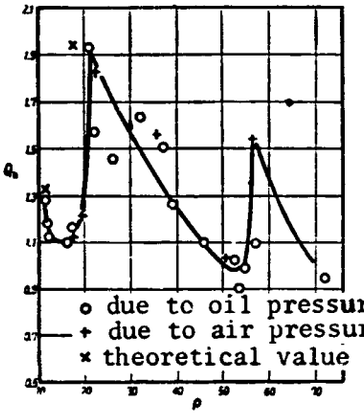 o due to oil pressure (initial load) + due to air pressure × theoretical value $\nu = 0.32$ 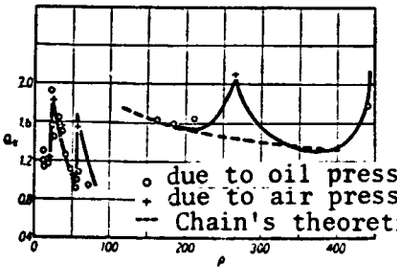 o due to oil pressure (initial load) + due to air pressure --- Chain's theoretical values	217 /657

No.	Graph & Boundary Cond.	Formula or Table of Results	Notes, Ref.
137	Spherical shell External pressure Plastic buckling	$\sigma_h = \frac{\eta E}{\sqrt{3(1-\nu_e^2)}} \frac{t}{r}$ $\eta = \left(\frac{1-\nu_e^2}{1-\nu^2}\right)^{\frac{1}{2}} \frac{E_s}{E} \left(\frac{E_t}{E_s}\right)^{\frac{1}{2}}$ (Notation) η = plasticity reduction factor E_t = tangent modulus E_s = secant modulus ν_e = Poisson's ratio (value in elastic region) = 0.3 ν = Poisson's ratio (plastic region)	210 Gerard
138	Spherical shell external pressure 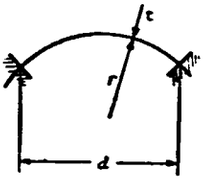 	In the elastic region, for all the $\sigma_h = \frac{K_p \pi^2 E}{12(1-\nu_e^2)} \left(\frac{t}{d}\right)^2$ where K_p found from the graph below. 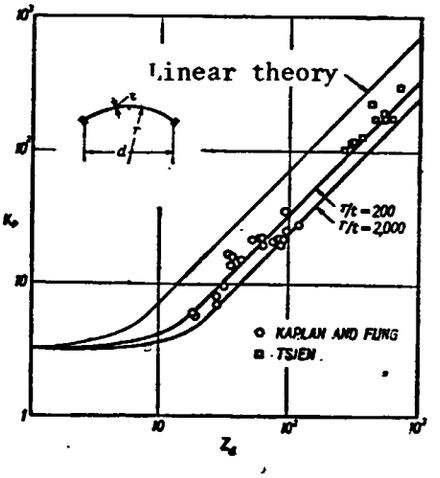 Here $Z_d = \frac{d^2}{rt}\sqrt{1-\nu_e^2}$ also in the case of $U_0 = \square\square$, the following equation may be used. $\eta = \frac{F_s}{E}\left[\frac{E_t}{E_s}\frac{(1-\nu_e^2)}{(1-\nu^2)}\right]^{\frac{1}{2}}$	219 /658

No.	Graph & Boundary Cond.	Formula or Table of Results	Notes, Ref.
		Where C determined from the following graph, 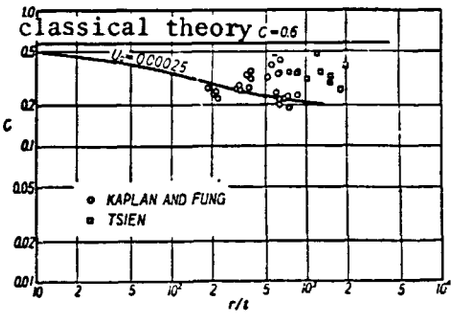 Here U_0 = uneveness factor and $\eta = \frac{E_s}{E}\left[\frac{E_t}{E_s}\cdot\frac{(1-\nu_s^2)}{(1-\nu^2)}\right]^{\frac{1}{3}}$	

No.	Graph & Boundary Cond.	Formula or Table of Results	Notes, Ref.
	CIRCULAR ARC SECTION CYLINDERS (supplement)		
	Bending		/659
139	Circular arc section cylinder Bending 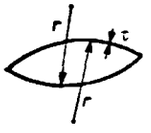	For long circular arc section cylinders $\sigma_k = 0.285\, E\frac{t}{r}$ Where r = radius of curvature of each arc within doublet	219
	SHELLS WITH HYPERBOLIC PARABOLOID SURFACE		
	Buckling Due to Dead Weight		
140	Shell with hyperbolic paraboloid surface (saddle type) (buckling due to dead weight) $z = C\frac{x}{a}\cdot\frac{y}{b}$ when a = b	$P_0 = \frac{4E\beta^2 P}{\sqrt{12(1-\nu^2)}}\frac{C}{b^4}$ P_0: weight (dead weight) per unit surface area $\beta = \frac{h}{C}$	197

No.	Graph & Boundary Cond.	Formula or Table of Results	Notes, Ref.
	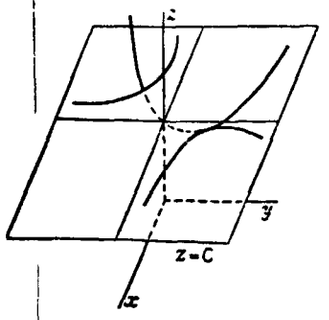	h : shell thickness (uniform) P: buckling load coefficient P is given by the function of β. 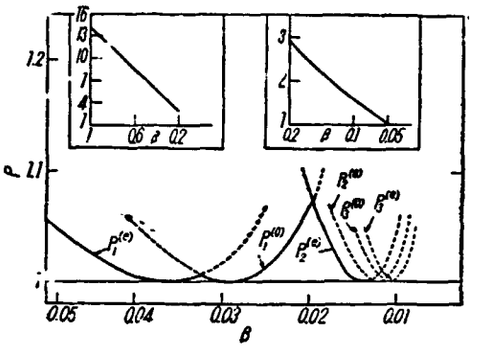	

REINFORCED CURVED PLATES (supplement)
Compression

No.	Graph & Boundary Cond.	Formula or Table of Results	Notes, Ref.
141	Reinforced curved plates Compression End revolving around straight edge 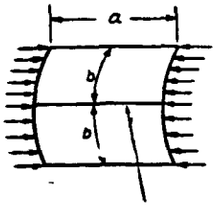 reinforcement	$\sigma_k = \frac{K\pi^2 E}{12(1-\nu_e^2)}\left(\frac{t}{b}\right)$ 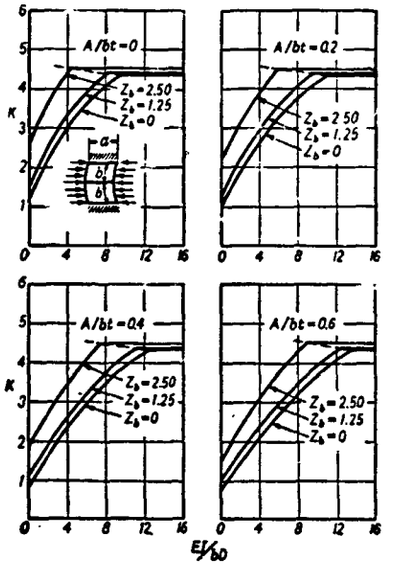 when (a) a/b = 4/3	218 /660

No	Graph & Boundary Cond.	Formula or Table of Results	Notes, Ref.

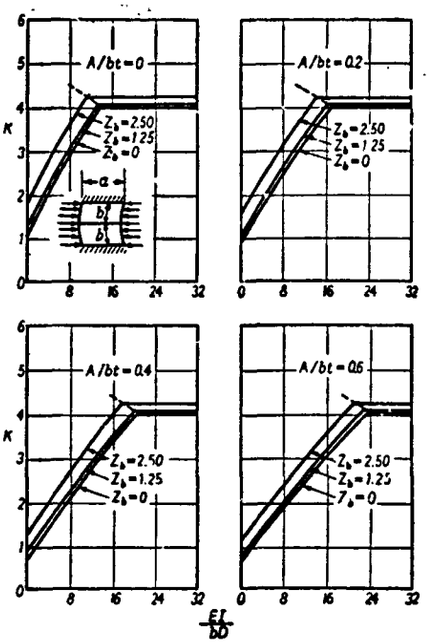

(b) when $\frac{a}{b} = 2$

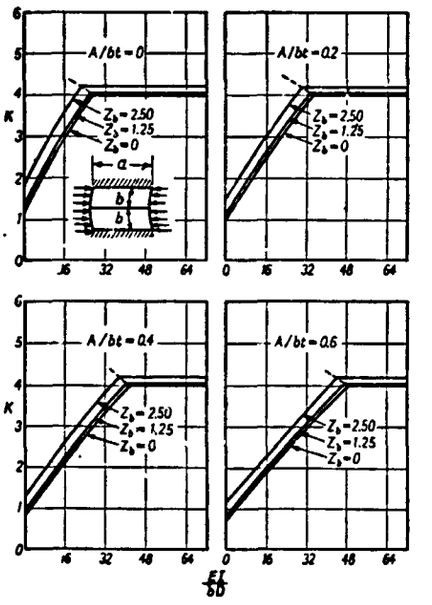

(c) when $\frac{a}{b} = 3$

/661

No.	Graph & Boundary Cond.	Formula or Table of Results	Notes, Ref.
		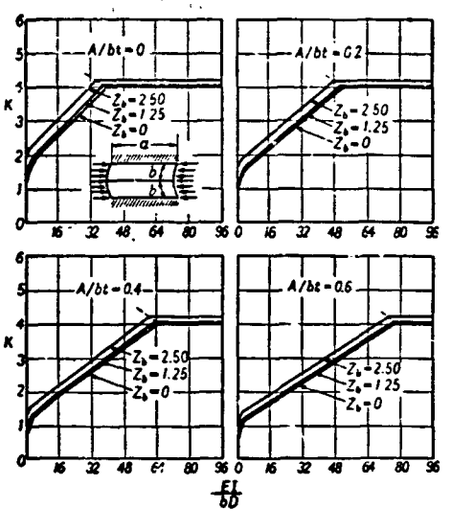	
		(d) when $\frac{a}{b} = 4$	
		(notation)	
		K = coefficient A = cross-section area of reinforcement t = thickness Z_b = plate curvature parameter $=\frac{b^2}{rt}\sqrt{1-\nu_e^2}$ /662 D = bending stiffness of plate per unit width $=\frac{Et^3}{12(1-\nu_e^2)}$ r = radius of curvature of curved plate E = Young's modulus I = moment of inertia of reinforcement cross-section ν_e = Poisson's ratio (elastic region)	

SHEAR

No.	Graph & Boundary Cond.	Formula or Table of Results	Notes, Ref.
142	Reinforced curved plate (shear) 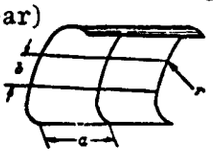	$\tau_b = KE\left(\frac{t}{b}\right)^2$ $K = 5.25 + \left(\frac{\pi}{4}\right)\left(\frac{b}{a}\right)^2 S^{\frac{1}{2}}$ $S = \frac{a^2}{rt}$ (shell parameter)	192

No.	Graph & Boundary Cond.	Formula or Table of Results	Notes, Ref.
143	Curved plate Shear	Results of Chiarito's experiment (24S-T)	209

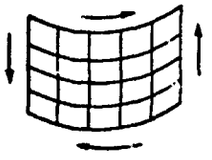

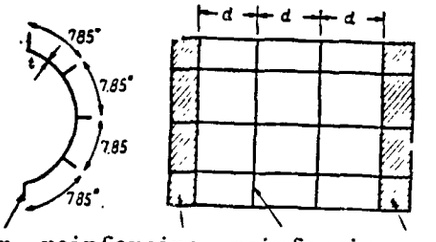

Specimen	t in.	d in.	Reinforcing hoop cr. sec.	Reinforcing hoop Dim. (in.)	Stringer cr. sec.	Stringer Dim. (in.)
1	0.0154	15.0	Z	$\frac{9}{16}\times\frac{9}{16}\times 0.040$	L	$\frac{3}{4}\times\frac{3}{4}\times\frac{3}{32}$
2	0.0145	7.5	L	"	L	"
3	0.0143	7.5	Z	"	L	"
6	0.0154	15.0	Z	$\frac{11}{16}\times\frac{3}{4}\times 0.064$	L	"
7	0.0395	7.5	Z	$\frac{11}{16}\times\frac{3}{4}\times 0.080$	L	"
8	0.0150	15.0	Z	$\frac{11}{16}\times\frac{3}{4}\times 0.051$	L	"
10	0.0154	1".0	Z	$\frac{11}{16}\times\frac{3}{4}\times 0.040$	L	"

Experiment values (KSI = 10^3 lb/in^2) | 208 | /663

Specimen	τ_b (KSI) (a)	(b)	(c)	τ_{all} (KSI)	Form of failure
1	1.40	5.22	1.63	18.95	A
2	1.82	3.45	2.00	20.45	B
3	1.50	3.75	2.50	25.00	A
6	0.93	2.32	2.09	22.75	A
7	7.10	14.20	7.10	24.90	B
8	1.43	2.14	2.02	22.20	A
10	1.76	2.29	2.23	17.65	B

No.	Graph & Boundary Cond.	Formula or Table of Results	Notes, Ref.
		(a) when buckling occurs first in some panel (b) when all panels of the center stringers buckle (c) when buckling first occurs in the center stringers A with web cracks, buckling of reinforcing hoop and stringers B no web cracks, buckling of both reinforcing hoops and stringers	
144	Reinforced curved plate Shear Simple support 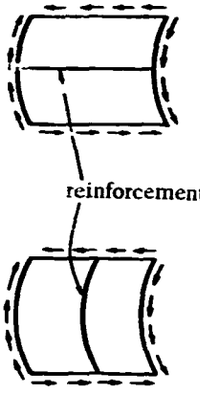 	$\tau_b = K\frac{\pi^2 E}{12(1-\nu_e^2)}\left(\frac{t}{b}\right)^2$ 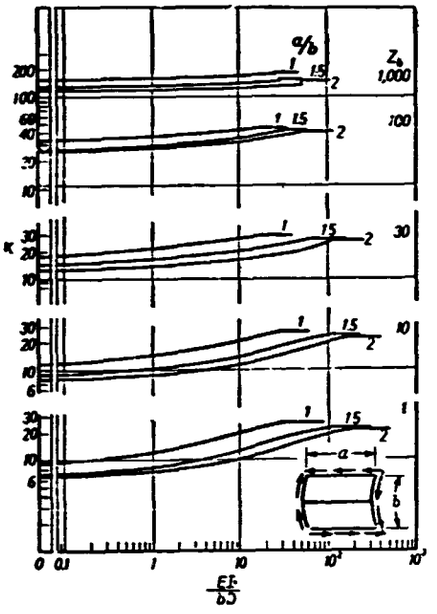 (a) reinforcement in direction of center axis Case in which the length in the direction of the axis is greater than the width in the direction of the circumference	218

No.	Graph & Boundary Cond.	Formula or Table of Results	Notes, Ref.

/664

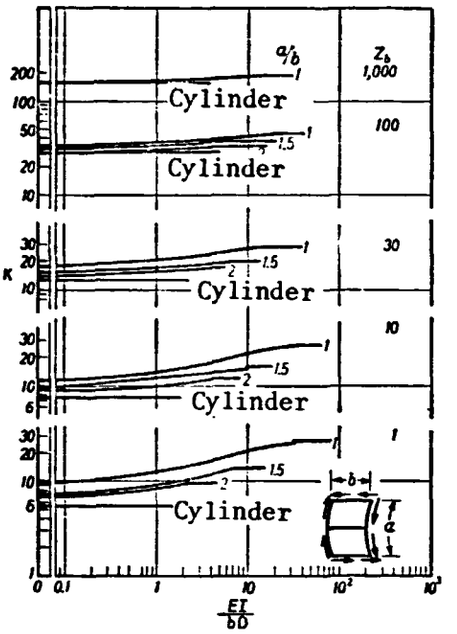

(b) reinforcement in direction of center axis Case in which the width in the direction of the circumference is greater than length in direction of axis

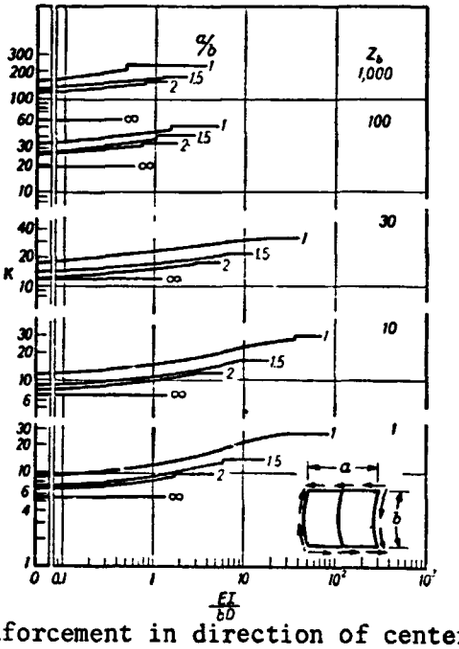

(c) Reinforcement in direction of center of circumference. Case in which the length in the direction of the axis is greater than width in the direction of the circumference.

No.	Graph & Boundary Cond.	Formula or Table of Results	Notes, Ref.

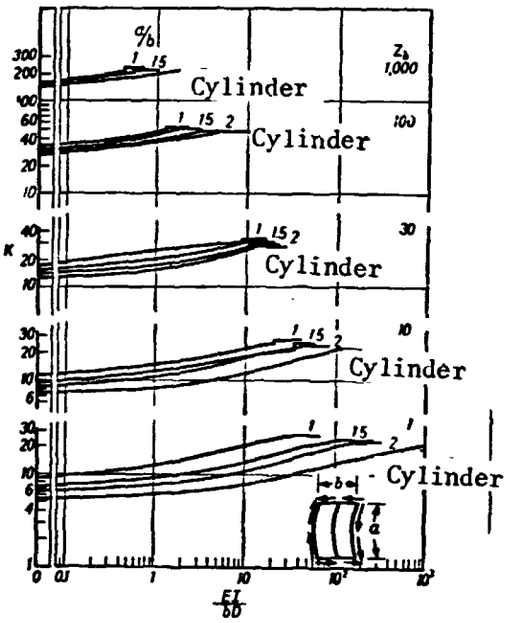

/665

(d) Reinforcement in direction of central circumference. Case in which the width in the direction of the circumference is greater than the length in the direction of the axis.

(Notation)

K = coefficient
t = thickness
Z_b = plate curvature parameter
$= \frac{b^2}{rt}\sqrt{1-\nu_e^2}$
D = bending stiffness of plate per unit width
$= \frac{Et^3}{12(1-\nu_e^2)}$
r = radius of curvature of curved plate
E = Young's modulus
ν_e = Poisson's ratio (elastic region)
I = moment of inertia of reinforcement cross-section

REINFORCED CYLINDERS(supplement)

Torsion

No.	Graph & Boundary Cond.	Formula or Table of Results	Notes,Ref.
145	Reinforced cylinders Torsion Simple support 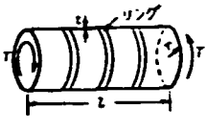 	Theoretical equation $\tau_k = \frac{T}{2\pi r^2 t} = K\frac{\pi^2 D}{l^2 t}$ Reinforced by rings placed at same equal intervals as when the torsion stiffness is zero. Solution for K by Galerkin's method, adding the term expressing the bending stiffness of the ring to the equilibrium equation for a circular columnar curved plate. T_k: shear buckling stress K : coefficient T : torsion moment $D = \frac{Et^3}{12(1-\nu^2)}$: bending stiffness of outer wall of cylinder 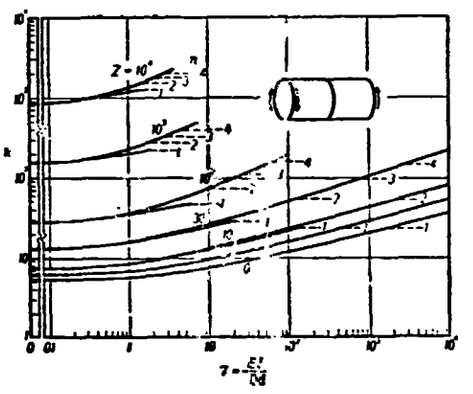 n = number of rings I = effective geometric moment of inertia of rings $d = \frac{l}{n+1}$ $Z = \frac{l^2}{rt}\sqrt{1-\nu^2}$ ν = Poisson's ratio	188 /666

No.	Graph & Boundary Cond.	Formula or Table of Results	Notes, Ref.
		Compared with the experiment values, the τ_k of the experiment values is about 15% lower. Comparison with experiment. 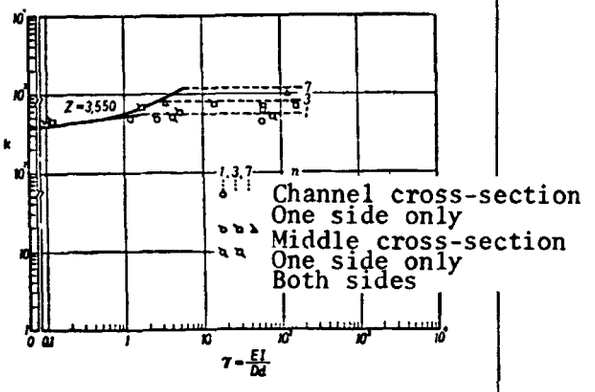	

EXTERNAL PRESSURE

No.	Graph & Boundary Cond.	Formula or Table of Results	Notes, Ref.
146	Reinforced cylinder External pressure (simultaneously in direction of circumference and in direction of axis) 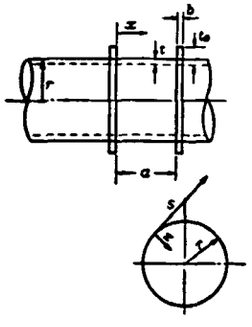 Found from the minimum conditions of total potential	1) When the stiffness of the reinforcing rings is infinitely large When the displacement can be expressed as follows $u = A\cos\frac{ms}{r}\sin 2\delta x$ $v = B\sin\frac{ms}{r}(1-\cos 2\delta x)$ $w = C\cos\frac{ms}{r}(1-\cos 2\delta x)$ Where A,B.C.: arbritrary constants m: number of waves in direction of circumference $\delta = \frac{n\pi}{a}$ For simplification, the following notation is introduced	189 /667

No.	Graph & Boundary Cond.	Formula or Table of Results	Notes, Ref.

$$k_1=\frac{Et}{2(1-\nu^2)} \qquad k_{12}=\frac{4(1-\nu)\delta^2m^2\pi a}{r}$$

$$k_2=2\delta^2\pi ra \qquad k_{13}=\frac{Et}{4(1+\nu)}$$

$$k_3=\frac{3m^2\pi a}{2r} \qquad k_{14}=\frac{m^2\pi a}{2r}$$

$$k_4=\frac{3\pi a}{2r} \qquad k_{15}=2\delta m\pi a$$

$$k_5=2\nu\delta m\pi a \qquad k_{16}=2\delta^2\pi ra$$

$$k_6=2\nu\delta\pi a \qquad k_{17}=\frac{3pm^2\pi a}{4}$$

$$k_7=\frac{3m\pi a}{r} \qquad k_{18}=\frac{3p\pi a}{4}$$

$$k_8=\frac{Et^3}{24(1-\nu^2)} \qquad k_{19}=pr\delta\pi a$$

$$k_9=8\delta^4\pi ra \qquad k_{20}=\frac{p\delta^2\pi r^2a}{2}$$

$$k_{10}=\frac{3m^4\pi a}{2r^3} \qquad k_{21}=\frac{3\pi a}{2r^3}$$

$$k_{11}=\frac{4\nu\delta^2m^2\pi a}{r} \qquad k_{22}=\frac{3m^2\pi a}{r^3}$$

Moreover

$$k_{23}=2k_1k_2+2k_{12}k_{14}$$
$$k_{24}=-k_1k_5-k_{13}k_{15}$$
$$k_{25}=k_1k_6+k_{13}$$
$$k_{26}=2k_1k_3+2k_{13}k_{16}$$
$$k_{27}=-k_1k_7$$
$$k_{28}=2k_1k_4+2k_3k_9+28_4k_{10}+2k_1k_{21}-2k_9k_{22}+2k_9k_{11}+2k_9k_{12}-2k_{17}+2k_{18}-2k_{20}$$

The buckling condition in the equation becomes as follows

$$\begin{vmatrix} k_{23} & k_{24} & k_{25} \\ k_{24} & k_{26} & k_{27} \\ k_{25} & k_{27} & k_{28} \end{vmatrix}=0$$

In this matrix, assuming n = 1, the buckling pressure can be determined if one finds the minimum value of p for the variable end. 189 /668

2) Case in which the stiffness of the reinforcing rings is finite

The displacement is

No.	Graph & Boundary Cond.	Formula or Table of Results	Notes, Ref.

$$u = A\sin\frac{ms}{r}\sin 2\delta x + B\sin\frac{ms}{r}\cos\delta x + C\cos\frac{ms}{r}\sin 2\delta x + D\cos\frac{ms}{r}\cos\delta x + \frac{Fx}{a}$$

$$v = \sin\frac{ms}{r}(G + H\sin 2\delta x + J\cos 2\delta x)$$

$$w = \left(K\sin\frac{ms}{r} + M\cos\frac{ms}{r}\right)(1-\cos 2\delta x) + N$$

Now, for simplification

$$k_1 = \frac{Et}{2(1-\nu^2)} \qquad k_{22} = \frac{3m^2\pi a}{r^3}$$

$$k_2 = 2\delta^2\pi ra \qquad k_{24} = \frac{4(1-\nu)\delta^2m^2\pi a}{r}$$

$$k_3 = \frac{\delta^2\pi ra}{2} \qquad k_{25} = \frac{Et}{4(1+\nu)}$$

$$k_4 = \frac{2\pi r}{a} \qquad k_{26} = \frac{8m^2a}{3r}$$

$$k_5 = \frac{8\delta\pi r}{3} \qquad k_{27} = 2\delta^2\pi ra$$

$$k_6 = \frac{m^2\pi a}{r} \qquad k_{28} = 2\delta m\pi a$$

$$k_7 = \frac{m^2\pi a}{2r} \qquad k_{29} = \frac{16m\pi}{3}$$

$$k_8 = \frac{3\pi a}{2r} \qquad k_{30} = \frac{3m^2\pi ap}{4}$$

$$k_9 = \frac{2\pi a}{r} \qquad k_{31} = \frac{3\pi ap}{4}$$

$$k_{10} = 4\nu\pi m \qquad k_{32} = \pi ap$$

$$k_{11} = 2\delta m\pi a\nu \qquad k_{33} = \delta\pi apr$$

$$k_{12} = \frac{4\nu\pi m}{3} \qquad k_{34} = \frac{8\delta pra}{3}$$

$$k_{13} = 2\delta\pi\nu a \qquad k_{35} = 2\pi rp$$

$$k_{14} = \frac{16\nu\pi}{3} \qquad k_{36} = \frac{\pi r^2a\delta^2p}{2}$$

$$k_{15} = \frac{2\pi a}{r^3} \qquad k_{37} = -\frac{bt_2E}{2}$$

$$k_{16} = -\frac{2m\pi a}{r} \qquad k_{38} = \frac{\pi m^2}{r^4}$$

$$k_{17} = -\frac{2\pi a}{r} \qquad k_{39} = \frac{2m^2\pi r_1^3}{r^4}$$

$$k_{18} = \frac{Et^3}{24(1-\nu^2)} \qquad k_{40} = \frac{2\pi}{r_1}$$

$$k_{19} = 8\delta^4\pi ra \qquad k_{41} = b\pi p$$

$$k_{20} = \frac{3m^4\pi a}{2r^3} \qquad k_{42} = \frac{E^2t^3}{24r^4}$$

$$k_{21} = \frac{4\nu\delta^2m^2\pi a}{r} \qquad k_{43} = m^4\pi r_1$$

$$k_{22} = \frac{3\pi a}{3r^3}$$

No.	Graph & Boundary Cond.	Formula or Table of Results	Notes, Ref.
			189

Furthermore

$$h_{44}=2h_1h_2+2h_{23}h_7$$
$$h_{45}=h_1h_5+h_{23}h_{26}$$
$$h_{46}=h_1h_{13}+h_{32}$$
$$h_{47}=2h_1h_3+2h_{23}h_7+2h_{42}h_{43}$$
$$h_{48}=h_1h_{14}+h_{34}$$
$$h_{49}=h_1h_{11}+h_{23}h_{26}$$
$$h_{50}=h_1h_{12}+h_{23}h_{29}$$
$$h_{51}=-h_1h_{10}$$
$$h_{52}=2h_1h_4$$
$$h_{53}=2h_1h_6+2h_{27}h_{34}$$
$$h_{54}=h_{27}h_{29}$$
$$h_{55}=-h_1h_{16}$$
$$h_{56}=2h_1h_7+2h_{15}h_{27}+2h_{27}h_{29}$$
$$h_{57}=h_1h_{17}$$
$$h_{58}=2h_1h_8+2h_{18}h_{19}+2h_{18}h_{20}+2h_{18}h_{21}+2h_{19}h_{32}$$
$$-2h_{19}h_{23}+2h_{18}h_{24}-2h_{30}+2h_{31}-2h_{34}$$
$$h_{59}=2h_1h_9+2h_{18}h_{19}+2h_{32}+2h_{27}h_{40}+2h_{41}$$
$$h_{60}=2h_1h_7+2h_{23}h_{27}$$

/669

Where

r_1: radius as far as the center of the mass of the cross-section of the shell with reinforcing rings

I_{z0}: geometric moment of inertia of shell with reinforcing rings passing through the cross-section center of mass, around the axis corresponding to the diameter of the shell

The buckling matrix is

	A	B	C	D	F	G	H	J	K	M	N	
1	h_{44}	h_{45}							h_{46}			$=0$
2	h_{46}	h_{47}							h_{48}			$=0$
3			h_{44}	h_{45}				h_{49}		h_{46}		$=0$
4			h_{45}	h_{47}		h_{51}		h_{50}		h_{48}		$=0$
5					h_{52}						h_{55}	$=0$
6				h_{51}		h_{53}		h_{54}		h_{55}		$=0$
7							h_{60}					$=0$
8			h_{49}	h_{50}		h_{54}		h_{56}		h_{57}		$=0$
9	h_{46}	h_{48}							h_{50}			$=0$
10			h_{46}	h_{48}		h_{55}		h_{57}		h_{58}		$=0$
11					h_{56}						h_{59}	$=0$

No.	Graph & Boundary Cond.	Formula or Table of Results	Notes, Ref.
		As above, the buckling load is obtained if one finds the minimum value of p for the number of waves m.	

BENDING

No.	Graph & Boundary Cond.	Formula or Table of Results	Notes, Ref.
147	Reinforced shell Pure bending (Spring substitutes for frame) 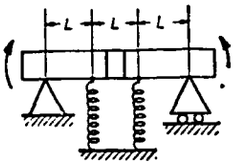 Experiment results	$C_f = \frac{(EI)_f \cdot L}{MD^2}$ M: bending moment D: shell diameter L: distance between frames C_f: coefficient I_f: moment of inertia of frame f: frame Aluminum alloy E = 10^7 PSI P = expresses panel failure G = expresses buckling overall $\frac{P}{G}$ = expresses combination of both	198 /670

TABLE 1

D(In)	L(In)	I_f·In⁴ ×10⁴	Mult (In-Lb)	$C_f \times 10^4$	Form of failure
31.84	8	1.537	219,000	0.554	G
31.84	4	1.537	27,000	0.225	G
31.84	2	1.537	340,000	0.809	G
31.84	16	1.537	168,500	1.438	P/G
31.84	16	1.537	123,000	1.972	P
31.84	8	1.537	107,500	1.128	G
31.84	4	1.537	137,500	0.441	G
31.84	2	1.537	185,000	0.164	G
31.84	16	1.537	45,000	5.376	P/G
31.84	8	1.537	58,500	2.074	G
31.84	4	1.537	75,000	0.808	G
31.84	2	1.537	100,000	0.303	G
31.84	1	1.537	209,000	0.072	G
31.84	1	1.537	397,000	0.038	G
31.84	16	1.537	222,300	1.091	P
31.84	8	1.537	283,600	0.428	G
31.84	4	1.537	336,500	0.180	G
31.84	2	1.537	380,000	0.080	G

No.	Graph & Boundary Cond.	Formula or Table of Results	Notes, Ref.

D(In)	L(In)	I_f·In^4 $\times 10^3$	Mult (In-Ld)	$C_f \times 10^3$	Form of failure
31.84	16	1.537	108,000	2.247	*P*
31.84	8	1.537	163,000	0.744	*G*
31.84	4	1.537	186,000	0.326	*G*
31.84	2	1.537	263,000	0.115	*G*
31.84	16	1.537	59,000	4.115	*P*
31.84	8	1.537	82,000	1.479	*G*
31.84	4	1.537	97,500	0.622	*G*
31.84	2	1.537	153,000	0.198	*G*
32.00	16	31.194	165,000	29.411	*P*
32.00	8	31.194	[illegible],000	8.403	*P*
32.00	4	31.194	434,000	2.808	*G*
32.00	2	31.194	460,000	1.324	*G*
32.00	16	31.194	75,000	66.667	*P*
32.00	8	31.194	134,000	18.131	*P*
32.00	4	31.194	220,000	5.524	*G*
32.00	2	31.194	284,000	2.145	*G*
32.00	8	27.400	169,000	12.658	*P*
32.00	4	27.400	256,000	4.184	*G*
32.00	4	27.400	436,000	2.457	*G*
32.00	2	27.400	500,000	1.070	*G*
20.00	4	1.537	110,000	1.396	*G*
20.00	2	1.537	140,000	0.549	*G*
20.00	4	1.537	66,500	2.309	*G*
20.00	2	1.537	79,000	0.973	*G*
20.00	4	1.537	117,000	1.314	*G*
20.00	2	1.537	150,000	0.512	*G*

/671

The above from E. E. Sechler.
Aluminum alloy, E = 10^7PSI

P = panel failure, G = overall buckling

$\frac{P}{G}$ = combination of both

No.	Graph & Boundary Cond.	Formula or Table of Results	Notes, Ref.

TABLE 2

D(In)	L(In)	I_f(In⁴ $\times 10^5$)	Mult (In-Lb)	$C_f \times 10^4$	Form of failure
20	7.07	6.10	273,000	3.96	*G*
20	7.07	8.15	280,000	5.15	*G*
20	7.07	41.30	280,500	19.22	*P/G*
20	7.07	16.30	337,500	8.55	*G*
20	7.07	65.00	403,500	28.60	*P*
20	5.79	8.15	251,500	4.70	*G*
20	6.43	8.15	246,500	5.32	*G*
20	5.79	8.15	486,500	2.43	*G*
20	9.00	6.10	508,500	2.70	*G*
20	6.43	6.10	553,500	1.77	*G*
20	5.79	8.15	553,300	2.14	*G*
20	9.00	12.20	460,600	5.95	*P/G*
20	9.00	8.15	451,000	4.07	*P/G*
20	9.00	27.50	451,000	13.70	*P*
20	9.00	6.10	403,000	3.40	*G*

No.	Graph & Boundary Cond.	Formula or Table of Results	Notes, Ref.
148	Reinforced cylinder (moncoque construction) Bending	According to Shanley, the buckling of a cylindrical shell with stringers and ribs is	204 /672

$$E_f I_f = C_f \frac{MD^2}{L}$$

I_f = moment of inertia of ribs around axis parallel to plate with stringers attached
E_f = Young's modulus of ribs
L = distance between rib centers
M = bending moment
D = shell diameter
C_f = experimentally determined coefficient

Values of C_f

i) From the results of Shanley's experiments, generally

$C_f > 6.25 \times 10^{-4}$ buckling at panel
$C_f < 6.25 \times 10^{-4}$ inward bulge type buckling
$C_f = 6.25 \times 10^{-4}$ it was found that both occur simultaneously.

No.	Graph & Boundary Cond.	Formula or Table of Results	Notes, Ref.
	Inward bulge type buckling 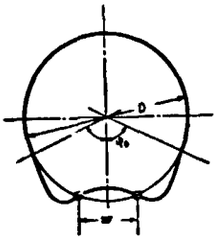	ii) Hoff's analysis $C_f=\left(\frac{2}{3n}\right)^4\cdot\frac{1}{\pi}$ n = number of buckling waves in direction of circumference If n > 5.5, only buckling as a panel n ≤ 5.5, I ward bulge type buckling When n = 5.5, $C_f = 6.84 \times 10^{-5}$ Moreover, in the case of inward bulge type buckling, the following relationship obtains. $\frac{w}{\pi D}=\frac{1}{3n}$	

SHEAR

No.	Graph & Boundary Cond.	Formula or Table of Results	Notes, Ref.
149	Reinforced cylinder Shear	Chiarito's experiment results (24S-T) 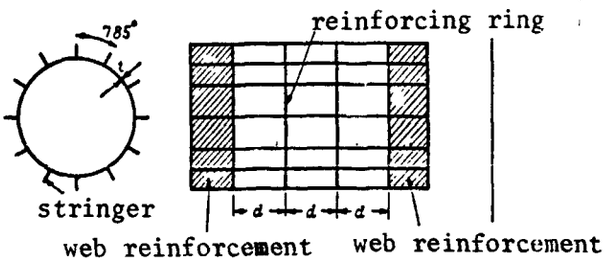	209

Specimen	in.	in.	Reinforcing rings cr. sec.	Dim. (in)	Stringers cr. sec.	Dim. (in)
1	0.0150	15.0	Z	$\frac{9}{16}\times\frac{9}{16}\times 0.040$	L	$\frac{3}{4}\times\frac{3}{4}\times\frac{3}{32}$
2	0.0157	7.5	L	〃	L	〃

No.	Graph & Boundary Cond.	Formula or Table of Results	Notes, Ref.

/673

Experiment Values

Specimen	τ_b (KSI) (a)	τ_b (KSI) (b)	τ_{all} (KSI)	Form of failure
1	0.49	2.82	15.25	A
2	1.68	3.38	18.70	A

(a) case in which buckling first occurs in some panel
(b) case in which buckling occurs in all panels
A with web cracks both reinforcing rings and stringers buckle.

SANDWICH COLUMNS (supplement)

Compression

No.	Graph & Boundary Cond.	Formula or Table of Results	Notes, Ref.
150	Sandwich columns Axial compression (axially symmetrical buckling)	1) when $\frac{E_f \cdot t}{G_c a} \geq \sqrt{1-\nu_f^2}$ $\sigma_b = \frac{(h+t)G_c}{2t}$ $N_b = (h+t)G_c$	195
	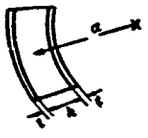	2) otherwise $\sigma_b = k_s E_f \left[\frac{(h+t)}{a}\right]$ $k_s = \frac{\frac{\lambda^2(h+t)}{4(1-\nu_f^2)a} + \frac{a}{\lambda^2(h+t)} + \frac{E_f \cdot t}{2(1-\nu_f^2)G_c a}}{1+\frac{E_f \cdot t}{2(1-\nu_f^2)G_c a}\lambda^2 \frac{(h+t)}{a}}$ $\lambda = \frac{m\pi a}{l}$	
	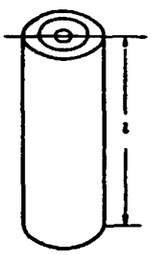	(m: half wave length number around generatrix of shell)	
	f = facing index c = core index	i) $\frac{E_f t}{G_c a} \geq 0.95$ $(\nu_f = 0.3)$ Assuming that the core is especially weak with respect to shear. $N_b = (h+t)G_c$	

No.	Graph & Boundary Cond.	Formula or Table of Results	Notes, Ref.
		ii) $0.1<\frac{E_f \cdot t}{G_c a}<0.95$ Assuming that the core is appropriately weak with respect to shear.	
		iii) $\frac{E_f \cdot t}{G_c a}<0.1$ Assuming that the core is relatively strong with respect to shear. In this case, the cylinder may be considered a homogeneous cylinder. $\sigma_b=\frac{1}{\sqrt{1-\nu^2}} \cdot \frac{E(h+t)}{a}$	/674
		k_c in the case of (ii) is $k_c=-\left(\frac{2\beta\alpha}{\tau^2}+\frac{0.178+0.932\beta}{0.178+1.257\beta+1.694\beta^2}\right)$ $\alpha=\frac{(h+t)^2}{a^2}$ $\beta=\frac{\tau}{\alpha\lambda^2}$ $\tau=\frac{(h+t)G_c}{E_f t}$	
151	Sandwich cylinder Compression Case where core is weak, facing is thin	Applying thin membrane theory to the facing, it is assumed that the core only undergoes shear buckling. i) when $\frac{1}{\sqrt{1-\nu_f^2}}\frac{t_f}{t_c}\frac{h}{a}\frac{E_f}{G_c}\leqq 1$ $\sigma_b=\frac{E_f}{\sqrt{1-\nu_f^2}}\frac{h}{a}\left\{2-\frac{1}{\sqrt{1-\nu_f^2}}\frac{t_f}{t_c}\frac{h}{a}\frac{E_f}{G_c}\right\}$ $N_b=k_c(h+t)G_c$ ii) when $\frac{1}{\sqrt{1-\nu_f^2}}\frac{t_f}{t_c}\frac{h}{a}\frac{E_f}{G_c}\geqq 1$ $\sigma_b=\frac{t_c}{t_f}G_c$ t_f = thickness of facing $2t_c$ = thickness of core	206

No.	Graph & Boundary Cond.	Formula or Table of Results	Notes, Ref.
		2h = distance between neutral planes of two face plates a = radius of neutral plane of cylinder E_f = face plate Young's modulus G_c = shear elasticity modulus of core ν_f = face plate Poisson's ratio	

TORSION

No.	Graph & Boundary Cond.	Formula or Table of Results	Notes, Ref.
152	Sanwich cylinder Torsion Case in which core is weak, face plate thin	Thin membrame theory applied for facing, only shear deformation considered for core. when $1 > \frac{9}{2}K' > 0$ $\tau_k = 1.05\left(1-\frac{9}{2}K'\right)^{\frac{3}{4}} \frac{E_f}{(1-\nu_f^2)^{\frac{3}{4}}} \left(\frac{k}{a}\right)^{\frac{3}{4}}$ $K' = \frac{D'}{2t_c G_c} \cdot \frac{1}{a^2}$ $D' = \frac{2E_f t_f \cdot h^2}{1-\nu_f^2}$ t_f = thickness of facing $2t_c$ = thickness of core 2h = distance between neutral planes of two face plates a = radius of neutral plane of cylinder E_f = face plate, Young's modulus G_c = shear elasticity modulus of core ν_f = face plate, Poisson's ratio	206

No.	Graph & Boundary Cond.	Formula or Table of Results	Notes, Ref.
153	Sandwich cylinder Combination of compression, torsion and bending	$R_c = \frac{N_1}{C} = \frac{\text{Compressive buckling stress}}{\text{Buckling stress in the case of comp. only}}$ $R_B = \frac{2Mrt}{IC} = \frac{\text{Buckling bending moment}}{\text{Buckling moment in case of bending only}}$ $R_t = \frac{T}{2\pi r^2 C} = \frac{\text{Buckling torsion moment}}{\text{Buckling moment in case of torsion only}}$	196 /675

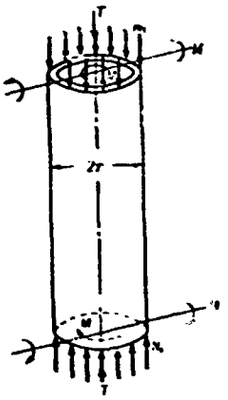

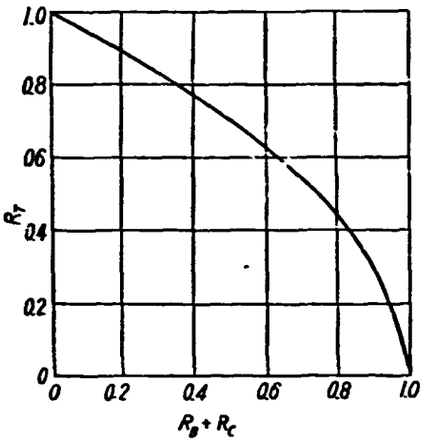

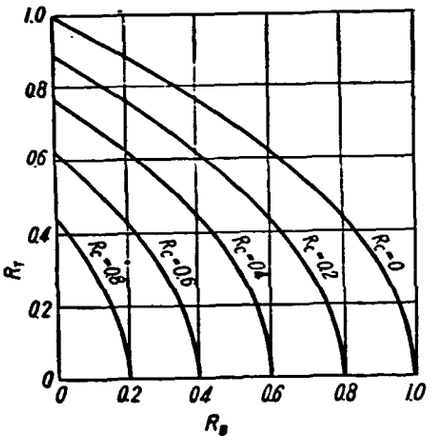

Notation

C = Gt,
G = shear elasticity modulus of core
t = distance between centerplanes of face plate
r = radius from center to neutral plane (of outside plate)
I = moment of inertia of cross-section of sandwich cylinder taken with respect to the diameter
N_1 = vertical forces (compressive force) acting per unit width in direction of axis
M = bending moment
T = torsion moment
N_1, M, T are the values during buckling when they act in combination

REFERENCES

General Theory of Buckling of Shells, Finite Deformation Theory, Tension Shell Structures

1. Lorenz, R.: "Axisymmetrical Distortion in Thin-walled cylinders." /677
   Zeit. V.D.I., Vol. 52, pp. 1706-1713, 1908.
2. Timoshenko, S.: "Some stability Problems of Elasticity Theory."
   Z. Math. Phys., Bd. 58, pp. 337-385, 1910.
3. Lorenz, R.: "Non-axisymmetrical bending of thin-walled cylinders."
   Physik. Zeitschrift., Vol. 12, pp. 241-260, 1911.
4. Southwell, R.v.: "On the General Theory of Elastic Stability", *Phil. Trans. Roy. Soc.*, London, Ser. A., Vol. 213, pp. 187-244, 1914.
5. Mises, R.v.: "The Critical Pressure of Cylindrical Tubes."
   Z. V.D.I., Vol. 58, pp. 750-755, 1914.
6. Zoelly, R.: "The Bending Problem of Round Cups."
   Diss., Zurich Technische Hochschule, 1915.
7. Dean, W.R.: "On the Theory of Elastic Stability", *Proc. Roy. Soc. Lond. Ser. A*, Vol. 102, pp. 734-760, 1925.
8. Rayleigh, L.: *Prox. London Math. Soc.*, Vol. 13, 1881; *Proc. Roy. Soc. Lond. Ser. A.*, Vol. 45, 1889.
9. Love, A.E.H.: "Mathematical Theory of Elasticity" Fourth Edition, Cambridge University Press, 1927.
10. Donnell, L.H.: "A New Theory for the Buckling of Thin Cylinders under Axial Compression and Bending", *Trans. Amer. Soc. Mech. Engr.*, Vol. 56, No. 11, pp. 795-806, 1934.
11. Trefftz, E.: "The Conclusion of the Stability Criterion of Elastic Equilibrium From the Elasticity Theory of Final Deformations."
    Verh. 3. Intern. Kongr. Techn. Mech. Stockholm, pp. 623-629, 1930.
12. Trefftz, E.: "The Theory of The Stability of Elastic Equilibrium."
    Z.A.M.M., Vol. 13, No. 2, pp. 160-165, 1933.
13. Marguerre, K. and E. Trefftz: "The Bearing Ability of a Longitudinally loaded Flat-Strip After Shifting of Ballast."
    Z.A.M.M., Vol. 17, No. 2, pp. 85-100, 1937.
14. Marguerre, K.: "Width of Pressed Plates."
    Lufo., Vol. 14, No. 3, pp. 121-128, 1937.
15. Marguerre: "The Theory of Sharply Deformed Bent Plates."
    Proc. 5. Intern. Congr. Appl. Mech., pp. 93-101, 1938.
16. Biot, M.A.: "Theory of Elasticity with Large Displacements and Rotations", *Proc. 5. Intern. Congr. Appl. Mech.*, pp. 117-122, 1938.
17. Marguerre, K.: "Treatment of Stability Problems by Energetic Methods."
    Z.A.M.M., Vol. 18, No. 1, pp. 57-73, 1938.
18. Marguerre, K.: "Application of Energetic Methods to Stability Problems."
    Jahrbh. d. Deutsche Vesuchsanstalt fur Luftfahrt, pp. 433-443, 1938.
19. Marguerre, K.: "Puncture of Resistance of a Slightly Bent Bar."
    Sitzungsberichte der Berliner Mathematischen Gesellschaft, Vol. 37, p. 22, 1938.
20. Biezeno, C.B.: "Determination of Puncture Resistanceof Slightly Bent, Circular Plate." *Z.A.M.M.*, Vol. 15, No. 2, pp. 13-30, 1938.

21. Kappus, R.: "Elasticity Theory of Finite Shifts."
I. Teil Z.A.M.M., Vol. 19, No. 5, pp. 271-285, 1939-10.
II. Tei. Z.A.M.M., Vol. 19, No. 6, pp. 344-361, 1939-12. /678
22. Karman, Th.v. and H.S. Tsien: "The Buckling of Spherical Shells by External Pressure", *Jour. Aero Sci.*, Vol. 7, No. 2, pp. 43-50, 1939-12.
23. Karman, Th.V., L. G. Dunn and H. S. Tsien: "The Influence of Curvature on the Buckling Characteristics of Structures", *Jour. Aero. Sci.*, Vol. 7, No. 7, pp. 276-289, 1940.
24. Karman, Th. V. and H. S. Tsien: "The Buckling of Thin Cylindrical Shells under Axial Compression", *Jour. Aero. Sci.*, Vol. 8, pp. 303-312, 1941.
25. Shibuya: "Buckling Phenomena in Curved Plates", *Journal of the Japan Aeronautic Society*, Vol. 8, No. 69, p. 53, 1941.
26. Kawano: "Theoretical Considerations of Elastic Instability Phenomena in Curved Plates," *Journal of the Japan Aeronautical Society*, Vol. 8, No. 70, pp. 178-199, 1941.
27. Kondo, K.: "Memorandum Concerning Deformation of Thin Walled Bodies," *Journal of the Japan Aeronautical Society*, Vol. 8, No. 80, pp. 1273-1284, 1941
28. Hiashi, S. and K. Imanaka: Dissertation of the Applied Mathematics Section The First Engineering Department of Tokyo University, 1948.
29. Donnell, L.H. and C.C. Wan: "Effect of Imperfections on Buckling of Thin Cylinders and Colymns under Axial Compression," *Jour. Appl. Mech.*, Vol. 17, No.1, pp. 73-83, 1950.
30. Ebner, H.: "Theory and Experiments of Strength of Fuselage Shells." *Lufo*, Vol. 14, No. 3, pp. 93-115, 1937.
31. Ebner, H. and H. Koller: "Calculation of Strength Curve in Stiffened Cylindrical Shells." *Lufo.*, Vol. 14, No. 12, pp. 607-626, 1937.
32. Ebner, H. and H. Koller: "Strength Curve in Longitudinally and Sectionally Stiffened Sections," *Lufo.*, Vol. 15, No. 10, 11, pp. 527-542, 1938.
33. Schapitz E. and G. Krummling: "Loading Experiments With Strengthened Cylindrical Shells With Loading At Individual Points." *Lufo*, Vol. 14, No. 12, pp. 593-606, 1937.
34. Schapitz, E., H. Feller and H. Koller: "Experimental and Calculation Investigation of Shells Fuselage Model Limited In Bending."

Lufo. 15, No. 12, pp. 563-576, 1938.
35. Ffugge, W.: *Statik und Dynamik der Schalen* [Statistics and Dynamics of Shells." , Julius Springer Press, 1934.
36. Timoshenko, S.: *Theory of Elastic Stability*, McGraw Hill, 1936.
37. Timoshenko, S.: *Theory of Plates and Shells*, New York and London, 1940.
38. Tokugawa, T.: *Elastic Stability Theory*, Published by the Shipbuilding Research Institute of the Naval Engineering Institute, 1940.
39. Kuranishi, N.: *Elasticity*, Published by the Mechanical Society of Japan, 1948.

Compressive Buckling of Curved Plates

40. Newell, J.S.: "Note on the Design of Metal Plate for Use in Airplane Construction," Report on Aircraft Material Research, Massachusetts INst. of Tech., 1931-32.

41. Redshaw, S.C.: "The Elastic Instability of a Thin Curved Panel," *R & M*, No. 1565, 1933.
42. Pollard, H.J.: "Some Developments in Aircraft Construction," *J. Roy. Aeron. Soc.*, Vol. 38, pp. -51-686, 1934.
43. Timoshenko, S.: *Theory of Elastic Stability*, p. 470, 1936.
44. Kromm, A.: "Influence of Rivet Distribution on Pressure Strength of Reinforced Shells of Duraluminum." *Lufo.*, Vol. 14, pp. 116-120, 1937.
45. Ebner, H.: "Theory and Experiments on the Strength of Fuselage Shells." *Lufo.*, Vol. 14, pp. 93-115, 1937.
46. Wenzek, W.A.: "Average Width After Bustling in Curved Plates." *Lufo.*, Vol. 14, pp. 340-344, 1938.
47. Redshaw, S.C.: "The Elastic Stability of a Curved Plate under Axial Thrusts" *Jour. Roy. Aeron. Soc.*, Vol. 42, 1938.
48. Shibuya, T.: "On the Elastic Stability of Thin Walled Cylinders," *Journal of the Japan Aeronautical Society*, Vol. 7, No. 58, pp. 97-135, February 1940.
49. Kawano, T.: "Theoretical Considerations of Concerning the Elastic Instability of Curved Plates," *Journal of the Japan Aeronautical Society*, Vol. 8, No. 70, pp. 178-199, February 1941.
50. Yokoo, T.: "Considering the Effective Width of Flat Plates and Curved Plates," *Journal of the Japan Aeronautical Society*, Vol. 8, No. 70, pp. 200-203, February 1941. /679
51. Kuranishi, N.: *Elasticity*, Published by the Mechanical Society of Japan, p. 523, 1948.

Shear Buckling of Curved Plates

52. Wagner, H.: "Design and Calculation Problems of Plate Structures." *Johrbh. wiss. Ges. Luftft.*, pp. 113-125, 1928.
53. Smith, C.M.: "Strength in Shear of Thin Curved Sheets of Alclad," *NACA Techn. Note*, No. 343, 1930.
54. Leggett, D.M.A.: "The Elastic Stability of a Long and Slightly Bend Rectangular Plate under Uniform Shear," *Proc. Roy. Soc. London*, Ser. A., Vol. 162 No. 908,pp. 62-83, 1937.
55. Ebner, H.: "Theory and Experiments on the Strength of Fuselage Shells." *Lufo.*, Vol. 14, No. 3, pp. 93-115, 1937.
56. Zahorski, A.: "Torsional Stability of Cylindrical Shells," *J. Aero. Sci.*, Vol. 5, No. 2, pp. 62-67, 1937.
57. Kromm, A.: "Stability Boundary of Bent Plates in Compression Loading." *Lufo.*, Vol. 15, No. 11-11, pp. 517-526, 1938.

Buckling Due to External Pressure in Curved Plates

58. Hurlbring, E.: "Strength Calculation of Tubular Bodies under Surrounding *Schiffbau*, Vol. 9, pp. 517-523, 1908.
59. Nicolai, E.L.: *Bull. Polytech. Inst. St. Petersburg*, Vol. 28, 1918; "Stability Problems of the Theory of Elasticity." *Z.A.M.M.*, Vol. 3, pp. 227-229, 1923.
60. Timoshenko, S.: *Theory of Elastic Stability*, p. 227, 1936.

Effective Width of Curved Plates

61. Ebner, H.: " Theory and Experiments on the Strength of Fuselage Shells." *Lufo.*, Vol. , pp. 93-115, 1937.
62. Kromm, A.: "Influence of Rivet distribution on Compressive Strength of Rein-

63. Wenzek, W.A.: *Lufo.*, Vol. 15, pp. 340-353, 1938.
64. Kawano, T.: "Theoretical Considerations of Concerning the Elastic Instability of Curved Plates ," *Journal of the Japan Aeronautical Society*, Vol. 8, No. 70, pp. 178-199, February 1941.

Flexural Buckling of Open Cross-Section Shells

65. Shibuya, T.: "On the Collapse of Partitioning Rings," *Journal of the Japan Aeronautical Society*, Vol. 8, No. 70, pp. 928-935, September 1941.

Compressive Buckling of Cylinders

66. Lorenz, R.: "Axisymmetrical Faults in Thin-Walled Cylinders." *Z.V.D.I.*, Vol. 52, pp. 1706-1713, 1908.
67. Tomoshenko, S.: "Individual Stability Problems of the Theory of Elasticity." *Z. Math. Physik*, Vol. 58, pp. 337-385, 1910.
68. Lorenz, R.: "Non-Axisymmetrical Buckling of Thin-Walled Cylinders." *Physik. Z.*, Vol. 12, pp. 241-260, 1911.
69. Southwell, R.v.: "On the General Theory of Elastic Stability," *Phil. Trans. Roy. Soc. London. Ser. A.*, Vol. 213, pp. 187-244, 1914.
70. Dean, W.R.: "On the Theory of Elastic Stability," *Proc. Roy. Soc. Lond. Ser. A.*, Vol. 102, pp. 734, 760, 1925. /680
71. Foppl, L.: *Sitzungsber. Bayr. Akad. Wissensch. math. naturwiss. Abt.*, pp. 27-40,1926.
72. Robertson, A.: "The Strength of Tubular Struts," *R & M*, No. 1185, 1927.
73. Geckeler, J.W.: "Plastic Buckling of Walls in Cylinders and other fault phenomena in Shells and Plates." *Z.A.M.M.*, Vol. 8, pp. 341-352, 1928.
74. Sander, K.v. and F. Tolke: "Stability Problems in Thin Cylindrical Shells." *Ing. Arcv.*, Vol. 3, No. 1, pp. 24-66, 1932.
75. Flugge, W.: "Stability of Circular Cylinders." *Ing. Arcv.*, Vol. 3, No. 5, pp. 463-506, 1932.
76. Lundquist, E.E.: "strength Test of Thin-walled Duralumin Cylinders in Compression," *N.A.C.A. T.R.*, No. 473, Washington, 1933.
77. Donnell, L.H.: "A New Thoery for the Buckling of Thin cylinders under Axial Compression and Bending," *Trans. Amer. Soc. Mecha. Engr.*, Vol. 56, No. 11, pp. 795-806, 1934.
78. Kaufmann, W.: "Notes on the Stability of Thin-Walled Circular Cylindrical Shells above the Proportionality limit." *Ing. Arcv.* Vol. 6, pp. 419-430.
79. Kaufmann, W.: "The Stability of Thin-Walled Cylinders and Flat Plates above the Proportionality Limit." *Stahlbau*, pp. 1-4, 1937.
80. Marguerre, K.: "Theory of Curved Plates at High Distortion." *Proc. 5, Intern. Congr. Appl. Mech.*, Cambridge, 1938.
81. Donnell, L.H.: "A Discussion of Thin Shell Theory," *Proc. 5. Intern. Congr. Appl. Mecha.*, Cambridge, 1938.

82. Karman, Th.v. L. G. Dunn and H.S. Tsien: "The Influence of Curvature on the Buckling Characteristics of Structures," *Jour. Aero. Sci.*, Vol. 7, pp. 276-289, 1940.
83. Karman, Th.v. and H. S. Tsien: "The Buckling of Thin Cylindrical Shells under Axial Compression," *Jour. Aero. Sci.*, Vol. 8, pp. 303-312, 1941.
84. Donnell, L.H. and C.C. Wan: "Effect of Imperfections on Buckling of Thin Cylinders and Columns under Axial Compression," *Jour. Appl. Mecha.*, Vol. 17, No. 1, pp. 73-83, 1950-3.

Torsional Buckling of Cylinders

85. Greenhill, A.G.: "On the Strength of Shafting When Exposed both to Torsion and to End Thrust," *Prox. Inst. Mech. Engrs.*, p. 182, London, 1883.
86. Schwerin, E.: "Torsion of Thin-Walled Tubes." *Rep. Intern. Congr. Appl. Mech. Delft*, 1924; *Z.A.M.M.*, Vol. 5, pp. 235-243, 1925.
87. Sezawa, K and K. Kubo: "The Buckling of a Cylindrical Shell under Torsion," *Aero. Res. Inst. Tokyo Univ.*, Report No. 76, 1931.
88. Sanden, K.v. and F. Tolke: "Stability Problems of Thinned Circular Cylindrical Shells." *Ing. Arcv.*, Vol. 3, pp. 24-66, 1932.
89. Sezawa, K.: "The Nature of the Torsional Stability of a Monocoque Fuselage", *J. Roy. Aero. Soc.*, Vol. 37, pp. 411-422, 1933.
90. Donnell, L.H.: "Stability of Thin-walled Tubes under Torsion," *N.A.C.A. T.R. No. 479*, Washington, 1933.
91. Lundquist, E.E.: "Strength Tests of Thin-walled Duralumin Cylinders in Torsion," *N.A.C.A. Tech. Note.*, No. 427, 1932.
92. Younger, J.E.: "Principle of Similitude as Applied to Research on Thin-sheet Structures," *Aeron. Engng.*, Vol. 5, pp. 163-169, 1933.
93. Ballerstedt W. and H. Wagner: "Experiments on Strength of Thin, Unstiffened Cylinders Under Compression and Tension." *Lufo.*, Vol. 13, pp. 309-312.
94. Flugge, W.: "Statics and Dynamics of Shells." p. 191, 1934.
95. Stang, A.H., W. Ramberg and G. Back: "Tests of Tubes,: N.A.C.A. T.R., No. 601, 1937. /681

Flexural Buckling of Cylinders

96. Brazier, L.G.: "On the Flexure of Thin Cylindrical Shells and Other Thin Sections," *Proc. Roy. Soc. London Ser. A.*, Vol. -16, pp. 104-114, 1927 or *R. & M.*, No. 1081, 1927.
97. Timoshenko, S.: "Stability and Strength of Thin-walled Constructions," *Proc. 3. Intern. Congr. Appl. Mech.*, Vol. 3, pp. 3-15, Stockholm, 1930.
98. Flugge, W.: "Stability of Circular Cylindrical Shells." *Ing. Arcv.*, Vol. 3, p. 463, 1932.
99. Mossman, R.W. and R. G. Robinson: "Bending Tests of Metal Monocoque Construction," *N.A.C.A. Tech. Note.*, No. 479, Washington, 1933.
100. Chwalla, E.: "Pure Bending of Thin, Thin-Walled Tubes with Straight Axis." *Z.A.M.M.*, Vol. 13, No. 1, pp. 48-58, 1933.
101. Lundquist, E.E.: "Strength Tests of Thin-walled Duralumin Cylinders in Pure Bending," *N.A.C.A. Tech. Note.*, No. 478, Washington, 1933.

102. Younger, J.E.: "Principle of Similitude as Applied to Research on Thin-sheet Structures," *Aeron. Engng.*, Vol. 5, No. 4, pp. 163-169, 1933.
103. Donnell, L.H.: "A New Theory for the Buckling of Thin Cylinders under Axial Compression and Bending," *Trans. A.S.M.E.*, Vol. 56, pp. 795-806, 1934.

Buckling of Cylinders Due to External Pressure

104. Bryan, H.: "On the Stability of Elastic Systems," *Proc. Cambridge Phil. Soc.*, Vol. 6, p. 287, 1888; Theory of Elastic Stability, by Timoshenko, p. 220.
105. Lorenz, R.: "Non-Axisymmetrical Buckling of Thin-Walled Cylinders." *Physik. Z.*, Vol. 12, pp. 241-260, 1911.
106. Southwell, R.v.: "On the Collapse of Tubes by External Pressure,"
Part I. *Phil. Mag.*, Series 6, Vol. 25, pp. 687-698, May 1913.
Part II. *Phil Mag. Series 6*, Vol. 25, pp. 502-511, Sept. 1913.
Part III. *Phil. Mag. Series 6*, Vol. 29, pp. 67-77, Jan. 1915.
107. South well, R.v.: "On the General Theory of Elastic Stability," *Phil. Trans. Roy. Soc. London*, Series A., Vol. 213, pp. 187-214, 1913.
108. Cook, G.: "The Resistance of Tube to Collapse," *Report of British Assoc. for the Advancement of Science*, p. 213, 1913.
109. Cook, G.: "The Collapse of Short Tubes by External Pressure," *Phil. Mag.*, Vol. 28, No. 163, p. 51, 1914.
110. Mises, R.v.: "Critical External Pressure for Surrounding Tubes." *Z.V.D.I.*, Vol. 58, No. 19, pp. 750-755, 1914.
111. Sanden K.v. and K. Gunther: "Strength Problems of Sec-ionally Strengthened Cylinders Under Even-Surrounding External Pressure." *Werft-Reederei-Hafen*
I. January 1920, No. 8, pp. 163-168.
" No. 9, pp. 189-198.
" No. 10, pp. 216-221.
II. January 1921, No. 17, pp. 505-510.
112. Tokugawa, T.: "Elastic Stability of a Thin Circular Ring and of an Infinitely Long Thin Circular Cylindrical Shell under Radial External Pressure," *Papers of the Shipbuilding Society*, No. 45, 1925.
113. Tokugawa, T.: "Model Experiments on the Elastic Stability of Closed and Cross-stiffened Circular Cylinders under Uniform External Pressure," *International Industrial Conference in Tokoyo, Papers*, Paper No. 651, Section 16-Shipbuilding & Marine Engng., Part. I, pp. 249-279, 1931.
114. Tokugawa, T.: "Experiments on the Elastic Stability of Thin Plate Cones /682
Under Uniform Normal External Pressure from Four Sides and Methods of Calculating the Collapse Pressure," *Special Publication No. 125 of the Shipbuilding Society for the Conference on Applied Dynamics* (1931), Collection of Lectures Delivered by the Shipbuilding Society at the Conference on Applied Dynamics, pp. 151-169, 1932.
115. A.S.M.E. Research Committee on the Strength of Vessels under External Pressure, *A.S.M.E.*, Dec. 1933.
116. Westergoard, H.M.: Proc. 4th Intern. Congr. Appl. Mech., p. 274, 1934.
117, Flugge, W.: "Statics and Dynamics of Shells."
Julius Springer, p. 199, Berlin, 1934.
118. Tokugawa, T.: "Experiments on the Compression Failure of Thin Plate

Spherical Cylinders under External Pressure and Methods for Calculating the Collapse Pressure," *Report of the Shipbuilding Society*, No. 59, pp. 179-194, 1936.
119. Tokugawa, T.: "Methods for Calculating Approximately the Collapse Pressure of Thin Plate Cylinders, Cones and Spherical Shells under Uniform External Pressure," *Report of the Shipbuilding Society*, No. 67, pp. 231-240, 1940.

Buckling of Cylinders due to Combined Loads

120. Mises, R.v.: "Critical External Pressure of Cylindrical Tubes." *Z.V.D.I.*, Vol. 58, No. 19, pp. 750-755, 1914.
121. Mises, R.v.: "The Critical External Pressure of Evenly Loaded Cylindrical Tubes."
122. Sanden, K.v. and F. Tolke: "Stability Problems of Thin Circular Cylindrical Shells." *Ing. Arcv.*, Vol. 3, No. 1, pp. 24-66, 1932.
123. Flugge, W.: "Stability of Circular Cylindrical Shells." *Ing. Arcv.*, Vol. 3, No. 5, pp. 463-506, 1932.
124. Yamana, M.: "On the Elastic Stability of Aeroplane Structures," *Jour. Fac. Engng. Tokyo Univ.*, Vol. 20, No. 8, p. 113, 1933.
125. Bridget, F. J. C.C. Jerome and A.B. Vosseller: "Some New Experiments on Buckling of Thin-wall Constructions," *Trans. Amer. Soc. Mech. Engr.*, Vol. 56, No. 8, pp. 569-578, 1934.
126. Windenburg, D.F and C. Trilling: "Collapse by Instability of Thin Cylindrical Shells under External Pressure," *Trans. Amer. Soc. Mech. Engrs.*, Vol. 56, No. 11, pp. 819-825, 1934.
127. Heck, O.S. and H. Ebner: "Formulas and the Calculation Procedures of Plate and Shell Construction in Aircraft." Vol. 11, pp. 211-222, 1935.
128. Ballerstedt, W. and H. Wagner: "Experiments on the Strength of Thinned, Unstiffed Cylinders Under Compression and Tension." *Lufo*. Vol. 13, No. 9
129. Ikeda, T.: "The Bending of Thin-walled Cylinders under Internal or External Pressure," *Journal of the Japan Aeronautical Society*, Vol. 7, No. 68, pp. 1109-1120, 1940.
130. Yoshimura, K. Mori: "The Torsional Buckling of Thin-walled Cylinders under Internal or External Pressure," *Reports of the Aeronautical Research Institute*, Vol. 19, No. 264, 1943.
130'. Kromm, A.: *Beulfestigkeit vor Versteiften Zylinderschalen unter Schud und Innendruck* [Strength of Stiffened Cylindrical Shells Under Compression and Internal Pressure." Jd. Luftf.-Forschg. I., p. 596, 1942.
131. Chwalls, E.: *Erlauterungen zur Begrundung des Normblattentwurfs 2*, Tiel, p. 12.

Compressive Buckling of Elliptical Cylinders

132. Shibuya, T.: "On the Elastic Stability of Thin-walled Cylinders," *Journal of the Japan Aeronautical Society*, Vol. 7, No. 58, pp. 97-135, 1940.

Buckling of Spherical Shells due to Concentrated Force

133. Biezeno, C.B.: "Determination of Puncture Resistance of Slightly Curved, Circular Plates." *Z.A.M.M.*, Vol. 15, No. 1-2, pp. 13-30, 1938.

134. Biezeno, C.B. and R. Grammel: *Technische Dynamik*, pp. 591-600.

Buckling of Spherical Shells due to External Pressure

135. Zoelly, R.:"A Buckling Problem of Spherical Shells."
Zurich Techn. Hochschule, 1915.
136. Schwerin, E.:"The Stability of Thin-Walled Spherical Shells Under Equal Surroundings Pressure." *Z.A.M.M.*, Vol. 2, pp. 81091, 1922. /683
137. Tokugawa, T.: "Experiments on the Compression Failure of Thin Plate Spherical Cylinders under External Pressure and Methods for Calculating the Collapse Pressure," *Report of the Shipbuilding Society*, No. 59, pp. 199-194, 1939.
138. Karman, Th.v. and H.S. Tsien: "The Buckling of Spherical Shells by External Pressure," *Jour. Aero. Sci.*, Vol. 7, No. 2., pp. 43-50, 1939.
139.Tokugawa, T.: "Methods for Calculating Approximately the Collapse Pressure of Thin Plate Cylinders, Cones and Spherical Shells under Uniform External Pressure," *Report of the Shipbuilding Society*, No. 67, pp. 231-240, 1940.

Buckling of Revolving Shells due to External Pressure

140. Geckeler, J.W.:"Plastic Buckling of Walls of Cylinders and Other Failures of Shells and Plates."
Z.A.M.M , Vol. 8, pp. 341-352, 1928.
141. Pfluger, A.: "Stability of Thin Cylindrical Shells."
Ing. Arcv., Vol. 8, pp. 151-172, 1937.
142. Tokugawa, T.: "Methods for Calculating Approximately the Collapse Pressure of Thin Plate Cylinders, Cones and Spherical Shells under Uniform External Pressure," *Report of the Shipbuilding Society*, No. 67, pp. 231-240, 1940.

Torsional Yield Phenomena in Closed Cross-section Shells

143. Ikeda, T.: "On the Failure of Non-circular Thin-walled Cylinders under Torsion," *Journal of the Japan Aeroanutical Society*, Vol. 7, No. 61, pp. 426-439, 1940.
144. Ikeda, T.: "On the Failure of triangular Thin-walled Hollow Cylinders under Torsion," *Journal of the Japan Aeronautical Society*, Vol. 8, No. 79, pp. 1183-1188, 1941.
145. Shibuya, T.: "On the Limits of Instability Phenomena in Thin-walled Angular Cylinders Caused by Torsion," *Journal of the Japan Aeronautical Society*, Vol. 8, No. 76, pp. 815-828, 1941.

Compressive Buckling of Reinforced circular Plates

146. Yamana, M.: "On the Elastic Stability of Aeroplane Structures," *Jour. Fac. Engng. Tokyo Univ.*, Vol. 20. No. 8, 1933.
147. Dschou, D.D.:"Compressive Strength of Reinforced Cylindrical Shells." *Lufo.*, Vol. 11, pp. 223-234, 1935.

148. Shibuya, T.: "On the Elastic Stability of Thin-walled Cylinders," *Journal of the Japan Aeronautical Society*, Vol. 7, No. 58, pp. 97-135, 1940.
149. Lundquist, E.E.: "Comparison of Three Methods for Calculating the Compressive Strength of Flat and Slightly Curved Sheet and Stiffner Corbinations," *N.A.C.A. Tech. Note*, No. 455, Washington, 1933.
150. Newell, J.S.: "The Strength of Aluminium-alloy Sheets," *Airway Age*, Vol. 11, pp. 1420-1424, 1467, 1548-1551, 1574, 1930.

Strength of Reinforced Curved Plates After Buckling

151. Ballerstedt, W. and H. Wagner:"Strength Fields In Curved Thin Plates Under Compressive Loading." *Lufo.*, Vol. 12, No. 2, pp. 70-74, 1935.
152, Eber, H. "Theory and Experiments of the Strength of Fuselage Shells." *Lufo.*, Vol. 14, No. 3, pp. 93-115, 1937.

Compressive Buckling of Reinforced Shells

153. Yamana, M.: "On the Elastic Stability of Aeroplane Structures," *Jour. Fac. Engng. Tokyo Univ.*, Vol. 20, No. 8, 1933.
154.Dschou, D.D.: "Strength of Reinforced Cylindrical Tubes." *Lufo.*, Vol. 11, pp. 223-234, 1935.
155. Hiashi, S.: "On the Buckling of Orthotropic Cylinders," *Reports of the Shipbuilding Society*, No. 81, pp. 85-98, 1949.
156. Taylor, J.L. "The Stability of a Monocoque in Compression," *Aero. Res. Comm. R & M*, No. 1679, 1935.
157. Sezawa, K. and Murakami, M: "The Buckling of Basket Shaped Cylinders Under Axial Pressure," *Report of the Institute of Aeronautics*, No. 168, pp. 427-451, 1938.
158. Hiashi, S., H. Murakami: Dissertation of the Applied Mathematics Section of the first Engineering Department of Tokyo University, 1947.

Torsional Buckling of Reinforced Shells

159. Schapitz, E.: "The Drilling of Thin Walls Reinforced Circular Cylindrical Shells." *Jahrbh. Lilienthal Ges. f. Luftfahrtforschung*, pp. 94-132, 1936.
160. Inoue, S. et al.: "On the strength of Plywood Cylinders," *Journal of the Japan Aeronautical Society*, Vol. 9, No. 91, pp. 1239-1253, 1942.
161. Hiashi, S.: "On the Buckling of Orthotropic Cylinders," *Reports of the Shipbuilding Society*, No. 81, pp. 85-98, 1949.

Flexural Buckling of Reinforced Shells

162. Hech, O.S.: " Stability of Orthotropic Eliptrical Cylindrical in Pure Bend." *Jahrbh. Lilienthal Ges. f, Luftfahrtforschung*, p. 94, 1936; *Lufo.*, Vol. 14, pp. 137-147, 1937.
163. Hoff, N.T.: "Instability of Monocoque Structures in Pure Bending," *J. Roy. Aero. Soc.*, Vol. 52, pp. 291-346, 1938.
164. Inoue, S. et al.: "On the strength of Plywood Cylinders," *Journal of the Japan Aeronautical Society*, Vol. 9, No. 91, pp. 1239-1253, 1942.

165. Hiashi, S.: "On the Buckling of Orthotropic Cylinders," *Reports of the Shipbuilding Society*, No. 81, pp. 85-98, 1949.

Buckling of Reinforced Shells due to Combined Loads

166. Flugge, W.: "The Stability of Circular Cylindrical Shells." *Ing. Arcv.*, Vol. 3, pp. 463-506, 1932.
167. Inoue, S. et al.: "On the Strength of Plywood Cylinders," *Journal of the Japan Aeronautical Society*, Vol. 9, No. 91, pp. 1239-1253, 1942.

Strength of Reinforced Shells after Buckling

168. Heck, O.S. and H. Ebner: "Formulas and Calculation Processes for the Plates and Shell Construction in Aircraft." *Lufo.*, Vol. 11, pp. 211-222, 1935.
169. Schapitz, E.: "The Drilling of Thin-Walled, Reinforced Circular Cylindrical Shells." *Johrbh. Lilienthal Ges. f. Luftfahrtforschung*, pp. 94-132, 1936.
170. Schapitz, E.: "The Theory of Incomplete Stress Fields." *Lufo*, Vol. 14, No. 3, pp. 129-136, 1937.
171, Ebner, H.: "Theory and Experiments of the Strength of Fuselage Shells." *Lufo.*, Vol. 14, No. 3, pp. 93-115, 1937.
172. Kromm, A.: "Influence of Rivet Distribution on the Strength of Reinforced Shells of Duraluminum." *Lufo.* Vol. 14, pp. 116-120, 1937.

General Theory of Corrugated Plates

173. Steel Machinery Data, 1943.
174. Brazier, L.G.: "On the Flexure of Thin Cylindrical Shells and Other Thin Sections," *Proc. Roy. Soy.*, Vol. 116, pp. 104-114, 1927.

Compressive Buckling of Corrugated Plates

175. Steel Machinery Data, 1943.
176. Shibuya, T.: "The Bending of Corrugated Plates and Problems Related to It," *Journal of the Japan Aeronautical Society*, Vol. 9, No. 85, pp. 519-531, 1942.
177. Nissen, O.: "Buckling Experiments of Reinforced Plate Shells with Fewer Compressive Loading." *D.V.L.-Jahrbuch*, Vol. 1, pp. 452-458, 1937.

Buckling of Corrugated Plates Due to Combined Loads

178. Ebner, H.: "The Strength of Shells and Tubular Fuselages." *Lufo.*, Vol. 14, pp. 179-190, 1937.

REFERENCES (Supplement)

179. Batdorf, S.B.: "A Simplified Method of Elastic-Stability Analysis for Thin /685 Cylindrical Shells", *N.A.C.A. Rept.*, NO. 874, March, 1947.
180. Batdorf, S.B., M. Scholdcrout and M. Stein: "Critical Stress of Thin-Walled Cylinders in Axial Compression", *N.A.C.A.*, Rept. 887, March, 1947.
181. Boley, B.A.: "The Shearing Rigidity of Buckled Sheet Panels", *J.A.S.*, Vol. 17, pp. 356-362, June 1950.
182. Krivetsky, A.: "Plasticity Coefficients for the Plastic Buckling of Plates and Shells," *J.A.S.*, Vol. 22, pp. 432-435, June 1955.
183. Yoshimura, Y.: "Local Buckling of Circular Cylindrical Shells and Scale Effects," Proc. 1st Japan National Congress for Applied Mechanics, pp. 69-74, 1951.
184. Nash, W.A.: "Buckling of Thin Cylindrical Shells subject to Hydrostatic Pressure," *J.A.S.*, Vol. 21, pp. 354-355, May, 1954.
185. Bijlaard, P.P.: "Buckling Stress of Thin Cylindrical Clamped Shells Subject to Hrdyostatic Pressure," *J.A.S.*, Vol. 21, pp. 852-853, Dec. 1954.
186. Crate, H., S.B. Batdorf and G. W. Baab: "The Effect of Internal Pressure on the Buckling Stress of Thin-walled Circular Cylinders Under Torsion," *N.A.C.A. Wartime Rept. L-67* (L 4 E 27) May 1944.
187. Klein, B.: "Interaction Equation for the Buckling of Unstiffened Cylinders Under Combined Bending, Torsion and Internal Pressure", *J.A.S.*, Vol. 22, p. 583, Aug. 1955.
188. Stein, M. J. L. Sanders, Jr. and H. Crate: "Critical Stress of Ring-Stiffened Cylinders in Torsion," *N.A.C.A. Rept. 989*, Sept. 1949.
189. Nash, W. A.: "Buckling of Multiple-Bay Ring-Reinforced Cylindrical Shells Subject ot Hydrostatic Pressure," *J. of Applied Mechanics*, pp. 469-474, Dec. 1953.
190. Onat, B.T. and D.C. Drucker: "Inelastic Instability and Incremental Theories of Plasticity," *J.A.S.*, Vol. 20, pp. 181-186, Mar. 1953.
191. Rafel, N.: "Effect of Normal Pressure on the Critical Compressive Stress of Curved Sheet," *N.A.C.A. Wartime Rept. L-258*, Nov. 1942.
192. Melcon, M.A. and A.F. Ensrud: "Analysis of Stiffened Curved Panels Under Shear and Compression," *J.A.S.*, Vol. 20, pp. 111-119, Feb. 1953.
193. Kuhn, P. and L.R. Levin: "An Empirical Formula for the Critical Shear Stress of Curved Sheets," *N.A.C.A. Wartime Rept. L-58*, Jan. 1945.
194. Schuette, E.H.: "Buckling of Curved Sheet in Compression and Its Relation to the Secant Modulus," *J.A.S.*, Vol. 15, pp. 18-22, Jan. 1948.
195. Teichmann, F.K., Chi-Teh Wang and G. Gerard: "Buckling of Sandwich Cylinders Under Axial Compression," *J.A.S.*, Vol. 18, pp. 398-406., June 1951.
196. Wang, C.T., R.J. Vaccaro and D.F. De Santo: "Buckling of Sandwich Cylinders Under Combined Compression, Torsion, and Bending Loads," *J. of Applied Mechanics*, pp. 324-328, Sept. 1955.
197. Ralston, A.: "On the Problem of Buckling of Hyperbolic Paraboloidal Shell Loaded by its own Weight," *J. of Mathematics and Physics*, Pp. 53-59, April 1956.
198. Shanley, F.R.: "Simplified Analaysis of General Instability of Stiffened

Shells in Pure Bending," *J.A.S.*, Vol. 16, pp. 590-592, Oct. 1949.
199. Levy, S. and W. D. Kroll: "Primary Instability of Open-section Stringers Attached to Sheet," *J.A.S.*, Vol. 15, pp. 581-591, Oct. 1948.
200. Tyler, C.M., Jr. and T.J. Walker: "Lateral Elastic Instability of Hat-Section Stringers," *J.A.S.*, Vol. 18, p. 633, Sept. 1951. /686
201. Uemura, M. and Y. Yoshimura: "The Buckling of Shells by External Pressure" Proc. 2nd Japan National Congress for Applied Mechanics, pp. 145-148, 1952.
202. Uemura, M.: "The Buckling of Spherical Shells by External Pressure 3rd Report: Buckling Mechanism of Spherical Shell Segments," Proc. 3rd Japan National Congress for Applied Mechanics, pp. 113-118, 1953.
203. Kanemitsu, S. and H. Nojima: "Axial Compression Tests of Thin Circular Cylinders," Thesis. Calif. Inst. of Tech., 1939.
204. Gerard, G.: "Minimum Weight Analysis of Compression Structures," pp. 119-131, 1956.
205. Kuhn, P.: "Stresses in Aircraft and Shell Structures," p. 352, 1956.
206. Kuranishi, M., H. Nagao: "The Buckling of Sandwich Rods, Plates and Shells," *Aeronautic Society*, 11. 10., 1956.
207. Gerard, G.: "Compressive and Torsional Buckling of Thin-walled Cylinders in Yield Region," *N.A.C.A. T.N. 3726*, Aug. 1956.
208. Batdorf, S.B.: "A Simplified Method of Elastic-Stability Analysis for Thin Cylindrical Shells 1-Donnell's Equation," *N.A.C.A. T.N. 1341*, 1947.
209. Chiarito, P. T.: "Some Strength Tests of Stiffened Curved Sheets Loaded in Shear," *N.A.C.A. Wartime Report L-259*, Apr. 1944.
210. Gerard, G.: "Plastic Stability Theory of Thin Shells," *J.A.S.*, Vol. 24, pp. 269-274, April 1957.
211. Lee, L. H. N. and C. S. Ades: "Plastic Torsional Buckling Strength of Cylinders Including the Effects of Imperfections,: *J.A.S.*, Vol. 24, pp. 241-248, April 1957.
212. Fung, Y.C and E.E. Sechler: "Buckling of Thin-walled Circular Cylinders under Axial Compression and Internal Pressure," *J.A.S.*, Vol. 24, pp. 351-356, May 1957.
213. Zuk, W.: "Thermal Buckling of Clamped Cylindrical Shells," *J.A.S.*, Vol.24 p. 389, May 1957.
214. Loo, Tsu-Tao: "An Extension of Donnell's Equation for a Circular Cylindrical Shell," *J.A.S.*, Vol. 24, pp. 390-391, May 1957.
215. Lo, H. Crate, H. and E. B. Schwartz: "Buckling of Thin-walled Cylinder under Axial Compression and Internal Pressure," *N.A.C.A. Rept. 1027*, 1951.
216. Radhakrishnan, S.: "Plastic Buckling of Circular Cylinders," *J.A.S.*, Vol. 23, pp. 892-894, Sept. 1956.
217. Reiss, E.L.: "On the Nonlinear Buckling of Shallow Spherical Domes," *J.A.S.* Vol. 23, pp. 973-975, Oct. 1956.
218. Becker, H.: "Handbook of Structural Stability, Part II....Buckling of Composite Elements," *N.A.C.A. T.N.3782*, 1957.
219. Gerard, G. and H. Becker: "Handbook of Structural Stability, Part III.... Buckling of Curved Plates and Shells," *N.A.C.A T.N. 3783*, 1957.
220. Gerard, G.: "Handbook of Structural Stability, Part, IV....Failure of Plates and Composite Elements," *N.A.C.A. T.N. 3784*, 1957.